CHARACTERIZING THE MULTI-FACETED DYNAMICS OF TUMOR CELL PLASTICITY

EDITED BY: Satyendra Chandra Tripathi, Mohit Kumar Jolly, Herbert Levine and Sendurai A. Mani

PUBLISHED IN: Frontiers in Molecular Biosciences, Frontiers in Oncology and Frontiers in Cell and Developmental Biology

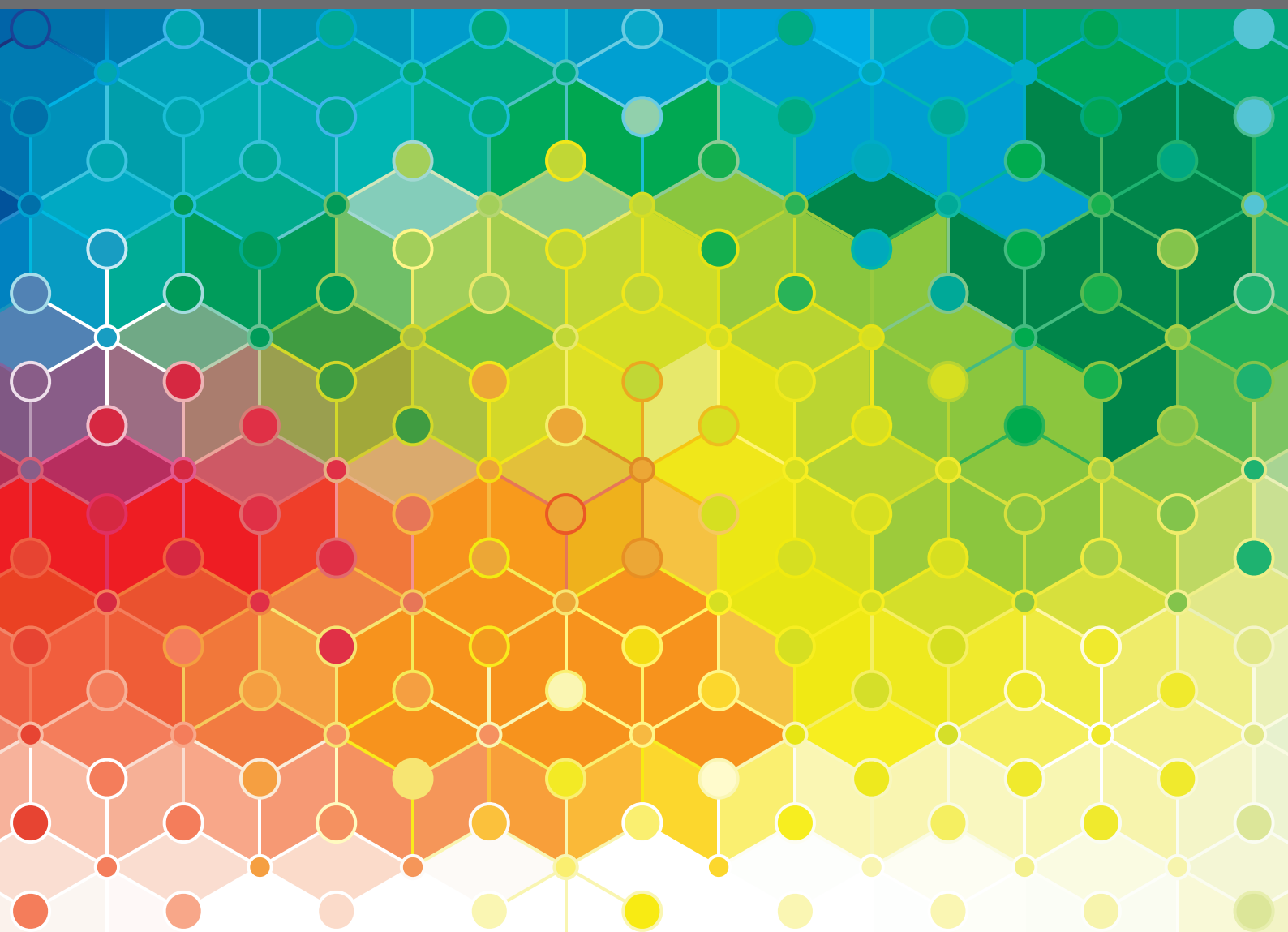

frontiers Research Topics

frontiers

Frontiers eBook Copyright Statement

The copyright in the text of individual articles in this eBook is the property of their respective authors or their respective institutions or funders. The copyright in graphics and images within each article may be subject to copyright of other parties. In both cases this is subject to a license granted to Frontiers.

The compilation of articles constituting this eBook is the property of Frontiers.

Each article within this eBook, and the eBook itself, are published under the most recent version of the Creative Commons CC-BY licence. The version current at the date of publication of this eBook is CC-BY 4.0. If the CC-BY licence is updated, the licence granted by Frontiers is automatically updated to the new version.

When exercising any right under the CC-BY licence, Frontiers must be attributed as the original publisher of the article or eBook, as applicable.

Authors have the responsibility of ensuring that any graphics or other materials which are the property of others may be included in the CC-BY licence, but this should be checked before relying on the CC-BY licence to reproduce those materials. Any copyright notices relating to those materials must be complied with.

Copyright and source acknowledgement notices may not be removed and must be displayed in any copy, derivative work or partial copy which includes the elements in question.

All copyright, and all rights therein, are protected by national and international copyright laws. The above represents a summary only. For further information please read Frontiers' Conditions for Website Use and Copyright Statement, and the applicable CC-BY licence.

ISSN 1664-8714
ISBN 978-2-88966-523-5
DOI 10.3389/978-2-88966-523-5

About Frontiers

Frontiers is more than just an open-access publisher of scholarly articles: it is a pioneering approach to the world of academia, radically improving the way scholarly research is managed. The grand vision of Frontiers is a world where all people have an equal opportunity to seek, share and generate knowledge. Frontiers provides immediate and permanent online open access to all its publications, but this alone is not enough to realize our grand goals.

Frontiers Journal Series

The Frontiers Journal Series is a multi-tier and interdisciplinary set of open-access, online journals, promising a paradigm shift from the current review, selection and dissemination processes in academic publishing. All Frontiers journals are driven by researchers for researchers; therefore, they constitute a service to the scholarly community. At the same time, the Frontiers Journal Series operates on a revolutionary invention, the tiered publishing system, initially addressing specific communities of scholars, and gradually climbing up to broader public understanding, thus serving the interests of the lay society, too.

Dedication to Quality

Each Frontiers article is a landmark of the highest quality, thanks to genuinely collaborative interactions between authors and review editors, who include some of the world's best academicians. Research must be certified by peers before entering a stream of knowledge that may eventually reach the public - and shape society; therefore, Frontiers only applies the most rigorous and unbiased reviews.
Frontiers revolutionizes research publishing by freely delivering the most outstanding research, evaluated with no bias from both the academic and social point of view. By applying the most advanced information technologies, Frontiers is catapulting scholarly publishing into a new generation.

What are Frontiers Research Topics?

Frontiers Research Topics are very popular trademarks of the Frontiers Journals Series: they are collections of at least ten articles, all centered on a particular subject. With their unique mix of varied contributions from Original Research to Review Articles, Frontiers Research Topics unify the most influential researchers, the latest key findings and historical advances in a hot research area! Find out more on how to host your own Frontiers Research Topic or contribute to one as an author by contacting the Frontiers Editorial Office: frontiersin.org/about/contact

CHARACTERIZING THE MULTI-FACETED DYNAMICS OF TUMOR CELL PLASTICITY

Topic Editors:
Satyendra Chandra Tripathi, All India Institute of Medical Sciences Nagpur, India
Mohit Kumar Jolly, Indian Institute of Science (IISc), India
Herbert Levine, Rice University, United States
Sendurai A. Mani, University of Texas MD Anderson Cancer Center, United States

Citation: Tripathi, S. C., Jolly, M. K., Levine, H., Mani, S. A., eds. (2021). Characterizing the Multi-faceted Dynamics of Tumor Cell Plasticity. Lausanne: Frontiers Media SA. doi: 10.3389/978-2-88966-523-5

Table of Contents

05 ***Editorial: Characterizing the Multi-Faceted Dynamics of Tumor Cell Plasticity***
Satyendra Chandra Tripathi, Mohit Kumar Jolly, Sendurai A. Mani and Herbert Levine

08 ***Multifaceted Roles of Asporin in Cancer: Current Understanding***
Shaohua Zhan, Jinming Li and Wei Ge

18 ***Inhibition of CYR61-S100A4 Axis Limits Breast Cancer Invasion***
Johanna W. Hellinger, Silke Hüchel, Lena Goetz, Gerd Bauerschmitz, Günter Emons and Carsten Gründker

35 ***Ping-Pong—Tumor and Host in Pancreatic Cancer Progression***
Wei Mu, Zhe Wang and Margot Zöller

81 ***High Frequency of Cell-in-Cell Formation in Heterogeneous Human Breast Cancer Tissue in a Patient With Poor Prognosis: A Case Report and Literature Review***
Banzhan Ruan, Zubiao Niu, Xiaoyi Jiang, Zhuo Li, Yanhong Tai, Hongyan Huang and Qiang Sun

87 ***Mitochondrial Involvement in Migration, Invasion and Metastasis***
Tatiana V. Denisenko, Anna S. Gorbunova and Boris Zhivotovsky

104 ***Integrative Transcriptomic Analysis Reveals a Multiphasic Epithelial–Mesenchymal Spectrum in Cancer and Non-tumorigenic Cells***
Nicholas Panchy, Cassandra Azeredo-Tseng, Michael Luo, Natalie Randall and Tian Hong

125 ***Single Tumor Cells With Epithelial-Like Morphology are Associated With Breast Cancer Metastasis***
Liubov A. Tashireva, Marina V. Zavyalova, Olga E. Savelieva, Tatyana S. Gerashchenko, Evgeniya V. Kaigorodova, Evgeny V. Denisov and Vladimir M. Perelmuter

137 ***LOXL2 Expression Status is Correlated With Molecular Characterizations of Cervical Carcinoma and Associated With Poor Cancer Survival via Epithelial-Mesenchymal Transition (EMT) Phenotype***
Canhui Cao, Shitong Lin, Wenhua Zhi, Cordelle Lazare, Yifan Meng, Ping Wu, Peipei Gao, Juncheng Wei and Peng Wu

150 ***Integrative Analysis of Breast Cancer Cells Reveals an Epithelial-Mesenchymal Transition Role in Adaptation to Acidic Microenvironment***
Mehdi Sadeghi, Bryce Ordway, Ilyia Rafiei, Punit Borad, Bin Fang, John L. Koomen, Chaomei Zhang, Sean Yoder, Joseph Johnson and Mehdi Damaghi

164 ***ZEB1: A Critical Regulator of Cell Plasticity, DNA Damage Response, and Therapy Resistance***
Stanislav Drápela, Jan Bouchal, Mohit Kumar Jolly, Zoran Culig and Karel Souček

174 ***New Insights Into the Role of Phenotypic Plasticity and EMT in Driving Cancer Progression***
Sugandha Bhatia, Peiyu Wang, Alan Toh and Erik W. Thompson

192 ***Toward Modeling Context-Specific EMT Regulatory Networks Using Temporal Single Cell RNA-Seq Data***
Daniel Ramirez, Vivek Kohar and Mingyang Lu

206 ***Cellular Plasticity in Breast Cancer Progression and Therapy***
Deguang Kong, Connor J. Hughes and Heide L. Ford

229 ***Cancer Stem Cell Plasticity – A Deadly Deal***
Archana P. Thankamony, Kritika Saxena, Reshma Murali, Mohit Kumar Jolly and Radhika Nair

245 ***Hybrid Stem Cell States: Insights Into the Relationship Between Mammary Development and Breast Cancer Using Single-Cell Transcriptomics***
Tasha Thong, Yutong Wang, Michael D. Brooks, Christopher T. Lee, Clayton Scott, Laura Balzano, Max S. Wicha and Justin A. Colacino

260 ***Senescence-Associated Pro-inflammatory Cytokines and Tumor Cell Plasticity***
Jean Paul Vernot

275 ***Dynamics of Cellular Plasticity in Prostate Cancer Progression***
Ritika Tiwari, Nishat Manzar and Bushra Ateeq

290 ***Slug and E-Cadherin: Stealth Accomplices?***
Esta Sterneck, Dipak K. Poria and Kuppusamy Balamurugan

298 ***Id Proteins Promote a Cancer Stem Cell Phenotype in Mouse Models of Triple Negative Breast Cancer via Negative Regulation of Robo1***
Wee S. Teo, Holly Holliday, Nitheesh Karthikeyan, Aurélie S. Cazet, Daniel L. Roden, Kate Harvey, Christina Valbirk Konrad, Reshma Murali, Binitha Anu Varghese, Archana P. Thankamony, Chia-Ling Chan, Andrea McFarland, Simon Junankar, Sunny Ye, Jessica Yang, Iva Nikolic, Jaynish S. Shah, Laura A. Baker, Ewan K. A. Millar, Matthew J. Naylor, Christopher J. Ormandy, Sunil R. Lakhani, Warren Kaplan, Albert S. Mellick, Sandra A. O'Toole, Alexander Swarbrick and Radhika Nair

315 ***Spotlight on the Granules (Grainyhead-Like Proteins) – From an Evolutionary Conserved Controller of Epithelial Trait to Pioneering the Chromatin Landscape***
Vignesh Sundararajan, Qing You Pang, Mahesh Choolani and Ruby Yun-Ju Huang

frontiers in Molecular Biosciences

EDITORIAL
published: 20 January 2021
doi: 10.3389/fmolb.2020.630276

Editorial: Characterizing the Multi-Faceted Dynamics of Tumor Cell Plasticity

Satyendra Chandra Tripathi[1]*, *Mohit Kumar Jolly*[2]*, *Sendurai A. Mani*[3] and *Herbert Levine*[4]

[1]Department of Biochemistry, All India Institute of Medical Sciences, Nagpur, India, [2]Centre for BioSystems Science and Engineering, Indian Institute of Science, Bangalore, India, [3]UT MD Anderson Cancer Center, Houston, TX, United States, [4]Center for Theoretical Biological Physics, Northeastern University, Boston MA, United States

Keywords: cellular plasticity, cancer, epithelial to mesenchymal transition, transcription factor, hybrid states, metastasis, drug resistance, epithelial-mesenchymal plasticity

Editorial on the Research Topic

Characterizing the Multi-faceted Dynamics of Tumor Cell Plasticity

Cellular plasticity – the ability to dynamically adapt to various changing biochemical and biomechanical, intracellular and extracellular conditions – is a hallmark of cancer aggressiveness. Metastasis, tumor relapse, and resistance against various therapies are manifestations of this multi-faceted phenomenon. Modes of tumor cell plasticity include transitions among phenotypes on the epithelial-mesenchymal spectrum, different subsets of cancer stem cells (CSCs) and non-CSCs, and various metabolic states. These modes depend on a complex interplay between multistable genetic networks, epigenetic regulation and cellular physiology. Furthermore, there is a reciprocal interaction between tumor cell plasticity and plasticity of the microenvironment, as illustrated for example in the alternative polarization states available for macrophages and CD4+ T-helper cells.

Recent in silico, in vitro, and in vivo studies have highlighted that all the processes mentioned above - Epithelial-to-Mesenchymal Transition (EMT), macrophage polarization, and metabolic flexibility related to the Warburg effect - are not binary as originally hypothesized. Instead, cells can acquire a variety of hybrid phenotype(s) with mixed molecular and cellular properties. The hybrid epithelial/mesenchymal (E/M) phenotypes may underpin collective cell migration during metastasis, leading to clusters of circulating tumor cells or emboli, and are typically more 'stem-like' and aggressive than cells on either end of the spectrum of this Epithelial-Mesenchymal Plasticity (EMP). Similarly, metabolic phenotypes exhibiting hybrid glycolytic/oxidative phosphorylation processes can drive aggressiveness and therapy resistance. Finally, reversible transitions among non-CSCs and different subsets of CSCs represent a population-level equilibrium maintained among various tumor cell populations.

Progress in charting the underlying regulatory networks mediating these interconnected manifestations of plasticity has facilitated detailed computational studies to identify various nodes in these networks that can potentially serve as biomarkers or therapeutic targets. However, a comprehensive characterization of the dynamics of these transitions and other associated traits such as drug resistance, immune evasion, epigenetic modifications, genetic instability, and cell migration and invasion, and identification of the molecular factors that coordinate these associations, remains incomplete. In this Research Topic, we focus on the molecular and cellular aspects of the multi-dimensional nature of tumor cell plasticity and its implications for cancer progression, metastasis, and tumor relapse. The crucial contributions contained herein cover a broad range of topics related to characterizing the multifaceted dynamics of cellular plasticity.

OPEN ACCESS

Edited and reviewed by:
William C. Cho,
QEH, Hong Kong
Mahendra K. Singh,
University of Miami, United States

***Correspondence:**
Satyendra Chandra Tripathi
sctripathi@aiimsnagpur.edu.in
Mohit Kumar Jolly
mkjolly@iisc.ac.in

Specialty section:
This article was submitted to a section of the journal Frontiers in Molecular Biosciences

Received: *17 November 2020*
Accepted: *21 December 2020*
Published: *20 January 2021*

Citation:
Tripathi SC, Jolly MK, Mani SA and Levine H (2021) Editorial: Characterizing the Multi-Faceted Dynamics of Tumor Cell Plasticity. Front. Mol. Biosci. 7:630276. doi: 10.3389/fmolb.2020.630276

Sadeghi et al. (2020) performed an integrative analysis to establish the role of EMT within the breast cancer acidic microenvironment. A partial EMT phenotype was observed in the acid-adapted cellular populations, indicating cellular plasticity leading to metastatic competence. The authors also proposed the S100A6 and S100B proteins as key players during the acid-induced EMT phenotypic alteration. Tashireva et al. (2020) categorized molecular subtypes of breast cancer to evaluate stemness and epithelial-mesenchymal transition (EMT) in single tumor cells (STCs). They found that in comparison to mesenchymal-like STCs, cells with epithelial-like morphology more effectively contribute towards breast cancer metastasis. Hellinger et al. (2019) identified an interaction of CYR61 with metastasis-associated protein S100A4 in invasive breast cancer cells. Their findings suggest that inhibiting EMT induced CYR61 reduces ERK1/2 phosphorylation, thereby suppressing S100A4 and hence invasiveness in mesenchymal-ransformed breast cancer cells. In a breast cancer case report, Ruan et al. (2019) focused on a rare pathological phenomenon called cell cannibalism. The authors reported a high frequency of cell-in-cell (CIC) structures with considerable heterogeneity associated with active cell proliferation and poor prognosis. Teo et al. (2020) utilized the 4T1 murine model of TNBC to reveal that Inhibitor of Differentiation Protein (ID1) is expressed in rare neoplastic cells within ER-negative breast cancers. They unveiled a novel mechanism where ID proteins negatively regulate Robo1, activating a Myc transcriptional program. Thong et al. (2020) used single-cell RNA-sequencing to quantify cell state distributions and hybrid stem cell states of the normal mammary (NM) gland throughout the developmental stages of breast and cancer. Their analysis highlighted the phenotypic plasticity of normal mammary stem cells, where E/M hybrids are the most developmentally immature type and play an important role in mammary morphogenesis. Among the breast cancer subtypes, basal tumors expressed a distinct developmentally immature signature.

Cao et al. (2020) identified LOXL2 as a therapeutic target in cervical carcinoma where it is positively correlated with EMT phenotype. They showed that LOXL2 silencing inhibits the proliferation and migration of cancer cells. Panchy et al. (2019) provided insights into the mechanistic basis of cancer cell heterogeneity and plasticity. They combined cancer cell transcriptomics from time course data of EMT in non-tumorigenic epithelial cells, and from epithelial cells with perturbations of key EMT factors in order to perform an integrative analysis. They noticed a wide distribution of cancer cells spread across the EMT spectrum, with ZEB1 playing a key role. Ramirez et al. (2020) used a bioinformatical approach combined with mathematical modelling to analyze a time-series of single-cell RNA-sequencing data of EMT induced cancer cell lines. They constructed common context-specific EMT gene regulatory circuits and identified transcriptional regulators contributing to drive or reverse EMT.

In addition to these original research contributions, the collection of articles also included comprehensive research articles on various axes of plasticity. Kong et al. presented an overall picture of cellular plasticity mediated by the MAPK, PI3K, STAT3, Wnt, Hedgehog, and Notch pathways during breast cancer progression. Drapela et al. discussed the role of ZEB1, a key EMT-inducing transcription factor involved in cell plasticity, response to DNA damage, and in enabling resistance to various therapies. Similarly, Sundararajan et al. (2019) reviewed the roles of GRHL2, an evolutionarily conserved regulator of the epithelial phenotype. Sterneck et al. investigated the respective roles of SLUG, a mediator of partial EMT, and E-cadherin. Zhan et al. (2019) reviewed the role of Asporin in various cancers including breast, colorectal, and pancreatic cancer, where it modulates the EMT transition and hence the migration and invasiveness of tumor cells. After reviewing the increasing amount of evidence for the significance of partial EMT states, Bhatia et al. also discussed clinical developments in targeting epithelial-mesenchymal plasticity (EMP). Clinical and therapeutic implicates of EMP are becoming increasingly crucial, thus indicating that the therapeutic window in the context of EMP needs to be investigated carefully. One proposed idea can be to 'fix the cells' on their position of the EMP axis, which may be possible by breaking feedback loops embedded in a cancer cell circuitry (Williams et al., 2019; Hari et al., 2020). Another recent approach can be re-differentiation of cancer cells into normal epithelial cells. Recent approaches include the forced trans-differentiation of EMT-derived breast cancer cells to being adipocytes (Ishay-Ronen et al., 2019).

Beyond EMP, plasticity along the axes of cancer cell stemness was discussed by Thankamony et al. and plasticity along neuroendocrine prostate cancer was highlighted by Tiwari et al. The association of tumor plasticity with senescence-associated pro-inflammatory cytokines was reviewed by Vernot et al. and with mitochondrial involvement was discussed by Denisenko et al. (2019). Finally, non-cell-autonomous mechanisms of cell plasticity i.e., tumor-host interactions, were reflected upon by Mu et al. (2019) focusing on mechanisms related to pancreatic cancer progression. The increasing realization of the plasticity of the TME and especially of its immune components is one of the critical topics ripe for future investigations. We hope you enjoy this series of articles and recognize that the concept of cell plasticity is engendering a revolution in how we think about cancer and how we might be able to create robust interventional strategies.

AUTHOR CONTRIBUTIONS

ST and MJ conceived, wrote, and edited the final version of this editorial. SM and HL edited and approved the final version of this editorial.

REFERENCES

Cao, C., Lin, S., Zhi, W., Lazare, C., Meng, Y., Wu, P., et al. (2020). LOXL2 Expression status is correlated with molecular characterizations of cervical Carcinoma and associated with Poor Cancer survival via Epithelial-Mesenchymal transition (EMT) phenotype. *Front. Oncol.* 10, 284. doi:10.3389/fonc.2020.0028

Denisenko, T. V., Gorbunova, A. S., and Zhivotovsky, B. (2019). Mitochondrial involvement in migration, invasion and metastasis. *Front. Cell Dev. Biol.* 7, 355. doi:10.3389/fcell.2019.00355

Hari, K., Sabuwala, B., Subramani, B. V., Porta, C. A., Zapperi, S., Font-Clos, F., et al. (2020). Identifying inhibitors of epithelial–mesenchymal plasticity using a network topology-based approach. npj. *Syst. Biol. Appl.* 6, 15. doi:10.1038/s41540-020-0132-1

Hellinger, J. W., Hüchel, S., Goetz, L., Bauerschmitz, G., Emons, G., and Gründker, C. (2019). Inhibition of CYR61-S100A4 axis limits Breast Cancer invasion. *Front. Oncol.* 9, 1074. doi:10.3389/fonc.2019.01074

Ishay-Ronen, D., Diepenbruck, M., Kalathur, R. K. R., Sugiyama, N., Tiede, S., and Ivanek, R., (2019). Gain fat—lose metastasis: converting invasive breast cancer cells into *Adipocytes* inhibits cancer metastasis. *Cancer Cell* 35, 17–32. doi:10.1016/j.ccell.2018.12.002

Mu, W., Wang, Z., and Zöller, M. (2019). Ping-Pong—Tumor and host in Pancreatic Cancer progression. *Front. Oncol.* 9, 1359. doi:10.3389/fonc.2019.01359

Panchy, N., Azeredo-Tseng, C., Luo, M., Randall, N., and Hong, T. (2019). Integrative transcriptomic analysis reveals a multiphasic Epithelial -Mesenchymal spectrum in Cancer and non-tumorigenic cells. *Front. Oncol.* 9, 1479. doi:10.3389/fonc.2019.01479

Ramirez, D., Kohar, V., and Lu, M. (2020). Toward modeling context-specific EMT regulatory networks using temporal single cell RNA-seq data. *Front. Mol. Biosci.* 7, 54. doi:10.3389/fmolb.2020.00054

Ruan, B., Niu, Z., Jiang, X., Li, Z., Tai, Y., Huang, H., et al. (2019). High frequency of cell-in-cell formation in heterogeneous human Breast Cancer tissue in a patient with poor prognosis: a case report and literature review. *Front. Oncol.* 9, 1444. doi:10.3389/fonc.2019.01444

Sadeghi, M., Ordway, B., Rafiei, I., Board, P., Fang, B., and Koomen, J. L. (2020). Integrative analysis of Breast Cancer cells reveals an Epithelial-Mesenchymal transition role in adaptation to acidic microenvironment. *Front. Oncol.* 10, 304. doi:10.3389/fonc.2020.00304

Sundararajan, V., Tan, M., Tan, T. Z., Ye, J., Thiery, J. P., and Huang, R. Y.-J. (2019). SNAI1 recruits HDAC1 to suppress SNAI2 transcription during epithelial to mesenchymal transition. *Sci. Rep.* 9, 8295. doi:10.1038/s41598-019-44826-8

Tashireva, L. A., Zavyalova, M. V., Savelieva, O. E., Gerashchenko, T. S., Kaigorodova, E. V., Denisov, E. V., et al. (2020). Single tumor cells with Epithelial-Like morphology are associated with Breast Cancer metastasis. *Front. Oncol.* 10, 50. doi:10.3389/fonc.2020.00050

Teo, W. S., Holliday, H., Karthikeyan, N., Cazet, A. S., Roden, D. L., et al. (2020). Id proteins promote a cancer stem cell phenotype in mouse models of triple negative Breast Cancer via negative regulation of Robo1. *Front. Cell. Dev. Biol.* 8, 552. doi:10.3389/fcell.2020.00552

Thong, T., Wang, Y., Brooks, M. D., Lee, C. T., Scott, C., Balzano, L., et al. (2020). Hybrid stem cell states: insights into the relationship between mammary development and Breast Cancer using single-cell transcriptomics. *Front. Cell. Dev. Biol.* 8, 288. doi:10.3389/fcell.2020.00288

Williams, E. D., Gao, D., Redfern, A., and Thompson, EW. (2019). Controversies around epithelial–mesenchymal plasticity in cancer metastasis. *Nat. Rev. Cancer* 19, 716–732. doi:10.1038/s41568-019-0213-x

Zhan, S., Li, J., and Ge, W. (2019). Multifaceted roles of asporin in cancer: current understanding. *Front. Oncol.* 9, 948. doi:10.3389/fonc.2019.00948

Conflict of Interest: The authors declare that the research was conducted in the absence of any commercial or financial relationships that could be construed as a potential conflict of interest.

Copyright © 2021 Tripathi, Jolly, Mani and Levine. This is an open-access article distributed under the terms of the Creative Commons Attribution License (CC BY). The use, distribution or reproduction in other forums is permitted, provided the original author(s) and the copyright owner(s) are credited and that the original publication in this journal is cited, in accordance with accepted academic practice. No use, distribution or reproduction is permitted which does not comply with these terms.

frontiers in Oncology

REVIEW
published: 24 September 2019
doi: 10.3389/fonc.2019.00948

Multifaceted Roles of Asporin in Cancer: Current Understanding

Shaohua Zhan[1,2], *Jinming Li*[2*] *and Wei Ge*[1,3*]

[1] National Key Laboratory of Medical Molecular Biology, Department of Immunology, Institute of Basic Medical Sciences, Chinese Academy of Medical Sciences, Beijing, China, [2] National Center for Clinical Laboratories, Beijing Hospital, National Center of Gerontology, Beijing, China, [3] Affiliated Hospital of Hebei University, Baoding, China

The small leucine-rich proteoglycan (SLRP) family consists of 18 members categorized into five distinct classes, the traditional classes I–III, and the non-canonical classes IV–V. Unlike the other class I SLRPs (decorin and biglycan), asporin contains a unique and conserved stretch of aspartate (D) residues in its N terminus, and germline polymorphisms in the D-repeat-length are associated with osteoarthritis and prostate cancer progression. Since the first discovery of asporin in 2001, previous studies have focused mainly on its roles in bone and joint diseases, including osteoarthritis, intervertebral disc degeneration and periodontal ligament mineralization. Recently, *asporin* gene expression was also reported to be dysregulated in tumor tissues of different types of cancer, and to act as oncogene in pancreatic, colorectal, gastric, and prostate cancers, and some types of breast cancer, though it is also reported to function as a tumor suppressor gene in triple-negative breast cancer. Furthermore, asporin is also positively or negatively correlated with tumor proliferation, migration, invasion, and patient prognosis through its regulation of different signaling pathways, including the TGF-β, EGFR, and CD44 pathways. In this review, we seek to elucidate the signaling pathways and functions regulated by asporin in different types of cancer and to highlight some important issues that require investigation in future research.

Keywords: SLRP, aspirin, cell migration and invasion, metastasis, signaling pathways

OPEN ACCESS

Edited by:
Satyendra Chandra Tripathi, All India Institute of Medical Sciences Nagpur, India

Reviewed by:
Giuseppe Palma, National Cancer Institute G. Pascale Foundation (IRCCS), Italy
Prasanna Ekambaram, University of Pittsburgh, United States
Chandra Prakash Prasad, All India Institute of Medical Sciences, India

***Correspondence:**
Jinming Li
jmli@nccl.org.cn
Wei Ge
wei.ge@chem.ox.ac.uk

Specialty section:
This article was submitted to Molecular and Cellular Oncology, a section of the journal Frontiers in Oncology

Received: *08 July 2019*
Accepted: *09 September 2019*
Published: *24 September 2019*

Citation:
Zhan S, Li J and Ge W (2019) Multifaceted Roles of Asporin in Cancer: Current Understanding. Front. Oncol. 9:948. doi: 10.3389/fonc.2019.00948

INTRODUCTION

Cancer is the leading cause of death from non-communicable disease, with an estimated 18.1 million new cases of cancer and 9.6 million cancer deaths, according to GLOBOCAN 2018 (1). Therefore, an in-depth understanding of tumor pathogenesis will be beneficial for the development of new pharmacological agents of therapeutic interventions, to decrease the global burden of cancer. The extracellular matrix (ECM) is a complex network of macromolecules with distinct physical and biochemical properties that participate in various cellular behaviors, including cell growth, survival, motility, and differentiation (2). Although tightly regulated in tissue development and homeostasis, the ECM influences the classical hallmarks of cancers, such as self-sufficient growth, insensitivity to growth inhibitors, evasion of apoptosis, limitless replicative potential, sustained angiogenesis, and tissue invasion and metastasis (3, 4). SLRP constitutes a major non-collagen component of the ECM and is ubiquitously distributed throughout the ECM in many tissues (5). Similarly, SLRP is also involved in various pathological processes resulting in skin fragility, cardiovascular disease, osteoporosis, osteoarthritis, and cancer (6–9). The SLRP family consists of 18 members categorized into five distinct classes: the traditional classes I-III and the

non-canonical classes IV-V. This categorization is based on N-terminal cysteine-rich clusters, core leucine-rich repeats (LRR), C-terminal ear repeat motifs, and genomic organization (10, 11). Most SLRP proteins are proteoglycans containing chondroitin/dermatan sulfate or keratan sulfate chains, while others are glycoproteins containing N-linked oligosaccharides (9). SLRPs have been shown to interact with various extracellular receptors or ligands through their bare β-sheets present on the concave surface of LRR, such as collagens, fibronectin, bone morphogenic protein-4 (BMP-4), and transforming growth factor-β1 (TGF-β1) (12–14). This interaction then involves several signaling pathways that regulate the cell-matrix function. Class I SLRPs, which have the highest homology (∼50% identity) based on the amino acid sequence, contains three classical members: decorin, biglycan, and asporin (9, 15). These three class I members contain 10 LRRs and are distinguished by a unique cysteine-rich cluster in the N terminus consensus (CX_3CXCX_6C). The N-terminal regions of decorin and biglycan carry one and two chondroitin/dermatan sulfate chains, respectively (9, 15, 16). Decorin is a natural receptor tyrosine kinase (RTK) inhibitor that functions through binding the epidermal growth factor receptor (EGFR), insulin like growth factor-1R (IGF-1R), fibroblast growth factor receptor (FGFR), and c-met. Thus, decorin blocks several biological processes, such as cell growth, cell evasion, and migration, through the induction of p21 via EGFR and downregulation of the c-met/β-catenin/myc pathway (17). Furthermore, decorin also modulates cancer through its interaction with TGF-β (18). Therefore, decorin is regarded as the "endogenous guardian" of the matrix, due to its anti-proliferative, anti-metastatic, and angio-suppressive effects. In contrast, biglycan acts as a danger signal by affecting both immune responses and tumor characteristics (17, 18). Various studies have shown that the upregulation of biglycan in cancer stroma is positively correlated with cell proliferation, migration, metastasis, and angiogenesis through the regulation of the TLR/NF-κB, MAPK, and the FAK signaling pathway (18). It has also been demonstrated that high biglycan expression is positively associated with pro-malignant potential and poor patient prognosis (19, 20). However, asporin exerts negative and positive roles in the pathogenesis and prognosis of different cancers (**Figure 1**). Therefore, we will narrow the focus of this review to asporin, simply describing its sequence, structure, and functions, and primarily highlighting its multifaceted roles in cancers. Although asporin has been reported using another name PLAP-1 (21), the term asporin is used exclusively in this review.

SEQUENCE, STRUCTURE, AND FUNCTIONS OF ASPORIN

Asporin was initially identified as an extracellular secreted protein in human articular cartilage or periodontal tissue by three independent groups in 2001 (15, 16, 21). The name "asporin" refers to the unique aspartic acid residues in its N terminus and its similarity to decorin. The human *asporin* gene has eight exons and spans 26 kilobases on chromosome region 9q22.31 (16). Asporin protein consists of 380 amino acids and its amino acid sequence is 54%/60% identical to decorin and biglycan, respectively. However, compared to decorin and biglycan, asporin cannot be considered as a proteoglycan in the strictest sense because it lacks the serine/glycine dipeptide sequence for O-linked glycosaminoglycan binding. Furthermore, unlike other proteoglycans, asporin contains a unique and conserved stretch (8–19) of aspartate residues (D-repeat) in its N terminus (12, 22). Two studies have demonstrated that asporin D14 variants increase susceptibility to and severity of knee osteoarthritis in Japanese and Chinese Han populations, whereas D13 was found to be significantly protective against osteoarthritis in some Japanese populations (12, 23). However, these findings were not confirmed in other populations in the United States (24), Spain (25), and Iran (26). Therefore, the relationship between asporin polymorphisms and osteoarthritis still needs to be investigated in large-scale studies of different ethnic populations.

The pathogenesis of osteoarthritis is characterized by an imbalance between the degradation and synthesis of the cartilage ECM, with type II collagen and aggrecan being the primary components that play critical roles in the viscoelasticity and tensile strength of cartilage (27). The same research group indicated that amino acids 159–205 of asporin interact directly with TGF-β1 and, compared with other alleles, its D14 allele significantly inhibits TGF-β1-induced expression of genes including type II collagen and aggrecan (12, 28). Furthermore, this inhibition is due to asporin blockade of TGF-β1 binding to its receptor TβRII (29). Interestingly, TGF-β1 indirectly induces an asporin expression at both the mRNA and protein levels through its downstream Smad pathway, particularly involving Smad3 (29, 30). Therefore, asporin and TGF-β1 form a functional feedback loop in cartilage and play vital roles in homeostasis and the pathogenesis of osteoarthritis. There is an additional regulatory feedback loop between asporin and BMP-2, which is also correlated with the severity of osteoarthritis (31, 32). In 2007, Yamada et al. demonstrated that asporin co-localize with BMP-2 *in vitro* (33). Previous studies also indicate that asporin acts as a negative regulator of cytodifferentiation and mineralization by regulating BMP-2 activity (33), and that asporin D14 inhibits BMP-2 signal transduction more efficiently than D13 (34). Conversely, BMP-2 also upregulates asporin mRNA and protein expression (35). As for the TGF-β1–mediated cartilage matrix gene, type I and type II collagen also bind to asporin (28, 36). Furthermore, the D-repeat domain of asporin interacts with calcium to stimulate the biomineralization of collagen. It may appear intriguing that, unlike biglycan, another class I SLRP member, decorin, inhibits asporin-induced collagen mineralization (36). Thus, although asporin shows significant associations with osteoarthritis, functional differences among D-repeat polymorphisms in asporin are still unclear. It is speculated that asporin D-repeat-length may influence conformational changes that consequently alter processes such as BMP-2 signaling, TGF-β1 signaling, and collagen mineralization, although further studies are required to clarify the underlying molecular mechanisms. Nevertheless, all these previous studies have a good implication for the following cancer research, which will be discussed in detail.

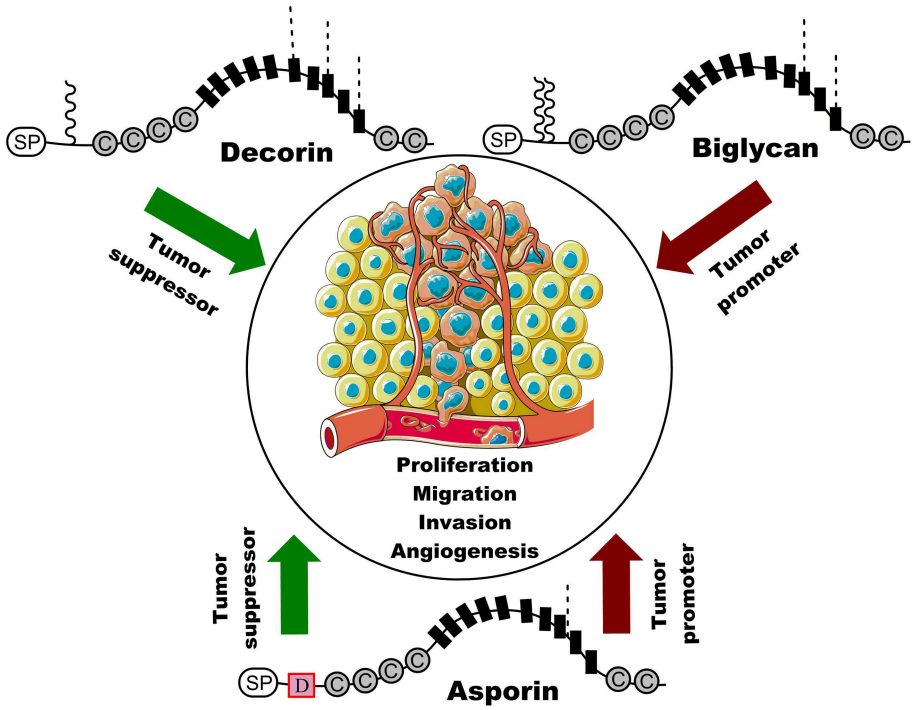

FIGURE 1 | Schematic representation of the structure of three class I SLRP members and their roles in cancer. Decorin suppresses cancer cell proliferation, migration, invasion, and angiogenesis, whereas biglycan is positively associated with cancer cell proliferation, migration, invasion, and angiogenesis. Interestingly, asporin serves as tumor suppressor gene or oncogene in different types of cancer. SP indicates signal peptides and C represents cysteine region. Black boxes indicate a leucine rich repeat (LRR) motif and D represents the unique and conserved aspartic acid (D)-repeats in asporin. Waved line indicates O-linked glycosylation site and dashed line represents N-linked glycosylation. Original elements used in this diagram are from Servier Medical Art (http://smart.servier.com/).

EMERGING ROLES OF ASPORIN IN CANCER

Bioinformatics analysis of microarray data indicate the potential of asporin as a biomarker for colorectal cancer detection and prevention (37). Recently, two studies also demonstrated that asporin is a potential biomarker in gastric cancer based on the integrated analysis of gene expression profiles (38, 39). Turtoi et al. found that asporin was upregulated in pancreatic ductal adenocarcinoma (PDAC) tissues compared to the corresponding normal tissues based on proteomics analysis and confirmed by immunohistochemistry (40). A recent report by Klee and colleagues indicated that serum asporin was upregulated in men with advanced prostate cancer (41). Furthermore, two studies demonstrated that asporin was not only elevated in invasive ducal breast carcinoma compared to ductal carcinoma *in situ* but also responded to aromatase inhibitor treatment (42, 43). All these studies suggest that asporin plays vital roles in the pathogenesis of different types of cancer, and a considerable amount of research has indicated that asporin acts as an oncogene in pancreatic (44), colorectal (45, 46), gastric (47, 48), and prostate cancer (49), as well as some types of breast cancer (50–52), but as a tumor suppressor gene in triple-negative breast cancer (52) via different signaling pathways. Therefore, here, we seek to elucidate the signaling pathways and different functions regulated by asporin in different types of cancer and to highlight some important issues that still need to be investigated.

CANCER-RELATED PATHWAYS REGULATED BY ASPORIN

Numerous studies have indicated that deregulated signaling pathways result in proliferation, invasion, and metastasis of cancer cells. The most significant cancer-related pathways regulated by asporin are TGF-β, EGFR, and CD44 signaling pathways; altered expression of components of these signaling pathways and the regulatory roles of asporin are illustrated in **Figure 2**.

TGF-β SIGNALING

The TGF-β/Smad2/3 signaling pathway plays critical roles in cancer cell behavior through the unique TGF-β serine-threonine kinases and exerts both tumor suppressor and promoter activity in tumor progression and invasion. Furthermore, TGF-β secreted by tumor cells acts not only on elements of the tumor microenvironment in a paracrine fashion, but also on the tumor cell itself via autocrine effects (53, 54). In the early stages of breast cancer, TGF-β1 shows anti-tumor activity by

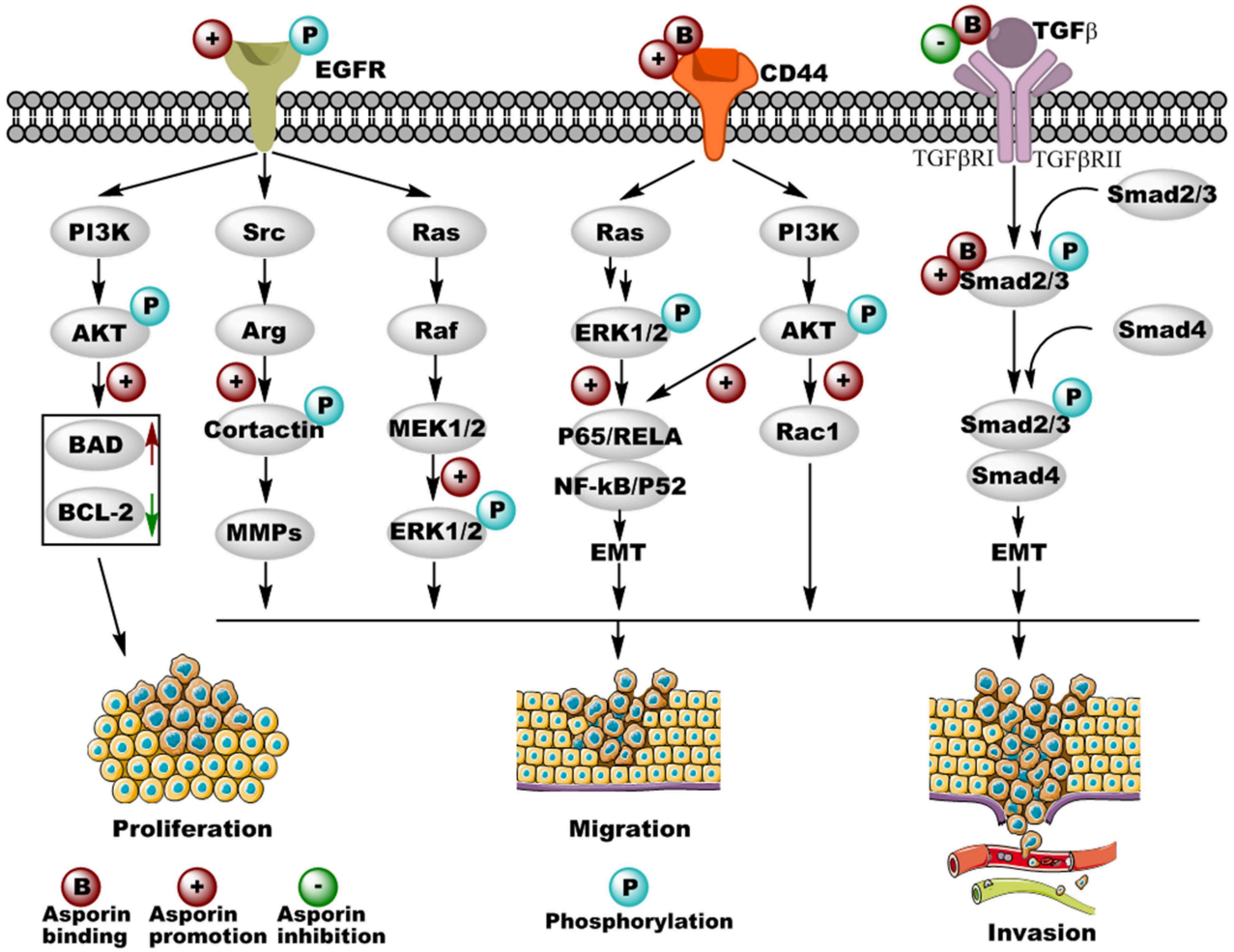

FIGURE 2 | Cancer-related pathways regulated by asporin in different types of cancer. Asporin not only promotes cancer cell proliferation, migration, and invasion by binding with CD44 and Smad 2/3 as well as promoting the phosphorylation of EGFR, but also inhibits cancer cell migration and invasion by binding with TGF-β in the extracellular matrix. Upregulated and downregulated proteins are shown in solid red and green arrows, respectively. Original elements used in this diagram are from Servier Medical Art (http://smart.servier.com/).

mediating growth arrest and cancer cell apoptosis; however, in the late stages, TGF-β1 enhances the malignancy of breast cancer cells (55). Previous studies have demonstrated that asporin interacts directly with TGF-β1 and inhibits downstream gene expression of aggrecan and collagen in osteoarthritis (12). In breast cancer, Maris et al. reported that asporin was upregulated in the stroma of breast cancer lesions but not in normal tissues, indicating that asporin influences the tumor microenvironment. This group also found that asporin expression was promoted by TGF-β1 and inhibited by IL-1β in normal breast fibroblasts, as well as cancer-associated fibroblasts (CAFs) (52). Furthermore, asporin inhibited triple-negative breast tumor growth and metastasis *in vivo*, via a molecular mechanism in which asporin may interact with TGF-β1 to inhibit its downstream Smad2 activation, resulting in the suppression of epithelial-to-mesenchymal transition (EMT) and stemness in triple-negative breast cancer cells (52). Similarly, dysregulated TGF-β signaling pathway plays pivotal roles in the development of colorectal cancer (56). Li et al. indicated that asporin enhances cell growth, migration, and invasion via activation of the TGF-β/Smad2/3 signaling pathway in colorectal cancer (45). Experimental evidence revealed that asporin interacts directly with Smad2/3 and facilitates the entry of p-Smad2/3 into the nucleus, which induces EMT and colorectal cancer progression (45). This was the first study to show the function of asporin as an intracellular molecule and not as an extracellular matrix component in cancer. Altogether, these results indicate that asporin binds directly to extracellular TGF-β1 or cytoplasmic Smad2/3, resulting in the inhibition or activation of the TGF-β signaling pathway, respectively. It is therefore not surprising that under different conditions, asporin acts as a tumor suppressor gene in triple-negative breast cancer and as an oncogene in colorectal cancer.

EGFR SIGNALING

EGFR is a tyrosine kinase receptor that drives many types of epithelial tumors, including metastatic colorectal cancer, non-small-cell lung cancer, pancreatic cancer, and breast cancer (57). Aberrant activation of the EGFR signaling pathway is critical for cancer cell apoptosis, proliferation, differentiation, and motility via the downstream RAS/RAF/MEK/ERK and AKT/PI3K/mTOR pathways (57, 58), and tremendous amounts of research have implicated EGFR as a potential target for cancer therapy (59). Upregulated expression and activation of EGFR are correlated with tumor invasion and poor prognosis, indicating that the EGFR signaling pathway is also critical in gastric cancer (60). In 2015, Ding et al. found that asporin promotes the activation of p-EGFR and its downstream p-ERK1/2 but not their corresponding total proteins (48). Small inhibitory RNA-mediated silencing of asporin in gastric cell lines not only inhibits cell proliferation and survival through the downregulation of anti-apoptotic Bcl-2 and the upregulation of pro-apoptotic Bad, but also blocks cell migration by the downregulation of the EGFR/ERK/MMP2-mediated signaling axis (48). As recently shown, Zhang et al. found that asporin is also located in the cytoplasm and nuclei of gastric cancer cell lines and could promote their proliferation. The underlying mechanism is that asporin interacts with PSMD2 and enhances PSMD2 mediated degradation of tumor suppressor factors (DUSP7, WIP1, and PTEN), resulting in the activation of MAPK/ERK, P38/MAPK, and PI3K/AKT signaling pathways (61). In colorectal cancer, Wu et al. suggested that asporin promotes cancer cell endothelial tube formation by upregulating VEGF expression (46). Furthermore, asporin has been shown to facilitate colorectal cancer cell migration and invasion by successively activating p-EGFR^{Tyr1173}, p-Src^{Tyr416}, and p-Cortactin^{Tyr421} (46), which is important for the formation of invadopodia and secretion of matrix metalloproteinases (MMPs) (62, 63). These results indicate that asporin-mediated EGFR/Src/Cortactin signaling is critical for colorectal cancer metastasis. Therefore, EGF and PP2 (Src inhibitor) inhibit the activation of the EGFR/Src/Cortactin pathway mediated by asporin (46). However, the molecular mechanism by which asporin activates the EGFR signaling pathway in gastric and colorectal cancer remains to be investigated both *in vitro* and *in vivo*.

CD44 SIGNALING

CD44 is a non-kinase transmembrane glycoprotein that exerts its cellular functions via interactions with several ligands, including hyaluronic acid (HA), osteopontin (OPN), collagen, and MMPs (64). By binding with CD44, HA induces conformational changes leading to adaptor protein recruitment to the intracellular cytoplasmic tail of CD44 and the subsequent activation of various signaling pathways involved in tumor progression (65). CD44 is involved in several types of cancers, including pancreatic, colorectal, breast, and prostate cancer, as well as head and neck squamous cell carcinoma, and gastrointestinal cancer (66). Furthermore, CD44 regulates tumor progression, metastasis, angiogenesis, and chemoresistance by activation of different cytoskeletal changes and signaling pathways, including MAPK, Hippo, β-catenin, AKT, TGF-β, MMPs, and STAT3 (66). In scirrhous gastric cancer, asporin is also an important ligand of CD44 (47). Satoyoshi et al. indicated that asporin was primarily expressed in cancer stroma but was not observed in normal tissues (47), which is consistent with the patterns of expression in pancreatic and breast cancer (44, 52). Experimental evidence shows that the gastric cancer cell line 44As3 promotes asporin expression in CAFs via a mechanism in which, asporin as a unique class I SLRP, enhances the co-invasion of CAFs and cancer cells both *in vitro* and *in vivo* through the CD44/Rac1 mediated axis (47). In pancreatic cancer, asporin was also shown to interact directly with CD44 in co-precipitation assays (44), and asporin not only facilitated cancer cell migration and invasion *in vitro* but also enhanced tumor metastasis *in vivo*. Although the binding motifs are unclear, asporin-CD44 binding is known to activate the CD44/AKT/NF-κB/p65 and CD44/ERK/NF-κB/p65 axes to promote EMT in a paracrine/autocrine pattern, resulting in the upregulated expression of ZEB1, N-catenin, vimentin, slug, and snail as well as the downregulated expression of ZO-1 and E-cadherin. Therefore, from a molecular perspective, the asporin/CD44/EMT signaling pathway could be considered as a potential therapeutic target axis to decrease tumor migration and invasion in pancreatic and gastric cancer.

FUTURE POTENTIAL DIRECTIONS OF ASPORIN MEDIATED SIGNALING PATHWAYS IN CANCER

Recently, Hughes and co-workers found that asporin could not only sustain the self-renewal capacity of the mesenchymal stromal cell but also restrict early mesenchymal stromal cell differentiation via inhibiting the BMP-4-induced signaling pathway (67). Furthermore, in asporin null mice, they also found that there are decreased tumor-associated mesenchymal stromal cells, fewer cancer stem cells, reduced tumor vasculature, and increased infiltrating $CD8^+$T cells in the prostate tumor allografts (67). All these results indicate that asporin is a critical regulator in the tumor microenvironment possibly by regulating different signaling pathways except for TGF-β, EGFR, and CD44 pathways, and we can get some clues from previous studies not associated with cancer. As a secreted extracellular protein, it has been demonstrated that asporin could interact with several ligands as well as with surface receptors, including BMP-2, BMP-4, FGF-2, WNT8, Nodal, IGF, and IGF1R (33, 67–69). Whether asporin could interact with these proteins and regulate the corresponding signaling pathways in cancer needs to be investigated in the future. Furthermore, the previous review indicated that SLRP could affect several RTKs, including the ErbB family, the hepatocyte growth factor receptor (Met) and IGF1R (70). Thus, we wonder whether asporin could regulate Met and ErbB2 signaling pathways in cancer, especially in breast cancer. As an intracellular protein, asporin could interact with PSMD2, which is responsible for substrate recognition and binding (61). Therefore, whether asporin could mediate another intracellular

substrate proteasomal degradation via binding with PSMD2 in different types of cancer, still needs to be uncovered. Collectively, because asporin could bind additional and currently unidentified proteins to regulate different signaling pathways in cancer, it is an interesting direction to globally screen additional asporin-interactive partners through quantitative (measuring dissociation constants) and proteomics (identifying interacting proteins) analyses.

PERSPECTIVES ON THE POTENTIAL ROLE OF ASPORIN IN THE DIAGNOSIS AND PROGNOSIS OF CANCER

From a clinical perspective, Maris et al. demonstrated that the areas under the curves (AUC) of asporin, to discriminate breast cancer patients with different outcomes was 0.87, and that low asporin expression is significantly correlated with reduced overall survival (52). However, another study showed that asporin has a dual role in the progression of breast cancer. In 2016, Simkova et al. demonstrated that a high expression of asporin correlated with good relapse-free survival (RFS) in grades I/II in breast cancer patients, but was associated with worse RFS in grade III patients regardless of tumor ER status (51). The dual role of asporin in breast cancer progression may be due to its D-repeat polymorphism, which has been described in prostate cancer progression (22); however, this hypothesis needs to be further investigated in large-scale population studies. Recently, elevated asporin gene expression was shown to be significantly correlated with worse overall survival and disease-free survival in gastric cancer (39). In colorectal cancer, high asporin expression showed a positive relationship with lymph node metastasis and high TNM stage, but not with sex, age and tumor size (46). Furthermore, upregulated asporin expression was correlated with worse overall and disease-free survival, and was implicated as an independent indicator of a worse prognosis through a multivariate analysis (45). In pancreatic cancer, asporin is mainly expressed in the cancer stroma, but only in cancer cells in a small proportion of patients (44). Furthermore, high asporin expression in the cancer stroma is positively correlated with poor overall survival, while there is no relationship between asporin expression in cancer cells and clinical outcome (44). Similarly, asporin is primarily expressed in the tumor stroma in prostate cancer, but not in benign tissue (22, 49). Interestingly, asporin is also positively associated with the presence of a reactive stroma (49), which is associated with disease progression and mortality in prostate cancer (71). Furthermore, two studies also demonstrated that elevated expression of asporin mRNA or protein was correlated with biochemical recurrence and higher Gleason score in independent prostate cancer cohorts (22, 49). A multivariable Cox proportional hazard analysis indicated that asporin expression in the stroma was an independent prognostic factor for biochemical recurrence (49). Moreover, Hurley et al. suggested that homozygous germline asporin D14 and heterozygous D13/14 were significantly associated with lymph node involvement and metastatic recurrence in prostate cancer, whereas homozygous D13 was significantly protective against metastatic recurrence in a multivariable analysis (22). Additionally, in an orthotopic xenograft model, co-injection of overexpressed asporin D14 fibroblast and PC-3 cancer cells increased the number of metastases to lymph nodes and other organs, including lung, liver, and pancreas compared to asporin D13, although the underlying molecular mechanisms are still unclear (22). Our current understanding of the dual role of asporin in cancer diagnosis and prognosis is summarized in **Table 1**.

THE THERAPEUTIC POTENTIAL OF ASPORIN MODULATION IN CANCER

Asporin could enhance the proliferation, migration, and invasion capacity of pancreatic, colorectal, gastric, prostate, and breast cancer cells (44–50, 61, 67), indicating it could be regarded as a valuable therapeutic target. Although non-drugs are currently in clinical trials for the treatment of patients with asporin dysregulation cancers, there are several potential strategies to reduce asporin functional dose in future cancer studies: (1) inhibition of asporin protein-protein interactions; (2) targeting *asporin* mRNA. Previous studies indicate that asporin could interact with CD44, TGF-β, BMP-2, BMP-4, FGF-2, WNT8, Nodal, IGF, and IGF1R in different microenvironments to regulate different signaling pathways. Therefore, peptide antagonists derived from asporin or its interaction partners may block asporin protein-protein interactions to inhibit corresponding signaling pathways. Additionally, the application of RNAi strategies are potential approaches to decrease asporin translational level, including antisense oligonucleotides, short interfering RNA, and short hairpin RNA. Furthermore, a revolutionary gene-editing tool CRISPR/Cas9 could be explored to deplete asporin expression in a tissue-specific manner (72). As asporin exerts tumor suppression in triple-negative breast cancer (52), increasing the asporin function dose may also be an anti-cancer strategy. Previous studies demonstrated that IL-1β, miR-21, and miR-101 could downregulate the asporin protein and mRNA level, respectively (52, 73). Antisense oligonucleotides toward IL-1β, miR-21, and miR-101 may be useful therapeutic applications when asporin acts as a tumor suppressor. In pre-clinical studies, different types of models could be valuable in order to test these potential therapeutic strategies in regulating asporin expression, including xenograft mouse models, allograft mouse models, genetically engineered mouse models, patient-derived models (PDX), and PDX 3D spheroids (67, 74). Altogether, further studies, especially mouse models and clinical trials, are needed to investigate the therapeutic potential of asporin modulation in cancer.

CONCLUSIONS

Class I SLRP members are ubiquitously distributed in the ECM of many tissues and play critical roles in tumor proliferation, migration, invasion, and angiogenesis. Although decorin is

TABLE 1 | Experimental evidence of asporin expression in human malignancies.

Cancer types	Asporin expression	Cell lines/models	Outcome	Clinical functions	References
Breast cancer	Up-regulation in tumor stroma	NBF/CAF cells MCF-7/T47D/ZR751/SKBR3/BT-474/MB-231/MB-468/BT-549/MCF-10A cell lines NOD-SCID mouse model	Inhibiting EMT transition, and stemness *in vitro* Reducing growth and metastasis *in vivo*	(+) good outcome (+) increased overall survival	(52)
Breast cancer	Up-regulation in tumor stroma and tumor cells	CAF cells Hs578T/MDA-MA-231/BT549/T47D cell lines PyMT mouse model	Promoting invasion *in vitro*	(+) better relapse free survival in low-grade patients (+) worse relapse free survival in high-grade patients	(50, 51)
Prostate cancer	Up-regulation in tumor stroma and blood	CAF/EPF/PrSC cells PC-3/LNCaP cell lines p53 null mouse model	(+) aggressive prostate cancer (+) neuroendocrine marker expression	(+) higher biochemical recurrence (+) higher Gleason score (+) reactive stroma	(41, 49)
Prostate cancer (asporin D13/14 or D14)	Up-regulation in tumor stroma	CAF cells WPMY1/PC3 cell lines NSG mouse model	(+) distant lymph nodes (+) distant organ metastasis	(+) worse metastasis free survival (+) lymph node involvement (+) higher Gleason score	(22)
Gastric cancer	Up-regulation in tumor stroma	NF/CAF cells 44As3/GES/SGC-7901/BGC-823/AGS/MKN45/N87 cell lines BALB/c nude mouse model	Promoting survival, proliferation, migration, and invasion *in vitro* Promoting invasion *in vivo*	(+) worse overall survival (+)worse disease-free survival	(39, 47, 48, 61)
Colorectal cancer	Up-regulation in tumor stroma and tumor cells	CAF cells HCT-8/RKO/HT-29/LoVo /Caco2 /HCT116/SW1116/ SW480/RKO/SW620 cell lines BALB/c nude mouse model	Promoting EMT transition, cell viability, migration, invasion, and endothelial tube formation *in vitro* Promoting liver metastasis *in vivo*	(+) higher TNM stage (+) lymph node involvement (+) worse overall survival (+) worse disease-free survival	(45, 46)
Pancreas cancer	Up-regulation in tumor stroma	PSC/CAF cells AsPC-1/BxPC-3/MIA PaCa-2/PANC-1 cell lines Nude mouse model	Promoting EMT transition, migration, and invasion *in vitro* Promoting tumor invasion *in vivo*	(+) worse overall survival	(44)

EMT, epithelial-to-mesenchymal transition; TNM, TNM classification of malignant tumors; EPF, fetal prostate fibroblasts; PrSC, primary prostate stromal cells; CAF, cancer associated fibroblast; PSC, pancreatic stellate cells.

regarded as the "endogenous guardian" and biglycan acts as a danger signal in cancer, asporin acts as an oncogene in some types of cancer (breast, pancreatic, colorectal, gastric, and prostate), but as a tumor suppressor gene in triple-negative breast cancer (75). Since the first discovery of asporin in 2001, studies have focused mainly on its role in bone and joint diseases, including osteoarthritis, intervertebral disc degeneration, and periodontal ligament mineralization (76, 77). Recently, asporin expression was also shown to be dysregulated in tumor tissues and positively or negatively correlated with tumor proliferation, migration, invasion, and patient prognosis by regulating different signaling pathways, including the TGF-β, EGFR, and CD44 pathway. However, various important issues associated with asporin in cancer remain to be investigated in future studies. First, asporin contains a unique and conserved stretch of aspartate residues in its N terminus, and germline polymorphisms in D-repeat-length are associated with osteoarthritis and prostate cancer progression; however, functional differences and the molecular mechanisms underlying the influence of different D-repeat polymorphisms remain to be clarified. Second, although asporin is primarily expressed in the ECM, asporin expression is also observed in the cytoplasm and nucleus (45, 46, 50, 61). The biological function of asporin inside cancer cells was largely neglected until it was found that asporin interacts with intracellular Smad2/3 and PSMD2 to facilitate gastric and colorectal cancer progression. Thus, the intracellular function of asporin in cancer and whether asporin subcellular localization is controlled by its post-translational modifications, still needs to be investigated. Third, as TGF-β, EGFR, and CD44 pathways play vital roles in other types of cancer, including head and neck cancer, gall bladder cancer, glioblastoma, lung cancer, gastrointestinal cancer, and so on, whether asporin is an oncogenic driver or tumor suppressor in these cancers still need to be investigated in the future. Finally, due to the function of asporin as a tumor suppressor gene and oncogene in different types of cancer, the exact molecular mechanisms of its dual role in different tumor microenvironments remain to be elucidated. Overall, only dedicated studies that investigate the molecular mechanisms underlying the roles of asporin in cancer will pave the way for the development of new pharmacological agents for therapeutic interventions.

AUTHOR CONTRIBUTIONS

SZ prepared the table and figures. SZ, JL, and WG wrote, read, and approved the final manuscript.

FUNDING

This work was supported by the CAMS Innovation Fund for Medical Sciences (2016-I2M-1-003), the National Natural Science Foundation of China (Nos. 81974319, 81772273, and 81971023), and the Beijing Municipal Administration of Hospitals' Youth Program (No. QML20161103).

ACKNOWLEDGMENTS

We thank all lab members for active discussions and critical reading.

REFERENCES

1. Bray F, Ferlay J, Soerjomataram I, Siegel RL, Torre LA, Jemal A. Global cancer statistics 2018: GLOBOCAN estimates of incidence and mortality worldwide for 36 cancers in 185 countries. *CA Cancer J Clin.* (2018) 68:394–424. doi: 10.3322/caac.21492
2. Lu P, Weaver VM, Werb Z. The extracellular matrix: a dynamic niche in cancer progression. *J Cell Biol.* (2012) 196:395–406. doi: 10.1083/jcb.201102147
3. Pickup MW, Mouw JK, Weaver VM. The extracellular matrix modulates the hallmarks of cancer. *EMBO Rep.* (2014) 15:1243–53. doi: 10.15252/embr.201439246
4. Hanahan D, Weinberg RA. The hallmarks of cancer. *Cell.* (2000) 100:57–70. doi: 10.1016/S0092-8674(00)81683-9
5. Ni GX, Li Z, Zhou YZ. The role of small leucine-rich proteoglycans in osteoarthritis pathogenesis. *Osteoarthr Cartil.* (2014) 22:896–903. doi: 10.1016/j.joca.2014.04.026
6. Ameye L, Young MF. Mice deficient in small leucine-rich proteoglycans: novel *in vivo* models for osteoporosis, osteoarthritis, Ehlers-Danlos syndrome, muscular dystrophy, and corneal diseases. *Glycobiology.* (2002) 12:107r−16. doi: 10.1093/glycob/cwf065
7. Reed CC, Iozzo RV. The role of decorin in collagen fibrillogenesis and skin homeostasis. *Glycoconj J.* (2002) 19:249–55. doi: 10.1023/A:1025383913444
8. Nikitovic D, Berdiaki K, Chalkiadaki G, Karamanos N, Tzanakakis G. The role of SLRP-proteoglycans in osteosarcoma pathogenesis. *Connect Tissue Res.* (2008) 49:235–8. doi: 10.1080/03008200802147589
9. Iozzo RV. The biology of the small leucine-rich proteoglycans. Functional network of interactive proteins. *J Biol Chem.* (1999) 274:18843–6. doi: 10.1074/jbc.274.27.18843
10. Schaefer L, Iozzo RV. Biological functions of the small leucine-rich proteoglycans: from genetics to signal transduction. *J Biol Chem.* (2008) 283:21305–9. doi: 10.1074/jbc.R800020200
11. McEwan PA, Scott PG, Bishop PN, Bella J. Structural correlations in the family of small leucine-rich repeat proteins and proteoglycans. *J Struct Biol.* (2006) 155:294–305. doi: 10.1016/j.jsb.2006.01.016
12. Kizawa H, Kou I, Iida A, Sudo A, Miyamoto Y, Fukuda A, et al. An aspartic acid repeat polymorphism in asporin inhibits chondrogenesis and increases susceptibility to osteoarthritis. *Nat Genet.* (2005) 37:138–44. doi: 10.1038/ng1496
13. Gallagher JT, Gasiunas N, Schor SL. Specific association of iduronic acid-rich dermatan sulphate with the extracellular matrix of human skin fibroblasts cultured on collagen gels. *Biochem J.* (1983) 215:107–16. doi: 10.1042/bj2150107
14. Schmidt G, Robenek H, Harrach B, Glossl J, Nolte V, Hormann H, et al. Interaction of small dermatan sulfate proteoglycan from fibroblasts with fibronectin. *J Cell Biol.* (1987) 104:1683–91. doi: 10.1083/jcb.104.6.1683
15. Henry SP, Takanosu M, Boyd TC, Mayne PM, Eberspaecher H, Zhou W, et al. Expression pattern and gene characterization of asporin. A newly discovered member of the leucine-rich repeat protein family. *J Biol Chem.* (2001) 276:12212–21. doi: 10.1074/jbc.M011290200
16. Lorenzo P, Aspberg A, Onnerfjord P, Bayliss MT, Neame PJ, Heinegard D. Identification and characterization of asporin. A novel member of the leucine-rich repeat protein family closely related to decorin and biglycan. *J Biol Chem.* (2001) 276:12201–11. doi: 10.1074/jbc.M010932200
17. Schaefer L, Iozzo RV. Small leucine-rich proteoglycans, at the crossroad of cancer growth and inflammation. *Curr Opin Genet Develop.* (2012) 22:56–7. doi: 10.1016/j.gde.2011.12.002
18. Appunni S, Anand V, Khandelwal M, Gupta N, Rubens M, Sharma A. Small leucine rich proteoglycans (decorin, biglycan and lumican) in cancer. *Clin Chim Acta.* (2019) 491:1–7. doi: 10.1016/j.cca.2019.01.003
19. Sun H, Wang X, Zhang Y, Che X, Liu Z, Zhang L, et al. Biglycan enhances the ability of migration and invasion in endometrial cancer. *Arch Gynecol Obstetr.* (2016) 293:429–38. doi: 10.1007/s00404-015-3844-5
20. Zhu Y-H, Yang F, Zhang S-S, Zeng T-T, Xie X, Guan X-Y. High expression of biglycan is associated with poor prognosis in patients with esophageal squamous cell carcinoma. *Int J Clin Exp Pathol.* (2013) 6:2497–505.
21. Yamada S, Murakami S, Matoba R, Ozawa Y, Yokokoji T, Nakahira Y, et al. Expression profile of active genes in human periodontal ligament and isolation of PLAP-1, a novel SLRP family gene. *Gene.* (2001) 275:279–86. doi: 10.1016/S0378-1119(01)00683-7
22. Hurley PJ, Sundi D, Shinder B, Simons BW, Hughes RM, Miller RM, et al. Germline variants in asporin vary by race, modulate the tumor microenvironment, and are differentially associated with metastatic prostate cancer. *Clin Cancer Res.* (2016) 22:448–58. doi: 10.1158/1078-0432.CCR-15-0256
23. Jiang Q, Shi D, Yi L, Ikegawa S, Wang Y, Nakamura T, et al. Replication of the association of the aspartic acid repeat polymorphism in the asporin gene with knee-osteoarthritis susceptibility in Han Chinese. *J Hum Genet.* (2006) 51:1068–72. doi: 10.1007/s10038-006-0065-6
24. Atif U, Philip A, Aponte J, Woldu EM, Brady S, Kraus VB, et al. Absence of association of asporin polymorphisms and osteoarthritis susceptibility in US Caucasians. *Osteoarthr Cartil.* (2008) 16:1174–7. doi: 10.1016/j.joca.2008.03.007
25. Rodriguez-Lopez J, Pombo-Suarez M, Liz M, Gomez-Reino JJ, Gonzalez A. Lack of association of a variable number of aspartic acid residues in the asporin gene with osteoarthritis susceptibility: case-control studies in Spanish Caucasians. *Arthr Res Ther.* (2006) 8:R55. doi: 10.1186/ar1920
26. Jazayeri R, Qoreishi M, Hoseinzadeh HR, Babanejad M, Bakhshi E, Najmabadi H, et al. Investigation of the asporin gene polymorphism as a risk factor for knee osteoarthritis in Iran. *Am J Orthop.* (2013) 42:313–6.
27. Grimaud E, Heymann D, Redini F. Recent advances in TGF-beta effects on chondrocyte metabolism. Potential therapeutic roles of TGF-beta in cartilage disorders. *Cytokine Growth Factor Rev.* (2002) 13:241–57. doi: 10.1016/S1359-6101(02)00004-7
28. Kou I, Nakajima M, Ikegawa S. Binding characteristics of the osteoarthritis-associated protein asporin. *J Bone Mineral Metab.* (2010) 28:395–402. doi: 10.1007/s00774-009-0145-8
29. Nakajima M, Kizawa H, Saitoh M, Kou I, Miyazono K, Ikegawa S. Mechanisms for asporin function and regulation in articular cartilage. *J Biol Chem.* (2007) 282:32185–92. doi: 10.1074/jbc.M700522200
30. Kou I, Nakajima M, Ikegawa S. Expression and regulation of the osteoarthritis-associated protein asporin. *J Biol Chem.* (2007) 282:32193–9. doi: 10.1074/jbc.M706262200
31. Liu Y, Hou R, Yin R, Yin W. Correlation of bone morphogenetic protein-2 levels in serum and synovial fluid with disease severity of knee osteoarthritis. *Med Sci Monit.* (2015) 21:363–70. doi: 10.12659/MSM.892160
32. van der Kraan PM, Blaney Davidson EN, van den Berg WB. Bone morphogenetic proteins and articular cartilage: to serve and

protect or a wolf in sheep clothing's? *Osteoarthr Cartil.* (2010) 18:735–41. doi: 10.1016/j.joca.2010.03.001
33. Yamada S, Tomoeda M, Ozawa Y, Yoneda S, Terashima Y, Ikezawa K, et al. PLAP-1/asporin, a novel negative regulator of periodontal ligament mineralization. *J Biol Chem.* (2007) 282:23070–80. doi: 10.1074/jbc.M611181200
34. Kajikawa T, Yamada S, Tauchi T, Awata T, Yamaba S, Fujihara C, et al. Inhibitory effects of PLAP-1/asporin on periodontal ligament cells. *J Dental Res.* (2014) 93:400–5. doi: 10.1177/0022034513520549
35. Yamada S, Ozawa Y, Tomoeda M, Matoba R, Matsubara K, Murakami S. Regulation of PLAP-1 expression in periodontal ligament cells. *J Dental Res.* (2006) 85:447–51. doi: 10.1177/154405910608500510
36. Kalamajski S, Aspberg A, Lindblom K, Heinegard D, Oldberg A. Asporin competes with decorin for collagen binding, binds calcium and promotes osteoblast collagen mineralization. *Biochem J.* (2009) 423:53–9. doi: 10.1042/BJ20090542
37. Wang J, Yu H, Ye L, Jin L, Yu M, Lv Y. Integrated regulatory mechanisms of miRNAs and targeted genes involved in colorectal cancer. *Int J Clin Exp Pathol.* (2015) 8:517–29.
38. Liu X, Wu J, Zhang D, Bing Z, Tian J, Ni M, et al. Identification of potential key genes associated with the pathogenesis and prognosis of gastric cancer based on integrated bioinformatics analysis. *Front. Genet.* (2018) 9:265. doi: 10.3389/fgene.2018.00265
39. Jiang K, Liu H, Xie D, Xiao Q. Differentially expressed genes ASPN, COL1A1, FN1, VCAN and MUC5AC are potential prognostic biomarkers for gastric cancer. *Oncol Lett.* (2019) 17:3191–202. doi: 10.3892/ol.2019.9952
40. Turtoi A, Musmeci D, Wang Y, Dumont B, Somja J, Bevilacqua G, et al. Identification of novel accessible proteins bearing diagnostic and therapeutic potential in human pancreatic ductal adenocarcinoma. *J Proteome Res.* (2011) 10:4302–13. doi: 10.1021/pr200527z
41. Klee EW, Bondar OP, Goodmanson MK, Dyer RB, Erdogan S, Bergstralh EJ, et al. Candidate serum biomarkers for prostate adenocarcinoma identified by mRNA differences in prostate tissue and verified with protein measurements in tissue and blood. *Clin Chem.* (2012) 58:599–609. doi: 10.1373/clinchem.2011.171637
42. Mackay A, Urruticoechea A, Dixon JM, Dexter T, Fenwick K, Ashworth A, et al. Molecular response to aromatase inhibitor treatment in primary breast cancer. *Breast Cancer Res.* (2007) 9:R37. doi: 10.1186/bcr1732
43. Turashvili G, Bouchal J, Baumforth K, Wei W, Dziechciarkova M, Ehrmann J, et al. Novel markers for differentiation of lobular and ductal invasive breast carcinomas by laser microdissection and microarray analysis. *BMC Cancer.* (2007) 7:55. doi: 10.1186/1471-2407-7-55
44. Wang L, Wu H, Wang L, Zhang H, Lu J, Liang Z, et al. Asporin promotes pancreatic cancer cell invasion and migration by regulating the epithelial-to-mesenchymal transition (EMT) through both autocrine and paracrine mechanisms. *Cancer Lett.* (2017) 398:24–36. doi: 10.1016/j.canlet.2017.04.001
45. Li H, Zhang Z, Chen L, Sun X, Zhao Y, Guo Q, et al. Cytoplasmic Asporin promotes cell migration by regulating TGF-beta/Smad2/3 pathway and indicates a poor prognosis in colorectal cancer. *Cell Death Dis.* (2019) 10:109. doi: 10.1038/s41419-019-1376-9
46. Huo WU, Jing X, Cheng X, He Y, Hu L, Wu H, et al. Asporin enhances colorectal cancer metastasis through activating the EGFR/src/cortactin signaling pathway. *Oncotarget.* (2016) 7:73402–73413. doi: 10.18632/oncotarget.12336
47. Satoyoshi R, Kuriyama S, Aiba N, Yashiro M, Tanaka M. Asporin activates coordinated invasion of scirrhous gastric cancer and cancer-associated fibroblasts. *Oncogene.* (2015) 34:650–60. doi: 10.1038/onc.2013.584
48. Ding Q, Zhang M, Liu C. Asporin participates in gastric cancer cell growth and migration by influencing EGF receptor signaling. *Oncol Rep.* (2015) 33:1783–90. doi: 10.3892/or.2015.3791
49. Rochette A, Boufaied N, Scarlata E, Hamel L, Brimo F, Whitaker HC, et al. Asporin is a stromally expressed marker associated with prostate cancer progression. *Br J Cancer.* (2017) 116:775. doi: 10.1038/bjc.2017.15
50. Castellana B, Escuin D, Peiro G, Garcia-Valdecasas B, Vazquez T, Pons C, et al. ASPN and GJB2 are implicated in the mechanisms of invasion of ductal breast carcinomas. *J Cancer.* (2012) 3:175–83. doi: 10.7150/jca.4120
51. Simkova D, Kharaishvili G, Korinkova G, Ozdian T, Suchánková-Kleplová T, Soukup T, et al. The dual role of asporin in breast cancer progression. *Oncotarget.* (2016) 7, 52045–52060. doi: 10.18632/oncotarget.10471
52. Maris P, Blomme A, Palacios AP, Costanza B, Bellahcène A, Bianchi E, et al. Asporin is a fibroblast-derived TGF-β1 inhibitor and a tumor suppressor associated with good prognosis in breast cancer. *PLoS Med.* (2015) 12:e1001871. doi: 10.1371/journal.pmed.1001871
53. Derynck R, Akhurst RJ, Balmain A. TGF-beta signaling in tumor suppression and cancer progression. *Nat Genet.* (2001) 29:117–29. doi: 10.1038/ng1001-117
54. de Caestecker MP, Piek E, Roberts AB. Role of transforming growth factor-beta signaling in cancer. *J Natl Cancer Inst.* (2000) 92:1388–402. doi: 10.1093/jnci/92.17.1388
55. Zarzynska JM. Two faces of TGF-beta1 in breast cancer. *Mediat Inflamm.* (2014) 2014:141747. doi: 10.1155/2014/141747
56. Jung B, Staudacher JJ, Beauchamp D. Transforming growth factor beta superfamily signaling in development of colorectal cancer. *Gastroenterology.* (2017) 152:36–52. doi: 10.1053/j.gastro.2016.10.015
57. Wee P, Wang Z. Epidermal growth factor receptor cell proliferation signaling pathways. *Cancers.* (2017) 9:E52. doi: 10.3390/cancers9050052
58. Sigismund S, Avanzato D, Lanzetti L. Emerging functions of the EGFR in cancer. *Mol Oncol.* (2018) 12:3–20. doi: 10.1002/1878-0261.12155
59. Scaltriti M, Baselga J. The epidermal growth factor receptor pathway: a model for targeted therapy. *Clin Cancer Res.* (2006) 12:5268–72. doi: 10.1158/1078-0432.CCR-05-1554
60. Barnard JA, Beauchamp RD, Russell WE, Dubois RN, Coffey RJ. Epidermal growth factor-related peptides and their relevance to gastrointestinal pathophysiology. *Gastroenterology.* (1995) 108:564–80. doi: 10.1016/0016-5085(95)90087-X
61. Zhang Z, Li H, Zhao Y, Guo Q, Yu Y, Zhu S, et al. Asporin promotes cell proliferation via interacting with PSMD2 in gastric cancer. *Front Biosci.* (2019) 24:1178–89. doi: 10.2741/4774
62. Artym VV, Zhang Y, Seillier-Moiseiwitsch F, Yamada KM, Mueller SC. Dynamic interactions of cortactin and membrane type 1 matrix metalloproteinase at invadopodia: defining the stages of invadopodia formation and function. *Cancer Res.* (2006) 66:3034–43. doi: 10.1158/0008-5472.CAN-05-2177
63. Clark ES, Whigham AS, Yarbrough WG, Weaver AM. Cortactin is an essential regulator of matrix metalloproteinase secretion and extracellular matrix degradation in invadopodia. *Cancer Res.* (2007) 67:4227–35. doi: 10.1158/0008-5472.CAN-06-3928
64. Senbanjo LT, Chellaiah MA. CD44: a multifunctional cell surface adhesion receptor is a regulator of progression and metastasis of cancer cells. *Front Cell Develop Biol.* (2017) 5:18. doi: 10.3389/fcell.2017.00018
65. Ponta H, Sherman L, Herrlich PA. CD44: from adhesion molecules to signalling regulators. *Nat Rev Mol Cell Biol.* (2003) 4:33–45. doi: 10.1038/nrm1004
66. Chen C, Zhao S, Karnad A, Freeman JW. The biology and role of CD44 in cancer progression: therapeutic implications. *J Hematol Oncol.* (2018) 11:64. doi: 10.1186/s13045-018-0605-5
67. Hughes RM, Simons BW, Khan H, Miller R, Kugler V, Torquato S, et al. Asporin restricts mesenchymal stromal cell differentiation, alters the tumor microenvironment, and drives metastatic progression. *Cancer Res.* (2019) 79:3636–50. doi: 10.1158/0008-5472.CAN-18-2931
68. Awata T, Yamada S, Tsushima K, Sakashita H, Yamaba S, Kajikawa T, et al. PLAP-1/Asporin positively regulates FGF-2 activity. *J Dental Res.* (2015) 94:1417–24. doi: 10.1177/0022034515598507
69. Luehders K, Sasai N, Davaapil H, Kurosawa-Yoshida M, Hiura H, Brah T, et al. The small leucine-rich repeat secreted protein Asporin induces eyes in Xenopus embryos through the IGF signalling pathway. *Development.* (2015) 142:3351–61. doi: 10.1242/dev.124438
70. Iozzo RV, Schaefer L. Proteoglycans in health and disease: novel regulatory signaling mechanisms evoked by the small leucine-rich proteoglycans. *FEBS J.* (2010) 277:3864–75. doi: 10.1111/j.1742-4658.2010.07797.x
71. Ayala G, Tuxhorn JA, Wheeler TM, Frolov A, Scardino PT, Ohori M, et al. Reactive stroma as a predictor of biochemical-free recurrence in prostate cancer. *Clin Cancer Res.* (2003) 9:4792–801.

72. Hsu PD, Lander ES, Zhang F. Development and applications of CRISPR-Cas9 for genome engineering. *Cell*. (2014) 157:1262–78. doi: 10.1016/j.cell.2014.05.010
73. Li C, Li C, Yue J, Huang X, Chen M, Gao J, et al. miR-21 and miR-101 regulate PLAP-1 expression in periodontal ligament cells. *Mol Med Rep*. (2012) 5:1340–6. doi: 10.3892/mmr.2012.797
74. Rea D, Del Vecchio V, Palma G, Barbieri A, Falco M, Luciano A, et al. Mouse models in prostate cancer translational research: from xenograft to PDX. *Bio Med Res Int*. (2016). 2016:9750795. doi: 10.1155/2016/9750795
75. Simkova D, Kharaishvili G, Slabakova E, Murray PG, Bouchal J. Glycoprotein asporin as a novel player in tumour microenvironment and cancer progression. *Biomed Papers*. (2016) 160:467–73. doi: 10.5507/bp.2016.037
76. Ikegawa S. Expression, regulation and function of asporin, a susceptibility gene in common bone and joint diseases. *Curr Med Chem*. (2008) 15:724–8. doi: 10.2174/092986708783885237
77. Xu L, Li Z, Liu S-Y, Xu S-Y, Ni G-X. Asporin and osteoarthritis. *Osteoarthr Cartil*. (2015) 23:933–9. doi: 10.1016/j.joca.2015.02.011

Conflict of Interest: The authors declare that the research was conducted in the absence of any commercial or financial relationships that could be construed as a potential conflict of interest.

Copyright © 2019 Zhan, Li and Ge. This is an open-access article distributed under the terms of the Creative Commons Attribution License (CC BY). The use, distribution or reproduction in other forums is permitted, provided the original author(s) and the copyright owner(s) are credited and that the original publication in this journal is cited, in accordance with accepted academic practice. No use, distribution or reproduction is permitted which does not comply with these terms.

frontiers in Oncology

ORIGINAL RESEARCH
published: 23 October 2019
doi: 10.3389/fonc.2019.01074

Inhibition of CYR61-S100A4 Axis Limits Breast Cancer Invasion

*Johanna W. Hellinger, Silke Hüchel, Lena Goetz, Gerd Bauerschmitz, Günter Emons and Carsten Gründker**

Department of Gynecology and Obstetrics, University Medicine Göttingen, Göttingen, Germany

Background and Objective: Matricellular proteins modulate the micro environment of tumors and are recognized to contribute to tumor cell invasion and dissemination. The cysteine-rich angiogenic inducer 61 (CYR61) is upregulated in mesenchymal transformed and invasive breast cancer cells. CYR61 correlates with poor prognosis of breast cancer patients. The signaling mechanism that causes invasive properties of cancer cells regarding to epithelial-mesenchymal transition (EMT) needs further research. In this study, we investigated the signaling mechanism, which is responsible for reduced cell invasion after suppression of CYR61 in mesenchymal transformed breast cancer cells and in triple negative breast cancer cells.

Methods: We addressed this issue by generating a mesenchymal transformed breast cancer cell line using prolonged mammosphere cultivation. Western blotting and quantitative PCR were used to analyze gene expression alterations. Transient gene silencing was conducted using RNA interference. Proliferation was assessed using AlamarBlue assay. Invasiveness was analyzed using 2D and 3D invasion assays. Immune-histochemical analysis of patient tissue samples was performed to examine the prognostic value of CYR61 expression.

Results: In this study, we investigated whether CYR61 could be used as therapeutic target and prognostic marker for invasive breast cancer. We discovered an interaction of CYR61 with metastasis-associated protein S100A4. Suppression of CYR61 by RNA interference reduced the expression of S100A4 dependent on ERK1/2 activity regulation. Non-invasive breast cancer cells became invasive due to extracellular CYR61 supplement. Immune-histochemical analysis of 239 patient tissue samples revealed a correlation of higher CYR61 and S100A4 expression with invasive breast cancer and metastasis.

Conclusion: Our data suggest that suppression of CYR61 impedes the formation of an invasive cancer cell phenotype by reducing ERK1/2 phosphorylation thereby suppressing S100A4. These findings identify mechanisms by which CYR61 suppresses cell invasion and suggest it to be a potential therapeutic target and prognostic marker for invasive breast cancer and metastasis.

Keywords: breast cancer, CYR61, invasion, EMT, triple negative breast cancer

OPEN ACCESS

Edited by:
Mohit Kumar Jolly,
Indian Institute of Science (IISc), India

Reviewed by:
Saurav Kumar,
Indian Institute of Science (IISc), India
Daniele Vergara,
University of Salento, Italy
Bisrat G. Debeb,
University of Texas MD Anderson Cancer Center, United States

****Correspondence:***
Carsten Gründker
grundker@med.uni-goettingen.de

Specialty section:
This article was submitted to Molecular and Cellular Oncology, a section of the journal Frontiers in Oncology

Received: *22 July 2019*
Accepted: *30 September 2019*
Published: *23 October 2019*

Citation:
Hellinger JW, Hüchel S, Goetz L, Bauerschmitz G, Emons G and Gründker C (2019) Inhibition of CYR61-S100A4 Axis Limits Breast Cancer Invasion. Front. Oncol. 9:1074. doi: 10.3389/fonc.2019.01074

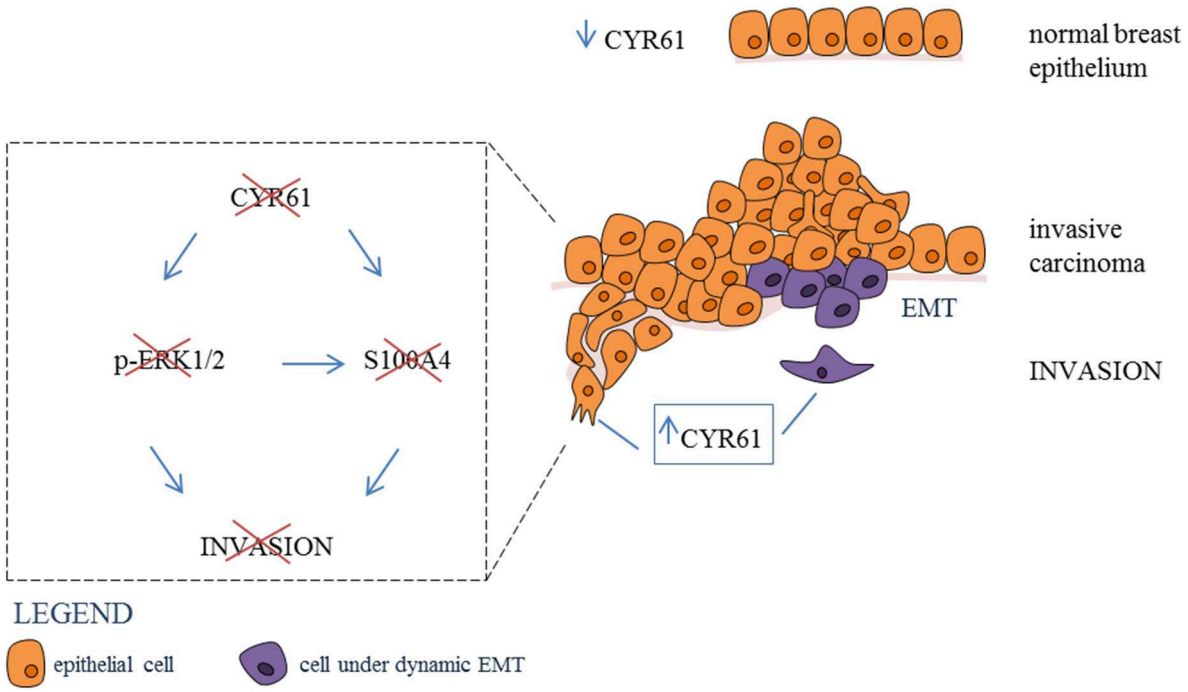

GRAPHICAL ABSTRACT | Inhibtion of CYR61-S100A4 axis limitis breast cancer Invasion. CYR61 expression is low in normal breast epithelium, while expression is increased in invasive breast carcinoma. Suppression of CYR61 leads to reduced ERK1/2 phosphorylation and S100A4 expression thereby reducing breast cancer invasion. EMT, epithelial-mesenchymal transition.

INTRODUCTION

In 2019, approximately 271270 woman and men in the United States will be diagnosed with breast cancer. Due to improved early detection techniques and treatment options 5-year-survival rates for local and regional breast cancer are 84–99 %. However, only 27of patients diagnosed with distant metastasis survive a period of 5 years (1). Consequently it is necessary to identify prognostic markers for the early detection of breast cancer metastasis and new treatment options for this indications which accounts for more than 90% of cancer related death (2).

The first key event in the multi-step process of metastasis is the separation of tumor cells from the primary tumor and the dissemination into the surrounding tissue. Cells gain the ability to migrate and invade by altering their cytoskeletal organization, cell-cell-contacts, contacts with the extracellular matrix (ECM) and surrounding stroma (3). Epithelial-mesenchymal transition (EMT) is a transient dynamic program induced by different transcription factors (TFs). EMT-TFs orchestrate tumor-promoting micro environmental changes, cancer cell stemness, and chemo resistance (4, 5). The contribution of EMT programs to the metastatic cascade regarding breast cancer is supported by several publications (6–8). However, it is still under debate if an involvement of EMT programs is indispensable for creating an invasive phenotype (4). Therefore it is necessary to study cancer cell invasion with regards to EMT complexity (9, 10).

The cysteine rich angiogenic inducer (CYR61) belongs to the CCN family (CYR61, CTGF /CCN12, NOV/CCN3, WISP-1/CCN4, WISP-2/CCN5, WISP-3/CCN6) of matricellular proteins and is localized on cell surface, cytoplasm and as a secreted protein in the extracellular matrix. The functions of CYR61 are cell type and context-dependent (11). They are transmitted through binding to integrin and heparin sulfate proteoglycans (HSPGs). CYR61 was shown to be involved in facilitating EMT programs in different cancer entities (12–14). It is known that elevated CYR61 expression promotes tumor progression, proliferation, migration and invasion of breast cancer (15, 16), whereas the role of CYR61 in breast cancer EMT programs remains elusive. Otherwise, CYR61 can act as a tumor suppressor in non-small cell lung cancer (17) and in fibroblasts by inducing apoptosis and senescence during wound healing (18, 19). The role of CYR61 signaling in cancer invasion and EMT programs regarding to a potential use as therapeutic target and prognostic marker needs further evaluation.

We hypothesize that CYR61 is a key regulator of breast cancer invasion. We want to identify the mechanisms by which CYR61 facilitates an invasive phenotype. Furthermore, we want to investigate the value of CYR61 as a therapeutic target and prognostic marker for invasive and metastatic breast cancer.

MATERIALS AND METHODS

Cell Lines and Cell Culture

Human breast cancer cell lines MCF-7, T47D, MDA-MB-231, and HCC1806 were obtained from American Type Cell Collection (ATCC; Manassas, VA, USA) and cultured in minimum essential medium (MEM; biowest, Nuaillé, France) supplemented with 10% fetal bovine serum (FBS; biochrom, Berlin, Germany), 1% Penicillin/Streptomycin (P/S; Gibco, Carlsbad, CA, USA), 0,1% Transferrin (Sigma, St. Louis, USA) and 26 IU Insulin (Sanofi, Frankfurt, Germany). Human osteosarcoma cell line MG-63 was purchased from ATCC and cultured Dulbecco's modified eagle medium (DMEM; Gibco) supplemented with 10% FBS (biochrom) and 1% Penicillin/Streptomycin (Gibco). To retain identity of cell lines, purchased cells were expanded and aliquots were frozen in liquid nitrogen. A new frozen stock was used every half year and Mycoplasma testing of cultured cell lines was performed routinely using PCR Mycoplasma Test Kit I/C (PromoCell GmbH, Heidelberg, Germany). All cells were cultured in a humidified atmosphere with 5% CO_2 at 37°C.

Generation of Mesenchymal Transformed MCF-7 Cells

Mesenchymal transformed MCF-7 breast cancer cells (MCF-7-EMT) were generated as described earlier (20). Briefly, 4×10^4 cells/ml were cultured in prolonged mammosphere culture (5–6 weeks) in ultralow adherence six well plates (Corning, Lowell, MA, USA) in DMEM/F12 (Gibco) supplemented with 10% charcoal-stripped fetal calf serum (cs-FCS;PAN-biotech, Aiden Bach, Germany), 2% B27 supplement (Invitrogen, Darmstadt, Germany), 1% penicillin/streptomycin, 0.5 mg/ml hydrocortisone (Sigma, St. Louis, MO, USA), 5 µg/ml insulin, 20 ng/ml epidermal growth factor (EGF; Sigma, St. Louis, MO, USA).

Treatment With rhCYR61 and U0126

Human breast cancer cells were seeded at 5×10^5 cells/ml in MEM supplemented with 10% FB, 1% P/S, 0,1% Transferrin 26 IU Insulin. Cells treated with 1 µg/ml rhCYR61 (recombinant human CYR61; C-63398; PromoKine; Heidelberg; Germany) were serum-deprived 24 h prior to treatment and lysed 24 h after treatment. Cells treated with 10 µM U0126 (#tlrl-u0126; InvivoGen; San Diego; USA) were lysed 24 h after treatment.

Transwell Invasion Assay

Using co-culture transwell assay as described earlier (21), 1×10^4 breast cancer cells were seeded in DMEM w/o phenol red (Gibco), supplemented with 10% cs-FCS into a cell cultural insert (upper well) with a polycarbonate membrane (8 µm pore diameter, Merck Millipore, Cork, Ireland) coated with 30 µL of a Matrigel® (BD Bioscience, Bedford, MA, USA) solution (1:2 in serum-free DMEM). The osteosarcoma cells were seeded (2.5×10^4) in DMEM supplemented with 10% cs-FCS into the lower well (24-well-plate). After 24 h cells were co-cultured for 48 h or 96 h. Stably transfected cells (overexpressing CYR61 or S100A4) were seeded at a density of 1×10^4 per well in DMEM w/o phenol red cell cultural insert (upper well, Matrigel-coated with a polycarbonate membrane), with the lower well containing DMEM w/o phenol red supplemented with 10% cs-FBS and cultured for 96 h. Invaded cells on the lower side of the insert were stained with hematoxylin and the number of cells in four randomly selected fields of each insert was counted.

3D Spheroid Assay

Assessment of 3D cell invasion was pursued as describes earlier with minor changes (22). Briefly 1×10^3 breast cancer cells were seeded in 100 µL in a well of an ultra-low-adherence 96-well plate (ULA; Nexcelom, Cenibra GmbH, Bramsche, Germany). After 48 h spheroid formation was visually confirmed and 50 µL of media was removed. Thereafter 50 µL Matrigel were added to the spheroid wells. Central position of the spheroids was checked visually and Matrigel was allowed to solidify for 1 h at 37°C and 5% CO_2. Afterwards 50 µL media were added to each well and a picture was taken marking time point 0 (t0h). When indicated 1µg/ml rhCYR61 or 10µM U0126 were added. Spheroid growth area was analyzed using ImageJ polygonal selection and measurement. Mean values were calculated and compared to respective control.

Small Interfering RNA Transfection

Breast cancer cell lines MCF-7-EMT (5×10^5 cells/ml) and MDA-MB-231 (2.5×10^5 cells/ml) were seeded in 2 ml of MEM with 10% FBS (-P/S) in 25 cm^2 cell culture flask. The cells were transiently transfected with siRNA specific to S100A4 (sc-106781 pool of three S100A4-specific siRNAs; Santa Cruz Biotechnology, Dallas, USA), CYR61 (sc-39331 pool of three CYR61-specific siRNAs; Santa Cruz Biotechnology) or YAP1 (sc38637 pool of three YAP1 specific siRNAs; Santa Cruz Biotechnologies) in OPTI-MEM I medium (Gibco, Carlsbad, CA, USA) with siRNA transfection reagent (sc-29528; Santa Cruz Biotechnology, Dallas, USA). A non-targeting siRNA was used as control (sc-37007 control-A; Santa Cruz Biotechnology, Dallas, TX, USA). After an incubation period of 6 h, MEM supplemented with 20% FBS and 20% penicillin/streptomycin was added.

Immune-Histochemical Staining

Immune-histochemical staining of human tissue array slides (T087a; BR20837; BR248a; US Biomax, Derwood, MD, USA) was performed as described earlier (23). Sample sections were deparaffinized and rehydrated. Then antigens were retrieved by slide incubation in 0.01 M citrate buffer (pH 6.0) in microwave (700W) for 5 min. Using 3% hydrogen peroxidase solution for 6 min the endogenous peroxidase activity was quenched. Sample sections were incubated over night with primary labeled antibodies against S100A4 (NBP2-54580AF488; Alexa Fluor 488 labeled; 5 µg/ml; Novus Biologicals, Centennial, CO, USA) and CYR61 (NB100-356R; DyLight labeled; 5 µg/ml; Novus Biologicals) at 4°C. Staining was visualized using a Zeiss Scope A1 Axio microscope (ZEISS, Oberkochen, Germany) with an oil EC PLAN-NEOFLUAR 100x (ZEISS, Oberkochen, Germany) objective and the ZEN software (ZEISS, Oberkochen, Germany).

Real-Time Quantitative PCR Analysis

Total RNA was extracted using an RNeasy mini kit (Qiagen, Hilden, Germany) and 2 µg were reverse transcribed with

high capacity cDNA reverse transcription kit (Qiagen, Hilden, Germany). Real- time qPCR was performed using SYBR green PCR master mix kit (Qiagen, Hilden, Germany). Primer were, for S100A4 5′- GTACTCGGGCAAAGAGGGTG−3′ (forward) 5′- TTGTCCCTGTTGCTGTCCAA−3′ (reverse), for CYR61 5′-CTCCCTGTTTTTGGAATGGA−3′ (forward) 5′- TGGTCTTG CTGCATTTCTTG−3′ (reverse), for YAP1 5′- TCCCAGATG AACGTCACAGC−3′ (forward) 5′- TCATGGCAAAACGAGG GTCA−3′ (reverse), E-cadherin 5′-CCTCCTGAAAAGAGAG TGGA−3′ (forward) 5′-GTGTCCGGATTAATCTCCAG−3′ (reverse), Vimentin 5′-GCTGCTAACTACCAAGACAC−3′ (forward) 5′-TCAGGTTCAGGGAGGAAAAG−3′ (reverse), Zeb1 5′-AAGACAAACTGCATATTGTGGAAG−3′ (forward) 5′-CTGCTTCATCTGCCTGAGCTT−3′ (reverse), SNAI1 5′-GCCAAACTACAGCGAACTGG−3′ (forward) 5′- GAGA GAGGCCATTGGGTAGC-3′ (reverse), SNAI2 5′- AAGATGCA CATCCGAAGCCA-3′ (forward) 5′- CATTCGGGAGAAGGTC CGAG−3′ (reverse) and GAPDH 5′- GAAGGTCGGAGTCAAC GGAT−3′ (forward) 5′- TGGAATTTGCCATGGGTGGA−3′ (reverse). PCR conditions were: denaturing once at 95°C (2 min), 95°C (5 s), and 60°C (15 s) for 40 cycles.

Western Blot Analysis

Cells were lysed in cell lytic M buffer (Sigma, St. Louis, USA) supplemented with 0.1% phosphatase-inhibitor (Sigma, St. Louis, MO, USA) and 0.1% protease-inhibitor (Sigma, St. Louis, MO, USA). Isolated proteins (40 μg) were fractioned using 12% SDS gels and electro-transferred to a polyvinylidene difluoride membrane (Merck Millipore, Cork, Ireland). Primary antibodies against S100A4 1:250 (HPA007973; Sigma, St. Louis, USA), CYR61 1:250 (HPA029853; Sigma, St. Louis, MO, USA), YAP 1:250 (sc-398182; Santa Cruz Biotechnology, Dallas, TX, USA), ERK1/2 1:1000 (4695S;Cell Signaling Technologies Inc., Danvers, MA, USA), Phospho-ERK1/2(Thr202/Tyr204) 1:1000 (9101S; Cell Signaling Technologies Inc.), and GAPDH 1:2000 (5174; Cell Signaling Technologies Inc) were used. The membrane was washed and incubated in horseradish peroxidase-conjugated secondary antibodies (GE Healthcare, Buckinghamshire, UK). Antibody-bond protein bands were assayed using a chemiluminescent luminol enhancer solution (Cyanagen, Bologna, Italy).

ECM Degradation

Wells of a 96-well plate were coated at room temperature for 20 min with 0.05 mg/ml Poly-L-lysine in DPBS (Sigma) and 15 min with glutaraldehyde 0.5% in DPBS. Gelatin (2 mg/ml; G9391; Sigma) was FITC conjugated as recommend by manufacture (#343210; EMD Millipore Corp., Billeria, MA, USA). Wells were coated with 60 μL FITC-conjugated gelatin (2 mg/ml; Invitrogen, Milpitas, CA, USA) diluted 1:5 with unlabeled gelatin (Sigma) and incubated for 10 min at RT. Solution was discarded and wells were incubated for 30 min in 70% ethanol and afterwards free aldehydes were quenched with culture media for 30 min at room temperature before cells were seeded. Cells were seeded (4.4×10^3 cells per Well) and treated with rhCTGF (1 μg/ml; R&D systems). After 24 h proteolytic activity was detected by measuring fluorescence (extinction 490 nm/emission 520 nm) using Synergy (BioTek Instruments, Bad Friedrichshall, Germany). Each experiment was performed in duplicates for at least three times. Mean values were compared to the respective control.

AlamarBlue Assay

3D spheroids were grown as described above and 48 h after adding Matrigel AlamarBlue (BioRad, Hercules, USA) was added and incubated for 4 h at 37°C 5% CO_2. The colorimetric change of resazurin to resorufin upon cellular metabolic reduction was measured by absorbance reading at 540 nm and 630 nm, using Synergy (BioTek Instruments). Relative AlamarBlue Reduction was calculated as indicated by manufacturer.

KM Plotter Analysis

The database of the Kaplan-Meier plotter (www.kmplot.com) downloads information of gene expression and overall survival from Gene Expression Omnibus (GEO; only Affymetrix microarrays), the European Genome- Phenome Archive (EGA) and The Cancer Genome Atlas (TCGA). To be able to analyze the prognostic value (overall survival) of CYR61 in 1,402 patient samples, the samples were split into two cohorts according to the expression of quantiles of CYR61 where all possible cutoff values between the lower and the upper quantiles are computed and the best performing threshold is used as a cutoff. These groups are compared by a Kaplan-Meier survival plot and the hazard ratio with 95% confidence intervals. Redundant samples were removed, biased arrays excluded and the proportional hazard assumption was set to zero (24).

Statistical Analysis

All experiments were performed at least in three biological and technical replicates. Data were analyzed by GraphPad Prism (GraphPad software Inc., v. 7.03, La Jolla, Ca, USA) using unpaired, two-tailed, parametric *t*-test comparing two groups (treatment to respective control) by assuming both populations have the same standard derivation. $P < 0.05$ was considered statistically significant.

RESULTS

CYR61 Expression Correlates With Altered Breast Cancer Cell Invasion

Mesenchymal transformed breast cancer cells show a TGFβ-dependent increased invasive and metastatic potential (20). Despite, it is still under debate, if EMT programs are indispensable for cell invasion (4) and which key players are crucial for pathological EMT programs. We investigated whether within dynamic EMT programs or triple-negative breast cancer (TNBC; no expression of estrogen or progesterone and no overexpression of Her2neu) cells show changes in CYR61 expression. It was shown before that non-invasive breast cancer cells gain invasiveness when co-cultured with primary osteoblasts or osteosarcoma cells (21). Gründker et al. suggested that mesenchymal transformed non-invasive MCF-7 cells (MCF-7-EMT) show an increased invasiveness and elevated CYR61 expression (23). Increased invasiveness could be suppressed by reducing extracellular CYR61 using blocking antibodies. Despite, it remains elusive, if targeting intracellular CYR61

alters cell invasiveness in 2D transwell co-culture invasion assay. Two non-invasive estrogen positive cell lines (MCF-7, T47D) were mesenchymal transformed (MCF-7-EMT; T47D-EMT) and altered expression of EMT-Transcriptionfactors (EMT-TFs) was assessed. Mesenchymal transformation using prolonged mammosphere culture leads to a decreased E-cadherin expression (**Figure 1**, **Figure S1B**) in two different estrogen positive breast cancer cells lines. Transforming growth factor induced (TGFBI), Zinc Finger E-Box Binding Homeobox 1 (Zeb1) and Snail Family Transcriptional Repressor 2 (Snai2) expression was increased after mesenchymal transformation (**Figure 1**, **Figures S1A,D–F**), while vimentin expression was upregulated in MCF-7-EMT breast cancer cells (**Figure 1**, **Figure S1C**) and Snail Family Transcriptional Repressor 1 (Snai1) was upregulated in T47D-EMT cells. In addition CYR61 expression is upregulated in mesenchymal transformed breast cancer cells (**Figure 1A**; MCF-7-EMT: 2.18 ± 0.2 SEM relative expression compared to MCF-7; $n = 5$; T47D-EMT: 3.04 ± 0.62 SEM relative expression compared to T47D) and in TNBC cells (**Figure 1A**; MDA-MB-231: 68.67±11.27 SEM relative expression compared to MCF-7; $n = 4$; HCC1806: 1.3 ± 0.09 SEM relative expression compared to MCF-7; $n = 3$). Moreover, mesenchymal transformed and TNBC cell lines show increased invasiveness in a 2D transwell co-culture invasion assay (**Figure 1B**; MCF-7-EMT: 683.9 ± 53.25 SEM invaded cells in % to MCF-7; $n = 36$; $P < 0.0001$; T47D-EMT: 11881 ± 155.8 SEM invaded cells in % to T47D; $n = 36$; $P = 0.0022$; MDA-MB-231: 466.7 ± 58.52 SEM invaded cells in % to MCF-7; $n = 24$; $P < 0.0001$; HCC1806: 2277 ± 237.4 SEM invaded cells in % to MCF-7; $n = 54$; $P < 0.0001$). To determine whether intracellular suppressed CYR61 regulates breast cancer cell invasion, we transiently reduced CYR61 (see verification of CYR61 suppression **Figure 1**, **Figure S2A**) in different invasive breast cancer cell lines and analyzed invasiveness using 2D invasion co-culture assay. Reducing CYR61 results in decreases cell invasion (**Figure 1C**; MCF-7-EMT CYR61$^-$: 59.01 ± 4.34 SEM invaded cells in % to MCF-7-EMT control; $n = 36$; $P < 0.0001$; T47D-EMT CYR61$^-$: 50.73 ± 8.71 SEM invaded cells in % to T47D-EMT control; $n = 36$; $P = 0.002$; MDA-MB-231 CYR61$^-$: 31.44 ± 4.22 SEM invaded cells in % to MDA-MB-231 control; $n = 18$; $P < 0.0001$; HCC1806 CYR61$^-$:18.51 ± 2.96; $n = 18$; $P < 0.0001$). To confirm the impact of CYR61 suppression on breast cancer cell invasion, we assessed whether CYR61 suppression leads to a reduced 3D spheroid invasion growth. Reducing CYR61 results in a decreased 3D spheroid invasion area (**Figure 1D**; MCF-7-EMT CYR61$^-$: 87.93 ± 2.54 SEM invaded area in % to MCF-7-EMT control; $n = 5$; $P = 0.0014$; T47D-EMT CYR61$^-$: 61.56 ± 4.3 SEM invaded area in % to T47D-EMT control; $n = 6$; $P < 0.0001$; MDA-MB-231 CYR61$^-$:50.37 ± 13.29; $n = 5$; $P = 0.006$; HCC1806 CYR61$^-$:82.24 ± 4.81 SEM invaded area in % to HCC1806 control; $n = 6$; $P = 0.004$). To determine whether decreased 3D spheroid invaded area is due to altered proliferation AlamarBlue Assay was conducted. Transient reduces CYR61 does not alter proliferation in 3D breast cancer cell spheroids after 96 h (**Figure 1**, **Figure S2B**). Furthermore, increased extracellular CYR61 expression increases 3D spheroid invaded area of non-invasive estrogen positive breast cancer cells (**Figure 1E**; MCF-7 rhCYR61: 119.7 ± 2.93 SEM invaded area in % to MCF-7 control; $n = 5$; $P = 0.001$; T47D rhCYR61: 128.6 ± 4.38 SEM invaded area in % to T47D control; $n = 4$; $P = 0.0006$). The underlying mechanism of cell invasion into the surrounding tissue evolve different processes including altered cell-cell adhesion, cell-ECM adhesion and ECM degradation (3). Proteolytic activity of estrogen positive breast cancer cells treated with extracellular CYR61 was increased (**Figure 1F**; MCF-7 rhCYR61: 110.8 ± 2.65 SEM relative proteolytic activity in % compared to MCF-7 control; $n = 3$; $P = 0.015$; T47D rhCYR61: 106.2 ± 1.806 SEM relative proteolytic activity compared to T47D control; $n = 3$; $P = 0.026$), while proliferation was not altered (**Figure 1**, **Figure S2C**). Collectively, these data indicate that suppression CYR61 decreases invasiveness in mesenchymal transformed and TNBC cells. Furthermore, increased extracellular CYR61 expression increases invasiveness of non-invasive estrogen positive breast cancer cells.

Suppression of CYR61 Reduces S100A4 Expression

Identically to CYR61, S100A4 is upregulated during EMT programs in breast cancer and correlates with bone metastasis (23, 25). Blocking extracellular signaling of S100A4 reduced invasiveness of breast cancer cells in a 2D transwell invasion assay (23). Both CYR61 and S100A4 alter breast cancer invasiveness but the underlying molecular mechanisms remain elusive. Chen et al. suggested that CTGF regulates S100A4 through regulation of extracellular regulated kinases ERK1 and ERK2 (26). CYR61 and CTGF both bind to integrinαV (12, 26, 27). We wanted to elucidate, whether suppression of CYR61 decreases S100A4 expression (**Figure 2A**). S100A4 was upregulated in mesenchymal transformed and TNBC cells (**Figure 2B**; MCF-7-EMT: 1.84 ± 0.27 SEM relative expression compared to MCF-7;$n = 5$; $P = 0.014$; T47D-EMT: 1.47 ± 0.16 SEM relative expression compared to T47D;$n = 5$; $P = 0.0185$; HCC1806: 1.89 ± 0.38 relative expression compared to MCF-7; $n = 6$; $P = 0.0403$; MDA-MB-231: 90.31 ± 13.3 SEM relative expression compared to MCF-7; $n = 4$; $P = 0.0005$). To elucidate the impact of CYR61 expression on S100A4, relative S100A4 expression was assessed after transient CYR61 suppression. Decreased CYR61 expression resulted in decreased S100A4 expression (**Figure 2C**; MCF-7-EMT CYR61$^-$:0.64 ± 0.05 SEM relative S100A4 expression compared to MCF-7-EMT control; $n = 4$; $P = 0.0002$; T47D-EMT CYR61$^-$: 0.79 ± 0.04 SEM relative S100A4 expression compared to T47D-EMT control; $n = 3$; $P = 0.0078$; MDA-MB-231 CYR61$^-$:0.78 ± 0.08 SEM relative S100A4 expression compared to MDA-MB-231 control; $n = 4$; $P = 0.0297$; HCC1806 CYR61-: 0.63 ± 0.07 SEM relative S100A4 expression compared to HCC1806 control; $n = 3$; $P = 0.0066$), while suppresses S100A4 had no impact on CYR61 expression (**Figure 2**, **Figure S3D**). We investigated whether decreased S100A4 suppresses cell invasion in a 2D transwell co-culture assay. Decreased S100A4 expression (verification **Figure 2**, **Figures S1–S3**) suppressed the invasiveness of mesenchymal transformed und TNBC cells (**Figure 2D**; MCF-7-EMT S100A4$^-$: 83.81 ± 4.9 SEM invaded

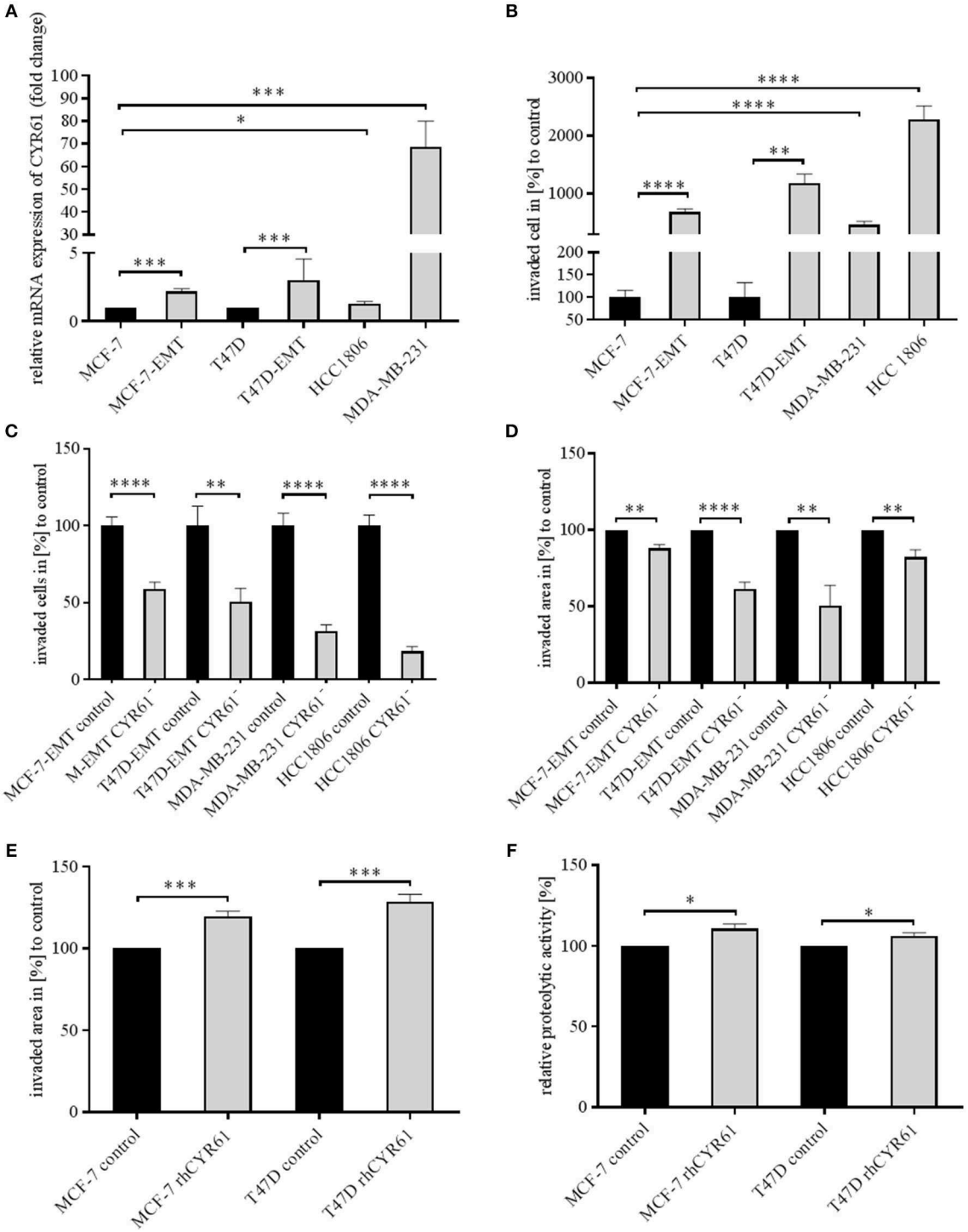

FIGURE 1 | CYR61 expression correlates with breast cancer cell invasiveness. **(A)** Relative CYR61 expression of invasive breast cancer cell lines compared to non-invasive controls. Data represent mean ± SEM. Using unpaired, two-tailed *t*-test analysis. MCF-7-EMT $n = 5$; T47D-EMT $n = 6$; MDA-MB-231 $n = 4$; HCC1806 $n = 3$; $^{*}P < 0.05$; $^{***}P < 0.005$ **(B)** 2D Invasion analysis of co-cultured (MG-63, osteosarcoma cells) breast cancer cells for 96 h. Percentage of cell invasion compared to controls was assessed by counting invaded cells under the filter in 4 random filter regions. Data represent mean ± SEM. Using unpaired, two-tailed *t*-test analysis. MCF-7-EMT $n = 36$; T47D-EMT $n = 36$; MDA-MB-231 $n = 24$; HCC1806 $n = 54$; $^{**}P < 0.01$; $^{****}P < 0.0001$ **(C)** 2D Invasion analysis of co-cultured (MG-63, osteosarcoma cells) breast cancer cells transient transfected with CYR61 siRNA for 96 h. Percentage of cell invasion compared to controls was assessed by counting invaded cells under the filter in 4 random filter regions. Data represent mean ± SEM. MCF-7-EMT $n = 36$; T47D-EMT $n = 18$; MDA-MB-231 $n = 18$;

(Continued)

FIGURE 1 | HCC1806 $n = 36$; $^{**}P < 0.01$; $^{****}P < 0.0001$ **(D)** 3D invasion analysis of breast cancer spheroids seeded after transient siRNA transfection. Spheroid area was assessed 48 h after adding Matrigel using polygonal selection and compared to spheroid area at time point 0 (adding of Matrigel). Area growth was compared to area growth of control spheroids. Data represent mean ± SEM. Using unpaired, two-tailed *t*-test analysis. MCF-7-EMT $n = 5$; T47D-EMT $n = 6$; MDA-MB-231 $n = 5$; HCC1806 $n = 6$; $^{**}P < 0.01$; $^{***}P < 0.005$ **(E)** 3D invasion analysis of breast cancer spheroids treated with recombinant human CYR61 (rhCYR61). Spheroid area was assessed 48 h after adding Matrigel and rhCYR61 using polygonal selection and compared to spheroid area at time point 0 (adding of Matrigel+ rhCYR61). Area growth was compared to area growth of control spheroids. Data represent mean ± SEM. Using unpaired, two-tailed *t*-test analysis. MCF-7 $n = 3$; T47D $n = 3$; $^{***}P<0.005$ **(F)** Proteolytic activity of non-invasive breast cancer cells treated with rhCYR61 was asses by measurement of fluorescence 24 h after seeding cells on wells coated with FITC-labeled gelatin. Relative proteolytic activity of rhCYR61 treated cells was compared to proteolytic activity of control cells. Data represent mean ± SEM. Using unpaired, two-tailed *t*-test analysis. MCF-7 $n = 3$; T47D $n = 3$ $^{*}P < 0.05$.

cell in % compared to MCF-7-EMT control; $n = 36$; $P = 0.0321$; T47D-EMT S100A4^{-}:66.29 ± 8.52 SEM invaded cells in % to T47D-EMT control; $n = 36$; $P = 0.0303$; MDA-MB-231 S100A4^{-}:65.02 ± 5.58 SEM invaded cells in % to MDA-MB-231 control; $n = 24$; $P = 0.0003$; HCC1806 S100A4^{-}: 51.84 ± 4.62 invaded cells in % to HCC1806 control; $n = 36$; $P < 0.0001$). Furthermore, decreased S100A4 expression reduces 3D spheroid invasion area of mesenchymal transformed and TNBC cells (**Figure 2E**; MCF-7-EMT S100A4^{-}: 82.77 ± 2.82 SEM invaded area in % compared to MCF-7-EMT control; $n = 6$; $P = 0.0001$; T47D-EMT S100A4^{-}: 78.24 ± 4.17 SEM invaded area in % to T47D-EMT control; $n = 6$; $P = 0.0004$; MDA-MB-231 S100A4^{-}: 47.93 ± 7.95 SEM invaded area in % to MDA-MB-231 control; $n = 12$; $P < 0.0001$; HCC1806 S100A4^{-}: 67.97 ± 5.46 invaded area in % to HCC1806 control; $n = 6$; $P = 0.0002$), while proliferation was not altered (**Figure 2**, **Figure S3E**). To assess whether extracellular CYR61 can counteract the S100A4 suppressive effect on 3D spheroid invaded area, spheroids with suppressed S100A4 were treated with rhCYR61. Decreased S100A4 expression and additional increased extracellular CYR61 expression lead to an increased spheroid invaded area (**Figure 2F**; MCF-7-EMT S100A4^{-}+rhCYR61: 112.8 ± 4.97 SEM invaded area in % compared to MCF-7-EMT S100A4^{-}; $n = 4$; $P = 0.0415$; T47D-EMT S100A4^{-}+rhCYR61: 118.9 ± 4.36 SEM invaded area in % compared to T47D-EMT S100A4^{-}; $n = 6$; $P = 0.0015$; MDA-MB-231 S100A4^{-}+rhCYR61: 174.2 ± 33.83 invaded area in % compared to MDA-MB-231 S100A4^{-}; $n = 5$; $P = 0.0596$; HCC1806 S100A4^{-}+rhCYR61: 116.3 ± 6.85 invaded area in % compared to HCC1806 S100A4^{-}; $n = 6$; $P = 0.0383$). These data indicate a close correlation between CYR61 and S100A4 expression and the invasiveness of mesenchymal transformed and TNBC cells *in vitro*.

ERK1/2 Activity Is Transducer of CYR61 Mediated S100A4 Regulation

We found that decreased CYR61 resulted in a decreased S100A4 expression. Despite it remains elusive how CYR61 regulates S100A4 expression. To elucidate underlying intracellular mechanism we tested, whether decreased CYR61 expression reduces the phosphorylation of ERK1/2 thereby regulating S100A4 expression (**Figure 3A**). Mesenchymal transformed and TNBC cells shows a decreased ERK1/2 expression, while ERK1/2 phosphorylation was increased compared to non-invasive estrogen positive breast cancer cells (**Figure 3B**). Reducing CYR61 expression led to a decreased ERK1/2 phosphorylation (**Figure 3C**). MEK1 and MEK2 are upstream regulators of ERK1/2 activity (28) By using U0126 inhibitor, ERK phosphorylation can be diminished (29). Blocking ERK1/2 phosphorylation due to an MEK1 and MEK2 specific inhibitor U0126 (verification of U0126 induced blocking of ERK1/2 phosphorylation **Figure 3**, **Figure S4A**) resulted in a decreased S100A4 expression (**Figure 3D**; MCF-7-EMT U0126: 0.89 ± 0.02 SEM relative S100A4 expression compared to MCF-7-EMT DMSO; $n = 3$; $P = 0.0114$; T47D-EMT U0126: 0.38 ± 0.07 SEM relative S100A4 expression compared to T47D-EMT DMSO control; $n = 3$; $P = 0.0009$; MDA-MB-231 U0126: 0.85 ±0.02 SEM relative S100A4 expression compared to MDA-MB-231 DMSO; $n = 3$; $P = 0.0026$; HCC1806 U0126: 0.71 ± 0.06 SEM relative S100A4 expression compared to HCC1806 DMSO; $n = 3$; $P = 0.0076$). Furthermore, U0126 treatment reduced 3 D spheroid invaded area (**Figure 3E**; MCF-7-EMR U0126: 47.52 ± 5.77 SEM invaded area in % compared to MCF-7-EMT DMSO; $n = 6$; $P < 0.0001$; T47D-EMT U0126: 71.51 ± 2.61 SEM invaded area in % compared to T47D-EMT DMSO; $n = 5$; $P < 0.0001$; MDA-MB-231 U0126: 35.31 ± 10.91 SEM invaded area in % compared to MDA-MB-231 DMSO; $n = 6$; $P = 0.0002$; HCC1806 U0126: 85.01 ± 4.05 SEM invaded area in % compared to HCC1806 DMSO; $n = 5$; $P = 0.006$). Treatment with U0126 reduced proliferation in 3D spheroids (**Figure 3F**; MCF-7-EMT U0126: 86.57 ± 2.11 SEM relative AlamarBlue reduction in % compared to MCF-7-EMT DMSO; $n = 3$; $P = 0.0031$; T47D-EMT U0126: 67.53 ± 8.61 SEM relative AlamarBlue reduction compared to T47D-EMT DMSO; $n = 4$; $P = 0.0093$; MDA-MB-231 U0126:52.23 ± 13.32 SEM relative AlamarBlue reduction in % compared to MDA-MB-231 DMSO; $n = 3$; $P = 0.023$; HCC1806 U0126: 70.37 ± 9.29 SEM relative AlamarBlue reduction in % compared to HCC1806 DMSO; $n = 3$; $P = 0.0332$). Moreover, treating non-invasive estrogen positive breast cancer cell spheroids with rhCYR61 lead to increased ERK1/2 phosphorylation (**Figure 3**, **Figure S4B**). These results suggest that decreased ERK1/2 phosphorylation suppresses S100A4 expression. Moreover, ERK1/2 phosphorylation is reduced by decreased CYR61 expression.

Suppression of YAP1 Reduces Invasiveness Through Altering CYR61-S100A4-pERK1/2 Signaling

Yes-associated protein (YAP) is a known upstream target of CYR61 in breast cancer (30). Validating that the observed results can be reproduced by altering YAP expression (**Figure 4A**), YAP was transiently decreased (verification **Figure 4**, **Figure S5A**). Decreased YAP expression reduced invaded area of 3 D spheroids

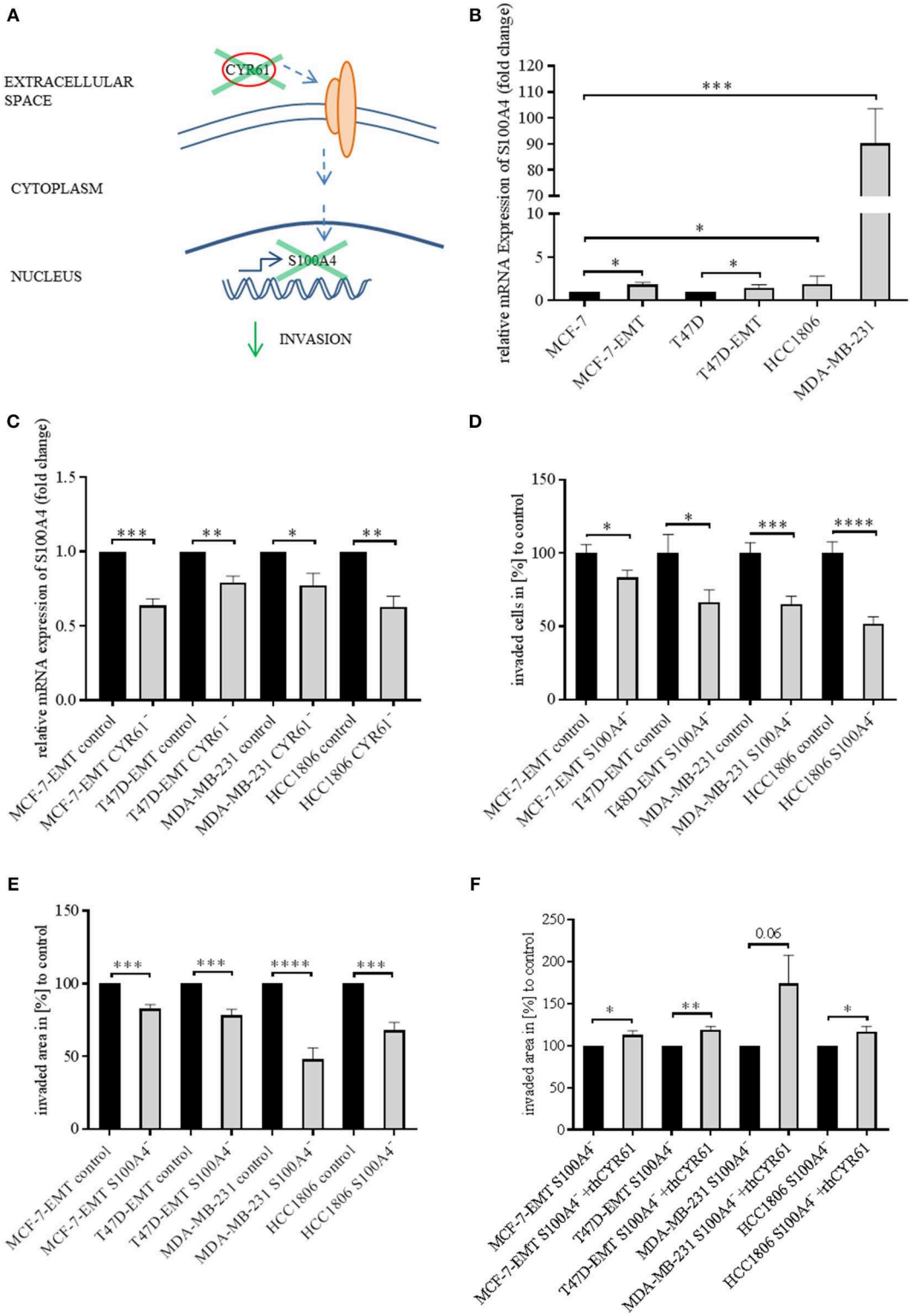

FIGURE 2 | Suppression of CYR61 reduces S100A4 expression. **(A)** Scheme illustrating hypothesis of CYR61-dependent cell invasion regulation. **(B)** Relative S100A4 expression of invasive breast cancer cell lines compared to non-invasive controls. Data represent mean ± SEM. Using unpaired, two-tailed *t*-test analysis. MCF-7-EMT $n = 5$; T47D-EMT $n = 5$; MDA-MB-231 $n = 4$; HCC1806 $n = 6$; $^{*}P < 0.05$; $^{***}P < 0.005$ **(C)** Relative S100A4 expression of invasive breast cancer cell lines 96 h after transient CYR61 transfection compared to non-invasive controls. Data represent mean ± SEM. Using unpaired, two-tailed *t*-test analysis. MCF-7-EMT

(Continued)

FIGURE 2 | $n = 4$; T47D-EMT $n = 3$; MDA-MB-231 $n = 4$; HCC1806 $n = 3$; $^{*}P < 0.05$; $^{**}P < 0.01$; $^{***}P < 0.005$ **(D)** 2D Invasion analysis of co-cultured (MG-63, osteosarcoma cells) breast cancer cells transient transfected with S100A4 siRNA for 96 h. Percentage of cell invasion compared to controls was assessed by counting invaded cells under the filter in 4 random filter regions. Data represent mean ± SEM. MCF-7-EMT $n = 36$; T47D-EMT $n = 36$; MDA-MB-231 $n = 24$; HCC1806 $n = 36$; $^{*}P < 0.05$; $^{***}P < 0.005$; $^{****}P < 0.0001$ **(E)** 3D invasion analysis of breast cancer spheroids seeded after transient siRNA transfection. Spheroid area was assessed 48 h after adding Matrigel using polygonal selection and compared to spheroid area at time point 0 (adding of Matrigel). Area growth was compared to area growth of control spheroids. Data represent mean ± SEM. Using unpaired, two-tailed *t*-test analysis. MCF-7-EMT $n = 6$; T47D-EMT $n = 6$; MDA-MB-231 $n = 12$; HCC1806 $n = 6$; $^{***}P < 0.005$; $^{****}P < 0.0001$ **(F)** 3D invasion analysis of breast cancer spheroids seeded after transient S100A4 siRNA transfection and treated with rhCYR61. Spheroid area was assessed 48 h after adding Matrigel and rhCYR61 using polygonal selection and compared to spheroid area at time point 0 (adding of Matrigel + rhCYR61). Area growth was compared to area growth of S100A4- spheroids. Data represent mean ± SEM. Using unpaired, two-tailed *t*-test analysis. MCF-7-EMT $n = 4$; T47D-EMT $n = 4$; MDA-MB-231 $n = 5$; HCC1806 $n = 6$; $^{*}P < 0.05$; $^{**}P < 0.001$.

(**Figure 4B**; MCF-7-EMT YAP^{-}:87.48 ± 3.84 SEM invaded area in % compared to MCF-7-EMT control; $n = 4$; $P = 0.0172$; T47D-EMT YAP^{-}: 76.23 ± 5.1 SEM invaded area in % compared to T47D-EMT control; $n = 5$; $P = 0.0016$; MDA-MB-231 YAP^{-}: 47 ± 12.39 SEM invaded area in % compared to MDA-MB-231 control; $n = 12$; $P = 0.0003$; HCC1806 YAP^{-}: 60.67 ± 7.38 SEM invaded area in % compared to HCC1806 control), while proliferation was not altered (**Figure 4**, **Figure S5B**). Decreased YAP expression reduces CYR61 expression (**Figure 4C**; MCF-7-EMT YAP^{-}: 0.79 ± 0.05 SEM relative CYR61 expression compared to MCF-7-EMT control; $n = 3$; $P = 0.01$; T47D-EMT YAP^{-}: 0.82 ± 0.05 SEM relative CYR61 expression compared to T47D-EMT control; $n = 3$; $P = 0.0269$; MDA-MB-231 YAP^{-}: 0.74 ± 0.03 SEM relative CYR61 expression compared to MDA-MB-231 control; $n = 3$; $P = 0.0008$; HCC1806 YAP^{-}: 0.54 ± 0.12 SEM relative CYR61 expression compared to HCC1806 control; $n = 3$; $P = 0.0198$) and S100A4 expression (**Figure 4D**; MCF-7-EMT YAP^{-}: 0.86 ± 0.04 SEM relative S100A4 expression compared to MCF-7-EMT control; $n = 3$; $P = 0.0362$; T47D-EMT YAP^{-}: 0.72 ± 0.08 SEM relative S100A4 expression compared to T47D-EMT control; $n = 3$; $P = 0.0289$; MDA-MB-231 YAP^{-}: 0.88 ± 0.03 SEM relative S100A4 expression compared to MDA-MB-231 control; $n = 3$; $P = 0.0179$; HCC1806 YAP^{-}: 0.78 ± 0.04 SEM relative S100A4 expression compared to HCC1806 control; $n = 3$; $P = 0.0067$). Furthermore, decreased YAP expression reduces ERK1/2 phosphorylation (**Figure 4E**). Transient decreased YAP expression in mesenchymal transformed and TNBC cells treated with rhCYR61 show no impact on spheroid invaded area (**Figure 4F**). Collectively, these data suggest that decreased YAP expression leads to a CYR61, pERK1/2 and S100A4 suppression. The effect of decreased YAP expression on spheroid invaded area can be restored be supplemented extracellular CYR61.

CYR61 and S100A4 as Prognostic Markers for Invasive and Metastatic Breast Cancer

To assess the value of CYR61 and S100A4 as prognostic marker meta-analysis were conducted. Reduced CYR61 expression increases the probability of distant-metastasis free survival (DMFS) of breast cancer patients with a lymph node positive status (**Figure 5A**; dataset 213226_at; $n = 382$; FDR 1%; $P = 2.8\ e^{-07}$). Reduced S100A4 expression increases the probability of DMFS of breast cancer patients with a lymph node positive status but shows a higher FDR (**Figure 5B**; dataset 203186_s_at; $n = 382$; FDR > 50%; $P = 0.024$, cut-off values see **Figure 5**, **Figure S6**). Analyzing the effects of decreases CYR61 or S100A4 expression with regards to the relapse free survival (RFS) shows comparable results (**Figures 5C,D**; CYR61: dataset 213226_at; $n = 1133$; FDR 1%; $P = 6.8\ e^{-09}$; S100A4: dataset 203186_s_at; FDR > 50%; $P = 0.0012$, cut-off values see **Figure 5**, **Figure S6**). These data demonstrate that CYR61 could act as a prognostic marker in breast cancer.

CYR61 and S100A4 as Therapeutic Target for Invasive and Metastatic Breast Cancer

CYR61 and S100A4 are drivers for breast cancer cell invasion *in vitro*. Consequently, we examined the value of CYR61 and/or S100A4 as a potential therapeutic target for advanced breast cancer. Analyzing the expression in 239 paraffin-fixed patient breast tissue sections (104 invasive breast cancer sections with corresponding metastatic lymph node section and progesterone receptor-, estrogen receptor- and Her2neu expression, BR20837; 17 invasive ductal,1 medullary carcinoma and 6 normal breast tissue sections, BR248a; 2 invasive ductal carcinomas, 1 invasive lobular carcinoma and 2 normal breast tissue section, T087a). Analyzing if expression was detected (immunofluorescence signal for CYR61 and/or S100A4 1-5 spots +; 5-10 spots ++; >10 spots + + +) or not (−), we find the following pattern: 90.2% of invasive ductal carcinomas were positive for CYR61 expression, 82% were positive for S100A4 expression and 78% showed both CYR61 and S100A4 expression (**Figure 6A** and **Figure S7**). Corresponding metastatic lymph node sections were in 96% positive for CYR61, in 75% positive for S100A4 and in 74% for both CYR61 and S100A4. TNBC tissue sections were in 97% positive for CYR61, in 75.8% positive for S100A4, and in 75.8% expressing both CYR61 and S100A4. Interestingly, CYR61 expression was only detected in 12.5% of normal breast tissue samples and S100A4 expression in none (**Figure 6D**, detailed list **Figure S7**). Visual expression of CYR61 and S100A4 in blood vessels (**Figure 6D**) could be found throughout all tissue sections. We find that the CYR61 and S100A4 expression appeared in very close localization to each other (**Figure 6**, white arrows) or even co-localized (**Figure 6**, white stars). These studies demonstrate that CYR61 and S100A4 could be valuable therapeutic targets and prognostic marker for invasive breast cancer and metastasis.

DISCUSSION

CYR61 is best recognized as regulator of inflammation and wound healing (31, 32). Several studies indicate that CYR61 can facilitate invasion and is crucial for EMT programs regarding

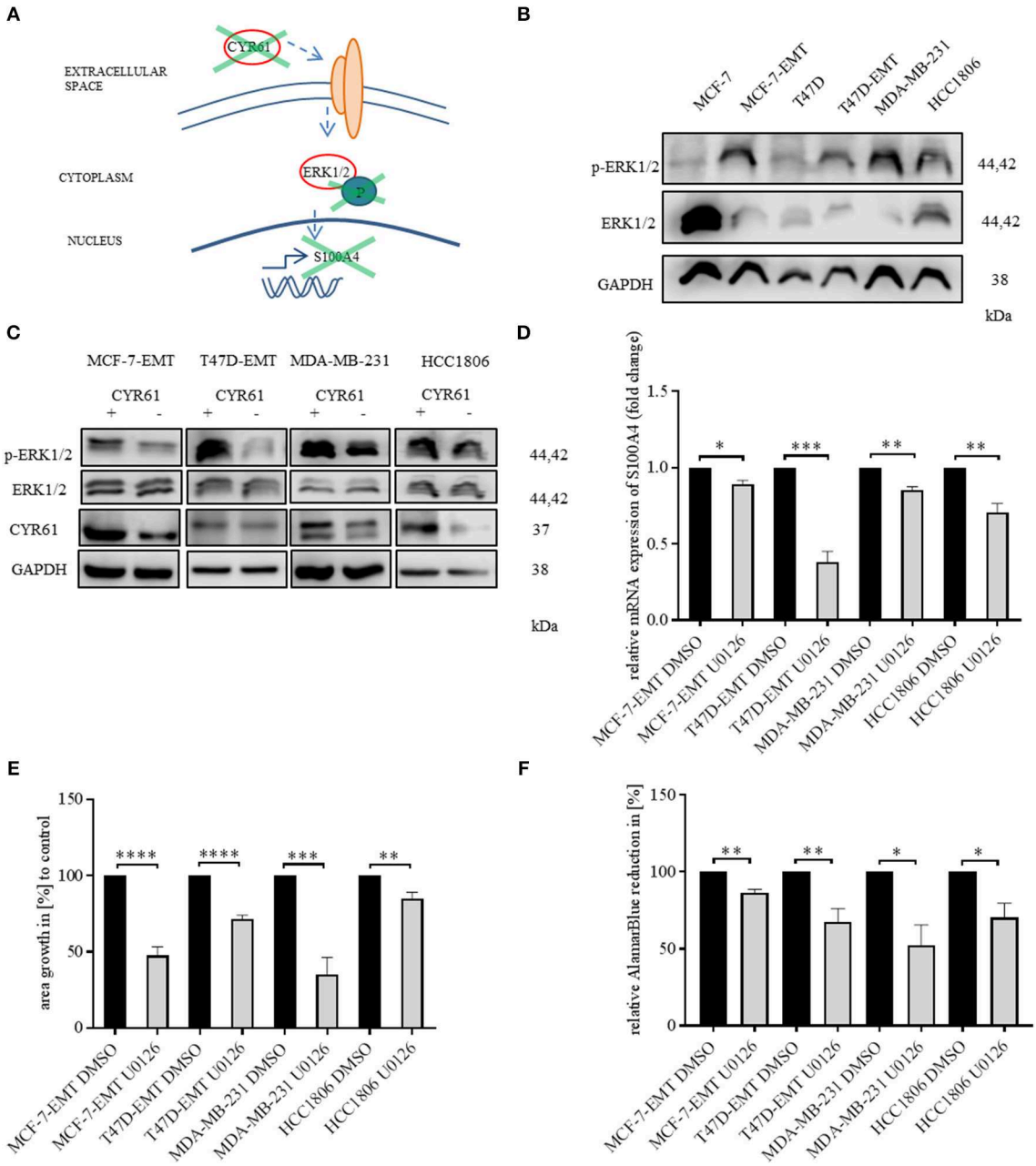

FIGURE 3 | ERK1/2 activity is transducer of CYR61 mediated S100A4 regulation. **(A)** Scheme illustrating hypothesis of CYR61 regulating S100A4 in a p-ERK1/2 dependent manner. **(B)** ERK1/2 and p-Erk1/2 (Thr202/Tyr204) expression in different breast cancer cell lines detected by western blotting. **(C)** ERK1/2 and p-Erk1/2 (Thr202/Tyr204) and CYR61 expression in different breast cancer cell lines after transient CYR61 transfection detected by western blotting. **(D)** Relative S100A4 expression of invasive breast cancer cell lines treated with 10 μM U0126 compared to DMSO controls. Data represent mean ± SEM. Using unpaired, two-tailed *t*-test analysis. $n = 3$; $^{*}P < 0.05$; $^{**}P < 0.01$; $^{***}P < 0.005$ **(E)** 3D invasion analysis of breast cancer spheroids seeded after U0126 treatment. Spheroid area was assessed 48 h after adding Matrigel using polygonal selection and compared to spheroid area at time point 0 (adding of Matrigel + 10 μM U0126). Area growth was compared to area growth of control spheroids. Data represent mean ± SEM. Using unpaired, two-tailed *t*-test analysis. MCF-7-EMT $n = 6$; T47D-EMT $n = 5$; MDA-MB-231 $n = 6$; HCC1806 $n = 5$; $^{**}P < 0.01$; $^{***}P < 0.005$; $^{****}P < 0.0001$ **(F)** Analysis of relative AlamarBlue reduction as indicator for cell viability. Breast cancer cell spheroids were grown and AlamarBlue reduction was assessed 48 h after adding Matrigel and 10 μM U0126 at 4 h incubation. Relative AlamarBlue reduction was calculated compared to DMSO control spheroids. Data represent mean ± SEM. MCF-7-EMT $n = 3$; T47D-EMT $n = 4$; MDA-MB-231 $n = 3$; HCC1806 $n = 3$; $^{*}P < 0.05$; $^{**}P < 0.01$.

cancer progression (12, 15, 16, 23). The question remains how CYR61 facilitates invasion in breast cancer and which role it possesses regarding EMT complexity (4). Since CYR61 has known oncogenic functions in serval tumor entities (12, 13), including breast cancer (15, 16), the question appeared if CYR61 might be a valuable therapeutic target in aggressive breast cancer

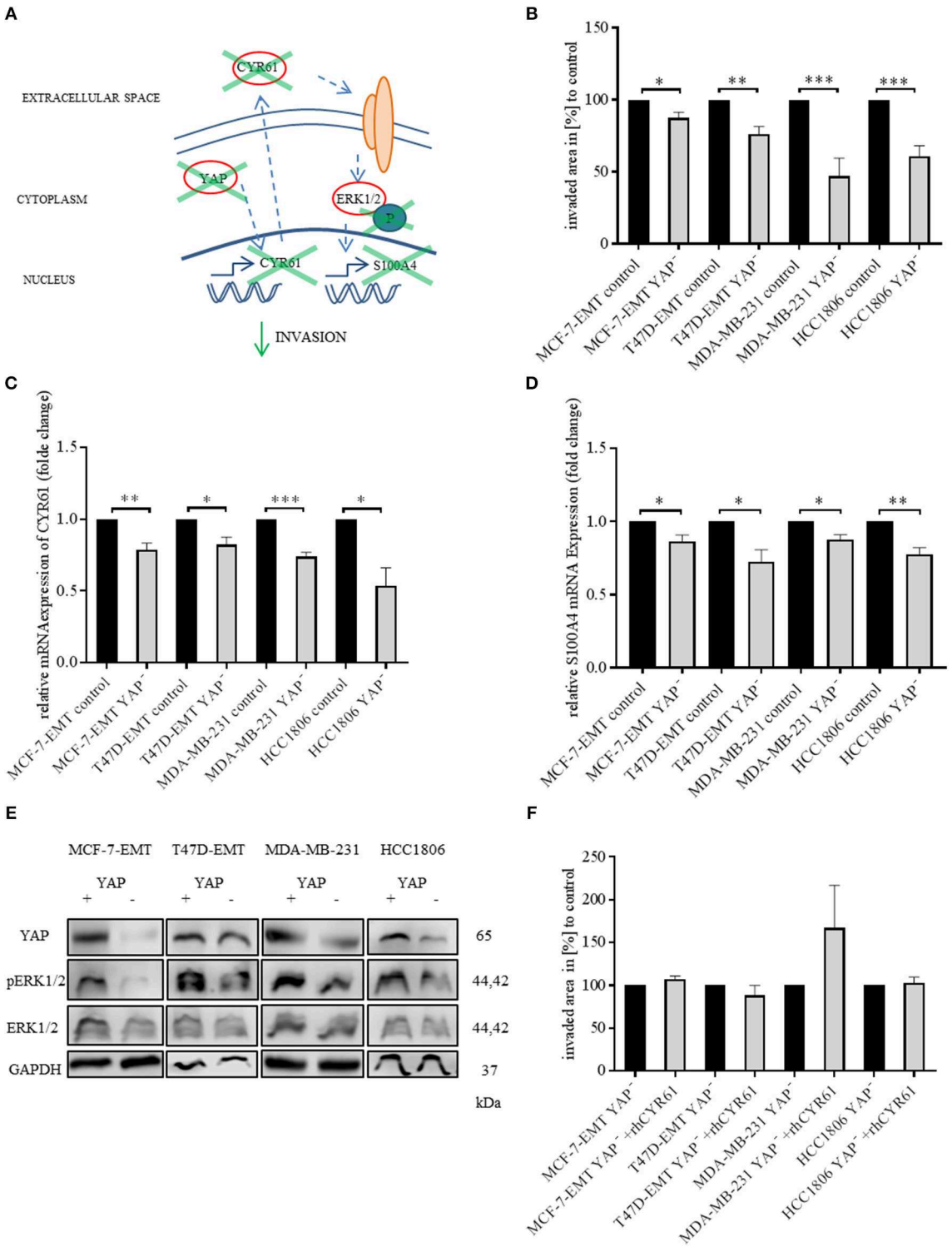

FIGURE 4 | Suppression of YAP reduces invasiveness through blocking CYR61-S100A4-pERK1/2 signaling. **(A)** Scheme illustrating hypothesis of YAP regulating S100A4 in a CYR61 - p-ERK1/2 dependent manner. **(B)** 3D invasion analysis of breast cancer spheroids seeded after transient YAP siRNA transfection. Spheroid area was assessed 48 h after adding Matrigel using polygonal selection and compared to spheroid area at time point 0 (adding of Matrigel). Area growth was compared to area growth of control spheroids. Data represent mean ± SEM. Using unpaired, two-tailed *t*-test analysis. MCF-7-EMT $n = 4$; T47D-EMT $n = 5$; MDA-MB-231 $n = 12$; HCC1806 $n = 8$; $^{*}P < 0.05$; $^{**}P < 0.01$; $^{***}P < 0.005$ **(C)** Relative CYR61 expression of invasive breast cancer cell lines 48 h after transient YAP siRNA compared to controls. Data represent mean ± SEM. Using unpaired, two-tailed *t*-test analysis. $n = 3$; $^{*}P < 0.05$; $^{**}P < 0.01$; $^{***}P < 0.005$ **(D)** Relative S100A4 expression of invasive breast cancer cell lines 48 h after transient YAP siRNA compared to controls. Data represent mean ± SEM. Using unpaired, two-tailed *t*-test analysis.

(Continued)

FIGURE 4 | $n = 3$; $^{*}P < 0.05$; $^{**}P < 0.01$; **(E)** ERK1/2, p-Erk1/2 (Thr202/Tyr204) and YAP expression in different breast cancer cell lines after transient YAP siRNA transfection detected by western blotting. **(F)** 3D invasion analysis of breast cancer spheroids seeded after transient YAP siRNA transfection and treated with rhCYR61. Spheroid area was assessed 48 h after adding Matrigel and rhCYR61 using polygonal selection and compared to spheroid area at time point 0 (adding of Matrigel + rhCYR61). Area growth was compared to area growth of YAP- spheroids. Data represent mean ± SEM. Using unpaired, two-tailed *t*-test analysis. MCF-7-EMT $n = 6$; T47D-EMT $n = 6$; MDA-MB-231 $n = 4$; HCC1806 $n = 6$.

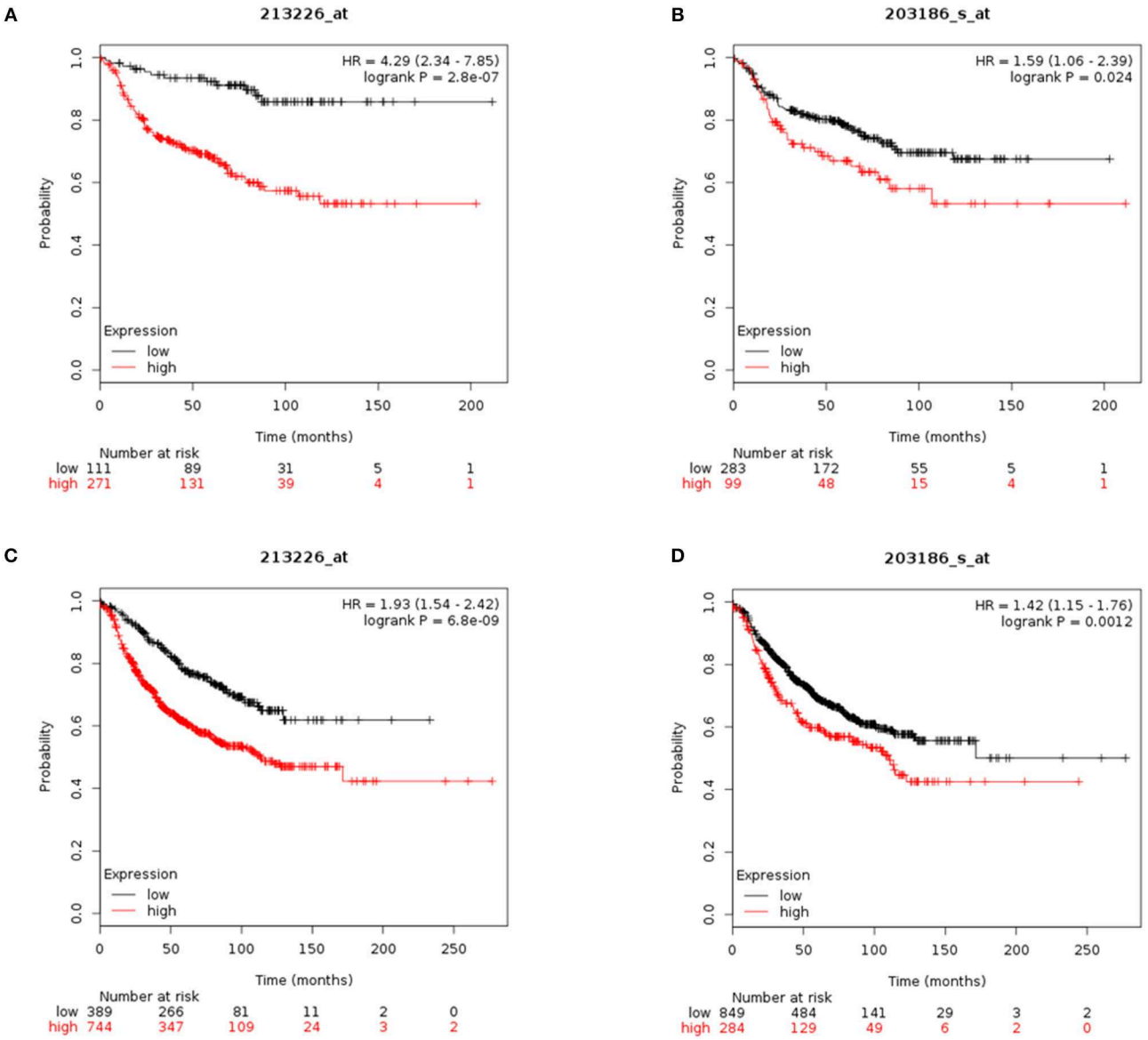

FIGURE 5 | CYR61 and S100A4 as prognostic marker for breast cancer progression. **(A)** Probability of distant metastasis free survival (DMFS) in 382 breast cancer patients with lymph node positive status according to CYR61expression level. Kaplan–Meier plots were generated using Kaplan–Meier plotter (www.kmplot.com) data set 213226_at with a false-discovery rate (FDR) of 1%. Black line illustrates high CYR61 expression group and red line illustrates low CYR61 expression group. **(B)** Probability of DMFS in 382 breast cancer patients with lymph node positive status according to S100A4 expression level. Kaplan–Meier plots were generated using Kaplan–Meier plotter (www.kmplot.com) data set 203186_at with a false-discovery rate (FDR) over 50%. Black line illustrates high S100A4 expression group and red line illustrates low S100A4 expression group. **(C)** Probability of remission free survival (RFS) in 1133 breast cancer patients with lymph node positive status according to CYR61 expression level. Kaplan–Meier plots were generated using Kaplan–Meier plotter (www.kmplot.com) data set 213226_at with a false-discovery rate (FDR) of 1%. Black line illustrates high CYR61 expression group and red line illustrates low CYR61 expression group. **(D)** Probability of RFS in 1133 breast cancer patients with lymph node positive status according to CYR61 expression level. Kaplan–Meier plots were generated using Kaplan–Meier plotter (www.kmplot.com) data set 203186_at with a false-discovery rate (FDR) over 50 %. Black line illustrates high S100A4 expression group and red line illustrates low S100A4 expression group. HR, hazard ratio.

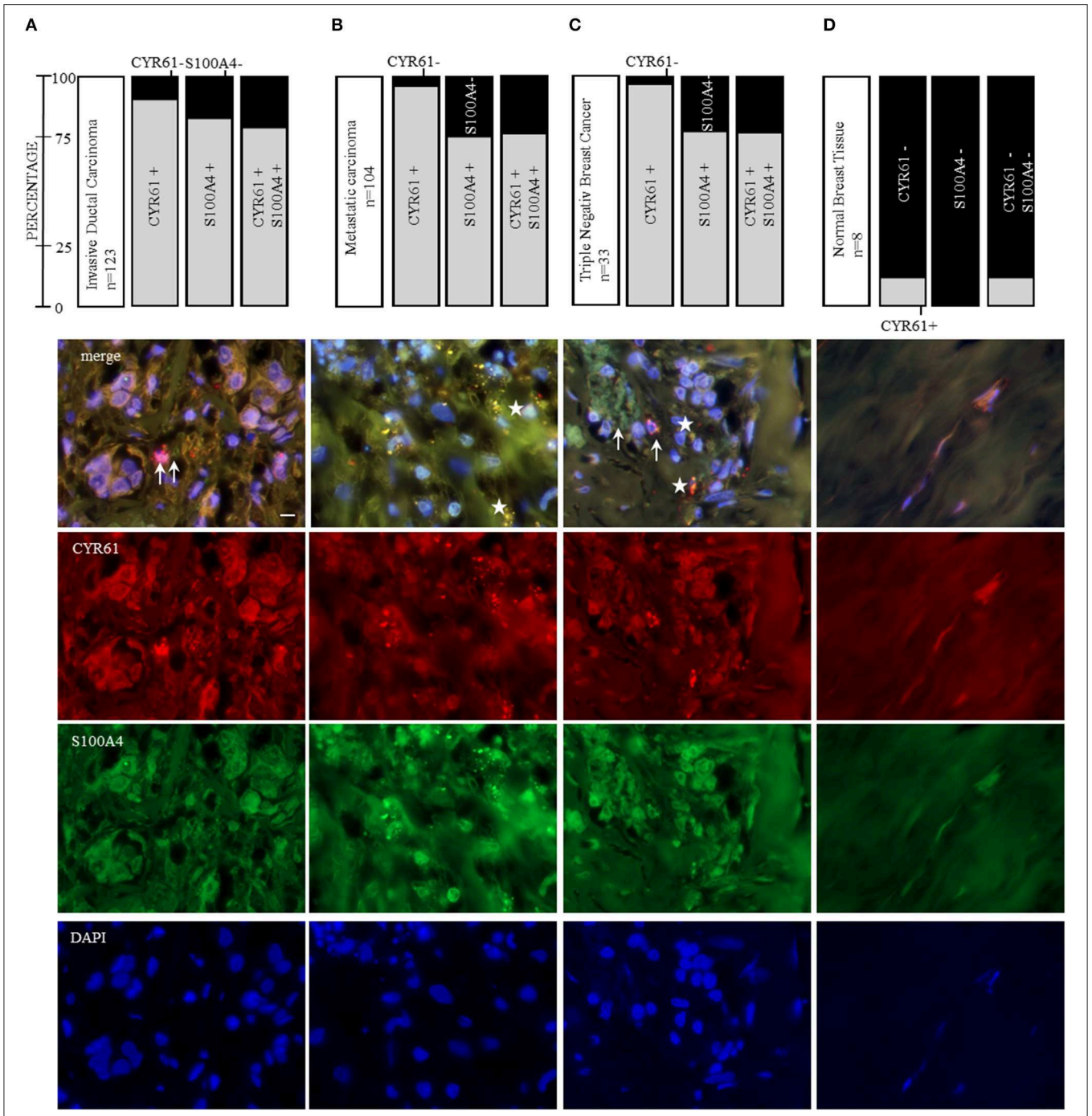

FIGURE 6 | CYR61 and S100A4 as therapeutic target for invasive and metastatic breast cancer. Immunofluorescence staining of three tissue arrays (biomax) containing 104 invasive ductal carcinoma tissue sections with corresponding metastatic carcinomas, further 21 invasive ductal carcinoma tissue sections and 8 normal breast tissue sections. With 33 of the carcinoma tissue sections being negative for the estrogen receptor and progesterone receptor and do not overexpress the Her2neu receptor (triple negative breast cancer, TNBC). **(A)** CYR61 and/or S100A4 expression analysis in 123 invasive ductal carcinoma tissue sections and corresponding lymph node sections from 104 patients **(B)** and representative immunofluorescence staining analyzed with a 100x oil objective (Axio ZEISS). **(C)** Within the 123 invasive ductal carcinomas patient tissue sections 33 were stated as being TNBC. **(D)** Normal breast tissue sections ($n = 8$) were analyzed for their CYR61 and/ or S100A4 expression using immunofluorescence staining. Scale bar gauges 20 μm.

and if it could be a prognostic marker for these indications. We report that a higher CYR61 expression correlates with a poor prognosis of breast cancer patients. Moreover, we found that reducing the CYR61 expression leads to a decreased invasion in 2D and 3D invasion analysis setups, showing comparable results. Suggesting that reduced invasion upon CYR61 suppression is

due to reduces ERK1/2 phosphorylation and S100A4 expression. CYR61 might be a valuable therapeutic target and prognostic marker for invasive and metastatic breast cancer.

Triple negative breast cancers (TNBC) account for 15–20% of all breast cancer incidents and there is no specific targeted therapy available (33). There is a need for identifying new targets for future therapy options. Consistent with previous published results we could demonstrate that CYR61 expression is increased in TNBC cell line MDA-MB-231 (34) and further more in the TNBC cell line HCC1806. The contribution of EMT-induced expression changes to the invasion and metastatic cascade regarding cancer progression is highly debated and needs to be interpreted cell and tissue specific (4, 8, 35). Mesenchymal transformed breast cancer cells show an increased expression of CYR61 and S100A4 (23), which we could reproduce in our setting. It was shown that S100A4 facilitates breast cancer invasion (36). Gründker et al. demonstrated that suppressing extracellular signaling of CYR61 and S100A4 decreased the ability of breast cancer cell invasion in a co-cultural setting mimicking bone metastasis (23). It was not tested how the intracellular signaling is affected when CYR61 or S100A4 expression is reduced. We report here that transient gene silencing of either CYR61 or S100A4 can reduce invasiveness in mesenchymal transformed and TNBC cells. To further assess the impact of CYR61 on breast cancer cell invasion we increased extracellular CYR61 expression in non-invasive breast cancer cells and could show that this led to an increased invasive behavior. These findings indicate that CYR61 could be a regulator of breast cancer cells invasion. We showed that reversing EMT-induced upregulation of CYR61 and S100A4 leads to reduced invasive behavior in breast cancer cells in different invasion setups. This could indicate a role of EMT within this process. Further research is necessary to assess, if modulating CYR61 regulates EMT-TFs and thereby facilitates cellular plasticity. It has been suggested that targeting EMT-TFs could help to overcome chemo resistance and recent findings suggest an involvement of CYR61 in resistance to certain therapies in different tumor entities (5, 37, 38).

Despite, it was unclear how CYR61 regulates invasiveness of breast cancer cells. We suggest that CYR61 regulates S100A4 expression in mesenchymal transformed and TNBC cells through regulating ERK1/2 phosphorylation. Reducing S100A4 expression leads to decreased 3 D spheroid invasion and invasiveness of breast cancer cells in co-culture with osteosarcoma cells. Adding extracellular CYR61 to breast cancer spheroids with transient decreased S100A4 expression could restore the effect und led to a slightly increased invaded area. Hou et al. suggested that regulating CYR61 in osteosarcoma cells targets the MEK-ERK pathway (12). ERK1/2 signaling is gaining higher interest since the unique ERK1/2 position within cellular signaling. Targeting ERK1/2 could be valuable for therapy-resistant cancer to known clinically used BRAF and MEK inhibitors (39). We could show that inhibition of ERK1/2 phosphorylation led to decreased 3D spheroid invasion and reduced spheroid proliferation. Inhibition of ERK1/2 phosphorylation led to decreased S100A4 expression. But S100A4 decreased expression by itself had no impact on spheroid proliferation, neither had CYR61 or YAP transient suppression.

YAP is regulated negatively through the Hippo-Pathway, which regulates key events of organ size, development and angiogenesis (40–42). Regarding breast cancer YAP is reported to have dual function as oncogene and tumor suppressor (43). Higher YAP expression correlates with increased EMT marker expression (44). We suggest that reduced YAP expression leads to decreased 3D spheroid invasion by suppression of CYR61, p-ERK1/2 and S100A4. The effect of reduced YAP expression on 3D invasion could be restored by extracellular CYR61 addition.

CYR61 or S100A4 are suggested to be valuable prognostic markers regarding several tumor entities (45–48). Egeland et al. suggested the use of S100A4 as a prognostic marker for early-stage breast cancer (49). We examined whether CYR61 and S100A4 could be valuable prognostic marker for invasive and metastatic breast cancer. CYR61 and S100A4 are highly expressed in invasive-ductal carcinomas, including TNBC, and both are expressed in metastatic lymph node sections. Of all analyzed tissue sections 82.2% expressing CYR61 did express S100A4, respectively, which lead to the conclusion, that CYR61 together with S100A4 would be valuable prognostic marker for breast cancer and breast cancer metastasis. Moreover, we found that expression of CYR61 and S100A4 is closely located (**Figure 6**, indicated by arrow) or even co-localized (**Figure 6**, indicated by star). Considering that CYR61 regulates cancer invasion and the findings, that it may be a valuable prognostic marker in different cancer entities (45, 46, 50, 51), It was suggested before, that CYR61 regulates E-cadherin, N-cadherin and Twist in osteosarcoma cells (12). Further investigations should clarify if CYR61 suppression regulates EMT-TFs in breast cancer and facilitates invasion by altering ECM degradation and adhesion. Secretome analysis of co-cultured cancer cells could identify secreted proteins, like matricellular proteins, that are drivers for invasion and promote metastasis.

Our findings suggest that CYR61 plays a major role in breast cancer invasion. This impact is facilitated through the regulation of ERK phosphorylation and S100A4 expression. Moreover, targeting YAP, a CYR61 upstream regulator, regulates CYR61, ERK phosphorylation and S100A4. We could identify a close correlation between CYR61 and S100A4 expression and breast cancer invasion and metastasis in breast cancer patients. CYR61 together with S100A4 might be utilized as therapeutic target and prognostic marker for invasive breast cancer and metastasis.

DATA AVAILABILITY STATEMENT

The datasets used and/or analyzed during the current study are available from the corresponding author on reasonable request.

AUTHOR CONTRIBUTIONS

Conception and design of the reported work was done by JH and CG. JH, GB, and CG did the development of methodology used. JH and SH performed invasion assays. JH and LG

contributed to protein expression analysis. JH contributed to immune histochemical staining, gene expression analysis, proliferation analysis, *in silico* and network analysis. Analysis and interpretation of data was performed by JH, SH, LG, GB, GE, and CG. All authors read and approved the final manuscript.

FUNDING

Research reported in this publication was supported, by the Deutsche Krebshilfe grant 70112534.

ACKNOWLEDGMENTS

We would like to thank Sonja Blume for her excellent technical assistance. The group of Dr. Florian Wegwitz for fruitful discussions. Moreover, we appreciate the valuable suggestions of the reviewers.

SUPPLEMENTARY MATERIAL

The Supplementary Material for this article can be found online at: https://www.frontiersin.org/articles/10.3389/fonc.2019.01074/full#supplementary-material

Figure S1 | CYR61 expression correlates with breast cancer cell invasiveness. **(A)** Relative transforming growth factor beta induced (TGFBI) expression of mesenchymal transformed breast cancer cell lines compared to non-invasive controls was assessed using real-time quantitative PCR. Data represent mean ± SEM. Using unpaired, two-tailed *t*-test analysis. MCF-7-EMT $n = 3$; T47D-EMT $n = 6$; $^{***}P < 0.0005$; $^{****}P < 0.0001$ **(B)** Relative E-cadherin expression of mesenchymal transformed breast cancer cell lines compared to non-invasive controls was assessed using real-time quantitative PCR. Data represent mean ± SEM. Using unpaired, two-tailed *t*-test analysis. MCF-7-EMT $n = 4$; T47D-EMT $n = 3$; $^{*}P < 0.05$; $^{****}P < 0.0001$ **(C)** Relative Vimentin expression of mesenchymal transformed breast cancer cell lines compared to non-invasive controls was assessed using real-time quantitative PCR. Data represent mean ± SEM. Using unpaired, two-tailed *t*-test analysis. MCF-7-EMT $n = 5$; T47D-EMT $n = 3$; $^{*}P < 0.05$ **(D)** Relative Zeb1 expression of mesenchymal transformed breast cancer cell lines compared to non-invasive controls was assessed using real-time quantitative PCR. Data represent mean ± SEM. Using unpaired, two-tailed *t*-test analysis. MCF-7-EMT $n = 4$; T47D-EMT $n = 3$; $^{*}P < 0.05$ **(E)** Relative SNAI1 expression of mesenchymal transformed breast cancer cell lines compared to non-invasive controls was assessed using real-time quantitative PCR. Data represent mean ± SEM. Using unpaired, two-tailed *t*-test analysis. MCF-7-EMT $n = 4$; T47D-EMT $n = 5$; $^{***}P < 0.0005$ **(F)** Relative SNAI2 expression of mesenchymal transformed breast cancer cell lines compared to non-invasive controls was assessed using real-time quantitative PCR. Data represent mean ± SEM. Using unpaired, two-tailed *t*-test analysis. MCF-7-EMT $n = 3$; T47D-EMT $n = 4$; $^{*}P < 0.05$.

Figure S2 | CYR61 expression correlates with breast cancer cell invasiveness. **(A)** Relative CYR61 expression 96 h after transient CYR61 siRNA transfection compared to control was assessed using real-time quantitative PCR. Data represent mean ± SEM. Using unpaired, two-tailed *t*-test analysis. MCF-7-EMT $n = 8$; T47D-EMT $n = 7$; MDA-MB-231 $n = 3$; HCC1806 $n = 4$; $^{**}P < 0.01$; $^{***}P < 0.0001$ **(B)** Analysis of relative AlamarBlue reduction as indicator for cell viability. Transient transfected breast cancer cell spheroids were grown and AlamarBlue reduction was assessed 48 hours after adding Matrigel at 4 h incubation. Relative AlamarBlue reduction was calculated compared to control spheroids. Data represent mean ± SEM. $n = 3$ **(C)** Analysis of relative AlamarBlue reduction as indicator for cell viability. Breast cancer cell spheroids were grown and AlamarBlue reduction was assessed 48 h after adding Matrigel and 1μg/ml rhCYR61 at 4 h incubation. Relative AlamarBlue reduction was calculated compared to control spheroids. Data represent mean ± SEM. $n = 3$.

Figure S3 | Suppression of CYR61 reduces S100A4 expression. **(A)** Immunoblot analysis of S100A4 mRNA expression levels in different breast cancer cell lines 96 h after S100A4 siRNA transfection was detected using western blotting. Date represent mean ± SEM. Using unpaired, two-tailed *t*-test analysis. MCF-7-EMT $n = 4$; T47D-EMT $n = 4$; MDA-MB-231 $n = 3$; HCC1806 $n = 3$; $^{*}P < 0.05$; $^{**}P < 0.01$; $^{***}P < 0.005$ **(B)** Representative experiments of S100A4 protein expression quantification corresponding to **(A)**. **(C)** S100A4 mRNA expression analysis 96 h after siRNA transfection using quantitative PCR. Date represent mean ± SEM. Using unpaired, two-tailed *t*-test analysis. MCF-7-EMT $n = 4$; T47D-EMT $n = 4$; MDA-MB-231 $n = 3$; HCC1806 $n = 3$; $^{***}P<0.005$; $^{****}P<0.0001$ **(D)** CYR61 mRNA expression analysis 96 h after S100A4 siRNA transfection using quantitative PCR. Date represent mean ± SEM. MCF-7-EMT $n = 5$; T47D-EMT $n = 6$; MDA-MB-231 $n = 3$; HCC1806 $n = 3$ **(E)** Analysis of relative AlamarBlue reduction as indicator for cell viability. Breast cancer cell spheroids transient transfected with S100A4 siRNA were grown and AlamarBlue reduction was assessed 48 h after adding Matrigel at 4 h incubation. Relative AlamarBlue reduction was calculated compared to control spheroids. Data represent mean ± SEM. $n = 3$.

Figure S4 | ERK1/2 activity is transducer of CYR61 mediated S100A4 regulation. **(A)** ERK1/2 and p-Erk1/2 (Thr202/Tyr204) expression in different breast cancer cell lines with or without 10μM U0126 treatment detected by western blotting. **(B)** ERK1/2 and p-Erk1/2 (Thr202/Tyr204) expression in non-invasive breast cancer cell lines with or without 1μg/ml rhCYR61 treatment detected by western blotting.

Figure S5 | Suppression of YAP reduces invasiveness through blocking CYR61-S100A4-pERK1/2 signaling. **(A)** Relative YAP expression 96 h after transient YAP siRNA transfection compared to control was assessed using real-time quantitative PCR. Data represent mean ± SEM. Using unpaired, two-tailed *t*-test analysis. MCF-7-EMT $n = 5$; T47D-EMT $n = 3$; MDA-MB-231 $n = 3$; HCC1806 $n = 3$; $^{*}P < 0.05$; $^{**}P < 0.01$; $^{****}P < 0.001$ **(B)** Analysis of relative AlamarBlue reduction as indicator for cell viability. Breast cancer cell spheroids were grown and AlamarBlue reduction was assessed 48 hours after adding Matrigel at 4 h incubation. Relative AlamarBlue reduction was calculated compared to control spheroids. Data represent mean ± SEM. $n = 3$.

Figure S6 | CYR61 and S100A4 as prognostic marker for breast cancer progression. Cut-off values were downloaded from kmplot.com after target (dataset 213226_at = CYR61; dataset 203186_s_at = S100A4) specific analysis. RFS, relapse free survival; DMFS, distant metastasis free survival.

Figure S7 | CYR61 and S100A4 are highly expressed in invasive and metastatic B cancer patient tissue samples. Expression analysis of CYR61 and S100A4 via fluorescence staining using biomax tissue arrays (BR 20837,BR 248a, T087a) with paraffin-embedded patient samples. Table shows Arraytyp of analyzed samples, patients age, sex, the organic tissue site, pathology diagnosis, classification of M tumors (TNM), grading, stage, typ, tisse ID and for most analyzed tiised the xpression of estrogen(ER), progesteron (PR) and Herceptinreceptor2 (Her2). Expression of CYR61 and S100A4 was assessed as (–) not expressed, (+) low expression, (++) medium expression, (+ + +) high expression.

REFERENCES

1. Noone AM, Howlader N, Krapcho M, Miller D, Brest A, Yu M, et al. (eds.). *SEER Cancer Statistics Review, 1975-2015*. Bethesda, MD: National Cancer Institute. Available online at: https://seer.cancer.gov/csr/1975_2015/ (accessed September 10, 2018).
2. Gupta GP, Massague J. Cancer metastasis: building a framework. *Cell.* (2006) 127:679–95. doi: 10.1016/j.cell.2006.11.001
3. Hanahan D, Weinberg RA. Hallmarks of cancer: the next generation. *Cell.* (2011) 144:646–74. doi: 10.1016/j.cell.2011.02.013
4. Brabletz T, Kalluri R, Nieto MA, Weinberg RA. Emt in cancer. *Nat Rev Cancer.* (2018) 18:128–34. doi: 10.1038/nrc.2017.118

5. Van Staalduinen J, Baker D, Ten Dijke P, Van Dam H. Epithelial–mesenchymal-transition-inducing transcription factors: new targets for tackling chemoresistance in cancer? *Oncogene.* (2018) 37:6195–211. doi: 10.1038/s41388-018-0378-x
6. Fischer KR, Durrans A, Lee S, Sheng J, Li F, Wong ST, et al. Epithelial-to-mesenchymal transition is not required for lung metastasis but contributes to chemoresistance. *Nature.* (2015) 527:472–6. doi: 10.1038/nature15748
7. Tran HD, Luitel K, Kim M, Zhang K, Longmore GD, Tran DD. Transient snail1 expression is necessary for metastatic competence in breast cancer. *Cancer Res.* (2014) 74:6330–40. doi: 10.1158/0008-5472.CAN-14-0923
8. Ye X, Brabletz T, Kang Y, Longmore GD, Nieto MA, Stanger BZ, et al. Upholding A role for emt in breast cancer metastasis. *Nature.* (2017) 547:E1–E3. doi: 10.1038/nature22816
9. Garg M. Epithelial, mesenchymal and hybrid epithelial/mesenchymal phenotypes and their clinical relevance in cancer metastasis. *Expert Rev Mol Med.* (2017) 19:E3. doi: 10.1017/erm.2017.6
10. Simeone P, Trerotola M, Franck J, Tristan C, Fournier I, Salzet M, et al. The multiverse nature of epithelial to mesenchymal transition. In: Vincent T, editor. *Seminars in Cancer Biology*. London: Academic Press Ltd-Elsevier Science Ltd (2018).
11. Kim YN, Choe SR, Cho KH, Cho DY, Kang J, Park CG, et al. Resveratrol suppresses breast cancer cell invasion by inactivating A Rhoa/yap signaling axis. *Exp Mol Med.* (2017) 49:E296. doi: 10.1038/emm.2016.151
12. Hou CH, Lin LL, Hou SM, Liu LF. Cyr61 promotes epithelial-mesenchymal transitionand tumor metastasis of osteosarcoma byraf-1/Mek/Erk/Elk-1/Twist-1 signaling pathway. *Mol Cancer.* (2014) 13:13. doi: 10.1186/1476-4598-13-236
13. Haque I, Mehta S, Majumder M, Dhar K, De A, Mcgregor D, et al. Cyr61/Ccn1 signaling is critical for epithelial-mesenchymal transition and stemness and promotes pancreatic carcinogenesis. *Mol Cancer.* (2011) 10:8. doi: 10.1186/1476-4598-10-8
14. Huang X, Xiang L, Li Y, Zhao Y, Zhu H, Xiao Y, et al. Snail/Foxk1/Cyr61 signaling axis regulates the epithelial-mesenchymal transition and metastasis in colorectal cancer. *Cell Physiol Biochem.* (2018) 47:590–603. doi: 10.1159/000490015
15. Tsai M-S, Bogart DF, Castañeda JM, Li P, Lupu R. Cyr61 promotes breast tumorigenesis and cancer progression. *Oncogene.* (2002) 21:8178. doi: 10.1038/sj.onc.1205682
16. Huang HT, Lan Q, Lorusso G, Duffey N, Rugg C. The matricellular protein Cyr61 promotes breast cancer lung metastasis by facilitating tumor cell extravasation and suppressing anoikis. *Oncotarget.* (2017) 8:16. doi: 10.18632/oncotarget.13677
17. Tong X, Xie D, O'kelly J, Miller CW, Muller-Tidow C, Koeffler HP. Cyr61, A member of Ccn family, is A tumor suppressor in non-small cell lung cancer. *J Biol Chem.* (2001) 276:47709–14. doi: 10.1074/jbc.M107878200
18. Jun JI, Lau LF. The matricellular protein Ccn1 induces fibroblast senescence and restricts fibrosis in cutaneous wound healing. *Nat Cell Biol.* (2010) 12:676–85. doi: 10.1038/ncb2070
19. Todorovic V, Chen CC, Hay N, Lau LF. The matrix protein Ccn1 (Cyr61) induces apoptosis in fibroblasts. *J Cell Biol.* (2005) 171:559–68. doi: 10.1083/jcb.200504015
20. Ziegler E, Hansen MT, Haase M, Emons G, Grundker C. Generation of Mcf-7 cells with aggressive metastatic potential *in vitro* and *in vivo*. *Breast Cancer Res Treat.* (2014) 148:269–77. doi: 10.1007/s10549-014-3159-4
21. Von Alten J, Fister S, Schulz H, Viereck V, Frosch KH, Emons G, et al. Gnrh analogs reduce invasiveness of human breast cancer cells. *Breast Cancer Res Treat.* (2006) 100:13–21. doi: 10.1007/s10549-006-9222-z
22. Vinci M, Box C, Eccles SA. Three-dimensional (3D) tumor spheroid invasion assay. *J Vis Exp.* (2015) e52686. doi: 10.3791/52686
23. Grundker C, Bauerschmitz G, Schubert A, Emons G. Invasion and increased expression of S100a4 and Cyr61 in mesenchymal transformed breast cancer cells is downregulated By Gnrh. *Int J Oncol.* (2016) 48:2713–21. doi: 10.3892/ijo.2016.3491
24. Gyorffy B, Lanczky A, Eklund AC, Denkert C, Budczies J, Li Q, et al. An online survival analysis tool to rapidly assess the effect of 22,277 genes on breast cancer prognosis using microarray data Of 1,809 patients. *Breast Cancer Res Treat.* (2010) 123:725–31. doi: 10.1007/s10549-009-0674-9
25. Chen A, Wang L, Li BY, Sherman J, Ryu JE, Hamamura K, et al. Reduction in migratory phenotype in a metastasized breast cancer cell line via downregulation of S100a4 and Grm3. *Sci Rep.* (2017) 7:3459. doi: 10.1038/s41598-017-03811-9
26. Chen PS, Wang MY, Wu SN, Su JL, Hong CC, Chuang SE, et al. Ctgf enhances the motility of breast cancer cells via an integrin-α vβ3–Erk1/2-dependent S100a4-upregulated pathway. *J Cell Sci.* (2007) 120:2053–65. doi: 10.1242/jcs.03460
27. Jim Leu S-J, Sung J-S, Huang M-L, Chen M-Y, Tsai T-W. A novel anti-Ccn1 monoclonal antibody suppresses Rac-dependent cytoskeletal reorganization and migratory activities in breast cancer cells. *Biochem Biophy Res Commun.* (2013) 434:885–91. doi: 10.1016/j.bbrc.2013.04.045
28. Shaul YD, Seger R. The Mek/Erk cascade: from signaling specificity to diverse functions. *Biochim et Biophys Acta Mol Cell Res.* (2007) 1773:1213–26. doi: 10.1016/j.bbamcr.2006.10.005
29. Favata MF, Horiuchi KY, Manos EJ, Daulerio AJ, Stradley DA, Feeser WS, et al. Identification of A novel inhibitor of mitogen-activated protein kinase kinase. *J Biol Chem.* (1998) 273:18623–32. doi: 10.1074/jbc.273.29.18623
30. Shen J, Cao B, Wang Y, Ma C, Zeng Z, Liu L, et al. Hippo component yap promotes focal adhesion and tumour aggressiveness via transcriptionally activating Thbs1/fak signalling in breast cancer. *J Exp Clin Cancer Res Cr.* (2018) 37:175–175. doi: 10.1186/s13046-018-0850-z
31. Emre Y, Imhof BA. Matricellular protein Ccn1/Cyr61: a new player in inflammation and leukocyte trafficking. *Semin Immunopathol.* (2014) 36:253–9. doi: 10.1007/s00281-014-0420-1
32. Bornstein P. Matricellular proteins: an overview. *J Cell Commun Signal.* (2009) 3:163–5. doi: 10.1007/s12079-009-0069-z
33. Yao H, Guangchun HE, Shichao Y, Chen C, Liujiang S, Thomas J, et al. Triple-negative breast cancer: is there a treatment on the horizon? *Oncotarget.* (2016) 8:12. doi: 10.18632/oncotarget.12284
34. Xie D, Nakachi K, Wang H, Elashoff R, Koeffler HP. Elevated levels of connective tissue growth factor, WISP-1, and CYR61 in primary breast cancers associated with more advanced features. *Cancer Res.* (2001) 61:8917–23.
35. Nieto MA. Context-specific roles of emt programmes in cancer cell dissemination. *Nat Cell Biol.* (2017) 19:416–8. doi: 10.1038/ncb3520
36. Jenkinson SR, Barraclough R, West CR, Rudland PS. S100a4 regulates cell motility and invasion in an in vitro model for breast cancer metastasis. *Br J Cancer.* (2004) 90:253–62. doi: 10.1038/sj.bjc.6601483
37. Maity G, Ghosh A, Gupta VG, Haque I, Sarkar S, Das A, et al. Cyr61/Ccn1 regulates Dck And Ctgf and causes gemcitabine resistant phenotype in pancreatic ductal adenocarcinoma. *Mol Cancer Therapeut Molcanther*. (2019) 0899:2018. doi: 10.1158/1535-7163.MCT-18-0899
38. Long X, Yu Y, Perlaky L, Man T-K, Redell MS. Stromal Cyr61 confers resistance to mitoxantrone via spleen tyrosine kinase activation in human acute myeloid leukaemia. *Br J Haematol.* (2015) 170:704–18. doi: 10.1111/bjh.13492
39. Liu F, Yang X, Geng M, Huang M. Targeting Erk, an achilles' heel of the mapk pathway, in cancer therapy. *Acta Pharmaceut Sin B.* (2018) 8:552–62. doi: 10.1016/j.apsb.2018.01.008
40. Boopathy GTK, Hong W. Role of hippo pathway-Yap/Taz signaling in angiogenesis. *Front Cell Dev Biol.* (2019) 7:49 doi: 10.3389/fcell.2019.00049
41. Halder G, Johnson RL. Hippo signaling: growth control and beyond. *Development.* (2011) 138:9–22. doi: 10.1242/dev.045500
42. Pan D. The hippo signaling pathway in development and cancer. *Dev Cell.* (2010) 19:491–505. doi: 10.1016/j.devcel.2010.09.011
43. Cao L, Sun PL, Yao M, Jia M, Gao H. Expression of yes-associated protein (Yap) and its clinical significance in breast cancer tissues. *Hum Pathol.* (2017) 68:166–74. doi: 10.1016/j.humpath.2017.08.032
44. Warren JSA, Xiao Y, Lamar JM. Yap/Taz activation as a target for treating metastatic cancer. *Cancers.* (2018) 10:E115. doi: 10.3390/cancers10040115
45. Mayer S, Gabriel B, Erbes T, Timme-Bronsert S, Jager M, Rucker G, et al. Cyr61 expression pattern and association with clinicopathological factors in patients with cervical cancer. *Anticancer Res.* (2017) 37:2451–6. doi: 10.21873/anticanres.11585

46. Wei J, Yu G, Shao G, Sun A, Chen M, Yang W, et al. Cyr61 (Ccn1) is a metastatic biomarker of gastric cardia adenocarcinoma. *Oncotarget*. (2016) 7:31067–78. doi: 10.18632/oncotarget.8845
47. Destek S, Gul VO. S100a4 may be a good prognostic marker and a therapeutic target for colon cancer. *J Oncol*. (2018) 2018:1828791. doi: 10.1155/2018/1828791
48. Ai KX, Lu LY, Huang XY, Chen W, Zhang HZ. Prognostic significance of S100a4 and vascular endothelial growth factor expression in pancreatic cancer. *World J Gastroenterol*. (2008) 14:1931–5. doi: 10.3748/wjg.14.1931
49. Egeland EV, Boye K, Park D, Synnestvedt M, Sauer T, Oslo Breast Cancer C, et al. Prognostic significance of S100a4-expression and subcellular localization in early-stage breast cancer. *Breast Cancer Res Treat*. (2017) 162:127–37. doi: 10.1007/s10549-016-4096-1
50. Monnier Y, Farmer P, Bieler G, Imaizumi N, Sengstag T, Alghisi GC, et al. Cyr61 and alphavbeta5 integrin cooperate to promote invasion and metastasis of tumors growing in preirradiated stroma. *Cancer Res*. (2008) 68:7323–31. doi: 10.1158/0008-5472.CAN-08-0841
51. Kassis JN, Virador VM, Guancial EA, Kimm D, Ho AS, Mishra M, et al. Genomic and phenotypic analysis reveals A key role for Ccn1 (Cyr61) In bag3-modulated adhesion and invasion. *J Pathol*. (2009) 218:495–504. doi: 10.1002/path.2557

Conflict of Interest: The authors declare that the research was conducted in the absence of any commercial or financial relationships that could be construed as a potential conflict of interest.

Copyright © 2019 Hellinger, Hüchel, Goetz, Bauerschmitz, Emons and Gründker. This is an open-access article distributed under the terms of the Creative Commons Attribution License (CC BY). The use, distribution or reproduction in other forums is permitted, provided the original author(s) and the copyright owner(s) are credited and that the original publication in this journal is cited, in accordance with accepted academic practice. No use, distribution or reproduction is permitted which does not comply with these terms.

frontiers in Oncology

REVIEW
published: 16 December 2019
doi: 10.3389/fonc.2019.01359

Ping-Pong—Tumor and Host in Pancreatic Cancer Progression

Wei Mu[1]*, *Zhe Wang*[2] and *Margot Zöller*[2]

[1] School of Public Health, Shanghai Jiao Tong University School of Medicine, Shanghai, China, [2] Department of Oncology, The First Affiliated Hospital of Guangdong, Pharmaceutical University, Guangzhou, China

Metastasis is the main cause of high pancreatic cancer (PaCa) mortality and trials dampening PaCa mortality rates are not satisfying. Tumor progression is driven by the crosstalk between tumor cells, predominantly cancer-initiating cells (CIC), and surrounding cells and tissues as well as distant organs, where tumor-derived extracellular vesicles (TEX) are of major importance. A strong stroma reaction, recruitment of immunosuppressive leukocytes, perineural invasion, and early spread toward the peritoneal cavity, liver, and lung are shared with several epithelial cell-derived cancer, but are most prominent in PaCa. Here, we report on the state of knowledge on the PaCIC markers Tspan8, alpha6beta4, CD44v6, CXCR4, LRP5/6, LRG5, claudin7, EpCAM, and CD133, which all, but at different steps, are engaged in the metastatic cascade, frequently via PaCIC-TEX. This includes the contribution of PaCIC markers to TEX biogenesis, targeting, and uptake. We then discuss PaCa-selective features, where feedback loops between stromal elements and tumor cells, including distorted transcription, signal transduction, and metabolic shifts, establish vicious circles. For the latter particularly pancreatic stellate cells (PSC) are responsible, furnishing PaCa to cope with poor angiogenesis-promoted hypoxia by metabolic shifts and direct nutrient transfer via vesicles. Furthermore, nerves including Schwann cells deliver a large range of tumor cell attracting factors and Schwann cells additionally support PaCa cell survival by signaling receptor binding. PSC, tumor-associated macrophages, and components of the dysplastic stroma contribute to perineural invasion with signaling pathway activation including the cholinergic system. Last, PaCa aggressiveness is strongly assisted by the immune system. Although rich in immune cells, only immunosuppressive cells and factors are recovered in proximity to tumor cells and hamper effector immune cells entering the tumor stroma. Besides a paucity of immunostimulatory factors and receptors, immunosuppressive cytokines, myeloid-derived suppressor cells, regulatory T-cells, and M2 macrophages as well as PSC actively inhibit effector cell activation. This accounts for NK cells of the non-adaptive and cytotoxic T-cells of the adaptive immune system. We anticipate further deciphering the molecular background of these recently unraveled intermingled phenomena may turn most lethal PaCa into a curatively treatable disease.

Keywords: pancreatic cancer, metastasis, exosomes, cancer-initiating cell markers, stellate cells, metabolism, perineural invasion, immunosuppression

OPEN ACCESS

Edited by:
Mohit Kumar Jolly,
Indian Institute of Science (IISc), India

Reviewed by:
Sabarish Ramachandran,
Texas Tech University Health Sciences Center, United States
Abhinav Achreja,
University of Michigan, United States
Dongya Jia,
Rice University, United States

***Correspondence:**
Wei Mu
weimu@shsmu.edu.cn

Specialty section:
This article was submitted to Molecular and Cellular Oncology, a section of the journal Frontiers in Oncology

Received: *09 August 2019*
Accepted: *18 November 2019*
Published: *16 December 2019*

Citation:
Mu W, Wang Z and Zöller M (2019) Ping-Pong—Tumor and Host in Pancreatic Cancer Progression. Front. Oncol. 9:1359. doi: 10.3389/fonc.2019.01359

INTRODUCTION

The Metastatic Cascade and Tumor Cell Dissemination

More than 90% of cancer mortality is related to metastasis (1), which in carcinoma requires completion of the metastatic cascade starting with local invasion of the surrounding extracellular matrix (ECM) and cells and processing through intravasation, surviving transport in vessels, arrest at distant organs, extravasation, surviving in the foreign environment and reinitiating tumor growth (2). These complex biological events are orchestrated by cell autonomous and non-autonomous signaling cascades. Local invasion requires breaching the basal membrane (BM) promoted by tumor-derived proteases and leading to liberation of growth factors and integrin activation affecting cell polarity and survival (3). Alternatively, tumor cells may use a protease- and integrin-independent, Rho[1]/ROCK[1]-dependent amoeboid invasion program (4). For local invasion of individual cells, tumor cells adopt a developmental epithelial-mesenchymal transition (EMT) program, which orchestrates activation of sets of transcription factors (Tf) that repress cell-cell adhesion molecules and induce expression of mesenchymal markers (5). Having passed the BM, tumor cells encounter the tumor stroma, which consists of endothelial cells (EC), pericytes, adipocytes, fibroblasts (FB), and bone marrow mesenchymal cells. Tumor cells push the reactive stroma toward pro-tumorigenic factor secretion and pro-tumorigenic cell recruitment. Thus, contact with the surrounding stroma is the first step where tumor cells receive a self-amplifying feedback (6, 7). The following step of invasion is strongly promoted by tumor-induced angiogenesis/lymphangiogenesis, the newly formed vessels being tortuous, leaky and continuously reconfiguring themselves, weak interactions between adjacent EC and the incomplete pericyte coverage facilitate tumor cell intravasation. EC wall passage is assisted by TGFβ[1] and tumor-associated macrophages (TAM), providing CFS1/MCSF[1] and EGF[1]. In addition, metabolic adaptations of growing and sprouting EC support (lymph)angiogenesis (8–10). In the vasculature, tumor cells are exposed to a variety of stresses. In the absence of cell-cell or cell-matrix adhesion, epithelial cell would undergo apoptosis/anoikis, which is circumvented by metabolic shifts toward the pentosephosphate pathway and anaerobic glycolysis. Matrix detachment-forced reduced glucose uptake assists LKB1[1] activation, which increases protein kinase AMP[1] catalytic subunit PRKAA[1] activity. This inhibits acetyl-CoA carboxylases ACACA/B[1], lowers NADPH[1] consumption in fatty acid (FA) synthesis, but increases NADPH generation through an alternative pathway. This process reduces reactive oxygen species (ROS), essential for precluding detached cancer cell anoikis (10–13). Shear stress and the attack by the innate immune system are circumvented by tumor cell tissue factor (TF[1]) and selectins binding to platelets to form microemboli, which act as protective shields for the tumor cells (14, 15). Tumor cells mostly extravasate between adjacent EC. Adhesion to EC is facilitated by selectins, cadherins, integrins, CD44, Ig superfamily members, CD146/MUC18[1], and by homophilic interactions between JAM[1]. Interactions between tumor cell-provided factors such as ANGPTL4[1] and α5β1, CDH5/CD144[1], CLDN5[1], EREG[1], COX2[1], and MMP[1] support extravasation. Actin remodeling, opening of junctions, necroptosis and APP[1]-DR6[1]-assisted EC death are discussed as underlying mechanisms. Platelet-, neutrophil- and monocyte-provided cytokines and chemokines also assist extravasation (16, 17).

Metastatic Growth

There is ample evidence that migrating cancer cells leave the circulation for well-prepared soil, known as premetastatic niche. It is arranged in advance of cancer cell arrival by receiving information via tumor exosomes (TEX). Integrins, tetraspanins, receptor tyrosine kinases (RTK) and G-protein coupled receptors (GPCR) are important for message transfer (18–21). Established micrometastases may persist for weeks to years in a state of long-term dormancy. This dormancy relies on resting state persistence or failure to initiate angiogenesis, or on apoptosis-promoting host cells. Macroscopic metastatic outgrowth requires a multitude of adaptive programs that vary depending on the organ site of the metastasis and the original tumor. No metastasis-specific genetic changes being observed, outgrowth is supposed relying on epigenetic changes, like aberrant DNA methylation, altered chromatin structure, and activation of transcriptional programs that can be facilitated/guided by long non-coding (lnc)RNA. Two prerequisites must be fulfilled. One is the presence of cancer-initiating cells (CIC) with the capacity for self-renewal that in part is promoted by EMT-related Tf. The other is the establishment of adaptive programs enabling growth in the foreign environment. This includes some common traits such as metabolic adaptation and survival pathway activation. Other adaptive programs vary with the site of metastasis. Thus, similar to primary tumor growth,

Abbreviations: AA, amino acid; a, activated; ADCC, antibody-dependent cellular cytotoxicity; ASC, adult stem cells; BM, basal membrane; BMC, bone marrow cells; CAF, cancer-associated fibroblasts; CIC, cancer–initiating cells/cancer stem cells; CNS, central nervous system; CoCa, colorectal cancer; CRD, carbohydrate recognition domain; CTL, cytotoxic T lymphocytes; DC, dendritic cells; DFS, disease free survival; DR, desmoplastic reaction; EC, endothelial cells; ECM, extracellular matrix; EE, early endosome; EMT, epithelial mesenchymal transition; ER, endoplasmic reticulum; ERM, ezrin, radixin, moesin; eRNA, enhancer lncRNA; ESC, embryonic stem cells; ESCRT, endosomal sorting complex required for transport; EV, extracellular vesicles; Exo, exosome; FA, fatty acid; FB, fibroblast; FN, fibronectin; GPCR, G protein-coupled receptor; HCC, hepatocellular carcinoma; HNRNP, heterogeneous ribonucleoprotein; ICD, intracellular domain; ILV, intraluminal vesicle; kd, knockdown; ko, knockout; LN, laminin; lnc, long noncoding; LNC, lymph node cells; MDSC, myeloid-derived suppressor cell; MET, mesenchymal-epithelial transition; Mϕ, macrophage; MHC, major histocompatibility complex; miRNA, microRNA; MS, mass spectrometry; MV, microvesicles; MVB, multivesicular body; nc, non-coding; NEAA, non-essential amino acids; NK, natural killer cells; Non-CIC, non-metastasizing tumor cells; PaCa, pancreatic cancer; PanIN, pancreatic intraepithelial neoplasia; PNI, perineural invasion; PSC, pancreatic stellate cells; RISC, RNA induced silencing complex; RBP, RNA binding proteins; RNP, ribonucleoprotein; ROS, reactive oxygen species; RTK, receptor tyrosine kinase; SC, stem cells; SNS, sympathetic nervous system; TAM, tumor-associated macrophages; TCA, tricarboxylic acid; TEM, tetraspanin- and glycolipid-enriched membrane microdomain; TEX, tumor exosomes; Tf, transcription factor; Th, helper T cells; TJ, tight junction; Treg, regulatory T cells.

[1]Alphabetic list of gene/protein full names: **Table S1**.

metastatic outgrowth is supported by the surrounding stroma including TGFβ1 and periostin, pro-inflammatory cells, local fibroblasts, and supportive ECM components (22–24). There remains a last query. CIC-derived metastases frequently reflect the mixed phenotype of the primary tumor. This may be due to the reversibility of EMT, called mesenchymal-epithelial transition (MET). However, further studies are required to elucidate tumor-inherent and surrounding-supported MET reprogramming (25–27).

Twenty-five years ago, the metastatic cascade was described as sequential processes in microecosystems (28). This still holds true, where striking progress in molecular characterization, important insights into stem cell (SC)/CIC plasticity, signaling pathways, networking connectivity and the modes of epigenetic regulation allowed deciphering the paths toward tumor progression.

After briefly introducing the clinical features of PaCa and exosome composition, we discuss current theories on the molecular mechanisms underlying the steps of the metastatic cascade particularly in PaCa.

CLINICAL FEATURES OF PANCREATIC CANCER GROWTH AND METASTASIS

Pancreatic cancer (PaCa) is the most lethal cancer, with a mortality rate close to the incidence rate. The overall 5-year survival rate is ∼5% (29) and does not exceed 15–20% after surgery, the only curative treatment option, owing to local recurrence and metastatic spread. Furthermore, 80% of patients are inoperable at diagnosis (30). Though mortality rates for several common cancers decreased over the last decades (29), mortality rates increased for PaCa. Ductal PaCa, the most frequent subtype, is expected to be the second cancer-related cause of death after lung cancer by 2030 (31). The high mortality, due to early spread and radio- and chemotherapy resistance (32), is caused by a small population of CIC (33). Three additional contributing features are abundant stroma reactions, preferential dissemination along intrapancreatic nerves and pronounced immune deviation.

Unlike most tumors, PaCa cells may form only small islands within an abundant tumor stroma. The main cellular components are cancer-associated fibroblasts (CAF), predominantly deriving from pancreatic stellate cells (PSC) and inflammatory cells. The ECM consists of collagens, laminin (LN), fibronectin (FN), proteoglycans, and glycosaminoglycans and harbors soluble factors affecting tumor and host cells (34, 35). The PaCa stroma reaction, primarily promoting tumor growth, may hamper tumor progression in certain circumstances, indicating the need for further studies on composition and activities (36).

Perineural invasion (PNI) is most common in PaCa and an indicator of aggressive tumors and short survival (37). The pancreatic nerve fibers from the splanchnic nerves, dorsal root ganglion and the vagus become hyperinnervated and hypertrophic. The nervous system participates in all stages of PaCa development with neurotrophic factors and axon guidance genes overrepresentation or mutation. CAF and intrapancreatic immune cells also affect the intrapancreatic neurons (38), but intrapancreatic neurons and Schwann cells also signal toward the tumor cells (39, 40).

Finally, the PaCa stroma is replete with immune cells (41) that are almost exclusively immunosuppressive (42).

The steeply increasing incidence of most malignant PaCa demands intensifying efforts to clarify the underlying mechanisms. PaCa shares the consecutive steps of the metastatic cascade with most epithelial carcinoma, but also displays several peculiarities. Extensive stroma dysplasia, preferred routing of migrating tumor cells along intrapancreatic nerves and striking deviations toward immunosuppressive cells and factors account for the early spread. We will discuss those features, which quantitatively differentiate PaCa from the majority of epithelial cancer. Exosomes and PaCIC markers, both essentially contributing to the selective features, are introduced in advance.

THE IMPORTANCE OF EXOSOMES IN TUMOR PROGRESSION

Contact between single tumor cells detaching from the tumor mass and distinct non-transformed tissues and cells is an essential prerequisite for tumor progression. The crosstalk between metastasizing and non-metastasizing tumor cells and non-transformed cells mostly relies on message delivery by TEX and stroma cell-derived Exo.

Exo, small 40–100 nm vesicles delivered by live cells (43), disperse throughout the body, which allows for short and long-range communication (44). Exo expressing donor cell-derived components allows differentiating non-transformed cell-derived Exo from TEX (45). Exo components are function-competent (46) and highly effective intercellular communicators (47). Delivered messages modulate the ECM, non-metastasizing tumor cells (Non-CIC), and non-transformed cells including hematopoietic cells, EC, FB, nerves, and epithelial cells (48–51).

Exo biogenesis starts with early endosome (EE) formation. EE derive from the trans-Golgi network or internalized membrane microdomains (52). Distinct transport machineries guide EE toward multivesicular bodies (MVB) (53). Exo collect their cargo during inward budding of endosomes, called intraluminal vesicles (ILV), into MVB (54–56). LPAR1[1], Alix/PDCD6IP[1], and HSP70[1] spur inward budding and SGPP1[1] and diaglycerol[1] are engaged in cargo sorting (57, 58). Loading are nonrandom processes. Protein loading is facilitated by mono-ubiquitination, acylation, myristoylation, higher order oligomerization, or sphingolipids forming ceramide (59–61). Annexin-II supports RNA sorting (62). Optionally, RNA becomes incorporated by affinity for the outer (cytoplasmic) raft-like MVB membrane (63). MiRNA loading is guided by a zip code in the 3′-UTR and coupling of RISC (RNA induced silencing complex) to specific EXO motifs binding to HNRNP (heterogeneous ribonucleoprotein) (55, 64). Selective lncRNA recruitment requires clarification (65, 66). ILV are guided toward the proteasome for degradation or toward the plasma membrane, supported by microtubules and Rab[1] proteins (53, 67). SNARE[1] and synaptogamins assist fusion with the plasma membrane (52, 53, 67). Released vesicles are called exosomes.

Exosome Composition

The Exo membrane lipid bilayer contains integrated membrane proteins and lipid- or membrane protein-attached cytoskeletal and cytosolic signaling molecules. The Exo lipid envelop is composed of phosphatidylcholine, -ethanolamine, -inositol, prostaglandins, lysobisphosphatidic acid, sphingomyelin, cholesterol, GM3[1]/GRM6[1], and PS[1] (phosphatidylserine) (68), high PS levels differentiating Exo from microvesicles (69). Lipids are organized along with lipid carriers such as lipid-transporting FABP[1]. Lipid second messengers are involved in biogenesis, some requiring a link to lipids during ILV invagination, e.g., HSPA8 needs battenin (CLN3[1]) (70), formed by PLD2[1] (71, 72). Ceramide triggers an ESCRT (endosomal sorting complex required for transport)-independent pathway of Exo biogenesis (73). Cholesterol enhances flotillin-2 positive Exo secretion (74). Lipid transporters such as ABCA3[1] are also involved in Exo production (75). Thus, Exo carry bioactive lipids, related enzymes, fatty acid transporters, and lipid-related enzyme carriers and use lipids to fuse with target cells (76–78).

Exo protein characterization profited from improved mass spectrometry (MS) (79) to be followed by the exocharta database [http://exocarta.org/exosome_markers]. Exo also contain proteins engaged in biogenesis and vesicle transport and proteins actively recruited during ILV invagination. Tetraspanins are most strongly enriched constitutive Exo component (80–82). Other abundant proteins include adhesion molecules, proteases, major histocompatibility complex (MHC) molecules, HSP, TSG101[1], ALIX, annexins, cytoskeleton proteins, metabolic enzymes, cytosolic signal transduction molecules, and ribosomal proteins (82, 83). Finally, PaCIC biomarkers are enriched in TEX (84–86). This is important as CIC drive the metastatic process (87–90), where Tspan8 (86, 91) and associated α6β4 (92–94), CD44v6 (95, 96), and linked cMET[1] (96, 97), CD184/CXCR4[1] that can associate with Tspan8 and CD44v6 (98–100), cldn7 (84, 101, 102), and associated EpCAM[1] (84, 103, 104), LGR5/GPR49[1] (105, 106) and CD133/PROM1[1] (107, 108) are engaged in distinct steps of tumor progression.

Exo also contain mRNA. mRNA is produced and processed in the nucleus, transported to the cytoplasm and translated. These processes are controlled by proteins, mostly RNA binding proteins (RBP), which interact with mRNA (109) and together with additional regulatory RNA constitute the mRNA binding protein code (110–113). Notably, the activity of RBP varies depending on the cell's activation state. Thus, GAPDH[1] binds the 3′UTR of IFNγ[1] and represses translation in inactive, but not activated T-cells (114). RBP also account for localization and trafficking of RNA-protein complexes in cells (115, 116). Finally, the mRNA profile of Exo differs from that of cells (117), metabolic enzymes and proteins engaged in cell-cell and cell-matrix adhesion being frequently overrepresented (118–120), and possibly translated in Exo (121, 122).

Exo contain a large range of non-coding (nc)RNA. Most abundant are microRNA (miRNA) and lncRNA. miRNA host genes are transcribed by RNA polymerase II to form primary (pri)-miRNA. The Drosha[1] endonuclease associates with the RBP DGCR8[1] releasing the stemloop precursor from the flanking pri-miRNA transcript sequence. After export from the nucleus by exportin-5, Dicer in association with TRBP[1] cleaves the precursor loop releasing the mature miRNA (123). One strand of this duplex RNA is integrated into the RISC complex, which contains argonaute linking the miRNA to target mRNA (124, 125). Importantly, miRNA with sequence motifs for sorting into ILV are efficiently transferred into Exo, some miRNA becoming undetectable in the donor cell (126, 127). Most miRNA bind to a large number of mRNA and most mRNA are targeted by more than one miRNA, providing hurtles for their potential therapeutic use, aggravated by the discussed mode whereby miRNA affect target cells (117, 128).

LncRNA, defined by a length of >200 bp, are abundantly recovered from Exo (129). LncRNA are involved in a large range of activities, including chromatin organization, gene transcription, mRNA turnover, protein translation, and macromolecular complex assembly (130–132). LncRNA can also be grouped according to functioning as signal, decoy, scaffold, guide, enhancer RNA, and short peptides (133). Signaling lncRNA regulate transcription (134). Decoy lncRNA sequesters regulatory factors including Tf, catalytic proteins, subunits of larger chromatin modifying complexes and miRNA (135). Scaffold lncRNA provide platforms for assembly of multiple-component complexes, e.g., ribonucleoprotein (RNP) complexes (136). Guide lncRNA drive RNP to specific target genes (137). Enhancer lncRNA (eRNA) influence the 3-dimensional organization of DNA, which may result from lncRNA being not released and tethering interacting proteins to enhancer regions (138). Finally, lncRNA can encode function-competent short peptides (139). Evidence for selective recruitment into Exo derives from enrichment of some lncRNA harboring seed regions for miRNA in Exo (140, 141). LncRNA recovery in Exo only recently receiving attention, important information on the multiple functions of lncRNA can be expected in the near future.

Exo contain mitochondrial, genomic, or retrotransposon double and single stranded DNA (142, 143). Without hints toward sorting and disputed functionality, a possible contribution of Exo DNA to tumor progression remains to be elaborated.

Taken together, TEX are optimally furnished to drive all steps of the metastatic cascade using their lipid, protein and RNA armament, where PaCIC markers contribute to biogenesis (Tspan8), miRNA loading (CD44v6), and lipid transport (cldn7) (144, 145) (**Figures 1A–C**).

Exosome Targeting and Uptake

Exosomes bind to the ECM and cells, using for both a similar appurtenance.

Exo binding mostly relies on surface receptor and adhesion molecules, such as tetraspanins, integrins, proteoglycans, and lectins, docking to appropriate ligands on the ECM and cells (146). Tetraspanin-associated adhesion molecules account for target-selective binding. Thus, Tspan8-α4 preferentially binds

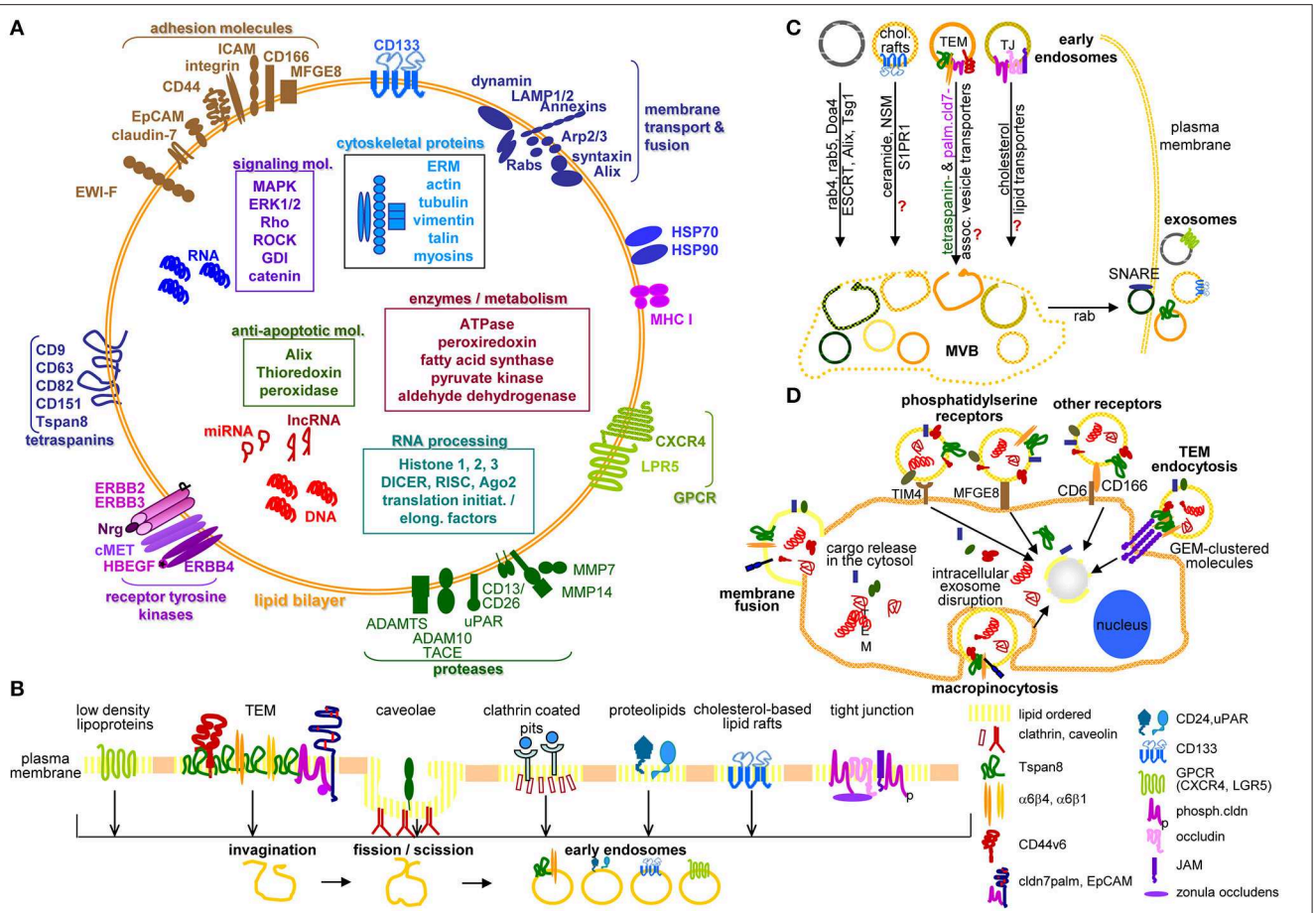

FIGURE 1 | Exosome characterization, biogenesis, and targeting. **(A)** Exosomes are composed of a lipid bilayer, transmembrane protein and the cytoplasm containing proteins, mRNA, non-coding RNA like miRNA and lncRNA and DNA, where PaCIC-TEX, express the CIC markers Tspan8, integrin α6β1/α6β4, CD44v6, CD133, CXCR4, LRP5, EpCAM, and cldn7. Other transmembrane proteins are linked to Exo biogenesis. **(B)** Exo biogenesis starts with the invagination of membrane microdomains that are characterized by ordered lipids, like low-density lipoprotein, caveolae, clathrin-coated pits, cholesterol-based lipid rafts, and others. **(C)** After fission and scission of invaginated membrane domains, the EE are guided toward MVB, the traffic differs between the origins from distinct lipid-enriched domains. Most abundant is rab4, rab5, Doa4 promoted migration and invagination into MVB via the ESCRT system. Components of cholesterol-based lipid raft-, TJ-, or TEM-derived EE are not completely explored. Guidance from MVB to the plasma membrane involves rab proteins, phospholipase D, and SNARE. **(D)** The contact between Exo and target cells can proceed via fusion of the Exo membrane with the cell membrane, by macropinocytosis, receptor ligand binding such as phosphatidylserine binding to TIM4 or MFGE8 or CD166 binding to CD6 or may be facilitated by Exo membrane protein complexes binding to invagination-prone complexes as described for TEM binding to the TCR complex. Exo also bind to the ECM or matricellular proteins, CD44 and integrins being most frequently involved. Full name of proteins are listed in **Table S1**. In brief, cells use a variety of pathways for the generation of EE, the traffic toward MVB, the loading of ILV with proteins, coding and non-coding RNA and DNA. Exo may preferentially bind to and be taken up by receptor-ligand binding, uptake being facilitated by the engagement of protein complexes at both the Exo and the target cell.

EC, whereas Tspan8-α6β4 preferentially binds FB (147, 148). Integrins, receptors for ECM proteins, also are involved in Tspan8-independent Exo binding (149), e.g., preventing α5β1-FN binding inhibits anchorage independent growth (150). ECM-binding proteins also guide Exo docking and uptake by recipient cells, demonstrated for β_1, α_v, β_3, and α_L integrin chains and ICAM1[1] (151). Recipient cell integrins contribute to Exo binding. PaCa-TEX preferentially bind ADGRE1[1] and CD11b[1] on Kupffer cells (152). Premetastatic niche formation relies on an integrin-dependent TEX tropism. (Tspan8)/β4 preferentially binds to lung (148, 153), αvβ5 preferentially to liver cells (153).

A second Exo docking system also is highly relevant (154). Exo proteoglycans bind to their receptors such as galectins, CD62E[1], CD169/SIGLEC1[1] (155, 156), and CD44 binds to hyaluronan (HA[1]) (157). Blocking Exo heparan sulfate proteoglycan (HSPG), the proteoglycan CD44 or the target cell ligands interferes with Exo binding *in vitro* and *in vivo* (157–160). PS binding TIM4[1], TIM1[1], TIM3[1], GAS6[1], MFGE8[1], Stabilin1, ADGRB1[1], and RAGE/AGER[1] also contributes to Exo docking (146, 154, 161). Furthermore, we want to stress that protein complexes rather than individual molecules, many of which are abundantly expressed, likely account for the selectivity of Exo binding. This is well-demonstrated for tetraspanin

complexes in glycolipid-enriched membrane domains (TEM), the multiple interactions between clustered proteins and target ligands strengthening and stabilizing docking (162). Finally, in view of the ongoing discussion on rapid Exo clearance *in vivo*, which could interfere with their therapeutic efficacy, an excellent report on CD47 binding to SIRPα[1] preventing Exo clearance should be mentioned. Particularly in PaCa, oncogenic KRAS contributes to Exo uptake by yet undefined mechanisms such that long-term persisting Exo manipulated to target oncogenic KRAS is currently the most efficient therapeutics (163).

Exo uptake proceeds by Exo fusion (164, 165) or preferentially endocytosis, a process requiring actin modulation (166). Endocytosis occurs via phagocytosis, macropinocytosis, or clathrin-dependent lipid raft/caveolae endocytosis (167). Phagocytosis, facilitated by LAMP1[1] and TIM4 proceeds by forming cup-like extensions, the tips fusing and becoming internalized (168, 169). Macropinocytosis relies on lamellipodia folding back and fusing with the plasma membrane. Dynamin, Na+H+ exchange, RAC1[1], EGF, and SDF1[1] are also engaged in uptake (170). Endocytosis via clathrin-coated pits, rafts, TEM or caveolae are most frequent (171, 172). In clathrin-dependent endocytosis, the membrane invagination becomes coated with clathrin. Clathrin-coated pits are released after scission by dynamin, dominant-negative forms of clathrin reducing Exo uptake (146). Ligand clustering in TEM also supports Exo uptake (162, 171) and a caveolin knockdown (kd) reduces exosome uptake (173, 174). Uptaken Exo are targeted to lysosomes for degradation. Exo content can directly modulate target cells or stimulate target cells' signaling cascades, transcription and silencing processes (175–177) (**Figure 1D**).

Exo/TEX binding and uptake drastically influence targets. In PaCa, TEX, but also PSC/CAF, immune cell and nerve Exo contribute to PaCa progression.

PANCREATIC CANCER-INITIATING CELL MARKERS AND THE METASTATIC CASCADE

Metastasis depends on CIC. Stem cells are a rare cell population with the capacity for self-renewal and differentiation, which relies mostly on Tf activation, the nuclear equivalent remaining unaltered (178–180). This also accounts for CIC (181, 182), characterized by infrequent division (183, 184), longevity (185), drug and radiation resistance (186–192), and migratory activity (193–196). Since CIC depend on crosstalk with surrounding tissues (197, 198), we wondered whether the PaCIC biomarkers CD44v6 (**Figure 2A**), Tspan8 (**Figure 2B**) and associated α6β4 (**Figure 2C**), LGR5/GPR49 (**Figure 2D**), CXCR4/CD184 that associates with Tspan8 and CD44v6 (**Figure 2E**), cldn7 (**Figure 2F**), EpCAM and cld7-associated EpCAM (**Figure 2G**), and CD133 (**Figure 2H**) might provide hints toward feedback communications between PaCIC and the stroma.

Tspan8 and the α6β4 Integrin

Tetraspanins are highly conserved 4-transmembrane proteins with a small and a large extracellular loop (199). The latter accounts for dimerization and association with non-tetraspanin molecules (200, 201). Prominent partners are integrins, proteases, cytoskeleton, and cytosolic signal transduction molecules (202–205). Intracellular, juxtamembrane cysteine palmitoylation supports tetraspanin-tetraspanin web formation, protects tetraspanins from lysosomal degradation and provides a link to cholesterol and gangliosides, tetraspanins mostly acting as molecular facilitators for associated molecules (206–209). As mentioned, Tspan8 contributes to Exo biogenesis (210) and is upregulated in PaCIC and -TEX (211–214).

Tspan8-promoted PaCa migration, invasion, and progression (215–220) relies on the recruitment of additional CIC markers. Tspan8 associates with CD44v6 (213), which recruits cMET and VEGFR2[1] via CD44v6-bound HGF[1] and VEGF[1] (216, 221, 222), α6β1 and α6β4 (213, 223, 224), cldn7 and EpCAM (225–227). Some associations depend on the cells' activation state in particular α6β4 (228), a major hemidesmosome component in non-activated cells (229, 230). Upon association with Tspan8, integrins become activated and initiate downstream signaling (231, 232). The tight junction (TJ) component cldn7 (233, 234) only associates upon palmitoylation (234) and recruits EpCAM (235–238). Tspan8 also cooperates with proteases (239–241).

Tspan8/Tspan8-TEX engage in crosstalk with the tumor stroma and premetastatic niche tissue (210) and promote EC progenitor maturation and activation (147, 148, 242). The interaction with the ECM is initiated by Tspan8-associated integrins. Collagen crosslinking assists associated protease activation, which degrade collagen and LN (243). Tspan8-associated α6β4 binding to the LN332[1]-rich BM promotes tumor cell migration. Liberation of growth factors, chemokines and proteases deposited in the ECM supports tumor cell migration and distant organ settlement (157). TEX Tspan8-integrin and -protease complexes distinctly affect gene expression in different target cells. Tumor cells respond with vimentin, Snail[1], and Slug[1] expression. In FB proteases (ADAM17[1], MMP14, TIMP1, and 2[1]) are mainly upregulated (240). Bone marrow cells (BMC) respond with TNFα[1] upregulation and STAT4[1] activation. Lymph node cells (LNC) upregulate TNFα, TGFβ, and FoxP3[1] expression (240). TEX Tspan8-α4β1/α5β1 (147, 148) targeting EC/EC progenitors induce CXCL5[1], MIF[1], vWF[1], and CCR1[1] mRNA translation. The increase in mRNA after 1d−5d indicates induction of transcription (147). *In vivo*, EC/lymphatic EC respond with FGF2[1], VEGFR1, VEGFR2, and VEGFR3 upregulation (244).

In brief, Tspan8 contributes to tumor progression at different levels of the metastatic cascade. Tspan8 is engaged in TEX biogenesis and binding/uptake and acts by clustering integrins, RTK, and proteases, which facilitate downstream signaling (**Figure 3**).

The α6β4 integrin was one of the first genes described to be metastasis-associated (245, 246). It is expressed in several normal epithelia, Schwann cells and EC, the β4 chain being characterized by a long cytoplasmic tail (245). A6β4

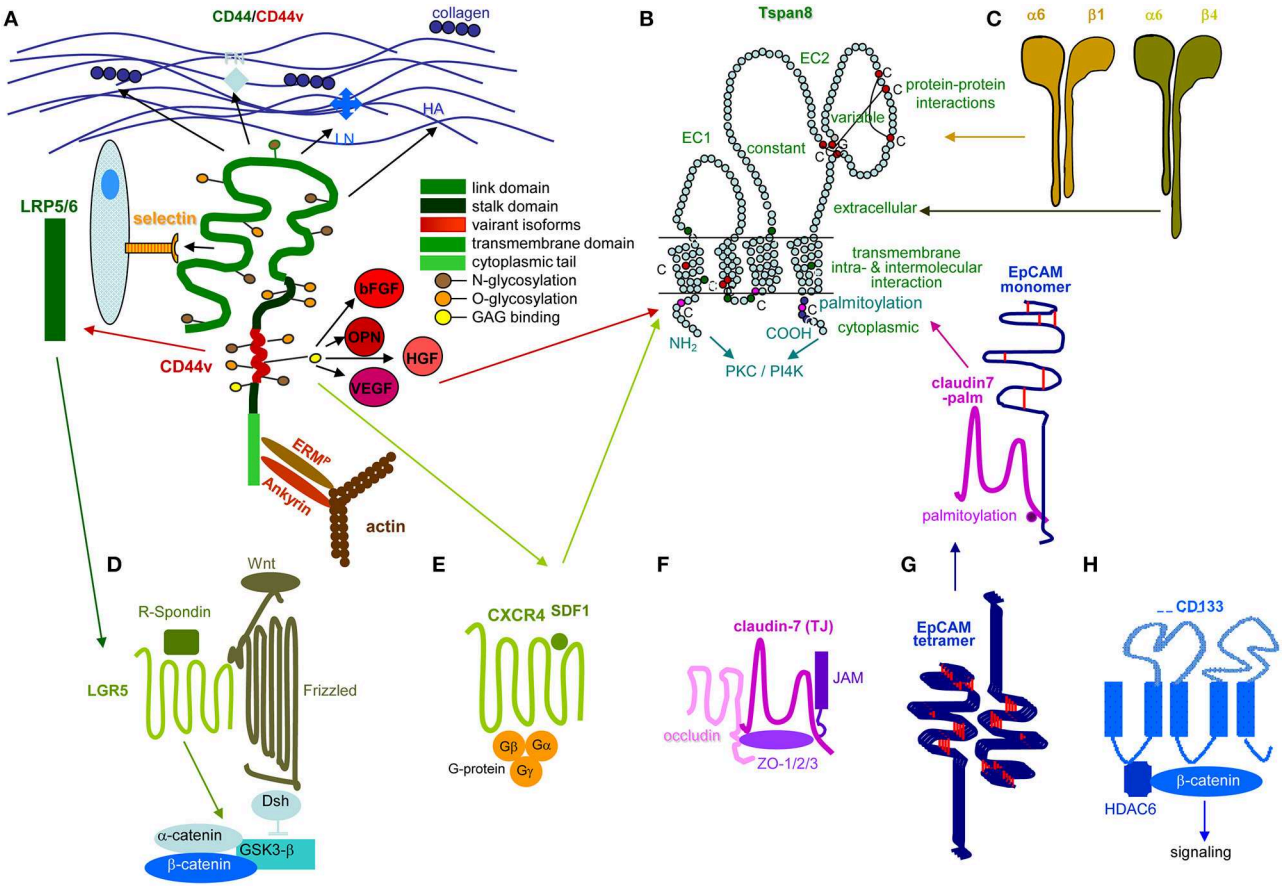

FIGURE 2 | Prominent PaCIC markers. **(A)** The lead PaCIC marker is CD44v6, a type I transmembrane protein that contributes to the crosstalk with the ECM via its link domain and the HA binding site. It has binding sites for selectins and LRP5/6. The v6 exon product carries binding sites for several growth factors. The cytoplasmic tail has binding sites for ankyrin and ERM proteins including merlin, which promote cytoskeleton association and downstream signaling. **(B)** Tspan8 is a tetraspanin with a small and a large extracellular loop, the latter mostly accounts for protein-protein interactions. The four transmembrane regions account for intramolecular and intermolecular interactions. The cytoplasmic tail binds PKC and PI4K. Main activities rely on the association with a large range of proteins. Dominant are integrins, but also CD44v6 and an EpCAM-cldn7 complex. **(C)** Particularly α6β4 is known as a PaCIC marker. Similar to other integrins, it binds matrix proteins, particularly LN. It is a major component of hemidesmosomes anchoring epithelial cells in the basal membrane. Upon activation, it leaves the desmosome complex and associates preferentially with Tspan8. It differs from other integrins by a long cytoplasmic domain of the β4 chain, which promotes multiple signaling pathways. **(D)** LGR5 is a seven transmembrane protein located close to frizzled. Upon R-spondin binding, it contributes via Wnt activation to ß-catenin liberation. LGR5 activity is supported by CD44v6-associated LRP5/6. **(E)** CXCR4 is another seven transmembrane protein. This GPCR becomes activated by SDF1 binding. It predominantly signals via trimeric G-proteins. CD44 crosslinking via HA promotes CXCR4 recruitment and strengthens activation of downstream signaling cascades. Activated CXCR4 also associates with Tspan8 **(F)** Claudin7 is a 4 transmembrane protein, which can be integrated in TJ, where it associates with other claudins, JAM, and occludin and the cytoplasmic zonula occludens proteins. Cldn7 is also recovered outside of TJ. Upon palmitoylation, it associates via a direct protein-protein interaction in the transmembrane region with monomeric EpCAM. The cldn7-EpCAM complex is recruited into TEM and associates with Tspan8. **(G)** EpCAM is a type I transmembrane protein of many epithelial cells. It forms tetramers, which promote homophilic binding to EpCAM on neighboring cells. It is engaged in signal transduction, predominantly via the liberated cytoplasmic tail that acts as cotranscription factor. **(H)** CD133 is a five transmembrane protein located in cholesterol-rich membrane domains. It is associated with HDAC6 that stabilizes a ternary CD133-HDAC6-β-catenin complex and β-catenin target activation, which present one of the signaling cascades initiated via CD133. The seven most prominent PaCIC markers belong to distinct protein families and exert non-related functions. Five of these molecules can become recruited into TEM, where they associate via weak, non-protein-protein interactions with Tspan8. This significantly expands the range of activities of TEM and TEM-derived Exo. Of note, all seven CIC markers contribute via different routes to maintain stem cell features.

binds to LN in the BM facilitating adhesion through the formation of hemidesmosomes, nucleating the connection between LN and cytokeratin intermediate filaments (247). Upon stimulation, hemidesmosomes are dismantled allowing leading edge migration (248, 249). Hemidesmosome disassembly is accompanied by α6β4 forming a complex with MST1R/RON[1], which interrupts its association with plectin (250). β4-linked activated ERBB2[1] associates with src[1], which initiates phosphorylation of the three components and signaling toward STAT3, which accounts for the breakdown of cell-cell junctions and initiation of invasion (251). Motility involves PI3K[1] catalytic subunit beta activation, proceeding via α6β4 promoted IRS1 and−2[1] phosphorylation (252), PI3K localization into lipid rafts or TEM (253, 254), or ERBB2/ERBB3 activation

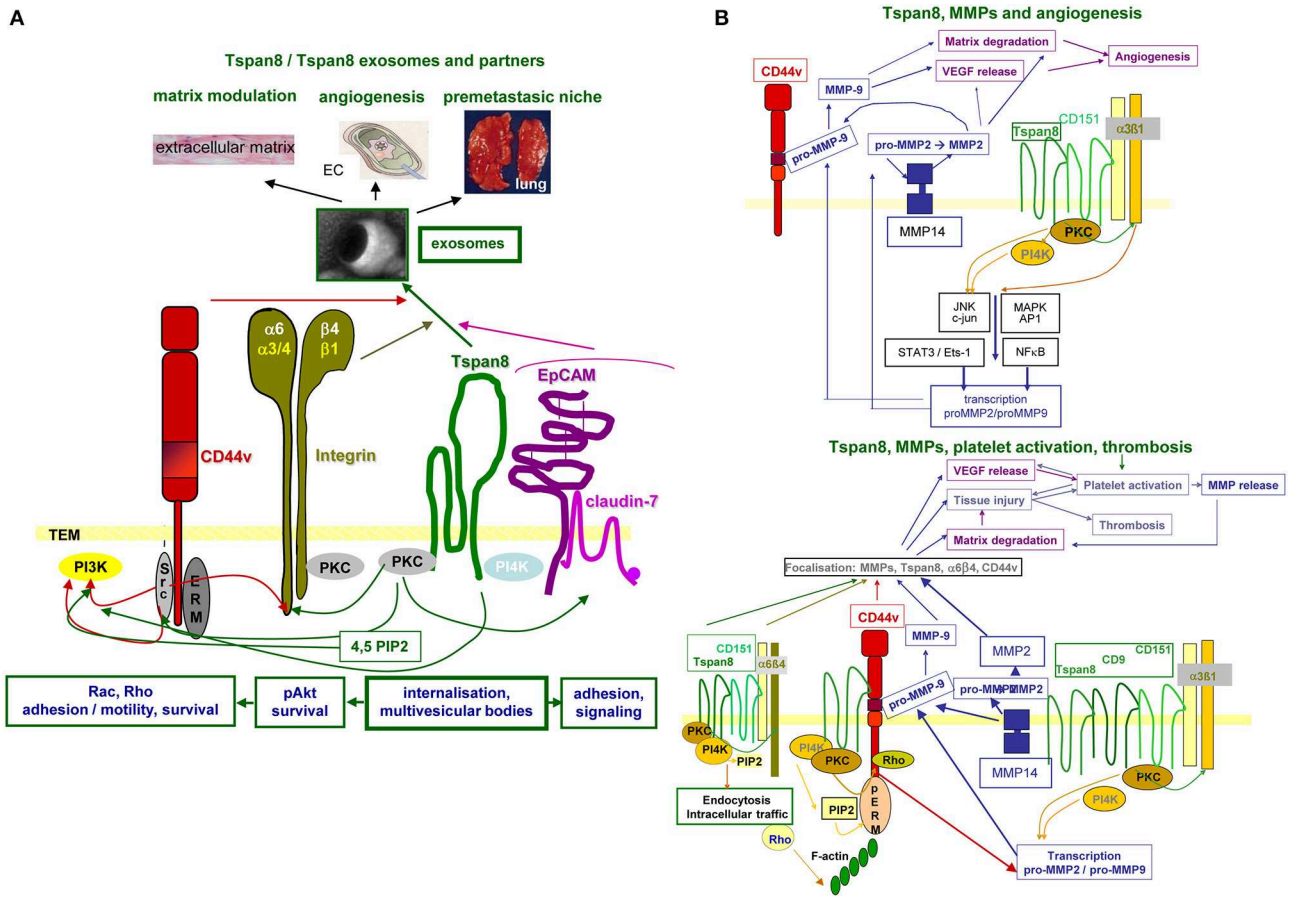

FIGURE 3 | Tspan8 promoted tumor progression. **(A)** Tspan8 acts as a facilitator. This accounts for membrane bound Tspan8, where it strengthens CD44v6, integrin, and cldn7palm/EpCAM complex signaling activity via its association with PKC and PI4K. This also holds true for the Exo-recruited TEM complex described to modulate the ECM, to promote or inhibit angiogenesis and to contribute actively to premetastatic niche formation. **(B)** Tspan8 is associated with MMP14 and the association of Tspan8 with α6β1 promotes, besides other the transcription of MMP2 and MMP9. Upon proform activation, also assisted by the proximity to CD44v6, matrix proteins become degraded and VEGF is released. VEGF, in collaboration with collagen degradation products, promotes angiogenesis. In addition, a complex between Tspan8, CD44v6, α6β4, and MMP is found in focal contact. The matrix degradation promoted tissue injury contributes to platelet activation and thrombosis, where together with the release of VEGF a positive feedback loop is created further pushing platelet activation and thrombus formation. Full name of proteins are listed in **Table S1**. With the multitude of Tspan8 associating molecules, we only present one example building on the association with MMP, which strengthens angiogenesis and thrombus formation. However, it should at least be mentioned that Tspan8 also associates with TACE, which strongly affect e.g., the delivery of the NOTCH and the EpCAM ICD, both acting as cotranscription factors.

(255, 256). RAC1 activation strengthens the formation of F-actin-rich motility structures by the cooperation of α6β4 with RTK (257). α6β4-increased cAMP-specific phosphodiesterase activity decreases cAMP and activates RhoA (258). FAK[1] regulates β4 tyrosine phosphorylation, which further promotes migration (259). Intravasation and extravasation are assisted by β4 cytoplasmic domain-dependent upregulation of VEGF enhancing transendothelial permeability (260). TEX Tspan8-α6β4 supports premetastatic niche preparations in the lung (92, 261).

β4 contributes to apoptosis resistance via tyrosine phosphorylation of the C-terminal segment of β4 by src family kinases downstream of RTK, but also by syndecan, which directly binds to the β4 cytoplasmic domain (262). Regardless of the initial signals, apoptosis resistance progresses by antiapoptotic PI3K pathway activation (263). TEX β4-vinculin complexes also cope with resistance toward a complex diterpene alkaloid, likely via plectin transfer by TEX (264).

Finally, α6β4 regulates transcription of invasion/metastasis-associated molecules by controlling promoter DNA demethylation. This was demonstrated for NFAT1[1] (265), which assists autotoxin expression, a motility factor stimulating lipoproteinA production (266). Metastasin1/S100A4[1] (267) spurs membrane ruffling via rhotekin (268), regulated through NFAT5 in conjunction with S100A4 promoter demethylation (269). S100A4 is also engaged in ERBB2 translation (270).

A6β4 is expressed on mature EC, a contribution to angiogenesis being disputed (271). Although reported to inhibit angiogenesis (148, 272, 273), α6β4 may be engaged in an early

stage of angiogenesis (274) via stimulating VEGF translation and signaling (275). The β4 C-terminal domain is important for responding to FGF2 and VEGF (276) and arteriolar remodeling is defective in β4 knockout (ko) cells due to altered TGFβ signaling (271).

Long-known as metastasis-associated, molecular pathways of α6β4 are not fully unraveled. Central are the signaling domain of the β4 tail and the dislodgement from hemidesmosomes. In PaCIC/-TEX, we consider the linkage to Tspan8 as a central coordinator (**Figure 4**).

CD44v6 and CD44v6-Associated Receptor Tyrosine Kinases

CD44v6, the alternatively spliced isoform of the adhesion molecule CD44 is a PaCIC marker involved in several steps of the metastatic cascade (277, 278). CD44, a type I transmembrane glycoprotein, varies in size by *N*- and *O*-glycosylation and insertion of alternatively spliced exon products between exons 5 and 6 of the CD44 standard isoform (CD44s) (279–281). CD44 belongs to the cartilage link protein family (282), the globular structure being stabilized by conserved cysteines (283). After the globular domain a heavily glycosylated stalk-like structure has putative proteolytic cleavage sites (284) and contains the variable exon products (285). The transmembrane region facilitates oligomerisation and recruitment into TEM, important for the interaction between CD44 and extracellular ligands and other transmembrane and cytoplasmic molecules (286). The cytoplasmic tail binds signaling and cytoskeletal linker proteins (287, 288). Most CD44s activities are maintained by CD44v.

CD44 has multiple ligands, which contribute to tumor progression. The link domain binds collagen, LN, FN, E-, and L-selectin (289, 290). CD44 has binding sites for glycosaminoglycans (GAG) and is the major HA receptor that binds to a basic motif outside the link domain (291–293). CD44v6 binds HGF, VEGF, and osteopontin (294–296). These associations are of central importance for its lateral associations with RTK. HGF binding brings CD44v6 into proximity with cMET and expedites cMET activation, which requires interaction between the CD44 cytoplasmic tail and ERM (ezrin, radixin, moesin) proteins for Ras[1]-MAPK[1] pathway activation (297). CD44v6-ECM binding also contributes to cMET transcription (298). Lateral association-initiated signal transduction also accounts for IGFR1[1] and PDGFR[1] (299). The HA crosslinking-initiated CD44 association with CXCR4 promotes SDF1 binding (300). The association with the low-density lipoprotein (LDL[1]) receptor-related LRP6[1] strengthened activation of the EMT-related Wnt[1] signaling pathway (301). Cytoplasmic tail-bound ankyrin contacts with spectrin support HA-dependent adhesion and motility (287). ERM proteins regulate migration, cell shape, and protein resorting (302, 303). The N-terminus of activated ERM proteins binds CD44, the C-terminus F-actin (304). Cytoskeletal linker protein binding expands the range of CD44-mediated downstream signaling pathways (303, 305), which can also proceed directly from TEM-located CD44v (306–308) or associated non-RTK (309, 310). The CD44/CD44v6-associated membrane-bound proteases MMP14 and Hyal2[1] (311) support tumor cell migration through matrix degradation and remodeling (312). CD44 contributes to drug resistance (313) by associating with ABC[1] transporters (314, 315) and additional antiapoptotic proteins (316, 317). Last, not least, the CD44 cytoplasmic tail (CD44ICD) moves toward the nucleus functioning as a cotranscription factor (318). Alternatively, the CD44v6 cytoplasmic tail can affect transcription by activation of signal-transducing complexes. With regard to the metastatic cascade, CD44v6 was described to directly or indirectly activate Tspan8, MMP9, MDR1[1], and NOTCH1[1] transcription (221, 319–321). Finally, CD44v6, but not CD44s, is engaged in loading ILV with miRNA (159, 322), which might rely on its association with Dicer (322) and contributes to tumor progression (323).

In brief, CD44v6 engages in EMT induction by supporting Wnt signaling and Nanog and Notch activation (324–326). It contributes to intravasation through binding and degradation via associated proteases. It supports extravasation by selectin binding to EC, allowing crawling toward EC-EC gaps. It assists tumor stroma formation and premetastatic niche preparation by HA, matrix-remodeling enzyme, cytokine, and chemokine provision (91, 327). Recruiting miRNA into ILV expands the range of TEX activities (322). A few of the many CD44v6 activities in tumor progression are shown in the accompanying figure (**Figure 5**).

CXCR4 and Its Association With Tspan8 and CD44v6

CXCR4 has been tied to tumor progression and poor prognosis (328, 329) and expression of its ligand SDF1 correlates with poor survival (97).

CXCR4 is expressed in BMC/-precursors, lymphocytes, resident macrophages (Mϕ), EC precursors, FB, and CIC. CXCR4 is a seven transmembrane GPCR (330), transcription increasing in response to several signaling molecules such as cyclic AMP, some cytokines including TGFβ and the growth factors FGF2 and VEGF (331). Upon ligand binding, CXCR4 undergoes a conformational change activating the intracellular trimeric G protein leading to the Gαi dissociation, which stimulates src, Ras/Raf[1]/MAPK (332) and PI3K pathways (331, 333). Gβγ triggers PLC, which catalyzes PIP2 into IP3 and DAG leading to Ca++ mobilization and PKC[1] and MAPK activation (334). CXCR4 also triggers a G-protein-independent pathway (335) promoting recruitment of GRK2[1] that phosphorylates the C-terminus resulting in β-arrestin association. CXCR4 thereby uncouples from G proteins and becomes internalized (336, 337). GRK2 is supported by PKC, PKA, and src (338). β-arrestin serves as a scaffold for downstream signaling promoting ERK/MAPK1 and p38/MAPK14 activation (339). Proper folding depends on HSP90, a chaperone for members of the CXCR4 phosphorylation cascade (340). Colocalization of these complexes in cholesterol-enriched lipid rafts (341) facilitates signal transfer (342).

CXCR4 contributes to tumor progression at multiple levels. CXCR4 sustains proliferation through direct activation of MAPK, PI3K, Wnt, and HH[1] signaling (343), where HH additionally induces SDF1 expression in the tumor surrounding (344) and activation of the intrinsic anti-apoptotic pathway

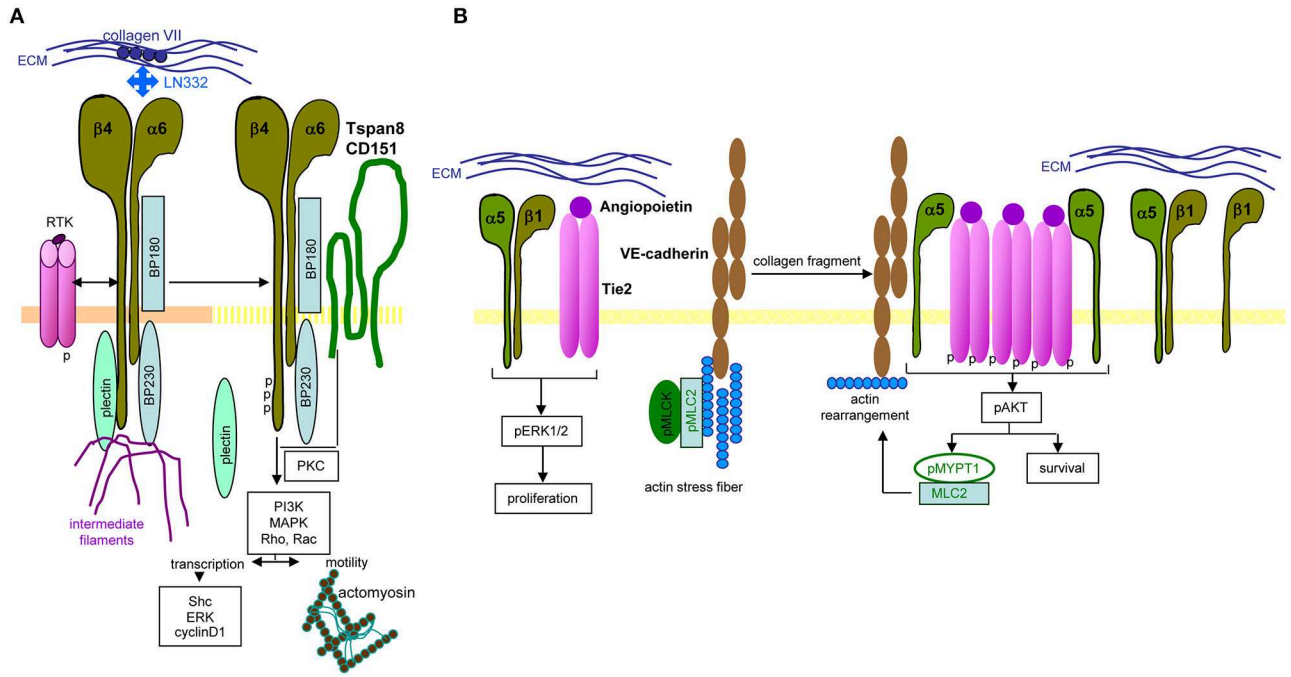

FIGURE 4 | Distinct integrin signaling in PaCIC. **(A)** Hemidesomosome-integrated α6β4 is associated with BP160/320 and plectin, the complex being linked to intermediate filament. Upon contact with RTK, the β4 cytoplasmic tail becomes phosphorylated, plectin is released from the complex and phosphorylated β4, supported by Tspan8-associated PKC promotes PI3K, MAPK, Rho, and RAC activation. Besides initiating transcription, the complex assists the association with actomyosin and motility. **(B)** Instead, when α5β1 associates with angiopoietin-activated Tie2, proliferation is initiated via ERK phosphorylation. In the presence of VE-cadherin, linked to actin stress fibers, pMLCK, and pMLC2 collagen fragments initiate actin rearrangement that promotes dissociation of the α5 from the β1 chain, which enclose phosphorylated Tie2. The phosphorylated Tie2 promotes Akt phosphorylation, which supports MYPT1 phosphorylation and MLC2 association that evoke actin rearrangement. Full name of proteins are listed in **Table S1**. In brief, only parts of integrin-mediated activities are affected by the association with Tspan8. Notably, the same stimulus distinctly affects integrin activation depending on the α or β chain of the integrin.

via ERK and Akt[1] (344, 345). CXCR4 assists invasion, HH signaling being associated with EMT and loss of adhesion (344). SDF1 increases MMP2, MMP9, and urokinase expression (346, 347). Particularly in PaCa, CXCR4 expression is linked to a subpopulation of migrating, metastasis-promoting PaCIC (348) that is highly chemotherapy resistant (349–351).

The involvement of CXCR4 in tumor progression is not restricted to tumor cells. EC respond to HIF1α[1] with CXCR4 upregulation (352). The SDF1-CXCR4 axis enhances VEGF and MMP production through ERK and Akt signaling (353), which promotes EC migration and capillary tube formation (354). Activated PSC (aPSC) promote SDF1 secretion, which binds to EC CXCR4 and is supported by PAUF[1]. SDF1 together with VEGFC also attracts lymphatic EC (354). Furthermore, tumor stroma cell-secreted SDF1 assists CXCR4 activation in tumor cells and CXCR4-induced HH expression stimulates CAF recruitment (344). By stimulating IL6[1] production, CXCR4 assists TAM recruitment (343) and mast cell recruitment and activation. Mast cells release IL13, which activates PSC, further promoting tumor growth (355). Other CXCR4-recruited immune cells force CXCR4 expression via IFNγ creating a positive feedback loop (356). The link between high CXCR4 expression and bone metastases relies on circulating tumor cells passing through the bone vessels, hematopoietic and mesenchymal progenitors highly expressing SDF1 (357). Another CXCR4 ligand is SDF1-associated HMGB1[1], which is also a ligand for AGER (358) and TLR2, 4, and 9[1] (359, 360). SDF1/HMGB1 complex binding to CXCR4 promotes inflammatory cell recruitment (361) (**Figure 6**).

In 2007, a first series of reviews pointed out the special role of CXCR4 in subpopulations of migrating/metastasizing CIC (348, 362, 363). Great progress over the last decade extended original findings toward the involvement of tumor stroma and EC. Although the extent of CXCR4 heterocomplex engagement in leukocyte recruitment awaits further exploration (364), based on promising results, great efforts are taken toward therapeutic translation (100, 365, 366).

Claudin7 and EpCAM

Claudins, including cldn7, are a four-pass proteins, which are the central TJ components (232, 367). TJ are found in epithelial and endothelial cells, cldn7 expression being particularly high in the gastrointestinal tract and lymphatic vessels (368). TJ, composed of the transmembrane proteins occludin, JAM and cldn, linked to zonula occludens proteins (ZO[1]), are located in the most apical lateral region of cell-cell contact sites (367). The transmembrane proteins are laterally linked via claudins,

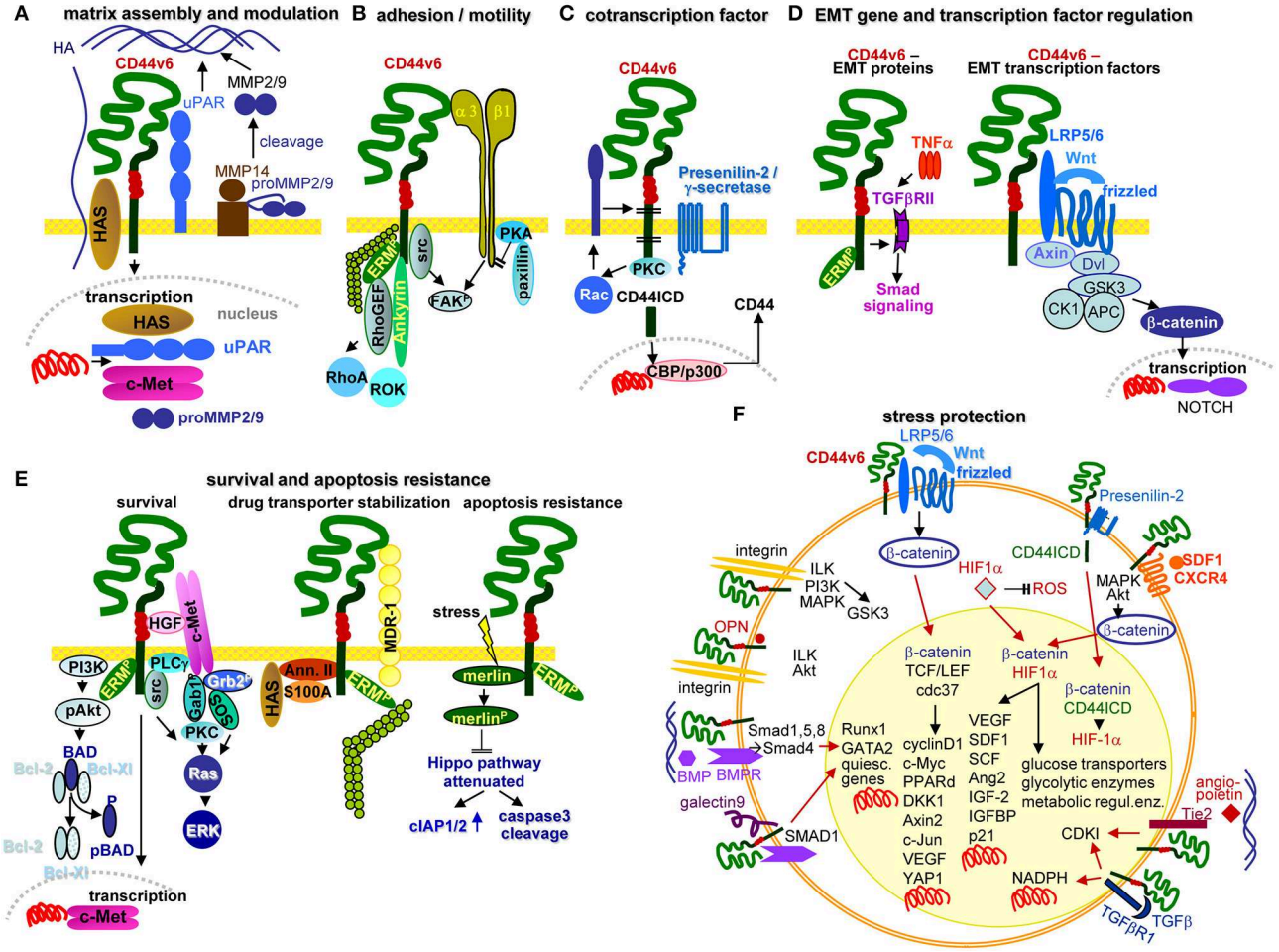

FIGURE 5 | Multifaceted activities of CD44v6 in PaCIC. **(A)** Upon HA crosslinking, CD44v6 initiates HAS, uPAR, MMP2, and MMP9 transcriptions, which promote HA assembly and matrix remodeling, where MMP14 contributes to proMMP2 and MMP9 cleavages. **(B)** CD44v6 can associate with α3β1 such that both molecules jointly contribute to FAK activation and motility. **(C)** CD44v6 can be cleaved by TACE and subsequently by the presenilin2 complex. The CD44ICD acts as a cotranscription factor, which together with CBP/p300 promotes CD44 transcription **(D)** By TNFα associating with TGFβRII, EMT protein expression is supported via Smad signaling. The association of CD44v6 with LRP5/6 supports Wnt/frizzled activation such that β-catenin leaves the suppressive complex and acts as cotranscription factor in NOTCH transcription. **(E)** There are several pathways whereby CD44v6 strengthens PaCIC survival and apoptosis resistance. cMET comes into proximity of CD44v6 via CD44v6-bound HGF. This initiates activation of the PI3K/Akt anti-apoptotic and of the Ras-ERK pathways. In addition, CD44v6 supports cMET transcription. A complex of CD44v6 with HAS, Annexin II, S100A, and activated ERM stabilizes MDR1 expression, which contributes to drug efflux. Finally, stress induces the association with and dephosphorylation of merlin, which attenuates the HIPPO pathway with upregulation of cIAP1/2 and caspace3 cleavage. **(F)** Some of the multiple activities of CD44v6 in stress protection via affecting the cells metabolism are summarized indicating whether altered metabolism is promoted by signaling cascades in the cytosol or depends on transcriptional activation (red arrows). The latter accounts particularly for β-catenin-TCF/LEF, β-catenin-HIF1α, and β-catenin-CD44ICD complexes, but also for the cooperation of CD44v6 with Tie2, TGFβR1, galectin 9, and BMPR, which affect transcription of a large range of distinct genes. Full name of proteins are listed in **Table S1**. CD44v6 is engaged in most steps of the metastatic cascade. The strongest impacts are seen in terms of survival, EMT induction and metabolic changes that guarantee unimpaired survival under hypoxic and poor nutrient conditions.

and tightly associate with TJ on opposing cells (369). TJ seal the organism from the outside and are involved in paracellular transport (370). The latter is determined by the polarity of the β-sheet of the extracellular loops of cldn, which differs between individual cldn and is adjusted to selective organs' demands (371). Both barrier and channel functions of TJ-integrated cldn are vital. Cldn7ko mice die within 10 days after birth due to gut destruction that might rely on a missing association with integrins and strong MMP3 upregulation or on enhanced paracellular influx of colonic inflammation-inducing bacterial products (372, 373). Apart from sealing and paracellular transport (370, 371, 374–376), few reports explore cldn-Exo/TEX activities. It was recently realized that a comparably large amount of continuously remodeled TJ components is recovered insight the cell and at distinct membrane locations (377–379). TJ remodeling rests on claudins being PKA, PKC, and MLCK[1] targets, cldn phosphorylation prohibiting TJ integration (380–385). Furthermore, TJ formation depends on sphingomyelin with long-chain fatty acids and cholesterol enrichment in membrane subdomains, cholesterol depletion affecting cldn

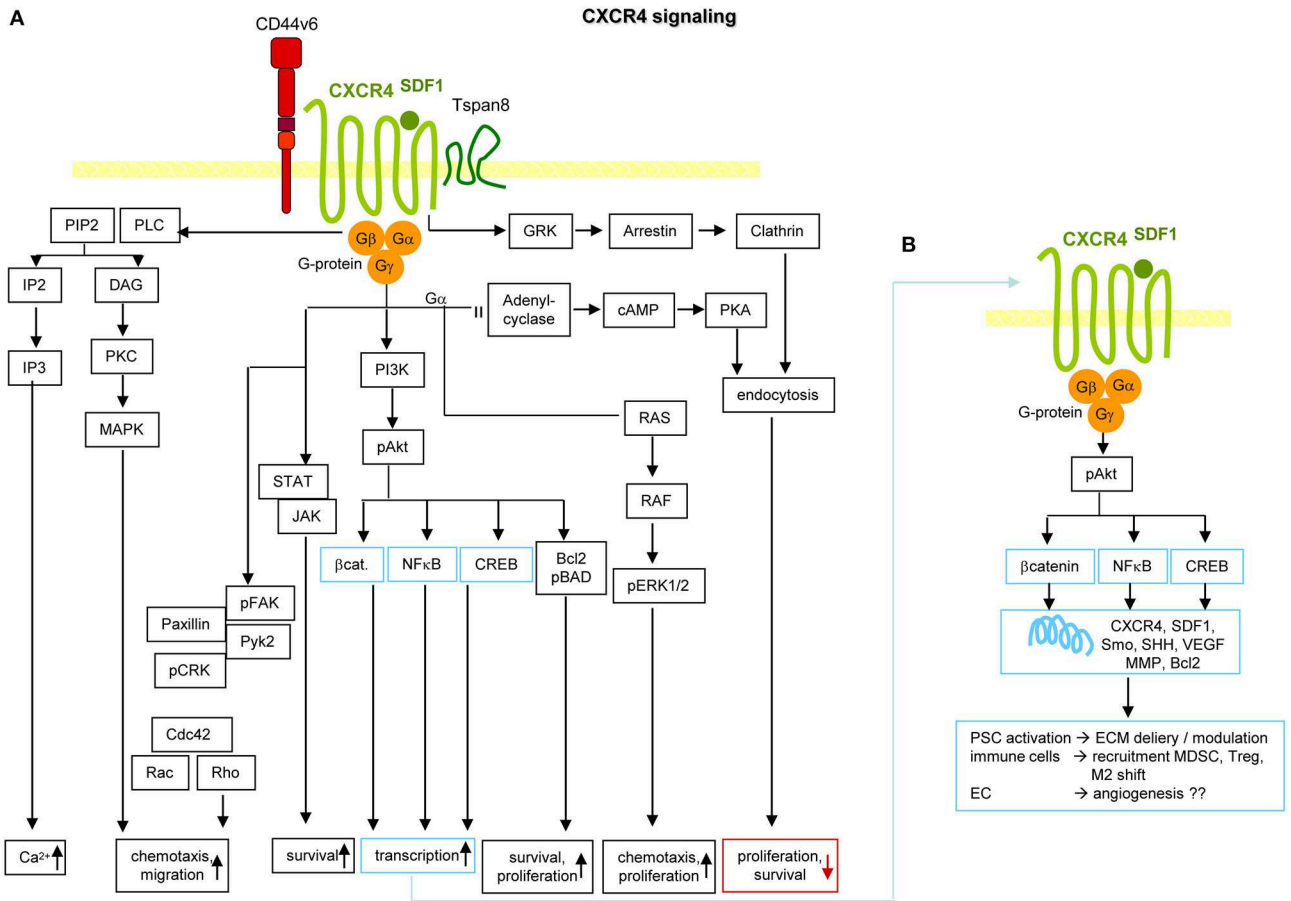

FIGURE 6 | CXCR4 and PaCIC survival and motility. **(A)** CXCR4 is a G-protein coupled receptor (GPCR) that in PaCa is mostly recovered in association with CD44v6 and/or Tspan8. Activation is initiated by binding of its ligand SDF1. Signals are transferred via the G protein subunits, which promote Ca2+ influx, and either via MAPK or Rho chemotaxis and migration. Chemotaxis and proliferation can also proceed via the Gα, Ras, Raf, pERK1,2 activation route. Activation of PI3K/Akt, Bcl2/pBAD promotes proliferation and survival. The latter is also supported by activation of the STAT-Jak pathway. PI3K/Akt can also initiate activation of transcription factors. Independent of the trimeric G-protein complex, CXCR4 associates with GRK, arrestin and clathrin. The complex becomes internalized, which is accompanied by reduced proliferation and survival. **(B)** Activation of β-catenin, NFκB and CREB supports transcription of CXCR4, SDF1, Smo, SHH, VEGF, MMP, and Bcl2. These genes are important in PSC activation, recruitment of immunosuppressive MDSC and Treg and the shift of M1 to M2 and in supporting angiogenesis, which may not be dominating in PaCa. Full name of proteins are listed in **Table S1**. It should be noted that the dominant activity of CXCR4 in promoting chemotaxis and motility covers only one, not essentially dominating feature in PaCIC.

integration and abolishing TJ formation (386). Finally, cldn7 is also located in the plasma membrane outside of TJ. Cldn7 palmitoylation is a precondition for partitioning into TEM, where palmitoylated cldn7 associates with EpCAM and tetraspanins (234, 387).

Internalized, TJ-derived cldn can be degraded, recycle or integrate into EE and, after passage through MVB, into Exo. In fact, TEM-located, palmitoylated and EpCAM-associated cldn7 is exclusively recovered from apical plasma membrane derived TEX (388, 389). In organoids, a second population of cldn7+/EpCAM- TEX is delivered at the basal membrane (389), which might derive from internalized TJ, facilitated by the high cholesterol content. Intracellular vesicle traffic remains to be defined (378). Alternatively, Exo-recruitment during biogenesis is not excluded (390) and would be consistent with pronounced coimmunoprecipitation of cldn7 with Golgi-endoplasmic reticulum (ER) transporters (391).

Pinpointing the activity of cldn7 in the metastatic cascade is difficult. Palmitoylated, EpCAM-associated cldn7 might favor signaling by supporting EpCAM cleavage and EPICD cotranscription factor activity in EMT. However, it is hard to demarcate from support by other TEM-located CIC markers. TJ-integrated and phosphorylated cldn7 is associated with a wide range of transporters, which likely impacts altered metabolism and signal transduction of CIC (**Figures 7A,C**). These options await untangling exploration.

The epithelial cell adhesion molecule EpCAM, overexpressed in many epithelial cancer, serves as diagnostic and therapeutic target (392). EpCAM mediates homophilic cell-cell adhesion (393, 394) and fulfills condition-dependent distinct functions (395). An initial, straight-forward explanation that oncogenic

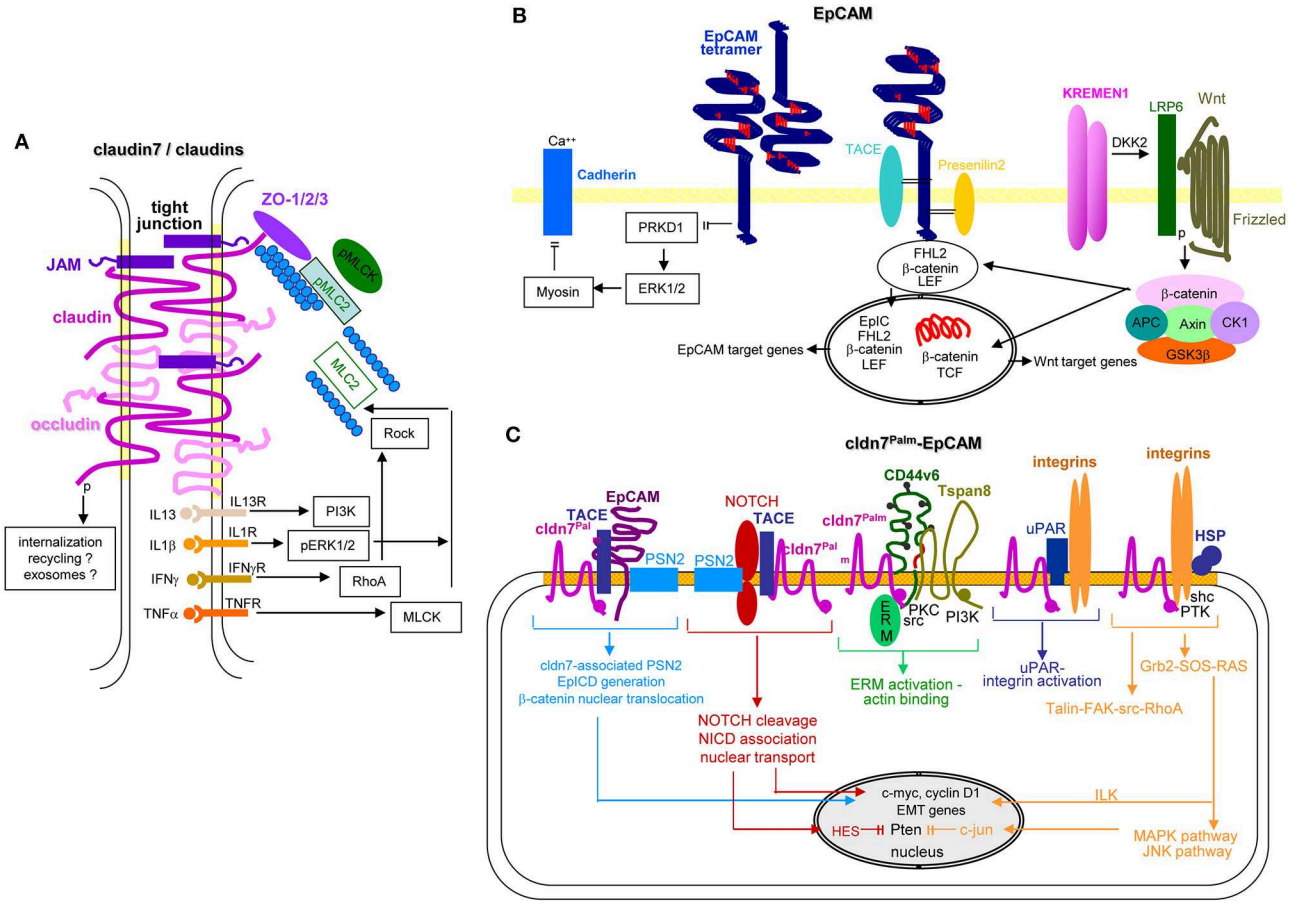

FIGURE 7 | EpCAM, claudin7 and their cooperation in PaCa. **(A)** In tight junctions, cldn7 is associated with additional cldns, occludin, JAM, and ZO1, 2, and 3, the latter being associated with pMIC2 and the cytoskeleton. Upon stimulation by several cytokine receptors, PI3K, ERK, RhoA/Rock, and MLCK promote MLC2 dephosphorylation, which promotes reorganization of the cytoskeleton with consequences on the cldn associated transporter activity. A stress response provokes internalization of the TJ complex. It is suggested that the internalized complex may be partly digested, recycle and become integrated into Exo. **(B)** EpCAM form tetramers, which with low affinity bind to EpCAM tetramers on neighboring cells and concomitantly prevent PRKD1 activation that leads to ERK1/2 and myosin activation, which inhibits Ca++-dependent Cadherin adhesion. Alternatively, EpCAM becomes cleaved by TACE and subsequently by PSN2. The cotranscription factor EpICD becomes supported by LEF and ß-catenin that might derive from Kremen1-DKK2-LRP6 promoted Wnt-Frizzled activation. This transcription factor complex mostly supports EpCAM and Wnt target gene expression. **(C)** Palmitoylated cld7 associates with monomeric EpCAM. As cldn7 is associated with PSN2, EpICD generation is augmented. Palmitoylated cldn7 may also contribute to NICD generation that acts as cotranscription factor. In association with CD44v6 and Tspan8, cldn7palm associates with ERM and contributes to ERM activation and actin binding. In association with uPAR and integrins it promotes both uPAR and integrin activation. Finally, a cldn7Palm-integrin-HSP complex assists talin-FAK-src-RhoA activation and by activation of the Grb2-SOS-RAS pathway ILK and the MAPK-JNK pathway. EpICD, NICD, and ILK contribute to c-myc, cyclinD1 and EMT gene transcription; NICD via HES and c-jun interfere with Pten transcription. Full name of proteins are listed in **Table S1**. Thus, TJ cldn7 is important particularly in lipid transport and cytoskeleton organization, EpCAM by promoting oncogenes and EMT genes, which also accounts for cldn7Palm-associated EpCAM. Cldn7Palm additionally contributes to Pten silencing.

and tumor progression supporting EpCAM activities rest on interfering with E-cadherin-mediated adhesion required revisiting, when it was realized that EpCAM can be cleaved by TACE and subsequently presenilin1, which generates EpICD (396). EpICD functions together with TCF/LEF[1] as a cotranscription factor for MYC, cyclinA/E, Oct4[1], and Nanog amongst others (397, 398). EpICD is also engaged in hypermethylation and activation of BMP[1] promoters (399) and can promote EMT through increased Slug and PTEN/Akt/mTOR[1] signaling pathway activation (400) and engagement in Wnt signaling. PKC downregulation and MMP7 upregulation backs EpCAM-promoted motility (401–406). Indicating its regulatory effect on another major pathway, EpCAM silencing reduces Ras/Raf/ERK signaling (407). However, EpCAM expression is transiently downregulated during EMT (401, 408, 409), which could argue for EpCAM prohibiting tumor cell dissemination (410, 411). Nonetheless, strong overexpression on embryonic SC endorses a contribution to pluripotency maintenance (412, 413).

EpCAM expression is epigenetically regulated. High EpCAM expression correlates with hypomethylation of a fragment of exon 1 and the proximal promoter, lack of EpCAM

expression correlates with methylation at a proposed Sp1 binding site (414, 415). Furthermore, activating histone modifications acH4[1], acH3[1], and H3K4me3[1] correlate and repressive histone modifications H3K9me3[1] and H3K27me3[1] inversely correlate with EpCAM expression (413, 416, 417). Additionally, EpCAM regulation by ncRNA might be relevant to the crosstalk between TEX and targets. LncRNA LINC00152 activates mTOR through binding to the EpCAM promoter region (418). Furthermore, miR-150, miR-155, miR-181, and miR-223 expression is increased in EpCAM+ hepatocellular carcinoma (HCC). MiR-155 contributes to EpCAM-promoted migration and invasion (419) and miR-29b to proliferation and inhibition of liver progenitor cell differentiation (418). Since miR-16-5p, miR-23a-3p, miR-23b-3p, miR-27a-3p, miR-27b-3p, miR-30b-5p, miR-30c-5p, and miR-222-3p are high in EpCAM+ colorectal cancer (CoCa) TEX, an EpCAM-dependent recruitment is discussed (420).

In brief, possibly due to abundant expression in most epithelial cells and upregulated expression in many primary tumors, the CIC features of EpCAM are more difficult to define than originally expected. Notwithstanding, EpICD contributes to the metastatic process by acting as a cotranscription factor. We personally interpret the transient downregulation during EMT as evidence for EpCAM not contributing to intravasation, intravascular traffic or extravasation. Expression during settlement of migrating tumor cells in distant organs could indicate a share in premetastatic niche preparation (**Figures 7B,C**). An interpretation of EpCAM regulation by lncRNA and miRNA might be premature.

LGR5

The leucin-rich repeat containing GPCR-5 (LGR5[1]) is a Rhodopsin GPCR, expressed in adult SC and best explored in intestinal SC and CIC (421). Secreted Wnt proteins interact with the Wnt receptor complex consisting of Frizzled and LPR5/6. Wnt binding sustains dissolving the downstream destruction complex and liberated β-catenin acts together with TCF/LEF as Tf (422). LGR5 is one of the targets of TCF4[1] (423), which regulates Wnt signaling. In the absence of Wnt, Frizzled, LPR5/6 and the RING-type E3 ubiquitin ligases RNF43[1] and ZNRF3[1] form a complex, which promotes Frizzled ubiquitination and degradation. Upon soluble R-spondin binding to LGR5, RNF43 becomes phosphorylated and sequestered generating a more stable complex between R-spondin, LRP5/6, and Wnt-Frizzled, which promotes β-catenin liberation (424, 425). This suggests LGR5 elimination hampering tumor progression. LGR5 elimination transiently retarded local tumor growth, possibly reflecting CIC plasticity, where differentiated cells can revert to LGR5+ CIC. Instead, metastatic growth was enduringly inhibited (426, 427).

Briefly, by regulating Wnt signaling, LGR5 is important for CIC maintenance and thereby tumor progression (**Figure 8**).

CD133

CD133 (Prominin1) is a hematopoietic SC and CIC marker in many malignancies (428, 429), high expression being associated with poor prognosis (430). CD133 is a 5-transmembrane molecule in protruding membrane subdomains, where it interacts with cholesterol-based lipid rafts (428, 431). CD133 contributes to cell polarity, cell-cell and cell-ECM interactions (432) and signaling cascade activation (433). Expression is enhanced by binding to HDAC6[1] that stabilizes β-catenin in a ternary CD133-HDAC6-β-catenin complex promoting β-catenin target activation. Loss of CD133 is accompanied by reduced SLUG, LAMC1[1], and MMP7 expression and a shift toward MET (434). CD133 activity is regulated by the tyrosine phosphatase receptor PTPRK[1], which dephosphorylates tyrosines 828 and 852. Low PTPRK expression in patients with cancer is associated with pronounced AKT activation and poor prognosis (435).

CD133 interferes with CIC differentiation by suppressing NTRK2 via p38MAPK and PI3K signaling (436). A CD133kd is also accompanied by a strong decrease in invasion and TIMP2 expression, the pathway remaining to be explored (437). CD133 affects migration via Akt or src activation and FAK phosphorylation (438, 439). A suggested engagement in drug resistance might proceed via CD133 directly interacting with PI3K-p85, resulting in multidrug resistance (440). Finally, neighboring cells support CD133 activities, e.g., EC secrete a soluble form of Jagged1[1] promoting Notch activation (441).

According to the location in internalization-prone rafts, CD133 is recovered in Exo/TEX (442–444). CD133 intracellular traffic follows an ESCRT-independent pathway and requires ceramide, neutral sphingomyelinases and the sphingosine-1 phosphate receptor S1PR1[1], confirmed by reduced MVB formation upon expulsion of S1PR1 by α-synuclein[1] (445, 446). The expected CD133-TEX contribution to intercellular communication requires exploration (107). However, endosomal CD133 at the pericentrosomal region captures GABARAP[1], an initiator of autophagy. This prevents GABARAP from mediating ULK1[1] activation and autophagy, whereby pericentrosomal CD133 sustains CIC undifferentiated state maintenance (447).

CD133 shares with several metastasis-associated markers the recovery in SC and CIC. It is engaged in CIC maintenance, Wnt/β-catenin signaling and contributes to migration and invasion, molecular mechanisms being not fully elucidated.

CIC Markers, Stemness, and EMT

Before summarizing the importance of PaCIC markers in tumor progression, we need commending on the linkage between CIC and EMT. Partial activation of the embryonic EMT program was considered a central feature of CIC and a prerequisite for metastasis formation (5). This was recently questioned for PaCa, where the EMT-related Tf Snail and Twist do not contribute to PaCa metastasis, but promote proliferation (448). On the other hand Notch2 and its ligand Jagged-1 are highly upregulated in drug-resistant PaCa cells and a NOTCH2 kd is associated with a partial reversion of the EMT phenotype with decreased vimentin, ZEB1, Slug, Snail, and NFκB expression (449). A more recent publication, describing ZEB1 being essential for PaCa progression, offers a plausible explanation, proposing context-dependent complementary subfunctions of distinct EMT-related

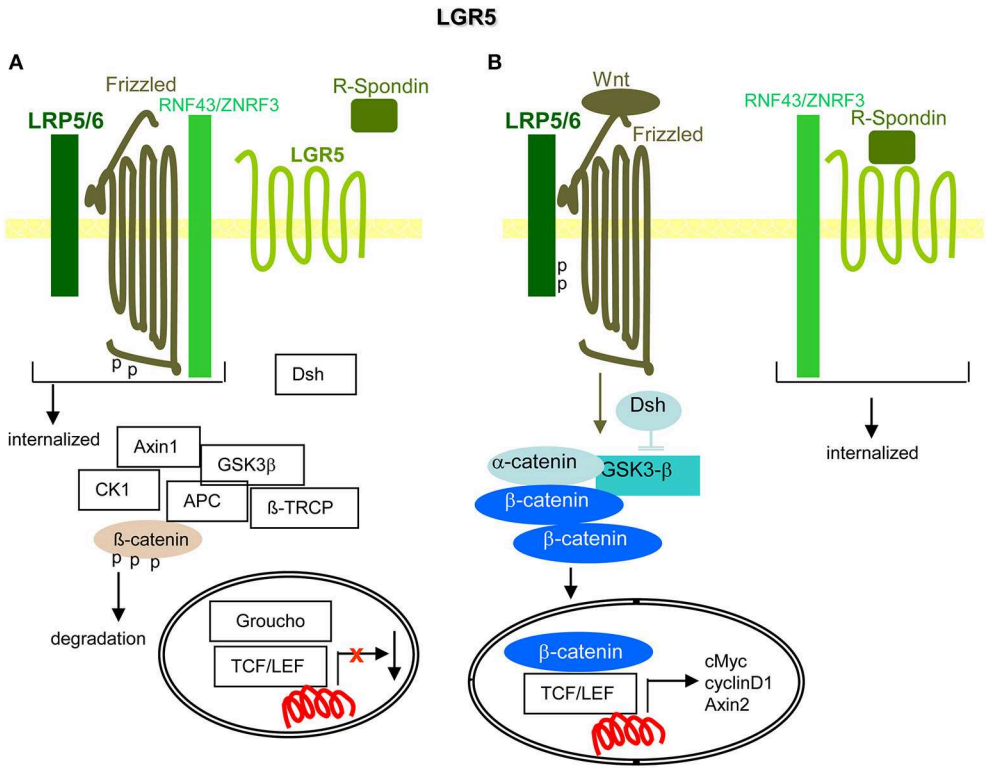

FIGURE 8 | LGR5 and the contribution to PaCIC maintenance. **(A)** The leucine-rich repeat-containing GPCR is engaged in Wnt signaling. Its ligand is R-Spondin. In the absence of R-Spondin, the transmembrane E ligases RNF43/ZNRF3 associate with Frizzled and LRP5/6 that leads to Frizzled phosphorylation and internalization of the complex. **(B)** However, in the presence of R-Spondin, RNF43/ZNRF3 is recruited toward LGR5 such that Wnt can bind to Frizzled and LRP5/6 becomes phosphorylated. Dsh blocks GSK3-β and β-catenin is liberated to move to the nucleus, where it together with TCF/LEF promotes cMyc, cyclinD1, and Axin1 transcription. Full name of proteins are listed in **Table S1**. The upregulated expression of LGR5 in PaCIC suggests its engagement in PaCIC maintenance.

Tf (450). Thus, the suggestions of CIC stemness and (partial) EMT requirement in supporting tumor progression, are not yet unambiguously answered (5). Taking the frequently unimpaired growth of the primary tumor mass and of established metastases after therapeutic trials to deplete CIC markers and/or selected Tf, we expect that both stemness markers and partial EMT greatly facilitate tumor progression.

Despite remaining open questions, we want to close this chapter with a personal experience, dating back to 1978, where a local tumor and ascites of a spontaneously arising PaCa were isolated from a rat (451). After subcutaneous transfer, rats receiving local tumor tissue developed local tumors, but not metastases. Rats receiving ascites did not develop a local tumor, but metastases in draining and distant lymph nodes and became moribund due to thousands of miliary lung metastases (452). The local tumor does not, the metastasizing tumor expresses all previously listed PaCIC markers (453). While overexpression of CD44v6, Tspan8, β4, EpCAM, and cld7 supported selective metastasis-associated features, but not the full-fledged metastatic profile (242, 454–457), a kd of each of these markers was accompanied by loss or strongly reduced metastasis formation (240, 388, 458, 459). CIC being unknown at that time, our "blind" studies may convincingly demonstrate the strong impact of CIC markers in tumor progression, their interdependent activities, and importantly, the requirement for a tumor-host crosstalk, the topic of the following chapters.

STROMA DYSPLASIA IN PANCREATIC CANCER

PaCa is characterized by an exuberant desmoplastic stroma reaction (DR) that may occupy far more space than the tumor cells, which form small nodules embedded in the dense DR (460). The DR is composed of ECM proteins, PSC, FB, EC, immune cells, and neurons (461).

PSC, quiescent in the healthy pancreas, are located in the basolateral region of acinar cells (462, 463). They are characterized by GFAP[1], desmin, vimentin, nestin, NGF, and NCAM[1] (464). During pancreatic injury, PSC develop a myofibroblast phenotype expressing αSMA[1], actively proliferate and migrate. Activation of PSC is promoted by TGFβ, HGF, FGF, EGF, and sHH[1] (465) (**Figures 9A,B**).

Activated PSC (aPSC) modulate the tumor matrix. They secrete ECM proteins including collagen I, III, and IV, FN and LN (464). Matrix deposition is supported by epithelial cell secreted SERPINE2[1], which activates PSC resulting in enlarged ECM protein deposits (466). PSC secrete MMP2, MMP9, MMP13,

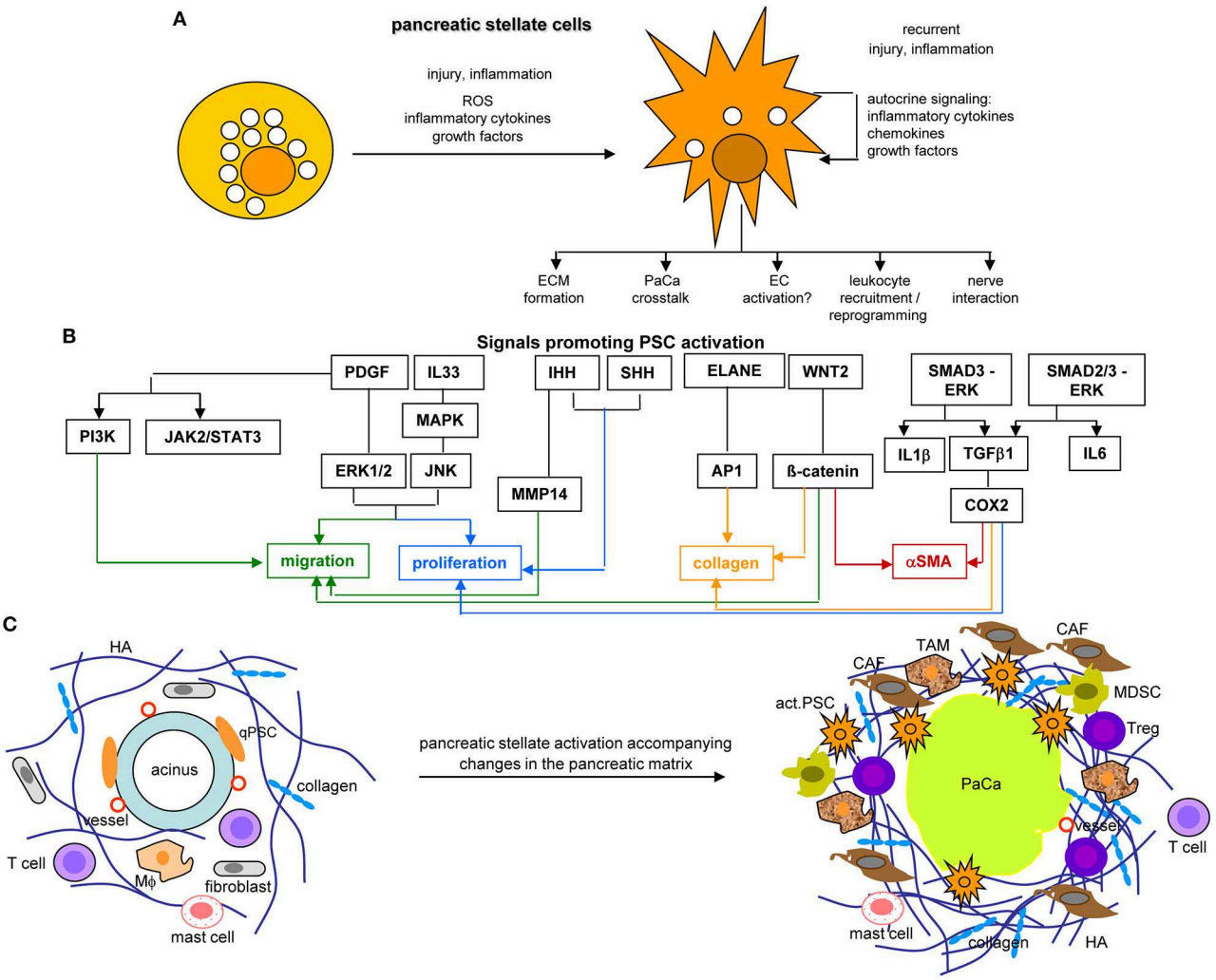

FIGURE 9 | The core position of pancreatic stellate cells in the dysplastic stroma reaction in PaCa. **(A)** PSC abundantly contain lipid droplets and lay close to the acinar cells in the healthy pancreas. They become activated by injury or inflammation, with a contribution of inflammatory cytokines, growth factors and ROS. Recurrent injury promotes autokrine signaling with further provision of growth factors, inflammatory cytokines, and chemokines. They partly loose the lipid droplets and become dispersed throughout the pancreatic stroma, where they affect the ECM, PaCa cells, leukocytes, and nerves. **(B)** Main factors contributing to PSC activation are PDGF and IL33 that assist proliferation and migration, Wnt2-β-catenin and IHH-MMP14 also contribute to the migratory phenotype and IHH-/SHH-Cox2 to proliferation. ELANE-AP1, Wnt2-β-catenin, and Smad3-ERK-TGFß1-Cox2 support collagen secretion, the latter two also support αSMA expression. **(C)** PSC activation is accompanied by the generation of a very dense ECM rich in HA and collagen, the recruitment of CAF, TAM, MDSC, and Treg, but a paucity of T cells in the dense ECM. Finally, they are engaged in a most intense crosstalk with the PaCa cells. Full name of proteins are listed in **Table S1**. PSC become activated at an early stage of PaCa initiation. Signals promoting PSC activation contribute to PSC collagen and αSMA expression, proliferation, and migration. aPSC are supposed to account for the ECM formation, to crosstalk with the tumor cells, to recruit and reprogram of leukocytes and to interact with the intrapancreatic nerves, some of these activities are detailed in the following figures.

TIMP1, and TIMP2, which account for matrix modulation (467–470). aPSC also affect immune cells. They express TLR2-5, required for non-adaptive immune cell activation (471), but also TLR9, which is protumorigenic via CCL11. CCL11 recruits regulatory T-cells (Treg) and promotes myeloid-derived suppressor cell (MDSC) proliferation (472). aPSC express MHCII and present tumor antigen peptides (473). However, in the absence of costimulatory signals MHC II presentation is not sufficient for helper T-cells (Th) activation (474). Further supporting immunosuppression, aPSC express high level of CXCL10/IP10[1], which correlates with a Treg increase and reduced CTL (cytotoxic T lymphocyte) and NK (natural killer cell) activity (475). aPSC also express T-cell apoptosis-inducing GAL1 (476, 477). Nonetheless, the impact of PSC on the immune system is still debated, as reverting activated to resting PSC appears superior to PSC elimination (478–480) (**Figure 9C**).

Taken together aPSC/CAF account for the dense stroma formation and ECM modulation. The DR provides a barrier for immune cells, but also for chemotherapy by poor drug access (481). Beyond this "passive action," aPSC/CAF contribute

to the acquisition of major hallmarks of PaCa via cytokines, chemokines, growth factors, and their receptors that promote tumor cell proliferation and chemoresistance, accelerate intrapancreatic nerve invasion and distant metastatic growth and assist establishing an inflammatory milieu that forces immune destruction (482). aPSC/CAF supply essential nutrients and promote metabolic reprogramming backing tumor cell survival and proliferation (483), which is assisted by aPSC/CAF miRNA (484). These activities are briefly elaborated in the following sections. Despite overwhelming evidences for aPSC/CAF supporting PaCa growth and progression, under selected circumstances they may provide a host defense against the tumor, the hypothesis building on poorer prognosis after HH depletion and in αSMA-ko mice (485, 486).

ACTIVATED PANCREATIC STELLATE CELLS AND THE CROSSTALK WITH TUMOR CELLS

The extensive crosstalk between aPSC and the embedded tumor cells is pivotal for PaCa survival and progression. Provision of TGFβ, PDGF, FGF2, profibrinogenic factors, serpin2, galectins3, and 9 sustain persisting PSC activation, proliferation, migration, and collagen synthesis. The aPSC also provide growth factors and nutritients (**Figure 10A**). aPSC/CAF secrete SPARC[1], involved in cell migration and proliferation (487), and periostin, which modulates invasion via AKT signaling and EMT (488, 489). Most abundant chemokines are CXC/CC family members CCL2/MCP1[1], CXCL8/IL8, CXCL1[1], and CXCL2/MIP2[1], all engaged in PaCa progression (490–492). Increased radioresistance by aPSC/CAF relies on ß1 integrin-FAK activation and DNA damage response regulation (493, 494). An impact on chemotherapy resistance hinges on accessibility (495), activation of the SDF1-CXCR4 axis with subsequent upregulation of IL6, increased HH expression, and IL1β-IRAK4[1] or mTOR/EIF4E[1] pathway activation (496–501). Finally, aPSC/CAF support metastasis formation via the HGF/cMET/survivin pathway, which is regulated by TP53[1]/CDKN1A[1] (502) or through altered lipid metabolism, particularly oleic-, palmitoleic-, and linoleic-acid upregulation (503). Tumor progression is further supported by CAF through partial EMT induction by HH signaling (504) and through aPSC-Exo delivering tumor growth promoting miRNA and lncRNA, which liberate oncogenic/metastasis-promoting mRNA from suppressive miRNA to name only one of the lncRNA functional activities (133). Furthermore, aPSC accompanying migrating tumor cells provide in loco support in establishing premetastatic niches (505, 506).

Nutrient provision by altered metabolic pathways is another important aPSC contribution to PaCa cell progression. This proceeds through increased glycolysis, amino acid (AA) production from protein degradation, by glycosylation and fatty acid synthesis, called the metabolic switch (507). Accordingly, glycolytic enzymes such as hexokinase-2, enolase-2, LDHA, and B[1] (508) and glycolytic metabolites are elevated (509). In addition, mitochondria adapt and account for energy supply. We recommend a most informative report on the different options, which tumor cells use to alter metabolic pathways (510), and give some examples on specific aPSC contributions. First, aPSC deliver cytokines that by binding to receptors initiate signaling cascades toward activation of the PI3K/Akt pathway, which is central for glycolysis, ATP level maintenance, stabilization of the mitochondrial potential, and tumor cell survival. Two examples are aPSC-derived IGF binding to the IGF1R and Gas6[1] binding to Axl. Gas6 is a member of the vitamin K-dependent protein family that resembles blood coagulation factors rather than typical growth factors (511). Both, IGF and Gas6 binding promote via PI3K/Akt activation Asp provision (512). Second, uptake of glucose and essential AA is facilitated by transporters either for delivery by aPSC or for uptake by PaCa cells that may also expulse unwanted byproducts, transporter families and their activities being profoundly reviewed (513). An example are glutamine transporters, which are supported by the glutamine-utilizing enzymes glutaminase GLS1[1], phosphoribosyl pyrophosphate synthetase PRPS2[1], and carbamoyl-phosphate synthetase 2 CAD converting glutamine to glutamate. Glutamate cannot exit and its accumulation replaces the TCA (tricarboxylic acid) cycle to generate citrate, which also can derive from the pyruvate-PDK-Ac-CoA pathway. Glutamate also stimulates cysteine uptake. Lactate, delivered via lactate transporters supports glutamine and glucose generation, GSH upregulation and ROS reduction. Glucose transporters in the tumor cells further assist glucose enrichment. Promoted by PKM2, NADH, and ATP support the generation of pyruvate. Excellent reviews unravel the current state of knowledge on the TCA cycle and the mitochondrial contribution in detail (508, 514–517). Autophagy accounts for a third support by CAF for nutrient supply. Autophagy is a cytoplasmic recycling process, where unfolded macromolecules, dysfunctional aggregates and organelles are sequestered in a double membrane organelle, called autophagosome, which fuses with lysosomes (518). The released breakdown products, AA, FA, nucleotides, and sugars are reused or released. One of the released AA, alanine is converted into pyruvate that is integrated into the TCA cycle (519). As far as aPSC deliver autophagosomes rather than the single components generated by lysosome degradation, autophagosomes are taken up by macropinocytosis, the nutrients becoming available after degradation in the tumor cell's lysosomes (520). Lysosome degradation is also required for access to nutrients provided by aPSC-derived Exo that modify the metabolic machinery of cancer cells increasing glycolysis and glutamine-dependent reductive carboxylation by providing AA, lipids, and TCA cycle intermediates (521). Finally, PaCa cells essentially depend on large amounts of lipids. FA uptake proceeds via different pathways. Besides gaining access by lysosome degradation of autophagosomes and Exo, the fatty acid translocase CD36 transports circulating free FA across the cell membrane (522, 523). FA sequestered in lipoproteins can be released by low density lipoprotein receptors before uptake by CD36. Alternatively and more frequently in PaCA, lipoproteins are internalized via LDL receptor-mediated endocytosis or macropinocytosis (524, 525). Notably the Exo transfer requires

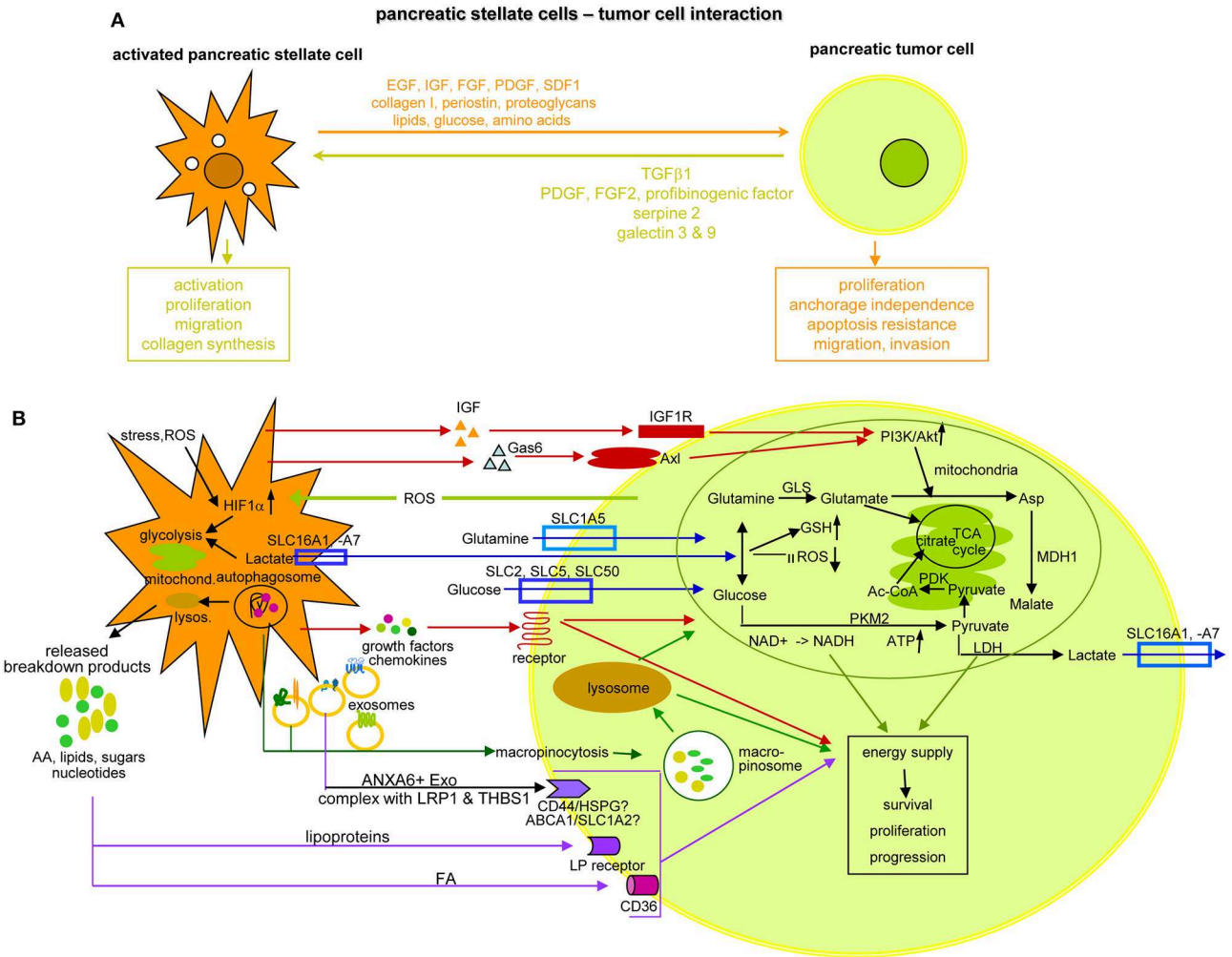

FIGURE 10 | The crosstalk between PSC and pancreatic cancer cells. **(A)** Overview of the support provided by aPSC to PaCa survival, expansion and gain in aggressiveness and feedback by the tumor cell, which sustains PSC activation, expansion and matrix protein synthesis. **(B)** Some of the important components delivered by aPSC toward tumor cells and the initiated changes with a focus on altered metabolism. Glutamate derived from influxed glutamine can replace the TCA cycle to generate citrate, which also can derive from the pyruvate-PDK-Ac-CoA pathway. Lactate, delivered via lactate transporters supports glutamine and glucose generation, GSH upregulation and ROS reduction. Glucose also becomes enriched by glucose transporter in the tumor cell, where PKM2 via NADH and ATP promotes pyruvate generation. After lysosome degradation of aPSC autophagosomes, a plethora of AA, lipids, lipoproteins, sugars, and nucleotides is delivered that in part are taken up by specific receptors, not all being identified so far. Alternatively, autophagosomes are taken up by macropinocytosis, the macropinosome content being delivered after lysosome degradation. Lysosome degradation is also required for the delivery of the aPSC Exo content. Another option is receptor-mediated uptake of selective transmembrane complexes as ANXA6[1] bound LRP1[1] and THBS1[1]. The predominant route of transfer from aPSC in PaCa cells is indicated by a color code: red: signaling receptor mediated uptake; blue: delivery or uptake by transporters; vesicle uptake: green; violet: receptor-mediated lipid and lipoprotein uptake; an olive circle encloses for a few of the aPSC-delivered components the pathway, whereby they contribute to the altered metabolism of PaCa cells; others may directly support PaCa survival and aggressiveness. Full name of proteins are listed in **Table S1**. aPSC support PaCa survival, expansion and progression, which to a considerable degree relies on their input of components initiating energy generation by altered metabolic pathways. Despite the focus on PSC-promoted metabolic adaptation of PaCa cells, the presented data cover only a minor part of the present state of knowledge and additional information can be expected by improved proteomic methodologies combined with organoid cultures.

ANXA6+ Exo derived from CAF, where ANXA6 forms a complex with LRP1[1] and THBS1[1], the complex being only recovered in aPSC from patient with PaCa (526) (**Figure 10B**). Thus, though free nutrients are rare in the stroma, embedded aPSC provide a potent source.

In brief, PaCa cells express surface molecules and secrete factors that sustain PSC activation and expansion. aPSC, in turn, support PaCa proliferation, survival and progression. They promote proliferation and migration via cytokine and chemokine delivery, and apoptosis/drug resistance as well as a shift toward EMT via integrin and RTK activation. Ample provision of nutrients supports tumor cell survival and expansion mostly by sustaining altered metabolic pathways. Exo delivered by aPSC add to nutrient supply. Exo miRNA and lncRNA

contribute to inactivation of tumor suppressor and liberation of metastasis-associated gene mRNA. lncRNA additionally support chromosome accessibility and transcription initiation, which adds to access of metabolism driving genes. Obviously, stress signals from PaCa cells suffice for aPCS/CAF responding with a plethora of supports.

ANGIOGENESIS IN PANCREATIC CANCER

PaCa cells can support angiogenesis (527–529) and microvessel density after PaCa resection correlates with recurrence and poor survival (530). Nonetheless, PaCa are mostly hypovascular and hypoxic, due to a dominance of negative angiogenesis modulators (531, 532).

Several angiogenesis inhibitory factors, elegantly reviewed by Walia et al. (533), are enriched in PaCa. They originate from ECM degradation, poor vascularization being a secondary phenomenon to the fibrotic microenvironment (534). Angiostatin, a 38-kDa tumor cell-derived plasminogen fragment, inhibits primary and metastatic tumor growth by blocking angiogenesis (535–537). Fibstatin, another endogenous angiogenesis inhibitor, is a FN fragment containing the type III domains 12–14 (538). Fibstatin cooperates with CXCL4L1/PF4V1[1], inhibiting EC proliferation, migration and tubulogenesis *in vitro* and both angiogenesis and lymphangiogenesis *in vivo* (539). Endostatin, another matricellular protein regulating cell function without contributing to ECM structural integrity (533), is a collagen XVIII fragment (540, 541). MMP12 is engaged in endostatin and angiostatin generation (542), VEGF and FGF2 support secretion (543). Endostatin binds both endogenous angiogenesis inhibitors thrombospondin-1 and SPARC (544, 545) and upregulates thrombospondin-1 expression (546). Endostatin also binds VEGFR2 on EC and VEGFR3 on lymphatic vessels preventing activation and downstream signaling (533, 547, 548). By occupying integrin-ECM binding sites, initiation of the tyrosine phosphorylation cascade, src activation, and EC migration are interrupted (549, 550). Endostatin additionally prevents clustering with caveolin-1 and downstream signaling activation (551). A different mechanism underlies the antiangiogenic effect of RNASET2[1]. Independent of its ribonuclease activity, RNASET2 arrests tube formation, accompanied by disruption of the actin network. The authors suggest RNASET2 competing or cooperating with angiogenin (552). Statins, HMGCR[1] inhibitors, interfere with angiogenesis via VEGF downregulation. Moreover, statins prevent adhesion to the ECM by blocking intercellular adhesion molecules (553). There is, at least, one exception to angiogenesis/lymphangiogenesis inhibition by the PaCa stroma. Stroma embedded mast cells enhance angiogenesis by inducing pro-angiogenic VEGF, FGF2, PDGF, and angiopoietin-1 expression (554).

It may appear surprising that angiogenesis inhibition is a special features of most malignant PaCa with an intensive desmoplasia leading to hypoxia and nutrition deprivation. However, there is no evidence of cell death. PaCa being most well-equipped to cope with nutrient deficits, already outlined in the preceding section, only PaCa cell autonomous programs will be added here. Reuse of vesicle-enclosed nutrients can be liberated in the PaCa cell lysosomes (520). PaCa cell also make use of autonomous autophagy driven by a transcriptional program. Master regulators in converging autophagic and lysosomal functions are MITF[1] and TFE[1]. A prerequisite for fulfilling these distinct functions relates to their shuttling between the surface of lysosomes, the cytoplasm, and the nucleus in response to nutrient fluctuations and various forms of cellular stress. Shuttling depends on changes in the phosphorylation of multiple conserved amino acids, phosphorylation being mainly promoted by mTOR, ERK, GSK3, and AKT, and dephosphorylation by calcineurin (555, 556). Furthermore, in contrast to most non-transformed tissue, tumor cells engage in *de novo* FA synthesis under hypoxic conditions (517, 557). This occurs particularly when the PI3K-Akt-mTOR pathway is constitutively active as in PaCa. mTOR signaling activates transcription factors of the sterol-regulatory element-binding protein family, which induce expression of the lipogenic genes ACACA[1], FASN[1], and SCD[1] (558, 559).

Taken together, hypoxia-dependent and -independent mechanisms of metabolic reprogramming account for poor vascularization not hindering PaCa progression. Metabolic reprogramming is predominantly promoted by aPSC/CAF and their Exo and is supported by tumor cell autonomous programs.

NEURAL INVASION IN PANCREATIC CANCER

Innervation of the digestive tract is composed of the intrinsic, enteric nervous system, and afferent extrinsic nerves, transferring information to the central nervous system (CNS) and efferent nerves conveying commands from the CNS to the digestive organs (560). The healthy pancreas has an abundant nerve supply. Ganglia (aggregates of neural cell bodies), the intrinsic component of the pancreatic innervation, are randomly distributed throughout the parenchyma. The afferent system, thin unmyelinated fibers run with the parasympathetic vagus or the sympathetic input splanchnic nerves, the cell bodies are located in the spinal or vagal afferent ganglia. Extrinsic parasympathetic fibers derive from the vagus or the stem brain and end in the synapse of the intrapancreatic ganglia. Postganglionic parasympathetic fibers distribute with sympathetic fibers. Postganglionic sympathetic fibers mostly run with blood vessels (561, 562). Innervation is increased in PaCa (563, 564), nerve fibers forming a dense network that interacts with tumor cells and supports tumor growth and dissemination (565–567). In fact, PaCa metastasize by PNI. Also reported in other cancer, with recovery in 80–100% of patients, PNI is most frequent in PaCa and associated with poor prognosis (37, 568–571). PNI is seen in early stages of PaCa (572, 573) and is independent of lymphatic or vascular metastasis (573, 574) (**Figures 11A–C**).

PNI is defined as the existence of tumor cells in the epineural, perineural and endoneural spaces of the neuronal sheath (566, 575) and results from mutual message transfer

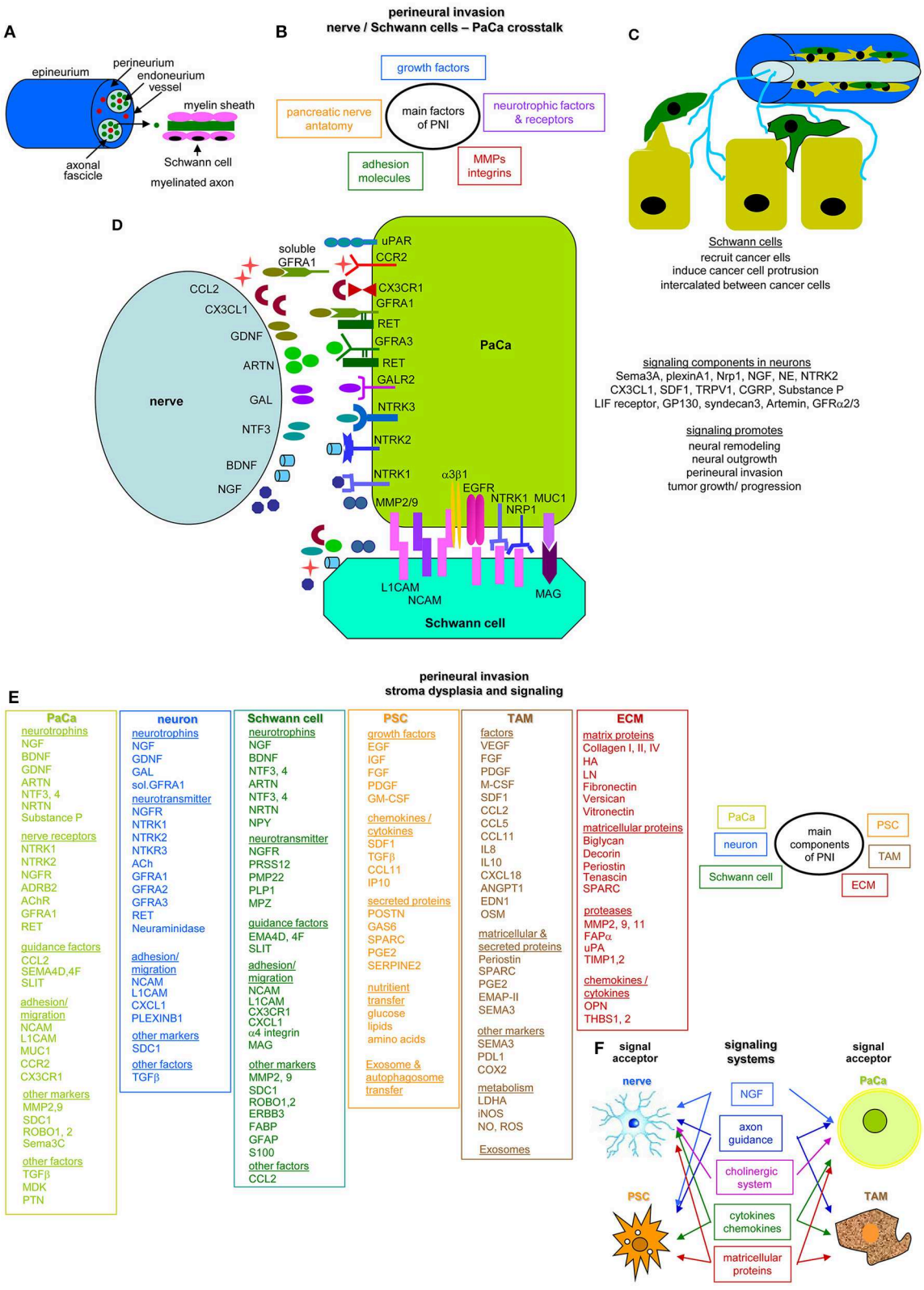

FIGURE 11 | The nervous system and perineural invasion in pancreatic cancer. **(A)** Overview of nerve anatomy. The endoneurium surrounds all axons and serves to separate individual nerve fibers. The axons are covered by Schwann cells, where Schwann cells myelinate the axons. Non-myelinating axons mostly ensheath multiple

(Continued)

FIGURE 11 | small caliber axons. **(B)** The anatomy of the pancreatic nerves, neurotrophic factors and receptors as well as growth factors expressed by the engaged cells all contribute to perineural invasion and are supported by adhesion molecules and proteases as demonstrated in **(C)** for Schwann cells that intercalate between tumor cells promoting destruction of the adhesive matrix and actively recruiting tumor cells toward the nerve by signaling via adhesion molecules that promote cytoskeleton reorganization associated with acquisition of a motile phenotype. **(D)** Overview of abundantly delivered neurotrophic factors, cytokines, and chemokines by neurons and the corresponding receptors on PaCa tumor cells that promote tumor cell growth and invasion; dominating in the interaction between Schwann cells and tumor cells are L1CAM and NCAM. Besides homophilic binding, they bind integrins and RTK. MAG binding MUC1 on tumor cells mainly contributes to adhesion. For detailed information on signaling cascade initiation in PaCa, please see reviews mentioned in the text file. **(E)** Besides the direct engagement of neurons, Schwann cells and tumor cells, PSC, TAM, and the dysplastic tumor matrix contribute to PNI. Molecules predominantly contributing to PNI are listed. Selective contributions of aPSC rely predominantly on the transfer of nutrients, Exo and autophagosomes; TAM contribute by the delivery of matricellular proteins like EMAP-II and metabolism regulators such as LDHA and iNOS, the ECM supports PNI by embedded matricellular proteins and proteases. **(F)** All engaged cell populations are also acceptors of signaling cascade activators such as NGF, axon guidance cytokines/chemokines, and matricellular proteins. Activation of the cholinergic system is of major relevance for nerves and tumor cells. Full name of proteins are listed in **Table S1**. PNI is one of the dominating pathways of PaCa invasion. It is supported by neurotrophins and neurotransmitters delivered by neurons and Schwann cells, the latter in addition providing guidance factors and membrane integrated proteins that promote adhesion and migration. aPSC are essential in nutrient transfer and TAM provide cue enzymes to cope with ROS and NO. TAM and the ECM contribute by matricellular proteins and proteases that facilitate PaCa cell migration toward the nerve.

between nerves and tumor cells (566). Though not fully elaborated, many contributing components are known. Nerve growth factor family NGF, BDNF[1], neurotrophin-3 and−4 (576) bind NTRK1/TRKA[1] with high- and NGFR/p75NTR[1] with low affinity (577–580), NTRK1 being highly expressed on nerves and tumor cells (581). Glial cell-derived neurotrophic factors GDNF[1], NRTN, artemin and persephin are secreted by neural tissue and bind to GFRA1-A4 (582). GDNF expression strongly affects PNI in PaCa (583). This relies on RET receptor-mediated activation of downstream RAS, MAPK/ERK, JNK[1], PI3K/Akt, and NFκB[1] pathway activation (584–586). Anti-NGF treatment decreased expression of PNI-involved NTRK1, NGFR, TAC1[1], and calbindin in neural cells, reduced PNI and inhibited metastases in mice (587). The CXCR4-SDF1 axis also contributes to PNI. CXCR4 promotes tumor cell migration toward nerve cells (588, 589) and SDF1 increases NGF expression (588). Shown in an autochthonous model, PNI plays a significant role in initiation and progression of early PaCa stages, inflammation and neuronal damage in the peripheral and central nervous system already occurring in pancreatic intraepithelial neoplasia (PanIN)2, where acinar-derived cells frequently invade along sensory neurons into the spinal cord and migrate caudally to the lower thoracic and upper lumbar regions. Sensory neuron ablation prevents PNI, astrocyte activation, and neuronal damage, suggesting sensory neurons conveying inflammatory signals from the tumor to the CNS. Neuron ablation also significantly delays PanIN. These data indicate a reciprocal signaling loop between PaCa and the nervous system, including the CNS (590). Axon guidance genes semaphorins and plexins also are frequently altered in PaCa. Semaphorin3C increases PaCa proliferation, invasion, and EMT through ERK1/2 signaling pathway activation (591). Semaphorin3D secretion is regulated by AnnexinA2 phosphorylation. It acts autocrine by binding to the coreceptors plexinD1 and neuropilin-1 (592). Parakrine signaling of Semaphorin3D and plexinD1 between tumor cells and neurons mediates increased innervation, PNI and PaCa metastasis (593). Activation of the peripheral sympathetic nervous system (SNS) also assists PNI. In the healthy pancreas the SNS regulates digestive enzyme and endocrine hormone secretion (594, 595). In PaCa, β-adrenergic receptor activation of the SNS contributes to tumor progression via release of norepinephrine and epinephrine (**Figure 11D**). In view of the abundance of information coupled with many remaining questions we recommend readers particularly interested in PNI some recent, excellent reviews (38, 596, 597).

Beside tumor cells, nerves, Schwann cells, aPSC, TAM, and the ECM contribute to PNI. The contributing components, sorted according to molecular families and subcellular units are listed (**Figure 11E**). The complex contribution of dysplastic stroma elements to PNI being not fully unraveled, we only mention few examples. Tumor cells, aPSC, and TAM express GPCR β-adrenergic receptors ADRBA1,-A2, -B1, -B2[1] that signal via the associated trimeric G-proteins (598–600), HIF-1α (601), and ERK/MAPK (574), which in concert promote tumor growth and metastasis (39). aPSC-derived TGFβ induces NGF via the TGFBR1/ALK5[1] pathway and HGF-cMET activation (602, 603) that contribute to neural plasticity (604). TAM infiltration also correlates with PNI (605), where TAM-secreted IL8 assists PNI through MMP1-PAR1[1] signaling via ERK1/2 (606). Schwann cells highly express MAG[1] (607), which is a receptor for abundant mucin-1 on PaCa (608), MAG-mucin-1 signaling promoting PNI (609). Furthermore, PaCa-derived NGF attracts Schwann cells via NGFR/p75NTR (40), which might be interpreted as the recruitment of nerve cells toward the tumor being the first step in PNI (40, 609). Finally, long distance nerve recruitment predominantly depends on Exo/MV (microvesicles) (610, 611) for several cancer (612, 613). This is best explored for glioblastoma-TEX, which are taken up by tumor cells, EC, and Mϕ, but also by healthy neural cells, and microglia (614). Furthermore, non-transformed cell-derived Exo/MV contribute to message transfer. Oligodendrocytes, glial cells in the brain accounting for axon myelination, shuttle messages between myelinating glia and neurons (615, 616) and between neurons (617). Microglia, the brain's Mϕ defense mechanism, also acts via released MV (618). Microglial MV additionally regulate neuronal excitability accompanied by neuronal ceramide and sphingosine production (618). Schwann cells, too, communicate with the peripheral nervous system via Exo (619).

In brief, the review "Splitting out the demons" is concerned about glioblastoma (620), but may well be of general relevance, particularly for PNI in PaCa. The authors demonstrate that

the major signaling systems are NGF, axon guidance molecules, cytokines/chemokines, the cholinergic system, and matricellular proteins that are also delivered by several components of PaCa. Searching for signal acceptors in PaCa revealed that tumor cells, nerves, aPSC, and TAM can all be acceptors of these signaling systems creating a malicious feedback loop in PaCa (**Figure 11F**).

Spurred by the poor prognosis and PaCa-associated pain (620–623) and PNI being an early event in PaCa development, PNI recently received increasing attention (595). For a long time uncovered molecular pathways due to technical difficulties in culturing engaged cellular components and isolating Exo from defined subpopulations may become unraveled in the near future. Success in culturing Schwann cells particularly opens access to a hitherto inaccessible, important contributor. We consider Exo/MV as an additional promising option to interrupt PNI (618), where improved techniques for isolating and characterizing single stroma cell derived Exo will be of great help in deciphering a PNI-forcing contribution. Despite strong progress, supported by elegant autochthonous mouse models, there is still great need to unravel the complex interactions underlying PNI, which is a prerequisite for therapeutic interference (587, 624).

PANCREATIC CANCER AND IMMUNOSUPPRESSION

Immune cells are abundant in the PaCa stroma (625, 626), but are immunosuppressive (627, 628), whereas effector cells are rare (629). This accounts for the innate and the adaptive immune system.

NK

NK are discussed as a therapeutic option in PaCa (630, 631). However, several constraints need clarification as NK are reduced in the juxta tumoral area compared to the stroma, possibly due to sequestration by aPSC (632) and NK apoptosis via FASL^1-positive tumor cells (613). In addition, cytotoxic activity of NK cells is severely impaired (633).

Activated NK cells bind via activating receptors NKG2D^1, NKp30^1, and NKp46^1 to their ligands major histocompatibility complex class I-related chain MICA/B^1 and ULBP1-6^1 (634). NKG2D having a very short cytoplasmic tail uses the adaptor molecules DAP10^1 and/or DAP12^1 to initiate downstream signaling (635). In addition, activated NK cells secrete IFNγ, TNFα, GM-CSF^1, the chemokine ligands CCL1-5^1, and CXCL8^1, which trigger activation and recruitment of other innate and adaptive immune cells, broadening and strengthening anti-tumor immune responses (636). In PaCa, instead, decreased NK activity is accompanied by low level NKp46, NKp30, granzymeB, and perforin expression (637). Lactate, a by-product of tumor metabolism also causes NKp46 downregulation (638). Another important group of NK receptors are nectin and nectin-like binding molecule DNAM1^1. DNAM1 downregulation on NK correlates with PaCa progression (639). Furthermore, though MICA/B is expressed in >70% of PaCa, it is also expressed on PSC (640). NK cells preferentially migrating toward PSC become sequestered in the stroma before reaching the tumor nodules (641). Moreover, ADAM10 and ADAM17 cause shedding of MICA/B and PSC inhibit NK cells via IL6 (642). Finally, NK cells tend to target (Pa)CIC due to enhanced MICA/B expression (643). In view of the CIC plasticity, it remains to be explored, whether CIC targeting by NK is of therapeutic benefit (**Figure 12A**).

Due to preferentially targeting tumor cells, NK-based immunotherapy was discussed just few years after their discovery (644), hope being fostered by their contribution to antibody-dependent cellular cytotoxicity (645). Further unraveling the impact of their surrounding, efficient use of NK cytotoxic potential may become reality in PaCa.

Mϕ

TAM are increased in the PaCa stroma (646), high numbers being associated with poor prognosis (647–649). TAM mostly exhibit the suppressive phenotype of CD163+ and CD204+ M2 (650, 651), M2 differentiation being supported by tumor- and Treg-derived IL4, IL10, and IL13 (652). TAM suppress the adaptive immune response via TGFβ, IL10, CCL17, CCL18, CCL22, and PDL1^1 secretion (653, 654). In addition, CCL2 and CCL20^1 through chemokine receptor CCR6^1 binding promote MMP9 upregulation and thereby invasiveness (655, 656) and can contribute to EMT (657, 658). In PaCa, TAM also secrete the serine protease FAP^1, which stimulates CAF (659) and induces CDA^1, contributing to drug resistance by metabolizing the active to the inactive form of Gemcitabine (660).

Briefly, the main feature of TAM is the shift to and the preponderance of immunosuppressive M2 in PaCa. Besides suppressing adaptive immune responses, TAM promote CAF and in a positive feedback loop Treg expansion. TAM also strengthen the aggressiveness of PaCa and support drug resistance. Reviews are recommended for a comprehensive overview of special TAM features in PaCa (661, 662) (**Figures 12B,C**).

MDSC

MDSC are a heterogeneous group of cells, characterized by myeloid origin, immature state and mostly functional activity. Two subgroups, defined as monocytic (M) and granulocytic (G) MDSC are differentiated by Ly6C^{high} (M-MDSC) or Ly6G^{high} (G-MDSC), M-MDSC exerting stronger suppressive activity (663–665). MDSC are abundant in the PaCa stroma (666). MDSC are recruited toward PaCa via CAF-derived CXCL12 and tumor-derived GM-CSF (588, 667). MDSC hamper T-cell recruitment and activation, which are their major targets and promote Treg expansion (668, 669). MDSC expansion is expedited by M-CSF^1, GM-CSF, SCF^1, IL6, IFNγ, IL1β, VEGF, HSP72, IL13, C5a^1, PGE2^1, and S100A8/A9 (664, 670). Inhibition of differentiation into mature myeloid cells is spurred by downstream activation of the JAK^1-STAT3/STAT5 pathway with stimulation of cyclinD1, BCLXL^1, survivin, c-myc, and S100A8/A9. CCL2 and SDF1 support MDSC recruitment, GM-CSF plays a major role in inflammatory milieu maintenance (667). Prominent signaling molecules engaged in MDSC activity are STAT3, COX2, HIF1α, C/EBPB^1, HMOX1^1, and IDO^1 (654, 670, 671). MDSC interfere at several levels with immune response induction (672).

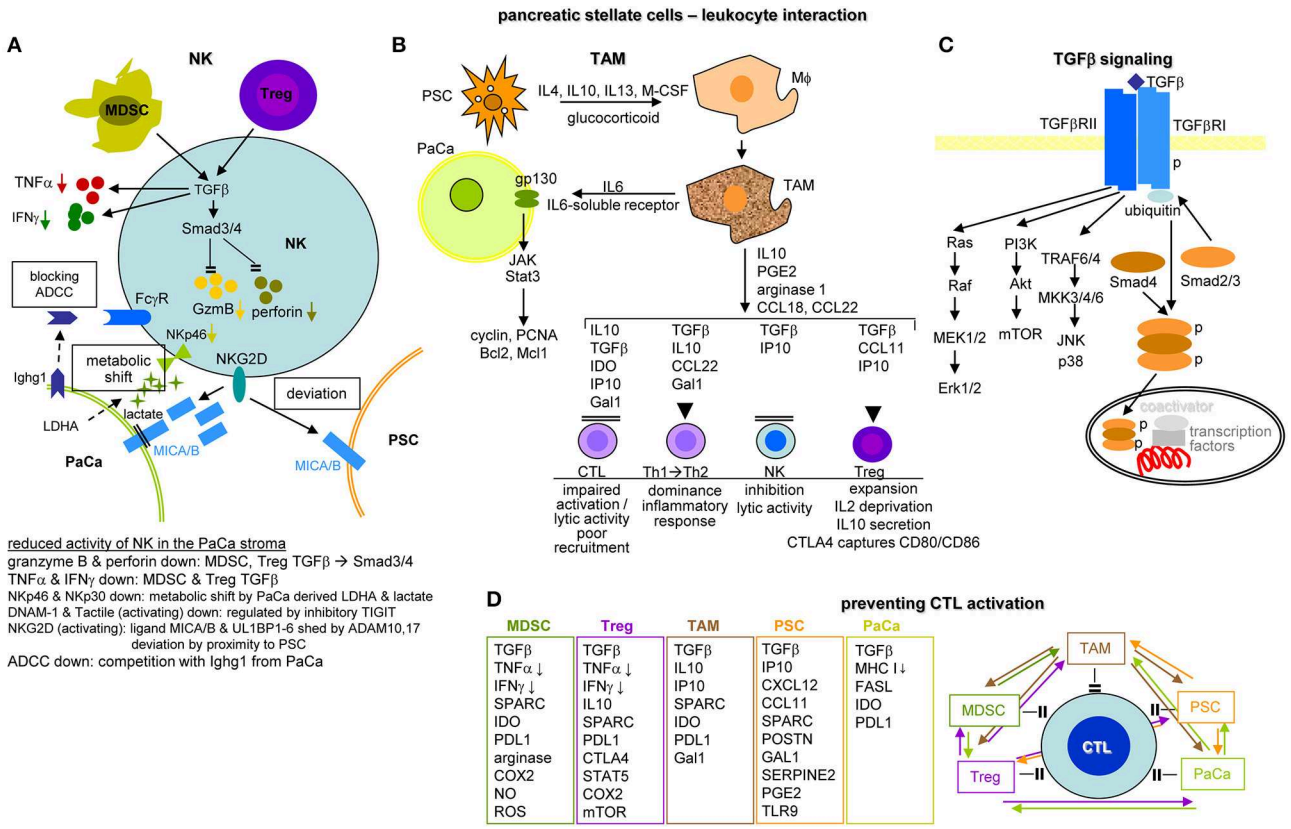

FIGURE 12 | The impact of PSC and tumor cells on immune cells in the pancreatic cancer stroma. **(A)** NK cells in the stroma display reduced activity. This is mainly due to MDSC and Treg that by TGFβ delivery affect TNFα and IFNγ secretion and SMAD3/4 activation, which inhibit GzmB and perforin transcription. The activating NKG2D receptor become deviated toward PSC due to higher expression of MICAB, where MICAB in tumor cells can become shed by ADAM17, free MICAB fragments further deviating NK cells from attacking the tumor cell. The activating receptors NKp46 and NKp30 become downregulated due to a metabolic shift induced by tumor cell derived LDHA and lactate. Activating receptor can also become occupied by inhibitory receptor, like TIGIT. Finally, tumor cells deliver an IgG like molecule, Ighg1, occupying the FcγR of NK cells and thereby interfering with ADCC. **(B)** PSC have a strong impact on driving Mϕ into TAM by the delivery of IL4, IL10, IL13, mCSF, and glucocorticoids. TAM deliver IL6 and soluble IL6 receptor binding to gp130 on tumor cells, which activates the JAK/Stat3 pathway promoting tumor cell survival and expansion by cyclin, PCNA Bcl2, and Mcl1 expression. TAM also affect the activity of additional immune cells. Lytic NK cell activity becomes inhibited by TGFβ and IP10. A shift of Th1 to Th2 is supported by TGFβ, IL10, CCL22, and Gal1. Expansion and activity of Treg is assisted by TGFβ, IP10, and CCL11. Finally, CTL recruitment, activation and lytic activity are impaired by TAM-derived TGFβ, IL10, IP10, IDO, and Gal1. **(C)** A central role of TGFβ in immune deviations relies on binding to the TGFβRII, which promotes RAS, PI3K, and TRAF6/4 pathway activation and on TGFβR1 binding, where phosphorylated Smad4 forms a complex with Smad2/3, the complex migrating into the nucleus promoting together with additional coactivators and transcription factor besides other transcription of NOS, PAI-1 and PDGF. **(D)** CTL activation is prohibited by tumor cells, PSC and immunosuppressive MDSC, Treg and TAM. The major inhibitory factors and membrane molecules are listed. PSC particularly contribute via POSTN, GAL1, SERPINE2, PGE2, and TLR9. Low level MHCI expression on tumor cells hampers CTL activation, high FASL expression contributes to CTL lysis and IDO and PDL1 are inhibitory receptors. As shown in the overview diagram, preventing CTL activation is the result of coordinated activities between all contributing components. Full name of proteins are listed in **Table S1**. The dense stroma and poor angiogenesis may hamper leukocyte recruitment. However, there is no paucity of immunosuppressive leukocyte, such that changes in metabolism and activation of signaling cascades are dominating immunosuppression. Feedback circles between all contributing elements create a self-replenishing vicious circle.

Downstream effector molecules arginase-1 and iNOS[1] account for L-arginine depletion and ζ-chain downregulation in T-cells (673). iNOS-induced NO and ROS inhibit T-cell proliferation and promote apoptosis. HMOX1 hampers T-cell proliferation by CO production (670, 674). Membrane-bound TGFβ1 assists NK anergy (675). IL10 and TGFβ foster Treg expansion, which become recruited by CXCL10 (676). TGFβ and IL10 also account for IFNγ downregulation (670, 674). IL10 promotes TH2 deviation (677) and M2 polarization (678). Finally, MDSC Exo characterization uncovered MDSC activities being efficiently transferred by Exo (679–681).

Thus, MDSC hamper mostly T-cell, but also B-cell (682) and NK activity, at least in part by supporting Treg expansion and activation. There are several well-established options to combat MDSC induction and activities, frequently used in combination with chemotherapy whose efficacy increases by eliminating MDSC-promoted drug resistance (683, 684).

Dendritic Cells

Dendritic cells (DC) are professional antigen presenting cells, directly linking the innate and adaptive immune systems, where particularly Th activation essentially depends on processed

antigen peptide presentation (685–687) and costimulatory signals provided by DC (688, 689). However, DC activity is severely impaired in cancer (690, 691). In the PaCa stroma, DC are rare and mostly located at the edge of the tumor (692). DC maturation and activation is also hindered by confrontation with immunosuppressive cytokines TGFß, IL6, IL10, and GM-CSF, which activate the STAT3 pathway (693–695). Furthermore, costimulatory molecule CD40 and CD80 expression is reduced in DC, hampering T-cell activation (696). Instead, DC produce CCL22, which recruits Treg (697, 698). Several options for coping with the DC deficit are clinically evaluated, mostly based on the transfer of antigen/peptide-loaded DC, where in PaCa mucin1 and Wilms tumor protein are promising antigen candidates. Loading DC with the patient's TEX is another option that guarantees presentation of the individual tumor's immunogenic antigens/peptides (699–701). The finding that DC-derived Exo are equipped to stimulate T-cells (702), spurred research focusing on DC transfer to overcome poor T-cell responses in PaCa (703–705).

Besides supporting Treg recruitment, DC do not actively contribute to PaCa progression. Unfortunately, their paucity in the tumor stroma, impaired antigen processing and presentation and the insufficient costimulatory molecule supply significantly hamper immune response induction. There is hope for circumventing these drawbacks by DC or DC-Exo transfer, the latter having the advantage of a technically easier implementation in the clinic.

T-Cells

The adaptive immune system, T-cells and B-cells, is the body's most specialized and efficient defense mechanism. B-cells, secreting antibodies, account for the humoral defense, T-cells for the cellular defense, where CD8+ CTL lyse their targets and CD4+ Th provide soluble factors supporting CTL, B-cells and NK. T-cells are rare in PaCa (706) and PaCa actively inhibit CD4+ T-cell proliferation and migration (707). Furthermore, PaCa tumor cells and the stroma skew Th from cell-mediated responses inducing Th1 toward Th2, which might support tolerance induction (708). The shift toward Th2 is assisted by PaCa-delivered IL10 and TGFβ (709) and by CAF-delivered lymphopoietin (710). Furthermore, lower numbers of T-cells in PaCa (706) may rely on aPSC affecting T-cell migration toward the tumor nodules (631). The Th2 cytokines IL4, IL5, IL6, MIP1α, GM-CSF, MCP1[1], IL17, IP10, and IL1β are dominant and are associated with poor immune responsiveness and a shorter DFS (disease free survival) (711). Moreover, PaCa inhibit CTL activity. PaCa-derived TGFβ interferes with perforin and granzyme expression (712, 713) and PDL1 on PaCa binds PD1[1] on CTL, spurring T-cell anergy or death (714). There are subtypes of PaCa that display higher T-cell levels, but the tumor evades the immune response due to amplification of PDL1/2 or upregulation of inhibitory cytokines and the JAK/STAT signaling pathway (715). aPSC also stimulate T-cell apoptosis, decrease IL2 and IFNγ secretion by Th1, but increase IL4 and IL5 secretion by Th2, which is linked to galectin-1 expression on PSC (716, 717).

Though mucin-16 tumor antigen-specific CTL were recovered in few long term survivors, supporting the efficacy of CTL in defending the body's integrity (718), PaCa and aPSC skew toward Th2 and promote T-cell anergy and apoptosis, low level T-cell recovery correlating with a poor prognosis (719) (**Figure 12D**).

Treg

Treg are CD4+CD25^{high}Foxp3+ cells (720, 721). They contribute to immunosuppression via CD152/CTLA4[1] (722, 723) and TGFβ and IL10 secretion, which affects Th, CTL, Mϕ, NK, and DC (626, 724–726). In PaCa, Treg are already present at the PanIN stage, expand during tumor progression (727, 728) and are preferentially located surrounding the tumor (729). Treg promote EMT (730) and inhibit Th1 and Th17 effector functions (731). Migration toward the tumor is assisted by tumor chemokines and EC addressins and their ligands on Treg (732). PaCa secrete elevated levels of CCR5 ligands/CCL28, which increases Treg chemotaxis (733). EC in the tumor tissue express high level of mucosal VCAM-1, E-selectin and CD116/CSF2RA[1], which foster Treg transmigration (734). Increased levels of Treg in the circulation (735) and the tumor stroma (731, 735) correlate with poor prognosis.

There are other unmentioned immune deviations related to PaCa. We recommend overviews focusing on cytokines and chemokines (736–739) and additional immunosuppressive molecules (740), where we only mention a few. RIP1 and 3[1], highly expressed in PaCa, are key mediators of necroptosis, a caspase-independent cell death. Interestingly, while an *in vitro* blockade of the necrosome was accompanied by increased PaCa aggressiveness, *in vivo* deletion was associated with increased immunogenic myeloid and T-cell infiltrates. The authors suggest that this is due to RIP1/3 signaling through CXCL1 ligation of its receptor CLEC4E/Mincle[1] that is also expressed on TAM. Thus, TAM lose their immunosuppressive features in the absence of either RIP3 or CLEC4E, which is accompanied by regain of immune defense promoting signaling in T-cells (741). A clinical study showed that an IDO1 inhibitor prevented disease progression. IDO1 catalyzes the degradation of tryptophan to kynurenine (742). Tryptophan is essential for T-cells, but kynurenine supports immunosuppression. Accordingly, IDO1 suppresses effector T-cells and NK and promotes induction, activation and recruitment of Treg and MDSC, the signaling pathways differing between leukocyte subsets (743). An elegant study recently reported on Treg signaling in the tumor environment. Tumor Treg undergo apoptosis and apoptotic Treg exhibit stronger immunosuppressive features than live Treg. Treg apoptosis is due to high oxidative stress susceptibility by weak NRF2[1] Tf and antioxidant system-associated gene expression. Apoptotic Treg-promoted immunosuppression relies on release and conversion of a large amount of ATP to adenosine by CD39 and CD73, and ADORA2A[1] pathway activation (744). Galectins are another family of secreted proteins contributing to immune evasion in PaCa (745). Galectins have high affinity for β-galactoside residues, sharing a consensus carbohydrate recognition domain (CRD) responsible for glycan binding, most of their biological functions relying on interactions with glycosylated proteins (746). aPSC account for galectin1 secretion and overexpression in the tumor microenvironment (716). Galectin1 recognizes glycoproteins

on T-cells, inhibits transendothelial migration and promotes apoptosis of activated Th1 cells, tilting the immune balance toward a Th2 profile. Galectin1 also impairs NK cell recruitment, induces Treg differentiation, M2 macrophage polarization, and MDSC expansion (747, 748), suggesting galectin1 a key driver in immune evasion in PaCa (748). Galectin9 also is crucial for immune deviation in PaCa. Galectin9 is a ligand for dectin1[1], highly expressed in PaCa Mϕ. Dectin ligation promotes signaling via syk[1], PLCγ, and the JNK pathway. The dectin1-galectin9 axis is central in directing the differentiation of TAM to a M2-like phenotype, which suffices for reprogramming CD4+ and CD8+ T-cells (749). Finally, we list some reviews helpful as starting information on PaCa-selective metabolic changes that affect immune responses in PaCa (739, 750–754).

Summarizing at least some aspects of immune modulation by the particular stroma reaction in PaCa, PSC/CAF secrete SDF1 that coats the tumor cells and prevents T-cell infiltration (640, 755). PSC also secrete galectin1 forcing T-cell apoptosis and Th2 deviation (716), but recruiting Treg (485) and supporting mononuclear cell differentiation toward MDSC (756), with suppressive myeloid cells being most abundant in PaCa, TAM accounting for 15–20% and MDSC for 5–10% (716, 757). Tumor-derived GM-CSF and MIP2 account for MDSC (716, 757), CSF1 and BAG3[1] for TAM (757, 758) recruitment and expansion, GM-CSF being also provided by tumor-associated mesenchymal cells (759). Both MDSC and TAM direct suppression through factors and tumor-cell-specific PDL1 expression (625, 760–762). B-cells are recruited via tumor-derived CXCL13 (763). A shift toward M2 via PI3Kγ-activated BTK[1] in B-cells and TAM supports PaCa growth and progression (764).

Taken together, PaCa and the dysplastic stroma hamper leukocyte infiltration and skew toward immunosuppressive components. This accounts for the non-adaptive and the adaptive immune system. The strong impact of PaCa and the stroma is reflected by low onco-immunotherapy efficacy, which fosters research on combined therapeutic approaches. With 416 reviews total and 86 in the last 18 months, on immunotherapy in PaCa, we apologize not mentioning this aspect, which goes beyond the scope of our trial giving an overview of the particularly dense crosstalk between PaCa and the stroma. Nonetheless, the body's defense mechanism being highly efficient at maintaining health and coping with a wide range of diseases, there is some hope that after unraveling the complex and intertwined contributions of individual components and signaling pathways, immunotherapy may shortly contribute in defeating PaCa (765).

CONCLUSION AND OUTLOOK

PaCa has a dismal prognosis and incidence is rapidly increasing. This fostered utmost intense research aiming elaborating the underlying mechanisms, which unequivocally demonstrated the lead role of the PaCa stroma, frequently displaying rebound effects on the tumor cells and between the individual stroma elements. These features seriously aggravate pinpointing single molecular mechanisms such that despite strong progress, we are still tickling the top of a non-melting iceberg. In brief,

1. Unlike most cancer, angiogenesis is reduced in PaCa. Pressure from the dense dysplastic reaction may be partly responsible for inadequate angiogenesis. We assume an active contribution of PaCa-TEX, which interfere with EC migration, expansion and sprouting *in vitro* and *in vivo*. The underlying mechanism remains to be clarified. A comparative analysis of the proteome, coding and noncoding RNA of PaCa-TEX and TEX of a strongly vascularized tumor might be a starting point depicting active contributors to poor PaCa vascularization. Irrespective of the suggested PaCa interference with angiogenesis, the stroma provides copious nutrients and redirects the tumor cells' metabolic pathways such that hypoxia-promoted damages are completely waved.
2. PSC/CAF are central for PaCa stroma dysplasia. The dysplastic stroma strongly adds to immune defense deviation and supports PNI. Progress in suppressing the overshooting stroma reaction may be achieved by a profound analysis of signaling/metabolic pathways linked to aPSC. The discussion still being ongoing, we only mentioned few examples of aPSC/CAF-promoted metabolic reprogramming and possible contributions of aPSC/CAF miRNA and lncRNA (483, 484). Nonetheless and despite overwhelming evidences for PaCa-promoting activities of aPSC/CAF, the dysplastic stroma could serve as a protective barrier for the host against the tumor under selected circumstances. Thus, in the growing list of therapeutic reagents interfering with the metabolism and/or signaling cascades in aPSC (766), the option of reverting PSC to their quiescent state by supporting FA synthesis could be of particular interest (767).
3. PaCa shares with many tumors a paucity of immunogenic tumor-associated antigens and excessive tumor-promoted immunosuppression. These drawbacks for immunotherapy are aggravated in PaCa by the dysplastic stroma. As immunosuppressive cells are enriched in the PaCa stroma, the stroma density may not considerably contribute excluding immune cells. In fact, it is within the stroma that immune cells are killed or deviate toward immunosuppression. Tumor immunotherapy with a strong focus on the transfer of activated DC and T-cells to circumvent low tumor antigen immunogenicity, requires in depth elaboration of in loco deviation to find pathways allowing activation of transferred immune cells within PaCa. This also accounts for the transfer of DC-Exo, where physical barriers are no hindrance, and for antibody-based therapies, where BTK activation by binding to FcRγ+ TAM needs to be bypassed. However, as good progress is already achieved in MDSC elimination, there is hope that remaining hurdles may be solved.
4. PNI, though not unique, is the dominant metastatic route already at early stages of PaCa development. Elaboration of underlying mechanisms is aggravated by an active contribution of the neuronal components. Comparative analyses to brain tumors, particularly glioblastoma, may provide hints for unraveling the crosstalk between tumor cells and nerves including Schwann cells and ganglia. With strong evidence for synaptic information transfer by EV, a

focus on the impact of nerve-, microglia-, and Schwann cell-derived Exo/MV on tumor cells could help unraveling the neural system contribution in diverting PaCa cells toward this particular metastatic route.

5. Many studies on PaCIC markers and the feedback on the tumor matrix, EC, the adaptive, and non-adaptive immune system point toward these markers severely affecting host matrix and cells. PaCIC markers are engaged in regulation of transcription, activation of signaling cascades, and metabolic shifts, spurring adhesion, migration, and invasion. Abundantly recovered PaCIC markers on TEX contribute to TEX biogenesis including loading, target binding, and TEX uptake (86). Intensifying studies on cooperation-based peculiarities of PaCIC-TEX markers may uncover a central switch in the PaCIC-stroma interplay, allowing for a unifying concept of PaCIC-TEX-based therapies.
6. We apologize for sparse discussion on signaling pathways in the PaCa-stroma crosstalk. First, signaling pathways are often connected and can be mutually affecting. More importantly, *in vivo* studies only depict the overall changes on tumor cells or stroma, even organoid cultures having some limits in depicting individual components. Nonetheless, organoid cultures provide an excellent method for unraveling the complex and mutual interactions between PaCa cells and their surrounding components (768, 769). It can be expected that continuing advancement in organoid research will markedly increase knowledge of the molecular features of the mutual crosstalk between the distinct components and pave the way for large scale therapeutic screenings that may prove reliable for clinical translation (770).
7. Though providing up-to-date references to the date of submission, for the sake of clarity and length we kindly ask scientists working on special topics gathering additional information. This request particularly applies to ncRNA, where multiple targets for most miRNA hamper coordination and the diverse range of lncRNA functions awaits comprehensive examination (86, 136, 139, 771–773). Furthermore, in view of many eminent reviews, we skipped information on therapeutic translation. Finally, we apologize for not citing numerous outstanding studies.

AUTHOR CONTRIBUTIONS

MZ planned the organization of the review and wrote the first draft. WM and ZW helped with data collection and corrected the first draft. All authors approved the final version.

FUNDING

This work was supported by grants from the National Natural Science Foundation of China (81803269) (WM), the Shanghai Sailing Program (18YF1412100) (WM), and the National Natural Science Foundation of China (NSFC. 81702877) (ZW).

SUPPLEMENTARY MATERIAL

The Supplementary Material for this article can be found online at: https://www.frontiersin.org/articles/10.3389/fonc.2019.01359/full#supplementary-material

REFERENCES

1. Gupta GP, Massagué J. Cancer metastasis: building a framework. *Cell.* (2006) 127:679–95. doi: 10.1016/j.cell.2006.11.001
2. Valastyan S, Weinberg RA. Tumor metastasis: molecular insights and evolving paradigms. *Cell.* (2011) 147:275–92. doi: 10.1016/j.cell.2011.09.024
3. Bissell MJ, Hines WC. Why don't we get more cancer? A proposed role of the microenvironment in restraining cancer progression. *Nat Med.* (2011) 17:320–9. doi: 10.1038/nm.2328
4. Te Boekhorst V, Friedl P. Plasticity of cancer cell invasion-mechanisms and implications for therapy. *Adv Cancer Res.* (2016) 132:209–64. doi: 10.1016/bs.acr.2016.07.005
5. Lamouille S, Xu J, Derynck R. Molecular mechanisms of epithelial-mesenchymal transition. *Nat Rev Mol Cell Biol.* (2014) 15:178–96. doi: 10.1038/nrm3758
6. Tao L, Huang G, Song H, Chen Y, Chen L. Cancer associated fibroblasts: an essential role in the tumor microenvironment. *Oncol Lett.* (2017) 14:2611–20. doi: 10.3892/ol.2017.6497
7. Bussard KM, Mutkus L, Stumpf K, Gomez-Manzano C, Marini FC. Tumor-associated stromal cells as key contributors to the tumor microenvironment. *Breast Cancer Res.* (2016) 18:84. doi: 10.1186/s13058-016-0740-2
8. Fiorio Pla A, Gkika D. Emerging role of TRP channels in cell migration: from tumor vascularization to metastasis. *Front Physiol.* (2013) 4:311. doi: 10.3389/fphys.2013.00311
9. Vaahtomeri K, Karaman S, Mäkinen T, Alitalo K. Lymphangiogenesis guidance by paracrine and pericellular factors. *Genes Dev.* (2017) 31:1615–34. doi: 10.1101/gad.303776.117
10. Draoui N, de Zeeuw P, Carmeliet P. Angiogenesis revisited from a metabolic perspective: role and therapeutic implications of endothelial cell metabolism. *Open Biol.* (2017) 7:170219. doi: 10.1098/rsob.170219
11. Paoli P, Giannoni E, Chiarugi P. Anoikis molecular pathways and its role in cancer progression. *Biochim Biophys Acta.* (2013) 1833:3481–98. doi: 10.1016/j.bbamcr.2013.06.026
12. Hawk MA, Schafer ZT. Mechanisms of redox metabolism and cancer cell survival during extracellular matrix detachment. *J Biol Chem.* (2018) 293:7531–7. doi: 10.1074/jbc.TM117.000260
13. Elia I, Doglioni G, Fendt SM. Metabolic hallmarks of metastasis formation. *Trends Cell Biol.* (2018) 28:673–84. doi: 10.1016/j.tcb.2018.04.002
14. Lou XL, Sun J, Gong SQ, Yu XF, Gong R, Deng H. Interaction between circulating cancer cells and platelets: clinical implication. *Chin J Cancer Res.* (2015) 27:450–60. doi: 10.3978/j.issn.1000-9604.2015.04.10
15. Leblanc R, Peyruchaud O. Metastasis: new functional implications of platelets and megakaryocytes. *Blood.* (2016) 128:24–31. doi: 10.1182/blood-2016-01-636399
16. Reymond N, d'Água BB, Ridley AJ. Crossing the endothelial barrier during metastasis. *Nat Rev Cancer.* (2013) 13:858–70. doi: 10.1038/nrc3628
17. Strilic B, Offermanns S. Intravascular survival and extravasation of tumor cells. *Cancer Cell.* (2017) 32:282–93. doi: 10.1016/j.ccell.2017.07.001
18. Thuma F, Zöller M. Outsmart tumor exosomes to steal the cancer initiating cell its niche. *Semin Cancer Biol.* (2014) 28:39–50. doi: 10.1016/j.semcancer.2014.02.011
19. Liu Y, Cao X. Characteristics and significance of the pre-metastatic niche. *Cancer Cell.* (2016) 30:668–81. doi: 10.1016/j.ccell.2016.09.011

20. Peinado H, Zhang H, Matei IR, Costa-Silva B, Hoshino A, Rodrigues G, et al. Pre-metastatic niches: organ-specific homes for metastases. *Nat Rev Cancer.* (2017) 17:302–17. doi: 10.1038/nrc.2017.6
21. Lobb RJ, Lima LG, Möller A. Exosomes: key mediators of metastasis and pre-metastatic niche formation. *Semin Cell Dev Biol.* (2017) 67:3–10. doi: 10.1016/j.semcdb.2017.01.004
22. Lambert AW, Pattabiraman DR, Weinberg RA. Emerging biological principles of metastasis. *Cell.* (2017) 168:670–91. doi: 10.1016/j.cell.2016.11.037
23. Nandy SB, Lakshmanaswamy R. Cancer stem cells and metastasis. *Prog Mol Biol Transl Sci.* (2017) 151:137–76. doi: 10.1016/bs.pmbts.2017.07.007
24. Dhamija S, Diederichs S. From junk to master regulators of invasion: lncRNA functions in migration, EMT and metastasis. *Int J Cancer.* (2016) 139:269–80. doi: 10.1002/ijc.30039
25. Brabletz T. To differentiate or not–routes towards metastasis. *Nat Rev Cancer.* (2012) 12:425–36. doi: 10.1038/nrc3265
26. Kim DH, Xing T, Yang Z, Dudek R, Lu Q, Chen YH. Epithelial mesenchymal transition in embryonic development, tissue repair and cancer: a comprehensive overview. *J Clin Med.* (2017) 7:E1. doi: 10.3390/jcm7010001
27. Jolly MK, Ware KE, Gilja S, Somarelli JA, Levine H. EMT and MET: necessary or permissive for metastasis? *Mol Oncol.* (2017) 11:755–69. doi: 10.1002/1878-0261.12083
28. Mareel MM, Van Roy FM, Bracke ME. How and when do tumor cells metastasize? *Crit Rev Oncog.* (1993) 4:559–94.
29. Siegel RL, Miller KD, Jemal A. Cancer statistics, 2016. *CA Cancer J Clin.* (2016) 66:7–30. doi: 10.3322/caac.21332
30. Strijker M, Chen JW, Mungroop TH, Jamieson NB, van Eijck CH, Steyerberg EW, et al. Systematic review of clinical prediction models for survival after surgery for resectable pancreatic cancer. *Br J Surg.* (2019) 106:342–54. doi: 10.1002/bjs.11111
31. Rahib L, Smith BD, Aizenberg R, Rosenzweig AB, Fleshman JM, Matrisian LM. Projecting cancer incidence and deaths to 2030: the unexpected burden of thyroid, liver, and pancreas cancers in the United States. *Cancer Res.* (2014) 74:2913–21. doi: 10.1158/0008-5472.CAN-14-0155
32. Del Chiaro M, Segersvärd R, Lohr M, Verbeke C. Early detection and prevention of pancreatic cancer: is it really possible today? *World J Gastroenterol.* (2014) 20:12118–31. doi: 10.3748/wjg.v20.i34.12118
33. Ajani JA, Song S, Hochster HS, Steinberg IB. Cancer stem cells: the promise and the potential. *Semin Oncol.* (2015) 42(Suppl. 1):S3–17. doi: 10.1053/j.seminoncol.2015.01.001
34. Nielsen MF, Mortensen MB, Detlefsen S. Key players in pancreatic cancer-stroma interaction: Cancer-associated fibroblasts, endothelial and inflammatory cells. *World J Gastroenterol.* (2016) 22:2678–700. doi: 10.3748/wjg.v22.i9.2678
35. Pothula SP, Xu Z, Goldstein D, Pirola RC, Wilson JS, Apte MV. Key role of pancreatic stellate cells in pancreatic cancer. *Cancer Lett.* (2016) 381:194–200. doi: 10.1016/j.canlet.2015.10.035
36. Vennin C, Murphy KJ, Morton JP, Cox TR, Pajic M, Timpson P. Reshaping the tumor stroma for treatment of pancreatic cancer. *Gastroenterology.* (2018) 154:820–38. doi: 10.1053/j.gastro.2017.11.280
37. Liang D, Shi S, Xu J, Zhang B, Qin Y, Ji S, et al. New insights into perineural invasion of pancreatic cancer: more than pain. *Biochim Biophys Acta.* (2016) 1865:111–22. doi: 10.1016/j.bbcan.2016.01.002
38. Jurcak N, Zheng L. Signaling in the microenvironment of pancreatic cancer: transmitting along the nerve. *Pharmacol Ther.* (2019) 200:126–134. doi: 10.1016/j.pharmthera.2019.04.010
39. Chen SH, Zhang BY, Zhou B, Zhu CZ, Sun LQ, Feng YJ. Perineural invasion of cancer: a complex crosstalk between cells and molecules in the perineural niche. *Am J Cancer Res.* (2019) 9:1–21.
40. Deborde S, Wong RJ. How Schwann cells facilitate cancer progression in nerves. *Cell Mol Life Sci.* (2017) 74:4405–20. doi: 10.1007/s00018-017-2578-x
41. Parente P, Parcesepe P, Covelli C, Olivieri N, Remo A, Pancione M, et al. Crosstalk between the tumor microenvironment and immune system in pancreatic ductal adenocarcinoma: potential targets for new therapeutic approaches. *Gastroenterol Res Pract.* (2018) 2018:7530619. doi: 10.1155/2018/7530619
42. Foucher ED, Ghigo C, Chouaib S, Galon J, Iovanna J, Olive D. Pancreatic ductal adenocarcinoma: a strong imbalance of good and bad immunological cops in the tumor microenvironment. *Front Immunol.* (2018) 9:1044. doi: 10.3389/fimmu.2018.01044
43. Théry C, Zitvogel L, Amigorena S. Exosomes: composition, biogenesis and function. *Nat Rev Immunol.* (2002) 2:569–79. doi: 10.1038/nri855
44. Boukouris S, Mathivanan S. Exosomes in bodily fluids are a highly stable resource of disease biomarkers. *Proteomics Clin Appl.* (2015) 9:358–67. doi: 10.1002/prca.201400114
45. Jia S, Zocco D, Samuels ML, Chou MF, Chammas R, Skog J, et al. Emerging technologies in extracellular vesicle-based molecular diagnostics. *Expert Rev Mol Diagn.* (2014) 14:307–21. doi: 10.1586/14737159.2014.893828
46. Valadi H, Ekström K, Bossios A, Sjöstrand M, Lee JJ, Lötvall JO. Exosome-mediated transfer of mRNAs and microRNAs is a novel mechanism of genetic exchange between cells. *Nat Cell Biol.* (2007) 9:654–9. doi: 10.1038/ncb1596
47. Lo Cicero A, Stahl PD, Raposo G. Extracellular vesicles shuffling intercellular messages: for good or for bad. *Curr Opin Cell Biol.* (2015) 35:69–77. doi: 10.1016/j.ceb.2015.04.013
48. Javeed N, Mukhopadhyay D. Exosomes and their role in the micro-/macro-environment: a comprehensive review. *J Biomed Res.* (2017) 31:386–94. doi: 10.7555/JBR.30.20150162
49. Burrello J, Monticone S, Gai C, Gomez Y, Kholia S, Camussi G. stem cell-derived extracellular vesicles and immune-modulation. *Front Cell Dev Biol.* (2016) 4:83. doi: 10.3389/fcell.2016.00083
50. Todorova D, Simoncini S, Lacroix R, Sabatier F, Dignat-George F. Extracellular vesicles in angiogenesis. *Circ Res.* (2017) 120:1658–73. doi: 10.1161/CIRCRESAHA.117.309681
51. Rajagopal C, Harikumar KB. The origin and functions of exosomes in cancer. *Front Oncol.* (2018) 8:66. doi: 10.3389/fonc.2018.00066
52. Colombo M, Raposo G, Théry C. Biogenesis, secretion, and intercellular interactions of exosomes and other extracellular vesicles. *Annu Rev Cell Dev Biol.* (2014) 30:255–89. doi: 10.1146/annurev-cellbio-101512-122326
53. van Niel G, D'Angelo G, Raposo G. Shedding light on the cell biology of extracellular vesicles. *Nat Rev Mol Cell Biol.* (2018) 19:213–28. doi: 10.1038/nrm.2017.125
54. Abels ER, Breakefield XO. Introduction to extracellular vesicles: biogenesis, RNA cargo selection, content, release, and uptake. *Cell Mol Neurobiol.* (2016) 36:301–12. doi: 10.1007/s10571-016-0366-z
55. Villarroya-Beltri C, Baixauli F, Gutiérrez-Vázquez C, Sánchez-Madrid F, Mittelbrunn M. Sorting it out: regulation of exosome loading. *Semin Cancer Biol.* (2014) 28:3–13. doi: 10.1016/j.semcancer.2014.04.009
56. Choi DS, Kim DK, Kim YK, Gho YS. Proteomics of extracellular vesicles: exosomes and ectosomes. *Mass Spectrom Rev.* (2015) 34:474–90. doi: 10.1002/mas.21420
57. Nabhan JF, Hu R, Oh RS, Cohen SN, Lu Q. Formation and release of arrestin domain-containing protein 1-mediated microvesicles (ARMMs) at plasma membrane by recruitment of TSG101 protein. *Proc Natl Acad Sci USA.* (2012) 109:4146–51. doi: 10.1073/pnas.1200448109
58. Egea-Jimenez AL, Zimmermann P. Phospholipase D and phosphatidic acid in the biogenesis and cargo loading of extracellular vesicles. *J Lipid Res.* (2018) 59:1554–60. doi: 10.1194/jlr.R083964
59. Shen B, Fang Y, Wu N, Gould SJ. Biogenesis of the posterior pole is mediated by the exosome/microvesicle protein-sorting pathway. *J Biol Chem.* (2011) 286:44162–76. doi: 10.1074/jbc.M111.274803
60. Guo BB, Bellingham SA, Hill AF. The neutral sphingomyelinase pathway regulates packaging of the prion protein into exosomes. *J Biol Chem.* (2015) 290:3455–67. doi: 10.1074/jbc.M114.605253
61. Moreno-Gonzalo O, Fernandez-Delgado I, Sanchez-Madrid F. Post-translational add-ons mark the path in exosomal protein sorting. *Cell Mol Life Sci.* (2018) 75:1–19. doi: 10.1007/s00018-017-2690-y
62. Vedeler A, Hollås H, Grindheim AK, Raddum AM. Multiple roles of annexin A2 in post-transcriptional regulation of gene expression. *Curr Protein Pept Sci.* (2012) 13:401–12. doi: 10.2174/138920312801619402
63. Janas T, Janas MM, Sapon K, Janas T. Mechanisms of RNA loading into exosomes. *FEBS Lett.* (2015) 589:1391–8. doi: 10.1016/j.febslet.2015.04.036
64. Villarroya-Beltri C, Gutierrez-Vazquez C, Sanchez-Cabo F, Pérez-Hernández D, Vázquez J, Martin-Cofreces N, et al. Sumoylated hnRNPA2B1 controls the

sorting of miRNAs into exosomes through binding to specific motifs. *Nat Commun.* (2013) 4:2980. doi: 10.1038/ncomms3980
65. Gezer U, Özgür E, Cetinkaya M, Isin M, Dalay N. Long non-coding RNAs with low expression levels in cells are enriched in secreted exosomes. *Cell Biol Int.* (2014) 38:1076–9. doi: 10.1002/cbin.10301
66. Dragomir M, Chen B, Calin GA. Exosomal lncRNAs as new players in cell-to-cell communication. *Transl Cancer Res.* (2018) 7(Suppl 2):S243–52. doi: 10.21037/tcr.2017.10.46
67. Hessvik NP, Llorente A. Current knowledge on exosome biogenesis and release. *Cell Mol Life Sci.* (2018) 75:193–208. doi: 10.1007/s00018-017-2595-9
68. Subra C, Grand D, Laulagnier K, Stella A, Lambeau G, Paillasse M, et al. Exosomes account for vesicle-mediated transcellular transport of activatable phospholipases and prostaglandins. *J Lipid Res.* (2010) 51:2105–20. doi: 10.1194/jlr.M003657
69. Skotland T, Hessvik NP, Sandvig K, Llorente A. Exosomal lipid composition and the role of ether lipids and phosphoinositides in exosome biology. *J Lipid Res.* (2018) 60:9–18. doi: 10.1194/jlr.R084343
70. Laulagnier K, Grand D, Dujardin A, Hamdi S, Vincent-Schneider H, Lankar D, et al. PLD2 is enriched on exosomes and its activity is correlated to the release of exosomes. *FEBS Lett.* (2004) 572:11–4. doi: 10.1016/j.febslet.2004.06.082
71. Carayon K, Chaoui K, Ronzier E, Lazar I, Bertrand-Michel J, Roques V, et al. Proteolipidic composition of exosomes changes during reticulocyte maturation. *J Biol Chem.* (2011) 286:34426–39. doi: 10.1074/jbc.M111.257444
72. Paillasse MR, de Medina P, Amouroux G, Mhamdi L, Poirot M, Silvente-Poirot S. Signaling through cholesterol esterification: a new pathway for the cholecystokinin 2 receptor involved in cell growth and invasion. *J Lipid Res.* (2009) 50:2203–11. doi: 10.1194/jlr.M800668-JLR200
73. Bowden KL, Bilbey NJ, Bilawchuk LM, Boadu E, Sidhu R, Ory DS, et al. Lysosomal acid lipase deficiency impairs regulation of ABCA1 gene and formation of high density lipoproteins in cholesteryl ester storage disease. *J Biol Chem.* (2011) 286:30624–35. doi: 10.1074/jbc.M111.274381
74. Costa Verdera H, Gitz-Francois JJ, Schiffelers RM, Vader P. Cellular uptake of extracellular vesicles is mediated by clathrin-independent endocytosis and macropinocytosis. *J Control Release.* (2017) 266:100–8. doi: 10.1016/j.jconrel.2017.09.019
75. Strauss K, Goebel C, Runz H, Möbius W, Weiss S, Feussner I, et al. Exosome secretion ameliorates lysosomal storage of cholesterol in Niemann-Pick type C disease. *J Biol Chem.* (2010) 285:26279–88. doi: 10.1074/jbc.M110.134775
76. Record M, Silvente-Poirot S, Poirot M, Wakelam MJO. Extracellular vesicles: lipids as key components of their biogenesis and functions. *J Lipid Res.* (2018) 59:1316–24. doi: 10.1194/jlr.E086173
77. Skotland T, Sandvig K, Llorente A. Lipids in exosomes: current knowledge and the way forward. *Prog Lipid Res.* (2017) 66:30–41. doi: 10.1016/j.plipres.2017.03.001
78. Pollet H, Conrard L, Cloos AS, Tyteca D. Plasma membrane lipid domains as platforms for vesicle biogenesis and shedding? *Biomolecules.* (2018) 8:E94. doi: 10.3390/biom8030094
79. Choi D, Spinelli C, Montermini L, Rak J. Oncogenic regulation of extracellular vesicle proteome and heterogeneity. *Proteomics.* (2019) 19:e1800169. doi: 10.1002/pmic.201800169
80. Zöller M. Tetraspanins: push and pull in suppressing and promoting metastasis. *Nat Rev Cancer.* (2009) 9:40–55. doi: 10.1038/nrc2543
81. Andreu Z, Yáñez-Mó M. Tetraspanins in extracellular vesicle formation and function. *Front Immunol.* (2014) 5:442. doi: 10.3389/fimmu.2014.00442
82. Greening DW, Xu R, Gopal SK, Rai A, Simpson RJ. Proteomic insights into extracellular vesicle biology - defining exosomes and shed microvesicles. *Expert Rev Proteomics.* (2017) 14:69–95. doi: 10.1080/14789450.2017.1260450
83. Rosa-Fernandes L, Rocha VB, Carregari VC, Urbani A, Palmisano G. A perspective on extracellular vesicles proteomics. *Front Chem.* (2017) 5:102. doi: 10.3389/fchem.2017.00102
84. Heiler S, Wang Z, Zöller M. Pancreatic cancer stem cell markers and exosomes - the incentive push. *World J Gastroenterol.* (2016) 22:5971–6007. doi: 10.3748/wjg.v22.i26.5971
85. Sun Z, Wang L, Dong L, Wang X. Emerging role of exosome signalling in maintaining cancer stem cell dynamic equilibrium. *J Cell Mol Med.* (2018). doi: 10.1111/jcmm.13676. [Epub ahead of print].
86. Wang Z, Zöller M. Exosomes, metastases, and the miracle of cancer stem cell markers. *Cancer Metastasis Rev.* (2019) 38:259–95. doi: 10.1007/s10555-019-09793-6
87. Lee SY, Jeong EK, Ju MK, Jeon HM, Kim MY, Kim CH, et al. Induction of metastasis, cancer stem cell phenotype, and oncogenic metabolism in cancer cells by ionizing radiation. *Mol Cancer.* (2017) 16:10. doi: 10.1186/s12943-016-0577-4
88. Lathia JD, Liu H. Overview of cancer stem cells and stemness for community oncologists. *Target Oncol.* (2017) 12:387–99. doi: 10.1007/s11523-017-0508-3
89. Najafi M, Mortezaee K, Ahadi R. Cancer stem cell (a)symmetry & plasticity: tumorigenesis and therapy relevance. *Life Sci.* (2019) 231:116520. doi: 10.1016/j.lfs.2019.05.076
90. Rao CV, Mohammed A. New insights into pancreatic cancer stem cells. *World J Stem Cells.* (2015) 7:547–55. doi: 10.4252/wjsc.v7.i3.547
91. Wang Z, Zhao K, Hackert T, Zöller M. CD44/CD44v6 a reliable companion in cancer-initiating cell maintenance and tumor progression. *Front Cell Dev Biol.* (2018) 6:97. doi: 10.3389/fcell.2018.00097
92. Hoshino A, Costa-Silva B, Shen TL, Rodrigues G, Hashimoto A, Tesic Mark M, et al. Tumour exosome integrins determine organotropic metastasis. *Nature.* (2015) 527:329–35. doi: 10.1038/nature15756
93. Paolillo M, Schinelli S. Integrins and exosomes, a dangerous liaison in cancer progression. *Cancers.* (2017) 9: E95. doi: 10.3390/cancers9080095
94. Ma B, Zhang L, Zou Y, He R, Wu Q, Han C, et al. Reciprocal regulation of integrin β4 and KLF4 promotes gliomagenesis through maintaining cancer stem cell traits. *J Exp Clin Cancer Res.* (2019) 38:23. doi: 10.1186/s13046-019-1034-1
95. Eom BW, Joo J, Park B, Jo MJ, Choi SH, Cho SJ, et al. Nomogram incorporating CD44v6 and clinicopathological factors to predict lymph node metastasis for early gastric cancer. *PLoS ONE.* (2016) 11:e0159424. doi: 10.1371/journal.pone.0159424
96. Matsumoto K, Umitsu M, De Silva DM, Roy A, Bottaro DP. Hepatocyte growth factor/MET in cancer progression and biomarker discovery. *Cancer Sci.* (2017) 108:296–307. doi: 10.1111/cas.13156
97. Giovannetti E, van der Borden CL, Frampton AE, Ali A, Firuzi O, Peters GJ. Never let it go: Stopping key mechanisms underlying metastasis to fight pancreatic cancer. *Semin Cancer Biol.* (2017) 44:43–59. doi: 10.1016/j.semcancer.2017.04.006
98. Guo F, Wang Y, Liu J, Mok SC, Xue F, Zhang W. CXCL12/CXCR4: a symbiotic bridge linking cancer cells and their stromal neighbors in oncogenic communication networks. *Oncogene.* (2016) 35:816–26. doi: 10.1038/onc.2015.139
99. Li YP, Pang J, Gao S, Bai PY, Wang WD, Kong P, et al. Role of CXCR4 and SDF1 as prognostic factors for survival and the association with clinicopathology in colorectal cancer: a systematic meta-analysis. *Tumour Biol.* (2017) 39:1010428317706206. doi: 10.1177/1010428317706206
100. Sleightholm RL, Neilsen BK, Li J, Steele MM, Singh RK, Hollingsworth MA, et al. Emerging roles of the CXCL12/CXCR4 axis in pancreatic cancer progression and therapy. *Pharmacol Ther.* (2017) 179:158–70. doi: 10.1016/j.pharmthera.2017.05.012
101. Liu H, Jiang F, Jia X, Lan J, Guo H, Li E, et al. Cycling hypoxia affects cell invasion and proliferation through direct regulation of claudin1/claudin7 expression, and indirect regulation of P18 through claudin7. *Oncotarget.* (2017) 8:10298–311. doi: 10.18632/oncotarget.14397
102. Wu Z, Shi J, Song Y, Zhao J, Sun J, Chen X, et al. Claudin-7 (CLDN7) is overexpressed in gastric cancer and promotes gastric cancer cell proliferation, invasion and maintains mesenchymal state. *Neoplasma.* (2018) 65:349–59. doi: 10.4149/neo_2018_170320N200
103. Rassouli FB, Matin MM, Saeinasab M. Cancer stem cells in human digestive tract malignancies. *Tumour Biol.* (2016) 37:7–21. doi: 10.1007/s13277-015-4155-y
104. Zarour LR, Anand S, Billingsley KG, Bisson WH, Cercek A, Clarke MF, et al. Colorectal cancer liver metastasis: evolving paradigms and future directions. *Cell Mol Gastroenterol Hepatol.* (2017) 3:163–73. doi: 10.1016/j.jcmgh.2017.01.006

105. Katoh M. Canonical and non-canonical WNT signaling in cancer stem cells and their niches: Cellular heterogeneity, omics reprogramming, targeted therapy and tumor plasticity (Review). *Int J Oncol.* (2017) 51:1357–69. doi: 10.3892/ijo.2017.4129
106. Basu S, Haase G, Ben-Ze'ev A. Wnt signaling in cancer stem cells and colon cancer metastasis. *F1000Res.* (2016) 5:F1000 Faculty Rev-699. doi: 10.12688/f1000research.7579.1
107. Rappa G, Mercapide J, Anzanello F, Pope RM, Lorico A. Biochemical and biological characterization of exosomes containing prominin-1/CD133. *Mol Cancer.* (2013) 12:62. doi: 10.1186/1476-4598-12-62
108. Li X, Zhao H, Gu J, Zheng L. Prognostic value of cancer stem cell marker CD133 expression in pancreatic ductal adenocarcinoma (PDAC): a systematic review and meta-analysis. *Int J Clin Exp Pathol.* (2015) 8:12084–92.
109. Mitchell SF, Parker R. Principles and properties of eukaryotic mRNPs. *Mol Cell.* (2014) 54:547–58. doi: 10.1016/j.molcel.2014.04.033
110. Gerstberger S, Hafner M, Tuschl T. A census of human RNA-binding proteins. *Nat Rev Genet.* (2014) 15:829–45. doi: 10.1038/nrg3813
111. Castello A, Horos R, Strein C, Fischer B, Eichelbaum K, Steinmetz LM, et al. Comprehensive identification of RNA-binding proteins by RNA interactome capture. *Methods Mol Biol.* (2016) 1358:131–9. doi: 10.1007/978-1-4939-3067-8_8
112. Yamashita A, Takeuchi O. Translational control of mRNAs by 3'-Untranslated region binding proteins. *BMB Rep.* (2017) 50:194–200. doi: 10.5483/BMBRep.2017.50.4.040
113. Castello A, Hentze MW, Preiss T. Metabolic enzymes enjoying new partnerships as RNA-binding proteins. *Trends Endocrinol Metab.* (2015) 26:746–57. doi: 10.1016/j.tem.2015.09.012
114. Chang CH, Curtis JD, Maggi LB Jr, Faubert B, Villarino AV, O'Sullivan D, et al. Posttranscriptional control of T cell effector function by aerobic glycolysis. *Cell.* (2013) 153:1239–51. doi: 10.1016/j.cell.2013.05.016
115. Chin A, Lécuyer E. RNA localization: making its way to the center stage. *Biochim Biophys Acta Gen Subj.* (2017) 1861:2956–70. doi: 10.1016/j.bbagen.2017.06.011
116. Eliscovich C, Singer RH. RNP transport in cell biology: the long and winding road. *Curr Opin Cell Biol.* (2017) 45:38–46. doi: 10.1016/j.ceb.2017.02.008
117. Di Liegro CM, Schiera G, Di Liegro I. Extracellular vesicle-associated RNA as a carrier of epigenetic information. *Genes.* (2017) 8:E240. doi: 10.3390/genes8100240
118. Sadik N, Cruz L, Gurtner A, Rodosthenous RS, Dusoswa SA, Ziegler O, et al. Extracellular RNAs: a new awareness of old perspectives. *Methods Mol Biol.* (2018) 1740:1–15. doi: 10.1007/978-1-4939-7652-2_1
119. Castello A, Frese CK, Fischer B, Järvelin AI, Horos R, Alleaume AM, et al. Identification of RNA-binding domains of RNA-binding proteins in cultured cells on a system-wide scale with RBDmap. *Nat Protoc.* (2017) 12:2447–64. doi: 10.1038/nprot.2017.106
120. Varela-Eirin M, Varela-Vazquez A, Rodríguez-Candela Mateos M, Vila-Sanjurjo A, Fonseca E, Mascareñas JL, et al. Recruitment of RNA molecules by connexin RNA-binding motifs: implication in RNA and DNA transport through microvesicles and exosomes. *Biochim Biophys Acta Mol Cell Res.* (2017) 1864:728–36. doi: 10.1016/j.bbamcr.2017.02.001
121. Schiera G, Di Liegro CM, Puleo V, Colletta O, Fricano A, Cancemi P, et al. Extracellular vesicles shed by melanoma cells contain a modified form of H1.0 linker histone and H1.0 mRNA-binding proteins. *Int J Oncol.* (2016) 49:1807–14. doi: 10.3892/ijo.2016.3692
122. Ragni E, Banfi F, Barilani M, Cherubini A, Parazzi V, Larghi P, et al. extracellular vesicle-shuttled mRNA in mesenchymal stem cell communication. *Stem Cells.* (2017) 35:1093–105. doi: 10.1002/stem.2557
123. Schwarzenbach H, Gahan PB. MicroRNA shuttle from cell-to-cell by exosomes and its impact in cancer. *Noncoding RNA.* (2019) 5:E28. doi: 10.3390/ncrna5010028
124. Lee YS Pressman S, Andress AP, Kim K, White JL, Cassidy JJ, et al. Silencing by small RNAs is linked to endosomal trafficking. *Nat Cell Biol.* (2009) 11:1150–6. doi: 10.1038/ncb1930
125. Kosaka N. Iguchi H, Yoshioka Y, Takeshita F, Matsuki Y, Ochiya T. Secretory mechanisms and intercellular transfer of microRNAs in living cells. *J Biol Chem.* (2010) 285:17442–52. doi: 10.1074/jbc.M110.107821
126. Villarroya-Beltri C, Guerra S, Sánchez-Madrid F. ISGylation - a key to lock the cell gates for preventing the spread of threats. *J Cell Sci.* (2017) 130:2961–9. doi: 10.1242/jcs.205468
127. Santangelo L, Giurato G, Cicchini C, Montaldo C, Mancone C, Tarallo R, et al. The RNA-binding protein SYNCRIP is a component of the hepatocyte exosomal machinery controlling MicroRNA sorting. *Cell Rep.* (2016) 17:799–808. doi: 10.1016/j.celrep.2016.09.031
128. Bhome R, Del Vecchio F, Lee GH, Bullock MD, Primrose JN, Sayan AE, et al. Exosomal microRNAs (exomiRs): small molecules with a big role in cancer. *Cancer Lett.* (2018) 420:228–35. doi: 10.1016/j.canlet.2018.02.002
129. Akhade VS, Pal D, Kanduri C. Long noncoding RNA: genome organization and mechanism of action. *Adv Exp Med Biol.* (2017) 1008:47–74. doi: 10.1007/978-981-10-5203-3_2
130. Kino T, Hurt DE, Ichijo T, Nader N, Chrousos GP. Noncoding RNA gas5 is a growth arrest- and starvation-associated repressor of the glucocorticoid receptor. *Sci Signal.* (2010) 3:ra8. doi: 10.1126/scisignal.2000568
131. Ng SY, Johnson R, Stanton LW. Human long non-coding RNAs promote pluripotency and neuronal differentiation by association with chromatin modifiers and transcription factors. *EMBO J.* (2012) 31:522–33. doi: 10.1038/emboj.2011.459
132. Martianov I, Ramadass A, Serra Barros A, Chow N, Akoulitchev A. Repression of the human dihydrofolate reductase gene by a non-coding interfering transcript. *Nature.* (2007) 445:666–70. doi: 10.1038/nature05519
133. Fang Y, Fullwood MJ. Roles, functions, and mechanisms of long non-coding RNAs in cancer. *Genomics Proteomics Bioinformatics.* (2016) 14:42–54. doi: 10.1016/j.gpb.2015.09.006
134. Pandey RR, Mondal T, Mohammad F, Enroth S, Redrup L, Komorowski J. Kcnq1ot1 antisense noncoding RNA mediates lineage-specific transcriptional silencing through chromatin-level regulation. *Mol Cell.* (2008) 32:232–46. doi: 10.1016/j.molcel.2008.08.022
135. Kallen AN, Zhou XB, Xu J, Qiao C, Ma J, Yan L. The imprinted H19 lncRNA antagonizes let-7 microRNAs. *Mol Cell.* (2013) 52:101–12. doi: 10.1016/j.molcel.2013.08.027
136. Kopp F, Mendell JT. Functional classification and experimental dissection of long noncoding RNAs. *Cell.* (2018) 172:393–407. doi: 10.1016/j.cell.2018.01.011
137. Grote P, Wittler L, Hendrix D, Koch F, Wahrisch S, Beisaw A. The tissue-specific lncRNA Fendrr is an essential regulator of heart and body wall development in the mouse. *Dev Cell.* (2013) 24:206–214. doi: 10.1016/j.devcel.2012.12.012
138. Li XL, Wu ZQ, Fu XB, Han WD. LncRNAs: insights into their function and mechanics in underlying disorders. *Mutat Res Rev Mut Res.* (2014) 762:1–21. doi: 10.1016/j.mrrev.2014.04.002
139. Tay Y, Rinn J, Pandolfi PP. The multilayered complexity of ceRNA crosstalk and competition. *Nature.* (2014) 505:344–52. doi: 10.1038/nature12986
140. Xie Y, Dang W, Zhang S, Yue W, Yang L, Zhai X, et al. The role of exosomal noncoding RNAs in cancer. *Mol Cancer.* (2019) 18:37. doi: 10.1186/s12943-019-0984-4
141. Ahadi A, Brennan S, Kennedy PJ, Hutvagner G, Tran N. Long non-coding RNAs harboring miRNA seed regions are enriched in prostate cancer exosomes. *Sci Rep.* (2016) 6:24922. doi: 10.1038/srep24922
142. Kawamura Y, Yamamoto Y, Sato TA, Ochiya T. Extracellular vesicles as trans-genomic agents: emerging roles in disease and evolution. *Cancer Sci.* (2017) 108:824–30. doi: 10.1111/cas.13222
143. Lee TH, Chennakrishnaiah S, Meehan B, Montermini L, Garnier D, D'Asti E, et al. Barriers to horizontal cell transformation by extracellular vesicles containing oncogenic H-ras. *Oncotarget.* (2016) 7:51991–2002. doi: 10.18632/oncotarget.10627
144. Penfornis P, Vallabhaneni KC, Whitt J, Pochampally R. Extracellular vesicles as carriers of microRNA, proteins and lipids in tumor microenvironment. *Int J Cancer.* (2016) 138:14–21. doi: 10.1002/ijc.29417
145. Bakhshandeh B, Kamaleddin MA, Aalishah K. A comprehensive review on exosomes and microvesicles as epigenetic factors. *Curr Stem Cell Res Ther.* (2017) 12:31–36. doi: 10.2174/1574888X11666160709211528
146. Mulcahy LA, Pink RC, Carter DRF. Routes and mechanisms of extracellular vesicle uptake. *J Extracell Vesicles.* (2014) 3. doi: 10.3402/jev.v3.24641

147. Nazarenko I, Rana S, Baumann A, McAlear J, Hellwig A, Trendelenburg M, et al. Cell surface tetraspanin Tspan8 contributes to molecular pathways of exosome-induced endothelial cell activation. *Cancer Res.* (2010) 70:1668–78. doi: 10.1158/0008-5472.CAN-09-2470
148. Gesierich S, Berezovskiy I, Ryschich E, Zöller M. Systemic induction of the angiogenesis switch by the tetraspanin D6.1A/CO-029. *Cancer Res.* (2006) 66:7083–94. doi: 10.1158/0008-5472.CAN-06-0391
149. Buck CA, Horwitz AF. Cell surface receptors for extracellular matrix molecules. *Annu Rev Cell Biol.* (1987) 3:179–205. doi: 10.1146/annurev.cb.03.110187.001143
150. Antonyak MA, Li B, Boroughs LK, Johnson JL, Druso JE, Bryant KL, et al. Cancer cell-derived microvesicles induce transformation by transferring tissue transglutaminase and fibronectin to recipient cells. *Proc Natl Acad Sci USA*. (2011) 108:4852–7. doi: 10.1073/pnas.1017667108
151. Morelli AE, Larregina AT, Shufesky WJ, Sullivan MLG, Stolz DB, Papworth GD, et al. Endocytosis, intracellular sorting, and processing of exosomes by dendritic cells. *Blood.* (2004) 104:3257–66. doi: 10.1182/blood-2004-03-0824
152. Costa-Silva B, Aiello NM, Ocean AJ, Singh S, Zhang H, Thakur BK, et al. Pancreatic cancer exosomes initiate pre-metastatic niche formation in the liver. *Nat Cell Biol.* (2015) 17:816–26. doi: 10.1038/ncb3169
153. Han W, Duan Z. Roles of exosomes in liver metastases: novel diagnosis and treatment choices. *J Cell Physiol.* (2019) 234:21588–600. doi: 10.1002/jcp.28785
154. French KC, Antonyak MA, Cerione RA. Extracellular vesicle docking at the cellular port: extracellular vesicle binding and uptake. *Semin Cell Dev Biol.* (2017) 67:48–55. doi: 10.1016/j.semcdb.2017.01.002
155. Bruno S, Grange C, Deregibus MC, Calogero RA, Saviozzi S, Collino F, et al. Mesenchymal stem cell-derived microvesicles protect against acute tubular injury. *J Am Soc Nephrol.* (2009) 20:1053–67. doi: 10.1681/ASN.2008070798
156. Melo SA, Luecke LB, Kahlert C, Fernandez AF, Gammon ST, Kaye J, et al. Glypican-1 identifies cancer exosomes and detects early pancreatic cancer. *Nature*. (2015) 523:177–82. doi: 10.1038/nature14581
157. Mu W, Rana S, Zöller M. Host matrix modulation by tumor exosomes promotes motility and invasiveness. *Neoplasia*. (2013) 15:875–87. doi: 10.1593/neo.13786
158. Barrès C, Blanc L, Bette-Bobillo P, André S, Mamoun R, Gabius HJ, et al. Galectin-5 is bound onto the surface of rat reticulocyte exosomes and modulates vesicle uptake by macrophages. *Blood*. (2010) 115:696–705. doi: 10.1182/blood-2009-07-231449
159. Rana S, Malinowska K, Zöller M. Exosomal tumor MicroRNA modulates premetastatic organ cells. *Neoplasia*. (2013) 15:281–95. doi: 10.1593/neo.122010
160. Saunderson SC, Dunn AC, Crocker PR, McLellan AD. CD169 mediates the capture of exosomes in spleen and lymph node. *Blood*. (2014) 123:208–16. doi: 10.1182/blood-2013-03-489732
161. Moller-Tank S, Maury W. Phosphatidylserine receptors: enhancers of enveloped virus entry and infection. *Virology*. (2014) 468–70: 565–80. doi: 10.1016/j.virol.2014.09.009
162. Rana S, Yue S, Stadel D, Zöller M. Toward tailored exosomes: the exosomal tetraspanin web contributes to target cell selection. *Int J Biochem Cell Biol.* (2012) 44:1574–84. doi: 10.1016/j.biocel.2012.06.018
163. Kamerkar S, LeBleu VS, Sugimoto H, Yang S, Ruivo CF, Melo SA, et al. Exosomes facilitate therapeutic targeting of oncogenic KRAS in pancreatic cancer. *Nature*. (2017) 546:498–503. doi: 10.1038/nature22341
164. Montecalvo A, Larregina AT, Shufesky WJ, Stolz DB, Sullivan ML, Karlsson JM, et al. Mechanism of transfer of functional microRNAs between mouse dendritic cells via exosomes. *Blood.* (2012) 119:756–66. doi: 10.1182/blood-2011-02-338004
165. Del Conde I, Shrimpton CN, Thiagarajan P, López JA. Tissue-factor-bearing microvesicles arise from lipid rafts and fuse with activated platelets to initiate coagulation. *Blood*. (2012) 106:1604–11. doi: 10.1182/blood-2004-03-1095
166. Tian T, Zhu YL, Hu FH, Wang YY, Huang NP, Xiao ZD. Dynamics of exosome internalization and trafficking. *J Cell Physiol.* (2013) 228:1487–95. doi: 10.1002/jcp.24304
167. Christianson HC, Svensson KJ, van Kuppevelt TH, Li JP, Belting M. Cancer cell exosomes depend on cell-surface heparan sulfate proteoglycans for their internalization and functional activity. *Proc Natl Acad Sci USA*. (2013) 110:17380–5. doi: 10.1073/pnas.1304266110
168. Feng D, Zhao WL, Ye YY, Bai XC, Liu RQ, Chang LF, et al. Cellular internalization of exosomes occurs through phagocytosis. *Traffic*. (2010) 11:675–87. doi: 10.1111/j.1600-0854.2010.01041.x
169. Freeman SA, Grinstein S. Phagocytosis: receptors, signal integration, and the cytoskeleton. *Immunol Rev.* (2014) 262:193–215. doi: 10.1111/imr.12212
170. Nakase I, Kobayashi NB, Takatani-Nakase T, Yoshida T. Active macropinocytosis induction by stimulation of epidermal growth factor receptor and oncogenic Ras expression potentiates cellular uptake efficacy of exosomes. *Sci Rep*. (2015) 5:10300. doi: 10.1038/srep10300
171. Zech D, Rana S, Büchler MW, Zöller M. Tumor-exosomes and leukocyte activation: an ambivalent crosstalk. *Cell Commun Signal.* (2012) 10:37. doi: 10.1186/1478-811X-10-37
172. Horibe S, Tanahashi T, Kawauchi S, Murakami Y, Rikitake Y. Mechanism of recipient cell-dependent differences in exosome uptake. *BMC Cancer*. (2018) 18:47. doi: 10.1186/s12885-017-3958-1
173. Nanbo A, Kawanishi E, Yoshida R, Yoshiyama H. Exosomes derived from Epstein-Barr virus-infected cells are internalized via caveola-dependent endocytosis and promote phenotypic modulation in target cells. *J Virol.* (2013) 87:10334–47. doi: 10.1128/JVI.01310-13
174. Zheng Y, Tu C, Zhang J, Wang J. Inhibition of multiple myeloma-derived exosomes uptake suppresses the functional response in bone marrow stromal cell. *Int J Oncol.* (2019) 54:1061–70. doi: 10.3892/ijo.2019.4685
175. Heusermann W, Hean J, Trojer D, Steib E, von Bueren S, Graff-Meyer A, et al. Exosomes surf on filopodia to enter cells at endocytic hot spots, traffic within endosomes, and are targeted to the ER. *J Cell Biol.* (2016) 213:173–84. doi: 10.1083/jcb.201506084
176. Holder B, Jones T, Sancho Shimizu V, Rice TF, Donaldson B, Bouqueau M, et al. Macrophage exosomes induce placental inflammatory cytokines: a novel mode of maternal-placental messaging. *Traffic*. (2016) 17:168–78. doi: 10.1111/tra.12352
177. Leone DA, Peschel A, Brown M, Schachner H, Ball MJ, Gyuraszova M, et al. Surface LAMP-2 is an endocytic receptor that diverts antigen internalized by human dendritic cells into highly immunogenic exosomes. *J Immunol.* (2017) 199:531–46. doi: 10.4049/jimmunol.1601263
178. Takahashi K, Yamanaka S. Induction of pluripotent stem cells from mouse embryonic and adult fibroblast cultures by defined factors. *Cell*. (2006) 126:663–76. doi: 10.1016/j.cell.2006.07.024
179. Park IH, Zhao R, West JA, Yabuuchi A, Huo H, Ince TA, et al. Reprogramming of human somatic cells to pluripotency with defined factors. *Nature*. (2008) 451:141–6. doi: 10.1038/nature06534
180. Daley GQ. Stem cells and the evolving notion of cellular identity. *Philos Trans R Soc Lond B Biol Sci.* (2015) 370:20140376. doi: 10.1098/rstb.2014.0376
181. Verga Falzacappa MV, Ronchini C, Reavie LB, Pelicci PG. Regulation of self-renewal in normal and cancer stem cells. *FEBS J.* (2012) 279:3559–72. doi: 10.1111/j.1742-4658.2012.08727.x
182. Liu J. The dualistic origin of human tumors. *Semin Cancer Biol.* (2018) 53:1–16. doi: 10.1016/j.semcancer.2018.07.004
183. Reya T, Morrison SJ, Clarke MF, Weissman IL. Stem cells, cancer, and cancer stem cells. *Nature*. (2001) 414:105–11. doi: 10.1038/35102167
184. Ratajczak MZ, Bujko K, Mack A, Kucia M, Ratajczak J. Cancer from the perspective of stem cells and misappropriated tissue regeneration mechanisms. *Leukemia*. (2018) 32:2519–26. doi: 10.1038/s41375-018-0294-7
185. Soteriou D, Fuchs Y. A matter of life and death: stem cell survival in tissue regeneration and tumour formation. *Nat Rev Cancer.* (2018) 18:187–201. doi: 10.1038/nrc.2017.122
186. Bourguignon LY, Shiina M, Li JJ. Hyaluronan-CD44 interaction promotes oncogenic signaling, microRNA functions, chemoresistance, and radiation resistance in cancer stem cells leading to tumor progression. *Adv Cancer Res.* (2014) 123:255–75. doi: 10.1016/B978-0-12-800092-2.00010-1
187. Mitra A, Mishra L, Li S. EMT, CTCs and CSCs in tumor relapse and drug-resistance. *Oncotarget*. (2015) 6:10697–711. doi: 10.18632/oncotarget.4037
188. Skvortsova I, Debbage P, Kumar V, Skvortsov S. Radiation resistance: cancer stem cells (CSCs) and their enigmatic pro-survival signaling. *Semin Cancer Biol.* (2015) 35:39–44. doi: 10.1016/j.semcancer.2015.09.009
189. Lipinska N, Romaniuk A, Paszel-Jaworska A, Toton E, Kopczynski P, Rubis B. Telomerase and drug resistance in cancer. *Cell Mol Life Sci.* (2017) 74:4121–32. doi: 10.1007/s00018-017-2573-2

190. Prieto-Vila M, Takahashi RU, Usuba W, Kohama I, Ochiya T. Drug resistance driven by cancer stem cells and their niche. *Int J Mol Sci.* (2017) 18:E2574. doi: 10.3390/ijms18122574
191. Batlle E, Clevers H. Cancer stem cells revisited. *Nat Med.* (2017) 23:1124–34. doi: 10.1038/nm.4409
192. Zhou P, Li B, Liu F, Zhang M, Wang Q, Liu Y, et al. The epithelial to mesenchymal transition (EMT) and cancer stem cells: implication for treatment resistance in pancreatic cancer. *Mol Cancer.* (2017) 16:52. doi: 10.1186/s12943-017-0624-9
193. Li H, Peyrollier K, Kilic G, Brakebusch C. Rho GTPases and cancer. *Biofactors.* (2014) 40:226–35. doi: 10.1002/biof.1155
194. Yan Y, Zuo X, Wei D. Concise review: emerging role of CD44 in cancer stem cells: a promising biomarker and therapeutic target. *Stem Cells Transl Med.* (2015) 4:1033–43. doi: 10.5966/sctm.2015-0048
195. de Lucas B, Pérez LM, Gálvez BG. Importance and regulation of adult stem cell migration. *J Cell Mol Med.* (2018) 22:746–54. doi: 10.1111/jcmm.13422
196. Hamidi H, Ivaska J. Every step of the way: integrins in cancer progression and metastasis. *Nat Rev Cancer.* (2018) 18:533–48. doi: 10.1038/s41568-018-0038-z
197. Albini A, Bruno A, Gallo C, Pajardi G, Noonan DM, Dallaglio K. Cancer stem cells and the tumor microenvironment: interplay in tumor heterogeneity. *Connect Tissue Res.* (2015) 56:414–25. doi: 10.3109/03008207.2015.1066780
198. Correnti M, Raggi C. Stem-like plasticity and heterogeneity of circulating tumor cells: current status and prospect challenges in liver cancer. *Oncotarget.* (2017) 8:7094–115. doi: 10.18632/oncotarget.12569
199. Stipp CS, Kolesnikova TV, Hemler ME. Functional domains in tetraspanin proteins. *Trends Biochem Sci.* (2003) 28:106–12. doi: 10.1016/S0968-0004(02)00014-2
200. Hemler ME. Tetraspanin functions and associated microdomains. *Nat Rev Mol Cell Biol.* (2005) 6:801–11. doi: 10.1038/nrm1736
201. Levy S, Shoham T. Protein-protein interactions in the tetraspanin web. *Physiology.* (2005) 20:218–24. doi: 10.1152/physiol.00015.2005
202. Berditchevski F, Odintsova E. Tetraspanins as regulators of protein trafficking. *Traffic.* (2007) 8:89–96. doi: 10.1111/j.1600-0854.2006.00515.x
203. Yáñez-Mó M, Gutiérrez-López MD, Cabañas C. Functional interplay between tetraspanins and proteases. *Cell Mol Life Sci.* (2011) 68:3323–35. doi: 10.1007/s00018-011-0746-y
204. Bassani S, Cingolani LA. Tetraspanins: interactions and interplay with integrins. *Int J Biochem Cell Biol.* (2012) 44:703–8. doi: 10.1016/j.biocel.2012.01.020
205. Halova I, Draber P. tetraspanins and transmembrane adaptor proteins as plasma membrane organizers-mast cell case. *Front Cell Dev Biol.* (2016) 4:43. doi: 10.3389/fcell.2016.00043
206. Scheffer KD, Gawlitza A, Spoden GA, Zhang XA, Lambert C, Berditchevski F, et al. Tetraspanin CD151 mediates papillomavirus type 16 endocytosis. *J Virol.* (2013) 87:3435–46. doi: 10.1128/JVI.02906-12
207. Stepanek O, Draber P, Horejsi V. Palmitoylated transmembrane adaptor proteins in leukocyte signaling. *Cell Signal.* (2014) 26:895–902. doi: 10.1016/j.cellsig.2014.01.007
208. Schmidt TH, Homsi Y, Lang T. Oligomerization of the tetraspanin CD81 via the flexibility of Its δ-loop. *Biophys J.* (2016) 110:2463–74. doi: 10.1016/j.bpj.2016.05.003
209. Termini CM, Gillette JM. Tetraspanins function as regulators of cellular signaling. *Front Cell Dev Biol.* (2017) 5:34. doi: 10.3389/fcell.2017.00034
210. Yue S, Zhao K, Erb U, Rana S, Zöller M. Joint features and complementarities of Tspan8 and CD151 revealed in knockdown and knockout models. *Biochem Soc Trans.* (2017) 45:437–47. doi: 10.1042/BST20160298
211. Greco C, Bralet MP, Ailane N, Dubart-Kupperschmitt A, Rubinstein E, Le Naour F, et al. E-cadherin/p120-catenin and tetraspanin Co-029 cooperate for cell motility control in human colon carcinoma. *Cancer Res.* (2010) 70:7674–83. doi: 10.1158/0008-5472.CAN-09-4482
212. Serewko-Auret MM, Mould AW, Loffler KA, Duncan R, Kay GF, Hayward NK. Alterations in gene expression in MEN1-associated insulinoma development. *Pancreas.* (2010) 39:1140–6. doi: 10.1097/MPA.0b013e3181dc67fc
213. Wang H, Rana S, Giese N, Büchler MW, Zöller M. Tspan8, CD44v6 and alpha6beta4 are biomarkers of migrating pancreatic cancer-initiating cells. *Int J Cancer.* (2013) 133:416–26. doi: 10.1002/ijc.28044
214. Madhavan B, Yue S, Galli U, Rana S, Gross W, Müller M, et al. Combined evaluation of a panel of protein and miRNA serum-exosome biomarkers for pancreatic cancer diagnosis increases sensitivity and specificity. *Int J Cancer.* (2015) 136:2616–27. doi: 10.1002/ijc.29324
215. Ailane N, Greco C, Zhu Y, Sala-Valdés M, Billard M, Casal I, et al. Effect of an anti-human Co-029/tspan8 mouse monoclonal antibody on tumor growth in a nude mouse model. *Front Physiol.* (2014) 5:364. doi: 10.3389/fphys.2014.00364
216. Berthier-Vergnes O, El Kharbili M, de la Fouchardière A, Pointecouteau T, Verrando P, Wierinckx A, et al. Gene expression profiles of human melanoma cells with different invasive potential reveal TSPAN8 as a novel mediator of invasion. *Br J Cancer.* (2011) 104:155–65. doi: 10.1038/sj.bjc.6605994
217. Wei L, Li Y, Suo Z. TSPAN8 promotes gastric cancer growth and metastasis via ERK MAPK pathway. *Int J Clin Exp Med.* (2015) 8:8599–607.
218. Pan SJ, Wu YB, Cai S, Pan YX, Liu W, Bian LG, et al. Over-expression of tetraspanin 8 in malignant glioma regulates tumor cell progression. *Biochem Biophys Res Commun.* (2015) 458:476–82. doi: 10.1016/j.bbrc.2015.01.128
219. Park CS, Kim TK, Kim HG, Kim YJ, Jeoung MH, Lee WR, et al. Therapeutic targeting of tetraspanin8 in epithelial ovarian cancer invasion and metastasis. *Oncogene.* (2016) 35:4540–8. doi: 10.1038/onc.2015.520
220. Akiel MA, Santhekadur PK, Mendoza RG, Siddiq A, Fisher PB, Sarkar D. Tetraspanin 8 mediates AEG-1-induced invasion and metastasis in hepatocellular carcinoma cells. *FEBS Lett.* (2016) 590:2700–8. doi: 10.1002/1873-3468.12268
221. Wang Z, von Au A, Schnölzer M, Hackert T, Zöller M. CD44v6-competent tumor exosomes promote motility, invasion and cancer-initiating cell marker expression in pancreatic and colorectal cancer cells. *Oncotarget.* (2016) 7:55409–36. doi: 10.18632/oncotarget.10580
222. Zhu Y, Ailane N, Sala-Valdés M, Haghighi-Rad F, Billard M, Nguyen V, et al. Multi-factorial modulation of colorectal carcinoma cells motility - partial coordination by the tetraspanin Co-029/tspan8. *Oncotarget.* (2017) 8:27454–70. doi: 10.18632/oncotarget.16247
223. Gesierich S, Paret C, Hildebrand D, Weitz J, Zgraggen K, Schmitz-Winnenthal FH, et al. Colocalization of the tetraspanins, CO-029 and CD151, with integrins in human pancreatic adenocarcinoma: impact on cell motility. *Clin Cancer Res.* (2005) 11:2840–52. doi: 10.1158/1078-0432.CCR-04-1935
224. Claas C, Wahl J, Orlicky DJ, Karaduman H, Schnölzer M, Kempf T, et al. The tetraspanin D6.1A and its molecular partners on rat carcinoma cells. *Biochem J.* (2005) 389:99–110. doi: 10.1042/BJ20041287
225. Drapkin R, Crum CP, Hecht JL. Expression of candidate tumor markers in ovarian carcinoma and benign ovary: evidence for a link between epithelial phenotype and neoplasia. *Hum Pathol.* (2004) 35:1014–21. doi: 10.1016/j.humpath.2004.04.014
226. Le Naour F, André M, Greco C, Billard M, Sordat B, Emile JF, et al. Profiling of the tetraspanin web of human colon cancer cells. *Mol Cell Proteomics.* (2006) 5:845–57. doi: 10.1074/mcp.M500330-MCP200
227. Kanatsu-Shinohara M, Takashima S, Ishii K, Shinohara T. Dynamic changes in EPCAM expression during spermatogonial stem cell differentiation in the mouse testis. *PLoS ONE.* (2011) 6:e23663. doi: 10.1371/journal.pone.0023663
228. Rana S, Claas C, Kretz CC, Nazarenko I, Zöller M. Activation-induced internalization differs for the tetraspanins CD9 and Tspan8: Impact on tumor cell motility. *Int J Biochem Cell Biol.* (2011) 43:106–19. doi: 10.1016/j.biocel.2010.10.002
229. Nievers MG, Schaapveld RQ, Sonnenberg A. Biology and function of hemidesmosomes. *Matrix Biol.* (1999) 18:5–17. doi: 10.1016/S0945-053X(98)00003-1
230. Margadant C, Frijns E, Wilhelmsen K, Sonnenberg A. Regulation of hemidesmosome disassembly by growth factor receptors. *Curr Opin Cell Biol.* (2008) 20:589–96. doi: 10.1016/j.ceb.2008.05.001
231. Pan SJ, Zhan SK, Pan YX, Liu W, Bian LG, Sun B, et al. Tetraspanin 8-rictor-integrin α3 complex is required for glioma cell migration. *Int J Mol Sci.* (2015) 16:5363–74. doi: 10.3390/ijms16035363

232. Van Itallie CM, Anderson JM. Architecture of tight junctions and principles of molecular composition. *Semin Cell Dev Biol*. (2014) 36:157–65. doi: 10.1016/j.semcdb.2014.08.011
233. Ladwein M, Pape UF, Schmidt DS, Schnölzer M, Fiedler S, Langbein L, et al. The cell-cell adhesion molecule EpCAM interacts directly with the tight junction protein claudin-7. *Exp Cell Res*. (2005) 309:345–57. doi: 10.1016/j.yexcr.2005.06.013
234. Heiler S, Mu W, Zöller M, Thuma F. The importance of claudin-7 palmitoylation on membrane subdomain localization and metastasis-promoting activities. *Cell Commun Signal*. (2015) 13:29. doi: 10.1186/s12964-015-0105-y
235. Kuhn S, Koch M, Nübel T, Ladwein M, Antolovic D, Klingbeil P, et al. A complex of EpCAM, claudin-7, CD44 variant isoforms, and tetraspanins promotes colorectal cancer progression. *Mol Cancer Res*. (2007) 5:553–67. doi: 10.1158/1541-7786.MCR-06-0384
236. Le Naour F, Zöller M. The tumor antigen EpCAM: tetraspanins and the tight junction protein claudin-7, new partners, new functions. *Front Biosci*. (2008) 13:5847–65. doi: 10.2741/3121
237. Wu CJ, Mannan P, Lu M, Udey MC. Epithelial cell adhesion molecule (EpCAM) regulates claudin dynamics and tight junctions. *J Biol Chem*. (2013) 288:12253–68. doi: 10.1074/jbc.M113.457499
238. Okada T, Nakamura T, Watanabe T, Onoda N, Ashida A, Okuyama R, et al. Coexpression of EpCAM, CD44 variant isoforms and claudin-7 in anaplastic thyroid carcinoma. *PLoS ONE*. (2014) 9:e94487. doi: 10.1371/journal.pone.0094487
239. Fang T, Lin J, Wang Y, Chen G, Huang J, Chen J, et al. Tetraspanin-8 promotes hepatocellular carcinoma metastasis by increasing ADAM12m expression. *Oncotarget*. (2016) 7:40630–43. doi: 10.18632/oncotarget.9769
240. Yue S, Mu W, Zöller M. Tspan8 and CD151 promote metastasis by distinct mechanisms. *Eur J Cancer*. (2013) 49:2934–48. doi: 10.1016/j.ejca.2013.03.032
241. Schmidt F, Müller M, Prox J, Arnold P, Schönherr C, Tredup C, et al. Tetraspanin 8 is an interactor of the metalloprotease meprin β within tetraspanin-enriched microdomains. *Biol Chem*. (2016) 397:857–69. doi: 10.1515/hsz-2016-0126
242. Claas C, Seiter S, Claas A, Savelyeva L, Schwab M, Zöller M. Association between the rat homologue of CO-029, a metastasis-associated tetraspanin molecule and consumption coagulopathy. *J Cell Biol*. (1998) 141:267–80. doi: 10.1083/jcb.141.1.267
243. Yao L, Damodaran G, Nikolskaya N, Gorman AM, Windebank A, Pandit A. The effect of laminin peptide gradient in enzymatically cross-linked collagen scaffolds on neurite growth. *J Biomed Mater Res A*. (2010) 92:484–92. doi: 10.1002/jbm.a.32359
244. Wang Z, Sun H, Provaznik J, Hackert T, Zöller M. Pancreatic cancer-initiating cell exosome message transfer into noncancer-initiating cells: the importance of CD44v6 in reprogramming. *J Exp Clin Cancer Res*. (2019) 38:132. doi: 10.1186/s13046-019-1129-8
245. Stewart RL, O'Connor KL. Clinical significance of the integrin α6β4 in human malignancies. *Lab Invest*. (2015) 95:976–86. doi: 10.1038/labinvest.2015.82
246. Ramovs V, Te Molder L, Sonnenberg A. The opposing roles of laminin-binding integrins in cancer. *Matrix Biol*. (2017) 57–58:213–43. doi: 10.1016/j.matbio.2016.08.007
247. Dowling J, Yu QC, Fuchs E. Beta4 integrin is required for hemidesmosome formation, cell adhesion and cell survival. *J Cell Biol*. (1996) 134:559–72. doi: 10.1083/jcb.134.2.559
248. Tsuruta D, Hashimoto T, Hamill KJ, Jones JC. Hemidesmosomes and focal contact proteins: functions and cross-talk in keratinocytes, bullous diseases and wound healing. *J Dermatol Sci*. (2011) 62:1–7. doi: 10.1016/j.jdermsci.2011.01.005
249. Rabinovitz I, Mercurio AM. The integrin alpha6beta4 functions in carcinoma cell migration on laminin-1 by mediating the formation and stabilization of actin-containing motility structures. *J Cell Biol*. (1997) 139:1873–84. doi: 10.1083/jcb.139.7.1873
250. Yu PT, Babicky M, Jaquish D, French R, Marayuma K, Mose E, et al. The RON-receptor regulates pancreatic cancer cell migration through phosphorylation-dependent breakdown of the hemidesmosome. *Int J Cancer*. (2012) 131:1744–54. doi: 10.1002/ijc.27447
251. Guo W, Pylayeva Y, Pepe A, Yoshioka T, Muller WJ, Inghirami G, et al. Beta 4 integrin amplifies ErbB2 signaling to promote mammary tumorigenesis. *Cell*. (2006) 126:489–502. doi: 10.1016/j.cell.2006.05.047
252. Shaw LM. Identification of insulin receptor substrate 1 (IRS-1) and IRS-2 as signaling intermediates in the alpha6beta4 integrin-dependent activation of phosphoinositide 3-OH kinase and promotion of invasion. *Mol Cell Biol*. (2001) 21:5082–93. doi: 10.1128/MCB.21.15.5082-5093.2001
253. Lee SS, Lee SJ, Lee SH, Ryu JM, Lim HS, Kim JS, et al. Netrin-1-induced stem cell bioactivity contributes to the regeneration of injured tissues via the lipid raft-dependent integrin α6β4 signaling pathway. *Sci Rep*. (2016) 6:37526. doi: 10.1038/srep37526
254. Laval S, Laklai H, Fanjul M, Pucelle M, Laurell H, Billon-Galés A, et al. Dual roles of hemidesmosomal proteins in the pancreatic epithelium: the phosphoinositide 3-kinase decides. *Oncogene*. (2014) 33:1934–44. doi: 10.1038/onc.2013.146
255. Hintermann E, Yang N, O'Sullivan D, Higgins JM, Quaranta V. Integrin alpha6beta4-erbB2 complex inhibits haptotaxis by up-regulating E-cadherin cell-cell junctions in keratinocytes. *J Biol Chem*. (2005) 280:8004–15. doi: 10.1074/jbc.M406301200
256. Folgiero V, Bachelder RE, Bon G, Sacchi A, Falcioni R, Mercurio AM. The α6β4 integrin can regulate ErbB-3 expression: implications for alpha6beta4 signaling and function. *Cancer Res*. (2007) 67:1645–52. doi: 10.1158/0008-5472.CAN-06-2980
257. O'Connor KL, Chen M, Towers LN. Integrin α6β4 cooperates with LPA signaling to stimulate Rac through AKAP-Lbc-mediated RhoA activation. *Am J Physiol Cell Physiol*. (2012) 302:C605–14. doi: 10.1152/ajpcell.00095.2011
258. Tan X, Xu A, Zhao T, Zhao Q, Zhang J, Fan C, et al. Simulated microgravity inhibits cell focal adhesions leading to reduced melanoma cell proliferation and metastasis via FAK/RhoA-regulated mTORC1 and AMPK pathways. *Sci Rep*. (2018) 8:3769. doi: 10.1038/s41598-018-20459-1
259. Tai YL, Chu PY, Lai IR, Wang MY, Tseng HY, Guan JL, et al. An EGFR/Src-dependent β4 integrin/FAK complex contributes to malignancy of breast cancer. *Sci Rep*. (2015) 5:16408. doi: 10.1038/srep16408
260. Fan J, Cai B, Zeng M, Hao Y, Giancotti FG, Fu BM. Integrin β4 signaling promotes mammary tumor cell adhesion to brain microvascular endothelium by inducing ErbB2-mediated secretion of VEGF. *Ann Biomed Eng*. (2011) 39:2223–41. doi: 10.1007/s10439-011-0321-6
261. Yue S, Mu W, Erb U, Zöller M. The tetraspanins CD151 and Tspan8 are essential exosome components for the crosstalk between cancer initiating cells and their surrounding. *Oncotarget*. (2015) 6:2366–84. doi: 10.18632/oncotarget.2958
262. Wang H, Jin H, Beauvais DM, Rapraeger AC. Cytoplasmic domain interactions of syndecan-1 and syndecan-4 with α6β4 integrin mediate human epidermal growth factor receptor (HER1 and HER2)-dependent motility and survival. *J Biol Chem*. (2014) 289:30318–32. doi: 10.1074/jbc.M114.586438
263. Bhatia V, Mula RV, Weigel NL, Falzon M. Parathyroid hormone-related protein regulates cell survival pathways via integrin alpha6beta4-mediated activation of phosphatidylinositol 3-kinase/Akt signaling. *Mol Cancer Res*. (2009) 7:1119–31. doi: 10.1158/1541-7786.MCR-08-0568
264. Kawakami K, Fujita Y, Kato T, Mizutani K, Kameyama K, Tsumoto H, et al. Integrin β4 and vinculin contained in exosomes are potential markers for progression of prostate cancer associated with taxane-resistance. *Int J Oncol*. (2015) 47:384–90. doi: 10.3892/ijo.2015.3011
265. Jauliac S, López-Rodriguez C, Shaw LM, Brown LF, Rao A, Toker A. The role of NFAT transcription factors in integrin-mediated carcinoma invasion. *Nat Cell Biol*. (2002) 4:540–4. doi: 10.1038/ncb816
266. Houben AJ, Moolenaar WH. Autotaxin and LPA receptor signaling in cancer. *Cancer Metastasis Rev*. (2011) 30:557–65. doi: 10.1007/s10555-011-9319-7
267. Boye K, Maelandsmo GM. S100A4 and metastasis: a small actor playing many roles. *Am J Pathol*. (2010) 176:528–35. doi: 10.2353/ajpath.2010.090526
268. Chen M, Bresnick AR, O'Connor KL. Coupling S100A4 to Rhotekin alters Rho signaling output in breast cancer cells. *Oncogene*. (2013) 32:3754–64. doi: 10.1038/onc.2012.383

269. Chen M, Sinha M, Luxon BA, Bresnick AR, O'Connor KL. Integrin alpha6beta4 controls the expression of genes associated with cell motility, invasion, and metastasis, including S100A4/metastasin. *J Biol Chem.* (2009) 284:1484–94. doi: 10.1074/jbc.M803997200
270. Yoon SO, Shin S, Lipscomb EA. A novel mechanism for integrin-mediated ras activation in breast carcinoma cells: the alpha6beta4 integrin regulates ErbB2 translation and transactivates epidermal growth factor receptor/ErbB2 signaling. *Cancer Res.* (2006) 66:2732–9. doi: 10.1158/0008-5472.CAN-05-2941
271. Welser-Alves JV, Boroujerdi A, Tigges U, Wrabetz L, Feltri ML, Milner R. Endothelial β4 integrin is predominantly expressed in arterioles, where it promotes vascular remodeling in the hypoxic brain. *Arterioscler Thromb Vasc Biol.* (2013) 33:943–53. doi: 10.1161/ATVBAHA.112.300566
272. Feng C, Ye C, Liu X, Ma H, Li M. Beta4 integrin is involved in statin-induced endothelial cell death. *Biochem Biophys Res Commun.* (2004) 323:858–64. doi: 10.1016/j.bbrc.2004.08.171
273. Wang L, Dong Z, Zhang Y, Miao J. The roles of integrin β4 in vascular endothelial cells. *J Cell Physiol.* (2012) 227:474–8. doi: 10.1002/jcp.22769
274. Nikolopoulos SN, Blaikie P, Yoshioka T, Guo W, Giancotti FG. Integrin beta4 signaling promotes tumor angiogenesis. *Cancer Cell.* (2004) 6:471–83. doi: 10.1016/j.ccr.2004.09.029
275. Mercurio AM, Lipscomb EA, Bachelder RE. Non-angiogenic functions of VEGF in breast cancer. *J Mamm Gland Biol Neoplasia.* (2005) 10:283–90. doi: 10.1007/s10911-006-9001-9
276. Roberts JE, Nikolopoulos SN, Oktem O, Giancotti F, Oktay K. Integrin beta-4 signaling plays a key role in mouse embryogenesis. *Reprod Sci.* (2009) 16:286–93. doi: 10.1177/1933719108325506
277. Todaro M, Gaggianesi M, Catalano V, Benfante A, Iovino F, Biffoni M, et al. CD44v6 is a marker of constitutive and reprogrammed cancer stem cells driving colon cancer metastasis. *Cell Stem Cell.* (2014) 14:342–56. doi: 10.1016/j.stem.2014.01.009
278. O'Brien CA, Pollett A, Gallinger S, Dick JE. A human colon cancer cell capable of initiating tumour growth in immunodeficient mice. *Nature.* (2007) 445:106–10. doi: 10.1038/nature05372
279. Idzerda RL, Carter WG, Nottenburg C, Wayner EA, Gallatin WM, John T. Isolation and DNA sequence of a cDNA clone encoding a lymphocyte adhesion receptor for high endothelium. *Proc Natl Acad Sci. USA.* (1989) 86:4659–63. doi: 10.1073/pnas.86.12.4659
280. Goldstein LA, Butcher EC. Identification of mRNA that encodes an alternative form of H-CAM (CD44) in lymphoid and nonlymphoid tissues. *Immunogenetics.* (1990) 32:389–97. doi: 10.1007/BF00241632
281. Screaton GR, Bell MV, Jackson DG, Cornelis FB, Gerth U, Bell JI. Genomic structure of DNA encoding the lymphocyte homing receptor CD44 reveals at least 12 alternatively spliced exons. *Proc Natl Acad Sci USA.* (1992) 89:12160–4. doi: 10.1073/pnas.89.24.12160
282. Peach RJ, Hollenbaugh D, Stamenkovic I, Aruffo A. Identification of hyaluronic acid binding sites in the extracellular domain of CD44. *J Cell Biol.* (1993) 122:257–64. doi: 10.1083/jcb.122.1.257
283. Ishii S, Ford R, Thomas P, Nachman A, Steele G Jr, Jessup JM. CD44 participates in the adhesion of human colorectal carcinoma cells to laminin and type IV collagen. *Surg Oncol.* (1993) 2:255–64. doi: 10.1016/0960-7404(93)90015-Q
284. Neame SJ, Isacke CM. The cytoplasmic tail of CD44 is required for basolateral localization in ephitelial MDCK cells but does not mediate association with the detergent-insoluble cytoskeleton of fibroblasts. *J Cell Biol.* (1993) 121:1299–310. doi: 10.1083/jcb.121.6.1299
285. Bennett KL, Jackson DG, Simon JC, Tanczos E, Peach R, Modrell B, et al. CD44 isoforms containing exon v3 are responsible for the presentation of heparin-binding growth factor. *J Cell Biol.* (1995) 128:687–98. doi: 10.1083/jcb.128.4.687
286. Föger N, Marhaba R, Zöller M. Raft associated interaction of CD44 with the cytoskeleton. *J Cell Sci.* (2001) 114:1169–78.
287. Oliferenko S, Paiha K, Harder T, Gerke V, Schwärzler C, Schwarz H, et al. Analysis of CD44-containing lipid rafts: Recruitment of annexin II and stabilization by the actin cytoskeleton. *J Cell Biol.* (1999) 146:843–54. doi: 10.1083/jcb.146.4.843
288. Lokeshwar VB, Fregien, N, Bourguignon LY. Ankyrin-binding domain of CD44(Gp85) is required for the expression of hyaluronic acid-mediated adhesion function. *J Cell Biol.* (1994) 126:1099–109. doi: 10.1083/jcb.126.4.1099
289. Jalkanen S, Jalkanen M. Lymphocyte CD44 binds the COOH-terminal heparin-binding domain of fibronectin. *J Cell Biol.* (1992) 116:817–25. doi: 10.1083/jcb.116.3.817
290. Toyama-Sorimachi N, Miyasaka M. A novel ligand for CD44 is sulfated proteoglycan. *Int Immunol.* (1994) 6:655–60. doi: 10.1093/intimm/6.4.655
291. Aruffo A, Stamenkovic I, Melnick M, Underhill CB, Seed B. CD44 is the principal cell surface receptor for hyaluronate. *Cell.* (1990) 61:1303–13. doi: 10.1016/0092-8674(90)90694-A
292. Greenfield B, Wang WC, Marquardt H, Piepkorn M, Wolff EA, Aruffo A, et al. Characterization of the heparan sulfate and chondroitin sulfate assembly sites in CD44. *J Biol Chem.* (1999) 274:2511–7. doi: 10.1074/jbc.274.4.2511
293. Higman VA, Briggs DC, Mahoney DJ, Blundell CD, Sattelle BM, Dyer DP, et al. A refined model for the TSG-6 link module in complex with hyaluronan: use of defined oligosaccharides to probe structure and function. *J Biol Chem.* (2014) 289:5619–34. doi: 10.1074/jbc.M113.542357
294. Tremmel M, Matzke A, Albrecht I, Laib AM, Olaku V, Ballmer-Hofer K, et al. A CD44v6 peptide reveals a role of CD44 in VEGFR-2 signaling and angiogenesis. *Blood.* (2009) 114:5236–44. doi: 10.1182/blood-2009-04-219204
295. Kim MS, Park MJ, Moon EJ, Kim SJ, Lee CH, Yoo H, et al. Hyaluronic acid induces osteopontin via the phosphatidylinositol 3-kinase/Akt pathway to enhance the motility of human glioma cells. *Cancer Res.* (2005) 65:686–91.
296. Yuan J, Gu K, He J, Sharma S. Preferential up-regulation of osteopontin in primary central nervous system lymphoma does not correlate with putative receptor CD44v6 or CD44H expression. *Hum Pathol.* (2013) 44:606–11. doi: 10.1016/j.humpath.2012.07.007
297. Orian-Rousseau V, Morrison H, Matzke A, Kastilan T, Pace G, Herrlich P, et al. Hepatocyte growth factor-induced Ras activation requires ERM proteins linked to both CD44v6 and F-actin. *Mol Biol Cell.* (2007) 18:76–83. doi: 10.1091/mbc.e06-08-0674
298. Adamia S, Maxwell CA, Pilarski LM. Hyaluronan and hyaluronan synthases: potential therapeutic targets in cancer. *Curr Drug Targets Cardiovasc Haematol Disord.* (2005) 5:3–14. doi: 10.2174/1568006053005056
299. Misra S, Toole BP, Ghatak S. Hyaluronan constitutively regulates activation of multiple receptor tyrosine kinases in epithelial and carcinoma cells. *J Biol Chem.* (2006) 281:34936–41. doi: 10.1074/jbc.C600138200
300. Orian-Rousseau V. CD44 Acts as a signaling platform controlling tumor progression and metastasis. *Front Immunol.* (2015) 6:154. doi: 10.3389/fimmu.2015.00154
301. Xu H, Tian Y, Yuan X, Wu H, Liu Q, Pestell RG, et al. The role of CD44 in epithelial-mesenchymal transition and cancer development. *Onco Targets Ther.* (2015) 8:3783–92. doi: 10.2147/OTT.S95470
302. Fehon RG, McClatchey AI, Bretscher A. Organizing the cell cortex: the role of ERM proteins. *Nat Rev Mol Cell Biol.* (2010) 11:276–87. doi: 10.1038/nrm2866
303. Stamenkovic I, Yu Q. Merlin, a "Magic" linker between extracellular cues and intracellular signaling pathways that regulate cell. motility, proliferation, and survival. *Curr Protein Pept Sci.* (2010) 11:471–84. doi: 10.2174/138920310791824011
304. Mori T, Kitano K, Terawaki S, Maesaki R, Fukami Y, Hakoshima T. Structural basis for CD44 recognition by ERM proteins. *J Biol Chem.* (2008) 283:29602–12. doi: 10.1074/jbc.M803606200
305. Horta S, Agostinho AL, Mateus R, Pereira L, Pereira C, Capinha L, et al. Looking out for cancer stem cells' properties: the value-driving role of CD44 for personalized medicines. *Curr Cancer Drug Targets.* (2015) 14:832–49. doi: 10.2174/1568009614666141111154713
306. Ingley E. Src family kinases: Regulation of their activities, levels and identification of new pathways. *Biochim Biophys Acta.* (2008) 1784:56–65. doi: 10.1016/j.bbapap.2007.08.012
307. Ekyalongo RC, Nakayama H, Kina K, Kaga N, Iwabuchi K. Organization and functions of glycolipid-enriched microdomains in phagocytes. *Biochim Biophys Acta.* (2015) 1851:90–7. doi: 10.1016/j.bbalip.2014.06.009
308. Korcsmaros T, Schneider MV, Superti-Furga G. Next generation of network medicine: interdisciplinary signaling approaches. *Integr Biol.* (2017) 9:97–108. doi: 10.1039/c6ib00215c

309. Cooper JA, Qian H. A mechanism for SRC kinase-dependent signaling by noncatalytic receptors. *Biochemistry*. (2008) 47:5681–8. doi: 10.1021/bi8003044
310. Nastase MV, Janicova A, Wygrecka M, Schaefer L. Signaling at the crossroads: matrix-derived proteoglycan and reactive oxygen species signaling. *Antioxid Redox Signal*. (2017) 27:855–73. doi: 10.1089/ars.2017.7165
311. Heldin P, Basu K, Kozlova I, Porsch H. HAS2 and CD44 in breast tumorigenesis. *Adv Cancer Res*. (2014) 123:211–29. doi: 10.1016/B978-0-12-800092-2.00008-3
312. Binder MJ, McCoombe S, Williams ED, McCulloch DR, Ward AC. The extracellular matrix in cancer progression: role of hyalectan proteoglycans and ADAMTS enzymes. *Cancer Lett*. (2017) 385:55–64. doi: 10.1016/j.canlet.2016.11.001
313. Vitale D, Kumar Katakam S, Greve B, Jang B, Oh ES, Alaniz L, et al. Proteoglycans and glycosaminoglycans as regulators of cancer stem cell function and therapeutic resistance. *FEBS J*. (2019) 286:2870–82. doi: 10.1111/febs.14967
314. Grass GD, Dai L, Qin Z, Parsons C, Toole BP. CD147: regulator of hyaluronan signaling in invasiveness and chemoresistance. *Adv Cancer Res*. (2014) 123:351–73. doi: 10.1016/B978-0-12-800092-2.00013-7
315. Bates RC, Elith CA, Thorne RF, Burns GF. Engagement of variant CD44 confers resistance to anti-integrin antibody-mediated apoptosis in a colon carcinoma cell line. *Cell Adhes Commun*. (1998) 6:21–38. doi: 10.3109/15419069809069758
316. Teoh SL, Das S. The emerging role of the hippo pathway in lung cancers: clinical implications. *Curr Drug Targets*. (2017) 18:1880–92. doi: 10.2174/1389450117666160907153338
317. Fan F, Xiuwen Z, Yongyi L, Weiping C, Lu G, Yueqin L, et al. The CD44 variant induces K562 cell acquired with resistance to adriamycin via NF-κB/Snail/Bcl-2 pathway. *Med Hypotheses*. (2018) 121:142–8. doi: 10.1016/j.mehy.2018.09.002
318. Lee JL, Wang MJ, Chen JY. Acetylation and activation of STAT3 mediated by nuclear translocation of CD44. *J Cell Biol*. (2009) 185:949–57. doi: 10.1083/jcb.200812060
319. Zhang Y, Han X, Wu H, Zhou Y. Bioinformatics analysis of transcription profiling of solid pseudopapillary neoplasm of the pancreas. *Mol Med Rep*. (2017) 16:1635–42. doi: 10.3892/mmr.2017.6800
320. Bourguignon LY, Xia W, Wong G. Hyaluronan-mediated CD44 interaction with p300 and SIRT1 regulates beta-catenin signaling and NFkappaB-specific transcription activity leading to MDR1 and Bcl-xL gene expression and chemoresistance in breast tumor cells. *J Biol Chem*. (2009) 284:2657–71. doi: 10.1074/jbc.M806708200
321. Ibrahim SA, Gadalla R, El-Ghonaimy EA, Samir O, Mohamed HT, Hassan H, et al. Syndecan-1 is a novel molecular marker for triple negative inflammatory breast cancer and modulates the cancer stem cell phenotype via the IL-6/STAT3, Notch and EGFR signaling pathways. *Mol Cancer*. (2017) 16:57. doi: 10.1186/s12943-017-0621-z
322. Sun H, Rana S, Wang Z, Schnölzer M, Provaznik J, Hackert T, et al. The pancreatic cancer stem cell marker CD44v6 affects Tspan8 transcription: consequences on exosome composition and delivery. *J Oncol*. (2019) 2019:3516973. doi: 10.1155/2019/3516973
323. Karousou E, Misra S, Ghatak S, Dobra K, Götte M, Vigetti D, et al. Roles and targeting of the HAS/hyaluronan/CD44 molecular system in cancer. *Matrix Biol*. (2017) 59:3–22. doi: 10.1016/j.matbio.2016.10.001
324. Schmitt M, Metzger M, Gradl D, Davidson G, Orian-Rousseau V. CD44 functions in Wnt signaling by regulating LRP6 localization and activation. *Cell Death Differ*. (2015) 22:677–89. doi: 10.1038/cdd.2014.156
325. Yong X, Tang B, Xiao YF, Xie R, Qin Y, Luo G, et al. Helicobacter pylori upregulates Nanog and Oct4 via Wnt/β-catenin signaling pathway to promote cancer stem cell-like properties in human gastric cancer. *Cancer Lett*. (2016) 374:292–303. doi: 10.1016/j.canlet.2016.02.032
326. Kashyap T, Pramanik KK, Nath N, Mishra P, Singh AK, Nagini S, et al. Crosstalk between Raf-MEK-ERK and PI3K-Akt-GSK3β signaling networks promotes chemoresistance, invasion/migration and stemness via expression of CD44 variants (v4 and v6) in oral cancer. *Oral Oncol*. (2018) 86:234–43. doi: 10.1016/j.oraloncology.2018.09.028
327. Senbanjo LT, Chellaiah MA. cd44: a multifunctional cell surface adhesion receptor is a regulator of progression and metastasis of cancer cells. *Front Cell Dev Biol*. (2017) 5:18. doi: 10.3389/fcell.2017.00018
328. Zhang NH, Li J, Li Y, Zhang XT, Liao WT, Zhang JY, et al. Co-expression of CXCR4 and CD133 proteins is associated with poor prognosis in stage II-III colon cancer patients. *Exp Ther Med*. (2012) 3:973–82. doi: 10.3892/etm.2012.527
329. Popple A, Durrant LG, Spendlove I, Rolland P, Scott IV, Deen S, et al. The chemokine, CXCL12, is an independent predictor of poor survival in ovarian cancer. *Br J Cancer*. (2012) 106:1306–13. doi: 10.1038/bjc.2012.49
330. Wu B, Chien EY, Mol CD, Fenalti G, Liu W, Katritch V, et al. Structures of the CXCR4 chemokine GPCR with small-molecule and cyclic peptide antagonists. *Science*. (2010) 330:1066–71. doi: 10.1126/science.1194396
331. Busillo JM, Benovic JL. Regulation of CXCR4 signaling. *Biochim Biophys Acta*. (2007) 1768:952–63. doi: 10.1016/j.bbamem.2006.11.002
332. Cheng M, Huang K, Zhou J, Yan D, Tang YL, Zhao TC, et al. A critical role of Src family kinase in SDF-1/CXCR4-mediated bone-marrow progenitor cell recruitment to the ischemic heart. *J Mol Cell Cardiol*. (2015) 81:49–53. doi: 10.1016/j.yjmcc.2015.01.024
333. Teicher BA, Fricker SP. CXCL12 (SDF-1)/CXCR4 pathway in cancer. *Clin Cancer Res*. (2010) 16:2927–31. doi: 10.1158/1078-0432.CCR-09-2329
334. Sun Y, Cheng Z, Ma L, Pei G. Beta-arrestin2 is critically involved in CXCR4-mediated chemotaxis, and this is mediated by its enhancement of p38 MAPK activation. *J Biol Chem*. (2002) 277:49212–9. doi: 10.1074/jbc.M207294200
335. Cojoc M, Peitzsch C, Trautmann F, Polishchuk L, Telegeev GD, Dubrovska A. Emerging targets in cancer management: role of the CXCL12/CXCR4 axis. *Onco Targets Ther*. (2013) 6:1347–61. doi: 10.2147/OTT.S36109
336. Krupnick JG, Benovic JL. The role of receptor kinases and arrestins in G protein-coupled receptor regulation. *Annu Rev Pharmacol Toxicol*. (1998) 38:289–319. doi: 10.1146/annurev.pharmtox.38.1.289
337. Liebick M, Henze S, Vogt V, Oppermann M. Functional consequences of chemically-induced β-arrestin binding to chemokine receptors CXCR4 and CCR5 in the absence of ligand stimulation. *Cell Signal*. (2017) 38:201–11. doi: 10.1016/j.cellsig.2017.07.010
338. Penela P, Murga C, Ribas C, Lafarga V, Mayor F Jr. The complex G protein-coupled receptor kinase 2 (GRK2) interactome unveils new physiopathological targets. *Br J Pharmacol*. (2010) 160:821–32. doi: 10.1111/j.1476-5381.2010.00727.x
339. DeWire SM, Ahn S, Lefkowitz RJ, Shenoy SK. Beta-arrestins and cell signaling. *Annu Rev Physiol*. (2007) 69:483–510. doi: 10.1146/annurev.physiol.69.022405.154749
340. Mandawat A, Fiskus W, Buckley KM, Robbins K, Rao R, Balusu R, et al. Pan-histone deacetylase inhibitor panobinostat depletes CXCR4 levels and signaling and exerts synergistic antimyeloid activity in combination with CXCR4 antagonists. *Blood*. (2010) 116:5306–15. doi: 10.1182/blood-2010-05-284414
341. Wysoczynski M, Reca R, Ratajczak J, Kucia M, Shirvaikar N, Honczarenko M, et al. Incorporation of CXCR4 into membrane lipid rafts primes homing-related responses of hematopoietic stem/progenitor cells to an SDF-1 gradient. *Blood*. (2005) 105:40–8. doi: 10.1182/blood-2004-04-1430
342. Chinni SR, Yamamoto H, Dong Z, Sabbota A, Bonfil RD, Cher ML. CXCL12/CXCR4 transactivates HER2 in lipid rafts of prostate cancer cells and promotes growth of metastatic deposits in bone. *Mol Cancer Res*. (2008) 6:446–57. doi: 10.1158/1541-7786.MCR-07-0117
343. Getts DR, Terry RL, Getts MT, Deffrasnes C, Müller M, van Vreden C, et al. Therapeutic inflammatory monocyte modulation using immune-modifying microparticles. *Sci Transl Med*. (2014) 6:219ra7. doi: 10.1126/scitranslmed.3007563
344. Singh AP, Arora S, Bhardwaj A, Srivastava SK, Kadakia MP, Wang B, et al. CXCL12/CXCR4 protein signaling axis induces sonic hedgehog expression in pancreatic cancer cells via extracellular regulated kinase- and Akt kinase-mediated activation of nuclear factor κB: implications for bidirectional tumor-stromal interactions. *J Biol Chem*. (2012) 287:39115–24. doi: 10.1074/jbc.M112.409581
345. Wang Z, Ma Q, Liu Q, Yu H, Zhao L, Shen S, et al. Blockade of SDF-1/CXCR4 signalling inhibits pancreatic cancer progression *in vitro* via inactivation of canonical Wnt pathway. *Br J Cancer*. (2008) 99:1695–703. doi: 10.1038/sj.bjc.6604745

346. Pan F, Ma S, Cao W, Liu H, Chen F, Chen X, et al. SDF-1α upregulation of MMP-2 is mediated by p38 MAPK signaling in pancreatic cancer cell lines. *Mol Biol Rep*. (2013) 40:4139–46. doi: 10.1007/s11033-012-2225-4
347. Li X, Ma Q, Xu Q, Liu H, Lei J, Duan W, et al. SDF-1/CXCR4 signaling induces pancreatic cancer cell invasion and epithelial-mesenchymal transition *in vitro* through non-canonical activation of Hedgehog pathway. *Cancer Lett*. (2012) 322:169–76. doi: 10.1016/j.canlet.2012.02.035
348. Hermann PC, Huber SL, Herrler T, Aicher A, Ellwart JW, Guba M, et al. Distinct populations of cancer stem cells determine tumor growth and metastatic activity in human pancreatic cancer. *Cell Stem Cell*. (2007) 1:313–23. doi: 10.1016/j.stem.2007.06.002
349. Weekes CD, Song D, Arcaroli J, Wilson LA, Rubio-Viqueira B, Cusatis G, et al. Stromal cell-derived factor 1α mediates resistance to mTOR-directed therapy in pancreatic cancer. *Neoplasia*. (2012) 14:690–701. doi: 10.1593/neo.111810
350. Pozzobon T, Goldoni G, Viola A, Molon B. CXCR4 signaling in health and disease. *Immunol Lett*. (2016) 177:6–15. doi: 10.1016/j.imlet.2016.06.006
351. Teixidó J, Martínez-Moreno M, Díaz-Martínez M, Sevilla-Movilla S. The good and bad faces of the CXCR4 chemokine receptor. *Int J Biochem Cell Biol*. (2018) 95:121–31. doi: 10.1016/j.biocel.2017.12.018
352. Tu TC, Nagano M, Yamashita T, Hamada H, Ohneda K, Kimura K, et al. A chemokine receptor, CXCR4, which is regulated by hypoxia-inducible factor 2α, is crucial for functional endothelial progenitor cells migration to ischemic tissue and wound repair. *Stem Cells Dev*. (2016) 25:266–76. doi: 10.1089/scd.2015.0290
353. Billadeau DD, Chatterjee S, Bramati P, Sreekumar R, Shah V, Hedin K, et al. Characterization of the CXCR4 signaling in pancreatic cancer cells. *Int J Gastrointest Cancer*. (2006) 37:110–9. doi: 10.1007/s12029-007-0011-7
354. Kim SJ, Lee Y, Kim NY, Hwang Y, Hwang B, Min JK, et al. Pancreatic adenocarcinoma upregulated factor, a novel endothelial activator, promotes angiogenesis and vascular permeability. *Oncogene*. (2013) 32:3638–47. doi: 10.1038/onc.2012.366
355. Ma Y, Hwang RF, Logsdon CD, Ullrich SE. Dynamic mast cell-stromal cell interactions promote growth of pancreatic cancer. *Cancer Res*. (2013) 73:3927–37. doi: 10.1158/0008-5472.CAN-12-4479
356. Chen HC, Chou AS, Liu YC, Hsieh CH, Kang CC, Pang ST, et al. Induction of metastatic cancer stem cells from the NK/LAK-resistant floating, but not adherent, subset of the UP-LN1 carcinoma cell line by IFN-γ. *Lab Invest*. (2011) 91:1502–13. doi: 10.1038/labinvest.2011.91
357. Shi J, Wei Y, Xia J, Wang S, Wu J, Chen F, et al. CXCL12-CXCR4 contributes to the implication of bone marrow in cancer metastasis. *Future Oncol*. (2014) 10:749–59. doi: 10.2217/fon.13.193
358. Unlu S, Tang S, Wang E, Martinez I, Tang D, Bianchi ME, et al. Damage associated molecular pattern molecule-induced microRNAs (DAMPmiRs) in human peripheral blood mononuclear cells. *PLoS ONE*. (2012) 7:e38899. doi: 10.1371/annotation/18ec64ae-e086-446c-b63c-a71fa2bba046
359. Kang R, Zhang Q, Hou W, Yan Z, Chen R, Bonaroti J, et al. Intracellular Hmgb1 inhibits inflammatory nuleosome release and limits acute pancreatitis in mice. *Gastroenterology*. (2014) 146:1097–107. doi: 10.1053/j.gastro.2013.12.015
360. Hou W, Zhang Q, Yan Z, Chen R, Zeh Iii HJ, Kang R, et al. Strange attractors: DAMPs and autophagy link tumor cell death and immunity. *Cell Death Dis*. (2013) 4:e966. doi: 10.1038/cddis.2013.493
361. Shakir M, Tang D, Zeh HJ, Tang SW, Anderson CJ, Bahary N, et al. The chemokine receptors CXCR4/CXCR7 and their primary heterodimeric ligands CXCL12 and CXCL12/high mobility group box 1 in pancreatic cancer growth and development: finding flow. *Pancreas*. (2015) 44:528–34. doi: 10.1097/MPA.0000000000000298
362. Dalerba P, Dylla SJ, Park IK, Liu R, Wang X, Cho RW, et al. Phenotypic characterization of human colorectal cancer stem cells. *Proc Natl Acad Sci USA*. (2007) 104:10158–63. doi: 10.1073/pnas.0703478104
363. Ricci-Vitiani L, Lombardi DG, Pilozzi E, Biffoni M, Todaro M, Peschle C, et al. Identification and expansion of human colon-cancer-initiating cells. *Nature*. (2007) 445:111–5. doi: 10.1038/nature05384
364. D'Agostino G, Cecchinato V, Uguccioni M. Chemokine heterocomplexes and cancer: a novel chapter to be written in tumor immunity. *Front Immunol*. (2018) 9:2185. doi: 10.3389/fimmu.2018.02185
365. Xu D, Li R, Wu J, Jiang L, Zhong HA. Drug design targeting the CXCR4/CXCR7/CXCL12 pathway. *Curr Top Med Chem*. (2016) 16:1441–51. doi: 10.2174/1568026615666150915120218
366. Xue LJ, Mao XB, Ren LL, Chu XY. Inhibition of CXCL12/CXCR4 axis as a potential targeted therapy of advanced gastric carcinoma. *Cancer Med*. (2017) 6:1424–36. doi: 10.1002/cam4.1085
367. Günzel D, Fromm M. Claudins and other tight junction proteins. *Compr Physiol*. (2012) 2:1819–52. doi: 10.1002/cphy.c110045
368. Nelson GM, Padera TP, Garkavtsev I, Shioda T, Jain RK. Differential gene expression of primary cultured lymphatic and blood vascular endothelial cells. *Neoplasia*. (2007) 9:1038–45. doi: 10.1593/neo.07643
369. Yano T, Kanoh H, Tamura A, Tsukita S. Apical cytoskeletons and junctional complexes as a combined system in epithelial cell sheets. *Ann N Y Acad Sci*. (2017) 1405:32–43. doi: 10.1111/nyas.13432
370. Rosenthal R, Günzel D, Theune D, Czichos C, Schulzke JD, Fromm M. Water channels and barriers formed by claudins. *Ann N Y Acad Sci*. (2017) 1397:100–9. doi: 10.1111/nyas.13383
371. Tsukita S, Tanaka H, Tamura A. The claudins: from tight junctions to biological systems. *Trends Biochem Sci*. (2019) 44:141–52. doi: 10.1016/j.tibs.2018.09.008
372. Ding L, Lu Z, Foreman O, Tatum R, Lu Q, Renegar R, et al. Inflammation and disruption of the mucosal architecture in claudin-7-deficient mice. *Gastroenterology*. (2012) 142:305–15. doi: 10.1053/j.gastro.2011.10.025
373. Tanaka H, Takechi M, Kiyonari H, Shioi G, Tamura A, Tsukita S. Intestinal deletion of Claudin-7 enhances paracellular organic solute flux and initiates colonic inflammation in mice. *Gut*. (2015) 64:1529–38. doi: 10.1136/gutjnl-2014-308419
374. Günzel D. Claudins: vital partners in transcellular and paracellular transport coupling. *Pflugers Arch*. (2017) 469:35–44. doi: 10.1007/s00424-016-1909-3
375. Baumholtz AI, Gupta IR, Ryan AK. Claudins in morphogenesis: forming an epithelial tube. *Tissue Barriers*. (2017) 5:e1361899. doi: 10.1080/21688370.2017.1361899
376. Tanaka H, Tamura A, Suzuki K, Tsukita S. Site-specific distribution of claudin-based paracellular channels with roles in biological fluid flow and metabolism. *Ann N Y Acad Sci*. (2017) 1405:44–52. doi: 10.1111/nyas.13438
377. Chelakkot C, Ghim J, Ryu SH. Mechanisms regulating intestinal barrier integrity and its pathological implications. *Exp Mol Med*. (2018) 50:103. doi: 10.1038/s12276-018-0126-x
378. Hagen SJ. Non-canonical functions of claudin proteins: beyond the regulation of cell-cell adhesions. *Tissue Barriers*. (2017) 5:e1327839. doi: 10.1080/21688370.2017.1327839
379. Stamatovic SM, Johnson AM, Sladojevic N, Keep RF, Andjelkovic AV. Endocytosis of tight junction proteins and the regulation of degradation and recycling. *Ann N Y Acad Sci*. (2017) 1397:54–65. doi: 10.1111/nyas.13346
380. Van Itallie CM, Anderson JM. Claudin interactions in and out of the tight junction. *Tissue Barriers*. (2013) 1:e25247. doi: 10.4161/tisb.25247
381. Sjö A, Magnusson KE, Peterson KH. Protein kinase C activation has distinct effects on the localization, phosphorylation and detergent solubility of the claudin protein family in tight and leaky epithelial cells. *J Membr Biol*. (2010) 236:181–9. doi: 10.1007/s00232-010-9289-7
382. Su L, Nalle SC, Shen L, Turner ES, Singh G, Breskin LA, et al. TNFR2 activates MLCK-dependent tight junction dysregulation to cause apoptosis-mediated barrier loss and experimental colitis. *Gastroenterology*. (2013) 145:407–15. doi: 10.1053/j.gastro.2013.04.011
383. Shen L. Tight junctions on the move: molecular mechanisms for epithelial barrier regulation. *Ann N Y Acad Sci*. (2012) 1258:9–18. doi: 10.1111/j.1749-6632.2012.06613.x
384. Manabe A, Furukawa C, Endo S, Marunaka K, Nishiyama T, Fujii N, et al. Chlorpheniramine increases paracellular permeability to marker fluorescein lucifer yellow mediated by internalization of occludin in murine colonic epithelial cells. *Biol Pharm Bull*. (2017) 40:1299–305. doi: 10.1248/bpb.b17-00244
385. Li J, Li YX, Chen MH, Li J, Du J, Shen B, et al. Changes in the phosphorylation of claudins during the course of experimental colitis. *Int J Clin Exp Pathol*. (2015) 8:12225–33.
386. Shigetomi K, Ono Y, Inai T, Ikenouchi J. Adherens junctions influence tight junction formation via changes in membrane lipid composition. *J Cell Biol*. (2018) 217:2373–81. doi: 10.1083/jcb.201711042

387. Thuma F, Heiler S, Schnölzer M, Zöller M. Palmitoylated claudin7 captured in glycolipid-enriched membrane microdomains promotes metastasis via associated transmembrane and cytosolic molecules. *Oncotarget*. (2016) 7:30659–77. doi: 10.18632/oncotarget.8928
388. Philip R, Heiler S, Mu W, Büchler MW, Zöller M, Thuma F. Claudin-7 promotes the epithelial-mesenchymal transition in human colorectal cancer. *Oncotarget*. (2015) 6:2046–63. doi: 10.18632/oncotarget.2858
389. Tauro BJ, Greening DW, Mathias RA, Mathivanan S, Ji H, Simpson RJ. Two distinct populations of exosomes are released from LIM1863 colon carcinoma cell-derived organoids. *Mol Cell Proteomics*. (2013) 12:587–98. doi: 10.1074/mcp.M112.021303
390. Kowal J, Tkach M, Théry C. Biogenesis and secretion of exosomes. *Curr Opin Cell Biol*. (2014) 29:116–25. doi: 10.1016/j.ceb.2014.05.004
391. Kyuno D, Bauer N, Schnölzer M, Provaznik J, Ryschich E, Hackert T, et al. Distinct origin of claudin7 in early tumor endosomes affects exosome assembly. *Int J Biol Sci*. (2019) 15:2224–39. doi: 10.7150/ijbs.35347
392. Patriarca C, Macchi RM, Marschner AK, Mellstedt H. Epithelial cell adhesion molecule expression (CD326) in cancer: a short review. *Cancer Treat Rev*. (2012) 38:68–75. doi: 10.1016/j.ctrv.2011.04.002
393. Munz M, Baeuerle PA, Gires O. The emerging role of EpCAM in cancer and stem cell signaling. *Cancer Res*. (2009) 69:5627–9. doi: 10.1158/0008-5472.CAN-09-0654
394. Litvinov SV, Velders MP, Bakker HA, Fleuren GJ, Warnaar SO. Ep-CAM: a human epithelial antigen is a homophilic cell-cell adhesion molecule. *J Cell Biol*. (1994) 125:437–46. doi: 10.1083/jcb.125.2.437
395. Boesch M, Spizzo G, Seeber A. Concise review: aggressive colorectal cancer: role of epithelial cell adhesion molecule in cancer stem cells and epithelial-to-mesenchymal transition. *Stem Cells Transl Med*. (2018) 7:495–501. doi: 10.1002/sctm.17-0289
396. Maetzel D, Denzel S, Mack B, Eggert C, Bärr G, Gires O. Nuclear signalling by tumour-associated antigen EpCAM. *Nat Cell Biol*. (2009) 11:162–71. doi: 10.1038/ncb1824
397. Lin CW, Liao MY, Lin WW, Wang YP, Lu TY, Wu HC. Epithelial cell adhesion molecule regulates tumor initiation and tumorigenesis via activating reprogramming factors and epithelial-mesenchymal transition genes expression in colon cancer. *J Biol Chem*. (2012) 287:39449–59. doi: 10.1074/jbc.M112.386235
398. Gires O, Stoecklein NH. Dynamic EpCAM expression on circulating and disseminating tumor cells: causes and consequences. *Cell Mol Life Sci*. (2014) 71:4393–402. doi: 10.1007/s00018-014-1693-1
399. Hsu YT, Gu F, Huang YW, Liu J, Ruan J, Huang RL, et al. Promoter hypomethylation of EpCAM-regulated bone morphogenetic protein gene family in recurrent endometrial cancer. *Clin Cancer Res*. (2013) 19:6272–85. doi: 10.1158/1078-0432.CCR-13-1734
400. Sankpal NV, Fleming TP, Sharma PK, Wiedner HJ, Gillanders WE. A double-negative feedback loop between EpCAM and ERK contributes to the regulation of epithelial-mesenchymal transition in cancer. *Oncogene*. (2017) 36:3706–17. doi: 10.1038/onc.2016.504
401. Herreros-Pomares A, Aguilar-Gallardo C, Calabuig-Fariñas S, Sirera R, Jantus-Lewintre E, Camps C. EpCAM duality becomes this molecule in a new Dr. Jekyll and Mr. Hyde tale. *Crit Rev Oncol Hematol*. (2018) 126:52–63. doi: 10.1016/j.critrevonc.2018.03.006
402. Denzel S, Mack B, Eggert C, Massoner P, Stöcklein N, Kemming D, et al. MMP7 is a target of the tumour-associated antigen EpCAM. *Int J Exp Pathol*. (2012) 93:341–53. doi: 10.1111/j.1365-2613.2012.00826.x
403. Imrich S, Hachmeister M, Gires O. EpCAM and its potential role in tumor-initiating cells. *Cell Adh Migr*. (2012) 6:30–8. doi: 10.4161/cam.18953
404. Maghzal N, Vogt E, Reintsch W, Fraser JS, Fagotto F. The tumor-associated EpCAM regulates morphogenetic movements through intracellular signaling. *J Cell Biol*. (2010) 191:645–59. doi: 10.1083/jcb.201004074
405. Huang L, Yang Y, Yang F, Liu S, Zhu Z, Lei Z, et al. Functions of EpCAM in physiological processes and diseases (Review). *Int J Mol Med*. (2018) 42:1771–85. doi: 10.3892/ijmm.2018.3764
406. Yahyazadeh Mashhadi SM, Kazemimanesh M, Arashkia A, Azadmanesh K, Meshkat Z, Golichenari B, et al. Shedding light on the EpCAM: an overview. *J Cell Physiol*. (2019) 234:12569–80. doi: 10.1002/jcp.28132
407. Gao J, Liu X, Yang F, Liu T, Yan Q, Yang X. By inhibiting Ras/Raf/ERK and MMP-9, knockdown of EpCAM inhibits breast cancer cell growth and metastasis. *Oncotarget*. (2015) 6:27187–98. doi: 10.18632/oncotarget.4551
408. Wang H, Stoecklein NH, Lin PP, Gires O. Circulating and disseminated tumor cells: diagnostic tools and therapeutic targets in motion. *Oncotarget*. (2017) 8:1884–912. doi: 10.18632/oncotarget.12242
409. Biddle A, Liang X, Gammon L, Fazil B, Harper LJ, Emich H, et al. Cancer stem cells in squamous cell carcinoma switch between two distinct phenotypes that are preferentially migratory or proliferative. *Cancer Res*. (2011) 71:5317–26. doi: 10.1158/0008-5472.CAN-11-1059
410. Gires O, Klein CA, Baeuerle PA. On the abundance of EpCAM on cancer stem cells. *Nat Rev Cancer*. (2009) 9:143. doi: 10.1038/nrc2499-c1
411. Driemel C, Kremling H, Schumacher S, Will D, Wolters J, Lindenlauf N, et al. Context-dependent adaption of EpCAM expression in early systemic esophageal cancer. *Oncogene*. (2014) 33:4904–15. doi: 10.1038/onc.2013.441
412. González B, Denzel S, Mack B, Conrad M, Gires O. EpCAM is involved in maintenance of the murine embryonic stem cell phenotype. *Stem Cells*. (2009) 27:1782–91. doi: 10.1002/stem.97
413. Lu TY, Lu RM, Liao MY, Yu J, Chung CH, Kao CF, et al. Epithelial cell adhesion molecule regulation is associated with the maintenance of the undifferentiated phenotype of human embryonic stem cells. *J Biol Chem*. (2010) 285:8719–32. doi: 10.1074/jbc.M109.077081
414. van der Gun BTF, Wasserkort R, Monami A, Jeltsch A, Raskó T, Slaska-Kiss K, et al. Persistent downregulation of the pancarcinoma-associated epithelial cell adhesion molecule via active intranuclear methylation. *Int J Cancer*. (2008) 123:484–9. doi: 10.1002/ijc.23476
415. Yu G, Zhang X, Wang H, Rui D, Yin A, Qiu G, et al. CpG island methylation status in the EpCAM promoter region and gene expression. *Oncol Rep*. (2008) 20:1061–7.
416. van der Gun BT, de Groote ML, Kazemier HG, Arendzen AJ, Terpstra P, Ruiters MH, et al. Transcription factors and molecular epigenetic marks underlying EpCAM overexpression in ovarian cancer. *Br J Cancer*. (2011) 105:312–9. doi: 10.1038/bjc.2011.231
417. Roche J, Nasarre P, Gemmill R, Baldys A, Pontis J, Korch C, et al. Global decrease of histone H3K27 acetylation in ZEB1-induced epithelial to mesenchymal transition in lung cancer cells. *Cancers*. (2013) 5:334–56. doi: 10.3390/cancers5020334
418. Ji J, Tang J, Deng L, Xie Y, Jiang R, Li G, et al. LINC00152 promotes proliferation in hepatocellular carcinoma by targeting EpCAM via the mTOR signaling pathway. *Oncotarget*. (2015) 6:42813–24. doi: 10.18632/oncotarget.5970
419. Qian NS, Liu WH, Lv WP, Xiang X, Su M, Raut V, et al. Upregulated microRNA-92b regulates the differentiation and proliferation of EpCAM-positive fetal liver cells by targeting C/EBPß. *PLoS ONE*. (2013) 8:e68004. doi: 10.1371/journal.pone.0068004
420. Ostenfeld MS, Jensen SG, Jeppesen DK, Christensen LL, Thorsen SB, Stenvang J, et al. miRNA profiling of circulating EpCAM(+) extracellular vesicles: promising biomarkers of colorectal cancer. *J Extracell Vesicles*. (2016) 5:31488. doi: 10.3402/jev.v5.31488
421. Koo BK, Clevers H. Stem cells marked by the R-spondin receptor LGR5. *Gastroenterology*. (2014) 147:289–302. doi: 10.1053/j.gastro.2014.05.007
422. Cruciat CM, Niehrs C. Secreted and transmembrane wnt inhibitors and activators. *Cold Spring Harb Perspect Biol*. (2013) 5:a015081. doi: 10.1101/cshperspect.a015081
423. Kemper K, Prasetyanti PR, De Lau W, Rodermond H, Clevers H, Medema JP. Monoclonal antibodies against Lgr5 identify human colorectal cancer stem cells. *Stem Cells*. (2012) 30:2378–86. doi: 10.1002/stem.1233
424. de Lau W, Barker N, Low TY, Koo BK, Li VS, Teunissen H, et al. Lgr5 homologues associate with Wnt receptors and mediate R-spondin signalling. *Nature*. (2011) 476:293–7. doi: 10.1038/nature10337
425. de Lau W, Peng WC, Gros P, Clevers H. The R-spondin/Lgr5/Rnf43 module: regulator of Wnt signal strength. *Genes Dev*. (2014) 28:305–16. doi: 10.1101/gad.235473.113
426. de Sousa e Melo F, Kurtova AV, Harnoss JM, Kljavin N, Hoeck JD, Hung J, et al. A distinct role for $Lgr5_+$ stem cells in primary and metastatic colon cancer. *Nature*. (2017) 543:676–80. doi: 10.1038/nature21713
427. Leung C, Tan SH, Barker N. Recent advances in $Lgr5_+$ stem cell research. *Trends Cell Biol*. (2018) 28:380–91. doi: 10.1016/j.tcb.2018.01.010

428. Corbeil D, Röper K, Hellwig A, Tavian M, Miraglia S, Watt SM, et al. The human AC133 hematopoietic stem cell antigen is also expressed in epithelial cells and targeted to plasma membrane protrusions. *J Biol Chem*. (2000) 275:5512–20. doi: 10.1074/jbc.275.8.5512
429. Ren F, Sheng WQ, Du X. CD133: a cancer stem cells marker, is used in colorectal cancers. *World J Gastroenterol*. (2013) 19:2603–11. doi: 10.3748/wjg.v19.i17.2603
430. Chen S, Song X, Chen Z, Li X, Li M, Liu H, et al. CD133 expression and the prognosis of colorectal cancer: a systematic review and meta-analysis. *PLoS ONE*. (2013) 8:e56380. doi: 10.1371/journal.pone.0056380
431. Röper K, Corbeil D, Huttner WB. Retention of prominin in microvilli reveals distinct cholesterol-based lipid micro-domains in the apical plasma membrane. *Nat Cell Biol*. (2000) 2:582–92. doi: 10.1038/35023524
432. Giebel B, Corbeil D, Beckmann J, Höhn J, Freund D, Giesen K, et al. Segregation of lipid raft markers including CD133 in polarized human hematopoietic stem and progenitor cells. *Blood*. (2004) 104:2332–8. doi: 10.1182/blood-2004-02-0511
433. Simons K, Toomre D. Lipid rafts and signal transduction. *Nat Rev Mol Cell Biol*. (2000) 1:31–9. doi: 10.1038/35036052
434. Mak AB, Nixon AM, Kittanakom S, Stewart JM, Chen GI, Curak J, et al. Regulation of CD133 by HDAC6 promotes β-catenin signaling to suppress cancer cell differentiation. *Cell Rep*. (2012) 2:951–63. doi: 10.1016/j.celrep.2012.09.016
435. Shimozato O, Waraya M, Nakashima K, Souda H, Takiguchi N, Yamamoto H, et al. Receptor-type protein tyrosine phosphatase κ directly dephosphorylates CD133 and regulates downstream AKT activation. *Oncogene*. (2015) 34:1949–60. doi: 10.1038/onc.2014.141
436. Takenobu H, Shimozato O, Nakamura T, Ochiai H, Yamaguchi Y, Ohira M, et al. CD133 suppresses neuroblastoma cell differentiation via signal pathway modification. *Oncogene*. (2011) 30:97–105. doi: 10.1038/onc.2010.383
437. Zhang M, Liu Y, Feng H, Bian X, Zhao W, Yang Z, et al. CD133 affects the invasive ability of HCT116 cells by regulating TIMP-2. *Am J Pathol*. (2013) 182:565–76. doi: 10.1016/j.ajpath.2012.10.015
438. Li C, Wang C, Xing Y, Zhen J, Ai Z. CD133 promotes gallbladder carcinoma cell migration through activating Akt phosphorylation. *Oncotarget*. (2016) 7:17751–9. doi: 10.18632/oncotarget.7474
439. Liu C, Li Y, Xing Y, Cao B, Yang F, Yang T, et al. The interaction between cancer stem cell marker CD133 and Src protein promotes Focal Adhesion Kinase (FAK) phosphorylation and cell migration. *J Biol Chem*. (2016) 291:15540–50. doi: 10.1074/jbc.M115.712976
440. Song S, Pei G, Du Y, Wu J, Ni X, Wang S, et al. Interaction between CD133 and PI3K-p85 promotes chemoresistance in gastric cancer cells. *Am J Transl Res*. (2018) 10:304–14.
441. Lu J, Ye X, Fan F, Xia L, Bhattacharya R, Bellister S, et al. Endothelial cells promote the colorectal cancer stem cell phenotype through a soluble form of Jagged-1. *Cancer Cell*. (2013) 23:171–85. doi: 10.1016/j.ccr.2012.12.021
442. Fonseca AV, Bauer N, Corbeil D. The stem cell marker CD133 meets the endosomal compartment–new insights into the cell division of hematopoietic stem cells. *Blood Cells Mol Dis*. (2008) 41:194–5. doi: 10.1016/j.bcmd.2008.04.004
443. Shmelkov SV, St Clair R, Lyden D, Rafii S. AC133/CD133/Prominin-1. *Int J Biochem Cell Biol*. (2005) 37:715–9. doi: 10.1016/j.biocel.2004.08.010
444. Corbeil D, Joester A, Fargeas CA, Jászai J, Garwood J, Hellwig A, et al. Expression of distinct splice variants of the stem cell marker prominin-1 (CD133) in glial cells. *Glia*. (2009) 57:860–74. doi: 10.1002/glia.20812
445. Trajkovic K, Hsu C, Chiantia S, Rajendran L, Wenzel D, Wieland F, et al. Ceramide triggers budding of exosome vesicles into multivesicular endosomes. *Science*. (2008) 319:1244–7. doi: 10.1126/science.1153124
446. Badawy SMM, Okada T, Kajimoto T, Hirase M, Matovelo SA, Nakamura S, et al. Extracellular α-synuclein drives sphingosine 1-phosphate receptor subtype 1 out of lipid rafts, leading to impaired inhibitory G-protein signaling. *J Biol Chem*. (2018) 293:8208–16. doi: 10.1074/jbc.RA118.001986
447. Izumi H, Li Y, Shibaki M, Mori D, Yasunami M, Sato S, et al. Recycling endosomal CD133 functions as an inhibitor of autophagy at the pericentrosomal region. *Sci Rep*. (2019) 9:2236. doi: 10.1038/s41598-019-39229-8
448. Zheng X, Carstens JL, Kim J, Scheible M, Kaye J, Sugimoto H, et al. Epithelial-to-mesenchymal transition is dispensable for metastasis but induces chemoresistance in pancreatic cancer. *Nature*. (2015) 527:525–30. doi: 10.1038/nature16064
449. Wang Z, Li Y, Kong D, Banerjee S, Ahmad A, Azmi AS, et al. Acquisition of epithelial-mesenchymal transition phenotype of gemcitabine-resistant pancreatic cancer cells is linked with activation of the notch signaling pathway. *Cancer Res*. (2009) 69:2400–7. doi: 10.1158/0008-5472.CAN-08-4312
450. Krebs AM, Mitschke J, Lasierra Losada M, Schmalhofer O, Boerries M, Busch H, et al. The EMT-activator Zeb1 is a key factor for cell plasticity and promotes metastasis in pancreatic cancer. *Nat Cell Biol*. (2017) 19:518–29. doi: 10.1038/ncb3513
451. Zöller M, Matzku S, Goerttler K. High incidence of spontaneous transplantable tumours in BDX rats. *Br J Cancer*. (1978) 37:61–6. doi: 10.1038/bjc.1978.9
452. Matzku S, Komitowski D, Mildenberger M, Zöller M. Characterization of BSp73, a spontaneous rat tumor and its *in vivo* selected variants showing different metastasizing capacities. *Invasion Metast*. (1983) 3:109–23.
453. Matzku S, Wenzel A, Liu S, Zöller M. Antigenic differences between metastatic and nonmetastatic BSp73 rat tumor variants characterized by monoclonal antibodies. *Cancer Res*. (1989) 49:1294–9.
454. Günthert U, Hofmann M, Rudy W, Reber S, Zöller M, Haussmann I, et al. A new variant of glycoprotein CD44 confers metastatic potential to rat carcinoma cells. *Cell*. (1991) 65:13–24. doi: 10.1016/0092-8674(91)90403-L
455. Herlevsen M, Schmidt DS, Miyazaki K, Zöller M. The association of the tetraspanin D6.1A with the alpha6beta4 integrin supports cell motility and liver metastasis formation. *J Cell Sci*. (2003) 116:4373–90. doi: 10.1242/jcs.00760
456. Würfel J, Rösel M, Seiter S, Claas C, Herlevsen M, Weth R, et al. Metastasis-association of the rat ortholog of the human epithelial glycoprotein antigen EGP314. *Oncogene*. (1999) 18:2323–34. doi: 10.1038/sj.onc.1202542
457. Nübel T, Preobraschenski J, Tuncay H, Weiss T, Kuhn S, Ladwein M, et al. Claudin-7 regulates EpCAM-mediated functions in tumor progression. *Mol Cancer Res*. (2009) 7:285–99. doi: 10.1158/1541-7786.MCR-08-0200
458. Klingbeil P, Marhaba R, Jung T, Kirmse R, Ludwig T, Zöller M. CD44 variant isoforms promote metastasis formation by a tumor cell-matrix cross-talk that supports adhesion and apoptosis resistance. *Mol Cancer Res*. (2009) 7:168–79. doi: 10.1158/1541-7786.MCR-08-0207
459. Thuma F, Zöller M. EpCAM-associated claudin-7 supports lymphatic spread and drug resistance in rat pancreatic cancer. *Int J Cancer*. (2013) 133:855–66. doi: 10.1002/ijc.28085
460. Rasheed ZA, Matsui W, Maitra A. Pathology of pancreatic stroma in PDAC. In: Grippo PJ, Munshi HG, editors. *Pancreatic Cancer and Tumor Microenvironment*. Trivandrum: Transworld Research Network (2012). p. 1–6.
461. Xu M, Zhou BP, Tao M, Liu J, Li W. The role of stromal components in pancreatic cancer progression. *Anticancer Agents Med Chem*. (2016) 16:1117–24. doi: 10.2174/1871520616666160404115532
462. Pang TCY, Wilson JS, Apte MV. Pancreatic stellate cells: what's new? *Curr Opin Gastroenterol*. (2017) 33:366–73. doi: 10.1097/MOG.0000000000000378
463. Allam A, Thomsen AR, Gothwal M, Saha D, Maurer J, Brunner TB. Pancreatic stellate cells in pancreatic cancer: in focus. *Pancreatology*. (2017) 17:514–22. doi: 10.1016/j.pan.2017.05.390
464. Bachem MG, Schneider E, Gross H, Weidenbach H, Schmid RM, Menke A, et al. Identification, culture, and characterization of pancreatic stellate cells in rats and humans. *Gastroenterology*. (1998) 115:421–32. doi: 10.1016/S0016-5085(98)70209-4
465. Bailey JM, Mohr AM, Hollingsworth MA. Sonic hedgehog paracrine signaling regulates metastasis and lymphangiogenesis in pancreatic cancer. *Oncogene*. (2009) 28:3513–25. doi: 10.1038/onc.2009.220
466. Neesse A, Wagner M, Ellenrieder V, Bachem M, Gress TM, Buchholz M. Pancreatic stellate cells potentiate proinvasive effects of SERPINE2 expression in pancreatic cancer xenograft tumors. *Pancreatology*. (2007) 7:380–5. doi: 10.1159/000107400
467. Mahadevan D, Von Hoff DD. Tumor-stroma interactions in pancreatic ductal adenocarcinoma. *Mol Cancer Ther*. (2007) 6:1186–97. doi: 10.1158/1535-7163.MCT-06-0686

468. Shields MA, Dangi-Garimella S, Krantz SB, Bentrem DJ, Munshi HG. Pancreatic cancer cells respond to type I collagen by inducing snail expression to promote membrane type 1 matrix metalloproteinase-dependent collagen invasion. *J Biol Chem*. (2011) 286:10495–504. doi: 10.1074/jbc.M110.195628
469. Tjomsland V, Pomianowska E, Aasrum M, Sandnes D, Verbeke CS, Gladhaug IP. Profile of MMP and TIMP expression in human pancreatic stellate cells: regulation by IL-1α and TGFβ and implications for migration of pancreatic cancer cells. *Neoplasia*. (2016) 18:447–56. doi: 10.1016/j.neo.2016.06.003
470. Li Y, Song T, Chen Z, Wang Y, Zhang J, Wang X. Pancreatic stellate cells activation and matrix metallopeptidase 2 expression correlate with lymph node metastasis in pancreatic carcinoma. *Am J Med Sci*. (2019) 357:16–22. doi: 10.1016/j.amjms.2018.10.001
471. Masamune A, Kikuta K, Watanabe T, Satoh K, Satoh A, Shimosegawa T. Pancreatic stellate cells express Toll-like receptors. *J Gastroenterol*. (2008) 43:352–62. doi: 10.1007/s00535-008-2162-0
472. Zambirinis CP, Levie E, Nguy S, Avanzi A, Barilla R, Xu Y, et al. TLR9 ligation in pancreatic stellate cells promotes tumorigenesis. *J Exp Med*. (2015) 212:2077–94. doi: 10.1084/jem.20142162
473. Winau F, Hegasy G, Weiskirchen R, Weber S, Cassan C, Sieling PA, et al. Ito cells are liver-resident antigen-presenting cells for activating T cell responses. *Immunity*. (2007) 26:117–29. doi: 10.1016/j.immuni.2006.11.011
474. Shimizu K, Hashimoto K, Tahara J, Imaeda H, Andoh A, Shiratori K. Pancreatic stellate cells do not exhibit features of antigen-presenting cells. *Pancreas*. (2012) 41:422–7. doi: 10.1097/MPA.0b013e31822e673b
475. Lunardi S, Lim SY, Muschel RJ, Brunner TB. IP-10/CXCL10 attracts regulatory T cells: implication for pancreatic cancer. *Oncoimmunology*. (2015) 4:e1027473. doi: 10.1080/2162402X.2015.1027473
476. Tang D, Gao J, Wang S, Yuan Z, Ye N, Chong Y, et al. Apoptosis and anergy of T cell induced by pancreatic stellate cells-derived galectin-1 in pancreatic cancer. *Tumour Biol*. (2015) 36:5617–26. doi: 10.1007/s13277-015-3233-5
477. Jiang ZJ, Shen QH, Chen HY, Yang Z, Shuai MQ, Zheng S. Galectin-1 restores immune tolerance to liver transplantation through activation of hepatic stellate cells. *Cell Physiol Biochem*. (2018) 48:863–79. doi: 10.1159/000491955
478. Saison-Ridinger M, DelGiorno KE, Zhang T, Kraus A, French R, Jaquish D, et al. Reprogramming pancreatic stellate cells via p53 activation: a putative target for pancreatic cancer therapy. *PLoS ONE*. (2017) 12:e0189051. doi: 10.1371/journal.pone.0189051
479. Pothula SP, Xu Z, Goldstein D, Merrett N, Pirola RC, Wilson JS, et al. Targeting the HGF/c-MET pathway: stromal remodelling in pancreatic cancer. *Oncotarget*. (2017) 8:76722–39. doi: 10.18632/oncotarget.20822
480. Schnittert J, Heinrich MA, Kuninty PR, Storm G, Prakash J. Reprogramming tumor stroma using an endogenous lipid lipoxin A4 to treat pancreatic cancer. *Cancer Lett*. (2018) 420:247–58. doi: 10.1016/j.canlet.2018.01.072
481. Bynigeri RR, Jakkampudi A, Jangala R, Subramanyam C, Sasikala M, Rao GV, et al. Pancreatic stellate cell: Pandora's box for pancreatic disease biology. *World J Gastroenterol*. (2017) 23:382–405. doi: 10.3748/wjg.v23.i3.382
482. Sun Q, Zhang B, Hu Q, Qin Y, Xu W, Liu W, et al. The impact of cancer-associated fibroblasts on major hallmarks of pancreatic cancer. *Theranostics*. (2018) 8:5072–87. doi: 10.7150/thno.26546
483. Fu Y, Liu S, Zeng S, Shen H. The critical roles of activated stellate cells-mediated paracrine signaling, metabolism and onco-immunology in pancreatic ductal adenocarcinoma. *Mol Cancer*. (2018) 17:62. doi: 10.1186/s12943-018-0815-z
484. Schoepp M, Ströse AJ, Haier J. Dysregulation of miRNA expression in cancer associated fibroblasts (CAFs) and its consequences on the tumor microenvironment. *Cancers*. (2017) 9:E54. doi: 10.3390/cancers9060054
485. Özdemir BC, Pentcheva-Hoang T, Carstens JL, Zheng X, Wu CC, Simpson TR, et al. Depletion of carcinoma-associated fibroblasts and fibrosis induces immunosuppression and accelerates pancreas cancer with reduced survival. *Cancer Cell*. (2014) 25:719–34. doi: 10.1016/j.ccr.2014.04.005
486. Rhim AD, Oberstein PE, Thomas DH, Mirek ET, Palermo CF, Sastra SA, et al. Stromal elements act to restrain, rather than support, pancreatic ductal adenocarcinoma. *Cancer Cell*. (2014) 25:735–47. doi: 10.1016/j.ccr.2014.04.021
487. Seux M, Peuget S, Montero MP, Siret C, Rigot V, Clerc P, et al. TP53INP1 decreases pancreatic cancer cell migration by regulating SPARC expression. *Oncogene*. (2011) 30:3049–61. doi: 10.1038/onc.2011.25
488. Kanno A, Satoh K, Masamune A, Hirota M, Kimura K, Umino J, et al. Periostin, secreted from stromal cells, has biphasic effect on cell migration and correlates with the epithelial to mesenchymal transition of human pancreatic cancer cells. *Int J Cancer*. (2008) 122:2707–18. doi: 10.1002/ijc.23332
489. Saini F, Argent RH, Grabowska AM. Sonic hedgehog ligand: a role in formation of a mesenchymal niche in human pancreatic ductal adenocarcinoma. *Cells*. (2019) 8:E424. doi: 10.3390/cells8050424
490. Sato N, Maehara N, Goggins M. Gene expression profiling of tumor-stromal interactions between pancreatic cancer cells and stromal fibroblasts. *Cancer Res*. (2004) 64:6950–6. doi: 10.1158/0008-5472.CAN-04-0677
491. Qian D, Tian L, Lu Z, Miao Y. Cytokine profiling and orthotopic xenografing of pancreatic stellate cells. *Methods Mol Biol*. (2019) 1882:157–60. doi: 10.1007/978-1-4939-8879-2_14
492. Tang D, Wu Q, Yuan Z, Xu J, Zhang H, Jin Z, et al. Identification of key pathways and genes changes in pancreatic cancer cells (BXPC-3) after cross-talked with primary pancreatic stellate cells using bioinformatics analysis. *Neoplasma*. (2019) 66:681–93. doi: 10.4149/neo_2018_181020N786
493. Al-Assar O, Demiciorglu F, Lunardi S, Gaspar-Carvalho MM, McKenna WG, Muschel RM, et al. Contextual regulation of pancreatic cancer stem cell phenotype and radioresistance by pancreatic stellate cells. *Radiother Oncol*. (2014) 111:243–51. doi: 10.1016/j.radonc.2014.03.014
494. Zhang H, Yue J, Jiang Z, Zhou R, Xie R, Xu Y, et al. CAF-secreted CXCL1 conferred radioresistance by regulating DNA damage response in a ROS-dependent manner in esophageal squamous cell carcinoma. *Cell Death Dis*. (2017) 8:e2790. doi: 10.1038/cddis.2017.180
495. Amrutkar M, Aasrum M, Verbeke CS, Gladhaug IP. Secretion of fibronectin by human pancreatic stellate cells promotes chemoresistance to gemcitabine in pancreatic cancer cells. *BMC Cancer*. (2019) 19:596. doi: 10.1186/s12885-019-5803-1
496. Duluc C, Moatassim-Billah S, Chalabi-Dchar M, Perraud A, Samain R, Breibach F, et al. Pharmacological targeting of the protein synthesis mTOR/4E-BP1 pathway in cancer-associated fibroblasts abrogates pancreatic tumour chemoresistance. *EMBO Mol Med*. (2015) 7:735–53. doi: 10.15252/emmm.201404346
497. Liu Y, Li F, Gao F, Xing L, Qin P, Liang X, et al. Periostin promotes the chemotherapy resistance to gemcitabine in pancreatic cancer. *Tumour Biol*. (2016) 37:15283–91. doi: 10.1007/s13277-016-5321-6
498. Zhang D, Li L, Jiang H, Li Q, Wang-Gillam A, Yu J, et al. Tumor-stroma IL1β-IRAK4 feedforward circuitry drives tumor fibrosis, chemoresistance, and poor prognosis in pancreatic cancer. *Cancer Res*. (2018) 78:1700–12. doi: 10.1158/0008-5472.CAN-17-1366
499. Neumann CCM, von Hörschelmann E, Reutzel-Selke A, Seidel E, Sauer IM, Pratschke J, et al. Tumor-stromal cross-talk modulating the therapeutic response in pancreatic cancer. *Hepatobiliary Pancreat Dis Int*. (2018) 17:461–72. doi: 10.1016/j.hbpd.2018.09.004
500. Hernandez-Unzueta I, Benedicto A, Romayor I, Herrero A, Sanz E, Arteta B, et al. Ocoxin oral solution exerts an antitumoral effect in pancreatic cancer and reduces the stromal-mediated chemoresistance. *Pancreas*. (2019) 48:555–67. doi: 10.1097/MPA.0000000000001277
501. Hwang HJ, Oh MS, Lee DW, Kuh HJ. Multiplex quantitative analysis of stroma-mediated cancer cell invasion, matrix remodeling, and drug response in a 3D co-culture model of pancreatic tumor spheroids and stellate cells. *J Exp Clin Cancer Res*. (2019) 38:258. doi: 10.1186/s13046-019-1225-9
502. Yang XP, Liu SL, Xu JF, Cao SG, Li Y, Zhou YB. Pancreatic stellate cells increase pancreatic cancer cells invasion through the hepatocyte growth factor /c-Met/survivin regulated by P53/P21. *Exp Cell Res*. (2017) 357:79–87. doi: 10.1016/j.yexcr.2017.04.027
503. Okumura T, Ohuchida K, Sada M, Abe T, Endo S, Koikawa K, et al. Extra-pancreatic invasion induces lipolytic and fibrotic changes in the adipose microenvironment, with released fatty acids enhancing the invasiveness of pancreatic cancer cells. *Oncotarget*. (2017) 8:18280–95. doi: 10.18632/oncotarget.15430

504. Shan T, Chen S, Chen X, Lin WR, Li W, Ma J, et al. Prometastatic mechanisms of CAF-mediated EMT regulation in pancreatic cancer cells. *Int J Oncol.* (2017) 50:121–8. doi: 10.3892/ijo.2016.3779
505. Suetsugu A, Snyder CS, Moriwaki H, Saji S, Bouvet M, Hoffman RM. Imaging the interaction of pancreatic cancer and stellate cells in the tumor microenvironment during metastasis. *Anticancer Res.* (2015) 35:2545–51.
506. Pang TCY, Xu Z, Pothula S, Becker T, Goldstein D, Pirola RC, et al. Circulating pancreatic stellate (stromal) cells in pancreatic cancer-a fertile area for novel research. *Carcinogenesis.* (2017) 38:588–91. doi: 10.1093/carcin/bgx030
507. Vaziri-Gohar A, Zarei M, Brody JR, Winter JM. Metabolic dependencies in pancreatic cancer. *Front Oncol.* (2018) 8:617. doi: 10.3389/fonc.2018.00617
508. Cameron ME, Yakovenko A, Trevino JG. Glucose and lactate transport in pancreatic cancer: glycolytic metabolism revisited. *J Oncol.* (2018) 2018:6214838. doi: 10.1155/2018/6214838
509. Chan AK, Bruce JI, Siriwardena AK. Glucose metabolic phenotype of pancreatic cancer. *World J Gastroenterol.* (2016) 22:3471–85. doi: 10.3748/wjg.v22.i12.3471
510. Pavlova NN, Thompson CB. The emerging hallmarks of cancer metabolism. *Cell Metab.* (2016) 23:27–47. doi: 10.1016/j.cmet.2015.12.006
511. Sasaki T, Knyazev PG, Clout NJ, Cheburkin Y, Göhring W, Ullrich A, et al. Structural basis for Gas6-Axl signalling. *EMBO J.* (2006) 25:80–7. doi: 10.1038/sj.emboj.7600912
512. Wu G, Ma Z, Cheng Y, Hu W, Deng C, Jiang S, et al. Targeting Gas6/TAM in cancer cells and tumor microenvironment. *Mol Cancer.* (2018) 17:20. doi: 10.1186/s12943-018-0769-1
513. Kandasamy P, Gyimesi G, Kanai Y, Hediger MA. Amino acid transporters revisited: new views in health and disease. *Trends Biochem Sci.* (2018) 43:752–89. doi: 10.1016/j.tibs.2018.05.003
514. Zong WX, Rabinowitz JD, White E. Mitochondria and cancer. *Mol Cell.* (2016) 61:667–76. doi: 10.1016/j.molcel.2016.02.011
515. Corbet C, Feron O. Cancer cell metabolism and mitochondria: Nutrient plasticity for TCA cycle fueling. *Biochim Biophys Acta Rev Cancer.* (2017) 1868:7–15. doi: 10.1016/j.bbcan.2017.01.002
516. Trotta AP, Chipuk JE. Mitochondrial dynamics as regulators of cancer biology. *Cell Mol Life Sci.* (2017) 74:1999–2017. doi: 10.1007/s00018-016-2451-3
517. Michalopoulou E, Bulusu V, Kamphorst JJ. Metabolic scavenging by cancer cells: when the going gets tough, the tough keep eating. *Br J Cancer.* (2016) 115:635–40. doi: 10.1038/bjc.2016.256
518. Chun Y, Kim J. autophagy: an essential degradation program for cellular homeostasis and life. *Cells.* (2018) 7:E278. doi: 10.3390/cells7120278
519. Sousa CM, Biancur DE, Wang X, Halbrook CJ, Sherman MH, Zhang L, et al. Pancreatic stellate cells support tumour metabolism through autophagic alanine secretion. *Nature.* (2016) 536:479–83. doi: 10.1038/nature19084
520. Perera RM, Stoykova S, Nicolay BN, Ross KN, Fitamant J, Boukhali M, et al. Transcriptional control of autophagy-lysosome function drives pancreatic cancer metabolism. *Nature.* (2015) 524:361–5. doi: 10.1038/nature14587
521. Zhao H, Yang L, Baddour J, Achreja A, Bernard V, Moss T, et al. Tumor microenvironment derived exosomes pleiotropically modulate cancer cell metabolism. *Elife.* (2016) 5:e10250. doi: 10.7554/eLife.10250
522. Glatz JF, Luiken JJ. From fat to FAT (CD36/SR-B2): Understanding the regulation of cellular fatty acid uptake. *Biochimie.* (2017) 136:21–6. doi: 10.1016/j.biochi.2016.12.007
523. Wang R, Tao B, Fan Q, Wang S, Chen L, Zhang J, et al. Fatty-acid receptor CD36 functions as a hydrogen sulfide-targeted receptor with its Cys333-Cys272 disulfide bond serving as a specific molecular switch to accelerate gastric cancer metastasis. *EBioMedicine.* (2019) 45:108–23. doi: 10.1016/j.ebiom.2019.06.037
524. Mattijssen F, Georgiadi A, Andasarie T, Szalowska E, Zota A, Krones-Herzig A, et al. Hypoxia-inducible lipid droplet-associated (HILPDA) is a novel peroxisome proliferator-activated receptor (PPAR) target involved in hepatic triglyceride secretion. *J Biol Chem.* (2014) 289:19279–93. doi: 10.1074/jbc.M114.570044
525. Vasseur S, Guillaumond F. LDL receptor: an open route to feed pancreatic tumor cells. *Mol Cell Oncol.* (2015) 3:e1033586. doi: 10.1080/23723556.2015.1033586
526. Leca J, Martinez S, Lac S, Nigri J, Secq V, Rubis M, et al. Cancer-associated fibroblast-derived annexin A6+ extracellular vesicles support pancreatic cancer aggressiveness. *J Clin Invest.* (2016) 126:4140–56. doi: 10.1172/JCI87734
527. Yamazaki M, Nakamura K, Mizukami Y, Ii M, Sasajima J, Sugiyama Y, et al. Sonic hedgehog derived from human pancreatic cancer cells augments angiogenic function of endothelial progenitor cells. *Cancer Sci.* (2008) 99:1131–8. doi: 10.1111/j.1349-7006.2008.00795.x
528. Patel MB, Pothula SP, Xu Z, Lee AK, Goldstein D, Pirola RC, et al. The role of the hepatocyte growth factor/c-MET pathway in pancreatic stellate cell-endothelial cell interactions: antiangiogenic implications in pancreatic cancer. *Carcinogenesis.* (2014) 35:1891–900. doi: 10.1093/carcin/bgu122
529. Zhou R, Curry JM, Roy LD, Grover P, Haider J, Moore LJ, et al. A novel association of neuropilin-1 and MUC1 in pancreatic ductal adenocarcinoma: role in induction of VEGF signaling and angiogenesis. *Oncogene.* (2016) 35:5608–18. doi: 10.1038/onc.2015.516
530. Ntellas P, Dadouli K, Perivoliotis K, Sogka E, Pentheroudakis G, Ioannou M, et al. Microvessel density and impact of angiogenesis on survival of resected pancreatic cancer patients: a systematic review and meta-analysis. *Pancreas.* (2019) 48:233–41. doi: 10.1097/MPA.0000000000001237
531. Erkan M, Kurtoglu M, Kleeff J. The role of hypoxia in pancreatic cancer: a potential therapeutic target? *Expert Rev Gastroenterol Hepatol.* (2016) 10:301–16. doi: 10.1586/17474124.2016.1117386
532. Longo V, Brunetti O, Gnoni A, Cascinu S, Gasparini G, Lorusso V, et al. Angiogenesis in pancreatic ductal adenocarcinoma: a controversial issue. *Oncotarget.* (2016) 7:58649–58. doi: 10.18632/oncotarget.10765
533. Walia A, Yang JF, Huang YH, Rosenblatt MI, Chang JH, Azar DT. Endostatin's emerging roles in angiogenesis, lymphangiogenesis, disease, and clinical applications. *Biochim Biophys Acta.* (2015) 1850:2422–38. doi: 10.1016/j.bbagen.2015.09.007
534. Ruge T, Carlsson AC, Larsson A, Ärnlöv J. Endostatin: a promising biomarker in the cardiovascular continuum? *Biomark Med.* (2017) 11:905–16. doi: 10.2217/bmm-2017-0025
535. O'Reilly MS, Holmgren L, Shing Y, Chen C, Rosenthal RA, Moses M, et al. Angiostatin: a novel angiogenesis inhibitor that mediates the suppression of metastases by a Lewis lung carcinoma. *Cell.* (1994) 79:315–28. doi: 10.1016/0092-8674(94)90200-3
536. Cao Y, Xue L. Angiostatin. *Semin Thromb Hemost.* (2004) 30:83–93. doi: 10.1055/s-2004-822973
537. Yadav L, Puri N, Rastogi V, Satpute P, Sharma V. Tumour angiogenesis and angiogenic inhibitors: a review. *J Clin Diagn Res.* (2015) 9:XE01–5. doi: 10.7860/JCDR/2015/12016.6135
538. Bossard C, Van den Berghe L, Laurell H, Castano C, Cerutti M, Prats AC, et al. Antiangiogenic properties of fibstatin, an extracellular FGF-2-binding polypeptide. *Cancer Res.* (2004) 64:7507–12. doi: 10.1158/0008-5472.CAN-04-0287
539. Prats AC, Van den Berghe L, Rayssac A, Ainaoui N, Morfoisse F, Pujol F, et al. CXCL4L1-fibstatin cooperation inhibits tumor angiogenesis, lymphangiogenesis and metastasis. *Microvasc Res.* (2013) 89:25–33. doi: 10.1016/j.mvr.2013.05.005
540. Sasaki T, Hohenester E, Timpl R. Structure and function of collagen-derived endostatin inhibitors of angiogenesis. *IUBMB Life.* (2002) 53:77–84. doi: 10.1080/15216540211466
541. Heljasvaara R, Aikio M, Ruotsalainen H, Pihlajaniemi T. Collagen XVIII in tissue homeostasis and dysregulation - Lessons learned from model organisms and human patients. *Matrix Biol.* (2017) 57–58:55–75. doi: 10.1016/j.matbio.2016.10.002
542. Tsuji T, Kelly NJ, Takahashi S, Leme AS, Houghton AM, Shapiro SD. Macrophage elastase suppresses white adipose tissue expansion with cigarette smoking. *Am J Respir Cell Mol Biol.* (2014) 51:822–9. doi: 10.1165/rcmb.2014-0083OC
543. Yan C, Wang C, Dong M, Liu S, Qi C, Zhao Y. RNA interference-mediated silencing of VEGF and bFGF suppresses endostatin secretion in pancreatic carcinoma cells. *Oncol Lett.* (2013) 5:1031–5. doi: 10.3892/ol.2013.1102
544. Ramirez MU, Stirling ER, Emenaker NJ, Roberts DD, Soto-Pantoja DR. Thrombospondin-1 interactions regulate eicosanoid metabolism and signaling in cancer-related inflammation. *Cancer Metastasis Rev.* (2018) 37:469–76. doi: 10.1007/s10555-018-9737-x

545. Rossi MK, Gnanamony M, Gondi CS. The 'SPARC' of life: analysis of the role of osteonectin/SPARC in pancreatic cancer (Review). *Int J Oncol.* (2016) 48:1765–71. doi: 10.3892/ijo.2016.3417
546. Faye C, Chautard E, Olsen BR, Ricard-Blum S. The first draft of the endostatin interaction network. *J Biol Chem.* (2009) 284:22041–7. doi: 10.1074/jbc.M109.002964
547. Kim YM, Hwang S, Kim YM, Pyun BJ, Kim TY, Lee ST, et al. Endostatin blocks vascular endothelial growth factor-mediated signaling via direct interaction with KDR/Flk-1. *J Biol Chem.* (2002) 277:27872–9. doi: 10.1074/jbc.M202771200
548. Han KY, Chang JH, Dugas-Ford J, Alexander JS, Azar DT. Involvement of lysosomal degradation in VEGF-C-induced down-regulation of VEGFR-3. *FEBS Lett.* (2014) 588:4357–63. doi: 10.1016/j.febslet.2014.09.034
549. Sudhakar A, Sugimoto H, Yang C, Lively J, Zeisberg M, Kalluri R. Human tumstatin and human endostatin exhibit distinct antiangiogenic activities mediated by alpha v beta 3 and alpha 5 beta 1 integrins. *Proc Natl Acad Sci USA*. (2003) 100:4766–71. doi: 10.1073/pnas.0730882100
550. Morais C, Ebrahem Q, Anand-Apte B, Parat MO. Altered angiogenesis in caveolin-1 gene-deficient mice is restored by ablation of endothelial nitric oxide synthase. *Am J Pathol.* (2012) 180:1702–14. doi: 10.1016/j.ajpath.2011.12.018
551. Hu J, Cheng T, Zhang L, Sun B, Deng L, Xu H. Anti-tumor peptide AP25 decreases cyclin D1 expression and inhibits MGC-803 proliferation via phospho-extracellular signal-regulated kinase-, Src-, c-Jun N-terminal kinase- and phosphoinositide 3-kinase-associated pathways. *Mol Med Rep.* (2015) 12:4396–402. doi: 10.3892/mmr.2015.3912
552. Nesiel-Nuttman L, Schwartz B, Shoseyov O. Human recombinant truncated RNASET2, devoid of RNase activity) A potential cancer therapeutic agent. *Oncotarget.* (2014) 5:11464–78. doi: 10.18632/oncotarget.2562
553. Vallianou NG, Kostantinou A, Kougias M, Kazazis C. Statins and cancer. *Anticancer Agents Med Chem.* (2014) 14:706–12. doi: 10.2174/1871520613666131129105035
554. Longo V, Tamma R, Brunetti O, Pisconti S, Argentiero A, Silvestris N, et al. Mast cells and angiogenesis in pancreatic ductal adenocarcinoma. *Clin Exp Med*. (2018) 18:319–23. doi: 10.1007/s10238-018-0493-6
555. Yang M, Liu E, Tang L, Lei Y, Sun X, Hu J, et al. Emerging roles and regulation of MiT/TFE transcriptional factors. *Cell Commun Signal.* (2018) 16:31. doi: 10.1186/s12964-018-0242-1
556. Puertollano R, Ferguson SM, Brugarolas J, Ballabio A. The complex relationship between TFEB transcription factor phosphorylation and subcellular localization. *EMBO J.* (2018) 37:e98804. doi: 10.15252/embj.201798804
557. Munir R, Lisec J, Swinnen JV, Zaidi N. Lipid metabolism in cancer cells under metabolic stress. *Br J Cancer*. (2019) 120:1090–8. doi: 10.1038/s41416-019-0451-4
558. Yin F, Sharen G, Yuan F, Peng Y, Chen R, Zhou X, et al. TIP30 regulates lipid metabolism in hepatocellular carcinoma by regulating SREBP1 through the Akt/mTOR signaling pathway. *Oncogenesis*. (2017) 6:e347. doi: 10.1038/oncsis.2017.49
559. Siqingaowa, Sekar S, Gopalakrishnan V, Taghibiglou C. Sterol regulatory element-binding protein 1 inhibitors decrease pancreatic cancer cell viability and proliferation. *Biochem Biophys Res Commun.* (2017) 488:136–40. doi: 10.1016/j.bbrc.2017.05.023
560. Salvioli B, Bovara M, Barbara G, DePont F, Stanghellini V, Tomini M, et al. Neurology and neuropathology of the pancreatic innervation. *JOP*. (2002) 3:26–33.
561. Niebergall-Roth E, Singer MV. Central and peripheral neural control of pancreatic exocrine secretion. *J Physiol Pharmacol.* (2001) 52:523–38.
562. Grundy D. Neuroanatomy of visceral nociception: vagal and splanchnic afferent. *Gut*. (2002) 51 (Suppl. 1):i2–5. doi: 10.1136/gut.51.suppl_1.i2
563. Stopczynski RE, Normolle DP, Hartman DJ, Ying H, DeBerry JJ, Bielefeldt K, et al. Neuroplastic changes occur early in the development of pancreatic ductal adenocarcinoma. *Cancer Res.* (2014) 74:1718–27. doi: 10.1158/0008-5472.CAN-13-2050
564. Demir IE, Friess H, Ceyhan GO. Neural plasticity in pancreatitis and pancreatic cancer. *Nat Rev Gastroenterol Hepatol.* (2015) 12:649–59. doi: 10.1038/nrgastro.2015.166
565. Lindsay TH, Halvorson KG, Peters CM, Ghilardi JR, Kuskowski MA, Wong GY, et al. A quantitative analysis of the sensory and sympathetic innervation of the mouse pancreas. *Neuroscience*. (2006) 137:1417–26. doi: 10.1016/j.neuroscience.2005.10.055
566. Ceyhan GO, Bergmann F, Kadihasanoglu M, Altintas B, Demir IE, Hinz U, et al. Pancreatic neuropathy and neuropathic pain—A comprehensive pathomorphological study of 546 cases. *Gastroenterology*. (2009) 136:177–86. doi: 10.1053/j.gastro.2008.09.029
567. Iwasaki T, Hiraoka N, Ino Y, Nakajima K, Kishi Y, Nara S, et al. Reduction of intrapancreatic neural density in cancer tissue predicts poorer outcome in pancreatic ductal carcinoma. *Cancer Sci*. (2019) 110:1491–502. doi: 10.1111/cas.13975
568. Chatterjee D, Katz MH, Rashid A, Wang H, Iuga AC, Varadhachary GR, et al. Perineural and intraneural invasion in posttherapy pancreaticoduodenectomy specimens predicts poor prognosis in patients with pancreatic ductal adenocarcinoma. *Am J Surg Pathol*. (2012) 36:409–17. doi: 10.1097/PAS.0b013e31824104c5
569. Lee SR, Kim HO, Son BH, Yoo CH, Shin JH. Prognostic factors associated with long-term survival and recurrence in pancreatic adenocarcinoma. *Hepatogastroenterology*. (2013) 60:358–62.
570. Chang ST, Jeffrey RB, Patel BN, DiMaio MA, Rosenberg J, Willmann JK, et al. preoperative multidetector ct diagnosis of extrapancreatic perineural or duodenal invasion is associated with reduced postoperative survival after pancreaticoduodenectomy for pancreatic adenocarcinoma: preliminary experience and implications for patient care. *Radiology*. (2016) 281:816–25. doi: 10.1148/radiol.2016152790
571. Schorn S, Demir IE, Haller B, Scheufele F, Reyes CM, Tieftrunk E, et al. The influence of neural invasion on survival and tumor recurrence in pancreatic ductal adenocarcinoma - A systematic review and meta-analysis. *Surg Oncol.* (2017) 26:105–15. doi: 10.1016/j.suronc.2017.01.007
572. Pour PM, Bell RH, Batra SK. Neural invasion in the staging of pancreatic cancer. *Pancreas*. (2003) 26:322–5. doi: 10.1097/00006676-200305000-00002
573. Liebig C, Ayala G, Wilks JA, Berger DH, Albo D. Perineural invasion in cancer: a review of the literature. *Cancer*. (2009) 115:3379–91. doi: 10.1002/cncr.24396
574. Chang A, Kim-Fuchs C, Le CP, Hollande F, Sloan EK. Neural regulation of pancreatic cancer: a novel target for intervention. *Cancers*. (2015) 7:1292–312. doi: 10.3390/cancers7030838
575. Amit M, Na'Ara S, Gil Z. Mechanisms of cancer dissemination along nerves. *Nat Rev Cancer*. (2016) 16:399–408. doi: 10.1038/nrc.2016.38
576. Liu H, Li X, Xu Q, Lv S, Li J, Ma Q. Role of glial cell line-derived neurotrophic factor in perineural invasion of pancreatic cancer. *Biochim Biophys Acta.* (2012) 1826:112–20. doi: 10.1016/j.bbcan.2012.03.010
577. Farina AR, Cappabianca L, Ruggeri P, Gneo L, Pellegrini C, Fargnoli MC, et al. The oncogenic neurotrophin receptor tropomyosin-related kinase variant, TrkAIII. *J Exp Clin Cancer Res.* (2018) 37:119. doi: 10.1186/s13046-018-0786-3
578. Griffin N, Faulkner S, Jobling P, Hondermarck H. Targeting neurotrophin signaling in cancer: the renaissance. *Pharmacol Res.* (2018) 135:12–17. doi: 10.1016/j.phrs.2018.07.019
579. Wislet S, Vandervelden G, Rogister B. From neural crest development to cancer and vice versa: how $p75_{NTR}$ and (Pro)neurotrophins could act on cell migration and invasion? *Front Mol Neurosci.* (2018) 11:244. doi: 10.3389/fnmol.2018.00244
580. Magnon C, Hall SJ, Lin J, Xue X, Gerber L, Freedland SJ, Frenette PS. Autonomic nerve development contributes to prostate cancer progression. *Science*. (2013) 341:1236361. doi: 10.1126/science.1236361
581. Gil Z, Cavel O, Kelly K, Brader P, Rein A, Gao SP, et al. Paracrine regulation of pancreatic cancer cell invasion by peripheral nerves. *J Natl Cancer Inst*. (2010) 102:107–18. doi: 10.1093/jnci/djp456
582. Fielder GC, Yang TW, Razdan M, Li Y, Lu J, Perry JK, et al. The GDNF family: a role in cancer? *Neoplasia*. (2018) 20:99–117. doi: 10.1016/j.neo.2017.10.010
583. Ceyhan GO, Schäfer KH, Kerscher AG, Rauch U, Demir IE, Kadihasanoglu M, et al. Nerve growth factor and artemin are paracrine mediators of pancreatic neuropathy in pancreatic adenocarcinoma. *Ann Surg.* (2010) 251:923–31. doi: 10.1097/SLA.0b013e3181d974d4

584. Okada Y, Eibl G, Duffy JP, Reber HA, Hines OJ. Glial cell-derived neurotrophic factor upregulates the expression and activation of matrix metalloproteinase-9 in human pancreatic cancer. *Surgery*. (2003) 134:293–9. doi: 10.1067/msy.2003.239
585. Veit C, Genze F, Menke A, Hoeffert S, Gress TM, Gierschik P, et al. Activation of phosphatidylinositol 3-kinase and extracellular signal-regulated kinase is required for glial cell line-derived neurotrophic factor-induced migration and invasion of pancreatic carcinoma cells. *Cancer Res.* (2004) 64:5291–300. doi: 10.1158/0008-5472.CAN-04-1112
586. Takahashi H, Funahashi H, Sawai H, Sakamoto M, Matsuo Y, Yamamoto M, et al. Glial cell line-derived neurotrophic factor enhances nuclear factor-kappaB activity and invasive potential in human pancreatic cancer cells. *Pancreas*. (2004) 29:22–7. doi: 10.1097/00006676-200407000-00051
587. Saloman JL, Singhi AD, Hartman DJ, Normolle DP, Albers KM, Davis BM. systemic depletion of nerve growth factor inhibits disease progression in a genetically engineered model of pancreatic ductal adenocarcinoma. *Pancreas*. (2018) 47:856–63. doi: 10.1097/MPA.0000000000001090
588. Xu Q, Wang Z, Chen X, Duan W, Lei J, Zong L, et al. Stromal-derived factor-1α/CXCL12-CXCR4 chemotactic pathway promotes perineural invasion in pancreatic cancer. *Oncotarget*. (2015) 6:4717–32. doi: 10.18632/oncotarget.3069
589. Wang J, Wang H, Cai J, Du S, Xin B, Wei W, et al. Artemin regulates CXCR4 expression to induce migration and invasion in pancreatic cancer cells through activation of NF-κB signaling. *Exp Cell Res.* (2018) 365:12–23. doi: 10.1016/j.yexcr.2018.02.008
590. Saloman JL, Albers KM, Li D, Hartman DJ, Crawford HC, Muha EA, et al. Ablation of sensory neurons in a genetic model of pancreatic ductal adenocarcinoma slows initiation and progression of cancer. *Proc Natl Acad Sci USA*. (2016) 113:3078–83. doi: 10.1073/pnas.1512603113
591. Xu X, Zhao Z, Guo S, Li J, Liu S, You Y, et al. Increased semaphorin 3c expression promotes tumor growth and metastasis in pancreatic ductal adenocarcinoma by activating the ERK1/2 signaling pathway. *Cancer Lett*. (2017) 397:12–22. doi: 10.1016/j.canlet.2017.03.014
592. Foley K, Rucki AA, Xiao Q, Zhou D, Leubner A, Mo G, et al. Semaphorin 3D autocrine signaling mediates the metastatic role of annexin A2 in pancreatic cancer. *Sci Signal.* (2015) 8:ra77. doi: 10.1126/scisignal.aaa5823
593. Jurcak NR, Rucki AA, Muth S, Thompson E, Sharma R, Ding D, et al. Axon guidance molecules promote perineural invasion and metastasis of orthotopic pancreatic tumors in mice. *Gastroenterology*. (2019) 157:838–50.e6. doi: 10.1053/j.gastro.2019.05.065
594. Sabbatini ME, Villagra A, Davio CA, Vatta MS, Fernandez BE, Bianciotti LG. Atrial natriuretic factor stimulates exocrine pancreatic secretion in the rat through NPR-C receptors. *Am J Physiol Gastrointest Liver Physiol*. (2003) 285:G929–37. doi: 10.1152/ajpgi.00010.2003
595. Rossi J, Santamäki P, Airaksinen MS, Herzig KH. Parasympathetic innervation and function of endocrine pancreas requires the glial cell line-derived factor family receptor alpha2 (GFRalpha2). *Diabetes*. (2005) 54:1324–30. doi: 10.2337/diabetes.54.5.1324
596. Haas SL, Fitzner B, Jaster R, Wiercinska E, Gaitantzi H, Jesnowski R, et al. Transforming growth factor-beta induces nerve growth factor expression in pancreatic stellate cells by activation of the ALK-5 pathway. *Growth Factors.* (2009) 27:289–99. doi: 10.1080/08977190903132273
597. Gasparini G, Pellegatta M, Crippa S, Lena MS, Belfiori G, Doglioni C, et al. Nerves and pancreatic cancer: new insights into a dangerous relationship. *Cancers*. (2019) 11:E893. doi: 10.3390/cancers11070893
598. Al-Wadei HA, Ullah MF, Al-Wadei M. GABA (γ-aminobutyric acid), a non-protein amino acid counters the β-adrenergic cascade-activated oncogenic signaling in pancreatic cancer: a review of experimental evidence. *Mol Nutr Food Res.* (2011) 55:1745–58. doi: 10.1002/mnfr.201100229
599. Lin X, Luo K, Lv Z, Huang J. Beta-adrenoceptor action on pancreatic cancer cell proliferation and tumor growth in mice. *Hepatogastroenterology*. (2012) 59:584–8.
600. Shan T, Ma J, Ma Q, Guo K, Guo J, Li X, et al. β2-AR-HIF-1α: a novel regulatory axis for stress-induced pancreatic tumor growth and angiogenesis. *Curr Mol Med.* (2013) 13:1023–34. doi: 10.2174/15665240113139990055
601. Lucki A, Klein E, Karry R, Ben-Shachar D. Dexamethasone in the presence of desipramine enhances MAPK/ERK1/2 signaling possibly via its interference with β-arrestin. *J Neural Transm*. (2014) 121:289–98. doi: 10.1007/s00702-013-1099-5
602. Nan L, Qin T, Xiao Y, Qian W, Li J, Wang Z, et al. Pancreatic stellate cells facilitate perineural invasion of pancreatic cancer via HGF/c-Met pathway. *Cell Transplant*. (2019) 28:1289–98. doi: 10.1177/0963689719851772
603. Demir IE, Ceyhan GO, Rauch U, Altintas B, Klotz M, Müller MW, et al. The microenvironment in chronic pancreatitis and pancreatic cancer induces neuronal plasticity. *Neurogastroenterol Motil*. (2010) 22:480–90. doi: 10.1111/j.1365-2982.2009.01428.x
604. Zeng L, Guo Y, Liang J, Chen S, Peng P, Zhang Q, et al. Perineural invasion and TAMs in pancreatic ductal adenocarcinomas: review of the original pathology reports using immunohistochemical enhancement and relationships with clinicopathological features. *J Cancer*. (2014) 5:754–60. doi: 10.7150/jca.10238
605. Cavel O, Shomron O, Shabtay A, Vital J, Trejo-Leider L, Weizman N, et al. Endoneurial macrophages induce perineural invasion of pancreatic cancer cells by secretion of GDNF and activation of RET tyrosine kinase receptor. *Cancer Res.* (2012) 72:5733–43. doi: 10.1158/0008-5472.CAN-12-0764
606. Swanson BJ, McDermott KM, Singh PK, Eggers JP, Crocker PR, Hollingsworth MA. MUC1 is a counter-receptor for myelin-associated glycoprotein (Siglec-4a) and their interaction contributes to adhesion in pancreatic cancer perineural invasion. *Cancer Res.* (2007) 67:10222–9. doi: 10.1158/0008-5472.CAN-06-2483
607. Stolt CC, Wegner M. Schwann cells and their transcriptional network: evolution of key regulators of peripheral myelination. *Brain Res*. (2016) 1641:101–10. doi: 10.1016/j.brainres.2015.09.025
608. Demir IE, Boldis A, Pfitzinger PL, Teller S, Brunner E, Klose N, et al. Investigation of Schwann cells at neoplastic cell sites before the onset of cancer invasion. *J Natl Cancer Inst*. (2014) 106:dju184. doi: 10.1093/jnci/dju184
609. Madeo M, Colbert PL, Vermeer DW, Lucido CT, Cain JT, Vichaya EG, et al. Cancer exosomes induce tumor innervation. *Nat Commun*. (2018) 9:4284. doi: 10.1038/s41467-018-06640-0
610. Vermeer PD. Exosomal induction of tumor innervation. *Cancer Res.* (2019) 79:3529–35. doi: 10.1158/0008-5472.CAN-18-3995
611. Lucido CT, Wynja E, Madeo M, Williamson CS, Schwartz LE, Imblum BA, et al. Innervation of cervical carcinoma is mediated by cancer-derived exosomes. *Gynecol Oncol.* (2019) 154:228–35. doi: 10.1016/j.ygyno.2019.04.651
612. Zhang Z, Yan C, Li B, Li L. Potential biological functions of microvesicles derived from adenoid cystic carcinoma. *Oncol Lett.* (2018) 15:7900–8.
613. Ohta T, Elnemr A, Kitagawa H, Kayahara M, Takamura H, Fujimura T, et al. Fas ligand expression in human pancreatic cancer. *Oncol Rep*. (2004) 12:749–54. doi: 10.3892/or.12.4.749
614. Budnik V, Ruiz-Cañada C, Wendler F. Extracellular vesicles round off communication in the nervous system. *Nat Rev Neurosci*. (2016) 17:160–72. doi: 10.1038/nrn.2015.29
615. Fruhbeis C, Fröhlich D, Kuo WP, Amphornrat J, Thilemann S, Saab AS, et al. Neurotransmitter-triggered transfer of exosomes mediates oligodendrocyte–neuron communication. *PLoS Biol.* (2013) 11:e1001604. doi: 10.1371/journal.pbio.1001604
616. Chivet M, Javalet C, Laulagnier K, Blot B, Hemming FJ, Sadoul R. Exosomes secreted by cortical neurons upon glutamatergic synapse activation specifically interact with neurons. *J Extracell Vesicles*. (2014) 3:24722. doi: 10.3402/jev.v3.24722
617. Bianco F, Pravettoni E, Colombo A, Schenk U, Möller T, Matteoli M, et al. Astrocyte-derived ATP induces vesicle shedding and IL-1β release from microglia. *J Immunol.* (2005) 174:7268–77. doi: 10.4049/jimmunol.174.11.7268
618. Antonucci F, Turola E, Riganti L, Caleo M, Gabrielli M, Perrotta C, et al. Microvesicles released from microglia stimulate synaptic activity via enhanced sphingolipid metabolism. *EMBO J.* (2012) 31:1231–40. doi: 10.1038/emboj.2011.489
619. Lopez-Verrilli MA, Court FA. Transfer of vesicles from schwann cells to axons: a novel mechanism of communication in the peripheral nervous system. *Front Physiol*. (2012) 3:205. doi: 10.3389/fphys.2012.00205

620. André-Grégoire G, Gavard J. Spitting out the demons: extracellular vesicles in glioblastoma. *Cell Adh Migr*. (2017) 11:164–72. doi: 10.1080/19336918.2016.1247145
621. Seufferlein T, Hammel P, Delpero JR, Macarulla T, Pfeiffer P, Prager GW, et al. Optimizing the management of locally advanced pancreatic cancer with a focus on induction chemotherapy: expert opinion based on a review of current evidence. *Cancer Treat Rev*. (2019) 77:1–10. doi: 10.1016/j.ctrv.2019.05.007
622. Springfeld C, Jäger D, Büchler MW, Strobel O, Hackert T, Palmer DH, et al. Chemotherapy for pancreatic cancer. *Presse Med*. (2019) 48(3 Pt 2):e159–74. doi: 10.1016/j.lpm.2019.02.025
623. Boldrini L, Cusumano D, Cellini F, Azario L, Mattiucci GC, Valentini V. Online adaptive magnetic resonance guided radiotherapy for pancreatic cancer: state of the art, pearls and pitfalls. *Radiat Oncol*. (2019) 14:71. doi: 10.1186/s13014-019-1275-3
624. Alcántara-Hernández R, Hernández-Méndez A. Adrenergic signaling molecular complexes. *Gac Med Mex*. (2018) 154:223–35. doi: 10.24875/GMM.M18000135
625. Chang JH, Jiang Y, Pillarisetty VG. Role of immune cells in pancreatic cancer from bench to clinical application: an updated review. *Medicine*. (2016) 95:e5541. doi: 10.1097/MD.0000000000005541
626. Ino Y, Yamazaki-Itoh R, Shimada K, Iwasaki M, Kosuge T, Kanai Y, et al. Immune cell infiltration as an indicator of the immune microenvironment of pancreatic cancer. *Br J Cancer*. (2013) 108:914–23. doi: 10.1038/bjc.2013.32
627. Chen ML, Pittet MJ, Gorelik L, Flavell RA, Weissleder R, von Boehmer H, et al. Regulatory T cells suppress tumor-specific CD8 T cell cytotoxicity through TGF-beta signals *in vivo*. *Proc Natl Acad Sci USA*. (2005) 102:419–24. doi: 10.1073/pnas.0408197102
628. Sinha P, Clements VK, Ostrand-Rosenberg S. Interleukin-13-regulated M2 macrophages in combination with myeloid suppressor cells block immune surveillance against metastasis. *Cancer Res*. (2005) 65:11743–51. doi: 10.1158/0008-5472.CAN-05-0045
629. Soares KC, Rucki AA, Wu AA, Olino K, Xiao Q, Chai Y, et al. PD-1/PD-L1 blockade together with vaccine therapy facilitates effector T-cell infiltration into pancreatic tumors. *J Immunother*. (2015) 38:1–11. doi: 10.1097/CJI.0000000000000062
630. Van Audenaerde JRM, Roeyen G, Darcy PK, Kershaw MH, Peeters M, Smits ELJ. Natural killer cells and their therapeutic role in pancreatic cancer: a systematic review. *Pharmacol Ther*. (2018) 189:31–44. doi: 10.1016/j.pharmthera.2018.04.003
631. Davis M, Conlon K, Bohac GC, Barcenas J, Leslie W, Watkins L, et al. Effect of pemetrexed on innate immune killer cells and adaptive immune T cells in subjects with adenocarcinoma of the pancreas. *J Immunother*. (2012) 35:629–40. doi: 10.1097/CJI.0b013e31826c8a4f
632. Ene-Obong A, Clear AJ, Watt J, Wang J, Fatah R, Riches JC, et al. Activated pancreatic stellate cells sequester CD8+ T cells to reduce their infiltration of the juxtatumoral compartment of pancreatic ductal adenocarcinoma. *Gastroenterology*. (2013) 145:1121–32. doi: 10.1053/j.gastro.2013.07.025
633. Peng YP, Zhu Y, Zhang JJ, Xu ZK, Qian ZY, Dai CC, et al. Comprehensive analysis of the percentage of surface receptors and cytotoxic granules positive natural killer cells in patients with pancreatic cancer, gastric cancer, and colorectal cancer. *J Transl Med*. (2013) 11:262. doi: 10.1186/1479-5876-11-262
634. Wensveen FM, Jelenčić V, Polić B. NKG2D: a master regulator of immune cell responsiveness. *Front Immunol*. (2018) 9:441. doi: 10.3389/fimmu.2018.00441
635. Paul S, Lal G. The molecular mechanism of natural killer cells function and its importance in cancer immunotherapy. *Front Immunol*. (2017) 8:1124. doi: 10.3389/fimmu.2017.01124
636. Peng YP, Zhang JJ, Liang WB, Tu M, Lu ZP, Wei JS, et al. Elevation of MMP-9 and IDO induced by pancreatic cancer cells mediates natural killer cell dysfunction. *BMC Cancer*. (2014) 14:738. doi: 10.1186/1471-2407-14-738
637. Husain Z, Huang Y, Seth P, Sukhatme VP. Tumor-derived lactate modifies antitumor immune response: effect on myeloid-derived suppressor cells and NK cells. *J Immunol*. (2013) 191:1486–95. doi: 10.4049/jimmunol.1202702
638. Blake SJ, Dougall WC, Miles JJ, Teng MW, Smyth MJ. Molecular pathways: targeting CD96 and TIGIT for cancer immunotherapy. *Clin Cancer Res*. (2016) 22:5183–8. doi: 10.1158/1078-0432.CCR-16-0933
639. Peng YP, Xi CH, Zhu Y, Yin LD, Wei JS, Zhang JJ, et al. Altered expression of CD226 and CD96 on natural killer cells in patients with pancreatic cancer. *Oncotarget*. (2016) 7:66586–94. doi: 10.18632/oncotarget.11953
640. Van Audenaerde JRM, De Waele J, Marcq E, Van Loenhout J, Lion E, Van den Bergh JMJ, et al. Interleukin-15 stimulates natural killer cell-mediated killing of both human pancreatic cancer and stellate cells. *Oncotarget*. (2017) 8:56968–79. doi: 10.18632/oncotarget.18185
641. Lu Y, Hu J, Sun W, Duan X, Chen X. Hypoxia-mediated immune evasion of pancreatic carcinoma cells. *Mol Med Rep*. (2015) 11:3666–72. doi: 10.3892/mmr.2015.3144
642. Huang Q, Huang M, Meng F, Sun R. Activated pancreatic stellate cells inhibit NK cell function in the human pancreatic cancer microenvironment. *Cell Mol Immunol*. (2019) 16:87–9. doi: 10.1038/s41423-018-0014-2
643. Ames E, Canter RJ, Grossenbacher SK, Mac S, Chen M, Smith RC, et al. NK cells preferentially target tumor cells with a cancer stem cell phenotype. *J Immunol*. (2015) 195:4010–9. doi: 10.4049/jimmunol.1500447
644. Herberman RB, Holden HT, Ting CC, Lavrin DL, Kirchner H. Cell-mediated immunity to leukemia virus- and tumor-associated antigens in mice. *Cancer Res*. (1976) 36:615–21.
645. Aya T, Matsuo T, Takada K, Osato T, Mizuno F. Antibody-dependent autologous lymphocyte cytotoxicity against cells freshly transformed by Epstein-Barr virus. *IARC Sci Publ*. (1978) 24:711–9.
646. Karnevi E, Andersson R, Rosendahl AH. Tumour-educated macrophages display a mixed polarisation and enhance pancreatic cancer cell invasion. *Immunol Cell Biol*. (2014) 92:543–52. doi: 10.1038/icb.2014.22
647. Bailey P, Chang DK, Nones K, Johns AL, Patch AM, Gingras MC, et al. Genomic analyses identify molecular subtypes of pancreatic cancer. *Nature*. (2016) 531:47–52. doi: 10.1038/nature16965
648. Knudsen ES, Vail P, Balaji U, Ngo H, Botros IW, Makarov V, et al. Stratification of pancreatic ductal adenocarcinoma: combinatorial genetic, stromal, and immunologic markers. *Clin Cancer Res*. (2017) 23:4429–40. doi: 10.1158/1078-0432.CCR-17-0162
649. Candido JB, Morton JP, Bailey P, Campbell AD, Karim SA, Jamieson T, et al. CSF1R+macrophages sustain pancreatic tumor growth through T cell suppression and maintenance of key gene programs that define the squamous subtype. *Cell Rep*. (2018) 23:1448–60. doi: 10.1016/j.celrep.2018.03.131
650. Barros MH, Hauck F, Dreyer JH, Kempkes B, Niedobitek G. Macrophage polarisation: an immunohistochemical approach for identifying M1 and M2 macrophages. *PLoS ONE*. (2013) 8:e80908. doi: 10.1371/journal.pone.0080908
651. Attri KS, Mehla K, Singh PK. Evaluation of macrophage polarization in pancreatic cancer microenvironment under hypoxia. *Methods Mol Biol*. (2018) 1742:265–76. doi: 10.1007/978-1-4939-7665-2_23
652. Sun W, Wei FQ, Li WJ, Wei JW, Zhong H, Wen YH, et al. A positive-feedback loop between tumour infiltrating activated Treg cells and type 2-skewed macrophages is essential for progression of laryngeal squamous cell carcinoma. *Br J Cancer*. (2017) 117:1631–43. doi: 10.1038/bjc.2017.329
653. Ginhoux F, Schultze JL, Murray PJ, Ochando J, Biswas SK. New insights into the multidimensional concept of macrophage ontogeny, activation and function. *Nat Immunol*. (2016) 17:34–40. doi: 10.1038/ni.3324
654. Jones KI, Tiersma J, Yuzhalin AE, Gordon-Weeks AN, Buzzelli J, Im JH, et al. Radiation combined with macrophage depletion promotes adaptive immunity and potentiates checkpoint blockade. *EMBO Mol Med*. (2018) 10:e9342. doi: 10.15252/emmm.201809342
655. Kimsey TF, Campbell AS, Albo D, Wilson M, Wang TN. Co-localization of macrophage inflammatory protein-3alpha (Mip-3alpha) and its receptor, CCR6, promotes pancreatic cancer cell invasion. *Cancer J*. (2004) 10:374–80. doi: 10.1097/00130404-200411000-00007
656. Lee S, Lee E, Ko E, Ham M, Lee HM, Kim ES, et al. Tumor-associated macrophages secrete CCL2 and induce the invasive phenotype of human breast epithelial cells through upregulation of ERO1-α and MMP-9. *Cancer Lett*. (2018) 437:25–34. doi: 10.1016/j.canlet.2018.08.025
657. Liu CY, Xu JY, Shi XY, Huang W, Ruan TY, Xie P, et al. M2-polarized tumor-associated macrophages promoted epithelial-mesenchymal transition in pancreatic cancer cells, partially through TLR4/IL-10 signaling pathway. *Lab Invest*. (2013) 93:844–54. doi: 10.1038/labinvest.2013.69

658. Helm O, Held-Feindt J, Grage-Griebenow E, Reiling N, Ungefroren H, Vogel I, et al. Tumor-associated macrophages exhibit pro- and anti-inflammatory properties by which they impact on pancreatic tumorigenesis. *Int J Cancer*. (2014) 135:843–61. doi: 10.1002/ijc.28736
659. Arnold JN, Magiera L, Kraman M, Fearon DT. Tumoral immune suppression by macrophages expressing fibroblast activation protein-α and heme oxygenase-1. *Cancer Immunol Res.* (2014) 2:121–6. doi: 10.1158/2326-6066.CIR-13-0150
660. Weizman N, Krelin Y, Shabtay-Orbach A, Amit M, Binenbaum Y, Wong RJ, et al. Macrophages mediate gemcitabine resistance of pancreatic adenocarcinoma by upregulating cytidine deaminase. *Oncogene*. (2014) 33:3812–9. doi: 10.1038/onc.2013.357
661. Najafi M, Hashemi Goradel N, Farhood B, Salehi E, Nashtaei MS, Khanlarkhani N, et al. Macrophage polarity in cancer: a review. *J Cell Biochem*. (2019) 120:2756–65. doi: 10.1002/jcb.27646
662. Yu M, Guan R, Hong W, Zhou Y, Lin Y, Jin H, et al. Prognostic value of tumor-associated macrophages in pancreatic cancer: a meta-analysis. *Cancer Manag Res*. (2019) 11:4041–58. doi: 10.2147/CMAR.S196951
663. Talmadge JE, Gabrilovich DI. History of myeloid-derived suppressor cells. *Nat Rev Cancer*. (2013) 13:739–52. doi: 10.1038/nrc3581
664. Zhao Y, Wu T, Shao S, Shi B, Zhao Y. Phenotype, development, and biological function of myeloid-derived suppressor cells. *Oncoimmunology*. (2015) 5:e1004983. doi: 10.1080/2162402X.2015.1004983
665. Bronte V, Brandau S, Chen SH, Colombo MP, Frey AB, Greten TF, et al. Recommendations for myeloid-derived suppressor cell nomenclature and characterization standards. *Nat Commun.* (2016) 7:12150. doi: 10.1038/ncomms12150
666. Clark CE, Hingorani SR, Mick R, Combs C, Tuveson DA, Vonderheide RH. Dynamics of the immune reaction to pancreatic cancer from inception to invasion. *Cancer Res*. (2007) 67:9518–27. doi: 10.1158/0008-5472.CAN-07-0175
667. Bayne LJ, Beatty GL, Jhala N, Clark CE, Rhim AD, Stanger BZ, et al. Tumor-derived granulocyte-macrophage colony-stimulating factor regulates myeloid inflammation and T cell immunity in pancreatic cancer. *Cancer Cell*. (2012) 21:822–35. doi: 10.1016/j.ccr.2012.04.025
668. Boros P, Ochando J, Zeher M. Myeloid derived suppressor cells and autoimmunity. *Hum Immunol.* (2016) 77:631–6. doi: 10.1016/j.humimm.2016.05.024
669. Chen W, Jiang J, Xia W, Huang J. Tumor-related exosomes contribute to tumor-promoting microenvironment: an immunological perspective. *J Immunol Res*. (2017) 2017:1073947. doi: 10.1155/2017/1073947
670. Condamine T, Gabrilovich DI. Molecular mechanisms regulating myeloid-derived suppressor cell differentiation and function. *Trends Immunol*. (2011) 32:19–25. doi: 10.1016/j.it.2010.10.002
671. Trikha P, Carson WE 3rd. Signaling pathways involved in MDSC regulation. *Biochim Biophys Acta.* (2014) 1846:55–65. doi: 10.1016/j.bbcan.2014.04.003
672. Draghiciu O, Lubbers J, Nijman HW, Daemen T. Myeloid derived suppressor cells-An overview of combat strategies to increase immunotherapy efficacy. *Oncoimmunology*. (2015) 4:e954829. doi: 10.4161/21624011.2014.954829
673. Shi H, Dong G, Yan F, Zhang H, Li C, Ma Q, et al. Arctigenin ameliorates inflammation by regulating accumulation and functional activity of MDSCs in endotoxin shock. *Inflammation*. (2018) 41:2090–100. doi: 10.1007/s10753-018-0852-1
674. Chen J, Ye Y, Liu P, Yu W, Wei F, Li H, et al. Suppression of T cells by myeloid-derived suppressor cells in cancer. *Hum Immunol.* (2017) 78:113–9. doi: 10.1016/j.humimm.2016.12.001
675. Li H, Han Y, Guo Q, Zhang M, Cao X. Cancer-expanded myeloid-derived suppressor cells induce anergy of NK cells through membrane-bound TGF-beta 1. *J Immunol*. (2009) 182:240–9. doi: 10.4049/jimmunol.182.1.240
676. Hatziioannou A, Alissafi T, Verginis P. Myeloid-derived suppressor cells and T regulatory cells in tumors: unraveling the dark side of the force. *J Leukoc Biol.* (2017) 102:407–21. doi: 10.1189/jlb.5VMR1116-493R
677. Ren JP, Zhao J, Dai J, Griffin JW, Wang L, Wu XY, et al. Hepatitis C virus-induced myeloid-derived suppressor cells regulate T-cell differentiation and function via the signal transducer and activator of transcription 3 pathway. *Immunology*. (2016) 148:377–86. doi: 10.1111/imm.12616
678. Roussel M, Ferrell PB Jr, Greenplate AR, Lhomme F, Le Gallou S, Diggins KE, et al. Mass cytometry deep phenotyping of human mononuclear phagocytes and myeloid-derived suppressor cells from human blood and bone marrow. *J Leukoc Biol.* (2017) 102:437–47. doi: 10.1189/jlb.5MA1116-457R
679. Chauhan S, Danielson S, Clements V, Edwards N, Ostrand-Rosenberg S, Fenselau C. Surface glycoproteins of exosomes shed by myeloid-derived suppressor cells contribute to function. *J Proteome Res.* (2017) 16:238–46. doi: 10.1021/acs.jproteome.6b00811
680. Geis-Asteggiante L, Belew AT, Clements VK, Edwards NJ, Ostrand-Rosenberg S, El-Sayed NM, et al. Differential content of proteins, mRNAs, and miRNAs suggests that MDSC and their exosomes may mediate distinct immune suppressive functions. *J Proteome Res.* (2018) 17:486–98. doi: 10.1021/acs.jproteome.7b00646
681. Zöller M. Janus-faced myeloid-derived suppressor cell exosomes for the good and the bad in cancer and autoimmune disease. *Front Immunol*. (2018) 9:137. doi: 10.3389/fimmu.2018.00137
682. Roussel M, Irish JM, Menard C, Lhomme F, Tarte K, Fest T. Regulatory myeloid cells: an underexplored continent in B-cell lymphomas. *Cancer Immunol Immunother*. (2017) 66:1103–11. doi: 10.1007/s00262-017-2036-5
683. Pergamo M, Miller G. Myeloid-derived suppressor cells and their role in pancreatic cancer. *Cancer Gene Ther*. (2017) 24:100–5. doi: 10.1038/cgt.2016.65
684. Wang Z, Liu Y, Zhang Y, Shang Y, Gao Q. MDSC-decreasing chemotherapy increases the efficacy of cytokine-induced killer cell immunotherapy in metastatic renal cell carcinoma and pancreatic cancer. *Oncotarget*. (2016) 7:4760–9. doi: 10.18632/oncotarget.6734
685. Amigorena S, Savina A. Intracellular mechanisms of antigen cross presentation in dendritic cells. *Curr Opin Immunol.* (2010) 22:109–17. doi: 10.1016/j.coi.2010.01.022
686. Mellman I. Dendritic cells: master regulators of the immune response. *Cancer Immunol Res*. (2013) 1:145–9. doi: 10.1158/2326-6066.CIR-13-0102
687. Neefjes J, Jongsma ML, Paul P, Bakke O. Towards a systems understanding of MHC class I and MHC class II antigen presentation. *Nat Rev Immunol.* (2011) 11:823–36. doi: 10.1038/nri3084
688. Verboogen DR, Dingjan I, Revelo NH, Visser LJ, ter Beest M, van den Bogaart G. The dendritic cell side of the immunological synapse. *Biomol Concepts.* (2016) 7:17–28. doi: 10.1515/bmc-2015-0028
689. Ugur M, Mueller SN. T cell and dendritic cell interactions in lymphoid organs: more than just being in the right place at the right time. *Immunol Rev*. (2019) 289:115–28. doi: 10.1111/imr.12753
690. Gardner A, Ruffell B. Dendritic cells and cancer immunity. *Trends Immunol.* (2016) 37:855–65. doi: 10.1016/j.it.2016.09.006
691. Bandola-Simon J, Roche PA. Dysfunction of antigen processing and presentation by dendritic cells in cancer. *Mol Immunol.* (2019) 113:31–7. doi: 10.1016/j.molimm.2018.03.025
692. Dallal RM, Christakos P, Lee K, Egawa S, Son YI, Lotze MT. Paucity of dendritic cells in pancreatic cancer. *Surgery*. (2002) 131:135–8. doi: 10.1067/msy.2002.119937
693. Wang T, Niu G, Kortylewski M, Burdelya L, Shain K, Zhang S, et al. Regulation of the innate and adaptive immune responses by Stat-3 signaling in tumor cells. *Nat Med.* (2004) 10:48–54. doi: 10.1038/nm976
694. Gabrilovich D. Mechanisms and functional significance of tumour-induced dendritic-cell defects. *Nat Rev Immunol.* (2004) 4:941–52. doi: 10.1038/nri1498
695. Bharadwaj U, Li M, Zhang R, Chen C, Yao Q. Elevated interleukin-6 and G-CSF in human pancreatic cancer cell conditioned medium suppress dendritic cell differentiation and activation. *Cancer Res*. (2007) 67:5479–88. doi: 10.1158/0008-5472.CAN-06-3963
696. Bellone G, Carbone A, Smirne C, Scirelli T, Buffolino A, Novarino A, et al. Cooperative induction of a tolerogenic dendritic cell phenotype by cytokines secreted by pancreatic carcinoma cells. *J Immunol.* (2006) 177:3448–60. doi: 10.4049/jimmunol.177.5.3448

697. Wiedemann GM, Knott MM, Vetter VK, Rapp M, Haubner S, Fesseler J, et al. Cancer cell-derived IL-1α induces CCL22 and the recruitment of regulatory T cells. *Oncoimmunology*. (2016) 5:e1175794. doi: 10.1080/2162402X.2016.1175794
698. Ghiringhelli F, Puig PE, Roux S, Parcellier A, Schmitt E, Solary E, et al. Tumor cells convert immature myeloid dendritic cells into TGF-beta-secreting cells inducing CD4+ CD25+ regulatory T cell proliferation. *J Exp Med*. (2005) 202:919–29. doi: 10.1084/jem.20050463
699. Murgaski A, Bardet PMR, Arnouk SM, Clappaert EJ, Laoui D. Unleashing tumour-dendritic cells to fight cancer by tackling their three A's: abundance, activation and antigen-delivery. *Cancers*. (2019) 11:E670. doi: 10.3390/cancers11050670
700. Deicher A, Andersson R, Tingstedt B, Lindell G, Bauden M, Ansari D. Targeting dendritic cells in pancreatic ductal adenocarcinoma. *Cancer Cell Int*. (2018) 18:85. doi: 10.1186/s12935-018-0585-0
701. Xiao L, Erb U, Zhao K, Hackert T, Zöller M. Efficacy of vaccination with tumor-exosome loaded dendritic cells combined with cytotoxic drug treatment in pancreatic cancer. *Oncoimmunology*. (2017) 6:e1319044. doi: 10.1080/2162402X.2017.1319044
702. Zitvogel L, Regnault A, Lozier A, Wolfers J, Flament C, Tenza D, et al. Eradication of established murine tumors using a novel cell-free vaccine: dendritic cell-derived exosomes. *Nat Med*. (1998) 4:594–600. doi: 10.1038/nm0598-594
703. Shenoda BB, Ajit SK. Modulation of immune responses by exosomes derived from antigen-presenting cells. *Clin Med Insights Pathol*. (2016) 9(Suppl. 1):1–8. doi: 10.4137/CPath.S39925
704. Tkach M, Kowal J, Zucchetti AE, Enserink L, Jouve M, Lankar D, et al. Qualitative differences in T-cell activation by dendritic cell-derived extracellular vesicle subtypes. *EMBO J*. (2017) 36:3012–28. doi: 10.15252/embj.201696003
705. Lindenbergh MFS, Stoorvogel W. Antigen presentation by extracellular vesicles from professional antigen-presenting cells. *Annu Rev Immunol*. (2018) 36:435–59. doi: 10.1146/annurev-immunol-041015-055700
706. Helm O, Mennrich R, Petrick D, Goebel L, Freitag-Wolf S, Röder C, et al. Comparative characterization of stroma cells and ductal epithelium in chronic pancreatitis and pancreatic ductal adenocarcinoma. *PLoS ONE*. (2014) 9:e94357. doi: 10.1371/journal.pone.0094357
707. Fogar P, Basso D, Fadi E, Greco E, Pantano G, Padoan A, et al. Pancreatic cancer alters human CD4+ T lymphocyte function: a piece in the immune evasion puzzle. *Pancreas*. (2011) 40:1131–7. doi: 10.1097/MPA.0b013e31822077b8
708. Suzuki D, Furukawa K, Kimura F, Shimizu H, Yoshidome H, Ohtsuka M, et al. Effects of perioperative immunonutrition on cell-mediated immunity, T helper type 1 (Th1)/Th2 differentiation, and Th17 response after pancreaticoduodenectomy. *Surgery*. (2010) 148:573–81. doi: 10.1016/j.surg.2010.01.017
709. Pu N, Zhao G, Gao S, Cui Y, Xu Y, Lv Y, et al. Neutralizing TGF-β promotes anti-tumor immunity of dendritic cells against pancreatic cancer by regulating T lymphocytes. *Cent Eur J Immunol*. (2018) 43:123–31. doi: 10.5114/ceji.2018.77381
710. De Monte L, Reni M, Tassi E, Clavenna D, Papa I, Recalde H, et al. Intratumor T helper type 2 cell infiltrate correlates with cancer-associated fibroblast thymic stromal lymphopoietin production and reduced survival in pancreatic cancer. *J Exp Med*. (2011) 208:469–78. doi: 10.1084/jem.20101876
711. Piro G, Simionato F, Carbone C, Frizziero M, Malleo G, Zanini S, et al. A circulating TH2 cytokines profile predicts survival in patients with resectable pancreaticadenocarcinoma. *Oncoimmunology*. (2017) 6:e1322242. doi: 10.1080/2162402X.2017.1322242
712. Trapani JA. The dual adverse effects of TGF-beta secretion on tumor progression. *Cancer Cell*. (2005) 8:349–50. doi: 10.1016/j.ccr.2005.10.018
713. Thomas DA, Massague J. TGF-beta directly targets cytotoxic T cell functions during tumor evasion of immune surveillance. *Cancer Cell*. (2005) 8:369–80. doi: 10.1016/j.ccr.2005.10.012
714. Dong H, Strome SE, Salomao DR, Tamura H, Hirano F, Flies DB, et al. Tumor-associated B7-H1 promotes T-cell apoptosis: a potential mechanism of immune evasion. *Nat Med*. (2002) 8:793–800. doi: 10.1038/nm730
715. Spranger S, Gajewski TF. Impact of oncogenic pathways on evasion of antitumour immune responses. *Nat Rev Cancer*. (2018) 18:139–47. doi: 10.1038/nrc.2017.117
716. Tang D, Yuan Z, Xue X, Lu Z, Zhang Y, Wang H, et al. High expression of Galectin-1 in pancreatic stellate cells plays a role in the development and maintenance of an immunosuppressive microenvironment in pancreatic cancer. *Int J Cancer*. (2012) 130:2337–48. doi: 10.1002/ijc.26290
717. Seicean A, Popa D, Mocan T, Cristea V, Neagoe I. Th1 and Th2 profiles in patients with pancreatic cancer compared with chronic pancreatitis. *Pancreas*. (2009) 38:594–5. doi: 10.1097/MPA.0b013e31819313d0
718. Balachandran VP, Łuksza M, Zhao JN, Makarov V, Moral JA, Remark R, et al. Identifica-tion of unique neoantigen qualities in long-term survivorsof pancreatic cancer. *Nature*. (2017) 551:512–6. doi: 10.1038/nature24462
719. Carstens JL, Correa de Sampaio P, Yang D, Barua S, Wang H, Rao A, et al. Spatial computation of intratumoral T cells correlates with survival of patients with pancreatic cancer. *Nat Commun*. (2017) 8:15095. doi: 10.1038/ncomms15095
720. Fontenot JD, Gavin MA, Rudensky AY. Foxp3 programs the development and function of CD4+CD25+ regulatory T cells. *Nat Immunol*. (2003) 4:330–6. doi: 10.1038/ni904
721. Hori S, Nomura T, Sakaguchi S. Control of regulatory T cell development by the transcription factor Foxp3. *Science*. (2003) 299:1057–61. doi: 10.1126/science.1079490
722. Lo B, Abdel-Motal UM. Lessons from CTLA-4 deficiency and checkpoint inhibition. *Curr Opin Immunol*. (2017) 49:14–19. doi: 10.1016/j.coi.2017.07.014
723. Mitsuiki N, Schwab C, Grimbacher B. What did we learn from CTLA-4 insufficiency on the human immune system? *Immunol Rev*. (2019) 287:33–49. doi: 10.1111/imr.12721
724. Ghiringhelli F, Menard C, Terme M, Flament C, Taieb J, Chaput N, et al. CD4+CD25+ regulatory T cells inhibit natural killer cell functions in a transforming growth factor-beta-dependent manner. *J Exp Med*. (2005) 202:1075–85. doi: 10.1084/jem.20051511
725. Azuma T, Takahashi T, Kunisato A, Azuma T, Takahashi T. Human CD4+ CD25+ regulatory T cells suppress NKT cell functions. *Cancer Res*. (2003) 63:4516–20.
726. Liang B, Workman C, Lee J, Chew C, Dale BM, Colonna L, et al. Regulatory T cells inhibit dendritic cells by lymphocyte activation gene-3 engagement of MHC class II. *J Immunol*. (2008) 180:5916–26. doi: 10.4049/jimmunol.180.9.5916
727. Hiraoka N, Onozato K, Kosuge T, Hirohashi S. Prevalence of FOXP3+ regulatory T cells increases during the progression of pancreatic ductal adenocarcinoma and its premalignant lesions. *Clin Cancer Res*. (2006) 12:5423–34. doi: 10.1158/1078-0432.CCR-06-0369
728. Kobayashi N, Kubota K, Kato S, Watanabe S, Shimamura T, Kirikoshi H, et al. FOXP3+ regulatory T cells and tumoral indoleamine 2,3-dioxygenase expression predicts the carcinogenesis of intraductal papillary mucinous neoplasms of the pancreas. *Pancreatology*. (2010) 10:631–40. doi: 10.1159/000308966
729. Tang Y, Xu X, Guo S, Zhang C, Tang Y, Tian Y, et al. An increased abundance of tumor-infiltrating regulatory T cells is correlated with the progression and prognosis of pancreatic ductal adenocarcinoma. *PLoS ONE*. (2014) 9:e91551. doi: 10.1371/journal.pone.0091551
730. Wartenberg M, Zlobec I, Perren A, Koelzer VH, Lugli A, Karamitopoulou E. Accumulation of FOXP3+T-cells in the tumor microenvironment is associated with an epithelial-mesenchymal-transition-type tumor budding phenotype and is an independent prognostic factor in surgically resected pancreatic ductal adenocarcinoma. *Oncotarget*. (2015) 6:4190–201. doi: 10.18632/oncotarget.2775

731. Amedei A, Niccolai E, Benagiano M, Della Bella C, Cianchi F, Bechi P, et al. Ex vivo analysis of pancreatic cancer-infiltrating T lymphocytes reveals that ENO-specific Tregs accumulate in tumor tissue and inhibit Th1/Th17 effector cell functions. *Cancer Immunol Immunother*. (2013) 62:1249–60. doi: 10.1007/s00262-013-1429-3
732. Tan MC, Goedegebuure PS, Belt BA, Flaherty B, Sankpal N, Gillanders WE, et al. Disruption of CCR5-dependent homing of regulatory T cells inhibits tumor growth in a murine model of pancreatic cancer. *J Immunol.* (2009) 182:1746–55. doi: 10.4049/jimmunol.182.3.1746
733. Facciabene A, Peng X, Hagemann IS, Balint K, Barchetti A, Wang L, et al. Tumour hypoxia promotes tolerance and angiogenesis via CCL28 and T(reg) cells. *Nature.* (2011) 475:226–30. doi: 10.1038/nature10169
734. Nummer D, Suri-Payer E, Schmitz-Winnenthal H, Bonertz A, Galindo L, Antolovich D, et al. Role of tumor endothelium in CD4+ CD25+ regulatory T cell infiltration of human pancreatic carcinoma. *J Natl Cancer Inst.* (2007) 99:1188–99. doi: 10.1093/jnci/djm064
735. Yamamoto T, Yanagimoto H, Satoi S, Toyokawa H, Hirooka S, Yamaki S, et al. Circulating CD4+CD25+ regulatory T cells in patients with pancreatic cancer. *Pancreas.* (2012) 41:409–15. doi: 10.1097/MPA.0b013e3182373a66
736. Gabitass RF, Annels NE, Stocken DD, Pandha HA, Middleton GW. Elevated myeloid-derived suppressor cells in pancreatic, esophageal and gastric cancer are an independent prognostic factor and are associated with significant elevation of the Th2 cytokine interleukin-13. *Cancer Immunol Immunother.* (2011) 60:1419–30. doi: 10.1007/s00262-011-1028-0
737. Roshani R, McCarthy F, Hagemann T. Inflammatory cytokines in human pancreatic cancer. *Cancer Lett.* (2014) 345:157–63. doi: 10.1016/j.canlet.2013.07.014
738. Wörmann SM, Diakopoulos KN, Lesina M, Algül H. The immune network in pancreatic cancer development and progression. *Oncogene.* (2014) 33:2956–67. doi: 10.1038/onc.2013.257
739. Padoan A, Plebani M, Basso D. Inflammation and pancreatic cancer: focus on metabolism, cytokines, and immunity. *Int J Mol Sci.* (2019) 20:E676. doi: 10.3390/ijms20030676
740. Lyssiotis CA, Kimmelman AC. Metabolic interactions in the tumor microenvironment. *Trends Cell Biol.* (2017) 27:863–75. doi: 10.1016/j.tcb.2017.06.003
741. Seifert L, Werba G, Tiwari S, Giao Ly NN, Alothman S, Alqunaibit D, et al. The necrosome promotes pancreatic oncogenesis via CXCL1 and Mincle-induced immune suppression. *Nature.* (2016) 532:245–9. doi: 10.1038/nature17403
742. Beatty GL, O'Dwyer PJ, Clark J, Shi JG, Bowman KJ, Scherle PA, et al. First-in-human phase I study of the oral inhibitor of indoleamine 2,3-dioxygenase-1 epacadostat (INCB024360) in patientswith advanced solid malignancies. *Clin Cancer Res.* (2017) 23:3269–76. doi: 10.1158/1078-0432.CCR-16-2272
743. Labadie BW, Bao R, Luke JJ. Reimagining IDO pathway inhibition in cancer immunotherapy via downstream focus on the Tryptophan-Kynurenine-Aryl hydrocarbon axis. *Clin Cancer Res.* (2019) 25:1462–71. doi: 10.1158/1078-0432.CCR-18-2882
744. Maj T, Wang W, Crespo J, Zhang H, Wang W, Wei S, et al. Oxidative stress controls regulatory T cell apoptosis and suppressor activity and PD-L1-blockade resistance in tumor. *Nat Immunol.* (2017) 18:1332–41. doi: 10.1038/ni.3868
745. Martinez-Bosch N, Vinaixa J, Navarro P. Immune evasion in pancreatic cancer: from mechanisms to therapy. *Cancers.* (2018) 10:E6. doi: 10.3390/cancers10010006
746. Cerliani JP, Blidner AG, Toscano MA, Croci DO, Rabinovich GA. Translating the "Sugar Code" into immune and vascular signaling programs. *Trends Biochem Sci.* (2017) 42:255–73. doi: 10.1016/j.tibs.2016.11.003
747. Martínez-Bosch N, Fernández-Barrena MG, Moreno M, Ortiz-Zapater E, Munné-Collado J, Iglesias M, et al. Galectin-1 drives pancreatic carcinogenesis through stroma remodeling and hedgehog signaling activation. *Cancer Res.* (2014) 74:3512–24. doi: 10.1158/0008-5472.CAN-13-3013
748. Méndez-Huergo SP, Blidner AG, Rabinovich GA. Galectins: emerging regulatory checkpoints linking tumor immunity and angiogenesis. *Curr Opin Immunol.* (2017) 45:8–15. doi: 10.1016/j.coi.2016.12.003
749. Daley D, Mani VR, Mohan N, Akkad N, Ochi A, Heindel DW, et al. Dectin 1 activation on macrophages by galectin 9 promotes pancreatic carcinoma and peritumoral immune tolerance. *Nat Med.* (2017) 23:556–67. doi: 10.1038/nm.4314
750. Zeligs KP, Neuman MK, Annunziata CM. Molecular pathways: the balance between cancer and the immune system challenges the therapeutic specificity of targeting nuclear factor-κB signaling for cancer treatment. *Clin Cancer Res.* (2016) 22:4302–8. doi: 10.1158/1078-0432.CCR-15-1374
751. Flint TR, Fearon DT, Janowitz T. Connecting the metabolic and immune responses to cancer. *Trends Mol Med.* (2017) 23:451–64. doi: 10.1016/j.molmed.2017.03.001
752. Mohamed E, Cao Y, Rodriguez PC. Endoplasmic reticulum stress regulates tumor growth and anti-tumor immunity: a promising opportunity for cancer immunotherapy. *Cancer Immunol Immunother.* (2017) 66:1069–78. doi: 10.1007/s00262-017-2019-6
753. Wang K, Baldwin GS, Nikfarjam M, He H. p21-activated kinase signalling in pancreatic cancer: new insights into tumour biology and immune modulation. *World J Gastroenterol.* (2018) 24:3709–23. doi: 10.3748/wjg.v24.i33.3709
754. Daniel SK, Sullivan KM, Labadie KP, Pillarisetty VG. Hypoxia as a barrier to immunotherapy in pancreatic adenocarcinoma. *Clin Transl Med.* (2019) 8:10. doi: 10.1186/s40169-019-0226-9
755. Feig C, Jones JO, Kraman M, Wells RJ, Deonarine A, Chan DS, et al. Targeting CXCL12 from FAP-expressing carcinoma-associated fibroblasts synergizes with anti-PD-L1 immunotherapy in pancreatic cancer. *Proc Natl Acad Sci USA.* (2013) 110:20212–7. doi: 10.1073/pnas.1320318110
756. Mace TA, Ameen Z, Collins A, Wojcik S, Mair M, Young GS, et al. Pancreatic cancer-associated stellate cells promote differentiation of myeloid-derived suppressor cells in a STAT3-dependent manner. *Cancer Res.* (2013) 73:3007–18. doi: 10.1158/0008-5472.CAN-12-4601
757. Mitchem JB, Brennan DJ, Knolhoff BL, Belt BA, Zhu Y, Sanford DE, et al. Targeting tumor-infiltrating macrophages decreases tumor-initiating cells, relieves immunosuppression, and improves chemotherapeutic responses. *Cancer Res.* (2013) 73:1128–41. doi: 10.1158/0008-5472.CAN-12-2731
758. Rosati A, Basile A, D'Auria R, d'Avenia M, De Marco M, Falco A, et al. BAG3 promotes pancreatic ductal adenocarcinoma growth by activating stromal macrophages. *Nat Commun.* (2015) 6:8695. doi: 10.1038/ncomms9695
759. Su S, Liu Q, Chen J, Chen J, Chen F, He C, et al. A positive feedback loop between mesenchymal-like cancer cells and macrophages is essential to breast cancer metastasis. *Cancer Cell.* (2014) 25:605–20. doi: 10.1016/j.ccr.2014.03.021
760. Zhang Y, Velez-Delgado A, Mathew E, Li D, Mendez FM, Flannagan K, et al. Myeloid cells are required for PD-1/PD-L1 checkpoint activation and the establishment of an immunosuppressive environment in pancreatic cancer. *Gut.* (2017) 66:124–36. doi: 10.1136/gutjnl-2016-312078
761. Sanford DE, Belt BA, Panni RZ, Mayer A, Deshpande AD, Carpenter D, et al. Inflammatory monocyte mobilization decreases patient survival in pancreatic cancer: a role for targeting the CCL2/CCR2Axis. *Clin Cancer Res.* (2013) 19:3404–15. doi: 10.1158/1078-0432.CCR-13-0525
762. Takeuchi S, Baghdadi M, Tsuchikawa T, Wada H, Nakamura T, Abe H, et al. Chemo-therapy-derived inflammatory responses accelerate the formation of immunosuppressive myeloid cells in the tissue microenvironment of human pancreatic cancer. *Cancer Res.* (2015) 75:2629–40. doi: 10.1158/0008-5472.CAN-14-2921
763. Pylayeva-Gupta Y, Das S, Handler JS, Hajdu CH, Coffre M, Koralov SB, et al. IL35-producing B cells promote the development of pancreatic neoplasia. *Cancer Discov.* (2016) 6:247–55. doi: 10.1158/2159-8290.CD-15-0843
764. Gunderson AJ, Kaneda MM, Tsujikawa T, Nguyen AV, Affara NI, Ruffell B, et al. Brutontyrosine kinase-dependent immune cell cross-talk drives pancreas cancer. *Cancer Discov.* (2016) 6:270–85. doi: 10.1158/2159-8290.CD-15-0827
765. Tan E, El-Rayes B. Pancreatic cancer and immunotherapy: resistance mechanisms and proposed solutions. *J Gastrointest Cancer.* (2019) 50:1–8. doi: 10.1007/s12029-018-0179-z
766. Heinemann V, Reni M, Ychou M, Richel DJ, Macarulla T, Ducreux M. Tumour-stroma interactions in pancreatic ductal adenocarcinoma: rationale and current evidence for new therapeutic strategies. *Cancer Treat Rev.* (2014) 40:118–28. doi: 10.1016/j.ctrv.2013.04.004

767. Sunami Y, Rebelo A, Kleeff J. Lipid metabolism and lipid droplets in pancreatic cancer and stellate cells. *Cancers*. (2017) 10:E3. doi: 10.3390/cancers10010003
768. Tsai S, McOlash L, Palen K, Johnson B, Duris C, Yang Q, et al. Development of primary human pancreatic cancer organoids, matched stromal and immune cells and 3D tumor microenvironment models. *BMC Cancer*. (2018) 18:335. doi: 10.1186/s12885-018-4238-4
769. Tiriac H, Plenker D, Baker LA, Tuveson DA. Organoid models for translational pancreatic cancer research. *Curr Opin Genet Dev*. (2019) 54:7–11. doi: 10.1016/j.gde.2019.02.003
770. Tuveson D, Clevers H. Cancer modeling meets human organoid technology. *Science*. (2019) 364:952–5. doi: 10.1126/science.aaw6985
771. Ali S, Suresh R, Banerjee S, Bao B, Xu Z, Wilson J, et al. Contribution of microRNAs in understanding the pancreatic tumor microenvironment involving cancer associated stellate and fibroblast cells. Am J *Cancer Res*. (2015) 5:1251–64
772. Li Y, Yang X, Kang X, Liu S. The regulatory roles of long noncoding RNAs in the biological behavior of pancreatic cancer. *Saudi J Gastroenterol*. (2019) 25:145–51. doi: 10.4103/sjg.SJG_465_18
773. Zappulli V, Friis KP, Fitzpatrick Z, Maguire CA, Breakefield XO. Extracellular vesicles and intercellular communication within the nervous system. *J Clin Invest*. (2016) 126:1198–207. doi: 10.1172/JCI81134

Conflict of Interest: The authors declare that the research was conducted in the absence of any commercial or financial relationships that could be construed as a potential conflict of interest.

Copyright © 2019 Mu, Wang and Zöller. This is an open-access article distributed under the terms of the Creative Commons Attribution License (CC BY). The use, distribution or reproduction in other forums is permitted, provided the original author(s) and the copyright owner(s) are credited and that the original publication in this journal is cited, in accordance with accepted academic practice. No use, distribution or reproduction is permitted which does not comply with these terms.

frontiers in Oncology

CASE REPORT
published: 19 December 2019
doi: 10.3389/fonc.2019.01444

High Frequency of Cell-in-Cell Formation in Heterogeneous Human Breast Cancer Tissue in a Patient With Poor Prognosis: A Case Report and Literature Review

Banzhan Ruan[1,2,3†], *Zubiao Niu*[3†], *Xiaoyi Jiang*[1,3†], *Zhuo Li*[4], *Yanhong Tai*[4], *Hongyan Huang*[1*] and *Qiang Sun*[3*]

[1] Department of Oncology, Beijing Shijitan Hospital of Capital Medical University, Beijing, China, [2] Department of Biology, Hainan Medical University, Haikou, China, [3] Laboratory of Cell Engineering, Institute of Biotechnology, Beijing, China, [4] The Fifth Medical Center of the Chinese PLA General Hospital, Beijing, China

Cell cannibalism is a unique pathological phenomenon that has been observed at low frequency in a variety of human tumor samples (<0.5%), including breast cancer. Cannibalistic cells typically form cell-in-cell (CIC) structures characterized by enclosure of one cell or more by another, mediating a novel type of cell death "entosis," which was proposed as the type IV cell death. A large number of CIC structures are generally associated with malignant transformation and progression, and they are believed to be primed by and form among heterogeneous cells. However, there is currently no *in vivo* evidence from human tumor samples. In this case report, covering a 37-year-old female breast cancer patient, we observed considerable heterogeneity and proliferative activity (>70% Ki-67 positivity) in her breast cancer cells, accompanied by high frequency of CIC formation (∼6%) and poor prognosis. We consider this a typical example of cell cannibalism, supporting a role of heterogeneity in cell-in-cell formation and malignant progression. It may serve as a pretest basis for further investigations of cell-in-cell biology and breast cancer treatment.

Keywords: cell-in-cell formation, cell cannibalism, entosis, heterogeneity, breast cancer, poor prognosis

OPEN ACCESS

Edited by:
Mohit Kumar Jolly,
Indian Institute of Science (IISc), India

Reviewed by:
Hanumantha Rao Madala,
Harvard Medical School,
United States
Nan-Shan Chang,
National Cheng Kung
University, Taiwan
Mary C. Farach-Carson,
University of Texas Health Science
Center at Houston, United States

***Correspondence:**
Hongyan Huang
hhongy1999@126.com
Qiang Sun
sunq@bmi.ac.cn

†These authors have contributed equally to this work

Specialty section:
This article was submitted to Molecular and Cellular Oncology, a section of the journal Frontiers in Oncology

Received: *18 July 2019*
Accepted: *03 December 2019*
Published: *19 December 2019*

Citation:
Ruan B, Niu Z, Jiang X, Li Z, Tai Y, Huang H and Sun Q (2019) High Frequency of Cell-in-Cell Formation in Heterogeneous Human Breast Cancer Tissue in a Patient With Poor Prognosis: A Case Report and Literature Review. Front. Oncol. 9:1444. doi: 10.3389/fonc.2019.01444

INTRODUCTION

Breast cancer tissues display profound heterogeneity, which is important for clinical diagnosis and therapy. Cell cannibalism is a unique pathological phenomenon that has been observed in various types of human tumors, including breast cancer (1). Cannibalistic cells typically form cell-in-cell (CIC) structures, characterized by enclosure of cells by another one, and this affects patient prognosis (2, 3). CIC structures have not only been found in human tumors but also in animal tumors (4), suggesting that CIC is a general malignant phenomenon across species. Recent advances have shown that CIC structures play important roles in not only tumor evolution and genome instability but also embryonic development and immune homeostasis (5).

Multiple mechanisms, such as entosis, emperitosis, and homotypical cell cannibalism, have been proposed to promote CIC formation either homotypically between tumor cells or heterotypically between lymphocytes and tumor cells, which generally leads to the death of the internalized

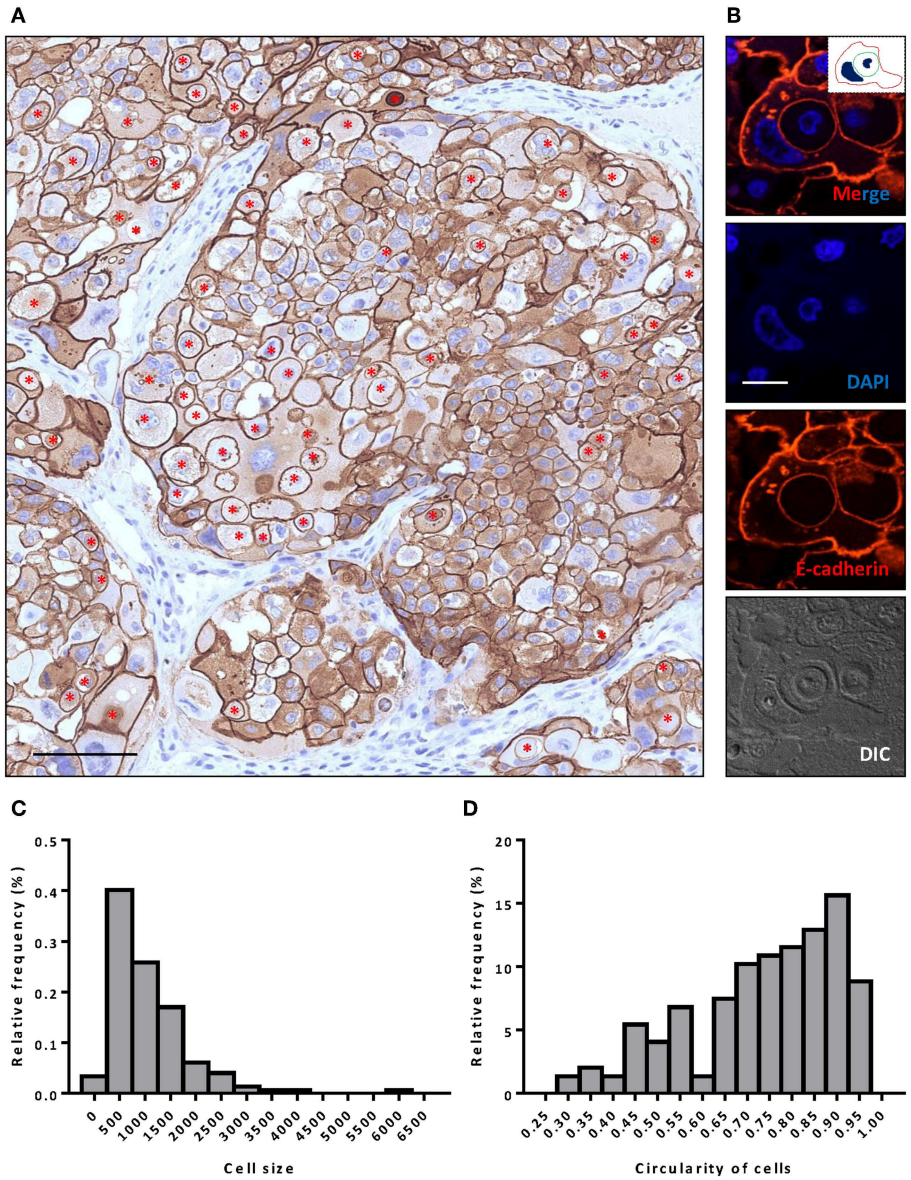

FIGURE 1 | Extensive CIC formation in heterogeneous cancer tissue. **(A)** Representative image for HER-2 staining. Inner cells of CIC structures are indicated with red asterisks. Scale bar: 100 μm. **(B)** Representative image for a typical CIC depicted with E-cadherin staining. Inserted picture of the top merged image is a schematic cartoon for the indicated CIC structure. Scale bar: 20 μm. **(C,D)** Histogram plots of cell size **(C)** and cell circularity **(D)** for **(A)**.

cells (5, 6). The death of the engulfed cells was believed to be executed non-autonomously by the engulfing cells, so CIC structures are believed to mediate a novel type of cell death process that parallels the existing cell-autonomous death processes apoptosis, necrosis, and autosis (7). Entosis is the best studied mechanism underlying the formation of CIC structures between tumor cells, and it is driven by polarized actomyosin that is compartmentalized by p190A RhoGAP recruited to E-cadherin-mediated adherens junction (8, 9). Factors regulating either actomyosin or adherens junctions have turned out to more or less affect entotic CIC formation (10, 11), and these effects can be induced by either matrix detachment, aberrant mitosis, or glucose starvation. Although these three inducers initiate entosis via distinct molecular mechanisms, the signal transduction converges eventually onto RhoA-ROCKs-regulated actomyosin (5, 11), suggesting that the cytoskeleton plays a pivotal role in controlling entosis. Activation of entosis probably serves as a competition mechanism that targets abnormal less fit cells for internalization and subsequent death to promote the selection of fitter cell clones. In this way, entosis was implicated in the evolution of heterogeneous tumors (6, 12, 13).

Since matrix detachment is a strong inducer of entotic CIC formation (14), tumor cells in effusion fluids are likely to form a high frequency of CIC structures (2). As for solid tumor tissues,

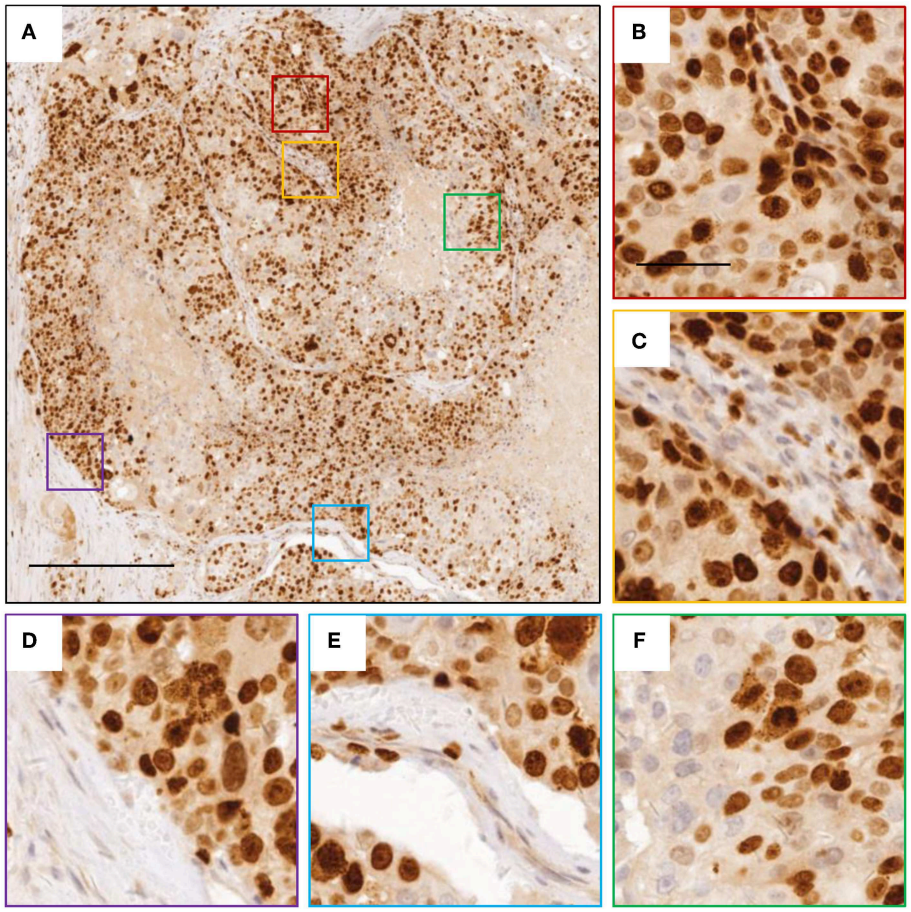

FIGURE 2 | Images of Ki-67 staining indicating active cell division. **(A)** representative image for breast cancer tissue with Ki-67 staining. **(B–F)** zoomed in images for boxed regions in **(A)**. The scale bars are 400 and 100 μm, respectively.

these types of cannibalistic structures were generally identified in low frequency (<0.5%) (15), probably due to complex cell adhesions that prevent asymmetric cell internalization. Here, we reported an unusual case of breast cancer patient whose tumor was highly heterogeneous and contained a considerable amount of complex CIC structures (∼6%), which may be related to active cell proliferation and may be involved in unfavorable prognosis.

CASE REPORT

A 37-year-old female was diagnosed with breast cancer 2 years ago. She had no family history. A tumor was found in the left chest, with lung metastases, but none were found in the axillary lymph nodes, so it was initially diagnosed as invasive ductal carcinoma of grade 3. Computerized tomography (CT) of the chest identified single tumor (4.9 × 3.1 × 4.5 cm). While the focal dermal layer of inner skin was involved, the nipple and striated muscle within mammary glands did not. Biopsy tissues displayed a large degree of cellular heterogeneity with tumor cells varying significantly in shape and size (**Figure 1**) and a high rate of Ki-67 positivity indicating active proliferation (**Figure 2**). Immunohistochemistry indicated the expression of HER-2 (3+), E-cadherin (+), Ki-67 (>70%), CK5/6 (+), EGFR (Weak +), and Top-IIα (+, 60%).

Like E-cadherin, HER-2 staining labeling cell boundary depicts a number of unique structures morphologically resembling CIC structures (**Figures 1A,B**). The overall frequency reached 6% of all tumor cells counted, which is pretty rare for solid tumors. The structures identified were complex. While most of them contained one cell (**Figures 3A,B**), some contained two or more (**Figures 3C–E**), which may have been caused by multiple internalization events or a single internalization event followed by mitotic cell division. Furthermore, some cells seemed to internalize sequentially to form superposition structures (**Figure 3F**). The outer cell nuclei were generally abnormal (**Figures 3B,D**) or irregular with some being split or multiple (**Figures 3C,E,F**), indicating aneuploidy or multi-ploidy, consistent with the report that CIC could induce aneuploidy by blocking cytokinesis of the engulfing cells (16).

The patient had an unfavorable prognosis. After diagnosis, she was given four cycles of TXH (T = docetaxel, X = capecitabine, H = herceptin) rescue chemotherapy, and then two cycles of XH treatment due to hand–foot syndrome. However, the

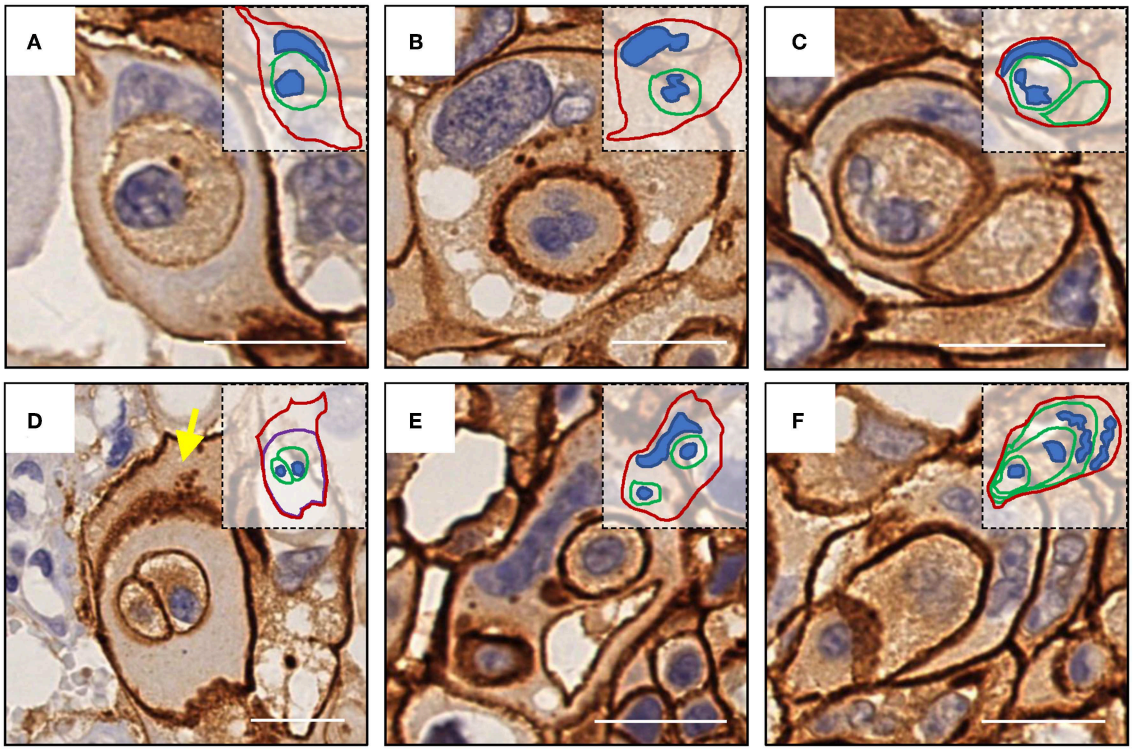

FIGURE 3 | Complex morphologies of CIC structures. **(A)** One cell was internalized. **(B)** abnormal nucleus of the outer cell. **(C)** Two cells were internalized, and the nucleus of one of them was missing. **(D)** The cell enclosing two cells was inside of another cell (yellow arrow) without nucleus. **(E)** Two cells were internalized, and the nucleus of the outer cell was deformed. **(F)** Sequential internalization of three cells. Inserted pictures are schematic cartoons for the indicated CIC structures, respectively. Scale bar: 20 μm.

disease progressed. Two cycles of vinorelbine plus trastuzumab were then applied, and tumor volume kept increasing. Next, palliative resection was performed, followed by 26 weeks of paclitaxel and lapatinib. *Staphylococcus aureus* infection occurred in the peripherally inserted central catheters. After anti-infection treatment, the patient reached a stable condition which was maintained for 5 weeks after 3 weeks of paclitaxel. Due to poor tolerance, therapy was changed to etoposide plus lapatinib. Nearly 4 months later, chest CT showed lung metastasis, and some lesions got larger in the following 2 months. Finally, gamma knife treatment (DT5600Gy/8f) was performed.

DISCUSSION

The roles of CIC in human cancers had been controversial (6), while the initial studies proposed a tumor suppressive role based on its nature of cell death, subsequent researches also identified tumor promotive functions for CIC-mediated engulfment. This discrepancy was resolved recently by the concept of cell competition (12, 17). Heterogeneous tumors generally contain multiple clones that compete with each other for limited space and nutrients. During the early stage, CIC death limited tumor growth. By CIC-mediated engulfment, the winner tumor cell clones that harbor oncogenic mutations such as *Kras*V12 (12) repetitively internalized and outcompeted those that were less malignant, leading to a slowing of tumor growth. CIC-induced aneuploidy endows the winner cells more opportunity to acquire new mutations and malignant phenotypes, such as metastasis. As a result, the malignant winner clones with oncogenic mutations eventually populate the tumor tissues and undergo distant metastasis during the late stage of cancer (18). Accordingly, high frequency of CIC structures precedes malignant transformation and progression, which is consistent with the case reported here, in which the tumor kept growing and progressing to lung metastasis despite sustained therapy.

Whereas, heterogeneities within tumor clones drive CIC formation, the process has been shown to be complex and genetically controlled (19). E-cadherin-mediated adherens junctions bring cells together, and set up asymmetric RhoA activity to drive cell internalization (8, 9) with the assistance of optimal membrane cholesterol and lipids (20) and the inflammatory cytokine IL-8 (21). Durgan et al. (22), and our unpublished work as well, identified cell division as a potent inducer of entotic CIC formation, the mechanism might also work in this case as the tumor cells are undergoing active division as indicated by >70% Ki-67 positivity. A review of the limited literature on CIC formation in breast cancer (**Table 1**) showed that CIC structures were also frequently associated with active cell proliferation (3, 22, 24) and, to an extent, cellular

TABLE 1 | Reports on CIC in human breast carcinoma.

Authors	Year	Case	Cancer type	Sample	CIC	Main finding	References
Fujii et al.	1986	1	Invasive ductal carcinoma	Nipple discharge	Present	Malignant epithelial cells and cell clusters were observed	(23)
Abodief et al.	2006	50	Ductal breast carcinoma	Tissue sections	<0.7%*	Cell cannibalism index associates with high grade of breast carcinoma	(15)
Overholtzer et al.	2007	4	Primary human breast carcinomas	Pleural effusions, tissue sections	2.5%#	CIC invasion mediates nonapoptotic death of internalized cells	(14)
Krajcovic et al.	2011	15	High grade or metastatic breast carcinoma	Pleural effusions, tissue sections	Present	CIC formation blocks outer cell cytokinesis to promote aneuploidy	(16)
Almeida and Rotta	2015	1	Metastatic breast carcinoma	Cerebrospinal fluid	Present	Cell cannibalism in the cerebrospinal fluid of a patient with metastatic breast adenocarcinoma	(24)
Durgan et al.	2017	75	Invasive ductal carcinomas	Tissue microarray	17/mm^2#	Mitosis can drive cell cannibalism through entosis	(22)
Kinoshita et al.	2018	25	Squamous cell, apocrine, invasive ductal carcinoma	Tissue sections	Present	Cannibalism are useful indicators for the differential diagnosis of SCC of the breast	(25)
Zhang et al.	2019	148	Ductal breast carcinoma	Tissue microarray	14/mm^2*	Subtyped CIC structures are independent prognostic markers that impact patient survival	(3)
Ruan et al.	2019	1	Invasive ductal carcinoma of grade 3	Tissue section	6%*	High frequency of CIC formation in heterogeneous breast carcinoma	(26)

#*Highest CIC structure.* **Mean CIC structure.*

heterogeneity (15, 16, 24, 25); and the frequencies of CIC structure, although difficult to compare due to the different types of calculation, span a wide range from presence (24, 25, 27) to 6% in this study.

In conclusion, the case reported here is a typical example of cell cannibalism, and its pathological features fit well current studies on CIC formation and functional implications, supporting the role of heterogeneity in CIC formation and malignant progression. It may serve as a pretest basis for further investigations on CIC biology and breast cancer treatment.

METHODS

Tissue Processing and Staining

Tissues were fixed in 10% (v/v) neutral phosphate-buffered formalin and then embedded in paraffin. Tissue sections of 5 μm were routinely de-paraffinized following standard Xylene-Ethonal method after being baked in 65°C for 1.5 h. Antigen retrieval was performed in citrate acid buffer by the microwaving method for 15 min after boiling. Then, the slides were blocked with 5% (w/v) BSA for 1 h at room temperature followed by incubation with the primary antibodies overnight at 4°C. For immunofluorescence (IF) staining, Alexa Fluor 568 anti-mouse secondary antibody (1:500) was applied for 1 h at room temperature before mounted with Prolong Gold antifade reagent with DAPI (Invitrogen). For immunohistochemistry (IHC) staining, HRP-conjugated secondary antibodies (1:2000) were applied for 1 h at room temperature before developed by DAB reagent.

Image Capture and Processing

IHC slides were scanned with NanoZoomer S60 (Hamamatzu Photonics) and analyzed with NDP.view 2.6.13 (Hamamatzu Photonics). Confocal images were captured on Ultraview Vox spinning disc confocal system (Perkin Elmer) on a Nikon Ti-E microscope and processed with Volocity 6.0 software. Cell size and morphology were analyzed using NIS Elements 4.5 software (Nikon). Briefly, images in JPG format were opened by the Element 4.5 software, and the irregular shape tool in the Object Catalog was selected and applied to individual cells, following the marking of cell contours. The information on cell size and circularity could be exported for further analysis and plotting with GraphPad Prism 6.01 (GraphPad). The carton print of images were made by curve painting in PowerPoint (Microsoft).

DATA AVAILABILITY STATEMENT

All datasets generated for this study are included in the article/supplementary material.

ETHICS STATEMENT

The studies involving human participants were reviewed and approved by Institutional Review Board of Affiliated Hospital of Academy of Military Medical Sciences [Beijing]. The patients/participants provided their written informed consent to participate in this study.

AUTHOR CONTRIBUTIONS

QS, HH, and BR prepared the figures and wrote the manuscript. ZN performed histological examination with the help of XJ. ZL and YT collected clinical data. BR performed immunohistochemistry analyses. All authors read and approved the final manuscript.

FUNDING

This work was supported by the National Key Research & Development Program of China (2016YFC1303303, 2018YFA0900804), the National Basic Research Program of China (2015CB553704), and the National Natural Science Foundation of China (81572799, 31671432, 31770975, 81471578, 81872314, 31970685, 81972485).

REFERENCES

1. Huang H, Chen A, Wang T, Wang M, Ning X, He M, et al. Detecting cell-in-cell structures in human tumor samples by E-cadherin/CD68/CD45 triple staining. *Oncotarget*. (2015) 6:20278–87. doi: 10.18632/oncotarget.4275
2. Gupta K, Dey P. Cell cannibalism: diagnostic marker of malignancy. *Diag Cytopathol*. (2003) 28:86–7. doi: 10.1002/dc.10234
3. Zhang X, Niu Z, Qin H, Fan J, Wang M, Zhang B, et al. Subtype-based prognostic analysis of cell-in-cell structures in early breast cancer. *Front Oncol*. (2019) 9:895. doi: 10.3389/fonc.2019.00895
4. Ferreira FC, Soares MJ, Carvalho S, Borralho L, Vicente G, Branco S, et al. Four cases of cell cannibalism in highly malignant feline and canine tumors. *Diag Pathol*. (2015) 10:199. doi: 10.1186/s13000-015-0429-3
5. Fais S, Overholtzer M. Cell-in-cell phenomena in cancer. *Nat Rev Cancer*. (2018) 18:758–66. doi: 10.1038/s41568-018-0073-9
6. Huang H, Chen Z, Sun Q. Mammalian cell competitions, cell-in-cell phenomena and their biomedical implications. *Curr Mol Med*. (2015) 15:852–60. doi: 10.2174/1566524015666151026101101
7. Martins I, Raza SQ, Voisin L, Dakhli H, Law F, De Jong D, et al. Entosis: The emerging face of non-cell-autonomous type IV programmed death. *Biomed J*. (2017) 40:133–40. doi: 10.1016/j.bj.2017.05.001
8. Sun Q, Cibas ES, Huang H, Hodgson L, Overholtzer M. Induction of entosis by epithelial cadherin expression. *Cell Res*. (2014) 24:1288–98. doi: 10.1038/cr.2014.137
9. Wang M, Ning X, Chen A, Huang H, Ni C, Zhou C, et al. Impaired formation of homotypic cell-in-cell structures in human tumor cells lacking alpha-catenin expression. *Sci Rep*. (2015) 5:12223. doi: 10.1038/srep12223
10. Liang J, Fan J, Wang M, Niu Z, Zhang Z, Yuan L, et al. CDKN2A inhibits formation of homotypic cell-in-cell structures. *Oncogenesis*. (2018) 7:1–8. doi: 10.1038/s41389-018-0056-4
11. Mackay HL, Muller PAJ. Biological relevance of cell-in-cell in cancers. *Biochem Soc Trans*. (2019) 47:725–32. doi: 10.1042/BST20180618
12. Sun Q, Luo T, Ren Y, Florey O, Shirasawa S, Sasazuki T, et al. Competition between human cells by entosis. *Cell Res.* (2014) 24:1299–310. doi: 10.1038/cr.2014.138
13. Mackay HL, Moore D, Hall C, Birkbak NJ, Jamal-Hanjani M, Karim SA, et al. Genomic instability in mutant p53 cancer cells upon entotic engulfment. *Nat Commun*. (2018) 9:3070. doi: 10.1038/s41467-018-05368-1
14. Overholtzer M, Mailleux AA, Mouneimne G, Normand G, Schnitt SJ, King RW, et al. A nonapoptotic cell death process, entosis, that occurs by cell-in-cell invasion. *Cell*. (2007) 131:966–79. doi: 10.1016/j.cell.2007.10.040
15. Abodief WT, Dey P, Al-Hattab O. Cell cannibalism in ductal carcinoma of breast. *Cytopathology*. (2006) 17:304–5. doi: 10.1111/j.1365-2303.2006.00326.x
16. Krajcovic M, Johnson NB, Sun Q, Normand G, Hoover N, Yao E, et al. A non-genetic route to aneuploidy in human cancers. *Nat Cell Biol*. (2011) 13:324–30. doi: 10.1038/ncb2174
17. Kroemer G, Perfettini JL. Entosis, a key player in cancer cell competition. *Cell Res*. (2014) 24:1280–1. doi: 10.1038/cr.2014.133
18. Sun Q, Huang H, Overholtzer M. Cell-in-cell structures are involved in the competition between cells in human tumors. *Mol Cell Oncol*. (2015) 2:e1002707. doi: 10.1080/23723556.2014.1002707
19. Ning X, Luo T, Chen Z, Sun Q. The physics for the formation of cell-in-cell structures. *Curr Mol Med*. (2015) 15:867–72. doi: 10.2174/1566524015666151026105123
20. Ruan B, Zhang B, Chen A, Yuan L, Liang J, Wang M, et al. Cholesterol inhibits entotic cell-in-cell formation and actomyosin contraction. *Biochem Biophys Res Commun*. (2018) 495:1440–6. doi: 10.1016/j.bbrc.2017.11.197
21. Ruan B, Wang C, Chen A, Liang J, Niu Z, Zheng Y, et al. Expression profiling identified IL-8 as a regulator of homotypic cell-in-cell formation. *BMB Rep*. (2018) 51:412–7. doi: 10.5483/BMBRep.2018.51.8.089
22. Durgan J, Tseng YY, Hamann JC, Domart MC, Collinson L, Hall A, et al. Mitosis can drive cell cannibalism through entosis. *eLife*. (2017) 6:1–26. doi: 10.7554/eLife.27134.031
23. Fujii M, Ishii Y, Wakabayashi T, Itoyanagi N, Hagiwara K, Saito M, et al. Cytologic diagnosis of male breast cancer with nipple discharge. A case report. *Acta Cytol*. (1986) 30:21–4.
24. Almeida SM, Rotta I. Cerebrospinal fluid cell cannibalism in metastatic breast adenocarcinoma. *Arquivos Neuro-psiquiatr*. (2015) 73:469. doi: 10.1590/0004-282X20150028
25. Kinoshita M, Matsuda Y, Arai T, Soejima Y, Sawabe M, Honma N. Cytological diagnostic clues in poorly differentiated squamous cell carcinomas of the breast: Streaming arrangement, necrotic background, nucleolar enlargement and cannibalism of cancer cells. *Cytopathology*. (2018) 29:22–7. doi: 10.1111/cyt.12461
26. Ruan B, Niu Z, Jiang X, Li Z, Tai Y, Huang H, et al. High frequency of cell-in-cell formation in heterogeneous human breast cancer tissue in a patient with poor prognosis: a case report and literature review. *Front Oncol*. (2019) 9:1444. doi: 10.3389/fonc.2019.01444
27. Uei Y, Watanabe Y, Hirota T, Yamamoto H, Watanabe H. Cytologic diagnosis of breast carcinoma with nipple discharge: special significance of the spherical cell cluster. *Acta Cytol*. (1980) 24:522–8.

Conflict of Interest: The authors declare that the research was conducted in the absence of any commercial or financial relationships that could be construed as a potential conflict of interest.

Copyright © 2019 Ruan, Niu, Jiang, Li, Tai, Huang and Sun. This is an open-access article distributed under the terms of the Creative Commons Attribution License (CC BY). The use, distribution or reproduction in other forums is permitted, provided the original author(s) and the copyright owner(s) are credited and that the original publication in this journal is cited, in accordance with accepted academic practice. No use, distribution or reproduction is permitted which does not comply with these terms.

frontiers in Cell and Developmental Biology

REVIEW
published: 20 December 2019
doi: 10.3389/fcell.2019.00355

Mitochondrial Involvement in Migration, Invasion and Metastasis

*Tatiana V. Denisenko[1], Anna S. Gorbunova[1] and Boris Zhivotovsky[1,2]**

[1] Faculty of Medicine, Lomonosov Moscow State University, Moscow, Russia, [2] Institute of Environmental Medicine, Division of Toxicology, Karolinska Institute, Stockholm, Sweden

Mitochondria in addition to be a main cellular power station, are involved in the regulation of many physiological processes, such as generation of reactive oxygen species, metabolite production and the maintenance of the intracellular Ca^{2+} homeostasis. Almost 100 years ago Otto Warburg presented evidence for the role of mitochondria in the development of cancer. During the past 20 years mitochondrial involvement in programmed cell death regulation has been clarified. Moreover, it has been shown that mitochondria may act as a switchboard between various cell death modalities. Recently, accumulated data have pointed to the role of mitochondria in the metastatic dissemination of cancer cells. Here we summarize the modern knowledge concerning the contribution of mitochondria to the invasion and dissemination of tumor cells and the possible mechanisms behind that and attempts to target metastatic cancers involving mitochondria.

Keywords: cell death, invasion, metastasis, migration, mitochondria

OPEN ACCESS

Edited by:
Satyendra Chandra Tripathi, All India Institute of Medical Sciences Nagpur, India

Reviewed by:
Ildikò Szabò, University of Padua, Italy
Carlos Villalobos, Spanish National Research Council (CSIC), Spain

***Correspondence:**
Boris Zhivotovsky
Boris.Zhivotovsky@ki.se

Specialty section:
This article was submitted to Molecular and Cellular Oncology, a section of the journal Frontiers in Cell and Developmental Biology

Received: *20 August 2019*
Accepted: *05 December 2019*
Published: *20 December 2019*

Citation:
Denisenko TV, Gorbunova AS and Zhivotovsky B (2019) Mitochondrial Involvement in Migration, Invasion and Metastasis. Front. Cell Dev. Biol. 7:355. doi: 10.3389/fcell.2019.00355

INTRODUCTION

Mitochondria are intracellular organelles that produce the majority of the energy in the cells, providing synthesis of ATP by oxidative phosphorylation (OXPHOS) (Mitchell, 1961). Beyond energy production mitochondria have multiple functions including the generation of reactive oxygen species (ROS), metabolite production, the regulation of intracellular Ca^{2+} homeostasis and modulation of cell death pathways. Additionally, mitochondria contribute to the regulation of signaling pathways linked to the cell proliferation, differentiation, and many others (Porporato et al., 2018). The multiple functions of mitochondria allow cells to adapt to the changing of environment, including the availability of nutrients and oxygen, making them perfect stress sensors (Vyas et al., 2016). These functions also determine the crucial role of mitochondria in development and progression of cancer. Indeed, mitochondria may drive tumor progression through adaptation to changing metabolic demand, contributing to chemoresistance, and regulating cell death pathways (Gogvadze et al., 2008). Furthermore, mitochondria have been shown to be linked to the metastatic dissemination of cancer cells. Importantly, mitochondrial turnover, i.e., fission/fusion, is deeply involved in the regulation of different mitochondrial functions and metastatic cascade. However, the role of mitochondrial dynamics in cancer cell invasion and metastasis remains highly controversial. Here we took an attempt to summarize the present knowledge about the functions of mitochondria that contribute to the metastatic dissemination and invasion including mitochondrial dynamics, cell death, oxidative stress, metabolism and bioenergetics, Ca^{2+} signaling, and mtDNA (**Figure 1**). Additionally, we highlight the existing therapy approaches to target metastatic cancers involving mitochondria.

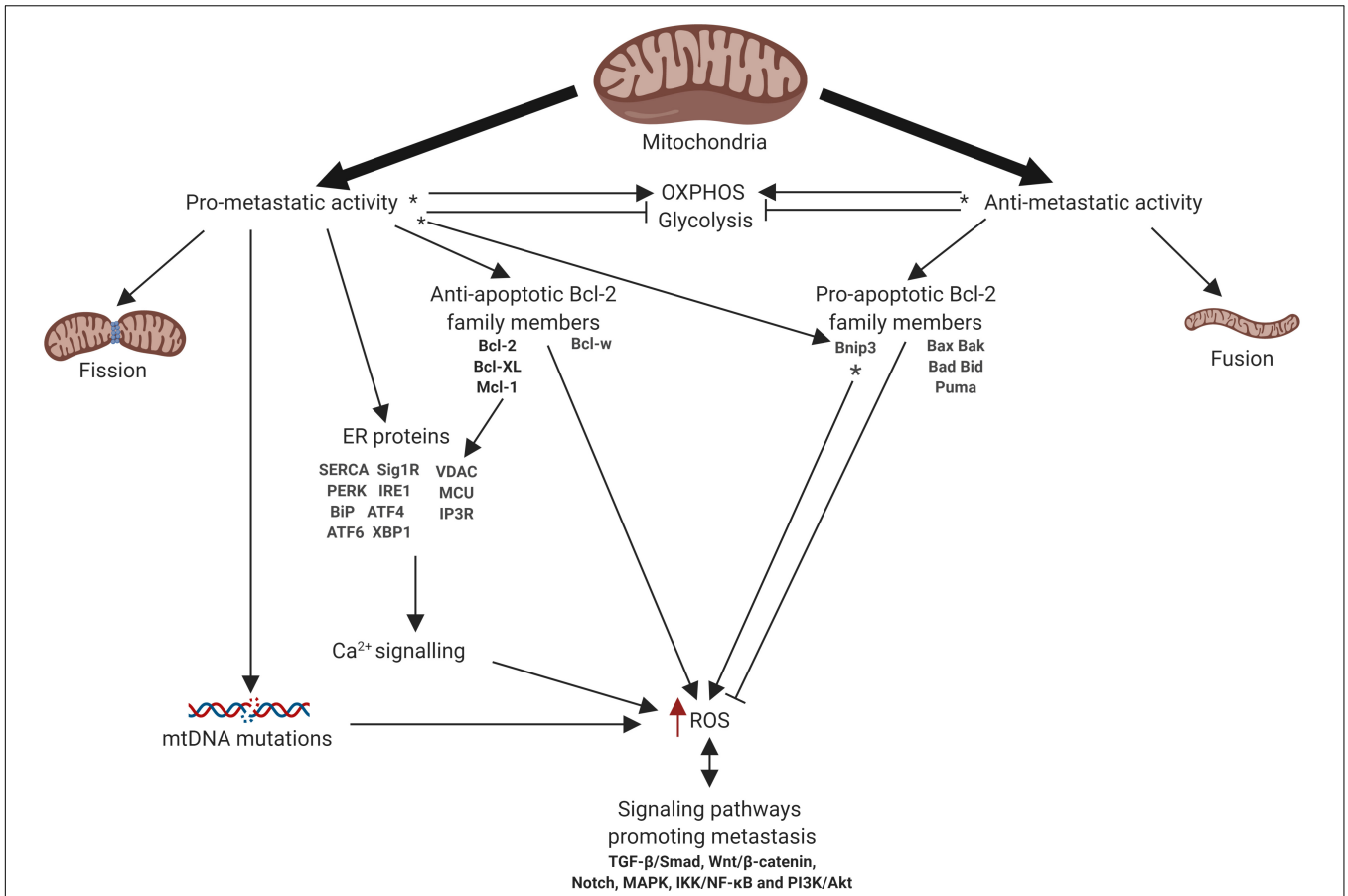

FIGURE 1 | Schematic representation of mitochondrial involvement in metastasis. Arrows or blunt ends indicate activation or inhibition, respectively. Red arrow indicates increased level. * - function depends on the tumor type. OXPHOS, oxidative phosphorylation; ER, endoplasmic reticulum; ROS, reactive oxygen species. For details, see text. Figure is created using BioRender.

MITOCHONDRIA AND MIGRATION

Metastasis is one of the main cause of cancer patients' death. Metastatic dissemination is characterized by cell detachment from the primary tumor mass, further migration through blood and lymphatic vessels and colonization of different tissues. The metastatic cascade can be subdivided into different stages, including local invasion, intravasation, survival in the circulation, extravasation, survival at a second site and finally outgrowth at this site. The epithelial to mesenchymal transition (EMT) is a biological phenomenon occurring during embryonic development but also associated with cancer metastasis (Chaffer and Weinberg, 2011). During EMT cancer cells lose their epithelial features and temporally acquire mesenchymal characteristics which allow them to migrate from the original site in order to colonize different tissues.

Epithelial to mesenchymal transition is regulated by various molecular pathways including TGF-β/Smad, Wnt/β-catenin, Notch, mitogen-activated protein kinase (MAPK), IKK/NF-κB and PI3K/Akt (Lamouille et al., 2014), cytokines (e.g., TGF-β and EGF) and transcription factors Snail (Snai1), Slug (Snai2), Twist (helix-loop-helix factor), and ZEB1/2 (zinc-finger E-box-binding homeobox) (Lu and Kang, 2019), etc. Overexpression of EMT transcriptional factors leads to the downregulation of epithelial markers and Tight Junction proteins, such as E-cadherin, occludin, and claudins, which in turn results in the loose of apical cell polarity (Lu and Kang, 2019). On the other hand, EMT activation provides the upregulation of mesenchymal markers: N-cadherin, vimentin, and fibronectin. In addition, EMT is accompanied by increased expression of matrix metalloproteinases (MMPs) and urokinase plasminogen activator (uPA), which contribute to the degradation of the extracellular matrix (ECM) and the basal membrane of epithelial tissue (Lu and Kang, 2019). These events lead to the loss of cell-cell and cell matrix adhesion contacts and an increase in cell motility and cell migration, which are the hallmarks of metastasis (Chaffer and Weinberg, 2011).

Mitochondrial Dynamics and Migration

Mitochondria have been shown to contribute to carcinogenesis including metastatic dissemination and EMT by different mechanisms. Being extremely dynamic organelles mitochondria

continuously change their morphology undergoing fission (fragmentation) and fusion (elongation). These processes are regulated by highly conserved guanosine triphosphatases (GTPases) (Senft and Ronai, 2016). Fission is controlled by cytosolic dynamin-related protein 1 (Drp1), which is recruited to mitochondria by adapter proteins, including mitochondrial fission factor (Mff) and mitochondrial dynamics proteins of 49 and 51 kDa (Mid49/51), where it forms oligomeric ring structures and executes mitochondrial fission. Fusion is mediated by two GTPases in the outer mitochondrial membrane (OMM), i.e., mitofusins 1 and 2 (Mfn1, 2), whereas the inner mitochondrial membrane (IMM) fusion is promoted by the cristae-shaping protein Opa1 (Losón et al., 2013). In cancer cells, mitochondrial fission/fusion is unbalanced due to the mitochondrial dysfunction (Srinivasan et al., 2017). Several studies have demonstrated that increased fission and/or reduced fusion are associated with malignant transformation in different types of cancer (Senft and Ronai, 2016). Furthermore, upregulation of mitochondrial fission and increased expression of Drp1 was shown to promote cancer metastasis (Zhao et al., 2013; Sun et al., 2018a). For example, overexpression of Drp1 was detected in breast cancer metastatic cells compared to the non-metastatic, whereas silencing of Drp1 or overexpression of Mfn1 resulted in mitochondrial elongation and significantly suppressed the metastatic properties of breast cancer cells (Zhao et al., 2013). Similarly, increased mitochondrial fission was observed in hepatocellular carcinoma (HCC) metastatic cells. Comparison of levels of Drp1 in tumor samples and in the normal tissues revealed its higher expression in the former, which is associated with the promotion of tumor cell survival and metastasis formation (Sun et al., 2018a). In addition, downregulation of Drp1 inhibits glioma cells invasive properties affecting cytoskeleton remodeling through the RhoA/ROCK1 pathway (Yin et al., 2016). Recent data have also suggested the existence of a link between mitochondrial fission and hypoxia-induced migration. The inhibition of Drp1 by Mdivi-1 leads to the decreased migration induced by hypoxia (Han et al., 2015). Taken together, these studies provide the evidence that mitochondrial fission is required for cancer cell migration and to support the metastatic potential of cancer cells. In migrating cancer cells, mitochondria localize at the leading edge along microtubules, where the energy demand is higher, providing necessary supply (Senft and Ronai, 2016). Unfortunately, the mechanism involving Drp1 in regulation of the process of cancer metastasis remains not fully understood. Different studies suggest that fission is required for efficient redistribution of mitochondria, and the upregulation/activation of Drp1 is associated with the migration of cancer cells (Zhao et al., 2013; Senft and Ronai, 2016). Another study has shown that inhibition of mitochondrial fusion may abolish invasion of syntaphilin-depleted prostate adenocarcinoma cells. Syntaphilin suppresses mitochondrial dynamics, cancer cell dissemination *in vivo*. Moreover, its downregulation correlates with poor outcome of cancer patients. Thereby, the silencing of both Mfn1, 2 and syntaphilin abolished mitochondrial trafficking and abrogated the migratory response (Caino et al., 2016). Thus, mitochondrial dynamics are linked to cancer cell migration, and the relative contribution of fission or fusion depends on tumor type and molecular context.

ROS Contributes to Migration and Metastasis

Reactive oxygen species constantly generated during the metabolic process and play a crucial role in the regulation of various cellular functions (Vyas et al., 2016). Mitochondrial electron transport chain (ETC) is the main source of ROS (Vyas et al., 2016). Complexes I and III are often regarded as the major sites of mitochondrial ROS (mtROS) production, but more recent studies indicate that at least ten other mitochondrial enzymes also contribute to ROS generation, including Complex II (Quinlan et al., 2013). The role of ROS in cancer remains highly controversial. First, in cancer cells a higher level of ROS is detected compared to their normal counterparts (Cannito et al., 2010; Vyas et al., 2016). A moderate increase of ROS level was shown to support cancer cell proliferation and migration and to activate different signaling pathways associated with cell survival, contributing to tumor growth and malignant transformation (Kumari et al., 2018). Indeed, the level of ROS has been shown to activate the PI3K pathway. The primary known ROS target in the PI3K pathway is phosphatase and tensin homolog (PTEN). ROS promote the inactivation of the tumor suppressor PTEN by oxidizing active-site cysteine residues, causing the formation of a disulfide bond, which prevents PTEN from inactivating the PI3K pathway (Lee et al., 2002; Sullivan and Chandel, 2014). Since ROS can inactivate protein tyrosine phosphatases through oxidation of cysteine residues, ROS may have many yet-to-be discovered effects on diverse, mitogen-activated pathways that are normally inhibited by phosphatases (Sullivan and Chandel, 2014). ROS can stimulate the phosphorylation of MAPK and extracellular signal-regulated kinase (ERK), cyclin D1 expression and JUN N-terminal kinase (JNK) activation, all of which are linked to tumor cell survival and growth (Gorrini et al., 2013). ROS may activate different processes associated with metastatic dissemination and invasion. They may be involved in cytoskeleton remodeling. The cell cytoskeleton is dynamic structure composed of microtubules and filaments. Cytoskeletal rearrangements are important for driving cell migration and invasion through the formation of different types of cellular protrusions including filopodia, lamellipodia, and invadopodia (Ridley, 2011). Recent studies have shown that Rac-mediated actin remodeling is attributed to increased O_2^- levels (Jiang et al., 2017). Specifically, Rho activation leads to the filopodia formation, while induction of Rac contributes to the formation of lamellipodia (Kozma et al., 1995; Narumiya et al., 2009; Galadari et al., 2017). Another mechanism by which ROS may promote tumor cell invasion is by stimulation of the proteolytic degradation of ECM components such as glycosaminoglycan (GAG), contributing to metastatic dissemination (Galadari et al., 2017).

Increased ROS levels can activate different pathways that induce morphological changes associated with the EMT (Jiang et al., 2017). For example, increased ROS generation stimulates the acquisition of invasive properties by pancreatic cancer

cells through the activation of NF-κB signaling. In turn, treatment with antioxidants leads to the suppression of EMT and attenuates metastasis (Shimojo et al., 2013). NF-κB signaling is strongly associated with the EMT process by promoting the expression of the main EMT-related transcription factors Snail, Slug, Twist1, and ZEB1/2, which is also involved in the disruption of the cell–cell junctions (Min et al., 2008; Jiang et al., 2017). Furthermore, NF-κB activation may contribute to the transcription of vimentin and MMPs such as MMP-2, MMP-9, to maintain the mesenchymal phenotype and promote tumor cell migration (Jiang et al., 2017). Another pathway involved in EMT and regulated by ROS is the transcription factor hypoxia inducible factor 1-alpha (HIF-1α) (Jiang et al., 2017), which is induced under hypoxic conditions and can stimulate cancer cell EMT by activating EMT-inducing transcription factors such as Twist, Snail and ZEB1/2 (Joseph et al., 2015; Zhang et al., 2015). Thus, NF-κB is activated under hypoxic conditions, and thereby, in the presence of hypoxia, may co-regulate many of EMT-linked transcription factors (D'Ignazio et al., 2017). Importantly, ROS accumulation leads to the stabilization of HIF-1 due to inhibition of the HIF-degrading enzyme prolyl hydroxylase (Comito et al., 2011).

There is a complex interplay between the level of ROS and the TGF-β signaling pathway exists, which is the one of the most important pathways involved in EMT regulation. It was reported that ROS mediate TGF-β-induced EMT in cancer (Corcoran and Cotter, 2013; Liu and Desai, 2015). ROS may affect the activation of TGF-β downstream effector Smad, while treatment with the ROS scavenger N-acetyl cysteine (NAC) abolishes Smad phosphorylation (Krstiæ et al., 2015). Additionally, ROS may regulate TGF-β activation through different signaling pathways as described above, including MAPK and NF-κB (Corcoran and Cotter, 2013). Conversely, TGF-β can induce ROS production by many alterations in mitochondrial functioning and antioxidant protection. For example, TGF-β affects ROS levels by blocking of ETC Complex IV and upregulation of NADPH oxidase 4 (NOX4) (Yoon et al., 2005). Further, it was revealed that TGF-β increases ROS levels inhibiting ETC Complex III (Jain et al., 2013). TGF-β also downregulates the synthesis of the antioxidant glutathione (GSH) and several antioxidant enzymes contributing to cellular redox misbalance and EMT-related processes, such as fibrosis (Liu and Desai, 2015). Using the mitochondria-targeted antioxidant SkQ1 was also shown that oxidative stress is implicated in EMT induced by TGF-β. In cervical carcinoma SiHa cells depletion of ROS leads to increase of E-cadherin and downregulation of Snail, the main negative regulator of E-cadherin (Shagieva et al., 2017). Similarly, pretreatment with the ROS scavenger carotenoid astaxanthin (AST) leads to the suppression of EMT and the production of inflammatory cytokines by mesothelial cells (Hara et al., 2017). Thus, TGF-β, as inducer of EMT, is likely to affect this process through the ROS production.

Reactive oxygen species accumulation may influence migration and metastasis of cancer cells through different mechanisms affecting cytoskeleton remodeling, ECM degradation and the activation of signaling pathways. However, in conditions of strong oxidative stress, ROS suppress metastatic dissemination, due to induction of cell death or cellular senescence (Piskounova et al., 2015). Furthermore, elevated ROS levels may activate antioxidant pathways (Vyas et al., 2016). Indeed, oncogenic K- Ras-, B- Raf-, and c-Myc-mediated pathways may downregulate ROS production through regulation of nuclear factor (erythroid-derived 2)-like 2 (Nrf2), one of the main regulators of the antioxidant response (Vyas et al., 2016). Nrf2 provides a transcriptional activation of several genes involved in glutathione (GSH) synthesis. It promotes tumorigenesis contributing to the cancer cell protection against oxidative stress and chemotherapeutic agents (Rojo de la Vega et al., 2018). Recent data have demonstrated that Nrf2 activation can stimulate cancer cell migration and metastasis and Nrf2 deletion attenuates metastatic potential breast cancer cells suppressing RhoA GTPases activity (Zhang et al., 2016). Altogether, these observations demonstrate that the role of ROS in tumor progression and metastasis remains highly controversial. It has been suggested that tumors should maintain the ROS at a definite level in order to sustain their growth and metastasis without causing cytotoxicity (Vyas et al., 2016). Moreover, for tumor promotion it also necessary to provide the right balance between ROS production and antioxidants.

Mitochondrial DNA Mutations Contribute to the Migration and Metastasis

It is known that mtDNA mutations can contribute to tumor initiation and progression (Vyas et al., 2016). Variations in copy number of mtDNA are associated with tumorigenesis and depend on tumor type (Sun et al., 2018b). Thus, decreased copy number of mtDNA was detected in breast cancer, HCC, non-small cell lung cancer (NSCLC) and gastric cancer (Mambo et al., 2005). On the other hand, increased copy number of mtDNA was found in prostate, head and neck, and colorectal cancers (Sun et al., 2018b). Mutations and variations in mtDNA content might be associated with regulation of the metastatic properties of tumor cells (Ishikawa et al., 2008). Replacement of mtDNA from a highly metastatic to a poorly metastatic cell line led to an increase in the metastatic potential in the recipient cell line (Ishikawa et al., 2008). mtDNA mutations are also associated with EMT of cancer cells. Indeed, EMT induced by TGF-β leads to an increase of mtDNA copy number in NSCLC cells (Xu and Lu, 2015). Conversely, knockdown of mitochondrial transcription factor A (TFAM) leads to a decrease in mtDNA copy number, upregulation of E-cadherin expression, and suppression of cell migration rate in esophageal squamous cell carcinoma (Lin et al., 2012). Increased mtDNA content in this type of tumor is associated with the higher energy required for EMT. Furthermore, mtDNA mutations contribute to the acquisition of an aggressive phenotype in oncocytic thyroid tumors leading to their bioenergetic crisis (De Luise et al., 2017). As a consequence, mitochondrial dysfunction may lead to the activation of glycolysis (Smolková et al., 2011). Thus, oxygen deprivation may provide positive selective pressure for cancer cells carrying damaging mtDNA mutations. However, another study provided the evidence that EMT could also be induced in mtDNA-depleted cells. Indeed,

it has been demonstrated that TGF-β–induced EMT occurs in mitochondria-depleted cell lines leading to the stimulation of invasive properties through activation of Raf/MAPK (Naito et al., 2008). These data are consistent with the observation that in human mammary epithelial cells (hMECs) a decrease in mtDNA copy number promotes calcineurin-mediated mitochondrial retrograde signaling, which initiates EMT (Guha et al., 2014). Likewise, reduction of mtDNA content by suppression of mitochondrial pyrimidine nucleotide carrier 1 (PNC1), which is responsible for mitochondrial DNA replication, leads to EMT induction in hMECs (Favre et al., 2010). A recent study has revealed that increased mtDNA copy number may sustain tumor progression and metastasis by upregulating OXPHOS function in cancer cells that rely on mitochondrial OXPHOS. On the other hand, in cancer cells that depend on glycolytic type of metabolism reduction of mtDNA was shown to promote proliferation and chemoresistance (Sun et al., 2018b). Summing up, mtDNA mutations and variations of mtDNA copy number are associated with EMT, increased invasiveness and metastasis in different types of cancer. The opposite role of mtDNA content in cancer progression and metastatic dissemination depends on metabolic pattern of different types of cancer.

Bcl-2 AND METASTASIS

B-cell lymphoma/leukemia gene 2 (Bcl-2) family proteins are considered to be regulators of the apoptotic mitochondrial pathway. This family includes both anti-apoptotic Bcl-2, Bcl-XL, Bcl-w, Mcl-1, Bcl-B, and pro-apoptotic multidomain Bax and Bak proteins. In addition, the pro-apoptotic subfamily includes so-called BH3-only domain proteins, such as Bim, Puma, Noxa, Bad, Bid, and Bnip3. The ratio between these proteins with opposite functions determines the success of apoptosis (Adams and Cory, 2018). Upregulation of anti-apoptotic and downregulation of pro-apoptotic proteins is a hallmark of cancer, and their misbalance is contributed to the chemo-, immune-, and radio-resistance of anticancer therapies (Opferman and Kothari, 2018). However, further evidence has demonstrated that the functions of Bcl-2 family proteins are not limited to cell death control and tumor resistance. It has been established, that Bcl-2 family proteins play crucial roles in the regulation of migration, invasion and metastasis (Um, 2016) (**Figure 2**).

Indeed, the overexpression of Bcl-2, Bcl-XL, Bcl-w, and Mcl-1 in different cancers, including glioma, neuroblastoma, melanoma, squamous carcinoma, and breast, lung, and colorectal cancer cells, leads to significant increase in their migratory and invasive properties (Sun et al., 2011; Lee et al., 2013; Um, 2016; Young et al., 2016; Trisciuoglio et al., 2017). On the other hand, downregulation of these proteins attenuates invasiveness without affecting apoptosis or tumor growth, indicating that their pro-survival functions are not linked to regulation of cell migration and invasion (Um, 2016). Importantly, several studies have demonstrated that overexpression of the Bcl-2 family proteins is not always sufficient to induce pro-invasive properties of cancer cells, and could require the co-expression of other proteins stimulating invasiveness, such as c-Myc (Lu and Hong, 2009), N-Myc (Noujaim et al., 2002), or Twist1 (Sun et al., 2011). In certain cases, the exposure to hypoxic conditions may also be essential (Trisciuoglio et al., 2005). It has been suggested that the pro-invasive activity of pro-survival Bcl-2 family members appears to vary depending on the cell type and environment (Um, 2016).

The mechanisms involved in Bcl-2 proteins-mediated regulation of invasiveness and metastasis remain incompletely understood. Anti-apoptotic Bcl-2 family proteins have been shown to activate different signaling pathways controlling migration, invasiveness and metastasis ability in cancer. Indeed, Bcl-2 may modulate the EMT program by direct interaction with Twist1 through the helix-loop-helix DNA binding domain of Twist1 and two domains of Bcl-2 in hepatocellular and oral squamous cells (Sun et al., 2011; Duan et al., 2017). In addition, almost all anti-apoptotic Bcl-2 family members regulate the PI3K pathway involved in metastasis progression (Um, 2016). Interplay between Bcl-2 and the p110α subunit of PI3K regulates human colorectal cancer cell migration through actin polymerization and filopodia formation (Wan et al., 2015). Likewise, in lung cancer cells, Bcl-XL increases PI3K and p38 MAPK activities, which subsequently stimulate MMP-2 expression via Akt (Ho et al., 2010). Specifically, Bcl-w was shown to affect migration and invasion pathways through regulation of PI3K, EGF, Src, MMP-2, uPA, and focal adhesion kinase (FAK) (Um, 2016). Furthermore, Bcl-w promotes migration and invasion of glioblastoma cells through β-catenin signaling via its translocation into the nucleus to act as transcription factor for MMP-2 and mesenchymal marker expression (Lee et al., 2013). Additionally, Mcl-1 supports breast cancer cell migration and invasion via Src family kinases (SFKs) and their targets, and also by alteration of the phosphorylation state of the cytoskeletal protein cofilin (Young et al., 2016).

It has been reported that Bcl-2 family members are capable of regulating the functioning of mitochondria, during cellular respiration and of stimulating ROS generation in the form of the superoxide anion radical O_2^- and H_2O_2 (Um, 2016). Thus, multidomain pro-apoptotic proteins Bax and Bak have been shown to bind to the ETC Complex-I resulting in decreased ROS production, whereas anti-apoptotic Bcl-w and Bcl-XL interact with Bax and Bak, and abolish their binding to the Complex-I, stimulating ROS production and PI3K-, Src-, and EGFR-dependent cell migration and invasion (Jung et al., 2018; Kim et al., 2018).

Analysis of patients' clinical samples confirmed the involvement of pro-survival Bcl-2 family members in metastasis. Bcl-2 expression is associated with lymph node metastases of bladder (Kiss et al., 2015) and gastric (Geng et al., 2013) cancer, liver metastases of colorectal cancer (Ishijima et al., 1999) and lymphovascular invasion of patients with breast cancer (Neri et al., 2006). Upregulation of Bcl-XL was observed in lymph node metastases and venous permeation in colorectal cancer (Jin-Song et al., 2011), hematogenous metastases of osteosarcoma patients (Wang et al., 2010) and lymph node metastases in oral tongue squamous cell carcinoma (Zhang et al., 2014). Overexpression of Bcl-w is associated with the infiltrative morphotypes of gastric cancer (Lee et al., 2003) and is overexpressed in patients with

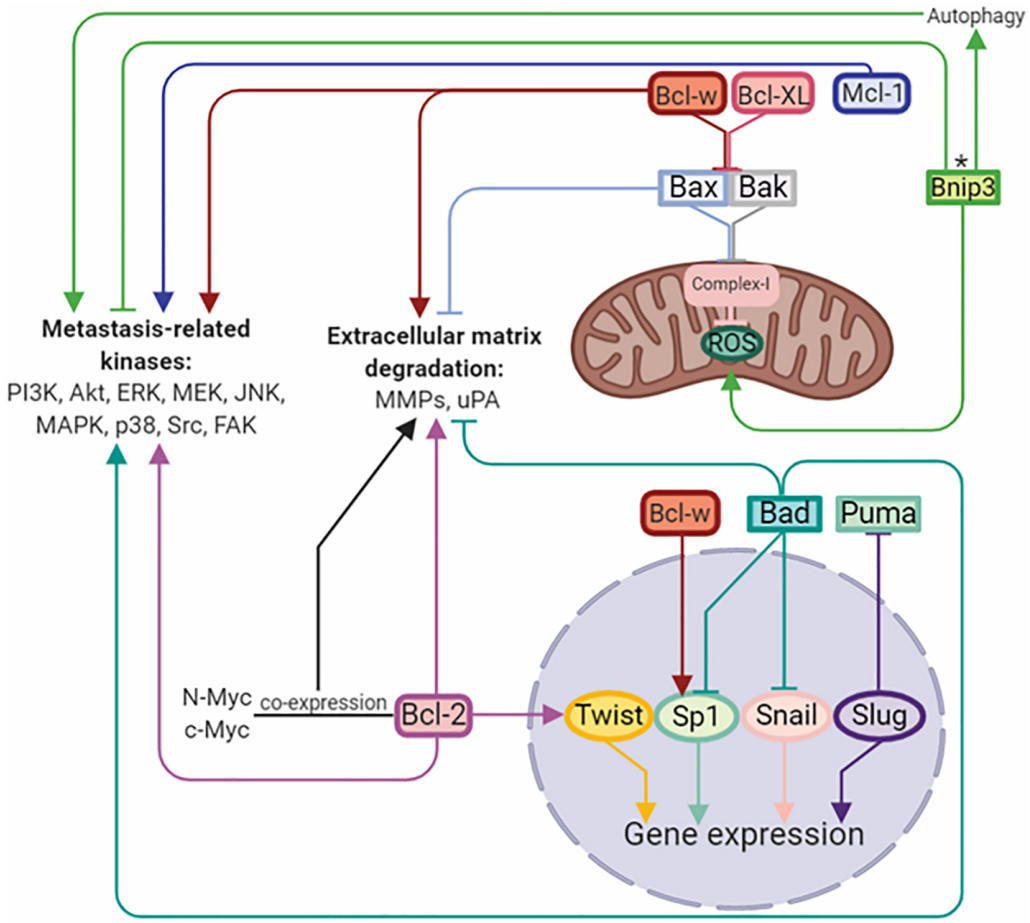

FIGURE 2 | Bcl-2 family members regulate metastasis by activation/inhibition of signaling kinases, matrix-degrading enzymes, and transcriptional factors. Arrows or blunt ends indicate activation or inhibition, respectively. Colored lines corresponds to each protein. * - function depends on the tumor type. Bcl-2, B-cell lymphoma 2; Mcl-1, myeloid cell leukemia 1; Bcl-XL, B-cell lymphoma-extra large; Bcl-w, Bcl-2-like protein 2; Bnip3, BCL2/adenovirus E1B 19 kDa protein-interacting protein 3; Bax, Bcl-2-like protein 4; Bak, Bcl-2 homologous antagonist/killer; Bad, Bcl-2-associated death promoter; Puma, p53 upregulated modulator of apoptosis; Twist, class A basic helix-loop-helix protein 38; Sp1, specificity protein 1; Snail, zinc finger protein SNAI1; Slug, zinc finger protein SNAI2. For details, see text. Figure is created using BioRender.

lung and breast cancers (Kim et al., 2019). Mcl-1 is upregulated among III–IV a stage of esophageal squamous cell carcinoma patients with lymph node metastases (Xu et al., 2017).

Conversely, pro-apoptotic proteins of this family may suppress cancer cell invasion and metastatic dissemination. Thus, Bax and Bad expression is associated with downregulation of MMP-2, -9, and -10 (Lee et al., 2010; Cekanova et al., 2015). Interestingly, Bax and Bid may downregulate tumor cell invasiveness, indirectly repressing the gene expression of c-Jun, cyclin D1, β-catenin, and Sp1, which are known to stimulate invasive properties and metastasis in breast cancer (Cekanova et al., 2015). In addition, Bad, Bim, and Puma were shown to suppress EMT, inhibiting related transcription factors, including Snai1, Sp1, Snai2, and Slug, and subsequent upregulation of epithelial phenotype markers (Kim et al., 2014; Cekanova et al., 2015; Merino et al., 2015).

Another member of the Bcl-2 family implicated in cancer cell migration, invasion and metastasis is Bnip3 (Maes et al., 2014; Chourasia et al., 2015), which is considered to be a pro-apoptotic Bcl-2 protein. Bnip3 also plays an important role in autophagy and mitophagy regulation (Chourasia et al., 2015). However, its role in cancer progression and metastasis remains highly controversial. Thus, in human triple-negative breast cancer (TNBC) the lack of Bnip3 results in tumor progression and metastasis via storage of dysfunctional mitochondria and subsequent ROS accumulation; the events that, as was discussed earlier, lead to expression of HIF-inducible genes including metastasis-related angiogenesis genes (Chourasia et al., 2015). Conversely, in melanoma cells Bnip3 silencing reduces the formation of lamellipodia and filopodia as well as cell migration through the downregulation of integrin-associated glycoprotein CD47, Rac1 and Cdc42 (Maes et al., 2014). Bnip3 in HCC may suppress metastasis through the JNK/Bnip3/SERCA/CaMKII axis, leading further to the cofilin/F-actin/lamellipodia inhibition (Shi et al., 2018). As mentioned above, Bnip3 is involved in autophagy, the process, which is tightly linked to EMT, migration

and metastasis. Specifically, Bnip3-dependent autophagy via hypoxia-induced ROS-modulated p38 MAPK and JNK activation contributes to keratinocytes migration (Zhang et al., 2019). In NSCLC Bnip3 supports metastasis via its modulation by aryl hydrocarbon receptor (AhR), which has an impact on Bnip3 proteasomal degradation and subsequent autophagy disturbance. These events result in decreased EMT progress (Tsai et al., 2017). Thus, Bnip3, depending on cancer cell type and hypoxic conditions, fulfills opposite functions in metastasis.

Analysis of clinical samples confirmed the participation of Bcl-2 pro-apoptotic members in metastasis formation. Increased expression of Bax, Bak and Puma is associated with a lack of vascular invasion in patients with oral squamous cell carcinoma (Coutinho-Camillo et al., 2010). Loss of Bax protein was demonstrated in retinoblastoma specimens with massive choroidal invasion (Singh et al., 2015). Downregulation of Bnip3 is characteristic of lymph node metastases in breast cancer (Koop et al., 2009). Conversely, in patients with renal cell carcinomas Bnip3 expression is correlated with lymph node metastasis (Macher-Goeppinger et al., 2017). Methylation of Bim and Bnip3 genes is associated with metastasis and the gene methylation rate is increased among colorectal and pancreatic cancer patients compared to healthy individuals (Shimizu et al., 2010; Mhaidat et al., 2017; Zhu et al., 2017). Interestingly, overexpression of pro-apoptotic Bcl-2 family members, except Bnip3, frequently correlates with decreased metastasis and favorable outcomes in patients with various cancer types (Chi et al., 2016).

Thus, anti-apoptotic members of the Bcl-2 family, including Bcl-2, Bcl-XL, Bcl-w, and Mcl-1, support the invasion and metastasis in various types of cancer. This positive influence is achieved through EMT, subsequent cytoskeleton rearrangement, overexpression of MMPs and uPA, and regulation of PI3K, p38 MAPK, Akt, and ERK. In contrast to anti-apoptotic proteins, almost all pro-apoptotic members, such as Bax, Bak, Bad, Bid, and Puma, were characterized by suppression of the metastatic potential of cancer cells. Despite Bnip3 being considered a pro-apoptotic member, its influence on metastasis remains highly controversial, likely due to its atypical BH3-domain contributing to autophagy-dependent processes (Mazure and Pouysségur, 2009). Bcl-2 family members play important role in the regulation of ROS production and activity of mitochondrial complexes leading to the activation of molecular pathways controlling invasion and metastasis. Moreover, the Bcl-2 family proteins affect cell migration of both malignant and normal tissues. Analysis of patient specimens with tumors confirms the participation of Bcl-2 family members in invasion and metastasis, which gives a reason to consider these proteins for target therapy.

ER-MITOCHONDRIA NETWORK AND METASTASIS

The endoplasmic reticulum (ER) is a crucial cellular Ca^{2+} reservoir, that coordinates Ca^{2+} signaling, protein synthesis and folding and traffic of properly folded proteins to the Golgi apparatus. Accumulation of misfolded proteins in the ER lumen triggers unfolded protein response (UPR), which is an adaptive signaling pathway to restore protein homeostasis (proteostasis). If accumulation of misfolded proteins remains unresolved activation of UPR signaling may lead to the initiation of apoptotic cascades. Crosstalk between apoptosis and UPR is maintained by mitochondria functioning partly due to contact sites with ER. These so-called mitochondria-associated ER membranes (MAMs) are key for Ca^{2+} transport between the ER and mitochondria to maintain cellular homeostasis and regulate ER stress. Moreover, MAMs form functional networks essential in determining pro-survival/pro-death and inflammation signaling (Malhotra and Kaufman, 2011).

As mentioned above, ER is a multifunctional organelle, the main function of which is to control protein-folding quality. Numerous factors may affect proper protein folding in the ER, including oxidative stress, hypoxia, glucose deficiency, viral infections and other physical/chemical stresses. As a result, it leads to ER stress and subsequent UPR. In mammals the UPR is carried out by three distinct ER-related transmembrane proteins, including protein kinase RNA-like ER kinase (PERK), endoribonuclease inositol-requiring enzyme 1 alpha (IRE1α/IRE1), and activating transcription factor 6 (ATF6) (Malhotra and Kaufman, 2011). In unstressed cell, ER-related transmembrane proteins including PERK, IRE1α/IRE1, and ATF6 are bound to immunoglobulin heavy chain protein/glucose-regulated protein 78 (BiP/GRP78). Under ER stress BiP dissociates from these proteins to trigger signaling pathways that result in the reduction of global protein synthesis, degradation of unfolded proteins and increase of protein-folding capacity of the ER (Lee, 2005).

Endoplasmic reticulum plays an important role in mitochondrial calcium signaling via the contact sites between mitochondria and ER (MERCs). The portion of membranes involved in these interactions defines the MAMs, which, as mentioned above, provide Ca^{2+} traffic between these organelles (Martinvalet, 2018). The transport of extracellular Ca^{2+} into the cytosol occurs through the voltage-gated, ligand-gated, and store-operated Ca^{2+}-channels (SOCCs) including Orai and/or transient receptor potential channels (TRPC). Orai1 and TRPC are activated through their binding to the stromal interaction molecule 1 (STIM1), which is the ER Ca^{2+}-sensor. Ca^{2+} transport from the cytosol and its accumulation in the ER depends on the action of ATP-driven sarco/ER Ca^{2+}-ATPase (SERCA) (Bower et al., 2017). Ca^{2+} is transported from the ER via 1,4,5-trisphosphate (IP3) and ryanodine receptors (IP3Rs, RyRs), after which Ca^{2+} invades the mitochondria through the voltage-dependent anion channels (VDACs) on the OMM (Báthori et al., 2006). Ca^{2+} then is transferred by the mitochondrial calcium uniporter (MCU) on the IMM (Martinvalet, 2018). Expression levels of these calcium-signaling proteins are frequently altered in numerous types of tumor cells (Singh et al., 2017) and most of all govern metastasis-related processes.

As mentioned above, ER is the main cellular Ca^{2+}-store. Decreased Ca^{2+} level in the ER results in STIM1 oligomerization and its transfer from ER to the plasma membrane where it promotes Orai1-dependent store-operated Ca^{2+} entry (SOCE) (Yang, 2018). A growing body of evidence indicates the existence

of an interplay between mitochondria and SOCE. Indeed, SOCE activation is accompanied by TRPC-modulated increase in cytosolic Na^+ level that in turn promotes the activation of mitochondrial Na^+/Ca^{2+} exchanger (NCLX) leading to mitochondrial Na^+ influx and Ca^{2+} efflux. Therefore, NCLX tightly regulates mitochondrial Ca^{2+} level and prevents excessive Ca^{2+} accumulation in mitochondria that can lead to the increase of the mtROS level and subsequent SOCE suppression via oxidation of redox-sensitive Cys195 of Orai1 (Ben-Kasus Nissim et al., 2017). Besides NCLX, the activity of SOCE-related proteins is regulated by Bcl-2. The mutations in BH1 domain of Bcl-2 protein leads to STIM1, Orai1-3, TRPC1 overexpression and SOCE enhancement (Chiu et al., 2018). It has been established, that hyperactive SOCE induced by STIM1 and Orai1 overexpression correlates with increased metastasis in different types of cancer. Intensified SOCE supports tumor cell invasion and migration by cytoskeleton rearrangement, ECM degradation and tumor microenvironment remodeling (Yang, 2018).

Sarco/ER Ca^{2+}-ATPase is a well-known regulator of Ca^{2+} stores in the ER and maintains the level of Ca^{2+} uptake and leak properties. Furthermore, SERCA inactivation associated with Yap deficiency has been shown to inhibit HCC metastasis through the cofilin/F-actin/lamellipodium pathway (Shi et al., 2018). Additionally, the downregulation of SERCA leads to a significant decrease in Ca^{2+} level in migrating cells that in turn inhibits cell migration and tracheogenesis (Bower et al., 2017). Other proteins localized to MAMs are VDAC and IP3R, the action of which is dependent on Bcl-2 family proteins and, in addition to their role in apoptosis, partly regulate Ca^{2+} signaling via their complex with MAM proteins (Monaco et al., 2015; Bittremieux et al., 2019). Anti-apoptotic family members Bcl-2, Bcl-XL, and Mcl-1 bind to VDACs and suppress mitochondrial Ca^{2+} transport that in turn supports cell migration and invasion (Huang et al., 2013, 2014; Fouqué et al., 2016). Both Bcl-2 and Bcl-XL interact with VDAC1 through BH4 domain; however, Bcl-XL BH4 is more effective than Bcl-2-BH4 in targeting VDAC1 activity (Monaco et al., 2015). Dissociation between these anti-apoptotic Bcl-2 family members and VDACs results in decreased migration of TNBC (Fouqué et al., 2016) and NSCLC cells (Huang et al., 2014). Bcl-2 family proteins could also interact with IP3R suppressing Ca^{2+}-release. Like VDACs, Bcl-2 binds IP3R through its BH4 domain inhibiting its activity. Besides Bcl-2, other anti-apoptotic family members, including Bcl-XL and Mcl-1, are able to influence IP3R activity and Ca^{2+} signaling, but their role in mitochondria-associated ER membrane-related calcium signaling still remains controversial (Eckenrode et al., 2010; Monaco et al., 2012). Also like VDACs, IP3R may regulate cell migration separately from its complex with Bcl-2 family members. It has been revealed, that inhibition of ryanodine receptor subtype IP3R3 and subsequent decrease in Ca^{2+} release results in suppression of the invasion and migration of glioblastoma cell lines and metastasis in glioblastoma mouse model (Kang et al., 2010). Overexpression of IP3R3, but not of IP3R1 and IP3R2, leads to stimulation of the migration properties of breast cancer cells sustaining Ca^{2+} signaling (Mound et al., 2017). Thus, IP3R could regulate cancer cell migration and metastasis through modifying calcium ER level.

Another MAM-related protein is Sig1R (stress-activated chaperone sigma-1 receptor). When ER stress is not activated, Sig1R cooperates with MAMs chaperone BiP/GRP78, whereas under activation of IP3Rs Sig1R dissociates from chaperone BiP and binds to IP3R3, leading to its stabilization at the MAM and increasing Ca^{2+} flux to the mitochondria (De Pinto and Palmieri, 1992; Naon and Scorrano, 2014). The expression level of MAM-associated Sig1R is increased in metastatic breast and colorectal cancer cells as compared to normal tissues (Gueguinou et al., 2017). Consistently with the above-mentioned MAM-related proteins, MCU also affects migration, invasion and metastasis. Silencing of this uniporter results in decreased mitochondrial Ca^{2+} level and ROS production, as well as migratory and invasiveness capacities. These findings are in good agreement with *in vivo* experiment. MCU gene deletion reduces tumor metastasis in TNBC MDA-MB-231 xenografts via HIF-1-dependent gene expression (Tosatto et al., 2016). Yu et al. (2017) demonstrated similar results in breast cancer MCF-7 cells by MCU overexpression, which leads to enhanced migratory and invasiveness potential *in vitro* and lung metastasis mouse model *in vivo*. Furthermore, overexpressed MCU was found in specimens from breast cancer patients with metastases. Thus, MCU expression correlates with migration and invasion of cancer cells, as well as with tumor metastasis, which has been proved by both *in vitro* and *in vivo* studies. Besides MAM-anchored proteins, UPR regulators, including PERK, IRE1 and BiP/GRP78, all influence the migration and metastasis. PERK as a key UPR sensor, also participates in MAM signaling (Verfaillie et al., 2012). A growing amount of evidence proves that UPR signaling and EMT reprogramming mutually activate each other. In gastric cancer cells knockdown of UPR-related proteins such as PERK, ATF4, and ATF6, decrease TGF-β expression and abrogates EMT under severe hypoxia (Shen et al., 2015). The inverse pattern in this UPR-EMT axis has been demonstrated in both *in vivo* and *in vitro* models of breast cancer: cells undergoing EMT have a branched ER structure and activated PERK–eIF2α link of the UPR, which helps cells to metastasize. Analysis of specimens from patients with breast, gastric, colon and lung metastatic tumors revealed correlations between expression of EMT and PERK–eIF2α genes (Feng et al., 2014). Additionally, ATF4, ATF6, another ER-transmembrane protein IRE1 and its-related X-box binding protein-1 (XBP1) play a role in metastatic progression. IRE1α regulates actin cytoskeleton rearrangement and influences the cell migration via filamin A in MEFs, fly, and zebrafish models (Urra et al., 2018). IRE1-XBP1 pathway is regulated by lysyl oxidase-like 2 (LOXL2) overexpression, and activates EMT via Snai1/2, ZEB2 and TCF3 transcription factors in breast carcinoma cells (Cuevas et al., 2017). Notably, XBP1 expression is significantly upregulated in tumor and lymph node metastases compared to normal tissues from patients with oral squamous cell carcinoma, and downregulated XBP1 expression results in decreased cell invasion capacity (Sun et al., 2018c). Thus, proteins of three distinct UPR branches, including PERK, ATF4, ATF6, IRE1, XBP1, and BiP/GRP78, contribute to cancer cell invasive properties and metastatic dissemination regulating MAM signaling (**Figure 3**).

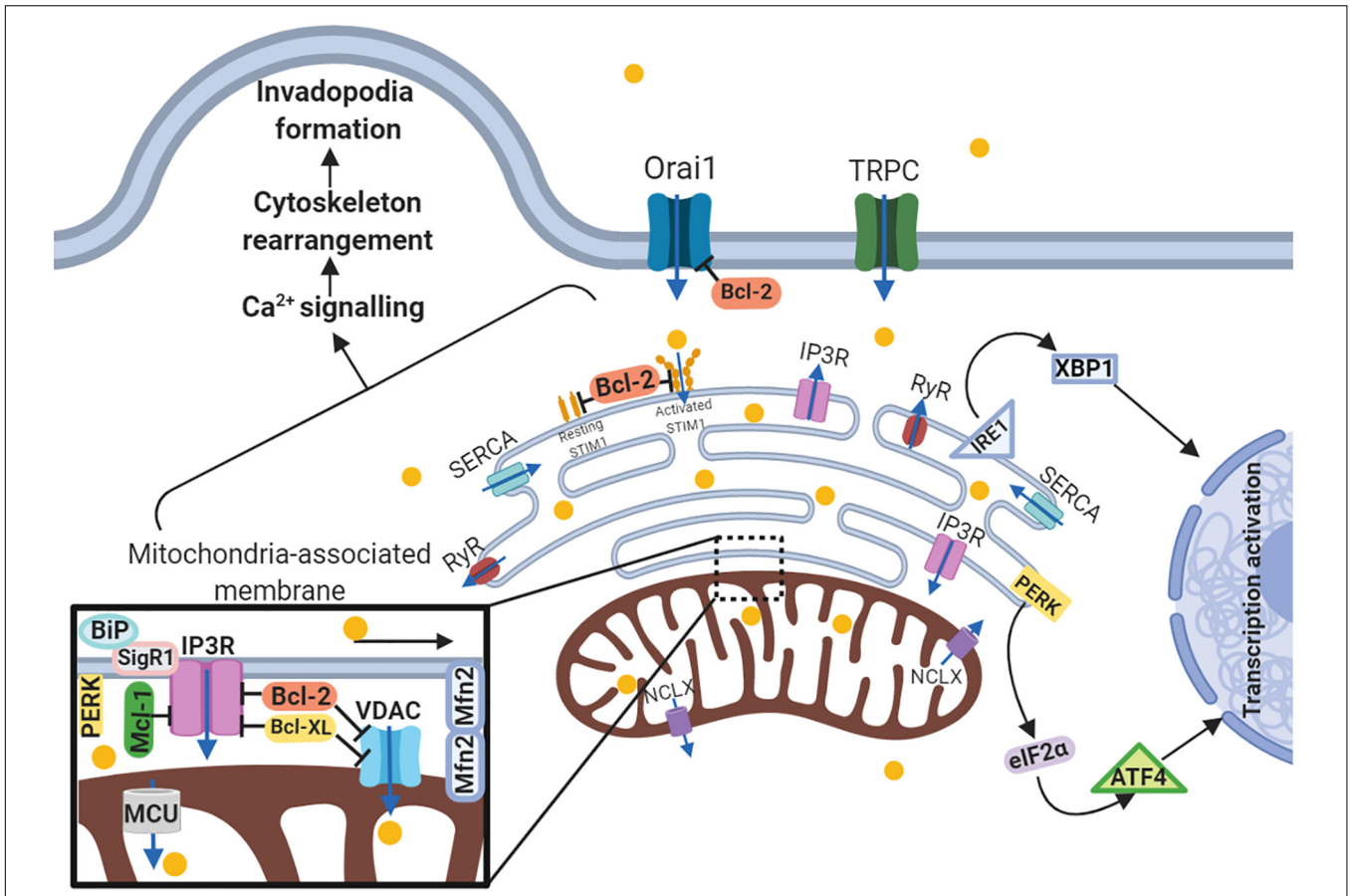

FIGURE 3 | Schematic representation of the link between ER-mitochondria network and motility of cancer cells. Arrows or blunt ends indicate activation or inhibition, respectively. Blue arrows indicate direction of Ca^{2+} current. Yellow circles – Ca^{2+}. MAM, mitochondria-associated ER membrane; Orai1, calcium release-activated calcium channel protein 1; TRPC, transient receptor potential cation channel; SERCA, sarco/endoplasmic reticulum Ca^{2+}-ATPase; STIM1, stromal interaction molecule 1; IP3R, inositol trisphosphate receptor; RyR, ryanodine receptor; IRE1, serine/threonine-protein kinase/endoribonuclease inositol-requiring enzyme 1; XBP1, X-box binding protein 1; PERK, protein kinase RNA-like endoplasmic reticulum kinase; eIF2α, eukaryotic translation initiation factor 2; ATF4, activating transcription factor 4; NCLX, mitochondrial Na^{+}/Ca^{2+} exchanger; BiP, binding immunoglobulin protein; SigR1, sigma receptor 1; Mfn2, mitofusin2; VDAC, voltage-dependent anion-selective channel; MCU, mitochondrial calcium uniporter. For details, see text. Figure is created using BioRender.

METABOLISM AND METASTASIS

Altered metabolic activity is one of the hallmarks of cancer. Cancer cells change their metabolism in order to satisfy increasing of bioenergetic and biosynthetic demand and maintain tumor growth (DeBerardinis and Chandel, 2016). Unlike normal cells, which generate much of their ATP via mitochondrial-dependent OXPHOS, cancer cells often demonstrate upregulation of glycolysis even under conditions when oxygen concentration is not limited (Lehuédé et al., 2016; Teoh and Lunt, 2018). This phenomenon was observed in the 1920s by Otto Warburg, who demonstrated that tumor tissues metabolize approximately ten-fold more glucose to lactate in a given time than do normal tissues, which led him to conclude that cancer cells rely on glycolysis more than do healthy cells. Enhanced aerobic glycolysis has been detected in many types of cancer and is correlated with worse clinical outcome (Yu et al., 2019). However, further studies have demonstrated that cancer cells may also engage mitochondrial respiration in addition to glycolysis (Jia et al., 2018). Indeed, breast cancer cells produce most of their ATP through mitochondrial oxidation (Park et al., 2016). Similarly, glioma cell lines are strongly dependent on mitochondrial OXPHOS for ATP production (Griguer et al., 2005). Moreover, cancer cells may display distinct metabolic characteristics depending on the tissue of origin (Elia et al., 2015). Thus, lung, liver and colorectal cancers, and leukemias depend on glycolysis, whereas, melanomas, lymphomas, and glioblastomas are characterized as oxidative tumors (Elia et al., 2015; Obre and Rossignol, 2015; Lehuédé et al., 2016). Tumor cells can also switch from one type of metabolism to another under glucose-limiting conditions as observed in cervical cancer, breast carcinoma, hepatoma and pancreatic cancer cells (Rossignol et al., 2004; Beckner et al., 2005; Jose et al., 2011; Smolková et al., 2010). A growing number of studies provide the evidence that cancer cell migration is associated with significant metabolic alterations supporting metastatic dissemination (Morandi et al., 2017; Teoh

and Lunt, 2018). Thus, it was reported that increased motility of cancer cells requires the shift toward utilization of glycolytic pathways (Shiraishi et al., 2015). Glycolytic genes activation has been detected in different tumors and is often associated with malignant and aggressive phenotypes (Jose et al., 2011). For example, expression of hexokinase 2 (HK2), the embryonic isoform of hexokinase, the enzyme which defines the start of glycolysis, is associated with increased risk of recurrence, and adverse clinical outcome for breast cancer, pancreatic cancer, and neuroblastoma patients (Teoh and Lunt, 2018). Further studies have demonstrated that glycolytic enzymes also contribute to the metastatic progression of cancer cells (Teoh and Lunt, 2018). For example, pyruvate kinase isozyme M2 (PKM2), which mediates the final rate-limiting step of glycolysis, promotes aggressive phenotype and metastasis in different types of tumors (Zhou et al., 2012; Yu et al., 2015; Teoh and Lunt, 2018). This enzyme also acts as a transcriptional coactivator of HIF-1α in cancer cells, thus promoting glycolysis and inducing EMT (Xu et al., 2012; Morandi et al., 2017). Furthermore, EMT stimulation induced by TGF-β leads to the nuclear translocation of PKM2 in colon cancer cells, where it interacts with TGIF2 and other transcription factors, promoting EMT and supporting the malignant properties of tumor cells (Hamabe et al., 2014). Phosphohexose isomerase (PHI) is another glycolytic enzyme that involved in stimulation of invasion and metastatic dissemination through extracellular autocrine motility factor (AMF) (Watanabe et al., 1996). The overexpression of PHI leads to the increased invasion and metastasis of colon cancer cells (Tsutsumi, 2009). Additionally, PHI/AMF overexpression has been reported to promote the EMT activation through the NF-κB pathway and increased expression of EMT markers such as Snai1 and ZEB1/2 (Ahmad et al., 2011). In keeping with these observations, high PHI levels in the serum correlate positively with metastases of colorectal and esophageal squamous cells, and lung tumors (Nakamori et al., 1994; Takanami et al., 1998). Conversely, downregulation of glycolytic enzymes including PKM2 and PHI, inhibit the proliferation and migration of cancer cells (Zhou et al., 2012; Teoh and Lunt, 2018). Inhibition of glycolysis attenuates cell motility even while mitochondrial ATP synthesis remains intact, and inhibition of mitochondrial respiration reduces cell motility only minimally compared to inhibition of glycolysis (Shiraishi et al., 2015).

Glycolysis regulates different stages of metastatic dissemination, contributing to the different stages of the metastatic cascade. Thus, prostate cancer cells undergoing EMT and acquiring mesenchymal features exhibit higher glycolytic activity than their epithelial counterparts. High glycolysis rate is associated with increased cytoskeletal rearrangement and cell migration. In turn, inhibition of glycolysis suppresses the migration properties of prostate cancer cells (Shiraishi et al., 2015). In addition, an interrelation between EMT induced by TGF-β, activation of the glycolytic pathway, and repression of mitochondrial function was demonstrated (Morandi et al., 2017). In breast cancer, loss of fructose-1,6-bisphosphatase together with the loss of E-cadherin promotes cancer stem cell (CSC)-like features and cancer cell dissemination by enhancing β-catenin signaling and the EMT program. These events are concomitant with the induction of glycolysis, increase in glucose uptake, and inhibition of oxygen consumption (Dong et al., 2013).

Although it is known that metastasis requires activation of the glycolytic program, recent studies demonstrate an equal importance of OXPHOS for metastatic dissemination (Porporato et al., 2018). For example, the strong correlation between expression of PGC-1*a* (peroxisome proliferator-activated receptor gamma coactivator-1*a*), a key regulator of mitochondrial biogenesis and OXPHOS, and invasive properties was observed in breast cancer cells (LeBleu et al., 2014). PGC-1*a* supports migration of cancer cells, stimulating mitochondrial biogenesis and respiration, whereas downregulation of PGC-1*a* decreases the frequency of metastasis. Elevated OXPHOS activity is also linked to the high metastatic potential in mouse melanoma and human cervical cancer cells (Porporato et al., 2014). In turn, prostate cancer cells exhibit a mixed phenotype, where both glycolysis and OXPHOS are required for energy metabolism at different stages of disease progression (Costello and Franklin, 2005). This hybrid metabolic state, also called metabolic plasticity, can sustain tumor cell survival under different micro-environmental conditions, while at the same time supporting tumor metastasis and therapy-resistance. Thus, a hybrid metabolic phenotype, characterized by high HIF-1/AMPK activities and high glycolysis/OXPHOS (glucose oxidation and FAO) activities, allows cancer cells to acquire metabolic plasticity and utilize different types of nutrients (Jia et al., 2019). Furthermore, it permits the cells to produce energy efficiently through multiple metabolic pathways and meanwhile synthesize biomass for rapid proliferation using by-products from glycolysis. A hybrid metabolic phenotype maintains the cellular ROS at a moderate level so that cancer cells can benefit from ROS signaling and avoid DNA damage due to excessive ROS (Vyas et al., 2016).

Finally, different metabolic profiles may dictate metastatic fitness to distinct organ sites (Lehuédé et al., 2016). It has been shown that metastatic breast cancer cells may display different metabolic pathways depending on the site of metastasis. Hence, breast cancer cells obtained from bone and lung metastases rely on OXPHOS, whereas liver-metastatic breast cancer cells engage a glycolytic type of metabolism (Dupuy et al., 2015).

In consequence, metabolic pathways of migrating cancer cells appear to be inter-connected and characterized by plasticity depending on different factors, i.e., tumor type, microenvironment, site of metastasis formation, etc. A better understanding of this metabolic plasticity will permit the design of specific therapy approaches in order to target metastatic cancer cells more efficiently.

THERAPEUTIC TARGETING METASTASIS

Metastasis is associated with poor outcome of cancer patients (Porporato et al., 2014). Existing therapeutic approaches are often ineffective or provide limited clinical benefit. Hence, mitochondria play an important role in metastatic dissemination, the targeting mitochondria might represent an attractive

approach for the development of new strategies for treatment of metastatic cancers.

Metastatic tumors have been shown to reprogram their metabolism in order to successfully metastasize (Lehuédé et al., 2016). Accordingly, significant efforts have been made to target cancer cell metabolism in different tumors for the prevention of metastasis progression. For example, the anti-diabetic drug metformin has been shown to possess anticancer properties in different types of cancer (Rattan et al., 2011; Schexnayder et al., 2018; Thakur et al., 2018). Metformin is a Complex I inhibitor, providing cancer metabolism suppression through downregulation of mitochondrial glycerophosphate dehydrogenase (mGPDH) and OXPHOS inhibition, leading to decreased metastasis levels in a thyroid cancer mouse model (Thakur et al., 2018). Metformin also attenuates the growth of lung metastatic nodules in an ovarian cancer mouse model by inhibiting the mTOR signaling pathway (Rattan et al., 2011). At low concentrations metformin inhibits breast cancer invasion and metastasis by suppressing ROS production, suggesting the use of metformin as a chemopreventive agent to block cancer cell invasiveness (Schexnayder et al., 2018). Although, the precise mechanisms of action of metformin are still debated, a number of clinical studies have confirmed its antitumor properties (Pollak, 2012). At present metformin is used during the treatment of different cancer types in order compound to inhibit hypoglycemia non-target effect of various chemotherapy drugs (da Veiga Moreira et al., 2019). Further clinical studies are required to clarify its anti-metastatic properties.

Glycolysis inhibition has been shown to suppress metastasis in several types of cancer (Caino and Altieri, 2016). For example, HKII inhibitor lonidamine (TH-070), a derivative of indazole-3-carboxylic acid, provided significant effectiveness in preclinical studies when the drug was administered in combination with paclitaxel and cisplatin (Sborov et al., 2015; Caino and Altieri, 2016). However, despite promising early stage results, further phase II and phase III trials targeting lung cancer with lonidamine have shown its limited efficacy and hepatic toxicity (Cervantes-Madrid et al., 2015). Importantly, a more recent study demonstrated that the use of modified lonidamine is significantly more efficacious in inhibiting mitochondrial bioenergetics in lung cancer cells, leading to suppression of lung cancer progression and metastasis. Mitochondrial-lonidamine activates the generation of ROS in lung cancer cells, which leads to the inactivation of the Akt/mTOR/p70S6K signaling pathways and autophagic cell death (Cheng et al., 2019). Glycolysis can be targeted by 2-deoxyglucose (2-DG), a non-metabolizable glucose analog, which is also pursued in the clinic. However, dose-escalation phase I trials in patients with castrate-resistant prostate cancer and other advanced solid tumors resulted in asymptomatic QTc prolongation that limited further drug evaluation (Sborov et al., 2015). Since tumors may shift from glycolysis to OXPHOS, or even engage hybrid metabolisms, several studies have proposed the dual inhibition of cancer metabolism using metformin and 2-DG (Cheong et al., 2011; Jia et al., 2019). Indeed, combined treatment with metformin and 2-DG led to the significant suppression of tumor growth and metastasis in preclinical models (Cheong et al., 2011).

Mitochondrial ROS have been reported to function as signaling molecules implicated in the regulation of tumor growth and metastasis (Porporato et al., 2014). The different mechanisms by which ROS contribute to tumor growth and metastatic dissemination were discussed above. Thus, targeting mtROS seems to be an attractive approach for cancer therapy. However, contrary to the expected results, the use of antioxidants for anticancer treatment led to increased risk of cancer (Klein et al., 2011; Sullivan and Chandel, 2014). Furthermore, the treatment with NAC was shown to enhance the metastatic dissemination of human melanoma cells, providing evidence that oxidative stress may, in certain circumstances, stimulate metastasis (Piskounova et al., 2015). The cause of the failure of treatment with antioxidants could be their lack of specificity. They also may regulate many different processes involved in tumor growth and metastasis (Sullivan and Chandel, 2014). On the other hand, it has been shown that inhibition of ROS with antioxidants that target precisely mitochondrial oxidative stress may stop metastatic spread. Scavenging with MitoTempo, specific mitochondrial antioxidant, significantly reduced cancer cell invasion and prevented metastasis (Porporato et al., 2014). Thus, ROS targeting appears to be more complex than believed before and requires further detailed investigation.

Another therapeutic agent that has shown promising results in preclinical studies is an inhibitor of mitochondrial heat shock protein 90 (Hsp90) Gamitrinib (Kang et al., 2011). This compound induces mitochondrial dysfunction, providing depolarization of inner membrane potential that in turn regulates the release of cytochrome *c*. In mouse model of prostate cancer, Gamitrinib administration inhibited tumor growth and metastasis affecting mitochondria (Kang et al., 2011). Furthermore, targeting Hsp90 with Gamitrinib suppresses cancer cell migration and metastasis preventing metabolic reprogramming and increasing AMPK phosphorylation (Caino et al., 2013), Gamitrinib is also effective in combination therapies with inhibitors of both TRAIL and PI3K (Siegelin et al., 2011; Ghosh et al., 2015).

Since the expression of Bcl-2 family proteins has been detected in metastases of different tumors, another possible approach for cancer therapy may be focused on targeting Bcl-2 family members. BH3-mimetics are promising therapeutic drugs that mimic endogenous Bcl-2 family member antagonists, thereby target some of them and abrogating their anti-apoptotic functions. Initially, BH3-mimetics displayed encouraged results in hematological malignancies including lymphoma lymphocytic leukemia, acute myeloid leukemia, small lymphocytic lymphoma and mantle-cell lymphoma (Cang et al., 2015; Mullard, 2016; DiNardo et al., 2018; Tam et al., 2018). Thus, first-generation BH3-mimetics such as ABT-737 and its orally available derivative navitoclax (ABT-263), which are inhibitors of Bcl-2 and Bcl-W, have shown clinical efficacy (Billard, 2013). However, in several cases the treatment with these agents was limited by severe thrombocytopenia (Mullard, 2016). Clinical studies of ABT-199 in chronic lymphocytic leukemia and non-Hodgkin's lymphoma have shown impressive antitumor efficacy, with higher response rates than navitoclax and without thrombocytopenia (Besbes et al., 2015). Several clinical trials have also demonstrated

the efficacy of BH3-mimetics in solid tumors (Boisvert-Adamo et al., 2009; McKee et al., 2013; Mukherjee et al., 2018). In particular Mcl-1 has emerged as a promising target for the treatment of melanoma (Boisvert-Adamo et al., 2009; McKee et al., 2013). Additionally, a novel gossypol derivative and BH3-mimetic ch282-5 (2-aminoethanesulfonic acid sodium-gossypolone) induced colon cancer cell death *in vitro* and *in vivo*. Ch282-5 treatment activated mitochondria-dependent apoptotic pathway accompanied by mitophagy disruption and mTOR pathway activation. Furthermore, Ch282-5 provided suppression of colon cancer cell migration, invasion and liver metastasis (Wang et al., 2016). Notably, Bcl-2 family members were shown to interact with Drp1 and treatment with BH3-mimetic A-1210477 led to Drp1-dependent mitochondria fragmentation, whereas Drp1 silencing significantly reduced apoptosis induced by BH3-mimetic in lung, cervical, and breast cancer cell lines (Milani et al., 2018). Conversely, inhibition of Drp1 in combination with BH3-mimetic treatment significantly enhanced apoptotic response in melanoma cells (Mukherjee et al., 2018). Additionally, inhibition of Drp1 by Mdivi-1 increased the cytotoxic effect of combination treatment with A-1210477 and ABT-263 in different melanoma cell lines (Mukherjee et al., 2018).

Another interesting approach to target metastatic cancers is the regulation of mitochondrial K^+/H^+ exchange. Salinomycin is an antibiotic from the polyether ionophores group widely used in agriculture (Managò et al., 2015). Recently, it has been revealed that it possesses anticancer properties in different types of cancer (Klose et al., 2019; Tang et al., 2011). Salinomycin may target chemoresistant tumor cells, inhibiting Wnt/β-catenin and Sonic Hedgehog signaling pathways (Managò et al., 2015). Furthermore, it suppresses the migration of colorectal, breast, lung and colon cancer cell lines as well the invasion of nasopharyngeal carcinoma and bladder cancer cells *in vitro* (Kopp et al., 2014; Wu et al., 2014; Qu et al., 2015; Klose et al., 2016). Consistently, *in vivo* studies proved that salinomycin may reduce metastasis formation in mammary tumor mouse model, bladder tumor rat model and intravenous mouse tumor model (Gupta et al., 2009; Kopp et al., 2014; Qu et al., 2015). Importantly, salinomycin is able to suppress the late stages of autophagy contributing to the ROS generation and mitochondria dysfunction (Klose et al., 2019). This might explain the mechanism by which salinomycin targets mitochondrial K^+/H^+ exchange and prevents migration, invasion and metastasis.

Summarizing, mitochondria contribute to tumor progression and metastasis through different mechanisms including redox signaling, mitochondrial biogenesis, regulating Bcl-2 family members, metabolic reprogramming and mitochondrial K^+/H^+ exchange. The better understanding of these mechanisms and the possible interplay between them may provide new therapeutic approaches to target metastatic diseases.

CONCLUSION

Mitochondria are very important and complex organelles that affect tumorigenesis and metastatic dissemination through different mechanisms including regulation of metabolism, redox status, signaling and cell death pathways. Recent evidence has demonstrated the existence of complex interplay between mitochondria-related functions and mitochondrial dynamics. Thus, dysregulated mitochondrial turnover contributes to tumorigenesis and metastases. However, the mechanisms connecting mitochondrial dynamics to the development of metastasis remain poorly understood. In addition, the flexibility of mitochondria that allow cancer cells to adapt to the changing microenvironment and stresses should be considered in order to combat cancer successfully. Consequently, a better understanding of the processes regulated by mitochondria and their complex interplay with mitochondrial biogenesis may offer new promising therapeutic strategies for cancer treatment.

AUTHOR CONTRIBUTIONS

All authors discussed the outline of the manuscript and involved in the preparation of the final version of the manuscript. TD and AG prepared the first draft, figure, and table.

FUNDING

This work was supported by the Grant from the Russian Science Foundation (19-15-00125). The work in the authors' laboratories is also supported by the Grant from the Russian Foundation for Basic Research (19-015-00332\19), the Swedish (190345) and Stockholm (181301) Cancer Societies. We apologize to those authors whose primary works could not be cited owing to space limitations.

REFERENCES

Adams, J. M., and Cory, S. (2018). The BCL-2 arbiters of apoptosis and their growing role as cancer targets. *Cell Death Differ.* 25, 27–36. doi: 10.1038/cdd.2017.161

Ahmad, A., Aboukameel, A., Kong, D., Wang, Z., Sethi, S., Chen, W., et al. (2011). Phosphoglucose Isomerase/Autocrine Motility factor mediates epithelial-mesenchymal transition regulated by miR-200 in breast cancer cells. *Cancer Res.* 71, 3400–3409. doi: 10.1158/0008-5472.CAN-10-0965

Báthori, G., Csordás, G., Garcia-Perez, C., Davies, E., and Hajnóczky, G. (2006). Ca^{2+} -dependent control of the permeability properties of the mitochondrial outer membrane and voltage-dependent anion-selective channel (VDAC). *J. Biol. Chem.* 281, 17347–17358. doi: 10.1074/jbc.M600906200

Beckner, M. E., Gobbel, G. T., Abounader, R., Burovic, F., Agostino, N. R., Laterra, J., et al. (2005). Glycolytic glioma cells with active glycogen synthase are sensitive to PTEN and inhibitors of PI3K and gluconeogenesis. *Lab. Invest.* 85, 1457–1470. doi: 10.1038/labinvest.3700355

Ben-Kasus Nissim, T., Zhang, X., Elazar, A., Roy, S., Stolwijk, J. A., Zhou, Y., et al. (2017). Mitochondria control store-operated Ca^{2+} entry through Na + and redox signals. *EMBO J.* 36, 797–815. doi: 10.15252/embj.201592481

Besbes, S., Mirshahi, M., Pocard, M., and Billard, C. (2015). New dimension in therapeutic targeting of BCL-2 family proteins. *Oncotarget* 6, 12862–12871. doi: 10.18632/oncotarget.3868

Billard, C. (2013). BH3 mimetics: status of the field and new developments. *Mol. Cancer Ther.* 12, 1691–1700. doi: 10.1158/1535-7163.MCT-13-0058

Bittremieux, M., La Rovere, R. M., Akl, H., Martines, C., Welkenhuyzen, K., Dubron, K., et al. (2019). Constitutive IP3 signaling underlies the sensitivity of B-cell cancers to the Bcl-2/IP3 receptor disruptor BIRD-2. *Cell Death Differ.* 26, 531–547. doi: 10.1038/s41418-018-0142-3

Boisvert-Adamo, K., Longmate, W., Abel, E. V., and Aplin, A. E. (2009). Mcl-1 is required for melanoma cell resistance to anoikis. *Mol. Cancer Res.* 7, 549–556. doi: 10.1158/1541-7786.MCR-08-0358

Bower, D. V., Lansdale, N., Navarro, S., Truong, T. V., Bower, D. J., Featherstone, N. C., et al. (2017). SERCA directs cell migration and branching across species and germ layers. *Biol. Open* 6, 1458–1471. doi: 10.1242/bio.026039

Caino, M. C., and Altieri, D. C. (2016). Molecular pathways: mitochondrial reprogramming in tumor progression and therapy. *Clin. Cancer Res.* 22, 540–545. doi: 10.1158/1078-0432.CCR-15-0460

Caino, M. C., Chae, Y. C., Vaira, V., Ferrero, S., Nosotti, M., Martin, N. M., et al. (2013). Metabolic stress regulates cytoskeletal dynamics and metastasis of cancer cells. *J. Clin. Invest.* 123, 2907–2920. doi: 10.1172/JCI67841

Caino, M. C., Seo, J. H., Aguinaldo, A., Wait, E., Bryant, K. G., Kossenkov, A. V., et al. (2016). A neuronal network of mitochondrial dynamics regulates metastasis. *Nat. Commun.* 7:13730. doi: 10.1038/ncomms13730

Cang, S., Iragavarapu, C., Savooji, J., Song, Y., and Liu, D. (2015). ABT-199 (venetoclax) and BCL-2 inhibitors in clinical development. *J. Hematol. Oncol.* 8:129. doi: 10.1186/s13045-015-0224-3

Cannito, S., Novo, E., di Bonzo, L. V., Busletta, C., Colombatto, S., and Parola, M. (2010). Epithelial–mesenchymal transition: from molecular mechanisms. Redox regulation to implications in human health and disease. *Antioxid. Redox Signal.* 12, 1383–1430. doi: 10.1089/ars.2009.2737

Cekanova, M., Fernando, R. I, Siriwardhana, N., Sukhthankar, M., De la Parra, C., Woraratphoka, J., et al. (2015). BCL-2 family protein, BAD is down-regulated in breast cancer and inhibits cell invasion. *Exp. Cell Res* 331, 1–10. doi: 10.1016/j.yexcr.2014.11.016

Cervantes-Madrid, D., Romero, Y., and Dueñas-González, A. (2015). Reviving lonidamine and 6-Diazo-5-oxo-L-norleucine to be used in combination for metabolic cancer therapy. *Biomed. Res. Int.* 2015, 1–13. doi: 10.1155/2015/690492

Chaffer, C. L., and Weinberg, R. A. (2011). A perspective on cancer cell metastasis. *Science* 331, 1559–1564. doi: 10.1126/science.1203543

Cheng, G., Zhang, Q., Pan, J., Lee, Y., Ouari, O., Hardy, M., et al. (2019). Targeting lonidamine to mitochondria mitigates lung tumorigenesis and brain metastasis. *Nat. Commun.* 10:2205. doi: 10.1038/s41467-019-10042-1

Cheong, J.-H., Park, E. S., Liang, J., Dennison, J. B., Tsavachidou, D., Nguyen-Charles, C., et al. (2011). Dual inhibition of tumor energy pathway by 2-deoxyglucose and metformin is effective against a broad spectrum of preclinical cancer models. *Mol. Cancer Ther.* 10, 2350–2362. doi: 10.1158/1535-7163.MCT-11-0497

Chi, H.-C., Chen, S.-L., Cheng, Y.-H., Lin, T.-K., Tsai, C.-Y., Tsai, M.-M., et al. (2016). Chemotherapy resistance and metastasis-promoting effects of thyroid hormone in hepatocarcinoma cells are mediated by suppression of FoxO1 and Bim pathway. *Cell Death Dis.* 7:e2324. doi: 10.1038/cddis.2016.227

Chiu, W.-T., Chang, H.-A., Lin, Y.-H., Lin, Y.-S., Chang, H.-T., Lin, H.-H., et al. (2018). Bcl-2 regulates store-operated Ca^{2+} entry to modulate ER stress-induced apoptosis. *Cell Death Discov.* 4:37. doi: 10.1038/s41420-018-0039-4

Chourasia, A. H., Tracy, K., Frankenberger, C., Boland, M. L., Sharifi, M. N., Drake, L. E., et al. (2015). Mitophagy defects arising from BNip3 loss promote mammary tumor progression to metastasis. *EMBO Rep.* 16, 1145–1163. doi: 10.15252/embr.201540759

Comito, G., Calvani, M., Giannoni, E., Bianchini, F., Calorini, L., Torre, E., et al. (2011). HIF-1α stabilization by mitochondrial ROS promotes Met-dependent invasive growth and vasculogenic mimicry in melanoma cells. *Free Radic. Biol. Med.* 51, 893–904. doi: 10.1016/j.freeradbiomed.2011.05.042

Corcoran, A., and Cotter, T. G. (2013). Redox regulation of protein kinases. *FEBS J.* 280, 1944–1965. doi: 10.1111/febs.12224

Costello, L. C., and Franklin, R. B. (2005). Why do tumour cells glycolyse?": from glycolysis through citrate to lipogenesis. *Mol. Cell. Biochem.* 280, 1–8. doi: 10.1007/s11010-005-8841-8

Coutinho-Camillo, C. M., Lourenço, S. V., Nishimoto, I. N., Kowalski, L. P., and Soares, F. A. (2010). Expression of Bcl-2 family proteins and association with clinicopathological characteristics of oral squamous cell carcinoma. *Histopathology* 57, 304–316. doi: 10.1111/j.1365-2559.2010.03621.x

Cuevas, E. P., Eraso, P., Mazón, M. J., Santos, V., Moreno-Bueno, G., Cano, A., et al. (2017). LOXL2 drives epithelial-mesenchymal transition via activation of IRE1-XBP1 signalling pathway. *Sci. Rep.* 7:44988. doi: 10.1038/srep44988

da Veiga Moreira, J., Hamraz, M., Abolhassani, M., Schwartz, L., Jolicoeur, M., et al. (2019). Metabolic therapies inhibit tumor growth in vivo and in silico. *Sci. Rep.* 9:3153. doi: 10.1038/s41598-019-39109-1

De Luise, M., Girolimetti, G., Okere, B., Porcelli, A. M., Kurelac, I., and Gasparre, G. (2017). Molecular and metabolic features of oncocytomas: seeking the blueprints of indolent cancers. *Biochim. Biophys. Acta Bioenerg.* 1858, 591–601. doi: 10.1016/j.bbabio.2017.01.009

De Pinto, V. D., and Palmieri, F. (1992). Transmembrane arrangement of mitochondrial porin or voltage-dependent anion channel (VDAC). *J. Bioenerg. Biomembr.* 24, 21–26. doi: 10.1007/bf00769526

DeBerardinis, R. J., and Chandel, N. S. (2016). Fundamentals of cancer metabolism. *Sci. Adv.* 2:e1600200. doi: 10.1126/sciadv.1600200

D'Ignazio, L., Batie, M., and Rocha, S. (2017). Hypoxia and inflammation in cancer, focus on HIF and NF-κB. *Biomedicines* 5:21. doi: 10.3390/biomedicines5020021

DiNardo, C. D., Pratz, K. W., Letai, A., Jonas, B. A., Wei, A. H., Thirman, M., et al. (2018). Safety and preliminary efficacy of venetoclax with decitabine or azacitidine in elderly patients with previously untreated acute myeloid leukaemia: a non-randomised, open-label, phase 1b study. *Lancet Oncol.* 19, 216–228. doi: 10.1016/S1470-2045(18)30010-X

Dong, C., Yuan, T., Wu, Y., Wang, Y., Fan, T. W. M., Miriyala, S., et al. (2013). Loss of FBP1 by snail-mediated repression provides metabolic advantages in basal-like breast cancer. *Cancer Cell* 23, 316–331. doi: 10.1016/j.ccr.2013.01.022

Duan, Y., He, Q., Yue, K., Si, H., Wang, J., Zhou, X., et al. (2017). Hypoxia induced Bcl-2/Twist1 complex promotes tumor cell invasion in oral squamous cell carcinoma. *Oncotarget* 8, 7729–7739. doi: 10.18632/oncotarget.13890

Dupuy, F., Tabariès, S., Andrzejewski, S., Dong, Z., Blagih, J., Annis, M. G., et al. (2015). PDK1-dependent metabolic reprogramming dictates metastatic potential in breast cancer. *Cell Metab.* 22, 577–589. doi: 10.1016/j.cmet.2015.08.007

Eckenrode, E. F., Yang, J., Velmurugan, G. V., Foskett, J. K., and White, C. (2010). Apoptosis protection by Mcl-1 and Bcl-2 modulation of inositol 1,4,5-trisphosphate receptor-dependent Ca^{2+} signaling. *J. Biol. Chem.* 285, 13678–13684. doi: 10.1074/jbc.M109.096040

Elia, I., Schmieder, R., Christen, S., and Fendt, S.-M. (2015). Organ-specific cancer metabolism and its potential for therapy. *Hand. Exp. Pharmacol.* 233, 321–353. doi: 10.1007/164_2015_10

Favre, C., Zhdanov, A., Leahy, M., Papkovsky, D., and O'Connor, R. (2010). Mitochondrial pyrimidine nucleotide carrier (PNC1) regulates mitochondrial biogenesis and the invasive phenotype of cancer cells. *Oncogene* 29, 3964–3976. doi: 10.1038/onc.2010.146

Feng, Y.-X., Sokol, E. S., Del Vecchio, C. A., Sanduja, S., Claessen, J. H. L., Proia, T. A., et al. (2014). Epithelial-to-mesenchymal transition activates PERK-eIF2 and sensitizes cells to endoplasmic reticulum stress. *Cancer Discov.* 4, 702–715. doi: 10.1158/2159-8290.CD-13-0945

Fouqué, A., Lepvrier, E., Debure, L., Gouriou, Y., Malleter, M., Delcroix, V., et al. (2016). The apoptotic members CD95. BclxL and Bcl-2 cooperate to promote cell migration by inducing Ca2+ flux from the endoplasmic reticulum to mitochondria. *Cell Death Differ.* 23, 1702–1716. doi: 10.1038/cdd.2016.61

Galadari, S., Rahman, A., Pallichankandy, S., and Thayyullathil, F. (2017). Reactive oxygen species and cancer paradox: to promote or to suppress? *Free Radic. Biol. Med.* 104, 144–164. doi: 10.1016/j.freeradbiomed.2017.01.004

Geng, M., Wang, L., and Li, P. (2013). Correlation between chemosensitivity to anticancer drugs and Bcl-2 expression in gastric cancer. *Int. J. Clin. Exp. Pathol.* 6, 2554–2559.

Ghosh, J. C., Siegelin, M. D., Vaira, V., Faversani, A., Tavecchio, M., Chae, Y. C., et al. (2015). adaptive mitochondrial reprogramming and resistance to PI3K therapy. *JNCI J. Natl. Cancer Inst.* 107, doi: 10.1093/jnci/dju502

Gogvadze, V., Orrenius, S., and Zhivotovsky, B. (2008). Mitochondria in cancer cells: what is so special about them? *Trends Cell Biol.* 18, 165–173. doi: 10.1016/j.tcb.2008.01.006

Gorrini, C., Harris, I. S., and Mak, T. W. (2013). Modulation of oxidative stress as an anticancer strategy. *Nat. Rev. Drug Discov.* 12, 931–947. doi: 10.1038/nrd4002

Griguer, C. E., Oliva, C. R., and Gillespie, G. Y. (2005). Glucose metabolism heterogeneity in human and mouse malignant glioma cell lines. *J. Neurooncol.* 74, 123–133. doi: 10.1007/s11060-004-6404-6

Gueguinou, M., Crottès, D., Chantôme, A., Rapetti-Mauss, R., Potier-Cartereau, M., Clarysse, L., et al. (2017). The SigmaR1 chaperone drives breast and colorectal cancer cell migration by tuning SK3-dependent Ca^{2+} homeostasis. *Oncogene* 36, 3640–3647. doi: 10.1038/onc.2016.501

Guha, M., Srinivasan, S., Ruthel, G., Kashina, A. K., Carstens, R. P., Mendoza, A., et al. (2014). Mitochondrial retrograde signaling induces epithelial–mesenchymal transition and generates breast cancer stem cells. *Oncogene* 33, 5238–5250. doi: 10.1038/onc.2013.467

Gupta, P. B., Onder, T. T., Jiang, G., Tao, K., Kuperwasser, C., Weinberg, R. A., et al. (2009). Identification of selective inhibitors of cancer stem cells by high-throughput screening. *Cell* 138, 645–659. doi: 10.1016/j.cell.2009.06.034

Hamabe, A., Konno, M., Tanuma, N., Shima, H., Tsunekuni, K., Kawamoto, K., et al. (2014). Role of pyruvate kinase M2 in transcriptional regulation leading to epithelial-mesenchymal transition. *Proc. Natl. Acad. Sci. U.S.A.* 111, 15526–15531. doi: 10.1073/pnas.1407717111

Han, X.-J., Yang, Z.-J., Jiang, L.-P., Wei, Y.-F., Liao, M.-F., Qian, Y., et al. (2015). Mitochondrial dynamics regulates hypoxia-induced migration and antineoplastic activity of cisplatin in breast cancer cells. *Int. J. Oncol.* 46, 691–700. doi: 10.3892/ijo.2014.2781

Hara, K., Hamada, C., Wakabayashi, K., Kanda, R., Kaneko, K., Horikoshi, S., et al. (2017). Scavenging of reactive oxygen species by astaxanthin inhibits epithelial–mesenchymal transition in high glucose-stimulated mesothelial cells. *PLoS One* 12:e0184332. doi: 10.1371/journal.pone.0184332

Ho, J.-N., Kang, G. Y., Lee, S.-S., Kim, J., Bae, I. H., Hwang, S.-G., et al. (2010). Bcl-XL and STAT3 mediate malignant actions of γ-irradiation in lung cancer cells. *Cancer Sci.* 101, 1417–1423. doi: 10.1111/j.1349-7006.2010.01552.x

Huang, H., Hu, X., Eno, C. O., Zhao, G., Li, C., and White, C. (2013). An interaction between Bcl-x L and the voltage-dependent anion channel (VDAC) promotes mitochondrial Ca^{2+} uptake. *J. Biol. Chem.* 288, 19870–19881. doi: 10.1074/jbc.M112.448290

Huang, H., Shah, K., Bradbury, N. A., Li, C., and White, C. (2014). Mcl-1 promotes lung cancer cell migration by directly interacting with VDAC to increase mitochondrial Ca^{2+} uptake and reactive oxygen species generation. *Cell Death Dis.* 5:e1482. doi: 10.1038/cddis.2014.419

Ishijima, N., Miki, C., Ishida, T., Kinoshita, T., and Suzuki, H. (1999). The immunohistochemical expression of BCL-2 oncoprotein in colorectal adenocarcinoma. *Surg. Today* 29, 682–684. doi: 10.1007/BF02483002

Ishikawa, K., Takenaga, K., Akimoto, M., Koshikawa, N., Yamaguchi, A., Imanishi, H., et al. (2008). ROS-generating mitochondrial DNA mutations can regulate tumor cell metastasis. *Science* 320, 661–664. doi: 10.1126/science.1156906

Jain, M., Rivera, S., Monclus, E. A., Synenki, L., Zirk, A., Eisenbart, J., et al. (2013). Mitochondrial reactive oxygen species regulate transforming growth factor-β signaling. *J. Biol. Chem.* 288, 770–777. doi: 10.1074/jbc.M112.431973

Jia, D., Lu, M., Jung, K. H., Park, J. H., Yu, L., Onuchic, J. N., et al. (2019). Elucidating cancer metabolic plasticity by coupling gene regulation with metabolic pathways. *Proc. Natl. Acad. Sci. U.S.A.* 116, 3909–3918. doi: 10.1073/pnas.1816391116

Jia, L., Huang, S., Yin, X., Zan, Y., Guo, Y., and Han, L. (2018). Quercetin suppresses the mobility of breast cancer by suppressing glycolysis through Akt-mTOR pathway mediated autophagy induction. *Life Sci.* 208, 123–130. doi: 10.1016/j.lfs.2018.07.027

Jiang, J., Wang, K., Chen, Y., Chen, H., Nice, E. C., and Huang, C. (2017). Redox regulation in tumor cell epithelial–mesenchymal transition: molecular basis and therapeutic strategy. *Signal Transduct. Target. Ther.* 2:17036. doi: 10.1038/sigtrans.2017.36

Jin-Song, Y., Zhao-Xia, W., Cheng-Yu, L., Xiao-Di, L., Ming, S., Yuan-Yuan, G., et al. (2011). Prognostic significance of Bcl-xL gene expression in human colorectal cancer. *Acta Histochem.* 113, 810–814. doi: 10.1016/j.acthis.2011.01.002

Jose, C., Bellance, N., and Rossignol, R. (2011). Choosing between glycolysis and oxidative phosphorylation: a tumor's dilemma? *Biochim. Biophys. Acta - Bioenerg.* 1807, 552–561. doi: 10.1016/j.bbabio.2010.10.012

Joseph, J. V., Conroy, S., Pavlov, K., Sontakke, P., Tomar, T., Eggens-Meijer, E., et al. (2015). Hypoxia enhances migration and invasion in glioblastoma by promoting a mesenchymal shift mediated by the HIF1α–ZEB1 axis. *Cancer Lett.* 359, 107–116. doi: 10.1016/j.canlet.2015.01.010

Jung, C.-H., Kim, E. M., Um, H.-D., Song, J.-Y., and Park, J. K. (2018). Pro-apoptotic Bax promotes mesenchymal-epithelial transition by binding to respiratory complex-I and antagonizing the malignant actions of pro-survival Bcl-2 proteins. *Cancer Lett.* 424, 127–135. doi: 10.1016/j.canlet.2018.03.033

Kang, B. H., Tavecchio, M., Goel, H. L., Hsieh, C.-C., Garlick, D. S., Raskett, C. M., et al. (2011). Targeted inhibition of mitochondrial Hsp90 suppresses localised and metastatic prostate cancer growth in a genetic mouse model of disease. *Br. J. Cancer* 104, 629–634. doi: 10.1038/bjc.2011.9

Kang, S. S., Han, K.-S., Ku, B. M., Lee, Y. K., Hong, J., Shin, H. Y., et al. (2010). Caffeine-mediated inhibition of calcium release channel inositol 1,4,5-trisphosphate receptor subtype 3 blocks glioblastoma invasion and extends survival. *Cancer Res.* 70, 1173–1183. doi: 10.1158/0008-5472.CAN-09-2886

Kim, E. M., Jung, C.-H., Song, J.-Y., Park, J. K., and Um, H.-D. (2018). Pro-apoptotic Bax promotes mesenchymal-epithelial transition by binding to respiratory complex-I and antagonizing the malignant actions of pro-survival Bcl-2 proteins. *Cancer Lett.* 424, 127–135. doi: 10.1016/j.canlet.2018.03.033

Kim, E. S., Choi, J. Y., Hwang, S. J., and Bae, I. H. (2019). Hypermethylation of miR-205-5p by IR governs aggressiveness and metastasis via regulating Bcl-w and Src. *Mol. Ther. Nucleic Acids* 14, 450–464. doi: 10.1016/j.omtn.2018.12.013

Kim, S., Yao, J., Suyama, K., Qian, X., Qian, B.-Z., Bandyopadhyay, S., et al. (2014). Slug promotes survival during metastasis through suppression of Puma-mediated apoptosis. *Cancer Res.* 74, 3695–3706. doi: 10.1158/0008-5472.CAN-13-2591

Kiss, B., Skuginna, V., Fleischmann, A., Bell, R. H., Collins, C., Thalmann, G. N., et al. (2015). Bcl-2 predicts response to neoadjuvant chemotherapy and is overexpressed in lymph node metastases of urothelial cancer of the bladder. *Urol. Oncol. Semin. Orig. Investig* 33:166.e1-8. doi: 10.1016/j.urolonc.2014.12.005

Klein, E. A., Thompson, I. M., Tangen, C. M., Crowley, J. J., Lucia, M. S., Goodman, P. J., et al. (2011). Vitamin E and the risk of prostate cancer. *JAMA* 306:1549. doi: 10.1001/jama.2011.1437

Klose, J., Eissele, J., Volz, C., Schmitt, S., Ritter, A., Ying, S., et al. (2016). Salinomycin inhibits metastatic colorectal cancer growth and interferes with Wnt/β-catenin signaling in CD133+ human colorectal cancer cells. *BMC Cancer* 16:896. doi: 10.1186/s12885-016-2879-8

Klose, J., Trefz, S., Wagner, T., Steffen, L., Preißendörfer Charrier, A., Radhakrishnan, P., et al. (2019). Salinomycin: anti-tumor activity in a pre-clinical colorectal cancer model. *PLoS One* 14:e0211916. doi: 10.1371/journal.pone.0211916

Koop, E. A., van Laar, T., van Wichen, D. F., de Weger, R. A., Wall, E., van der, et al. (2009). Expression of BNIP3 in invasive breast cancer: correlations with the hypoxic response and clinicopathological features. *BMC Cancer* 9:175. doi: 10.1186/1471-2407-9-175

Kopp, F., Hermawan, A., Oak, P. S., Herrmann, A., Wagner, E., and Roidl, A. (2014). Salinomycin treatment reduces metastatic tumor burden by hampering cancer cell migration. *Mol. Cancer* 13:16. doi: 10.1186/1476-4598-13-16

Kozma, R., Ahmed, S., Best, A., and Lim, L. (1995). The Ras-related protein Cdc42Hs and bradykinin promote formation of peripheral actin microspikes and filopodia in Swiss 3T3 fibroblasts. *Mol. Cell. Biol.* 15, 1942–1952. doi: 10.1128/MCB.15.4.1942

Krstić, J., Trivanović, D., Mojsilović, S., and Santibanez, J. F. (2015). Transforming growth factor-beta and oxidative stress interplay: implications in tumorigenesis and cancer progression. *Oxid. Med. Cell. Longev.* 2015, 1–15. doi: 10.1155/2015/654594

Kumari, S., Badana, A. K., G, M. M., G, S., and Malla, R. (2018). Reactive oxygen species: a key constituent in cancer survival. *Biomark. Insights* 13:117727191875539. doi: 10.1177/1177271918755391

Lamouille, S., Xu, J., and Derynck, R. (2014). Molecular mechanisms of epithelial–mesenchymal transition. *Nat. Rev. Mol. Cell Biol.* 15, 178–196. doi: 10.1038/nrm3758

LeBleu, V. S., O'Connell, J. T., Gonzalez Herrera, K. N., Wikman, H., Pantel, K., Haigis, M. C., et al. (2014). PGC-1α mediates mitochondrial biogenesis and oxidative phosphorylation in cancer cells to promote metastasis. *Nat. Cell Biol.* 16, 992–1003. doi: 10.1038/ncb3039

Lee, A. S. (2005). The ER chaperone and signaling regulator GRP78/BiP as a monitor of endoplasmic reticulum stress. *Methods* 35, 373–381. doi: 10.1016/j.ymeth.2004.10.010

Lee, G.-H., Yan, C., Shin, S.-J., Hong, S.-C., Ahn, T., Moon, A., et al. (2010). BAX inhibitor-1 enhances cancer metastasis by altering glucose metabolism and activating the sodium-hydrogen exchanger: the alteration of mitochondrial function. *Oncogene* 29, 2130–2141. doi: 10.1038/onc.2009.491

Lee, H. W., Lee, S.-S., Lee, S. J., and Um, H.-D. (2003). Bcl-w is expressed in a majority of infiltrative gastric adenocarcinomas and suppresses the cancer cell death by blocking stress-activated protein kinase/c-Jun NH2-terminal kinase activation. *Cancer Res* 63, 1093–1100.

Lee, S.-R., Yang, K.-S., Kwon, J., Lee, C., Jeong, W., and Rhee, S. G. (2002). Reversible inactivation of the tumor suppressor PTEN by H 2 O 2. *J. Biol. Chem.* 277, 20336–20342. doi: 10.1074/jbc.M111899200

Lee, W. S., Woo, E. Y., Kwon, J., Park, M.-J., Lee, J.-S., Han, Y.-H., et al. (2013). Bcl-w enhances mesenchymal changes and invasiveness of glioblastoma cells by inducing nuclear accumulation of β-Catenin. *PLoS One* 8:e68030. doi: 10.1371/journal.pone.0068030

Lehuédé, C., Dupuy, F., Rabinovitch, R., Jones, R. G., and Siegel, P. M. (2016). Metabolic plasticity as a determinant of tumor growth and metastasis. *Cancer Res.* 76, 5201–5208. doi: 10.1158/0008-5472.CAN-16-0266

Lin, C.-S., Lee, H.-T., Lee, S.-Y., Shen, Y.-A., Wang, L.-S., Chen, Y.-J., et al. (2012). High mitochondrial DNA copy number and bioenergetic function are associated with tumor invasion of esophageal squamous cell carcinoma cell lines. *Int. J. Mol. Sci.* 13, 11228–11246. doi: 10.3390/ijms130911228

Liu, R.-M., and Desai, L. P. (2015). Reciprocal regulation of TGF-β and reactive oxygen species: a perverse cycle for fibrosis. *Redox Biol.* 6, 565–577. doi: 10.1016/j.redox.2015.09.009

Losón, O. C., Song, Z., Chen, H., and Chan, D. C. (2013). Fis1. Mff, MiD49, and MiD51 mediate Drp1 recruitment in mitochondrial fission. *Mol. Biol. Cell* 24, 659–667. doi: 10.1091/mbc.e12-10-0721

Lu, Q., and Hong, W. (2009). Bcl2 enhances c-Myc-mediated MMP-2 expression of vascular smooth muscle cells. *Cell. Signal.* 21, 1054–1059. doi: 10.1016/j.cellsig.2009.02.020

Lu, W., and Kang, Y. (2019). Epithelial-mesenchymal plasticity in cancer progression and metastasis. *Dev. Cell* 49, 361–374. doi: 10.1016/j.devcel.2019.04.010

Macher-Goeppinger, S., Keith, M., Hatiboglu, G., Hohenfellner, M., Schirmacher, P., Roth, W., et al. (2017). Expression and functional characterization of the BNIP3 protein in renal cell carcinomas. *Transl. Oncol.* 10, 869–875. doi: 10.1016/j.tranon.2017.08.008

Maes, H., Van Eygen, S., Krysko, D. V., Vandenabeele, P., Nys, K., Rillaerts, K., et al. (2014). BNIP3 supports melanoma cell migration and vasculogenic mimicry by orchestrating the actin cytoskeleton. *Cell Death Dis.* 5, e1127. doi: 10.1038/cddis.2014.94

Malhotra, J. D., and Kaufman, R. J. (2011). ER stress and its functional link to mitochondria: role in cell survival and death. *Cold Spring Harb. Perspect. Biol.* 3:a004424. doi: 10.1101/cshperspect.a004424

Mambo, E., Chatterjee, A., Xing, M., Tallini, G., Haugen, B. R., Yeung, S.-C. J., et al. (2005). Tumor-specific changes in mtDNA content in human cancer. *Int. J. Cancer* 116, 920–924. doi: 10.1002/ijc.21110

Managò, A., Leanza, L., Carraretto, L., Sassi, N., Grancara, S., Quintana-Cabrera, R., et al. (2015). Early effects of the antineoplastic agent salinomycin on mitochondrial function. *Cell Death Dis.* 6:e1930. doi: 10.1038/cddis.2015.263

Martinvalet, D. (2018). The role of the mitochondria and the endoplasmic reticulum contact sites in the development of the immune responses. *Cell Death Dis.* 9:336. doi: 10.1038/s41419-017-0237-7

Mazure, N. M., and Pouysségur, J. (2009). Atypical BH3-domains of BNIP3 and BNIP3L lead to autophagy in hypoxia. *Autophagy* 5, 868–869. doi: 10.4161/auto.9042

McKee, C. S., Hill, D. S., Redfern, C. P. F., Armstrong, J. L., and Lovat, P. E. (2013). Oncogenic BRAF signalling increases Mcl-1 expression in cutaneous metastatic melanoma. *Exp. Dermatol.* 22, 767–769. doi: 10.1111/exd.12254

Merino, D., Best, S. A., Asselin-Labat, M.-L., Vaillant, F., Pal, B., Dickins, R. A., et al. (2015). Pro-apoptotic Bim suppresses breast tumor cell metastasis and is a target gene of SNAI2. *Oncogene* 34, 3926–3934. doi: 10.1038/onc.2014.313

Mhaidat, N. M., Al Sheyab, F. M., Zyoud, A. M., Alzoubi, K. H., Khabour, O. F., Al-Quraan, N. A., et al. (2017). Study the epigenetic down-regulation of Bim on colorectal cancer chemotherapy response. *J. King Saud Univ. Sci.* 31, 308–313. doi: 10.1016/j.jksus.2017.09.012

Milani, M., Byrne, D. P., Greaves, G., Butterworth, M., Cohen, G. M., Eyers, P. A., et al. (2018). DRP-1 is required for BH3 mimetic-mediated mitochondrial fragmentation and apoptosis. *Cell Death Dis.* 8:e2552. doi: 10.1038/cddis.2016.485

Min, C., Eddy, S. F., Sherr, D. H., and Sonenshein, G. E. (2008). NF-κB and epithelial to mesenchymal transition of cancer. *J. Cell. Biochem.* 104, 733–744. doi: 10.1002/jcb.21695

Mitchell, P. (1961). Coupling of phosphorylation to electron and hydrogen transfer by a chemi-osmotic type of mechanism. *Nature* 191, 144–148. doi: 10.1038/191144a0

Monaco, G., Beckers, M., Ivanova, H., Missiaen, L., Parys, J. B., De Smedt, H., et al. (2012). Profiling of the Bcl-2/Bcl-XL-binding sites on type 1 IP3 receptor. *Biochem. Biophys. Res. Commun.* 428, 31–35. doi: 10.1016/j.bbrc.2012.10.002

Monaco, G., Decrock, E., Arbel, N., van Vliet, A. R., La Rovere, R. M., De Smedt, H., et al. (2015). The BH4 Domain of Anti-apoptotic Bcl-XL, but Not That of the Related Bcl-2. Limits the Voltage-dependent Anion Channel 1 (VDAC1)-mediated Transfer of Pro-apoptotic Ca 2+ Signals to Mitochondria. *J. Biol. Chem.* 290, 9150–9161. doi: 10.1074/jbc.M114.622514

Morandi, A., Taddei, M. L., Chiarugi, P., and Giannoni, E. (2017). Targeting the metabolic reprogramming that controls epithelial-to-mesenchymal transition in aggressive tumors. *Front. Oncol.* 7:40. doi: 10.3389/fonc.2017.00040

Mound, A., Vautrin-Glabik, A., Foulon, A., Botia, B., Hague, F., Parys, J. B., et al. (2017). Downregulation of type 3 inositol (1,4,5)-trisphosphate receptor decreases breast cancer cell migration through an oscillatory Ca2+ signal. *Oncotarget* 8, 72324–72341. doi: 10.18632/oncotarget.20327

Mukherjee, N., Strosnider, A., Vagher, B., Lambert, K. A., Slaven, S., Robinson, W. A., et al. (2018). BH3 mimetics induce apoptosis independent of DRP-1 in melanoma. *Cell Death Dis.* 9:907. doi: 10.1038/s41419-018-0932-z

Mullard, A. (2016). Pioneering apoptosis-targeted cancer drug poised for FDA approval. *Nat. Rev. Drug Discov.* 15, 147–149. doi: 10.1038/nrd.2016.23

Naito, A., Cook, C. C., Mizumachi, T., Wang, M., Xie, C., Evans, T. T., et al. (2008). Progressive tumor features accompany epithelial-mesenchymal transition induced in mitochondrial DNA-depleted cells. *Cancer Sci.* 99, 1584–1588. doi: 10.1111/j.1349-7006.2008.00879.x

Nakamori, S., Watanabe, H., Kameyama, M., Imaoka, S., Furukawa, H., Ishikawa, O., et al. (1994). Expression of autocrine motility factor receptor in colorectal cancer as a predictor for disease recurrence. *Cancer* 74, 1855–1862. doi: 10.1002/1097-0142(19941001)74:7<1855

Naon, D., and Scorrano, L. (2014). At the right distance: ER-mitochondria juxtaposition in cell life and death. *Biochim. Biophys. Acta Mol. Cell Res.* 1843, 2184–2194. doi: 10.1016/j.bbamcr.2014.05.011

Narumiya, S., Tanji, M., and Ishizaki, T. (2009). Rho signaling. ROCK and mDia1, in transformation, metastasis and invasion. *Cancer Metastasis Rev.* 28, 65–76. doi: 10.1007/s10555-008-9170-7

Neri, A., Marrelli, D., Roviello, F., De Marco, G., Mariani, F., De Stefano, A., et al. (2006). Bcl-2 expression correlates with lymphovascular invasion and long-term prognosis in breast cancer. *Breast Cancer Res. Treat.* 99, 77–83. doi: 10.1007/s10549-006-9183-2

Noujaim, D., van Golen, C. M., van Golen, K. L., Grauman, A., and Feldman, E. L. (2002). N-Myc and Bcl-2 coexpression induces MMP-2 secretion and activation in human neuroblastoma cells. *Oncogene* 21, 4549–4557. doi: 10.1038/sj.onc.1205552

Obre, E., and Rossignol, R. (2015). Emerging concepts in bioenergetics and cancer research: metabolic flexibility, coupling, symbiosis, switch, oxidative tumors, metabolic remodeling, signaling and bioenergetic therapy. *Int. J. Biochem. Cell Biol.* 59, 167–181. doi: 10.1016/j.biocel.2014.12.008

Opferman, J. T., and Kothari, A. (2018). Anti-apoptotic BCL-2 family members in development. *Cell Death Differ.* 25, 37–45. doi: 10.1038/cdd.2017.170

Park, J. H., Vithayathil, S., Kumar, S., Sung, P.-L., Dobrolecki, L. E., Putluri, V., et al. (2016). Fatty acid oxidation-driven src links mitochondrial energy reprogramming and oncogenic properties in triple-negative breast cancer. *Cell Rep.* 14, 2154–2165. doi: 10.1016/j.celrep.2016.02.004

Piskounova, E., Agathocleous, M., Murphy, M. M., Hu, Z., Huddlestun, S. E., Zhao, Z., et al. (2015). Oxidative stress inhibits distant metastasis by human melanoma cells. *Nature* 527, 186–191. doi: 10.1038/nature15726

Pollak, M. N. (2012). Investigating metformin for cancer prevention and treatment: the end of the beginning. *Cancer Discov.* 2, 778–790. doi: 10.1158/2159-8290.CD-12-0263

Porporato, P. E., Filigheddu, N., Pedro, J. M. B.-S., Kroemer, G., and Galluzzi, L. (2018). Mitochondrial metabolism and cancer. *Cell Res.* 28, 265–280. doi: 10.1038/cr.2017.155

Porporato, P. E., Payen, V. L., Pérez-Escuredo, J., De Saedeleer, C. J., Danhier, P., Copetti, T., et al. (2014). A mitochondrial switch promotes tumor metastasis. *Cell Rep.* 8, 754–766. doi: 10.1016/j.celrep.2014.06.043

Qu, H., Ma, B., Yuan, H.-F., Wang, Z.-Y., Guo, S.-J., and Zhang, J. (2015). Effect of salinomycin on metastasis and invasion of bladder cancer cell line T24. *Asian Pac. J. Trop. Med.* 8, 578–582. doi: 10.1016/j.apjtm.2015.06.004

Quinlan, C. L., Perevoshchikova, I. V., Hey-Mogensen, M., Orr, A. L., and Brand, M. D. (2013). Sites of reactive oxygen species generation by mitochondria oxidizing different substrates. *Redox Biol.* 1, 304–312. doi: 10.1016/j.redox.2013.04.005

Rattan, R., Graham, R. P., Maguire, J. L., Giri, S., and Shridhar, V. (2011). Metformin suppresses ovarian cancer growth and metastasis with enhancement of cisplatin cytotoxicity in vivo. *Neoplasia* 13, 483–491.

Ridley, A. J. (2011). Life at the leading edge. *Cell* 145, 1012–1022. doi: 10.1016/j.cell.2011.06.010

Rojo de la Vega, M., Chapman, E., and Zhang, D. D. (2018). NRF2 and the Hallmarks of Cancer. *Cancer Cell* 34, 21–43. doi: 10.1016/j.ccell.2018.03.022

Rossignol, R., Gilkerson, R., Aggeler, R., Yamagata, K., Remington, S. J., and Capaldi, R. A. (2004). Energy substrate modulates mitochondrial structure and oxidative capacity in cancer cells. *Cancer Res.* 64, 985–993. doi: 10.1158/0008-5472.can-03-1101

Sborov, D. W., Haverkos, B. M., and Harris, P. J. (2015). Investigational cancer drugs targeting cell metabolism in clinical development. *Expert Opin. Investig. Drugs* 24, 79–94. doi: 10.1517/13543784.2015.960077

Schexnayder, C., Broussard, K., Onuaguluchi, D., Poché, A., Ismail, M., McAtee, L., et al. (2018). Metformin inhibits migration and invasion by suppressing ROS production and COX2 expression in MDA-MB-231 breast cancer cells. *Int. J. Mol. Sci.* 19:3692. doi: 10.3390/ijms19113692

Senft, D., and Ronai, Z. A. (2016). Regulators of mitochondrial dynamics in cancer. *Curr. Opin. Cell Biol.* 39, 43–52. doi: 10.1016/j.ceb.2016.02.001

Shagieva, G., Domnina, L., Makarevich, O., Chernyak, B., Skulachev, V., and Dugina, V. (2017). Depletion of mitochondrial reactive oxygen species downregulates epithelial-to-mesenchymal transition in cervical cancer cells. *Oncotarget* 8, 4901–4913. doi: 10.18632/oncotarget.13612

Shen, X., Xue, Y., Si, Y., Wang, Q., Wang, Z., Yuan, J., et al. (2015). The unfolded protein response potentiates epithelial-to-mesenchymal transition (EMT) of gastric cancer cells under severe hypoxic conditions. *Med. Oncol.* 32:447. doi: 10.1007/s12032-014-0447-0

Shi, C., Cai, Y., Li, Y., Li, Y., Hu, N., Ma, S., et al. (2018). Yap promotes hepatocellular carcinoma metastasis and mobilization via governing cofilin/F-actin/lamellipodium axis by regulation of JNK/Bnip3/SERCA/CaMKII pathways. *Redox Biol.* 14, 59–71. doi: 10.1016/j.redox.2017.08.013

Shimizu, S., Iida, S., Ishiguro, M., Uetake, H., Ishikawa, T., Takagi, Y., et al. (2010). Methylated BNIP3 gene in colorectal cancer prognosis. *Oncol. Lett.* 1, 865–872. doi: 10.3892/ol_00000153

Shimojo, Y., Akimoto, M., Hisanaga, T., Tanaka, T., Tajima, Y., Honma, Y., et al. (2013). Attenuation of reactive oxygen species by antioxidants suppresses hypoxia-induced epithelial-mesenchymal transition and metastasis of pancreatic cancer cells. *Clin. Exp. Metastasis* 30, 143–154. doi: 10.1007/s10585-012-9519-8

Shiraishi, T., Verdone, J. E., Huang, J., Kahlert, U. D., Hernandez, J. R., Torga, G., et al. (2015). Glycolysis is the primary bioenergetic pathway for cell motility and cytoskeletal remodeling in human prostate and breast cancer cells. *Oncotarget* 6, 130–143. doi: 10.18632/oncotarget.2766

Siegelin, M. D., Dohi, T., Raskett, C. M., Orlowski, G. M., Powers, C. M., Gilbert, C. A., et al. (2011). Exploiting the mitochondrial unfolded protein response for cancer therapy in mice and human cells. *J. Clin. Invest.* 121, 1349–1360. doi: 10.1172/JCI44855

Singh, A., Sharma, R. K., Chagtoo, M., Agarwal, G., George, N., Sinha, N., et al. (2017). 1H NMR metabolomics reveals association of high expression of inositol 1, 4, 5 trisphosphate receptor and metabolites in breast cancer patients. *PLoS One* 12:e0169330. doi: 10.1371/journal.pone.0169330

Singh, L., Pushker, N., Saini, N., Sen, S., Sharma, A., Bakhshi, S., et al. (2015). Expression of pro-apoptotic Bax and anti-apoptotic Bcl-2 proteins in human retinoblastoma. *Clin. Exp. Ophthalmol.* 43, 259–267. doi: 10.1111/ceo.12397

Smolková, K., Bellance, N., Scandurra, F., Génot, E., Gnaiger, E., Plecitá-Hlavatá, L., et al. (2010). Mitochondrial bioenergetic adaptations of breast cancer cells to aglycemia and hypoxia. *J. Bioenerg. Biomembr.* 42, 55–67. doi: 10.1007/s10863-009-9267-x

Smolková, K., Plecitá-Hlavatá, L., Bellance, N., Benard, G., Rossignol, R., and Ježek, P. (2011). Waves of gene regulation suppress and then restore oxidative phosphorylation in cancer cells. *Int. J. Biochem. Cell Biol.* 43, 950–968. doi: 10.1016/j.biocel.2010.05.003

Srinivasan, S., Guha, M., Kashina, A., and Avadhani, N. G. (2017). Mitochondrial dysfunction and mitochondrial dynamics-The cancer connection. *Biochim. Biophys. Acta - Bioenerg.* 1858, 602–614. doi: 10.1016/j.bbabio.2017.01.004

Sullivan, L. B., and Chandel, N. S. (2014). Mitochondrial reactive oxygen species and cancer. *Cancer Metab.* 2:17. doi: 10.1186/2049-3002-2-17

Sun, T., Sun, B., Zhao, X., Zhao, N., Dong, X., Che, N., et al. (2011). Promotion of tumor cell metastasis and vasculogenic mimicry by way of transcription coactivation by Bcl-2 and Twist1: a study of hepatocellular carcinoma. *Hepatology* 54, 1690–1706. doi: 10.1002/hep.24543

Sun, X., Cao, H., Zhan, L., Yin, C., Wang, G., Liang, P., et al. (2018a). Mitochondrial fission promotes cell migration by Ca^{2+} /CaMKII/ERK/FAK pathway in hepatocellular carcinoma. *Liver Int.* 38, 1263–1272. doi: 10.1111/liv.13660

Sun, X., Zhan, L., Chen, Y., Wang, G., He, L., Wang, Q., et al. (2018b). Increased mtDNA copy number promotes cancer progression by enhancing mitochondrial oxidative phosphorylation in microsatellite-stable colorectal cancer. *Signal Transduct. Target. Ther.* 3:8. doi: 10.1038/s41392-018-0011-z

Sun, Y., Jiang, F., Pan, Y., Chen, X., Chen, J., Wang, Y., et al. (2018c). XBP1 promotes tumor invasion and is associated with poor prognosis in oral squamous cell carcinoma. *Oncol. Rep.* 40, 988–998. doi: 10.3892/or.2018.6498

Takanami, I., Takeuchi, K., Naruke, M., Kodaira, S., Tanaka, F., Watanabe, H., et al. (1998). Autocrine motility factor in pulmonary adenocarcinomas: results of an immunohistochemical study. *Tumor Biol.* 19, 384–389. doi: 10.1159/000030031

Tam, C. S., Anderson, M. A., Pott, C., Agarwal, R., Handunnetti, S., Hicks, R. J., et al. (2018). Ibrutinib plus venetoclax for the treatment of mantle-cell lymphoma. *N. Engl. J. Med.* 378, 1211–1223. doi: 10.1056/NEJMoa1715519

Tang, Q.-L., Zhao, Z.-Q., Li, J.-C., Liang, Y., Yin, J.-Q., Zou, C.-Y., et al. (2011). Salinomycin inhibits osteosarcoma by targeting its tumor stem cells. *Cancer Lett.* 311, 113–121. doi: 10.1016/j.canlet.2011.07.016

Teoh, S. T., and Lunt, S. Y. (2018). Metabolism in cancer metastasis: bioenergetics, biosynthesis, and beyond. *Wiley Interdiscip. Rev. Syst. Biol. Med.* 10:e1406. doi: 10.1002/wsbm.1406

Thakur, S., Daley, B., Gaskins, K., Vasko, V. V., Boufraqech, M., Patel, D., et al. (2018). Metformin targets mitochondrial glycerophosphate dehydrogenase to control rate of oxidative phosphorylation and growth of thyroid cancer in vitro and in vivo. *Clin. Cancer Res.* 24, 4030–4043. doi: 10.1158/1078-0432.CCR-17-3167

Tosatto, A., Sommaggio, R., Kummerow, C., Bentham, R. B., Blacker, T. S., Berecz, T., et al. (2016). The mitochondrial calcium uniporter regulates breast cancer progression via HIF−1α. *EMBO Mol. Med.* 8, 569–585. doi: 10.15252/emmm.201606255

Trisciuoglio, D., Desideri, M., Ciuffreda, L., Mottolese, M., Ribatti, D., Vacca, A., et al. (2005). Bcl-2 overexpression in melanoma cells increases tumor progression-associated properties and in vivo tumor growth. *J. Cell. Physiol.* 205, 414–421. doi: 10.1002/jcp.20413

Trisciuoglio, D., Tupone, M. G., Desideri, M., Di Martile, M., Gabellini, C., Buglioni, S., et al. (2017). BCL-XL overexpression promotes tumor progression-associated properties. *Cell Death Dis.* 8, 3216. doi: 10.1038/s41419-017-0055-y

Tsai, C.-H., Li, C.-H., Cheng, Y.-W., Lee, C.-C., Liao, P.-L., Lin, C.-H., et al. (2017). The inhibition of lung cancer cell migration by AhR-regulated autophagy. *Sci. Rep.* 7:41927. doi: 10.1038/srep41927

Tsutsumi. (2009). Phosphoglucose isomerase enhances colorectal cancer metastasis. *Int. J. Oncol.* 35, 1117–1121. doi: 10.3892/ijo_00000427

Um, H.-D. (2016). Bcl-2 family proteins as regulators of cancer cell invasion and metastasis: a review focusing on mitochondrial respiration and reactive oxygen species. *Oncotarget* 7, 5193–5203. doi: 10.18632/oncotarget.6405

Urra, H., Henriquez, D. R., Cánovas, J., Villarroel-Campos, D., Carreras-Sureda, A., Pulgar, E., et al. (2018). IRE1α governs cytoskeleton remodelling and cell migration through a direct interaction with filamin A. *Nat. Cell Biol.* 20, 942–953. doi: 10.1038/s41556-018-0141-0

Verfaillie, T., Rubio, N., Garg, A. D., Bultynck, G., Rizzuto, R., Decuypere, J.-P., et al. (2012). PERK is required at the ER-mitochondrial contact sites to convey apoptosis after ROS-based ER stress. *Cell Death Differ.* 19, 1880–1891. doi: 10.1038/cdd.2012.74

Vyas, S., Zaganjor, E., and Haigis, M. C. (2016). Mitochondria and cancer. *Cell* 166, 555–566. doi: 10.1016/j.cell.2016.07.002

Wan, G., Mahajan, A., Lidke, D., and Rajput, A. (2015). Bcl-2 together with PI3K p110α regulates cell morphology and cell migration. *Cell Death Dis.* 6:e2006. doi: 10.1038/cddis.2015.345

Wang, X., Zhang, C., Yan, X., Lan, B., Wang, J., Wei, C., et al. (2016). A novel bioavailable BH3 mimetic efficiently inhibits colon cancer via cascade effects of mitochondria. *Clin. Cancer Res.* 22, 1445–1458. doi: 10.1158/1078-0432.CCR-15-0732

Wang, Z.-X., Yang, J.-S., Pan, X., Wang, J.-R., Li, J., Yin, Y.-M., et al. (2010). Functional and biological analysis of Bcl-xL expression in human osteosarcoma. *Bone* 47, 445–454. doi: 10.1016/j.bone.2010.05.027

Watanabe, H., Takehana, K., Date, M., Shinozaki, T., and Raz, A. (1996). Tumor cell autocrine motility factor is the neuroleukin/phosphohexose isomerase polypeptide. *Cancer Res.* 56, 2960–2963.

Wu, D., Zhang, Y., Huang, J., Fan, Z., Shi, F., and Wang, S. (2014). Salinomycin inhibits proliferation and induces apoptosis of human nasopharyngeal carcinoma cell in vitro and suppresses tumor growth in vivo. *Biochem. Biophys. Res. Commun.* 443, 712–717. doi: 10.1016/j.bbrc.2013.12.032

Xu, C., Liu, Y., Huang, J., Wang, H., Tan, L., Xu, Y., et al. (2017). The prognostic significance of MCL1 copy number gain in esophageal squamous cell carcinoma. *Oncotarget* 8, 87699–87709. doi: 10.18632/oncotarget.21181

Xu, Y., and Lu, S. (2015). Transforming growth factor-β1-induced epithelial to mesenchymal transition increases mitochondrial content in the A549 non-small cell lung cancer cell line. *Mol. Med. Rep.* 11, 417–421. doi: 10.3892/mmr.2014.2678

Xu, Y., Zhao, F., Wang, Z., Song, Y., Luo, Y., Zhang, X., et al. (2012). MicroRNA-335 acts as a metastasis suppressor in gastric cancer by targeting Bcl-w and specificity protein 1. *Oncogene* 31, 1398–1407. doi: 10.1038/onc.2011.340

Yang, S. (2018). The store-operated calcium channels in cancer metastasis from cell migration invasion to metastatic colonization. *Front. Biosci.* 23:4641. doi: 10.2741/4641

Yin, M., Lu, Q., Liu, X., Wang, T., Liu, Y., and Chen, L. (2016). Silencing Drp1 inhibits glioma cells proliferation and invasion by RHOA/ ROCK1 pathway. *Biochem. Biophys. Res. Commun.* 478, 663–668. doi: 10.1016/j.bbrc.2016.08.003

Yoon, Y.-S., Lee, J.-H., Hwang, S.-C., Choi, K. S., and Yoon, G. (2005). TGF beta1 induces prolonged mitochondrial ROS generation through decreased complex IV activity with senescent arrest in Mv1Lu cells. *Oncogene* 24, 1895–1903. doi: 10.1038/sj.onc.1208262

Young, A. I. J., Law, A. M. K., Castillo, L., Chong, S., Cullen, H. D., Koehler, M., et al. (2016). MCL-1 inhibition provides a new way to suppress breast cancer metastasis and increase sensitivity to dasatinib. *Breast Cancer Res.* 18:125. doi: 10.1186/s13058-016-0781-6

Yu, C., Wang, Y., Peng, J., Shen, Q., Chen, M., Tang, W., et al. (2017). Mitochondrial calcium uniporter as a target of microRNA-340 and promoter of metastasis via enhancing the Warburg effect. *Oncotarget* 8, 83831–83844. doi: 10.18632/oncotarget.19747

Yu, G., Yu, W., Jin, G., Xu, D., Chen, Y., Xia, T., et al. (2015). PKM2 regulates neural invasion of and predicts poor prognosis for human hilar cholangiocarcinoma. *Mol. Cancer* 14:193. doi: 10.1186/s12943-015-0462-6

Yu, M., Chen, S., Hong, W., Gu, Y., Huang, B., Lin, Y., et al. (2019). Prognostic role of glycolysis for cancer outcome: evidence from 86 studies. *J. Cancer Res. Clin. Oncol.* 145, 967–999. doi: 10.1007/s00432-019-02847-w

Zhang, C., Wang, H.-J., Bao, Q.-C., Wang, L., Guo, T.-K., Chen, W.-L., et al. (2016). NRF2 promotes breast cancer cell proliferation and metastasis by increasing RhoA/ROCK pathway signal transduction. *Oncotarget* 7, 73593–73606. doi: 10.18632/oncotarget.12435

Zhang, J., Zhang, C., Jiang, X., Li, L., Zhang, D., Tang, D., et al. (2019). Involvement of autophagy in hypoxia-BNIP3 signaling to promote epidermal keratinocyte migration. *Cell Death Dis.* 10:234. doi: 10.1038/s41419-019-1473-9

Zhang, K., Jiao, K., Xing, Z., Zhang, L., Yang, J., Xie, X., et al. (2014). Bcl-xL overexpression and its association with the progress of tongue carcinoma. *Int. J. Clin. Exp. Pathol.* 7, 7360–7377.

Zhang, W., Shi, X., Peng, Y., Wu, M., Zhang, P., Xie, R., et al. (2015). HIF-1α promotes epithelial-mesenchymal transition and metastasis through direct regulation of ZEB1 in colorectal cancer. *PLoS One* 10:e0129603. doi: 10.1371/journal.pone.0129603

Zhao, J., Zhang, J., Yu, M., Xie, Y., Huang, Y., Wolff, D. W., et al. (2013). Mitochondrial dynamics regulates migration and invasion of breast cancer cells. *Oncogene* 32, 4814–4824. doi: 10.1038/onc.2012.494

Zhou, C.-F., Li, X.-B., Sun, H., Zhang, B., Han, Y.-S., Jiang, Y., et al. (2012). Pyruvate kinase type M2 is upregulated in colorectal cancer and promotes proliferation and migration of colon cancer cells. *IUBMB Life* 64, 775–782. doi: 10.1002/iub.1066

Zhu, D., Li, Y., Zhang, L., Zhu, Y., Li, D., Zhou, J., et al. (2017). Methylation of BNIP3 in pancreatic cancer inhibits the induction of mitochondrial-mediated tumor cell apoptosis. *Oncotarget* 8, 63208–63222. doi: 10.18632/oncotarget.18736

Conflict of Interest: The authors declare that the research was conducted in the absence of any commercial or financial relationships that could be construed as a potential conflict of interest.

Copyright © 2019 Denisenko, Gorbunova and Zhivotovsky. This is an open-access article distributed under the terms of the Creative Commons Attribution License (CC BY). The use, distribution or reproduction in other forums is permitted, provided the original author(s) and the copyright owner(s) are credited and that the original publication in this journal is cited, in accordance with accepted academic practice. No use, distribution or reproduction is permitted which does not comply with these terms.

frontiers in Oncology

ORIGINAL RESEARCH
published: 22 January 2020
doi: 10.3389/fonc.2019.01479

Integrative Transcriptomic Analysis Reveals a Multiphasic Epithelial–Mesenchymal Spectrum in Cancer and Non-tumorigenic Cells

Nicholas Panchy[1,2], *Cassandra Azeredo-Tseng*[3,4], *Michael Luo*[5], *Natalie Randall*[6] *and Tian Hong*[1,2]*

[1] Department of Biochemistry & Cellular and Molecular Biology, The University of Tennessee, Knoxville, Knoxville, TN, United States, [2] National Institute for Mathematical and Biological Synthesis, Knoxville, TN, United States, [3] Department of Biochemistry, New College of Florida, Sarasota, FL, United States, [4] Department of Applied Mathematics, New College of Florida, Sarasota, FL, United States, [5] Department of Mathematics & Statistics, The College of New Jersey, Ewing Township, NJ, United States, [6] Department of Mathematics and Computer Science, Austin College, Sherman, TX, United States

OPEN ACCESS

Edited by:
Mohit Kumar Jolly,
Indian Institute of Science (IISc), India

Reviewed by:
Mingyang Lu,
Jackson Laboratory, United States
David Jordan Wooten,
Pennsylvania State University (PSU), United States

***Correspondence:**
Tian Hong
hongtian@utk.edu

Specialty section:
This article was submitted to Molecular and Cellular Oncology, a section of the journal Frontiers in Oncology

Received: *10 October 2019*
Accepted: *09 December 2019*
Published: *22 January 2020*

Citation:
Panchy N, Azeredo-Tseng C, Luo M, Randall N and Hong T (2020) Integrative Transcriptomic Analysis Reveals a Multiphasic Epithelial–Mesenchymal Spectrum in Cancer and Non-tumorigenic Cells. Front. Oncol. 9:1479. doi: 10.3389/fonc.2019.01479

Epithelial–mesenchymal transition (EMT), the conversion between rigid epithelial cells and motile mesenchymal cells, is a reversible cellular process involved in tumorigenesis, metastasis, and chemoresistance. Numerous studies have found that several types of tumor cells show a high degree of cell-to-cell heterogeneity in terms of their gene expression signatures and cellular phenotypes related to EMT. Recently, the prevalence and importance of partial or intermediate EMT states have been reported. It is unclear, however, whether there is a general pattern of cancer cell distribution in terms of the overall expression of epithelial-related genes and mesenchymal-related genes, and how this distribution is related to EMT process in normal cells. In this study, we performed integrative transcriptomic analysis that combines cancer cell transcriptomes, time course data of EMT in non-tumorigenic epithelial cells, and epithelial cells with perturbations of key EMT factors. Our statistical analysis shows that cancer cells are widely distributed in the EMT spectrum, and the majority of these cells can be described by an EMT path that connects the epithelial and the mesenchymal states via a hybrid expression region in which both epithelial genes and mesenchymal genes are highly expressed overall. We found that key patterns of this EMT path are observed in EMT progression in non-tumorigenic cells and that transcription factor ZEB1 plays a key role in defining this EMT path via diverse gene regulatory circuits connecting to epithelial genes. We performed Gene Set Variation Analysis to show that the cancer cells at hybrid EMT states also possess hybrid cellular phenotypes with both high migratory and high proliferative potentials. Our results reveal critical patterns of cancer cells in the EMT spectrum and their relationship to the EMT process in normal cells, and provide insights into the mechanistic basis of cancer cell heterogeneity and plasticity.

Keywords: hybrid EMT states, ZEB1, breast cancer, cell migration and proliferation, tumor cell heterogeneity

INTRODUCTION

Epithelial–mesenchymal transition (EMT) is a fundamental cellular process in which rigid epithelial cells convert to motile mesenchymal forms. Canonical EMT and its reversal, mesenchymal–epithelial transition (MET), occur in embryogenesis, and they are critical for the formation of body plans and new organs in metazoans (1, 2). Numerous reports have shown that EMT is also activated during acquisition of a metastatic phenotype by tumor cells (3–5). In this scenario, EMT enables cells to migrate to distant organs or invade adjacent tissues, whereas MET allows cells to settle and proliferate (6). Inhibitions of EMT or MET have been shown to reduce the metastatic potentials of tumor cells (7–9). In addition, EMT was shown to promote chemoresistance (10, 11), suggesting the multifaceted roles of EMT in cancer progression and treatment.

Recent data and theoretical studies suggest a remarkable diversity of normal and cancer epithelial cells in terms of their E and M properties. Particularly, mathematical models and experiments show that partial forms of EMT give rise to intermediate (or hybrid, or transition) cellular phenotypes that exist between the extreme E and extreme M states, and that such phenotypes can be stable (12–18). These intermediate phenotypes were observed in non-tumorigenic epithelial cells during the EMT process induced by extracellular stimuli, such as transforming growth factor beta (TGF-β) (19). While the precise roles of EMT and its associated cellular states in cancer progression may be complex, recent single-cell transcriptomic analysis showed that various tumor cells are enriched with intermediate EMT cellular phenotypes (20), suggesting the prevalence of such cell states during cancer progression. In addition, previous survival analysis has shown that the intermediate EMT states are associated with poor prognosis of breast cancer patients (21, 22). Together, these studies suggest the importance of understanding an EMT spectrum that contains intermediate cell states in cancer cells.

During EMT, cellular properties such as adhesion, motility, and proliferation are altered dramatically through the coordination of two major molecular programs (E and M). Previous transcriptomic studies showed that several hundred epithelial-related genes (E-genes) and mesenchymal-related genes (M-genes) are down-regulated and up-regulated, respectively (14, 23–25). Previously, one-dimensional EMT spectrums were used to describe the cellular diversity in EMT (14, 26). This approach is useful to understand multiple EMT phenotypes in a concise manner. However, given the complexity and importance of E- and M-gene coordination, the one-dimensional spectrums do not provide a complete view of EMT process and its associated cellular diversity. In more recent studies, landscapes of cellular states in both E-gene activity and M-gene activity are used to describe cancer cell transcriptomes and specific perturbations leading to EMT/MET (27). Nonetheless, general patterns of cancer cell distributions in the two-dimensional EMT spectrum are unclear, and it is not known how such distributions are related to the EMT process in normal cells. In addition, it is not clear whether the multiple steps of EMT marked by the intermediate EMT state(s) involve the same degree of the coordination between E and M programs.

In this study, we performed integrative transcriptomic analysis that combines cancer cell transcriptomes, time course data during EMT induction, and transcriptomic changes upon perturbations of EMT factors. We systematically characterized the distributions of cancer and non-tumorigenic cells in terms of their E-gene and M-gene activities with Gene Set Variation Analysis (GSVA) and statistical models. We found that there is a significant diversity of cancer cells in their E-gene and M-gene activities, which cannot be described by an EMT spectrum that assumes linear coordination between E and M programs. We identified a non-linear EMT path that connects E and M, and hybrid cell states can be used to describe a large fraction of cancer cells in multiple organs. Notably, this EMT path involves a region in which the activities of E-genes and M-genes are both relatively high, and the pattern of this path is consistent with the EMT process in non-tumorigenic epithelial cells with respect to time. We identified key regulators that may contribute the multiphasic EMT that is elucidated by the EMT path. We found that the hybrid EMT gene expression region also corresponds to cell states with hybrid cellular phenotypes, including high motility and proliferative potentials. Together, our analyses characterized the multiphasic nature of EMT in a comprehensive and quantitative manner, and elucidated the connection between the diversity of cancer cells and the normal EMT progression in gene expression space, suggesting that multiple attractors in EMT are an intrinsic property that is reflected in both cancer and normal cells.

METHODS

Transcriptomic Data

RNA-seq-based gene expression data were obtained for 1,215 invasive breast carcinoma samples (BRCA), 183 pancreas adenocarcinoma samples (PAAD), 576 lung adenocarcinoma samples (LUAD), 309 cervical squamous cell carcinoma and endocervical adenocarcinoma samples (CESC), and 550 prostate adenocarcinoma samples (PRAD) from The Cancer Genome Atlas (TCGA) using the R package "TCGABiolinks" (28, 29). These data were pre-processed via upper quartile normalization of RNA-Seq by Expectation Maximization (RSEM). Previous studies using TCGA transcriptome data have elucidated key factors contributing to cancer cell plasticity (24, 30, 31). As a control for non-EMT cancer cell types, we also obtained 173 acute myeloid leukemia cell samples (LAML) from TCGA. Time course transcriptomic data for TGF-β-treated MCF10A cells were obtained from a recent study by Zhang et al. (32). Transcriptome data for combinatorial perturbations of TGF-β and ZEB1 in MCF10A cells were obtained from a recent study by Watanabe et al. (23). Both of the Zhang et al. and Watanabe et al. studies employed RNA-Seq data and normalized the results as fragments per kilobase million (FPKM).

E and M Scores

We computed scores for E and M scores with GSVA (33). For each sample (one transcriptome), we used a list of E-genes and a list of M-genes from Tan et al. (26) as two signature gene sets

to compute the two scores, respectively. Briefly, GSVA estimates a cumulative density function for each gene using all samples, ranks genes across samples, and then calculates a score between −1 and 1 for each gene set using the Kolmogorov–Smirnov random walk statistic. GSVA scoring was implemented using the R package "GSVA" (33). The scoring procedure is illustrated in **Figure 1**.

Gaussian Mixture Model

We built Gaussian Mixture Models (GMMs) for cancer cell transcriptomes in terms of their E and M scores to infer the subpopulations in the EMT spectrum. We tested one to nine subpopulations, and we used Bayesian Information Criteria to select the optimal number of subpopulations (**Supplementary Tables 1–5**). For each number of subpopulations, we tested six different models based on various assumptions on covariance [excluding those that allowed for non-diagonal or cluster-specific relationships among E and M scores between models (34)]. Among the models with different numbers of subpopulations, we selected the best subpopulation number using the best score based on Bayesian Information Criterion (BIC). We found that the five-cluster models had the lowest BIC scores in terms of both mean score in covariance models and the minimum score (**Supplementary Figure 1**). We therefore selected five-cluster models for the subsequent analysis. To select the most representative model with a particular assumption of covariance from the models with the best subpopulation number, we compared the distributions of all candidate models and selected those with the most consistent distribution across all models. We found that the covariance assumptions EII, EEI, VEI, and VVI (34) generated the most robust models within data sets, except for the LUAD data where there was a significant difference between equal volume models (EII, EEI) and unequal variance (VEI and VVI) (**Supplementary Figure 2**). While the unequal variance models had slightly better BIC, model predictions overall had higher uncertainty values (**Supplementary Figure 3**). As such, we chose to exclude unequal volume models and used EII for clustering transcriptome data except BRCA, where it was outscored by EEI but gave similar results. GMMs were implemented using the "mclust" package in R (34). To show that our main conclusions are not sensitive to the choice of the five-cluster models, we performed additional analysis with four-cluster and six-cluster models, which had BIC scores moderately higher than those with five-cluster models (**Supplementary Figure 1**). Although our main analysis focused on five-cluster models, additional comparisons of these models were performed, and they are described in later sections.

Segmented Regression

To infer the one-dimensional EMT spectrums (EMT paths) from the two-dimensional scores, we used segmented regression models (35). For cancer cells with ample amount of data and significant heterogeneity of multiple possible EMT paths, the models were based on consecutive sample clusters that can be sequentially ordered in the E–M space by adjacency, and the assumption that paths must proceed from the most extreme E to the most extreme M state by passing through the minimum number of clusters (i.e., four clusters in BRCA, three clusters in all others). In the regression model, we chose the independent variable to be the projection of a pair of E–M scores onto a straight line crossing with the origin with slope of −1, representing a hypothetical linear progression of EMT, and the dependent variable to be the projection onto its orthogonal line, representing the deviation from the linear EMT progression. For time course TGF-β-driven EMT data with the time labels as the unambiguous independent variable, all data points were used to infer two models (E and M scores as functions of time). In all models, piecewise relationships between E and M scores were obtained. To test the existence of non-zero difference in slope parameter, we employed the Davies' test and a pseudo Score statistic test with a null hypothesis that there is a zero difference in slopes (36–38). Models with one to four breakpoints were then tested, and the respective maximum adjusted R^2 values were used to select the best model (see **Supplementary Table 6**). For time course data, we used the E score and M scores relative to time to estimate breakpoints between 2 and 3 days (stating value = 2.5 days) and between 8 and 12 days (stating value = 10 days) for both E and M, respectively, and compared them to models with only one breakpoint. We found that the E scores only supported a segmented breakpoint when both breakpoints were used, while the two-breakpoint M score model outperformed a model with one breakpoint, which was always placed around 8 days (adjusted R^2, 0.941 vs. 0.939). The approach we use to estimate breakpoint positions calculate a 95% confidence interval using a score-based approach that accounts for the non-differentiable, non-concave nature of likelihood function for breakpoints (35, 39) and we found that the confidence interval of the first E break point (0–4.6 days) covered the most sampled time points and therefore had the greatest impact on the time course model. Therefore, to find the upper and lower bound for the time course model, we modified the model by placing the first E break point at the extremes of the confidence interval (i.e., 0 days and 4.6 days). Comparably, the confidence interval of other breakpoints was either too small (0–1.25 days for the first M) or the range was between time samples (i.e., between 8 and 12 days for the second E and M breakpoint), such that varying them had little impact on the model as they did not alter the division of samples into different segments. Segmented models and analysis were implemented using the "segmented" package in R (39).

Differences in TES Scores and EMT Factors Expression Between Clusters

Differences in TES scores and EMT gene expression between clusters were assessed using Welch's *t*-test, and the resulting *p*-values were adjusted using Benjamini–Hochberg correction for multiple hypothesis testing. Expression of individual genes in TCGA data sets was measured using normalized RSEM values derived from the TCGA processing pipeline (40).

Clustering of E- and M-Genes

To infer clusters of E- and M-genes controlled by different regulatory circuits that connect to TGF-β and ZEB1, we employed a semi-supervised learning method that we used in

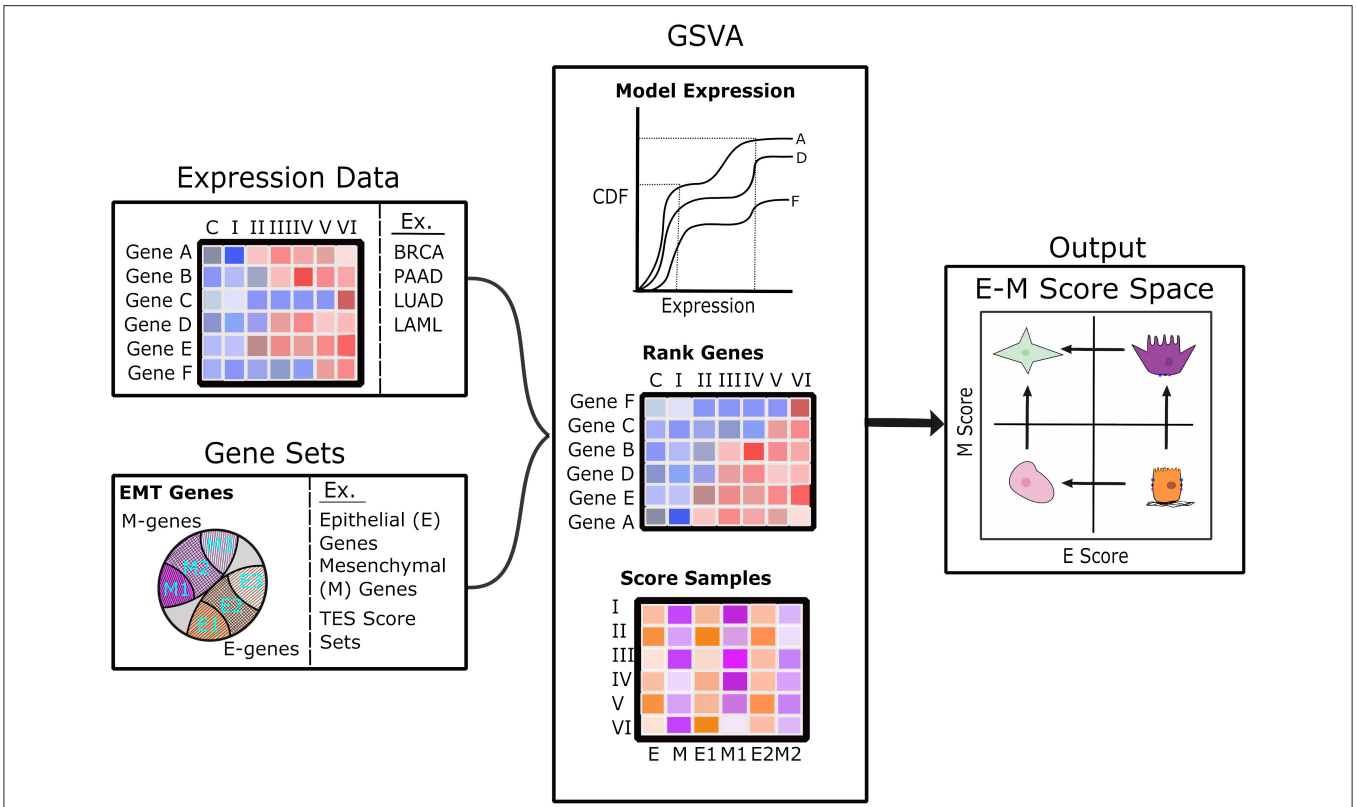

FIGURE 1 | Diagram of the analysis pipeline to map transcriptome samples to E–M score space. The left panels show the scoring pipeline including transcriptomic data (top) and various gene sets (bottom). The center panels show a brief description of the GSVA scoring process that includes modeling gene expression as a cumulative distribution function, ranking of genes across samples, and the estimation of scores using Kolmogorov–Smirnov statistics. The right panel shows E–M score space annotated with possible cell states in each quadrant: terminal-E (lower right), terminal-M (upper left), hybrid intermediate (upper right), and characterless intermediate (lower left).

our previous study. Briefly, EMT genes were clustered using a transcriptome data set obtained from combinatorially perturbed MCF10A cells with up- or down-regulation of TGF-β and ZEB1 (23). This unsupervised clustering was achieved by using a Self-Organizing Maps (SOM) algorithm on a 10 × 10 grid (41, 42). Each node was classified by counting the number of previously annotated E or M genes and computing their ratios (this supervised step is essentially a *k*-nearest-neighbors algorithm). To obtain gene clusters among E-gene nodes and M-gene nodes, respectively, we used the hierarchical clustering method and we selected the optimal numbers of clusters (four E-gene clusters and four M-gene clusters) using the within-cluster sums of squares error (the elbow criterion). Tables of EMT related scores and cluster classifications for samples in TCGA and EMT time course are available in **Supplementary Files 1**, **2**, respectively.

GSVA for Phenotypic Inference

To infer phenotypic changes when cells move along the EMT path, we employed GSVA in a way similar to what we used for computing E and M scores. We focused specifically on cancer samples for the BRCA data set, because the presence of normal tissue samples had a significant effect on functional scoring, specifically with respect to migration (see **Supplementary Figure 4**). We obtained curated gene sets from the Broad Institute and selected four representative gene sets each for cell migration and for cell proliferation to quantify the phenotypic enrichment of the corresponding cellular properties in each subpopulation along the EMT paths (for a full description of gene sets, see **Supplementary Table 7**) (43). Differences in score between clusters were assessed using the same test and correction procedure as EMT factors. To exclude the possibility that gene sets carry redundant information with the E- and M-genes, we calculated the percentages of overlapping genes between the phenotypic and pathway gene sets and the EMT gene sets, and in no case did more than 20% of genes in a phenotypic set belong to the E-gene set or M-gene set.

RESULTS

Multimodal Distribution of Cancer Cells in the EMT Spectrum

To examine how breast cancer cells are distributed in terms of the degree of EMT, we obtained 1,215 samples from the TCGA breast cancer project (BRCA), which focuses on invasive carcinomas, and we computed a pair of scores that summarize the overall transcriptional activities of E- and M-genes for each cancer cell

sample, respectively. These scores are based on GSVA using a list of 228 E-genes and a list of 188 M-genes as signature gene sets (26). We found that the BRCA sample transcriptomes are widely distributed across the space of E and M scores (**Figure 2A**). In particular, all four quadrants of the E–M score space contain at least 10% of the samples, reflecting the heterogeneity of cancer cells in terms of the degree of EMT. Nonetheless, the quadrant corresponding to low-E–low-M gene expression contains fewest samples with 187 (15.4%), whereas the high-E–high-M quadrant contains 248 (20.4%) samples. To exclude the possibility that the wide distribution and the low density of samples in the low-E–low-M region is due to the normalization in the scoring scheme, we combined these breast cancer samples with 173 acute myeloid leukemia samples (LAML), which have hematopoietic lineage origins that are distant from that of epithelial cells. We found that the distribution of BRCA samples is consistent with the previous results even in the presence of LAML samples (**Figure 2B**). BRCA samples remain widely distributed in high-E and/or high-M quadrants with fewer samples in the low-E–low-M quadrant that are close to but do not overlap with LAML samples. We found that the distribution of the M scores is wider than that of the E scores (**Figure 2**). This is consistent with a previous observation that M-gene expression is more divergent than E-gene expression during EMT (23).

We next asked how many subpopulations these breast cancer samples may contain in terms of the degree of EMT. We built a series of Gaussian Mixture Models (GMMs) based on the E and M scores of these samples. We evaluated these models using BIC, the consistency of clusters across different variance assumptions, and the number of cells that can be assigned to subpopulations (clusters) with high confidence (see Methods). We found that a five-cluster model best describes the overall distribution of BRCA samples. Our GMM model of BRCA (**Figure 2C**) includes an extreme E cluster (orange), an extreme M cluster (green), and three intermediate clusters (I0, I1, and I2, which are pink, purple, and blue, respectively). The I0 cluster contains most (178 of 187) samples that are in the low-E–low-M region, whereas the I1 and I2 clusters contain all (248 of 248) samples with the high-E–high-M expression profiles. Most of these samples (237 of 248) belong to the I1 clusters, with I2 lying along the border between high-E–high-M and low-E–high-M. To exclude the possibility that our conclusions are sensitive to the choice of number of clusters, we analyzed the GMMs for four and six clusters and we found that they had distributions of clusters similar to that of the five-cluster model (**Supplementary Figure 5**).

Although EMT is a process involving gene expression changes in high-dimensional space, it is useful to construct one-dimensional EMT spectrums (paths) to quantify the degree of EMT. Moreover, if these one-dimensional spectrums can be mapped to the overall E- and M-gene activities, one can further infer the changes of the (anti-)correlation between E- and M-gene activities during EMT/MET. Therefore, we constructed models that describe possible EMT spectrums quantitatively. We assumed that a path will connect E and M states by joining neighboring clusters as cells go from the extreme E-state and to the extreme M-state. We also assumed that paths will take the fewest possible steps between neighboring clusters (loops and backtracking were not considered). With these assumptions, two possible three-step paths of EMT can exist: E–I0–I2–M (the lower path) and E–I1–I2–M (the upper path). We built two piecewise linear models using segmented regression with data from these two sets of clusters (see Methods). Our assumption concerning EMT progression is supported by a non-linear relationship between the E and M score (Davies's test, $p = 8.6 \times 10^{-3}$) and the possible existence of a breakpoint in the relationship between E and M along each path (pseudo Score stat, $p = 3.7 \times 10^{-8}$ and $p = 1.3 \times 10^{-3}$ for upper and lower paths, respectively). Models for the upper (light red, **Figure 2D**) and lower (light blue, **Figure 2D**) paths had reasonable performance in fitting to their respective data points ($R^2 = 0.5$ and 0.52 for upper and lower paths, respectively). The overall distribution of BRCA samples had an R^2 of 0.29 with a single segmented model (black, **Figure 2D**).

Note that these paths do not necessary contain information about how cancer cells change their expression over time, because EMT and MET can occur one after the other at any stage of EMT/MET. Rather, they predict how the overall E- and M-gene activities are likely to change at any given state when cancer cells alter their expression profiles in an incremental fashion. These steady-state and transient changes may be triggered by changes of microenvironment or mutations in cancer cells.

We next asked whether the pattern of distributions of cancer cells in the E–M space is consistent across tumors from different organs. We obtained samples of pancreas (PAAD), cervical (CESC), prostate (PRAD), and lung carcinoma (LUAD) from TCGA, all of which were shown to involve EMT (8, 44–49). Samples from these cancers show similar distributions to that of the breast cancer samples (**Supplementary Figure 6**) and GMMs consistently generated four populations as the optimal models (**Supplementary Figure 7**) with rough correspondence to BRCA populations (excluding I2). Using the same approach that we applied to BRCA, we found that a segmented model with two distinct EMT paths fits better than a single segmented model in all cases (**Supplementary Figure 8**). Notably, the samples in the high-E–high-M states are the main population of the cells at the intermediate EMT states in PAAD (42 of 56, 75.0%) and PRAD (147 of 212, 69.3%). In contrast, high-E–high-M and low-E–low-M populations are comparable in LUAD (104 of 192, 54.1% low-E–low-M) and CESC (66 of 125, 52.8% low-E–low-M). As such, both the upper and lower paths could be possible routes of E/M variations in our cancer data.

An EMT Path Involving a High-E–High-M State Revealed by Time Course EMT Data

To further examine whether the variation in E and M scores among the populations of BRCA samples is driven by the canonical EMT (e.g., TGF-β induced) pathway, we applied GSVA to calculate TGFβ-EMT scores (TES) in order to track progression through EMT (24). This score has two components, one for genes that increase during TGF-β-induced EMT (TES_UP) and the other for genes that decrease during the same process (TES_DOWN). Importantly, while there is overlap between these gene sets and our E- and M-gene sets, the majority

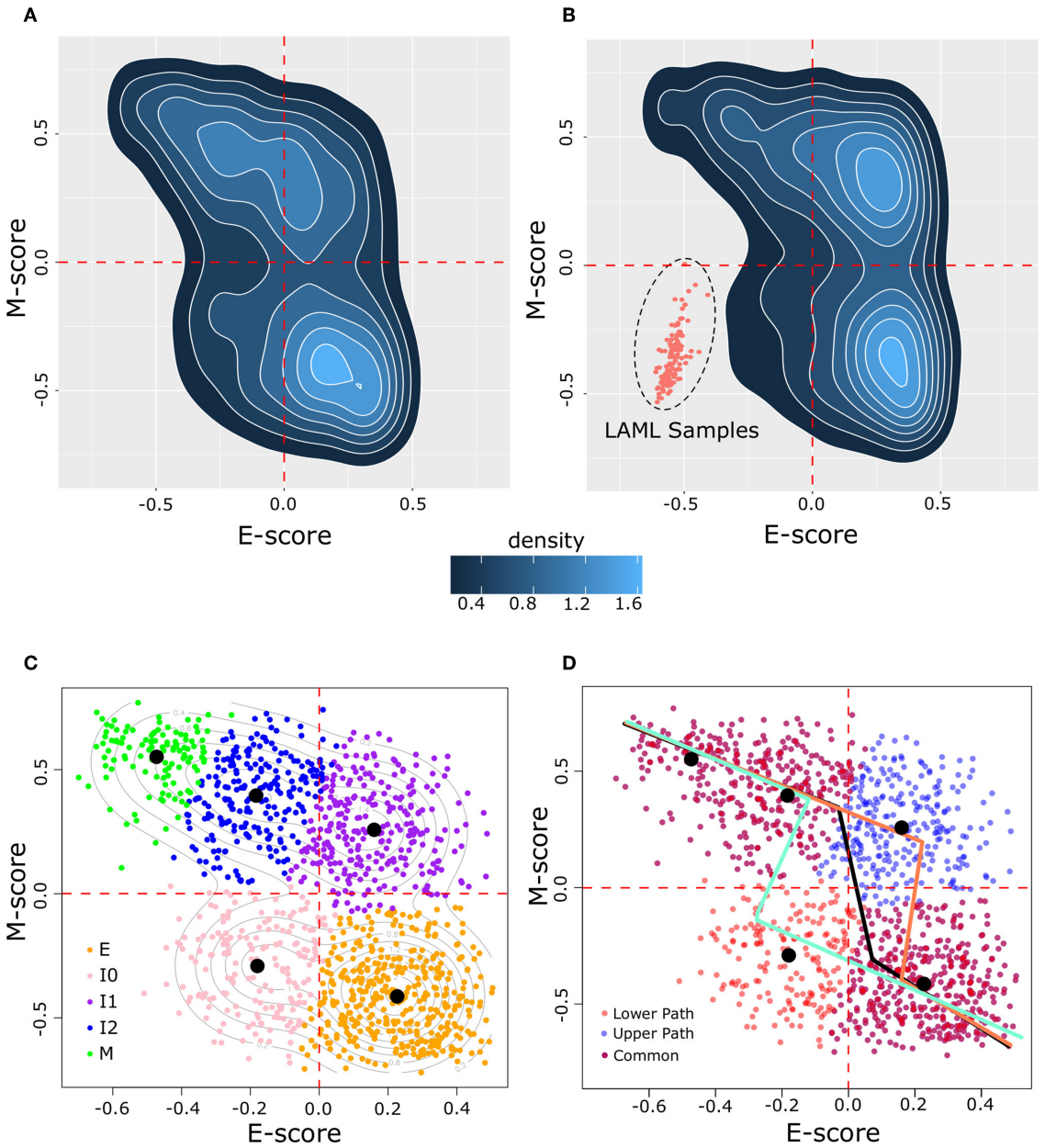

FIGURE 2 | Distribution of BRCA samples in E–M score space following GSVA scoring. **(A)** Density of BRCA samples in E–M score space. Lighter blue color indicates higher density and darker blue indicates lower density. **(B)** Density of samples in a merged BRCA-LAML data set demonstrating the positioning of samples of a non-epithelial origin in the lower left (low-E–low-M) quadrant beyond the distribution of BRCA samples. **(C)** Clustering of BRCA samples by GMM. Individual samples are indicated by points in E–M score space with their assigned cluster indicated by color (E = orange, I0 = pink, I1 = purple, I2 = blue, M = green). Contour lines indicate the predicted distribution of the underlying models. Black dots denote the center of each Gaussian distribution. **(D)** Segmented models E–M score relationship among BRCA samples. Three models are shown: one based on all BRCA samples (black line), one excluding I0 samples (upper path, light red line), and one excluding I1 samples (lower path, light blue line). Individual samples are shown by points with the color corresponding to whether the point is unique to the upper path (blue) or to the lower path (red), or common to both paths (purple).

of both TES_UP (155, 81.7%) and TES_DOWN (70, 64.8%) genes are not used to define our E and M scores. With the distribution of these scores across the BRCA populations, we observed a pattern that follows our previous two-path model of EMT progression (**Figure 3**). TES_UP and TES_DOWN values were compared between each cluster using Welch's *t*-test; the *p*-values and 95% CIs for each comparison can be found in **Supplementary Table 8**. I0 samples have significantly decreased TES_DOWN relative to E samples (Welch's *t*-test, $p = 1.97 \times 10^{-42}$), consistent with a decrease in E-gene expression, while

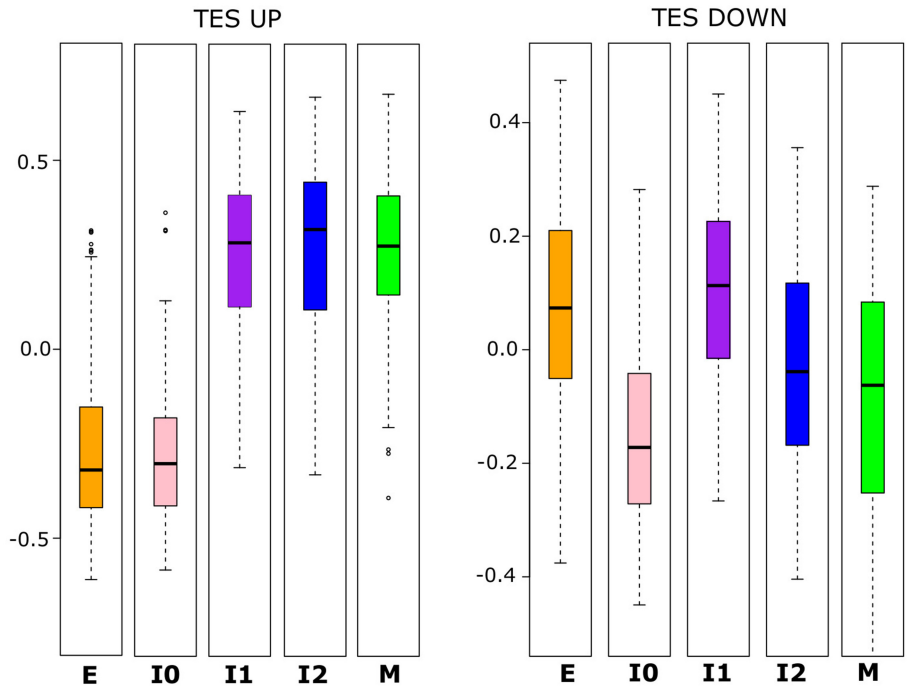

FIGURE 3 | Boxplots showing the distribution of TES_UP (left) and TES_DOWN (right) scores that reflect the activating and repressing programs of TGF-β-induced EMT, respectively. Note that there is a significant difference (Welch's *t*-test, $\alpha < 0.05$) in TES_UP between E and I1 and I0 and I2, but no significant difference among I1, I2, and M. For TES_DOWN, there is no significant difference between E and I1, but there are significant differences between E and I0, and between I1 and I2. I0 has a significantly lower TES_DOWN score than all other clusters do, but the magnitude of the difference is smaller between M and I0 than for E and I0. A full table of *p*-values and 95% confidence intervals can be found in **Supplementary Table 8**.

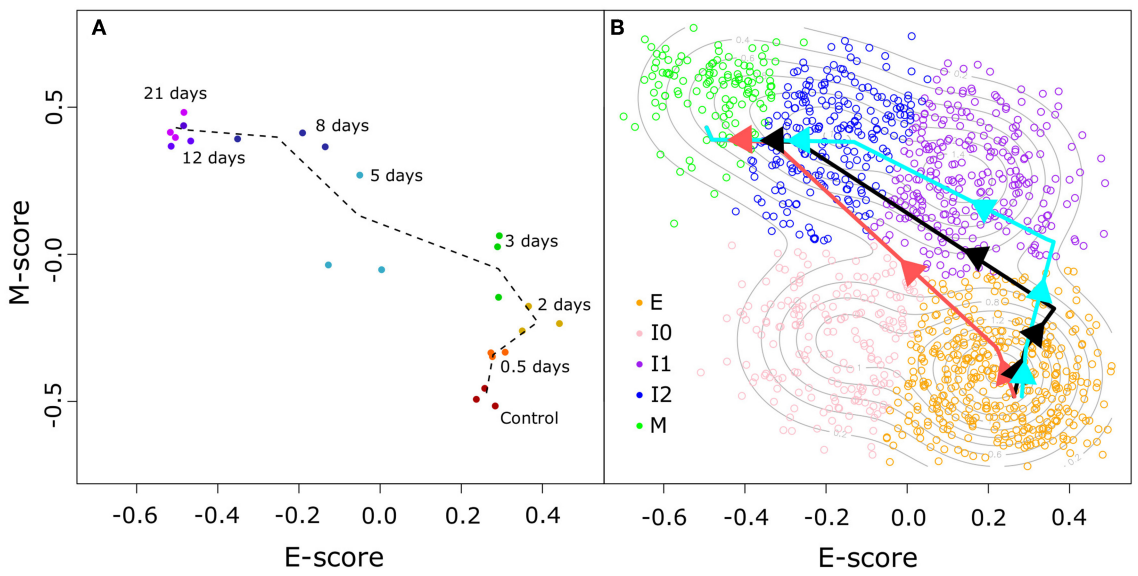

FIGURE 4 | TGF-β-induced EMT time course in E–M score space. **(A)** Time course samples projected in E–M space. Progression of samples through time is indicated by color (from red to purple) and adjacent time points are linked by a dotted black line. **(B)** Segmented models of the relationship between the time since TGF-β induction of EMT and the E–M scores of treated cells. Different colored lines correspond to the best fit (black), lower bound (light red), and upper bound (light blue) models. Individual BRCA samples are indicated as open points with their color corresponding to the assigned cluster (E = orange, I0 = pink, I1 = purple, I2 = blue, M = green).

I1 has significantly increased TES_UP (Welch's t-test, $p = 1.98 \times 10^{-132}$), consistent with an increase in M-gene expression. As a consequence, transition from I1 to M involves a significant repression of E-gene activity, while transition from I0 to M involves a significant increase of M-gene activity along with a relatively small change of E-gene activity in terms of magnitude (lower bound = +0.015 E score), compared to the transition from I1 (lower bound = −0.217 E-score). Nevertheless, these results are consistent with an "upper path" of E–M variance where the initial changes result from EMT-driven activation of mesenchymal genes and a "lower path" of E–M variance where the initial changes result from EMT-driven repression of epithelial genes. These results suggest that canonical EMT is an underlying factor of E/M variation in our cancer samples. However, it remains unclear whether TGF-β-driven EMT in non-tumorigenic cells resembles either of the putative paths (24, 50).

To address this, we used a time course transcriptome data set for MCF10A cells (non-tumorigenic human breast epithelial cells) treated with TGF-β (32) to compute E and M score for time points across EMT using the same procedure described earlier. The distribution of these time course data points in E–M score space (**Figure 4A**) shows that the TGF-β-driven EMT process involves an initial phase of significant increase of M-gene expression with a moderate change of E-gene activities, as well as a final phase of significant decrease of E-gene expression with a moderate change of M-gene activities. The middle phase of this process involves change of cell states near or within the high-E–high-M region. We next built a segmented regression model for all data points with time as the reference independent variable (see Methods). We found that the model generated a triphasic pattern with two break points with respect to both E and M scores (**Figure 4B**). Varying the placement of the first E score breakpoint was used to examine the upper (**Figure 4B**, light blue) and lower (**Figure 4B**, light red) bounds of the model of TGF-β-driven EMT, and in all cases, cell states primarily evolve through the high-E–high-M region when compared to our GMM models of BRCA samples (**Supplementary Figure 9**). Together with the EMT paths that we constructed for BRCA samples, our analyses show that the TGF-β-driven EMT primarily involves a path that crosses a high-E–high-M state, and this process is reflected in the distribution of a large fraction of cancer samples. These results imply that some intrinsic intermediate EMT attractors may govern both normal EMT process and a large number of cancer cells, and that a major population of cells at the intermediate EMT states may possess hybrid phenotypes in which the overall activities of E-genes and M-genes are both high.

Divergence of EMT Genes in Multiphasic Transitions Regulated by Key EMT Factors

We next asked which EMT factors may be responsible for the multiphasic EMT that we observed with the time course data as well as cancer cells. We first examined the time course expression of several core EMT promoting transcription factors, ZEB1/2, SNAIL1/2, and TWIST1/2 (**Figure 5**), which were shown to be critical for EMT and EMT-related physiological or pathological processes (51–57). Consistent with the pattern of overall M score,

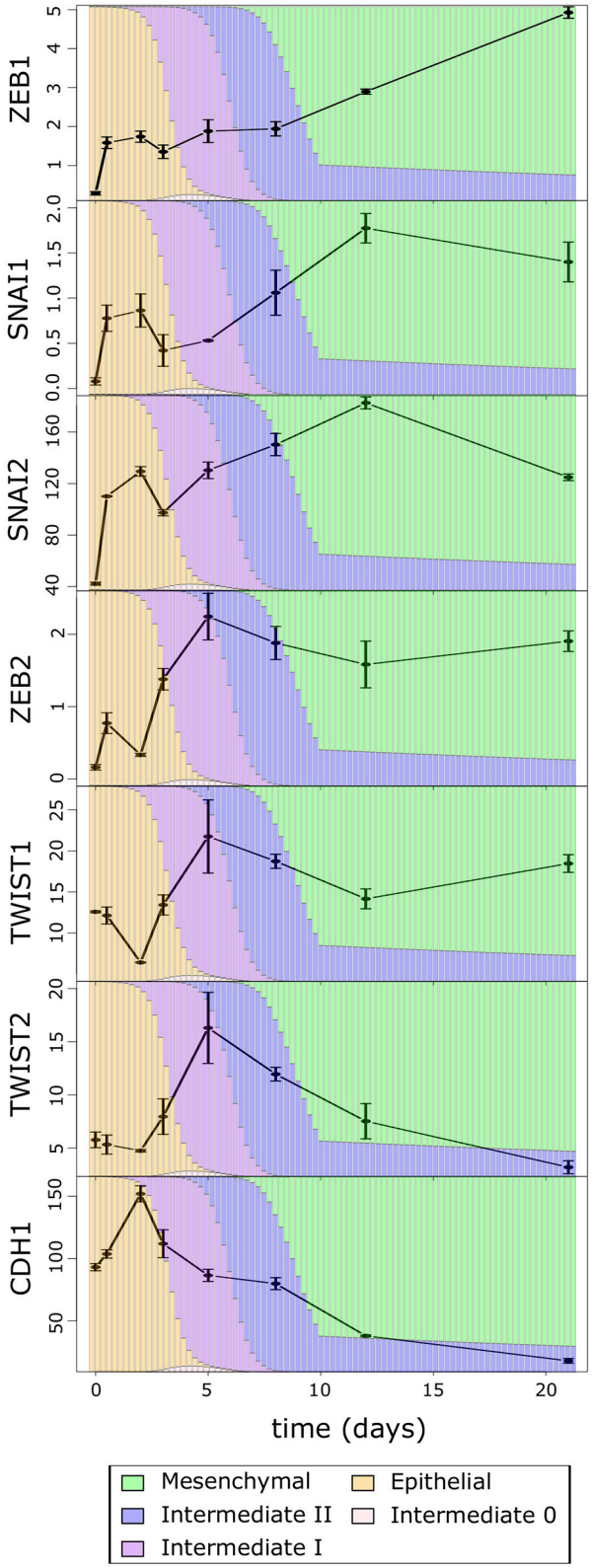

FIGURE 5 | The average expression of EMT factors over the TGF-β-induced EMT time course. The color of the background bars in each plot indicates the *(Continued)*

FIGURE 5 | predicated probability of samples at the point in time belonging to each cell state cluster. The probabilities were calculated by applying the BRCA GMM model to the segmented model of E–M scores with respect to time after TGF-β induction. Expression values are FPKM and bars indicate standard error of the mean.

all these EMT factors show significant increase in the first phase (Day 0 to Day 5), although some (ZEB2, TWIST1, and TWIST2) only increase after a delay (Day 2), which is consistent with the transition into and through the high-E–high-M intermediates. Conversely, the late-phase expression of these factors is more divergent (Day 8 to Day 21): ZEB2 and TWIST1 do not show dramatic increase, while TWIST2 and SNAI1/2 decrease during the late-phase EMT. This is consistent with our analysis of EMT paths in BRCA samples where the increase in M scores becomes moderate after passing through the intermediate states. We found that the transcription factor ZEB1 showed robust increasing dynamics even in the late phase. Given the significant decrease in overall E-gene activity in late-phase EMT (e.g., E score and CDH1), the dynamical pattern of ZEB1 suggests its close association with the dynamics of many E-genes. In fact, in our recent perturbation analysis with MCF10A cells, we found that most of the annotated E-genes are down-regulated by ZEB1 in a causal fashion (23), and this is consistent with the dynamical anticorrelation that we found in the time course data.

We then asked whether the robust increase of ZEB1 also exists near the M-end of the EMT path in cancer cells, and we compared the distributions of ZEB1 expression across the five cancer cell clusters along the EMT paths (**Figure 6**). The p-values for comparing expression change between clusters by Welch's t-test can be found in **Supplementary Table 9**. Consistent with the time course EMT dynamics, ZEB1 showed an increase in each of the three steps of the E–I1–I2–M transition in BRCA (Welch's t-test, $p = 3.97 \times 10^{-66}$, 1.85×10^{-4}, and 2.85×10^{-15}, respectively). In contrast, SNAIL1/2 showed a significant increase from I1 to M (Welch's t-test, $p = 3.84 \times 10^{-3}$ and 4.96×10^{-5}, respectively), but not I2 to M (Welch's t-test, $p = 9.61 \times 10^{-2}$ and 7.13×10^{-2}, respectively), which reflects the long run decay of SNAI1/2 from their initial peak in M in the time course. We found that, in TWIST1, there is no significant difference between E and I1 (Welch's t-test, $p = 1.43 \times 10^{-1}$), consistent with the delay in the time course, but both TWIST1 and TWIST2 had a significant increase from I2 to M in BRCA samples (Welch's t-test, $p = 5.93 \times 10^{-9}$ and 7.39×10^{-2}, respectively), a pattern not observed with time course data. In fact, TWIST1 and TWIST2 mirror ZEB1 in terms of their expression patterns in E, I1, I2, and M clusters. This dissimilarity between the cancer cells and the time course data was also observed for ZEB2, which showed the largest absolute change in mean between I2 and M. Consistent with the moderate increase of M score from E to I0, expression of ZEB1, TWIST1, and TWIST2 was not significantly different between I0 and E clusters (Welch's t-test, $p = 2.66 \times 10^{-1}$, 1.43×10^{-1}, and 4.20×10^{-1} respectively). While the behavior of ZEB2 and TWIST1/2 was not consistent across data sets, unlike these EMT factors, ZEB1 has significant dynamical changes at the M-end of EMT path in both normal and cancer cells, indicating its primary role in robustly controlling E-gene expression at this phase of canonical EMT. On the other hand, the lack of ZEB1 variation in E–I0 suggests that if transition through low-E–low-M quadrant represents an alternative path of EMT, it accomplishes repression of E-genes through a ZEB1 independent pathway.

To gain deeper understanding of the divergent expression patterns that contribute to the moderate change of E-gene expression in early-phase EMT, and/or to the moderate change of M-gene in late-phase EMT, we focused on gene clusters that are differentially controlled by TGF-β, a canonical EMT promoting factor important for metastasis (58), and ZEB1, a factor involved in regulation of most E-genes (23). Using a semi-supervised learning algorithm applied to a transcriptome data set for MCF10A cells that were combinatorially perturbed with up-/down-regulation of TGF-β and/or ZEB1 (23), we classified E- and M-genes into six major gene clusters [**Figure 7A**, **Supplementary Figure 10**, note that our previously analysis focused on M-gene clusters but not E-gene clusters (23)]. These gene clusters are regulated by TGF-β and ZEB1 with distinct circuits. Notably, the three E-gene clusters show a divergent expression pattern in early-phase EMT. In particular, the E2 cluster containing 80 E-genes show a significant increase from Day 0 to Day 3 (**Figure 7B**). The genes in this cluster are up-regulated by TGF-β via a ZEB-1-independent pathway and down-regulated by ZEB1, thereby forming an incoherent feed-forward loop. This network motif is likely responsible for the transient increase of this gene cluster around Day 3 as well as the overall increase in E score during the initial phase of EMT. Divergent expression patterns were also observed for M-genes: there is a significant difference between the M1/2 clusters and the M3 cluster, which is primarily regulated by ZEB1 (**Figure 7C**). M3 genes (e.g., TWIST1/2) do not exhibit increased expression until the intermediate phase of EMT progression, and this may be a general pattern of ZEB1 responsive M-genes. Furthermore, in contrast to M1 and M2, M3 still increases during Day 12 to Day 21, further reflecting the dynamics of ZEB1. Together, these results show that the heterogeneity of gene expression pattern contributes to the moderation of changes in E-gene expression during early-phase EMT and M-gene expression during late-phase EMT. The analysis further suggests that distinct gene regulatory circuits that connect EMT genes to ZEB1 and TGF-β are part of the mechanistic basis of such heterogeneity.

Phenotypic Implications of Multiphasic EMT Spectrums

Since the intermediate cancer cell populations favor hybrid expression patterns with a high-E–high-M profile, we asked whether these cells possess hybrid cellular properties related to the EMT transcriptional program. We first performed GSVA with the breast cancer cell transcriptomes using several functional gene sets related to cell migration and proliferation from the Broad Institute GSEA database (see Methods). These two cellular properties are closely related to EMT and tumorigenesis, respectively. We used four curated cell migration gene sets

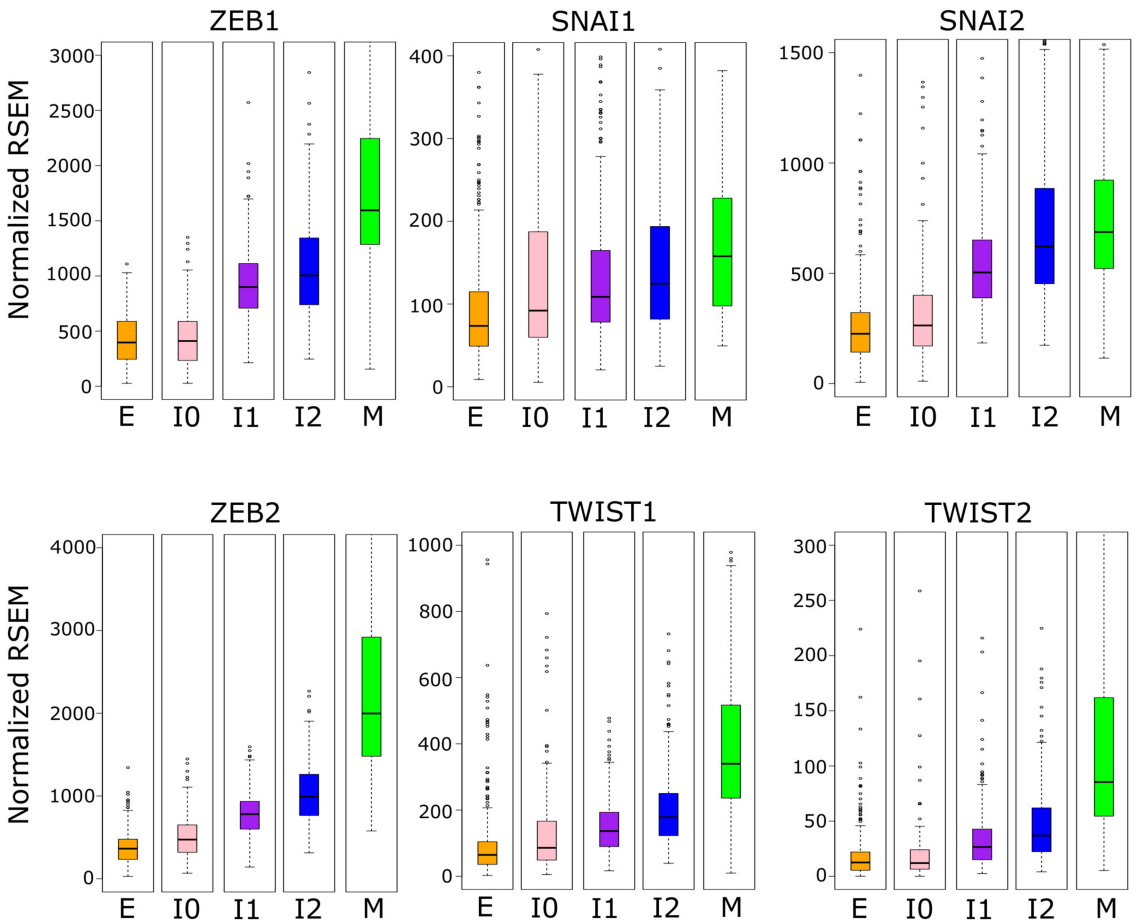

FIGURE 6 | Boxplots showing the distribution of EMT factor expression across different clusters of BRCA samples indicated by color (E = orange, I0 = pink, I1 = purple, I2 = blue, M = green). Note that the difference between E–I1–I2–M clusters are significant for ZEB1, but SNAI1/2 show no significant difference between I2 and M, and TWIST1 is not significantly different between E and I1 but is between I2 and M. Expression values are normalized RSEM (RNA-Seq by Expectation Maximization) values (see Methods). A full table of *p*-values can be found in **Supplementary Table 9**.

including RUNX2, RUNX3, and SEMA4D-mediated pathways as well as a general migration gene set from Wu et al. (59) (**Figure 8A**). As cells progress from E-state to M-state, these migration-related genes are up-regulated significantly (Welch's *t*-test, see **Supplementary Table 10**). Remarkably, the I1 and I2 intermediate cell clusters show high activities of migration-related genes and their overall expression is comparable to that in the M state in all cases except for the RUNX3 pathway. Additionally, we observe a large increase in the expression of migration-related genes from E to I1, but not E to I0, except for the RUNX3 pathway, which shows a linear progression from E to M. We next applied GSVA to gene sets related to cell proliferation. Since there were no available gene sets for breast epithelial cells, we first used two gene sets describing the proliferation of other cell types: lymphocytes [Goldrath, (60)] and mice liver cells [Fujiwara, (61)]. In both cases (**Figure 8B**), as cells progress from E-state to M-state, proliferation-related genes are down-regulated significantly (Welch's *t*-test, see **Supplementary Table 11**), but I1 cells score significantly higher than M cells, and I1 is not significantly different from E with the Goldrath set. We observed the same pattern of proliferation driven by MYC pathway genes and a similar pattern among VEGFR2 pathway genes, though in the latter set, the proliferation of intermediate states is slightly higher than the extreme E state. We also observed that I0 has a higher proliferation score than all other clusters in the MYC pathway do, but in other proliferation sets, it is indistinguishable from E or is between E and I1. Taken together, our analysis of both proliferation and migration gene sets suggests that cancer cells in I1 and I2 may exhibit the same migratory potential of full-differentiated mesenchymal cells with only a partial reduction in proliferation compared to epithelial cells.

To exclude the possibility that the consistency of the observed pattern is simply due to overlap between the migration, proliferation, and E/M gene sets, we examined the number of overlapping genes between phenotypic gene sets, and between

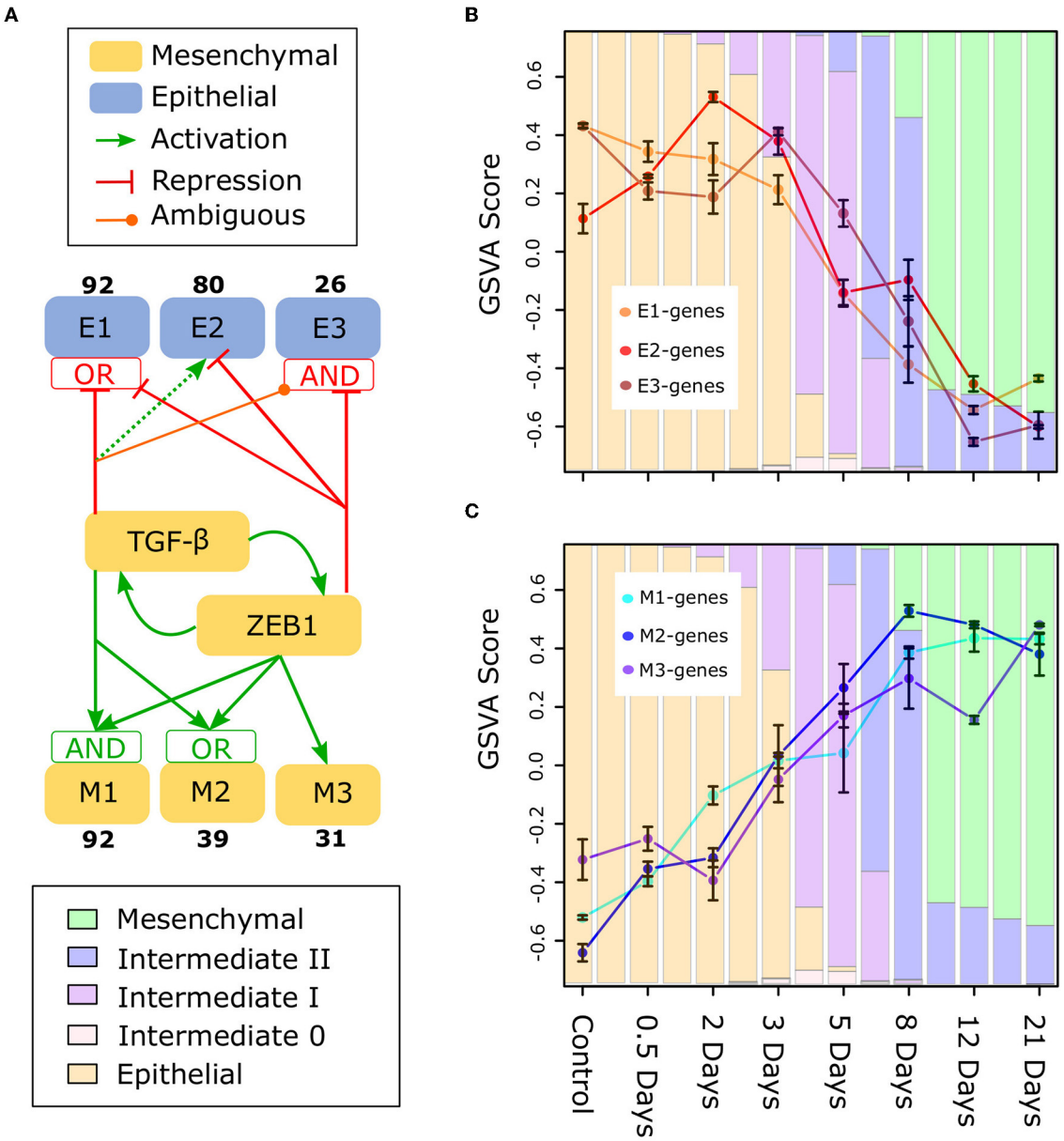

FIGURE 7 | Subclusters of E and M genes in TGF-β induced EMT **(A)** A model of the regulation of subclusters of E (E1, E2, E3) and M (M1, M2, M3) genes by TGF-β and ZEB1 based on perturbation analysis (23). The boxes containing "AND" and "OR" indicate the type of logic gate integrating the regulatory signals of TGF-β and ZEB1: "OR" indicates that one factor can drive activation/repression independently, while "AND" indicates both are required. However, in the case of both "AND" gates, TGF-β alone can regulate the subcluster, either with reduced (M1) or with opposite (E3) affect (the latter is indicated by TGF-β being ambiguous for E3). Also, there is no gate integrating TGF-β and ZEB1 for E2 because ZEB1 suppresses activation by TGF-β when present (indicated by the dotted line for TGF-β). For the data and methodology underlying this regulatory model, see **Supplementary Figure 10** for E-genes. **(B)** GSVA scores of E1, E2, and E3 subclusters across the TGF-β-induced EMT time course. **(C)** GSVA scores of M1, M2, and M3 subclusters across the TGF-β-induced EMT time course. The color of the background bars in each plot indicates the predicated probability of samples at the point in time belonging to each cell state cluster. The probabilities were calculated by applying the BRCA GMM model to the segmented model of E–M scores with respect to time after TGF-β induction. Bars that align with points on the line graph represent the predicated probabilities at the time point while columns between sample time points represented the predicated probabilities at the middle point of two neighboring time points (i.e., 0.25, 1.75, 2.5, etc.). Bars around each point indicate standard error of the mean.

phenotypic gene sets and the EMT gene sets. The largest overlap occurs between the Wu gene set and E-gene (42, 22.9%) and M-genes (27, 14.7%). In the remaining pairwise comparisons of gene sets, there was either no or a small overlap (one to three genes) (**Supplementary Table 12**). This suggests that our phenotypic scores are generally independent from one another and from E–M scores, such that the functionally hybrid potentials of the I1 and I2 states are not likely due to an artifact in

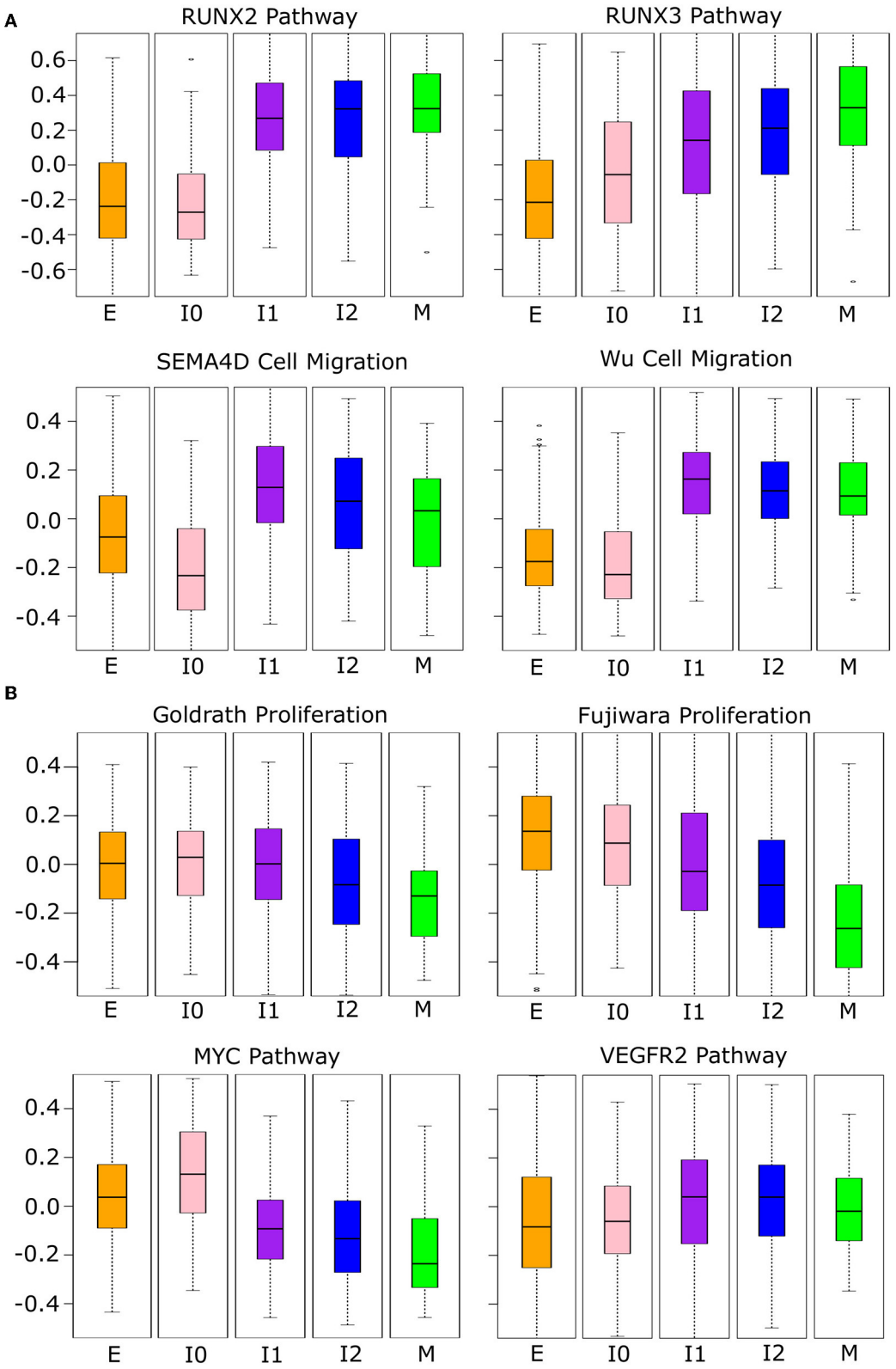

FIGURE 8 | Phenotypic scores BRCA cancer samples. **(A)** Boxplots showing the distribution of migration-related gene set scores across different clusters of BRCA samples indicated by color (E = orange, I0 = pink, I1 = purple, I2 = blue, M = green). Note that, in all cases, there is a significant jump in score between E–I0 and

(Continued)

FIGURE 8 | I1–I2–M, except for RUNX3 where there is a constant, significant growth in scores from E to M. A full table of *p*-values can be found in **Supplementary Table 10**. **(B)** Boxplots showing the distribution of proliferation-related gene set scores across different clusters of BRCA samples indicated by color as in **(A)**. Note that proliferation scores of I1 samples are consistently higher than M samples and, in two cases, are comparable to that of E samples (Goldrath and VEGFR2). A full table of *p*-values can be found in **Supplementary Table 11**.

our method. Furthermore, this hybrid potential appears to be specific to cancer cells: the time course data showed the same pattern of an early gain of migration (**Figure 9A**), but only in the Fujiwara proliferation set did the intermediate EMT phase show high proliferation relative to the terminal mesenchymal states. In contrast, the intermediate EMT phase has lower proliferation capacity than either terminal E or M in scores obtained with the Goldrath set as well as the MYC and VEGFR2 pathways (**Figure 9B**), suggesting that the combined proliferative and migratory potential may be specific to cancerous intermediate states. Furthermore, this phenotypic combination may contribute to the "fitness" of the tumorigenic intermediate EMT states in metastasis (62).

While the analysis of proliferative and migratory genes implies the functional significance of the upper path of EMT, the lower path remains largely undescribed due to the similarity of I0 to E in these measures. We performed further analysis with other high-level functional gene sets, and we found that I0 samples are distinct from other EMT clusters in the expressions of cell cycle and DNA repair genes (**Figure 10A**). Cell cycle genes are significantly up-regulated in I0 compared to all other EMT clusters (see **Supplementary Table 13**) and there is a significant decrease in DNA repair associated gene expression from E to I1 (Welch's *t*-test, $p = 4.16 \times 10^{-26}$) that is not seen from E to I0 (Welch's *t*-test, $p = 3.51 \times 10^{-1}$). We next analyzed three sets of proto-oncogene pathways (E2Fs, MCM, and CDC25; **Figure 10B**) and three sets of tumor suppressor pathways (RB, P53, PTEN; **Figure 10C**) that are related to the cell cycle and cell survival. All proto-oncogene pathways showed increased expression in I0 compared to other EMT clusters, while pathways of tumor suppressors were decreased, except for RB, which also had increased expression (see **Supplementary Table 14**). The higher expression of RB associated genes may be due to the significant overlap in the RB pathway with those of CDC25 (66.7%) and E2F (58.3%). In general, there is a large degree of overlap between proto-oncogene pathways, but not within tumor suppressor pathways or between tumor suppressors and proto-oncogene pathways, except for RB (**Supplementary Table 12**). In terms of the expression of these tumor suppressors themselves, both RB and PTEN are down-regulated in I0 compared to I1, I2, and M, but not P53 (**Supplementary Figure 11**, **Supplementary Table 15**). RB and PTEN were previously shown to be mutated or down-regulated in triple-negative breast cancer (also known as basal-like) (63–66). These results further suggest that different intermediate EMT states or paths have distinct signatures that can be potentially used for diagnosis or treatment of particular cancer subtypes (67, 68).

To explore the relationship between these tumor suppressors and cancer subtypes, we obtained the subtype annotation of BRCA samples from TCGA and analyzed frequency of each subtype among our EMT clusters. We used a chi-squared test to evaluate the distribution of subtypes against a null model where the frequency in each cluster matched the background distribution (**Figure 11A**) and found that the distribution of Luminal A ($p = 4.05 \times 10^{-8}$), Luminal B ($p = 7.90 \times 10^{-10}$), and Basal ($p = 2.55 \times 10^{-19}$) subtypes differed significantly across EMT clusters (HER2 Enriched was also significant, $p = 0.72 \times 10^{-3}$, but violated the assumptions of chi-squared test due to low counts in I0 and M). In general, we observed an increase in Her2 subtypes (Luminal A and Basal) from E to M, but Basal samples specifically are enriched in I0, which accounts for 41.5% of all I0 samples and 38.7% of all Basal samples. Compared to other I0 samples, Basal I0 samples have decreased RB (Welch's *t*-test, $p = 1.84 \times 10^{-9}$) and PTEN (Welch's *t*-test, $p = 1.69 \times 10^{-3}$) expression, but P53 is not significantly different in either direction (Welch's *t*-test, $p = 9.68 \times 10^{-2}$), though P53 is more variable among I0 Basal samples (**Figure 11B**). Taken together, these results indicate that I0 samples are enriched in the loss of clinically significant features, including both hormone receptors and tumor suppressors, though it is unclear if this is directly related to the down-regulation EMT genes in general or if the correlation arises from some linkage to additional factors.

DISCUSSION

The diversity of cancer cells regarding their relationship to EMT has been found in numerous previous studies (14, 21, 24, 26). However, the distribution of cancer cells in terms of the overall activities of E- and M-genes was unclear. In this study, we used integrative transcriptomic data analysis to show that cancer cells from various organs are widely distributed across the E- and M-gene expression space and that a non-linear path connecting E and M via a high-E–high-M region describes a large fraction of breast, lung, pancreas, cervical, and prostate cancer cells. With further transcriptomic analysis using non-tumorigenic cells, we found that this EMT path is consistent with the progression of TGF-β-induced EMT in normal cells over time. A previous study with breast cancer cells also showed a similar consistency in terms of a binary model between E and M states (69). These results suggest that the gene regulatory network in epithelial cells govern high-E–high-M cellular states intrinsically, and a large fraction of cancer cells show this expression pattern. Nonetheless, future experiments are warranted to demonstrate the existence of and the relationship between the cancerous intermediate EMT states and their normal counterparts. Previous mathematical models based on core EMT regulatory networks have explained the hybrid nature of partial EMT states (15–18, 70, 71). Our analyses complement these mechanistic dynamical models by demonstrating that the hybrid EMT states in terms of the overall transcriptional activity are prevalent in cancer cells. These EMT states not only show significant activities of E- and M-genes comparable to those at extreme E and M states, respectively, but are also associated with gene expression patterns corresponding

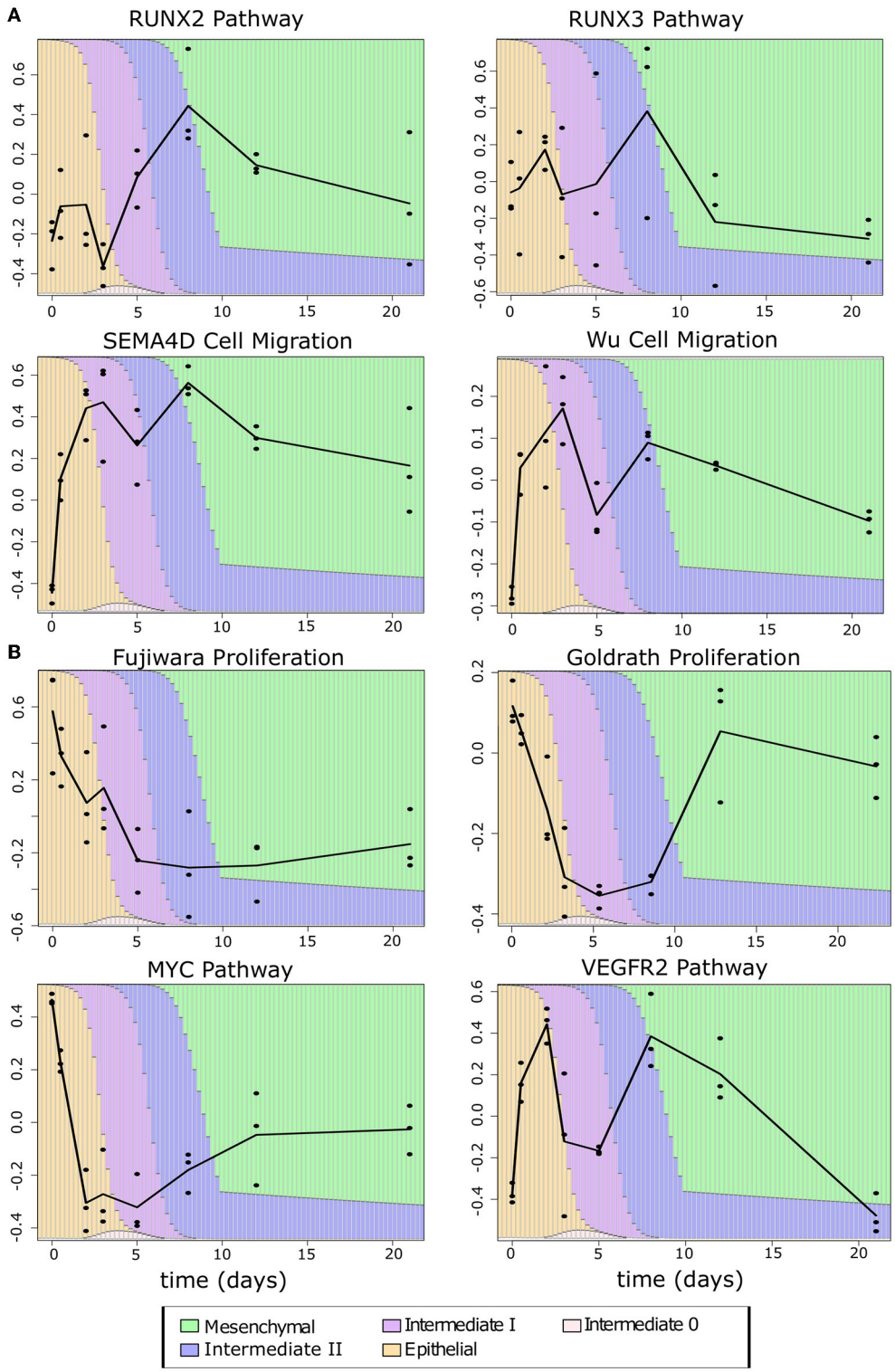

FIGURE 9 | Phenotypic scores of EMT time course samples **(A)** Migration scores across the samples in the TGF-β-induced EMT time course. **(B)** Proliferation scores across the samples in the TGF-β-induced EMT time course. The color of the background bars in each line plot indicates the predicated probability of samples at the point in time belonging to each cell state cluster. The probabilities were calculated by applying the BRCA GMM model to the segmented model of E–M scores with respect to time after TGF-β induction. The black line indicates the change between sample averages at each experimental time point.

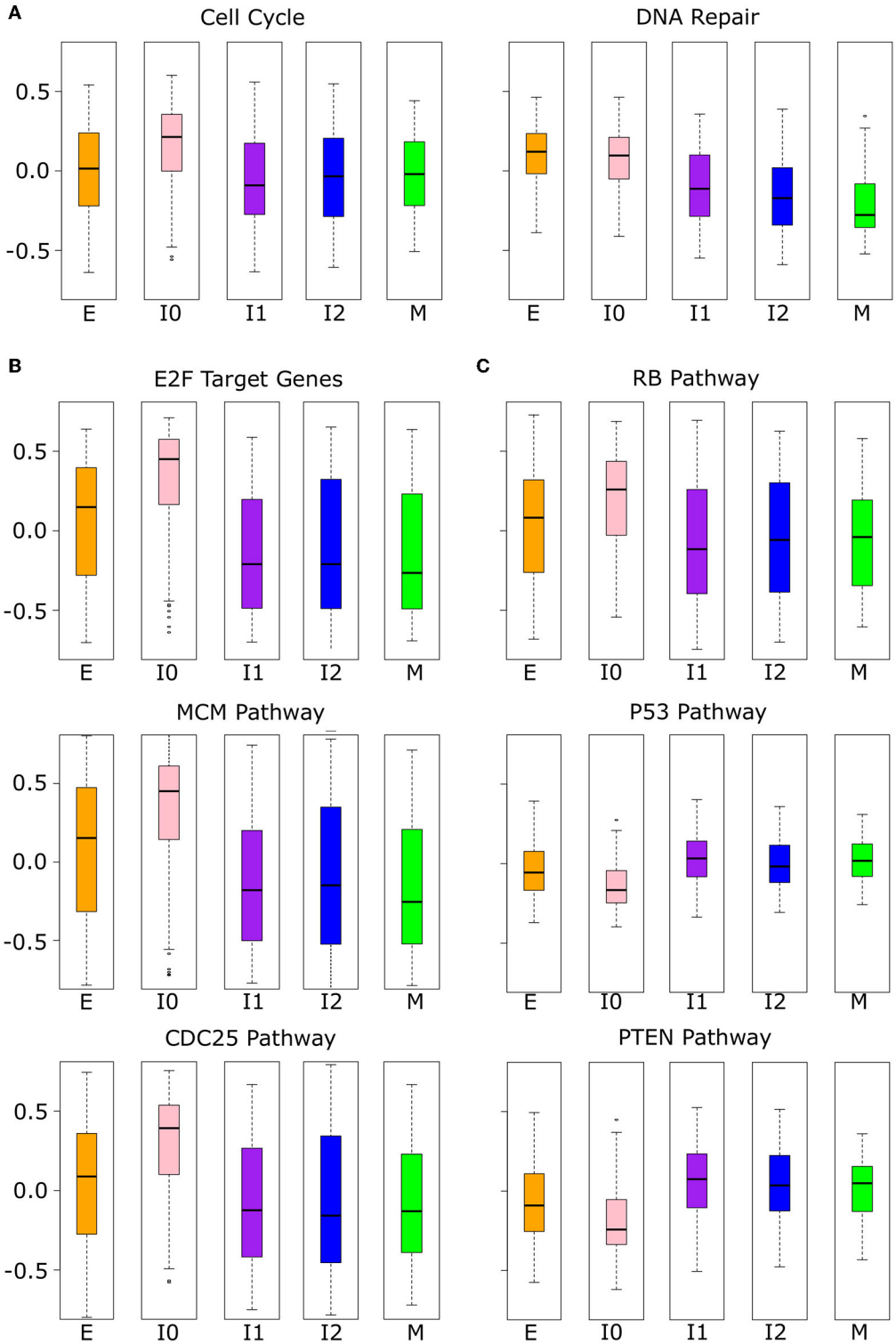

FIGURE 10 | Phenotypic scores were significant in I0 BRCA cancer samples. **(A)** Boxplots showing the distribution of cell cycle and DNA repair-related gene set scores across different clusters of BRCA samples indicated by color (E = orange, I0 = pink, I1 = purple, I2 = blue, M = green). **(B)** Boxplots showing the distribution of proto-oncogene (CDC24, E2F, and MCM) pathways across different clusters of BRCA samples indicated by color as in **(A)**. **(C)** Boxplots showing the distribution of tumor suppressor (P53, PTEN, and RB) pathway scores across different clusters of BRCA samples indicated by color as in **(A)**. The *p*-values of the comparison of scores between clusters can be found in **Supplementary Tables 13**, **14**.

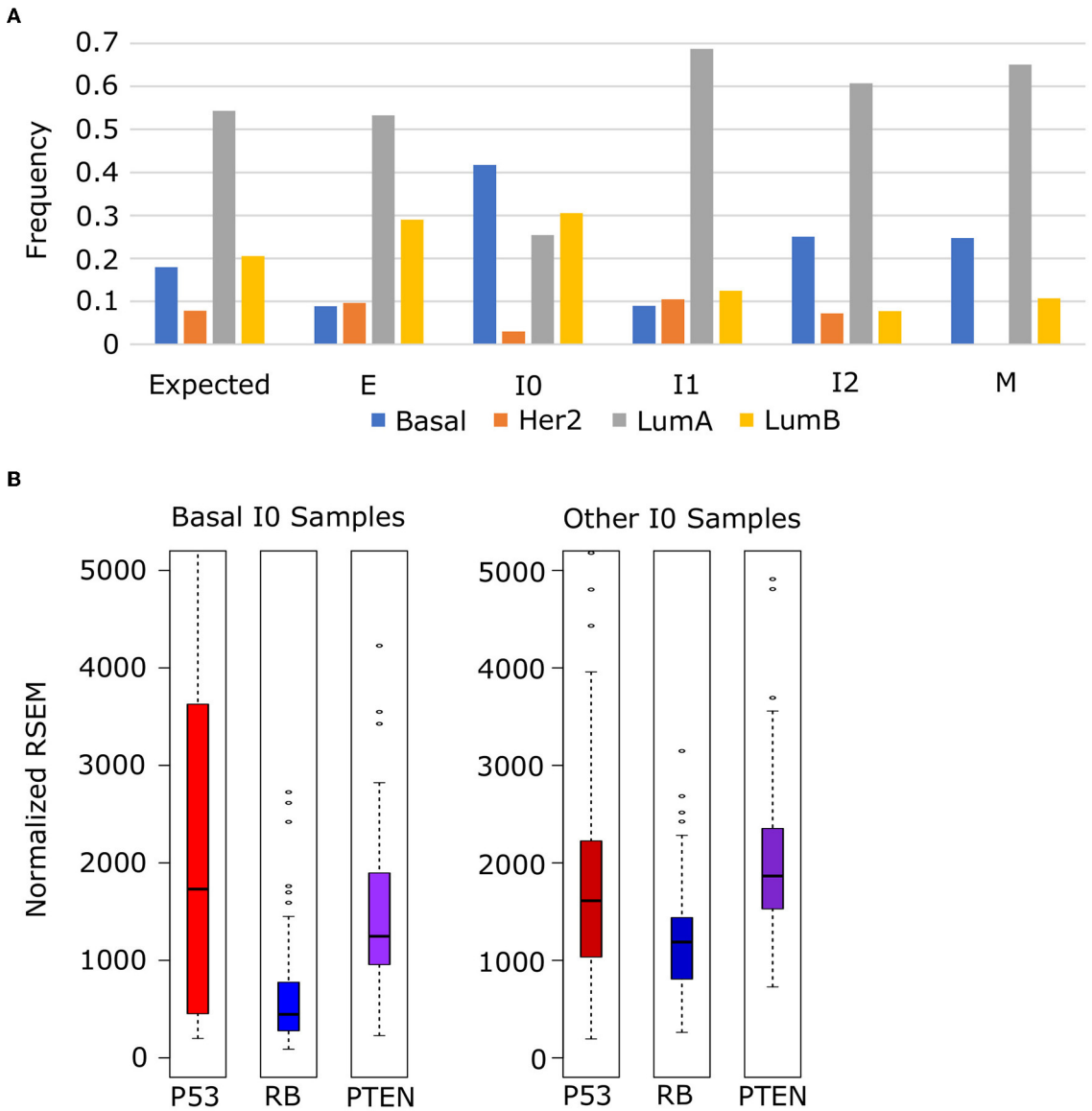

FIGURE 11 | Enrichment of basal-subtype BRCA tumors in the I0 cluster. **(A)** The frequency of Luminal A (gray), Luminal B (yellow), Basal (blue), and Her2 Enriched (orange) breast cancer subtypes among breast cancer samples in each of the five EMT clusters. **(B)** The expression of tumor suppressors P53 (red), RB (blue), and PTEM (purple) in Basal I0 samples vs. all other I0 samples.

to high motility and proliferation potentials, suggesting their hybrid cellular phenotypes.

Our analyses of breast cancer samples focused on a GMM with five clusters. Although this model was the best-performing model among models with one to nine clusters (see Methods), we extended our analyses to a four-cluster model and a six-cluster model (**Supplementary Figures 5**, **12–14**). The distribution of the four clusters in the former model is clearly consistent with the non-linear EMT paths that we obtained with the five-cluster model (**Supplementary Figure 5**). Since it is less obvious whether the six-cluster model generates results inconsistent with our main conclusions, we performed segmented regression, analyzed the key EMT gene expression, made comparison with time course data, and examined the functional enrichment of all clusters with the six-cluster model (**Supplementary Figures 12–14**). All results were consistent with those obtained with the five-cluster model. Therefore, the main conclusions of this study do not depend on the exact number of clusters in the GMM.

We used statistical models to describe possible subpopulations in the cancer cell transcriptomes. It is possible that these subpopulations (clusters) of cells correspond to attractors in the EMT spectrum. In particular, both the normal EMT process and some cancer cell subpopulations show high-E–high-M expression pattern, suggesting the existence of attractors within that expression pattern. Future work is needed to relate the

subpopulations in the statistical models to attractors (e.g., stable steady states) in dynamical systems, which would require a combination of transcriptomic measurement and tests of stability of the cell phenotypes. Previous work has shown the stability of a hybrid E/M phenotype in lung cancer cells (17). More systematic analysis will be needed to draw a general conclusion about the attractor property of the hybrid cancer cells in various other organs.

We found that the EMT path through a high-E–high-M region can be a major EMT path in both cancer and normal cells. This conclusion does not exclude the possibility that other EMT paths exist in significant populations of cancer cells. In fact, clusters of cells near the low-E–low-M region were found in the EMT spectrum, and they may also contribute to the transition EMT states observed in tumor cells (20). Future work involving single cell analysis is needed to reveal EMT paths in the cancer settings at higher resolutions (72–74). It is also possible that frequent transitions involving both EMT and MET, and those between intermediate states (e.g., high-E–high-M from/to low-E–low-M) occur in tumorigenesis (69, 75, 76). These transitions may be driven by paradoxical signals, such as simultaneous up-regulation or down-regulation of both EMT promoting and inhibiting factors in the microenvironment or the decoupling of the activating and repressing functions of EMT, as seen in the TES scores of the I0 and I1 clusters. The correlations between cancer and non-tumorigenic cells in the EMT spectrum do not imply the similarity of the dynamics of EMT between cancer and normal cells. In fact, genetic perturbations are likely to be a major factor contributing to the diversity of cancer cell transcriptomes. The EMT paths in the cancer samples suggest the directions of changes of cellular properties upon the gradual genetic or non-genetic perturbations to these cells. In addition, these correlations suggest that the existing regulatory pathways may channel the perturbed cells into some defined states, so long as the disruption of EMT pathways is not dramatic.

The summary scores that we used to quantify the overall activities of E- and M-genes are based on the expression of a list of EMT genes. The advantage of such metrics is that the scoring is robust to the change of individual genes. However, performing clustering on cells based on low-dimensional scores has the disadvantage of missing useful information in high-dimensional gene expression space, which has even greater potentials to reveal multiple attractors (77). This can be seen in part in the scores of E and M gene subclusters, in that the initial increase in E score during the time course appears to be driven by a specific subset of epithelial genes with distinct regulation by EMT factors. Moreover, the diversity of cancer cells must be beyond their status in the EMT spectrum (30, 78). Nonetheless, in case of proliferation and migration, we found that the activity of many functional gene sets is highly correlated with EMT status despite little or no overlap with annotated EMT genes. Overall, our clustering method is not aimed to provide a general clustering framework for analyzing cancer cells. Instead, given that the goal of our study is to find the overall patterns in the EMT spectrum for better understanding cancer cell diversity, the E- and M-gene scores serve as a concise approach to summarize the gene expression in cancer cells.

It was proposed in earlier studies that the mesenchymal state is associated with tumorigenesis (79). More recently, there was a refinement of the concept in terms of the roles of EMT in cancer progression. Multiple studies involving tumorigenesis models or analysis of tumor cells suggest the critical roles of partial EMT in metastatic processes (3, 80, 81). In addition, cellular functions of both epithelial and mesenchymal genes contribute to the formation of secondary tumors (7, 81). This suggests that metastasis may involve synergy among various cell types in multiple positions on the EMT spectrum. Our work further suggests that a significant population of cancer cells possess hybrid functions. Although it is likely that tumor formation requires interactions of multiple types of cells, the multifunctional nature of the hybrid cells, in particular their potential to migrate and proliferate, might be an important factor contributing to the invasiveness of cancer cells.

DATA AVAILABILITY STATEMENT

The results shown here are in whole or part based upon data generated by the TCGA Research Network: https://www.cancer.gov/tcga. All datasets generated for this study are included in the article/**Supplementary Material**. All computer code for data analysis is available upon request.

AUTHOR CONTRIBUTIONS

NP, CA-T, ML, NR, and TH performed the research. NP and TH wrote the manuscript. TH conceived the study. All authors have read and approved the final manuscript.

FUNDING

TH was partially supported by the Bio Medical Seed Research Program at The University of Tennessee, Knoxville. This work was conducted, in part, during the 2019 Summer Research Experience (SRE) for undergraduates program at the National Institute for Mathematical and Biological Synthesis, an Institute sponsored by the National Science Foundation through NSF Award #DBI-1300426, with additional support from The University of Tennessee, Knoxville.

SUPPLEMENTARY MATERIAL

The Supplementary Material for this article can be found online at: https://www.frontiersin.org/articles/10.3389/fonc.2019.01479/full#supplementary-material

Supplementary Figure 1 | Graphs of the Bayesian Information Criterion (BIC) against the number of clusters in the model of BRCA samples. **(A)** The BIC of six different variance model, indicated by the color the line (EII = red, VII = orange, EEI = green, VEI = blue, EVI = purple, VVI = pink). **(B)** The average BIC across all six models. Note that, in both graphs, the BIC of the five cluster models have the minimum value and occurs at the cusp of the graph, where additional cluster cease to produce large reduction in BIC.

Supplementary Figure 2 | Clustering of LUAD transcriptome samples using different variance models. Note the difference between models with equal volume (top) and varying volume (bottom).

Supplementary Figure 3 | Histogram of uncertainty (1—max probability of cluster membership) for different GMM models of LUAD transcriptome samples using different variance models. Note decreased uncertain for models with equal volume (top) compared to those with varying volume (bottom).

Supplementary Figure 4 | Migration score for RUNX2 pathway in BRCA samples including only cancer samples (left) and all samples (right). Note the decrease in proliferation scores for M and I2 when normal samples are included as most of these samples are clustered with M or I2. This suggest that these samples are functional different from cancer samples and therefore were excluded from further functional analysis.

Supplementary Figure 5 | Clustering of BRCA samples by GMM using four **(A)** and six **(B)** clusters. Individual samples are indicated by points in E-M score space with their assigned cluster indicated by color (E = orange, I0 = pink, I1 = purple, I1' = blue, I2 = green, M = red). Contour lines indicate the predicted distribution of the underlying models. Black dots denote the center of each Gaussian distribution. Note that the major difference in the four clusters model is that the most extreme low E, high M cluster now include the majority (69%) of I2 samples from five-cluster GMM, the remainder being split between I1 and I0. Similarly, in the six-cluster GMM model, I1 samples from the five-cluster GMM model are divided into two clusters, I1 and I1', with I1' consisting of samples with the most extreme E and M expression.

Supplementary Figure 6 | Contour plots of LUAD (top-left), PAAD (top-right), CESC (bottom-left), and PRAD (bottom-right) samples in E-M score space.

Supplementary Figure 7 | GMM models of LUAD (top-left), PAAD (top-right), CESC (bottom-left), and PRAD (bottom-right) samples in E-M score space. Individual samples are indicated by points in E-M score space with their assigned cluster indicated by color which roughly correspond to the clusters assigned to BRCA but for the absence of an I2 intermediate state (E = orange, I0 = pink, I1 = purple, M = green).

Supplementary Figure 8 | Segmented models E-M score relationship among LUAD (top-left), PAAD (top-right), CESC (bottom-left), and PRAD (bottom-right) samples. Three models are shown: one based on all samples (black line), one excluding I0 samples (upper path, light red line), and on excluding I1 samples (light blue lines). Individual samples are shown by points with the color of the point corresponding to the whether the point is unique the upper path (blue), lower path (red), or common to both paths (purple).

Supplementary Figure 9 | Probabilities of cluster membership across segmented models of E-M scores in the TGF-β induced EMT time course. Three segmented models are evaluated, the best fit and the upper and lowers bounds, which are based on the confidence interval of the time of the first breakpoint in the relationship between time after TGF-β induction and E-score. Probabilities are estimated by evaluating the segmented model every 0.25 days from 0 to 21 days and clustering the resulting E-M scores using the BRCA GMM model.

Supplementary Figure 10 | The response of subculsters of epithelial (E1, E2, E3) and mesenchymal (M1, M2, M3) genes to TGF-β and ZEB1. Each boxplot shows the distribution of fold change of expression to eight contrast conditions between TGF-β induction (TGFβ) ZEB1 induction (DOX), TGF-β inhibition (SB), and ZEB1 inhibition (dZEB) and their respective controls (WT for TGF-β induction and DMSO for ZEB1 induction). Note that, for M3 genes, the distribution of fold change is highest for DOX vs. DMSO and DOX + SB vs. SB, indicating increased expression in response to ZEB1 regardless of TGF-β expression and that, for E2 genes, the distribution of TGF-β + dZEB vs. dZEb is most positive, indicating that, when dZEB is absent or repressed, TGF-β can induced expression of these epithelial genes. Following the methodology applied to M-genes in (23), the regulation of E-gene subclusters was inferred from their response to each condition. The response of E1 to each factor is independent of the other factor (compare TGF-β vs. WT to TGF-β + dZEB vs. dZEB and DOX vs. DSMO to DOX + SB vs. SB), similar to M2, so we infer regulation occurs via an "OR" gate. E3 genes are repressed by expression TGF-β in the presence of ZEB1 (TGF-β vs. WT), but unaffected by ZEB1 in the presence (DOX vs. DMSO) or absence (DOX + SB vs. SB) of TGF-β. As such, E3 regulation is similar to M1, requiring integration of TGF-β and ZEB1 via an "AND" style logic gate. However, unlike M1, the absence of ZEB1 doesn't suppress the TGF-β effect on E3. Rather, TGF-β has the opposite effect on E3 genes without ZEB1 (TGF-β + dZEB vs. dZEb). Finally, E2 genes are repressed by ZEB1 (DOX vs. DMSO), independent of TGF-β (DOX + SB vs. SB), while TGF-β activates E2 (TGF-β + dZEB vs. dZEB), though this effect is suppressed in the absence of ZEB1 (TGF-β vs. WT). While this pattern is difficult to describe using a single logical gate, it is easy to understand as ZEB1 regulating E2 both directly and by suppressing the activating function of ZEB1. Therefore, E2 is similar to M3 in that ZEB1 plays the dominant role in regulating the expression.

Supplementary Figure 11 | Boxplots showing the distribution of P53, PTEN, and RB expression across different clusters of BRCA samples indicated by color (E = orange, I0 = pink, I1 = purple, I2 = blue, M = green). A full table of *p*-values can be found in **Supplementary Table 15**.

Supplementary Figure 12 | TGF-β induced EMT time course in E-M score space with six GMM clusters. **(A)** Segmented models of the relationship between the time since TGF-β induction of EMT and the E-M scores of treated cells. Different colored lines correspond to the best fit (black), lower bound (light red), and upper bound (light blue) models. Individual BRCA samples are indicated as by open points with their color corresponding to the assigned cluster (E = orange, I0 = pink, I1 = purple, I1' = blue, I2 = green, M = red). Note that, much like the 5-cluster GMM models, the models pass from E to I1 to I2 to M, with only the upper bound intersecting with I1'. **(B)** The predicated probability of samples at a point in segmented model TGF-β induced EMT belonging to each cell state cluster from the six cluster GMM model of BRCA samples. The probabilities were calculated by applying the BRCA GMM model to segmented model of E-M scores with respect to time after TGF-β induction. Note that I1' appears for a small period of time between I1 and I2 and never accounts for the majority predictions of the cell state at any point during TGF-β induced EMT.

Supplementary Figure 13 | Boxplots showing the distribution of ZEB1 expression across six clusters of BRCA samples indicated by color (E = orange, I0 = pink, I1 = purple, I1' = blue, I2 = green, M = red). As with the five cluster GMM model of BRCA samples, the differences between E-I1-I2-M clusters are significant. The I1' cluster has significantly higher expression than I1 and significantly lower expression than M, but is not different from I2. Expression values are normalized RSEM (RNA-Seq by Expectation Maximization) values.

Supplementary Figure 14 | Phenotypic scores BRCA cancer samples in the six cluster GMM model. **(A)** Boxplots showing the distribution of migration related gene set scores across different clusters of BRCA samples indicated by color (E = orange, I0 = pink, I1 = purple, I2 = blue, M = green). **(B)** Boxplots showing the distribution of proliferation related gene set scores across different clusters of BRCA samples indicated by color as in **(A)**. Note that in both cases, the association between BRCA clusters and phenotypic data is the same, with proliferation being maintained through I1 and migration increasing at I1, though I1 occasionally represents a peak of migration at or above the level of M.

Supplementary Table 1 | BIC Scores for BRCA sample models.

Supplementary Table 2 | BIC Scores for PAAD sample models.

Supplementary Table 3 | BIC Scores for LUAD sample models.

Supplementary Table 4 | BIC Scores for CESC sample models.

Supplementary Table 5 | BIC Scores for PRAD sample models.

Supplementary Table 6 | Adjusted R-squared values for different breakpoint models.

Supplementary Table 7 | Description of phenotypic gene sets from the Broad Institute.

Supplementary Table 8 | *P*-values and 95% CI values for TES scores between clusters.

Supplementary Table 9 | *P*-values for EMT Factor expression between clusters.

Supplementary Table 10 | *P*-values for migration scores between clusters.

Supplementary Table 11 | *P*-values for proliferation scores between clusters.

Supplementary Table 12 | Overlap between E-M gene sets and Broad Institute gene sets.

Supplementary Table 13 | *P*-values for cell cycle and DNA repair scores between clusters.

Supplementary Table 14 | *P*-values for proto onco-gene and tumor suppressor pathway scores between clusters.

Supplementary Table 15 | *P*-values for tumor suppressor gene expression between clusters.

Supplementary File 1 | EMT related scores and cluster classifications for samples in TCGA.

Supplementary File 2 | EMT related scores for EMT time course data.

REFERENCES

1. Nakaya Y, Sheng G. EMT in developmental morphogenesis. *Cancer Lett.* (2013) 341:9–15. doi: 10.1016/j.canlet.2013.02.037
2. Lim J, Thiery JP. Epithelial-mesenchymal transitions: insights from development. *Development.* (2012) 139:3471–86. doi: 10.1242/dev.071209
3. Lambert AW, Pattabiraman DR, Weinberg RA. Emerging biological principles of metastasis. *Cell.* (2017) 168:670–91. doi: 10.1016/j.cell.2016.11.037
4. Guo D, Xu B-L, Zhang X-H, Dong M-M. Cancer stem-like side population cells in the human nasopharyngeal carcinoma cell line cne-2 possess epithelial mesenchymal transition properties in association with metastasis. *Oncol Rep.* (2012) 28:241–7. doi: 10.3892/or.2012.1781
5. Thiery JP, Acloque H, Huang RYJ, Nieto MA. Epithelial-mesenchymal transitions in development and disease. *Cell.* (2009) 139:871–90. doi: 10.1016/j.cell.2009.11.007
6. Nieto MA. Epithelial plasticity: a common theme in embryonic and cancer cells. *Science.* (2013) 342:1234850. doi: 10.1126/science.1234850
7. Shinde A, Libring S, Alpsoy A, Abdullah A, Schaber JA, Solorio L, et al. Autocrine fibronectin inhibits breast cancer metastasis. *Mol Cancer Res.* (2018) 78(Suppl 13):2128. doi: 10.1158/1538-7445.AM2018-2128
8. Wang J, Zhou F, Yin L, Zhao L, Zhang Y, Wang J. MicroRNA-199b targets the regulation of ZEB1 expression to inhibit cell proliferation, migration and invasion in nonsmall cell lung cancer. *Mol Med Rep.* (2017) 16:5007–14. doi: 10.3892/mmr.2017.7195
9. Celià-Terrassa T, Bastian C, Liu D, Ell B, Aiello NM, Wei Y, et al. Hysteresis control of epithelial-mesenchymal transition dynamics conveys a distinct program with enhanced metastatic ability. *Nat Commun.* (2018) 9:5005. doi: 10.1038/s41467-018-07538-7
10. Fischer KR, Durrans A, Lee S, Sheng J, Li F, Wong ST, et al. Epithelial-to-mesenchymal transition is not required for lung metastasis but contributes to chemoresistance. *Nature.* (2015) 527:472–6. doi: 10.1038/nature15748
11. Zheng X, Carstens JL, Kim J, Scheible M, Kaye J, Sugimoto H, et al. Epithelial-to-mesenchymal transition is dispensable for metastasis but induces chemoresistance in pancreatic cancer. *Nature.* (2015) 527:525–30. doi: 10.1038/nature16064
12. Grande MT, Sanchez-Laorden B, Lopez-Blau C, De Frutos CA, Boutet A, Arevalo M, et al. Snail1-induced partial epithelial-to-mesenchymal transition drives renal fibrosis in mice and can be targeted to reverse established disease. *Nat Med.* (2015) 21:989–97. doi: 10.1038/nm.3901
13. Futterman MA, Garcia AJ, Zamir EA. Evidence for partial epithelial-to-mesenchymal transition (pEMT) and recruitment of motile blastoderm edge cells during avian epiboly. *Dev Dyn.* (2011) 240:1502–11. doi: 10.1002/dvdy.22607
14. Huang RY, Wong MK, Tan TZ, Kuay KT, Ng AH, Chung VY, et al. An EMT spectrum defines an anoikis-resistant and spheroidogenic intermediate mesenchymal state that is sensitive to e-cadherin restoration by a src-kinase inhibitor, saracatinib (AZD0530). *Cell Death Dis.* (2013) 4:e915. doi: 10.1038/cddis.2013.442
15. Lu M, Jolly MK, Levine H, Onuchic JN, Ben-Jacob E. MicroRNA-based regulation of epithelial-hybrid-mesenchymal fate determination. *Proc Natl Acad Sci USA.* (2013) 110:17874–9. doi: 10.1073/pnas.1318192110
16. Steinway SN, Zanudo JGT, Michel PJ, Feith DJ, Loughran TP, Albert R. Combinatorial interventions inhibit TGFbeta-driven epithelial-to-mesenchymal transition and support hybrid cellular phenotypes. *NPJ Syst Biol Appl.* (2015) 1:15014. doi: 10.1038/npjsba.2015.14
17. Jolly MK, Tripathi SC, Jia D, Mooney SM, Celiktas M, Hanash SM, et al. Stability of the hybrid epithelial/mesenchymal phenotype. *Oncotarget.* (2016) 7:27067. doi: 10.18632/oncotarget.8166
18. Hong T, Watanabe K, Ta CH, Villarreal-Ponce A, Nie Q, Dai X. An Ovol2-Zeb1 mutual inhibitory circuit governs bidirectional and multi-step transition between epithelial and mesenchymal states. *PLoS Comput Biol.* (2015) 11:e1004569. doi: 10.1371/journal.pcbi.1004569
19. Zhang J, Tian XJ, Zhang H, Teng Y, Li R, Bai F, et al. TGF-β -induced epithelial-to-mesenchymal transition proceeds through stepwise activation of multiple feedback loops. *Sci Signal.* (2014) 7:ra91-ra. doi: 10.1126/scisignal.2005304
20. Pastushenko I, Brisebarre A, Sifrim A, Fioramonti M, Revenco T, Boumahdi S, et al. Identification of the tumour transition states occurring during EMT. *Nature.* (2018) 556:463–8. doi: 10.1038/s41586-018-0040-3
21. Grosse-Wilde A, Fouquier d'Herouel A, McIntosh E, Ertaylan G, Skupin A, Kuestner RE, et al. Stemness of the hybrid epithelial/mesenchymal state in breast cancer and its association with poor survival. *PLoS ONE.* (2015) 10:e0126522. doi: 10.1371/journal.pone.0126522
22. George JT, Jolly MK, Xu S, Somarelli JA, Levine H. Survival outcomes in cancer patients predicted by a partial EMT gene expression scoring metric. *Cancer Res.* (2017) 77:6415–28. doi: 10.1158/0008-5472.CAN-16-3521
23. Watanabe K, Panchy N, Noguchi S, Suzuki H, Hong T. Combinatorial perturbation analysis reveals divergent regulations of mesenchymal genes during epithelial-to-mesenchymal transition. *NPJ Syst Biol Appl.* (2019) 5:21. doi: 10.1038/s41540-019-0097-0
24. Foroutan M, Cursons J, Hediyeh-Zadeh S, Thompson EW, Davis MJ. A transcriptional program for detecting TGFβ-induced EMT in Cancer. *Mol Cancer Res.* (2017) 15:619–31. doi: 10.1158/1541-7786.MCR-16-0313
25. Zhao M, Kong L, Liu Y, Qu H. dbEMT: an epithelial-mesenchymal transition associated gene resource. *Sci Rep.* (2015) 5:11459. doi: 10.1038/srep11459
26. Tan TZ, Miow QH, Miki Y, Noda T, Mori S, Huang RYJ, et al. Epithelial-mesenchymal transition spectrum quantification and its efficacy in deciphering survival and drug responses of cancer patients. *EMBO Mol Med.* (2014) 6:1279–93. doi: 10.15252/emmm.201404208
27. Cursons J, Pillman KA, Scheer KG, Gregory PA, Foroutan M, Hediyeh-Zadeh S, et al. Combinatorial targeting by microRNAs co-ordinates post-transcriptional control of EMT. *Cell Systems.* (2018) 7:77–91.e7. doi: 10.1016/j.cels.2018.05.019
28. Colaprico A, Silva TC, Olsen C, Garofano L, Cava C, Garolini D, et al. TCGAbiolinks: an R/Bioconductor package for integrative analysis of TCGA data. *Nucleic Acids Res.* (2016) 44:e71. doi: 10.1093/nar/gkv1507
29. Mounir M, Lucchetta M, Silva TC, Olsen C, Bontempi G, Chen X, et al. New functionalities in the TCGAbiolinks package for the study and integration of cancer data from GDC and GTEx. *PLoS Comput Biol.* (2019) 15:e1006701. doi: 10.1371/journal.pcbi.1006701
30. Jia D, Lu M, Jung KH, Park JH, Yu L, Onuchic JN, et al. Elucidating cancer metabolic plasticity by coupling gene regulation with metabolic pathways. *Proc Natl Acad Sci USA.* (2019) 116:3909. doi: 10.1073/pnas.1816391116
31. Yu L, Lu M, Jia D, Ma J, Ben-Jacob E, Levine H, et al. Modeling the genetic regulation of cancer metabolism: interplay between glycolysis and oxidative phosphorylation. *Cancer Res.* (2017) 77:1564–74. doi: 10.1158/0008-5472.CAN-16-2074
32. Zhang J, Chen H, Li R, Taft DA, Yao G, Bai F, et al. Spatial clustering and common regulatory elements correlate with coordinated gene expression. *PLoS Comput Biol.* (2019) 15:e1006786. doi: 10.1371/journal.pcbi.1006786
33. Hänzelmann S, Castelo R, Guinney J. GSVA: gene set variation analysis for microarray and RNA-Seq data. *BMC Bioinformatics.* (2013) 14:7. doi: 10.1186/1471-2105-14-7
34. Scrucca L, Fop M, Murphy TB, Raftery AE. mclust 5: clustering, classification and density estimation using Gaussian finite mixture models. *R J.* (2016) 8:289–317. doi: 10.32614/RJ-2016-021

35. Muggeo VMR. Interval estimation for the breakpoint in segmented regression: a smoothed score-based approach. *Aust NZ J Stat*. (2017) 59:311–22. doi: 10.1111/anzs.12200
36. Muggeo VMR. Testing with a nuisance parameter present only under the alternative: a score-based approach with application to segmented modelling. *J Stat Comput Simul*. (2016) 86:3059–67. doi: 10.1080/00949655.2016.1149855
37. Davies RB. Hypothesis testing when a nuisance parameter is present only under the alternative: linear model case. *Biometrika*. (2002) 89:484–9. doi: 10.1093/biomet/89.2.484
38. Davies RB. Hypothesis testing when a nuisance parameter is present only under the alternatives. *Biometrika*. (1987) 74:33–43. doi: 10.1093/biomet/74.1.33
39. Muggeo VM. Estimating regression models with unknown break-points. *Stat Med*. (2003) 22:3055–71. doi: 10.1002/sim.1545
40. Li B, Dewey CN. RSEM: accurate transcript quantification from RNA-Seq data with or without a reference genome. *BMC Bioinformatics*. (2011) 12:323. doi: 10.1186/1471-2105-12-323
41. Törönen P, Kolehmainen M, Wong G, Castrén E. Analysis of gene expression data using self-organizing maps. *FEBS Lett*. (1999) 451:142–6. doi: 10.1016/S0014-5793(99)00524-4
42. Kohonen T. The self-organizing map. *Neurocomputing*. (1998) 21:1–6. doi: 10.1016/S0925-2312(98)00030-7
43. Subramanian A, Tamayo P, Mootha VK, Mukherjee S, Ebert BL, Gillette MA, et al. Gene set enrichment analysis: a knowledge-based approach for interpreting genome-wide expression profiles. *Proc Natl Acad Sci USA*. (2005) 102:15545–50. doi: 10.1073/pnas.0506580102
44. Karacosta LG, Anchang B, Ignatiadis N, Kimmey SC, Benson JA, Shrager JB, et al. Mapping lung cancer epithelial-mesenchymal transition states and trajectories with single-cell resolution. *bioRxiv*. (2019) 570341. doi: 10.1101/570341
45. Krebs AM, Mitschke J, Lasierra Losada M, Schmalhofer O, Boerries M, Busch H, et al. The EMT-activator Zeb1 is a key factor for cell plasticity and promotes metastasis in pancreatic cancer. *Nat Cell Biol*. (2017) 19:518–29. doi: 10.1038/ncb3513
46. Maupin KA, Sinha A, Eugster E, Miller J, Ross J, Paulino V, et al. Glycogene expression alterations associated with pancreatic cancer epithelial-mesenchymal transition in complementary model systems. *PLoS ONE*. (2010) 5:e13002. doi: 10.1371/journal.pone.0013002
47. Zhau HE, Odero-Marah V, Lue H-W, Nomura T, Wang R, Chu G, et al. Epithelial to mesenchymal transition (EMT) in human prostate cancer: lessons learned from ARCaP model. *Clin Exp Metastasis*. (2008) 25:601–10. doi: 10.1007/s10585-008-9183-1
48. Chen CL, Mahalingam D, Osmulski P, Jadhav RR, Wang CM, Leach RJ, et al. Single-cell analysis of circulating tumor cells identifies cumulative expression patterns of EMT-related genes in metastatic prostate cancer. *The Prostate*. (2013) 73:813–26. doi: 10.1002/pros.22625
49. Qureshi R, Arora H, Rizvi MA. EMT in cervical cancer: its role in tumour progression and response to therapy. *Cancer Lett*. (2015) 356:321–31. doi: 10.1016/j.canlet.2014.09.021
50. Zavadil J, Böttinger EP. TGF-β and epithelial-to-mesenchymal transitions. *Oncogene*. (2005) 24:5764–774. doi: 10.1038/sj.onc.1208927
51. Wellner U, Schubert J, Burk UC, Schmalhofer O, Zhu F, Sonntag A, et al. The EMT-activator ZEB1 promotes tumorigenicity by repressing stemness-inhibiting microRNAs. *Nat Cell Biol*. (2009) 11:1487–95. doi: 10.1038/ncb1998
52. Leroy P, Mostov KE. Slug is required for cell survival during partial epithelial-mesenchymal transition of HGF-induced tubulogenesis. *Mol Biol Cell*. (2007) 18:1943–52. doi: 10.1091/mbc.e06-09-0823
53. Villarejo A, Cortés-Cabrera A, Molina-Ortíz P, Portillo F, Cano A. Differential role of Snail1 and Snail2 zinc fingers in E-cadherin repression and epithelial to mesenchymal transition. *J Biol Chem*. (2014) 289:930–41. doi: 10.1074/jbc.M113.528026
54. Cano A, Pérez-Moreno MA, Rodrigo I. The transcription factor snail controls epithelial–mesenchymal transitions by repressing E-cadherin expression. *Nature Cell*. (2000) 2:76–83. doi: 10.1038/35000025
55. Dave N, Guaita-Esteruelas S, Gutarra S, Frias A, Beltran M, Peiro S, et al. Functional cooperation between Snail1 and twist in the regulation of ZEB1 expression during epithelial to mesenchymal transition. *J Biol Chem*. (2011) 286:12024–32. doi: 10.1074/jbc.M110.168625
56. DaSilva-Arnold SC, Kuo C-Y, Davra V, Remache Y, Kim PCW, Fisher JP, et al. ZEB2, a master regulator of the epithelial–mesenchymal transition, mediates trophoblast differentiation. *MHR: Basic Sci Reprod Med*. (2018) 25:61–75. doi: 10.1093/molehr/gay053
57. Fang X, Cai Y, Liu J, Wang Z, Wu Q, Zhang Z, et al. Twist2 contributes to breast cancer progression by promoting an epithelial–mesenchymal transition and cancer stem-like cell self-renewal. *Oncogene*. (2011) 30:4707–20. doi: 10.1038/onc.2011.181
58. Padua D, Massagué J. Roles of TGFβ in metastasis. *Cell Res*. (2009) 19:89–102. doi: 10.1038/cr.2008.316
59. Wu Y, Siadaty MS, Berens ME, Hampton GM, Theodorescu D. Overlapping gene expression profiles of cell migration and tumor invasion in human bladder cancer identify metallothionein 1E and nicotinamide N-methyltransferase as novel regulators of cell migration. *Oncogene*. (2008) 27:6679–89. doi: 10.1038/onc.2008.264
60. Goldrath AW, Luckey CJ, Park R, Benoist C, Mathis D. The molecular program induced in T cells undergoing homeostatic proliferation. *Proc Natl Acad Sci USA*. (2004) 101:16885–90. doi: 10.1073/pnas.0407417101
61. Fujiwara M, Marusawa H, Wang HQ, Iwai A, Ikeuchi K, Imai Y, et al. Parkin as a tumor suppressor gene for hepatocellular carcinoma. *Oncogene*. (2008) 27:6002–11. doi: 10.1038/onc.2008.199
62. Jolly MK, Mani SA, Levine H. Hybrid epithelial/mesenchymal phenotype (s): the 'fittest'for metastasis? *Biochim Biophys Acta Rev Cancer*. (2018) 1870:151–7. doi: 10.1016/j.bbcan.2018.07.001
63. Shah SP, Roth A, Goya R, Oloumi A, Ha G, Zhao Y, et al. The clonal and mutational evolution spectrum of primary triple-negative breast cancers. *Nature*. (2012) 486:395–9. doi: 10.1038/nature10933
64. Nik-Zainal S, Davies H, Staaf J, Ramakrishna M, Glodzik D, Zou X, et al. Landscape of somatic mutations in 560 breast cancer whole-genome sequences. *Nature*. (2016) 534:47–54. doi: 10.1038/nature17676
65. Perren A, Weng L-P, Boag AH, Ziebold U, Thakore K, Dahia PLM, et al. Immunohistochemical evidence of loss of PTEN expression in primary ductal adenocarcinomas of the breast. *Am J Pathol*. (1999) 155:1253–60. doi: 10.1016/S0002-9440(10)65227-3
66. Hu X, Stern HM, Ge L, O'Brien C, Haydu L, Honchell CD, et al. Genetic alterations and oncogenic pathways associated with breast cancer subtypes. *Mol Cancer Res*. (2009) 7:511–22. doi: 10.1158/1541-7786.MCR-08-0107
67. Jolly MK, Somarelli JA, Sheth M, Biddle A, Tripathi SC, Armstrong AJ, et al. Hybrid epithelial/mesenchymal phenotypes promote metastasis and therapy resistance across carcinomas. *Pharmacol Ther*. (2019) 194:161–84. doi: 10.1016/j.pharmthera.2018.09.007
68. Karacosta LG, Anchang B, Ignatiadis N, Kimmey SC, Benson JA, Shrager JB, et al. Mapping lung cancer epithelial-mesenchymal transition states and trajectories with single-cell resolution. *Nat Commun*. (2019) 10:5587. doi: 10.1038/s41467-019-13441-6
69. Liu S, Cong Y, Wang D, Sun Y, Deng L, Liu Y, et al. Breast cancer stem cells transition between epithelial and mesenchymal states reflective of their normal counterparts. *Stem Cell Rep*. (2014) 2:78–91. doi: 10.1016/j.stemcr.2013.11.009
70. Li C, Hong T, Nie Q. Quantifying the landscape and kinetic paths for epithelial-mesenchymal transition from a core circuit. *Phys Chem Chem Phys*. (2016) 18:17949–56. doi: 10.1039/C6CP03174A
71. Tian X-J, Zhang H, Xing J. Coupled reversible and irreversible bistable switches underlying TGFβ-induced epithelial to mesenchymal transition. *Biophys J*. (2013) 105:1079–89. doi: 10.1016/j.bpj.2013.07.011
72. Font-Clos F, Zapperi S, La Porta CAM. Topography of epithelial–mesenchymal plasticity. *Proc Natl Acad Sci USA*. (2018) 115:5902–7. doi: 10.1073/pnas.1722609115
73. Chu L-F, Leng N, Zhang J, Hou Z, Mamott D, Vereide DT, et al. Single-cell RNA-seq reveals novel regulators of human embryonic stem cell differentiation to definitive endoderm. *Genome Biol*. (2016) 17:173. doi: 10.1186/s13059-016-1033-x

74. MacLean AL, Hong T, Nie Q. Exploring intermediate cell states through the lens of single cells. *Curr Opin Syst Biol.* (2018) 9:32–41. doi: 10.1016/j.coisb.2018.02.009
75. Ta CH, Nie Q, Hong T. Controlling stochasticity in epithelial-mesenchymal transition through multiple intermediate cellular states. *Discrete Continuous Dynamical Syst B.* (2016) 21:2275–91. doi: 10.3934/dcdsb.2016047
76. Gupta PB, Fillmore CM, Jiang G, Shapira SD, Tao K, Kuperwasser C, et al. Stochastic state transitions give rise to phenotypic equilibrium in populations of cancer cells. *Cell.* (2011) 146:633–44. doi: 10.1016/j.cell.2011.07.026
77. Hong T, Oguz C, Tyson JJ. A mathematical framework for understanding four-dimensional heterogeneous differentiation of CD4+ T cells. *Bull Math Biol.* (2015) 77:1046–64. doi: 10.1007/s11538-015-0076-6
78. Jolly MK, Ware KE, Gilja S, Somarelli JA, Levine H. EMT and MET: necessary or permissive for metastasis? *Mol Oncol*. (2017) 11:755–69. doi: 10.1002/1878-0261.12083
79. Mani Sa, Guo W, Liao M-J, Eaton EN, Ayyanan A, Zhou AY, et al. The epithelial-mesenchymal transition generates cells with properties of stem cells. *Cell.* (2008) 133:704–15. doi: 10.1016/j.cell.2008.03.027
80. Kröger C, Afeyan A, Mraz J, Eaton EN, Reinhardt F, Khodor YL, et al. Acquisition of a hybrid E/M state is essential for tumorigenicity of basal breast cancer cells. *Proc Natl Acad Sci USA*. (2019) 116:7353–62. doi: 10.1073/pnas.1812876116
81. Nieto MA, Huang RY, Jackson RA, Thiery JP. EMT: 2016. *Cell.* (2016) 166:21–45. doi: 10.1016/j.cell.2016.06.028

Conflict of Interest: The authors declare that the research was conducted in the absence of any commercial or financial relationships that could be construed as a potential conflict of interest.

Copyright © 2020 Panchy, Azeredo-Tseng, Luo, Randall and Hong. This is an open-access article distributed under the terms of the Creative Commons Attribution License (CC BY). The use, distribution or reproduction in other forums is permitted, provided the original author(s) and the copyright owner(s) are credited and that the original publication in this journal is cited, in accordance with accepted academic practice. No use, distribution or reproduction is permitted which does not comply with these terms.

frontiers in Oncology

ORIGINAL RESEARCH
published: 19 February 2020
doi: 10.3389/fonc.2020.00050

Single Tumor Cells With Epithelial-Like Morphology Are Associated With Breast Cancer Metastasis

Liubov A. Tashireva[1], Marina V. Zavyalova[1,2], Olga E. Savelieva[1], Tatyana S. Gerashchenko[3], Evgeniya V. Kaigorodova[1,4], Evgeny V. Denisov[3,5] and Vladimir M. Perelmuter[1]*

[1] Department of General and Molecular Pathology, Cancer Research Institute, Tomsk National Research Medical Center, Tomsk, Russia, [2] Department of Pathological Anatomy, Siberian State Medical University, Tomsk, Russia, [3] Laboratory of Cancer Progression Biology, Cancer Research Institute, Tomsk National Research Medical Center, Tomsk, Russia, [4] Department of Biochemistry and Molecular Biology, Siberian State Medical University, Tomsk, Russia, [5] Department of Organic Chemistry, Tomsk State University, Tomsk, Russia

Introduction: The identification of tumor cells that can be potential metastatic seeds would reach two key aims—prognosis of metastasis risk and appointment of the optimal adjuvant therapy to prevent metastatic disease. Single tumor cells (STCs) located out of multicellular structures can most likely demonstrate features that are needed to initiate metastasis.

Methods: One-hundred-and-thirty-five patients with invasive breast carcinoma of no special type have been enrolled. Molecular subtypes of breast cancer were categorized according to St. Gallen recommendations. Hematoxylin and eosin staining was used to identify STCs with epithelial-like morphology (eSTCs) in breast tumors. Immunofluorescence staining was applied to evaluate stemness and epithelial–mesenchymal transition (EMT) in STCs. The correlation between STCs and recurrence and metastasis-free survival (MFS) was performed using the Kaplan–Meier method and the log-rank test.

Results: Distant metastasis was more frequent in eSTC-positive than eSTC-negative patients (28.0% vs. 9.4%, $p = 0.007$). When tumor types were analyzed separately, distant metastasis tended to be more frequent in eSTC-positive than eSTC-negative patients for HER2-positive cancer [75.0% (3/4) vs. 12.5% (1/8), $p = 0.066$]. In luminal A [22.7% (5/22) vs. 10.0% (3/30), $p = 0.259$], luminal B [21.1% (4/19) vs. 6.7% (2/30), $p = 0.189$], and triple-negative [40.0% (2/5) vs. 11.8% (2/17), $p = 0.209$] cancers, distance metastasis was not associated with eSTCs. Median MFS was not reached in eSTC-positive and eSTC-negative patients. eSTC-positive patients had a higher risk of breast cancer metastasis [hazard ratio (HR) 3.57, 95% confidence interval (CI): 1.46–8.71; $p = 0.001$]. When tumor types were analyzed separately, a higher risk of breast cancer metastasis occurred only in HER2-positive patients (HR 8.49, 95% CI: 1.29–55.59; $p = 0.016$). Immunofluorescence analysis revealed mesenchymal-like STCs (mSTCs) and inter- and intra-tumor heterogeneity in STCs. There were breast tumors with either eSTCs or mSTCs and tumors with

OPEN ACCESS

Edited by:
Satyendra Chandra Tripathi, All India Institute of Medical Sciences Nagpur, India

Reviewed by:
Anna Zaczek, Medical University of Gdansk, Poland
Jason Somarelli, Duke University, United States
Saurav Kumar, Indian Institute of Science (IISc), India

***Correspondence:**
Liubov A. Tashireva
tashireva@oncology.tomsk.ru

Specialty section:
This article was submitted to Molecular and Cellular Oncology, a section of the journal Frontiers in Oncology

Received: *21 August 2019*
Accepted: *13 January 2020*
Published: *19 February 2020*

Citation:
Tashireva LA, Zavyalova MV, Savelieva OE, Gerashchenko TS, Kaigorodova EV, Denisov EV and Perelmuter VM (2020) Single Tumor Cells With Epithelial-Like Morphology Are Associated With Breast Cancer Metastasis. Front. Oncol. 10:50. doi: 10.3389/fonc.2020.00050

both types of STCs. Both eSTCs and mSTCs were represented by cells with different stem and/or EMT phenotypes.

Conclusions: STCs with epithelial-like morphology contribute to breast cancer metastasis and represent an attractive model for studying mechanisms of metastatic seeding. The assessment of STCs in histological sections of breast tumors can be a simple and effective method for the prediction of metastasis risk.

Keywords: single tumor cells, breast cancer, EMT, stem cell, distant metastasis

INTRODUCTION

The prediction of tumor progression risk, including lymph node and distant metastasis, remains one of the most important problems in modern oncology. Metastasis can occur not only by single tumor cells (STCs) but also by tumor cell clusters (1). In the past, metastasis was thought to occur by retention of metastatic cells in the capillary system of the first parenchymatous organ encountered (2). This hypothesis was subsequently dismissed as metastatic cells were shown to reach the vasculature of all organs (2). Moreover, clusters of tumor cells are able to pass through capillary-sized vessels (3). Recent findings give further support to the "seed and soil" hypothesis (2) that focuses on the dissemination of STCs.

STCs are a manifestation of intratumor morphological heterogeneity and most likely result from multicellular tumor structures through cancer invasion. In the last years, the appearance of STCs is described as tumor budding in the invasive front (4).

Invasive carcinoma of no special type (IC NST), the most common form of breast cancer (5), is highly heterogeneous in the morphological pattern. Previously, we showed that breast tumor cells can be either single, arranged in small (discrete) groups, or arranged in more complex structures (tubular, alveolar, solid, and trabecular) (6). In addition, we suggested that the intratumor morphological heterogeneity in breast cancer is a result of the unfolding of the invasion program during which epithelial–mesenchymal transition (EMT) leads to significant morphogenetic changes in the tumor landscape: from tubular structures that are close to normal mammary ducts to discrete groups of tumor cells demonstrating a strongly pronounced mesenchymal phenotype (7). The recent study hypothesized that the intratumor morphological heterogeneity can be an attractive model for studying the mechanisms of collective cell invasion (by focusing on solid and trabecular structures) and individual cell invasion (by focusing on discrete groups, namely, STCs) (8).

According to current understanding, STCs may be in a quiescent state or invade by mesenchymal, amoeboid, and hybrid mesenchymal–amoeboid motion (9, 10). The definition of these STC states could be an effective tool for studying the mechanisms of cancer invasion and intravasation and would help to predict metastasis risk.

Thus, the aim of this study was to assess morphological and phenotypical heterogeneity of STCs and their prognostic significance in breast cancer patients.

TABLE 1 | Clinicopathological characteristics of breast cancer patients.

Characteristics		No eSTCs, % (*n*)	Yes eSTCs, % (*n*)	*p*
Postoperative treatment	Adjuvant chemotherapy: CMF, FAC, CAX	80 (68)	82 (41)	NS
	Antiestrogen therapy with tamoxifen	20 (17)	18 (9)	NS
Age	<35 years	35 (30)	26 (13)	NS
	35–50 years	22 (19)	36 (18)	NS
	>50 years	43 (36)	38 (19)	NS
Menopausal status	Premenopausal	33 (28)	36 (18)	NS
	Postmenopausal	67 (57)	64 (32)	NS
Stage	I ($T_1N_0M_0$)	28 (24)	16 (8)	NS
	IIA ($T_{0-1}N_1M_0$, $T_2N_0M_0$)	39 (33)	32 (16)	NS
	IIB ($T_2N_1M_0$, $T_3N_0M_0$)	13 (11)	14 (7)	NS
	IIIA ($T_{0-2}N_2M_0$, $T_3N_{1-2}M_0$)	14 (12)	30 (15)	NS
	IIIB ($T_4N_{0-2}M_0$)	1 (1)	0 (0)	NS
	IIIC ($T_{1-4}N_3M_0$)	5 (4)	8 (4)	NS
Grade	I	7 (6)	10 (5)	NS
	II	74 (63)	80 (40)	NS
	III	19 (16)	10 (5)	NS
Tumor size	<2 cm	55 (47)	30 (15)	0.007
	2–5 cm	44 (37)	62 (31)	0.049
	>5 cm	1 (1)	8 (4)	NS
Molecular subtype	Luminal A	35 (30)	44 (22)	NS
	Luminal B	35 (30)	38 (19)	NS
	Triple-negative	20 (17)	10 (5)	NS
	HER2-positive	10 (8)	8 (4)	NS
Estrogen receptors	Positive	75 (64)	86 (43)	NS
	Negative	25 (20)	14 (7)	NS
Progesterone receptors	Positive	62 (53)	64 (32)	NS
	Negative	38 (32)	36 (18)	NS
HER2	Positive	20 (17)	26 (13)	NS
	Negative	80 (68)	74 (37)	NS
Ki-67	Expression < 20%	36 (31)	48 (24)	NS
	Expression > 20%	64 (54)	52 (26)	NS

CMF, cyclophosphamide, methotrexate, 5-fluorouracil; FAC, 5-fluorouracil, adriamycin, cyclophosphamide; CAX, cyclophosphamide, adriamycin, xeloda; NS, not significant.

MATERIALS AND METHODS

Patients and Specimens

The retrospective study included 135 patients with IC NST (stage I-IIIC, $T_{1-4}N_{0-3}M_0$) who were treated in the Cancer Research Institute, Tomsk NRMC between 2008 and 2015 (**Table 1**). The median age was 55 years (range: 29–85 years). All cases were reexamined, and IC NST was diagnosed and staged according to the World Health Organization's recommendations (5). Patients had not received neoadjuvant chemotherapy and were monitored using computed tomography (CT) scan every 6 months to identify metastatic lesions. Recurrence- and metastasis-free survival (RFS and MFS) was defined as the time window spanning between the diagnosis and the detection of the first recurrence or metastatic lesion on imaging or patient death, whichever occurred first.

Formalin-fixed, paraffin-embedded (FFPE) samples of breast tumors were used for morphological ($n = 135$), immunohistochemical ($n = 135$), and immunofluorescence analyses ($n = 25$).

The procedures followed in this study were in accordance with the Helsinki Declaration (1964, amended in 1975 and 1983). All patients signed informed consent for voluntary participation. The study was approved by the review board of the Cancer Research Institute, Tomsk NRMC on 17 June 2016 (the approval number is 8).

Morphological Analysis

The morphological analysis included the determination of STCs in breast tumors (**Figure 1**). Five-micrometer-thick hematoxylin and eosin (H&E)-stained sections of FFPE samples were used for the STC analysis using an Axio Lab.A1 light microscope (Carl Zeiss, Germany). STCs (or detached individual tumor cells) were determined in the entire tumor tissue in contrast to tumor buds residing in the invasive front and defined as tumor cells located out of multicellular tumor structures (tubular, alveolar, solid, and trabecular) but similar to them in cytological features. STCs with epithelial morphology (eSTCs) had eosin-stained cytoplasm of different volumes and were larger than immune and stromal cells (tumor cell nuclei $\geq 3 \times$ the size of lymphocyte). Tumor cells similar to fibroblasts/myofibroblasts or mononuclear leukocytes (lymphoid cells, macrophages) in shape and size were not possible to identify in H&E-stained sections and were revealed using the epithelial marker, cytokeratin 7 (CK7). We attributed these cells to STCs with mesenchymal morphology (mSTCs).

Immunohistochemical Analysis

Immunohistochemistry was used to assess the expression of estrogen and progesterone receptors (ER and PR),

TABLE 2 | Frequency of recurrences in breast cancer patients with eSTCs.

	No eSTCs	Yes eSTCs	*P*-values
Luminal A	3.33 (1/30)	4.54 (1/22)	1.000
Luminal B	0.00 (0/30)	0.00 (0/19)	1.000
Triple-negative	5.88 (1/17)	4.00 (2/5)	0.116
HER2-positive	12.50 (1/8)	0.00 (0/4)	1.000

P-values indicate differences between patients with the absence ("No") and presence ("Yes") of eSTCs.

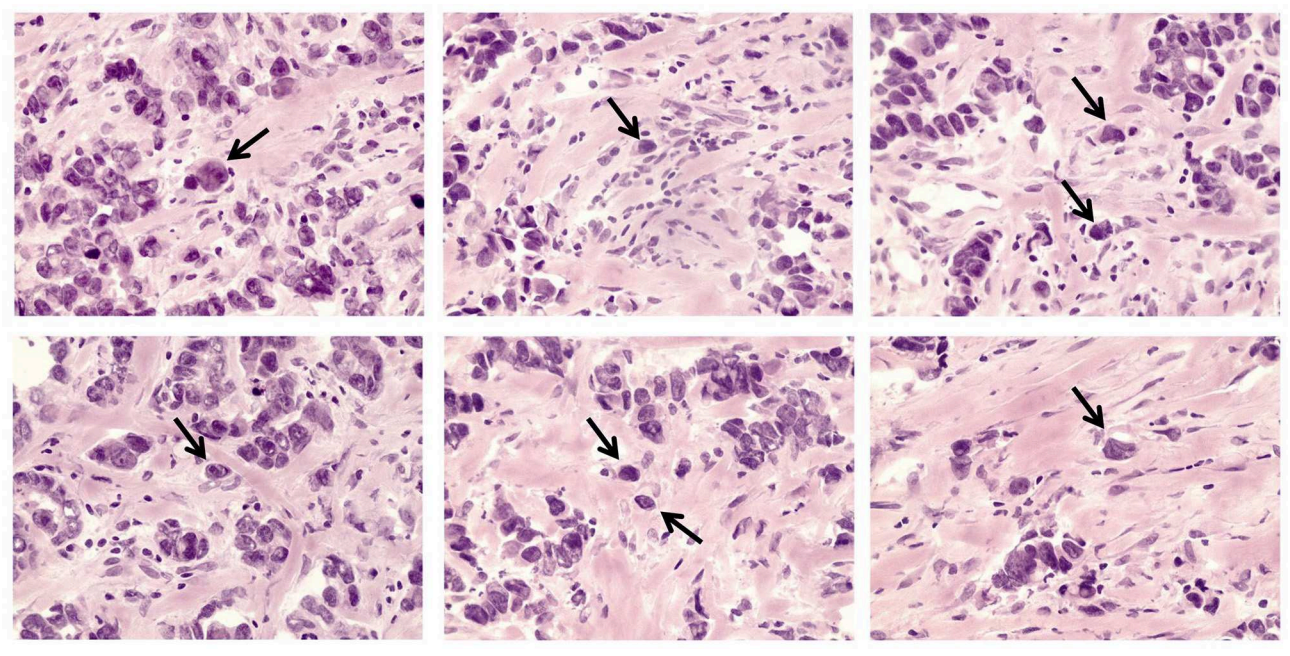

FIGURE 1 | eSTCs in invasive breast carcinoma of no special type. Arrows indicate eSTCs located out of multicellular structures. 400× magnification.

HER2, and Ki-67 in breast tumors using the following antibodies: mouse anti-ER (Dako, Cat. # IR084, clone 1D5, RTU), mouse anti-PR (Dako, Cat. # IR068, clone PgR636, RTU), rabbit anti-HER2 (Dako, Cat. # A0485, 1:800), and mouse anti-Ki-67 (Dako, Cat. # IR626, clone MIB-1, RTU). Immunohistochemistry was performed as previously described (11). ER and PR immunostaining was scored using ASCO/CAP Recommendations (12). HER2 immunostaining was scored using St. Gallen recommendations (13). Ki-67 immunostaining was expressed as the percentage of positively stained cells. At least 10 fields of view and at least 1,000 cells at 400× magnification (field area = 0.196 mm^2) were analyzed per sample. Molecular subtypes of the IC NST were categorized according to St. Gallen recommendations (13): luminal A (ER^+ and/or PR^+, $HER2^-$, and Ki-67 < 20%), luminal B (ER^+ and/or PR^+, $HER2^{-/+}$, and Ki-67 ≥ 20%), HER2-positive (ER^-, PR^-, and $HER2^+$), and triple-negative (ER^-, PR^-, and $HER2^-$).

Immunofluorescence Analysis

Immunofluorescence staining was used to analyze the morphological and phenotypical heterogeneity of STCs. Seven-micrometer-thick sections were prepared from FFPE tumor samples (n = 25), deparaffinized, rehydrated, processed for heat-induced epitope retrieval in PT Link (Dako, Denmark) with high pH buffer, and blocked with 3% bovine serum albumin (Amresco, USA) in PBS. Subsequently, the sections were incubated with a cocktail of primary antibodies: mouse anti-CD133 (MyBioSource, Cat. # MBS5305439, clone 3F10, 1:800), rabbit anti-Snail/Slug (Abcam ab180714, 1:400), and goat anti-CK7 (Santa Cruze, Cat. # sc-70936, 1:50) or mouse anti-CD133 (MyBioSource, Cat. # MBS5305439, 1:800), rabbit anti-N-cadherin (Abcam ab76057, 1:400), and goat anti-CK7 (Santa Cruze, Cat. # sc-70936, 1:50) followed by incubation with the appropriate secondary antibodies: goat anti-mouse IgG H&L (Alexa Fluor 488, Abcam ab150117, 1:200), goat

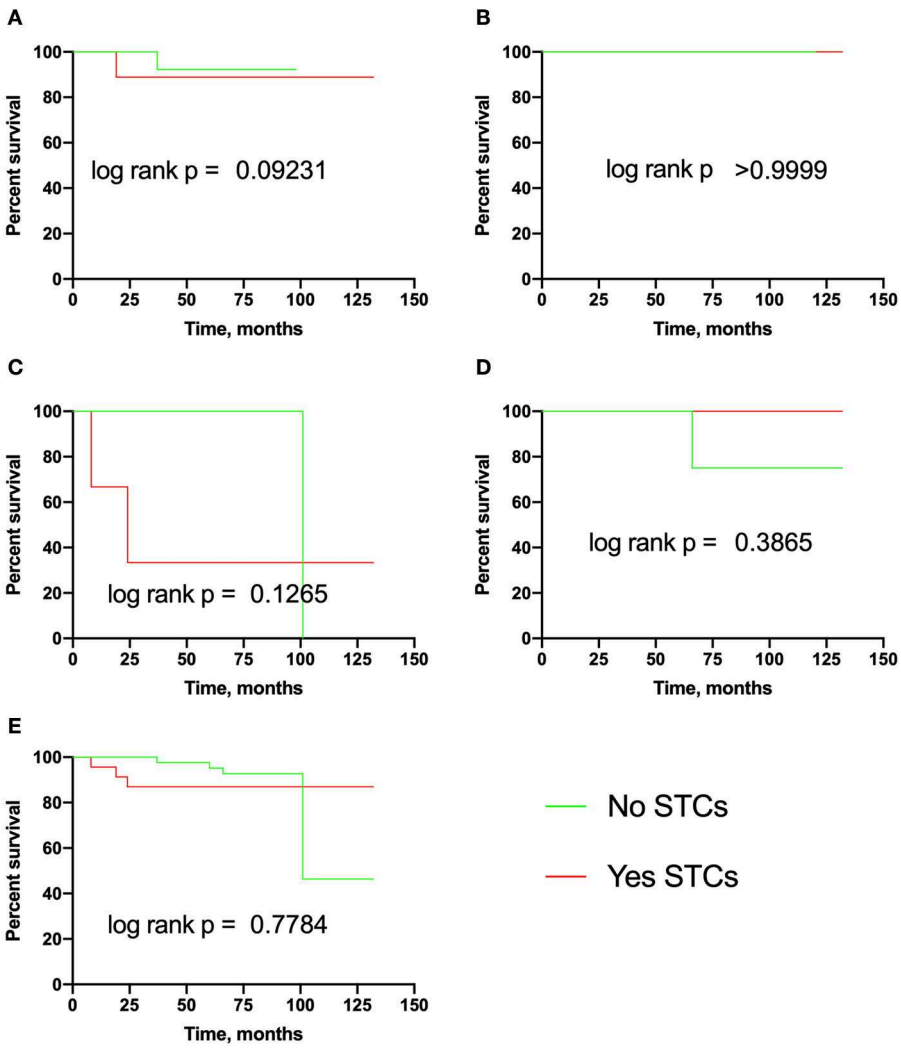

FIGURE 2 | Recurrence-free survival in breast cancer patients with eSTCs. **(A)** Luminal A. **(B)** Luminal B. **(C)** Triple-negative. **(D)** HER2-positive. **(E)** Total group.

anti-rabbit IgG H&L (Cy3, Abcam ab6939, 1:200), and donkey anti-goat IgG H&L (Alexa Fluor 647, Abcam ab150135, 1:200). Finally, Vectashield mounting medium (Vector Laboratories, USA) containing DAPI was used to detect nuclei and mount the specimens. The samples were analyzed using an LSM 780 NLO confocal microscope (Carl Zeiss, Germany).

Normal endometrial, liver, and tonsillar tissues were used as a positive control for anti-CD133, N-cadherin, and Snail antibodies, respectively. Human skin fibroblasts were used as a negative control for CD133 and N-cadherin staining. Snail expression was heterogeneous in cells of mammary acini and ducts. Negative control for Snail staining was acinar and ductal cells that did not express this protein.

Using CK7 staining, we identified STCs with distinct epithelial- and mesenchymal-like morphologies. eSTCs had abundant cytoplasm and were larger than immune and stromal cells (tumor cell nuclei $\geq 3 \times$ the size of the lymphocyte). mSTCs were detected as CK7-positive cells, in which the size and the cytological characteristics were similar to those of immune and stromal cells.

CD133-positive STCs were designated as stem cells. Snail was considered as a marker of early EMT (14), whereas N-cadherin—as a marker of advanced EMT (15, 16). Two parameters were used to evaluate the distribution of cells with stem and EMT phenotypes in eSTCs and mSTCs. First, we assessed how often stem and EMT cells were observed in eSTC- and mSTC-positive patients. Second, we calculated the percentage of stem and EMT cells among eSTCs and mSTCs.

Statistical Analysis

Statistical analysis was performed using STATISTICA 8.0 for Windows (StatSoft Inc., USA). Normal distribution was tested using the Shapiro–Wilk test. Fisher's exact test was applied to assess differences in the frequency of cell subpopulations both between STCs with various morphologies and different clinicopathological parameters. The Mann–Whitney U-test was applied to analyze differences in the percentage of cell subpopulations between STCs with various morphologies. MFS and RFS were evaluated using the Kaplan–Meier estimator with the log-rank test. Differences were considered significant at

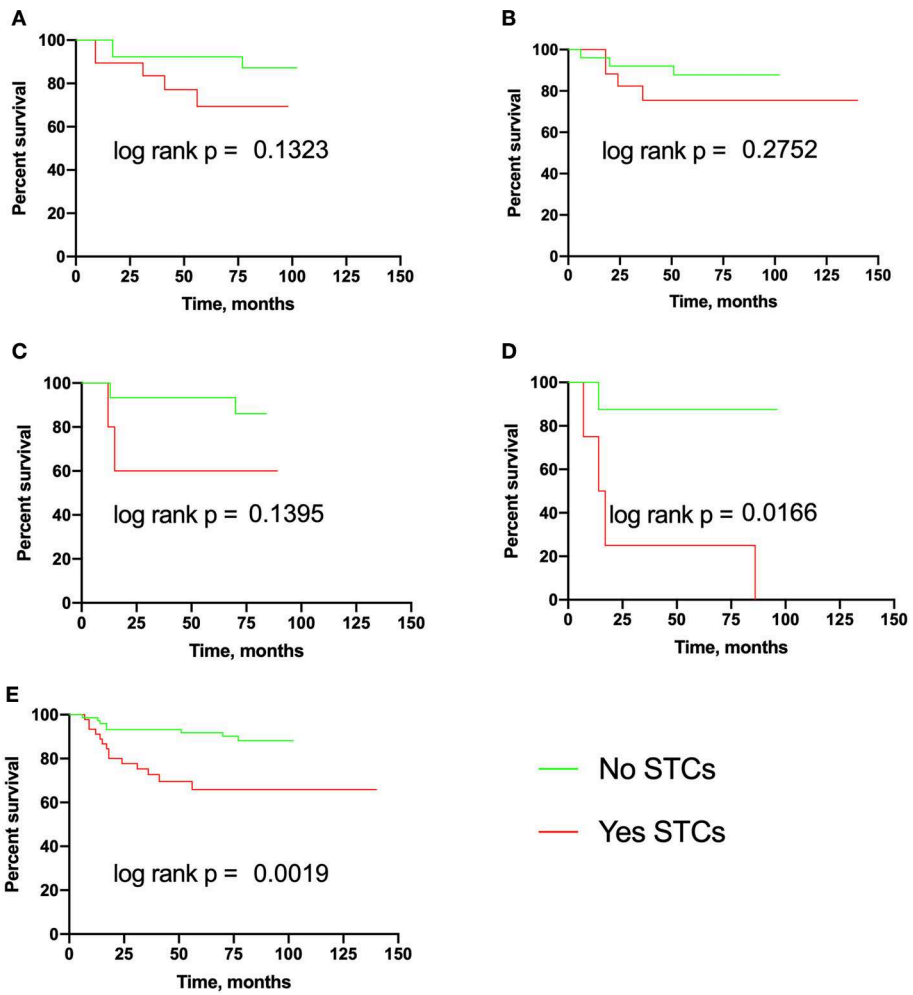

FIGURE 3 | Metastasis-free survival in breast cancer patients with eSTCs. **(A)** Luminal A. **(B)** Luminal B. **(C)** Triple-negative. **(D)** HER2-positive. **(E)** Total group.

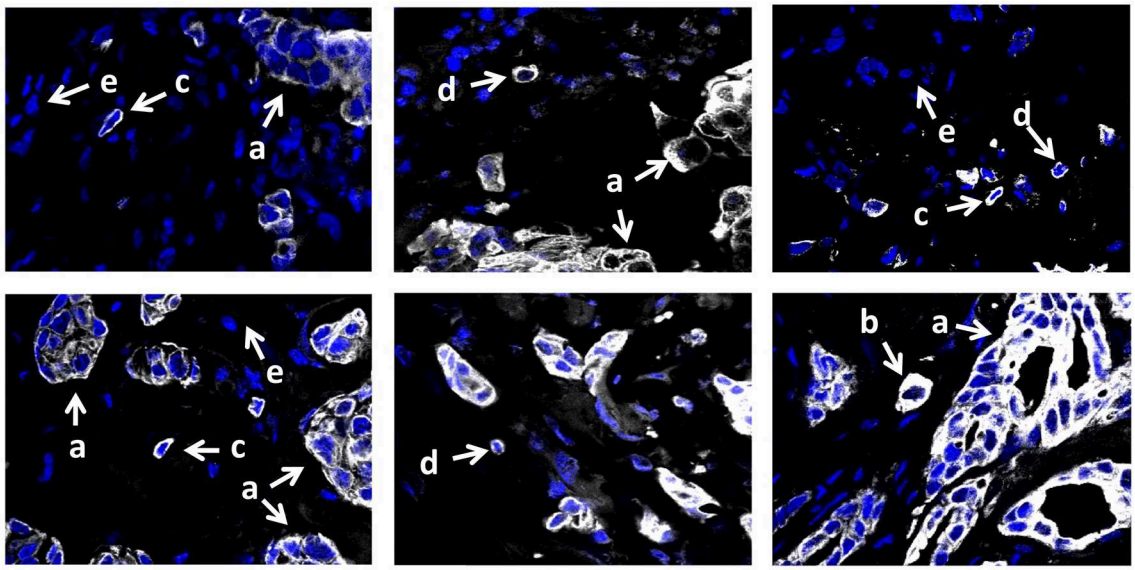

FIGURE 4 | CK7 expression in invasive breast carcinoma of no special type. Multicellular structures are formed by tumor cells with epithelial morphology (marked by the letter "a"). Few CK7-positive STCs have epithelial morphology and do not differ from tumor cells of multicellular structures (marked by the letter "b"). Numerous CK7-positive mSTCs with fibroblast- (marked by the letter "c") or lymphocyte-like (marked by the letter "d") morphology are similar to CK7-negative stromal cells (marked by the letter "e"). 400× magnification.

$p < 0.05$. Differences at $0.05 > p < 0.1$ were discussed as non-significant trends. Cox proportional hazard analysis was used to assess the association between eSTCs and MFS and RFS. Associations were reported as hazard ratios (HRs) with 95% confidence intervals (95% CIs) and *p*-values (likelihood ratio test).

RESULTS AND DISCUSSION

Frequency of eSTCs in Breast Cancer: an Association With Clinicopathological Parameters

Here, we assessed the frequency of STCs in breast tumors ($n = 135$). It must be noted that only eSTCs could be detected in the H&E sections of breast tumors (**Figure 1**). eSTCs were found in 37.0% (50/135) of the breast tumors. Their frequency did not vary between molecular subtypes of breast cancer: 42.3% (22/52)—luminal A, 38.8% (19/49)—luminal B, 22.7% (5/22)—triple-negative, and 33.3% (4/12)—HER2-positive tumors. The frequency of eSTCs did not depend on the parameters of the patients. However, eSTCs were more frequent in large-sized tumors (2–5 cm) (**Table 1**).

Association of eSTCs With Breast Cancer Progression

In this section, we assessed the association of eSTCs with recurrence, lymph node, and distant metastasis in breast cancer. It turned out that the probability of recurrence and RFS did not depend on eSTCs (**Table 2**, **Figure 2**).

By contrast, lymph node involvement was more frequent in eSTC-positive than in eSTC-negative patients [60.0% (30/50) vs. 32.1% (27/84), $p = 0.002$]. This association was significant only in luminal A [59.1% (13/22) vs. 23.3% (7/30), $p = 0.011$]. In luminal B [63.1% (12/19) vs. 44.8% (13/29), $p = 0.250$], triple-negative [60.0% (3/5) vs. 29.4% (5/17), $p = 0.308$], and HER2-positive cancer [50.0% (2/4) vs. 25.0% (2/8), $p = 0.547$], lymph node metastasis was not associated with eSTCs.

The frequency of distant metastasis was also higher in eSTC-positive than in eSTC-negative patients [28.0% (14/50) vs. 9.4% (8/85), $p = 0.007$]. This association was at a borderline significance in HER2-positive [75.0% (3/4) vs. 12.5% (1/8), $p = 0.066$] cancer and not significant in luminal A [22.7% (5/22) vs. 10.0% (3/30), $p = 0.259$], luminal B [21.1% (4/19) vs. 6.7% (2/30), $p = 0.189$], and triple-negative [40.0% (2/5) vs. 11.8% (2/17), $p = 0.209$] cancers.

The median MFS was not reached in eSTC-positive and eSTC-negative patients both in the total group and in any molecular subtypes (**Figure 3**). eSTC-positive patients had a higher risk of breast cancer metastasis (HR 3.57, 95% CI: 1.46–8.71; $p = 0.001$). When tumor types were analyzed separately, a higher risk of breast cancer metastasis occurred only in HER2-positive patients (HR 8.49, 95% CI: 1.29–55.59; $p = 0.016$).

Morphological Heterogeneity of STCs

To assess the morphological heterogeneity in STCs, we analyzed the expression of the epithelial marker, cytokeratin 7 (CK7), in 15 breast cancers with eSTCs and 10 cases without these cells. CK7-positive STCs were represented by cells with both distinct epithelial and mesenchymal (fibroblast- or lymphocyte-like) morphologies (**Figure 4**). In particular, 40.0% (10/25) of the

cases had eSTCs, 28.0% (7/25) of the cases had mSTCs, and 32.0% (8/25) of the cases had eSTCs and mSTCs simultaneously.

CK7-positive STCs tended to be observed more frequently in luminal B cancers, whereas CK7-negative STCs were more often in triple-negative cancers (**Table 3**). In HER2-positive cancer, the frequencies of $CK7^+$ and $CK7^-$ STCs were not compared due to small patient numbers in each group (**Table 3**).

Morphological and immunofluorescence analysis showed a high level of concordance (88%) in the identification of eSTCs. In 12% (3/25) of the cases, eSTCs were not detected morphologically but were observed by immunofluorescence staining with CK7. Most likely, it was related to the scarcity of CK7-positive STCs in H&E sections or their intermediate epithelial–mesenchymal morphology. It must be noted that immunofluorescence analysis not only confirmed the absence of eSTCs in H&E stained sections of some cases but also showed the presence of mSTCs in these cases.

Based on the morphological analysis, we classified breast cancer patients to three groups: with eSTCs (mSTCs−) only, with mSTCs (eSTCs−) only, and with eSTCs and mSTCs (eSTC+mSTC+) simultaneously.

TABLE 3 | Frequency of eSTCs and mSTCs in different molecular subtypes of breast cancer.

Patient groups		eSTC+mSTC–	eSTC–mSTC+	eSTC+mSTC+
Luminal A	1	20.0 (2/10)	30.0 (3/10)	50.0 (5/10)
Luminal B	2	66.7 (6/9) p_{2-1} =0.069 p_{2-3} = 0.181	11.1 (1/9)	22.2 (2/9)
Triple-negative	3	0.0 (0/3)	66.7 (2/3) p_{3-2} = 0.127	33.3 (1/3)

Fisher's exact test. p_{2-1}, p_{2-3}, and p_{3-2}, differences between luminal B (2), luminal A (1), and triple-negative (3) cancers.

Heterogeneity of STCs in Stem and EMT Features

Markers for stemness (CD133) and EMT (Snail and/or N-cadherin) were assessed in eSTCs and mSTCs (**Table 4**, **Figures 5**, **6**). However, the frequencies of tumors with stem and/or EMT cells did not differ between patient groups, eSTC (mSTC–) and mSTC (eSTC–) (**Table 4**). Nevertheless, the differences in the percentages of different subpopulations were observed among eSTCs and mSTCs (**Table 5**).

Stem cells with early ($CK7^+CD133^+Snail^+$) and late ($CK7^+CD133^+$N-cadherin$^+$) EMT were lower in the mSTC (eSTC–) group compared to the eSTC (mSTC–) group (**Table 5**). In the patient group with the simultaneous presence of eSTCs and mSTCs, $CK7^+CD133^+Snail^-$ and $CK7^+CD133^+$N-cadherin$^-$ cells tended to be rare among mSTCs compared to eSTCs (**Table 4**). Surprisingly, the percentage of these stem-like non-EMT cells did not differ between eSTCs and mSTCs in patients in which the tumor simultaneously contained eSTCs and mSTCs (**Table 5**).

Non-stem and non-EMT ($CK7^+CD133^-Snail^-$) cells were predominant among eSTCs and mSTCs in all three groups of patients: eSTC (mSTC–), mSTC (eSTC–), and eSTC+mSTC+ (**Tables 4**, **5**).

DISCUSSION

STCs, i.e., detached individual tumor cells, are widely recognized by pathologists in H&E-stained sections, but their phenotypic features and role in cancer progression remain to be elucidated. Some studies reported genetic analysis of STCs, but in many cases, these were not detached individual cells and were obtained from tumor samples by mechanical dissociation (17) or from multicellular structures by laser microdissection (18). Other studies described STCs at the invasive front, for example, in

TABLE 4 | Frequency of cells with stem and EMT phenotypes among eSTCs and mSTCs.

Cells	eSTC+mSTC– (1)	eSTC–mSTC+ (2)	eSTC+mSTC+	
			eSTCs (3)	mSTCs (4)
$CK7^+CD133^-Snail^-$	100 (9/9)	100 (5/5)	100 (7/7)	100 (8/8)
$CK7^+CD133^-Snail^+$	78 (7/9)	40 (2/5)	86 (6/7)	50 (4/8)
$CK7^+CD133^+Snail^-$	67 (6/9)	100 (5/5)	43 (3/7)	0 (0/8) p_{3-4} = 0.076 p_{2-4} = 0.0008
$CK7^+CD133^+Snail^+$	89 (8/9)	60 (3/5)	71 (5/7)	25 (2/8)
$CK7^+CD133^-$N-cadherin$^-$	100 (9/9)	100 (5/5)	100 (7/7)	88 (7/8)
$CK7^+CD133^-$N-cadherin$^+$	89 (8/9)	100 (5/5)	86 (6/7)	38 (3/8)
$CK7^+CD133^+$N-cadherin$^-$	56 (5/9)	40 (2/5)	71 (5/7)	13 (1/8) p_{3-4} = 0.040
$CK7^+CD133^+$N-cadherin$^+$	100 (9/9)	60 (3/5)	57 (4/7)	25 (2/8)

Fisher's exact test. p_{2-4} and p_{3-4}, differences between groups of patients with only mSTCs (2) and simultaneously with eSTCs (3) and mSTCs (4).

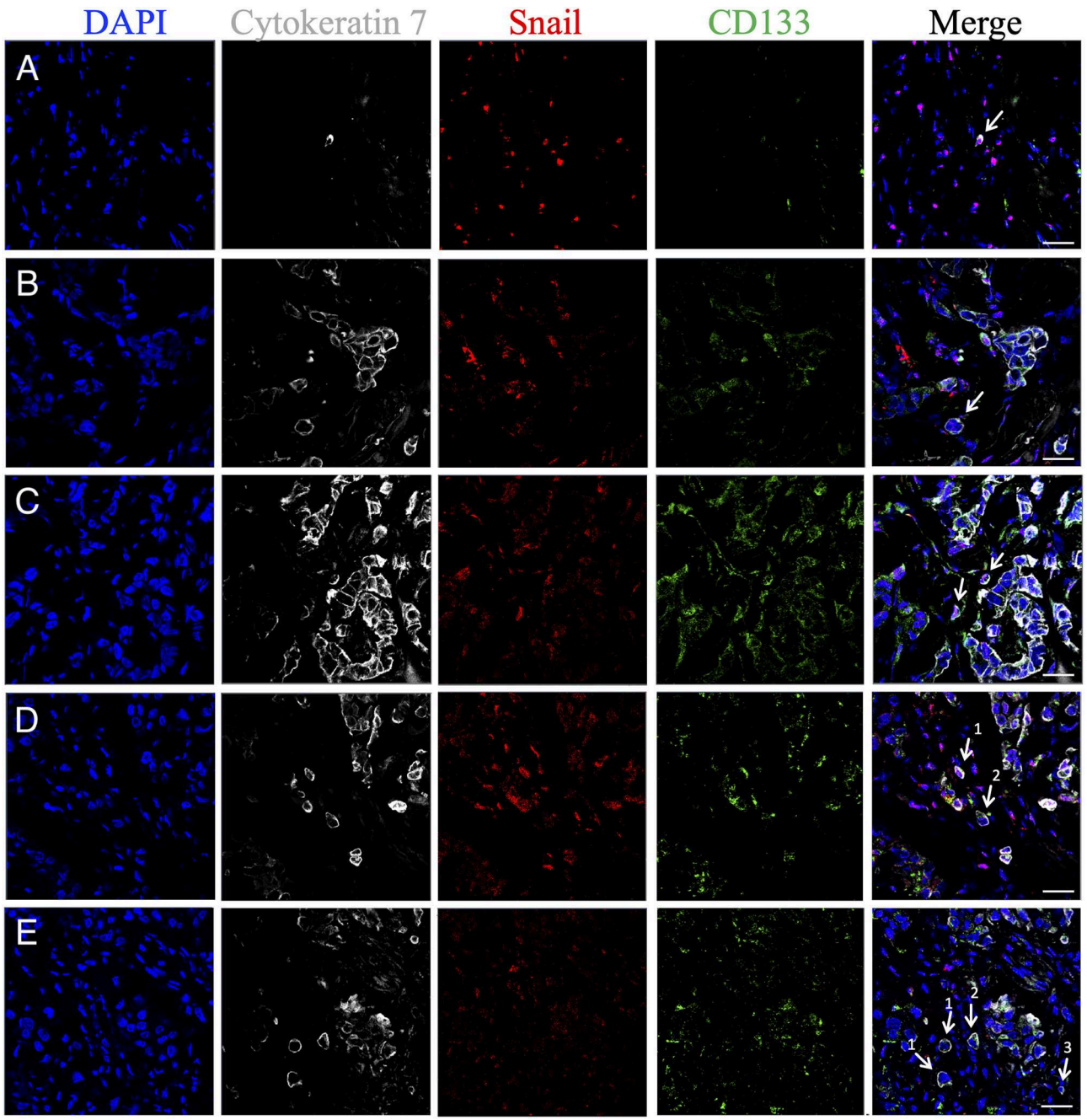

FIGURE 5 | Phenotypic heterogeneity of eSTCs and mSTCs in stem and early EMT features. **(A)** Nonstem mSTC with early EMT ($CK7^+CD133^-Snail^+$) surrounded by immune and stromal cells. **(B)** eSTC without stem and EMT features ($CK7^+CD133^-Snail^-$) near the multicellular structure. **(C)** Stem mSTC with early EMT ($CK7^+CD133^+Snail^+$) near the multicellular structure. **(D)** Stem mSTC with early EMT ($CK7^+CD133^+Snail^+$) among microenvironment cells (1) and stem eSTC without EMT ($CK7^+CD133^+Snail^-$) similar in size to tumor cells composing multicellular structures (2). **(E)** Nonstem eSTC without EMT ($CK7^+CD133^-Snail^-$) (1), stem eSTC without EMT ($CK7^+CD133^+Snail^-$) (2), and nonstem mSTC without EMT ($CK7^+CD133^-Snail^-$) among microenvironment cells. eSTCs were identified based on their similarity in size to tumor cells of multicellular structures, whereas mSTCs, to immune/stromal cells. Scale bar, 50 μm.

tumor budding (4), and investigated their genomic copy number profiles (19).

In this study, we determined STCs in the entire tumor tissue as cells with epithelial- or mesenchymal-like morphology that were represented by subpopulations with various EMT and stem phenotypes. However, only eSTCs were associated with breast cancer metastasis. In addition, eSTCs were prevalent in large-sized breast tumors. This finding may explain why large breast

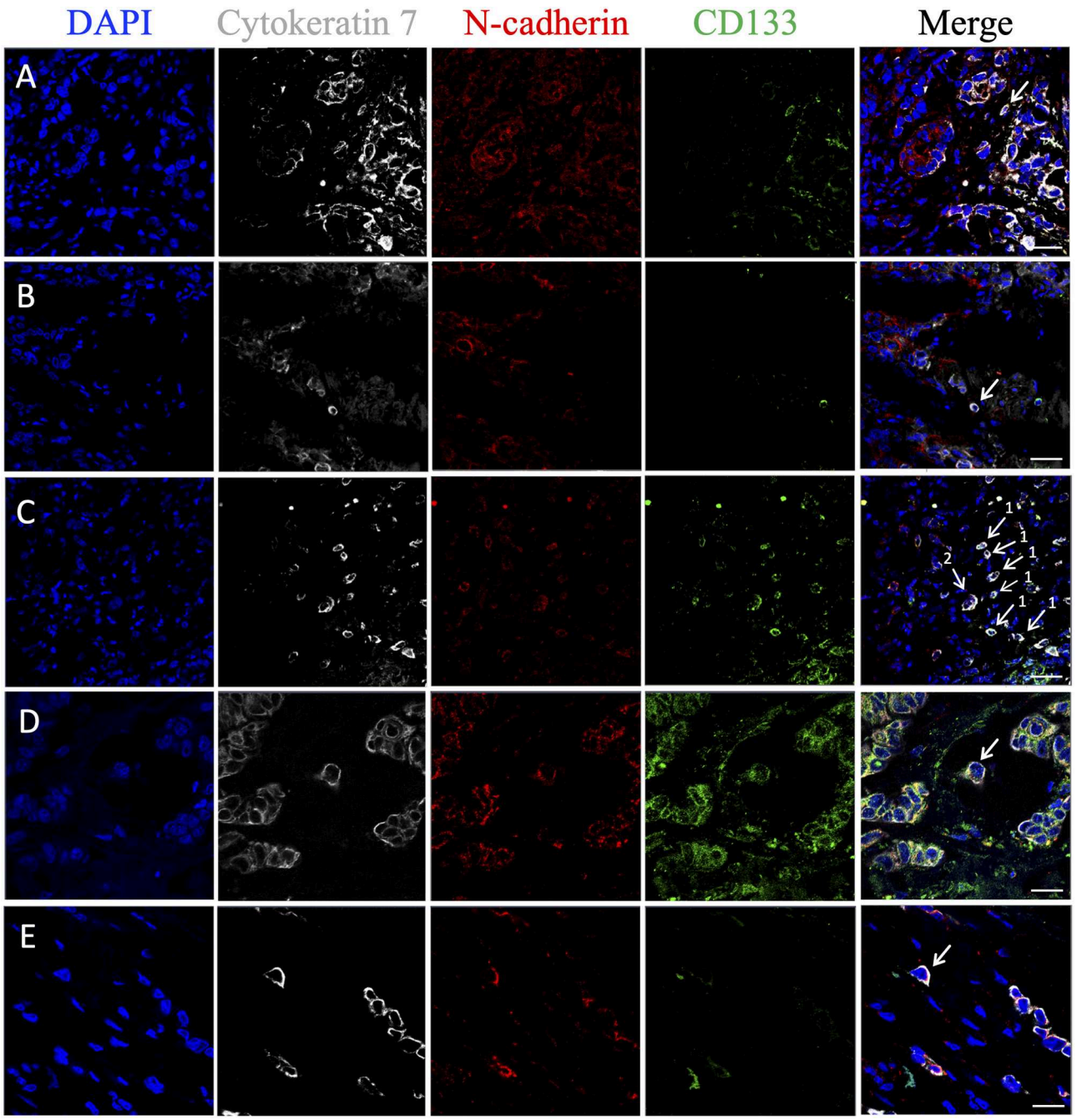

FIGURE 6 | Phenotypic heterogeneity of eSTCs and mSTCs in stem and advanced EMT features. **(A)** Stem mSTC with advanced EMT ($CK7^+CD133^+N\text{-}cadherin^+$) near the multicellular structures. **(B)** mSTC without the stem and EMT features ($CK7^+CD133^-N\text{-}cadherin^-$) among microenvironment cells. **(C)** Stem mSTC with advanced EMT ($CK7^+CD133^+N\text{-}cadherin^+$) (1) and the group of two tumor cells (were not considered as STCs in the study) with stem and advanced EMT features (2) among microenvironment cells. **(D)** Stem eSTC with advanced EMT ($CK7^+CD133^+N\text{-}cadherin^+$) near the multicellular structures. **(E)** Nonstem eSTC with advanced EMT ($CK7^+CD133^-N\text{-}cadherin^+$) near the multicellular structures. Scale bar, 50 μm **(A–C)** and 20 μm **(D,E)**.

tumors metastasize more often than small tumors (20). STCs probably appear in the tumor by detaching from multicellular tumor structures. Most likely, it may occur through two different mechanisms. The first mechanism, demonstrated by various studies, is that STCs are a result of detaching of leader cells at the invasive edge of multicellular tumor structures (21). The second mechanism is rather hypothetical and may be due to the pushing of tumor cells from multicellular structures to the stroma. As suggested by Rosenblatt and coauthors, such basal extrusion occurs in conditions of disrupting the S1P-S1P2 signaling

TABLE 5 | Percentage of cells with stem and EMT phenotypes among eSTCs and mSTCs.

	eSTC+mSTC– (1)	eSTC–mSTC+ (2)	eSTC+mSTC+	
			eSTCs (3)	mSTCs (4)
$CK7^+CD133^-Snail^-$	70.70 (24.20–80.00)	88.10 (80.00–94.00) $p_{1-2} = 0.031$	62.70 (46.50–78.20)	73.55 (51.30–100.00)
$CK7^+CD133^-Snail^+$	5.00 (1.70–7.50)	0.00 (0.00–1.40)	16.70 (6.40–24.10)	7.70 (0.00–37.45)
$CK7^+CD133^+Snail^-$	6.10 (0.00–19.00)	3.40 (2.00–4.50)	0.00 (0.00–8.60)	0.00
$CK7^+CD133^+Snail^+$	12.30 (9.40–29.30)	2.40 (0.00–8.50) $p_{1-2} = 0.025$	15.38 (0.00–21.60)	0.00 (0.00–3.20)
$CK7^+CD133^-$N-cadherin$^-$	50.00 (17.20–73.20)	68.30 (50.0–78.10)	64.30 (51.0–66.70)	95.45 (67.85–100.00)
$CK7^+CD133^-$N-cadherin$^+$	17.20 (15.60–33.30)	16.40 (7.30–22.70)	20.80 (13.60–33.30)	0.00 (0.00–13.65)
$CK7^+CD133^+$N-cadherin$^-$	1.20 (0.00–10.30)	1.20 (0.00–3.90)	6.60 (0.00–21.40)	0.00
$CK7^+CD133^+$N-cadherin$^+$	16.70 (7.70–21.70)	7.40 (0.00–12.20) $p_{1-2} = 0.011$	3.40 (0.00–17.70)	0.00 (0.00–3.05)

Percentages are given as medians and quartiles: Me (Q1–Q3). Mann–Whitney U-test. p_{1-2} and p_{3-4}, differences between groups of patients with eSTCs (1) only, with mSTCs (2) only, and with eSTCs (3) and mSTCs (4) simultaneously.

pathway underlying physiologically normal apical extrusion of cells that completed their life cycle (22, 23).

It is reasonable to assume that detaching cells from multicellular structures, or collective-individual transition, should be accompanied by EMT and following the inhibition of cell–cell adhesion. However, our results show that most STCs are not characterized by the expression of Snail or N-cadherin. This can be explained either by the fact that basal extrusion, if it occurs, is not related to EMT or by EMT reversibility (i.e., mesenchymal–epithelial transition, MET). In fact, the study of EMT in cancers resulted in the understanding of this process as a consecutive spectrum of cell states from initial epithelial through intermediate hybrid or metastable to terminal mesenchymal phenotypes (24, 25).

The term "epithelial–mesenchymal plasticity," which is more and more often used at the present time, most accurately describes the EMT–MET interconversion, with the possibility of phenotypic changes from epithelial to mesenchymal states and vice versa with a stop at any stage of the process (25, 26). The presence of cells with varying degrees of EMT among STCs with epithelial and mesenchymal morphology most likely reflects epithelial–mesenchymal plasticity.

At present, it is known that complete EMT is less effective for cancer progression than partial EMT that retains the molecular and morphological features of epithelial cells (26). Tumor cells with a hybrid epithelial–mesenchymal phenotype are more adaptive to the tumor microenvironment and resistant to immune reactions and demonstrate a pronounced colony-forming ability (27). In our study, eSTCs expressing Snail or N-cadherin most likely possess a hybrid (metastable) phenotype. This can explain the significant association between eSTCs and high probability of breast cancer metastasis. In addition, our results indicate that the presence of EMT features, particularly Snail or N-cadherin expression, is not accompanied by an obligatory transition from epithelial to fibroblast- or lymphocyte-like cell shape. The absence of spindle-like shape in tumor cells undergoing EMT was reported previously (28).

Nevertheless, tumor cells with mesenchymal morphology can be identified in H&E sections if they are located in multicellular structures together with epithelial-like cells. For example, the three-dimensional reconstruction of tumor tissue sections showed that tumor cells located at the invasive front of the collective invading structure rarely have spindle-like or round (mesenchymal) shape (29). In histological specimens, it is almost impossible to observe STCs with fibroblast- or lymphocyte-like morphology without epithelial markers. This fact should be considered when a pathologic response to neoadjuvant chemotherapy is assessed. It is well-known that a pathologic complete response (pCR) is a favorable prognostic factor. However, because pCR is determined by a pathologist based on the assessment of H&E sections, STCs with fibroblast- or lymphocyte-like morphology cannot be detected and the diagnosis can be inaccurate. Despite a high probability of this mistake, pCR remains a marker of good prognosis. Does it mean that mSTCs are not significant for cancer progression? The association between eSTCs and high frequency of breast cancer metastasis probably confirms the low importance of mSTCs in the formation of metastases. In reality, tumor cells with fibroblast-like shape were found to have a decreased aggressiveness (30). However, future studies should clarify the significance of eSTCs and mSTCs in metastasis.

According to our study, some eSTCs and mSTCs demonstrated features of either stemness, EMT, or simultaneous stemness and EMT that make them similar to circulating tumor cells (CTCs). For example, breast CTCs were found to express both epithelial and mesenchymal markers demonstrating EMT features (31). We also showed that CTCs are highly heterogeneous population in breast cancer and have similar phenotypes to STCs: various combinations of the stem and EMT features or the absence of these marks (32). The similarity of STC

and CTC phenotypes may indicate the high ability of STCs to intravasation (33).

The relationship between stemness and EMT in tumor cells is widely discussed (34); however, opinions about causal relationships between these processes are contradictory. The recent study showed that EMT inhibition results in the acquisition of stemness and the initiation of breast cancer metastasis. In contrast, EMT activation suppressed stem features (27). These findings are in agreement with our results that eSTCs are associated with breast cancer metastasis. Moreover, it was found that fibroblast-like cells with EMT features partially maintain the polarity, attach tightly to the extracellular matrix, and remain quiescent. It was assumed that these cells may irreversibly transform to cancer-associated fibroblasts (35).

CONCLUSIONS

STCs demonstrate morphological diversity and phenotypical heterogeneity in stem and EMT features. STCs with epithelial morphology are associated with breast cancer metastasis and probably demonstrate a hybrid (metastable) EMT phenotype. Given these findings, eSTCs represent an attractive object in the study of mechanisms and key features that are typical of metastatic "seeds." In general, the determination of eSTCs in histological sections of breast tumors may be considered as an available prognostic marker of metastasis.

DATA AVAILABILITY STATEMENT

The datasets generated for this study are available on request to the corresponding author.

ETHICS STATEMENT

The studies involving human participants were reviewed and approved by Ethic Committee of the Cancer Research Institute, Tomsk NRMC (the approval number is 8, on 17 June 2016). The patients/participants provided their written informed consent to participate in this study.

AUTHOR CONTRIBUTIONS

VP and MZ designed the research. MZ performed histology image analysis. LT, OS, and EK performed immunofluorescence analysis, score, and analysis of STCs in breast cancer samples. LT prepared confocal images. LT and TG performed data analysis. LT, ED, and VP drafted the work. VP supervised the study and the final approval of the version to be published.

FUNDING

This study was supported by the Russian Science Foundation (grant #19-75-30016).

REFERENCES

1. Aceto N, Bardia A, Miyamoto DT, Donaldson MC, Wittner BS, Spencer JA, et al. Circulating tumor cell clusters are oligoclonal precursors of breast cancer metastasis. *Cell*. (2014) 158:1110–22. doi: 10.1016/j.cell.2014.07.013
2. Psaila B, Lyden D. The metastatic niche: adapting the foreign soil. *Nat Rev Cancer*. (2009) 9:285–93. doi: 10.1038/nrc2621
3. Au SH, Storey BD, Moore JC, Tang Q, Chen YL, Javaid S, et al. Clusters of circulating tumor cells traverse capillary-sized vessels. *Proc Natl Acad Sci USA*. (2016) 113:4947–52. doi: 10.1073/pnas.1524448113
4. Grigore AD, Jolly MK, Jia D, Farach-Carson MC, Levine H. Tumor budding: the name is EMT. partial EMT. *J Clin Med*. (2016) 5:51. doi: 10.3390/jcm5050051
5. Lakhani SR, Ellis IO, Schnitt SJ, Tan PH, van de Vijver MJ. *World Health Organization (WHO) Classification of Tumours of the Breast*, 4 ed. Lyon: IARC Press (2012).
6. Zavyalova MV, Perelmuter VM, Vtorushin SV, Denisov EV, Litvyakov NV, Slonimskaya EM, et al. The presence of alveolar structures in invasive ductal NOS breast carcinoma is associated with lymph node metastasis. *Diagn Cytopathol*. (2013) 41:279–82. doi: 10.1002/dc.21852
7. Denisov EV, Skryabin NA, Gerashchenko TS, Tashireva LA, Wilhelm J, Buldakov MA, et al. Clinically relevant morphological structures in breast cancer represent transcriptionally distinct tumor cell populations with varied degrees of epithelial-mesenchymal transition and CD44(+)CD24(-) stemness. *Oncotarget*. (2017) 8:61163–80. doi: 10.18632/oncotarget.18022
8. Gerashchenko TS, Novikov NM, Krakhmal NV, Zolotaryova SY, Zavyalova MV, Cherdyntseva NV, et al. Markers of cancer cell invasion: are they good enough? *J Clin Med*. (2019) 8:1092. doi: 10.3390/jcm8081092
9. Chikina AS, Alexandrova AY. The cellular mechanisms and regulation of metastasis formation. *Mol Biol*. (2014) 48:165–80. doi: 10.1134/S0026893314020046
10. Krakhmal NV, Zavyalova MV, Denisov EV, Vtorushin SV, Perelmuter VM. Cancer invasion: patterns and mechanisms. *Acta Nat*. (2015) 7:17–28. doi: 10.32607/20758251-2015-7-2-17-28
11. Zavyalova MV, Denisov EV, Tashireva LA, Gerashchenko TS, Litviakov NV, Skryabin NA, et al. Phenotypic drift as a cause for intratumoral morphological heterogeneity of invasive ductal breast carcinoma not otherwise specified. *BioResearch Open Access*. (2013) 2:148–54. doi: 10.1089/biores.2012.0278
12. Hammond ME, Hayes DF, Dowsett M, Allred DC, Hagerty KL, Badve S, et al. American Society of Clinical Oncology/College of American Pathologists guideline recommendations for immunohistochemical testing of estrogen and progesterone receptors in breast cancer (unabridged version). *Arch Pathol Lab Med*. (2010) 134:e48–72. doi: 10.1043/1543-2165-134.7.e48
13. Coates AS, Winer EP, Goldhirsch A, Gelber RD, Gnant M, Piccart-Gebhart M, et al. Tailoring therapies–improving the management of early breast cancer: St Gallen International Expert Consensus on the Primary Therapy of Early Breast Cancer 2015. *Ann Oncol*. (2015) 26:1533–46. doi: 10.1093/annonc/mdv221
14. Peinado H, Olmeda D, Cano A. Snail, Zeb and bHLH factors in tumour progression: an alliance against the epithelial phenotype? *Nat Rev Cancer*. (2007) 7:415–28. doi: 10.1038/nrc2131
15. Huang RY, Wong MK, Tan TZ, Kuay KT, Ng AH, Chung VY, et al. An EMT spectrum defines an anoikis-resistant and spheroidogenic intermediate mesenchymal state that is sensitive to e-cadherin restoration by a src-kinase inhibitor, saracatinib (AZD0530). *Cell Death Dis*. (2013) 4:e915. doi: 10.1038/cddis.2013.442
16. Lindley LE, Briegel KJ. Molecular characterization of TGFbeta-induced epithelial-mesenchymal transition in normal finite lifespan human mammary epithelial cells. *Biochem Biophys Res Commun*. (2010) 399:659–64. doi: 10.1016/j.bbrc.2010.07.138
17. Hou Y, Guo H, Cao C, Li X, Hu B, Zhu P, et al. Single-cell triple omics sequencing reveals genetic, epigenetic, and transcriptomic heterogeneity in hepatocellular carcinomas. *Cell Res*. (2016) 26:304–19. doi: 10.1038/cr.2016.23

18. Foley JW, Zhu C, Jolivet P, Zhu SX, Lu P, Meaney MJ, et al. Gene expression profiling of single cells from archival tissue with laser-capture microdissection and Smart-3SEQ. *Genome Res*. (2019) 29:1816–25. doi: 10.1101/gr.234807.118
19. Casasent AK, Schalck A, Gao R, Sei E, Long A, Pangburn W, et al. Multiclonal invasion in breast tumors identified by topographic single cell sequencing. *Cell*. (2018) 172:205–17 e12. doi: 10.1016/j.cell.2017.12.007
20. Heimann R, Hellman S. Aging, progression, and phenotype in breast cancer. *J Clin Oncol*. (1998) 16:2686–92. doi: 10.1200/JCO.1998.16.8.2686
21. Mayor R, Etienne-Manneville S. The front and rear of collective cell migration. *Nat Rev Mol Cell Biol*. (2016) 17:97–109. doi: 10.1038/nrm.2015.14
22. Slattum G, Gu Y, Sabbadini R, Rosenblatt J. Autophagy in oncogenic K-Ras promotes basal extrusion of epithelial cells by degrading S1P. *Curr Biol*. (2014) 24:19–28. doi: 10.1016/j.cub.2013.11.029
23. Gudipaty SA, Rosenblatt J. Epithelial cell extrusion: pathways and pathologies. *Semin Cell Dev Biol*. (2017) 67:132–40. doi: 10.1016/j.semcdb.2016.05.010
24. Lambert AW, Pattabiraman DR, Weinberg RA. Emerging biological principles of metastasis. *Cell*. (2017) 168:670–91. doi: 10.1016/j.cell.2016.11.037
25. Nieto MA, Huang RY, Jackson RA, Thiery JP. Emt: 2016. *Cell*. (2016) 166:21–45. doi: 10.1016/j.cell.2016.06.028
26. Jolly MK, Boareto M, Huang B, Jia D, Lu M, Ben-Jacob E, et al. Implications of the hybrid epithelial/mesenchymal phenotype in metastasis. *Front Oncol*. (2015) 5:155. doi: 10.3389/fonc.2015.00155
27. Nan X, Wang J, Liu HN, Wong STC, Zhao H. Epithelial-mesenchymal plasticity in organotropism metastasis and tumor immune escape. *J Clin Med*. (2019) 8:E747. doi: 10.3390/jcm8050747
28. Clark AG, Vignjevic DM. Modes of cancer cell invasion and the role of the microenvironment. *Curr Opin Cell Biol*. (2015) 36:13–22. doi: 10.1016/j.ceb.2015.06.004
29. Bronsert P, Enderle-Ammour K, Bader M, Timme S, Kuehs M, Csanadi A, et al. Cancer cell invasion and EMT marker expression: a three-dimensional study of the human cancer-host interface. *J Pathol*. (2014) 234:410–22. doi: 10.1002/path.4416
30. Zhao Z, Zhu X, Cui K, Mancuso J, Federley R, Fischer K, et al. *In vivo* visualization and characterization of epithelial-mesenchymal transition in breast tumors. *Cancer Res*. (2016) 76:2094–104. doi: 10.1158/0008-5472.CAN-15-2662
31. Yu M, Bardia A, Wittner BS, Stott SL, Smas ME, Ting DT, et al. Circulating breast tumor cells exhibit dynamic changes in epithelial and mesenchymal composition. *Science*. (2013) 339:580–4. doi: 10.1126/science.1228522
32. Kaigorodova EV, Savelieva OE, Tashireva LA, Tarabanovskaya NA, Simolina EI, Denisov EV, et al. Heterogeneity of circulating tumor cells in neoadjuvant chemotherapy of breast cancer. *Molecules*. (2018) 23:E727. doi: 10.3390/molecules23040727
33. Zavyalova MV, Denisov EV, Tashireva LA, Savelieva OE, Kaigorodova EV, Krakhmal NV, et al. Intravasation as a key step in cancer metastasis. *Biochemistry*. (2019) 84:762–72. doi: 10.1134/S0006297919070071
34. Brabletz T, Kalluri R, Nieto MA, Weinberg RA. EMT in cancer. *Nat Rev Cancer*. (2018) 18:128–34. doi: 10.1038/nrc.2017.118
35. Kalluri R, Zeisberg M. Fibroblasts in cancer. *Nat Rev Cancer*. (2006) 6:392–401. doi: 10.1038/nrc1877

Conflict of Interest: The authors declare that the research was conducted in the absence of any commercial or financial relationships that could be construed as a potential conflict of interest.

Copyright © 2020 Tashireva, Zavyalova, Savelieva, Gerashchenko, Kaigorodova, Denisov and Perelmuter. This is an open-access article distributed under the terms of the Creative Commons Attribution License (CC BY). The use, distribution or reproduction in other forums is permitted, provided the original author(s) and the copyright owner(s) are credited and that the original publication in this journal is cited, in accordance with accepted academic practice. No use, distribution or reproduction is permitted which does not comply with these terms.

frontiers in Oncology

ORIGINAL RESEARCH
published: 06 March 2020
doi: 10.3389/fonc.2020.00284

LOXL2 Expression Status Is Correlated With Molecular Characterizations of Cervical Carcinoma and Associated With Poor Cancer Survival via Epithelial-Mesenchymal Transition (EMT) Phenotype

*Canhui Cao[1], Shitong Lin[1], Wenhua Zhi[1], Cordelle Lazare[1], Yifan Meng[1], Ping Wu[1], Peipei Gao[1], Juncheng Wei[1,2] and Peng Wu[1,2]**

[1] Cancer Biology Research Center (Key Laboratory of the Ministry of Education), Tongji Hospital, Tongji Medical College, Huazhong University of Science and Technology, Wuhan, China, [2] Department of Gynecologic Oncology, Tongji Hospital, Tongji Medical College, Huazhong University of Science and Technology, Wuhan, China

OPEN ACCESS

Edited by:
Mohit Kumar Jolly,
Indian Institute of Science (IISc), India

Reviewed by:
Christine Chaffer,
Garvan Institute of Medical Research, Australia
Dingcheng Gao,
Cornell University, United States

***Correspondence:**
Peng Wu
pengwu8626@tjh.tjmu.edu.cn

Specialty section:
This article was submitted to Molecular and Cellular Oncology, a section of the journal Frontiers in Oncology

Received: 18 November 2019
Accepted: 18 February 2020
Published: 06 March 2020

Citation:
Cao C, Lin S, Zhi W, Lazare C, Meng Y, Wu P, Gao P, Wei J and Wu P (2020) LOXL2 Expression Status Is Correlated With Molecular Characterizations of Cervical Carcinoma and Associated With Poor Cancer Survival via Epithelial-Mesenchymal Transition (EMT) Phenotype. Front. Oncol. 10:284. doi: 10.3389/fonc.2020.00284

As molecular analyses based on high-throughput sequencing have developed, the molecular classification of cancer has facilitated clinical work. The aim of the present study was to identify a new potential therapeutic target for cervical carcinoma by molecular analyses. We firstly tested the LOXL2 expression pattern in 50 paired normal cervix and cervical carcinoma via qPCR and immunohistochemistry, and the LOXL2 expression pattern was found to be in accordance with public datasets from Gene Expression Omnibus (GEO). Then, we comprehensively rewired the 176 cervical carcinoma samples from The Cancer Genome Atlas (TCGA), subsequently clustered the samples into two groups corresponding to LOXL2 expression to determined the associations between LOXL2 expression status and molecular characterizations of cervical carcinoma. *In vitro* assays for further verifying the correlations in SiHa-shLOXL2 and HeLa-shLOXL2 cell lines. In this study, we found that LOXL2 highly expressed in carcinoma tissue, with 14 CpG islands of LOXL2 promoter that were significantly and negatively associated with its expression in cervical carcinoma. And there were notable correlations among LOXL2 expression status and molecular characterizations of cervical carcinoma, including diagnostic age, HPV A7 types, mRNA molecular clusters, miRNA molecular clusters, and DNA methylation molecular clusters et al. In addition, high LOXL2 expression was negatively correlated with lower tumor mutation density, especially in EP300, ERBB2, EGFR and NOTCH2, and was negatively correlated with lower expression of APOBEC3 family genes, such as APOBEC3A, APOBEC3B, APOBEC3D, and APOBEC3G. Furthermore, high LOXL2 expression was associated with poor overall (OS) and poor disease-free survival (DFS) in cervical carcinoma, and was associated with higher epithelial-mesenchymal transition (EMT) score, enrichment of extracellular matrix (ECM) signaling, the phenotype that was found to be associated with poor prognosis

in cervical carcinoma from TCGA. Conversely, the ability of cell proliferation and cell migration were reversed in LOXL2 knock-down cervical cell lines via regulating the genes' expression of EMT phenotype *in vitro*. Overall, we demonstrated the correlation between LOXL2 expression status and cancer molecular characterizations of cervical carcinoma, and identified LOXL2 may serve as a therapeutic target for such carcinoma.

Keywords: LOXL2, molecular analyses, cervical cancer, EMT, APOBEC3 family genes, cancer survival

INTRODUCTION

Cervical cancer accounts for 265,700 cancer-related deaths in women worldwide, more than any other gynecological tumor, with 527,600 new cases reported every year (1). The association between intratumor heterogeneity and cancer molecular function varies substantially in cervical cancer among different HPV types (2–4), which in turn provides insight into carcinogenesis beyond histological subtype. With the development of high-throughput sequencing using a large cervical carcinoma cohort, The Cancer Genome Atlas (TCGA) research network has identified three clusters according to mRNA expression, three clusters corresponding to reverse phase protein array (RPPA), six clusters based on miRNA expression, and two clusters based on copy number variation (CNV) data. This has highlighted molecular heterogeneity of cervical cancer not only from a histological perspective but also in relation to the molecular characterizations of cervical cancer. Based on gynecological and breast cancer data, previous pan-cancer molecular study showed that, among gynecological cancers, cervical cancer exhibits a high median mutation (5.3 mutations/mbp), high degree of hypermethylation, and expresses high immune marker signatures (5).

Lysyl oxidase-like 2 (LOXL2) is a member of the lysyl oxidase (LOX) family, which plays a critical role in catalyzing the formation of cross-links of elastin and collagen in the extracellular matrix (ECM) (6). LOXL2 has been implicated in promoting cancer cell proliferation (7), invasion (8), metastasis (9), and angiogenesis (10) in many cancer types. In addition, increased expression of LOXL2 is significantly associated with decreased survival in laryngeal squamous cell carcinoma (11), gastric cancer (12), pancreatic carcinoma (13), hepatocellular carcinoma (9), colon tumor (14), and basal-like breast carcinoma (15). Moreover, LOXL2 may serve as a target in the development of antibodies or inhibitors for cancer therapeutics (16, 17), as characterized in ClinicalTrials.gov NCT01323933.

In the current study, by rewiring TCGA cervical carcinoma data, including clinical information, HPV status, established molecular clusters, tumor mutation density, and APOBEC3 family gene expression, we demonstrated the correlation between LOXL2 expression status and the molecular characterizations of cervical carcinoma, and found that LOXL2 expression was negatively correlated with the expression of APOBEC3 family genes, especially APOBEC3A, APOBEC3B, APOBEC3D, and APOBEC3G *in vitro*. More importantly, increased expression of LOXL2 was significantly associated with decreased survival in cervical carcinoma, which was further associated with EMT phenotype *in vitro*.

MATERIALS AND METHODS

Datasets

Integrated analyses were performed on a subset of 176 samples (the core-set) (**Supplementary Table 1**) from TCGA dataset (18), which included LOXL2 mRNA expression, clinical information of samples (age at initial pathologic diagnosis, lymph node status, pathology, and clinical stage), HPV status of samples (HPV categories, HPV integrated status, E6 ratio category), somatic genomic alterations density (non-silent mutation rate per MB, silent mutation rate per MB and total mutation rate per MB) of patients, molecular platform of established clusters (copy number clusters, methylation based clusters, mRNA based clusters, miRNA based clusters, uterine corpus endometrial-like (UCEC-like) based analysis and reverse phase protein array (RPPA) based clusters) and APOBEC family genes expression (APOBEC1, APOBEC3A, APOBEC3B, APOBEC3C, APOBEC3D, APOBEC3F, APOBEC3G, and APOBEC3H). All detail information was showed in **Supplementary Table 1**.

Cells Culture

The human cervical cancer cell lines (SiHa and HeLa) were purchased from American Type Culture Collection (ATCC) and authenticated at China Center for Type Culture Collection (Wu Han University). All of the cells were cultured in DMEM (11965084, Gibco) containing 10% fetal bovine serum (FBS, SH30406.05, Hyclone) and antibiotics (100 U/mL penicillin and 100 μg/mL streptomycin, 15140163, Gibco) at 37°C with 5% CO_2.

RNA Interference

Cells were cultured in six-well plates for transfecting with MCS-shLOXL2-SV40-firefly-Luciferase-IRES-Puromycin lentiviral particles (GeneChem, Shanghai, China) and screened by puromycin (0.1 μg/mL, A1113803, Gibco) for 2 weeks. The sequences targeted the LOXL2 (Human NM_002318) gene by shRNA were 5′-GAAACCCTCCAGTCTATTATA-3′.

Immunohistochemistry (IHC)

The cervical cancer samples and the paired adjacent normal cervix samples were obtained from The Biobank of Patients With Gynecologic Neoplasms (NCT01267851, ClinicalTrials.gov, https://clinicaltrials.gov/ct2/show/study/NCT01267851) in the department of gynecologic oncology of Tongji Hospital. The 4% paraformaldehyde fixed and paraffin-embedded sections (4 μm) were subjected to IHC assay according to the manufacturer's protocols. Briefly, The slides were put into the dewaxing solution

I/II, 100% ethanol, 90% ethanol, 85% ethanol and 75% ethanol for 5 min respectively. Antigen retrieval was performed in Tris-EDTA (PH 9.0) using heat-induced protocol. And the slides were incubated at 4°C with LOXL2 antibody (GTX105085, GeneTex, 1:400) overnight. Staining detection was performed using DAB (Servicebo). Characteristics of patients were displayed in **Supplementary Table 2**.

Immunofluorescence (IF)

Cells were seeded in glass coverslips that were placed in 24-well plates after 24 h for assay according to the protocols (http://media.cellsignal.com/www/pdfs/resources/product-literature/application-if-brochure.pdf). Briefly, cells were fixed by 4% paraformaldehyde for 30 min in room temperature, and penetrated by 0.3% Triton X-100 (T8200, Solarbio) for 30 min in 37°C before blocking step (5% bovine serum albumin (BSA) for 30 min in 37°C). Antibodies used for incubation were LOXL2 (GTX105085, GeneTex, 1:200) and Alexa Fluor Plus 488 (A32731, Invitrogen, 1:1000). Images were taken using Olympus microscope (BX53) equipped with FITC and DAPI filters.

Western Blot

Cells were lysed in RIPA lysis buffer (P0013B, Beyotime) with protease inhibitor cocktail (04693132001, Roche). The protein was performed in SDS-PAGE (8012011, BioSci) and was electrically transferred onto PVDF membrane (10600023, GE). The PVDF membrane was incubated with diluted GAPDH (A10471, ABclonal, 1:2000), LOXL2 antibody (A4708, ABclonal, 1:1000), SNAI1 antibody (A12301, ABclonal,1:1000), E-Cadherin (GTX100443, 1:1000), N-Cadherin (A10206, ABclonal, 1:1000), Vimentin (3932, CST,1:1000), APOBEC3A (A12399, ABclonal, 1:400), APOBEC3B (A9010, ABclonal, 1:1000), APOBEC3D (A11648, ABclonal, 1:1000), APOBEC3G (A17199, ABclonal, 1:1000), Ki 67 (273091-1-AP, proteintech, 1:4000), Caspase 3 (A19654, ABclonal, 1:1000) at 4°C overnight. After incubation with HRP Goat anti-rabbit IgG (H+L) (AS014, ABclonal, 1:1000) at 37°C for 1 h, the PVDF membrane was performed using western bright ECL HRP substrate (K-12045-C20, Advansta) and analyzed by Image Lab (v4.1).

RNA Extraction, PCR, and qRT-PCR

The total RNA of cells were extracted with Trizol reagent (15596026, Invitrogen) under the protocols of manufacturer. The cDNA was synthesized by HiScript II Q RT SuperMix (R223-01, Vazyme) according to the manufacturer's constructions. Bio-Rad CFX96 Real-Time System manager (C1000 Thermal Cycler) was used to detect the expression level of target genes using iTaq Universal SYBR Green (1725125, Bio-Rad), and GAPDH was used as the internal control. The specific primer sequences of targeted genes are displayed in **Supplementary Table 3**.

Cell Viability Assay

Cells ($n = 6{,}000$) were seeded in the 96-well plates. The relative viability of cells were assayed by Cell Counting Kit-8 (CK04, Dojindo Laboratories) at each time point according to the protocols, which were measured by Multiskan Spectrum (Spectra Max190, Molecular Devices) with the wavelength of 450 nm. Assay was performed using six replications.

Colony Formation Assays

Cells ($n = 1{,}000$) were seeded in six-well plates for 2 weeks to allow colony formation. Then, the plates were fixed with 4% paraformaldehyde for 10 min and stained with 0.1% crystal violet for 30 min.

Transwell Chamber Assay

The transwell (3422, Corning Incorporated Costar, 8.0 μm pore size) was used to assess the ability of migration for cells according to the protocols (https://www.corning.com/catalog/cls/documents/protocols/Transwell_InstructionManual.pdf.). Cells (5×10^4) were seeded in the upper chamber for incubation at each time point. Then the upper chamber was removed, fixed with paraformaldehyde for 10 min and stained with 0.1% crystal violet for 30 min. Finally, the upper chamber biofilm was cut off for further analysis.

Wound Healing Assay

The same number of cells (4×10^5) between the two groups were seeded in 6-well plates. Three horizontal and vertical scratches were made using 200 μL pipette tips in the plates, and the plates were washed with phosphate buffered saline (PBS) for three times. Then the cells were cultured in serum-free medium. The degree of cell migration to the blank was recorded by microscopy at 0 and 48 h, and analyzed with software Image J (v1.8.0).

Bioinformatic Analyses

The correlation of DNA methylation and LOXL2 expression was performed by MEXPRESS (v2019) (19, 20) with default setting. All results were showed in **Supplementary Table 4**. Correlation analyses were performed in the Gene Expression Profiling Interactive Analysis (GEPIA) dataset (21). Correlation coefficient was operated by Pearson's test. All parameters were computed at the default setting. Survival plots of LOXL2 gene in cervical cancer was performed in GEPIA with default setting. LOXL2 mRNA expression in the groups of normal cervix and cervical cancer were conducted in the GEO expression profiling dataset (GSE63514, GSE7803, and GSE9750). LOXL2 correlated genes were performed by LinkedOmics (22) with default setting. Functional enrichment of the LOXL2 positively correlated genes was performed by Metascape (23) with FDR< 0.05, $r > 0.3$.

EMT Score Analysis

The EMT score was downloaded from **Supplementary Data** of TCGA research network, and the EMT score algorism was computed as previously published (24). Briefly, the score was the value that the average expression of stromal genes minus the average expression of epithelial genes. Removed all unavailable data (NA) values from the calculation. Accordingly, a *t*-test and ANOVA test were applied to each comparison.

Statistical Analyses

Data were presented as mean ± standard deviation (SD) or standard error of mean (SEM). Results were calculated by GraphPad Prism 6 (version 6.02) software. The Student's *t*-test,

Mann-Whitney test, one-way ANOVA, Two-way ANOVA, log-rank test, Cox model or Chi-Square test as indicating in figure legends. The expression of APOBEC3 genes was shown with log2 of (RSEM (RNA-Seq by Expectation-Maximization)+1) according the TCGA research network. Mean and SD were shown. Single comparisons between the low- and high- LOXL2 groups were determined by Student's *t*-test. Kaplan–Meier curves were based on the log-rank test. The HR was performed using the Cox model. *P*-value < 0.05 was considered to be significant.

RESULTS

LOXL2 Expression Profile in Cervical Cancer Tissues

We first investigated the expression pattern of LOXL2 in the GEO dataset (**Figure 1A**) and in clinical samples of paired adjacent normal cervix and cancer tissues using quantitative polymerase chain reaction (qPCR) (**Figure 1B**) and immunohistochemical (IHC) assays (**Figures 1C,D** and **Supplementary Figure 1**). Integrative analyses of LOXL2 expression were conducted in three GEO expression profile datasets (i.e., GSE63514, GSE7803, and GSE9750), which included transcriptomic profiles of normal cervix and primary cancer tissue. We found that the average expression of LOXL2 was elevated in primary cancer compared with normal cervix tissue. Additionally, IHC staining demonstrated that 80% of adjacent normal cervix samples vs. 20% of primary cancer samples showed negative staining, 20% of normal samples vs. 60% of cancer samples showed weak staining, and 20% of cancer samples showed moderate staining (**Figures 1C,D**, and **Supplementary Figure 1**). In addition, LOXL2 also expression in the adjacent stroma of cervical cancer slide (**Figure 1D**, and **Supplementary Figure 1**). These results demonstrated that LOXL2 expression was significantly increased in cervical carcinoma.

To demonstrate the correlation between LOXL2 expression and DNA methylation of the LOXL2 promoter, we performed integrated visualization of LOXL2 expression and DNA methylation data in MEXPRESS (19, 20) based on 317 cervical squamous cell carcinomas and endocervical adenocarcinomas from TCGA (**Figure 1E**). We identified 14 CpG islands of LOXL2 (i.e., cg20981791, cg20142986, cg24531955, cg17804498, cg09535960, cg04028450, cg10090386, cg09042448, cg18233786, cg22996912, cg00558156, cg25074071, cg05365729, and cg04259752) that were significantly and negatively associated with LOXL2 gene expression in cervical carcinoma (**Supplementary Table 4**).

Multiplatform Integrative Analyses of Cervical Carcinoma Data Clustered by LOXL2 Expression Status

We integrated the LOXL2 mRNA expression levels, clinical information of patients (age at initial pathologic diagnosis, lymph node status, pathology, and clinical stage), HPV status of samples (HPV categories, HPV integrated status, E6 ratio category), somatic genomic alteration densities (non-silent, silent, and total mutation rates per MB) of patients, molecular platform of established clusters (copy number clusters, methylation-based clusters, mRNA-based clusters, miRNA-based clusters, UCEC-like-based analysis, and RPPA-based clusters) corresponding to TCGA clustering to analyze the molecular characterizations based on LOXL2 status in cervical carcinoma (**Figure 2**, **Supplementary Table 1**, **Supplementary Figure 2** and Methods). Samples were ordered by LOXL2 expression and classified into two clusters, i.e., low-LOXL2 cluster and high-LOXL2 cluster.

Many studies have identified the important role of APOBEC3 genes in HPV-related cancers (18, 25). There was direct evidence that APOBEC3 edited HPV DNA (25) and there were notable APOBEC mutagenesis patterns in cervical carcinoma sequencing (18). Therefore, we also integrated the APOBEC family (APOBEC1 APOBEC3A, APOBEC3B, APOBEC3C, APOBEC3D, APOBEC3F, APOBEC3G, and APOBEC3H) mRNA expression of 176 core-set cervical carcinoma samples for multiplatform integrative analyses (**Figure 2**, **Supplementary Table 1**, **Supplementary Figure 2**).

For clinical information, we found that the mean age at initial pathological diagnosis differed between the two clusters ($P = 0.0383$). For HPV infection, HPV A7 types were enriched in the high-LOXL2 cluster ($P = 0.0145$), consistent with the enrichment of HPV A7 type in low-keratin and adenocarcinoma clusters reported in TCGA (18). In addition, the E6 ratio category was significantly different ($P = 0.0272$), especially C2 in the low-LOXL2 cluster and C4 in the high-LOXL2 cluster (E6 category (31 = C1, 33 = C2, 31 = C3, 32 = C4, 49 = NA), **Supplementary Table 1**). However, HPV integration showed no correlation with LOXL2 expression status ($P = 0.8532$). For somatic mutation density divided by genome length (MB), the mean densities of the non-silent ($P = 0.0227$), silent ($P = 0.0260$), and total mutation rates ($P = 0.0275$) were correlated with LOXL2 expression. For molecular platform features, the mRNA-Seq ($P = 0.0164$), miRNA-Seq ($P = 0.0287$), and DNA-methylation clusters ($P = 0.0063$) based on unsupervised hierarchical clustering were significantly correlated with LOXL2 expression status. For the APOBEC3 family genes, the mean expression levels of APOBEC3A ($P < 0.0001$), APOBEC3B ($P < 0.0001$), APOBEC3D ($P < 0.0001$), APOBEC3F ($P = 0.0025$), APOBEC3G ($P = 0.0013$), and APOBEC3H ($P = 0.0112$) were different between the LOXL2 clusters.

Mean Diagnostic Age and Tumor Mutation Density Were Negatively Correlated With LOXL2 Expression Cluster

To identify the clinical characteristics associated with LOXL2 expression in cervical cancer, we arranged LOXL2 expression and diagnostic age of the 176 core-set samples, which were ordered by LOXL2 expression (**Figure 3A**). We then compared the mean age at initial pathological diagnosis between the two clusters (**Supplementary Figure 3A**), i.e., 49.64 ± 1.462 in low-LOXL2 cluster vs. 45.55 ± 1.305 in high-LOXL2 cluster and found that diagnostic age was negatively associated with LOXL2 expression status. According to the latest worldwide statistics, cervical cancer is the second leading cause of cancer deaths in the

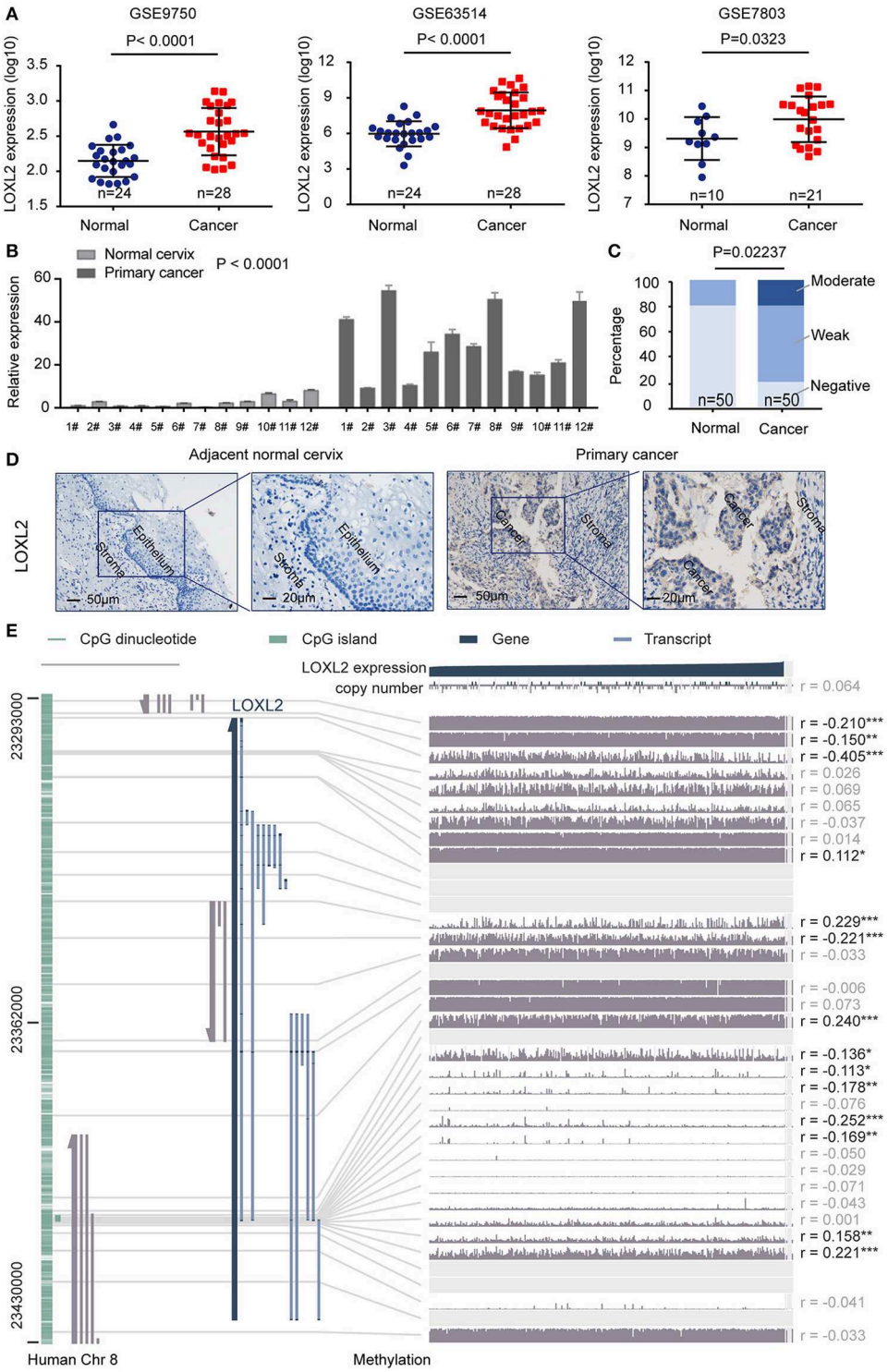

FIGURE 1 | LOXL2 expression profile in cervical cancer tissues. **(A)** Normalized expression of LOXL2 in the normal cervix and primary cancer using three expression profiling data (GSE63514, GSE7803, and GSE9750). *P*-values were calculated by Student's *t*-test Mean and SD were shown. **(B)** qPCR of LOXL2 relative expression in paired adjacent normal cervix and cancer tissues. Mean and SEM ($n = 3$) were shown. *P*-values were calculated by Two-way ANOVA test. #Means patients number. **(C)** Scoring of LOXL2 in the stained tissues. *P*-values were calculated by Chi-square test. **(D)** Representative images of IHC staining of LOXL2 in the adjacent normal cervix and primary cancer. **(E)** The correlation of LOXL2 expression and DNA methylation of LOXL2 promoter from MEXPRESS (19, 20), including 317 cervical squamous cell carcinoma and endocervical adenocarcinoma from TCGA datasets. The statistics (correlation coefficient (r) and *P*-value) on the right show how LOXL2 expression and DNA methylation of promoter were negatively correlated (* <0.05, ** <0.01, *** <0.001).

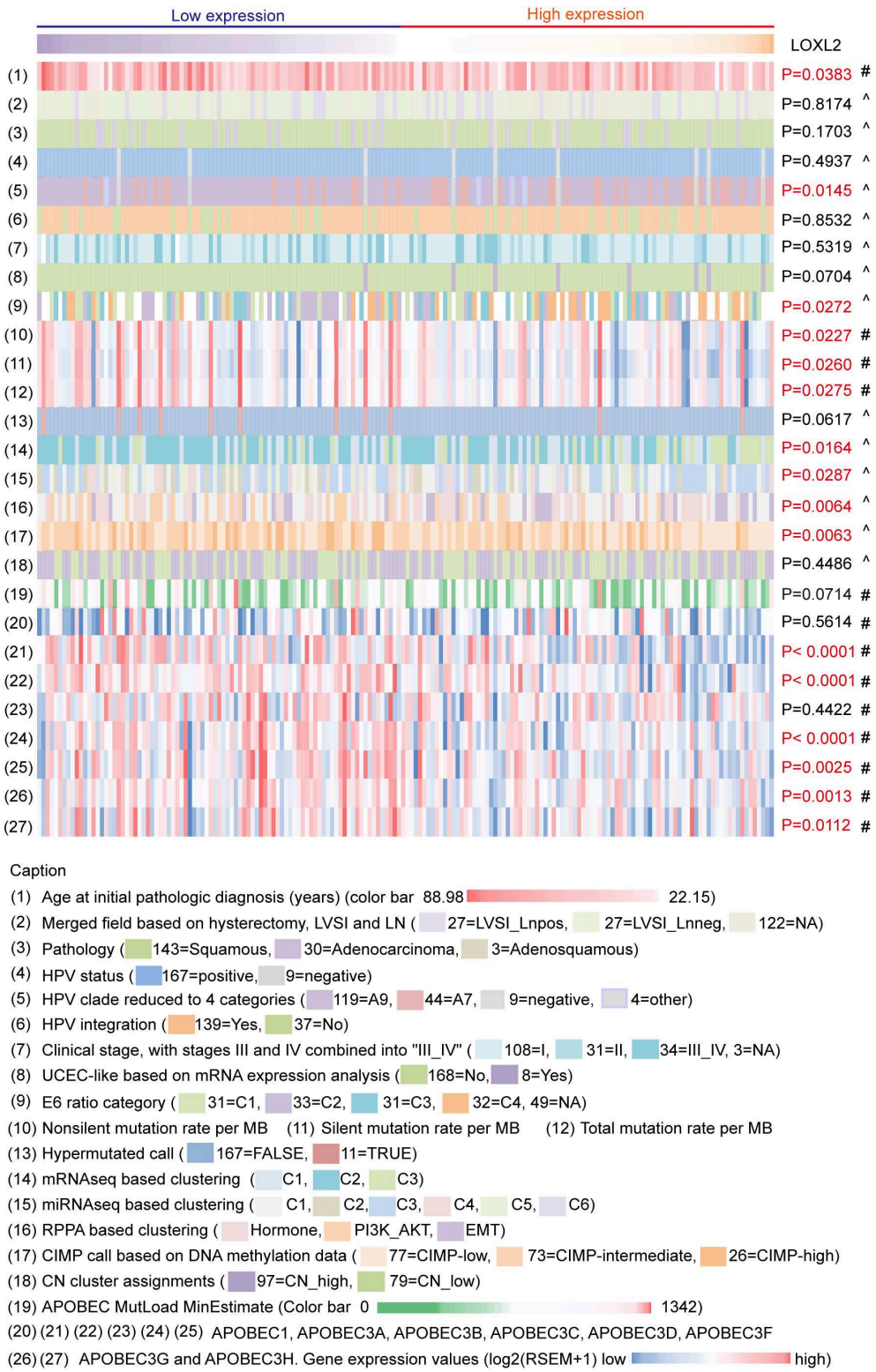

FIGURE 2 | Multiplatform integrative analyses of cervical cancer data clustered by LOXL2 expression. 176 core-set cervical cancer samples were clustered into two groups according to LOXL2 mRNA expression (low LOXL2 expression, high LOXL2 expression). Clinical information, HPV genotypes of samples, somatic genomic alterations, molecular platform features corresponding to the TCGA clustering and the APOBEC3 family genes expression were showed by color. Color captions were shown in the bottom. Each column represented a sample. #*P*-values were calculated by Mann–Whitney test. ^*P* values were calculated by Chi-Square Test. Red *P*-values indicate $P < 0.05$.

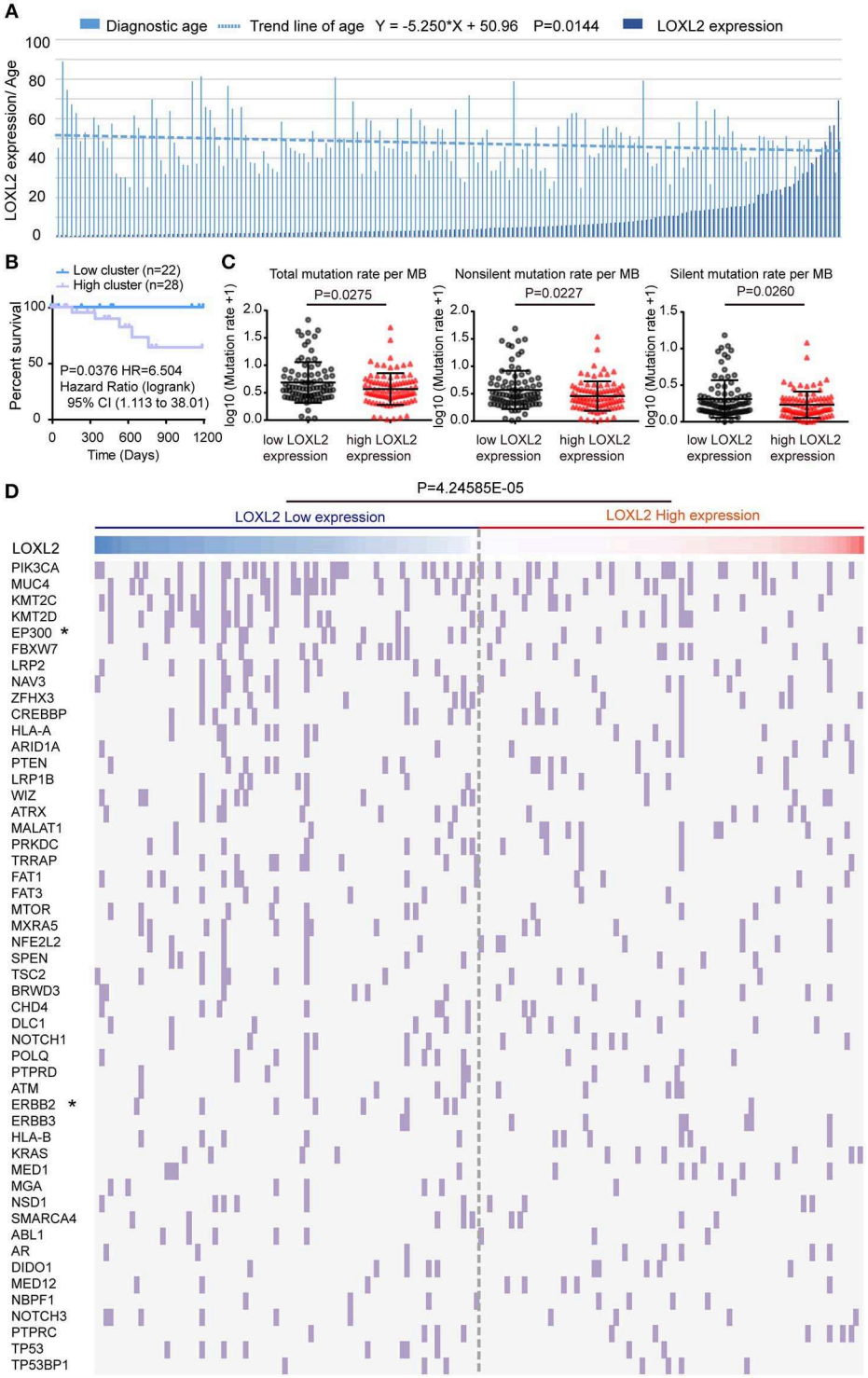

FIGURE 3 | The mean diagnostic age and tumor mutational density were negatively correlated with LOXL2 expression cluster. **(A)** Clustered column of LOXL2 expression and the diagnostic age of 176 core-set cervical cancer samples, which was ordered by the LOXL2 expression. *P*-values were calculated by linear regression about log10 of LOX2 expression and the diagnostic age. Equation was shown above. **(B)** Three years Kaplan–Meier survival curve between the LOXL2-high and -low groups corresponding to diagnostic age 20 to 39. **(C)** Scatter plots of samples' somatic genomic alterations intensity in the two LOXL2 subgroups, which represent total, non-silent, silent mutation rate per MB. Y axis shows the log10 of the mutation rate per MB. Mean and SD were shown. *P*-values were calculated by Mann-Whitney test. **(D)** 176 core-set cervical cancer samples (columns) arranged by LOXL2 expression, tumor mutation density corresponding to top 50 somatic genomic alteration genes (rows) of patients in cervical cancer were calculated. Each light purple column represents a somatic genomic alteration. *P*-values were calculated by Chi-square test.

TABLE 1 | Four mutation genes that were significant associated with the LOXL2 clusters.

Characteristics	Total patients		LOXL2 low expression		LOXL2 high expression		P value
	N = 176 (No. %)		*N* = 88 (No. %)		*N* = 88 (No. %)		
Genes	Mutation	Non-mutation	Mutation	Non-mutation	Mutation	Non-mutation	
EP300	19 (10.80%)	157 (89.20%)	14 (15.91%)	74 (84.09%)	5 (5.68%)	83 (94.32%)	0.0289
ERBB2	9 (5.11%)	167 (94.89%)	8 (9.09%)	80 (90.90%)	1 (1.14%)	87 (98.86%)	0.0166
EGFR	9 (5.11%)	167 (94.89%)	8 (9.09%)	80 (90.90%)	1 (1.14%)	87 (98.86%)	0.0166
NOTCH2	8 (4.55%)	168 (95.45%)	8 (9.09%)	80 (90.90%)	0 (0%)	88 (100%)	0.0113

P-values were calculated by Chi-Square Test.

20- to 39-year age group, with nine cases reported per week (26). Thus, we compared the three-year OS for the 20- to 39-year age group between the two clusters, with poorer outcomes found for the high-LOXL2 cluster (**Figure 3B**, **Supplementary Table 5**).

Cervical carcinoma exhibits a high tumor mutation burden (TMB) and microsatellite instability (MSI) stable carcinoma (27). Thus, we compared the mean somatic genomic mutation density between the two clusters (**Supplementary Table 6**). We found that the mean densities of the total, non-silent, and silent mutation rates (Figure 3**C**) were higher in the low-LOXL2 cluster than in the high-LOXL2 cluster.

By ordering the 176 core-set cervical cancer samples by LOXL2 expression, we found that the somatic alteration density was high in the low-LOXL2 cluster when considering the top 50 (P = 4.24585E-05) (**Figure 3D**), top 1-10 (P = 3.40597E-05), top 21-30 (P = 0.048011) (**Supplementary Figure 3B**, and **Supplementary Table 6**) mutation genes in the dataset. Furthermore, the EP300 (P = 0.0289), ERBB2 (P = 0.0166), EGFR (P = 0.0166), and NOTCH2 (P = 0.0113) mutations were significantly associated with both clusters (**Table 1** and **Supplementary Table 6**).

APOBEC3 Family Gene Expression Levels Were Negatively Correlated With LOXL2 Status in Cervical Carcinoma

Previous studies have indicated that APOBEC3 family genes play a key role in innate immunity (28, 29), HPV associated carcinogenesis (30), and development of chemoresistance in cancer (31, 32). By clustering the 176 core-set samples into two groups, we found that the mean expression of APOBEC3 family genes was higher in the low-LOXL2 cluster (**Figure 4A**), including APOBEC3A (8.384 ± 0.2478 in low cluster vs. 6.80 ± 0.2578 in high cluster), APOBEC3B (9.904 ± 0.1226 in low cluster vs. 8.588 ± 0.2501 in high cluster), APOBEC3D (7.273 ± 0.1367 in low cluster vs. 6.547 ± 0.1360 in high cluster), APOBEC3F (7.988 ± 0.09133 in low cluster vs. 7.597 ± 0.08861 in high cluster), APOBEC3G (8.929 ± 0.1288 in low cluster vs. 8.333 ± 0.1326 in high cluster), and APOBEC3H (4.163 ± 0.1426 in low cluster vs. 3.617 ± 0.1237 in high cluster). Our *in vitro* experiment also verified these associations at the mRNA level (**Figure 4B**).

To validate the expression patterns of APOBEC3 genes and LOXL2, we carried out correlation analysis using the GEPIA dataset, which included expression profiles of 306 cervical cancer tissues (21). Results showed that APOBEC3A (r = −0.14, P = 0.012), APOBEC3B (r = −0.21, P = 3e−4), APOBEC3D (r = −0.12, P = 0.033), and APOBEC3G (r = −0.11, P = 0.048) were statistically correlated with LOXL2 in cervical cancer (**Figure 4C**) and the APOBEC3C, APOBEC3F and APOBEC3H were not correlated (**Supplementary Figure 4**), the correlation coefficient seem to not be significantly correlated. Therefore, we performed the western blot assay in LOXL2 RNA-interference (**Figure 4D**) cells for further analysis. We found that the LOXL2-interference resulted in an increase in APOBEC3A, APOBEC3B, APOBEC3D, and APOBEC3G protein levels (**Figure 4E**) in the cervical cancer cells.

High Levels of LOXL2 Were Associated With Poor Cancer Survival, Which Was Associated With EMT Phenotype

As LOXL2 expression status was correlated with molecular characterizations of cervical cancer, we performed cancer survival analysis for the two clusters. High LOXL2 expression was found to be significantly correlated with poor OS (HR = 2.3, p(HR) = 6e−04) (**Figure 5A** and **Supplementary Figure 5A**) and with poor DFS (HR = 2.2, p(HR) = 0.0081) (**Figure 5A**) in the 292 cervical cancer TCGA dataset from GEPIA (21). Given that RPPA-based clustering was correlated with LOXL2 expression status, especially enrichment of the EMT cluster in the high-LOXL2 cluster, we performed correlation analysis between LOXL2 expression and EMT score and found that they were positively correlated (P < 0.0001, r = 0.4210) (**Figure 5B**). In addition, the EMT group exhibited poorer outcome (HR = 2.5, p(HR) = 0.0156) in OS (**Figure 5C**), which was well-established in TCGA network (18). Thus, we hypothesized that high LOXL2 expression showing poor cancer survival may be associated with the EMT phenotype.

To further explore the links between LOXL2 and the EMT phenotype, we detected protein levels *in vitro*. Results showed a decrease in N-cadherin (CHD2), SNAI1, and vimentin, and an increase in E-cadherin (CHD2) in the SiHa-sh-LOXL2 and HeLa-sh-LOXL2 cells (**Figure 5D**). Furthermore, these results showed the same tendency of LOXL2 positively correlated genes in cervical carcinoma (**Figure 5E**, **Supplementary Figures 5B–D**, and **Supplementary Table 7**), which was associated with ECM structural constituents (**Supplementary Tables 8**, **9**). In addition,

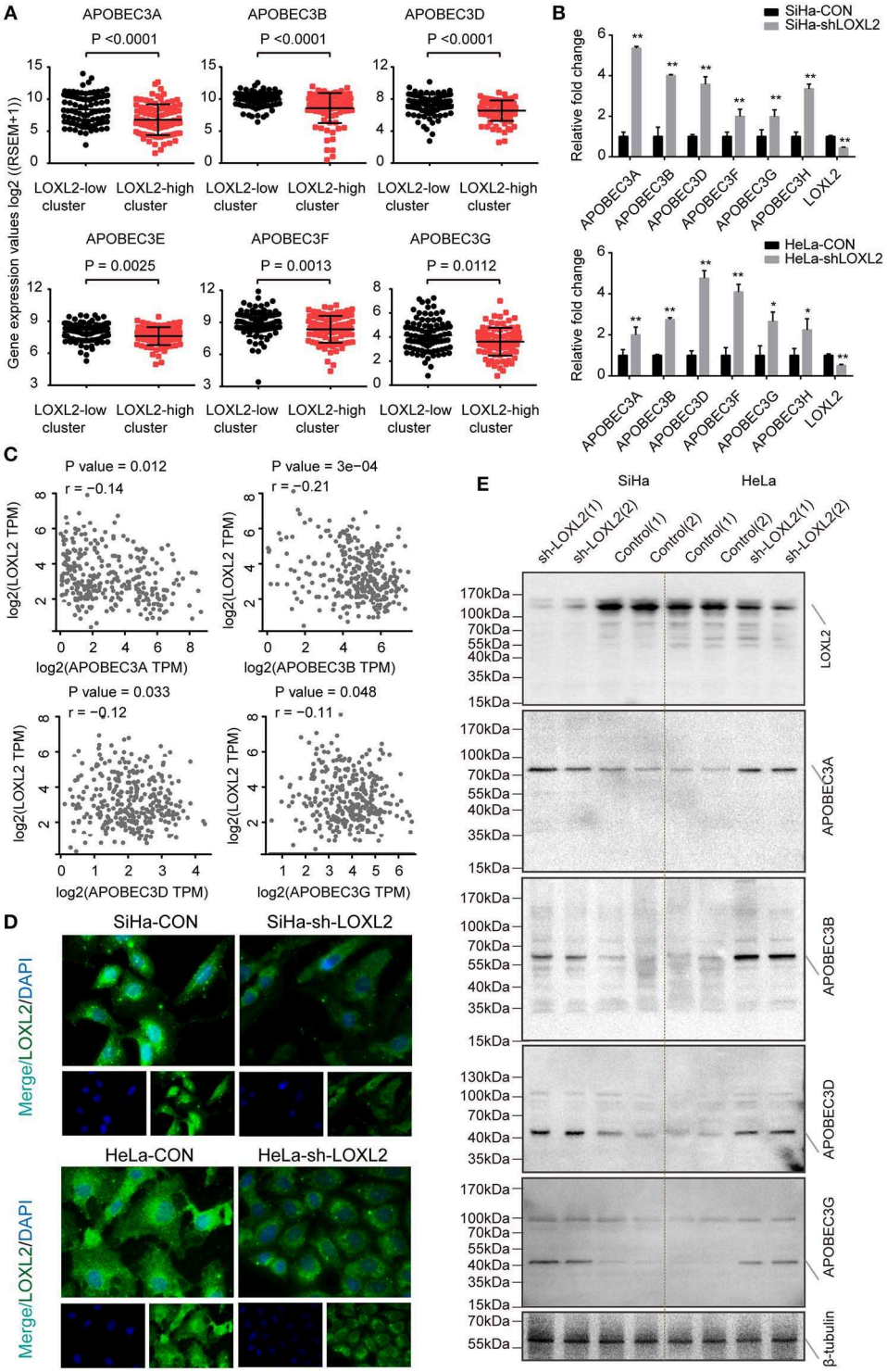

FIGURE 4 | The expression of APOBEC3 family genes negatively correlated with the LOXL2 status in cervical cancer. **(A)** Scatter plots of APOBEC3 family mRNA expression in the two groups clustered by LOXL2 expression in 176 core-set cervical cancer samples. Y axis shows the log2 of (RSEM (RNA-Seq by Expectation-Maximization)+1). Mean and SD were shown. *P*-values were calculated by Student's *t*-test. **(B)** qPCR of APOBEC3 family genes in SiHa from CON and sh-LOXL2 ($n = 3$). Mean and SEM were shown. *P*-values were calculated by Student's *t*-test. (* <0.05, ** <0.01) **(C)** Pearson correlation analysis of APOBEC3 family genes as APOBEC3A, APOBEC3B, APOBEC3D, and APOBEC3G with that of LOXL2 expression in TCGA dataset from GEPIA (21). *P*-value and Pearson correlation coefficient (r) were shown. **(D)** Representative images of IF assay in SiHa and HeLa cell lines. **(E)** Western blot assay of LOXL2, APOBEC3A, APOBEC3B, APOBEC3D, and APOBEC3G in SiHa and HeLa after transfected with sh-Con or sh-LOXL2. β-tubulin served as the loading control.

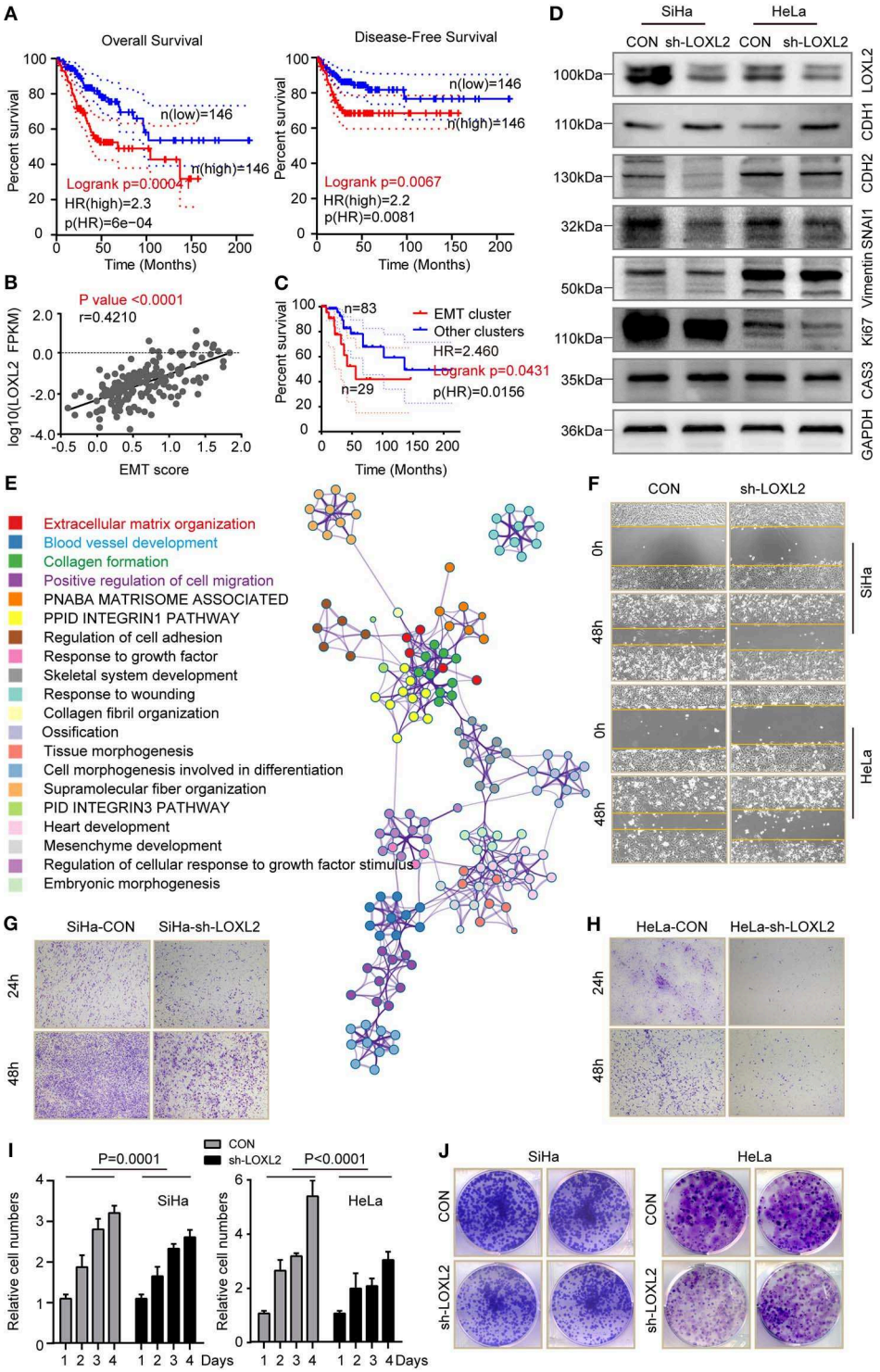

FIGURE 5 | High level of LOXL2 was associated with poor cancer survival, which was associated with EMT phenotype. **(A)** Overall survival and disease-free survival were compared between the LOXL2-high and -low groups corresponding to LOXL2 expression. **(B)** Spearman correlation analysis of LOXL2 expression with that of normalized EMT score in 176 core-set cervical cancer samples. *P*-value and Pearson correlation coefficient (r) were shown. **(C)** Kaplan–Meier survival curve comparing overall survival across RPPA clusters (EMT cluster and other clusters) using 115 data from 176 core-set cervical cancer samples. Kaplan–Meier curves were based on the log-rank test. The HR was performed using the Cox model. **(D)** Western blot assay of LOXL2, E-Cadherin (CHD1), N-Cadherin (CHD2), SNAI1, Vimentin, Ki67 and Caspase 3 in SiHa and HeLa after transfected with sh-Con or sh-LOXL2. GAPDH served as the loading control. **(E)** Enrichment terms of LOXL2 positive correlated genes and network of enriched terms (Colored by cluster of enriched terms). Representative images of wound healing assay **(F)**, cellular migration assay **(G,H)**, cell viability assay **(I)** and colony formation assay **(J)** of SiHa and HeLa in CON or sh-LOXL2 groups at 0 and 48 h time points. Each assay was displayed more than three times.

cell diminished in the SiHa and HeLa LOXL2-interfering cells (**Figures 5F-H** and **Supplementary Figure 5E**) and the cell viability (**Figure 5I**) and colony formation assays (**Figure 5J**) revealed that cell proliferation was attenuated after LOXL2 silencing. To further investigate the role of LOXL2 in cell proliferation, we performed Ki 67 and Caspase 3 blotting in LOXL2-interfering cells. Result showed that LOXL2 knockdown blocked cell division instead of promoting cell death in cervical cancer (**Figure 5D**, **Supplementary Figure 6**).

DISCUSSION

Precise classification of cervical carcinoma in combination with multiplatform profiling can help to identify novel clinical and molecular associations in functional phenotypes, as well as predict disease outcome and guide selection of tumor-specific therapeutic approaches (18, 33). By rewiring the TCGA and GEO datasets with multiplatform profiling corresponding to LOXL2 expression status, we identified the correlation between LOXL2 and the molecular clusters established in TCGA. And the different features in the same patient indicated that LOXL2 expression status may reflect a combination of tumor heterogeneity and tumor-associated functional phenotype and represent an opportunity to subtype stratified clustering.

The U.S. Food and Drug Administration (FDA) has officially approved Keytruda (pembrolizumab) for cervical cancer patients with recurrent or metastatic disease during or after chemotherapy. However, previous cervical cancer clinical trials have reported relatively low overall response rates (ORR) with this drug (34). It has been reported that PD-L1 is expressed in <50% of samples (35), except for the current predictive value of PD-L1 immunohistochemistry, the other biomarkers should be assessed. Here, LOXL2 clustering identified different mutational density between the two clusters, especially for the EP300, ERBB2, EGFR, and NOTCH2 genes. As high TMB is considered to be an emerging biomarker of sensitivity to PD-1 and PD-L1 blockades and immune checkpoint inhibitors (27), LOXL2 clustering may be a new biomarker for screening immunotherapy, accompanied by PD-1 or PD-L1 expression in clinical triage, which needs subsequent research.

In innate immunity, the role of APOBEC3 genes in HPV-related cancer is presumed to be an aberrant trigger and/or dysregulation that results in somatic mutation observed in cervical cancer (31). For the different mean expression patterns of APOBEC3 genes between the two LOXL2 clusters observed in our research and their negative correlation in the SiHa and HeLa cell lines, we tentatively put forward LOXL2 may be a trigger of APOBEC3 gene dysregulation in cervical cancer. Furthermore, HPV A7 type, a type including HPV 18, 39, 45, 59, 68 subtypes, was observed in the high-LOXL2 cluster. According to the lasted TCGA clustering (18), most HPV clade A7 samples were with low CpG island hypermethylated (CIMP-low). In our clustering, HPV A7 type ($P = 0.0145$) and the CIMP-low group ($P = 0.0063$) was enriched in the high-LOXL2 cluster. The high expression of LOXL2 may be associated with the infection of type of HPV A7 and CpG island methylation of genes, which is worthy of further investigation.

For predicting potency, the high-LOXL2 cluster showed younger mean diagnostic age, with poorer cancer outcome in the 20–39 age range. In addition, high LOXL2 expression was significantly correlated with poor OS and DFS in cervical cancer. However, the mortality of cervical cancer is related to age, older women were seen to have the highest mortality rates (36). In our study, we found that high-LOXL2 cluster showed younger mean diagnostic age, while high-LOXL2 cluster showed poor cancer survival, which meant the poor prognosis in high-LOXL2 cluster was not completely on account of age at initial pathological diagnosis. Therefore, we analyzed the poor prognosis of high-LOXL2 cluster in cervical cancer, such as EMT phenotype in cancer progression. It is well-known that LOXL2 is involved in SNAI1 interaction and CDH1 repression for EMT induction (37). We found that the expression of LOXL2 was positively correlated with EMT phenotype in cervical cancer, and the proliferation and migration of cells were attenuated after LOXL2 silencing. These results contributed to the prediction potency of LOXL2 in cervical cancer, in accordance with the finding that the EMT phenotype is significantly correlated with poor prognosis in cervical carcinoma (18).

In many cancer types, EMT became aberrantly activated during tumor invasion and metastasis or sped up the processes of metastatic colonization (38). It was reported that overexpression of LOXL2 drove EMT via upregulating the expression of SNAIL (SNAI1/2), ZEB (ZEB1/2) via IRE1-XBP1 signaling pathway or FAK/SRC signaling pathway in cancer cells (39, 40). Furthermore, there was an autocrine feedback loops among ESRP1, HAS2, CD44, and ZEB1 in the aberrant activation of EMT (41), which acted in the dynamics of EMT in cancer metastasis. In addition, LOXL2 was also involved in the process of extracellular matrix (ECM) remodeling (42). ECM contributes to EMT and enhances cellular invasion via altering mechanical stiffness of the ECM and weakening the cell to cell adhesion (43, 44). In turn, LOXL2 induced aberrant activation of EMT crosslinked collagen in ECM remodeling for tumor microenvironment (41). Furthermore, LOXL2, as a copper-dependent enzyme, could be inhibited by copper chelation agents, such as penicillamine, trientine, disulfiram, clioquinol, or tetrathiomolybdate (TM), which could be used in cancer treatment (45, 46). Although TM has been demonstrated as controversial observations in cancer clinical trials, especially in breast cancer, the phase II trial of breast cancer demonstrated that women who had a high risk of recurrence would get benefit from TM treatment via changing the tumor microenvironment to prevent metastasis (47). There was potential value of copper chelation agents in cervical cancer for further research.

It should be noted that, in this study, we has examined only the expression pattern of LOXL2 in cervical carcinoma or paired normal tissue, the specific application and the significance in clinical samples should be further accessed, such as routine immunostaining. And there was specificity of

LOXL2, high LOXL2 expression both in epithelial and stroma, which could be conducive to the epithelial–stromal cross talk and the malignant progression of cervical cancer (48, 49). We focused on the correlation between characterizations of carcinoma and LOXL2 expression status in cervical carcinoma, however, not all the results are significantly meaningful, especially in the stage, grade or histologic subtype of carcinoma, which is the evaluating indicator of carcinoma in clinical work. The correlation may reflect some part of molecular characterizations in cervical carcinoma. In addition, higher mutation burden is considered to be characteristic of high aggressive and mesenchymal cancers (50), there was a contradiction between TMB and LOXL2 expression status in our study. For low mutation density in high LOXL2 group, with poor outcome in high LOXL2 group, we tended to use the LOXL2 clustering as a biomarker for screening candidates for immunotherapy.

In summary, our results supported the relevance of LOXL2 expression status in multiplatform integrative analyses, prognosis of tumor mutation density, and survival prediction in cancer. And we showed the clinical and molecular associations as well as functionally altered features of LOXL2 expression, which may drive carcinogenesis and potentially serve as a therapeutic target in cervical carcinoma.

DATA AVAILABILITY STATEMENT

The datasets analyzed in this study can be found in the The Cancer Genome Atlas (https://portal.gdc.cancer.gov/).

ETHICS STATEMENT

The studies involving human participants were reviewed and approved by Medical Ethics Committee of Tongji Medical College, Huazhong University of Science and Technology. The patients/participants provided their written informed consent to participate in this study.

AUTHOR CONTRIBUTIONS

PeW designed the experiments and supervised the study. CC, SL, and WZ performed the experiments. CC, CL, and SL wrote the manuscript. PiW, YM, and PG contributed to samples' collection. JW and PeW for funding acquisition.

FUNDING

This work was supported by Natural Science Foundation of China (81630060 and 81772775), The research-oriented clinician funding program of Tongji Medical College, Huazhong University of Science and Technology for PeW. We are grateful for the public datasets obtained from TCGA and Gene Expression Omnibus.

SUPPLEMENTARY MATERIAL

The Supplementary Material for this article can be found online at: https://www.frontiersin.org/articles/10.3389/fonc.2020.00284/full#supplementary-material

REFERENCES

1. Torre LA, Bray F, Siegel RL, Ferlay J, Lortet-Tieulent J, Jemal A. Global cancer statistics, 2012. *CA Cancer J Clin*. (2015) 65:87–108. doi: 10.3322/caac.21262
2. Bachtiary B, Boutros PC, Pintilie M, Shi W, Bastianutto C, Li JH, et al. Gene expression profiling in cervical cancer: an exploration of intratumor heterogeneity. *Clin Cancer Res*. (2006) 12:5632–40. doi: 10.1158/1078-0432.CCR-06-0357
3. Kidd EA, Grigsby PW. Intratumoral metabolic heterogeneity of cervical cancer. *Clin Cancer Res*. (2008) 14:5236–41. doi: 10.1158/1078-0432.CCR-07-5252
4. Ojesina AI, Lichtenstein L, Freeman SS, Pedamallu CS, Imaz-Rosshandler I, Pugh TJ, et al. Landscape of genomic alterations in cervical carcinomas. *Nature*. (2014) 506:371–5. doi: 10.1038/nature12881
5. Berger AC, Korkut A, Kanchi RS, Hegde AM, Lenoir W, Liu W, et al. A comprehensive pan-cancer molecular study of gynecologic and breast cancers. *Cancer Cell*. (2018) 33:690–705 e9. doi: 10.1016/j.ccell.2018.03.014
6. Smith-Mungo LI, Kagan HM. Lysyl oxidase: properties, regulation and multiple functions in biology. *Matrix Biol*. (1998) 16:387–98. doi: 10.1016/S0945-053X(98)90012-9
7. Baker AM, Cox TR, Bird D, Lang G, Murray GI, Sun XF, et al. The role of lysyl oxidase in SRC-dependent proliferation and metastasis of colorectal cancer. *J Natl Cancer Inst*. (2011) 103:407–24. doi: 10.1093/jnci/djq569
8. Ahn SG, Dong SM, Oshima A, Kim WH, Lee HM, Lee SA, et al. LOXL2 expression is associated with invasiveness and negatively influences survival in breast cancer patients. *Breast Cancer Res Treat*. (2013) 141:89–99. doi: 10.1007/s10549-013-2662-3
9. Wong CC, Tse AP, Huang YP, Zhu YT, Chiu DK, Lai RK, et al. Lysyl oxidase-like 2 is critical to tumor microenvironment and metastatic niche formation in hepatocellular carcinoma. *Hepatology*. (2014) 60:1645–58. doi: 10.1002/hep.27320
10. Zaffryar-Eilot S, Marshall D, Voloshin T, Bar-Zion A, Spangler R, Kessler O, et al. Lysyl oxidase-like-2 promotes tumour angiogenesis and is a potential therapeutic target in angiogenic tumours. *Carcinogenesis*. (2013) 34:2370–9. doi: 10.1093/carcin/bgt241
11. Peinado H, Moreno-Bueno G, Hardisson D, Perez-Gomez E, Santos V, Mendiola M, et al. Lysyl oxidase-like 2 as a new poor prognosis marker of squamous cell carcinomas. *Cancer Res*. (2008) 68:4541–50. doi: 10.1158/0008-5472.CAN-07-6345
12. Peng L, Ran YL, Hu H, Yu L, Liu Q, Zhou Z, et al. Secreted LOXL2 is a novel therapeutic target that promotes gastric cancer metastasis via the Src/FAK pathway. *Carcinogenesis*. (2009) 30:1660–9. doi: 10.1093/carcin/bgp178
13. Ruckert F, Joensson P, Saeger HD, Grutzmann R, Pilarsky C. Functional analysis of LOXL2 in pancreatic carcinoma. *Int J Colorectal Dis*. (2010) 25:303–11. doi: 10.1007/s00384-009-0853-5
14. Fong SF, Dietzsch E, Fong KS, Hollosi P, Asuncion L, He Q, et al. Lysyl oxidase-like 2 expression is increased in colon and esophageal tumors and associated with less differentiated colon tumors. *Genes Chromosomes Cancer*. (2007) 46:644–55. doi: 10.1002/gcc.20444
15. Moreno-Bueno G, Salvador F, Martin A, Floristan A, Cuevas EP, Santos V, et al. Lysyl oxidase-like 2 (LOXL2), a new regulator of cell polarity required for metastatic dissemination of basal-like breast carcinomas. *EMBO Mol Med*. (2011) 3:528–44. doi: 10.1002/emmm.201100156
16. Barry-Hamilton V, Spangler R, Marshall D, McCauley S, Rodriguez HM, Oyasu M, et al. Allosteric inhibition of lysyl oxidase-like-2 impedes the development of a pathologic microenvironment. *Nat Med*. (2010) 16:1009–17. doi: 10.1038/nm.2208
17. Barker HE, Cox TR, Erler JT. The rationale for targeting the LOX family in cancer. *Nat Rev Cancer*. (2012) 12:540–52. doi: 10.1038/nrc3319

18. Cancer Genome Atlas Research Network, Albert Einstein College of Medicine, Analytical Biological Services, Barretos Cancer Hospital, Baylor College of Medicine, Beckman Research Institute of City of Hope, et al. Integrated genomic and molecular characterization of cervical cancer. *Nature*. (2017) 543:378–84. doi: 10.1038/nature21386
19. Koch A, Jeschke J, Van Criekinge W, van Engeland M, De Meyer T. MEXPRESS update 2019. *Nucleic Acids Res*. (2019) 47:W561–5. doi: 10.1093/nar/gkz445
20. Koch A, De Meyer T, Jeschke J, Van Criekinge W. MEXPRESS: visualizing expression, DNA methylation and clinical TCGA data. *BMC Genomics*. (2015) 16:636. doi: 10.1186/s12864-015-1847-z
21. Tang Z, Li C, Kang B, Gao G, Li C, Zhang Z. GEPIA: a web server for cancer and normal gene expression profiling and interactive analyses. *Nucleic Acids Res*. (2017) 45:W98–102. doi: 10.1093/nar/gkx247
22. Vasaikar SV, Straub P, Wang J, Zhang B. LinkedOmics: analyzing multi-omics data within and across 32 cancer types. *Nucleic Acids Res*. (2018) 46:D956–63. doi: 10.1093/nar/gkx1090
23. Zhou Y, Zhou B, Pache L, Chang M, Khodabakhshi AH, Tanaseichuk O, et al. Metascape provides a biologist-oriented resource for the analysis of systems-level datasets. *Nat Commun*. (2019) 10:1523. doi: 10.1038/s41467-019-09234-6
24. Cancer Genome Atlas Network. Comprehensive genomic characterization of head and neck squamous cell carcinomas. *Nature*. (2015) 517:576–82. doi: 10.1038/nature14129
25. Vartanian JP, Guetard D, Henry M, Wain-Hobson S. Evidence for editing of human papillomavirus DNA by APOBEC3 in benign and precancerous lesions. *Science*. (2008) 320:230–3. doi: 10.1126/science.1153201
26. Siegel RL, Miller KD, Jemal A. Cancer statistics, 2019. *CA Cancer J Clin*. (2019) 69:7–34. doi: 10.3322/caac.21551
27. Chalmers ZR, Connelly CF, Fabrizio D, Gay L, Ali SM, Ennis R, et al. Analysis of 100,000 human cancer genomes reveals the landscape of tumor mutational burden. *Genome Med*. (2017) 9:34. doi: 10.1186/s13073-017-0424-2
28. Narvaiza I, Landry S, Weitzman MD. APOBEC3 proteins and genomic stability: the high cost of a good defense. *Cell Cycle*. (2012) 11:33–8. doi: 10.4161/cc.11.1.18706
29. Harris RS. Enhancing immunity to HIV through APOBEC. *Nat Biotechnol*. (2008) 26:1089–90. doi: 10.1038/nbt1008-1089
30. Cannataro VL, Gaffney SG, Sasaki T, Issaeva N, Grewal NKS, Grandis JR, et al. APOBEC-induced mutations and their cancer effect size in head and neck squamous cell carcinoma. *Oncogene*. (2019) 38:3475–87. doi: 10.1038/s41388-018-0657-6
31. Smith NJ, Fenton TR. The APOBEC3 genes and their role in cancer: insights from human papillomavirus. *J Mol Endocrinol*. (2019) 62:R269–87. doi: 10.1530/JME-19-0011
32. Venkatesan S, Rosenthal R, Kanu N, McGranahan N, Bartek J, Quezada SA, et al. Perspective: APOBEC mutagenesis in drug resistance and immune escape in HIV and cancer evolution. *Ann Oncol*. (2018) 29:563–72. doi: 10.1093/annonc/mdy003
33. Spaans VM, Trietsch MD, Peters AA, Osse M, Ter Haar N, Fleuren GJ, et al. Precise classification of cervical carcinomas combined with somatic mutation profiling contributes to predicting disease outcome. *PLoS ONE*. (2015) 10:e0133670. doi: 10.1371/journal.pone.0133670
34. Lheureux S, Butler MO, Clarke B, Cristea MC, Martin LP, Tonkin K, et al. Association of ipilimumab with safety and antitumor activity in women with metastatic or recurrent human papillomavirus-related cervical carcinoma. *JAMA Oncol*. (2018) 4:e173776. doi: 10.1001/jamaoncol.2017.3776
35. Frenel JS, Le Tourneau C, O'Neil B, Ott PA, Piha-Paul SA, Gomez-Roca C, et al. Safety and efficacy of pembrolizumab in advanced, programmed death ligand 1-positive cervical cancer: results from the phase Ib KEYNOTE-028 trial. *J Clin Oncol*. (2017) 35:4035–41. doi: 10.1200/JCO.2017.74.5471
36. Arbyn M, Weiderpass E, Bruni L, de Sanjose S, Saraiya M, Ferlay J, et al. Estimates of incidence and mortality of cervical cancer in 2018: a worldwide analysis. *Lancet Glob Health*. (2019) 8:Pe191–e203. doi: 10.1016/S2214-109X(19)30482-6
37. Peinado H, Del Carmen Iglesias-de la Cruz M, Olmeda D, Csiszar K, Fong KS, Vega S, et al. A molecular role for lysyl oxidase-like 2 enzyme in snail regulation and tumor progression. *EMBO J*. (2005) 24:3446–58. doi: 10.1038/sj.emboj.7600781
38. Jolly MK, Ware KE, Gilja S, Somarelli JA, Levine H. EMT and MET: necessary or permissive for metastasis? *Mol Oncol*. (2017) 11:755–69. doi: 10.1002/1878-0261.12083
39. Cuevas EP, Eraso P, Mazon MJ, Santos V, Moreno-Bueno G, Cano A, et al. LOXL2 drives epithelial-mesenchymal transition via activation of IRE1-XBP1 signalling pathway. *Sci Rep*. (2017) 7:44988. doi: 10.1038/srep44988
40. Peng DH, Ungewiss C, Tong P, Byers LA, Wang J, Canales JR, et al. ZEB1 induces LOXL2-mediated collagen stabilization and deposition in the extracellular matrix to drive lung cancer invasion and metastasis. *Oncogene*. (2017) 36:1925–38. doi: 10.1038/onc.2016.358
41. Jolly MK, Preca BT, Tripathi SC, Jia D, George JT, Hanash SM, et al. Interconnected feedback loops among ESRP1, HAS2, and CD44 regulate epithelial-mesenchymal plasticity in cancer. *APL Bioeng*. (2018) 2:031908. doi: 10.1063/1.5024874
42. Park PG, Jo SJ, Kim MJ, Kim HJ, Lee JH, Park CK, et al. Role of LOXL2 in the epithelial-mesenchymal transition and colorectal cancer metastasis. *Oncotarget*. (2017) 8:80325–35. doi: 10.18632/oncotarget.18170
43. Kumar S, Das A, Sen S. Extracellular matrix density promotes EMT by weakening cell-cell adhesions. *Mol Biosyst*. (2014) 10:838–50. doi: 10.1039/C3MB70431A
44. Moon HJ, Finney J, Xu L, Moore D, Welch DR, Mure M. MCF-7 cells expressing nuclear associated lysyl oxidase-like 2 (LOXL2) exhibit an epithelial-to-mesenchymal transition (EMT) phenotype and are highly invasive *in vitro*. *J Biol Chem*. (2013) 288:30000–8. doi: 10.1074/jbc.C113.502310
45. Tapiero H, Townsend DM, Tew KD. Trace elements in human physiology and pathology. *Copper Biomed Pharmacother*. (2003) 57:386–98. doi: 10.1016/S0753-3322(03)00012-X
46. Turski ML, Thiele DJ. New roles for copper metabolism in cell proliferation, signaling, and disease. *J Biol Chem*. (2009) 284:717–21. doi: 10.1074/jbc.R800055200
47. Garber K. Biomedicine. Targeting copper to treat breast cancer. *Science*. (2015) 349:128–9. doi: 10.1126/science.349.6244.128
48. Martin A, Salvador F, Moreno-Bueno G, Floristan A, Ruiz-Herguido C, Cuevas EP, et al. Lysyl oxidase-like 2 represses Notch1 expression in the skin to promote squamous cell carcinoma progression. *EMBO J*. (2015) 34:1090–109. doi: 10.15252/embj.201489975
49. Mahjour F, Dambal V, Shrestha N, Singh V, Noonan V, Kantarci A, et al. Mechanism for oral tumor cell lysyl oxidase like-2 in cancer development: synergy with PDGF-AB. *Oncogenesis*. (2019) 8:34. doi: 10.1038/s41389-019-0144-0
50. Campbell BB, Light N, Fabrizio D, Zatzman M, Fuligni F, de Borja R, et al. Comprehensive analysis of hypermutation in human cancer. *Cell*. (2017) 171:1042–56 e10. doi: 10.1016/j.cell.2017.09.048

Conflict of Interest: The authors declare that the research was conducted in the absence of any commercial or financial relationships that could be construed as a potential conflict of interest.

Copyright © 2020 Cao, Lin, Zhi, Lazare, Meng, Wu, Gao, Wei and Wu. This is an open-access article distributed under the terms of the Creative Commons Attribution License (CC BY). The use, distribution or reproduction in other forums is permitted, provided the original author(s) and the copyright owner(s) are credited and that the original publication in this journal is cited, in accordance with accepted academic practice. No use, distribution or reproduction is permitted which does not comply with these terms.

frontiers in Oncology

ORIGINAL RESEARCH
published: 10 March 2020
doi: 10.3389/fonc.2020.00304

Integrative Analysis of Breast Cancer Cells Reveals an Epithelial-Mesenchymal Transition Role in Adaptation to Acidic Microenvironment

Mehdi Sadeghi[1†], *Bryce Ordway*[2†], *Ilyia Rafiei*[1], *Punit Borad*[2], *Bin Fang*[3], *John L. Koomen*[3], *Chaomei Zhang*[4], *Sean Yoder*[4], *Joseph Johnson*[5] and *Mehdi Damaghi*[2,6*]

[1] Department of Cell and Molecular Biology, Faculty of Science, Semnan University, Semnan, Iran, [2] Department of Cancer Physiology, Moffitt Cancer Center and Research Institute, Tampa, FL, United States, [3] Proteomics Core, Moffitt Cancer Center and Research Institute, Tampa, FL, United States, [4] Molecular Biology Core, Moffitt Cancer Center and Research Institute, Tampa, FL, United States, [5] Microscopy Core, Moffitt Cancer Center and Research Institute, Tampa, FL, United States, [6] Department of Oncologic Sciences, Morsani College of Medicine, University of South Florida, Tampa, FL, United States

OPEN ACCESS

Edited by:
Mohit Kumar Jolly,
Indian Institute of Science (IISc), India

Reviewed by:
Dongya Jia,
Rice University, United States
Prashant Kumar,
Institute of Bioinformatics (IOB), India

***Correspondence:**
Mehdi Damaghi
mehdi.damaghi@moffitt.org

[†]These authors have contributed equally to this work

Specialty section:
This article was submitted to Molecular and Cellular Oncology, a section of the journal Frontiers in Oncology

Received: 03 November 2019
Accepted: 20 February 2020
Published: 10 March 2020

Citation:
Sadeghi M, Ordway B, Rafiei I, Borad P, Fang B, Koomen JL, Zhang C, Yoder S, Johnson J and Damaghi M (2020) Integrative Analysis of Breast Cancer Cells Reveals an Epithelial-Mesenchymal Transition Role in Adaptation to Acidic Microenvironment. Front. Oncol. 10:304. doi: 10.3389/fonc.2020.00304

Early ducts of breast tumors are unequivocally acidic. High rates of glycolysis combined with poor perfusion lead to a congestion of acidic metabolites in the tumor microenvironment, and pre-malignant cells must adapt to this acidosis to thrive. Adaptation to acidosis selects cancer cells that can thrive in harsh conditions and are capable of outgrowing the normal or non-adapted neighbors. This selection is usually accompanied by phenotypic change. Epithelial mesenchymal transition (EMT) is one of the most important switches correlated to malignant tumor cell phenotype and has been shown to be induced by tumor acidosis. New evidence shows that the EMT switch is not a binary system and occurs on a spectrum of transition states. During confirmation of the EMT phenotype, our results demonstrated a partial EMT phenotype in our acid-adapted cell population. Using RNA sequencing and network analysis we found 10 dysregulated network motifs in acid-adapted breast cancer cells playing a role in EMT. Our further integrative analysis of RNA sequencing and SILAC proteomics resulted in recognition of S100B and S100A6 proteins at both the RNA and protein level. Higher expression of S100B and S100A6 was validated *in vitro* by Immunocytochemistry. We further validated our finding both *in vitro* and in patients' samples by IHC analysis of Tissue Microarray (TMA). Correlation analysis of S100A6 and LAMP2b as marker of acidosis in each patient from Moffitt TMA approved the acid related role of S100A6 in breast cancer patients. Also, DCIS patients with higher expression of S100A6 showed lower survival compared to lower expression. We propose essential roles of acid adaptation in cancer cells EMT process through S100 proteins such as S100A6 that can be used as therapeutic strategy targeting both acid-adapted and malignant phenotypes.

Keywords: acid adaptation, EMT, tumor microenvironment, breast cancer, S100 family proteins

INTRODUCTION

The principle driver of evolutionary processes is the concept of survival of the fittest. Those given populations that are the most well adapted to survive in an environment are the ones that will persist. In higher order organisms, the surviving populations are those that have a set of static traits that make them successful in a given environment. At a cellular selection level, organisms have the ability to acclimate to a given environment and alter their phenotype to be more successful in surviving. This ability to alter phenotype in order to acclimate to a given environment is particularly important in the context of cancer cell survival. In order for a cancerous cell population to persist, it must be able to adapt and evolve to maintain its' fitness within a given tumoral environment (1–3). Those cellular populations with the ability to more rapidly and efficiently adapt to the environment will have an advantage over the other cell populations when facing the challenges of a new or changing environment (4). Epithelial to mesenchymal transition (EMT) is one of the phenotypic switches that promote cancer progression, invasion and metastasis. EMT tests a cancer cells ability to efficiently change cellular states in response to changing conditions, also denoted as cellular plasticity, which also often referred to in the cancer stem cell model (5, 6). Although denoted as a transition, It has been recently observed that the EMT process is non-binary and occurs on a spectrum of transition states that can have the characteristics of both epithelial and mesenchymal phenotypes (7, 8). The transition to one of the intermediate states between epithelial and mesenchymal phenotype has been denoted partial EMT (pEMT), with cells expressing both markers of epithelial and mesenchymal cell status. pEMT states compared to complete EMT carry different migratory patterns during cancer metastasis (9, 10), and demonstrate the elevated plasticity of their epithelial progenitors (8). Another cause of EMT can be functional heterogeneity of cancer cells that is the result of genetic and epigenetic makeup as well as their interactions with the microenvironment. It has been recently shown that phenotypic heterogeneity is a dynamic reversible state of highly plastic cancer cells and their response to microenvironmental changes in GBM (11). Lately, there have been proposals for a strong connection between tumor plasticity and recreating intra-tumoral phenotypic heterogeneity (12) and also emphasizing the role of microenvironment in shaping spatial and temporal heterogeneity (13). It looks like the relationship between tumor cell plasticity, and intra-tumoral heterogeneity with emerging new phenotypes such as EMT or pEMT in everchanging cancer microenvironments is getting more attention and will be new area of research. It has been shown that growth factors, such as epidermal growth factor (EGF), transforming growth factor-β (TGF-β), and basic fibroblast growth factor (bFGF/FGF2) are also able to induce EMT (14, 15). It has also recently reported that tumor microenvironment conditions such as hypoxia and acidosis can induce EMT (16, 17).

Adenocarcinomas initiate and evolve within the hostile microenvironment of avascular ducts, which are characterized by acidosis, hypoxia, reactive oxygen species (ROS), and nutrient deprivation (18, 19). In particular, the acidic microenvironment of tumors strongly influences cancer progression and evolution. We have proposed that chronic acidosis induces genomic instability and selects for emergence of aggressive clones, leading to genomic diversity and increased tumor heterogeneity (20–24), a proximal cause of malignancy and resistance (25). Specifically, the acidified habitat imparts a Darwinian selection pressure that favors cells that adapt mechanisms to resist acid-mediated cell death. Further, the acidic microenvironment is also manifested in locally invasive cancers where it confers cancer cells a selective advantage over the stromal cells, leading them to invade to surrounding stroma. Indeed, an acidic microenvironment stimulates invasion and metastasis and also promotes remodeling of the extracellular matrix (ECM) (26–30). Further, acidosis promotes angiogenesis via the release of VEGF (31) and impairs immune surveillance (32, 33). Acid adaptation also pushes cancer cells toward a more aggressive phenotype through lysosomal redistribution (34) and plays a major role in subpopulation formation and evolution of solid tumors.

Integrative analysis has received a lot of attention lately in biology and cancer biology specifically, due to its nature of inter-validating data in different levels of biology such as genome, transcriptome, proteome, and metabolome (35). Different data integration approaches can help to combine various high throughput omics data to construct an integrative regulatory network. These networks can help to understand the molecular basis of carcinogenesis and provide a powerful framework for exploring new cancer biomarkers (36, 37). With the advancements in network inference and construction methods, network analysis, and interpretation approaches it is feasible now to explore authentic and accurate molecular signatures. Another advantage of such analysis is discovery of groups of co-regulated molecules as a sub-network biomarker for treatment, diagnosis or prognosis applications.

Expression profiling is a major key to unraveling gene expression patterns and the transcriptome. RNA sequencing is a next-generation sequencing (NGS) technology that sequences cDNA in order to provide accurate measurement of transcripts levels to define biological networks (38). Networks are the language of complex systems like biological systems. Biological networks are used widely to model biological interactions at the molecular level to understand biological processes particularly in the case of cancer (39). To assess biological networks different techniques have been developed; centrality analysis is one of them (40, 41). Centrality analysis ranks the nodes (genes in gene regulatory networks) based on their significance. In centrality analysis, adding topological parameters to biological data leads to sufficiently informative results that have been shown to be effective in exploring key signature molecules in biological processes (42). Such biological network analysis has been used in cancer biomarker discovery (43).

Here in, we studied the effect of acid adaptation on early stage breast cancer evolution using the MCF7 cancer cell line. We studied EMT phenotypic switches as regulators of acid adaptation using RNA sequencing data and gene regulatory network analysis and by integrating the results to SILAC proteomics data. For that reason, we compared acid-adapted MCF7 breast cancer cell line RNA profile to parental MCF7

cells. The differentially expressed genes in the acid-adapted cells were used to construct a gene regulatory network. This network was implemented to explore sub-network biomarkers related to EMT by a set of robust criteria. We then compared our findings with the SILAC proteomics results and found S100 family proteins such as S100A6 and S100B are abundant in both sets of omics data. We validated both S100B from RNA sequencing and S100A6 from proteomics data, by Immunocytochemistry (ICC). We further our validation using IHC of breast cancer patient TMAs with 160 biopsy cores. S100A6 expression was compared to LAMP2b as a biomarker of acidosis in solid tumors, and each core's LAMP2b expression was co-registered with S100A6 expression using Definiens tissue studio software analysis. The TMA co-registration analysis showed correlation of S100A6 with LAMP2b expression the most in early breast cancer stage, ductal carcinoma *in situ*, DCIS. Survival analysis of patients with different expression of S100A6 revealed correlation of high S100A6 expression with worse outcome in survival of breast cancer patients. When taken in total, we conclude that amongst many paths of EMT, S100 proteins play critical roles in acid-induced EMT that can be responsible for cancer progression and survival of cancer cells in their continuously changing microenvironments.

MATERIALS AND METHODS

Cell Culture and Acid Adaptation *in vitro*

MCF7 cells were acquired from American Type Culture Collection (ATCC, Manassas, VA, 2007–2010) and were grown in DMEM-F12 (Life Technologies) with 10% fetal bovine serum (HyClone Laboratories) and 1% peniciline/stroptomycine added. Growth medium was buffered with 25 mmol l^{-1} each of PIPES and HEPES and the pH adjusted to 7.4 or 6.5. Cells were tested for mycoplasma contamination and authenticated using short tandem repeat DNA typing according to ATCC's. To achieve acid adaptation, cells were chronically cultured and passaged directly in pH 6.5 medium for ∼2 months. Chronic low-pH-adapted cells underwent at least 20 passages.

RNA Sequencing

RNA sequencing was performed on MCF7 and acid-adapted MCF7 cells using the NuGen Ovation Encore Complete RNAseq kit, which generates strand-specific total RNAseq libraries (Nugen, Inc., San Carlos, CA). Following quality control screening on the NanoDrop to assess 260/230 and 260/280 ratios, the samples were screened on the Agilent BioAnalyzer RNA Nano chip to generate an RNA Integrity Number (RIN) (Agilent Technologies, Santa Clara, CA). Hundred nanogram of DNase-treated total RNA was then used to generate double-stranded cDNA, which was initiated with selective random priming allowing for the sequencing of total RNA, while avoiding rRNA and mitochondrial transcripts. After primer annealing at 65°C for 5 min, a first strand cDNA synthesis reaction was performed at 40°C for 30 min using kit-supplied reverse transcription reagents. Second strand cDNA synthesis was performed in a 70 μl reaction volume at 16°C for 1 h and the reaction was stopped by adding 45 μl of stop solution. The double-stranded cDNA was then fragmented to ∼200 bp with the Covaris M220 sonicator (Covaris, Inc., Woburn, MA), followed by purification with Agencourt RNAClean XP (Beckman Coulter Life Sciences, Indianapolis, IN). The fragmented DNA was suspended in 10 μl of water and end repair was performed in a 13 μl for 30 min at 25°C, followed by a heat inactivation of 70°C for 10 min. Sample-specific indexed adapter was ligated to the end-repaired DNA for 30 min at 25°C, followed by a two-step strand selection process with an intervening 1.8X volume RNAClean XP bead purification. 13 cycles of library amplification and a 1.2x volume RNAClean XP purification of the strand-selected library was performed, followed by resuspension of the library DNA in 30 μl of RNase-free water. Final libraries were screened for library fragment size distribution using an Agilent BioAnalyzer High sensitive DNA Chip. Libraries were then quantitated using the Kapa Library Quantification Kit (Roche Sequencing, Pleasanton, CA), normalized to 4 nM, and were sequenced on an Illumina NextSeq 500 150-cycle high-output flow cell in order to generate ∼40 million paired-end reads of 75-base per sample (Illumina, Inc., San Diego, CA) (44).

RNA Sequencing Data Processing and Analysis

The RNA-seq data analysis workflow has been provided schematically in **Supplementary Figure 1**. Raw reads were quality-filtered to obtain clear data via removal of adaptor sequences, ambiguous or low-quality reads and reads with more than 5% N, using FastQC version 0.11.8 (http://www.bioinformatics.babraham.ac.uk/projects/fastqc/) and Trimmomatic version 0.39) (45). Then clean reads were aligned to the reference genome (GRCh37) using HISAT2 version 2.1.0 (46). Finally, the read count values for aligned sequences of genes were computed to represent the expression levels of genes using HTSeq version 11.1 (47). Differentially expressed genes (DEGs) between two groups were explored using R (48) package DESeq2 version1.24.0 (49).

Genes with p-value <0.05 were selected as differentially expressed Genes. Benjamini-Hochberg (BH) multiple testing correction was applied on results.

PROTEOMICS

SILAC Labeling

Acid-adapted and naive cells were labeled by SILAC. Cells were cultured in heavy SILAC media (Δ6-lysine and Δ10-arginine) for eight doubling time of MCF7. Extent of labeling was determined by LC–MS/MS analysis of tryptic peptides from labeled samples to ensure >90% labeling.

Lysis and Digestion

Cells were lysed by sonication in a buffer of 50% trifluoroethanol and 50 mM ammonium bicarbonate, pH 8.0, and protein was measured by the Bradford method. Protein from heavy- and light-labeled cells was combined in equal amounts, and lysis buffer was added to bring the final volume to 200 μl. The combined protein was reduced with 100 μl of 40 mM TCEP/100 mM dithiothreitol for 1 h at 37°C. Proteins were

alkylated with 100 µl of 200 mM iodoacetamide for 30 min in the dark at ambient temperature. The volume of the reduced and alkylated sample was brought to 1 ml with 50 mM ammonium bicarbonate, pH 8.0. Trypsin was added at a ratio of 1:50 and samples were digested at 37°C overnight. Digests were frozen at −80°C and lyophilized. Dried peptides were resuspended in HPLC water with 0.1% TFA and desalted on 100-mg Thermo hypersep C18 columns. Eluted peptides were dried in a Speed-Vac and resuspended in HPLC water for isoelectric focusing fractionation.

Isoelectric Focusing Fractionation

Tryptic peptides were fractionated using a narrow-pH-range fractionation strategy. At the end of the isoelectric focusing programme, strips were manually cut into 20 fractions. Peptides were extracted and samples were combined in the following manner to achieve 15 fractions for LC–MS/MS analysis: (anode end) samples 1–2, 3–4, 5–6, 7–8, and 9–10 were combined to make five fractions, samples 11–20 were left as individual fractions.

LC–MS/MS

Samples were analyzed as duplicate injections for each fraction. A nano-flow ultra-high performance liquid chromatograph (RSLC, Dionex, Sunnyvale, CA) coupled to an electrospray ion trap mass spectrometer (LTQ-Orbitrap, Thermo Scientific, San Jose, CA) was used for tandem MS peptide-sequencing experiments. The sample was first loaded onto a pre-column (2 cm × 75 µm ID packed with C18 reversed-phase resin, 5 µm particle size, 100 Å pore size) and washed for 8 min with aqueous 2% acetonitrile and 0.04% trifluoroacetic acid. The trapped peptides were eluted onto the analytical column (C18 Pepmap 100, 75 µm × 50 cm ID, Dionex). The 120-min gradient was programmed as: 95% solvent A (2% acetonitrile + 0.1% formic acid) for 8 min, solvent B (90% acetonitrile + 0.1% formic acid) from 5 to 15% in 5 min, 15 to 40% in 85 min, then solvent B from 50 to 90% B in 7 min and held at 90% for 5 min, followed by solvent B from 90 to 5% in 1 min and re-equilibration for 10 min. The flow rate on the analytical column was 300 nl min^{-1}. Ten tandem mass spectra were collected in a data-dependent manner following each survey scan. The MS scans were performed in the Orbitrap to obtain accurate peptide mass measurements, and the MS/MS scans were performed in the linear ion trap using a 60-s exclusion for previously sampled peptide peaks. Mascot (www.matrixscience.com) searches were performed against the UniProt human database downloaded on 11 July 11 2012. Two missed tryptic cleavages were allowed, the precursor mass tolerance was 1.2 Da to accommodate selection of different isotopes of the peptide precursor. MS/MS mass tolerance was 0.6 Da. Dynamic modifications included carbamidomethylation (Cys), oxidation (Met), heavy lysine (Δ6) and heavy arginine (Δ10).

Quantification of differences in protein expression between SILAC-labeled samples was performed as described using MaxQuant. Results were filtered to require a posterior error probability (PEP) score < 0.05 and summed intensity > 0. Candidates were selected among proteins that consistently showed at least a 1.5-fold increase under low-pH conditions across label-flipping experiments.

Network Construction

The STRING database is a valuable resource for the exploration and analysis of functional gene/protein interactions (50). STRING database was used to find conserved experimentally validated gene-gene interaction networks for the explored DEGs. Since STRING builds protein-protein interaction (PPI) networks thereby our network was constructed upon coding RNAs.

Motif Exploring and Motif Ranking

Networks consist of smaller and repetitive structural units which are called motifs. Network motifs can be described as recurring circuits of interactions from which the networks are made (51). Motifs have important roles in biological networks and suggested that they accomplish overriding functions in biological networks. In this study, Cytoscape (52) NetMatchStar plugin (53) was used to find 3-node 3-edge network motifs in the gene regulatory network which retrieved from STRING database.

In order to further our network analysis, multiple topological and biological parameters were determined and used. Log2 fold change of differentially expressed genes associated in the gene regulatory network (**Supplementary Table 1**), association of network's genes with biological processes involved in EMT (based on explored GOBP terms related to EMT) (**Supplementary Table 2**) and gene prioritization score (**Supplementary Table 3**) which were obtained from Cytoscape GPEC (54) plugin (54), were considered as biological parameters. Betweenness centrality and node degree are two network topological parameters (**Supplementary Table 4**) which obtained using Cytoscape (52) NetworkAnalyzer (55) plugin and were considered besides biological parameters for network's robust motif ranking. Node degree indicates the number of connected edges to each node and betweenness centrality shows the control level of a node over interactions of other nodes in a network. This centrality parameter prefers the nodes that allow to connect non-directly connected clusters of a network.

The next step was to find the most important motifs in the network. For this purpose, a ranking scheme (56) was performed based on a multi objective weighting function. This scheme is based on parameters which we gathered before: (i) Topological parameters, node degree and betweenness centrality, (ii) the presence of motif genes in EMT related biological pathways (see "Discussion" for more detail), (iii) the gene prioritization score obtained from Cytoscape GPEC plugin (54), (iv) acid-adapted MCF7 cell lines gene expression log2 fold-changes (based on differential expression analysis of acid-adapted MCF7 cell lines vs. non-adapted cell lines). Using this weighted multi-objective function in Equation 1, the motif ranking was performed.

$$GS_{ij} = \frac{w_{1j}}{2}.\frac{\langle nD\rangle_i}{max(nD)} + \frac{w_{1j}}{2}.\frac{\langle nB\rangle_i}{max(nB)} + w_{2j}.\frac{\langle PP\rangle_i}{max(PP)} + w_{3j}.\frac{\langle GPS\rangle_i}{max(GPS)} + w_{4j}.\frac{\langle |LFC|\rangle_i}{max(LFC)}$$

GS_{ij} is the ranking score for each motif ($i = 1 \ldots n$) in different weighting scheme ($j = 1 \ldots 13$) as said in **Table 1**.

TABLE 1 | Weighting scenarios for motif ranking.

Sets	w_1	w_2	w_3	w_4
Set 1	1	0	0	0
	0	0	1	0
	0	0	0	1
Set 2	1.4	0	0	3.4
	0	1.4	0	3.4
	0	0	1.4	3.4
Set 3	1.8	1.8	0	3.4
	1.8	0	1.8	3.4
	0	1.8	1.8	3.4
Set 4	1.16	1.16	1.8	3.4
	1.16	1.8	1.16	3.4
	1.8	1.16	1.16	3.4
Set 5	1.4	1.4	1.4	1.4

Different weighting values including w_{1j} to w_{4j} are used to strike importance of used factors, $\langle nD \rangle_i$: average node degree for motif's node, $\langle nB \rangle_i$: average betweenness centrality of each node in a motif, $\langle PP \rangle_i$: number of genes in a motif involved in EMT related pathways, $\langle GPS \rangle_i$: average gene prioritization score obtained from GPEC, $\langle |LFC| \rangle_i$: average absolute log2 fold change for each motif.

Five different sets of weighting scenarios including 13 different weighting schemes were applied (**Table 1**) to remove biasness between used parameters in motif prioritization. Each set pays more attention to specific parameters in Equation (1). In the first set, only one parameter is more important for ranking. In the sets 2–4, two, three and four parameters are important, respectively, and constantly have higher weights to the absolute LFC of the motif to explore phenotype-specific top ranked motifs. In the fifth set, equal weights allocated to all the parameters. This weighting scheme leads to 13 ranking score for each motif. After removing duplicated motifs, we selected the top 10 motifs from each weighting scenario for further analysis (**Supplementary Table 5**).

PROTEOMICS AND TRANSCRIPTOMICS INTEGRATIVE DATA ANALYSIS

Integrative proteomics and transcriptomics data analysis was performed in roder to ensure about consistency of proteomic and transcriptomic data regarding explored motifs. In this regard 19 differentially expressed genes of the top 10 explored motifs cross referenced with SILAC proteomics data (DCIS and MCF7 cell lines) to see which of the following transcriptomes are alternatively translated in the proteomics level.

EXAMINING SURVIVAL AND GENE ALTERATION CHANGES

cBioportal.org was used to examine the survival and gene alteration changes in breast cancer patient samples. For non-invasive breast cancer sample data, the set from Razavi et al. (57) was used, and for invasive breast cancer sample data the set from Curtis et al. (58) was used.

IMMUNOFLUORESCENCE

Cells cultured at pH 6.5 chronically and pH 7.4 of with the same passage were rinsed with PBS, fixed in cold Methanol:Acetone (1:1) for 10 min and then blocked with 4% bovine serum albumin in PBS for 1 h. Samples were incubated with primary antibody of S100B and S100A6(1:100) and secondary Alexa-Fluor 488 antirabbit (1:500) antibody) for 1 h in room temperature. Coverslips were mounted using ProLong Gold Antifade Reagent (Life Technologies) and images were captured with a Leica TCS SP5 (Leica) confocal microscope.

IMMUNOHISTOCHEMISTRY

For human tissues, a TMA containing formalin-fixed and paraffin-embedded human breast tissue specimens was constructed in Moffitt Cancer Center histology core. The TMA contains 27 normal breast tissue, 30 DCIS, 48 invasive ductal carcinomas without metastasis, 49 invasive ductal carcinomas with metastasis and 48 lymph node macro-metastases of breast cancer. Cores were selected from viable tumor regions and did not contain necrosis. A 1:400 dilution of anti-LAMP2 (#ab18529, Abcam), anti-S100A6 antibody (Prestige Antibodies Powered by Atlas Antibodies, Sigma-Aldrich) and anti S100 protein were used as primary antibodies. Positive and negative controls were used. Normal placenta was used as a positive control for LAMP2, normal breast was used as a positive control for S100 and normal kidney was used as a positive control for S100A6. For the negative control, an adjacent section of the same tissue was stained without application of primary antibody, and any stain pattern observed was considered as non-specific binding of the secondary.

Immunohistochemical analysis was conducted using digitally scanning slides and scoring by three independent reviewers. The scoring method used by the pathologist reviewer to determine (1) the degree of positivity scored the positivity of each sample ranged from 0 to 3 and were derived from the product of staining intensity ($0–3^+$). A zero score was considered negative, score 1 was weak positive, score 2 was moderate positive, and score 3 was strong positive (2). The percentage of positive tumors stained (on a scale of 0–3).

STATISTICAL ANALYSIS

Statistical analysis and estimation of correlations in this study were performed using GraphPad Prism v.6. Correlation significance calculated by Pearson correlation. The *p*-values reported for survival analysis measured by cox regression hazard ratio and log rank tests. All paired tests were performed by Student's *t*-test.

RESULTS

RNA Sequencing of Acid-Adapted and Non-adapted MCF7 Cells Unravels the EMT Mechanism of Breast Cancer Cells

In order to study the effects of acidosis on EMT of breast cancer cells at early stages such as ductal carcinoma *in situ* (DCIS) we first probed the effect of chronic acid adaptation on EMT status of MCF7 breast cancer cell line using quantitative reverse transcription-polymerase chain reaction (qRT-PCR) (**Figure 1A**) and Immunofluorescent (IF) (**Figure 1B**) techniques. Acid adaptation showed some of the epithelial to mesenchymal phenotypes such as high expression of Vimentin or loss of membrane β-catenin and ZO-1 and didn't show some other's such as loss of E-Cadherins (**Figures 1A,B**). So, we concluded acid adaptation is a path to complete EMT and the status we observed can be explained as partial EMT induced by acid adaptation that can be completed by further adaptation to acid or other microenvironmental conditions (**Figures 1A,B**). The partial EMT is reported in other publications and referred as a measure of plasticity (8, 10). Then we carried out sequencing of RNA on a paired sample of MCF7 cells and its acid-adapted counterpart. MCF7 cells are ER, PR, and HER2 positive with many phenotypes of early neoplastic cells such as slow metabolism, and low rate of glycolysis and Warburg phenotype that makes them a proper model of studying acidosis at early stages of breast cancer (27, 59). They are also tumorigenic but not metastatic i.e., injection of MCF7 into immunodeficient mice will result in tumor growth but not metastasis. For RNA extraction we used acid-adapted and non-adapted MCF7 (parental) at the same passage number with similar growth rate at the time of experiment. We identified 1,928 differentially expressed genes in acid-adapted MCF7 cells compared to non-adapted MCF7 (**Supplementary Table 1**). Using STRING database, a regulatory interaction network based on experimentally validated interactions was plotted. The constructed network was replotted in Cytoscape software for better visualization (**Supplementary Figure 2**). Then we searched for EMT related markers in the RNA sequencing data and found that acid adapted cells show some of epithelial markers and some of the mesenchymal markers validating the partial EMT statues of acid adapted cells (**Figure 1C**).

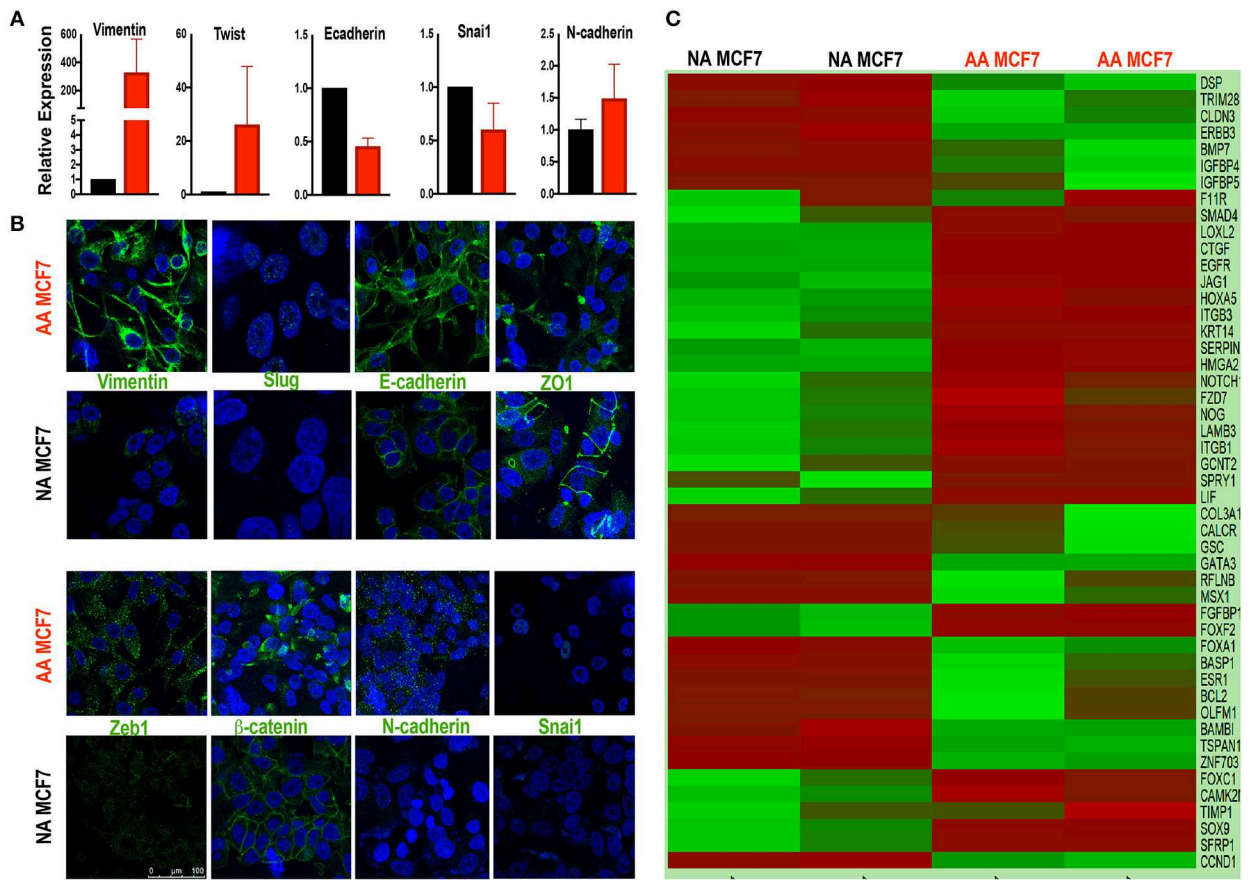

FIGURE 1 | Acid adapted cells show partial EMT phenotype. **(A)** q-RT-PCR-analysis and **(B)** IF of EMT marker at RNA and protein level respectively show both markers of epithelial and mesenchymal phenotype are present in acid adapted cells confirming their transient EMT phenotype. **(C)** Analysis of RNA sequencing shows a mixed epithelial and mesenchymal markers. Heatmap plot for EMT related deferentially expressed genes in AA-MCF7 compared to MCF7. Each row represents a gene and each columns stands for a sample. Cells color is correlated to gene count in the corresponding sample. Color code for gene count: red, high expression; green, low expression.

Gene Regulatory Network

To obtain an interaction network, an effort to unravel the regulatory core related to EMT under the influence of acidosis was made through identifying and ranking 3-node and 3-edge motifs (**Figure 2A**). To this end, $n = 3{,}320$ three member motifs were identified in the network using Cytoscape NetMatchStar plugin. In order to take the significance of motifs in cellular EMT into account, GOBO terms related to EMT were explored. Then for motif ranking scheme a factor was considered for each motif based on the membership of its genes in these terms. In order to place more emphasis on EMT Cytoscape GPEC plugin was used for gene prioritization based on explored GOBP terms. It works based on a random walk with restart algorithm. GPEC helps to rank genes based on their association with specific diseases or biological pathways (EMT in our case) The obtained scores were considered as another weight in scoring function (60). The log fold change, node degree and betweenness centrality were used in the scoring function as well. Using these factors in the scoring function the explored motifs were prioritized and ranked. The top 10 ranking motifs (**Figure 2B**) were selected for enrichment analysis toward EMT and acid adaptation. These motifs consist of 19 unique genes. Merging of these top ranked motifs leads to construct the underlying core subnetwork of the genes that were affected by acidosis and are related to EMT, differentiation and invasion of the tumor cells (**Figure 2C**).

Integrative Analysis of Transcriptomics and Proteomics of Acid-Adapted and Non-adapted MCF7 Cells Reveals the Role of S100 Proteins in Acid-Induced Epithelial to Mesenchymal Transition

For further validation of our findings in RNA sequencing and EMT related motif analysis at the protein level, we compared all the genes in the EMT motifs with their relative protein change in our SILAC discovery proteomics of the MCF7 cell line published previously (27) as well as the MCF-DCIS (DCIS) cell line which we conducted SILAC proteomics on for this

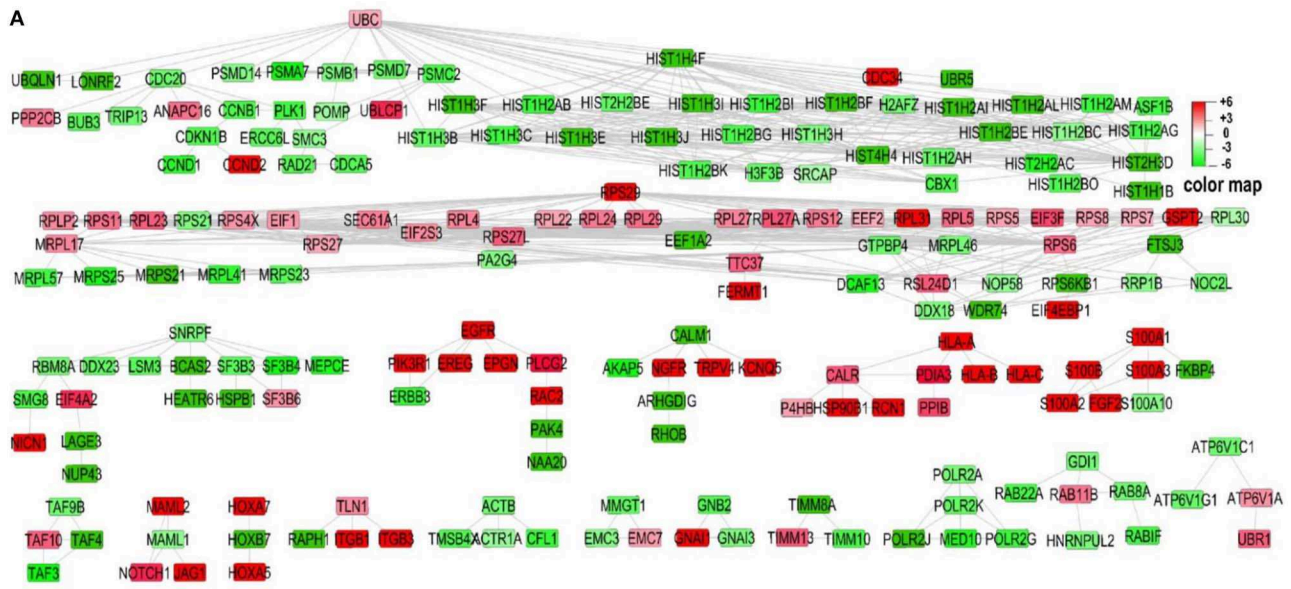

B

	Gene1	Gene2	Gene3
Motif1	PIK3R1	EGFR	ERBB3
Motif2	S100B	S100A1	S100A2
Motif3	S100A1	S100A2	S100A3
Motif4	CALR	HSP90B1	RCN1
Motif5	MAML1	NOTCH1	MAML2
Motif6	CALR	PDIA3	HLA-A
Motif7	CALR	HSP90B1	P4HB
Motif8	HSP90B1	P4HB	RCN1
Motif9	RPS6	RPS29	GSPT2
Motif10	CALR	P4HB	RCN1

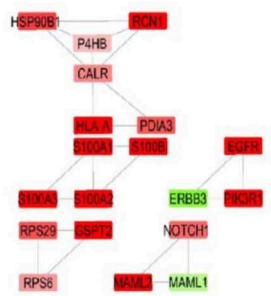

FIGURE 2 | RNA sequencing motif analysis unravels EMT related genes involved in acid adaptation. **(A)** Experimentally validated gene regulatory networks of differentially expressed genes. For better visualization Y files layout algorithm of cytoscape was used to organize the network. Two node interactions and disconnected nodes were ommited. **(B)** Top ten ranked motifs of our network, directed toward EMT. **(C)** Top 10 explored motifs based on ranking analysis were merged together. The association of some of genes like P4HB and CALR in multiple motifs which present in top 10 motifs leads to construct a small sub-network by merging of these motifs which leads to construct core regulatory subnetwork.

study. Since the focus of this study is on early adaption of breast cancer cells we selected DCIS cell lines and adapted them to acid for 3–6 months in the same process as the MCF7 cells. The SILAC proteomics approach was applied to compare the whole proteome of acid-adapted cancer cells to non-adapted counterparts. SILAC or stable isotope-labeled amino acids in cell culture is a quantitative mass spectrometry (MS) based technique that is used to compare the proteome of pairs of biological samples (61) which in our case is acid-adapted and acid-naive breast cancer cell lines. To minimize the rate of false-positive biomarker association, parallel SILAC experiments were conducted for each cell lines in which the acid-adapted or non-adapted cells were labeled by growing them in SILAC "heavy" media ($^{13}C_6$ lysine and $^{13}C_6^{14}N_4$ arginine), while the comparator cells (acid-naive or acid-adapted cells, respectively) were cultured in media containing the corresponding amino acids of naturally occurring isotopic distribution. The labeling strategy was reversed (flipped) to eliminate potential bias due to the media and incorporation of the stable isotope-labeled amino acids (**Figure 3A**) (62). MCF7 data was previously published for biomarker discovery of acid adaptation (27). In DCIS SILAC proteomics, 2,841 proteins were detected with 466 unique proteins for acid-adapted DCIS cells and 323 unique proteins for non-adapted ones (**Figures 3B,C** and **Supplementary Figure 3**). We used fold change to plot our data and used 1.5-fold change cut off (**Figure 3C**). The same analysis and cut off was applied for both DCIS and MCF7 cells. To do integrative analysis, we looked for any proteins related to the five explored motif packs isolated from RNA sequencing data (**Figure 2C**) in both MCF7 and DCIS proteomics with more than 1.5 ratio change in acid-adapted vs. non-adapted condition (**Figure 3C**). In order to perform integrative proteomics and transcriptomics data analysis we focused on 10 explored motifs based on motif ranking analysis (**Figure 2C**). This analysis has been conducted to ensure consistency of proteomics and transcriptomics data. Translational pattern of 19 differentially expressed genes were assessed in MCF7 and DCIS proteomics data. We plotted the interactome map for these altered proteins that were identified through integration of transcriptome and proteome data (**Figure 3D**). In this figure nodes in rectangular shape have both gene expression and protein translation alteration and oval nodes only present alterations in transcriptomics level. Ten proteins out of 19 discovered genes had more than 1.5-fold change in MCF7 and DCIS proteomics data (**Figure 3E**). Among these genes the ones presented in **Figure 3F** are differentially expressed at the proteomics level in the DCIS and MCF7 cell lines (**Figure 3F**). Due to abundancy of the S100 family proteins in both transcriptomics and proteomics data, this motif pack was chosen for further experimental validation.

Acid-Adapted MCF7 Cells Express Higher S100A6 and S100B Proteins

To further validate the S100 motif discovered in both RNA sequencing and proteomics data in acid-adapted EMT analysis, we performed Immunocytochemistry (ICC) experiments on our acid-adapted and non-adapted MCF7 cells. We chose S100A6 and S100B from the family because of over expression of S100A6 at the protein level in both MCF7 and DCIS cells and S100B as one marker discovered in RNA sequencing of MCF7 cells and the proteomics of DCIS. To do the experiment, both AA MCF7 and NA MCF7 were seeded on the one slide with eight chambers on it and were treated with exactly equal amounts of antibodies. Slides were imaged using a Leica TCS SP5 confocal microscope with exact settings for both cells, and samples were imaged the same day. We found higher expression of both S100B and S1006 in acid-adapted MCF7 cells (**Figures 4A,B**). To confirm the acid adaptation status of our cells, we also stained the acid-adapted MCF7 cells and the non-adapted MCF7 cells with the known marker of acid adaptation, LAMP2b. We observed membrane localization of LAMP2b in our acid-adapted MCF7 cells (**Figure 4C**), which is characteristic of acid-adapted cell populations.

S100A6 Expression Correlates With Survival in Breast Cancer Patients

We then sought to clinically validate our identified S100 proteins expression in breast cancer patient Tissue Micro Arrays (TMA) that we have available at the Moffitt Cancer Center tissue core bank. On the basis of our previous findings, we hypothesized that an acidity biomarker should have two characteristics. First, due to the increase in glycolytic rate with breast cancer progression, there should be an association of progression with marker of acidity and second, the expression of the proteins should correlate somehow with the expression pattern of LAMP2b as it is a known marker of acidosis (27, 34). In short, S100A6 and S100B proteins should increase with stage similar to LAMP2b. To test this, we analyzed protein expression of S100A6 and S100B via IHC of TMAs containing patient sample biopsies from different stages of breast cancer totaling 160 cores. While the protein expression of S100A6 showed statistically ($P < 0.0001$) higher in tumor samples compared with adjacent normal breast there was no difference for S100B. The negative results of S100B could be the cause of problems with antigen specificity or epitopes that were used. We then continued our analysis with S100A6 by measuring the positivity of each core in different stages of breast cancer. Increased S100A6 expression correlates with increased tumor progression from DCIS to invasive ductal carcinoma (**Figure 5A**). There were notably significant differences between normal breast and DCIS, Invasive Ductal Carcinomas (IDCs), and IDCs with local metastases indicating the role of this protein in cancer progression and invasiveness. We then compared the survival of patients with high and low expression of S100A6 for each biopsy cores in three categories of DCIS, IDC and IDC with local metastasis. For defining high vs. low expression, we use the median of all the cores in each category as middle point and anything below the media was taken as low and vice versa. The data was analyzed using two testing methods: Mantel-Cox and Gehan-Greslow-Willcoxon. The DCIS category showed significant difference between low and high expression (**Figure 5B**), which confirms our previous studies of DCIS as the most acidic tumors in breast cancer. The difference wasn't significant for survival of patients with breast cancer at IDC,

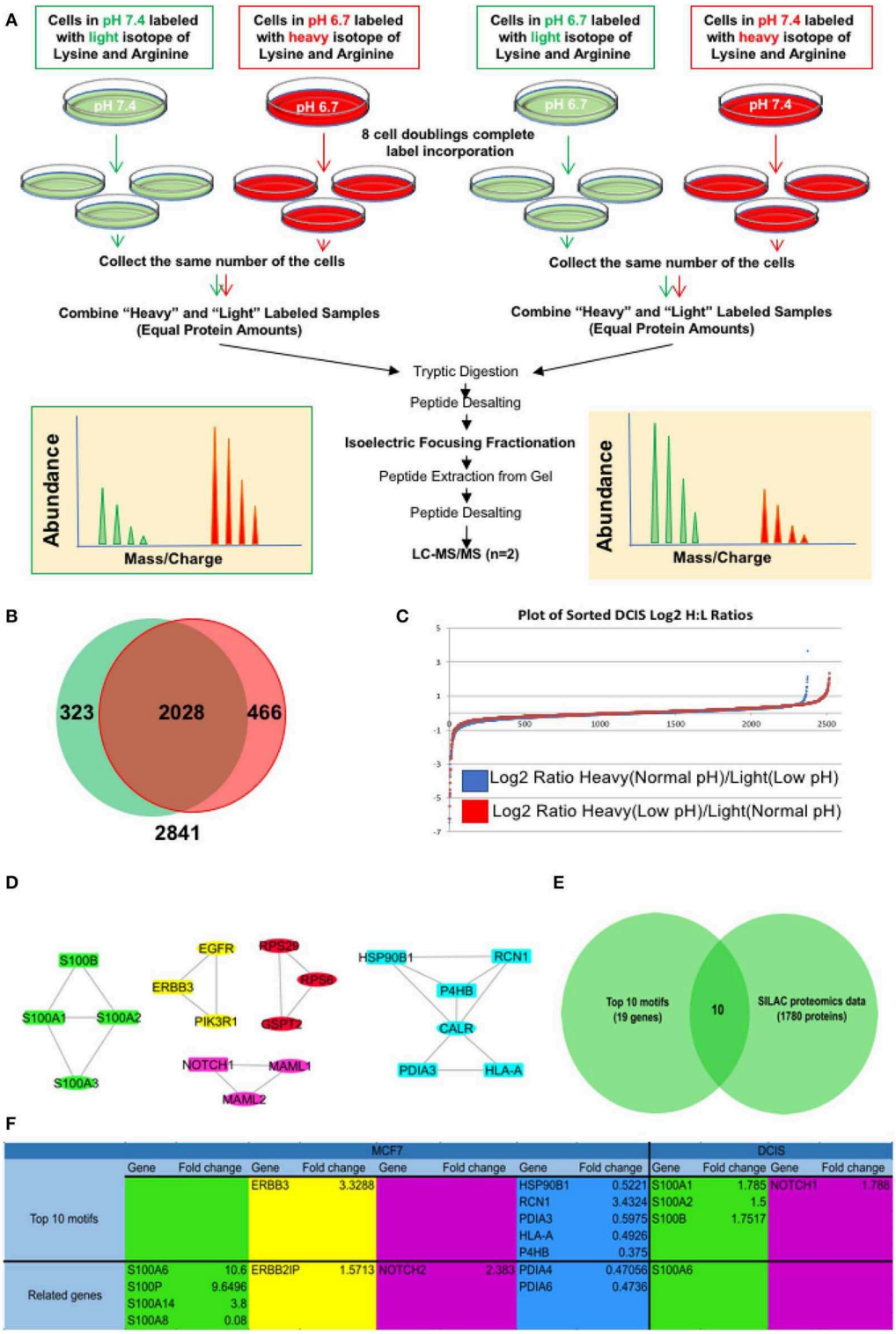

F

	MCF7								DCIS			
	Gene	Fold change	Gene	Fold change	Gene	Fold change	Gene	Fold change	Gene	Fold change	Gene	Fold change
Top 10 motifs			ERBB3	3.3288			HSP90B1	0.5221	S100A1	1.785	NOTCH1	1.768
							RCN1	3.4324	S100A2	1.5		
							PDIA3	0.5975	S100B	1.7517		
							HLA-A	0.4926				
							P4HB	0.375				
Related genes	S100A6	10.6	ERBB2IP	1.5713	NOTCH2	2.383	PDIA4	0.47056	S100A6			
	S100P	9.6496					PDIA6	0.4736				
	S100A14	3.8										
	S100A8	0.08										

FIGURE 3 | Integrative analysis of proteomics and transcriptomics data to discover the acidic microenvironment induced EMT genes. **(A)** A schematic of our SILAC proteomics design. We flipped the labeling to make sure the changes in protein expression is not affected by the type of labels. **(B)** Venn diagram and **(C)** Log 2 fold change of SILAC proteomics data discovered in each flipping experiment. **(D)** Integrated interaction map of the regulatory subnetwork and their related altered proteins in both DCIS and MCF7 cell lines. **(E)** Venn diagram indicating that among $n = 45$ transcripts (The subnetwork and it's near interactions) $n = 12$ proteins were differentially translated with the abundancy of S100 family. **(F)** The name of proteins that are discovered in DCIS and MCF7 proteomics and are correlated to the motif's from RNA sequencing data.

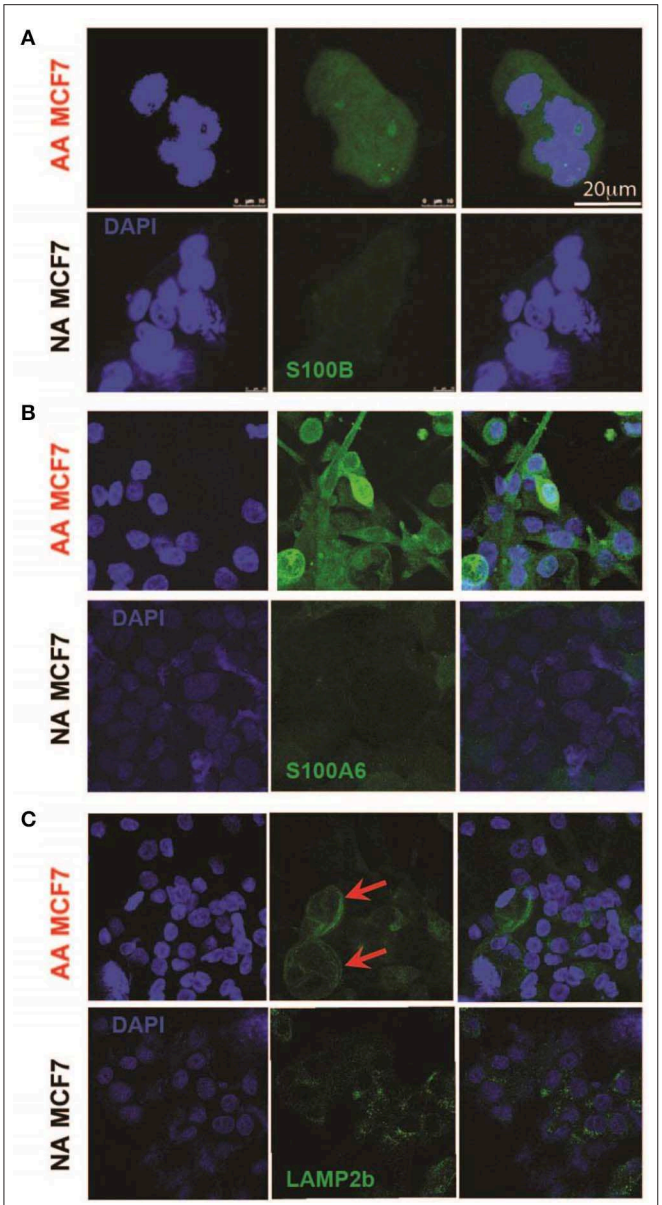

FIGURE 4 | Validation of higher expression of acid-induced EMT markers by Immunocytochemistry. **(A)** S100B protein expression in acid-adapted and non-adapted MCF7 cells with the analysis on right. S100B expression is significantly higher in acid adapted cells. **(B)** S100A6 ICC of acid-adapted and non-adapted MCF7 cancer cells shows higher expression of S100A6 in AA MCF7 cells. **(C)** LAMP2b ICC of acid-adapted and WT MCF7 cancer cells. Acid-adapted MCF7 cells display membrane localization of LAMP2b, compared to cytoplasmic localization in non-adapted MCF7 cells.

and IDC with local invasion stages, implying the importance of acidosis and acid related phenotype at early stages of cancer again (**Supplementary Figure 4**).

To further prove the correlation of S100A6 and acidosis we compared the positivity of LAMP2b as a marker of acidosis and S100A6 as our candidate, for each biopsy core in our TMA. Comparative analysis of S100A6 positivity from each biopsy core to LAMP2b expression of the same core showed a correlation between these two proteins (**Figures 5C,D**) validating the role of S100A6 in acid adaptation.

DISCUSSION

Deregulated energetics is a hallmark of cancer progression, and the deregulation of cellular energetics has a profound effect on the growth and progression of a tumor. The creation of an acidic tumor microenvironment (TME) is one of these major consequences of deregulated cancer cell energetics. When faced with the acidic TME the cancer cell population must either adapt or perish, with the former being the usual outcome due to the extraordinary ability of cancerous cell populations to adapt to a changing environment. This adaptation to an acidic TME is not a passive action and leads to permanent changes in the phenotype of the surviving population. Little is known about the phenotypic changes that occur throughout the arduous task of adapting to the acidic TME, and deeper insight into these changes will move us a step in the direction of targeting these aggressive populations therapeutically.

Although the concept of lower pH in the tumor microenvironment is not a new discovery, the specific studying of acid-adapted cancer cell phenotypic switch is a relatively new realm of science. Previous investigations have found numerous phenotypic changes that occur during cancer cell populations adapting to an acidic environment such as, chronic autophagy (63), increased presence of lysosomal proteins in the plasma membrane (27), and heightened aggressiveness (34). Acidity in the intratumoral environment, not associated with acid adaptation, has also been shown to foster the stemness of cancer cell populations in osteosarcoma (64).

The aim of this study was to understand the role of acidic microenvironment in the EMT phenotypic switch, a demonstration of cancer plasticity and heterogeneity of cancer cell populations, and study their role in patient survival. We used a unique approach to identify vital regulatory sub-networks that are involved in the acid adaptation of cancer cell populations using integrative analysis of transcriptomic and proteomic data of selected cancer cells under an acid microenvironment that mimics one of the harsh selection pressures amongst many in solid breast tumors. The advantage of our approach is that our network analysis workflow encompasses different layers of information such as log fold change in cells, involvement of genes in partial and complete EMT processes and network centrality parameters which reflects gene regulatory role in the whole network. These considerations led to isolation of the motifs that have a critical role in cancer cells' acid adaptation and pEMT. The discovered motifs also have significant regulatory function throughout the network from a structural perspective. Network centrality parameters were considered as a unique factor to weighting nodes. Log fold changes of motif genes were another parameter to rank motifs. Therefore, we have four parameters to rank the motifs: direct association of motif in EMT, motif prioritization score which is based on Cytoscape GPEC plugin and reflect indirect association of motif in EMT, centrality of the

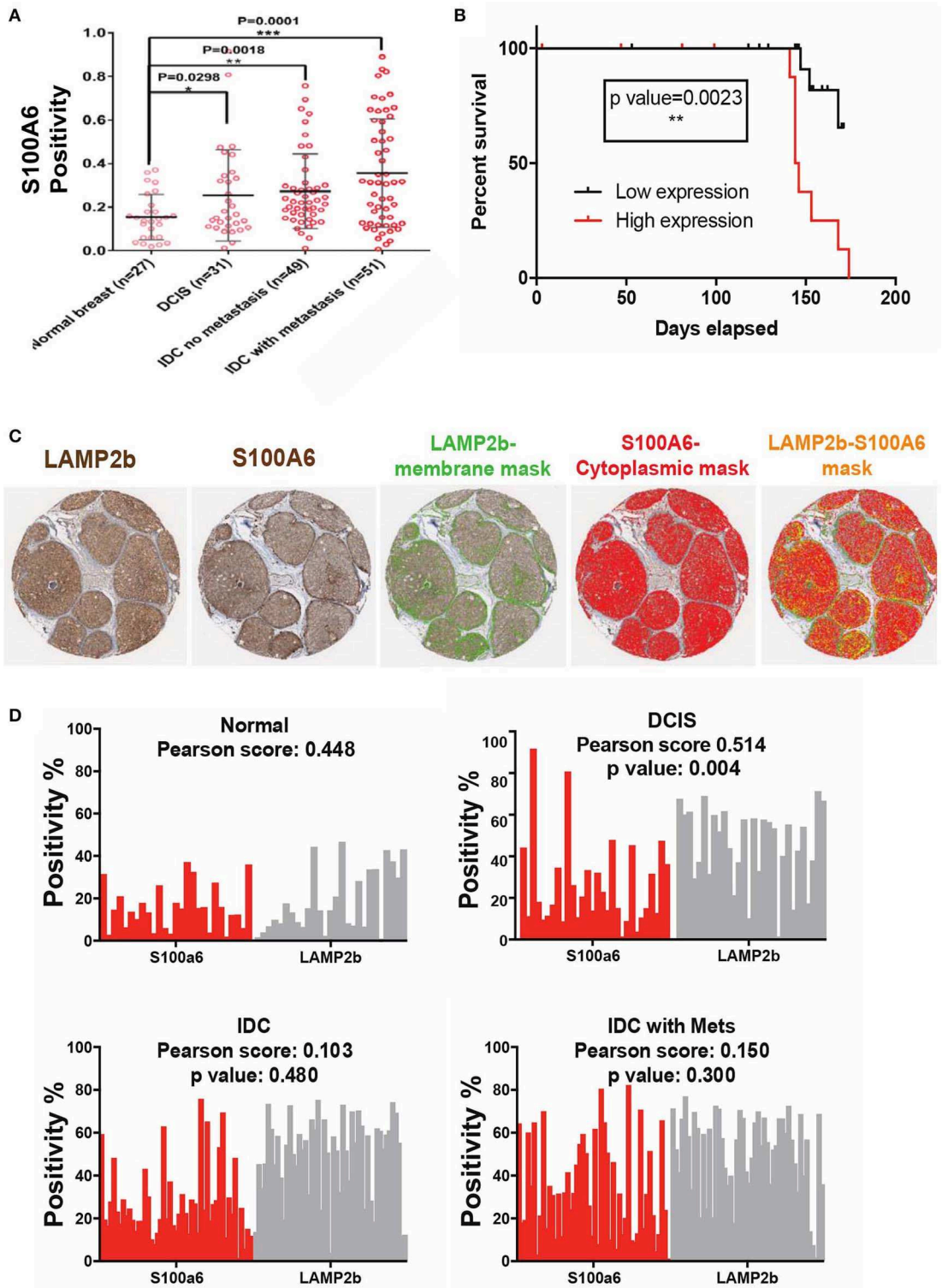

FIGURE 5 | Clinical validation of S100A6 expression correlation to acid phenotype in breast cancer. **(A)** TMA analysis of 160 biopsy cores stained with S100A6 antibody showed increased expression of this protein from normal to DCIS, IDC, and IDC with Mets. Data are shown as mean with standard deviation as error bar. **(B)** Kaplan-Meier graph comparing DCIS patient's survival with low expression of S100A6 (Below the average) to patients with high S100A6 expression. Patients with high expression survived less than patients with low expression. **(C)** Representative images of core biopsies stained for both LAMP2b and S100A6 on sequential cuts. **(D)** Correlation analysis of LAMP2b and S100A6 in different stages of breast cancer.

gene within the network, and expression behavior of motif in acidosis. When taken in total, these four parameters return the important motifs within the system.

Here in, we demonstrated the correlation of cancer cells acid adaptation, EMT and its driven heterogeneity with patient's survival. Our findings demonstrated a partial EMT phenotype in our acid-adapted cellular populations by correlation to EMT markers accepted in the field. This partial transition may represent a heightened degree of plasticity or metastatic ability, with cells carrying phenotypic characteristics of both epithelial and mesenchymal cells. We observed downregulation of Snai1 in the acid-adapted group, which negatively correlates with E-cadherin expression, and is not typical of a traditional EMT switch. While this was not typical of the EMT response, we did observe EMT characteristics with heightened vimentin and N-cadherin expression. Due to the observed changes in EMT markers caused by acid adaptation, we believe the acid adaptation may target specific pathways in the EMT process, while neglecting others. We also proposed one of the possible mechanisms of acid-induced EMT phenotypic alteration through S100 family proteins, specifically S100A6 and S100B proteins. These findings can be used for therapeutic advances targeting EMT and heterogeneity of breast tumors while also providing a better understanding of the mechanism behind microenvironment induced phenotypic changes toward EMT, and the role EMT plays in acid-induced cancer progression and evolution.

DATA AVAILABILITY STATEMENT

The datasets generated for this study can be found in the NCBI Gene Expression Omnibus (GSE145383).

ETHICS STATEMENT

All the patient data for breast TMA4 used in this study were deidentified by Moffitt Cancer Center and consent was obtained from the participants at the source. The authors of this manuscript had no access to patient information in any course of this study.

AUTHOR CONTRIBUTIONS

MD designed and accomplished the experiment and wrote the manuscript. MS and IR analyzed the data. BO, PB, BF, and CZ did the experiments. JJ analyzed the images. JK and SY supervised the proteomics and transcriptome analysis.

FUNDING

This work was supported by two grants from NCI: U54CA193489, Cancer as a Complex Adaptive System and R01CA077575, Causes & Consequences of Acid pH in Tumors.

ACKNOWLEDGMENTS

We thank Samantha Byrne for technical assistance.

SUPPLEMENTARY MATERIAL

The Supplementary Material for this article can be found online at: https://www.frontiersin.org/articles/10.3389/fonc.2020.00304/full#supplementary-material

REFERENCES

1. Gouirand V, Guillaumond F, Vasseur S. Influence of the tumor microenvironment on cancer cells metabolic reprogramming. *Front Oncol*. (2018) 8:117. doi: 10.3389/fonc.2018.00117
2. Gravenmier CA, Siddique M, Gatenby RA. Adaptation to stochastic temporal variations in intratumoral blood flow: the Warburg effect as a bet hedging strategy. *Bull Math Biol*. (2018) 80:954–70. doi: 10.1007/s11538-017-0261-x
3. Epstein T, Gatenby RA, Brown JS. The Warburg effect as an adaptation of cancer cells to rapid fluctuations in energy demand. *PLoS ONE*. (2017) 12:e0185085. doi: 10.1371/journal.pone.0185085
4. Brooks AN, Turkarslan S, Beer KD, Lo FY, Baliga NS. Adaptation of cells to new environments. *Wiley Interdiscip Rev Syst Biol Med*. (2011) 3:544–61. doi: 10.1002/wsbm.136
5. Marjanovic ND, Weinberg RA, Chaffer CL. Cell plasticity and heterogeneity in cancer. *Clin Chem*. (2013) 59:168–79. doi: 10.1373/clinchem.2012.184655
6. Cabrera MC, Hollingsworth RE, Hurt EM. Cancer stem cell plasticity and tumor hierarchy. *World J Stem Cells*. (2015) 7:27–36. doi: 10.4252/wjsc.v7.i1.27
7. Karacosta LG, Anchang B, Ignatiadis N, Kimmey SC, Benson JA, Shrager JB, et al. Mapping lung cancer epithelial-mesenchymal transition states and trajectories with single-cell resolution. *Nat Commun*. (2019) 10:5587. doi: 10.1038/s41467-019-13441-6
8. Lovisa S, Zeisberg M, Kalluri R. Partial epithelial-to-mesenchymal transition and other new mechanisms of kidney fibrosis. *Trends Endocrinol Metab*. (2016) 27:681–95. doi: 10.1016/j.tem.2016.06.004
9. Aiello NM, Maddipati R, Norgard RJ, Balli D, Li J, Yuan S, et al. EMT subtype influences epithelial plasticity and mode of cell migration. *Dev Cell*. (2018) 45:681–95.e4. doi: 10.1016/j.devcel.2018.05.027
10. Jolly MK, Somarelli JA, Sheth M, Biddle A, Tripathi SC, Armstrong AJ, et al. Hybrid epithelial/mesenchymal phenotypes promote metastasis and therapy resistance across carcinomas. *Pharmacol Ther*. (2019) 194:161–84. doi: 10.1016/j.pharmthera.2018.09.007
11. Dirkse A, Golebiewska A, Buder T, Nazarov PV, Muller A, Poovathingal S, et al. Stem cell-associated heterogeneity in Glioblastoma results from intrinsic tumor plasticity shaped by the microenvironment. *Nat Commun*. (2019) 10:1787. doi: 10.1038/s41467-019-09853-z
12. Gupta PB, Pastushenko I, Skibinski A, Blanpain C, Kuperwasser C. Phenotypic plasticity: driver of cancer initiation, progression, and therapy resistance. *Cell Stem Cell*. (2019) 24:65–78. doi: 10.1016/j.stem.2018.11.011
13. Enderling H. Cancer stem cells: small subpopulation or evolving fraction? *Integr Biol*. (2015) 7:14–23. doi: 10.1039/C4IB00191E
14. Tan EJ, Olsson AK, Moustakas A. Reprogramming during epithelial to mesenchymal transition under the control of TGFbeta. *Cell Adh Migr*. (2015) 9:233–46. doi: 10.4161/19336918.2014.983794
15. Valcourt U, Carthy J, Okita Y, Alcaraz L, Kato M, Thuault S, et al. Analysis of epithelial-mesenchymal transition induced by transforming growth factor beta. *Methods Mol Biol*. (2016) 1344:147–81. doi: 10.1007/978-1-4939-2966-5_9
16. Tang C, Liu T, Wang K, Wang X, Xu S, He D, et al. Transcriptional regulation of FoxM1 by HIF1alpha mediates hypoxiainduced EMT in prostate cancer. *Oncol Rep*. (2019) 42:1307–18. doi: 10.3892/or.2019.7248

17. Suzuki A, Maeda T, Baba Y, Shimamura K, Kato Y. Acidic extracellular pH promotes epithelial mesenchymal transition in Lewis lung carcinoma model. *Cancer Cell Int*. (2014) 14:129. doi: 10.1186/s12935-014-0129-1
18. Wykoff CC, Beasley NJ, Watson PH, Turner KJ, Pastorek J, Sibtain A, et al. Hypoxia-inducible expression of tumor-associated carbonic anhydrases. *Cancer Res*. (2000) 60:7075–83.
19. Gillies RJ, Gatenby RA, Hypoxia and adaptive landscapes in the evolution of carcinogenesis. *Cancer Metastasis Rev*. (2007) 26:311–7. doi: 10.1007/s10555-007-9065-z
20. Gerlinger M, Rowan AJ, Horswell S, Larkin J, Endesfelder D, Gronroos E, et al. Intratumor heterogeneity and branched evolution revealed by multiregion sequencing. *N Engl J Med*. (2012) 366:883–92. doi: 10.1056/NEJMoa1113205
21. Sottoriva A, Spiteri I, Piccirillo SG, Touloumis A, Collins VP, Marioni JC, et al. Intratumor heterogeneity in human glioblastoma reflects cancer evolutionary dynamics. *Proc Natl Acad Sci USA*. (2013) 110:4009–14. doi: 10.1073/pnas.1219747110
22. Baird RD, Caldas C. Genetic heterogeneity in breast cancer: the road to personalized medicine? *BMC Med*. (2013) 11:151. doi: 10.1186/1741-7015-11-151
23. Yachida S, Iacobuzio-Donahue CA. Evolution and dynamics of pancreatic cancer progression. *Oncogene*. (2013) 32:5253–60. doi: 10.1038/onc.2013.29
24. Ibrahim-Hashim A, Robertson-Tessi M, Enriquez-Navas PM, Damaghi M, Balagurunathan Y, Wojtkowiak JW, et al. Defining cancer subpopulations by adaptive strategies rather than molecular properties provides novel insights into intratumoral evolution. *Cancer Res*. (2017) 77:2242–54. doi: 10.1158/0008-5472.CAN-16-2844
25. Ercan D, Zejnullahu K, Yonesaka K, Xiao Y, Capelletti M, Rogers A, et al. Amplification of EGFR T790M causes resistance to an irreversible EGFR inhibitor. *Oncogene*. (2010) 29:2346–56. doi: 10.1038/onc.2009.526
26. Gatenby RA, Gillies RJ. A microenvironmental model of carcinogenesis. *Nat Rev Cancer*. (2008) 8:56–61. doi: 10.1038/nrc2255
27. Damaghi M, Tafreshi NK, Lloyd MC, Sprung R, Estrella V, Wojtkowiak JW, et al. Chronic acidosis in the tumour microenvironment selects for overexpression of LAMP2 in the plasma membrane. *Nat Commun*. (2015) 6:8752. doi: 10.1038/ncomms9752
28. Damaghi M, Wojtkowiak JW, Gillies RJ. pH sensing and regulation in cancer. *Front Physiol*. (2013) 4:370. doi: 10.3389/fphys.2013.00370
29. Gillies RJ, Robey I, Gatenby RA. Causes and consequences of increased glucose metabolism of cancers. *J Nucl Med*. (2008) 49 (Suppl. 2):4S−42S. doi: 10.2967/jnumed.107.047258
30. Estrella V, Chen T, Lloyd M, Wojtkowiak J, Cornnell HH, Ibrahim-Hashim A, et al. Acidity generated by the tumor microenvironment drives local invasion. *Cancer Res*. (2013) 73:1524–35. doi: 10.1158/0008-5472.CAN-12-2796
31. Xu L, Fukumura D, Jain RK. Acidic extracellular pH induces vascular endothelial growth factor (VEGF) in human glioblastoma cells via ERK1/2 MAPK signaling pathway: mechanism of low pH-induced VEGF. *J Biol Chem*. (2002) 277:11368–74. doi: 10.1074/jbc.M108347200
32. Lardner A. The effects of extracellular pH on immune function. *J Leukoc Biol*. (2001) 69:522–30.
33. Pilon-Thomas S, Kodumudi KN, El-Kenawi AE, Russell S, Weber AM, Luddy K, et al. Neutralization of tumor acidity improves antitumor responses to immunotherapeutic interventions. *Cancer Res*. (2015) 76:1381–90. doi: 10.1158/0008-5472.CAN-15-1743
34. Damaghi M, Gillies R. Phenotypic changes of acid adapted cancer cells push them toward aggressiveness in their evolution in the tumor microenvironment. *Cell Cycle*. (2016) 16:1739–43. doi: 10.1080/15384101.2016.1231284
35. Kelley DZ, Flam EL, Izumchenko E, Danilova LV, Wulf HA, Guo T, et al. Integrated analysis of whole-genome ChIP-Seq and RNA-Seq data of primary head and neck tumor samples associates HPV integration sites with open chromatin marks. *Cancer Res*. (2017) 77:6538–50. doi: 10.1158/0008-5472.CAN-17-0833
36. Wang J, Zuo Y, Man YG, Avital I, Stojadinovic A, Liu M, et al. Pathway and network approaches for identification of cancer signature markers from omics data. *J Cancer*. (2015) 6:54–65. doi: 10.7150/jca.10631
37. Wolchok JD, Kluger H, Callahan MK, Postow MA, Rizvi NA, Lesokhin AM, et al. Nivolumab plus ipilimumab in advanced melanoma. *N Engl J Med*. (2013) 369:122–33. doi: 10.1056/NEJMoa1302369
38. Wang Z, Gerstein M, Snyder M. RNA-seq: a revolutionary tool for transcriptomics. *Nat Rev Genet*. (2009) 10:57–63. doi: 10.1038/nrg2484
39. Kreeger PK, Lauffenburger DA. Cancer systems biology: a network modeling perspective. *Carcinogenesis*. (2009) 31:2–8. doi: 10.1093/carcin/bgp261
40. Patt A, Siddiqui J, Zhang B, Mathe E. Integration of metabolomics and transcriptomics to identify gene-metabolite relationships specific to phenotype. *Methods Mol Biol*. (2019) 1928:441–68. doi: 10.1007/978-1-4939-9027-6_23
41. Schmitz L, McCotter S, Kretschmer M, Kronstad JW, Heimel K. Transcripts and tumors: regulatory and metabolic programming during biotrophic phytopathogenesis. *F1000Research*. (2018) 7:F1000. doi: 10.12688/f1000research.16404.1
42. Sadeghi M, Ranjbar B, Ganjalikhany MR, Khan FM, Schmitz U, Wolkenhauer O, et al. MicroRNA and transcription factor gene regulatory network analysis reveals key regulatory elements associated with prostate cancer progression. *PLoS ONE*. (2016) 11:e0168760. doi: 10.1371/journal.pone.0168760
43. Guo NL, Wan YW. Network-based identification of biomarkers coexpressed with multiple pathways. *Cancer Inform*. (2014) 13 (Suppl. 5):37–47. doi: 10.4137/CIN.S14054
44. Armour CD, Castle JC, Chen R, Babak T, Loerch P, Jackson S, et al. Digital transcriptome profiling using selective hexamer priming for cDNA synthesis. *Nat Methods*. (2009) 6:647–9. doi: 10.1038/nmeth.1360
45. Bolger AM, Lohse M, Usadel B. Trimmomatic: a flexible trimmer for Illumina sequence data. *Bioinformatics*. (2014) 30:2114–20. doi: 10.1093/bioinformatics/btu170
46. Kim D, Langmead B, Salzberg SL. HISAT: a fast spliced aligner with low memory requirements. *Nat Methods*. (2015) 12:357. doi: 10.1038/nmeth.3317
47. Anders S, Pyl PT, Huber W. HTSeq–a Python framework to work with high-throughput sequencing data. *Bioinformatics*. (2015) 31:166–9. doi: 10.1093/bioinformatics/btu638
48. Team RC. A language and environment for statistical computing. *Computing*. (2006) 83:3097–107. doi: 10.1890/0012-9658(2002)083[3097:CFHIWS]2.0.CO;2
49. Love MI, Huber W, Anders S. Moderated estimation of fold change and dispersion for RNA-seq data with DESeq2. *Genome Biol*. (2014) 15:550. doi: 10.1186/s13059-014-0550-8
50. von Mering C, Huynen M, Jaeggi D, Schmidt S, Bork P, Snel B. STRING: a database of predicted functional associations between proteins. *Nucleic Acids Res*. (2003) 31:258–61.
51. Alon U. Network motifs: theory and experimental approaches. *Nat Rev Genet*. (2007) 8:450. doi: 10.1038/nrg2102
52. Shannon P, Markiel A, Ozier O, Baliga NS, Wang JT, Ramage D, et al. Cytoscape: a software environment for integrated models of biomolecular interaction networks. *Genome Res*. (2003) 13:2498–504.
53. Rinnone F, Micale G, Bonnici V, Bader GD, Shasha D, Ferro A, et al. NetMatchStar: an enhanced Cytoscape network querying app. *F1000Research*. (2015) 4:479. doi: 10.12688/f1000research.6656.1
54. Le D-H, Pham V-H. HGPEC: a Cytoscape app for prediction of novel disease-gene and disease-disease associations and evidence collection based on a random walk on heterogeneous network. *BMC Syst Biol*. (2017) 11:61. doi: 10.1186/s12918-017-0437-x
55. Assenov Y, Ramirez F, Schelhorn SE, Lengauer T, Albrecht M. Computing topological parameters of biological networks. *Bioinformatics*. (2008) 24:282–4.
56. Khan FM, Marquardt S, Gupta SK, Knoll S, Schmitz U, Spitschak A, et al. Unraveling a tumor type-specific regulatory core underlying E2F1-mediated epithelial-mesenchymal transition to predict receptor protein signatures. *Nat Commun*. (2017) 8:198. doi: 10.1038/s41467-017-00268-2
57. Razavi P, Chang MT, Xu G, Bandlamudi C, Ross DS, Vasan N, et al. The genomic landscape of endocrine-resistant advanced breast cancers. *Cancer Cell*. (2018) 34:427–38.e6. doi: 10.1016/j.ccell.2018.08.008
58. Curtis C, Shah SP, Chin SF, Turashvili G, Rueda OM, Dunning MJ, et al. The genomic and transcriptomic architecture of 2,000 breast tumours reveals novel subgroups. *Nature*. (2012) 486:346–52. doi: 10.1038/nature10983
59. Persi E, Duran-Frigola M, Damaghi M, Roush WR, Aloy P, Cleveland JL, et al. Systems analysis of intracellular pH vulnerabilities for cancer therapy. *Nat Commun*. (2018) 9:2997. doi: 10.1038/s41467-018-05261-x

60. Le D-H, Kwon Y-K. GPEC: A Cytoscape plug-in for random walk-based gene prioritization and biomedical evidence collection. *Comput Biol Cem*. (2012) 37:1–23. doi: 10.1016/j.compbiolchem.2012.02.004
61. Geiger T, Wisniewski JR, Cox J, Zanivan S, Kruger M, Ishihama Y, et al. Use of stable isotope labeling by amino acids in cell culture as a spike-in standard in quantitative proteomics. *Nat Protoc*. (2011) 6:147–57. doi: 10.1038/nprot.2010.192
62. Cox J, Matic I, Hilger M, Nagaraj N, Selbach M, Olsen JV, et al. A practical guide to the MaxQuant computational platform for SILAC-based quantitative proteomics. *Nat Protoc*. (2009) 4:698–705. doi: 10.1038/nprot.2009.36
63. Wojtkowiak JW, Rothberg JM, Kumar V, Schramm KJ, Haller E, Proemsey JB, et al. Chronic autophagy is a cellular adaptation to tumor acidic pH microenvironments. *Cancer Res*. (2012) 72:3938–47. doi: 10.1158/0008-5472.CAN-11-3881
64. Avnet S, Di Pompo G, Chano T, Errani C, Ibrahim-Hashim A, Gillies RJ, et al. Cancer-associated mesenchymal stroma fosters the stemness of osteosarcoma cells in response to intratumoral acidosis via NF-kappaB activation. *Int J Cancer*. (2017) 140:1331–45. doi: 10.1002/ijc.30540

Conflict of Interest: The authors declare that the research was conducted in the absence of any commercial or financial relationships that could be construed as a potential conflict of interest.

Copyright © 2020 Sadeghi, Ordway, Rafiei, Borad, Fang, Koomen, Zhang, Yoder, Johnson and Damaghi. This is an open-access article distributed under the terms of the Creative Commons Attribution License (CC BY). The use, distribution or reproduction in other forums is permitted, provided the original author(s) and the copyright owner(s) are credited and that the original publication in this journal is cited, in accordance with accepted academic practice. No use, distribution or reproduction is permitted which does not comply with these terms.

frontiers in Molecular Biosciences

MINI REVIEW
published: 19 March 2020
doi: 10.3389/fmolb.2020.00036

ZEB1: A Critical Regulator of Cell Plasticity, DNA Damage Response, and Therapy Resistance

Stanislav Drápela[1,2,3], *Jan Bouchal*[4], *Mohit Kumar Jolly*[5], *Zoran Culig*[2,6] *and Karel Souček*[1,2,3]*

[1] Department of Cytokinetics, Institute of Biophysics of the Czech Academy of Sciences, Brno, Czechia, [2] International Clinical Research Center, Center for Biomolecular and Cellular Engineering, St. Anne's University Hospital in Brno, Brno, Czechia, [3] Department of Experimental Biology, Faculty of Science, Masaryk University, Brno, Czechia, [4] Department of Clinical and Molecular Pathology, Faculty of Medicine and Dentistry, Institute of Molecular and Translational Medicine, Palacky University, Olomouc, Czechia, [5] Centre for BioSystems Science and Engineering, Indian Institute of Science, Bangalore, India, [6] Department of Urology, Experimental Urology, Innsbruck Medical University, Innsbruck, Austria

The predominant way in which conventional chemotherapy kills rapidly proliferating cancer cells is the induction of DNA damage. However, chemoresistance remains the main obstacle to therapy effectivity. An increasing number of studies suggest that epithelial-to-mesenchymal transition (EMT) represents a critical process affecting the sensitivity of cancer cells to chemotherapy. Zinc finger E-box binding homeobox 1 (ZEB1) is a prime element of a network of transcription factors controlling EMT and has been identified as an important molecule in the regulation of DNA damage, cancer cell differentiation, and metastasis. Recent studies have considered upregulation of ZEB1 as a potential modulator of chemoresistance. It has been hypothesized that cancer cells undergoing EMT acquire unique properties that resemble those of cancer stem cells (CSCs). These stem-like cells manifest enhanced DNA damage response (DDR) and DNA repair capacity, self-renewal, or chemoresistance. In contrast, functional experiments have shown that ZEB1 induces chemoresistance regardless of whether other EMT-related changes occur. ZEB1 has also been identified as an important regulator of DDR by the formation of a ZEB1/p300/PCAF complex and direct interaction with ATM kinase, which has been linked to radioresistance. Moreover, ATM can directly phosphorylate ZEB1 and enhance its stability. Downregulation of ZEB1 has also been shown to reduce the abundance of CHK1, an effector kinase of DDR activated by ATR, and to induce its ubiquitin-dependent degradation. In this perspective, we focus on the role of ZEB1 in the regulation of DDR and describe the mechanisms of ZEB1-dependent chemoresistance.

Keywords: ZEB1, plasticity, DNA damage response, therapy resistance, EMT-epithelial to mesenchymal transition

OPEN ACCESS

Edited by:
Robert M. Brosh, National Institute on Aging, National Institutes of Health (NIH), United States

Reviewed by:
Michael G. Kemp, Wright State University, United States
Chinnadurai Mani, Texas Tech University Health Sciences Center, United States

***Correspondence:**
Karel Souček
ksoucek@ibp.cz

Specialty section:
This article was submitted to Molecular Diagnostics and Therapeutics, a section of the journal Frontiers in Molecular Biosciences

Received: *12 December 2019*
Accepted: *14 February 2020*
Published: *19 March 2020*

Citation:
Drápela S, Bouchal J, Jolly MK, Culig Z and Souček K (2020) ZEB1: A Critical Regulator of Cell Plasticity, DNA Damage Response, and Therapy Resistance. Front. Mol. Biosci. 7:36. doi: 10.3389/fmolb.2020.00036

INTRODUCTION

Cancer is the second leading cause of death worldwide (Wang et al., 2016). Nevertheless, the basis of poor prognosis for cancer patients and the obstacle to a positive clinical outcome is not the primary tumor itself, but cancer cell plasticity, which enables local invasion, dissemination, and distant metastases. Evidence has accumulated that plasticity is driven by the process called

epithelial-mesenchymal transition (EMT). Activation of EMT is widely believed to contribute to invasion, metastasis, tumor relapse, and therapy resistance (Zheng et al., 2015). In many epithelial malignancies, EMT is associated with a change in phenotypic features such as loss of cell-cell adhesion and polarity, change from a cobblestone-like shape to an elongated one, and development of a generally more aggressive mesenchymal-like phenotype (Kalluri and Weinberg, 2009). EMT originally observed during embryogenesis (Hay, 1995), is a reversible, evolutionary conserved process that is tightly regulated through the interplay between environmental signals from Wnt, TGF, FGF family members, interleukins, and various EMT-transcription factors (EMT-TFs), including Zinc-finger E-box binding protein 1 (ZEB1), ZEB2, Snail, Slug, and Twist (Kalluri and Weinberg, 2009). All of these processes are fine-tuned by oncogenic and tumor-suppressive microRNAs (miRNA). ZEB1 is a core EMT-TF of the ZEB family and is implicated in cellular plasticity, dissemination, and a dormant-to-proliferative phenotypic switch at the distant site as well as being a determinant of worse clinical prognosis in most human cancers (Zhang et al., 2015; Katsura et al., 2017; Krebs et al., 2017). Furthermore, activation and stabilization of ZEB1 via a miRNA- or ATM-dependent axis contribute to the resistance to various anticancer therapies (Burk et al., 2008; Zhang et al., 2014a). With regards to clinical relevance, ZEB1 expression increases progressively through the different stages of cancer progression, e.g., ZEB1 expression dramatically increases in advanced castration-resistant prostate cancer (CRPC) and PCa metastasis compared to clinically localized prostate cancer (Figiel et al., 2017). Moreover, patients with ZEB1-expressing metastases have shorter overall survival compared to patients with ZEB1-negative tumors (Figiel et al., 2017). In this review, we outline recent studies on the molecular function of ZEB1 in cellular plasticity and metastasis and elucidate its role in DDR and therapy resistance in an EMT-dependent or EMT-independent manner.

STRUCTURE AND REGULATORY MECHANISMS OF ZEB1

ZEB1 protein (also known as TCF8), encoded by the ZEB1 gene in humans, is a transcription factor characterized by the presence of two C2H2-type flanking zinc finger clusters, which are responsible for interaction with paired CACCT(G) E-box-like promoter elements on DNA, and a centrally located POU-like homeodomain, not binding DNA (Vandewalle et al., 2009). Additionally, ZEB1 contains Smad- (SID), CtBP- (CID), and p300-P/CAF (CBD) interaction domains that are instrumental in the control of its transcriptional activity (Vandewalle et al., 2009; Zhang Y. et al., 2019). ZEB1 can either downregulate or upregulate the expression of its target genes by epigenetic mechanisms, including DNA methylation or histone modifications and recruitment of different co-suppressors or co-activators through SID, CID, or CBD (Postigo et al., 2003). For instance, ZEB1 can activate transcription of TGF-beta responsive genes through its interaction with co-activators such as Smad, p300, and P/CAF (Postigo et al., 2003; Caramel et al., 2018). Conversely, recruitment of CtBP transcriptional co-repressors (histone deacetylases HDAC1/2) following direct ZEB1 binding onto the *CDH1* gene promoter leads to repression of *CDH1* transcription, resulting in downregulation of E-cadherin protein expression and induction of EMT (Zhang et al., 2015). This dual activity, which fosters the expression of genes encoding components for tight cell junctions, desmosomes or intermediate filaments, is unique for ZEB1/2 transcription factors and crucial for the EMT program (Caramel et al., 2018).

Regulation of ZEB1 expression can be accomplished on different levels by transcriptional or post-transcriptional mechanisms. First, the feedback loop between ZEB1 and the miRNA-200 family is a well-described mechanism of the regulation of cellular plasticity, (de)differentiation, and EMT machinery (Tian et al., 2014; Zhang Y. et al., 2019). Second, ubiquitination by E3 ligase complex Skp1-Pam-Fbxo (Xu et al., 2015) or, conversely, deubiquitination by USP51 enzyme has also been shown to regulate ZEB1 and EMT (Zhou Z. et al., 2017). Expression of ZEB1 is under the control of different positive (TGF-beta, Wnt/beta-catenin, NF-κB, PI3K/Akt, Ras/Erk) as well as negative regulators, including miRNA signaling (Chua et al., 2007; Bullock et al., 2012; Horiguchi et al., 2012; Kahlert et al., 2012; Zhang and Ma, 2012; Zhang Y. et al., 2019). For instance, ZEB1 represents the direct downstream target of Wnt-activated beta-catenin in bone metastasis of lung cancer, resulting in decreased levels of E-cadherin and EMT (Yang et al., 2015). In parallel, TGF-beta induces the mesenchymal phenotype in glioblastoma cells via pSmad2- and ZEB1-dependent signaling, leading to tumor invasion (Joseph et al., 2014). Finally, Han et al. have reported that hepatocyte growth factor increases the invasive potential of prostate cancer cells via the ERK/MAPK-ZEB1 axis (Han et al., 2016). Besides well-known transcription factors, Grainyhead-like 2 (GRHL2) has been described as a potential key player associated with the epithelial phenotype and an important regulator of ZEB1 and EMT. Studies have shown that GRHL2 modulates the expression of E-cadherin and Claudin 4, which are crucial for differentiation and maintenance of cell junctions (Werth et al., 2010). In breast cancer, GRHL2 acts as an EMT suppressor by forming a double-negative feedback loop with the EMT driver ZEB1 via the miR-200 family (Cieply et al., 2012). Similarly, GRHL2 regulates epithelial plasticity along with stemness in pancreatic cancer progression by forming a mutual inhibitory loop with ZEB1 (Nishino et al., 2017). Whereas combined (over)expression of GRHL2 and miR-200s increases E-cadherin levels, inhibits ZEB1 expression and induces MET (Somarelli et al., 2016), GRHL2 knockdown is associated with downregulation of epithelial genes, upregulation of ZEB1 or vimentin, and the onset of EMT (Chung et al., 2019). Hence, the reciprocal repressive relationship between GRHL2 and ZEB1 is considered to be a significant regulator of EMT cell plasticity and chemoresistance (Chung et al., 2019). These regulatory mechanisms make ZEB1 the core downstream target of broad spectra of signaling pathways implicated in various cellular processes, including differentiation, proliferation, plasticity, and survival.

ZEB1 IN PLASTICITY AND DISSEMINATION

Enhanced plasticity of cancer cells is considered an important driving force of tumor progression, allowing continuous adaptations to the demanding conditions in the ever-changing tumor microenvironment. Cellular plasticity is exerted by a reciprocal feedback loop between the EMT driver ZEB1 and the miR-200 family as an inducer of epithelial differentiation (Burk et al., 2008; Gregory et al., 2008; Brabletz and Brabletz, 2010). Within this feedback loop, ZEB1 promotes EMT, plasticity, dissemination, and drug resistance via inhibition of the transcription of miR-200 family members, while miR-200 family members promote MET, differentiation, and drug sensitivity by inhibition of ZEB1 translation (Brabletz, 2012). Thus, this regulatory mechanism was proposed as a molecular "engine" of cellular plasticity and a driving force toward cancer metastasis (Brabletz and Brabletz, 2010). Mathematical modeling of this feedback loop suggests that cells need not necessarily attain just epithelial or mesenchymal states; rather, they can stably acquire a hybrid epithelial/mesenchymal phenotype (Lu et al., 2013). The coupled system of ZEB1, GRHL2, and miR-200 drives the cellular dynamics of epithelial-hybrid-mesenchymal transition (Jolly et al., 2016; Chung et al., 2019). ZEB1 forms two additional indirect feedback loops including epithelial splicing regulatory factor ESRP1 and an enzyme that produces hyaluronic acid, HAS2 (Preca et al., 2015, 2017; Jolly et al., 2018) Thus, ZEB1-mediated feedback loops function as a hub of cellular plasticity during metastasis.

From another point of view, it is increasingly evident that genomic regions that do not encode proteins and are often transcribed into long non-coding RNAs (lncRNAs) represent important regulators of cancer development, dissemination, and aggressiveness (Huarte, 2015). Moreover, lncRNAs can directly interact with proteins and thereby regulate their stability (Huarte, 2015). A recent study has reported a novel lncRNA, namely RP11-138 J23.1 (RP11), as a positive regulator of migration, invasion, and EMT in colorectal carcinoma cells *in vitro* and enhanced liver metastasis *in vivo* (Wu et al., 2019b). Mechanistically, epigenetic upregulation of RP11 (m6A modification) accelerates the degradation of two E3 ligases and thus attenuates proteasomal degradation of ZEB1, resulting in dissemination of CRC cells (Wu et al., 2019b).

Genome-wide screening of ZEB1 targets using TNBC cell line Hs578T revealed more than 2,000 genes that are positively or negatively regulated by this transcription factor. In the context of plasticity, ZEB1 contributed to the regulation of cell polarity via DLG2 and FAT3 proteins, cell-to-cell adhesion via transmembrane protein TENM2 or anchorage-independent growth through interaction with metalloproteinase inhibitor TIMP3 (Maturi et al., 2018). Moreover, strong evidence indicates that ZEB1, but not Snail or Slug, is the master regulator of phenotypic as well as metabolic plasticity of pancreatic cells, affecting cancer cell dissemination and metastasis (Krebs et al., 2017). Moreover, metastasis remains one of the main obstacles in cancer therapy. Hence, effective anti-ZEB1 immunotherapy might serve as a promising tool for the reduction of cancer cell dissemination and metastasis and thus could help to eradicate various types of cancer. Notably, ZEB1 depletion significantly reduces stemness and colonization capacity and locks the cells in the homogeneous epithelial state, limiting cell heterogeneity and plasticity (Krebs et al., 2017). However, the similarities and overlaps in molecular networks mediated by ZEB1 vs. other EMT-inducing transcription factors remain to be identified. Thus, ZEB1 may play context-specific roles in repressing epithelial genes and/or activating genes involved with a mesenchymal phenotype (Watanabe et al., 2019), given its ability to function both as a repressor and as an activator depending on available co-factors (Lehmann et al., 2016).

The detachment of tumor cells from the main tumor bulk and invasion through surrounding stroma is an important step for the development of distant metastasis. A growing body of evidence proves that the stroma plays a major role in the budding of quiescent tumor cells, resulting in dissemination. ZEB1 has been shown to be strongly associated with this complex process, wherein EMT-like stromal cells possessing high ZEB1 levels trigger the tumor-budding phenotype by tumor-stroma crosstalk (Galvan et al., 2015). Strikingly, ZEB1 also governs the inflammatory phenotype in breast cancer cells by regulating the secretion of pro-inflammatory cytokines IL-6 and IL-8 and induction of fibroblasts and growth of myeloid-derived suppressor cells, indicating its key role in the tumor microenvironment and formation of the pre-metastatic niche (Katsura et al., 2017; Carpenter et al., 2018). At the same time, it has been shown that in the post-dissemination events, inflammation orchestrates ZEB1-dependent escape of disseminated tumor cells from dormant to active phenotype and induces EMT-associated metastatic outgrowth, highlighting the importance of ZEB1 in the regulation of cell plasticity (De Cock et al., 2016). Functional studies revealed that ZEB1 overexpression drives melanoma phenotypic plasticity and is sufficient to drive resistance to BRAF and/or MEK inhibitors, whereas ZEB1 inhibition sensitizes naive melanoma cells to BRAF inhibitors, prevents the emergence of resistance, and decreases the viability of resistant cells (Richard et al., 2016). Finally, ZEB1-driven phenotypic plasticity of epithelial pancreatic cancer cells was also observed *in vivo*, where differentiated primary tumor cells underwent dedifferentiation associated with an upregulation of ZEB1 at the invasive front, resulting in liver metastasis (Krebs et al., 2017). Taken together, these findings reveal the crucial role of ZEB1 in the phenotypic plasticity important for the dissemination of cancer cells and the establishment of metastasis in distant sites.

Importantly, ZEB1-mediated mechanisms and feedback loops can also drive an irreversible EMT (Jia et al., 2019). However, the different impacts of reversible vs. irreversible EMT on associated traits such as therapy resistance, immune evasion, and tumor-initiating potential remain to be investigated. Breaking the ZEB1/miR-200 feedback loop has been shown to alter the dynamics of phenotypic plasticity in a cell population and curb metastasis *in vivo*, but the mechanisms involved here are still elusive (Celia-Terrassa et al., 2018).

MECHANISMS OF ZEB1-TRIGGED THERAPY RESISTANCE

Nowadays, a growing body of evidence implicates intratumoral heterogeneity, EMT, and increased ZEB1 levels as among the main drivers of therapy resistance, exemplified by EMT-induced docetaxel resistance in prostate cancer (Hanrahan et al., 2017), gemcitabine resistance in pancreatic cancer (Wang et al., 2017), and multiple types of resistance within various malignancies (Shibue and Weinberg, 2017; Cui et al., 2018; Zhang et al., 2018; Orellana-Serradell et al., 2019). Besides being a key contributor to the regulation of cancer cell differentiation and metastasis, the potential role of ZEB1 in the modulation of tumor chemoresistance is not yet fully understood.

Complex Role of ZEB1 in DNA Damage Response and DNA Repair

From previous studies, it is apparent that ZEB1 is required for DNA repair and the clearance of DNA breaks (Zhang et al., 2014b). Mechanistically, ZEB1 knockdown significantly reduces levels of both total and phosphorylated CHK1, a critical effector kinase implicated in DDR and HR-mediated DNA repair, while ZEB1 overexpression acts in the opposite way and promotes clearance of DNA breaks after IR therapy (Zhang et al., 2014b). Previous study showed that chemoresistant tumor cells possess constitutively activated ATM kinase (Svirnovski et al., 2010). This activation is induced and maintained by overexpressed ZEB1 recruiting the transcriptional coactivators p300/PCAF to the *ATM* promoter, which results in the chemoresistance of breast cancer cells (Zhang et al., 2018). Meanwhile, in the positive feedback loop, over-activated ATM stabilizes ZEB1, which acts as a repressor of poly-ubiquitination of endogenous CHK1 via direct interaction with the deubiquitinating enzyme USP7. In contrast, Song et al. claimed that ZEB1 inhibition promotes CHK1 phosphorylation and induces cell cycle arrest in the interphase and thus sensitizes p53-mutated pancreatic cancer cells to the therapy by ATR inhibitor, whereas ZEB1 overexpression attenuates chemotherapy-stimulated CHK1 phosphorylation (Song et al., 2018). This indirect regulation, mediated via interaction of ZEB1 with ATR adaptor protein TopBP1 triggering CHK1 phosphorylation (Song et al., 2018), underlines the pleiotropic and complex role of ZEB1 in the regulation of the response to various anticancer treatments. Importantly, the EMT program has also been shown to be involved in the normal mammary epithelial stem cell state. Morel et al. have shown that ZEB1 is expressed in normal human mammary stem cells and promotes a protective antioxidant program driven by the methionine sulfoxide reductase MSRB3 (Morel et al., 2017). This preemptive program prevents the formation of oncogene-induced DNA damage in stem cells. As a direct consequence, ZEB1 expression precludes the activation of the p53-dependent DNA damage response (DDR) and ensures the maintenance of genomic stability over the course of tumorigenesis. These findings provide a rational explanation for the existence of a subclass of aggressive breast neoplasms exhibiting high ZEB1 expression, a low frequency of p53 mutations, and a subnormal genomic landscape. Given these data, it is evident that ZEB1 plays a significant role in the regulation of DDR and DNA repair machinery, no matter of the p53 status. Considering that DDR is one of the most important signaling pathways in the maintenance of genomic integrity and regulation of cell response to the various anticancer therapies, ZEB1 represents a promising target for combined therapy with DNA-damaging drugs in order to decrease toxicity and undesirable side effects.

Interplay Between microRNAs, ZEB1, and DNA Damage Response

Cellular plasticity, EMT, and ZEB1 overexpression share one common denominator: microRNAs (miRNAs) (Zhang Y. et al., 2019). Many studies have considered miRNAs as key regulators of EMT through downregulation of EMT-driving transcription factors, including Twist, Snail, and ZEB1/2 (Bullock et al., 2012; Zhang and Ma, 2012; Khanbabaei et al., 2016). Recent studies have highlighted both radio- and chemotherapy when used alone as major factors in cancer cell plasticity, promoting *in vitro* invasion and migration in a ZEB1-dependent manner through the ERK1/2 signaling pathway (Song et al., 2017). For instance, exposure of triple-negative breast cancer cell lines to radiation triggered migration and progression via ATM-driven phosphorylation and stabilization of ZEB1 protein, while its mRNA levels remained unchanged (Lin et al., 2018). Moreover, complete loss or downregulation of different miRNAs was strongly associated with poor prognosis, metastasis, and resistance to various anticancer therapies. Although the mechanism of ZEB1-driven chemoresistance is not yet fully described, miR-203 has been considered an important ZEB1 target with stemness-inhibiting properties and a capability to restore drug sensitivity (Meidhof et al., 2015). Sensitivity to the chemotherapy drug gemcitabine can be restored by targeting the negative feedback loop miR-203-ZEB1 using histone-deacetylase (HDAC) inhibitor mocetinostat (MGCD0103). Mocetinostat interferes with ZEB1, downregulating its mRNA and protein levels, and upregulates tumor-suppressing miR-203, resulting in significantly enhanced sensitivity of pancreatic cancer cells to gemcitabine therapy (Meidhof et al., 2015). Also, miR-205 upregulation enhances radiation response in a prostate cancer cell line as well as in xenograft models by impairment of DDR and DNA repair as a consequence of ZEB1 inhibition (El Bezawy et al., 2019). Moreover, siRNA-mediated silencing of ZEB1 recapitulated the effect of miR-205 re-sensitization, confirming its functional role in radiotherapy of prostate cancer (El Bezawy et al., 2019). Similarly, reconstitution of miR-875-5p, whose expression is strongly down-regulated in prostate cancer clinical samples, led to enhanced radiation response in PCa cell lines and xenografts by disabling EGFR nuclear translocation and upstream signaling of ZEB1-triggered activation of CHK1 and DNA repair machinery (El Bezawy et al., 2017). At the same time, miR-875-5p, counteracts EMT by suppression of EGFR and ZEB1,

signaling molecules that are crucial for the preservation of a mesenchymal-like phenotype (El Bezawy et al., 2017). In regard of DDR, the tumor suppressor protein p53 is a crucial molecule in the regulation of the cell cycle (Chen, 2016) and cell differentiation and plasticity (Spike and Wahl, 2011), indicating that p53 deregulation might play a critical role in disease progression, activation of DNA damage, and chemoresistance. Moreover, p53 induces miR-200c transcription, which leads to ZEB1 inhibition and MET (Kim et al., 2011; Schubert and Brabletz, 2011). Thus, an intact p53-ZEB1 feedback loop represents an important regulatory mechanism for epithelial phenotype maintenance, suppression of metastasis, and protection against enhanced chemoresistance. Importantly, two independent studies with MDM2 inhibitors, which both reactivated p53 and downregulated ZEB1, also documented decreased stemness features and glioblastoma aggressiveness (Giacomelli et al., 2017; Her et al., 2018). Such effects of p53 reactivation on ZEB1 may be mediated via activation of microRNAs that p53 can activate such as miR-34, miR-145, and miR-200 (Chang et al., 2011; Siemens et al., 2011; Ren D. et al., 2013).

Further studies have reported other feedback loops whereby the miR-205 and miR-200 family of miRNAs directly target ZEB1 and, conversely, ZEB1 represses the transcription of miR-200 genes (Burk et al., 2008; Gregory et al., 2008). Consistently, irradiation therapy in breast cancer cells results in massive miR-205 downregulation, accompanied by upregulation of ZEB1, which can be completely reversed by inhibition of ATM or direct depletion of ZEB1 (Zhang et al., 2014a). This supports the scenario where ATM stabilizes ZEB1 upon irradiation, which in turn represses its negative regulator miR-205, leading to more robust activation of ZEB1, enhanced DNA repair, and radioresistance. Previous reports have shown that similarly to miRNA-205, miR-200c directly targets ZEB1 (Hurteau et al., 2007) and is crucial for the maintenance of sensitivity to chemotherapy. Since low levels of miR-200c are associated with chemoresistance, high ZEB1 levels, and EMT in advanced breast and ovarian cancer, restoration of its expression is considered as a promising therapeutic approach to overcome limited therapeutic response (Cochrane et al., 2009). In addition to those already mentioned, several other miRNAs including miR-15 (Pouliot et al., 2012), miR-16 (Lezina et al., 2013), miR155 (Pouliot et al., 2012), miR-26a (Lezina et al., 2013), and miR-424 (Xu et al., 2013), were also implicated in the direct targeting of CHK1, including dual targeting by miR-195 (Kim et al., 2018) of both ZEB1 and CHK1 at the same time. The loss of these miRNAs was associated with increased activity of the DNA damage and repair machinery and subsequent resistance to chemotherapy. Besides miRNAs, there is evidence that lncRNAs can also play a significant role in cancer progression, metastasis (Chen et al., 2018), and chemoresistance (Bermudez et al., 2019). For instance, overexpression of lncRNA SBF2-AS1 led to the promotion of temozolomide chemoresistance in glioblastoma cells and tissues via a ZEB1-dependent pathway. ZEB1 was found to directly bind to the *SBF2-AS1* promoter, induce its expression and stimulate double-strand-break DNA repair, thereby increasing chemoresistance spread by exosomes (Zhang Z. et al., 2019). Taken together, these results support the idea that miRNAs regulating ZEB1 expression represent a crucial mechanism controlling DDR, activation of DNA repair, and subsequent chemoresistance.

EMT: Effector or Bystander of Therapy Resistance?

The epithelial-to-mesenchymal transition refers to the highly conserved trans-differentiation program that culminates in increased tumorigenesis, invasiveness, and metastatic potential and can generate CSCs (Mani et al., 2008; Brabletz et al., 2018) with significantly enhanced potential to stimulate DNA repair and promote therapy resistance (Bao et al., 2006). Emerging evidence indicates that molecular and phenotypic changes during acquired drug resistance are associated with the differentiation state of the tumor, which is likely to reflect EMT and the emergence of chemorefractory cells with stem cell-like features in many cancer types (Voulgari and Pintzas, 2009; Singh and Settleman, 2010). EMT is a multi-dimensional, non-linear process where cells can acquire multiple states along the spectrum of the epithelial-mesenchymal landscape; the association of these states with drug resistance need not be universal but is dependent on cancer, drug, and also the inducer of EMT in that context (Huang et al., 2013).

As one of the major inducers of EMT (Yang and Weinberg, 2008), ZEB1 represents an important molecule that plays a crucial role in tumor progression and metastasis and the expression of which correlates with poor clinical outcome in cancer patients (Shibue and Weinberg, 2017). ZEB1 is also implicated in resistance to various anticancer therapies through both EMT-dependent and EMT-independent mechanisms, depending on specific cancer and treatment type. Thus, it remains unclear whether EMT by itself or specific EMT regulators are the main drivers of therapy resistance. Previous studies demonstrated that highly proliferative non-EMT breast cancer cells were sensitive to chemotherapy, while the emergence of recurrent EMT-derived metastases was associated with resistance to cyclophosphamide *in vivo* (Fischer et al., 2015). Also, miR-200 overexpression results in the switch toward cyclophosphamide sensitivity (Fischer et al., 2015). These results indicate potential relevance of EMT in the chemoresistance, as the main target of miR-200 is ZEB1, a crucial regulator of EMT that is capable of reversing the whole machinery (Bracken et al., 2014). Further studies have discovered various other mechanisms connecting EMT and chemoresistance. For instance, Snail, Slug, and ZEB1 were determined to be inducers of chemoresistance driven by inhibition of p53-mediated apoptosis via ATM and PTEN (Liu et al., 2015). Further, loss of miR-200c led to the induction of Snail and ZEB1, activation of EMT, and abnormal expression of beta-tubulin III (TUBB3), leading to paclitaxel resistance in ovarian cancer cell models (Izutsu et al., 2008). A SIRT6-driven EMT program is sufficient to enhance repair of carboplatin-induced DNA damage by activation of DNA repair enzyme, poly ADP-ribose polymerase

(PARP). This mechanism counteracts the cytotoxic effect of this chemotherapeutic agent and results in chemoresistance (Mao et al., 2011).

EMT is also associated with the expression of ATP-binding cassette (ABC) transporters, membrane proteins responsible for pumping xenobiotics out of the cells (Saxena et al., 2011). Indeed, the correlation between EMT, increased ZEB1/2-dependent expression of MDR1 and ABCG2, and resistance to platinum-based drugs was confirmed by the whole transcriptome profiling of ovarian and lung cancer tissues (Zhou Y. et al., 2017; Wu et al., 2019a). Finally, several recent studies demonstrated decreased sensitivity to chemotherapy of primary and metastatic tumor cells in an EMT-dependent manner in both lung and pancreatic cancers (Fischer et al., 2015; Zheng et al., 2015). These reports provide convincing data linking EMT to chemoresistance. Nevertheless, several studies have demonstrated EMT-independent ZEB1-driven chemoresistance. For instance, EMT by itself was considered as an important process contributing to metastasis formation, but not to the limited sensitivity of multiple drug-resistant gastric and breast cancer cell models (Xu et al., 2017). Notably, human lung carcinoma cells resistant to docetaxel possessed significantly increased expression of ZEB1, while other transcriptional factors associated with EMT, including Snail, Twist, and Slug, were not deregulated (Ren J. et al., 2013). Highly expressed ZEB1 was also implicated in several mechanisms leading to chemoresistance to paclitaxel (Sakata et al., 2017) or cisplatin (Cui et al., 2018) in various types of epithelial-like malignancies. Inhibition of ZEB1 in epithelial-like docetaxel-resistant SPC-A1/DTX cells reversed the chemoresistance and significantly enhanced sensitivity to docetaxel (Ren J. et al., 2013). There is increasing evidence that high ZEB1 expression is also one of the significant indicators of poor prognosis in chemoresistant glioblastoma disease (Siebzehnrubl et al., 2013). Experimentally, ZEB1 regulates expression of O-6-methylguanine DNA methyltransferase (MGMT) via a miR-200c- and c-MYB-dependent axis to promote resistance in a presumably EMT-independent context (Siebzehnrubl et al., 2013). Moreover, several studies also report higher sensitivity of mesenchymal-like tumors to neoadjuvant therapy

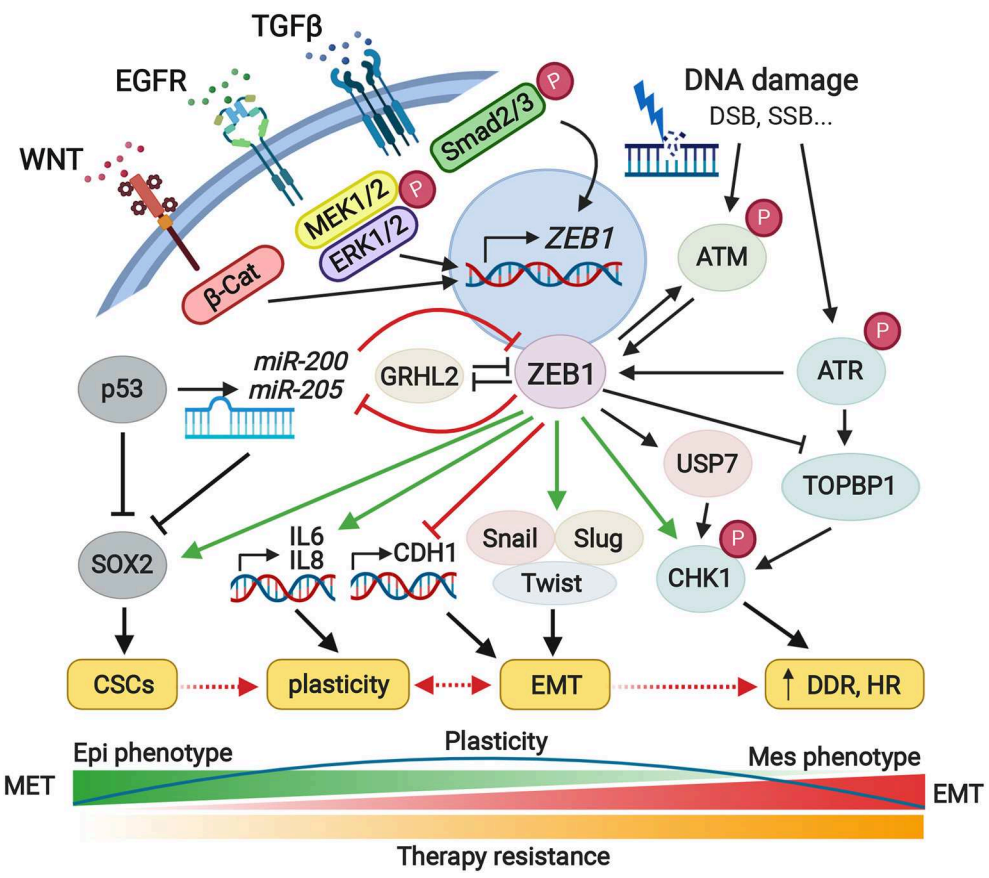

FIGURE 1 | Pleiotropic roles of ZEB1 in the cell plasticity, EMT, and therapy resistance. The ZEB1 represents a core transcriptional factor and central determinant of cell fate which controls fundamental intracellular processes including cell plasticity, EMT, or therapy resistance. Downstream signaling pathways triggered by ZEB1, regulate the activity of the proteins and miRNAs involved in cell differentiation, proliferation, or motility. ZEB1 overexpression is accompanied by overall changeover of the cell phenotype, higher tumorigenic potential, and increased migratory character. ZEB1 also promotes immune escape as well as contributes to the formation of a pre-metastatic niche. Given the tumor heterogeneity, ZEB1 plays an important role in the stemness of cancer cells and increased radio- and chemoresistance. Green and red arrows illustrate major activating or inhibitory effects of ZEB1, respectively. CSCs, cancer stem cells; EMT, epithelial-to-mesenchymal transition; MET, mesenchymal-to-epithelial transition; DDR, DNA damage response; HR, homologous recombination. Created with Biorender.com.

in comparison to epithelial-like subtypes of breast cancer (Carey et al., 2007; Li et al., 2008). Lastly, following previous findings, only ZEB1, but not other transcriptional factors, including Snail or Twist, conferred radioresistance to the breast cancer model MCF7, even without inducing EMT (Zhang et al., 2014b). These results suggest that ZEB1, but not necessarily EMT itself might indeed be the crucial regulator of therapy resistance.

CONCLUSION AND FUTURE DIRECTIONS

A growing body of publications has considered ZEB1 in normal and cancer cells to be a crucial regulator of fundamental intracellular processes as well a major denominator of plasticity, driving drug adaptation and phenotypic resistance to various types of anticancer therapy. Given the core downstream target of highly conserved pathways implicated in response to DNA damage and repair, proliferation, plasticity, and cell differentiation, ZEB1 plays a pivotal role in the determination of cell fate (**Figure 1**). Considering its phosphorylation and stabilization by ATM kinase, leading to a limited response to different types of anticancer therapy, combined targeting of ZEB1 with the ATR-CHK1 axis might represent an effective way to overcome these obstacles. Promising results were also obtained with MDM2 inhibitors, which could reactivate p53 tumor suppressor along with downregulating ZEB1 and decreasing stemness features and cancer aggressiveness. An additional possibility for reducing the expression of ZEB1 is inhibition of non-coding circular RNA (circRNA) hsa_circ_0057481, as shown in laryngeal cancer (Fu et al., 2019). Further studies are necessary in order to test clinical applicability. One could also consider inhibition of ZEB1 and EMT by down-regulation of valproic acid, which regulates the *ZEB1* promoter (Zhang S. et al., 2019). Multiple studies have also focused on BET inhibitors in cancer. In this context, it was observed that the DNA endonuclease Mus81, which regulates ZEB1, may be targeted by BET4 inhibitors (Yin et al., 2019). In general, miRNA-based therapeutic options targeting ZEB1 might represent promising tools for targeting ZEB1 but need to be further developed, and delivery methods and therapeutic agent stability should also be investigated with priority.

Despite the association of high ZEB1 expression, EMT, and chemoresistance described in many studies, the role of EMT by itself in therapy resistance is rather controversial. It is not necessarily the epithelial or mesenchymal state that dictates cancer stem-like properties such as drug resistance; instead, they depend on the functions and mechanisms of action of EMT regulators, including ZEB1. Moreover, underlying mechanisms should be investigated for individual context, as the roles of ZEB1 and other transcriptional factors are highly treatment- and cancer type-dependent. The mechanistic links between ZEB1 expression, plasticity, the emergence of CSCs and therapy resistance represent important areas for future investigation. A novel, more specific inhibitors and a better understanding of ZEB1-driven plasticity, inflammation, and vascularization within the tumor and/or pre-metastatic niche microenvironments are inevitably needed to more effectively control resistance to various types of therapies.

AUTHOR CONTRIBUTIONS

SD wrote a complete draft and first version of the manuscript. All authors contributed to the manuscript revision, read, and approved final version and contributed to the principle layout of the article.

FUNDING

This work was supported by funds from the Ministry of Health of the Czech Republic, grant nr. 17-28518A, NV18-08-00245, all rights reserved (ZC, KS), by projects no. LQ1605 from the National Program of Sustainability II (MEYS CR), and by the European Regional Development Fund—Project ENOCH (No. CZ.02.1.01/0.0/0.0/16_019/0000868). This work was further supported from European Structural and Investment Funds, Operational Programme Research, Development and Education—Preclinical Progression of New Organic Compounds with Targeted Biological Activity (Preclinprogress)-CZ.02.1.01/0.0/0.0/16_025/0007381. MJ was supported by the Ramanujan Fellowship provided by the Science and Engineering Research Board, Department of Science and Technology, Government of India (SB/S2/RJN-049/2018). Funders partly covered the wages of the authors. Open access publication fee is covered by FNUSA-ICRC (LQ1605).

ACKNOWLEDGMENTS

The authors would like to thank Dr. Eva Slabakova for proofreading the manuscript.

REFERENCES

Bao, S., Wu, Q., Mclendon, R. E., Hao, Y., Shi, Q., Hjelmeland, A. B., et al. (2006). Glioma stem cells promote radioresistance by preferential activation of the DNA damage response. *Nature* 444, 756–760. doi: 10.1038/nature05236

Bermudez, M., Aguilar-Medina, M., Lizarraga-Verdugo, E., Avendano-Felix, M., Silva-Benitez, E., Lopez-Camarillo, C., et al. (2019). LncRNAs as regulators of autophagy and drug resistance in colorectal cancer. *Front. Oncol.* 9:1008. doi: 10.3389/fonc.2019.01008

Brabletz, S., and Brabletz, T. (2010). The ZEB/miR-200 feedback loop–a motor of cellular plasticity in development and cancer? *EMBO Rep.* 11, 670–677. doi: 10.1038/embor.2010.117

Brabletz, T. (2012). To differentiate or not–routes towards metastasis. *Nat. Rev. Cancer* 12, 425–436. doi: 10.1038/nrc3265

Brabletz, T., Kalluri, R., Nieto, M. A., and Weinberg, R. A. (2018). EMT in cancer. *Nat. Rev. Cancer* 18, 128–134. doi: 10.1038/nrc.2017.118

Bracken, C. P., Li, X., Wright, J. A., Lawrence, D. M., Pillman, K. A., Salmanidis, M., et al. (2014). Genome-wide identification of miR-200 targets reveals a regulatory network controlling cell invasion. *EMBO J.* 33, 2040–2056. doi: 10.15252/embj.201488641

Bullock, M. D., Sayan, A. E., Packham, G. K., and Mirnezami, A. H. (2012). MicroRNAs: critical regulators of epithelial to mesenchymal (EMT) and mesenchymal to epithelial transition (MET) in cancer progression. *Biol. Cell* 104, 3–12. doi: 10.1111/boc.201100115

Burk, U., Schubert, J., Wellner, U., Schmalhofer, O., Vincan, E., Spaderna, S., et al. (2008). A reciprocal repression between ZEB1 and members of the miR-200 family promotes EMT and invasion in cancer cells. *EMBO Rep.* 9, 582–589. doi: 10.1038/embor.2008.74

Caramel, J., Ligier, M., and Puisieux, A. (2018). Pleiotropic roles for ZEB1 in Cancer. *Cancer Res.* 78, 30–35. doi: 10.1158/0008-5472.CAN-17-2476

Carey, L. A., Dees, E. C., Sawyer, L., Gatti, L., Moore, D. T., Collichio, F., et al. (2007). The triple negative paradox: primary tumor chemosensitivity of breast cancer subtypes. *Clin. Cancer Res.* 13, 2329–2334. doi: 10.1158/1078-0432.CCR-06-1109

Carpenter, R. A., Kwak, J. G., Peyton, S. R., and Lee, J. (2018). Implantable pre-metastatic niches for the study of the microenvironmental regulation of disseminated human tumour cells. *Nat. Biomed. Eng.* 2, 915–929. doi: 10.1038/s41551-018-0307-x

Celia-Terrassa, T., Bastian, C., Liu, D. D., Ell, B., Aiello, N. M., Wei, Y., et al. (2018). Hysteresis control of epithelial-mesenchymal transition dynamics conveys a distinct program with enhanced metastatic ability. *Nat. Commun.* 9:5005. doi: 10.1038/s41467-018-07538-7

Chang, C. J., Chao, C. H., Xia, W., Yang, J. Y., Xiong, Y., Li, C. W., et al. (2011). P53 regulates epithelial-mesenchymal transition and stem cell properties through modulating miRNAs. *Nat. Cell Biol.* 13, 317–323. doi: 10.1038/ncb2173

Chen, J. (2016). The cell-cycle arrest and apoptotic functions of p53 in tumor initiation and progression. *Cold Spring Harb. Perspect. Med.* 6:a026104. doi: 10.1101/cshperspect.a026104

Chen, X., Chen, Z., Yu, S., Nie, F., Yan, S., Ma, P., et al. (2018). Long noncoding RNA LINC01234 functions as a competing endogenous RNA to regulate CBFB expression by sponging miR-204-5p in gastric cancer. *Clin. Cancer Res.* 24, 2002–2014. doi: 10.1158/1078-0432.CCR-17-2376

Chua, H. L., Bhat-Nakshatri, P., Clare, S. E., Morimiya, A., Badve, S., and Nakshatri, H. (2007). NF-kappaB represses E-cadherin expression and enhances epithelial to mesenchymal transition of mammary epithelial cells: potential involvement of ZEB-1 and ZEB-2. *Oncogene* 26, 711–724. doi: 10.1038/sj.onc.1209808

Chung, V. Y., Tan, T. Z., Ye, J., Huang, R. L., Lai, H. C., Kappei, D., et al. (2019). The role of GRHL2 and epigenetic remodeling in epithelial-mesenchymal plasticity in ovarian cancer cells. *Commun. Biol.* 2:272. doi: 10.1038/s42003-019-0506-3

Cieply, B., Riley, P. T., Pifer, P. M., Widmeyer, J., Addison, J. B., Ivanov, A. V., et al. (2012). Suppression of the epithelial-mesenchymal transition by grainyhead-like-2. *Cancer Res.* 72, 2440–2453. doi: 10.1158/0008-5472.CAN-11-4038

Cochrane, D. R., Spoelstra, N. S., Howe, E. N., Nordeen, S. K., and Richer, J. K. (2009). MicroRNA-200c mitigates invasiveness and restores sensitivity to microtubule-targeting chemotherapeutic agents. *Mol. Cancer Ther.* 8, 1055–1066. doi: 10.1158/1535-7163.MCT-08-1046

Cui, Y., Qin, L., Tian, D., Wang, T., Fan, L., Zhang, P., et al. (2018). ZEB1 promotes chemoresistance to cisplatin in ovarian cancer cells by suppressing SLC3A2. *Chemotherapy* 63, 262–271. doi: 10.1159/000493864

De Cock, J. M., Shibue, T., Dongre, A., Keckesova, Z., Reinhardt, F., and Weinberg, R. A. (2016). Inflammation triggers Zeb1-Dependent escape from tumor latency. *Cancer Res.* 76, 6778–6784. doi: 10.1158/0008-5472.CAN-16-0608

El Bezawy, R., Cominetti, D., Fenderico, N., Zuco, V., Beretta, G. L., Dugo, M., et al. (2017). MiR-875-5p counteracts epithelial-to-mesenchymal transition and enhances radiation response in prostate cancer through repression of the EGFR-ZEB1 axis. *Cancer Lett.* 395, 53–62. doi: 10.1016/j.canlet.2017.02.033

El Bezawy, R., Tinelli, S., Tortoreto, M., Doldi, V., Zuco, V., Folini, M., et al. (2019). MiR-205 enhances radiation sensitivity of prostate cancer cells by impairing DNA damage repair through PKCε and ZEB1 inhibition. *J. Exp. Clin. Cancer Res.* 38:51. doi: 10.1186/s13046-019-1060-z

Figiel, S., Vasseur, C., Bruyere, F., Rozet, F., Maheo, K., and Fromont, G. (2017). Clinical significance of epithelial-mesenchymal transition markers in prostate cancer. *Hum. Pathol.* 61, 26–32. doi: 10.1016/j.humpath.2016.10.013

Fischer, K. R., Durrans, A., Lee, S., Sheng, J., Li, F., Wong, S. T., et al. (2015). Epithelial-to-mesenchymal transition is not required for lung metastasis but contributes to chemoresistance. *Nature* 527, 472–476. doi: 10.1038/nature15748

Fu, D., Huang, Y., and Gao, M. (2019). Hsa_circ_0057481 promotes laryngeal cancer proliferation and migration by modulating the miR-200c/ZEB1 axis. *Int. J. Clin. Exp. Pathol.* 12, 4066–4076.

Galvan, J. A., Zlobec, I., Wartenberg, M., Lugli, A., Gloor, B., Perren, A., et al. (2015). Expression of E-cadherin repressors SNAIL, ZEB1 and ZEB2 by tumour and stromal cells influences tumour-budding phenotype and suggests heterogeneity of stromal cells in pancreatic cancer. *Br. J. Cancer* 112, 1944–1950. doi: 10.1038/bjc.2015.177

Giacomelli, C., Daniele, S., Natali, L., Iofrida, C., Flamini, G., Braca, A., et al. (2017). Carnosol controls the human glioblastoma stemness features through the epithelial-mesenchymal transition modulation and the induction of cancer stem cell apoptosis. *Sci. Rep.* 7:15174. doi: 10.1038/s41598-017-15360-2

Gregory, P. A., Bert, A. G., Paterson, E. L., Barry, S. C., Tsykin, A., Farshid, G., et al. (2008). The miR-200 family and miR-205 regulate epithelial to mesenchymal transition by targeting ZEB1 and SIP1. *Nat. Cell Biol.* 10, 593–601. doi: 10.1038/ncb1722

Han, Y., Luo, Y., Wang, Y., Chen, Y., Li, M., and Jiang, Y. (2016). Hepatocyte growth factor increases the invasive potential of PC-3 human prostate cancer cells via an ERK/MAPK and Zeb-1 signaling pathway. *Oncol. Lett.* 11, 753–759. doi: 10.3892/ol.2015.3943

Hanrahan, K., O'neill, A., Prencipe, M., Bugler, J., Murphy, L., Fabre, A., et al. (2017). The role of epithelial-mesenchymal transition drivers ZEB1 and ZEB2 in mediating docetaxel-resistant prostate cancer. *Mol. Oncol.* 11, 251–265. doi: 10.1002/1878-0261.12030

Hay, E. D. (1995). An overview of epithelio-mesenchymal transformation. *Acta Anat.* 154, 8–20. doi: 10.1159/000147748

Her, N. G., Oh, J. W., Oh, Y. J., Han, S., Cho, H. J., Lee, Y., et al. (2018). Potent effect of the MDM2 inhibitor AMG232 on suppression of glioblastoma stem cells. *Cell Death Dis.* 9:792. doi: 10.1038/s41419-018-0825-1

Horiguchi, K., Sakamoto, K., Koinuma, D., Semba, K., Inoue, A., Inoue, S., et al. (2012). TGF-β drives epithelial-mesenchymal transition through deltaEF1-mediated downregulation of ESRP. *Oncogene* 31, 3190–3201. doi: 10.1038/onc.2011.493

Huang, R. Y., Wong, M. K., Tan, T. Z., Kuay, K. T., Ng, A. H., Chung, V. Y., et al. (2013). An EMT spectrum defines an anoikis-resistant and spheroidogenic intermediate mesenchymal state that is sensitive to e-cadherin restoration by a src-kinase inhibitor, saracatinib (AZD0530). *Cell Death Dis.* 4:e915. doi: 10.1038/cddis.2013.442

Huarte, M. (2015). The emerging role of lncRNAs in cancer. *Nat. Med.* 21, 1253–1261. doi: 10.1038/nm.3981

Hurteau, G. J., Carlson, J. A., Spivack, S. D., and Brock, G. J. (2007). Overexpression of the microRNA hsa-miR-200c leads to reduced expression of transcription factor 8 and increased expression of E-cadherin. *Cancer Res.* 67, 7972–7976. doi: 10.1158/0008-5472.CAN-07-1058

Izutsu, N., Maesawa, C., Shibazaki, M., Oikawa, H., Shoji, T., Sugiyama, T., et al. (2008). Epigenetic modification is involved in aberrant expression of class III beta-tubulin, TUBB3, in ovarian cancer cells. *Int. J. Oncol.* 32, 1227–1235. doi: 10.3892/ijo_32_6_1227

Jia, W., Deshmukh, A., Mani, S. A., Jolly, M. K., and Levine, H. (2019). A possible role for epigenetic feedback regulation in the dynamics of the epithelial-mesenchymal transition (EMT). *Phys. Biol.* 16:066004. doi: 10.1088/1478-3975/ab34df

Jolly, M. K., Preca, B. T., Tripathi, S. C., Jia, D., George, J. T., Hanash, S. M., et al. (2018). Interconnected feedback loops among ESRP1, HAS2, and CD44 regulate epithelial-mesenchymal plasticity in cancer. *APL Bioeng.* 2:031908. doi: 10.1063/1.5024874

Jolly, M. K., Tripathi, S. C., Jia, D., Mooney, S. M., Celiktas, M., Hanash, S. M., et al. (2016). Stability of the hybrid epithelial/mesenchymal phenotype. *Oncotarget* 7, 27067–27084. doi: 10.18632/oncotarget.8166

Joseph, J. V., Conroy, S., Tomar, T., Eggens-Meijer, E., Bhat, K., Copray, S., et al. (2014). TGF-β is an inducer of ZEB1-dependent mesenchymal transdifferentiation in glioblastoma that is associated with tumor invasion. *Cell Death Dis.* 5:e1443. doi: 10.1038/cddis.2014.395

Kahlert, U. D., Maciaczyk, D., Doostkam, S., Orr, B. A., Simons, B., Bogiel, T., et al. (2012). Activation of canonical WNT/β-catenin signaling enhances *in vitro* motility of glioblastoma cells by activation of ZEB1 and other activators of epithelial-to-mesenchymal transition. *Cancer Lett.* 325, 42–53. doi: 10.1016/j.canlet.2012.05.024

Kalluri, R., and Weinberg, R. A. (2009). The basics of epithelial-mesenchymal transition. *J. Clin. Invest.* 119, 1420–1428. doi: 10.1172/JCI39104

Katsura, A., Tamura, Y., Hokari, S., Harada, M., Morikawa, M., Sakurai, T., et al. (2017). ZEB1-regulated inflammatory phenotype in breast cancer cells. *Mol. Oncol.* 11, 1241–1262. doi: 10.1002/1878-0261.12098

Khanbabaei, H., Teimoori, A., and Mohammadi, M. (2016). The interplay between microRNAs and twist1 transcription factor: a systematic review. *Tumour Biol.* 37, 7007–7019. doi: 10.1007/s13277-016-4960-y

Kim, C., Hong, Y., Lee, H., Kang, H., and Lee, E. K. (2018). MicroRNA-195 desensitizes HCT116 human colon cancer cells to 5-fluorouracil. *Cancer Lett.* 412, 264–271. doi: 10.1016/j.canlet.2017.10.022

Kim, T., Veronese, A., Pichiorri, F., Lee, T. J., Jeon, Y. J., Volinia, S., et al. (2011). P53 regulates epithelial-mesenchymal transition through microRNAs targeting ZEB1 and ZEB2. *J. Exp. Med.* 208, 875–883. doi: 10.1084/jem.20110235

Krebs, A. M., Mitschke, J., Lasierra Losada, M., Schmalhofer, O., Boerries, M., Busch, H., et al. (2017). The EMT-activator Zeb1 is a key factor for cell plasticity and promotes metastasis in pancreatic cancer. *Nat. Cell Biol.* 19, 518–529. doi: 10.1038/ncb3513

Lehmann, W., Mossmann, D., Kleemann, J., Mock, K., Meisinger, C., Brummer, T., et al. (2016). ZEB1 turns into a transcriptional activator by interacting with YAP1 in aggressive cancer types. *Nat. Commun.* 7:10498. doi: 10.1038/ncomms10498

Lezina, L., Purmessur, N., Antonov, A. V., Ivanova, T., Karpova, E., Krishan, K., et al. (2013). MiR-16 and miR-26a target checkpoint kinases Wee1 and Chk1 in response to p53 activation by genotoxic stress. *Cell Death Dis.* 4:e953. doi: 10.1038/cddis.2013.483

Li, X., Lewis, M. T., Huang, J., Gutierrez, C., Osborne, C. K., Wu, M. F., et al. (2008). Intrinsic resistance of tumorigenic breast cancer cells to chemotherapy. *J. Natl. Cancer Inst.* 100, 672–679. doi: 10.1093/jnci/djn123

Lin, Y., Bai, X., Zhou, W., He, Y., Wu, Y., and Wang, X. (2018). Radiation exposure triggers the progression of triple negative breast cancer via stabilizing ZEB1. *Biomed. Pharmacother.* 107, 1624–1630. doi: 10.1016/j.biopha.2018.08.026

Liu, G., Yang, D., Rupaimoole, R., Pecot, C. V., Sun, Y., Mangala, L. S., et al. (2015). Augmentation of response to chemotherapy by microRNA-506 through regulation of RAD51 in serous ovarian cancers. *J. Natl. Cancer Inst.* 107, 1236–1247. doi: 10.1093/jnci/djv108

Lu, M., Jolly, M. K., Levine, H., Onuchic, J. N., and Ben-Jacob, E. (2013). MicroRNA-based regulation of epithelial-hybrid-mesenchymal fate determination. *Proc. Natl. Acad. Sci. U.S.A.* 110, 18144–18149. doi: 10.1073/pnas.1318192110

Mani, S. A., Guo, W., Liao, M. J., Eaton, E. N., Ayyanan, A., Zhou, A. Y., et al. (2008). The epithelial-mesenchymal transition generates cells with properties of stem cells. *Cell* 133, 704–715. doi: 10.1016/j.cell.2008.03.027

Mao, Z., Hine, C., Tian, X., Van Meter, M., Au, M., Vaidya, A., et al. (2011). SIRT6 promotes DNA repair under stress by activating PARP1. *Science* 332, 1443–1446. doi: 10.1126/science.1202723

Maturi, V., Enroth, S., Heldin, C. H., and Moustakas, A. (2018). Genome-wide binding of transcription factor ZEB1 in triple-negative breast cancer cells. *J. Cell. Physiol.* 233, 7113–7127. doi: 10.1002/jcp.26634

Meidhof, S., Brabletz, S., Lehmann, W., Preca, B. T., Mock, K., Ruh, M., et al. (2015). ZEB1-associated drug resistance in cancer cells is reversed by the class I HDAC inhibitor mocetinostat. *EMBO Mol. Med.* 7, 831–847. doi: 10.15252/emmm.201404396

Morel, A. P., Ginestier, C., Pommier, R. M., Cabaud, O., Ruiz, E., Wicinski, J., et al. (2017). A stemness-related ZEB1-MSRB3 axis governs cellular pliancy and breast cancer genome stability. *Nat. Med.* 23, 568–578. doi: 10.1038/nm.4323

Nishino, H., Takano, S., Yoshitomi, H., Suzuki, K., Kagawa, S., Shimazaki, R., et al. (2017). Grainyhead-like 2 (GRHL2) regulates epithelial plasticity in pancreatic cancer progression. *Cancer Med.* 6, 2686–2696. doi: 10.1002/cam4.1212

Orellana-Serradell, O., Herrera, D., Castellon, E. A., and Contreras, H. R. (2019). The transcription factor ZEB1 promotes chemoresistance in prostate cancer cell lines. *Asian J. Androl.* 21, 460–467. doi: 10.4103/aja.aja_1_19

Postigo, A. A., Depp, J. L., Taylor, J. J., and Kroll, K. L. (2003). Regulation of smad signaling through a differential recruitment of coactivators and corepressors by ZEB proteins. *EMBO J.* 22, 2453–2462. doi: 10.1093/emboj/cdg226

Pouliot, L. M., Chen, Y. C., Bai, J., Guha, R., Martin, S. E., Gottesman, M. M., et al. (2012). Cisplatin sensitivity mediated by WEE1 and CHK1 is mediated by miR-155 and the miR-15 family. *Cancer Res.* 72, 5945–5955. doi: 10.1158/0008-5472.CAN-12-1400

Preca, B. T., Bajdak, K., Mock, K., Lehmann, W., Sundararajan, V., Bronsert, P., et al. (2017). A novel ZEB1/HAS2 positive feedback loop promotes EMT in breast cancer. *Oncotarget* 8, 11530–11543. doi: 10.18632/oncotarget.14563

Preca, B. T., Bajdak, K., Mock, K., Sundararajan, V., Pfannstiel, J., Maurer, J., et al. (2015). A self-enforcing CD44s/ZEB1 feedback loop maintains EMT and stemness properties in cancer cells. *Int. J. Cancer* 137, 2566–2577. doi: 10.1002/ijc.29642

Ren, D., Wang, M., Guo, W., Zhao, X., Tu, X., Huang, S., et al. (2013). Wild-type p53 suppresses the epithelial-mesenchymal transition and stemness in PC-3 prostate cancer cells by modulating miR145. *Int. J. Oncol.* 42, 1473–1481. doi: 10.3892/ijo.2013.1825

Ren, J., Chen, Y., Song, H., Chen, L., and Wang, R. (2013). Inhibition of ZEB1 reverses EMT and chemoresistance in docetaxel-resistant human lung adenocarcinoma cell line. *J. Cell Biochem.* 114, 1395–1403. doi: 10.1002/jcb.24481

Richard, G., Dalle, S., Monet, M. A., Ligier, M., Boespflug, A., Pommier, R. M., et al. (2016). ZEB1-mediated melanoma cell plasticity enhances resistance to MAPK inhibitors. *EMBO Mol. Med.* 8, 1143–1161. doi: 10.15252/emmm.201505971

Sakata, J., Utsumi, F., Suzuki, S., Niimi, K., Yamamoto, E., Shibata, K., et al. (2017). Inhibition of ZEB1 leads to inversion of metastatic characteristics and restoration of paclitaxel sensitivity of chronic chemoresistant ovarian carcinoma cells. *Oncotarget* 8, 99482–99494. doi: 10.18632/oncotarget.20107

Saxena, M., Stephens, M. A., Pathak, H., and Rangarajan, A. (2011). Transcription factors that mediate epithelial-mesenchymal transition lead to multidrug resistance by upregulating ABC transporters. *Cell Death Dis.* 2:e179. doi: 10.1038/cddis.2011.61

Schubert, J., and Brabletz, T. (2011). P53 spreads out further: suppression of EMT and stemness by activating miR-200c expression. *Cell Res.* 21, 705–707. doi: 10.1038/cr.2011.62

Shibue, T., and Weinberg, R. A. (2017). EMT, CSCs, and drug resistance: the mechanistic link and clinical implications. *Nat. Rev. Clin. Oncol.* 14, 611–629. doi: 10.1038/nrclinonc.2017.44

Siebzehnrubl, F. A., Silver, D. J., Tugertimur, B., Deleyrolle, L. P., Siebzehnrubl, D., Sarkisian, M. R., et al. (2013). The ZEB1 pathway links glioblastoma initiation, invasion and chemoresistance. *EMBO Mol. Med.* 5, 1196–1212. doi: 10.1002/emmm.201302827

Siemens, H., Jackstadt, R., Hunten, S., Kaller, M., Menssen, A., Gotz, U., et al. (2011). MiR-34 and SNAIL form a double-negative feedback loop to regulate epithelial-mesenchymal transitions. *Cell Cycle* 10, 4256–4271. doi: 10.4161/cc.10.24.18552

Singh, A., and Settleman, J. (2010). EMT, cancer stem cells and drug resistance: an emerging axis of evil in the war on cancer. *Oncogene* 29, 4741–4751. doi: 10.1038/onc.2010.215

Somarelli, J. A., Shetler, S., Jolly, M. K., Wang, X., Bartholf Dewitt, S., Hish, A. J., et al. (2016). Mesenchymal-Epithelial transition in sarcomas is controlled by the combinatorial expression of MicroRNA 200s and GRHL2. *Mol. Cell. Biol.* 36, 2503–2513. doi: 10.1128/MCB.00373-16

Song, N., Jing, W., Li, C., Bai, M., Cheng, Y., Li, H., et al. (2018). ZEB1 inhibition sensitizes cells to the ATR inhibitor VE-821 by abrogating epithelial-mesenchymal transition and enhancing DNA damage. *Cell Cycle* 17, 595–604. doi: 10.1080/15384101.2017.1404206

Song, X. F., Chang, H., Liang, Q., Guo, Z. F., and Wu, J. W. (2017). ZEB1 promotes prostate cancer proliferation and invasion through ERK1/2 signaling pathway. *Eur. Rev. Med. Pharmacol. Sci.* 21, 4032–4038.

Spike, B. T., and Wahl, G. M. (2011). P53, stem cells, and reprogramming: tumor suppression beyond guarding the genome. *Genes Cancer* 2, 404–419. doi: 10.1177/1947601911410224

Svirnovski, A. I., Serhiyenka, T. F., Kustanovich, A. M., Khlebko, P. V., Fedosenko, V. V., Taras, I. B., et al. (2010). DNA-PK, ATM and MDR proteins inhibitors in overcoming fludarabine resistance in CLL cells. *Exp. Oncol.* 32, 258–262.

Tian, Y., Pan, Q., Shang, Y., Zhu, R., Ye, J., Liu, Y., et al. (2014). MicroRNA-200 (miR-200) cluster regulation by achaete scute-like 2 (Ascl2): impact on the epithelial-mesenchymal transition in colon cancer cells. *J. Biol. Chem.* 289, 36101–36115. doi: 10.1074/jbc.M114.598383

Vandewalle, C., Van Roy, F., and Berx, G. (2009). The role of the ZEB family of transcription factors in development and disease. *Cell Mol. Life Sci.* 66, 773–787. doi: 10.1007/s00018-008-8465-8

Voulgari, A., and Pintzas, A. (2009). Epithelial-mesenchymal transition in cancer metastasis: mechanisms, markers and strategies to overcome drug resistance in the clinic. *Biochim. Biophys. Acta* 1796, 75–90. doi: 10.1016/j.bbcan.2009.03.002

Wang, H., Naghavi, M., Allen, C., Barber, R., Bhutta, Z., Carter, A., et al. (2016). Global, regional, and national life expectancy, all-cause mortality, and cause-specific mortality for 249 causes of death, 1980-2015: a systematic analysis for the global burden of disease study 2015. *Lancet* 388, 1459–1544. doi: 10.1016/S0140-6736(16)31012-1

Wang, Z., Chen, Y., Lin, Y., Wang, X., Cui, X., Zhang, Z., et al. (2017). Novel crosstalk between KLF4 and ZEB1 regulates gemcitabine resistance in pancreatic ductal adenocarcinoma. *Int. J. Oncol.* 51, 1239–1248. doi: 10.3892/ijo.2017.4099

Watanabe, K., Panchy, N., Noguchi, S., Suzuki, H., and Hong, T. (2019). Combinatorial perturbation analysis reveals divergent regulations of mesenchymal genes during epithelial-to-mesenchymal transition. *NPJ Syst. Biol. Appl.* 5:21. doi: 10.1038/s41540-019-0097-0

Werth, M., Walentin, K., Aue, A., Schonheit, J., Wuebken, A., Pode-Shakked, N., et al. (2010). The transcription factor grainyhead-like 2 regulates the molecular composition of the epithelial apical junctional complex. *Development* 137, 3835–3845. doi: 10.1242/dev.055483

Wu, Y., Jin, D., Wang, X., Du, J., Di, W., An, J., et al. (2019a). UBE2C induces cisplatin resistance via ZEB1/2-dependent upregulation of ABCG2 and ERCC1 in NSCLC cells. *J. Oncol.* 2019:8607859. doi: 10.1155/2019/8607859

Wu, Y., Yang, X., Chen, Z., Tian, L., Jiang, G., Chen, F., et al. (2019b). M(6)A-induced lncRNA RP11 triggers the dissemination of colorectal cancer cells via upregulation of Zeb1. *Mol. Cancer* 18:87. doi: 10.1186/s12943-019-1014-2

Xu, J., Li, Y., Wang, F., Wang, X., Cheng, B., Ye, F., et al. (2013). Suppressed miR-424 expression via upregulation of target gene Chk1 contributes to the progression of cervical cancer. *Oncogene* 32, 976–987. doi: 10.1038/onc.2012.121

Xu, L., Zhang, Y., Qu, X., Che, X., Guo, T., Cai, Y., et al. (2017). E3 ubiquitin ligase Cbl-b prevents tumor metastasis by maintaining the epithelial phenotype in multiple drug-resistant gastric and breast cancer cells. *Neoplasia* 19, 374–382. doi: 10.1016/j.neo.2017.01.011

Xu, M., Zhu, C., Zhao, X., Chen, C., Zhang, H., Yuan, H., et al. (2015). Atypical ubiquitin E3 ligase complex Skp1-Pam-Fbxo45 controls the core epithelial-to-mesenchymal transition-inducing transcription factors. *Oncotarget* 6, 979–994. doi: 10.18632/oncotarget.2825

Yang, J., and Weinberg, R. A. (2008). Epithelial-mesenchymal transition: at the crossroads of development and tumor metastasis. *Dev. Cell* 14, 818–829. doi: 10.1016/j.devcel.2008.05.009

Yang, X., Li, L., Huang, Q., Xu, W., Cai, X., Zhang, J., et al. (2015). Wnt signaling through Snail1 and Zeb1 regulates bone metastasis in lung cancer. *Am. J. Cancer Res.* 5, 748–755.

Yin, Y., Liu, W., Shen, Q., Zhang, P., Wang, L., Tao, R., et al. (2019). The DNA endonuclease Mus81 regulates ZEB1 expression and serves as a target of BET4 inhibitors in gastric cancer. *Mol. Cancer Ther.* 18, 1439–1450. doi: 10.1158/1535-7163.MCT-18-0833

Zhang, J., and Ma, L. (2012). MicroRNA control of epithelial-mesenchymal transition and metastasis. *Cancer Metastasis Rev.* 31, 653–662. doi: 10.1007/s10555-012-9368-6

Zhang, P., Sun, Y., and Ma, L. (2015). ZEB1: at the crossroads of epithelial-mesenchymal transition, metastasis and therapy resistance. *Cell Cycle* 14, 481–487. doi: 10.1080/15384101.2015.1006048

Zhang, P., Wang, L., Rodriguez-Aguayo, C., Yuan, Y., Debeb, B. G., Chen, D., et al. (2014a). MiR-205 acts as a tumour radiosensitizer by targeting ZEB1 and Ubc13. *Nat. Commun.* 5:5671. doi: 10.1038/ncomms6671

Zhang, P., Wei, Y., Wang, L., Debeb, B. G., Yuan, Y., Zhang, J., et al. (2014b). ATM-mediated stabilization of ZEB1 promotes DNA damage response and radioresistance through CHK1. *Nat. Cell Biol.* 16, 864–875. doi: 10.1038/ncb3013

Zhang, S., Tang, Z., Qing, B., Tang, R., Duan, Q., Ding, S., et al. (2019). Valproic acid promotes the epithelial-to-mesenchymal transition of breast cancer cells through stabilization of Snail and transcriptional upregulation of Zeb1. *Eur. J. Pharmacol.* 865:172745. doi: 10.1016/j.ejphar.2019.172745

Zhang, X., Zhang, Z., Zhang, Q., Sun, P., Xiang, R., Ren, G., et al. (2018). ZEB1 confers chemotherapeutic resistance to breast cancer by activating ATM. *Cell Death Dis.* 9:57. doi: 10.1038/s41419-017-0087-3

Zhang, Y., Xu, L., Li, A., and Han, X. (2019). The roles of ZEB1 in tumorigenic progression and epigenetic modifications. *Biomed. Pharmacother.* 110, 400–408. doi: 10.1016/j.biopha.2018.11.112

Zhang, Z., Yin, J., Lu, C., Wei, Y., Zeng, A., and You, Y. (2019). Exosomal transfer of long non-coding RNA SBF2-AS1 enhances chemoresistance to temozolomide in glioblastoma. *J. Exp. Clin. Cancer Res.* 38:166. doi: 10.1186/s13046-019-1139-6

Zheng, X., Carstens, J. L., Kim, J., Scheible, M., Kaye, J., Sugimoto, H., et al. (2015). Epithelial-to-mesenchymal transition is dispensable for metastasis but induces chemoresistance in pancreatic cancer. *Nature* 527, 525–530. doi: 10.1038/nature16064

Zhou, Y., Zhu, Y., Fan, X., Zhang, C., Wang, Y., Zhang, L., et al. (2017). NID1, a new regulator of EMT required for metastasis and chemoresistance of ovarian cancer cells. *Oncotarget* 8, 33110–33121. doi: 10.18632/oncotarget.16145

Zhou, Z., Zhang, P., Hu, X., Kim, J., Yao, F., Xiao, Z., et al. (2017). USP51 promotes deubiquitination and stabilization of ZEB1. *Am. J. Cancer Res.* 7, 2020–2031.

Conflict of Interest: The authors declare that the research was conducted in the absence of any commercial or financial relationships that could be construed as a potential conflict of interest.

Copyright © 2020 Drápela, Bouchal, Jolly, Culig and Souček. This is an open-access article distributed under the terms of the Creative Commons Attribution License (CC BY). The use, distribution or reproduction in other forums is permitted, provided the original author(s) and the copyright owner(s) are credited and that the original publication in this journal is cited, in accordance with accepted academic practice. No use, distribution or reproduction is permitted which does not comply with these terms.

frontiers in Molecular Biosciences

REVIEW
published: 23 April 2020
doi: 10.3389/fmolb.2020.00071

New Insights Into the Role of Phenotypic Plasticity and EMT in Driving Cancer Progression

Sugandha Bhatia[1,2], Peiyu Wang[1,2], Alan Toh[1,2] and Erik W. Thompson[1,2]*

[1] *Institute of Health and Biomedical Innovation and School of Biomedical Sciences, Queensland University of Technology, Brisbane, QLD, Australia,* [2] *Translational Research Institute, Brisbane, QLD, Australia*

Tumor cells demonstrate substantial plasticity in their genotypic and phenotypic characteristics. Epithelial-mesenchymal plasticity (EMP) can be characterized into dynamic intermediate states and can be orchestrated by many factors, either intercellularly via epigenetic reprograming, or extracellularly via growth factors, inflammation and/or hypoxia generated by the tumor stromal microenvironment. EMP has the capability to alter phenotype and produce heterogeneity, and thus by changing the whole cancer landscape can attenuate oncogenic signaling networks, invoke anti-apoptotic features, defend against chemotherapeutics and reprogram angiogenic and immune recognition functions. We discuss here the role of phenotypic plasticity in tumor initiation, progression and metastasis and provide an update of the modalities utilized for the molecular characterization of the EMT states and attributes of cellular behavior, including cellular metabolism, in the context of EMP. We also summarize recent findings in dynamic EMP studies that provide new insights into the phenotypic plasticity of EMP flux in cancer and propose therapeutic strategies to impede the metastatic outgrowth of phenotypically heterogeneous tumors.

Keywords: EMT, EMP, stem cell, CTCs, hybrid EMT states, metastasis, metabolism, tumor cell heterogeneity

OPEN ACCESS

Edited by:
Satyendra Chandra Tripathi, All India Institute of Medical Sciences Nagpur, India

Reviewed by:
Surendra Kumar Shukla, University of Nebraska Medical Center, United States
Abhijit De, Tata Memorial Hospital, India

****Correspondence:***
Sugandha Bhatia
sugandha.bhatia@hdr.qut.edu.au; sugandhabhatia05@gmail.com

Specialty section:
This article was submitted to Molecular Diagnostics and Therapeutics, a section of the journal Frontiers in Molecular Biosciences

Received: *25 January 2020*
Accepted: *30 March 2020*
Published: *23 April 2020*

Citation:
Bhatia S, Wang P, Toh A and Thompson EW (2020) New Insights Into the Role of Phenotypic Plasticity and EMT in Driving Cancer Progression. Front. Mol. Biosci. 7:71. doi: 10.3389/fmolb.2020.00071

INTRODUCTION (EMT-MET)

Epithelial–mesenchymal transition (EMT), in which epithelial cells undergo dynamic cellular transition from a sessile epithelial state to a motile mesenchymal state allowing the formation of new tissues, is considered one of the pivotal processes during embryogenesis and organogenesis (Chaffer et al., 2007; Yang and Weinberg, 2008). The process of EMT (classified as three different subtypes) has been implicated in a broad range of normal and pathophysiological processes from development, wound healing and tissue regeneration (type I), to organ fibrosis (type 2), and cancer progression (type 3) (Kalluri and Weinberg, 2009). During cancer progression, it is postulated that epithelial-derived carcinoma cells undergo a reversible, trans-differentiation process with changes in cell–cell adhesion and polarity, cytoskeletal remodeling, migratory and invasive enhancement, and dissemination into secondary organs via local invasion, intravasation and transfer through the blood stream and lymphatics (Polyak and Weinberg, 2009). In addition to cellular migration during metastasis, EMT also influences resistance to anoikis and apoptosis, blocks senescence, enhances survival, facilitates genomic instability, causes cancer stem cell (CSC) activity, alters

metabolism, and induces drug resistance and immune suppression (Przybylo and Radisky, 2007; Ansieau et al., 2008; Gal et al., 2008; Kumar et al., 2011; Huang et al., 2013; Dongre et al., 2017; Lee et al., 2018; Redfern et al., 2018).

After invasion and spread, cancer recurrence at the metastatic site is thought to require the reverse process, termed mesenchymal to epithelial transition (MET) (Chaffer et al., 2007; Hugo et al., 2007; Brabletz, 2012). The reversal of EMT, referred to as MET, has received less attention than EMT in the establishment of metastasis. Microenvironmental cues are considered a major deterministic factor for the reversion of the migratory mesenchymal neoplastic cells and the subsequent development of macrometastases. However, the re-expression of E-cadherin, inhibition of SNAIL, and β-catenin sequestration have provided evidence of MET in liver metastasis from MDA-MB-231 (Chao et al., 2010; Brabletz, 2012), as has the anti-metastatic effects of sustained pro-mesenchymal signals (Ocana et al., 2012; Tsai et al., 2012). The concept of MET in metastasis is refuted in some of the cancer recurrence studies as no definitive proof of a MET requirement was obtained in the MMTV-PyMT genetically engineered mouse model (GEMMs) of metastatic breast cancer or in the KPC GEMM for metastatic pancreatic cancer (Fischer et al., 2015; Zheng et al., 2015). Nevertheless, recent data on EMP phenomena during metastatic cancer colonization is emerging (Chao et al., 2010; Rhim et al., 2012; Nieto, 2013; Beerling et al., 2016; Pastushenko et al., 2018) and could be of particular interest in breast and pancreatic carcinomas where EMT is considered an early event in tumorigenesis (Hüsemann et al., 2008; Rhim et al., 2012). Moreover, other studies have reported at least partial involvement of EMP in the breast model (Ye et al., 2015) and Zeb1 has been shown to contribute to metastasis in the pancreatic model (Krebs et al., 2017).

Considerably less information is available on the key intrinsic factors that drive MET *in vivo* and *in vitro*, while the drivers and transcriptional mediators of EMT are quite comprehensively documented (Stemmler et al., 2019). Bone morphogenetic protein 7 (BMP7) is reported to trigger MET in renal fibroblasts during kidney development (Zeisberg et al., 2005), and also in breast cancer cells, reducing their capability to form bone metastases (Buijs et al., 2007). Protein Kinase A was recently identified as an inducer of MET in human mammary epithelial cells (Pattabiraman et al., 2016). The role of Notch4 in melanoma cells to induce MET and suppress malignancy in mice has also been reported (Bonyadi Rad et al., 2016). The course of epigenetic reprograming is also supporting EMT and MET acquisition (Tamura et al., 2000). Reversible epigenetic changes acquired during EMT underpin the emergence of self-renewal and chemo-refractory stem cell-like features, which can revert to the MET phenotype for establishing metastasis (Voulgari and Pintzas, 2009; Sharma et al., 2010). Here, we discuss the role and the regulatory mechanisms of EMP, with the focus on recent emerging concepts that highlights the bidirectional dynamics of this phenomenon and the hybrid intermediate states. We also provide a brief overview of various techniques/modalities employed to analyze EMP in cancer. Understanding the phenotypic plasticity will provide insights for various therapeutic strategies that can be implemented to prevent/restrict spread of cancer by metastasis.

SIGNIFICANCE OF EMP AND HYBRID EMT STATES

Epithelial–mesenchymal transition, however, is not a two-step event through which cancer cells lose epithelial markers and acquire mesenchymal traits between two rigid phenotypes. Rather, studies performed within the last decade increasingly show that cancer cells sequentially acquire mesenchymal traits, but don't automatically dissipate all of their previously expressed epithelial features (Tam and Weinberg, 2013; Aiello and Kang, 2019). The term "epithelial–mesenchymal plasticity" (EMP) is more favored recently as compared to EMT-MET (Bhatia et al., 2017; Williams et al., 2019). The multiple signal transduction cascade for EMT-MET programing results in dynamic and intermediate transitional states wherein, the cancer cells can reside in all three EMP phenotypes (epithelial, mesenchymal and hybrid phenotype). EMP reflects the bidirectional flux often in a continuum across the full spectrum (Lee et al., 2006; Oltean et al., 2006). Thus, a full spectrum of EMP endows the formation of a new carcinomatous tumor at distant organ sites with similar histopathology as observed in primary tumor (Gunasinghe et al., 2012).

Hybrid epithelial-mesenchymal features of carcinoma cells have indeed been observed in various invasive carcinoma model systems (Lee et al., 2006; Klymkowsky and Savagner, 2009), in which individual cells co-express markers of both epithelial and mesenchymal lineages, and circulating tumor cells (CTCs) in particular have been shown to exhibit a spectrum of EMP states (Armstrong et al., 2011; Yu et al., 2014; Khoo et al., 2015; Bourcy et al., 2016); reviewed in McInnes et al. (2015); Hassan et al. (2020). The hybrid EMP state seen in carcinomas and CTCs, in which individual cells co-express markers of both epithelial and mesenchymal lineages, is predicted to have the highest tumourigenicity and metastatic potential (Lee et al., 2006; Klymkowsky and Savagner, 2009; Jolly et al., 2016; Kroger et al., 2019; Pastushenko and Blanpain, 2019). An emerging challenge is also to decipher correctly the contribution that intermediate states of the EMT spectrum make to tumor evolution for therapeutic interventions.

EXTRINSIC AND INTRINSIC MECHANISMS AND REGULATORS INVOLVED IN PLASTICITY

The crosstalk mediated by autocrine and/or paracrine factors secreted by cancer cells and tumor stroma has been widely proven to occur via extracellular mediators of EMT (Scheel et al., 2011). A host of extracellular mediators secreted by tumor stromal cells are already proven to elicit EMT induction. Examples of validated extracellular mediators as EMT inducers include TGF-β (Buonato et al., 2015), EGF (Hugo et al., 2009), FGF (Kurimoto et al., 2016), PDGF (Devarajan et al., 2012),

HGF (Suarez-Causado et al., 2015), IGF (Wang et al., 2016), Interleukin-6 (IL-6) (Miao et al., 2014), WNT (Ochoa-Hernandez et al., 2012), Hedgehog (Yoo et al., 2011), and Notch (Yuan et al., 2014). Other inducers of EMT include collagen types I and III, matrix metalloproteinases-2 (MMP-2), MMP-3, MMP-9, and MMP14/MT1-MMP (Thiery et al., 2009). YAP and TAZ are also emerging as key modulators in inducing plasticity and skin cancer initiation (Moroishi et al., 2015; Debaugnies et al., 2018). EMT of tumor cells can also be induced by various stimuli from the tumor microenvironment (Marcucci et al., 2014); Fabrizio Marcucci and his colleagues proposed five major classes of these stimuli in 2016 (Marcucci et al., 2016): hypoxia and low pH, innate and adaptive immune responses, mechanical stress, altered ECM and treatment with chemotherapeutics (**Figure 1**).

Interestingly, hypoxic features in the tumor microenvironment can stimulate EMT as a downstream consequence of upregulated hypoxia-inducible factor 1α (HIF1α) (Wong et al., 2012). Apart from tumor microenvironment stimuli for EMT induction, stimulus-independent activation of signaling pathways, caused by mutations or epigenetic modifications leading to overexpression of certain pathway components, can also trigger EMT (Wallin et al., 2012; Serrano-Gomez et al., 2016). Gain-of-function mutations in P53 has been reported to induce EMT via modulation of miR-130b-Zeb1 axis (Dong P. et al., 2013).

Epigenetic modifications can also cause a shift of epithelial to mesenchymal state; for example, aberrant DNA CpG island methylation correlated with the repression of the miR-200 cluster, which promotes EMT and contributes to tumor progression (Vrba et al., 2010). LSD1-dependent genome-scale epigenetic reprograming was also observed during EMT (McDonald et al., 2011; Tang et al., 2013; Boulding et al., 2019). Various other chromatin regulators (e.g., DNMT1, KDM6B, PHF8, EZH2, and HDAC) are also reported to regulate EMT, genomic stability and metastasis (Suvà et al., 2013; Lu and Kang, 2019). Apart from epigenetics and mutations, EMT can also be modulated at transcriptional, post-transcriptional, translational and post-translational levels. The intrinsic gene network regulators, via alternate splice isoforms of ESRP1/2, microRNAs and long non-coding RNAs, also acts as other distinctive mechanisms to induce EMT (Aiello et al., 2018; Aiello and Kang, 2019). It has been postulated that during chemotherapy regimens, undifferentiated cancer cells also commence EMT, causing therapy resistance, CSC-like behavior, and a high propensity for metastasize. Tumor relapse after drug treatment cessation is due to persistence of disseminated CSC with mesenchymal features (Witta et al., 2006). Redfern et al. (2018) have also recently shown shorter overall survival times in patients treated with EMT-inducing agents compared to agents known to inhibit EMT.

The expression changes of various key molecular markers during EMT, are represented in **Figure 1** (Christiansen and Rajasekaran, 2006; Pastushenko and Blanpain, 2019). The transition of epithelial cells to a more mesenchymal state is also characterized by reduced intracellular adhesion through the downregulation of E-cadherin (CDH1) and EpCAM, and gain of mesenchymal markers such as N-cadherin (CDH2), vimentin and FSP1/S100A4 (Francart et al., 2018). Repressors of E-cadherin can be divided into groups that modulate either directly or indirectly effects on gene transcription by binding to promoter sites. ZEBs, SNAIL1 and KLF8 repress expression by binding the E-cadherin promotor, thereby inactivating transcription, while E2.2, FOXC2, GOOSECOID, and TWIST repress E-cadherin transcription as indirect repressors (Peinado et al., 2004, 2007; Xu et al., 2019). These factors also share an elaborate interactome, in that SNAIL1 upregulates SNAIL2 and TWIST (Thuault et al., 2008; Smit et al., 2009), SNAIL1 and TWIST then induce ZEB1 and SNAIL2 (Casas et al., 2011; Dave et al., 2011), and SNAIL2 induces ZEB2 (Thuault et al., 2008). Although commonly serving as repressors of E-cadherin, these broader mechanisms also selectively modulate other programs

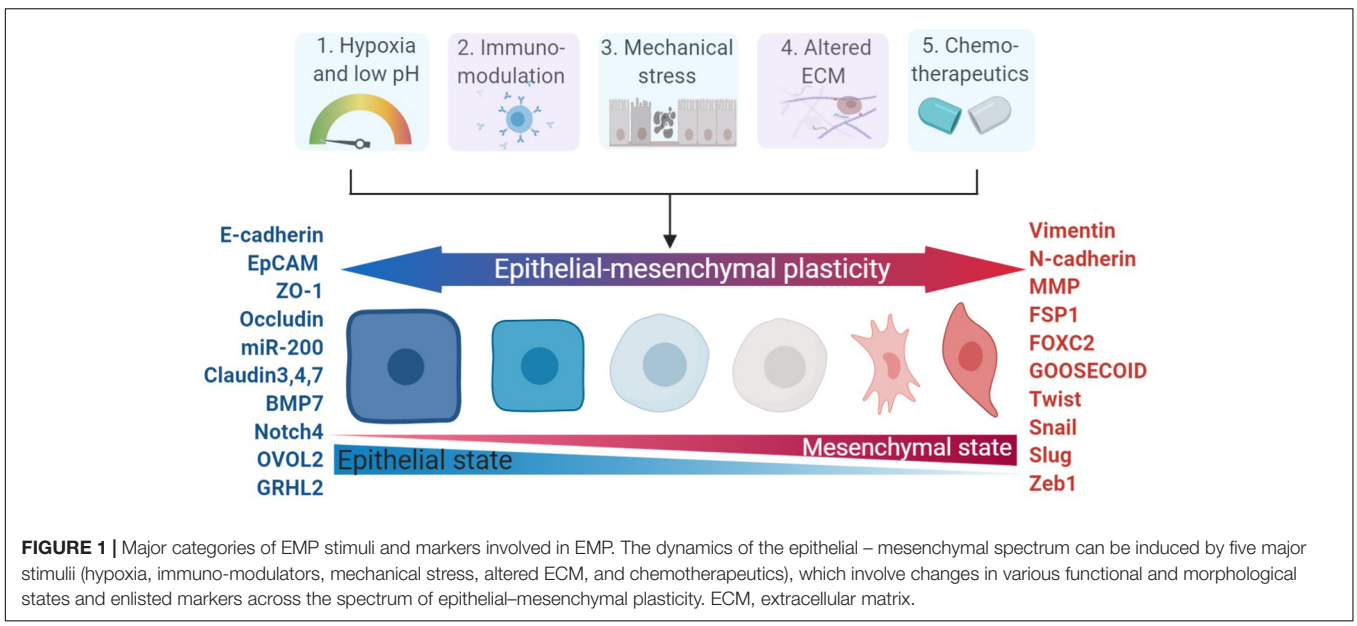

FIGURE 1 | Major categories of EMP stimuli and markers involved in EMP. The dynamics of the epithelial – mesenchymal spectrum can be induced by five major stimulii (hypoxia, immuno-modulators, mechanical stress, altered ECM, and chemotherapeutics), which involve changes in various functional and morphological states and enlisted markers across the spectrum of epithelial–mesenchymal plasticity. ECM, extracellular matrix.

involved in cell division, cell survival, and cell attachment, thereby resulting in a motile, invasive and resistant cell phenotype (Barrallo-Gimeno and Nieto, 2005).

ROLE OF EMT IN TUMOR INITIATION, PROGRESSION AND METASTASIS

Although much less studied than later tumor stages, a number of studies have made a connection between the linkage of EMT to stemness and tumor-initiating capacity (Mani et al., 2008; Morel et al., 2008). In some carcinoma cells, overexpression of EMT transcription factors (EMT-TFs) has been observed to drive and enhance tumorigenicity (Wellner et al., 2009), and in particular, EMT has been shown to cause avoidance of oncogene-induced senescence (Ansieau et al., 2008). In a mouse skin SCC model, low levels of TWIST was explicitly responsible for the tumor initiation process, whereas higher levels of TWIST induced EMT and tumor progression (Beck et al., 2015). In recent lineage tracing studies along with transcriptional and epigenomic profiling, Latil et al found disparities in the tumors generated from interfollicular epidermis (IFE) and hair follicle (HF) stem cells (Lgr5CreER). While IFE tumors showed a well-differentiated phenotype, tumors generated from HF stem cells displayed an EMT spectrum and increased metastatic potential (Latil et al., 2017).

The profound role of EMP in tumor progression and metastasis *in vivo* has remained a topic with various controversies (Brabletz et al., 2018; Williams et al., 2019). The number of mesenchymal cells observed in primary cancers in many xenograft studies had been observed to be less than 10%. Although the specific dissemination process of these cells is not yet well documented (Bhatia et al., 2019; Lourenco et al., 2020), enrichment of EMT in circulating tumor cells has supported a role for EMT in the initial steps of metastasis. Various studies have highlighted the role of key EMT TFs, such as Slug and Zeb1, in promoting metastasis of breast and colorectal cancer to liver and lung, respectively (Spaderna et al., 2008; Guo et al., 2012). Downregulation of TWIST expression in highly metastatic mammary carcinoma cells was found to inhibit their metastatic seeding ability in the lung (Yang et al., 2004). However, these studies are nuanced by observations that enforced overexpression or downregulation of EMT-TFs doesn't recapitulate the dynamic spectrum of transitional and/or partial EMT states discovered *in vivo* (Pastushenko et al., 2018). Similarly, the studies from the genetic abrogation of Twist or Snail in mouse models of pancreatic adenocarcinoma and from EMT lineage tracing using Fsp1 and β-actin promoter in breast cancer mouse model have questioned the indispensability of full mesenchymal transition in the metastasis process (Fischer et al., 2015; Zheng et al., 2015). The conclusions of these studies have been subsequently refuted by other studies where genetic depletion of Zeb1 in the same pancreatic model resulted in strong suppression of metastasis. Therefore, caution is required while interpreting such results as the context of EMT and other compensatory mechanisms may significantly influence their role in promoting metastasis (Aiello et al., 2017; Ye et al., 2017). With the advent of cell fate mapping studies using intra-vital imaging, plasticity was revealed in mouse breast tumor cells from primary site to its re-epithelisation upon metastasis (Beerling et al., 2016). Several other studies have also reported the direct evidence of EMP under physiological conditions (Rhim et al., 2012; Chaffer et al., 2013; Ye et al., 2015). Multiple tumor subpopulations screened from mammary and skin tumors suggested that tumor cells with hybrid phenotypes were more efficient in dissemination and metastasis (Pastushenko et al., 2018; Thompson and Nagaraj, 2018; Pastushenko and Blanpain, 2019; Rios et al., 2019). Similar, other relevant studies are also emerging to suggest that cancer cells mostly transition between epithelial/mesenchymal and hybrid intermediate states, but rarely undergo complete EMT during metastasis (Kroger et al., 2019).

EMP ANALYSIS OF CIRCULATING TUMOR CELLS (CTCS)

Generation of CTCs is regarded as a consequential effect of the multi-step processes that constitute the metastasic cascade (Lambert et al., 2017), and have become a particularly rich source of evidence and information regarding the role of EMP in cancer progression. Understanding the biology and characteristics of CTCs can provide important insights into the molecular and cellular requirements of cancer cells during metastatic spread. Observations of enriched levels of mesenchymal genes (e.g., N-cadherin, vimentin and Twist) and reduced expression of epithelial genes (e.g., E-cadherin, EpCAM and CK8/18/19) has been reported in the CTCs relative to cells in the tumors of origin in the breast cancer patients (Yu et al., 2013; Wang et al., 2018). Although many CTCs exhibit a mesenchymally enriched phenotype, some researchers have revealed that a small population of CTCs co-expressed both epithelial and mesenchymal (E/M) hybrid phenotype traits, which likely promoted cell migration, cell invasion and cell survival capabilities (Lecharpentier et al., 2011; Milano et al., 2018). Hence hybrid CTCs may be more metastatic than mesenchymal CTCs.

High numbers of CTCs in blood is significantly associated with poor prognosis in several carcinoma types, such as prostate cancer (Wang et al., 2011), breast cancer (Bulfoni et al., 2016), pancreatic cancer (Han et al., 2014), lung cancer (Naito et al., 2012), and increasingly these have taken account of CTC phenotypes (Tachtsidis et al., 2016). Pan et al. (2019) conducted a correlation study between CTC phenotypes and clinicopathological features of early cervical cancer, finding lower CTC counts in stage I patients than stage II patients with pelvic lymph node metastasis, but also that mesenchymal CTCs expressing vimentin and TWIST were more commonly found in the latter. Consistently, Markiewicz et al. (2014) selectively found of *VIM*, *SNAI1*, and *UPAR* expression in mesenchymal CTCs derived from breast cancer patient with lymph nodes metastases. Due to the low number of CTCs in blood, the greatest challenge in studying CTCs is the detection and isolation of these cells from patients' blood (Kowalik et al., 2017). Molecular profiling of EMT markers in CTCs has been used to establish tools to isolate

and classify CTCs. RNA *in situ* hybridization (RNA-ISH) is a detection method that employs specific probes targeting different epithelial and mesenchymal genes to detect multiple transcripts simultaneously (Lopez-Munoz and Mendez-Montes, 2013). An enhanced RNA-ISH-based detection system, CTCscope, was innovated to detect eight epithelial markers and three EMT markers (Payne et al., 2012), and has been employed successfully in the landmark breast cancer CTC study (Yu et al., 2013; Wang et al., 2018). The FDA-approved CELLSEARCH® system (Menarini-Silicon Biosystems, Inc.), which immunocaptures EpCAM-expressing CTCs for patient prognosis (Riethdorf et al., 2007), is intrinsically biased toward predominantly epithelial CTCs. However, recent CTC studies have employed microfluidic devices to capture and isolate CTCs according to their size and deformability, which allows for better coverage of different phenotypic states (Lemaire et al., 2018; Ribeiro-Samy et al., 2019).

Although the devices used to isolate CTCs have improved the quality and quantity assessment of CTCs, there are still limitations when studying CTCs. Over the past few years, use of the revolutionary single- cell RNA sequencing (scRNA-seq) has emerged to assess genome-wide expression profiles of isolated CTC populations and CTC clusters. Aceto et al. (2014) conducted scRNA-seq on endogenous CTCs generated using tumor xenografts of LM2 variant of MDA-MB-231 human breast cancer cells, showing that CTC clusters are oligoclonal and highly metastatic compared to single CTCs. It was found that the cell junction protein plakoglobin (JUP) mediates cell cluster formation, enhancing the metastatic potential of CTCs. Ting et al. (2014) performed scRNA-seq analysis on CTCs in a mouse pancreatic cancer model, and revealed a universal loss of the epithelial markers E-cadherin (*Cdh1*) and Mucin-1 (*Muc1)* across all CTCs compared with the primary xenograft tumors. Hugo et al. (2017) showed that both *in vitro* and *in vivo* knockdown of *Cdh1* in MDA- MB-468 breast cancer cells reduced proliferation, and this was also reported by Padmanaban et al. (2019), who further indicated that the loss of *Cdh1* increased invasion capacity while reducing cell survival, CTC number and metastasis spread in the breast cancer.

The interconnection between CTC, EMT and CSC has been actively studied and reported to harbor important mechanisms underlying tumourigenicity (Agnoletto et al., 2019). EMT generates stem-like cells (Mani et al., 2008) and tumor cells that features both EMT and stem-like characters are better equipped to induce metastasis (May et al., 2011; Barriere et al., 2014), while some CTCs have dynamic cellular plasticity expressing EMT traits and stemnicity (Alonso-Alconada et al., 2014). A minor fraction of EMT hybrid phenotype CTCs have been shown to exhibit stem-like features, and these cells have been shown to promote collective migration Kaigorodova et al. (2017); Quan et al. (2020), as well as enhanced survivability and chemoresistant (Papadaki et al., 2019). Papadaki et al. (2019) modeled four CTC subpopulations based on the co-expression of three different markers; cytokeratin (epithelial marker), ALDH1 (stemness marker) and TWIST1 (partial EMT marker), and revealed that CTCs co-expressing cytokeratin, high levels of ALDH1, and nuclear TWIST1 (CSC^+/partial-EMT^+) were enriched after the first-line chemotherapy, implying that they were the most chemoresistant subpopulation, and had a favored prognostic value in patients with metastatic breast cancer. Another study has showed that $EpCAM^{high}$ CTCs were significantly associated with poor prognosis compared to $EpCAM^{low}$ CTCs in patients with breast and prostate cancer (de Wit et al., 2018), however the level of mesenchymal co-expression was not measured. Ting et al. (2014) showed that the stem cell markers *Aldh1a1* and *Aldh1a2* were enriched in pancreatic CTCs, and they also demonstrated that *Igfbp5* (a transport protein of epithelial stroma) and *SPARC* (a collagen-binding glycoprotein related to ECM reorganization) were highly expressed in the CTCs. Although they stated that there was no intrinsic correlation between EMP state and stemness in their CTCs, other reports have shown expression of these genes were associated with Cdh1 reduction (Bradshaw, 2009; Sureshbabu et al., 2012). There still remains a lack of evidence to fully elucidate the mechanistic relationship between CTCs, EMT and CSCs through the association of their existing markers with functional features, although it seems clear that they represent only a small fraction of CTCs.

UNDERSTANDING DYNAMICS OF EMT

In the last two decades, many new concepts and findings have flourished around the dynamics of EMP. The dynamics of the stochastic state transitions, which allows cancer cells to switch between phenotypic states, is not yet explicitly described. However, novel concepts of dynamic equilibrium, asymmetrical dynamics of EMT-MET conversions, bet hedging, and hysteresis/cellular memory of cancer cells have heralded a deeper understanding of the phenotypic heterogeneity that cancer cells endow/possess (Jolly and Celià-Terrassa, 2019). This intrinsic mechanism of bi-directional transitions between epithelial (differentiated) and mesenchymal (stem-like) states is reported in different kinds of cancer (Polyak and Weinberg, 2009; Chaffer et al., 2011; Gupta et al., 2011; Yang et al., 2012; Ruscetti et al., 2016; Bhatia et al., 2019). Sequencing of breast cancer stem cell populations also indicates a dynamic conversion between differentiation states *in vivo* (Klevebring et al., 2014). A phenotypically stable equilibrium was observed in breast cancer cell lines, differentially segregated across cell state proportions (Gupta et al., 2011; Bhatia et al., 2019). DNA barcoding and subsequently high-throughput sequencing of breast cancer cell clones had also been employed to quantify the extent of intrinsic phenotypic plasticity exhibiting epithelial or mesenchymal phenotypes (Mathis et al., 2017; Rios et al., 2019). Various mechanism-based mathematical modeling and data-based statistical modeling approaches have been developed in an attempt to uncover the presence of these metastable states (Lu et al., 2013; Jolly et al., 2016; Jolly and Celià-Terrassa, 2019).

The presence of "multiple attractor states" based on Waddington landscape and intrinsic cellular variability also contributes to phenotypic plasticity (Huang et al., 2009; Ferrell, 2012; Li et al., 2016). The studies pertaining to EMT and MET reversion have also explained explicitly that the dynamics achieved for its reversion back may not follow the same path. For example, studies with a Snail-inducible expression system

in prostate cancer cells has identified metabolic plasticity and asymmetrical dynamics during their EMT-MET cycle (Stylianou et al., 2019). Other studies, where re-expression of significant epithelial markers such as E-cadherin, OVOL2 and GRHL2 after their knockout may not obtain the same spectrum of reversion also suggests asymmetrical dynamics (Qi et al., 2018; Chung et al., 2019; Jolly et al., 2019). The concept of bet hedging had been observed in bacterial persistence under different environmental stimulations by generating mutation-independent phenotypic heterogeneity (Veening et al., 2008). This pre-existing phenotypic heterogeneity is thought to be exploited by cancer cells in generating drug-persistence cells via non-genetic mechanism, which might lead to anti-drug resilience in clinical scenarios (Jolly et al., 2018). The property of hysteresis and "cellular memory" allows cells from the same clonal population to respond differently to the same strength and duration of a signal. The differential response again can be attributed to the cellular placement across different "attractor states" or the possibility of history of input stimuli (Chang et al., 2006; Jolly and Celià-Terrassa, 2019). The possibility of EMT occurring via non-linear hysteretic mode had been recently observed to result in different dynamics and increased metastasis in a breast cancer model (Celià-Terrassa et al., 2018). Thus, these dynamics impart a further layer of intricacies in understanding the causes and reasons of non-genetic heterogeneity in cancer in regard to phenotypic plasticity. An integrative understanding of the approaches to block this phenotypic plasticity and EMP dynamics could further aid in combating cancer resistance.

IMPLICATIONS OF METABOLIC PLASTICITY AND EMP

During the processes of EMP, there are numerous adaptations, not only in cell morphology and epigenetic changes, but also in metabolism (Cha et al., 2015). Among them, glucose and lipid metabolism alterations are crucial for the EMT induction (Kondaveeti et al., 2015; Sánchez-Martínez et al., 2015; Morandi et al., 2017; Kang et al., 2019). In terms of carbohydrate metabolism, it is well known that cancer cells prefer to reply on the glycolysis to generate ATP instead of oxidative phosphoruylation (OXPHOS), even under the well-oxygenated conditions, according to the Warburg effect (Warburg, 1956). However, apart from the Warburg effect, other glucose metabolic pathway adaptations have been observed during the last decade. When cancer cells undergo an EMP process, their metabolism will reprogram from aerobic glycolysis for proliferation to EMT-like metabolism to meet the increased energy needs. Both enhanced glucose and lipid uptake and increased glycolytic mediated biosynthesis and lipid synthesis are the characteristics of EMT-like metabolism. The correlation between metabolism and EMP is dynamic. EMP-associated genetic changes can stimulate metabolic adaptations, while the higher metabolic rate can support and facilitate the EMP process.

A number of studies illustrate the EMT-associated metabolic changes and their implications. According to the research of Dong et al., up-regulation of the EMT-driving transcription factor Snail-1 in basal-like breast cancer cells leads to the formation of a Snail-G9a-Dnmt1 complex to silence the expression of fructose-1,6-bisphosphatase (FBP1), which is an important enzyme of gluconeogenesis (Dong C. et al., 2013). The loss of the FBP1 caused an increase in glucose uptake for ATP production and glycolytic mediated biosynthesis, like the pentose phosphate pathway (PPP), serine and glycerol-3-phosphate. The reprogramed metabolism offers enough energy to fuel the invasion and metastasis processes.

For lipid metabolism, higher expression levels of lipid synthesis enzymes such as ATP-citrate lyase (ACLY), stearoyl-CoA desaturase (SCD), fatty acid synthase (FASN) and HMG-CoA reductase, have been detected in more aggressive tumor cells (Sánchez-Martínez et al., 2015). Jing et al. reported that overexpression of these proteins in association with mutated p53 in mostly mesenchymal cancer cells, along with aberrant expression of sterol regulatory element-binding proteins (SREBPs) (Hu et al., 2013). In normal tissue, wild type p53 can inhibit the expression of SREBP-1c, a transcription factor of FASN and ACLY (Horton et al., 2002), while the mutated p53 loses this capacity. Moreover, the mutated p53 can bind with SREBP-2 to enhance the cholesterol biosynthesis (Freed-Pastor et al., 2012). Thus, mutated p53 significantly upregulates both fatty acid (FA) and cholesterol levels in cancer cells, which generate more membrane lipid rafts to support cell motility during the EMT process. High levels of SREBP1 can also induce EMT, via recruiting a SNAIL1/HDAC1/2 complex to stop E-cadherin mRNA expression (Zhang et al., 2019). Chen et al., has proposed that drugs targeting SREBPs could suppress cancer cell metastasis (Chen et al., 2018).

Growth factors from the tumor microenvironment can also reprogram cancer cells from the Warburg-like metabolism to EMT-like metabolism. Activated PI3K/AKT/mTOR signaling due to growth factor stimulation can enhance the uptake of glucose and lipid, as well as the synthesis of FA and protein (Chen et al., 2018). The study of EMP relative metabolism changes can offer a promising target for cancer therapy.

CURRENT MODALITIES TO INVESTIGATE PLASTICITY

Many techniques recently employed in the field of cancer cellular plasticity have corroborated not only the epithelial and mesenchymal phenotypic states, but also the spectrum of intermediate and hybrid E/M states (Pastushenko et al., 2018; Karacosta et al., 2019). The molecular approaches widely used in the cancer EMT field are broadly divided into two categories: *in vitro* based molecular and functional assays and *in vivo* based cancer models. The *in vitro* assays routinely performed in EMP studies involve various molecular and functional assays. Molecular assays, using FACS and immunocytochemistry staining with microscopy analysis, relies on various validated EMP markers that are used to delineate the phenotypic state of cells (Celià-Terrassa et al., 2018; Pastushenko et al., 2018; Risom et al., 2018; Bhatia et al., 2019). Microscopy based snap-shot and real time analysis in conjunction with quantitative assessment

is an imperative technique. These optic techniques are widely employed to study the cellular localization of various molecular markers, such as E-cadherin presence at the cell junctions, and also the subtle dynamic changes of various markers in the absence or presence of various stimuli or inducers can be studied (Hirata et al., 2014; Labernadie et al., 2017; Liu et al., 2018). Microscopy approaches are also well integrated in various functional assays, such as *in vitro* wound closure, Transwell migration studies performed in the presence or absence of ECM, quantification of single cell migration and invasion studies in culture medium, spheroid assessment and co-culture assays with cancer associated fibroblasts or endothelial cells (Kramer et al., 2013; Tanner and Gottesman, 2015; Mitchell and O'Neill, 2016; Klymenko et al., 2017; Reynolds et al., 2017; Mason et al., 2019). Other *in vitro* assessment also include "soft agar assay" for anchorage independent growth studies, "ECM degradation assays" to measure MMP and other protease activity, and "trans-epithelial resistance" assays to study monolayer integrity and permeability (Narai et al., 1997; Anderl et al., 2012; Borowicz et al., 2014). In studies relevant to single cell colonization, plasticity generated from single cell clonal culture is also examined for differences in migration, invasion and chemoresistance assays, which can be extrapolated to the metastatic cascade (Kramer et al., 2013; Harner-Foreman et al., 2017; Bhatia et al., 2019). While *in vitro* studies are important to study cellular behavior in context of phenotypic plasticity and tumoural non-genetic heterogeneity, these routinely performed assays have the drawback of not presenting the whole landscape of cancer and the real EMP spectrum, where cancer cells are infiltrated with stromal and immune microenvironment.

Researchers in the field of EMP have employed various animal models, including as *C. elegans*, *Drosophila Melanogaster*, chick embryos, zebrafish and mice to study the *in vivo* dynamics of phenotypic plasticity in developmental EMT and cancer EMP (Jimenez et al., 2016; Gómez-Cuadrado et al., 2017; Nieto, 2018; Stuelten et al., 2018; Campbell et al., 2019). Genetically engineered mouse models and patient-derived xenografts (PDXs) have been observed to recapitulate metastatic and organ homing properties similar to clinical specimens (Sikandar et al., 2017). Orthotopic implantation strategies, such as inoculation into the mammary fat pad, has also improved the recapitulation of the breast cancer in mice (Proia et al., 2011). In conjunction with intravital imaging and fluorophore chemistry, various Cre-Lox lineage tracing approaches have been employed in cell lines, and in injected mouse and zebrafish models, to delineate EMP status of the cells at primary and metastatic sites, and also of encaptured CTCs (Lourenco et al., 2020). These reporter tags are valuable in identification of CTCs and in scenarios of low numbers of cells seeding at secondary niches during metastasis (Zheng et al., 2015; Sikandar et al., 2017). The inducible system utilized for Twist1 induction or deletion at different stages of skin carcinogenesis allowed flexibility in spatio-temporal tuning (Tsai et al., 2012; Beck et al., 2015). The use of confetti mouse models and lineage tracing can also aid in the determination of intratumoural heterogeneity owing to clonal variations, and in fate mapping of the cancer evolution studies (Janiszewska and Polyak, 2018; Marx, 2018; Rios et al., 2019). Technological advances in the fields of single cell transcriptomic analysis (Patel et al., 2014; Ting et al., 2014; Horning et al., 2018; Kim et al., 2018; Puram et al., 2018; Cook and Vanderhyden, 2019), single-cell methylome profiling or ChIP sequencing (Rotem et al., 2015; Angermueller et al., 2016; Grosselin et al., 2019) and multiplex *in situ* imaging (Tsujikawa et al., 2017; Schulz et al., 2018) has allowed researchers to gain insightful information of cellular phenotypic status from clinical specimens. Microfluidic modalities are also gaining attention recently and are of great help not only in detection and capturing of label-free CTCs from patients, but also to gauge the effects of fluid pressures, cancer cell motility assessment associated with

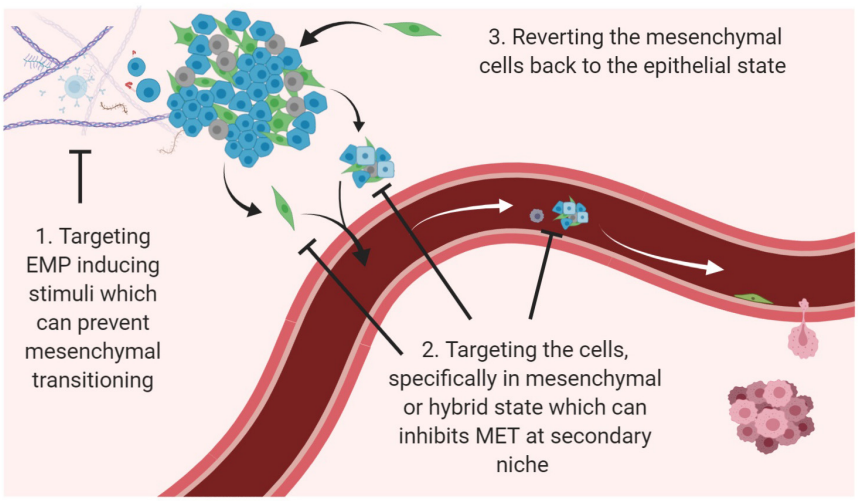

FIGURE 2 | Potential avenues to target EMP. Three main strategies for targeting cancer progression and recurrence with relevance to EMP dynamics are to use agents/compounds (i) that can target the inducers to prevent EMT; (ii) that can selectively kill mesenchymal phenotype and cells present within multiple transition states; (iii) that can revert the cells via MET.

TABLE 1 | List of the current active clinical trials targeting EGF and TGF-β signaling pathways in combination with chemotherapeutics.

Target class	Functional class	Drug name	chemotherapeutics combination	Cancer type	Clinical status (first posted, recruitment status)	Intervention/treatment
TGF-β/TGF-β Receptor inhibitors	Tyrosine kinase inhibitor	LY-2152799 (Galunisertib)	Fluorouracil/Capecitabine + Tumor specific mesorectal excision	Locally Advanced Rectal Adenocarcinoma	NCT02688712 (2016, Recruiting)	Drug: LY2157299Drug: Capecitabine Drug: Fluorouracil Procedure: Tumor specific mesorectal excision
			Paclitaxel/Carboplatin	Carcinosarcoma of the Uterus or Ovary	NCT03206177 (2017, Recruiting)	Drug: Galunisertib Drug: Paclitaxel Drug: Carboplatin
			Sorafenib	Advanced Hepatocellular Carcinoma	NCT02178358 (2014, Active, not recruiting)	Drug: LY2157299 Drug: Sorafenib Drug: Placebo
	TGF-β receptor inhibitor	TEW-7197	Pomalidomide	Relapsed or Relapsed and Refractory Multiple Myeloma	NCT03143985 (2017, Recruiting)	Drug: TEW-7197 Drug: Pomalidomide
EGF/EGFR inhibitors	EGFR tyrosine kinase inhibitor	Gefitinib	Pemetrexed	Advanced Non-Small Cell Lung Cancer	NCT01982955 (2013, Active, not recruiting)	Drug: Tepotinib Drug: Gefitinib Drug: Pemetrexed Drug: Cisplatin Drug: Carboplatin
		Icotinib	Pemetrexed, Carboplatin	III B/IV Non-Small Cell Lung Cancer	NCT03151161 (2017, Not yet recruiting)	Drug: Icotinib, Pemetrexed, Carboplatin Drug: Icotinib
			Cisplatin or Carboplatin	metastatic non-squamous non-small cell lung cancer who did not progress after pemetrexed combined with platinum chemotherapy	NCT03992885 (2019, Recruiting)	Drug: Icotinib Drug: Cisplatin Drug: Carboplatin
		Apatinib	Pemetrexed, Gemcitabine, Docetaxel	NSCLC Patients Without T790M Mutation	NCT03758677 (2018, Not yet recruiting)	Drug: Apatinib Drug: Chemotherapy with platinum-based double drugs (Pemetrexed, Gemcitabine, Docetaxel)
			Pemetrexed Plus Carboplatin	Advanced Non-small Cell Lung Cancer	NCT03164694 (2018, Recruiting)	Drug: Apatinib + Pemetrexed + Carboplatin Drug: Pemetrexed + Carboplatin
		Osimertinib	Cisplatin or Carboplatin	Metastatic EGFR Mutant Lung Cancers	NCT03567642 (2018, Recruiting)	Drug: Osimertinib Drug: Platinum Drug: Etoposide
			Platinum-based Doublet-Chemotherapy	Locally Advanced or Metastatic Non-Small Cell Lung Cancer	NCT02151981 (2018, Active, not recruiting)	Drug: Chemotherapy Drug: Cross-over to Osimertinib
			Pemetrexed + Cisplatin or Pemetrexed + Carboplatin	Locally Advanced Non-Small Cell Lung Cancer	NCT04035486 (2019, Recruiting)	Drug: Osimertinib Drug: Osimertinib + Pemetrexed + Cisplatin Drug: Osimertinib + Pemetrexed + Carboplatin
	Monoclonal antibody	Panitumumab	Carboplatin and Paclitaxel	Invasive Triple Negative Breast Cancer	NCT02876107 (2016, recruiting)	Drug: Carboplatin Other: Laboratory Biomarker Analysis Drug: Paclitaxel Biological: Panitumumab
		HLX07	Gemcitabine + Cisplatin/Paclitaxel + Carboplatin/mFOLFOX6	Advanced Solid Tumors	NCT03577704 (2018, Recruiting)	Drug: HLX07 + Gemcitabine + Cisplatin Drug: HLX07 + Paclitaxel + Carboplatin Drug: HLX07 + mFOLFOX6

TABLE 2 | Different categories of inhibitors that target stimuli and signaling pathways associated with EMT and are targeted in current clinical trials.

Target class	Functional class	Drug Name	Cancer type	Clinical status (first posted)
Inhibitors of extracellular mediators and their corresponding receptors				
TGF-β–TGF-β receptor inhibitors	TGF-β receptor inhibitor	TEW-7197	Urothelial Carcinoma Recurrent, Advanced Urothelial Carcinoma, Myelodysplastic Syndromes	NCT04064190(2019); NCT03074006(2017)
	TGFβ receptor ectodomain-IgG Fc fusion protein	AVID200	refractory advanced and metastatic malignancies, Myelofibrosis (Myeloproliferative Neoplasms Research Consortium [MPN-RC] 118)	NCT03834662(2019); NCT03895112(2019)
	a bifunctional fusion protein targeting PD-L1 and TGF-β	MSB0011359C (M7824)	Stage II-III HER2 Positive Breast Cancer, Locally Advanced or Metastatic Second Line (2L) Biliary Tract Cancer (Cholangiocarcinoma and Gallbladder Cancer), Solid Tumors, Recurrent Respiratory Papillomatosis, HPV Associated Malignancies	NCT03620201(2018); NCT03833661(2019); NCT02699515(2016); NCT02517398(2015); NCT03707587(2018); NCT03427411(2018)
	CAR-T cells that target GPC3 (GPC3-CART cell) and/or soluble TGFβ (GPC3/TGFβ-CART)	GPC3-T2-CAR-T	Hepatocellular Carcinoma, Squamous Cell Lung Cancer	NCT03198546(2017)
IL-6/IL-6R inhibitors	Monoclonal antibody	Siltuximab (CNTO-328, Tocilizumab)	Metastatic Pancreatic Cancer; multiple myeloma (MM) and systemic AL amyloidosis (AL)	NCT04191421(2019); NCT03315026(2017)
EGF/EGFR inhibitors	Tyrosine kinase inhibitor	Afatinib (BIBW2992)	Chordoma,	NCT03083678(2018)
		Dacomitinib (PF00299804)	EGFR Mutant Lung Cancer	NCT03755102(2018)
		Osimertinib	Stage I-IIIA EGFR-mutant Non-small Cell Lung Cancer, stage IIIB-IV or Recurrent Non-small Cell Lung Cancer	NCT03586453(2018); NCT03434418(2018); NCT03433469(2018); NCT03191149(2018)
		Brigatinib (AP26113)	Advanced Non-small Cell Lung Cancer (NSCLC), Anaplastic Large Cell Lymphoma, Advanced Malignant Neoplasm	NCT02737501(2016); NCT02706626(2017); NCT03719898(2018); NCT03868423(2019); NCT03707938(2018); NCT03596866(2019);
	inhibitor for (EGFR, HER2, and ErbB4)	Poziotinib (HM781-36B)	EGFR Exon 20 Mutant Advanced NSCLC, Breast Cancer, Stage IV Lung Adenocarcinoma with HER2 Mutation	NCT03066206(2017); NCT03066206(2017); NCT03744715(2018); NCT03318939(2017); NCT02979821(2016)
	Monoclonal antibody	Panitumumab	Anaplastic Lymphoma Kinase-Positive (ALK +), Advanced Non-Small-Cell Lung Cancer (NSCLC)	NCT03535740(2019)
		HLX07	Advanced Solid Cancers	NCT02648490(2016)
PDGF/PDGFR inhibitors	Tyrosine kinase inhibitor	Axitinib	Pheochromocytoma, Paraganglioma, Renal Cell Carcinoma, Hepatobiliary Neoplasm, Liver Neoplasm, Biliary Tract Neoplasms, Cervical Cancer, Non-Small Cell Lung Cancer, Urothelial Cancer	NCT03839498(2019); NCT03494816(2018); NCT04010071(2019); NCT03826589(2019); NCT03472560(2018); NCT03341845(2017)
FGF/FGFR inhibitors	Tyrosine kinase inhibitor	Lenvatinib	Advanced Biliary Tract Cancer, Thyroid Neoplasms, Advanced Gastric Cancer, Non-small Cell Lung Cancer, Solid Tumor, Thyroid Cancer	NCT04211168(2019); NCT03573960(2018); NCT03609359(2018); NCT03829332(2019); NCT03009292(2017); NCT03139747(2017)
		Nintedanib (BIBF1120)	Appendix Cancer, Lymphangioleiomyomatosis, Adenocarcinoma of the Lung	NCT03287947(2017); NCT03062943(2017); NCT04046614(2019)
		Pazopanib	Refractory Solid Tumors, Metastatic Sarcoma, Recurrent Sarcoma, Resectable Sarcoma, Advanced Renal Cell Carcinoma Metastatic Renal Cell Carcinoma	NCT02691767(2016); NCT04199026(2019); NCT03200717(2017)

(Continued)

TABLE 2 | Continued

Target class	Functional class	Drug Name	Cancer type	Clinical status (first posted)
		Ponatinib	Medullary Thyroid Cancer, Acute Myeloid Leukemia, Accelerated Phase Chronic Myeloid Leukemia, Blast Phase Chronic Myeloid Leukemia, GIST, Malignant, Chronic Myeloid Leukemia, Acute Lymphoblastic Leukemia, Philadelphia Chromosome-positive Acute Lymphoblastic Leukemia	NCT03838692(2019); NCT03934372(2019); NCT03171389(2017); NCT04233346(2020); NCT03709017(2018)
TNFα inhbitors	Monoclonal antibody	Infliximab	Advanced Melanoma	NCT03293784(2017)
Hedgehog/ Smoothened inhibitors	Smoothened antagonists (small-molecule inhibitor)	Vismodegib	Stomach Neoplasms, Basal Cell Carcinoma, Metastatic Basal Cell Carcinoma, Locally Advanced Basal Cell Carcinoma, Advanced Solid Tumors	NCT03052478(2017); NCT03035188(2017); NCT03610022(2018); NCT03297606(2017)
		Sonidegib	Clinical Stage III Cutaneous Melanoma AJCC v8, Clinical Stage III Gastric Cancer AJCC v8, Basal Cell Carcinoma	NCT04007744(2019); NCT04066504(2019)
Notch/Notch ligand (Delta-like and Jagged) inhibitors	Small-molecule inhibitor	γ-secretase inhibitor: LY3039478	Advanced Solid Tumor	NCT02836600(2016)
		γ-secretase inhibitor: PF-03084014	Desmoid Tumor, Aggressive Fibromatosis, Desmoid-Type Fibromatosis, Recurrent Desmoid-Type Fibromatosis, Unresectable Desmoid-Type Fibromatosis	NCT03785964(2018); NCT04195399(2019)
		PAN-Notch inhibitor BMS-906024	recurrent or metastatic Adenoid Cystic Carcinoma	NCT03691207(2018)
WNT/Frizzled inhibitors	Wnt5a mimetic	Foxy-5	Colon Cancer	NCT03883802(2019)
	Peptidomimetics	CWP232291	Acute Myeloid Leukemia	NCT03055286(2017)
	Inhibits the recruiting of β-catenin with its co-activator CBP	PRI-724	Liver Cirrhosis	NCT03620474(2018)
Inhibitors of intracellular signaling pathways				
SRC inhibitors	Tyrosine Kinase inhibitor	Dasatinib (BMS-354825)	Relapsed AML, Waldenstrom Macroglobulinemia, Relapsed CML	NCT03560908(2018); NCT04115059(2019); NCT03573596(2018)
		Bosutinib (SKI-606)	Metastatic Breast Cancer, Chronic Myeloid Leukemia, Advanced Solid Tumors	NCT03854903(2019); NCT02810990(2016); NCT03297606(2017)
FAK inhibitors	Tyrosine Kinase inhibitor	Defactinib (VS-6063)	Malignant Pleural Mesothelioma, Advanced Solid Tumors	NCT04201145(2019); NCT02546531(2015)
PI3K/AKT/mTOR inhibitors	PI3K inhibitor	Idelalisib	Follicular Non-Hodgkin's Lymphoma Refractory, Relapsed Diffuse Large B-cell Lymphoma, B-cell Lymphoma Recurrent, B-cell Chronic Lymphocytic Leukemia	NCT03568929(2018); NCT03576443(2018); NCT03757000(2018)
	AKT inhibitor	AZD5363	Advanced Solid Tumors, Advanced Breast Cancer	NCT03310541(2017); NCT03182634(2017)
		Temsirolimus	Non-muscle Invasive Bladder Cancer,	NCT02753309(2016)
	Tyrosine kinase inhibitor	CX-4945	Recurrent Medulloblastoma	NCT03904862(2019)
AURKA/SYK	Tyrosine kinase inhibitor	Midostaurin	Acute Myeloid Leukemia, AML/MDS	NCT03951961(2019); NCT04097470(2019)
AXL inhibitors	Tyrosine Kinase inhibitor	BGB324	Recurrent Glioblastoma Undergoing Surgery, Advanced NSCLC	NCT03965494(2019); NCT03184571(2017)
RAS/RAF/MAPK inhibitors	RAF inhibitor	Sorafenib	Recurrent or Metastatic Triple Negative Breast Cancer, Advanced Liver Cancer, Advanced Hepatic Carcinoma	NCT02624700(2015); NCT04163237(2019); NCT03164382(2017); NCT03211416(2017)
	MEK inhibitor	Trametinib	Advanced ALK-Positive NSCLC, Advanced/Metastatic Colorectal Cancer	NCT03087448(2017); NCT03714958(2018)
Inhibitors of transcription factors that indirectly induce EMP				
JAK and STAT3 inhibitors	Small molecule inhibitor	STAT3: BB1608 (Napabucasin)	Metastatic Colorectal Cancer, Metastatic Pancreatic Cancer	NCT03522649(2018); NCT03647839(2018); NCT03721744(2018)

(Continued)

TABLE 2 | Continued

Target class	Functional class	Drug Name	Cancer type	Clinical status (first posted)
Compounds acting on epigenetic modulators				
Histone deacetylase inhibitor		Vorinostat	Mutated Advanced Melanoma, Breast Cancer Metastatic	NCT02836548(2016); NCT03742245(2018)
		Romidepsin	Survey- Relapsed or Refractory Peripheral T-Cell Lymphoma	NCT03742921(2018); NCT03547700(2018)
		Mocetinostat	Advanced Lung Cancer, Unresectable Stage III or Stage IV Melanoma	NCT03220477(2017); NCT03565406(2018)
		Panobinostat	Multiple Myeloma	NCT02722941(2016); NCT04150289(2019);
Histone methyl transferases inhibitor	EZH2 inhibitor	E7438 (Tazemetostat, EPZ-6438)	Relapsed or Refractory B-cell Non-Hodgkin's Lymphoma, Relapsed/Refractory Follicular Lymphoma	NCT03009344(2017); NCT03456726(2018); NCT04224493(2020)
	EZH1/2 inhibitor	DS-3201b	Relapsed or Refractory Adult T-cell Leukemia/Lymphoma, Acute Leukemia Myeloid Leukemia, Acute Lymphocytic, Recurrent Small Cell Lung Cancer	NCT04102150(2019); NCT03110354(2017); NCT03879798(2019)
Inhibitors of stimuli from the tumor microenvironment				
HIF-1α inhibitors	Small molecule inhibitor	PT2385	Von Hippel-Lindau Disease-Associated Clear Cell Renal Cell Carcinoma, Recurrent Glioblastoma	NCT03108066(2017); NCT03216499(2017)
		Digoxin	Breast Cancer, Circulating Tumor Cells (CTCs), Advanced Pancreatic Cancer, Advanced Solid Tumor	NCT03928210(2019); NCT03889795(2019)

single cell or collective migration, and for co-culture studies (Sarioglu et al., 2015; Ma et al., 2018; Shang et al., 2019; Truong et al., 2019). Similarly, various mathematical approaches and modeling have been helpful in deciphering the significant genes and molecular networks associated with the spectrum of epithelial and mesenchymal states, as well as phenotypic plasticity (Jolly et al., 2017; Bocci et al., 2018; Jia et al., 2019; Yang et al., 2019). However, it is crucial to acknowledge that the modalities and analytical approaches utilized in the field of EMP present context-specific studies, such that inferences derived will not provide an overarching conclusion (Henkel et al., 2019). Inherent limitations of the employed assays should always be taken into consideration while extrapolating from the data.

THERAPEUTIC STRATEGIES FOR TARGETING EMP

The presence of plasticity in tumor cells and resultant heterogeneity is one of the utmost challenges in targeting cancer on a whole (Bhatia et al., 2017; Redfern et al., 2018). EMT and/or CSC have been reported to confer drug resistance characteristics against a number of conventional therapeutics like taxol, vincristine, oxaliplatin, gemcitabine, cisplatin and 5-fluorouracil in human pancreatic cell lines, and against EGFR-targeted therapies erlotinib, cetuximab and gefitinib in lung cancer (Fuchs et al., 2008; Sabbah et al., 2008; Arumugam et al., 2009). Similarly, studies have also reported that an active EMT program in breast cancer cell lines makes them unresponsive to tamoxifen, paclitaxel, and adriamycin treatment (Kajita et al., 2004; Hiscox et al., 2006; Cheng et al., 2007; Li Q. Q. et al., 2009). Breast cancer cells with EMT-associated CSC features ($CD44^{high}$, $CD24^{low}$) have been reported to remain after neoadjuvant chemotherapy and HER2 pharmacological inhibition, suggesting that they encode resistance (Li et al., 2008; Blick et al., 2010). Many reports have also shown basal, mesenchymal-like neoplasms to be more resistant to neoadjuvant chemotherapy than epithelial, luminal-like tumors (Yauch et al., 2005; Carey et al., 2007; Liedtke et al., 2008), and reversal of the EMT phenotype in resistant cell lines has re-established drug sensitivity (Arumugam et al., 2009; Li Y. et al., 2009). Therefore, three main strategies as combinatorial therapies that are being widely acknowledged and/or proposed in the field of combating plasticity are (i) Targeting EMP inducing stimuli which can prevent mesenchymal transitioning, (ii) Targeting the cells, specifically in mesenchymal or hybrid state which can inhibit MET at secondary niche, and (iii) Reverting the mesenchymal cells back to the epithelial state (Bhatia et al., 2017; Williams et al., 2019; **Figure 2**).

In the first scenario to target EMP inducing stimuli, many different approaches have been utilized to inhibit different signaling pathways that contribute to the induction and maintenance of EMT, such as TGFβ/TGFβR, EGF/EGFR, FGF/FGFR, IGF/IGFR, IL-6/IL-6R, HGF/MET, PDGF/PDGFR, TNFα, Wnt and Notch signaling (Marcucci et al., 2016; Bhatia et al., 2017). Of all, TGFβ and EGF pathway inhibitors have been most extensively studied and investigated, as these have been found to be common inducers of EMT in different cancer types (Li et al., 2015). **Table 1** details the current active clinical trials inhibiting these two EMT-inducing pathways in combination with chemotherapeutics.

Secondly, for therapies specifically targeting mesenchymal cells, different novel strategies such as EMP-targeting vaccines against transcription factors such as TWIST1 and Brachyury;

nutraceuticals; and the repurposing of drugs such as metformin, salinomycin and resveratrol, have been extensively discussed in our previous review (Bhatia et al., 2017). **Table 2** details current clinical trials (2015 onward) with the focus on targeting EMP in cancer patients, as an update from our previous review (Bhatia et al., 2017). New combinatorial approaches combining EMT inhibitors alongside targeting immunotherapy blockade are also being developed, as EMT is reported to induce PDL1 expression in carcinoma cells (Chen et al., 2014; Noman et al., 2017), and an EMT signature was seen in tumors that responded to anti PD1/PD-L1- and CTLA4-associated treatments (Lou et al., 2016).

For the third strategy, the detailed molecular knowledge of MET regulation will provide opportunities to curtail this event and prevent the development of metastasis, which is of high clinical relevance. Depending on the clinical scenario, MET-inducing/stabilizing factors may inhibit metastasis if they block the initial EMT stages that allow the dissemination, or promote the later stages of metastasis, which can cause some conflicting considerations (van Denderen and Thompson, 2013; Pattabiraman and Weinberg, 2016). An emerging challenge is then to determine the correct timings for therapeutic interventions, and also to decipher correctly the contribution that intermediate states of the EMT spectrum make to tumor evolution for therapeutic interventions (McGranahan and Swanton, 2015). A high-throughput screening approach is required to identify suitable drugs or "repurposable" small molecular agents in context of specifically targeting hybrid and/or partial EMP cells. The concept of intermittent dosing (drug holidays) is also resurfacing to prevent the plasticity and transitioning of cells in carcinoma. For example, resistance to the BRAF inhibitor vemurafenib in melanoma is remodeled to forestall drug resistance (Das Thakur et al., 2013). Thus, the development of combinatorial therapeutic interventions that can target dynamics and plasticity alongside proliferative tendency of cancer cells may pave the way to more promising treatment strategies.

CONCLUSION AND PERSPECTIVES

The crucial roles of EMT-MET during embryogenesis and organogenesis is hijacked during tumor progression and metastasis. The roles of various signaling cascades, intrinsic and extrinsic mechanisms, and regulators that contributes to EMP dynamics are reasonably well determined, but more refined studies and techniques need to be employed to recapitulate the MET behavior of cells while extravasating, seeding and colonizing at secondary niches. The intricacies associated with phenotypic plasticity, stemness and intratumoral heterogeneity further sheds light on several unresolved queries. The reliable features of cellular behavior relating to drug persistent states through the spectrum of EMT need to be verified. Is there a ubiquitous molecular feature of partial/hybrid EMT cells that can be identified and targeted across all different cancer context types? What actual mechanisms do cancer cells employ to intravasate from the primary sites, and how do EMT - MET programs cooperate to assist cancer cells through several stages of cancer progression? We are still lagging in obtaining a wider and more complete understanding of the contributions of EMP in cancer. The sophisticated developments in lineage tracing using confetti animal models and implementation of other novel technologies such as high-resolution intravital imaging, live cell imaging, inducible reporter systems and single-cell sequencing techniques will provide great avenues in the fields of plasticity and dynamics around EMP. Finally, it is imperative to determine how phenotypic plasticity can be exploited, as therapeutic interventions that push the conversion of cancer cells to fat cells or apoptosis, for example, (David et al., 2016; Ishay-Ronen et al., 2019) might be promising approaches in clinical settings.

AUTHOR CONTRIBUTIONS

SB wrote the manuscript, developed the first draft, and contributed significantly toward development of the whole manuscript. PW contributed significantly in content material, figures and tables preparation and drafted metabolomics section. AT contributed in providing content material and drafted CTC section. ET refined, edited the manuscript, and approved the final version to be published.

FUNDING

During the course of study, SB, PW and AT were supported by a QUTPRA scholarship.

REFERENCES

Aceto, N., Bardia, A., Miyamoto, D. T., Donaldson, M. C., Wittner, B. S., Spencer, J. A., et al. (2014). Circulating tumor cell clusters are oligoclonal precursors of breast cancer metastasis. *Cell* 158, 1110–1122. doi: 10.1016/j.cell.2014.07.013

Agnoletto, C., Corrà, F., Minotti, L., Baldassari, F., Crudele, F., Cook, W. J. J., et al. (2019). Heterogeneity in circulating tumor cells: the relevance of the stem-cell subset. *Cancer* 11:483. doi: 10.3390/cancers11040483

Aiello, N. M., Brabletz, T., Kang, Y., Nieto, M. A., Weinberg, R. A., and Stanger, B. Z. (2017). Upholding a role for EMT in pancreatic cancer metastasis. *Nature* 547, E7–E8. doi: 10.1038/nature22963

Aiello, N. M., and Kang, Y. (2019). Context-dependent EMT programs in cancer metastasis. *J. Exp. Med.* 216, 1016–1026. doi: 10.1084/jem.20181827

Aiello, N. M., Maddipati, R., Norgard, R. J., Balli, D., Li, J., Yuan, S., et al. (2018). EMT subtype influences epithelial plasticity and mode of cell migration. *Dev. Cell* 45, 681–695. doi: 10.1016/j.devcel.2018.05.027

Alonso-Alconada, L., Muinelo-Romay, L., Madissoo, K., Diaz-Lopez, A., Krakstad, C., Trovik, J., et al. (2014). Molecular profiling of circulating tumor cells links plasticity to the metastatic process in endometrial cancer. *Mol. Cancer* 13:223. doi: 10.1186/1476-4598-13-223

Anderl, J., Ma, J., Armstrong, L., and Millipore, E. J. N. M. (2012). Fluorescent gelatin degradation assays for investigating invadopodia formation. *Biol. Protoc.* 121007, 1–5.

Angermueller, C., Clark, S. J., Lee, H. J., Macaulay, I. C., Teng, M. J., Hu, T. X., et al. (2016). Parallel single-cell sequencing links transcriptional and epigenetic heterogeneity. *Brief Commun.* 13:229. doi: 10.1038/nmeth.3728

Ansieau, S., Bastid, J., Doreau, A., Morel, A. P., Bouchet, B. P., Thomas, C., et al. (2008). Induction of EMT by twist proteins as a collateral effect of tumor-promoting inactivation of premature senescence. *Cancer Cell* 14, 79–89. doi: 10.1016/j.ccr.2008.06.005

Armstrong, A. J., Marengo, M. S., Oltean, S., Kemeny, G., Bitting, R. L., Turnbull, J. D., et al. (2011). Circulating tumor cells from patients with advanced prostate and breast cancer display both epithelial and mesenchymal markers. *Mol. Cancer Res.* 9, 997–1007. doi: 10.1158/1541-7786.mcr-10-0490

Arumugam, T., Ramachandran, V., Fournier, K. F., Wang, H., Marquis, L., Abbruzzese, J. L., et al. (2009). Epithelial to mesenchymal transition contributes to drug resistance in pancreatic cancer. *Cancer Res.* 69, 5820–5828. doi: 10.1158/0008-5472.can-08-2819

Barrallo-Gimeno, A., and Nieto, M. A. (2005). The Snail genes as inducers of cell movement and survival: implications in development and cancer. *Development* 132, 3151–3161. doi: 10.1242/dev.01907

Barriere, G., Fici, P., Gallerani, G., Fabbri, F., Zoli, W., and Rigaud, M. (2014). Circulating tumor cells and epithelial, mesenchymal and stemness markers: characterization of cell subpopulations. *Ann. Transl. Med.* 2:109.

Beck, B., Lapouge, G., Rorive, S., Drogat, B., Desaedelaere, K., Delafaille, S., et al. (2015). Different levels of twist1 regulate skin tumor initiation, stemness, and progression. *Cell Stem Cell* 16, 67–79. doi: 10.1016/j.stem.2014.12.002

Beerling, E., Seinstra, D., de Wit, E., Kester, L., van der Velden, D., Maynard, C., et al. (2016). Plasticity between epithelial and mesenchymal states unlinks EMT from metastasis-enhancing stem cell capacity. *Cell Rep.* 14, 2281–2288. doi: 10.1016/j.celrep.2016.02.034

Bhatia, S., Monkman, J., Blick, T., Pinto, C., Waltham, M., Nagaraj, S. H., et al. (2019). Interrogation of phenotypic plasticity between epithelial and mesenchymal states in breast cancer. *J. Clin. Med.* 8:893. doi: 10.3390/jcm8060893

Bhatia, S., Monkman, J., Toh, A. K. L., Nagaraj, S. H., and Thompson, E. W. (2017). Targeting epithelial-mesenchymal plasticity in cancer: clinical and preclinical advances in therapy and monitoring. *Biochem. J.* 474, 3269–3306. doi: 10.1042/bcj20160782

Blick, T., Hugo, H., Widodo, E., Waltham, M., Pinto, C., Mani, S. A., et al. (2010). Epithelial mesenchymal transition traits in human breast cancer cell lines parallel the CD44(hi/)CD24 (lo/-) stem cell phenotype in human breast cancer. *J. Mammary Gland Biol. Neoplasia* 15, 235–252. doi: 10.1007/s10911-010-9175-z

Bocci, F., Jolly, M. K., George, J. T., Levine, H., and Onuchic, J. N. (2018). A mechanism-based computational model to capture the interconnections among epithelial-mesenchymal transition, cancer stem cells and Notch-Jagged signaling. *Oncotarget* 9, 29906–29920. doi: 10.18632/oncotarget.25692

Bonyadi Rad, E., Hammerlindl, H., Wels, C., Popper, U., Ravindran Menon, D., Breiteneder, H., et al. (2016). Notch4 signaling induces a mesenchymal-epithelial-like transition in melanoma cells to suppress malignant behaviors. *Cancer Res.* 76, 1690–1697. doi: 10.1158/0008-5472.can-15-1722

Borowicz, S., Van Scoyk, M., Avasarala, S., Karuppusamy Rathinam, M. K., Tauler, J., Bikkavilli, R. K., et al. (2014). The soft agar colony formation assay. *J. Vis. Exp.* 9:e51998. doi: 10.3791/51998

Boulding, T., McCuaig, R. D., Tan, A., Hardy, K., Wu, F., Dunn, J., et al. (2019). Author Correction: LSD1 activation promotes inducible EMT programs and modulates the tumour microenvironment in breast cancer. *Sci. Rep.* 9:18771. doi: 10.1038/s41598-019-55020-55021

Bourcy, M., Suarez-Carmona, M., Lambert, J., Francart, M. E., Schroeder, H., Delierneux, C., et al. (2016). Tissue factor induced by epithelial-mesenchymal transition triggers a procoagulant state that drives metastasis of circulating tumor cells. *Cancer Res.* 76, 4270–4282. doi: 10.1158/0008-5472.CAN-15-2263

Brabletz, T. (2012). To differentiate or not — routes towards metastasis. *Nat. Rev. Cancer* 12, 425–436. doi: 10.1038/nrc3265

Brabletz, T., Kalluri, R., Nieto, M. A., and Weinberg, R. A. (2018). EMT in cancer. *Nat. Rev. Cancer* 18, 128–134. doi: 10.1038/nrc.2017.118

Bradshaw, A. D. (2009). The role of SPARC in extracellular matrix assembly. *J. Cell Commun. Signal.* 3:239. doi: 10.1007/s12079-009-0062-6

Buijs, J. T., Henriquez, N. V., van Overveld, P. G. M., van der Horst, G., Que, I., Schwaninger, R., et al. (2007). Bone morphogenetic protein 7 in the development and treatment of bone metastases from breast cancer. *Cancer Res.* 67, 8742–8751.

Bulfoni, M., Gerratana, L., Del Ben, F., Marzinotto, S., Sorrentino, M., Turetta, M., et al. (2016). In patients with metastatic breast cancer the identification of circulating tumor cells in epithelial-to-mesenchymal transition is associated with a poor prognosis. *Breast Cancer Res* 18:30.

Buonato, J. M., Lan, I. S., and Lazzara, M. J. (2015). EGF augments TGFβ-induced epithelial-mesenchymal transition by promoting SHP2 binding to GAB1. *J. Cell Sci.* 128, 3898–3909. doi: 10.1242/jcs.169599

Campbell, K., Rossi, F., Adams, J., Pitsidianaki, I., Barriga, F. M., Garcia-Gerique, L., et al. (2019). Collective cell migration and metastases induced by an epithelial-to-mesenchymal transition in Drosophila intestinal tumors. *Nat. Commun.* 10:2311. doi: 10.1038/s41467-019-10269-y

Carey, L. A., Dees, E. C., Sawyer, L., Gatti, L., Moore, D. T., Collichio, F., et al. (2007). The triple negative paradox: primary tumor chemosensitivity of breast cancer subtypes. *Clin. Cancer Res.* 13, 2329–2334. doi: 10.1158/1078-0432.ccr-06-1109

Casas, E., Kim, J., Bendesky, A., Ohno-Machado, L., Wolfe, C. J., and Yang, J. (2011). Snail2 is an essential mediator of Twist1-induced epithelial mesenchymal transition and metastasis. *Cancer Res.* 71, 245–254. doi: 10.1158/0008-5472.can-10-2330

Celià-Terrassa, T., Bastian, C., Liu, D. D., Ell, B., Aiello, N. M., Wei, Y., et al. (2018). Hysteresis control of epithelial-mesenchymal transition dynamics conveys a distinct program with enhanced metastatic ability. *Nat. Commun.* 9:5005. doi: 10.1038/s41467-018-07538-7537

Cha, Y. H., Yook, J. I., Kim, H. S., and Kim, N. H. (2015). Catabolic metabolism during cancer EMT. *Arch. Pharm. Res.* 38, 313–320. doi: 10.1007/s12272-015-0567-x

Chaffer, C. L., Brueckmann, I., Scheel, C., Kaestli, A. J., Wiggins, P. A., Rodrigues, L. O., et al. (2011). Normal and neoplastic nonstem cells can spontaneously convert to a stem-like state. *Proc. Natl. Acad. Sci. U.S.A.* 108, 7950–7955. doi: 10.1073/pnas.1102454108

Chaffer, C. L., Marjanovic, N. D., Lee, T., Bell, G., Kleer, C. G., Reinhardt, F., et al. (2013). Poised chromatin at the ZEB1 promoter enables breast cancer cell plasticity and enhances tumorigenicity. *Cell* 154, 61–74. doi: 10.1016/j.cell.2013.06.005

Chaffer, C. L., Thompson, E. W., and Williams, E. D. (2007). Mesenchymal to epithelial transition in development and disease. *Cells Tissues Organs* 185, 7–19. doi: 10.1159/000101298

Chang, H. H., Oh, P. Y., Ingber, D. E., and Huang, S. (2006). Multistable and multistep dynamics in neutrophil differentiation. *BMC Cell Biol.* 7:11. doi: 10.1186/1471-2121-7-11

Chao, Y. L., Shepard, C. R., and Wells, A. (2010). Breast carcinoma cells re-express E-cadherin during mesenchymal to epithelial reverting transition. *Mol. Cancer* 9, 1–18. doi: 10.1186/1476-4598-9-179

Chen, L., Gibbons, D. L., Goswami, S., Cortez, M. A., Ahn, Y.-H., Byers, L. A., et al. (2014). Metastasis is regulated via microRNA-200/ZEB1 axis control of tumour cell PD-L1 expression and intratumoral immunosuppression. *Nat. Commun.* 5, 5241–5241. doi: 10.1038/ncomms6241

Chen, M., Zhang, J., Sampieri, K., Clohessy, J. G., Mendez, L., Gonzalez-Billalabeitia, E., et al. (2018). An aberrant SREBP-dependent lipogenic program promotes metastatic prostate cancer. *Nat. Genet.* 50, 206–218. doi: 10.1038/s41588-017-0027-22

Cheng, G. Z., Chan, J., Wang, Q., Zhang, W., Sun, C. D., and Wang, L. H. (2007). Twist transcriptionally up-regulates AKT2 in breast cancer cells leading to increased migration, invasion, and resistance to paclitaxel. *Cancer Res.* 67, 1979–1987. doi: 10.1158/0008-5472.can-06-1479

Christiansen, J. J., and Rajasekaran, A. K. (2006). Reassessing epithelial to mesenchymal transition as a prerequisite for carcinoma invasion and metastasis. *Cancer Res.* 66, 8319–8326. doi: 10.1158/0008-5472.can-06-0410

Chung, V. Y., Tan, T. Z., Ye, J., Huang, R. L., Lai, H. C., Kappei, D., et al. (2019). The role of GRHL2 and epigenetic remodeling in epithelial-mesenchymal plasticity in ovarian cancer cells. *Commun. Biol.* 2:272. doi: 10.1038/s42003-019-0506-503

Cook, D. P., and Vanderhyden, B. C. (2019). Comparing transcriptional dynamics of the epithelial-mesenchymal transition. *bioRxiv* [Preprint], doi: 10.1101/732412

Das Thakur, M., Salangsang, F., Landman, A. S., Sellers, W. R., Pryer, N. K., Levesque, M. P., et al. (2013). Modelling vemurafenib resistance in melanoma reveals a strategy to forestall drug resistance. *Nature* 494, 251–255. doi: 10.1038/nature11814

Dave, N., Guaita-Esteruelas, S., Gutarra, S., Frias, A., Beltran, M., Peiro, S., et al. (2011). Functional cooperation between Snail1 and twist in the regulation of

ZEB1 expression during epithelial to mesenchymal transition. *J. Biol. Chem.* 286, 12024–12032. doi: 10.1074/jbc.M110.168625

David, C. J., Huang, Y.-H., Chen, M., Su, J., Zou, Y., Bardeesy, N., et al. (2016). TGF-β Tumor Suppression through a Lethal EMT. *Cell* 164, 1015–1030. doi: 10.1016/j.cell.2016.01.009

de Wit, S., Manicone, M., Rossi, E., Lampignano, R., Yang, L., Zill, B., et al. (2018). EpCAMhigh and EpCAMlow circulating tumor cells in metastatic prostate and breast cancer patients. *Oncotarget* 9:35705.

Debaugnies, M., Sánchez-Danés, A., Rorive, S., Raphaël, M., Liagre, M., Parent, M.-A., et al. (2018). YAP and TAZ are essential for basal and squamous cell carcinoma initiation. *EMBO Rep.* 19, e45809. doi: 10.15252/embr.201845809

Devarajan, E., Song, Y. H., Krishnappa, S., and Alt, E. (2012). Epithelial-mesenchymal transition in breast cancer lines is mediated through PDGF-D released by tissue-resident stem cells. *Int. J. Cancer* 131, 1023–1031. doi: 10.1002/ijc.26493

Dong, C., Yuan, T., Wu, Y., Wang, Y., Fan, T. W., Miriyala, S., et al. (2013). Loss of FBP1 by Snail-mediated repression provides metabolic advantages in basal-like breast cancer. *Cancer Cell* 23, 316–331. doi: 10.1016/j.ccr.2013.01.022

Dong, P., Karaayvaz, M., Jia, N., Kaneuchi, M., Hamada, J., Watari, H., et al. (2013). Mutant p53 gain-of-function induces epithelial-mesenchymal transition through modulation of the miR-130b-ZEB1 axis. *Oncogene* 32, 3286–3295. doi: 10.1038/onc.2012.334

Dongre, A., Rashidian, M., Reinhardt, F., Bagnato, A., Keckesova, Z., Ploegh, H. L., et al. (2017). Epithelial-to-mesenchymal transition contributes to immunosuppression in breast carcinomas. *Cancer Res.* 77, 3982–3989. doi: 10.1158/0008-5472.can-16-3292

Ferrell, J. E. Jr. (2012). Bistability, bifurcations, and Waddington's epigenetic landscape. *Curr. Biol.* 22, R458–R466. doi: 10.1016/j.cub.2012.03.045

Fischer, K. R., Durrans, A., Lee, S., Sheng, J., Li, F., Wong, S. T., et al. (2015). Epithelial-to-mesenchymal transition is not required for lung metastasis but contributes to chemoresistance. *Nature* 527, 472–476. doi: 10.1038/nature15748

Francart, M.-E., Lambert, J., Vanwynsberghe, A. M., Thompson, E. W., Bourcy, M., Polette, M., et al. (2018). Epithelial-mesenchymal plasticity and circulating tumor cells: travel companions to metastases. *Dev. Dyn.* 247, 432–450. doi: 10.1002/dvdy.24506

Freed-Pastor, W. A., Mizuno, H., Zhao, X., Langerod, A., Moon, S. H., Rodriguez-Barrueco, R., et al. (2012). Mutant p53 disrupts mammary tissue architecture via the mevalonate pathway. *Cell* 148, 244–258. doi: 10.1016/j.cell.2011.12.017

Fuchs, B. C., Fujii, T., Dorfman, J. D., Goodwin, J. M., Zhu, A. X., Lanuti, M., et al. (2008). Epithelial-to-mesenchymal transition and integrin-linked kinase mediate sensitivity to epidermal growth factor receptor inhibition in human hepatoma cells. *Cancer Res.* 68, 2391–2399. doi: 10.1158/0008-5472.can-07-2460

Gal, A., Sjoblom, T., Fedorova, L., Imreh, S., Beug, H., and Moustakas, A. (2008). Sustained TGF beta exposure suppresses Smad and non-Smad signalling in mammary epithelial cells, leading to EMT and inhibition of growth arrest and apoptosis. *Oncogene* 27, 1218–1230. doi: 10.1038/sj.onc.1210741

Gómez-Cuadrado, L., Tracey, N., Ma, R., Qian, B., and Brunton, V. G. (2017). Mouse models of metastasis: progress and prospects. *Dis. Mod. Mech.* 10, 1061–1074. doi: 10.1242/dmm.030403

Grosselin, K., Durand, A., Marsolier, J., Poitou, A., Marangoni, E., Nemati, F., et al. (2019). High-throughput single-cell ChIP-seq identifies heterogeneity of chromatin states in breast cancer. *Nat. Genet.* 51, 1060–1066. doi: 10.1038/s41588-019-0424-429

Gunasinghe, N. P., Wells, A., Thompson, E. W., and Hugo, H. J. (2012). Mesenchymal-epithelial transition (MET) as a mechanism for metastatic colonisation in breast cancer. *Cancer Metast. Rev.* 31, 469–478. doi: 10.1007/s10555-012-9377-9375

Guo, W., Keckesova, Z., Donaher, J. L., Shibue, T., Tischler, V., Reinhardt, F., et al. (2012). Slug and Sox9 cooperatively determine the mammary stem cell state. *Cell* 148, 1015–1028. doi: 10.1016/j.cell.2012.02.008

Gupta, P. B., Fillmore, C. M., Jiang, G., Shapira, S. D., Tao, K., Kuperwasser, C., et al. (2011). Stochastic state transitions give rise to phenotypic equilibrium in populations of cancer cells. *Cell* 146, 633–644. doi: 10.1016/j.cell.2011.07.026

Han, L., Chen, W., and Zhao, Q. J. T. B. (2014). Prognostic value of circulating tumor cells in patients with pancreatic cancer: a meta-analysis. *Tumour Biol.* 35, 2473–2480. doi: 10.1007/s13277-013-1327-5

Harner-Foreman, N., Vadakekolathu, J., Laversin, S. A., Mathieu, M. G., Reeder, S., Pockley, A. G., et al. (2017). A novel spontaneous model of epithelial-mesenchymal transition (EMT) using a primary prostate cancer derived cell line demonstrating distinct stem-like characteristics. *Sci. Rep.* 7:40633. doi: 10.1038/srep40633

Hassan, S., Blick, T., Williams, E. D., and Thompson, E. W. (2020). Applications of RNA from circulating tumor cells. *Front. Biosci.* 25, 874–892. doi: 10.2741/4838

Henkel, L., Rauscher, B., and Boutros, M. (2019). Context-dependent genetic interactions in cancer. *Curr. Opin. Genet. Dev.* 54, 73–82. doi: 10.1016/j.gde.2019.03.004

Hirata, E., Park, D., and Sahai, E. (2014). Retrograde flow of cadherins in collective cell migration. *Nat. Cell Biol.* 16:621. doi: 10.1038/ncb2995

Hiscox, S., Jiang, W. G., Obermeier, K., Taylor, K., Morgan, L., Burmi, R., et al. (2006). Tamoxifen resistance in MCF7 cells promotes EMT-like behaviour and involves modulation of β-catenin phosphorylation. *Int. J. Cancer* 118, 290–301. doi: 10.1002/ijc.21355

Horning, A. M., Wang, Y., Lin, C.-K., Louie, A. D., Jadhav, R. R., Hung, C.-N., et al. (2018). Single-Cell RNA-seq reveals a subpopulation of prostate cancer cells with enhanced cell-Cycle-Related transcription and attenuated androgen response. *Cancer Res.* 78, 853–864. doi: 10.1158/0008-5472.can-17-1924

Horton, J. D., Goldstein, J. L., and Brown, M. S. (2002). SREBPs: activators of the complete program of cholesterol and fatty acid synthesis in the liver. *J. Clin. Invest.* 109, 1125–1131. doi: 10.1172/jci15593

Hu, J., Liu, Z., and Wang, X. (2013). Does TP53 mutation promote ovarian cancer metastasis to omentum by regulating lipid metabolism? *Med. Hypotheses* 81, 515–520. doi: 10.1016/j.mehy.2013.06.009

Huang, R. Y. J., Wong, M. K., Tan, T. Z., Kuay, K. T., Ng, A. H. C., Chung, V. Y., et al. (2013). An EMT spectrum defines an anoikis-resistant and spheroidogenic intermediate mesenchymal state that is sensitive to e-cadherin restoration by a src-kinase inhibitor, saracatinib (AZD0530). *Cell Death Dis.* 4:e915. doi: 10.1038/cddis.2013.442

Huang, S., Ernberg, I., and Kauffman, S. (2009). Cancer attractors: a systems view of tumors from a gene network dynamics and developmental perspective. *Semin. Cell Dev. Biol.* 20, 869–876. doi: 10.1016/j.semcdb.2009.07.003

Hugo, H., Ackland, M. L., Blick, T., Lawrence, M. G., Clements, J. A., Williams, E. D., et al. (2007). Epithelial–mesenchymal and mesenchymal–epithelial transitions in carcinoma progression. *J. Cell. Physiol.* 213, 374–383. doi: 10.1002/jcp.21223

Hugo, H., Gunasinghe, N., Hollier, B., Tanaka, T., Blick, T., Toh, A., et al. (2017). Epithelial requirement for in vitro proliferation and xenograft growth and metastasis of MDA-MB-468 human breast cancer cells: oncogenic rather than tumor-suppressive role of E-cadherin. *Breast Cancer Res.* 19, 86.

Hugo, H. J., Wafai, R., Blick, T., Thompson, E. W., and Newgreen, D. F. (2009). Staurosporine augments EGF-mediated EMT in PMC42-LA cells through actin depolymerisation, focal contact size reduction and Snail1 induction - a model for cross-modulation. *BMC Cancer* 9:235. doi: 10.1186/1471-2407-9-235

Hüsemann, Y., Geigl, J. B., Schubert, F., Musiani, P., Meyer, M., Burghart, E., et al. (2008). Systemic spread is an early step in breast cancer. *Cancer Cell* 13, 58–68. doi: 10.1016/j.ccr.2007.12.003

Ishay-Ronen, D., Diepenbruck, M., Kalathur, R. K. R., Sugiyama, N., Tiede, S., Ivanek, R., et al. (2019). Gain fat-lose metastasis: converting invasive breast cancer cells into adipocytes inhibits cancer metastasis. *Cancer Cell* 35, 17–32. doi: 10.1016/j.ccell.2018.12.002

Janiszewska, M., and Polyak, K. (2018). A confetti trail of tumour evolution. *Nat. Cell Biol.* 20, 639–641. doi: 10.1038/s41556-018-0110-117

Jia, D., Li, X., Bocci, F., Tripathi, S., Deng, Y., Jolly, M. K., et al. (2019). Quantifying cancer epithelial-mesenchymal plasticity and its association with stemness and immune response. *J. Clin. Med.* 8:725. doi: 10.3390/jcm8050725

Jimenez, L., Wang, J., Morrison, M. A., Whatcott, C., Soh, K. K., Warner, S., et al. (2016). Phenotypic chemical screening using a zebrafish neural crest EMT reporter identifies retinoic acid as an inhibitor of epithelial morphogenesis. *Dis. Model. Mech.* 9, 389–400. doi: 10.1242/dmm.021790

Jolly, M. K., and Celià-Terrassa, T. (2019). Dynamics of phenotypic heterogeneity associated with EMT and stemness during cancer progression. *J. Clin. med.* 8:1542. doi: 10.3390/jcm8101542

Jolly, M. K., Kulkarni, P., Weninger, K., Orban, J., and Levine, H. (2018). Phenotypic plasticity, bet-hedging, and androgen independence in prostate

cancer: role of non-genetic heterogeneity. *Front. Oncol.* 8:50. doi: 10.3389/fonc.2018.00050

Jolly, M. K., Tripathi, S. C., Jia, D., Mooney, S. M., Celiktas, M., Hanash, S. M., et al. (2016). Stability of the hybrid epithelial/mesenchymal phenotype. *Oncotarget* 7, 27067–27084. doi: 10.18632/oncotarget.8166

Jolly, M. K., Tripathi, S. C., Somarelli, J. A., Hanash, S. M., and Levine, H. (2017). Epithelial/mesenchymal plasticity: how have quantitative mathematical models helped improve our understanding? *Mol. Oncol.* 11, 739–754. doi: 10.1002/1878-0261.12084

Jolly, M. K., Ware, K. E., Xu, S., Gilja, S., Shetler, S., Yang, Y., et al. (2019). E-cadherin represses anchorage-independent growth in sarcomas through both signaling and mechanical mechanisms. *Mol. Cancer Res.* 17, 1391–1402. doi: 10.1158/1541-7786.Mcr-18-0763

Kaigorodova, E., Tarabanovskaya, N., Staheeva, M., Savelieva, O., Tashireva, L., Denisov, E., et al. (2017). Effect of small and radical surgical injury on the level of different populations of circulating tumor cells in the blood of breast cancer patients. *Neoplasma* 64, 437–443. doi: 10.4149/neo_2017_315

Kajita, M., McClinic, K. N., and Wade, P. A. (2004). Aberrant expression of the transcription factors snail and slug alters the response to genotoxic stress. *Mol. Cell. Biol.* 24, 7559–7566. doi: 10.1128/MCB.24.17.7559-7566.2004

Kalluri, R., and Weinberg, R. A. (2009). The basics of epithelial-mesenchymal transition. *J. Clin. Invest.* 119, 1420–1428. doi: 10.1172/jci39104

Kang, H., Kim, H., Lee, S., Youn, H., and Youn, B. (2019). Role of metabolic reprogramming in epithelial?mesenchymal transition (EMT). *Intern. J. Mol. Sci.* 20:2042. doi: 10.3390/ijms20082042

Karacosta, L. G., Anchang, B., Ignatiadis, N., Kimmey, S. C., Benson, J. A., Shrager, J. B., et al. (2019). Mapping lung cancer epithelial-mesenchymal transition states and trajectories with single-cell resolution. *Nat. Commun.* 10:5587. doi: 10.1038/s41467-019-13441-13446

Khoo, B. L., Lee, S. C., Kumar, P., Tan, T. Z., Warkiani, M. E., Ow, S. G., et al. (2015). Short-term expansion of breast circulating cancer cells predicts response to anti-cancer therapy. *Oncotarget* 6, 15578–15593. doi: 10.18632/oncotarget.3903

Kim, C., Gao, R., Sei, E., Brandt, R., Hartman, J., Hatschek, T., et al. (2018). Chemoresistance evolution in triple-negative breast cancer delineated by single-cell sequencing. *Cell* 173, 879–893.

Klevebring, D., Rosin, G., Ma, R., Lindberg, J., Czene, K., Kere, J., et al. (2014). Sequencing of breast cancer stem cell populations indicates a dynamic conversion between differentiation states in vivo. *Breast Cancer Res.* 16:R72. doi: 10.1186/bcr3687

Klymenko, Y., Johnson, J., Bos, B., Lombard, R., Campbell, L., Loughran, E., et al. (2017). Heterogeneous cadherin expression and multicellular aggregate dynamics in ovarian cancer dissemination. *Neoplasia* 19, 549–563. doi: 10.1016/j.neo.2017.04.002

Klymkowsky, M. W., and Savagner, P. (2009). Epithelial-mesenchymal transition: a cancer researcher's conceptual friend and foe. *Am. J. Pathol.* 174, 1588–1593.

Kondaveeti, Y., Guttilla Reed, I. K., and White, B. A. (2015). Epithelial-mesenchymal transition induces similar metabolic alterations in two independent breast cancer cell lines. *Cancer Lett.* 364, 44–58. doi: 10.1016/j.canlet.2015.04.025

Kowalik, A., Kowalewska, M., and Góźdź, S. J. T. R. (2017). Current approaches for avoiding the limitations of circulating tumor cells detection methods—implications for diagnosis and treatment of patients with solid tumors. *Transl. Res.* 185, 58.–84.

Kramer, N., Walzl, A., Unger, C., Rosner, M., Krupitza, G., Hengstschlager, M., et al. (2013). In vitro cell migration and invasion assays. *Mutat. Res.* 752, 10–24. doi: 10.1016/j.mrrev.2012.08.001

Krebs, A. M., Mitschke, J., Lasierra Losada, M., Schmalhofer, O., Boerries, M., Busch, H., et al. (2017). The EMT-activator Zeb1 is a key factor for cell plasticity and promotes metastasis in pancreatic cancer. *Nat. Cell Biol.* 19, 518–529. doi: 10.1038/ncb3513

Kroger, C., Afeyan, A., Mraz, J., Eaton, E. N., Reinhardt, F., Khodor, Y. L., et al. (2019). Acquisition of a hybrid E/M state is essential for tumorigenicity of basal breast cancer cells. *Proc. Natl. Acad. Sci. U.S.A.* 116, 7353–7362. doi: 10.1073/pnas.1812876116

Kumar, S., Park, S. H., Cieply, B., Schupp, J., Killiam, E., Zhang, F., et al. (2011). A pathway for the control of anoikis sensitivity by E-cadherin and epithelial-to-mesenchymal transition. *Mol. Cell. Biol.* 31, 4036–4051. doi: 10.1128/MCB.01342-1310

Kurimoto, R., Iwasawa, S., Ebata, T., Ishiwata, T., Sekine, I., Tada, Y., et al. (2016). Drug resistance originating from a TGF-beta/FGF-2-driven epithelial-to-mesenchymal transition and its reversion in human lung adenocarcinoma cell lines harboring an EGFR mutation. *Int. J. Oncol.* 48, 1825–1836. doi: 10.3892/ijo.2016.3419

Labernadie, A., Kato, T., Brugues, A., Serra-Picamal, X., Derzsi, S., Arwert, E., et al. (2017). A mechanically active heterotypic E-cadherin/N-cadherin adhesion enables fibroblasts to drive cancer cell invasion. *Nat. Cell Biol.* 19, 224–237. doi: 10.1038/ncb3478

Lambert, A. W., Pattabiraman, D. R., and Weinberg, R. A. J. C. (2017). Emerging biological principles of metastasis. *Cell* 168, 670–691. doi: 10.1016/j.cell.2016.11.037

Latil, M., Nassar, D., Beck, B., Boumahdi, S., Wang, L., Brisebarre, A., et al. (2017). Cell-type-specific chromatin states differentially prime squamous cell carcinoma tumor-initiating cells for epithelial to mesenchymal transition. *Cell Stem Cell* 20, 191–204. doi: 10.1016/j.stem.2016.10.018

Lecharpentier, A., Vielh, P., Perez-Moreno, P., Planchard, D., Soria, J., and Farace, F. J. B. (2011). Detection of circulating tumour cells with a hybrid (epithelial/mesenchymal) phenotype in patients with metastatic non-small cell lung cancer. *Br. J. Cancer* 105, 1338–1341. doi: 10.1038/bjc.2011.405

Lee, J. M., Dedhar, S., Kalluri, R., and Thompson, E. W. (2006). The epithelial-mesenchymal transition: new insights in signaling, development, and disease. *J. Cell Biol.* 172, 973–981. doi: 10.1083/jcb.200601018

Lee, S. Y., Ju, M. K., Jeon, H. M., Lee, Y. J., Kim, C. H., Park, H. G., et al. (2018). Oncogenic metabolism acts as a prerequisite step for induction of cancer metastasis and cancer stem cell phenotype. *Oxid. Med. Cell Longev.* 2018:1027453. doi: 10.1155/2018/1027453

Lemaire, C. A., Liu, S. Z., Wilkerson, C. L., Ramani, V. C., Barzanian, N. A., Huang, K.-W., et al. (2018). Fast and label-free isolation of circulating tumor cells from blood: from a research microfluidic platform to an automated fluidic instrument, VTX-1 liquid biopsy system. *SLAS Technol.* 23, 16–29. doi: 10.1177/2472630317738698

Li, L., Qi, L., Liang, Z., Song, W., Liu, Y., Wang, Y., et al. (2015). Transforming growth factor-beta1 induces EMT by the transactivation of epidermal growth factor signaling through HA/CD44 in lung and breast cancer cells. *Int. J. Mol. Med.* 36, 113–122. doi: 10.3892/ijmm.2015.2222

Li, Q., Wennborg, A., Aurell, E., Dekel, E., Zou, J.-Z., Xu, Y., et al. (2016). Dynamics inside the cancer cell attractor reveal cell heterogeneity, limits of stability, and escape. *Proc. Natl. Acad. Sci. U.S.A.* 113:2672. doi: 10.1073/pnas.1519210113

Li, Q. Q., Xu, J. D., Wang, W. J., Cao, X. X., Chen, Q., Tang, F., et al. (2009). Twist1-mediated adriamycin-induced epithelial-mesenchymal transition relates to multidrug resistance and invasive potential in breast cancer cells. *Clin. Cancer Res.* 15, 2657–2665. doi: 10.1158/1078-0432.ccr-08-2372

Li, Y., VandenBoom, T. G. II, Kong, D., Wang, Z., Ali, S., Philip, P. A., et al. (2009). Up-regulation of miR-200 and let-7 by natural agents leads to the reversal of epithelial-to-mesenchymal transition in gemcitabine-resistant pancreatic cancer cells. *Cancer Res.* 69, 6704–6712. doi: 10.1158/0008-5472.can-09-1298

Li, X., Lewis, M. T., Huang, J., Gutierrez, C., Osborne, C. K., Wu, M. F., et al. (2008). Intrinsic resistance of tumorigenic breast cancer cells to chemotherapy. *J. Natl. Cancer Inst.* 100, 672–679. doi: 10.1093/jnci/djn123

Liedtke, C., Mazouni, C., Hess, K. R., Andre, F., Tordai, A., Mejia, J. A., et al. (2008). Response to neoadjuvant therapy and long-term survival in patients with triple-negative breast cancer. *J. Clin. Oncol.* 26, 1275–1281. doi: 10.1200/jco.2007.14.4147

Liu, T. L., Upadhyayula, S., Milkie, D. E., Singh, V., Wang, K., Swinburne, I. A., et al. (2018). Observing the cell in its native state: imaging subcellular dynamics in multicellular organisms. *Science* 360:6386. doi: 10.1126/science.aaq1392

Lopez-Munoz, E., and Mendez-Montes, M. (2013). Markers of circulating breast cancer cells. *Adv. Clin. Chem.* 61, 175–224. doi: 10.1016/b978-0-12-407680-8.00007-5

Lou, Y., Diao, L., Cuentas, E. R., Denning, W. L., Chen, L., Fan, Y. H., et al. (2016). Epithelial-mesenchymal transition is associated with a distinct tumor microenvironment including elevation of inflammatory signals and multiple immune checkpoints in lung adenocarcinoma. *Clin. Cancer Res.* 22, 3630–3642. doi: 10.1158/1078-0432.Ccr-15-1434

Lourenco, A. R., Ban, Y., Crowley, M. J., Lee, S. B., Ramchandani, D., Du, W., et al. (2020). Differential contributions of pre- and post-EMT tumor cells in breast

cancer metastasis. *Cancer Res.* 80, 163–169. doi: 10.1158/0008-5472.Can-19-1427

Lu, M., Jolly, M. K., Levine, H., Onuchic, J. N., and Ben-Jacob, E. J. P. (2013). MicroRNA-based regulation of epithelial-hybrid-mesenchymal fate determination. *PNAS* 110, 18144–18149. doi: 10.1073/pnas.1318192110

Lu, W., and Kang, Y. (2019). Epithelial-mesenchymal plasticity in cancer progression and metastasis. *Dev. Cell* 49, 361–374. doi: 10.1016/j.devcel.2019.04.010

Ma, Y.-H. V., Middleton, K., You, L., and Sun, Y. (2018). A review of microfluidic approaches for investigating cancer extravasation during metastasis. *Microsyst. Nanoeng.* 4:17104.

Mani, S. A., Guo, W., Liao, M.-J., Eaton, E. N., Ayyanan, A., Zhou, A. Y., et al. (2008). The epithelial-mesenchymal transition generates cells with properties of stem cells. *Cell* 133, 704–715. doi: 10.1016/j.cell.2008.03.027

Marcucci, F., Bellone, M., Caserta, C. A., and Corti, A. (2014). Pushing tumor cells towards a malignant phenotype: stimuli from the microenvironment, intercellular communications and alternative roads. *Int. J. Cancer* 135, 1265–1276. doi: 10.1002/ijc.28572

Marcucci, F., Stassi, G., and De Maria, R. (2016). Epithelial-mesenchymal transition: a new target in anticancer drug discovery. *Nat. Rev. Drug Discov.* 15, 311–325. doi: 10.1038/nrd.2015.13

Markiewicz, A., Ksiazkiewicz, M., Welnicka-Jaskiewicz, M., Seroczynska, B., Skokowski, J., Szade, J., et al. (2014). Mesenchymal phenotype of CTC-enriched blood fraction and lymph node metastasis formation potential. *PLoS One* 9:e93901. doi: 10.1371/journal.pone.0093901

Marx, V. (2018). Stem cells: lineage tracing lets single cells talk about their past. *Nat. Methods* 15, 411–414. doi: 10.1038/s41592-018-0016-10

Mason, D. E., Collins, J. M., Dawahare, J. H., Nguyen, T. D., Lin, Y., Voytik-Harbin, S. L., et al. (2019). YAP and TAZ limit cytoskeletal and focal adhesion maturation to enable persistent cell motility. *J. Cell Biol.* 218, 1369–1389. doi: 10.1083/jcb.201806065

Mathis, R. A., Sokol, E. S., and Gupta, P. B. (2017). Cancer cells exhibit clonal diversity in phenotypic plasticity. *Open Biol.* 7:160283. doi: 10.1098/rsob.160283

May, C. D., Sphyris, N., Evans, K. W., Werden, S. J., Guo, W., and Mani, S. A. (2011). Epithelial-mesenchymal transition and cancer stem cells: a dangerously dynamic duo in breast cancer progression. *Breast Cancer Res.* 13:202.

McDonald, O. G., Wu, H., Timp, W., Doi, A., and Feinberg, A. P. (2011). Genome-scale epigenetic reprogramming during epithelial-to-mesenchymal transition. *Nat. Struct. Mol. Biol.* 18, 867–874. doi: 10.1038/nsmb.2084

McGranahan, N., and Swanton, C. (2015). Biological and therapeutic impact of intratumor heterogeneity in cancer evolution. *Cancer Cell* 27, 15–26. doi: 10.1016/j.ccell.2014.12.001

McInnes, L. M., Jacobson, N., Redfern, A., Dowling, A., Thompson, E. W., and Saunders, C. M. (2015). Clinical implications of circulating tumor cells of breast cancer patients: role of epithelial-mesenchymal plasticity. *Front. Oncol.* 5:42. doi: 10.3389/fonc.2015.00042

Miao, J. W., Liu, L. J., and Huang, J. (2014). Interleukin-6-induced epithelial-mesenchymal transition through signal transducer and activator of transcription 3 in human cervical carcinoma. *Int. J. Oncol.* 45, 165–176. doi: 10.3892/ijo.2014.2422

Milano, A., Mazzetta, F., Valente, S., Ranieri, D., Leone, L., Botticelli, A., et al. (2018). Molecular detection of EMT markers in circulating tumor cells from metastatic non-small cell lung cancer patients: potential role in clinical practice. *Anal. Cell Pathol.* 2018:3506874.

Mitchell, C. B., and O'Neill, G. M. (2016). Cooperative cell invasion: matrix metalloproteinase-mediated incorporation between cells. *Mol. Biol. Cell* 27, 3284–3292. doi: 10.1091/mbc.E16-03-0194

Morandi, A., Taddei, M. L., Chiarugi, P., and Giannoni, E. (2017). Targeting the metabolic reprogramming that controls epithelial-to-mesenchymal transition in aggressive tumors. *Front. Oncol.* 7:40. doi: 10.3389/fonc.2017.00040

Morel, A.-P., Lièvre, M., Thomas, C., Hinkal, G., Ansieau, S., and Puisieux, A. (2008). Generation of breast cancer stem cells through epithelial-mesenchymal transition. *PLoS One* 3:e2888. doi: 10.1371/journal.pone.0002888

Moroishi, T., Hansen, C. G., and Guan, K.-L. (2015). The emerging roles of YAP and TAZ in cancer. *Nat. Rev. Cancer* 15, 73–79. doi: 10.1038/nrc3876

Naito, T., Tanaka, F., Ono, A., Yoneda, K., Takahashi, T., Murakami, H., et al. (2012). Prognostic impact of circulating tumor cells in patients with small cell lung cancer. *J. Thor. Oncol.* 7, 512–519.

Narai, A., Arai, S., and Shimizu, M. (1997). Rapid decrease in transepithelial electrical resistance of human intestinal Caco-2 cell monolayers by cytotoxic membrane perturbents. *Toxicol. Vitro* 11, 347–354. doi: 10.1016/s0887-2333(97)00026-x

Nieto, M. A. (2013). Epithelial plasticity: a common theme in embryonic and cancer cells. *Science* 342:6159.

Nieto, M. A. (2018). A snail tale and the chicken embryo. *Int. J. Dev. Biol.* 62, 121–126. doi: 10.1387/ijdb.170301mn

Noman, M. Z., Janji, B., Abdou, A., Hasmim, M., Terry, S., Tan, T. Z., et al. (2017). The immune checkpoint ligand PD-L1 is upregulated in EMT-activated human breast cancer cells by a mechanism involving ZEB-1 and miR-200. *Oncoimmunology* 6:e1263412. doi: 10.1080/2162402x.2016.1263412

Ocana, O. H., Corcoles, R., Fabra, A., Moreno-Bueno, G., Acloque, H., Vega, S., et al. (2012). Metastatic colonization requires the repression of the epithelial-mesenchymal transition inducer Prrx1. *Cancer Cell* 22, 709–724. doi: 10.1016/j.ccr.2012.10.012

Ochoa-Hernandez, A. B., Juarez-Vazquez, C. I., Rosales-Reynoso, M. A., and Barros-Nunez, P. (2012). WNT-beta-catenin signaling pathway and its relationship with cancer. *Cir. Cir.* 80, 389–398.

Oltean, S., Sorg, B. S., Albrecht, T., Bonano, V. I., Brazas, R. M., Dewhirst, M. W., et al. (2006). Alternative inclusion of fibroblast growth factor receptor 2 exon IIIc in Dunning prostate tumors reveals unexpected epithelial mesenchymal plasticity. *Proc. Natl. Acad. Sci. U.S.A.* 103, 14116–14121. doi: 10.1073/pnas.0603090103

Padmanaban, V., Krol, I., Suhail, Y., Szczerba, B. M., Aceto, N., Bader, J. S., et al. (2019). E-cadherin is required for metastasis in multiple models of breast cancer. *Nature* 573, 439–444. doi: 10.1038/s41586-019-1526-3

Pan, L., Yan, G., Chen, W., Sun, L., Wang, J., and Yang, J. (2019). Distribution of circulating tumor cell phenotype in early cervical cancer. *Cancer Manag. Res.* 11:5531. doi: 10.2147/cmar.s198391

Papadaki, M. A., Stoupis, G., Theodoropoulos, P. A., Mavroudis, D., Georgoulias, V., and Agelaki, S. J. (2019). Circulating tumor cells with stemness and epithelial-to-mesenchymal transition features are chemoresistant and predictive of poor outcome in metastatic breast cancer. *Mol. Cancer Ther.* 18, 437–447. doi: 10.1158/1535-7163.mct-18-0584

Pastushenko, I., and Blanpain, C. (2019). EMT Transition states during tumor progression and metastasis. *Trends Cell Biol.* 29, 212–226. doi: 10.1016/j.tcb.2018.12.001

Pastushenko, I., Brisebarre, A., Sifrim, A., Fioramonti, M., Revenco, T., Boumahdi, S., et al. (2018). Identification of the tumour transition states occurring during EMT. *Nature* 556, 463–468. doi: 10.1038/s41586-018-0040-43

Patel, A. P., Tirosh, I., Trombetta, J. J., Shalek, A. K., Gillespie, S. M., Wakimoto, H., et al. (2014). Single-cell RNA-seq highlights intratumoral heterogeneity in primary glioblastoma. *Science* 344, 1396–1401. doi: 10.1126/science.1254257

Pattabiraman, D. R., Bierie, B., Kober, K. I., Thiru, P., Krall, J. A., Zill, C., et al. (2016). Activation of PKA leads to mesenchymal-to-epithelial transition and loss of tumor-initiating ability. *Science* 351:3680. doi: 10.1126/science.aad3680

Pattabiraman, D. R., and Weinberg, R. A. (2016). Targeting the Epithelial-to-Mesenchymal Transition: the Case for differentiation-based therapy. *Cold. Spring Harb. Symp. Quant. Biol.* 81, 11–19. doi: 10.1101/sqb.2016.81.030957

Payne, R., Wang, F., Su, N., Krell, J., Zebrowski, A., Yagüe, E., et al. (2012). Viable circulating tumour cell detection using multiplex RNA in situ hybridisation predicts progression-free survival in metastatic breast cancer patients. *Br. J. Cancer* 106, 1790–1797. doi: 10.1038/bjc.2012.137

Peinado, H., Marin, F., Cubillo, E., Stark, H. J., Fusenig, N., Nieto, M. A., et al. (2004). Snail and E47 repressors of E-cadherin induce distinct invasive and angiogenic properties in vivo. *J. Cell Sci.* 117(Pt 13), 2827–2839. doi: 10.1242/jcs.01145

Peinado, H., Olmeda, D., and Cano, A. (2007). Snail, Zeb and bHLH factors in tumour progression: an alliance against the epithelial phenotype? *Nat. Rev. Cancer* 7, 415–428. doi: 10.1038/nrc2131

Polyak, K., and Weinberg, R. A. (2009). Transitions between epithelial and mesenchymal states: acquisition of malignant and stem cell traits. *Nat. Rev. Cancer* 9, 265–273. doi: 10.1038/nrc2620

Proia, T. A., Keller, P. J., Gupta, P. B., Klebba, I., Jones, A. D., Sedic, M., et al. (2011). Genetic predisposition directs breast cancer phenotype by dictating progenitor cell fate. *Cell Stem Cell* 8, 149–163. doi: 10.1016/j.stem.2010.12.007

Przybylo, J. A., and Radisky, D. C. (2007). Matrix metalloproteinase-induced epithelial-mesenchymal transition: tumor progression at Snail's pace. *Int. J. Biochem. Cell Biol.* 39, 1082–1088. doi: 10.1016/j.biocel.2007.03.002

Puram, S. V., Parikh, A. S., and Tirosh, I. (2018). Single cell RNA-seq highlights a role for a partial EMT in head and neck cancer. *Mol. Cell Oncol.* 5:e1448244. doi: 10.1080/23723556.2018.1448244

Qi, X. K., Han, H. Q., Zhang, H. J., Xu, M., Li, L., Chen, L., et al. (2018). OVOL2 links stemness and metastasis via fine-tuning epithelial-mesenchymal transition in nasopharyngeal carcinoma. *Theranostics* 8, 2202–2216. doi: 10.7150/thno.24003

Quan, Q., Wang, X., Lu, C., Ma, W., Wang, Y., Xia, G., et al. (2020). Cancer stem-like cells with hybrid epithelial/mesenchymal phenotype leading the collective invasion. *Cancer Sci.* 111, 467. doi: 10.1111/cas.14285

Redfern, A. D., Spalding, L. J., and Thompson, E. W. (2018). The Kraken Wakes: induced EMT as a driver of tumour aggression and poor outcome. *Clin. Exp. Metastasis* 35, 285–308. doi: 10.1007/s10585-018-9906-x

Reynolds, D. S., Tevis, K. M., Blessing, W. A., Colson, Y. L., Zaman, M. H., and Grinstaff, M. W. (2017). Breast cancer spheroids reveal a differential cancer stem cell response to chemotherapeutic treatment. *Sci. Rep.* 7:10382. doi: 10.1038/s41598-017-10863-10864

Rhim, A. D., Mirek, E. T., Aiello, N. M., Maitra, A., Bailey, J. M., McAllister, F., et al. (2012). EMT and dissemination precede pancreatic tumor formation. *Cell* 148, 349–361. doi: 10.1016/j.cell.2011.11.025

Ribeiro-Samy, S., Oliveira, M. I., Pereira-Veiga, T., Muinelo-Romay, L., Carvalho, S., Gaspar, J., et al. (2019). Fast and efficient microfluidic cell filter for isolation of circulating tumor cells from unprocessed whole blood of colorectal cancer patients. *Sci. Rep.* 9, 1–12.

Riethdorf, S., Fritsche, H., Müller, V., Rau, T., Schindlbeck, C., Rack, B., et al. (2007). Detection of circulating tumor cells in peripheral blood of patients with metastatic breast cancer: a validation study of the CellSearch system. *Clin. Cancer Res.* 13, 920–928. doi: 10.1158/1078-0432.ccr-06-1695

Rios, A. C., Capaldo, B. D., Vaillant, F., Pal, B., van Ineveld, R., Dawson, C. A., et al. (2019). Intraclonal plasticity in mammary tumors revealed through large-scale single-cell resolution 3D imaging. *Cancer Cell* 35, 618–632. doi: 10.1016/j.ccell.2019.02.010

Risom, T., Langer, E. M., Chapman, M. P., Rantala, J., Fields, A. J., Boniface, C., et al. (2018). Differentiation-state plasticity is a targetable resistance mechanism in basal-like breast cancer. *Nat. Commun.* 9:3815. doi: 10.1038/s41467-018-05729-w

Rotem, A., Ram, O., Shoresh, N., Sperling, R. A., Goren, A., Weitz, D. A., et al. (2015). Single-cell ChIP-seq reveals cell subpopulations defined by chromatin state. *J. Cell Sci.* 33:1165. doi: 10.1038/nbt.3383

Ruscetti, M., Dadashian, E. L., Guo, W., Quach, B., Mulholland, D. J., Park, J. W., et al. (2016). HDAC inhibition impedes epithelial-mesenchymal plasticity and suppresses metastatic, castration-resistant prostate cancer. *Oncogene* 35, 3781–3795. doi: 10.1038/onc.2015.444

Sabbah, M., Emami, S., Redeuilh, G., Julien, S., Prevost, G., Zimber, A., et al. (2008). Molecular signature and therapeutic perspective of the epithelial-to-mesenchymal transitions in epithelial cancers. *Drug Resist. Updat.* 11, 123–151. doi: 10.1016/j.drup.2008.07.001

Sánchez-Martínez, R., Cruz-Gil, S., Gómez de Cedrón, M., Álvarez-Fernández, M., Vargas, T., Molina, S., et al. (2015). A link between lipid metabolism and epithelial-mesenchymal transition provides a target for colon cancer therapy. *Oncotarget* 6, 38719–38736. doi: 10.18632/oncotarget.5340

Sarioglu, A. F., Aceto, N., Kojic, N., Donaldson, M. C., Zeinali, M., Hamza, B., et al. (2015). A microfluidic device for label-free, physical capture of circulating tumor cell clusters. *Nat. Methods* 12, 685–691. doi: 10.1038/nmeth.3404

Scheel, C., Eaton, E. N., Li, S. H., Chaffer, C. L., Reinhardt, F., Kah, K. J., et al. (2011). Paracrine and autocrine signals induce and maintain mesenchymal and stem cell states in the breast. *Cell* 145, 926–940. doi: 10.1016/j.cell.2011.04.029

Schulz, D., Zanotelli, V. R. T., Fischer, J. R., Schapiro, D., Engler, S., Lun, X.-K., et al. (2018). Simultaneous multiplexed imaging of mRNA and proteins with subcellular resolution in breast cancer tissue samples by mass cytometry. *Cell Syst.* 6, 25–36. doi: 10.1016/j.cels.2017.12.001

Serrano-Gomez, S. J., Maziveyi, M., and Alahari, S. K. (2016). Regulation of epithelial-mesenchymal transition through epigenetic and post-translational modifications. *Mol. Cancer* 15:8. doi: 10.1186/s12943-016-0502-x

Shang, M., Soon, R. H., Lim, C. T., Khoo, B. L., and Han, J. (2019). Microfluidic modelling of the tumor microenvironment for anti-cancer drug development. *Lab. Chip.* 19, 369–386. doi: 10.1039/c8lc00970h

Sharma, S. V., Lee, D. Y., Li, B., Quinlan, M. P., Takahashi, F., Maheswaran, S., et al. (2010). A chromatin-mediated reversible drug-tolerant state in cancer cell subpopulations. *Cell* 141, 69–80. doi: 10.1016/j.cell.2010.02.027

Sikandar, S. S., Kuo, A. H., Kalisky, T., Cai, S., Zabala, M., Hsieh, R. W., et al. (2017). Role of epithelial to mesenchymal transition associated genes in mammary gland regeneration and breast tumorigenesis. *Nat. Commun.* 8:1669. doi: 10.1038/s41467-017-01666-1662

Smit, M. A., Geiger, T. R., Song, J. Y., Gitelman, I., and Peeper, D. S. (2009). A Twist-Snail axis critical for TrkB-induced epithelial-mesenchymal transition-like transformation, anoikis resistance, and metastasis. *Mol. Cell. Biol.* 29, 3722–3737. doi: 10.1128/mcb.01164-1168

Spaderna, S., Schmalhofer, O., Wahlbuhl, M., Dimmler, A., Bauer, K., Sultan, A., et al. (2008). The transcriptional repressor ZEB1 promotes metastasis and loss of cell polarity in cancer. *Cancer Res.* 68, 537–544. doi: 10.1158/0008-5472.Can-07-5682

Stemmler, M. P., Eccles, R. L., Brabletz, S., and Brabletz, T. (2019). Non-redundant functions of EMT transcription factors. *Nat. Cell Biol.* 21, 102–112. doi: 10.1038/s41556-018-0196-y

Stuelten, C. H., Parent, C. A., and Montell, D. J. (2018). Cell motility in cancer invasion and metastasis: insights from simple model organisms. *Nat. Rev. Cancer* 18, 296–312. doi: 10.1038/nrc.2018.15

Stylianou, N., Lehman, M. L., Wang, C., Fard, A. T., Rockstroh, A., Fazli, L., et al. (2019). A molecular portrait of epithelial-mesenchymal plasticity in prostate cancer associated with clinical outcome. *Oncogene* 38, 913–934. doi: 10.1038/s41388-018-0488-485

Suarez-Causado, A., Caballero-Diaz, D., Bertran, E., Roncero, C., Addante, A., Garcia-Alvaro, M., et al. (2015). HGF/c-Met signaling promotes liver progenitor cell migration and invasion by an epithelial-mesenchymal transition-independent, phosphatidyl inositol-3 kinase-dependent pathway in an in vitro model. *Biochim. Biophys. Acta* 1853(10 Pt A), 2453–2463. doi: 10.1016/j.bbamcr.2015.05.017

Sureshbabu, A., Okajima, H., Yamanaka, D., Tonner, E., Shastri, S., Maycock, J., et al. (2012). IGFBP5 induces cell adhesion, increases cell survival and inhibits cell migration in MCF-7 human breast cancer cells. *J. Cell Sci.* 125, 1693–1705. doi: 10.1242/jcs.092882

Suvà, M. L., Riggi, N., and Bernstein, B. E. (2013). Epigenetic reprogramming in cancer. *Science* 339:1567. doi: 10.1126/science.1230184

Tachtsidis, A., McInnes, L. M., Jacobsen, N., Thompson, E., and Saunders, C. M. J. (2016). Minimal residual disease in breast cancer: an overview of circulating and disseminated tumour cells. *Clin. Exp. Metast.* 33, 521–550. doi: 10.1007/s10585-016-9796-8

Tam, W. L., and Weinberg, R. A. (2013). The epigenetics of epithelial-mesenchymal plasticity in cancer. *Nat. Med.* 19, 1438–1449. doi: 10.1038/nm.3336

Tamura, G., Yin, J., Wang, S., Fleisher, A. S., Zou, T., Abraham, J. M., et al. (2000). E-Cadherin gene promoter hypermethylation in primary human gastric carcinomas. *J. Natl. Cancer Inst.* 92, 569–573. doi: 10.1093/jnci/92.7.569

Tang, M., Shen, H., Jin, Y., Lin, T., Cai, Q., Pinard, M. A., et al. (2013). The malignant brain tumor (MBT) domain protein SFMBT1 is an integral histone reader subunit of the LSD1 demethylase complex for chromatin association and epithelial-to-mesenchymal transition. *J. Biol. Chem.* 288, 27680–27691. doi: 10.1074/jbc.M113.482349

Tanner, K., and Gottesman, M. M. (2015). Beyond 3D culture models of cancer. *Sci. Transl. Med.* 7:283s289. doi: 10.1126/scitranslmed.3009367

Thiery, J. P., Acloque, H., Huang, R. Y., and Nieto, M. A. (2009). Epithelial-mesenchymal transitions in development and disease. *Cell* 139, 871–890. doi: 10.1016/j.cell.2009.11.007

Thompson, E. W., and Nagaraj, S. H. (2018). Transition states that allow cancer to spread. *Nature* 556, 442–444. doi: 10.1038/d41586-018-04403-x

Thuault, S., Tan, E. J., Peinado, H., Cano, A., Heldin, C. H., and Moustakas, A. (2008). HMGA2 and Smads co-regulate SNAIL1 expression during induction of epithelial-to-mesenchymal transition. *J. Biol. Chem.* 283, 33437–33446. doi: 10.1074/jbc.M802016200

Ting, D. T., Wittner, B. S., Ligorio, M., Jordan, N. V., Shah, A. M., Miyamoto, D. T., et al. (2014). Single-cell RNA sequencing identifies extracellular matrix

gene expression by pancreatic circulating tumor cells. *Cell Rep.* 8, 1905–1918. doi: 10.1016/j.celrep.2014.08.029

Truong, D. D., Kratz, A., Park, J. G., Barrientos, E. S., Saini, H., Nguyen, T., et al. (2019). A Human organotypic microfluidic tumor model permits investigation of the interplay between patient-derived fibroblasts and breast cancer cells. *Cancer Res.* 79, 3139–3151. doi: 10.1158/0008-5472.Can-18-2293

Tsai, J. H., Donaher, J. L., Murphy, D. A., Chau, S., and Yang, J. (2012). Spatiotemporal regulation of epithelial-mesenchymal transition is essential for squamous cell carcinoma metastasis. *Cancer Cell* 22, 725–736. doi: 10.1016/j.ccr.2012.09.022

Tsujikawa, T., Kumar, S., Borkar, R. N., Azimi, V., Thibault, G., Chang, Y. H., et al. (2017). Quantitative multiplex immunohistochemistry reveals myeloid-inflamed tumor-immune complexity associated with poor prognosis. *Cell Rep.* 19, 203–217. doi: 10.1016/j.celrep.2017.03.037

van Denderen, B. J., and Thompson, E. W. (2013). Cancer: the to and fro of tumour spread. *Nature* 493, 487–488. doi: 10.1038/493487a

Veening, J.-W., Smits, W. K., and Kuipers, O. P. (2008). Bistability, epigenetics, and bet-hedging in bacteria. *Annu. Rev. Microbiol.* 62, 193–210. doi: 10.1146/annurev.micro.62.081307.163002

Voulgari, A., and Pintzas, A. (2009). Epithelial-mesenchymal transition in cancer metastasis: mechanisms, markers and strategies to overcome drug resistance in the clinic. *Biochim. Biophys. Acta* 1796, 75–90. doi: 10.1016/j.bbcan.2009.03.002

Vrba, L., Jensen, T. J., Garbe, J. C., Heimark, R. L., Cress, A. E., Dickinson, S., et al. (2010). Role for DNA methylation in the regulation of miR-200c and miR-141 expression in normal and cancer cells. *PLoS One* 5:e8697. doi: 10.1371/journal.pone.0008697

Wallin, J. J., Guan, J., Edgar, K. A., Zhou, W., Francis, R., Torres, A. C., et al. (2012). Active PI3K pathway causes an invasive phenotype which can be reversed or promoted by blocking the pathway at divergent nodes. *PLoS One* 7:e36402. doi: 10.1371/journal.pone.0036402

Wang, F.-B., Yang, X.-Q., Yang, S., Wang, B.-C., Feng, M.-H., and Tu, J.-C. (2011). A higher number of circulating tumor cells (CTC) in peripheral blood indicates poor prognosis in prostate cancer patients–a meta-analysis. *Asian Pac. J. Cancer Prev.* 12, 2629–2635.

Wang, R., Li, H., Guo, X., Wang, Z., Liang, S., and Dang, C. (2016). IGF-I induces epithelial-to-mesenchymal transition via the IGF-IR-Src-MicroRNA-30a-E-cadherin pathway in nasopharyngeal carcinoma cells. *Oncol. Res.* 24, 225–231. doi: 10.3727/096504016x14648701447931

Wang, W.-C., Zhang, X.-F., Peng, J., Li, X.-F., Wang, A.-L., Bie, Y.-Q., et al. (2018). Survival mechanisms and influence factors of circulating tumor cells. *Biomed. Res. Interna.* 2018:9.

Warburg, O. (1956). On the origin of cancer cells. *Science* 123, 309–314. doi: 10.1126/science.123.3191.309

Wellner, U., Schubert, J., Burk, U. C., Schmalhofer, O., Zhu, F., Sonntag, A., et al. (2009). The EMT-activator ZEB1 promotes tumorigenicity by repressing stemness-inhibiting microRNAs. *Nat. Cell Biol.* 11, 1487–1495. doi: 10.1038/ncb1998

Williams, E. D., Gao, D., Redfern, A., and Thompson, E. W. (2019). Controversies around epithelial-mesenchymal plasticity in cancer metastasis. *Nat. Rev. Cancer* 19, 716–732. doi: 10.1038/s41568-019-0213-x

Witta, S. E., Gemmill, R. M., Hirsch, F. R., Coldren, C. D., Hedman, K., Ravdel, L., et al. (2006). Restoring E-cadherin expression increases sensitivity to epidermal growth factor receptor inhibitors in lung cancer cell lines. *Cancer Res.* 66, 944–950. doi: 10.1158/0008-5472.can-05-1988

Wong, C. C., Zhang, H., Gilkes, D. M., Chen, J., Wei, H., Chaturvedi, P., et al. (2012). Inhibitors of hypoxia-inducible factor 1 block breast cancer metastatic niche formation and lung metastasis. *J. Mol. Med.* 90, 803–815. doi: 10.1007/s00109-011-0855-y

Xu, R., Won, J.-Y., Kim, C.-H., Kim, D.-E., and Yim, H. (2019). Roles of the phosphorylation of transcriptional factors in epithelial-mesenchymal transition. *J. Oncol.* 2019:5810465. doi: 10.1155/2019/5810465

Yang, G., Quan, Y., Wang, W., Fu, Q., Wu, J., Mei, T., et al. (2012). Dynamic equilibrium between cancer stem cells and non-stem cancer cells in human SW620 and MCF-7 cancer cell populations. *Br. J. Cancer* 106, 1512–1519. doi: 10.1038/bjc.2012.126

Yang, J., Mani, S. A., Donaher, J. L., Ramaswamy, S., Itzykson, R. A., Come, C., et al. (2004). Twist, a master regulator of morphogenesis, plays an essential role in tumor metastasis. *Cell* 117, 927–939. doi: 10.1016/j.cell.2004.06.006

Yang, J., and Weinberg, R. A. (2008). Epithelial-mesenchymal transition: at the crossroads of development and tumor metastasis. *Dev. Cell* 14, 818–829. doi: 10.1016/j.devcel.2008.05.009

Yang, Y., Jolly, M. K., and Levine, H. (2019). Computational modeling of collective cell migration: mechanical and biochemical aspects. *Adv. Exp. Med. Biol.* 1146, 1–11. doi: 10.1007/978-3-030-17593-1_1

Yauch, R. L., Januario, T., Eberhard, D. A., Cavet, G., Zhu, W., Fu, L., et al. (2005). Epithelial versus mesenchymal phenotype determines in vitro sensitivity and predicts clinical activity of erlotinib in lung cancer patients. *Clin. Cancer Res.* 11(24 Pt 1), 8686–8698. doi: 10.1158/1078-0432.ccr-05-1492

Ye, X., Brabletz, T., Kang, Y., Longmore, G. D., Nieto, M. A., Stanger, B. Z., et al. (2017). Upholding a role for EMT in breast cancer metastasis. *Nature* 547, E1–E3. doi: 10.1038/nature22816

Ye, X., Tam, W. L., Shibue, T., Kaygusuz, Y., Reinhardt, F., Ng Eaton, E., et al. (2015). Distinct EMT programs control normal mammary stem cells and tumour-initiating cells. *Nature* 525, 256–260. doi: 10.1038/nature14897

Yoo, Y. A., Kang, M. H., Lee, H. J., Kim, B. H., Park, J. K., Kim, H. K., et al. (2011). Sonic hedgehog pathway promotes metastasis and lymphangiogenesis via activation of Akt, EMT, and MMP-9 pathway in gastric cancer. *Cancer Res.* 71, 7061–7070. doi: 10.1158/0008-5472.can-11-1338

Yu, M., Bardia, A., Aceto, N., Bersani, F., Madden, M. W., Donaldson, M. C., et al. (2014). Cancer therapy. Ex vivo culture of circulating breast tumor cells for individualized testing of drug susceptibility. *Science* 345, 216–220. doi: 10.1126/science.1253533

Yu, M., Bardia, A., Wittner, B. S., Stott, S. L., Smas, M. E., Ting, D. T., et al. (2013). Circulating breast tumor cells exhibit dynamic changes in epithelial and mesenchymal composition. *Science* 339, 580–584. doi: 10.1126/science.1228522

Yuan, X., Wu, H., Han, N., Xu, H., Chu, Q., Yu, S., et al. (2014). Notch signaling and EMT in non-small cell lung cancer: biological significance and therapeutic application. *J. Hematol. Oncol.* 7:87. doi: 10.1186/s13045-014-0087-z

Zeisberg, M., Shah, A. A., and Kalluri, R. (2005). Bone morphogenic protein-7 induces mesenchymal to epithelial transition in adult renal fibroblasts and facilitates regeneration of injured kidney. *J. Biol. Chem.* 280, 8094–8100. doi: 10.1074/jbc.M413102200

Zhang, N., Zhang, H., Liu, Y., Su, P., Zhang, J., Wang, X., et al. (2019). SREBP1, targeted by miR-18a-5p, modulates epithelial-mesenchymal transition in breast cancer via forming a co-repressor complex with Snail and HDAC1/2. *Cell Death Differ.* 26, 843–859. doi: 10.1038/s41418-018-0158-158

Zheng, X., Carstens, J. L., Kim, J., Scheible, M., Kaye, J., Sugimoto, H., et al. (2015). Epithelial-to-mesenchymal transition is dispensable for metastasis but induces chemoresistance in pancreatic cancer. *Nature* 527, 525–530. doi: 10.1038/nature16064

Conflict of Interest: The authors declare that the research was conducted in the absence of any commercial or financial relationships that could be construed as a potential conflict of interest.

Copyright © 2020 Bhatia, Wang, Toh and Thompson. This is an open-access article distributed under the terms of the Creative Commons Attribution License (CC BY). The use, distribution or reproduction in other forums is permitted, provided the original author(s) and the copyright owner(s) are credited and that the original publication in this journal is cited, in accordance with accepted academic practice. No use, distribution or reproduction is permitted which does not comply with these terms.

frontiers in Molecular Biosciences

ORIGINAL RESEARCH
published: 23 April 2020
doi: 10.3389/fmolb.2020.00054

Toward Modeling Context-Specific EMT Regulatory Networks Using Temporal Single Cell RNA-Seq Data

Daniel Ramirez[1†], Vivek Kohar[2†] and Mingyang Lu[2]*

[1] College of Health Solutions, Arizona State University, Tempe, AZ, United States, [2] The Jackson Laboratory for Mammalian Genetics, Bar Harbor, ME, United States

Epithelial-mesenchymal transition (EMT) is well established as playing a crucial role in cancer progression and being a potential therapeutic target. To elucidate the gene regulation that drives the decision making of EMT, many previous studies have been conducted to model EMT gene regulatory circuits (GRCs) using interactions from the literature. While this approach can depict the generic regulatory interactions, it falls short of capturing context-specific features. Here, we explore the effectiveness of a combined bioinformatics and mathematical modeling approach to construct context-specific EMT GRCs directly from transcriptomics data. Using time-series single cell RNA-sequencing data from four different cancer cell lines treated with three EMT-inducing signals, we identify context-specific activity dynamics of common EMT transcription factors. In particular, we observe distinct paths during the forward and backward transitions, as is evident from the dynamics of major regulators such as NF-KB (e.g., NFKB2 and RELB) and AP-1 (e.g., FOSL1 and JUNB). For each experimental condition, we systematically sample a large set of network models and identify the optimal GRC capturing context-specific EMT states using a mathematical modeling method named *Ra*ndom *Ci*rcuit *Pe*rturbation (RACIPE). The results demonstrate that the approach can build high quality GRCs in certain cases, but not others and, meanwhile, elucidate the role of common bioinformatics parameters and properties of network structures in determining the quality of GRCs. We expect the integration of top-down bioinformatics and bottom-up systems biology modeling to be a powerful and generally applicable approach to elucidate gene regulatory mechanisms of cellular state transitions.

Keywords: phenotypic plasticity, epithelial-mesenchymal transition, cancer, network modeling, single-cell RNA-seq

OPEN ACCESS

Edited by:
Sendurai A. Mani, The University of Texas MD Anderson Cancer Center, United States

Reviewed by:
Francesc Font Clos, University of Milan, Italy
Nikolay Mikhaylovich Borisov, I.M. Sechenov First Moscow State Medical University, Russia

***Correspondence:**
Mingyang Lu
mingyang.lu@jax.org

[†] These authors have contributed equally to this work

Specialty section:
This article was submitted to Molecular Diagnostics and Therapeutics, a section of the journal Frontiers in Molecular Biosciences

Received: *25 January 2020*
Accepted: *17 March 2020*
Published: *23 April 2020*

Citation:
Ramirez D, Kohar V and Lu M (2020) Toward Modeling Context-Specific EMT Regulatory Networks Using Temporal Single Cell RNA-Seq Data. Front. Mol. Biosci. 7:54. doi: 10.3389/fmolb.2020.00054

INTRODUCTION

Epithelial-mesenchymal transition (EMT) has been implicated in a number of biological phenomena including embryonic development, wound healing, and cancer metastasis (Thiery et al., 2009). During EMT, epithelial cells detach from their environment and gain more migratory and apoptosis-resistant qualities (Nieto et al., 2016) to become mesenchymal cells (Nistico et al., 2012). Recent studies have identified new hybrid EMT cellular states (Bartoschek et al., 2018; Dong et al., 2018) with the expression of both epithelial (E) and mesenchymal (M) genes.

The hybrid states in cancer have been associated with collective cell migration and aggressiveness of cancer (Jolly, 2015).

From extensive experimental (Ding et al., 2013; Bartoschek et al., 2018; Dong et al., 2018) and computational (Steinway et al., 2014; Burger et al., 2017; Jia et al., 2019) studies, it is now understood that the decision making of an EMT is usually driven by a gene regulatory circuit (GRC) consisting of master regulators, including transcription factors (TFs), such as ZEB, SNAIL, TWIST, and GRHL2, and microRNAs, such as miR200 and miR34. Remarkably, the core GRCs explain the existence of hybrid EMT cellular states (Lu et al., 2013). Although a generic gene regulatory network is expected for the same process in different contexts, the specific gene regulatory interactions that occur in an EMT could vary for different cell types, signaling states, and disease states (Cook and Vanderhyden, 2019). Indeed, an EMT can be induced by activating either one of the common signaling pathways, including TGFβ, EGF, TNF, Wnt, Notch, and Hedgehog signaling (Gonzalez and Medici, 2014; Steinway et al., 2014; Basu et al., 2018; Font-Clos et al., 2018). EMT has also been widely studied and observed in various types of cancer (Chung et al., 2016; Bartoschek et al., 2018; Brabletz et al., 2018), with different genetically modified mouse models (Zheng et al., 2015; Kersten et al., 2017; Chen et al., 2018) and a broad spectrum of cancer cell lines (Steinway et al., 2014; Chung et al., 2016; Bartoschek et al., 2018; Brabletz et al., 2018). Yet, little efforts have been made to identify the common and context-specific regulators and regulatory interactions during EMT and how these regulatory relationships contribute to the diversity of EMT. This investigation will help to further understand the regulatory mechanisms of EMT, elucidate the composition and stability of the various EMT states, and facilitate the discovery of new therapeutic drugs in different contexts.

Recent single-cell RNA sequencing (scRNA-seq) technology has enabled measurement of genome-wide gene expression at the single cell level. It is particularly relevant to this study, as single-cell data can not only reveal heterogeneity within cell populations but, when combined with time-series analysis, can provide a comprehensive view of the dynamics of EMT. For example, single-cell sequencing has been used to understand the intratumoral variation in cell localization and function, potentially unveiling biomarkers or drug targets (Patel et al., 2014; Bartoschek et al., 2018). A 2018 study observed a hybrid EMT state occurring during mouse organogenesis, identifying tissue type-specific regulatory elements in EMT such as *Prrx1* and *Lef1* (Dong et al., 2018). Another recent investigation found both broadly conserved regulatory elements of EMT and highly variable transcriptomic features using scRNA-seq on a melanoma dataset (Wouters et al., 2019).

A recently published dataset from Cook and Vanderhyden (2019) includes time-series scRNA-seq data from four different cancer cell lines (A549, DU145, MCF7, and OVCA420) undergoing EMT induced by one of three distinct signals (TGFB1, TNF, and EGF) for 7 days and subsequent MET induced by removing the corresponding signal. In this study, the different cell lines demonstrated distinct phenotypic trajectories with different TFs implicated in the process. The presence of context-dependent variations of the EMT trajectories confirms that the mechanism of EMT is not invariant with respect to the stimuli which induce it. The time-series data permits a thorough investigation of the path of cellular state transitions and GRCs driving the decision making of EMT in multiple experimental conditions.

Here, we will adopt a combined bioinformatics and systems-biology modeling approach to construct context-specific core GRCs using the above-mentioned time-series scRNA-seq data from multiple cell lines and signaling treatment conditions (**Figure 1**). Many previous computational studies have been conducted to build EMT GRCs from literature support (Steinway et al., 2014; Hong et al., 2015; Burger et al., 2017; Huang et al., 2017; Bocci et al., 2018; Kohar and Lu, 2018; Ramirez et al., 2019). However, this approach is not optimized for the goal of this project, as there might not be sufficient literature data for a specific experimental condition. To address this issue, we systematically constructed a large number of networks for each experimental condition by starting from a collection of common TFs and integrating context-specific regulatory links derived from the gene expression data and *cis*-regulatory motif analysis. Using a wide range of network construction parameters, we evaluated the performance of each network in comparison to experimental data and generated GRCs that are highly representative of specific experimental conditions. To achieve this, a mathematical modeling method named *Ra*ndom *Ci*rcuit *Per*turbation (RACIPE) (Huang et al., 2017; Kohar and Lu, 2018) was applied on each network model to simulate the gene expression profiles and quantitatively compare with experimentally observed gene expression profiles. RACIPE is a parameter agnostic ordinary differential equation-based method to simulate gene regulatory networks. RACIPE takes a network topology specifying the regulator, target, and interaction type (excitatory/inhibitory) as the input and generates a large ensemble of models, where kinetic parameters of the models are randomized within a range of possible values. By simulating each of these models, RACIPE generates stable steady-state gene expression profiles from which we identify the generic features of a network and predict possible phenotypic states (see section "Materials and Methods"). From this approach, we aim to identify key regulators of EMT across all conditions as well as specific actors in each cancer type.

RESULTS

Characterizing the Heterogeneity of Transcription Factor Dynamics

In this study, we focused on building GRCs using the single cell RNA sequencing (scRNA-seq) data collected from Cook and Vanderhyden (2019) for four cancer cell lines (A549, DU145, MCF7, and OVCA420) treated with EGF, TGFB1, and TNF. The data were collected at eight timepoints at 0 day, 8 h, 1 day, 3 days, and 7 days of exposure to the treatment and 8 h, 1 day, and 3 days post-signal termination at 7 days.

To evaluate the differences in the initial EMT and the backward transition occurring after the signals were removed, we separated each condition into two datasets, where the first

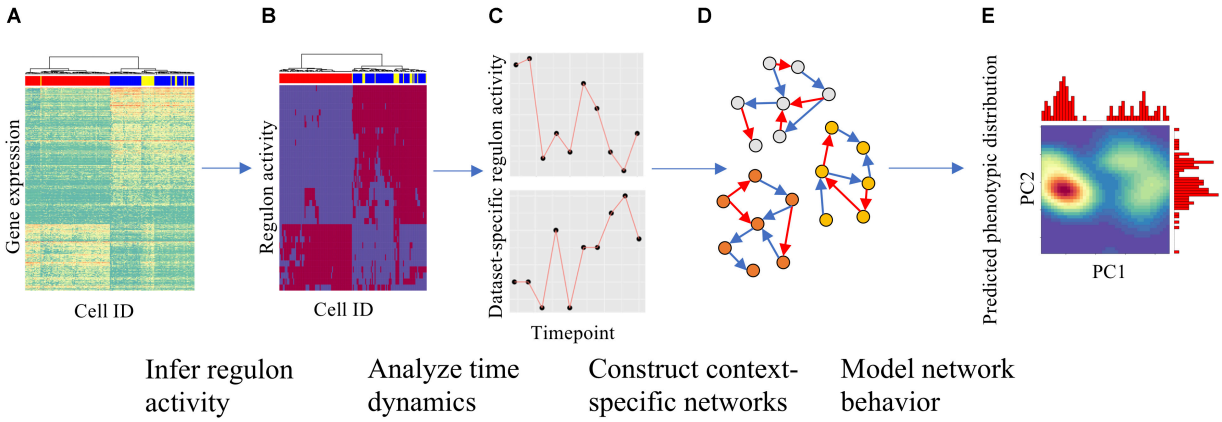

FIGURE 1 | Overall strategy for analyzing scRNA-seq data and constructing context-specific gene regulatory circuits (GRCs). **(A)** Gene expression heatmap with cells in columns and gene expression levels in rows, clustered hierarchically to group cells. **(B)** Using gene expression data and SCENIC, gene regulatory module (regulon) activity for each cell could be inferred and is shown in a similar heatmap. **(C)** The time dynamics of selected regulons were then compared across datasets to identify divergent regulatory trajectories. **(D)** After the role of each regulon across datasets was characterized, numerous context-specific circuit topologies were generated (nodes represent genes, blue and red arrows represent excitatory and inhibitory regulation, respectively) using different statistical cutoffs for network modeling. **(E)** Finally, dynamics simulations were performed on each circuit to identify the optimal circuit that captures the terminal cellular states from the experimental datasets. Using simulations, one can also predict the paths of cellular state transitions upon either signal induction or removal. Density maps show PCA on simulation results with marginal histograms.

dataset contains timepoints 0, 8 h, 1 day, 3 days, and 7 days during the signal induction, and the second dataset contains timepoints 7 days during the signal induction and 8 h, 1 day, and 3 days after the signal removal. The day 7 data were used twice here to recapitulate the dynamics in both directions. Thus, there are a collection of 24 experimental datasets in total (three treatments, four cell lines, and two directions). For each dataset, we applied SCENIC (Aibar et al., 2017) to infer the regulons or enriched transcription factors (TFs) and their corresponding TF activity for every cell. Differential analysis was then applied using Seurat (Butler et al., 2018; Stuart et al., 2019) to the activity profiles for cells at different time points. To capture the changes over time, we performed comprehensive differential activity analysis (see section "Materials and Methods") for the forward and backward directions to obtain a list of highly variable regulons for each of the 12 conditions. Interestingly, the response to signal induction and retrieval was quite heterogeneous and only 20–30% of the differentially active TFs in the forward direction were differentially active in the backward direction as well.

Moreover, canonical EMT marker genes like SNAIL, SLUG, ZEB, and TWIST were not consistently identified as regulons in the experimental data. This finding agrees with Cook and Vanderhyden's (2019) analysis of the datasets and suggests that complete EMT may not be taking place in the data, but with the initial response to the inductive signal leading toward partial EMT states.

EMT Across Signaling Conditions Is Similar Within Cell Lines

With the eventual goal of building context-specific GRCs, we first investigated which type of context was more relevant between the cell lines and the treatments. Our expectation was that the same cell line triggered by different signals may exhibit a varying response in relation to signal strength, but the nature of the transition will remain consistent across the signaling conditions. Extensive evidence exists to suggest that the three signal molecules examined in the dataset, i.e., TGFB1, EGF, and TNF, act on many of the same targets in EMT, most notably NF-κB, which comprises NFKB1 and RELB genes (Pires et al., 2017), and the AP-1 complex, which comprises FOS and JUN genes (Sun and Carpenter, 1998; Chen and Davis, 2003; Wu and Zhou, 2010; Romagnoli et al., 2012; Freudlsperger et al., 2013; Vervoort et al., 2018) (**Figure 2A**). On the other hand, the same signal applied to different cell lines may elicit different effects because of the unique genetic profile and mutations present in each cell line.

The overlap of differentially active TFs (DATFs) across the 12 conditions was then plotted (**Figure 2B**). Though a large number of DATFs are unique to each condition, more DATFs were shared across treatments of a single cell line than across cell lines for the same signal, supporting our initial hypothesis that different cell lines will have more context-specific regulatory activity than different signal treatments. In the original study, the authors also reported larger overlap among the highly variable genes for cell lines compared to signaling (Cook and Vanderhyden, 2019).

Further, we identified 28 common DATFs (**Supplementary Figure S4**), which frequently occur in differential analysis across timepoints (see section "Materials and Methods"). Among the most frequently identified DATFs are AP-1 genes, such as JUN and FOSL1, and NFκB genes, such as NFKB2 and RELB, consistent with the literature analysis mentioned above. Next, we annotated the TFs as E (i.e., an epithelial gene) or M (i.e., a mesenchymal gene) depending on whether the expression levels trended upward or downward over the course of the experiment. TFs whose activity increased and subsequently decreased during the transition were denoted intermediate (I)

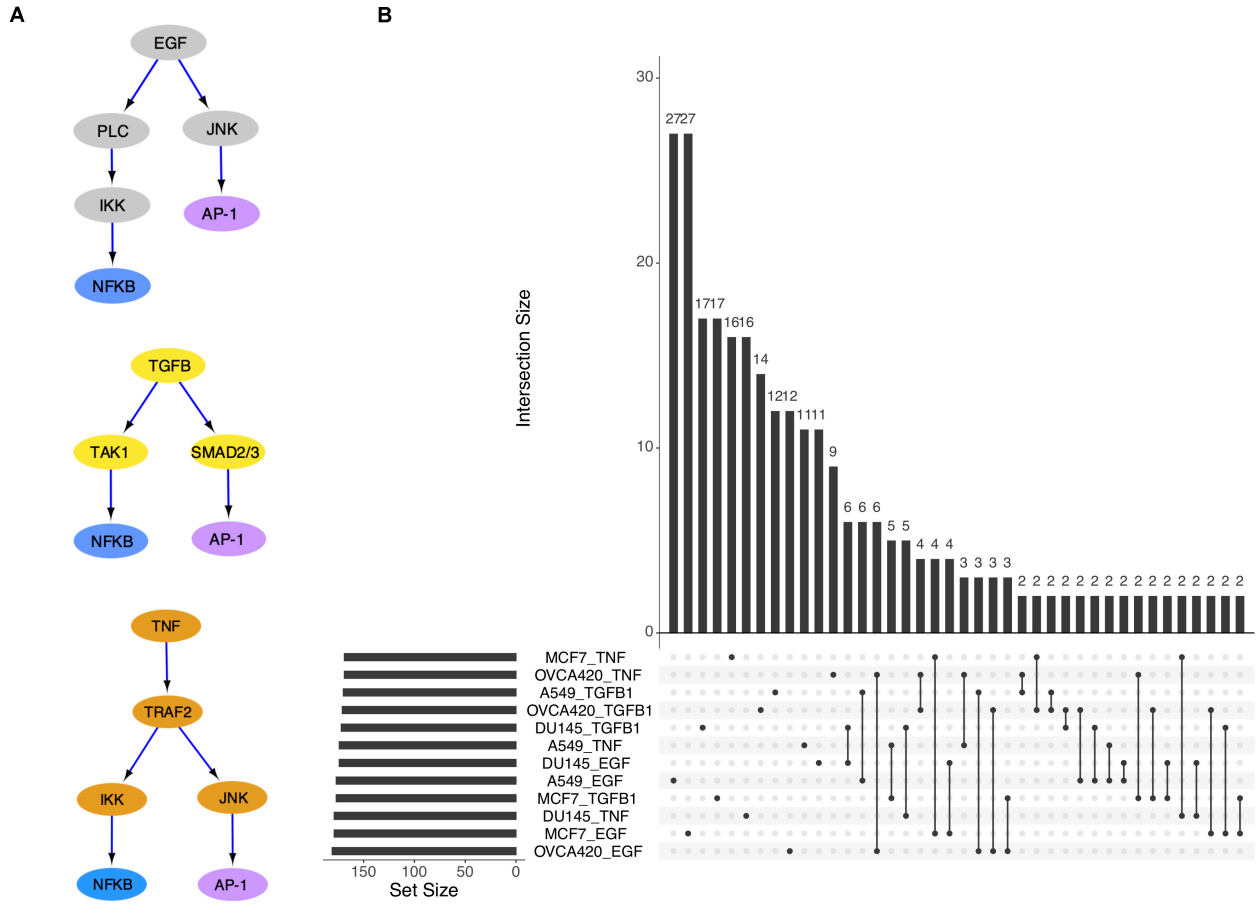

FIGURE 2 | The three signal pathways have convergent gene targets. **(A)** Simplified models of signal transduction pathways for EGF, TGFB1, and TNF based on published results in the literature. **(B)** Upset plot showing overlap of differentially activated regulons across cell lines and signal treatments.

and those whose activity decreased and then increased were denoted I2 (**Figures 3A,B**). Across the different experimental datasets, the roles of these TFs in EMT was observed changing depending on the context (**Supplementary Figure S1** for the activity time dynamics of every TF). Some TFs showed signal-specific activity profiles, such as NFKB2, which frequently served as an I gene in TNF-treated cases and an M gene in most other cases (**Figure 4A**). Others, such as SPDEF, showed cell line-dependent behaviors (**Figure 4B**). SPDEF only acted as a consistent M gene in OVCA420 and DU145, showing more E-like activity profiles in A549 and MCF7. Other genes from the overlapping TFs were more consistent across all contexts (**Figure 4C**); KLF6 behaved as an M gene in nearly all cases. These universally consistent genes were also generally among the well-documented EMT-related TFs, such as JUN and MYC (**Supplementary Table S1**).

Exploring Intermediate EMT States and Transition Paths

To break down the chronological progression of EMT and the backward transition, the activity of AP-1 and NF-KB across the different timepoints were examined (**Figure 5** for FOSL1 and JUNB vs. RELB and NFKB2, **Supplementary Figure S2** for RELB vs. FOSL1, and **Supplementary Figure S3** for RELB vs. JUNB). In multiple experimental conditions, cells exhibited an increase in activity of one signaling component before the next. During the backward transition, the order of the changes in activity is usually not consistent with the order for the forward transition, suggesting that EMT is not reversible and instead must transit through multiple distinct intermediate states depending on the direction of transition (**Figure 5**). The exact trajectory of the transition also varied with respect to both signaling treatment and cell line, confirming that context-specific features of EMT are present for both variables.

Constructing Context-Specific GRCs

Next, we constructed context-specific GRCs using a combined bioinformatics and mathematical modeling protocol. Each context-specific gene network was built based on the following rules (see section "Materials and Methods" for details). First, we started with the 28 common TFs that we previously identified from comparisons across time points and identified neighboring nodes of these TFs using SCENIC regulons, i.e., genes directly upstream or downstream of the TFs. Regulatory interactions

A

Cell Line	Treatment	BHLHE40	CEBPB	CREB3	CREM	ELK3	ESRRA	ETS1	ETS2	FOS	FOSB	FOSL1	IRF1	IRF2	IRF3	IRF7	JUN	JUNB	KLF6	MAFG	MYC	NFE2L3	NFKB2	RELB	SOX4	SPDEF	STAT1	STAT3	XBP1
A549	EGF_fwd	E	N	I	E	E	I	I	I	E	E	I	N	I	I	N	I	E	E	E	M	M	I	I		E	E	N	E
	EGF_rev	E	E	I2	N	M	N	M	M	E	E	M	E	I2	M	N	M	E	I2	E	M	M	I2	I2		E	I	E	I2
	TGFB1_fwd	M	I2	M	M	M	E	E	M	E	M	E	M	M	M	M	M	M	M	M	M	E	M	M	M	E	M	E	I2
	TGFB1_rev	M	N	M	I	M	N	E	N	N	M	M	M	M	N	E	M	M	M	N	N	I2	E	M	M	M	N	E	M
	TNF_fwd	M	M	I	N	M	N	I	M	E	I	M	I	I	M	I	M	M	M	E	M	I	I	I		E	I	M	E
	TNF_rev	E	M	M		M	N	I	M	E	I	M	M	M	M	M	M	M	M	I2	M	M	M	M	I	M	E	M	I
DU145	EGF_fwd	N	M	I	N	M	M	I		I	N	M	N	N	M	N	M	M	M	N	N	M	I	I	M	I	N	E	N
	EGF_rev	I2	M	M	I	M	M	M	M		N	M	N	E	E	M	M	M	M	N	M	M	I	I	M	N	I2	E	N
	TGFB1_fwd	M	I2	M	M	M	E	E	M	M	M	E	M	M	M	N	M	M	M	E	M		I	E	M	M	M		M
	TGFB1_rev	M	I2	M	M	M	E	M	M	M	N	E	M	M	N	M	M	M	M	M	I	M	M	M	M	I	M		M
	TNF_fwd	M	I	M	M	M	M	N	M	N	N	M	I	M	M	I	M	I	M	N	N	M	I	I		E	N	E	N
	TNF_rev	I2	M	M	M	M	M	M	M	I2	M	M	M	N	I2	I2	M	M	M	E	M	M	M	M			N	N	I2
MCF7	EGF_fwd	I	M	M	M	I	I		I	E	I2	I	E	E	N	E	E	I	I	N	N	N		N	I	I2	E	I	I
	EGF_rev	I	M	M	I2	N	I		I	E	I2	I	E	I	I2	E	E	I	I	M	N	N	N	N	I	E	E	N	I2
	TGFB1_fwd	M	M	N	E	M	M		M	M	M	M	M		N	M	M	M	M	M	M		M	M	M	E	M	I	E
	TGFB1_rev	M	N	N	E	M	M		I	E	E	M	M	M	E	M	M	M	M	I	E	I	I	M	M	E	M		E
	TNF_fwd	M	M	M	M	M	M		M	I2	I	M	M	M	I	M	M	M	M	E	M	M	I	M	M	E	M	M	E
	TNF_rev	M	M	M	M	N	N		M	M	E	E	M	M	I2	M	M	M	M	N	M	N	M	M	M	E	M	M	E
OVCA420	EGF_fwd	I	M	M	E	M	M	M	I	E	I2	M	M	M	I		I	M	M	N	N	E	M	M	M	M	I	E	E
	EGF_rev	M	M	M	E	M	I2	M	M	E	I2	M	I2	N	N	N	I2	M	M	M	I2	E	M	M		M	I2		E
	TGFB1_fwd	I	M	M	M	M	I2	M	I	I	M	M	I	E	M	M	I	I	M	M	M		M	M	M	M	M	I	M
	TGFB1_rev	N	M	M	I	M	I2	M	M	N	E	N	M	M	I2	M	N	M	M	M	I2	N	I	M	M	M	M	N	M
	TNF_fwd	I	I	M	E	I	I	I	I	E	E	I	I	I	I	E	I	I	E	I	I	E	I	I		E	E	I	I
	TNF_rev	I	M	M		I	I	I	M	E	I	I	M	I	I	E	M	M	N	I	I2	M	M	M	M		E	M	I2

B

Cell Line	Treatment	BHLHE40	CEBPB	CREB3	CREM	ELK3	ESRRA	ETS1	ETS2	FOS	FOSB	FOSL1	IRF1	IRF2	IRF3	IRF7	JUN	JUNB	KLF6	MAFG	MYC	NFE2L3	NFKB2	RELB	SOX4	SPDEF	STAT1	STAT3	XBP1
A549	EGF_fwd	E	N	I	E	E	I	I	I	E	E	I	N	I	I	N	I	E	E	E	M	M	I	I		E	E	N	E
	EGF_rev	E	E	I2	N	M	N	M	M	E	E	M	E	I2	M	N	M	E	I2	E	M	M	I2	I2		E	I	E	I2
DU145	EGF_fwd	N	M	I	N	M	M	I		I	N	M	N	N	M	N	M	M	M	N	N	M	I	I	M	I	N	E	N
	EGF_rev	I2	M	M	I	M	M	M	M		N	M	N	E	E	M	M	M	M	N	M	M	I	I	M	N	I2	E	N
MCF7	EGF_fwd	I	M	M	M	I	I		I	E	I2	I	E	E	N	E	E	I	I	N	N	N		N	I	I2	E	I	I
	EGF_rev	I	M	M	I2	N	I		I	E	I2	I	E	E	E	E	E	I	I	M	N	N	N	N	I	E	E	N	I2
OVCA420	EGF_fwd	I	M	M	E	M	M	I	I	E	I2	M	M	N	N		I	M	M	N	N	E	M	M	M	M	I	E	E
	EGF_rev	M	M	M	E	M	I2	M	M	E	I2	M	I2	E	M	N	I2	M	M	M	I2	E	M	M		M	I2		E
A549	TGFB1_fwd	M	I2	M	M	M	E	E	M	E	M	E	M	M	M	M	M	M	M	M	M	E	M	M	M	E	M	E	I2
	TGFB1_rev	M	N	M	I	M	N	E	N	N	M	M	M	M	N	E	M	M	M	N	N	I2	E	M	M	M	N	E	M
DU145	TGFB1_fwd	M	I2	M	M	M	E	E	M	M	M	E	M	M	M	N	M	M	M	E	M	I	E	M	M	M	I	M		M
	TGFB1_rev	M	I2	M	M	M	E	M	M	N	E	M	M	M	N	M	M	M	M	E	M	I	M	M	M	M	I	M		M
MCF7	TGFB1_fwd	M	M	N	E	M	M		M	M	M	M	M		N	M	M	M	M	M	M		M	M	M	E	M	I	E
	TGFB1_rev	M	N	N	E	M	M		I	E	E	M	M	M	E	M	M	M	M	I	E		I	M	M	E	M	I	E
OVCA420	TGFB1_fwd	I	M	M	M	M	I2	M	I	I	M	M	I	E	M	M	I	I	M	M	M		M	M	M	M	M	I	M
	TGFB1_rev	N	M	E	I	M	I2	M	M	N	E	N	M	M	I2	M	N	M	M	M	I2	N	I	M	M	E	M	N	M
A549	TNF_fwd	M	M	I	N	M	N	I	M	E	I	M	I	I	M	I	M	M	M	E	M	I	I	I		E	I	M	E
	TNF_rev	E	M	M		M	N	I	M	E	I	M	M	M	M	M	M	M	M	I2	M	M	M	M	I	M	E	M	I
DU145	TNF_fwd	M	I	M	M	M	M	N	M	N	N	M	I	M	M	I	M	I	M	N	N	M	I	I		E	N	E	N
	TNF_rev	I2	M	M	M	M	M	M	M	I2	M	M	M	N	I2	I2	M	M	M	E	M	M	M	M			N	N	I2
MCF7	TNF_fwd	M	M	M	M	M	M		M	I2	I	M	M	M	I	M	M	M	M	E	M	M	I	M	M	E	M	M	E
	TNF_rev	M	M	M	M	N	N		M	M	E	E	M	M	I2	M	M	M	M	N	M	N	M	M	M	E	M	M	E
OVCA420	TNF_fwd	I	I	M	E	I	I	I	I	E	E	I	I	I	I	E	I	I	E	I	I	E	I	I		E	E	I	I
	TNF_rev	I	M	N		I	I	I	M	E	I	I	M	I	I	E	M	M	N	I	I2	M	M	M	M		E	M	I2

FIGURE 3 | Gene expression time dynamics of common TFs for forward and backward transitions. **(A)** Table of the most common 28 TFs with state classifications sorted by cell line. While many genes play similar roles across all datasets, some, such as SPDEF and IRF3, show cell-line dependent behaviors. **(B)** 28 most common TFs with state classifications sorted by signal. As in **(A)**, some genes such as STAT1 and NFKB appear to play different roles in EMT according to the inducing signal.

between these nodes were scored based on mutual information (MI) of TF activities, and the sign (i.e., activation or inhibition) was determined based on the sign of the TF activity Spearman's correlations. Second, the networks for the forward and backward transitions were combined to form a unified network. Third, any TF which has only outgoing links was removed. This step was performed only once, and TFs that had only outgoing links afterward were kept in the model.

We generated a series of gene networks for each condition by varying the cutoff values of MI. From our initial exploration, we found that activating links were favored in the network construction, probably because of the nature of scRNA-seq data (Sanchez-Taltavull et al., 2019). To select different numbers of activating and inhibitory links, we varied the MI cutoffs for positive and negative interactions. These thresholds facilitated the construction of diverse networks having different number of TFs, interactions, ratio of positive and negative interactions, etc. We did an initial screening to ensure that a network contains at least 5 E or M TFs for that specific condition. However, we still investigate networks even when only positive or negative interactions are present.

The generated networks were simulated using the parameter-agnostic random circuit perturbation (RACIPE) approach. We evaluated the quality of gene networks by comparing the simulated and experimental gene expression data (see section "Materials and Methods"). From this extensive analysis, we identified representative GRCs containing both E and M TFs for each condition and yielding high accuracies (**Figure 6A**, network topology files are listed in **Supplementary Material**). These networks illustrate the heterogeneity in responses for different cell lines and treatments. Simulating the large number of networks provides unique insights into network structure and resultant dynamics (**Figure 6B**). We found that typically moderately sized networks have better accuracy compared to large or small networks. This is reflected in the accuracy plots for various number of nodes (**Figure 6B1**) or interactions in the network (**Figure 6B3**). Expectedly, accuracy increases if the fraction of nodes that can be assigned as E or M increases (**Figure 6B2**), as such networks capture a larger proportion of differentially active regulons. Similarly, very low or high mutual information cutoffs for inhibitory or excitatory interactions yield lower accuracies as the network becomes sparsely connected or very dense in such cases (**Figures 6B4,B5**). We observed that the accuracies are also context-specific, as shown in **Figure 6B6** and the performance for individual dataset shown in **Supplementary Figure S5**. More information on each network is given in **Supplementary Table S3**.

Taking the GRC from the OVCA420 TGFB1 condition [identified as having the highest EMT score by Cook and Vanderhyden (2019)] as an example (**Figure 7B**), we directly compared the simulation results from RACIPE with the experimental data (**Figure 7A**). We observed that the simulations not only capture the two major E and M states, but the simulated expression profiles are also very similar to the activities of the

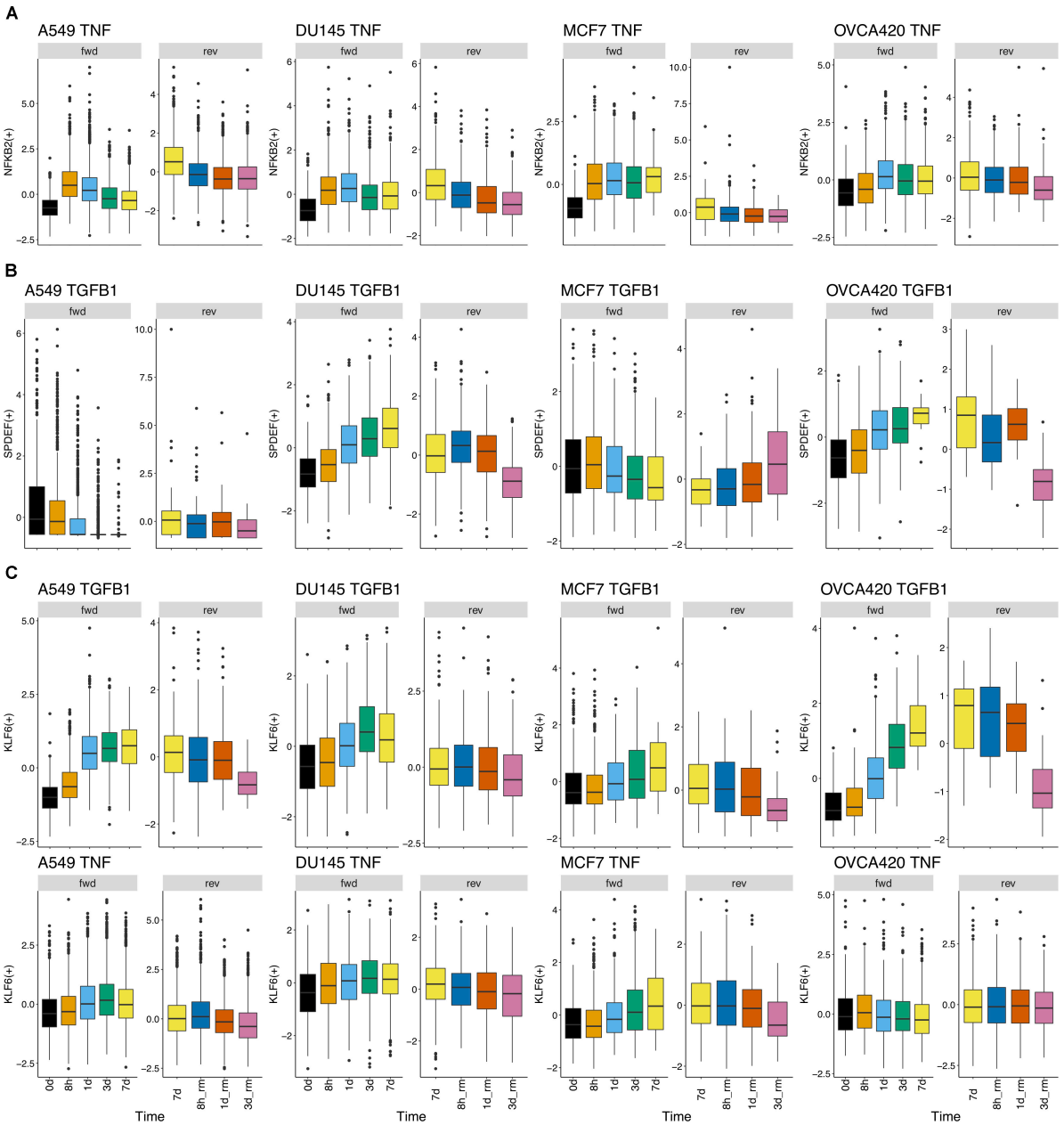

FIGURE 4 | Regulon activity profiles over time. **(A)** TF activity profile for NFKB2 over time in all cell lines treated with TNF. NFKB2 generally has similar gene activity dynamics across all cell lines treated with TNF. During signal induction, NFKB2 activity initially goes up and goes down at later time points; during signal removal, it gradually decreases. **(B)** TF activity profile for SPDEF over time in all cell lines treated with TGFB1. TGFB1 dynamics differ widely across cell lines; it acts like an M gene in DU145 and OVCA420, acts as an E gene in MCF7, and shows generally low activity in A549. **(C)** TF activity profile for KLF6 over time in all cell lines treated with TGFB1 or TNF. Across both cell lines and signal treatments, KLF6 activity follows a similar pattern throughout the transition: activity largely increases during the forward transition and decreases after signal removal.

TFs in the datasets for the forward and backward transitions (**Figure 7A**). We projected the experimental activities on the first two principal components of the simulated data and observed that the projected values identify the transition of cells from E to M upon signal induction and M to E during signal removal (**Figure 7C**). The average and standard deviation of the cells at each time point are shown in bottom panels highlighting the distinct trajectories during the forward and reverse transitions. Further, we observed that cells could not undergo a complete backward transition upon signaling removal.

To test whether we can identify similar features in our simulations, we used the E state models and applied a signal (i.e., TGFB1) to JUN and RELB and observed how the gene expressions change over time (**Figure 7E**). We observed the E

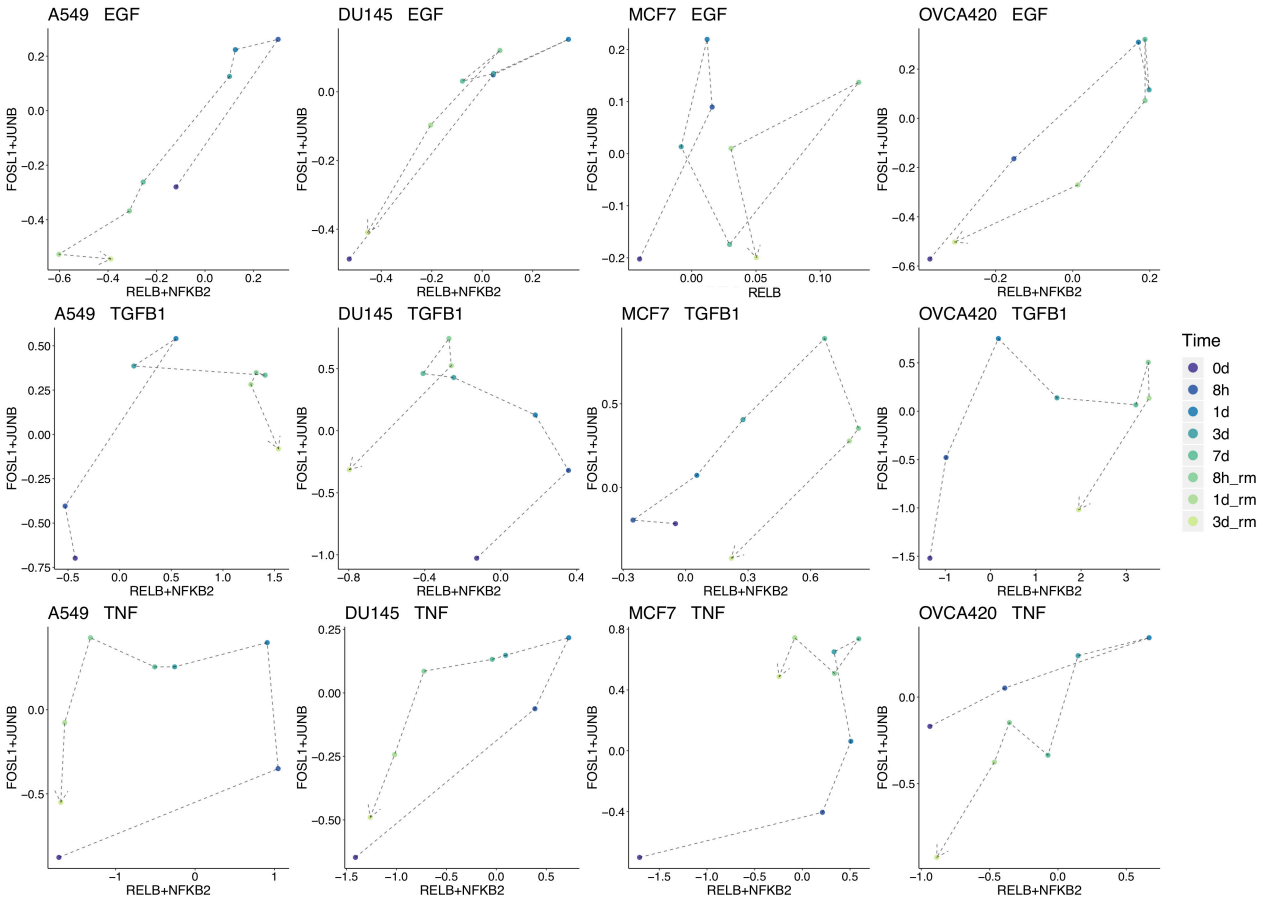

FIGURE 5 | Signal chronology across experimental conditions. Combined average TF activity of FOSL1 and JUNB vs. RELB and NFKB2 for each timepoint across each cell line and signal treatment. TF activity from 7 days onward (data from the backward direction) is scaled on a linear model to match the 7 days distributions for the forward direction. Some aspects of the EMT-MET trajectory are similar across cell lines, such as in A549, DU145, and MCF7 treated with TNF, which all follow a generally counterclockwise movement. On the other hand, the transition path is also in large part determined by cell line for all signaling conditions, such as in OVCA420, where the trajectory is generally clockwise for all inducing signals.

models gradually shift toward M over time, while some models undergo a complete transition to the M state. The number of models that transit to the M state depends on the strength of the signal and noise in the simulations. The strength of the signal induction and noise were selected so that the E-state models have significantly more transitions to the M state with both signal activation and noise than those for the cases with only signal activation or noise (**Supplementary Figure S7**). We also observe that signal removal doesn't result in MET in all the models that underwent EMT. When we inhibited the models by reducing the production rates of JUN and RELB below their original values, a larger fraction of models was able to transit back to the E state. The mean and standard deviation of the models at different times follow patterns quite similar to experimental activities and capture the distinct forward and backward trajectories. We found similar results when the statistics were performed to the subset of models that transit from the E state to the M state (**Supplementary Figure S8**). We also observed that the transition occurred at different time scales in both experiments and simulations where the cells (models) moved faster in the forward direction and slower in backward direction. The average expression of each TF at multiple time points in OVCA420 TGFB1 signal induction and removal in experiments and in simulations during signal induction, removal, and inhibition is shown in **Supplementary Figure S6**. Overall, these results highlight that our simulations are able to capture many aspects of experimental data.

A Common Gene Regulatory Circuit Driving a Multi-Step EMT

Although the canonical master regulators of EMT such as SNAIL and ZEB were not prevalent in the differential activity analysis, there is evidence suggesting that they are downstream targets of the signaling pathways triggered in the experiment (**Supplementary Table S2**) (Chen and Davis, 2003; Li et al., 2010; Wu and Zhou, 2010; Romagnoli et al., 2012). Using information from the literature and TFs identified in the experimental data, we constructed a core GRC to model the generic effect of the signals on driving EMT (**Figure 8A**).

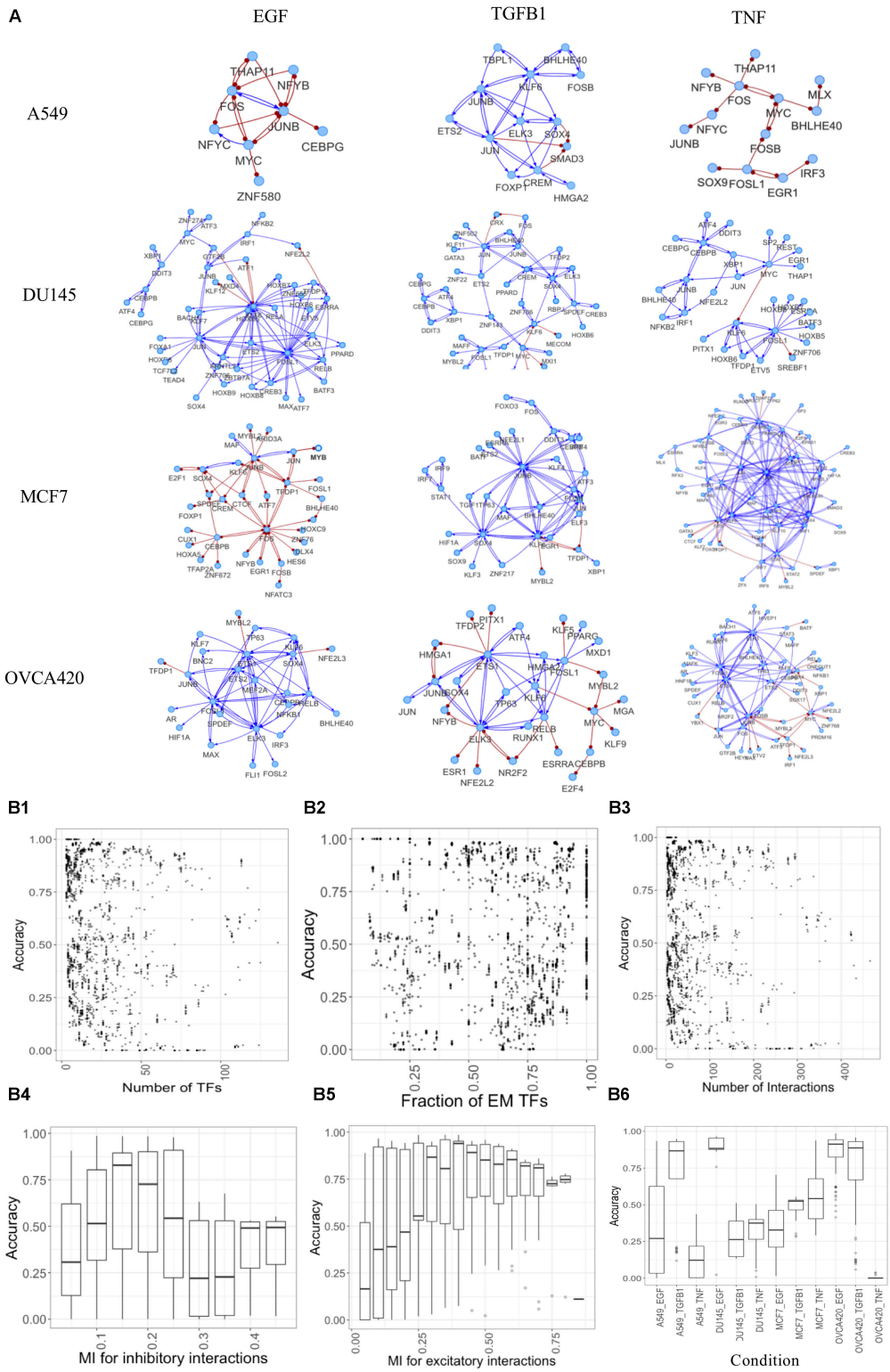

FIGURE 6 | Constructing context-specific gene regulatory networks. **(A)** Representative networks yielding high accuracy scores for various conditions. Activating interactions denoted as blue arrows and inhibitory interactions as red round-tipped arrows. **(B)** Accuracy dependence on various network properties for all conditions. **(B1–B3)** Points showing accuracy (measured as fraction of models that can be classified as E or M) of models for various **(B1)** number of TFs in the network, **(B2)** fraction of TFs assigned as E or M using experimental data, **(B3)** number of interactions in the network. **(B4–B6)** Box plots showing accuracy of networks for various **(B4)** mutual information cutoffs for inhibitory interactions, **(B5)** mutual information cutoffs for excitatory interactions, **(B6)** different experimental conditions.

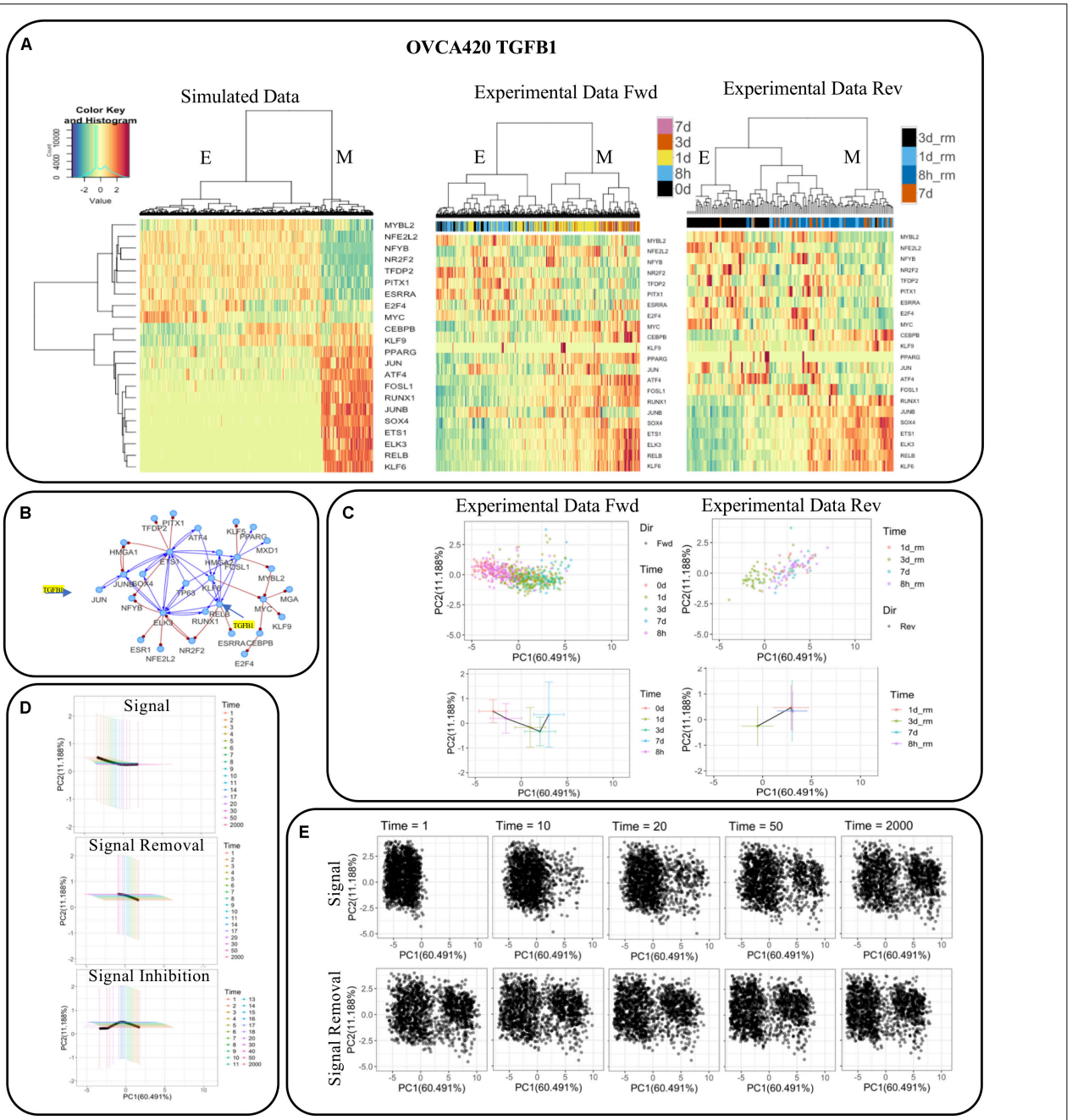

FIGURE 7 | Comparison of network simulations on 2000 RACIPE models with experimental observations for OVCA420 treated with TGFB1 signaling. **(A)** Hierarchical clustering of simulated and experimental activities. **(B)** The network topology, in which TGFB1 signaling is applied to JUN and RELB. **(C)** Experimental activities (top) and their mean and standard deviation (bottom) during signal induction (left) and removal (right) projected on first two principal components of the simulated data. **(D)** Mean and standard deviation of the simulated profiles of the E-state models during signal induction (top), removal (middle), and inhibition (bottom) at multiple time points projected on the first two principal components as in **(C)**. **(E)** Simulated profiles of the E-state models during signal removal and induction at multiple time points projected on the first two principal components as in **(C)**.

Using RACIPE, we performed network simulations and identified three distinct states. One state corresponds to E cells with high expression of CDH1 and low signal strength; as the signal strength increases, models are likely to enter one of the other states: an intermediate state where signal strength is high and NF-KB and AP-1 are expressed, but ZEB remains low, and finally a full M state with high expression of M marker genes (**Figure 8B**). The states in this network support the hypothesis that the EMT undergone in this experiment may not be complete and may only demonstrate an initial

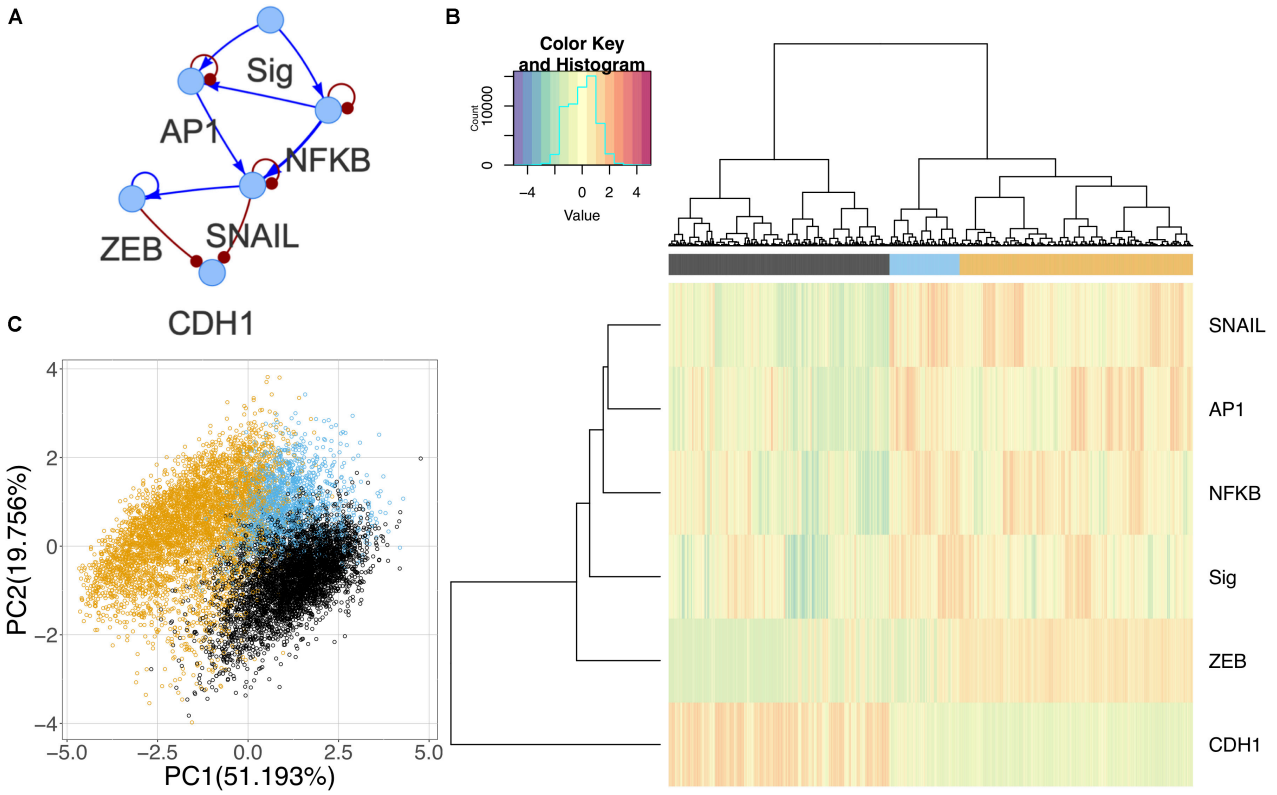

FIGURE 8 | Core network simulations with 2000 RACIPE models. **(A)** Core EMT network derived from published experimental results. Activating interactions denoted as blue arrows and inhibitory interactions as red round-tipped arrows. **(B)** Heatmap of core network simulation results with ward.D2 hierarchical clustering of models and genes (number of clusters $k = 3$). **(C)** PCA of core network simulation results color coded by cluster.

signaling response. On a PCA plot, the intermediate state occurs between the two extreme phenotypes in one corner of the plot (**Figure 8C**). It is possible that other intermediate states exist when cells undergo a different type or direction of EMT, and these context-specific states are simply not captured by the common core circuit.

DISCUSSION

In this study, we analyzed a recent collection of time-series single cell RNA sequencing (scRNA-seq) data sets for four different cancer cell lines and three types of treatments targeting different signaling pathways to model context-specific GRCs driving EMT. We developed a combined bioinformatics and mathematical modeling approach and explored its effectiveness in constructing GRCs that capture the essential temporal dynamics derived from the scRNA-seq data. We used bioinformatics analysis to construct networks of differentially active transcription factors using the transcription factor activities obtained through co-expression and *cis*-regulatory motif analysis and used the ODE-based mathematical modeling method RACIPE to simulate the gene expression of a large number of constructed networks. The consistency of experimental activities and simulated expressions of the transcription factors was used to evaluate the networks and identify optimal networks. Our study sheds light on the regulatory mechanisms of EMT that are common and context-specific and how the identified transcriptional regulators contribute to driving or reversing EMT.

In particular, we explored the options to construct GRCs directly from *cis*-regulatory motif analysis using gene expression data and subsequent *in silico* validation by comparing circuit simulations with experimental data. From our analysis, we found it is still challenging to build high-quality circuit models directly from bioinformatics tools, consistent with a recent benchmark test (Pratapa et al., 2020). Most existing bioinformatics methods rely on statistical tests to refine network topologies by removing spurious interactions. Instead of using simple statistic-based filtering, we applied RACIPE to evaluate whether the constructed GRCs can capture the gene expression states from the data. Using RACIPE, we found a gene network typically cannot recapitulate experimentally observed cellular states when the network is either too small or too large. The optimal GRCs were mostly derived from gene networks of medium size. In addition, higher accuracy was usually found in GRCs constructed using different cutoff values for excitatory and inhibitory interactions, likely because SCENIC produced an unbalanced amount of interactions by type. We expect that an iterative procedure between network building and modeling can further improve the quality of GRC modeling.

Both the bioinformatic analysis on the data sets from multiple conditions and the literature analysis indicate that the TGFB1, EGR, and TNF signaling pathways all converge to two transcription factor (TF) complexes AP-1 and NFκB. The activation of these two complexes induces a cellular state transition to an intermediate EMT state, an event presumably occurring prior to the induction of typical EMT master regulators, such as SNAIL, TWIST, and ZEB. Our findings are consistent with the picture of multi-step state transitions during EMT (Zhang and Weinberg, 2018). One way to further test the model is to inhibit AP-1 and NFκB and evaluate how the perturbation affects EMT and MET. Moreover, from both of our bioinformatics and mathematical modeling analyses, we found that the trajectories of the forward and backward transitions do not overlap but go along two different paths, a typical hysteresis phenomenon of a non-linear dynamical system (Kramer and Fussenegger, 2005). The distinct paths of EMT and MET can be clearly illustrated by the temporal activity dynamics of AP-1 and NFκB. Such an irreversible behavior has been also observed in lung cancer in a recent study (Karacosta et al., 2019). Also, from mathematical modeling, we found that, after the initial signaling induction to achieve the forward transition, signaling removal does not fully reverse the process, but signaling inhibition can. The incomplete reverse process is also evident from the single cell data for most conditions in this study. Further characterizing the transitional paths will expand our knowledge on driving or reversing EMT.

Further, we found the performance of network modeling is context dependent. For instance, accuracies for some conditions like OVCA420 TNF were quite low. This can happen if the identified common TFs are not differentially activated, resulting in low number of E and M TFs. Cook and Vanderhyden (2019) indeed discussed that the A549 TGFB1 and OVCA420 TNF conditions had low EMT scores. Another limitation of the current approach is that it relies on SCENIC for identifying regulons and thus utilizes regulatory interactions identified by only gene co-expression and *cis*-regulatory motif enrichment analysis. One way to improve the analysis is to incorporate regulatory interactions from the literature. The specific datasets analyzed here contain heterogeneous clusters, where cells from different time points do not fall into distinct clusters (**Supplementary Figure S9**), but are rather on a continuum; this can also limit the robustness of the analysis. Another potential caveat of the current approach is that transcriptomics data can only capture transcriptional regulations but fall short to discover new pathways of signaling induction and metabolic pathways. A potential solution is to integrate multi-omics data (Hawe et al., 2019) to improve network construction and modeling.

MATERIALS AND METHODS

Single Cell RNA-Seq Data Processing

Processed single cell RNA seq data were downloaded from the download link provided by Cook and Vanderhyden (2019) Normalized log counts were used in pySCENIC v0.9.19 to calculate the activities of transcription factors. We used 7-species hg19 mc9nr cisTargetDBs for the enrichment analysis. The activities obtained from SCENIC analysis were used as counts in Seurat v3.1.1 for downstream analysis. The differential activity analysis was conducted using Seurat. We used default settings except for the log fold change criteria which we reduced to zero, as the activity fold change is quite low. To capture the changes over time, we performed seven comparisons for each of the twelve conditions – four for the forward group (1) 0 vs. 8 h; (2) 0 vs. 1 day; (3) 0 vs. 3 days; (4) 0 vs. 7 days; and three for the backward group (5) 7 days vs. 8 h; (6) 7 days vs. 1 day; (7) 7 days vs. 3 days. From this comprehensive differential analysis for 84 comparisons, we selected top hundred DATFs (sorted based on adjusted *p*-values) for the forward and backward directions to obtain a list of highly variable TFs for each of the twelve conditions. Further, we identified 28 DATFs, each of which occurs in at least 24 of the 84 pairwise comparisons (**Supplementary Figure S5**). The TFs were annotated as E (i.e., an epithelial gene) depending on whether the log fold change in the 0 day vs. 7 days (7 days vs. 3 d_rm) comparison is negative (positive) with an adjusted *p*-value of 0.05. Similarly, TFs with log fold change positive (negative) in the 0 day vs. 7 days (7 days vs. 3 d_rm) comparison are annotated as M (i.e., a mesenchymal gene). Scaled activity values from Seurat were used for network analysis. We scaled the backward activities whenever the forward and backward activities were needed on the same scale (for example, in gene activity plots in **Figures 4**, **7**). As the 7 days cells were included in both forward and backward datasets, these were used to fit a linear model which was then used to scale the activities of cells from the other days where the signal is removed.

Network Construction

All the nearest neighboring TFs of the common DATFs were identified using the SCENIC regulons. Thus, for a TF (annotated as TF1), if either the forward or backward regulon for the TF includes another TF (annotated as TF2), then TF2 was identified as a target of TF1. Spearman's correlation between the activities of the TFs in a specific dataset was used for assigning an interaction as excitatory or inhibitory. Mutual information between the DATF activities was calculated with infotheo R package using "mm" correction (Meyer, 2014). The interactions in the network were filtered based on MI cut offs and any interaction with opposite sign in the forward and backward direction was removed from the network. Based on the maximum and minimum values of MI, we varied the positive MI cutoffs from 0.05 to 1 and the negative MI cutoffs from 0.05 to 0.5 incrementing by 0.05 at each step. If a TF in a network had only outgoing interactions with no incoming interactions, then the TF was removed from the network. This pruning was done only once – if removing a TF this way makes another TF with only outgoing interactions, then this new signaling TF is not removed.

Network Simulation

The network construction step generated a large number of networks with different number of nodes and interactions for each condition. The resulting networks, which specify the

interactions in the form of regulator, target, and interaction type, were simulated using the default settings in sRACIPEv1.3.1 (Huang et al., 2017; Kohar and Lu, 2018). Specifically, 2000 models with randomized kinetic parameters were generated for each network. The model kinetic parameters include two parameters for each gene – maximum production rate (1–100) and degradation rate (0.1–1) and three parameters for each interaction – Hill coefficient of co-operativity (1–6), fold change (1–100), and threshold. The numbers in brackets indicate the range from which the corresponding parameter was selected. The range for threshold for interactions was dynamically selected based on network topology to roughly satisfy the half functional rule (Huang et al., 2017). The initial condition for each gene in a model was selected from a log distribution over the minimum and maximum possible expression value for that gene in the model with given kinetic parameters. For more details, please refer to Huang et al. (2017). The ODEs with these kinetic parameters and initial conditions were solved using the fourth order Runge–Kutta method and the model state was recorded after 50 time units. These simulated gene expressions for all the models were log transformed and standardized for further analysis.

Network Evaluation

Gene networks were evaluated by comparing the simulated and experimental TF activity data. For each experimental condition, the activities at 0 and 7 days during signal induction and 3 days after signal removal were used to classify the network TFs as either E or M TFs. For the forward transition, a TF was defined as an M TF if the gene has differential activity (adjusted p-value < 0.05) with a positive log fold change when comparing the data from 0 and 7 days, and as an E TF if the log fold change is negative. Similarly, for the backward transition, a TF was defined as an M TF if the gene has differential activity with a negative log fold change when comparing the data from 7 and 3 days after signal removal, and as an E TF if the log fold change is positive. The EMT states were not assigned to TFs if there is a conflict between E and M assignment for the forward and backward transitions. Using these E and M classification, we defined two digitized gene expression vectors as references to represent the E and M states. Here, in the E reference state, E TFs have high expressions (denoted as 1) and M TFs have low expressions (denoted as 0), vice versa. These E and M reference states were used to identify whether the 2000 simulated profiles using RACIPE can generate models in the E and M states. The simulated profiles were binarized with the binarize R package and kMeans method with two clusters (Mundus et al., 2019). The fraction of models having expression profiles close to the E and M state were calculated to evaluate how accurately the constructed network can capture the EMT states. The similarity between the binarized expression profiles and the digitized E and M expression vectors was measured by calculating the hamming distance between the common TFs. The hamming distance cutoff for matching of simulated and experimental data is selected based on number of common TFs such that the probability of a match by random chance stays below 0.05.

To model the signal induction in simulations, we selected all of the E models obtained in the previous simulations and increased the production rates of JUN and RELB in the OVCA420 TGFB1 network. The productions rates of both were multiplied by 10,000 and the network was simulated keeping the other parameters same (**Figures 7D,E**). Steady state solutions obtained from previous simulations were used as the initial conditions. The trajectories were sampled at multiple time points to capture the dynamics. To account for intrinsic and extrinsic noise and facilitate the transition between the states we also added some noise (0.05) during the simulations. Then, the production rates were reverted back to their original values to reflect the removal of signals. In another set of simulations, using the steady state solutions of the signal induction models as the initial condition, the production rates of RELB and JUN were decreased (multiplied by 0.0001) below their original values to allow all the E state models to transit back (**Figures 7D,E**).

DATA AVAILABILITY STATEMENT

All sequencing data used in this study was generated by Cook and Vanderhyden (2019) and is available at https://drive.google.com/drive/folders/1lZ38Uj2ZjmFus7XbHGTATh8f9MqXLAf_. The python and R scripts used to perform the analyses here are available at https://lusystemsbio.github.io/EMT-Cancer-scRnaSeq/EMT-Cancer-scRnaSeq.html.

AUTHOR CONTRIBUTIONS

ML conceived the scope and design of the study. DR and VK conducted experimental data analysis and figure generation. VK generated network models and performed simulations. DR, VK, and ML contributed to drafting and revising the manuscript.

FUNDING

This study was supported by a startup fund from The Jackson Laboratory, by the National Cancer Institute of the National Institutes of Health under Award Number P30CA034196, and by the National Institute of General Medical Sciences of the National Institutes of Health under Award Number R35GM128717. DR was also partially supported by a Summer Student Fellowship at the Jackson Laboratory and by the National Cancer Institute of the National Institutes of Health under Award Number R25CA174584.

SUPPLEMENTARY MATERIAL

The Supplementary Material for this article can be found online at: https://www.frontiersin.org/articles/10.3389/fmolb.2020.00054/full#supplementary-material

REFERENCES

Aibar, S., González-Blas, C. B., Moerman, T., Huynh-Thu, V. A., Imrichova, H., Hulselmans, G., et al. (2017). SCENIC: single-cell regulatory network inference and clustering. *Nat. Methods* 14, 1083–1086. doi: 10.1038/nmeth.4463

Bartoschek, M., Oskolkov, N., Bocci, M., Lövrot, J., Larsson, C., Sommarin, M., et al. (2018). Spatially and functionally distinct subclasses of breast cancer-associated fibroblasts revealed by single cell RNA sequencing. *Nat. Commun.* 9:5150.

Basu, S., Cheriyamundath, S., and Ben-Ze'ev, A. (2018). Cell–cell adhesion: linking Wnt/β-catenin signaling with partial EMT and stemness traits in tumorigenesis. *F1000Res* 7:1488. doi: 10.12688/f1000research.15782.1

Bocci, F., Jolly, M. K., George, J. T., Levine, H., and Onuchic, J. N. (2018). A mechanism-based computational model to capture the interconnections among epithelial-mesenchymal transition, cancer stem cells and Notch-Jagged signaling. *Oncotarget* 9, 29906–29920.

Brabletz, T., Kalluri, R., Nieto, M. A., and Weinberg, R. A. (2018). EMT in cancer. *Nat. Rev. Cancer* 18, 128–134.

Burger, G. A., Danen, E. H. J., and Beltman, J. B. (2017). Deciphering epithelial–mesenchymal transition regulatory networks in cancer through computational approaches. *Front. Oncol.* 7:162. doi: 10.3389/fonc.2017.00162

Butler, A., Hoffman, P., Smibert, P., Papalexi, E., and Satija, R. (2018). Integrating single-cell transcriptomic data across different conditions, technologies, and species. *Nat. Biotechnol.* 36, 411–420. doi: 10.1038/nbt.4096

Chen, D., and Davis, J. S. (2003). Epidermal growth factor induces c-fos and c-jun mRNA via Raf-1/MEK1/ERK-dependent and -independent pathways in bovine luteal cells. *Mol. Cel. Endocrinol.* 200, 141–154. doi: 10.1016/s0303-7207(02)00379-9

Chen, Y., LeBleu, V. S., Carstens, J. L., Sugimoto, H., Zheng, X., Malasi, S., et al. (2018). Dual reporter genetic mouse models of pancreatic cancer identify an epithelial-to-mesenchymal transition-independent metastasis program. *EMBO Mol. Med.* 10:e9085.

Chung, V. Y., Tan, T. Z., Tan, M., Wong, M. K., Kuay, K. T., Yang, Z., et al. (2016). GRHL2-miR-200-ZEB1 maintains the epithelial status of ovarian cancer through transcriptional regulation and histone modification. *Sci. Rep.* 6:19943.

Cook, D. P., and Vanderhyden, B. C. (2019). Comparing transcriptional dynamics of the epithelial-mesenchymal transition. *Cancer Biol. biorxiv* [Preprint]. doi: 10.1101/732412

Ding, S., Zhang, W., Xu, Z., Xing, C., Xie, H., Guo, H., et al. (2013). Induction of an EMT-like transformation and MET in vitro. *J. Transl. Med.* 11:164. doi: 10.1186/1479-5876-11-164

Dong, J., Hu, Y., Fan, X., Wu, X., Mao, Y., Hu, B., et al. (2018). Single-cell RNA-seq analysis unveils a prevalent epithelial/mesenchymal hybrid state during mouse organogenesis. *Genome Biol.* 19:31

Font-Clos, F., Zapperi, S., and La Porta, C. A. M. (2018). Topography of epithelial–mesenchymal plasticity. *Proc,. Natl. Acad. Sci. U.S.A.* 115, 5902–5907. doi: 10.1073/pnas.1722609115

Freudlsperger, C., Bian, Y., Contag Wise, S., Burnett, J., Coupar, J., Yang, X., et al. (2013). TGF-β and NF-κB signal pathway cross-talk is mediated through TAK1 and SMAD7 in a subset of head and neck cancers. *Oncogene* 32, 1549–1559. doi: 10.1038/onc.2012.171

Gonzalez, D. M., and Medici, D. (2014). Signaling mechanisms of the epithelial-mesenchymal transition. *Sci. Signal.* 7:re8. doi: 10.1126/scisignal.005189

Hawe, J. S., Theis, F. J., and Heinig, M. (2019). Inferring interaction networks from multi-omics data. *Front. Genet.* 10:535. doi: 10.3389/fgene.2019.00535

Hong, T., Watanabe, K., Ta, C. H., Villarreal-Ponce, A., Nie, Q., and Dai, X. (2015). An Ovol2-Zeb1 mutual inhibitory circuit governs bidirectional and multi-step transition between epithelial and mesenchymal states. *PLoS Comput. Biol.* 11:e1004569. doi: 10.1371/journal.pcbi.1004569

Huang, B., Lu, M., Jia, D., Ben-Jacob, E., Levine, H., and Onuchic, J. N. (2017). Interrogating the topological robustness of gene regulatory circuits by randomization. *PLoS Comput. Biol.* 13:e1005456. doi: 10.1371/journal.pcbi.1005456

Jia, D., Li, X., Bocci, F., Tripathi, S., Deng, Y., Jolly, M. K., et al. (2019). Quantifying cancer epithelial-mesenchymal plasticity and its association with stemness and immune response. *JCM* 8:725. doi: 10.3390/jcm8050725

Jolly, M. K. (2015). Implications of the hybrid epithelial/mesenchymal phenotype in metastasis. *Front. Oncol.* 5:155. doi: 10.3389/fonc.2015.00155

Karacosta, L. G., Anchang, B., Ignatiadis, N., Kimmey, S. C., Benson, J. A., Shrager, J. B., et al. (2019). Mapping lung cancer epithelial-mesenchymal transition states and trajectories with single-cell resolution. *Nat. Commun.* 10:5587.

Kersten, K., Visser, K. E., Miltenburg, M. H., and Jonkers, J. (2017). Genetically engineered mouse models in oncology research and cancer medicine. *EMBO Mol. Med.* 9, 137–153. doi: 10.15252/emmm.201606857

Kohar, V., and Lu, M. (2018). Role of noise and parametric variation in the dynamics of gene regulatory circuits. *Syst. Biol. Appl.* 4:40.

Kramer, B. P., and Fussenegger, M. (2005). Hysteresis in a synthetic mammalian gene network. *Proc. Natl. Acad. Sci. U.S.A.* 102, 9517–9522. doi: 10.1073/pnas.0500345102

Li, Y., Liu, Y., Xu, Y., Voorhees, J. J., and Fisher, G. J. (2010). UV irradiation induces Snail expression by AP-1 dependent mechanism in human skin keratinocytes. *J. Dermatol. Sci.* 60, 105–113. doi: 10.1016/j.jdermsci.2010.08.003

Lu, M., Jolly, M. K., Levine, H., Onuchic, J. N., and Ben-Jacob, E. (2013). MicroRNA-based regulation of epithelial-hybrid-mesenchymal fate determination. *Proc. Natl. Acad. Sci. U.S.A.* 110, 18144–18149. doi: 10.1073/pnas.1318192110

Meyer, P. E. (2014). *infotheo: Information-Theoretic Measures*.

Mundus, S., Müssel, C., Schmid, F., Lausser, L., Blätte, T. J., Hopfensitz, M., et al. (2019). Binarize: Binarization of One-Dimensional Data. *R package version 1.3.* Available online at: https://CRAN.R-project.org/package=Binarize

Nieto, M. A., Huang, R. Y.-J., Jackson, R. A., and Thiery, J. P. (2016). EMT: 2016. *Cell* 166, 21–45.

Nistico, P., Bissell, M. J., and Radisky, D. C. (2012). Epithelial-mesenchymal transition: general principles and pathological relevance with special emphasis on the role of matrix metalloproteinases. *Cold Spring Harbor Perspect. Biol.* 4:a011908. doi: 10.1101/cshperspect.a011908

Patel, A. P., Tirosh, I., Trombetta, J. J., Shalek, A. K., Gillespie, S. M., Wakimoto, H., et al. (2014). Single-cell RNA-seq highlights intratumoral heterogeneity in primary glioblastoma. *Science* 344, 1396–1401. doi: 10.1126/science.1254257

Pires, B. R. B., Mencalha, A. L., Ferreira, G. M., de Souza, W. F., Morgado-Díaz, J. A., Maia, A. M., et al. (2017). NF-kappaB is involved in the regulation of EMT genes in breast cancer cells. *PLoS One* 12:e0169622. doi: 10.1371/journal.pone.0169622

Pratapa, A., Jalihal, A. P., Law, J. N., Bharadwaj, A., and Murali, T. M. (2020). Benchmarking algorithms for gene regulatory network inference from single-cell transcriptomic data. *Nat. Methods*. 17, 147–154. doi: 10.1038/s41592-019-0690-6

Ramirez, D., Kohar, V., Katebi, A., and Lu, M. (2019). Modeling a gene regulatory network of EMT hybrid states for mouse embryonic skin cells. *bioRxiv* [Preprint]. doi: 10.1101/799908.

Romagnoli, M., Belguise, K., Yu, Z., Wang, X., Landesman-Bollag, E., Seldin, D. C., et al. (2012). Epithelial-to-mesenchymal transition induced by TGF-β1 Is mediated by blimp-1–dependent repression of BMP-5. *Cancer Res.* 72, 6268–6278. doi: 10.1158/0008-5472.can-12-2270

Sanchez-Taltavull, D., Perkins, T. J., Dommann, N., Melin, N., Keogh, A., Candinas, D., et al. (2019). Bayesian Correlation is a robust similarity measure for single cell RNA-seq data. *Bioinformatics* 2:lqaa002.

Steinway, S. N., Zanudo, J. G. T., Ding, W., Rountree, C. B., Feith, D. J., Loughran, T. P., et al. (2014). Network modeling of TGF signaling in hepatocellular carcinoma epithelial-to-mesenchymal transition reveals joint sonic hedgehog and wnt pathway activation. *Cancer Res.* 74, 5963–5977. doi: 10.1158/0008-5472.can-14-0225

Stuart, T., Butler, A., Hoffman, P., Hafemeister, C., Papalexi, E., Mauck, W. M., et al. (2019). Comprehensive integration of single-cell data. *Cell* 177, 1888.e21–1902.e21.

Sun, L., and Carpenter, G. (1998). Epidermal growth factor activation of NF-κB is mediated through IκBα degradation and intracellular free calcium. *Oncogene* 16, 2095–2102. doi: 10.1038/sj.onc.1201731

Thiery, J. P., Acloque, H., Huang, R. Y. J., and Nieto, M. A. (2009). Epithelial-mesenchymal transitions in development and disease. *Cell* 139, 871–890. doi: 10.1016/j.cell.2009.11.007

Vervoort, S. J., Lourenço, A. R., Tufegdzic Vidakovic, A., Mocholi, E., Sandoval, J. L., Rueda, O. M., et al. (2018). SOX4 can redirect TGF-β-mediated SMAD3-transcriptional output in a context-dependent manner to promote tumorigenesis. *Nucleic Acids Res.* 46, 9578–9590. doi: 10.1093/nar/gky755

Wouters, J., Kalender-Atak, Z., Minnoye, L., Spanier, K. I., De Waegeneer, M., González-Blas, C. B., et al. (2019). Single-cell gene regulatory network analysis reveals new melanoma cell states and transition trajectories during phenotype switching. *Genomics. bioRxiv* [Preprint].

Wu, Y., and Zhou, B. P. (2010). TNF-α/NF-κB/Snail pathway in cancer cell migration and invasion. *Br. J. Cancer* 102, 639–644. doi: 10.1038/sj.bjc.6605530

Zhang, Y., and Weinberg, R. A. (2018). Epithelial-to-mesenchymal transition in cancer: complexity and opportunities. *Front. Med.* 12, 361–373. doi: 10.1007/s11684-018-0656-6

Zheng, X., Carstens, J. L., Kim, J., Scheible, M., Kaye, J., Sugimoto, H., et al. (2015). Epithelial-to-mesenchymal transition is dispensable for metastasis but induces chemoresistance in pancreatic cancer. *Nature* 527, 525–530. doi: 10.1038/nature16064

Conflict of Interest: The authors declare that the research was conducted in the absence of any commercial or financial relationships that could be construed as a potential conflict of interest.

Copyright © 2020 Ramirez, Kohar and Lu. This is an open-access article distributed under the terms of the Creative Commons Attribution License (CC BY). The use, distribution or reproduction in other forums is permitted, provided the original author(s) and the copyright owner(s) are credited and that the original publication in this journal is cited, in accordance with accepted academic practice. No use, distribution or reproduction is permitted which does not comply with these terms.

frontiers in Molecular Biosciences

REVIEW
published: 24 April 2020
doi: 10.3389/fmolb.2020.00072

Cellular Plasticity in Breast Cancer Progression and Therapy

Deguang Kong[1,2†], *Connor J. Hughes*[1,3,4†] *and Heide L. Ford*[1,3,4*]

[1] *Department of Pharmacology, University of Colorado Anschutz Medical Campus, Aurora, CO, United States,* [2] *Department of General Surgery, Zhongnan Hospital of Wuhan University, Wuhan, China,* [3] *Pharmacology Graduate Program, University of Colorado Anschutz Medical Campus, Aurora, CO, United States,* [4] *Medical Scientist Training Program, University of Colorado Anschutz Medical Campus, Aurora, CO, United States*

With the exception of non-melanoma skin cancer, breast cancer is the most frequently diagnosed malignant disease among women, with the majority of mortality being attributable to metastatic disease. Thus, even with improved early screening and more targeted treatments which may enable better detection and control of early disease progression, metastatic disease remains a significant problem. While targeted therapies exist for breast cancer patients with particular subtypes of the disease (Her2+ and ER/PR+), even in these subtypes the therapies are often not efficacious once the patient's tumor metastasizes. Increases in stemness or epithelial-to-mesenchymal transition (EMT) in primary breast cancer cells lead to enhanced plasticity, enabling tumor progression, therapeutic resistance, and distant metastatic spread. Numerous signaling pathways, including MAPK, PI3K, STAT3, Wnt, Hedgehog, and Notch, amongst others, play a critical role in maintaining cell plasticity in breast cancer. Understanding the cellular and molecular mechanisms that regulate breast cancer cell plasticity is essential for understanding the biology of breast cancer progression and for developing novel and more effective therapeutic strategies for targeting metastatic disease. In this review we summarize relevant literature on mechanisms associated with breast cancer plasticity, tumor progression, and drug resistance.

Keywords: breast cancer, plasticity, EMT, cancer stem cell, metastasis

OPEN ACCESS

Edited by:
Mohit Kumar Jolly,
Indian Institute of Science (IISc), India

Reviewed by:
Bramanandam Manavathi,
University of Hyderabad, India
Michael D. Brooks,
University of Michigan, United States

***Correspondence:**
Heide L. Ford
heide.ford@cuanschutz.edu

† These authors have contributed equally to this work

Specialty section:
This article was submitted to Molecular Diagnostics and Therapeutics, a section of the journal Frontiers in Molecular Biosciences

Received: *03 February 2020*
Accepted: *31 March 2020*
Published: *24 April 2020*

Citation:
Kong D, Hughes CJ and Ford HL (2020) Cellular Plasticity in Breast Cancer Progression and Therapy. Front. Mol. Biosci. 7:72. doi: 10.3389/fmolb.2020.00072

INTRODUCTION

With the exception of non-melanoma skin cancer, breast cancer is the most frequently diagnosed malignant disease among women (Bray et al., 2018). In 2018, there were about 2.1 million newly diagnosed cases worldwide (Bray et al., 2018). With the introduction of mammography coupled with improved treatment, breast cancer mortality rates have decreased 1.8 to 3.4% per year since 1990 (Hendrick et al., 2019). Nonetheless, breast cancer remains the leading cause of cancer death among females, claiming over 600,000 lives per year worldwide (Valastyan and Weinberg, 2011; Bray et al., 2018), with more than 90% of patients dying from metastatic disease (Valastyan and Weinberg, 2011). Currently, there are no effective treatment strategies for metastatic patients, regardless of breast cancer subtype, and the median overall survival remains at ∼1–5 years (Waks and Winer, 2019). Therefore, understanding the cellular and molecular mechanisms that mediate cancer cell escape from the primary tumor, and most importantly, outgrowth and maintenance at secondary sites, is critical for developing novel therapies that specifically target metastatic disease.

Metastasis is highly complex, requiring cells to adapt to numerous different microenvironments as they leave the primary site, invade into and disseminate through the vasculature, seed at a distant site, and finally colonize and expand to form macrometastases (Gupta and Massague, 2006; Micalizzi et al., 2017; Smigiel et al., 2019). To navigate all the steps of the metastatic cascade, tumor cells likely require significant plasticity (da Silva-Diz et al., 2018; Chu et al., 2019; Smigiel et al., 2019; Yuan et al., 2019) (**Figure 1**). Plasticity can be defined as the ability of cells to toggle between different phenotypes without altering genotype, and is widely observed in embryonic differentiation, wound repair, and cancer metastasis (Yuan et al., 2019). In part, plasticity may arise from a gain in progenitor or stem-like qualities and/or from induction of an epithelial-to-mesenchymal transition (EMT).

During development, stem cells with self-renewal capability generate progeny that differentiate into all the cells of the body (Thiery et al., 2009). Further, in the developing organism, a subset of epithelial cells undergo an EMT, and subsequently may undergo the reverse process (mesenchymal to epithelial transition [MET]), in order to enable epithelial sheets to fold and fuse to create the final shapes of the various tissues and organs (Thiery et al., 2009; Ray and Niswander, 2012). It has become increasingly appreciated that these developmental processes, which require cell plasticity, share commonalities with processes required for the progression of cancer (Ma et al., 2010; Manzo, 2019; Yuan et al., 2019). As the counterpart of normal stem cells, cancer stem cells (CSCs) are characterized by their ability to self-renew, in addition to their pluripotent and pro-tumorigenic properties (Mani et al., 2008; Morel et al., 2008). Similar to epithelial cells during development, carcinoma cells also perform EMT to become motile, enabling the spread of cells to distant organs (Thiery et al., 2009).

An association between EMT and cancer stem cells was first reported by Mani et al., where they demonstrated that transduction of human mammary epithelial cells with EMT transcription factors (Snail/Twist1) led not only to an increase in expression of mesenchymal markers and a phenotypic change toward mesenchymal morphology, but also led to an increase in the percentage of $CD44^{high}CD24^{low}$ cells with increased stemness properties (Mani et al., 2008). Other studies led to similar conclusions, where the induction of an EMT program in epithelial tumor cells increased the population of CSCs, enhancing their tumor initiation ability (Morel et al., 2008; Wellner et al., 2009). However, EMT cannot always be equated with cancer stemness. Nieto et al. demonstrated that the homeobox transcription factor Prrx1, which induced EMT and enabled invasiveness characteristics in a panel of human cancer cell lines, actually needed to be lost in order for breast cancer cells to metastasize *in vivo*. This loss of Prrx1 was associated with a reversion of EMT and induction of stem cell properties, suggesting that plasticity and EMT are not inextricably linked and the process of metastasis may require dynamic fluctuations between epithelial and mesenchymal states in cancer cells (Ocana et al., 2012).

In this review, we summarize current knowledge around cellular plasticity in breast cancer, specifically with regards to epithelial-mesenchymal plasticity (EMP) and plasticity of cancer stem cells, and the role of these processes in promoting tumor initiation, maintenance, and metastasis. We will also outline the impact of plasticity on drug resistance and explore recent findings in which targeting plasticity may be used to develop more effective therapeutic strategies.

CANCER STEM CELL AND EMT PLASTICITY IN BREAST TUMORIGENESIS

Breast cancer stem cells (BCSCs) are identified as a small population of cells that have specific molecular signatures such as $CD44^{+}/CD24^{-}$, Aldehyde dehydrogenase 1 high ($ALDH1^{high}$), and $CD133^{+}$ (Al-Hajj et al., 2003; Al-Hajj and Clarke, 2004; Butti et al., 2019). The origin of BCSCs is still controversial. Due to their ability to self-renew and to lead to differentiation when driving tumor growth, numerous researchers claim that BCSCs arise from mammary stem cells or progenitor cells (Liu et al., 2014; Bao et al., 2015; Sin and Lim, 2017). This claim is supported by the fact that BCSCs share specific cell markers and exhibit properties that are highly similar to normal mammary stem cells or partially differentiated mammary progenitor cells, such as self-renewal and long persistence in mammary tissue (Liu et al., 2014; Sin and Lim, 2017). In contrast to this hypothesis, other investigators argue that BCSCs can be derived from differentiated mammary cells. Indeed, several recent studies indicate that gene mutations, a damaging physical stimulus, or the tissue microenvironment can all transform differentiated cells into BCSCs (Lagadec et al., 2012; Chaffer et al., 2013; Koren et al., 2015). Thus, it is possible that BCSC may arise via several means, underscoring the plastic nature of cancer cells at various different stages of differentiation.

It is now well-understood that significant heterogeneity exists in tumors, and that only a subset of cells within primary breast tumors have tumor initiating potential. Because of the ability of BCSCs to self-renew and to also yield progeny that differentiate, a significant amount of research on these cells has revolved around their role in breast cancer initiation. The tumor initiating potential of BCSCs likely has important clinical relevance, as triple-negative breast cancer (TNBC), which has a

Abbreviations: EMT, epithelial-to-mesenchymal transition; MET, mesenchymal to epithelial transition; CSC, cancer stem cells; BCSCs, Breast cancer stem cells; ALDH1, Aldehyde dehydrogenase1; NOD/SCID, nonobese diabetic/severe combined immunodeficient; TNBC, triple-negative breast cancer; ECM, extracellular matrix; MMPs, matrix metalloproteinases; TGF-ß, transforming growth factor ß; CTC, circulating tumor cells; FLPs, filopodium-like protrusions; DTCs, disseminated tumor cells; LOXL2, Lysyl oxidase-like 2; iPSCs, induced pluripotent stem cells; E/M, epithelial/mesenchymal; Tregs, regulatory T cells; PD-L1, programmed death-ligand-1; TAMs, tumor-associated macrophages; ABC, ATP-binding cassette; ROS, reactive oxygen species; MR-3, 3,5,4′-trimethoxystilbene; MAPK, Mitogen-activated protein kinase; EGFR, epidermal growth factor receptor; MEK/ERK, mitogen-activated protein kinase kinase/extracellular signal-regulated kinase; MNK, MAPK interacting (Ser/Thr)-kinase; PI3K, phosphoinositide 3-kinase; AKT/PKB, protein kinase B; mTOR, mechanistic target of rapamycin; STAT3, signal transducer and activator of transcription 3; TCF4, T-cell factor 4; WAP, whey acidic protein; MMTV, mouse mammary tumor virus; PFS, progression free survival; NSAID, non-steroidal anti-inflammatory drug; DVL1, disheveled1; FDA, food and drug administration.

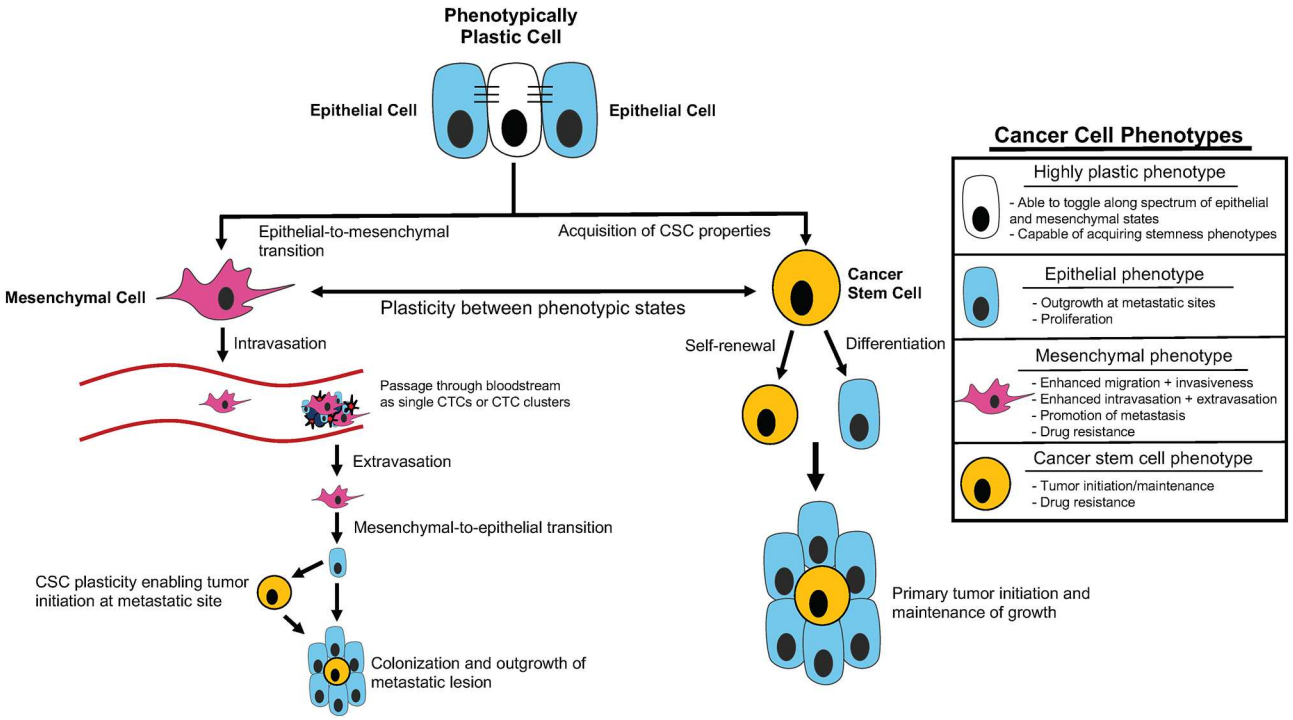

FIGURE 1 | Cancer cell plasticity throughout tumor initiation and the metastatic cascade. Outline of contribution of epithelial-mesenchymal plasticity (EMP) and acquisition of cancer stem cell (CSC) properties to tumor initiation and components of the metastatic cascade, including intravasation, extravasation, and metastatic colonization/outgrowth. Summary of distinct cellular phenotypes and characteristics associated with each.

higher population of BCSCs than other breast cancer subtypes, is more likely to relapse, providing an impetus for studies on this unique tumor cell population (Park et al., 2019).

In 2003, studies by Clarke and colleagues showed that breast tumor initiating stem cells ($CD44^{+}CD24^{-/low}$ lineage subpopulation) isolated from primary breast cancers could form tumors when transplanted into non-obese diabetic/severe combined immunodeficient (NOD/SCID) immunocompromised mice (Al-Hajj et al., 2003), however the remaining populations formed no detectable tumors even 29 weeks after injection into mice. Shortly after these studies, Dontu and colleagues discovered that ALDH1 could also mark BCSCs, and demonstrated that cells with high ALDH1 activity could generate mammospheres (a measure of anchorage-independent growth potential) *in vitro* and initiate tumors *in vivo* (Ginestier et al., 2007). Of note, different markers were used to define BCSC populations in these studies, and these markers do not identify the same populations. $CD44^{+}/CD24^{-}$ has been shown to mark mesenchymal-like CSCs, and $ALDH1^{high}$ has been shown to mark epithelial-like CSCs (Liu et al., 2014). Importantly, BCSCs display plasticity between these epithelial and mesenchymal CSC states, with BCSCs expressing both markers simultaneously having the highest tumor initiating potential (Liu et al., 2014). These data suggest that stemness and EMP may coordinately regulate elements of tumor initiation and it is possible that these same characteristics are important not only for establishing primary tumors, but also for the initiation of metastatic lesions. Since those initial studies, additional studies have demonstrated even greater plasticity for BCSCs than originally anticipated. For example, BCSCs have been shown to be capable of differentiating into endothelial cells to support the formation of new blood vessels and further contribute to tumor growth (Delgado-Bellido et al., 2017). Therefore, tumor initiating potential is likely not the only way that highly plastic BCSCs can contribute to tumor progression.

A number of studies have suggested that cells that undergo an EMT (and thus are plastic in nature), are often more CSC-like, having gained self-renewal capabilities (May et al., 2011; Mallini et al., 2015; Yuan et al., 2019). In addition, conditions (such as hypoxia or addition of transforming growth factor beta) that induce EMT in human breast cancers also increase the proportion of CSCs, leading to increased resistance to chemotherapies and increased proliferation *in vitro*, as well as enhanced tumorigenicity *in vivo* (Mani et al., 2008; Shuang et al., 2014). As such, it has been proposed that some properties of tumor aggressiveness, including metastatic potential and therapeutic resistance, which have been attributed to CSCs, may also be due to activation of EMT programs in these cells (Gupta et al., 2019). Work by our group supports the connection between EMT and BCSCs by demonstrating that overexpression of the homeobox transcription factor, Six1, in a mammary gland-specific Six1-overexpressing transgenic mouse model increased the CSC pool while simultaneously producing tumors that exhibited a partial EMT phenotype (McCoy et al.,

2009). Furthermore, several recent studies demonstrated that tumor-initiating ability of mesenchymal tumor-initiating cells was abolished when they were converted into epithelial counter parts (Avgustinova and Benitah, 2016; Chakraborty et al., 2016; Nilendu et al., 2018). These findings suggest contexts in which dynamic interplay between EMP and stemness can lead to distinct cancer cell populations with unique characteristics and activities.

However, while the tumor-initiating capacity of cancer cells may be dependent on the overall stemness of these cells, this stemness is not inextricably linked to an epithelial or mesenchymal state. A recent study by Weinberg et al. demonstrated that that hybrid epithelial/mesenchymal (E/M) breast cancer cells, which co-expressed both epithelial and mesenchymal markers, and were further defined by the antigen combination $CD104^{+}/CD44^{hi}$, were required for tumorigenicity. Mixing of cells expressing only epithelial or mesenchymal markers, respectively, did not recapitulate the tumorigenic potential of hybrid E/M cells which express both epithelial and mesenchymal markers simultaneously and likely represent an intermediate cell state with distinct phenotypic characteristics. Additionally, forcing hybrid E/M cells to a pure mesenchymal state through ectopic expression of Zeb1 abrogated the tumorigenic potential of these cells. This study suggests that the tumorigenic potential of CSCs may be more dependent on intrinsic cellular plasticity rather than EMT *per se* (Kroger et al., 2019).

With these studies in mind, it may be more appropriate to think of stemness and EMT as spectrums rather than distinct cell states, allowing for unique combinations of stem cell and E/M characteristics in a given subpopulation. Recent mathematical modeling approaches provide evidence for this line of thinking based on coupling of core decision-making modules of EMT (miR-200/ZEB) and stemness (LIN28/let-7) phenotypes. This modeling demonstrates that fine-tuning of the expression and interaction of these modules can alter the position of the "stemness window" on the "EMT axis" (Jolly et al., 2015). Additionally, these findings suggest that the position of the "stemness window" on the "EMT axis" is flexible and provides a unifying explanation for the seemingly contradictory connections between EMT, MET, and hybrid E/M states and stemness phenotypes (Jolly et al., 2015). Thus, it is possible that EMT and CSC phenotypes represent characteristics that define the overall EMP of a given cancer cell, and this plasticity may be the key driver of tumor progression related to EMT and cancer cell stemness (Ford and Thompson, 2010) (**Figure 1**).

STEM CELL AND EMT PLASTICITY IN PROGRESSION AND METASTASIS

It is well-established that tumor-host cell interactions influence the growth and spread of breast cancer. Tumor metastasis and ultimate outgrowth are very complex processes which require tumor cells to navigate numerous different environments and undergo a multitude of obstacles to survival and growth. Thus, those cancer cells that are able to alter their characteristics in response to different environments are likely to best navigate the multiple steps of the metastatic cascade (**Figure 1**). Plasticity, as well as the ability to cooperate with neighboring tumor cells or cells in the microenvironment, contributes to successful metastatic dissemination, and is important to understand if we are ever to develop means to treat this disease or prevent deadly progression.

Escape From the Primary Tumor Site and Intravasation Into the Vasculature

During breast cancer development (and the development of numerous carcinomas), a subset of tumor cells may undergo an EMT. This program can be initiated by EMT-associated transcription factors (often induced in response to microenvironmental signals) and results in decreased expression of E-cadherin, claudins, occludins, and other proteins that are key components of adherence junctions and desmosomes (Peinado et al., 2004; Thiery and Sleeman, 2006). Concomitant with the loss of epithelial proteins, mesenchymal-associated proteins such as N-cadherin, Vimentin, fibronectin, and α-smooth muscle actin, can become up-regulated. As a result, intercellular contacts and apical-basal polarity are lost, and tumor cell motility is enhanced via reorganization of the actin cytoskeleton and the intermediate filament network (Thiery et al., 2009; May et al., 2011). EMT-associated transcription factors can also stimulate secretion of gelatinases and matrix metalloproteinases (MMPs), leading to remodeling of the extracellular matrix (ECM) (Galindo-Hernandez et al., 2015; Shen et al., 2017). The induction of EMT in carcinomas can further increase tumor angiogenesis via enriching CSCs which possess the capacity to differentiate into endothelial cells and also upregulate the expression of the pro-angiogenic transcription factor VEGF-A (Fantozzi et al., 2014; Delgado-Bellido et al., 2017). Collectively, these changes disrupt the contiguity of the tissue epithelium and basement membrane and enable enhanced cancer cell motility, rendering the cells able to invade into bloodstream.

The existence of EMP in breast cancer has become evident both from animal model and human studies. Studies from our group demonstrated that overexpression of SIX1 in the breast cancer cell line MCF-7 converted transforming growth factor-ß (TGF-ß) signaling from tumor suppressive to tumor-promotional (Micalizzi et al., 2010), and this modification of TGF-ß signaling additionally promoted EMT and enhanced metastasis in both experimental and spontaneous mouse models (Micalizzi et al., 2009). In line with this data, and importantly in the setting of the human disease, Maheswaran and colleagues found that mesenchymal cells expressing known EMT regulators, including TGF-β pathway components and the FOXC1 transcription factor, were highly enriched in circulating tumor cells (CTCs) and these mesenchymal CTCs were associated with disease progression (Yu et al., 2013). Similarly, Agelaki and colleagues found that EMT markers (Twist and Vimentin) are expressed in CTCs of patients with metastatic disease and in early breast cancer patients (Kallergi et al.,

2011). Additionally, Maheswaran and colleagues also noticed small populations of CTCs that were positive for both epithelial and mesenchymal markers by RNA-*in situ* hybridization, and these hybrid E/M CTCs were often enriched in patients with progressive disease after chemotherapy (Yu et al., 2013). In this same study, an index patient demonstrated dynamic switching between mesenchymal and epithelial CTCs upon each cycle of therapy, suggesting that CTCs may maintain dynamic E/M plasticity (Yu et al., 2013; Hinohara and Polyak, 2019). This data aligns well with a recent study from Gupta and colleagues which utilized a DNA barcoding approach in the human breast cancer cell line MDA-MB-157 in order to demonstrate that distinct clonal populations of tumor cells can fluctuate between epithelial and mesenchymal states, demonstrating intrinsic E/M plasticity (Mathis et al., 2017). Additionally, they further demonstrated that progeny from a single clonal population maintain stable epithelial-to-mesenchymal ratios, suggesting that there may be an intrinsic component of distinct tumor clones which define their overall tropism for epithelial or mesenchymal states (Mathis et al., 2017). In fact, it is possible that cells maintaining both epithelial and mesenchymal characteristics may be the most metastatic, as a recent study demonstrated that intravenous injection of mammary tumor subpopulations from different stages of EMT saw the strongest increase in metastatic potential of early hybrid E/M states (Gupta et al., 2019; Pastushenko and Blanpain, 2019). After sorting, the majority of CTCs observed after IV injection exhibited an EpCAM-CD106-CD51-CD61 phenotype which is associated with co-expression of epithelial and mesenchymal markers (Gupta et al., 2019; Pastushenko and Blanpain, 2019). This study provides evidence that metastasis may be more dependent on maintaining EMP and hybrid E/M characteristics than it is on cells undergoing a complete EMT. Additionally, this plasticity may extend to stemness as well, as CTCs isolated from patients with breast cancer or from xenografts derived from patients with breast cancer overexpress both EMT markers and stem cell markers (Aktas et al., 2009; Baccelli et al., 2013). Together, these data suggest that highly plastic cells are more likely to make it to or survive in the bloodstream and represent the primary pool of cells from which metastatic lesions arise.

It is hypothesized that these highly metastatic hybrid E/M cells and cancer stem cells may be generated in or maintain local signaling in and around the primary tumor, which spatially primes tumors to seed cells into the bloodstream. Mathematical modeling experiments demonstrate that concentration gradients of EMT inducing signals (such as TGF-β) from the tumor-stroma boundary can generate distinct spatial patterning within tumors where complete EMT cells cluster toward the invasive edge and hybrid E/M cells are generated closer to the interior of the tumor where the concentrations of these signaling molecules are lower (Bocci et al., 2019). This may, in part, explain why mesenchymal cells are highly enriched in CTCs (Yu et al., 2013). In this model, CSC properties are generated in both the pure EMT and hybrid E/M populations, suggesting that both of these cell populations are intrinsically plastic. Subsequent addition of inflammatory cytokine signaling to this model enhances Notch signaling and stabilizes cells within the hybrid E/M state, offering an explanation for how stable hybrid E/M cells may reach the periphery of the tumor, form clusters, and dislodge from the primary tumor and enter the circulation without undergoing a complete EMT (Bocci et al., 2019). These mathematical findings suggest that cancer cell plasticity likely enables or facilitates movement of cancer cells from the primary tumor into the vasculature and may enhance survival of these cells in the circulation during therapy.

Plasticity as a Means to Survive in the Circulation

CTCs confront a harsh environment (shear stress, anoikis, and cytotoxic immune attack) making it difficult to survive as they move through the bloodstream, resulting in a large number of CTCs that are apoptotic in cancer patients (Francart et al., 2018). In breast cancer, Agelaki and colleagues found that a low percentage of apoptotic CTCs was associated with advanced clinical parameters, suggesting that having CTCs that are able to resist apoptosis may predict worse clinical disease (Kallergi et al., 2013). In this section, we will discuss how cellular plasticity contributes to survival of CTCs in the bloodstream.

Recent studies have demonstrated that undergoing an EMT in the initial invasion steps of metastasis may protect tumor cells from anoikis once in the bloodstream (Charpentier and Martin, 2013). For example, Weinberg and colleagues showed that loss of E-cadherin, one of the hallmarks of EMT, can enhance anoikis resistance of immortalized human mammary epithelial cells via inhibition of phosphorylation of β-catenin, thus stabilizing the protein by inhibiting its recognition by the proteasome (Onder et al., 2008). In an epithelium-specific p53 knock out mouse tumor model, Jonkers and colleagues similarly found that loss of E-cadherin could promote tumor metastasis by inducing increased anoikis resistance (Derksen et al., 2006). Furthermore, in breast cancer cell lines, loss of E-cadherin suppresses the activity of Ankyrin–NRAGE–p14ARF signaling to confer anoikis resistance (Kumar et al., 2011; Frisch et al., 2013). EMP and cancer stemness may act cooperatively to enhance anoikis resistance, as Frisch and colleagues showed that in breast cancer, the cancer stem cell marker CD44S, which is up-regulated in response to an EMT, can enhance cell survival under detached conditions (Cieply et al., 2015).

EMP affects numerous characteristics of tumor cells beyond the expression of epithelial and mesenchymal markers. For example, microtentacles, produced via dynamic microtubule-based extensions of the plasma membrane, have been shown to be critical for CTCs to resist shear stress and anoikis in circulation (Yamauchi et al., 2005; Charpentier and Martin, 2013). In human mammary epithelial cells or breast cancer cells, EMT-associated transcription factors, including Snail1 and Twist1, could up-regulate this cytoskeletal structure, and vimentin filaments, a known marker for EMT, supported extension of these microtentacles (Whipple et al., 2008, 2010).

As more studies on CTCs have been performed, it has become clear that CTCs can exist as single cells or in clusters containing mixes of tumor cells, immune cells, stromal cells, pericytes, platelets, and cancer-associated fibroblasts (Hong et al., 2016)

(**Figure 1**). In breast cancer, CTC clusters have been shown to be more metastatic than single CTCs, and their presence is associated with a poor prognosis (Aceto et al., 2014). Blackhall and colleagues have demonstrated that when compared to single CTCs, tumor cells within CTC clusters exhibit enhanced survival and decreased anoikis (Hou et al., 2011). Emerging evidence suggests that EMT, and its reverse program MET, play important roles in the formation of CTC clusters. Maheswaran and colleagues showed that the formation of CTC clusters relies on the expression of the cell–cell adhesion molecule plakoglobin in a mouse mammary carcinoma model (Aceto et al., 2014). However, in that study, they did not explore the EMT status in these CTCs cluster cells. Cheung and colleagues found that Keratin 14, an epithelial cytoskeletal protein, is highly expressed in murine breast cancer CTC clusters and that these Keratin 14 positive cells exhibit a hybrid E/M phenotype expressing both epithelial and EMT/stemness mesenchymal markers (Cheung et al., 2016), again indicating that plasticity may be a key feature for survival of tumor cells that leave the primary tumor. In contrast, Blackhall and colleagues found that lung carcinoma cells within CTC clusters primarily remain very mesenchymal, expressing Vimentin but not expressing E-cadherin. In addition, they also found that the EMT status of CTC cluster cells was more pronounced than that of single CTCs (Hou et al., 2011). There are many considerations for why these studies yielded divergent findings. First, the Blackhall study utilized human lung cancer patient blood samples, whereas the Cheung study utilized a murine breast cancer model, and thus it's possible the murine model doesn't accurately portray human cancer biology or that lung and breast cancer may utilize different strategies for CTC dispersal and survival. It is important to note that the Blackhall study uncovered a high degree of intra- and inter-patient heterogeneity with regards to staining for epithelial markers in CTC clusters. Thus, loss of membranous E-cadherin may not represent a complete loss of the epithelial phenotype of these cells as other epithelial markers can be expressed in this context to promote aggregation of these clusters. While there remains much to be understood about CTC cell plasticity, these studies suggest that carcinoma CTCs can exist in various states on the spectrum from epithelial to mesenchymal, underscoring the benefits of plasticity in the process of metastasis.

Emerging evidence suggests that coagulation activated by CTCs also plays an important role in enhancing the ability of CTCs to survive in the bloodstream. Many kinds of tumor cells, including breast cancer cells, express tissue factor, which is an important cell-associated activator of the coagulation cascade (Palumbo, 2008; Cole and Bromberg, 2013; Lambert et al., 2017). Once the tumor cells invade into the circulation, CTCs rapidly associate with platelets to activate the coagulation cascade and form platelet-rich thrombi around tumor cells in the vasculature. These thrombi are thought to physically protect CTCs from the stress of blood flow and from elimination by the immune system (Labelle and Hynes, 2012). This idea has also been supported by clinical studies. In a variety of malignant diseases, coagulation has been associated with a poor clinical prognosis and anticoagulants can reduce metastasis (Lee, 2010; Degen and Palumbo, 2012). Further, Cristofanilli and colleagues found that CTCs in metastatic breast cancer patients are associated with increased risk of thromboembolism (Mego et al., 2009). Strikingly, a relationship between EMT and tissue factor has been observed in several cancers (including breast cancer), again suggesting that plasticity is a key factor in mediating this phenotype. For example, in breast cancer cell lines, cells induced to undergo an EMT via introduction of Zeb1 increased the expression of tissue factor, which led to increased coagulant properties. Silencing Zeb1 inhibited both EMT-associated TF expression and coagulant activity (Bourcy et al., 2016). Taken together, these studies, as well as many others, suggest that EMP may be a key means by which cells survive the early steps of metastasis.

Tumor Cell Extravasation

After surviving in the circulation, CTCs must first attach to the capillary endothelium and then penetrate a physical barrier composed of an endothelial and pericyte cell layer to effectively develop into a metastatic lesion. Most circulating cancer cells become trapped in capillaries due to size restriction. Compared to single cells, cancer cell clusters are larger and travel more slowly, and can thus easily be trapped in small blood vessels in various organs (Yu, 2019). This entrapment and arrest may be one mechanism by which CTC clusters and CTC-containing-thrombi (regulated by EMT) promote metastases as this increased residence time may facilitate increased interaction with the endothelial wall and subsequent extravasation. In addition to a passive entrapment in the vasculature, under certain conditions cancer cells can undergo adhesive arrest in the capillary vessels that are larger than the cell diameter in an active manner (Yamauchi et al., 2005). Similar to leukocytes, CTCs can roll and adhere to endothelial cells. CTC clusters and CTC-containing- thrombi have a much lower rolling velocity, and are thus susceptible to increased interaction with the vascular wall (Francart et al., 2018). In addition, tumor cells express specific proteins such as selectins, integrins, and metadherin, which enable active adhesion to the vasculature (Orr and Wang, 2001; Brown and Ruoslahti, 2004; Wang et al., 2004; Labelle and Hynes, 2012). Weinberg and colleagues found that the EMT-associated transcription factors (Snail1 and Twist1), when expressed in murine mammary carcinoma lines, promote the formation of filopodia-like protrusions (FLPs) which contain integrin β1, enabling interaction with the ECM (Shibue et al., 2012). In contrast, Klemke and colleagues found that Twist1 expression in human breast tumor cells promoted tumor cell adherence to the vascular wall through a β1 integrin-independent mechanism (Stoletov et al., 2010). In addition, Twist1 positive cells formed large dynamic rounded membrane protrusions, promoting the ability for tumor cells to traverse capillary vessels (Stoletov et al., 2010). It is possible that the dependence or lack of dependence of this process on β1 integrin may depend on the species of origin or specific cell line, or that abundant expression of β1 integrin in murine FLPs doesn't necessarily imply that this expression is explicitly required for the adhesion function of these protrusions. In any case, it remains that EMT and cancer cell plasticity can facilitate extravasation through multiple, possibly synergistic, mechanisms.

Colonization of Distant Organ Sites

The microenvironment of the secondary site is often very different from the primary site, creating a significant challenge for disseminated tumor cell (DTC) survival. In 1889, Steven Paget first proposed the 'seed and soil' hypothesis, which proposed the need for a receptive microenvironment for the growth of metastases (Paget, 1989). In recent years, this hypothesis has been supported by experimental studies, leading to the more recently described concept of a pre-metastatic niche. The pre-metastatic niche has been shown to be educated by tumor-derived secreted factors, extracellular vesicles, bone marrow-derived cells, suppressive immune cells and host stromal cells, in order to become a receptive microenvironment for DTC colonization (Liu and Cao, 2016). Strikingly, Cano and colleagues uncovered a relationship between EMT and the formation of a premetastatic niche in breast cancer (Canesin et al., 2015). Tumor cell expression of lysyl oxidase-like 2 (LOXL2) has been shown to regulate the EMT transcription factor Snail1 and can additionally interact with the bHLH transcription factor E47 to downregulate E-cadherin and induce EMT (Canesin et al., 2015; Salvador et al., 2017). In addition to regulating EMT-associated transcription factors, LOXL2 additionally regulates the recruitment of bone marrow progenitor cells (c-kit$^+$/Sca-1$^+$) to the lungs and enhances premetastatic niche formation, demonstrating multiple, simultaneous means by which tumor cells may enhance their metastatic potential (Canesin et al., 2015).

While EMP appears to be critical in the earlier stages of metastasis, cancer stemness, which is associated with self-renewal and tumor initiation, is another form of plasticity that is likely most important in metastatic colonization. For example, our laboratory demonstrated that SIX2 overexpression in breast cancer cells leads to efficient metastatic colonization in the lung via its ability to induce a CSC phenotype through upregulation of SOX2 (Oliphant et al., 2019). Wong and colleagues also demonstrated a critical role for CSCs in metastatic colonization (Ren et al., 2018). The authors obtained triple-negative breast cancer patient-derived and cell line–derived CSC- enriched populations via growth as tumorspheres. CSCs obtained from tumorspheres formed brain metastases more rapidly after intracardiac injection into mice than their origin cell lines. It was observed that maintenance of stemness in these CSCs in this model occurred through activation of a tumor cell PCDH7-PLCβ-Ca^{2+}-CaMKII/S100A4 signaling axis. When stemness was inhibited through administration of a specific PLC inhibitor edelfosine which disrupted this axis, brain metastatic colonization was significantly decreased (Ren et al., 2018).

Recent studies suggest that EMT may only be critical for the initial steps of the metastatic cascade up to organ extravasation, while its reverse process, MET, is associated with the tumor-initiating ability required for metastatic colonization (Acloque et al., 2009; Thiery et al., 2009). This hypothesis is reinforced by histological examination in clinical specimens, as metastatic tumors exhibit epithelial characteristics that are similar to those seen in the primary tumors (Chui, 2013). Wells and colleagues showed mesenchymal-like MDA-MB-231 breast cancer cells re-express E-cadherin through loss of methylation in the E-cadherin promoter when the cells reach the secondary organ environment via tail vein injection (Chao et al., 2010). In a dynamic *in vivo* model of metastatic breast cancer, Gilles and colleagues found that tumor cells in vascular tumoral emboli all express Vimentin (a marker of mesenchymal cells), but macrometastases in the lung display heterogenous Vimentin expression, and thus resemble the primary tumor (Bonnomet et al., 2012). In addition, Lieberman and colleagues found that miR-200, which promotes an MET, enhances macroscopic metastases in mouse breast cancer cell lines (Dykxhoorn et al., 2009). But how does MET influence metastatic colonization, particularly when EMT has been associated with stemness? Somewhat counterintuitively, stemness caused by MET may be one of the reasons. Indeed, growing evidence supports that MET is also linked to stemness. For example, MET is required to reprogram fibroblasts to iPSCs (Li et al., 2010; Samavarchi-Tehrani et al., 2010). During the reprogramming process, Snail1, TGF-β1 and TGF-β receptor II are repressed, and E-cadherin is up-regulated (Li et al., 2010). In breast cancer, recent studies also indicate a relationship between MET and stemness. Benezra and colleagues showed that during metastatic colonization, inhibitor of differentiation 1 (Id1), enhances breast cancer cells' stem-like phenotype by suppressing Twist1 and inducing an MET (Stankic et al., 2013). While these findings seemingly contradict the relationship of EMT in promoting stemness (May et al., 2011; Delgado-Bellido et al., 2017; Yuan et al., 2019), the two ideas may be unified through the concept of the hybrid E/M state, which may be indicative of plasticity. As discussed previously, this concept is supported by mathematical modeling of EMT and stemness due to intrinsic signaling modules (Jolly et al., 2015) or concentration gradients of secreted signaling molecules in the tumor microenvironment (Bocci et al., 2019). Possibly as a consequence of MET, a subset of cells can be found in a hybrid E/M state (Grosse-Wilde et al., 2015). Therefore, it may be the case that a cell that has undergone an EMT and is more stem-like may also be more plastic and thus better able to undergo a MET or fluctuate along a spectrum of epithelial and mesenchymal states. Grosse-Wilde and colleagues demonstrated that in breast cancer, the hybrid E/M state reflects stemness and increased plasticity, as these cells demonstrate increased self-renewal, mammosphere formation, and can produce ALDH1$^+$ progeny. Further, such hybrid cells are associated with poor prognosis (Grosse-Wilde et al., 2015). Weinberg and colleagues also demonstrate that the hybrid E/M state is essential for tumorigenicity of breast cancer (Kroger et al., 2019) further entwining the relationship between EMP and stemness. This theory was verified in ovarian and prostate cancer cells as well (Strauss et al., 2011; Ruscetti et al., 2015). Another possible means by which MET may induce colonization is through its ability to relieve the repression of proliferation caused by EMT. Nieto and colleagues found that during EMT, Snail impaired cell proliferation via repressing Cyclin D2 transcription (Vega et al., 2004). Tulchinsky and colleagues demonstrated that induction of EMT by Zeb1 directly repressed cell division by inhibiting Cyclin D1 activity (Mejlvang et al., 2007). Thus, there are a host of distinct mechanisms through which complete EMT may suppress and MET/EMP may facilitate outgrowth and establishment of metastatic lesions.

Escape From Immune System

Evasion of the immune system is required if tumors are to recur or progress (Hanahan and Weinberg, 2011). Not surprisingly, cancer cell plasticity may be a key means through which tumor cells avoid detection by the immune system. Zhou and colleagues found that in cells enriched for BCSCs ($ALDH^+$ or $CD44+CD24^-$ cell populations), extracellular−5'- nucleotidase (CD73) was increased, which enzymatically produces extracellular adenosine and thus can activate adenosine signaling in immune cells. Adenosine signaling has been shown to suppress a variety of immune responses through a variety of distinct mechanisms including upregulation of the negative co-stimulatory molecules CTLA-4 and PD-1 in lymphocytes (Hasko et al., 2008; Zhang, 2010; Allard et al., 2013; Gajewski et al., 2013). These data suggest that BCSCs might promote breast cancer development and progression through immune evasion (Yu et al., 2017). In addition, Marcato and colleagues found that $ALDH^+$ BCSCs had decreased expression of antigen processing and co-stimulatory molecules when compared to non-CSCs (Sultan et al., 2018). As a result, BCSCs could be less susceptible to T cell-mediated cytotoxicity.

Immunosuppressive effects of BCSCs extend to the innate immune system as well. Semenza and colleagues found CD47 expressed on BCSCs could enable cancer cells to evade phagocytosis by tumor-associated macrophages (TAMs) (Zhang et al., 2015). Additionally, Bian and colleagues demonstrated that BCSCs were resistant to the attack mediated by autologous/allogeneic NK cells due to reduced expression of MICA and MICB which were the ligands for the stimulatory NK cell receptor NKG2D (Wang et al., 2014). In addition to direct suppression of immune cells, BCSCs may also be capable of immune suppression through modulation of cytokine signaling in the tumor microenvironment. Farrar and colleagues found that BCSCs ($CD44^+/CD24^-$) express increased levels of CD200 on their cell surface (Kawasaki et al., 2007). CD200 is a member of the immunoglobulin superfamily involved in immunoregulation and tolerance. Its expression on ovarian and melanoma cancer cells was shown to suppress the anti-tumor immune response through downregulation of Th1 cytokines IL-2 and IFN-γ (Kawasaki and Farrar, 2008).

In tumor immune escape, there is a close relationship between EMT and cancer stemness. EMT can reduce immune detection as well as increase the percentage of cells with CSC characteristics. Chouaib and colleagues found that acquisition of the EMT phenotype in MCF-7 cells is associated with increased $CD24^-/CD44^+/ALDH^+$ stem cell populations and is also associated with an inhibition of cytotoxic T lymphocytes (Akalay et al., 2013). This finding was strengthened by another study which found that immunoediting of breast tumor cells may be accompanied by both an EMT and the acquisition of a stem-like state in a neu-transgenic mouse model of breast cancer (Knutson et al., 2006). Further studies demonstrate that compared to non-CSCs, PD-L1 total protein and surface expression was enriched in BCSCs ($CD44^+/CD24^{-/low}$ population in human breast cancer and $CD44^+/CD24^+/ALDH1^+$ population in mouse breast cancer) and this enrichment was regulated in response to EMT through an EMT/ß-catenin/STT3/PD-L1 signaling axis. EMT-induced ß-catenin transcriptionally upregulates the N-glycosyltransferase STT3, which N-glycosylates and subsequently stabilizes PD-L1 from degradation (Hsu et al., 2018). Intriguingly, although the induction of an EMT could upregulate PD-L1 on the surface Of non-CSC breast cancer cells, EMT led to a more robust PD-L1 induction in the BCSC populations (Hsu et al., 2018). In addition to up-regulation of PD-L1, down-regulation of MHC-I on the surface of breast cancer cells has been observed in response to EMT, protecting these cells and their more epithelial counterparts from immune attack (Dongre et al., 2017). These data indicate that there are multiple means through which EMT and cancer stemness can protect tumor cells from immune attack, and it is likely that tumor cells that have undergone an EMT and possess CSC properties confer even greater protection from immune clearance by simultaneously engaging multiple of the aforementioned immunosuppressive mechanisms.

INFLUENCE OF THE MICROENVIRONMENT AND TUMOR CELL CROSSTALK ON BREAST CANCER CELL PLASTICITY

As described above, cancer cell plasticity is frequently regulated by dynamic cell-intrinsic EMT and stemness gene expression patterns. However, regulation of plasticity is also highly dependent on tumor cell-extrinsic microenvironmental influences. For example, an elegant *in vitro* study by Gupta and colleagues showed that in short-term 2D cultures, mammary epithelial cells spontaneously acquire stem-like traits. However, culturing of these same cells in 3D matrices more representative of *in vivo* tissue architecture preserves lineage identity (Sokol et al., 2016; Gupta et al., 2019). This finding suggests that tissue architecture may be capable of regulating cellular stemness, and this regulatory mechanism may also act to regulate generation or maintenance of BCSCs.

In addition to structural elements of the tumor microenvironment, local signaling between tumor cell subpopulations and between tumor cells and non-tumor cells can also influence cancer cell stemness, EMP, and tumor aggressiveness. Luo and colleagues demonstrated that tumor-associated macrophages (TAMs) were capable of paracrine activation of an EGFR-STAT3-SOX2 signaling axis in the 4T07 and 4T1 murine breast cancer cell lines leading to enhanced BCSC properties and tumor-initiating potential (Yang et al., 2013). Similarly, it was shown that estrogen could expand the BCSC pool in multiple human ER+ breast cancer cell lines through activation of a paracrine FGF/FGFR/Tbx3 axis in the cancer cell, greatly increasing tumorsphere formation potential of these cancer cells (Fillmore et al., 2010).

Recent work by our laboratory demonstrated that breast cancer cells that have undergone an EMT are capable of inducing EMT-like phenotypes and enhancing metastatic potential of non-EMT cells by activating GLI signaling in neighboring non-EMT cells (Neelakantan et al., 2017). In this way, signals from subsets of cells within a heterogeneous tumors could promote EMP and

enhanced tumor metastasis in cells not intrinsically expressing EMT-associated transcription factors (Neelakantan et al., 2017).

Similar to stemness, EMP can also be induced through microenvironmental signaling driven by non-tumor cells. Feng and colleagues found that cancer-associated fibroblasts isolated from breast cancer tissues secreted TGF-β1, which was capable of activating TGF-β/Smad signaling in multiple breast cancer cell lines, leading to upregulation of EMT-associated transcription factors, and promoting an EMT phenotype (Yu et al., 2014). Similarly, Aboussekhra and colleagues demonstrated that SDF-1/MMP-2 secreted by cancer-associated fibroblasts deficient in p16 could induce an EMT in MDA-MB-231 breast cancer cells, again suggesting mechanisms of paracrine regulation of EMT in breast cancer (Al-Ansari et al., 2013).

Treatment with exogenous therapies also represents an extrinsic factor which can modulate cancer cell plasticity. An example of this was demonstrated by Gupta and colleagues, who used mathematical modeling approaches to simulate treatment of breast cancer cells with epithelial or mesenchymal-specific targeting drugs. This simulation suggested that sequential treatment of E or M specific therapies would lead to selection of plastic E/M clones with enhanced therapeutic resistance (Mathis et al., 2017). Similarly, it was demonstrated *in vitro* that radiation therapy led to a dose-dependent increase in BCSCs in single cell suspensions of human breast cancer specimens, as quantified by ALDH1 positivity (Lagadec et al., 2012). These examples demonstrate that while cancer cell plasticity often results from changes in cell-intrinsic gene expression and signaling, extrinsic effects of the microenvironment and tumor cell crosstalk also play a crucial role in regulating cancer cell stemness and EMP.

CLINICAL CHALLENGES CAUSED BY BREAST CANCER CELL PLASTICITY

The presence of intratumor heterogeneity, which describes the coexistence of cells that are genetically, epigenetically, or phenotypically different within the primary tumor or the metastatic site, creates a significant challenge for clinical diagnosis and therapy (Hong et al., 2018). Such heterogeneity can cause incorrect diagnoses or treatment when a small biopsy is used for pathological examination. Heterogeneity can also lead to resistance to chemotherapy and radiotherapy, as minor clones can be selected for during the course of the treatment (McGranahan and Swanton, 2015; Yang et al., 2017; Hong et al., 2018). This phenomenon was observed in a recent study which used single-cell DNA-sequencing to show that pre-existing resistant cells were selected for by neo-adjuvant chemotherapy in TNBC, leading to the development of therapeutic resistance (Kim et al., 2018; Hinohara and Polyak, 2019). Some of these resistant subpopulations in tumors may be caused in part via the presence of cells with BCSC and/or EMT characteristics, largely obtained through non-genetic means and thus particularly difficult to detect and/or target (Hong et al., 2018).

BCSCs are associated with therapy resistance and relapse. Compared with highly proliferative breast cancer cells, BCSCs are thought to remain in the G0 phase of the cell cycle for long periods of time (a quiescent state also known as dormancy) which likely contributes to their ability to resist chemotherapy and/or radiation damage (Allan et al., 2006). For example, Chang and colleagues compared the biopsies of patients' primary tumors before and after 12 weeks of treatment with neoadjuvant chemotherapy and found that the percentage of BCSCs ($CD44^{high}/CD24^{low}$) was increased after chemotherapy (Li et al., 2008). Similarly, Noguchi and colleagues also found that chemotherapy increased the percentage of BCSCs, however their results suggest that ALDH1-positivity as a marker of BCSCs was significantly more predictive than $CD44^{+}/CD24^{-}$ (Tanei et al., 2009). As early as the 1990s, and well before ALDH was associated with cancer stem cell phenotypes, it was known to be associated with chemoresistance due at least in part to its ability to metabolically inactivate chemotherapeutic agents such as cyclophosphamide (Mirkes et al., 1991). More recently, it has been shown that ALDH enhances breast cancer cell resistance to chemotherapy via up-regulation of many therapy-resistance proteins (p-glycoprotein, GSTpi, and/or CHK1) (Croker and Allan, 2012). In addition, BCSCs are reported to express high levels of ATP-binding cassette (ABC) transporter proteins, which protect cells from drug damage via efflux pumping mechanisms (Hirschmann-Jax et al., 2004).

The resistance of CSCs to radiation is largely due to the heightened ability of these cells to activate the DNA damage checkpoint, increasing the repair of DNA damage and decreasing resultant cell death (Rich, 2007). For example, the repair of radiation-induced DNA damage in mammospheres (enriched for breast cancer stem cells and their progenitors) is dramatically increased when compared with monolayer cultures (Phillips et al., 2006). Furthermore, several studies have demonstrated that BCSCs also more efficiently reduce intracellular reactive oxygen species (ROS) induced by ionizing radiation (Phillips et al., 2006; Diehn et al., 2009). ROS is a critical mediator of cell killing after exposure to ionizing radiation, and thus decreasing ROS can enhance the resistance of cancer cells to radiation (Riley, 1994).

As outlined above, a strong association exists between EMT and CSC phenotypes, and thus it is not surprising that the two phenotypes have been linked to resistance in the same context. In basal/$HER2^{+}$ breast cancer cell lines, Menendez and colleagues showed that EMT-associated transcription factors (Snail2 and Slug) enhance resistance to trastuzumab via inducing a BCSC phenotype ($CD44^{+}CD24^{-/low}$) (Oliveras-Ferraros et al., 2012). In addition, recent studies also suggest that EMT may contribute to drug resistance directly. For example, it was found that EMT-associated markers, including Vimentin and MMP2, were increased in residual breast cancers after conventional therapy (Creighton et al., 2009), suggesting that breast cancer cells with molecular signatures associated with EMT may be more resistant to endocrine therapy (letrozole) or chemotherapy (docetaxel). Importantly, if EMT inhibits cancer cell proliferation (Vega et al., 2004; Mejlvang et al., 2007), this feature alone may

increase chemotherapy resistance. In an elegant study in which cells undergoing an EMT were fate-mapped in a genetically engineered mouse model of breast cancer (MMTV-PyMT), Gao and colleagues demonstrated that mammary carcinoma cells that had undergone an EMT were much more resistant to chemotherapy than carcinoma cells that had not undergone an EMT, likely due to reduced proliferation, apoptotic tolerance and increased expression of chemoresistance-related genes in the EMT cells (Fischer et al., 2015). Similarly, it has been shown that Twist1 (a master regulator of EMT) is associated with multi-drug resistance in breast cancer, however, the mechanism by which Twist1 leads to resistance was not explored (Li et al., 2009). In a separate study, it was found that Twist can increase the transcription of ABC transporters, enabling efflux of drugs and an association with multidrug resistance (Saxena et al., 2011). Further, mathematical modeling of sequential therapy targeted toward either epithelial or mesenchymal tumor cells was shown to actually increase E/M plasticity leading to therapy resistance of breast cancer cells (Mathis et al., 2017). Modification of the therapeutic schedule to use alternating rather than sequential therapy was able to overcome this effect by killing both epithelial and mesenchymal cells and preventing phenotypic switching (Mathis et al., 2017). These data suggest that cells that have undergone an EMT or cells with enhanced plasticity may display heightened resistance to conventional cancer therapies, potentially through both active and passive mechanisms. As such, therapies that can target these plastic tumor cell populations may enhance therapeutic efficacy in patients who have failed one or more lines of conventional therapy.

MECHANISMS THAT PROMOTE CANCER CELL PLASTICITY

Cancer cell plasticity can be regulated by numerous signaling pathways, and likely is a characteristic driven by the aggregate functions of multiple signaling pathways simultaneously. Below, we discuss the role of some of the pathways that appear to play very critical roles in the induction of plasticity in breast cancer by regulating CSC and EMT phenotypes. In addition to the following pathways, other pathways are also heavily implicated in both CSC and EMT cancer biology, including TGF-ß signaling, which is known to be critical for these processes. This pathway, as well as other pathways that we could not address due to space limitations of this review, have been extensively reviewed elsewhere (Wendt et al., 2009; Xu et al., 2009; Singh et al., 2015; Bellomo et al., 2016; Li et al., 2017).

Mitogen-Activated Protein Kinase (MAPK) Pathway

The MAPK pathway is evolutionarily conserved and controls cell growth, proliferation, differentiation, migration, and apoptosis (Dhillon et al., 2007). Aberrant activation of MAPK is known to play a significant role in breast tumor onset and progression (Dhillon et al., 2007). This may in part be due to a role for MAPK signaling in the promotion of maintenance of CSC populations in tumors. Arteaga and colleagues found that loss of dual specificity phosphatase-4 (DUSP4), a negative regulator of the MAPK pathway, promoted cancer stem cell-like phenotypes in basal-like breast cancer (Balko et al., 2013). Similarly, activation of epidermal growth factor receptor (EGFR) leads to an expansion of $CD44^{+}/CD24^{-}$ populations in TNBC (which is heavily enriched in basal-like breast cancer) in a mitogen-activated protein kinase kinase/extracellular signal-regulated kinase (MEK/ERK) dependent manner (Wise and Zolkiewska, 2017). But MAPK regulation of CSCs is not limited to the TNBC and/or basal subtype. Indeed, our own group demonstrated that a developmental homeoprotein, SIX1, induces a CSC phenotype in luminal B breast cancer cells through induction of MAPK/ERK signaling (Iwanaga et al., 2012). MAPK signaling has also been implicated in the plasticity of cells in inflammatory breast cancer, where the MAPK interacting (Ser/Thr)-kinase (MNK) can activate NFκB signaling via increasing the expression of X-linked inhibitor of apoptosis, resulting in increased stem cell like characteristics as measured by ALDH expression (Evans et al., 2018).

In addition to its role in cancer cell stemness, MAPK signaling has also been shown to play a role in promoting EMT and EMP. For example, overexpression of RAS in human mammary epithelial cells, and resultant induction of MAPK signaling, results in an EMT and endows cells with stem and tumorigenic characteristics (Milsom et al., 2008). Further, constitutive activation of Raf-1 in MCF-7 cells lead to the development of distant metastases in xenograft models by promoting EMT (Leontovich et al., 2012). Numerous molecules promote EMT and EMP via activation of MAPK signaling. Examples include YB-1 (Evdokimova et al., 2009) as well as Doublecortin-like kinase 1 (DCLK1) (Liu et al., 2019), which can induce an EMT at least in part via activating MAPK signaling.

While these data suggest that cell autonomous control of MAPK signaling can promote cancer cell stemness and plasticity, MAPK signaling, and subsequent cancer cell plasticity, is also regulated by signaling molecules in the tumor microenvironment. Lijun Hao's group found that in breast cancer, stem cell factor (SCF) released by adipose-derived stem cells promoted an EMT phenotype (increased expression of N-cadherin, vimentin, and Twist and decreased expression of E-cadherin) and increased pulmonary metastasis in mouse models by downregulation of miR-20b. The authors determined that SCF-induced miR-20b downregulation was dependent on activation of the c-Kit/MAPK-p38/E2F1 signaling cascade (Xu et al., 2019). This finding suggests that EMT and cancer cell plasticity may not only be a cell autonomous characteristic but also may depend on the composition of the microenvironment surrounding a given cell.

Phosphoinositide 3-Kinase (PI3K)/ AKT/Mechanistic Target of Rapamycin (mTOR) Pathway

Aberrations in the PI3K/AKT/mTOR pathway are common genomic abnormalities in the majority of human cancers

including breast cancer (Cancer Genome Atlas, 2012). Recent studies demonstrate that the PI3K/AKT/mTOR pathway plays an important role in breast cancer cell plasticity. For example, Wandosell and colleagues demonstrated that knockdown of AKT1 (and to a lesser extent AKT2) in the human triple negative breast cancer cell line MDA-MB-231 reduces CSC-like phenotypes and EMT characteristics in breast cancer cells, suggesting a reliance on flux through the PI3K/AKT pathway for maintenance of EMP and cancer cell stemness (Gargini et al., 2015). Similarly, Watson and colleagues showed that the inflammatory cytokine, oncostatin-M, mediates breast cancer cell stem and EMT characteristics via activation of PI3K signaling (West et al., 2014). Isolation of BCSCs ($CD44^+/CD24^-/CD45^-$) from primary ERα-positive breast cancer followed by next generation sequencing- and microarray-based gene expression profiling clearly demonstrate that PIK3CA and other PI3K pathway genes are overexpressed in this population and the pathway is known to be involved in maintaining cancer stem cells in ER-positive breast cancer (Hardt et al., 2012). Intriguingly, while many pathways involved in plasticity are not mediated via genetic alterations, PI3K signaling alterations are often found to be due to mutations. Indeed, PIK3CA mutations are frequent in breast cancer, occurring in 28–47% of hormone receptor-positive breast cancers, 25% of HER2-positive breast cancers, and 8% of basal-like tumors (Stemke-Hale et al., 2008). The large percentage of hormone receptor positive tumors carrying PIK3CA mutations alludes to a particularly important role for this pathway in CSCs in this subtype of the disease.

Signal Transducer and Activator of Transcription 3 (STAT3) Pathway

STAT3, a downstream effector of several receptor tyrosine kinases (RTKs) commonly activated by growth factors and cytokines, is persistently activated in all breast cancer subtypes (Walker et al., 2014; Banerjee and Resat, 2016). Constitutive STAT3 activation in breast cancer cells induces EMT and CSC properties. Compared with other breast cancer subtypes, STAT3 is most often associated with triple negative tumors, which are rich in cancer stem cells (Banerjee and Resat, 2016). However, some studies report that STAT3 is downstream of HER2 and may be associated with CSCs in this subtype of breast cancer also (Hartman et al., 2011; Chung et al., 2014). Therefore, it appears that STAT3 signaling is an important mediator of EMT and stemness across many genetically-distinct breast cancers.

In studying the relationship between STAT3 and CSCs, Polyak and colleagues found that the IL-6/JAK2/Stat3 pathway is preferentially active in $CD44^+CD24^-$ stem-enriched breast cancer cells, where it is required for their growth (Marotta et al., 2011). Additionally, work by the Slingerland group demonstrated that a VEGF/VEGFR2/STAT3 axis promotes breast and lung CSC self-renewal via upregulation of Myc and Sox2 (Zhao et al., 2015). In addition to stemness, STAT3 also regulates EMT. A study demonstrated that in breast cancer cells, phosphorylated STAT3 up-regulates the EMT associated protein, TWIST (Lo et al., 2007). Further, several studies have demonstrated that STAT3 up-regulates MMP2, MMP7 and MMP9 in breast cancer cell lines (Song et al., 2008; Yuan et al., 2008; Wang et al., 2012), proteins that are heavily associated with EMT. Additionally, through regulation of EMT/stemness, STAT3 may also play a role in regulating drug resistance, as it was shown that in human breast cancer, feedback activation of the IL6-STAT3 loop induced EMT and cancer stem cell features, leading to resistance to PI3K inhibitors (Yang et al., 2014).

Wnt Pathway

Wnt signaling, which regulates cell polarity, proliferation, migration, survival, and maintenance of somatic stem cells, is very important in normal embryonic development (Clevers and Nusse, 2012) and its aberrant activation is involved in many malignant diseases, including breast cancer (Clevers and Nusse, 2012; Blagodatski et al., 2014). A growing body of evidence suggests that dysregulation of Wnt signaling promotes mammary tumor formation (Nusse and Varmus, 1982; Lane and Leder, 1997; Theodorou et al., 2007). In addition, Wnt signaling contributes to breast cancer progression at least in part due to increases in CSC and EMT phenotypes, suggesting that Wnt signaling is critical for cell plasticity. An example of this was shown by Varmus and colleagues, who found that expression of Wnt-1 in mammary glands of transgenic mice expands a population of basal-like cells which are enriched in stem like cells (Li et al., 2003). Similarly, Hong and colleagues showed that Wnt/β-catenin activity in BCSCs (ALDH1 positive) is significantly higher than in bulk cancer cells, and that blockade of Wnt/β-catenin signaling suppresses CSC-like phenotypes in a mouse model of breast cancer (Jang et al., 2015a). Interestingly, SOX9, which is an important pluripotency factor, was identified as a Wnt-target in intestinal crypts (Blache et al., 2004). In breast cancer, SOX9 enhanced T-cell factor 4 (TCF4) transcription and Wnt/β-catenin signaling (Wang et al., 2013). These studies highlight the possibility of a feedback loop between Wnt/β-catenin and SOX9 in promoting BCSCs. Finally, Wnt signaling may similarly promote EMT, as Weiss and colleagues demonstrated that the Wnt–Axin2–GSK3β cascade induces an EMT-like program via up-regulating Snail1 in breast cancer cells (Yook et al., 2006). Functionally these alterations in stemness and EMT may facilitate tumor progression, as data from Leyland-Jones's group demonstrated that breast cancer patients whose tumors had elevated Wnt/β-catenin signaling are more likely to develop lung and brain secondary metastases (Dey et al., 2013).

The Hedgehog (Hh) Pathway

The Hh pathway is involved in embryonic mammary gland induction, development of ductal architecture and the differentiation that occurs prior to lactation (Lewis and Veltmaat, 2004). Emerging evidence suggests that dysregulation of Hh signaling is implicated in breast cancer development (Hatsell and Frost, 2007; Bhateja et al., 2019), though there is controversy around whether the primary role is in the tumor cells themselves or in the tumor microenvironment (Sun et al., 2014; Sims-Mourtada et al., 2015; Yang et al., 2016; Koike et al., 2017; Neelakantan et al., 2017). Multiple studies have linked Hh signaling to promotion and maintenance of CSC phenotypes in breast cancer. Wang and colleagues found that in

human estrogen receptor positive breast cancer cells, estrogen promotes a CSC and EMT phenotype via activation of Gli1, a downstream effector of the Hh pathway (Sun et al., 2014). Similarly, Sims-Mourtada and colleagues found that Hh pathway activation mediates the activity of BCSCs and clonogenic re-growth of breast cancer cells after chemotherapy treatment (Sims-Mourtada et al., 2015). Consistent with this finding, recent studies showed that inhibition of the Hh pathway attenuates stem cell phenotypes such as $CD44^{+}/CD24^{-}$ cells and sphere forming capacity in breast cancer cell lines (Yang et al., 2016; Koike et al., 2017).

In addition to promoting stemness, Hh pathway activation can also promote EMT in breast cancer cells. For example, Tan and colleagues found that Twist1 and Snail (important EMT-associated transcription factors) are direct transcriptional targets of Gli1 (Kong et al., 2015). Similarly, Frost and colleagues found that Gli1 enhances breast cancer cell EMT and metastasis via up-regulation of MMP-11 (Kwon et al., 2011), suggesting that GLI proteins regulate numerous genes associated with EMT. Our lab recently demonstrated a key role for Hh/Gli pathway signaling in cellular plasticity in breast cancer cells as we showed that breast cancer cells that had undergone an oncogenic EMT could increase metastasis of neighboring cancer cells via both canonical and non-canonical paracrine-mediated activation of GLI activity (Neelakantan et al., 2017). These data suggest rapid alterations in plasticity and metastatic characteristics in response to signals that emanate from neighboring tumor cells, underscoring the critical nature of cell-cell crosstalk in inducing a plastic phenotype. Importantly, co-expression of GLI1 and two GLI1 targets, EGFR and Snail, are associated with worse outcome in breast cancer patients (Rudolph et al., 2018), further underscoring the clinical relevance of this pathway.

Notch Pathway

The Notch signaling pathway, which is heavily associated with stemness, self-renewal, and differentiation during development, is essential for the development of multiple organ systems including mammary gland (Bolos et al., 2007). Activation of Notch signaling has been extensively linked to malignant progression in multiple solid cancer types, including breast cancer (Bigas and Espinosa, 2018). The breast tumorigenic ability of Notch has been known since the 1990s. Notch genes (Notch1 and Notch4), when expressed under the control of whey acidic protein (WAP) or mouse mammary tumor virus (MMTV) promoters in the mouse, result in the formation of mammary carcinoma (Jhappan et al., 1992; Gallahan et al., 1996; Dievart et al., 1999). Attempting to understand potential mechanisms through which Notch signaling may facilitate tumorigenesis, Tagliabue and colleagues found that Notch1 signaling equipped breast cancer cells with tumor-initiating cell properties due to HER2 gene amplification, and these effects were reduced after blockage of Notch signaling using either γ-secretase inhibition or Notch1-specific silencing (Magnifico et al., 2009). Multiple Notch family members may be involved in maintaining tumor-initiating potential in breast cancer cells, as Clarke and colleagues demonstrated that Notch4 has a more significant impact than Notch1 in BCSCs, and that Notch4 inhibition produces a more robust effect with a complete inhibition of tumor initiation (Harrison et al., 2010). Intriguingly, the same group demonstrated that estrogen increases BCSC activity by activating Notch signaling and showed that BCSCs induced by NOTCH signaling contribute to anti-estrogen resistance in human breast cells (Harrison et al., 2013; Simoes et al., 2015). In an attempt to understand regulation of Notch signaling in breast cancer, a recent study by our laboratory demonstrated that in both estrogen receptor positive and triple negative breast cancer, the miR-106b-25 miRNA cluster upregulates NOTCH1 through stabilizing the protein via direct repression of the E3 ubiquitin ligase NEDD4L. Further, we found that this upregulation of NOTCH1 was required for tumor initiating cell induction in multiple breast cancer cell lines (Guarnieri et al., 2018).

In addition to affecting cancer stem cell biology, Notch signaling is involved in the induction of EMT, again underscoring its role in mediating breast cancer cell plasticity. Slug and Snail, which are two critical EMT-associated transcription factors, have been shown to be regulated by Notch signaling in breast cancer cells (Chen et al., 2010; Shao et al., 2015). In addition, Karsan and colleagues showed that Slug is a direct target gene of Notch1 in breast cancer (Leong et al., 2007). In line with these findings, Suh and colleagues demonstrated that Notch2 up-regulates multiple EMT-associated markers including Twist, Snail1, Slug, Vimentin, and Zeb1 in basal type breast cancer cells (Lee et al., 2018). Clinical studies performed in breast cancer patients demonstrate that Notch signaling activation is associated with reduced overall survival and poor prognosis (Reedijk et al., 2005; Dickson et al., 2007), underscoring the importance of this signaling pathway for tumor progression in human breast cancer.

THERAPEUTIC STRATEGIES FOR TARGETING BREAST CANCER CELL PLASTICITY

Because BCSCs and cells known to have undergone an EMT likely represent cancer cells with high degrees of plasticity, and because of the role of BCSCs and EMT in driving tumor initiation, invasion, metastasis, escape from the immune system, and resistance to chemo- and radiotherapy, it is often argued that targeting cancer stem cells and EMT may be the best way to therapeutically target phenotypically plastic cancer cells and improve patient survival. Over the last decade, numerous studies have focused on therapeutic strategies that target pathways involved in BCSC and/or EMT programs as a means to inhibit cancer cell plasticity and to reduce the overall ability of these cells to navigate the multiple environments encountered during the metastatic cascade (**Figure 2**).

Targeting of the MAPK Pathway

Numerous small molecule compounds have been developed that target the MAPK pathway and based on the role of MAPK signaling in promoting EMP and stemness, inhibition of this pathway presents a logical therapeutic target. In line

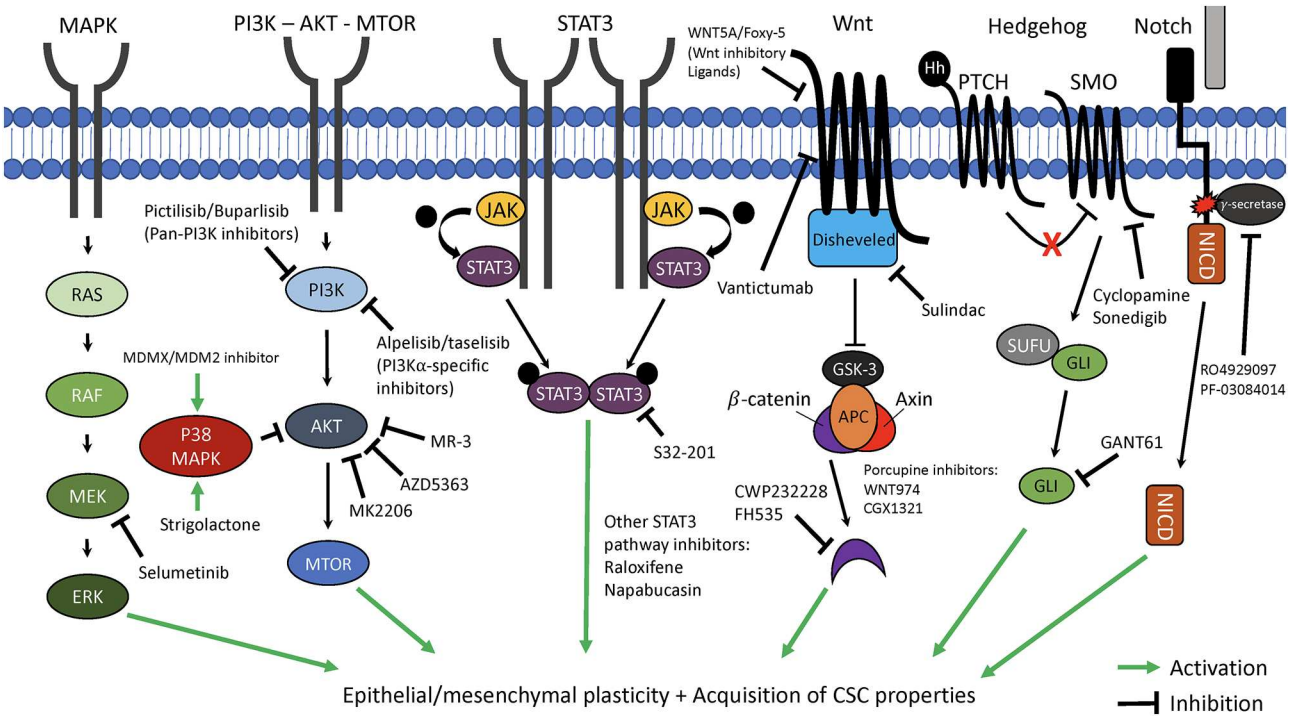

FIGURE 2 | Therapeutic targeting of key pathways involved in cancer cell plasticity. The critical cellular pathways, mitogen-activated protein kinase (MAPK), phosphoinositide 3-kinase—protein kinase B—mammalian target of rapamycin (PI3K—AKT—MTOR), signal transducer and activator of transcription 3 (STAT3), Wnt, Hedgehog, and Notch each have been demonstrated to play key roles in promotion of epithelial-mesenchymal plasticity (EMP) and acquisition of cancer stem cell (CSC) properties. Highlighted are novel targeted therapeutics which can interfere with these pathways and may be able to suppress EMP and CSC characteristics of cancer cells. MEK/ERK, mitogen-activated protein kinase kinase/extracellular signal-regulated kinase; JAK, Janus-activated kinasel APC, adenomatosis polyposis coli; GSK3, Glycogen synthase kinase 3; PTCH/SMO, Patched/smoothened; SUFU, Suppressor of fused; NICD, Notch intracellular domain.

with this thought, emerging evidence indicates that selumetinib, a MEK1/2 inhibitor which has been used for phase I and II clinic trials in several kinds of malignant diseases (Bodoky et al., 2012; Hayes et al., 2012; Catalanotti et al., 2013; Ho et al., 2013; Jänne et al., 2013; Janne et al., 2015, 2016; Carvajal et al., 2014, 2015; Gupta et al., 2014; Brown et al., 2019), might be a novel therapeutic strategy for breast cancer. For example, Zolkiewska and colleagues found that selumetinib blocked EGF-induced expansion of CD44+/CD24– breast cancer stem cell associated populations (Wise and Zolkiewska, 2017). Similarly, the Ueno laboratory found that selumetinib inhibits the acquisition of breast cancer stem cell phenotypes and protects mice from lung metastasis after transplantation with TNBC cells (Bartholomeusz et al., 2015).

Paradoxically, other therapeutic approaches suggest that activation of the P38 MAPK pathway may have therapeutic benefit in breast cancer. Yarden and colleagues showed that Strigolactone was able to inhibit the growth of BCSCs via activation of P38 (Pollock et al., 2012). While this seemingly contradicts the role of MAPK signaling in CSC promotion, activation of P38 in this context actually suppressed AKT survival signaling, and the authors suggest that it is the suppression of PI3K/AKT signaling through P38 activation that is responsible for the observed inhibition of BCSC growth and thus provides a therapeutic benefit in this context (Pollock et al., 2012). Similarly, the Dong laboratory found that a dual-target murine double minute 2 (MDM2) and murine double minute X (MDMX) inhibitor suppresses EMT, migration, and invasion of TNBC cells through activation of the p38 MAPK pathway (Fan et al., 2019). Thus, while the MAPK pathway remains an attractive target for inhibiting cancer cell plasticity, the complex downstream signaling and cross-activation of other key signaling pathways by MAPK components suggests that targeting this pathway must be done thoughtfully in order to maximize therapeutic benefit.

PI3K/AKT/mTOR Pathway

There are a number of different classes and isoforms of PI3Ks, and PI3Kα is the isoform predominantly mutated in cancer (Guerrero-Zotano et al., 2016). Currently, numerous compounds have been developed to inhibit PI3K signaling in breast cancer. Pictilisib and Buparlisib, which are orally available pan-PI3K inhibitors, have been studied in phase II or III clinic trials. Schmid and colleagues found that compared with use of the aromatase inhibitor anastrozole as a monotherapy, the combination of pictilisib and anastrozole significantly increases inhibition of tumor cell proliferation in luminal B primary breast cancer (Schmid et al., 2016). However, in the same year, another study found that in estrogen receptor-positive patients, the combination of pictisilib and fulvestrant did not increase

progression free survival (PFS) compared to fulvestrant and placebo (Krop et al., 2016). In addition, dosing was limited by significant toxicities. Patients in the pictisilib + fulvestrant group showed a much higher rate of serious side effects than those in the fulvestrant + placebo group—these included pneumonitis, diarrhea, stomatitis, rash, and transaminitis, which led to dose reduction in 45% of cases and treatment discontinuation in 24% of patients (Krop et al., 2016). Compared with pictisilib, buparlisib is reported to have a better therapeutic effect with less associated toxicities (Mayer et al., 2014; Guerrero-Zotano et al., 2016). Baselga and colleagues found that Buparlisib plus fulvestrant significantly improved progression free survival (PFS) by 1.9 months (6.9 vs. 5.0 months, $p < 0.001$) in patients with hormone receptor-positive, human epidermal growth factor receptor 2-negative advanced breast cancer (Baselga et al., 2017).

Alpelisib and taselisib are two PI3Kα specific inhibitors which are ideal drug candidates for patients with PIK3CA mutations. Studies demonstrate that these two drugs, either used as single agent or combined with endocrine therapy, showed preferential therapeutic effects against breast tumors harboring PIK3CA mutations, and as such, these drugs represent a means for personalized, tumor specific therapy (de Jonge et al., 2014; Mayer et al., 2017; Tamura et al., 2018; Baird et al., 2019; Saura et al., 2019). In addition to targeting PI3K itself, other therapeutic approaches have attempted to target the downstream target of PI3K, AKT. MK-2206, and AZD5363, two inhibitors of AKT, exhibited promising activity against breast cancer cells in preclinical studies (Crafter et al., 2015; Ribas et al., 2015; Choi et al., 2016; Baek et al., 2018; Chen et al., 2018). However, these drugs showed limited clinical efficacy in clinical trials (Kalinsky et al., 2018; Turner et al., 2019; Xing et al., 2019). A distinct attempt to target AKT activity was made by Chen and colleagues, who recently discovered that a natural methoxylated analog of resveratrol, 3,5,4′-trimethoxystilbene (MR-3), can block EMT and the invasion of breast cancer cells via restoring GSK3β activity and inhibiting the phosphorylation of AKT (Tsai et al., 2013). However, the effects of this compound have not yet been tested clinically. While PI3K and AKT remain promising drug targets for selective inhibition/elimination of phenotypically plastic cancer cells, high toxicity and mixed efficacy for many candidate therapeutics in clinical trials indicates a need for further research to better characterize the druggability of this key signaling pathway.

STAT3 Pathway

In breast cancer, most STAT3 pathway inhibitors are still in the preclinical phase of development, but represent a promising category of therapeutics due to the role of STAT3 in promoting cancer cell plasticity. Sun and colleagues found that pharmacological inhibition of STAT3 with S32-201 reduced breast cancer cell EMT and stem-like properties. In addition, disruption of the IL6-STAT3 signaling pathway can overcome resistance to PI3K inhibitors, suggesting that combined blockade of STAT3 and PI3K signaling might be a more efficient therapeutic strategy for breast cancer (Yang et al., 2014). Lin and colleagues found that Raloxifene, a selective estrogen receptor modulator which was approved for reducing the risk of invasive breast cancer, attenuates STAT3 phosphorylation and transcriptional activity via inhibiting IL-6/GP130 interaction in various cancer (including breast cancer) cell lines (Shi et al., 2017), suggesting that this inhibitor may work by influencing numerous critical pathways in hormone positive breast cancer cells. Strikingly, a phase Ib/II study showed that napabucasin, a first-in-class cancer stemness inhibitor that targets the STAT3 pathway, when given with weekly paclitaxel treatments, has shown promising effects in metastatic TNBC patients who have progressed on taxane-based treatment regimens (Becerra et al., 2016). Therefore, while we are just beginning to understand effective means of targeting STAT3, this may present a novel means for inhibiting cancer cell plasticity and associated tumor progression.

Wnt Pathway

Wnt pathway inhibitors have been an area of active investigation for many years, but have often proven difficult to use due to associated toxicities (particularly affecting the GI tract). Currently, Vantictumab, a first-in-class antibody that inhibits canonical Wnt signaling by blocking five Frizzled receptors (1, 2, 5, 7, 8) (Ram Makena et al., 2019) is being used in combination with paclitaxel in phase 1b clinical studies in patients with metastatic HER2-negative breast cancer (Mita et al., 2016). WNT5A is a WNT inhibitory ligand, and Foxy-5, a WNT5A mimicking peptide, has been shown to reduce metastatic spread of WNT5A-low breast cancer cells in mouse models (Safholm et al., 2008; Canesin et al., 2017). Currently, a phase 1 clinic study is ongoing to evaluate the safety, tolerability, and pharmacokinetic profiles of Foxy-5 in patients with metastatic breast, colorectal, or prostate cancer (Soerensen et al., 2014). Numerous groups continue to investigate novel Wnt inhibitors that may have a more tolerable side effect profile than earlier ones tested. For example, CWP232228, the Wnt/beta-catenin inhibitor which blocks β-catenin binding to TCF in the nucleus, inhibits proliferation and activity of BCSCs (Jang et al., 2015b) and treatment with CWP232228 after tail vein injection of 4T1 mammary carcinoma cells decreased metastatic burden and increased overall survival in pre-clinical studies (Jang et al., 2015b). Similarly, Hong and colleagues found that FH535, another β-catenin/TCF inhibitor, significantly suppressed tumor sphere formation and the $CD44^{+}/CD24^{-}$ BCSC subpopulation in mouse breast cancer cells (Jang et al., 2015a).

One class of drugs that has recently received a lot of attention are Porcupine inhibitors. Porcupine is an acyltransferase which is involved in enabling secretion of all Wnt ligands, and thus represents an ideal drug candidate for targeting the Wnt pathway (Solzak et al., 2017). WNT974, a novel small molecule Porcupine inhibitor, was shown to reduce lung metastatic burden and increase survival when combined with the pan-PI3K inhibitor buparlisib in triple negative breast cancer PDX models (Solzak et al., 2017). WNT974 and CGX1321, another small molecule Porcupine inhibitor, are

both currently in early stage clinical trials in advanced solid tumors[1, 2]. Other known drugs may also exhibit inhibitory effects on the Wnt pathway such as Sulindac, a non-steroidal anti-inflammatory drug (NSAID), which was shown be able to inhibit Wnt signaling by binding the PDZ domain of disheveled (DVL1) (Lee et al., 2009). Importantly, Yang and colleagues found that Sulindac inhibits cell proliferation via downregulation of Wnt signaling in breast, lung and colon cancer cells (Han et al., 2008). As more data is amassed and as more clinical trials aimed at targeting the Wnt pathway complete, we will gain a better understanding of the therapeutic efficacy of inhibition of the Wnt pathway in preventing tumor progression.

Hh Pathway

Compared with other signaling pathways, the strategies targeting the Hh pathway are more diverse. The Hh pathway can be inhibited via blocking Hh ligands, receptors (such as SMO), or downstream transcription factors (GLI) (Bhateja et al., 2019). A monoclonal antibody against Hh ligands (5E1) was shown to inhibit breast cancer growth and metastasis in mouse models (O'Toole et al., 2011). Cyclopamine, a naturally occurring chemical with a high affinity for SMO, can be used to block Hh pathway signaling and can reduce breast cancer cell viability (Mukherjee et al., 2006). However, the low potency and poor solubility of cyclopamine has limited its clinical use. Another SMO inhibitor, sonidegib, which is FDA-approved for the treatment of advanced and metastatic basal cell carcinoma, was evaluated in phase I and II clinical trials for patients with breast cancer (Stathis et al., 2017; Ruiz-Borrego et al., 2019). Unfortunately, it has been less efficacious in breast cancer, despite evidence for activated Hh signaling (Stathis et al., 2017). Our previous studies showed that GLI signaling is activated downstream of EMT transcription factors in both SMO-dependent and SMO-independent manners (Neelakantan et al., 2017), providing a potential explanation for why SMO inhibitors are not efficacious in breast cancers with evidence of activated Hh signaling. Instead, we found that GANT61, a GLI antagonist which interferes with GLI translocation to the nucleus, is more efficacious in PDX models of breast cancer than SMO inhibitors (Neelakantan et al., 2017). Consistent with our results, Bei and colleagues found that GANT61 inhibited Hh pathway activity and breast cancer cell survival more effectively than GDC-0449 (a SMO inhibitor) (Benvenuto et al., 2016). Furthermore, in a mouse breast cancer model (TUBO cells), GANT61 caused complete tumor regression in 80% of mice, and these mice remained tumor free for up to 30 weeks (Benvenuto et al., 2016).

Notch Pathway

γ-Secretase is a membrane-embedded aspartyl protease that cleaves the Notch receptor and results in the release and translocation of its intracellular domain into the nucleus and subsequent activation of target genes (Lu et al., 2014). Due to its important role in Notch pathway activation, to date, many different γ-secretase inhibitors have been evaluated and they exhibit promising results (Kontomanolis et al., 2018). Strikingly, several γ-secretase inhibitors were used in breast cancer clinic trails. For example, RO4929097 was recently used in a phase I study in patients with refractory metastatic or locally advanced solid tumors, including breast cancer and showed excellent tolerance (Tolcher et al., 2012). Subsequently another phase I study in patients with advanced solid tumors, including breast cancer, showed that RO4929097 and gemcitabine can be safely combined and 22.22% of patients achieving a partial response or stable disease more than 3 months after the combined treatment (Richter et al., 2013). A phase I clinical trial of another γ-secretase inhibitor (PF-03084014) in combination with docetaxel in patients with metastatic TNBC is ongoing. At present, the combination treatment is generally well-tolerated, and 16% of patients treated achieved a partial response (Curigliano et al., 2015; Locatelli et al., 2017). These studies suggest that use of γ-secretase inhibitors may be an effective and well-tolerated way to inhibit the Notch signaling pathway and to subsequently treat metastatic or locally advanced cancers.

CONCLUSION

In summary, due to the adaptability afforded by cellular plasticity, plastic breast cancer cells gain a fitness advantage during tumor progression, enabling them to adjust to an unfavorable microenvironment, evade immune attack, and spread from the primary tumor to a metastatic site. Further, such plasticity can enable escape from toxic effects of anticancer drugs. As a result, plasticity programs lead to the poor prognosis observed in patients with breast and other cancers. Targeting plasticity represents a promising therapeutic strategy to repress breast cancer metastasis and overcome therapy resistance and promote tumor regression.

AUTHOR CONTRIBUTIONS

DK: design and co-wrote draft manuscript. CH: design, co-wrote manuscript, editing, and drawing figures. HF: design, editing, and approval of final version.

FUNDING

HF was funded by the National Cancer Institute, R01CA224867 (MPI grant with Michael T. Lewis), to support her work on breast tumor cell plasticity and heterogeneity and by R01CA221282 to support her work related to the crosstalk between breast tumor cells and the immune microenvironment. CH was funded by the National Institute of Health Predoctoral Training Grant in Pharmacology, T32GM007635-41.

[1] *CGX1321 in Subjects With Advanced Solid Tumors and CGX1321 With Pembrolizumab in Subjects With Advanced GI Tumors (Keynote 596).* (2016) Available online at: https://clinicaltrials.gov/ct2/show/NCT02675946 (accessed January 25, 2020).

[2] *A Phase II Trial Evaluating WNT974 in Patients With Metastatic Head and Neck Squamous Cell Carcinoma.* (2016) Available online at: https://clinicaltrials.gov/ct2/show/study/NCT02649530 (accessed January 25, 2020).

REFERENCES

Aceto, N., Bardia, A., Miyamoto, D. T., Donaldson, M. C., Wittner, B. S., Spencer, J. A., et al. (2014). Circulating tumor cell clusters are oligoclonal precursors of breast cancer metastasis. *Cell* 158, 1110–1122. doi: 10.1016/j.cell.2014.07.013

Acloque, H., Adams, M. S., Fishwick, K., Bronner-Fraser, M., and Nieto, M. A. (2009). Epithelial-mesenchymal transitions: the importance of changing cell state in development and disease. *J. Clin. Invest*. 119, 1438–1449. doi: 10.1172/JCI38019

Akalay, I., Janji, B., Hasmim, M., Noman, M. Z., Andre, F., De Cremoux, P., et al. (2013). Epithelial-to-mesenchymal transition and autophagy induction in breast carcinoma promote escape from T-cell-mediated lysis. *Cancer Res*. 73, 2418–2427. doi: 10.1158/0008-5472.CAN-12-2432

Aktas, B., Tewes, M., Fehm, T., Hauch, S., Kimmig, R., and Kasimir-Bauer, S. (2009). Stem cell and epithelial-mesenchymal transition markers are frequently overexpressed in circulating tumor cells of metastatic breast cancer patients. *Breast Cancer Res*. 11:R46. doi: 10.1186/bcr2333

Al-Ansari, M. M., Hendrayani, S. F., Shehata, A. I., and Aboussekhra, A. (2013). p16(INK4A) represses the paracrine tumor-promoting effects of breast stromal fibroblasts. *Oncogene* 32, 2356–2364. doi: 10.1038/onc.2012.270

Al-Hajj, M., and Clarke, M. F. (2004). Self-renewal and solid tumor stem cells. *Oncogene* 23, 7274–7282. doi: 10.1038/sj.onc.1207947

Al-Hajj, M., Wicha, M. S., Benito-Hernandez, A., Morrison, S. J., and Clarke, M. F. (2003). Prospective identification of tumorigenic breast cancer cells. *Proc. Natl. Acad. Sci. U S A*. 100, 3983–3988. doi: 10.1073/pnas.0530291100

Allan, A. L., Vantyghem, S. A., Tuck, A. B., and Chambers, A. F. (2006). Tumor dormancy and cancer stem cells: implications for the biology and treatment of breast cancer metastasis. *Breast Dis*. 26, 87–98. doi: 10.3233/BD-2007-26108

Allard, B., Pommey, S., Smyth, M. J., and Stagg, J. (2013). Targeting CD73 enhances the antitumor activity of anti-PD-1 and anti-CTLA-4 mAbs. *Clin. Cancer Res*. 19, 5626–5635. doi: 10.1158/1078-0432.CCR-13-0545

Avgustinova, A., and Benitah, S. A. (2016). The epigenetics of tumour initiation: cancer stem cells and their chromatin. *Curr. Opin. Genet. Dev*. 36, 8–15. doi: 10.1016/j.gde.2016.01.003

Baccelli, I., Schneeweiss, A., Riethdorf, S., Stenzinger, A., Schillert, A., Vogel, V., et al. (2013). Identification of a population of blood circulating tumor cells from breast cancer patients that initiates metastasis in a xenograft assay. *Nat. Biotechnol*. 31, 539–544. doi: 10.1038/nbt.2576

Baek, H. J., Kim, S. E., Kim, J. K., Shin, D. H., Kim, T. H., Kim, K. G., et al. (2018). Inhibition of AKT suppresses the initiation and progression of BRCA1-associated mammary tumors. *Int. J. Biol. Sci*. 14, 1769–1781. doi: 10.7150/ijbs.29242

Baird, R. D., Schrier, M., van Rossum, A. G. J., Oliveira, M., Beelen, K., Gao, M., et al. (2019). POSEIDON trial phase 1b results: safety, efficacy and circulating tumor DNA response of the beta isoform-sparing PI3K inhibitor taselisib (GDC-0032) combined with tamoxifen in hormone receptor positive metastatic breast cancer patients. *Clin. Cancer Res*. 25, 6598–6605. doi: 10.1158/1078-0432.CCR-19-0508

Balko, J. M., Schwarz, L. J., Bhola, N. E., Kurupi, R., Owens, P., Miller, T. W., et al. (2013). Activation of MAPK pathways due to DUSP4 loss promotes cancer stem cell-like phenotypes in basal-like breast cancer. *Cancer Res*. 73, 6346–6358. doi: 10.1158/0008-5472.CAN-13-1385

Banerjee, K., and Resat, H. (2016). Constitutive activation of STAT3 in breast cancer cells: a review. *Int. J. Cancer* 138, 2570–2578. doi: 10.1002/ijc.29923

Bao, L., Cardiff, R. D., Steinbach, P., Messer, K. S., and Ellies, L. G. (2015). Multipotent luminal mammary cancer stem cells model tumor heterogeneity. *Breast Cancer Res*. 17:137. doi: 10.1186/s13058-015-0615-y

Bartholomeusz, C., Xie, X., Pitner, M. K., Kondo, K., Dadbin, A., Lee, J., et al. (2015). MEK inhibitor selumetinib (AZD6244; ARRY-142886) prevents lung metastasis in a triple-negative breast cancer xenograft model. *Mol. Cancer Ther*. 14, 2773–2781. doi: 10.1158/1535-7163.MCT-15-0243

Baselga, J., Im, S. A., Iwata, H., Cortés, J., De Laurentiis, M., Jiang, Z., et al. (2017). Buparlisib plus fulvestrant versus placebo plus fulvestrant in postmenopausal, hormone receptor-positive, HER2-negative, advanced breast cancer (BELLE-2): a randomised, double-blind, placebo-controlled, phase 3 trial. *Lancet Oncol*. 18, 904–916. doi: 10.1016/S1470-2045(17)30376-5

Becerra, C., Braiteh, F. S., Spira, A. I., Langleben, A., Panasci, L. C., Vukelja, S. J., et al. (2016). A Ib/II study of cancer stemness inhibitor napabucasin (BB608) combined with weekly paclitaxel in advanced triple negative breast cancer. *J. Clin. Oncol*. 34, 1094–1094. doi: 10.1200/JCO.2016.34.15_suppl.1094

Bellomo, C., Caja, L., and Moustakas, A. (2016). Transforming growth factor β as regulator of cancer stemness and metastasis. *Br. J. Cancer* 115, 761–769. doi: 10.1038/bjc.2016.255

Benvenuto, M., Masuelli, L., De Smaele, E., Fantini, M., Mattera, R., Cucchi, D., et al. (2016). *In vitro* and *in vivo* inhibition of breast cancer cell growth by targeting the hedgehog/GLI pathway with SMO (GDC-0449) or GLI (GANT-61) inhibitors. *Oncotarget* 7, 9250–9270. doi: 10.18632/oncotarget.7062

Bhateja, P., Cherian, M., Majumder, S., and Ramaswamy, B. (2019). The hedgehog signaling pathway: a viable target in breast cancer? *Cancers* 11:E1126. doi: 10.3390/cancers11081126

Bigas, A., and Espinosa, L. (2018). The multiple usages of Notch signaling in development, cell differentiation and cancer. *Curr. Opin. Cell Biol*. 55, 1–7. doi: 10.1016/j.ceb.2018.06.010

Blache, P., M., van de Wetering, M., Duluc, I., Domon, C., Berta, P., Freund, J. N., et al. (2004). SOX9 is an intestine crypt transcription factor, is regulated by the Wnt pathway, and represses the CDX2 and MUC2 genes. *J. Cell Biol*. 166, 37–47. doi: 10.1083/jcb.200311021

Blagodatski, A., Poteryaev, D., and Katanaev, V. L. (2014). Targeting the Wnt pathways for therapies. *Mol Cell Ther*. 2:28. doi: 10.1186/2052-8426-2-28

Bocci, F., Gearhart-Serna, L., Boareto, M., Ribeiro, M., Ben-Jacob, E., Devi, G. R., et al. (2019). Toward understanding cancer stem cell heterogeneity in the tumor microenvironment. *Proc. Natl. Acad. Sci. U S A*. 116, 148–157. doi: 10.1073/pnas.1815345116

Bodoky, G., Timcheva, C., Spigel, D. R., La Stella, P. J., Ciuleanu, T. E., Pover, G., et al. (2012). A phase II open-label randomized study to assess the efficacy and safety of selumetinib (AZD6244 [ARRY-142886]) versus capecitabine in patients with advanced or metastatic pancreatic cancer who have failed first-line gemcitabine therapy. *Invest. New Drugs* 30, 1216–1223. doi: 10.1007/s10637-011-9687-4

Bolos, V., Grego-Bessa, J., and de la Pompa, J. L. (2007). Notch signaling in development and cancer. *Endocr. Rev*. 28, 339–363. doi: 10.1210/er.2006-0046

Bonnomet, A., Syne, L., Brysse, A., Feyereisen, E., Thompson, E. W., Noel, A., et al. (2012). A dynamic *in vivo* model of epithelial-to-mesenchymal transitions in circulating tumor cells and metastases of breast cancer. *Oncogene* 31, 3741–3753. doi: 10.1038/onc.2011.540

Bourcy, M., Suarez-Carmona, M., Lambert, J., Francart, M. E., Schroeder, H., Delierneux, C., et al. (2016). Tissue factor induced by epithelial-mesenchymal transition triggers a procoagulant state that drives metastasis of circulating tumor cells. *Cancer Res*. 76, 4270–4282. doi: 10.1158/0008-5472.CAN-15-2263

Bray, F., Ferlay, J., Soerjomataram, I., Siegel, R. L., Torre, L. A., and Jemal, A. (2018). Global cancer statistics 2018: GLOBOCAN estimates of incidence and mortality worldwide for 36 cancers in 185 countries. *CA Cancer J. Clin*. 68, 394–424. doi: 10.3322/caac.21492

Brown, D. M., and Ruoslahti, E. (2004). Metadherin, a cell surface protein in breast tumors that mediates lung metastasis. *Cancer Cell* 5, 365–374. doi: 10.1016/S1535-6108(04)00079-0

Brown, S. R., Hall, A., Buckley, H. L., Flanagan, L., D., Gonzalez de Castro, Farnell, K., et al. (2019). Investigating the potential clinical benefit of Selumetinib in resensitising advanced iodine refractory differentiated thyroid cancer to radioiodine therapy (SEL-I-METRY): protocol for a multicentre UK single arm phase II trial. *BMC Cancer* 19:582. doi: 10.1186/s12885-019-5541-4

Butti, R., Gunasekaran, V. P., Kumar, T. V. S., Banerjee, P., and Kundu, G. C. (2019). Breast cancer stem cells: biology and therapeutic implications. *Int. J. Biochem. Cell Biol*. 107, 38–52. doi: 10.1016/j.biocel.2018.12.001

Cancer Genome Atlas, N. (2012). Comprehensive molecular portraits of human breast tumours. *Nature* 490, 61–70. doi: 10.1038/nature11412

Canesin, G., Cuevas, E. P., Santos, V., Lopez-Menendez, C., Moreno-Bueno, G., Huang, Y., et al. (2015). Lysyl oxidase-like 2 (LOXL2) and E47 EMT factor: novel partners in E-cadherin repression and early metastasis colonization. *Oncogene* 34, 951–964. doi: 10.1038/onc.2014.23

Canesin, G., Evans-Axelsson, S., Hellsten, R., Krzyzanowska, A., Prasad, C. P., Bjartell, A., et al. (2017). Treatment with the WNT5A-mimicking peptide Foxy-5 effectively reduces the metastatic spread of WNT5A-low prostate cancer cells in an orthotopic mouse model. *PLoS ONE* 12:e0184418. doi: 10.1371/journal.pone.0184418

Carvajal, R. D., Schwartz, G. K., Mann, H., Smith, I., and Nathan, P. D. (2015). Study design and rationale for a randomised, placebo-controlled, double-blind study to assess the efficacy of selumetinib (AZD6244; ARRY-142886) in combination with dacarbazine in patients with metastatic uveal melanoma (SUMIT). *BMC Cancer* 15:467. doi: 10.1186/s12885-015-1470-z

Carvajal, R. D., Sosman, J. A., Quevedo, J. F., Milhem, M. M., Joshua, A. M., Kudchadkar, R. R., et al. (2014). Effect of selumetinib vs chemotherapy on progression-free survival in uveal melanoma: a randomized clinical trial. *JAMA* 311, 2397–2405. doi: 10.1001/jama.2014.6096

Catalanotti, F., Solit, D. B., Pulitzer, M. P., Berger, M. F., Scott, S. N., Iyriboz, T., et al. (2013). Phase II trial of MEK inhibitor selumetinib (AZD6244, ARRY-142886) in patients with BRAFV600E/K-mutated melanoma. *Clin. Cancer Res.* 19, 2257–2264. doi: 10.1158/1078-0432.CCR-12-3476

Chaffer, C. L., Marjanovic, N. D., Lee, T., Bell, G., Kleer, C. G., Reinhardt, F., et al. (2013). Poised chromatin at the ZEB1 promoter enables breast cancer cell plasticity and enhances tumorigenicity. *Cell* 154, 61–74. doi: 10.1016/j.cell.2013.06.005

Chakraborty, C., Chin, K. Y., and Das, S. (2016). miRNA-regulated cancer stem cells: understanding the property and the role of miRNA in carcinogenesis. *Tumour Biol.* 37, 13039–13048. doi: 10.1007/s13277-016-5156-1

Chao, Y. L., Shepard, C. R., and Wells, A. (2010). Breast carcinoma cells re-express E-cadherin during mesenchymal to epithelial reverting transition. *Mol. Cancer* 9:179. doi: 10.1186/1476-4598-9-179

Charpentier, M., and Martin, S. (2013). Interplay of stem cell characteristics, EMT, and microtentacles in circulating breast tumor cells. *Cancers* 5, 1545–1565. doi: 10.3390/cancers5041545

Chen, J., Imanaka, N., Chen, J., and Griffin, J. D. (2010). Hypoxia potentiates Notch signaling in breast cancer leading to decreased E-cadherin expression and increased cell migration and invasion. *Br. J. Cancer* 102, 351–360. doi: 10.1038/sj.bjc.6605486

Chen, X., Cui, D., Bi, Y., Shu, J., Xiong, X., and Zhao, Y. (2018). AKT inhibitor MK-2206 sensitizes breast cancer cells to MLN4924, a first-in-class NEDD8-activating enzyme (NAE) inhibitor. *Cell Cycle* 17, 2069–2079. doi: 10.1080/15384101.2018.1515550

Cheung, K. J., Padmanaban, V., Silvestri, V., Schipper, K., Cohen, J. D., Fairchild, A. N., et al. (2016). Polyclonal breast cancer metastases arise from collective dissemination of keratin 14-expressing tumor cell clusters. *Proc. Natl. Acad. Sci. U S A.* 113, E854–E863. doi: 10.1073/pnas.1508541113

Choi, A. R., Kim, J. H., Woo, Y. H., Cheon, J. H., Kim, H. S., and Yoon, S. (2016). Co-treatment of LY294002 or MK-2206 with AZD5363 attenuates AZD5363-induced increase in the level of phosphorylated AKT. *Anticancer Res.* 36, 5849–5858. doi: 10.21873/anticanres.11170

Chu, P. Y., Hou, M. F., Lai, J. C., Chen, L. F., and Lin, C. S. (2019). Cell reprogramming in tumorigenesis and its therapeutic implications for breast cancer. *Int. J. Mol. Sci.* 20:E1827. doi: 10.3390/ijms20081827

Chui, M. H. (2013). Insights into cancer metastasis from a clinicopathologic perspective: epithelial-mesenchymal transition is not a necessary step. *Int. J. Cancer* 132, 1487–1495. doi: 10.1002/ijc.27745

Chung, S. S., Giehl, N., Wu, Y., and Vadgama, J. V. (2014). STAT3 activation in HER2-overexpressing breast cancer promotes epithelial-mesenchymal transition and cancer stem cell traits. *Int. J. Oncol.* 44, 403–411. doi: 10.3892/ijo.2013.2195

Cieply, B., Koontz, C., and Frisch, S. M. (2015). CD44S-hyaluronan interactions protect cells resulting from EMT against anoikis. *Matrix Biol.* 48, 55–65. doi: 10.1016/j.matbio.2015.04.010

Clevers, H., and Nusse, R. (2012). Wnt/β-catenin signaling and disease. *Cell* 149, 1192–1205. doi: 10.1016/j.cell.2012.05.012

Cole, M., and Bromberg, M. (2013). Tissue factor as a novel target for treatment of breast cancer. *Oncologist* 18, 14–18. doi: 10.1634/theoncologist.2012-0322

Crafter, C., Vincent, J. P., Tang, E., Dudley, P., James, N. H., Klinowska, T., et al. (2015). Combining AZD8931, a novel EGFR/HER2/HER3 signalling inhibitor, with AZD5363 limits AKT inhibitor induced feedback and enhances antitumour efficacy in HER2-amplified breast cancer models. *Int. J. Oncol.* 47, 446–454. doi: 10.3892/ijo.2015.3062

Creighton, C. J., Li, X., Landis, M., Dixon, J. M., Neumeister, V. M., Sjolund, A., et al. (2009). Residual breast cancers after conventional therapy display mesenchymal as well as tumor-initiating features. *Proc. Natl. Acad. Sci. U S A.* 106, 13820–13825. doi: 10.1073/pnas.0905718106

Croker, A. K., and Allan, A. L. (2012). Inhibition of aldehyde dehydrogenase (ALDH) activity reduces chemotherapy and radiation resistance of stem-like ALDHhiCD44(+) human breast cancer cells. *Breast Cancer Res. Treat.* 133, 75–87. doi: 10.1007/s10549-011-1692-y

Curigliano, G., Aftimos, P. G., Dees, E. C., LoRusso, P., Pegram, M. D., Awada, A., et al. (2015). Phase I dose-finding study of the gamma secretase inhibitor PF-03084014 (PF-4014) in combination with docetaxel in patients (pts) with advanced triple-negative breast cancer (TNBC). *J. Clin. Oncol.* 33:1068. doi: 10.1200/jco.2015.33.15_suppl.1068

da Silva-Diz, V., Lorenzo-Sanz, L., Bernat-Peguera, A., Lopez-Cerda, M., and Muñoz, P. (2018). Cancer cell plasticity: impact on tumor progression and therapy response. *Semin. Cancer Biol.* 53, 48–58. doi: 10.1016/j.semcancer.2018.08.009

de Jonge, M. J. A., van Herpen, C., Gietema, J. A., Shepherd, S., Koornstra, R., Jager, A., et al. (2014). 452pa study of Abt-767 in advanced solid tumors with Brca 1 and Brca 2 mutations and high grade serous ovarian, fallopian tube, or primary peritoneal cancer. *Ann. Oncol.* 25:iv150. doi: 10.1093/annonc/mdu331.12

Degen, J. L., and Palumbo, J. S. (2012). Hemostatic factors, innate immunity and malignancy. *Thromb Res.* 129(Suppl 1), S1–S5. doi: 10.1016/S0049-3848(12)70143-3

Delgado-Bellido, D., Serrano-Saenz, S., Fernandez-Cortes, M., and Oliver, F. J. (2017). Vasculogenic mimicry signaling revisited: focus on non-vascular VE-cadherin. *Mol. Cancer* 16:65. doi: 10.1186/s12943-017-0631-x

Derksen, P. W., Liu, X., Saridin, F., H., van der Gulden, Zevenhoven, J., Evers, B., et al. (2006). Somatic inactivation of E-cadherin and p53 in mice leads to metastatic lobular mammary carcinoma through induction of anoikis resistance and angiogenesis. *Cancer Cell* 10, 437–449. doi: 10.1016/j.ccr.2006.09.013

Dey, N., Barwick, B. G., Moreno, C. S., Ordanic-Kodani, M., Chen, Z., Oprea-Ilies, G., et al. (2013). Wnt signaling in triple negative breast cancer is associated with metastasis. *BMC Cancer* 13:537. doi: 10.1186/1471-2407-13-537

Dhillon, A. S., Hagan, S., Rath, O., and Kolch, W. (2007). MAP kinase signalling pathways in cancer. *Oncogene* 26, 3279–3290. doi: 10.1038/sj.onc.1210421

Dickson, B. C., Mulligan, A. M., Zhang, H., Lockwood, G., O'Malley, F. P., Egan, S. E., et al. (2007). High-level JAG1 mRNA and protein predict poor outcome in breast cancer. *Mod. Pathol.* 20, 685–693. doi: 10.1038/modpathol.3800785

Diehn, M., Cho, R. W., Lobo, N. A., Kalisky, T., Dorie, M. J., Kulp, A. N., et al. (2009). Association of reactive oxygen species levels and radioresistance in cancer stem cells. *Nature* 458, 780–783. doi: 10.1038/nature07733

Dievart, A., Beaulieu, N., and Jolicoeur, P. (1999). Involvement of Notch1 in the development of mouse mammary tumors. *Oncogene* 18, 5973–5981. doi: 10.1038/sj.onc.1202991

Dongre, A., Rashidian, M., Reinhardt, F., Bagnato, A., Keckesova, Z., Ploegh, H. L., et al. (2017). Epithelial-to-mesenchymal transition contributes to immunosuppression in breast carcinomas. *Cancer Res.* 77, 3982–3989. doi: 10.1158/0008-5472.CAN-16-3292

Dykxhoorn, D. M., Wu, Y., Xie, H., Yu, F., Lal, A., Petrocca, F., et al. (2009). miR-200 enhances mouse breast cancer cell colonization to form distant metastases. *PLoS ONE* 4:e7181. doi: 10.1371/journal.pone.0007181

Evans, M. K., Brown, M. C., Geradts, J., Bao, X., Robinson, T. J., Jolly, M. K., et al. (2018). XIAP Regulation by MNK links MAPK and NFkappaB signaling to determine an aggressive breast cancer phenotype. *Cancer Res.* 78, 1726–1738. doi: 10.1158/0008-5472.CAN-17-1667

Evdokimova, V., Tognon, C., Ng, T., and Sorensen, P. H. (2009). Reduced proliferation and enhanced migration: two sides of the same coin? Molecular mechanisms of metastatic progression by YB-1. *Cell Cycle* 8, 2901–2906. doi: 10.4161/cc.8.18.9537

Fan, Y., Li, M., Ma, K., Hu, Y., Jing, J., Shi, Y., et al. (2019). Dual-target MDM2/MDMX inhibitor increases the sensitization of doxorubicin and inhibits migration and invasion abilities of triple-negative breast cancer cells through activation of TAB1/TAK1/p38 MAPK pathway. *Cancer Biol. Ther.* 20, 617–632. doi: 10.1080/15384047.2018.1539290

Fantozzi, A., Gruber, D. C., Pisarsky, L., Heck, C., Kunita, A., Yilmaz, M., et al. (2014). VEGF-mediated angiogenesis links EMT-induced cancer stemness to tumor initiation. *Cancer Res.* 74, 1566–1575. doi: 10.1158/0008-5472.CAN-13-1641

Fillmore, C. M., Gupta, P. B., Rudnick, J. A., Caballero, S., Keller, P. J., Lander, E. S., et al. (2010). Estrogen expands breast cancer stem-like cells through

paracrine FGF/Tbx3 signaling. *Proc. Natl. Acad. Sci. U S A*. 107, 21737–21742. doi: 10.1073/pnas.1007863107

Fischer, K. R., Durrans, A., Lee, S., Sheng, J., Li, F., Wong, S. T., et al. (2015). Epithelial-to-mesenchymal transition is not required for lung metastasis but contributes to chemoresistance. *Nature* 527, 472–476. doi: 10.1038/nature15748

Ford, H. L., and Thompson, E. W. (2010). Mammary gland studies as important contributors to the cause of epithelial mesenchymal plasticity in malignancy. *J. Mamm. Gland Biol. Neoplasia* 15, 113–115. doi: 10.1007/s10911-010-9182-0

Francart, M. E., Lambert, J., Vanwynsberghe, A. M., Thompson, E. W., Bourcy, M., Polette, M., et al. (2018). Epithelial-mesenchymal plasticity and circulating tumor cells: travel companions to metastases. *Dev. Dyn*. 247, 432–450. doi: 10.1002/dvdy.24506

Frisch, S. M., Schaller, M., and Cieply, B. (2013). Mechanisms that link the oncogenic epithelial-mesenchymal transition to suppression of anoikis. *J. Cell Sci*. 126, 21–29. doi: 10.1242/jcs.120907

Gajewski, T. F., Schreiber, H., and Fu, Y. X. (2013). Innate and adaptive immune cells in the tumor microenvironment. *Nat. Immunol*. 14, 1014–1022. doi: 10.1038/ni.2703

Galindo-Hernandez, O., Gonzales-Vazquez, C., Cortes-Reynosa, P., Reyes-Uribe, E., Chavez-Ocana, S., Reyes-Hernandez, O., et al. (2015). Extracellular vesicles from women with breast cancer promote an epithelial-mesenchymal transition-like process in mammary epithelial cells MCF10A. *Tumor Biol*. 36, 9649–9659. doi: 10.1007/s13277-015-3711-9

Gallahan, D., Jhappan, C., Robinson, G., Hennighausen, L., Sharp, R., Kordon, E., et al. (1996). Expression of a truncated Int3 gene in developing secretory mammary epithelium specifically retards lobular differentiation resulting in tumorigenesis. *Cancer Res*. 56, 1775–1785.

Gargini, R., Cerliani, J. P., Escoll, M., Anton, I. M., and Wandosell, F. (2015). Cancer stem cell-like phenotype and survival are coordinately regulated by Akt/FoxO/Bim pathway. *Stem Cells* 33, 646–660. doi: 10.1002/stem.1904

Ginestier, C., Hur, M. H., Charafe-Jauffret, E., Monville, F., Dutcher, J., Brown, M., et al. (2007). ALDH1 is a marker of normal and malignant human mammary stem cells and a predictor of poor clinical outcome. *Cell Stem Cell* 1, 555–567. doi: 10.1016/j.stem.2007.08.014

Grosse-Wilde, A., Fouquier d'Herouel, A., McIntosh, E., Ertaylan, G., Skupin, A., Kuestner, R. E., et al. (2015). Stemness of the hybrid epithelial/mesenchymal state in breast cancer and its association with poor survival. *PLoS ONE* 10:e0126522. doi: 10.1371/journal.pone.0126522

Guarnieri, A. L., Towers, C. G., Drasin, D. J., Oliphant, M. U. J., Andrysik, Z., Hotz, T. J., et al. (2018). The miR-106b-25 cluster mediates breast tumor initiation through activation of NOTCH1 via direct repression of NEDD4L. *Oncogene* 37, 3879–3893. doi: 10.1038/s41388-018-0239-7

Guerrero-Zotano, A., Mayer, I. A., and Arteaga, C. L. (2016). PI3K/AKT/mTOR: role in breast cancer progression, drug resistance, and treatment. *Cancer Metastasis Rev*. 35, 515–524. doi: 10.1007/s10555-016-9637-x

Gupta, A., Love, S., Schuh, A., Shanyinde, M., Larkin, J. M., Plummer, R., et al. (2014). DOC-MEK: a double-blind randomized phase II trial of docetaxel with or without selumetinib in wild-type BRAF advanced melanoma. *Ann. Oncol*. 25, 968–974. doi: 10.1093/annonc/mdu054

Gupta, G. P., and Massague, J. (2006). Cancer metastasis: building a framework. *Cell* 127, 679–695. doi: 10.1016/j.cell.2006.11.001

Gupta, P. B., Pastushenko, I., Skibinski, A., Blanpain, C., and Kuperwasser, C. (2019). Phenotypic plasticity: driver of cancer initiation, progression, and therapy resistance. *Cell Stem Cell* 24, 65–78. doi: 10.1016/j.stem.2018.11.011

Han, A., Song, Z., Tong, C., Hu, D., Bi, X., Augenlicht, L. H., et al. (2008). Sulindac suppressesβ-catenin expression in human cancer cells. *Eur. J. Pharmacol*. 583, 26–31. doi: 10.1016/j.ejphar.2007.12.034

Hanahan, D., and Weinberg, R. A. (2011). Hallmarks of cancer: the next generation. *Cell* 144, 646–674. doi: 10.1016/j.cell.2011.02.013

Hardt, O., Wild, S., Oerlecke, I., Hofmann, K., Luo, S., Wiencek, Y., et al. (2012). Highly sensitive profiling of CD44+/CD24- breast cancer stem cells by combining global mRNA amplification and next generation sequencing: evidence for a hyperactive PI3K pathway. *Cancer Lett*. 325, 165–174. doi: 10.1016/j.canlet.2012.06.010

Harrison, H., Farnie, G., Howell, S. J., Rock, R. E., Stylianou, S., Brennan, K. R., et al. (2010). Regulation of breast cancer stem cell activity by signaling through the Notch4 receptor. *Cancer Res*. 70, 709–718. doi: 10.1158/0008-5472.CAN-09-1681

Harrison, H., Simoes, B. M., Rogerson, L., Howell, S. J., Landberg, G., and Clarke, R. B. (2013). Oestrogen increases the activity of oestrogen receptor negative breast cancer stem cells through paracrine EGFR and Notch signalling. *Breast Cancer Res*. 15:R21. doi: 10.1186/bcr3396

Hartman, Z. C., Yang, X. Y., Glass, O., Lei, G., Osada, T., Dave, S. S., et al. (2011). HER2 overexpression elicits a proinflammatory IL-6 autocrine signaling loop that is critical for tumorigenesis. *Cancer Res*. 71, 4380–4391. doi: 10.1158/0008-5472.CAN-11-0308

Hasko, G., Linden, J., Cronstein, B., and Pacher, P. (2008). Adenosine receptors: therapeutic aspects for inflammatory and immune diseases. *Nat. Rev. Drug Discov*. 7, 759–770. doi: 10.1038/nrd2638

Hatsell, S., and Frost, A. R. (2007). Hedgehog signaling in mammary gland development and breast cancer. *J. Mamm. Gland Biol. Neoplasia* 12, 163–173. doi: 10.1007/s10911-007-9048-2

Hayes, D. N., Lucas, A. S., Tanvetyanon, T., Krzyzanowska, M. K., Chung, C. H., Murphy, B. A., et al. (2012). Phase II efficacy and pharmacogenomic study of Selumetinib (AZD6244; ARRY-142886) in iodine-131 refractory papillary thyroid carcinoma with or without follicular elements. *Clin. Cancer Res*. 18, 2056–2065. doi: 10.1158/1078-0432.CCR-11-0563

Hendrick, R. E., Baker, J. A., and Helvie, M. A. (2019). Breast cancer deaths averted over 3 decades. *Cancer* 125, 1482–1488. doi: 10.1002/cncr.31954

Hinohara, K., and Polyak, K. (2019). Intratumoral heterogeneity: more than just mutations. *Trends Cell Biol*. 29, 569–579. doi: 10.1016/j.tcb.2019.03.003

Hirschmann-Jax, C., Foster, A. E., Wulf, G. G., Nuchtern, J. G., Jax, T. W., Gobel, U., et al. (2004). A distinct "side population" of cells with high drug efflux capacity in human tumor cells. *Proc. Natl. Acad. Sci. U S A*. 101, 14228–14233. doi: 10.1073/pnas.0400067101

Ho, A. L., Grewal, R. K., Leboeuf, R., Sherman, E. J., Pfister, D. G., Deandreis, D., et al. (2013). Selumetinib-enhanced radioiodine uptake in advanced thyroid cancer. *N. Engl. J. Med*. 368:623. doi: 10.1056/NEJMoa1209288

Hong, D., Fritz, A. J., Zaidi, S. K., van Wijnen, A. J., Nickerson, J. A., Imbalzano, A. N., et al. (2018). Epithelial-to-mesenchymal transition and cancer stem cells contribute to breast cancer heterogeneity. *J. Cell. Physiol*. 233, 9136–9144. doi: 10.1002/jcp.26847

Hong, Y., Fang, F., and Zhang, Q. (2016). Circulating tumor cell clusters: What we know and what we expect (Review). *Int. J. Oncol*. 49, 2206–2216. doi: 10.3892/ijo.2016.3747

Hou, J. M., Krebs, M., Ward, T., Sloane, R., Priest, L., Hughes, A., et al. (2011). Circulating tumor cells as a window on metastasis biology in lung cancer. *Am. J. Pathol*. 178, 989–996. doi: 10.1016/j.ajpath.2010.12.003

Hsu, J. M., Xia, W., Hsu, Y. H., Chan, L. C., Yu, W. H., Cha, J. H., et al. (2018). STT3-dependent PD-L1 accumulation on cancer stem cells promotes immune evasion. *Nat. Commun*. 9:1908. doi: 10.1038/s41467-018-04313-6

Iwanaga, R., Wang, C. A., Micalizzi, D. S., Harrell, J. C., Jedlicka, P., Sartorius, C. A., et al. (2012). Expression of Six1 in luminal breast cancers predicts poor prognosis and promotes increases in tumor initiating cells by activation of extracellular signal-regulated kinase and transforming growth factor-beta signaling pathways. *Breast Cancer Res*. 14:R100. doi: 10.1186/bcr3219

Jang, G. B., Hong, I. S., Kim, R. J., Lee, S. Y., Park, S. J., Lee, E. S., et al. (2015b). Wnt/β-catenin small-molecule inhibitor CWP232228 preferentially inhibits the growth of breast cancer stem-like cells. *Cancer Res*. 75, 1691–1702. doi: 10.1158/0008-5472.CAN-14-2041

Jang, G. B., Kim, J. Y., Cho, S. D., Park, K. S., Jung, J. Y., Lee, H. Y., et al. (2015a). Blockade of Wnt/β-catenin signaling suppresses breast cancer metastasis by inhibiting CSC-like phenotype. *Sci. Rep*. 5:12465. doi: 10.1038/srep12465

Janne, P. A., Mann, H., and Ghiorghiu, D. (2016). Study design and rationale for a randomized, placebo-controlled, double-blind study to assess the efficacy and safety of selumetinib in combination with docetaxel as second-line treatment in patients with KRAS-mutant advanced non-small cell lung cancer (SELECT-1). *Clin. Lung Cancer* 17, e1–e4. doi: 10.1016/j.cllc.2015.12.010

Jänne, P. A., Shaw, A. T., Pereira, J. R., Jeannin, G., Vansteenkiste, J., Barrios, C., et al. (2013). Selumetinib plus docetaxel for KRAS-mutant advanced non-small-cell lung cancer: a randomised, multicentre, placebo-controlled, phase 2 study. *Lancet Oncol*. 14, 38–47. doi: 10.1016/S1470-2045(12)70489-8

Janne, P. A., Smith, I., McWalter, G., Mann, H., Dougherty, B., Walker, J., et al. (2015). Impact of KRAS codon subtypes from a randomised phase II trial of selumetinib plus docetaxel in KRAS mutant advanced non-small-cell lung cancer. *Br. J. Cancer* 113, 199–203. doi: 10.1038/bjc.2015.215

Jhappan, C., Gallahan, D., Stahle, C., Chu, E., Smith, G. H., Merlino, G., et al. (1992). Expression of an activated Notch-related int-3 transgene interferes with cell differentiation and induces neoplastic transformation in mammary and salivary glands. *Genes Dev*. 6, 345–355. doi: 10.1101/gad.6.3.345

Jolly, M. K., Jia, D., Boareto, M., Mani, S. A., Pienta, K. J., Ben-Jacob, E., et al. (2015). Coupling the modules of EMT and stemness: a tunable 'stemness window' model. *Oncotarget* 6, 25161–25174. doi: 10.18632/oncotarget.4629

Kalinsky, K., Sparano, J. A., Zhong, X., Andreopoulou, E., Taback, B., Wiechmann, L., et al. (2018). Pre-surgical trial of the AKT inhibitor MK-2206 in patients with operable invasive breast cancer: a New York cancer consortium trial. *Clin. Transl. Oncol*. 20, 1474–1483. doi: 10.1007/s12094-018-1888-2

Kallergi, G., Konstantinidis, G., Markomanolaki, H., Papadaki, M. A., Mavroudis, D., Stournaras, C., et al. (2013). Apoptotic circulating tumor cells in early and metastatic breast cancer patients. *Mol. Cancer Ther*. 12, 1886–1895. doi: 10.1158/1535-7163.MCT-12-1167

Kallergi, G., Papadaki, M. A., Politaki, E., Mavroudis, D., Georgoulias, V., and Agelaki, S. (2011). Epithelial to mesenchymal transition markers expressed in circulating tumour cells of early and metastatic breast cancer patients. *Breast Cancer Res*. 13:R59. doi: 10.1186/bcr2896

Kawasaki, B. T., and Farrar, W. L. (2008). Cancer stem cells, CD200 and immunoevasion. *Trends Immunol*. 29, 464–468. doi: 10.1016/j.it.2008.07.005

Kawasaki, B. T., Mistree, T., Hurt, E. M., Kalathur, M., and Farrar, W. L. (2007). Co-expression of the toleragenic glycoprotein, CD200, with markers for cancer stem cells. *Biochem. Biophys. Res. Commun*. 364, 778–782. doi: 10.1016/j.bbrc.2007.10.067

Kim, C., Gao, R., Sei, E., Brandt, R., Hartman, J., Hatschek, T., et al. (2018). Chemoresistance evolution in triple-negative breast cancer delineated by single-cell sequencing. *Cell* 173, 879–893 e13. doi: 10.1016/j.cell.2018.03.041

Knutson, K. L., Lu, H., Stone, B., Reiman, J. M., Behrens, M. D., Prosperi, C. M., et al. (2006). Immunoediting of cancers may lead to epithelial to mesenchymal transition. *J. Immunol*. 177, 1526–1533. doi: 10.4049/jimmunol.177.3.1526

Koike, Y., Ohta, Y., Saitoh, W., Yamashita, T., Kanomata, N., Moriya, T., et al. (2017). Anti-cell growth and anti-cancer stem cell activities of the non-canonical hedgehog inhibitor GANT61 in triple-negative breast cancer cells. *Breast Cancer* 24, 683–693. doi: 10.1007/s12282-017-0757-0

Kong, Y., Peng, Y., Liu, Y., Xin, H., Zhan, X., and Tan, W. (2015). Twist1 and Snail link hedgehog signaling to tumor-initiating cell-like properties and acquired chemoresistance independently of ABC transporters. *Stem Cells* 33, 1063–1074. doi: 10.1002/stem.1955

Kontomanolis, E. N., Kalagasidou, S., Pouliliou, S., Anthoulaki, X., Georgiou, N., Papamanolis, V., et al. (2018). The notch pathway in breast cancer progression. *ScientificWorldJournal* 2018:2415489. doi: 10.1155/2018/2415489

Koren, S., Reavie, L., Couto, J. P., De Silva, D., Stadler, M. B., Roloff, T., et al. (2015). PIK3CA(H1047R) induces multipotency and multi-lineage mammary tumours. *Nature* 525, 114–118. doi: 10.1038/nature14669

Kroger, C., Afeyan, A., Mraz, J., Eaton, E. N., Reinhardt, F., Khodor, Y. L., et al. (2019). Acquisition of a hybrid E/M state is essential for tumorigenicity of basal breast cancer cells. *Proc. Natl. Acad. Sci. U S A*. 116, 7353–7362. doi: 10.1073/pnas.1812876116

Krop, I. E., Mayer, I. A., Ganju, V., Dickler, M., Johnston, S., Morales, S., et al. (2016). Pictilisib for oestrogen receptor-positive, aromatase inhibitor-resistant, advanced or metastatic breast cancer (FERGI): a randomised, double-blind, placebo-controlled, phase 2 trial. *Lancet Oncol*. 17, 811–821. doi: 10.1016/S1470-2045(16)00106-6

Kumar, S., Park, S. H., Cieply, B., Schupp, J., Killiam, E., Zhang, F., et al. (2011). A pathway for the control of anoikis sensitivity by E-cadherin and epithelial-to-mesenchymal transition. *Mol. Cell. Biol*. 31, 4036–4051. doi: 10.1128/MCB.01342-10

Kwon, Y. J., Hurst, D. R., Steg, A. D., Yuan, K., Vaidya, K. S., Welch, D. R., et al. (2011). Gli1 enhances migration and invasion via up-regulation of MMP-11 and promotes metastasis in ERα negative breast cancer cell lines. *Clin. Exp. Metastasis* 28, 437–449. doi: 10.1007/s10585-011-9382-z

Labelle, M., and Hynes, R. O. (2012). The initial hours of metastasis: the importance of cooperative host-tumor cell interactions during hematogenous dissemination. *Cancer Discov*. 2, 1091–1099. doi: 10.1158/2159-8290.CD-12-0329

Lagadec, C., Vlashi, E., Della Donna, L., Dekmezian, C., and Pajonk, F. (2012). Radiation-induced reprogramming of breast cancer cells. *Stem Cells*. 30, 833–844. doi: 10.1002/stem.1058

Lambert, A. W., Pattabiraman, D. R., and Weinberg, R. A. (2017). Emerging biological principles of metastasis. *Cell* 168, 670–691. doi: 10.1016/j.cell.2016.11.037

Lane, T. F., and Leder, P. (1997). Wnt-10b directs hypermorphic development and transformation in mammary glands of male and female mice. *Oncogene* 15, 2133–2144. doi: 10.1038/sj.onc.1201593

Lee, A. Y. (2010). Thrombosis in cancer: an update on prevention, treatment, and survival benefits of anticoagulants. *Hematol. Am. Soc. Hematol. Educ. Prog.* 2010, 144–149. doi: 10.1182/asheducation-2010.1.144

Lee, G. H., Yoo, K. C., An, Y., Lee, H. J., Lee, M., Uddin, N., et al. (2018). FYN promotes mesenchymal phenotypes of basal type breast cancer cells through STAT5/NOTCH2 signaling node. *Oncogene* 37, 1857–1868. doi: 10.1038/s41388-017-0114-y

Lee, H. J., Wang, N. X., Shi, D. L., and Zheng, J. J. (2009). Sulindac inhibits canonical Wnt signaling by blocking the PDZ domain of the protein Dishevelled. *Angew. Chem. Int. Ed Engl*. 48, 6448–6452. doi: 10.1002/anie.200902981

Leong, K. G., Niessen, K., Kulic, I., Raouf, A., Eaves, C., Pollet, I., et al. (2007). Jagged1-mediated Notch activation induces epithelial-to-mesenchymal transition through slug-induced repression of E-cadherin. *J. Exp. Med*. 204, 2935–2948. doi: 10.1084/jem.20071082

Leontovich, A. A., Zhang, S., Quatraro, C., Iankov, I., Veroux, P. F., Gambino, M. W., et al. (2012). Raf-1 oncogenic signaling is linked to activation of mesenchymal to epithelial transition pathway in metastatic breast cancer cells. *Int. J. Oncol*. 40, 1858–1864. doi: 10.3892/ijo.2012.1407

Lewis, M. T., and Veltmaat, J. M. (2004). Next stop, the twilight zone: hedgehog network regulation of mammary gland development. *J. Mamm. Gland Biol. Neoplasia* 9, 165–181. doi: 10.1023/B:JOMG.0000037160.24731.35

Li, Q. Q., Xu, J. D., Wang, W. J., Cao, X. X., Chen, Q., Tang, F., et al. (2009). Twist1-mediated adriamycin-induced epithelial-mesenchymal transition relates to multidrug resistance and invasive potential in breast cancer cells. *Clin. Cancer Res*. 15, 2657–2665. doi: 10.1158/1078-0432.CCR-08-2372

Li, R., Liang, J., Ni, S., Zhou, T., Qing, X., Li, H., et al. (2010). A mesenchymal-to-epithelial transition initiates and is required for the nuclear reprogramming of mouse fibroblasts. *Cell Stem Cell* 7, 51–63. doi: 10.1016/j.stem.2010.04.014

Li, X., Lewis, M. T., Huang, J., Gutierrez, C., Osborne, C. K., Wu, M. F., et al. (2008). Intrinsic resistance of tumorigenic breast cancer cells to chemotherapy. *J. Natl. Cancer Inst*. 100, 672–679. doi: 10.1093/jnci/djn123

Li, Y., Lin, Z., Chen, B., Chen, S., Jiang, Z., Zhou, T., et al. (2017). Ezrin/NF-kB activation regulates epithelial- mesenchymal transition induced by EGF and promotes metastasis of colorectal cancer. *Biomed. Pharmacother* 92, 140–148. doi: 10.1016/j.biopha.2017.05.058

Li, Y., Welm, B., Podsypanina, K., Huang, S., Chamorro, M., Zhang, X., et al. (2003). Evidence that transgenes encoding components of the Wnt signaling pathway preferentially induce mammary cancers from progenitor cells. *Proc. Natl. Acad. Sci. U S A*. 100, 15853–15858. doi: 10.1073/pnas.2136825100

Liu, H., Wen, T., Zhou, Y., Fan, X., Du, T., Gao, T., et al. (2019). DCLK1 plays a metastatic-promoting role in human breast cancer cells. *Biomed. Res. Int*. 2019:1061979. doi: 10.1155/2019/1061979

Liu, S. L., Cong, Y., Wang, D., Sun, Y., Deng, L., Liu, Y. J., et al. (2014). Breast cancer stem cells transition between epithelial and mesenchymal states reflective of their normal counterparts. *Stem Cell Rep*. 2, 78–91. doi: 10.1016/j.stemcr.2013.11.009

Liu, Y., and Cao, X. T. (2016). Characteristics and significance of the pre-metastatic niche. *Cancer Cell* 30, 668–681. doi: 10.1016/j.ccell.2016.09.011

Lo, H. W., Hsu, S. C., Xia, W., Cao, X., Shih, J. Y., Wei, Y., et al. (2007). Epidermal growth factor receptor cooperates with signal transducer and activator of transcription 3 to induce epithelial-mesenchymal transition in cancer cells via up-regulation of TWIST gene expression. *Cancer Res*. 67, 9066–9076. doi: 10.1158/0008-5472.CAN-07-0575

Locatelli, M. A., Aftimos, P., Dees, E. C., LoRusso, P. M., Pegram, M. D., Awada, A., et al. (2017). Phase I study of the gamma secretase inhibitor PF-03084014 in combination with docetaxel in patients with advanced triple-negative breast cancer. *Oncotarget* 8, 2320–2328. doi: 10.18632/oncotarget.13727

Lu, P., Bai, X. C., Ma, D., Xie, T., Yan, C., Sun, L., et al. (2014). Three-dimensional structure of human gamma-secretase. *Nature* 512, 166–170. doi: 10.1038/nature13567

Ma, Y. L., Zhang, P., Wang, F., Yang, J. J., Yang, Z., and Qin, H. L. (2010). The relationship between early embryo development and tumourigenesis. *J. Cell. Mol. Med.* 14, 2697–2701. doi: 10.1111/j.1582-4934.2010.01191.x

Magnifico, A., Albano, L., Campaner, S., Delia, D., Castiglioni, F., Gasparini, P., et al. (2009). Tumor-initiating cells of HER2-positive carcinoma cell lines express the highest oncoprotein levels and are sensitive to trastuzumab. *Clin. Cancer Res.* 15, 2010–2021. doi: 10.1158/1078-0432.CCR-08-1327

Mallini, P., Leonard, T., Kirby, J., and Meeson, A. (2015). Epithelial-to-mesenchymal transition: What is the impact on breast cancer stem cells and drug resistance. *Int. J. Mol. Med.* 36:S49. doi: 10.1016/j.ctrv.2013.09.008

Mani, S. A., Guo, W., Liao, M. J., Eaton, E. N., Ayyanan, A., Zhou, A. Y., et al. (2008). The epithelial-mesenchymal transition generates cells with properties of stem cells. *Cell* 133, 704–715. doi: 10.1016/j.cell.2008.03.027

Manzo, G. (2019). Similarities between embryo development and cancer process suggest new strategies for research and therapy of tumors: a new point of view. *Front Cell Dev. Biol.* 7:20. doi: 10.3389/fcell.2019.00020

Marotta, L. L., Almendro, V., Marusyk, A., Shipitsin, M., Schemme, J., Walker, S. R., et al. (2011). The JAK2/STAT3 signaling pathway is required for growth of CD44(+)CD24(-) stem cell-like breast cancer cells in human tumors. *J. Clin. Invest.* 121, 2723–2735. doi: 10.1172/JCI44745

Mathis, R. A., Sokol, E. S., and Gupta, P. B. (2017). Cancer cells exhibit clonal diversity in phenotypic plasticity. *Open Biol.* 7:160283. doi: 10.1098/rsob.160283

May, C. D., Sphyris, N., Evans, K. W., Werden, S. J., Guo, W. J., and Mani, S. A. (2011). Epithelial-mesenchymal transition and cancer stem cells: a dangerously dynamic duo in breast cancer progression. *Breast Cancer Res.* 13:202. doi: 10.1186/bcr2789

Mayer, I. A., Abramson, V. G., Formisano, L., Balko, J. M., Estrada, M. V., Sanders, M. E., et al. (2017). A phase Ib study of alpelisib (BYL719), a PI3Kα -specific inhibitor, with letrozole in ER+/HER2- metastatic breast cancer. *Clin. Cancer Res.* 23, 26–34. doi: 10.1158/1078-0432.CCR-16-0134

Mayer, I. A., Abramson, V. G., Isakoff, S. J., Forero, A., Balko, J. M., Kuba, M. G., et al. (2014). Stand up to cancer phase Ib study of pan-phosphoinositide-3-kinase inhibitor buparlisib with letrozole in estrogen receptor-positive/human epidermal growth factor receptor 2-negative metastatic breast cancer. *J. Clin. Oncol.* 32, 1202–1209. doi: 10.1200/JCO.2013.54.0518

McCoy, E. L., Iwanaga, R., Jedlicka, P., Abbey, N. S., Chodosh, L. A., Heichman, K. A., et al. (2009). Six1 expands the mouse mammary epithelial stem/progenitor cell pool and induces mammary tumors that undergo epithelial-mesenchymal transition. *J. Clin. Invest.* 119, 2663–2677. doi: 10.1172/JCI37691

McGranahan, N., and Swanton, C. (2015). Biological and therapeutic impact of intratumor heterogeneity in cancer evolution. *Cancer Cell* 27, 15–26. doi: 10.1016/j.ccell.2014.12.001

Mego, M., De Giorgi, U., Broglio, K., Dawood, S., Valero, V., Andreopoulou, E., et al. (2009). Circulating tumour cells are associated with increased risk of venous thromboembolism in metastatic breast cancer patients. *Br. J. Cancer* 101, 1813–1816. doi: 10.1038/sj.bjc.6605413

Mejlvang, J., Kriajevska, M., Vandewalle, C., Chernova, T., Sayan, A. E., Berx, G., et al. (2007). Direct repression of cyclin D1 by SIP1 attenuates cell cycle progression in cells undergoing an epithelial mesenchymal transition. *Mol. Biol. Cell* 18, 4615–4624. doi: 10.1091/mbc.e07-05-0406

Micalizzi, D. S., Christensen, K. L., Jedlicka, P., Coletta, R. D., Baron, A. E., Harrell, J. C., et al. (2009). The Six1 homeoprotein induces human mammary carcinoma cells to undergo epithelial-mesenchymal transition and metastasis in mice through increasing TGF-beta signaling. *J. Clin. Invest.* 119, 2678–2690. doi: 10.1172/JCI37815

Micalizzi, D. S., Maheswaran, S., and Haber, D. A. (2017). A conduit to metastasis: circulating tumor cell biology. *Genes Dev.* 31, 1827–1840. doi: 10.1101/gad.305805.117

Micalizzi, D. S., Wang, C. A., Farabaugh, S. M., Schiemann, W. P., and Ford, H. L. (2010). Homeoprotein Six1 increases TGF-beta type I receptor and converts TGF-beta signaling from suppressive to supportive for tumor growth. *Cancer Res.* 70, 10371–10380. doi: 10.1158/0008-5472.CAN-10-1354

Milsom, C. C., Yu, J. L., Mackman, N., Micallef, J., Anderson, G. M., Guha, A., et al. (2008). Tissue factor regulation by epidermal growth factor receptor and epithelial-to-mesenchymal transitions: effect on tumor initiation and angiogenesis. *Cancer Res.* 68, 10068–10076. doi: 10.1158/0008-5472.CAN-08-2067

Mirkes, P. E., Ellison, A., and Little, S. A. (1991). Role of aldehyde dehydrogenase (ALDH) in the detoxication of cyclophosphamide (CP) in rat embryos. *Adv. Exp. Med. Biol.* 284, 85–95. doi: 10.1007/978-1-4684-5901-2_11

Mita, M. M., Becerra, C., Richards, D. A., Mita, A. C., Shagisultanova, E., Osborne, C. R. C., et al. (2016). Phase 1b study of WNT inhibitor vantictumab (VAN, human monoclonal antibody) with paclitaxel (P) in patients (pts) with 1st- to 3rd-line metastatic HER2-negative breast cancer (BC). *J. Clin. Oncol.* 34, 2516–2516. doi: 10.1200/JCO.2016.34.15_suppl.2516

Morel, A. P., Lievre, M., Thomas, C., Hinkal, G., Ansieau, S., and Puisieux, A. (2008). Generation of breast cancer stem cells through epithelial-mesenchymal transition. *PLoS ONE* 3:e2888. doi: 10.1371/journal.pone.0002888

Mukherjee, S., Frolova, N., Sadlonova, A., Novak, Z., Steg, A., Page, G. P., et al. (2006). Hedgehog signaling and response to cyclopamine differ in epithelial and stromal cells in benign breast and breast cancer. *Cancer Biol. Ther.* 5, 674–683. doi: 10.4161/cbt.5.6.2906

Neelakantan, D., Zhou, H., M., Oliphant, U. J., Zhang, X., Simon, L. M., Henke, D. M., et al. (2017). EMT cells increase breast cancer metastasis via paracrine GLI activation in neighbouring tumour cells. *Nat. Commun.* 8:15773. doi: 10.1038/ncomms15773

Nilendu, P., Kumar, A., Kumar, A., Pal, J. K., and Sharma, N. K. (2018). Breast cancer stem cells as last soldiers eluding therapeutic burn: a hard nut to crack. *Int. J. Cancer.* 142, 7–17. doi: 10.1002/ijc.30898

Nusse, R., and Varmus, H. E. (1982). Many tumors induced by the mouse mammary tumor virus contain a provirus integrated in the same region of the host genome. *Cell* 31, 99–109. doi: 10.1016/0092-8674(82)90409-3

Ocana, O. H., Corcoles, R., Fabra, A., Moreno-Bueno, G., Acloque, H., Vega, S., et al. (2012). Metastatic colonization requires the repression of the epithelial-mesenchymal transition inducer Prrx1. *Cancer Cell.* 22, 709–724. doi: 10.1016/j.ccr.2012.10.012

Oliphant, M. U. J., Vincent, M. Y., Galbraith, M. D., Pandey, A., Zaberezhnyy, V., Rudra, P., et al. (2019). SIX2 mediates late-stage metastasis via direct regulation of SOX2 and induction of a cancer stem cell program. *Cancer Res.* 79, 720–734. doi: 10.1158/0008-5472.CAN-18-1791

Oliveras-Ferraros, C., Corominas-Faja, B., Cufi, S., Vazquez-Martin, A., Martin-Castillo, B., Iglesias, J. M., et al. (2012). Epithelial-to-mesenchymal transition (EMT) confers primary resistance to trastuzumab (Herceptin). *Cell Cycle* 11, 4020–4032. doi: 10.4161/cc.22225

Onder, T. T., Gupta, P. B., Mani, S. A., Yang, J., Lander, E. S., and Weinberg, R. A. (2008). Loss of E-cadherin promotes metastasis via multiple downstream transcriptional pathways. *Cancer Res.* 68, 3645–3654. doi: 10.1158/0008-5472.CAN-07-2938

Orr, F. W., and Wang, H. H. (2001). Tumor cell interactions with the microvasculature: a rate-limiting step in metastasis. *Surg. Oncol. Clin. N. Am.* 10, 357–381. doi: 10.1016/S1055-3207(18)30070-X

O'Toole, S. A., Machalek, D. A., Shearer, R. F., Millar, E. K., Nair, R., Schofield, P., et al. (2011). Hedgehog overexpression is associated with stromal interactions and predicts for poor outcome in breast cancer. *Cancer Res.* 71, 4002–4014. doi: 10.1158/0008-5472.CAN-10-3738

Paget, S. (1989). The distribution of secondary growths in cancer of the breast (1889). *Cancer Metastasis Rev.* 8, 98–101.

Palumbo, J. S. (2008). Mechanisms linking tumor cell-associated procoagulant function to tumor dissemination. *Semin. Thromb. Hemost.* 34, 154–160. doi: 10.1055/s-2008-1079255

Park, S. Y., Choi, J. H., and Nam, J. S. (2019). Targeting cancer stem cells in triple-negative breast cancer. *Cancers* 11:E965. doi: 10.3390/cancers11070965

Pastushenko, I., and Blanpain, C. (2019). EMT transition states during tumor progression and metastasis. *Trends Cell Biol.* 29, 212–226. doi: 10.1016/j.tcb.2018.12.001

Peinado, H., Portillo, F., and Cano, A. (2004). Transcriptional regulation of cadherins during development and carcinogenesis. *Int. J. Dev. Biol.* 48, 365–375. doi: 10.1387/ijdb.041794hp

Phillips, T. M., McBride, W. H., and Pajonk, F. (2006). The response of CD24(-/low)/CD44+ breast cancer-initiating cells to radiation. *J. Natl. Cancer Inst.* 98, 1777–1785. doi: 10.1093/jnci/djj495

Pollock, C. B., Koltai, H., Kapulnik, Y., Prandi, C., and Yarden, R. I. (2012). Strigolactones: a novel class of phytohormones that inhibit the growth and survival of breast cancer cells and breast cancer stem-like enriched mammosphere cells. *Breast Cancer Res. Treat*. 134, 1041–1055. doi: 10.1007/s10549-012-1992-x

Ram Makena, M., Gatla, H., Verlekar, D., Sukhavasi, S., Pandey, M., and Pramanik,. K. (2019). Wnt/β-catenin signaling: the culprit in pancreatic carcinogenesis and therapeutic resistance. *Int. J. Mol. Sci*. 20:E4242. doi: 10.3390/ijms20174242

Ray, H. J., and Niswander, L. (2012). Mechanisms of tissue fusion during development. *Development* 139, 1701–1711. doi: 10.1242/dev.068338

Reedijk, M., Odorcic, S., Chang, L., Zhang, H., Miller, N., McCready, D. R., et al. (2005). High-level coexpression of JAG1 and NOTCH1 is observed in human breast cancer and is associated with poor overall survival. *Cancer Res*. 65, 8530–8537. doi: 10.1158/0008-5472.CAN-05-1069

Ren, D., Zhu, X., Kong, R., Zhao, Z., Sheng, J., Wang, J., et al. (2018). Targeting brain-adaptive cancer stem cells prohibits brain metastatic colonization of triple-negative breast cancer. *Cancer Res*. 78, 2052–2064. doi: 10.1158/0008-5472.CAN-17-2994

Ribas, R., Pancholi, S., Guest, S. K., Marangoni, E., Gao, Q., Thuleau, A., et al. (2015). AKT antagonist AZD5363 influences estrogen receptor function in endocrine-resistant breast cancer and synergizes with fulvestrant (ICI182780) *in vivo*. *Mol. Cancer Ther*. 14, 2035–2048. doi: 10.1158/1535-7163.MCT-15-0143

Rich, J. N. (2007). Cancer stem cells in radiation resistance. *Cancer Res*. 67, 8980–8984. doi: 10.1158/0008-5472.CAN-07-0895

Richter, S., Bedard, P. L., Chen, E. X., Clarke, B. A., Tran, B., Hotte, S. J., et al. (2013). A phase I study of the oral gamma secretase inhibitor R04929097 in combination with gemcitabine in patients with advanced solid tumors (PHL-078/CTEP 8575). *Invest. New Drugs* 32, 243–249. doi: 10.1007/s10637-013-9965-4

Riley, P. A. (1994). Free radicals in biology: oxidative stress and the effects of ionizing radiation. *Int. J. Radiat. Biol*. 65, 27–33. doi: 10.1080/09553009414550041

Rudolph, M., Sizemore, S. T., Lu, Y., Teng, K. Y., Basree, M. M., Reinbolt, R., et al. (2018). A hedgehog pathway-dependent gene signature is associated with poor clinical outcomes in luminal A breast cancer. *Breast Cancer Res. Treat*. 169, 457–467. doi: 10.1007/s10549-018-4718-x

Ruiz-Borrego, M., Jimenez, B., Antolin, S., Garcia-Saenz, J. A., Corral, J., Jerez, Y., et al. (2019). A phase Ib study of sonidegib (LDE225), an oral small molecule inhibitor of smoothened or hedgehog pathway, in combination with docetaxel in triple negative advanced breast cancer patients: GEICAM/2012-12 (EDALINE) study. *Invest. New Drugs* 37, 98–108. doi: 10.1007/s10637-018-0614-9

Ruscetti, M., Quach, B., Dadashian, E. L., Mulholland, D. J., and Wu, H. (2015). Tracking and functional characterization of epithelial-mesenchymal transition and mesenchymal tumor cells during prostate cancer metastasis. *Cancer Res*. 75, 2749–2759. doi: 10.1158/0008-5472.CAN-14-3476

Safholm, A., Tuomela, J., Rosenkvist, J., Dejmek, J., Harkonen, P., and Andersson, T. (2008). The Wnt-5a-derived hexapeptide Foxy-5 inhibits breast cancer metastasis *in vivo* by targeting cell motility. *Clin. Cancer Res*. 14, 6556–6563. doi: 10.1158/1078-0432.CCR-08-0711

Salvador, F., Martin, A., Lopez-Menendez, C., Moreno-Bueno, G., Santos, V., Vazquez-Naharro, A., et al. (2017). Lysyl oxidase-like protein LOXL2 promotes lung metastasis of breast cancer. *Cancer Res*. 77, 5846–5859. doi: 10.1158/0008-5472.CAN-16-3152

Samavarchi-Tehrani, P., Golipour, A., David, L., Sung, H. K., Beyer, T. A., Datti, A., et al. (2010). Functional genomics reveals a BMP-driven mesenchymal-to-epithelial transition in the initiation of somatic cell reprogramming. *Cell Stem Cell*. 7, 64–77. doi: 10.1016/j.stem.2010.04.015

Saura, C., Hlauschek, D., Oliveira, M., Zardavas, D., Jallitsch-Halper, A., de la pena, L., et al. (2019). Neoadjuvant letrozole plus taselisib versus letrozole plus placebo in postmenopausal women with oestrogen receptor-positive, HER2-negative, early-stage breast cancer (LORELEI): a multicentre, randomised, double-blind, placebo-controlled, phase 2 trial. *Lancet Oncol*. 20, 1226–1238. doi: 10.1016/S1470-2045(19)30334-1

Saxena, M., Stephens, M. A., Pathak, H., and Rangarajan, A. (2011). Transcription factors that mediate epithelial-mesenchymal transition lead to multidrug resistance by upregulating ABC transporters. *Cell Death Dis*. 2:e179. doi: 10.1038/cddis.2011.61

Schmid, P., Pinder, S. E., Wheatley, D., Macaskill, J., Zammit, C., Hu, J., et al. (2016). Phase II randomized preoperative window-of-opportunity study of the PI3K inhibitor pictilisib plus anastrozole compared with anastrozole alone in patients with estrogen receptor-positive breast cancer. *J. Clin. Oncol*. 34, 1987–1994. doi: 10.1200/JCO.2015.63.9179

Shao, S., Zhao, X., Zhang, X., Luo, M., Zuo, X., Huang, S., et al. (2015). Notch1 signaling regulates the epithelial-mesenchymal transition and invasion of breast cancer in a slug-dependent manner. *Mol. Cancer* 14:28. doi: 10.1186/s12943-015-0295-3

Shen, C. J., Kuo, Y. L., Chen, C. C., Chen, M. J., and Cheng, Y. M. (2017). MMP1 expression is activated by Slug and enhances multi-drug resistance (MDR) in breast cancer. *PLoS ONE* 12:e0174487. doi: 10.1371/journal.pone.0174487

Shi, W., Yan, D., Zhao, C., Xiao, M., Wang, Y., Ma, H., et al. (2017). Inhibition of IL-6/STAT3 signaling in human cancer cells using evista. *Biochem. Biophys. Res. Commun*. 491, 159–165. doi: 10.1016/j.bbrc.2017.07.067

Shibue, T., Brooks, M. W., Inan, M. F., Reinhardt, F., and Weinberg, R. A. (2012). The outgrowth of micrometastases is enabled by the formation of filopodium-like protrusions. *Cancer Discov*. 2, 706–721. doi: 10.1158/2159-8290.CD-11-0239

Shuang, Z. Y., Wu, W. C., Xu, J., Lin, G., Liu, Y. C., Lao, X. M., et al. (2014). Transforming growth factor-β1-induced epithelial-mesenchymal transition generates ALDH-positive cells with stem cell properties in cholangiocarcinoma. *Cancer Lett*. 354, 320–328. doi: 10.1016/j.canlet.2014.08.030

Simoes, B. M., O'Brien, C. S., Eyre, R., Silva, A., Yu, L., Sarmiento-Castro, A., et al. (2015). Anti-estrogen resistance in human breast tumors is driven by JAG1-NOTCH4-dependent cancer stem cell activity. *Cell Rep*. 12, 1968–1977. doi: 10.1016/j.celrep.2015.08.050

Sims-Mourtada, J., Opdenaker, L. M., Davis, J., Arnold, K. M., and Flynn, D. (2015). Taxane-induced hedgehog signaling is linked to expansion of breast cancer stem-like populations after chemotherapy. *Mol. Carcinog*. 54, 1480–1493. doi: 10.1002/mc.22225

Sin, W. C., and Lim, C. L. (2017). Breast cancer stem cells-from origins to targeted therapy. *Stem Cell Investig*. 4:96. doi: 10.21037/sci.2017.11.03

Singh, S. K., Chen, N. M., Hessmann, E., Siveke, J., Lahmann, M., Singh, G., et al. (2015). Antithetical NFATc1-Sox2 and p53-miR200 signaling networks govern pancreatic cancer cell plasticity. *EMBO J*. 34, 517–530. doi: 10.15252/embj.201489574

Smigiel, J. M., Taylor, S. E., Bryson, B. L., Tamagno, I., Polak, K., and Jackson, M. W. (2019). Cellular plasticity and metastasis in breast cancer: a pre- and post-malignant problem. *J Cancer Metastasis Treat*. 5:47. doi: 10.20517/2394-4722.2019.26

Soerensen, P. G., Andersson, T., Buhl, U., Moelvadgaard, T., Jensen, P. B., Brunner, N., et al. (2014). Phase I dose-escalating study to evaluate the safety, tolerability, and pharmacokinetic and pharmacodynamic profiles of Foxy-5 in patients with metastatic breast, colorectal, or prostate cancer. *J. Clin. Oncol*. 32:TPS1140. doi: 10.1200/jco.2014.32.15_suppl.tps1140

Sokol, E. S., Miller, D. H., Breggia, A., Spencer, K. C., Arendt, L. M., and Gupta, P. B. (2016). Growth of human breast tissues from patient cells in 3D hydrogel scaffolds. *Breast Cancer Res*. 18:19. doi: 10.1186/s13058-016-0677-5

Solzak, J. P., Atale, R. V., Hancock, B. A., Sinn, A. L., Pollok, K. E., Jones, D. R., et al. (2017). Dual PI3K and Wnt pathway inhibition is a synergistic combination against triple negative breast cancer. *NPJ Breast Cancer* 3:17. doi: 10.1038/s41523-017-0016-8

Song, Y., Qian, L., Song, S., Chen, L., Zhang, Y., Yuan, G., et al. (2008). Fra-1 and Stat3 synergistically regulate activation of human MMP-9 gene. *Mol. Immunol*. 45, 137–143. doi: 10.1016/j.molimm.2007.04.031

Stankic, M., Pavlovic, S., Chin, Y., Brogi, E., Padua, D., Norton, L., et al. (2013). TGF-β-Id1 signaling opposes Twist1 and promotes metastatic colonization via a mesenchymal-to-epithelial transition. *Cell Rep*. 5, 1228–1242. doi: 10.1016/j.celrep.2013.11.014

Stathis, A., Hess, D., von Moos, R., Homicsko, K., Griguolo, G., Joerger, M., et al. (2017). Swiss group for clinical cancer, phase I trial of the oral smoothened inhibitor sonidegib in combination with paclitaxel in patients with advanced solid tumors. *Invest. New Drugs* 35, 766–772. doi: 10.1007/s10637-017-0454-z

Stemke-Hale, K., Gonzalez-Angulo, A. M., Lluch, A., Neve, R. M., Kuo, W. L., Davies, M., et al. (2008). An integrative genomic and proteomic analysis

of PIK3CA, PTEN, and AKT mutations in breast cancer. *Cancer Res*. 68, 6084–6091. doi: 10.1158/0008-5472.CAN-07-6854

Stoletov, K., Kato, H., Zardouzian, E., Kelber, J., Yang, J., Shattil, S., et al. (2010). Visualizing extravasation dynamics of metastatic tumor cells. *J Cell Sci*. 123(Pt 13), 2332–2341. doi: 10.1242/jcs.069443

Strauss, R., Li, Z. Y., Liu, Y., Beyer, I., Persson, J., Sova, P., et al. (2011). Analysis of epithelial and mesenchymal markers in ovarian cancer reveals phenotypic heterogeneity and plasticity. *PLoS ONE* 6:e16186. doi: 10.1371/journal.pone.0016186

Sultan, M., Vidovic, D., Paine, A. S., Huynh, T. T., Coyle, K. M., Thomas, M. L., et al. (2018). Epigenetic silencing of TAP1 in aldefluor(+) breast cancer stem cells contributes to their enhanced immune evasion. *Stem Cells* 36, 641–654. doi: 10.1002/stem.2780

Sun, Y., Wang, Y., Fan, C., Gao, P., Wang, X., Wei, G., et al. (2014). Estrogen promotes stemness and invasiveness of ER-positive breast cancer cells through Gli1 activation. *Mol. Cancer* 13, 137–137. doi: 10.1186/1476-4598-13-137

Tamura, K., Kodaira, M., Shimizu, C., Yonemori, K., Yunokawa, M., Shimomura, A., et al. (2018). Phase I study of taselisib in Japanese patients with advanced solid tumors or hormone receptor-positive advanced breast cancer. *Cancer Sci*. 109, 1592–1601. doi: 10.1111/cas.13561

Tanei, T., Morimoto, K., Shimazu, K., Kim, S. J., Tanji, Y., Taguchi, T., et al. (2009). Association of breast cancer stem cells identified by aldehyde dehydrogenase 1 expression with resistance to sequential paclitaxel and epirubicin-based chemotherapy for breast cancers. *Clin. Cancer Res*. 15, 4234–4241. doi: 10.1158/1078-0432.CCR-08-1479

Theodorou, V., Kimm, M. A., Boer, M., Wessels, L., Theelen, W., Jonkers, J., et al. (2007). MMTV insertional mutagenesis identifies genes, gene families and pathways involved in mammary cancer. *Nat. Genet*. 39, 759–769. doi: 10.1038/ng2034

Thiery, J. P., Acloque, H., Huang, R. Y., and Nieto, M. A. (2009). Epithelial-mesenchymal transitions in development and disease. *Cell* 139, 871–890. doi: 10.1016/j.cell.2009.11.007

Thiery, J. P., and Sleeman, J. P. (2006). Complex networks orchestrate epithelial-mesenchymal transitions. *Nat. Rev. Mol. Cell Biol*. 7, 131–142. doi: 10.1038/nrm1835

Tolcher, A. W., Messersmith, W. A., Mikulski, S. M., Papadopoulos, K. P., Kwak, E. L., Gibbon, D. G., et al. (2012). Phase I study of RO4929097, a gamma secretase inhibitor of Notch signaling, in patients with refractory metastatic or locally advanced solid tumors. *J. Clin. Oncol*. 30, 2348–2353. doi: 10.1200/JCO.2011.36.8282

Tsai, J. H., Hsu, L. S., Lin, C. L., Hong, H. M., Pan, M. H., Way, T. D., et al. (2013). 3,5,4'-trimethoxystilbene, a natural methoxylated analog of resveratrol, inhibits breast cancer cell invasiveness by downregulation of PI3K/Akt and Wnt/β-catenin signaling cascades and reversal of epithelial-mesenchymal transition. *Toxicol. Appl. Pharmacol*. 272, 746–756. doi: 10.1016/j.taap.2013.07.019

Turner, N. C., Alarcon, E., Armstrong, A. C., Philco, M., Lopez Chuken, Y. A., Sablin, M. P., et al. (2019). BEECH: a dose-finding run-in followed by a randomised phase II study assessing the efficacy of AKT inhibitor capivasertib (AZD5363) combined with paclitaxel in patients with estrogen receptor-positive advanced or metastatic breast cancer, and in a PIK3CA mutant sub-population. *Ann. Oncol*. 30, 774–780. doi: 10.1093/annonc/mdz086

Valastyan, S., and Weinberg, R. A. (2011). Tumor metastasis: molecular insights and evolving paradigms. *Cell* 147, 275–292. doi: 10.1016/j.cell.2011.09.024

Vega, S., Morales, A. V., Ocana, O. H., Valdes, F., Fabregat, I., and Nieto, M. A. (2004). Snail blocks the cell cycle and confers resistance to cell death. *Genes Dev*. 18, 1131–1143. doi: 10.1101/gad.294104

Waks, A. G., and Winer, E. P. (2019). Breast cancer treatment: a review. *JAMA* 321, 288–300. doi: 10.1001/jama.2018.19323

Walker, S. R., Xiang, M., and Frank, D. A. (2014). Distinct roles of STAT3 and STAT5 in the pathogenesis and targeted therapy of breast cancer. *Mol. Cell. Endocrinol*. 382, 616–621. doi: 10.1016/j.mce.2013.03.010

Wang, B., Wang, Q., Wang, Z., Jiang, J., Yu, S. C., Ping, Y. F., et al. (2014). Metastatic consequences of immune escape from NK cell cytotoxicity by human breast cancer stem cells. *Cancer Res*. 74, 5746–5757. doi: 10.1158/0008-5472.CAN-13-2563

Wang, H., Fu, W., Im, J. H., Zhou, Z., Santoro, S. A., Iyer, V., et al. (2004). Tumor cell alpha3beta1 integrin and vascular laminin-5 mediate pulmonary arrest and metastasis. *J. Cell Biol*. 164, 935–941. doi: 10.1083/jcb.200309112

Wang, H., He, L., Ma, F., Regan, M. M., Balk, S. P., Richardson, A. L., et al. (2013). SOX9 regulates low density lipoprotein receptor-related protein 6 (LRP6) and T-cell factor 4 (TCF4) expression and Wnt/β-catenin activation in breast cancer. *J. Biol. Chem*. 288, 6478–6487. doi: 10.1074/jbc.M112.419184

Wang, X., Zhang, Y., Zhang, X., Tian, W., Feng, W., and Chen, T. (2012). The curcumin analogue hydrazinocurcumin exhibits potent suppressive activity on carcinogenicity of breast cancer cells via STAT3 inhibition. *Int. J. Oncol*. 40, 1189–1195. doi: 10.3892/ijo.2011.1298

Wellner, U., Schubert, J., Burk, U. C., Schmalhofer, O., Zhu, F., Sonntag, A., et al. (2009). The EMT-activator ZEB1 promotes tumorigenicity by repressing stemness-inhibiting microRNAs. *Nat. Cell Biol*. 11, 1487–1495. doi: 10.1038/ncb1998

Wendt, M. K., Allington, T. M., and Schiemann, W. P. (2009). Mechanisms of the epithelial-mesenchymal transition by TGF-beta. *Fut. Oncol*. 5, 1145–1168. doi: 10.2217/fon.09.90

West, N. R., Murray, J. I., and Watson, P. H. (2014). Oncostatin-M promotes phenotypic changes associated with mesenchymal and stem cell-like differentiation in breast cancer. *Oncogene* 33, 1485–1494. doi: 10.1038/onc.2013.105

Whipple, R. A., Balzer, E. M., Cho, E. H., Matrone, M. A., Yoon, J. R., and Martin, S. S. (2008). Vimentin filaments support extension of tubulin-based microtentacles in detached breast tumor cells. *Cancer Res*. 68, 5678–5688. doi: 10.1158/0008-5472.CAN-07-6589

Whipple, R. A., Matrone, M. A., Cho, E. H., Balzer, E. M., Vitolo, M. I., Yoon, J. R., et al. (2010). Epithelial-to-mesenchymal transition promotes tubulin detyrosination and microtentacles that enhance endothelial engagement. *Cancer Res*. 70, 8127–8137. doi: 10.1158/0008-5472.CAN-09-4613

Wise, R., and Zolkiewska, A. (2017). Metalloprotease-dependent activation of EGFR modulates CD44(+)/CD24(-) populations in triple negative breast cancer cells through the MEK/ERK pathway. *Breast Cancer Res. Treat*. 166, 421–433. doi: 10.1007/s10549-017-4440-0

Xing, Y., Lin, N. U., Maurer, M. A., Chen, H., Mahvash, A., Sahin, A., et al. (2019). Phase II trial of AKT inhibitor MK-2206 in patients with advanced breast cancer who have tumors with PIK3CA or AKT mutations, and/or PTEN loss/PTEN mutation. *Breast Cancer Res*. 21:78. doi: 10.1186/s13058-019-1154-8

Xu, H., Li, W., Luo, S., Yuan, J., and Hao, L. (2019). Adipose derived stem cells promote tumor metastasis in breast cancer cells by stem cell factor inhibition of miR20b. *Cell Signal*. 62:109350. doi: 10.1016/j.cellsig.2019.109350

Xu, J., Lamouille, S., and Derynck, R. (2009). TGF-beta-induced epithelial to mesenchymal transition. *Cell Res*. 19, 156–172. doi: 10.1038/cr.2009.5

Yamauchi, K., Yang, M., Jiang, P., Yamamoto, N., Xu, M., Amoh, Y., et al. (2005). Real-time *in vivo* dual-color imaging of intracapillary cancer cell and nucleus deformation and migration. *Cancer Res*. 65, 4246–4252. doi: 10.1158/0008-5472.CAN-05-0069

Yang, F., Wang, Y., Li, Q., Cao, L., Sun, Z., Jin, J., et al. (2017). Intratumor heterogeneity predicts metastasis of triple-negative breast cancer. *Carcinogenesis* 38, 900–909. doi: 10.1093/carcin/bgx071

Yang, J., Liao, D., Chen, C., Liu, Y., Chuang, T. H., Xiang, R., et al. (2013). Tumor-associated macrophages regulate murine breast cancer stem cells through a novel paracrine EGFR/Stat3/Sox-2 signaling pathway. *Stem Cells* 31, 248–258. doi: 10.1002/stem.1281

Yang, L., Han, S., and Sun, Y. (2014). An IL6-STAT3 loop mediates resistance to PI3K inhibitors by inducing epithelial-mesenchymal transition and cancer stem cell expansion in human breast cancer cells. *Biochem. Biophys. Res. Commun*. 453, 582–587. doi: 10.1016/j.bbrc.2014.09.129

Yang, N., Zhou, T. C., Lei, X. X., Wang, C., Yan, M., Wang, Z. F., et al. (2016). Inhibition of sonic hedgehog signaling pathway by thiazole antibiotic thiostrepton attenuates the CD44+/CD24-stem-like population and sphere-forming capacity in triple-negative breast cancer. *Cell. Physiol. Biochem*. 38, 1157–1170. doi: 10.1159/000443066

Yook, J. I., Li, X. Y., Ota, I., Hu, C., Kim, H. S., Kim, N. H., et al. (2006). A Wnt-Axin2-GSK3beta cascade regulates Snail1 activity in breast cancer cells. *Nat. Cell Biol*. 8, 1398–1406. doi: 10.1038/ncb1508

Yu, J., Liao, X., Li, L., Lv, L., Zhi, X., Yu, J., et al. (2017). A preliminary study of the role of extracellular−5'- nucleotidase in breast cancer stem cells and epithelial-mesenchymal transition. *In Vitro Cell. Dev. Biol. Anim*. 53, 132–140. doi: 10.1007/s11626-016-0089-y

Yu, M. (2019). Metastasis stemming from circulating tumor cell clusters. *Trends Cell Biol.* 29, 275–276. doi: 10.1016/j.tcb.2019.02.001

Yu, M., Bardia, A., Wittner, B. S., Stott, S. L., Smas, M. E., Ting, D. T., et al. (2013). Circulating breast tumor cells exhibit dynamic changes in epithelial and mesenchymal composition. *Science* 339, 580–584. doi: 10.1126/science.1228522

Yu, Y., Xiao, C. H., Tan, L. D., Wang, Q. S., Li, X. Q., and Feng, Y. M. (2014). Cancer-associated fibroblasts induce epithelial-mesenchymal transition of breast cancer cells through paracrine TGF-βsignalling. *Br. J. Cancer* 110, 724–732. doi: 10.1038/bjc.2013.768

Yuan, G., Qian, L., Shi, M., Lu, F., Li, D., Hu, M., et al. (2008). HER2-dependent MMP-7 expression is mediated by activated STAT3. *Cell Signal.* 20, 1284–1291. doi: 10.1016/j.cellsig.2008.02.017

Yuan, S., Norgard, R. J., and Stanger, B. Z. (2019). Cellular plasticity in cancer. *Cancer Discov.* 9, 837–851. doi: 10.1158/2159-8290.CD-19-0015

Zhang, B. (2010). CD73: a novel target for cancer immunotherapy. *Cancer Res.* 70, 6407–6411. doi: 10.1158/0008-5472.CAN-10-1544

Zhang, H., Lu, H., Xiang, L., Bullen, J. W., Zhang, C., Samanta, D., et al. (2015). HIF-1 regulates CD47 expression in breast cancer cells to promote evasion of phagocytosis and maintenance of cancer stem cells. *Proc. Natl. Acad. Sci. U S A.* 112, E6215–E6223. doi: 10.1073/pnas.1520032112

Zhao, D., Pan, C., Sun, J., Gilbert, C., Drews-Elger, K., Azzam, D. J., et al. (2015). VEGF drives cancer-initiating stem cells through VEGFR-2/Stat3 signaling to upregulate Myc and Sox2. *Oncogene* 34, 3107–3119. doi: 10.1038/onc.2014.257

Conflict of Interest: The authors declare that the research was conducted in the absence of any commercial or financial relationships that could be construed as a potential conflict of interest.

Copyright © 2020 Kong, Hughes and Ford. This is an open-access article distributed under the terms of the Creative Commons Attribution License (CC BY). The use, distribution or reproduction in other forums is permitted, provided the original author(s) and the copyright owner(s) are credited and that the original publication in this journal is cited, in accordance with accepted academic practice. No use, distribution or reproduction is permitted which does not comply with these terms.

frontiers in Molecular Biosciences

REVIEW
published: 30 April 2020
doi: 10.3389/fmolb.2020.00079

Cancer Stem Cell Plasticity – A Deadly Deal

Archana P. Thankamony[1,2†], Kritika Saxena[3†], Reshma Murali[1], Mohit Kumar Jolly[3] and Radhika Nair[1*]*

[1] Cancer Research Program, Rajiv Gandhi Centre for Biotechnology, Thiruvananthapuram, India, [2] Manipal Academy of Higher Education (MAHE), Manipal, India, [3] Centre for BioSystems Science and Engineering, Indian Institute of Science, Bengaluru, India

Intratumoral heterogeneity is a major ongoing challenge in the effective therapeutic targeting of cancer. Accumulating evidence suggests that a fraction of cells within a tumor termed Cancer Stem Cells (CSCs) are primarily responsible for this diversity resulting in therapeutic resistance and metastasis. Adding to this complexity, recent studies have shown that there can be different subpopulations of CSCs with varying biochemical and biophysical traits resulting in varied dissemination and drug-resistance potential. Moreover, cancer cells can exhibit a high level of plasticity or the ability to dynamically switch between CSC and non-CSC states or among different subsets of CSCs. In addition, CSCs also display extensive metabolic plasticity. The molecular mechanisms underlying these different interconnected axes of plasticity has been under extensive investigation and the trans-differentiation process of Epithelial to Mesenchymal transition (EMT) has been identified as a major contributing factor. Besides genetic and epigenetic factors, CSC plasticity is also shaped by non-cell-autonomous effects such as the tumor microenvironment (TME). In this review, we discuss the latest developments in decoding mechanisms and implications of CSC plasticity in tumor progression at biochemical and biophysical levels, and the latest *in silico* approaches being taken for characterizing cancer cell plasticity. These efforts can help improve existing therapeutic approaches by taking into consideration the contribution of cellular plasticity/heterogeneity in enabling drug resistance.

Keywords: cancer stem cells, plasticity, epithelial-mesenchymal transition, metastasis, microenvironment, metabolic plasticity

OPEN ACCESS

Edited by:
Yong Teng,
Augusta University, United States

Reviewed by:
Aamir Ahmad,
Mitchell Cancer Institute, United States
Monica Venere,
The Ohio State University, United States

****Correspondence:***
Radhika Nair
radhikanair@rgcb.res.in
Mohit Kumar Jolly
mkjolly@iisc.ac.in

[†] These authors share first authorship

Specialty section:
This article was submitted to Molecular Diagnostics and Therapeutics, a section of the journal Frontiers in Molecular Biosciences

Received: *07 January 2020*
Accepted: *06 April 2020*
Published: *30 April 2020*

Citation:
Thankamony AP, Saxena K, Murali R, Jolly MK and Nair R (2020) Cancer Stem Cell Plasticity – A Deadly Deal. Front. Mol. Biosci. 7:79. doi: 10.3389/fmolb.2020.00079

INTRODUCTION

Heterogeneity in cancer biology has long been recognized and exploited in the clinical management of the disease (Rich, 2016). Intertumoral heterogeneity within breast cancer patients, for example, exhibiting different molecular subtypes based on immunohistochemical markers like Estrogen Receptor (ER) or Her2, has been the basis of successful targeted therapeutic approaches (Turashvili and Brogi, 2017; Januskeviciene and Petrikaite, 2019). The inbuilt cellular variation within a

tumor has been shown to be an important driver for the emergence of therapy resistant clones which ultimately lead to recurrence and spread of the cancer cells resulting in patient mortality (Somasundaram et al., 2012; Dagogo-Jack and Shaw, 2018; Akgul et al., 2019).

The development of intratumoral diversity in tumor cells has been widely attributed to two contrasting processes (Shackleton et al., 2009; Prasetyanti and Medema, 2017). The clonal evolution theory takes into account the intrinsic differences between all cells based on genetic and epigenetic programs as well as the influence of the tumor microenvironment (TME). The fitter clones are selected for and contribute to the diversity of the tumor cell population (McGranahan and Swanton, 2017). The second model – Cancer Stem Cell (CSC) model – proposes that there are a subset of cells (termed CSCs) which are predisposed to drive the tumor progression, metastatic and therapeutic resistance of the entire tumor. In this hierarchical model, CSCs can differentiate into less self-renewing populations of non-CSCs which form the bulk of the tumor, in an analogous fashion to stem cell development (Vermeulen et al., 2012). More recently, the ability of cells to switch states via different programs such as Epithelial-Mesenchymal Transition (EMT) has given rise to the concept that non-CSCs can also convert to being a CSC. Thus, CSCs need not be always *a priori* defined; rather stemness can be thought of as a cell state can that be reversibly gained or lost. In other words, cellular plasticity can allow CSCs and non-CSCs to switch among one another (Chaffer et al., 2011; Marjanovic et al., 2013; Gupta et al., 2019). Moreover, different subsets of CSCs can lie on various points on the epithelial-mesenchymal axis and can possibly interconvert (Liu et al., 2014; Bocci et al., 2018; Bocci et al., 2019). Therefore, clonal evolution and CSC models are not necessarily mutually exclusive and the plasticity model ushers in more complexity to the manner in which heterogeneous cell populations can possibly arise within a tumor (Cabrera et al., 2015; **Figure 1**).

A direct consequence of interconverting or plastic cellular populations in a tumor is the rise of drug resistant and/or metastatic cells which are ultimately responsible for the mortality associated with cancer (Biddle et al., 2016; Doherty et al., 2016). The need of the hour is hence to understand the molecular underpinnings for CSC plasticity and to decode the impact of bidirectional nature of CSC plasticity on the clinical management of the disease.

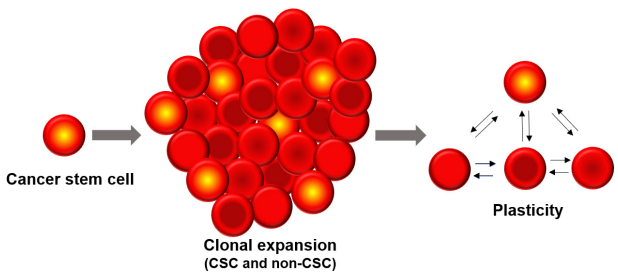

FIGURE 1 | Cancer stem cells (CSCs) constitute a minor sub-population of tumor mass. Phenotypic plasticity can enable CSCs and non-CSCs to interconvert among one another, depending on cell-intrinsic (e.g., epigenetic) and cell-extrinsic (e.g., tumor microenvironment) features.

CSC HETEROGENEITY AND PLASTICITY IN TUMOR PROGRESSION

The concept that CSCs are dynamic populations and can undergo spontaneous state transitions has been strengthened by various studies (Chaffer et al., 2011, 2013; Gupta et al., 2011). In the study done by Chaffer et al. (2011), using basal-like breast cancer cells, non-stem cells were shown to spontaneously switch to stem-like cells *in vitro* and *in vivo*; this plasticity was later found to be regulated by ZEB1 (Chaffer et al., 2013) – a key regulator of EMT (Jia et al., 2017). CSC heterogeneity and plasticity has been observed in different cancers. Just like their non-cancerous counterparts, identification of CSCs has been mainly based on the expression of cell surface markers (Chen W. et al., 2016). However, even within a single tumor type, different markers can identify distinct CSCs which are phenotypically distinct and could vary from patient to patient depending on the genetic make-up of the tumor (Tang, 2012). For instance, in glioblastoma, multiple markers like CD133, CD44, A2B5, SSEA have been utilized for identifying the stem cell populations (Singh et al., 2004; Ogden et al., 2008; Son et al., 2009). However, the use of CD133 marker is controversial as $CD133^-$ cells have also been shown to form tumors in glioma and $CD133^+$ cells could be derived from $CD133^-$ cells *in vivo,* implying the underlying plasticity (Wang et al., 2008). A recent study by Dirkse et al. (2019) found that in glioblastoma, the cell-membrane associated CSC markers such as CD133, A2B5, SSEA, and CD15 does not represent a clonal entity but a plastic state which can be adapted by most of the cells in response to varying conditions in the microenvironment. They also proposed that the enhanced tumorigenic potential of CSC-like state is a result of faster adaptation of the cells to the microenvironment.

The evidence for plasticity of CSC states comes from melanoma as well. A slow cycling population of melanoma CSC-like cells were identified using H3K4 demethylase JARID1B as a biomarker (Roesch et al., 2010). Intriguingly, the expression of this marker was dynamically regulated and JARID1B-negative cells could re-express the marker, thus indicating the dynamic nature of the stemness trait. Another seminal study done on melanoma supports the phenotypic plasticity model of CSCs. In this study, phenotypically distinct melanoma cells were shown to undergo reversible phenotypic changes *in vivo* and recapitulate the original tumor (Quintana et al., 2010). In breast cancer, different subsets of CSCs were identified based on ALDH1, CD44, and CD24; and the two subpopulations (epithelial-like ALDH1+, mesenchymal like $CD44^+/CD24^-$) were shown to be capable of inter converting among themselves as well as give rise to non-CSCs (Liu et al., 2014). Moreover, in breast cancer, CSCs and non-CSCs were shown to exhibit dynamic equilibrium maintained by cytokine-mediated crosstalk among these distinct populations (Iliopoulos et al., 2011). These results suggest that at least in

some cancers, phenotypic plasticity is reversible and does not necessarily depend on genetic alterations (Jolly et al., 2018a).

Another compelling evidence for CSC plasticity in tumor progression comes from studies on colorectal cancer. LGR5, a Wnt target gene, is used as a marker for colorectal CSCs. Kobayashi et al. (2012) has established human colon cancer cell lines that express LGR5 and possess CSC properties. However, treatment with an anticancer drug resulted in the conversion of the $LGR5^+$ cells into $LGR5^-$ cells; the absence of drug drove the transition back from $LGR5^-$ to $LGR5^+$ cells, suggesting the inherent plasticity. Both of these cell types could reconstitute the tumor *in vivo*. Consistently, targeted ablation of $Lgr5^+$ CSCs did not lead to tumor regression *in vivo* as the $Lgr5^-$ cells could give rise to $Lgr5^+$ cells and sustained the tumor growth. But interestingly, the $Lgr5^-$ cells could not form liver metastases (de Sousa e Melo et al., 2017), suggesting that the contribution of CSCs in primary tumor formation and that in metastatic settings may be different. However, contrary to these results, a very recent study has shown that majority of the colorectal cancer metastases were seeded by $Lgr5^-$ cells. Interestingly, these cells could re-establish cellular hierarchy by giving rise to $Lgr5^+$ cells and thereby reinforcing the concept of plasticity (Fumagalli et al., 2020). Therefore, the ability of CSCs and non-CSCs to switch among one another seems crucial both for the primary tumor and metastatic growth. More recently, some markers for metastatic CSCs have been identified across cancers (Celia-Terrassa and Jolly, 2019).

CSC plasticity has also been observed alongside vasculogenic mimicry (VM) – a hallmark process of cancer cell plasticity in which cancer cells transdifferentiate and acquire endothelial cell like characteristics (Fernandez-Cortes et al., 2019). In triple negative breast cancer, a $CD133^+$ cell population with CSC-like traits was found to show the ability to form tube-like structures (Liu et al., 2013). In renal cell carcinoma, using immunohistochemistry analysis of patient samples, the expression of stem cell like markers CD133 and CD44 was found to correlate with VM and high CSC marker expression and VM correlated with poor survival (Zhang et al., 2013). Thus, CSCs may not only interconvert among their sub-groups, but also give rise to different kinds of non-CSC differentiated cells.

MECHANISMS CONTROLLING CSC PLASTICITY

CSC plasticity is controlled by both cell-intrinsic and cell-extrinsic factors (Poli et al., 2018). Several studies have implied the importance of key transcription factors such as OCT3/4, SOX2, NANOG and KLF4 in modulating the generation of CSCs and regulation of cellular plasticity (Gu et al., 2007; Ben-Porath et al., 2008; Liu et al., 2013; Eun et al., 2017). For example, the introduction of OCT3/4, NANOG and KLF4 retrovirally into human colon cancer cells resulted in enhanced CSC properties and the xenografts of these cells actually resembled the original human tumor tissue (Oshima et al., 2014). Similarly, in glioblastoma, Suva et al. (2014) identified a core set of neurodevelopmental transcription factors (POU3F2, SOX2, SALL2, and OLIG2) that were sufficient to reprogram differentiated glioblastoma cells to CSCs. Tumor suppressor transcription factors like p53, pTEN has also been associated with CSC plasticity (Cabrera et al., 2015; da Silva-Diz et al., 2018; Santoro et al., 2019). Loss of p53 lead to increased expression of Nestin and enable the dedifferentiation of hepatocytes and thereby contributes to cellular plasticity in liver carcinogenesis (Tschaharganeh et al., 2014). Similarly, combined loss of p53/pTEN in clonal prostate epithelial cells caused transformation of multipotent progenitors and lead to epithelial to mesenchymal transition (EMT) (Martin et al., 2011). Moreover, genetic mutations of oncogene like KRAS and tumor suppressor like APC is also linked to the generation of stem-like cells (Easwaran et al., 2014).

Many studies have pointed out various mechanisms of epigenetic regulation such as bivalent chromatin state, DNA methylation, histone modifications in mediating CSC plasticity (Poli et al., 2018). For example, in basal like breast cancer cells, Chaffer and colleagues observed that ZEB1 promoter of non-CSCs is maintained in a bivalent configuration and in response to TGFβ, the chromatin switches to an active state leading to the transcription of ZEB1, consequently converting non-CSCs to CSCs (Chaffer et al., 2013). On the other hand, loss of function of HOXC8, a homeobox gene, in non-tumorigenic mammary epithelial cells due to its promoter DNA hypermethylation has been shown to be associated with CSC pool expansion, increased self-renewal and a transformed phenotype (Shah et al., 2017). A histone modifier, enhancer of zeste homolog 2 (EZH2) is a core member of polycomb repressor complex 2 (PRC2) and mediates transcriptional repression of target genes via the trimethylation of lysine 27 of histone 3 (H3K27me3) (Gan et al., 2018). EZH2 is upregulated in many cancers and its enhanced expression is associated with invasion, migration and stemness (Yamaguchi and Hung, 2014). In breast cancer, overexpression of EZH2 can increase mammosphere formation and self-renewal ability in CSCs (Chang et al., 2011; Wen et al., 2017). In glioblastoma, loss of H3K27me3 can lead to aberrant activation of Wnt pathway which is required for tumorigenicity and CSC maintenance (Rheinbay et al., 2013). On the other hand, in pediatric glioblastomas, the mutations in histone variants H3.1 and H3.3 results in reduced activity of EZH2 and consequently reprograms toward a stem cell-like state (Lewis et al., 2013). These observations suggest that CSCs are capable of exploiting the reversible nature of epigenetic modifications to achieve their plastic nature (Wainwright and Scaffidi, 2017). However, this reversibility also putatively offers an attractive opportunity that needs to be harnessed for therapeutic targeting.

CSC PLASTICITY AND EMT

EMT is a reversible, dynamic process which is critical during embryonic development and also aberrantly activated during various pathological processes like wound healing, fibrosis and cancer progression (Kalluri and Weinberg, 2009;

Jolly et al., 2018d). EMT is characterized by the loss of apico-basal polarity, rearrangements in the cytoskeleton and the acquisition of mesenchymal gene expression signature (Kalluri and Weinberg, 2009). The activation of EMT program is associated with the acquisition of stem like characteristics and has been implicated in different cancers (Mani et al., 2008; Shibue and Weinberg, 2017; Singla et al., 2018; Dongre and Weinberg, 2019). Initial reports suggested that activation of an EMT program endowed cells with traits similar to CSCs, such as enhanced colony formation *in vitro* and enhanced tumorigenesis *in vivo* (Shibue and Weinberg, 2017). Recent studies have, however, presented a more nuanced understanding of the interconnection between EMT and CSCs. Cells that undergo a more extreme version of EMT can lose the stemness gained during the initiation of EMT; thus, cells in a hybrid epithelial/mesenchymal phenotype are much more likely to be stem-like as compared to those on either end of the spectrum – pure epithelial or pure mesenchymal (Bierie et al., 2017; Jolly et al., 2018b). A recent study by Kroger et al. has found that the acquisition of a hybrid phenotype is a critical for the maintenance of tumorigenicity of basal breast cancer cells. Based on CD104/CD44 cell surface antigen expression and by regulating the expression of transcription factors like Zeb1 and Snail, they isolated highly tumorigenic cell population residing stably in a hybrid E/M state. This hybrid E/M cell population showed enhanced stemness which was mediated by increased expression of Snail and Wnt signaling pathway (Kroger et al., 2019). Another interesting study by Pastushenko et al. (2018) looked at the spectrum of EMT states that exist in a tumor rather than the binary fixed state that was accepted for long. The hybrid E/M tumor cells were associated with differences in their transcriptional and epigenetic programs, metastatic potential and also the location within a tumor (Pastushenko et al., 2018). It would be interesting to further understand whether these different hybrid states also respond differently to cues like chemotherapeutic treatment leading to resistance and ultimately relapse in cancer patients.

THE EFFECT OF THE TUMOR MICROENVIRONMENT ON CSC PLASTICITY

Besides juxtacrine crosstalk among cancer cells and stromal cells, there are factors secreted by the different cell types that form complex interacting networks in a TME (Swartz et al., 2012; Quail and Joyce, 2013; Peltanova et al., 2019). Accumulating evidence suggests that such crosstalk can modulate stem-like behavior and phenotypic plasticity of cancer cells (Pattabiraman and Weinberg, 2014; Cabrera et al., 2015; Prasetyanti and Medema, 2017). Cancer associated fibroblasts (CAFs) are a major component of the TME and play a pivotal role in various aspects of tumor progression (Kwa et al., 2019). CAFs were found to modulate the CSC plasticity in hepatocellular carcinoma through c-Met/FRA1/HEY1 signaling (Lau et al., 2016), in pancreatic adenocarcinoma through FAK signaling (Begum et al., 2019) and in lung cancer by IGF-II/IGF1R signaling pathway (Chen et al., 2014). In a recent study, the extent of intracellular Notch1 signaling in mesenchymal stem cell-derived dermal fibroblasts was found to determine the ability of these cells to regulate melanoma aggressiveness, stemness and phenotypic plasticity (Du et al., 2019). Another key component in TME is the immune system which plays a crucial role in regulating CSC plasticity. In response to chemotherapy, macrophages can secrete factor like Oncostatin-M (OSM), an IL-6 family cytokine which in turn can activate the dedifferentiation of triple negative breast cancer cells into aggressive stem cells (Doherty et al., 2019) and this activation could be mediated through co-operative STAT3/SMAD3 signaling (Junk et al., 2017). OSM can also be secreted by cancer associated adipocytes which can also promote stemness (Wolfson et al., 2015). Similarly, a crosstalk between macrophages of various polarizations (M1, M2) can alter the composition of tumor cells in terms of epithelial vs. mesenchymal populations, thus modulating stemness (Li et al., 2019).

The physical and chemical composition of the microenvironment such as acidic pH, low oxygen and nutrient availability, rigidity and porosity of the ECM can also play an important role in regulating the cancer stem cell behavior (Hjelmeland et al., 2011; Nallanthighal et al., 2019; Prager et al., 2019). A classic example would be hypoxia which is a hallmark of tumor progression in solid tumors and is associated with metastasis, therapeutic resistance and poor survival (Lequeux et al., 2019). A hypoxic microenvironment is known to regulate various aspects of malignant progression including cellular plasticity. In Glioblastoma, hypoxia was found to promote self-renewal in non-stem cells by upregulating important factors like OCT4, NANOG, and cMYC (Heddleston et al., 2009). Also, the hypoxic microenvironment can select the fate of breast cancer stem cells (CSCs) *in vivo* (Kim et al., 2018). Using flow cytometry, hypoxic and non-hypoxic breast cancer cells were isolated from hypoxia sensing xenografts of MDA-MB-231 and MCF7 breast cancer cell lines. Hypoxic tumor cells showed enhanced CSC characteristics compared to non-hypoxic cells which is attributed to the PI3K/AKT signaling. Interestingly, this differential cell fate was observed only in tumor cells isolated from hypoxic TME *in vivo* and not in tumor cells treated by hypoxia *in vitro* alone (Kim et al., 2018).

These studies underscore the importance of the microenvironment in sculpting intra-tumoral heterogeneity and CSC plasticity and highlight the need to better understand the tumor-microenvironment crosstalk for the development of effective therapeutic strategies (**Figure 2**). However, it is still controversial whether the CSC heterogeneity arises as a consequence of the microenvironment exerted selection pressure or whether plasticity is an intrinsic, default feature of the cancer cells that enable to adapt to varying cues from the microenvironment (Poli et al., 2018; Dirkse et al., 2019). Recent evidence from the study on glioblastoma suggests that intrinsic plasticity of tumor cells enables them to stochastically transition between different states defined by distinct expression of cancer stem cell markers and adapt to the microenvironment. Although all cell subpopulations are capable of phenotypic adjustment, they vary in their speed of adaptation (Dirkse et al., 2019).

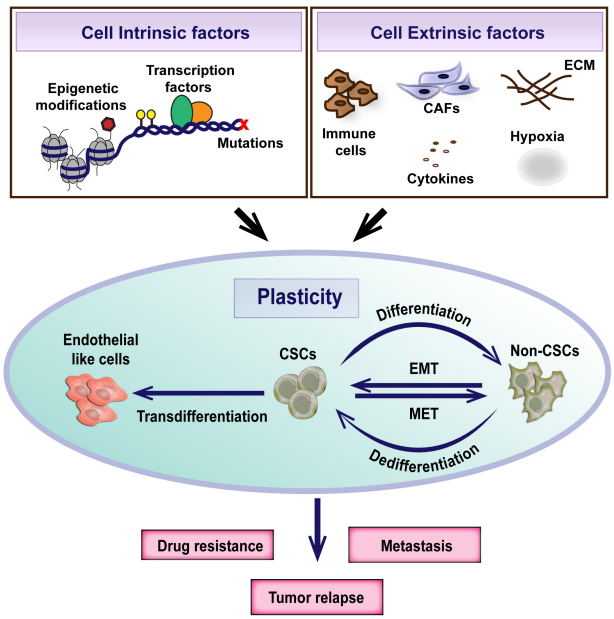

FIGURE 2 | Cancer stem cell plasticity is the ability to dynamically switch between CSC and non-CSC states. It is a complex process regulated by both cell intrinsic and extrinsic factors. Plasticity plays an important role in the evolution of therapeutic resistance, tumor relapse and metastasis.

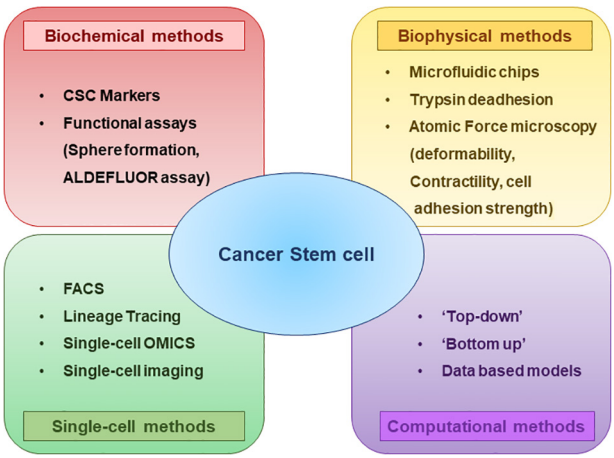

FIGURE 3 | Methods to characterize CSCs and their subsets at a glance. Biochemical and biophysical characteristics of the CSCs can be strikingly different and this diversity can be understood by using multiple assays. Analyzing the properties of CSCs at Single-cell resolution enables to better comprehend the CSC plasticity. Different computational and mathematical models are also being used which helps to gain insights regarding the CSC diversity and plasticity.

BIOCHEMICAL CHARACTERIZATION OF CANCER STEM CELLS AND THEIR SUBSETS

CSC plasticity can be instigated by various components in the microenvironment such as the secretion of cytokines and chemokines, communication with different stromal cell types and extracellular matrix and hypoxia (Agliano et al., 2017). Consequent activation of transcription factors and/or epigenetic modifications have been shown to mediate this interconversion (Cabrera et al., 2015). To understand the biology of CSC plasticity and the mechanisms underlying their functional phenotype with the aim of developing efficient treatment strategies, an essential requirement is the characterization and methods to selectively isolate the plastic CSC population from bulk tumors (**Figure 3**).

One of the serious and longstanding challenges in studying CSCs is the determination of appropriate methodology for the isolation and characterization of CSCs (Agliano et al., 2017). One of the most widely applied method to identify CSCs is to sort the cells based on the expression of cell surface markers such as CD44, CD133, CD24, CD26, EPCAM, CD166 (Jaggupilli and Elkord, 2012; Chen et al., 2013) or based on enzymatic activity of intracellular proteins like ALDH1 (Pattabiraman and Weinberg, 2014; **Table 1**). However, even these markers are not universally expressed on all CSCs, limiting their use in few cancers (Jaggupilli and Elkord, 2012). To overcome this limitation, more than one markers are used together in several cancers (Agliano et al., 2017). Although multiple markers have been described, the lack of reliable and accurate markers remains to be a stumbling block in the identification of CSCs. Moreover, recent single cell transcriptome analyses revealed that many CSC markers could be co-expressed by a single cell at the same time (Patel et al., 2014; Eun et al., 2017; **Table 2**) and the expression of CSC markers could vary *in vivo* as a consequence of plasticity and adaptation to the microenvironment (Dirkse et al., 2019). These observations clearly highlight the heterogeneity of CSCs and inefficiency of the markers currently in use in distinguishing CSCs and non-CSCs. Therefore, combining marker-based isolation strategies with functional assays such as *in vitro* clonogenic and *in vivo* limiting dilution xenotransplantation assays are of paramount importance to validate the stemness trait of the cells (Dirkse et al., 2019; Prager et al., 2019; **Table 2**).

BIOPHYSICAL CHARACTERIZATION OF CSCS AND THEIR SUBSETS

The properties of stem cells such as self-renewal and multipotency can be governed by intra-cellular and extracellular components constituting the stem cell niche (Morrison and Spradling, 2008). Similar to stem cells, properties of CSCs can be regulated by the TME to enhance their metastatic and tumor initiation capabilities (Aponte and Caicedo, 2017). CSCs, on the other hand, can also remodel ECM more strongly as compared to bulk cancer population (Srinivasan et al., 2017); thereby setting a complex feedback loop among the CSC and its niche. Biochemical constituents of such loops have been well-characterized earlier (Korkaya et al., 2011). Recent evidence suggests how biophysical cues such as matrix stiffness, cell contractility and cell-matrix adhesion strengths can regulate the tumor-initiating properties of CSCs. For instance, blocking ROCK (Rho-associated protein kinase) can inhibit cell

TABLE 1 | Commonly used markers for the isolation of cancer stem cells.

Cancer type	CSC markers	References
Breast	CD44, CD24, EPCAM, CD133, ALDH	Al-Hajj et al., 2003; Qiu et al., 2019
Glioblastoma	CD133, CD15, CD44, A2B5	Singh et al., 2004; Dirkse et al., 2019
Head and Neck	CD44, CD133, CD98, ALDH, Side population	Prince et al., 2007; Peitzsch et al., 2019
Lung	CD44, CD133, ALDH, CD90	Leung et al., 2010; Maiuthed et al., 2018
Colorectal	CD44, CD24, CD133, CD166, ALDH, EPCAM	Ricci-Vitiani et al., 2007; Zhou et al., 2018
Gastric	CD44, CD24, CD133, LGR5, CD90, CD71	Yang et al., 2007; Bekaii-Saab and El-Rayes, 2017
Pancreatic	CD44, CD24, CD133, ESA, DCLK1, ABCB1	Li et al., 2007; Di Carlo et al., 2018
Hepatocellular	CD44, CD133, CD13, CD45, CD90, EPCAM	Terris et al., 2010; Wang and Sun, 2018
Renal	CD105, CD133, ALDH1	Bussolati et al., 2008; Peired et al., 2016
Ovarian	CD44, CD24, CD117, EPCAM, ABCB1, ABCB2	Zhang et al., 2008; Roy and Cowden Dahl, 2018
Endometrial	CD44, CD117, CD55, CD133	Giannone et al., 2019
Prostate	CD133, CD44, α2β1, ABCG2, ALDH	Collins et al., 2005; Skvortsov et al., 2018
Melanoma	CD133, ALDH, CD271, ABCG2, JARID1B, CD20	Fang et al., 2005; Kumar et al., 2017
Leukemia	CD34, CD38, CD123, CD47, CD96	Lapidot et al., 1994; Wang et al., 2017

contractility and invasion potential of breast CSCs (Srinivasan et al., 2017). At a biophysical level, TME is often characterized by increased stiffness due to ECM remodeling, increased compressive stress due to confined growth, enhanced interstitial pressure and an increased interstitial fluid flow (Zanotelli et al., 2018). Extrinsic mechanical forces exerted by ECM constituents can trigger biochemical changes inside cells such as cytoskeleton rearrangement, and changes in gene expression, protein-protein interactions and enzyme modifications, thus converging on various mechano-transduction and mechano-chemical axes (Ogden et al., 2008; Broders-Bondon et al., 2018; Roy Choudhury et al., 2019).

Cancer cells display variations in response to extrinsic biomechanical stimuli, leading to heterogeneity in their biophysical properties, which influences the overall nature of cells such as stemness and differentiation. Recent studies have shown that mechano-transduction cues greatly influences the generation and maintenance of CSCs and eventually metastasis (Chen and Kumar, 2017). In addition, mechanical properties such as deformability and adhesiveness are different for CSCs as compared to the bulk tumor population (Saliba et al., 2010; Zhang et al., 2012; Babahosseini et al., 2014; Chen J. et al., 2016). These advances have enabled attempts to isolate and identify CSCs based on biophysical marker using engineering techniques such as microfluidic devices (Saliba et al., 2010; Gossett et al., 2012; Zhang et al., 2012; Liu et al., 2015; Chen J. et al., 2016) in a label-free manner.

For instance, CSCs were enriched based on their adhesive traits using a microfluid chip having micro-channels coated with basement membrane extract. The cells entered into the chip driven by hydrodynamic forces. While highly adhesive cells were captured in micro-channels, less adhesive cells were collected from the outlet, which were shown to be enriched in CSCs, had greater motility and were resistant to chemotherapeutic drugs (Zhang et al., 2015). This study emphasizes the interconnections between EMT, stemness, and drug resistance (Jolly et al., 2019), and the use of microfluidics in investigating these associations (Nath et al., 2019). Similarly, another microfluidic device fitted with microbarriers was used to isolate cancer cells based on their deformability *in vitro*. The more deformable flexible phenotype was associated with expression of many genes involved in motility, metastasis and greater mammosphere formation efficiency (Zhang et al., 2012). Consistently, *in vivo*, deformability has been shown to be crucial for efficient extravasation of tumor-repopulating cells during metastasis as seen in zebrafish models (Chen J. et al., 2016; **Figure 3**).

Similar to biochemical heterogeneity observed within CSCs (Bocci et al., 2019; Moreira et al., 2019), CSCs can be biophysically strikingly different too (**Table 2**). In a recent study, Chen et al. (2019) showed the association of biophysical properties of CSCs and their ability to invade, migrate, and initiate tumors, using the SUM149 inflammatory breast cancer (IBC) stem cells. In this study, the authors sorted SUM149 CSCs based on the expression of aldehyde dehydrogenase enzyme (ALDH) and assayed biophysical properties of ALDH+ and ALDH– cells in terms of deformability, adhesion strength and contractility. ALDH+ cells displayed greater deformability, lower adhesion strength and reduced contractility relative to ALDH– cells, and resulted into enhanced functional phenotypes *in vitro* and greater tumor development *in vivo*. In addition, the authors isolated IBC cells based on their adhesive property using a microfluidic device and showed that the less adhesive cell population was ALDH– enriched, displayed enhanced *in vitro* invasion and migration as well as increased *in vivo* tumor development. Further, exogenous alteration of cell stiffness also resulted in changes in metastatic potential of these cells with less stiff cells showing greater invasion and migration (Chen et al., 2019). The results observed in this study corroborated well with earlier studies showing that cancer cells with greater deformability, lower adhesion strength and lower contractile force show enhanced metastatic potential (Swaminathan et al., 2011; Kraning-Rush et al., 2012; Byun et al., 2013; Sun et al., 2016; Bongiorno et al., 2018).

Therefore, with increasingly detailed characterization of biomechanical properties of various subpopulations of cancer cells and ECM, a "mechanosome" or "matrisome" signature may

TABLE 2 | Biochemical and biophysical methods to characterize the CSCs and their subsets.

Method	Experiment	Cell-line/Cancer type	Biochemical/Biophysical property	Scale	References
Single-cell RNA sequencing	*In vitro*	Primary glioblastoma cells	CD133	Single cell	Patel et al., 2014
Multi-color flow cytometry	*In vitro*	Glioblastoma tissue isolated from PDX	CD195, CD15, CD95,CD133,A2B5, CD24,CD29, CD44,CD90,CD56	Single cell	Dirkse et al., 2019
Fluorescence activated cell sorting, spheroid assay, RT PCR	*In vitro*	MCF-7, MDA-MB-231, MDA-MB-453	CD44, CD24, Oct4, Nanog and Klf4	Single cell	Srinivasan et al., 2017
Trypsin de-adhesion assay, atomic force microscopy, collagen degradation assay	*In vitro*	MCF-7, MDA-MB-231, MDA-MB-453	ROCK pathway, cell contractility, stiffness, ECM remodeling	Single cell	Srinivasan et al., 2017
Microfluidics method with mechanical separation chip	*In vitro*	MDA-MB-436, MCF-7, SUM149	Deformability, stiffness	Single cell	Zhang et al., 2012
Atomic force microscopy (AFM)	*In vitro*	Murine ovarian surface epithelial (MOSE) cell line	Stiffness	Single cell	Babahosseini et al., 2014
In vitro transmigration assay, F-actin staining	Both	tfRFP B16 cells, zebra fish	CDC42, SOX2, deformability	Population	Chen W. et al., 2016
Microfluidic cytometry (MC) chip	*In vitro*	MCF-7, MCF-10A, MDA-MB–231, SUM 149, SUM 159	Cell stiffness and cell-surface frictional property	Single cell	Liu et al., 2015
Microfluidics method	*In vitro*	SUM-149 and SUM-159	Cell adhesion property	Single cell	Zhang et al., 2015
ALDEFLOUR assay, microfluidics method, PDMS micropost array	*In vitro*	SUM149	ALDH, deformability, adhesion strength, contractility, stiffness	Single cell	Chen et al., 2019
Intra-vital lineage tracing	*In vivo*	MMTV-PyMT mouse models of mammary tumor	Cell lineage	Population	Zomer et al., 2013
Lineage tracing, transcriptomic analysis	*In vivo*	Notch1 transgenic mouse models	Cell lineage, Notch1, Lgr5	Population	Mourao et al., 2019
Single-cell RNA sequencing	*In vitro*	Patient-derived primary oral squamous cell carcinomas (OSCC) cell lines	Single cell expression data-biomolecular and epigenetic markers	Single cell	Sharma et al., 2018
Single cell gene expression profiling combined with functional characterization	*In vitro*	ER^+, ER^- breast cancer cell lines	Markers of differentiation, EMT, proliferation, stemness, pluripotency	Single cell	Akrap et al., 2016
Single cell RNA sequencing combined with mammosphere formation assay and label-retention assay	*In vitro*	MDA-MB-231	Markers involved in cell-cycle regulation, stem-cell properties and differentiation	Single cell	Jonasson et al., 2019
High-throughput automated single cell imaging analysis (HASCIA)	*In vitro*	Glioblastoma (GBM) CSCs	CD133, SOX2, pSTAT3,EGFR	Single cell	Chumakova et al., 2019

be helpful in identifying and isolating the most aggressive cancer cell subpopulations (Roy Choudhury et al., 2019).

SINGLE-CELL METHODS TO IDENTIFY CSCS AND THEIR SUBSETS

Much of our current understanding about CSCs comes from studies performed on bulk cancer cell populations. However, bulk analysis masks the underlying intra-tumor heterogeneity and does not inform much about rare cell subpopulations within the tumor (Navin, 2015; Bhatia et al., 2019). Therefore, it becomes extremely critical to study the cancer cells at a single-cell resolution to better comprehend the CSC heterogeneity and plasticity (Etzrodt et al., 2014). Flow cytometry and Fluorescence-Activated Cell Sorting (FACS) is a widely used method for the isolation and characterization of single CSCs (Greve et al., 2012; Etzrodt et al., 2014). Also, lineage tracing can be used to follow the fate of individual cells (**Figure 3**; McKenna and Gagnon, 2019).

A recent study integrated FACS analysis of CSC markers with functional assays such as proliferation, self-renewal and multipotency tests, and observed that glioblastoma stem cell heterogeneity results from tumor plasticity which is determined by the microenvironment cues (Dirkse et al., 2019). Lineage tracing methods have also been utilized by researchers to decipher the properties of CSCs and has huge potential in understanding the transition of cellular states. Using intra-vital *in vivo* lineage tracing method in a genetic mouse model of breast cancer, Zomer et al. (2013) demonstrated the existence of CSCs in unperturbed mammary tumor. They also found that CSC state is plastic and can be

activated, lost or deactivated. In another study, lineage tracing and transcriptional analysis of Notch1 expressing cells of intestinal tumors has led to the identification of a previously uncharacterized and undifferentiated stem cell population that contribute to tumor progression and heterogeneity (Mourao et al., 2019).

The advent of single-cell omics approaches has revolutionized our knowledge on CSC biology. Single cell genomic and transcriptomic analyses have provided invaluable insights regarding intra-tumor heterogeneity and clonal evolution in different cancers (Patel et al., 2014; Eirew et al., 2015; Hou et al., 2016; Puram et al., 2017). In addition to discerning the dynamics of clonal evolution, single cell omics methods have also enabled the identification of transitioning CSCs and their contribution to drug resistance (Puram et al., 2018; Sharma et al., 2018). Considering the rarity of CSCs, combining single cell transcriptomics with enrichment strategies such as flow cytometry or sphere assays are capable of drastically improving the characterization of CSC (Akrap et al., 2016; Jonasson et al., 2019). Single cell multi-omics approaches involving obtaining information from multiple components within a single cell is also gaining interest, because it facilitates the assessment of genotype and phenotype relationship in regulating the individual cell states (Macaulay et al., 2017; Liu et al., 2019).

Nonetheless, most of the single-cell omics analyses does not preserve spatial information as it requires the cells to be isolated from their microenvironment (Yuan et al., 2017). Another limitation is that a snap-shot analysis is inadequate to evaluate the dynamic nature of cellular processes (Skylaki et al., 2016). Transcriptomic profiling of cells using fluorescence *in situ* hybridization or sequencing will enable the decoding of the spatial regulation of cellular heterogeneity at single-cell resolution (Lee et al., 2014; Chen et al., 2015; Suva and Tirosh, 2019). Single-cell RNA sequencing data can be mapped to spatial transcriptomic data using advanced computational methods (Satija et al., 2015; Edsgard et al., 2018). Using a newly developed high-throughput automated single cell image analysis (HASCIA), the spatio-temporal factors regulating glioblastoma stem cell state transitions has been recently investigated (Chumakova et al., 2019). Integrating the transcriptomic and spatial data can significantly improve the interpretation of the CSC plasticity (Satija et al., 2015; Yuan et al., 2017). A recent work coupling large scale single cell-resolution 3D imaging strategy, lineage tracing and RNA sequencing in pTEN/Trp53 deficient mice models, observed extensive molecular heterogeneity and clonal plasticity within tumors and found that EMT is not a rare event within the tumors (Rios et al., 2019). Live single-cell imaging techniques are also being developed which overcomes the limitation of static snap-shot analyses in studying the temporal regulation of cellular state changes (Fumagalli et al., 2019). The number of genes analyzed by such studies are much less than snap-shot studies and the lack of specialized tools and computational methods for handling the large amount of data generated through such studies is a major challenge (Skylaki et al., 2016).

With emerging evidence about the potential of single-cell analysis in understanding the biology of CSCs, development of newer tools and analysis methods and integrative approach are required for better comprehending the cell state transitions and improved therapeutic strategies.

COMPUTATIONAL METHODS TO IDENTIFY CSCS

With the deluge of preclinical and clinical data being generated at a high-dimensional level, computational approaches to extract meaningful information and generate testable hypotheses are becoming more common (Suhail et al., 2019). Various "top–down" and "bottom-up" computational methods provide a framework to unravel novel insights into various aspects of the dynamics of cancer progression such as role of intra-tumoral heterogeneity, dynamics of EMT, CSCs and its role in metastases, evolutionary dynamics of cancer initiation and progression, prediction of treatment response and therapy resistance (**Figure 3**). While "top–down" methods use high-dimensional data and apply an inferential metric to identify patterns through machine learning and/or network reconstruction, the "bottom-up" approaches aim to elucidate the emergent dynamics of a phenomenon based on its mechanism-based description through mathematical modeling. Both approaches can be synergistically used to predict and/or interpret cellular behavior (Altrock et al., 2015; Jolly et al., 2017). Mechanism-based, i.e., "bottom-up," mathematical models have been useful in understanding the dynamics of complex regulatory networks that modulate cancer stem cell behavior such as stem cell state transitions and dedifferentiation (Sehl and Wicha, 2018). Recent studies using mathematical models have predicted that cells in one or more hybrid E/M phenotypes are associated more with stemness as compared to cells in purely mesenchymal or purely epithelial (Jolly et al., 2014). These predictions have since been validated *in vitro* and *in vivo* (Grosse-Wilde et al., 2015; Bierie et al., 2017; Pastushenko et al., 2018; Kroger et al., 2019) and has been supported by clinical data (Jolly et al., 2019). How are the pathways of EMT and stemness interconnected with each other? These questions can be addressed by investigating *in silico* the coupling between core regulatory circuits of EMT, CSCs and other connected signaling pathways such as Notch signaling; this model predicted that altering the coupling strength between EMT and CSC networks and/or modulating Notch signaling can change the position of "stemness window" on the "EMT axis," thus generating various subsets of CSCs in terms of EMT phenotypes (Bocci et al., 2018). Such CSC heterogeneity has been extensively seen across cancers (Liu et al., 2014; Giraddi et al., 2018; Zheng et al., 2018). A common unifying principle that has emerged upon investigating the regulatory networks underlying EMT, CSCs and related traits such as drug resistance has been the role of interconnected feedback loops in enabling multiple phenotypes (i.e., heterogeneity) and the ability to switch among them (i.e., plasticity) (Mooney et al., 2017; Tripathi et al., 2017; Jolly et al., 2018c). Phenotypic plasticity can abet the generation and maintenance of phenotypic heterogeneity (Celia-Terrassa et al., 2018; Hari et al., 2019); thus, breaking these feedback loops can be thought of as a

novel potential therapeutic strategy to restrict phenotypic plasticity and/or heterogeneity (Celia-Terrassa et al., 2018; Hari et al., 2019).

"Data-based" models have also been valuable in decoding CSC signatures. A stemness index was derived using one-class logistic regression and observed to be higher in the metastatic breast cancer cells compared with primary tumors (Malta et al., 2018), suggesting the possibility of a signature specific to metastatic CSCs. Similar logistic regression models have been used to quantify the extent of EMT (George et al., 2017) that has revealed the heterogeneity of EMT phenotypes in various CSCs and their subsets (Bocci et al., 2018), hence strengthening the insights from "mechanism-based" or "bottom-up" models.

Another set of questions where mathematical models have been useful is estimating the fraction of CSCs in a tumor. Many studies have used population-level models to understand the difference in growth kinetics of CSCs and non-CSCs, and used that to offer a potential mechanistic underpinning of "tumor growth paradox," i.e., accelerated tumor growth with increased cell death (Hillen et al., 2013). Typically, CSC represent a minor cell population within a tumor, major population being the non-CSCs which compete with the CSCs for space and resources. While induction of cell death results into death of bulk of non-CSCs which facilitates increase in CSC division, ultimately resulting into expansion of CSC population and increase in tumor progression (Hillen et al., 2013). In contrary, another study showed that the CSC population within a tumor is homeostatically maintained such that reducing CSC population below a threshold triggers extensive phenotypic switching of non-CSC to CSC population (Sellerio et al., 2015). Thus, while the dynamics and mechanisms of CSC generation, plasticity and maintenance remain to be comprehensively understood (Enderling, 2015), integrating these different modeling approaches with one another and with experimental and clinical data shall contribute to revealing this complex behavior at an intracellular and at a population level. Such an improved dynamic understanding can help identify optimal treatment strategies to reduce tumor burden, such as a combination of radiation and differentiation therapies (Bachman and Hillen, 2013), or a sequential treatment of drugs to tackle the *de novo* generation of CSCs (Gupta et al., 2011) and their functional attributes (Goldman et al., 2015).

SPATIAL ORGANIZATION OF CSCS

Spatial heterogeneity is a fundamental feature of TME that contains diverse cell types (Yuan, 2016; Yuan et al., 2017). One canonical representation of spatial heterogeneity is the co-occurrence of vascular and hypoxic regions, as observed in solid tumors (Alfarouk et al., 2013). This heterogeneity can alter cellular phenotypes, for instance, glioblastoma cells in hypoxic regions have been shown to over-express epidermal growth factor receptor (EGFR) while those over-expressing platelet-derived growth factor receptor (PDGFRA) were enriched in vascular regions (Little et al., 2012). Similarly, hypoxic TME induced by anti-angiogenic agents can increase breast CSCs (Conley et al., 2012). Hypoxia can be acute, chronic or cyclic (intermittent), each with its unique effects on tumor progression (Saxena and Jolly, 2019). Thus, spatial heterogeneity of TME can give rise to differential spatial organization of cancer sub-populations within a tumor.

Varying levels of nuclear β-catenin expression was observed in different sub-populations of well-differentiated colorectal cancer, suggested to be regulated by TME (Brabletz et al., 2001). Cells in the invasive front of the primary tumor as well as metastases expressed high levels of nuclear β-catenin, and lacked the expression of membranous E-cadherin, indicative of an EMT. On the other hand, centrally located cells in the primary tumor and metastases showed cytoplasmic β-catenin and membranous E-cadherin expression, perhaps due to a mesenchymal-epithelial transition (MET) (Brabletz et al., 2001). Spatial heterogeneity with respect to EMT has been reported since in primary tumor (Jung et al., 2001; Schmalhofer et al., 2009; Bronsert et al., 2014; Liu et al., 2014; Grigore et al., 2016). Consistently, $CD24^{-}CD44^{+}$ mesenchymal breast CSCs were found in the invasive edge of the tumor, while the more epithelial or hybrid E/M CSCs, identified by ALDH1+, were localized in the interior regions of the tumor (Liu et al., 2014). Put together, these observations beg the question of what mechanisms might underlie such patterning. Recent efforts including a mathematical modeling analysis revealed that in the presence of a gradient of TGF-β (EMT inducing) signal, cell-cell communication among tumor cells mediated via Notch-Jagged signaling can recapitulate the experimentally observed spatial organization of CSCs sub-populations with varying EMT phenotypes (Bocci et al., 2019). *In vitro* knock down of JAG1 in SUM149 human breast cancer cells significantly reduced their tumor organoid formation, confirming the role of Notch-Jagged signaling in tumor progression (Bocci et al., 2019). Future studies can focus on gaining a understanding of other interconnected aspects of heterogeneity in TME.

Spatial heterogeneity of tumors can be used as a predictor of cancer prognosis and treatment response across different cancer types (Yuan, 2016). For example, colorectal cancer patients with high density of tumor infiltrating lymphocytes responded to anti-cancer therapy (Gong et al., 2018). Spatial heterogeneity can also significantly impact the time to occurrence in cancer cells exposed to continuous as well as adaptive therapies (Gallaher et al., 2018). Thus, the spatiotemporal dynamics of phenotypic changes induced by TME can be pivotal in aggravating aspects of tumor progression.

METABOLIC PLASTICITY OF CSCS

Ever since Otto Warburg's observation that cancer cells, unlike normal cells preferentially rely on glycolysis for energy production even under aerobic conditions, referred to as aerobic glycolysis or Warburg effect (Warburg et al., 1927), metabolic adaptation of cancer has been under extensive investigation (Liberti and Locasale, 2016; Peiris-Pages et al., 2016). To meet

the varying metabolic demands set by the microenvironment during the course of tumor progression and to survive, cancer cells must dynamically rewire their metabolic phenotype and has been recognized as a hallmark feature of cancer (Hanahan and Weinberg, 2011). This ability to adapt is critical for tumor growth, metastasis and response to therapy (Dupuy et al., 2015; Luo and Wicha, 2015). Metabolic plasticity, also contributes to the tumor heterogeneity (Lehuede et al., 2016; De Francesco et al., 2018). Emerging evidence suggest that CSCs display extensive metabolic plasticity and can reprogramme their metabolism in a context dependent manner in response to the cues from the microenvironment (Albini et al., 2015; Sancho et al., 2016). Also, non-CSCs can acquire a stem-like character through changing the metabolic phenotype. This acquired stemness by altering metabolism is an emerging hallmark of cancer, known as "metabostemness" and contributes to the CSC plasticity (Menendez and Alarcon, 2014; De Francesco et al., 2018). There is no consensus regarding the metabolic phenotype of CSCs (Peiris-Pages et al., 2016). Although many reports show that CSCs are more glycolytic than the other differentiated cells, several other conflicting reports suggest that they prefer mitochondrial oxidative phosphorylation (OXPHOS). For example, CSC from the breast, lung, and colon cancers have been found to show higher glycolytic activity than the other cells (Ciavardelli et al., 2014; Liu et al., 2014). On the other hand, CSCs from pancreatic cancer and leukemia depend on OXPHOS for energy production (Skrtic et al., 2011; Lonardo et al., 2013; Sancho et al., 2015). Also, studies have shown that CSCs could switch from one metabolic state to another in response to various challenges microenvironment like pH, hypoxia and nutritional status (Singh et al., 2004; Sancho et al., 2015; Chae and Kim, 2018). This apparent discrepancy in these observations could be due to multiple reasons. One reason could be the intrinsic differences between the metabolic phenotype of different cancer types from which they were derived (Kim and DeBerardinis, 2019). Another major reason could be the metabolic plasticity of CSCs, existence of multiple CSC subsets, each of which may have an increased proclivity to exhibit a particular metabolic phenotype, reminiscent of observations for varying degrees of stemness observed along the spectrum of EMT states (Gammon et al., 2013; Peiris-Pages et al., 2016; Bocci et al., 2018). The inherent limitation associated with the use of distinct markers/techniques for the isolation and characterization of CSCs in these studies can be another confounding factor (Sancho et al., 2016; Snyder et al., 2018; Martano et al., 2019). Also, the preference of metabolic states relies heavily on the microenvironmental conditions, differences in the nutrient availability at the primary and metastatic sites (Dupuy et al., 2015; Pascual et al., 2018) and the co-operation (Pavlides et al., 2009) or competition with the stromal cells (Chang et al., 2015). The cause for the differences in the metabolic states are also often attributed to alterations in the mitochondrial mass, mitochondrial dynamics, biogenesis and mitochondrial DNA content (Guha et al., 2014; De Luca et al., 2015; Farnie et al., 2015; De Francesco et al., 2018). Metabolic reprogramming can be orchestrated by a wide array of signaling pathways (Ito and Suda, 2014; Papa et al., 2019). For example, overexpression WNT1/FGF3 signaling in MCF7 resulted in increased stemness by increased mitochondrial mass and thereby increasing the mitochondrial respiration (Lamb et al., 2015). Thus, various different cell-intrinsic and cell-extrinsic factors may modulate the "metabostemness."

In addition to switching between glycolytic and OXPHOS phenotype, CSCs have also been shown to coopt these two pathways and exist in a hybrid metabolic state as suggested by recent studies (Yu et al., 2017). So, it is imperative to use drugs that block both glycolysis and OXPHOS to target CSC plasticity and has been found to inhibit tumor growth and metastasis (Cheong et al., 2011; Peiris-Pages et al., 2016). For instance, combining fasting induced hypoglycemia (to reduce glycolysis) with metformin, an OXPHOS inhibitor has impaired the metabolic plasticity of cancer cells by regulating PP2A-GSK3β-MCL-1 Axis (Elgendy et al., 2019).

Although most studies have focused on the glucose metabolism, the involvement of other metabolic pathways like lipid and amino acid metabolism still needs to be investigated further. A better understanding of the metabolic phenotypes and plasticity of CSC is required for the effective elimination of these cells.

DISCUSSION

The issue of phenotypic plasticity presents a clear and present danger in the treatment of cancer patients. Accumulating evidence suggests that CSCs consist of different sub-populations that can interconvert among different states through intracellular and intercellular regulatory networks. Over expression of one or more transcription factors or activating trans-differentiation processes such as EMT and metabolic alterations can drive the switch among CSCs and non-CSCs as well as between different subsets of CSCs. These adaptive strategies adopted by cells must be taken into account while devising new therapeutic strategies in the clinic in order to target all populations effectively.

The challenges to addressing this issue are multifold. The ability to identify the plastic CSC population using markers has its inherent problems which are further confounded by each individual patient's unique biochemical and biomechanical signatures. The general consensus is that drug resistance is achieved through a transition to a slow cycling state which is reversible once the stress is removed (De Angelis et al., 2019). Understanding how the cells switch from a slow cycling state and reenter the proliferative phase of the cell cycle will be key to targeting this population which contributes to minimal residual disease.

Using latest developments in computational and experimental methods will allow us to map the different states of tumor cells within multiple locations in a tumor, thus enabling a more comprehensive view of the genetic and non-genetic heterogeneity that exists within a cancer. Correlating such intratumoral heterogeneity with cellular phenotypes will be key to

devising better therapeutic options in patients to ablate the tumor cells stably within a patient.

AUTHOR CONTRIBUTIONS

RN and MJ designed the review. AT, KS, RM, MJ and RN wrote, read, and approved of the manuscript.

FUNDING

This work was supported by Ramanujan Fellowship awarded to RN (SB/S2/RJN/182/2014) and to MJ (SB/S2/RJN-049/2018) provided by Science and Engineering Research Board (SERB), Department of Science and Technology (DST), Government of India. AT was supported by CSIR (Council of Scientific Industrial Research) – Junior research fellowship.

REFERENCES

Agliano, A., Calvo, A., and Box, C. (2017). The challenge of targeting cancer stem cells to halt metastasis. *Semin. Cancer Biol.* 44, 25–42. doi: 10.1016/j.semcancer.2017.03.003

Akgul, S., Patch, A. M., D'Souza, R. C. J., Mukhopadhyay, P., Nones, K., Kempe, S., et al. (2019). Intratumoural heterogeneity underlies distinct therapy responses and treatment resistance in glioblastoma. *Cancers (Basel)* 11:190. doi: 10.3390/cancers11020190

Akrap, N., Andersson, D., Bom, E., Gregersson, P., Stahlberg, A., and Landberg, G. (2016). Identification of distinct breast cancer stem cell populations based on single-cell analyses of functionally enriched stem and progenitor pools. *Stem Cell Rep.* 6, 121–136. doi: 10.1016/j.stemcr.2015.12.006

Albini, A., Bruno, A., Gallo, C., Pajardi, G., Noonan, D. M., and Dallaglio, K. (2015). Cancer stem cells and the tumor microenvironment: interplay in tumor heterogeneity. *Connect. Tissue Res.* 56, 414–425. doi: 10.3109/03008207.2015.1066780

Alfarouk, K. O., Ibrahim, M. E., Gatenby, R. A., and Brown, J. S. (2013). Riparian ecosystems in human cancers. *Evol. Appl.* 6, 46–53. doi: 10.1111/eva.12015

Al-Hajj, M., Wicha, M. S., Benito-Hernandez, A., Morrison, S. J., and Clarke, M. F. (2003). Prospective identification of tumorigenic breast cancer cells. *Proc. Natl. Acad. Sci. U.S.A.* 100, 3983–3988.

Altrock, P. M., Liu, L. L., and Michor, F. (2015). The mathematics of cancer: integrating quantitative models. *Nat. Rev. Cancer* 15, 730–745. doi: 10.1038/nrc4029

Aponte, P. M., and Caicedo, A. (2017). Stemness in cancer: stem cells, cancer stem cells, and their microenvironment. *Stem Cells Int.* 2017:5619472.

Babahosseini, H., Ketene, A. N., Schmelz, E. M., Roberts, P. C., and Agah, M. (2014). Biomechanical profile of cancer stem-like/tumor-initiating cells derived from a progressive ovarian cancer model. *Nanomedicine* 10, 1013–1019.

Bachman, J. W., and Hillen, T. (2013). Mathematical optimization of the combination of radiation and differentiation therapies for cancer. *Front. Oncol.* 3:52. doi: 10.3389/fonc.2013.00052

Begum, A., McMillan, R. H., Chang, Y. T., Penchev, V. R., Rajeshkumar, N. V., Maitra, A., et al. (2019). Direct interactions with cancer-associated fibroblasts lead to enhanced pancreatic cancer stem cell function. *Pancreas* 48, 329–334. doi: 10.1097/mpa.0000000000001249

Bekaii-Saab, T., and El-Rayes, B. (2017). Identifying and targeting cancer stem cells in the treatment of gastric cancer. *Cancer* 123, 1303–1312. doi: 10.1002/cncr.30538

Ben-Porath, I., Thomson, M. W., Carey, V. J., Ge, R., Bell, G. W., Regev, A., et al. (2008). An embryonic stem cell-like gene expression signature in poorly differentiated aggressive human tumors. *Nat. Genet.* 40, 499–507. doi: 10.1038/ng.127

Bhatia, S., Monkman, J., Blick, T., Pinto, C., Waltham, M., Nagaraj, S. H., et al. (2019). Interrogation of phenotypic plasticity between epithelial and mesenchymal states in breast cancer. *J. Clin. Med.* 8:893. doi: 10.3390/jcm8060893

Biddle, A., Gammon, L., Liang, X., Costea, D. E., and Mackenzie, I. C. (2016). Phenotypic plasticity determines cancer stem cell therapeutic resistance in oral squamous cell carcinoma. *EBioMedicine* 4, 138–145. doi: 10.1016/j.ebiom.2016.01.007

Bierie, B., Pierce, S. E., Kroeger, C., Stover, D. G., Pattabiraman, D. R., Thiru, P., et al. (2017). Integrin-beta4 identifies cancer stem cell-enriched populations of partially mesenchymal carcinoma cells. *Proc. Natl. Acad. Sci. U.S.A.* 114, E2337–E2346.

Bocci, F., Gearhart-Serna, L., Boareto, M., Ribeiro, M., Ben-Jacob, E., Devi, G. R., et al. (2019). Toward understanding cancer stem cell heterogeneity in the tumor microenvironment. *Proc. Natl. Acad. Sci. U.S.A.* 116, 148–157. doi: 10.1073/pnas.1815345116

Bocci, F., Jolly, M. K., George, J. T., Levine, H., and Onuchic, J. N. (2018). A mechanism-based computational model to capture the interconnections among epithelial-mesenchymal transition, cancer stem cells and Notch-Jagged signaling. *Oncotarget* 9, 29906–29920.

Bongiorno, T., Gura, J., Talwar, P., Chambers, D., Young, K. M., Arafat, D., et al. (2018). Biophysical subsets of embryonic stem cells display distinct phenotypic and morphological signatures. *PLoS One* 13:e0192631. doi: 10.1371/journal.pone.0192631

Brabletz, T., Jung, A., Reu, S., Porzner, M., Hlubek, F., Kunz-Schughart, L. A., et al. (2001). Variable beta-catenin expression in colorectal cancers indicates tumor progression driven by the tumor environment. *Proc. Natl. Acad. Sci. U.S.A.* 98, 10356–10361. doi: 10.1073/pnas.171610498

Broders-Bondon, F., Nguyen, T. H., Ho-Bouldoires, M., Fernandez-Sanchez, E., and Farge, E. (2018). Mechanotransduction in tumor progression: the dark side of the force. *J. Cell Biol.* 217, 1571–1587. doi: 10.1083/jcb.201701039

Bronsert, P., Enderle-Ammour, K., Bader, M., Timme, S., Kuehs, M., Csanadi, A., et al. (2014). Cancer cell invasion and EMT marker expression: a three-dimensional study of the human cancer-host interface. *J. Pathol.* 234, 410–422. doi: 10.1002/path.4416

Bussolati, B., Bruno, S., Grange, C., Ferrando, U., and Camussi, G. (2008). Identification of a tumor-initiating stem cell population in human renal carcinomas. *FASEB J.* 22, 3696–3705. doi: 10.1096/fj.08-102590

Byun, S., Son, S., Amodei, D., Cermak, N., Shaw, J., Kang, J. H., et al. (2013). Characterizing deformability and surface friction of cancer cells. *Proc. Natl. Acad. Sci. U.S.A.* 110, 7580–7585. doi: 10.1073/pnas.1218806110

Cabrera, M. C., Hollingsworth, R. E., and Hurt, E. M. (2015). Cancer stem cell plasticity and tumor hierarchy. *World J. Stem Cells* 7, 27–36.

Celia-Terrassa, T., Bastian, C., Liu, D. D., Ell, B., Aiello, N. M., Wei, Y., et al. (2018). Hysteresis control of epithelial-mesenchymal transition dynamics conveys a distinct program with enhanced metastatic ability. *Nat. Commun.* 9:5005.

Celia-Terrassa, T., and Jolly, M. K. (2019). Cancer stem cells and epithelial-to-mesenchymal transition in cancer metastasis. *Cold Spring Harb. Perspect. Med.* doi: 10.1101/cshperspect.a036905

Chae, Y. C., and Kim, J. H. (2018). Cancer stem cell metabolism: target for cancer therapy. *BMB Rep.* 51, 319–326. doi: 10.5483/bmbrep.2018.51.7.112

Chaffer, C. L., Brueckmann, I., Scheel, C., Kaestli, A. J., Wiggins, P. A., Rodrigues, L. O., et al. (2011). Normal and neoplastic nonstem cells can spontaneously convert to a stem-like state. *Proc. Natl. Acad. Sci. U.S.A.* 108, 7950–7955. doi: 10.1073/pnas.1102454108

Chaffer, C. L., Marjanovic, N. D., Lee, T., Bell, G., Kleer, C. G., Reinhardt, F., et al. (2013). Poised chromatin at the ZEB1 promoter enables breast cancer cell plasticity and enhances tumorigenicity. *Cell* 154, 61–74. doi: 10.1016/j.cell.2013.06.005

Chang, C. H., Qiu, J., O'Sullivan, D., Buck, M. D., Noguchi, T., Curtis, J. D., et al. (2015). Metabolic competition in the tumor microenvironment is a driver of cancer progression. *Cell* 162, 1229–1241. doi: 10.1016/j.cell.2015.08.016

Chang, C. J., Yang, J. Y., Xia, W., Chen, C. T., Xie, X., Chao, C. H., et al. (2011). EZH2 promotes expansion of breast tumor initiating cells through activation of

RAF1-beta-catenin signaling. *Cancer Cell* 19, 86–100. doi: 10.1016/j.ccr.2010.10.035

Chen, J., and Kumar, S. (2017). Biophysical regulation of cancer stem/initiating cells: implications for disease mechanisms and translation. *Curr. Opin. Biomed. Eng.* 1, 87–95. doi: 10.1016/j.cobme.2017.02.006

Chen, J., Zhou, W., Jia, Q., Chen, J., Zhang, S., Yao, W., et al. (2016). Efficient extravasation of tumor-repopulating cells depends on cell deformability. *Sci. Rep.* 6:19304.

Chen, K., Huang, Y. H., and Chen, J. L. (2013). Understanding and targeting cancer stem cells: therapeutic implications and challenges. *Acta Pharmacol. Sin.* 34, 732–740. doi: 10.1038/aps.2013.27

Chen, K. H., Boettiger, A. N., Moffitt, J. R., Wang, S., and Zhuang, X. (2015). RNA imaging. Spatially resolved, highly multiplexed RNA profiling in single cells. *Science* 348:aaa6090. doi: 10.1126/science.aaa6090

Chen, W., Allen, S. G., Qian, W., Peng, Z., Han, S., Li, X., et al. (2019). Biophysical phenotyping and modulation of ALDH+ inflammatory breast cancer stem-like cells. *Small* 15:e1802891.

Chen, W., Dong, J., Haiech, J., Kilhoffer, M. C., and Zeniou, M. (2016). Cancer stem cell quiescence and plasticity as major challenges in cancer therapy. *Stem Cells Int.* 2016:1740936.

Chen, W. J., Ho, C. C., Chang, Y. L., Chen, H. Y., Lin, C. A., Ling, T. Y., et al. (2014). Cancer-associated fibroblasts regulate the plasticity of lung cancer stemness via paracrine signalling. *Nat. Commun.* 5:3472.

Cheong, J. H., Park, E. S., Liang, J., Dennison, J. B., Tsavachidou, D., Nguyen-Charles, C., et al. (2011). Dual inhibition of tumor energy pathway by 2-deoxyglucose and metformin is effective against a broad spectrum of preclinical cancer models. *Mol. Cancer Ther.* 10, 2350–2362. doi: 10.1158/1535-7163.mct-11-0497

Chumakova, A. P., Hitomi, M., Sulman, E. P., and Lathia, J. D. (2019). High-throughput Automated single-cell imaging analysis reveals dynamics of glioblastoma stem cell population during state transition. *Cytometry A* 95, 290–301. doi: 10.1002/cyto.a.23728

Ciavardelli, D., Rossi, C., Barcaroli, D., Volpe, S., Consalvo, A., Zucchelli, M., et al. (2014). Breast cancer stem cells rely on fermentative glycolysis and are sensitive to 2-deoxyglucose treatment. *Cell Death Dis.* 5:e1336. doi: 10.1038/cddis.2014.285

Collins, A. T., Berry, P. A., Hyde, C., Stower, M. J., and Maitland, N. J. (2005). Prospective identification of tumorigenic prostate cancer stem cells. *Cancer Res.* 65, 10946–10951. doi: 10.1158/0008-5472.can-05-2018

Conley, S. J., Gheordunescu, E., Kakarala, P., Newman, B., Korkaya, H., Heath, A. N., et al. (2012). Antiangiogenic agents increase breast cancer stem cells via the generation of tumor hypoxia. *Proc. Natl. Acad. Sci. U.S.A.* 109, 2784–2789. doi: 10.1073/pnas.1018866109

da Silva-Diz, V., Lorenzo-Sanz, L., Bernat-Peguera, A., Lopez-Cerda, M., and Munoz, P. (2018). Cancer cell plasticity: impact on tumor progression and therapy response. *Semin. Cancer Biol.* 53, 48–58. doi: 10.1016/j.semcancer.2018.08.009

Dagogo-Jack, I., and Shaw, A. T. (2018). Tumour heterogeneity and resistance to cancer therapies. *Nat. Rev. Clin. Oncol.* 15, 81–94. doi: 10.1038/nrclinonc.2017.166

De Angelis, M. L., Francescangeli, F., La Torre, F., and Zeuner, A. (2019). Stem cell plasticity and dormancy in the development of cancer therapy resistance. *Front. Oncol.* 9:626. doi: 10.3389/fonc.2019.00626

De Francesco, E. M., Sotgia, F., and Lisanti, M. P. (2018). Cancer stem cells (CSCs): metabolic strategies for their identification and eradication. *Biochem. J.* 475, 1611–1634. doi: 10.1042/bcj20170164

De Luca, A., Fiorillo, M., Peiris-Pages, M., Ozsvari, B., Smith, D. L., Sanchez-Alvarez, R., et al. (2015). Mitochondrial biogenesis is required for the anchorage-independent survival and propagation of stem-like cancer cells. *Oncotarget* 6, 14777–14795.

de Sousa e Melo, F., Kurtova, A. V., Harnoss, J. M., Kljavin, N., Hoeck, J. D., Hung, J., et al. (2017). A distinct role for Lgr5(+) stem cells in primary and metastatic colon cancer. *Nature* 543, 676–680. doi: 10.1038/nature21713

Di Carlo, C., Brandi, J., and Cecconi, D. (2018). Pancreatic cancer stem cells: perspectives on potential therapeutic approaches of pancreatic ductal adenocarcinoma. *World J. Stem Cells* 10, 172–182. doi: 10.4252/wjsc.v10.i11.172

Dirkse, A., Golebiewska, A., Buder, T., Nazarov, P. V., Muller, A., Poovathingal, S., et al. (2019). Stem cell-associated heterogeneity in glioblastoma results from intrinsic tumor plasticity shaped by the microenvironment. *Nat. Commun.* 10:1787.

Doherty, M. R., Parvani, J. G., Tamagno, I., Junk, D. J., Bryson, B. L., Cheon, H. J., et al. (2019). The opposing effects of interferon-beta and oncostatin-M as regulators of cancer stem cell plasticity in triple-negative breast cancer. *Breast Cancer Res.* 21:54.

Doherty, M. R., Smigiel, J. M., Junk, D. J., and Jackson, M. W. (2016). Cancer stem cell plasticity drives therapeutic resistance. *Cancers (Basel)* 8:8. doi: 10.3390/cancers8010008

Dongre, A., and Weinberg, R. A. (2019). New insights into the mechanisms of epithelial-mesenchymal transition and implications for cancer. *Nat. Rev. Mol. Cell. Biol.* 20, 69–84. doi: 10.1038/s41580-018-0080-4

Du, Y., Shao, H., Moller, M., Prokupets, R., Tse, Y. T., and Liu, Z. J. (2019). Intracellular Notch1 signaling in cancer-associated fibroblasts dictates the plasticity and stemness of melanoma stem/initiating cells. *Stem Cells* 37, 865–875. doi: 10.1002/stem.3013

Dupuy, F., Tabaries, S., Andrzejewski, S., Dong, Z., Blagih, J., Annis, M. G., et al. (2015). PDK1-Dependent metabolic reprogramming dictates metastatic potential in breast cancer. *Cell Metab.* 22, 577–589. doi: 10.1016/j.cmet.2015.08.007

Easwaran, H., Tsai, H. C., and Baylin, S. B. (2014). Cancer epigenetics: tumor heterogeneity, plasticity of stem-like states, and drug resistance. *Mol. Cell* 54, 716–727. doi: 10.1016/j.molcel.2014.05.015

Edsgard, D., Johnsson, P., and Sandberg, R. (2018). Identification of spatial expression trends in single-cell gene expression data. *Nat. Methods* 15, 339–342. doi: 10.1038/nmeth.4634

Eirew, P., Steif, A., Khattra, J., Ha, G., Yap, D., Farahani, H., et al. (2015). Dynamics of genomic clones in breast cancer patient xenografts at single-cell resolution. *Nature* 518, 422–426.

Elgendy, M., Ciro, M., Hosseini, A., Weiszmann, J., Mazzarella, L., Ferrari, E., et al. (2019). Combination of hypoglycemia and metformin impairs tumor metabolic plasticity and growth by modulating the PP2A-GSK3beta-MCL-1 Axis. *Cancer Cell* 35, 798–815.e5. doi: 10.1016/j.ccell.2019.03.007

Enderling, H. (2015). Cancer stem cells: small subpopulation or evolving fraction? *Integr. Biol. (Camb)* 7, 14–23. doi: 10.1039/c4ib00191e

Etzrodt, M., Endele, M., and Schroeder, T. (2014). Quantitative single-cell approaches to stem cell research. *Cell Stem Cell* 15, 546–558. doi: 10.1016/j.stem.2014.10.015

Eun, K., Ham, S. W., and Kim, H. (2017). Cancer stem cell heterogeneity: origin and new perspectives on CSC targeting. *BMB Rep.* 50, 117–125. doi: 10.5483/bmbrep.2017.50.3.222

Fang, D., Nguyen, T. K., Leishear, K., Finko, R., Kulp, A. N., Hotz, S., et al. (2005). A tumorigenic subpopulation with stem cell properties in melanomas. *Cancer Res.* 65, 9328–9337. doi: 10.1158/0008-5472.can-05-1343

Farnie, G., Sotgia, F., and Lisanti, M. P. (2015). High mitochondrial mass identifies a sub-population of stem-like cancer cells that are chemo-resistant. *Oncotarget* 6, 30472–30486.

Fernandez-Cortes, M., Delgado-Bellido, D., and Oliver, F. J. (2019). Vasculogenic mimicry: become an endothelial cell but not so much. *Front. Oncol.* 9:803. doi: 10.3389/fonc.2019.00803

Fumagalli, A., Bruens, L., Scheele, C., and van Rheenen, J. (2019). Capturing stem cell behavior using intravital and live cell microscopy. *Cold Spring Harb. Perspect. Biol.* doi: 10.1101/cshperspect.a035949

Fumagalli, A., Oost, K. C., Kester, L., Morgner, J., Bornes, L., Bruens, L., et al. (2020). Plasticity of Lgr5-negative cancer cells drives metastasis in colorectal cancer. *Cell Stem Cell* 26, 569–578.e7.

Gallaher, J. A., Enriquez-Navas, P. M., Luddy, K. A., Gatenby, R. A., and Anderson, A. R. A. (2018). Spatial heterogeneity and evolutionary dynamics modulate time to recurrence in continuous and adaptive cancer therapies. *Cancer Res.* 78, 2127–2139. doi: 10.1158/0008-5472.can-17-2649

Gammon, L., Biddle, A., Heywood, H. K., Johannessen, A. C., and Mackenzie, I. C. (2013). Sub-sets of cancer stem cells differ intrinsically in their patterns of oxygen metabolism. *PLoS One* 8:e62493. doi: 10.1371/journal.pone.0062493

Gan, L., Yang, Y., Li, Q., Feng, Y., Liu, T., and Guo, W. (2018). Epigenetic regulation of cancer progression by EZH2: from biological insights to therapeutic potential. *Biomark Res.* 6:10.

George, J. T., Jolly, M. K., Xu, S., Somarelli, J. A., and Levine, H. (2017). Survival outcomes in cancer patients predicted by a partial EMT gene expression scoring metric. *Cancer Res.* 77, 6415–6428. doi: 10.1158/0008-5472.can-16-3521

Giannone, G., Attademo, L., Scotto, G., Genta, S., Ghisoni, E., Tuninetti, V., et al. (2019). Endometrial cancer stem cells: role, characterization and therapeutic implications. *Cancers (Basel)* 11:1820. doi: 10.3390/cancers11111820

Giraddi, R. R., Chung, C. Y., Heinz, R. E., Balcioglu, O., Novotny, M., Trejo, C. L., et al. (2018). Single-cell transcriptomes distinguish stem cell state changes and lineage specification programs in early mammary gland development. *Cell Rep.* 24, 1653–1666.e7. doi: 10.1016/j.celrep.2018.07.025

Goldman, A., Majumder, B., Dhawan, A., Ravi, S., Goldman, D., Kohandel, M., et al. (2015). Temporally sequenced anticancer drugs overcome adaptive resistance by targeting a vulnerable chemotherapy-induced phenotypic transition. *Nat. Commun.* 6:6139.

Gong, C., Anders, R. A., Zhu, Q., Taube, J. M., Green, B., Cheng, W., et al. (2018). Quantitative characterization of CD8+ T cell clustering and spatial heterogeneity in solid tumors. *Front. Oncol.* 8:649. doi: 10.3389/fonc.2018.00649

Gossett, D. R., Tse, H. T., Lee, S. A., Ying, Y., Lindgren, A. G., Yang, O. O., et al. (2012). Hydrodynamic stretching of single cells for large population mechanical phenotyping. *Proc. Natl. Acad. Sci. U.S.A.* 109, 7630–7635. doi: 10.1073/pnas.1200107109

Greve, B., Kelsch, R., Spaniol, K., Eich, H. T., and Gotte, M. (2012). Flow cytometry in cancer stem cell analysis and separation. *Cytometry A* 81, 284–293. doi: 10.1002/cyto.a.22022

Grigore, A. D., Jolly, M. K., Jia, D., Farach-Carson, M. C., and Levine, H. (2016). Tumor budding: the name is EMT. Partial EMT. *J. Clin. Med.* 5:51. doi: 10.3390/jcm5050051

Grosse-Wilde, A., d'Herouel, A., McIntosh, E., Ertaylan, G., Skupin, A., Kuestner, R. E., et al. (2015). Stemness of the hybrid epithelial/mesenchymal state in breast cancer and its association with poor survival. *PLoS One* 10:e0126522. doi: 10.1371/journal.pone.0126522

Gu, G., Yuan, J., Wills, M., and Kasper, S. (2007). Prostate cancer cells with stem cell characteristics reconstitute the original human tumor in vivo. *Cancer Res* 67, 4807–4815. doi: 10.1158/0008-5472.can-06-4608

Guha, M., Srinivasan, S., Ruthel, G., Kashina, A. K., Carstens, R. P., Mendoza, A., et al. (2014). Mitochondrial retrograde signaling induces epithelial-mesenchymal transition and generates breast cancer stem cells. *Oncogene* 33, 5238–5250. doi: 10.1038/onc.2013.467

Gupta, P. B., Fillmore, C. M., Jiang, G., Shapira, S. D., Tao, K., Kuperwasser, C., et al. (2011). Stochastic state transitions give rise to phenotypic equilibrium in populations of cancer cells. *Cell* 146, 633–644. doi: 10.1016/j.cell.2011.07.026

Gupta, P. B., Pastushenko, I., Skibinski, A., Blanpain, C., and Kuperwasser, C. (2019). Phenotypic plasticity: driver of cancer initiation, progression, and therapy resistance. *Cell Stem Cell* 24, 65–78. doi: 10.1016/j.stem.2018.11.011

Hanahan, D., and Weinberg, R. A. (2011). Hallmarks of cancer: the next generation. *Cell* 144, 646–674. doi: 10.1016/j.cell.2011.02.013

Hari, K., Sabuwala, B., Subramani, B. V., La Porta, C. A. M., Zapperi, S., Font-Clos, F., et al. (2019). Identifying inhibitors of epithelial-mesenchymal plasticity using a network topology based approach. *bioRxiv* [Preprint]. doi: 10.1101/854307

Heddleston, J. M., Li, Z., McLendon, R. E., Hjelmeland, A. B., and Rich, J. N. (2009). The hypoxic microenvironment maintains glioblastoma stem cells and promotes reprogramming towards a cancer stem cell phenotype. *Cell Cycle* 8, 3274–3284. doi: 10.4161/cc.8.20.9701

Hillen, T., Enderling, H., and Hahnfeldt, P. (2013). The tumor growth paradox and immune system-mediated selection for cancer stem cells. *Bull. Math. Biol.* 75, 161–184. doi: 10.1007/s11538-012-9798-x

Hjelmeland, A. B., Wu, Q., Heddleston, J. M., Choudhary, G. S., MacSwords, J., Lathia, J. D., et al. (2011). Acidic stress promotes a glioma stem cell phenotype. *Cell Death Differ.* 18, 829–840. doi: 10.1038/cdd.2010.150

Hou, Y., Guo, H., Cao, C., Li, X., Hu, B., Zhu, P., et al. (2016). Single-cell triple omics sequencing reveals genetic, epigenetic, and transcriptomic heterogeneity in hepatocellular carcinomas. *Cell Res.* 26, 304–319. doi: 10.1038/cr.2016.23

Iliopoulos, D., Hirsch, H. A., Wang, G., and Struhl, K. (2011). Inducible formation of breast cancer stem cells and their dynamic equilibrium with non-stem cancer cells via IL6 secretion. *Proc. Natl. Acad. Sci. U.S.A.* 108, 1397–1402. doi: 10.1073/pnas.1018898108

Ito, K., and Suda, T. (2014). Metabolic requirements for the maintenance of self-renewing stem cells. *Nat. Rev. Mol. Cell. Biol.* 15, 243–256. doi: 10.1038/nrm3772

Jaggupilli, A., and Elkord, E. (2012). Significance of CD44 and CD24 as cancer stem cell markers: an enduring ambiguity. *Clin. Dev. Immunol.* 2012:708036.

Januskeviciene, I., and Petrikaite, V. (2019). Heterogeneity of breast cancer: the importance of interaction between different tumor cell populations. *Life Sci.* 239:117009. doi: 10.1016/j.lfs.2019.117009

Jia, D., Jolly, M. K., Tripathi, S. C., Den Hollander, P., Huang, B., Lu, M., et al. (2017). Distinguishing mechanisms underlying EMT tristability. *Cancer Converg.* 1:2.

Jolly, M. K., Huang, B., Lu, M., Mani, S. A., Levine, H., and Ben-Jacob, E. (2014). Towards elucidating the connection between epithelial-mesenchymal transitions and stemness. *J. R. Soc. Interface* 11:20140962. doi: 10.1098/rsif.2014.0962

Jolly, M. K., Kulkarni, P., Weninger, K., Orban, J., and Levine, H. (2018a). Phenotypic plasticity, bet-hedging, and androgen independence in prostate cancer: role of non-genetic heterogeneity. *Front. Oncol.* 8:50. doi: 10.3389/fonc.2018.00050

Jolly, M. K., Mani, S. A., and Levine, H. (2018b). Hybrid epithelial/mesenchymal phenotype(s): the 'fittest' for metastasis? *Biochim. Biophys. Acta Rev. Cancer* 1870, 151–157. doi: 10.1016/j.bbcan.2018.07.001

Jolly, M. K., Preca, B. T., Tripathi, S. C., Jia, D., George, J. T., Hanash, S. M., et al. (2018c). Interconnected feedback loops among ESRP1, HAS2, and CD44 regulate epithelial-mesenchymal plasticity in cancer. *APL Bioeng.* 2:031908. doi: 10.1063/1.5024874

Jolly, M. K., Somarelli, J. A., Sheth, M., Biddle, A., Tripathi, S. C., Armstrong, A. J., et al. (2019). Hybrid epithelial/mesenchymal phenotypes promote metastasis and therapy resistance across carcinomas. *Pharmacol. Ther.* 194, 161–184. doi: 10.1016/j.pharmthera.2018.09.007

Jolly, M. K., Tripathi, S. C., Somarelli, J. A., Hanash, S. M., and Levine, H. (2017). Epithelial/mesenchymal plasticity: how have quantitative mathematical models helped improve our understanding? *Mol. Oncol.* 11, 739–754. doi: 10.1002/1878-0261.12084

Jolly, M. K., Ward, C., Eapen, M. S., Myers, S., Hallgren, O., Levine, H., et al. (2018d). Epithelial-mesenchymal transition, a spectrum of states: role in lung development, homeostasis, and disease. *Dev. Dyn.* 247, 346–358. doi: 10.1002/dvdy.24541

Jonasson, E., Ghannoum, S., Persson, E., Karlsson, J., Kroneis, T., Larsson, E., et al. (2019). Identification of breast cancer stem cell related genes using functional cellular assays combined with single-cell RNA sequencing in MDA-MB-231 cells. *Front. Genet.* 10:500. doi: 10.3389/fgene.2019.00500

Jung, A., Schrauder, M., Oswald, U., Knoll, C., Sellberg, P., Palmqvist, R., et al. (2001). The invasion front of human colorectal adenocarcinomas shows co-localization of nuclear beta-catenin, cyclin D1, and p16INK4A and is a region of low proliferation. *Am. J. Pathol.* 159, 1613–1617. doi: 10.1016/s0002-9440(10)63007-6

Junk, D. J., Bryson, B. L., Smigiel, J. M., Parameswaran, N., Bartel, C. A., and Jackson, M. W. (2017). Oncostatin M promotes cancer cell plasticity through cooperative STAT3-SMAD3 signaling. *Oncogene* 36, 4001–4013. doi: 10.1038/onc.2017.33

Kalluri, R., and Weinberg, R. A. (2009). The basics of epithelial-mesenchymal transition. *J Clin Invest* 119, 1420–1428. doi: 10.1172/jci39104

Kim, H., Lin, Q., Glazer, P. M., and Yun, Z. (2018). The hypoxic tumor microenvironment in vivo selects the cancer stem cell fate of breast cancer cells. *Breast Cancer Res.* 20:16.

Kim, J., and DeBerardinis, R. J. (2019). Mechanisms and implications of metabolic heterogeneity in cancer. *Cell Metab.* 30, 434–446. doi: 10.1016/j.cmet.2019.08.013

Kobayashi, S., Yamada-Okabe, H., Suzuki, M., Natori, O., Kato, A., Matsubara, K., et al. (2012). LGR5-positive colon cancer stem cells interconvert with drug-resistant LGR5-negative cells and are capable of tumor reconstitution. *Stem Cells* 30, 2631–2644. doi: 10.1002/stem.1257

Korkaya, H., Liu, S., and Wicha, M. S. (2011). Breast cancer stem cells, cytokine networks, and the tumor microenvironment. *J. Clin. Invest.* 121, 3804–3809.

Kraning-Rush, C. M., Califano, J. P., and Reinhart-King, C. A. (2012). Cellular traction stresses increase with increasing metastatic potential. *PLoS One* 7:e32572. doi: 10.1371/journal.pone.0032572

Kroger, C., Afeyan, A., Mraz, J., Eaton, E. N., Reinhardt, F., Khodor, Y. L., et al. (2019). Acquisition of a hybrid E/M state is essential for tumorigenicity of basal breast cancer cells. *Proc. Natl. Acad. Sci. U.S.A.* 116, 7353–7362. doi: 10.1073/pnas.1812876116

Kumar, D., Gorain, M., Kundu, G., and Kundu, G. C. (2017). Therapeutic implications of cellular and molecular biology of cancer stem cells in melanoma. *Mol. Cancer* 16:7.

Kwa, M. Q., Herum, K. M., and Brakebusch, C. (2019). Cancer-associated fibroblasts: how do they contribute to metastasis? *Clin. Exp. Metastasis* 36, 71–86.

Lamb, R., Bonuccelli, G., Ozsvari, B., Peiris-Pages, M., Fiorillo, M., Smith, D. L., et al. (2015). Mitochondrial mass, a new metabolic biomarker for stem-like cancer cells: understanding WNT/FGF-driven anabolic signaling. *Oncotarget* 6, 30453–30471.

Lapidot, T., Sirard, C., Vormoor, J., Murdoch, B., Hoang, T., Caceres-Cortes, J., et al. (1994). A cell initiating human acute myeloid leukaemia after transplantation into SCID mice. *Nature* 367, 645–648. doi: 10.1038/367645a0

Lau, E. Y., Lo, J., Cheng, B. Y., Ma, M. K., Lee, J. M., Ng, J. K., et al. (2016). Cancer-associated fibroblasts regulate tumor-initiating cell plasticity in hepatocellular carcinoma through c-Met/FRA1/HEY1 signaling. *Cell Rep.* 15, 1175–1189. doi: 10.1016/j.celrep.2016.04.019

Lee, J. H., Daugharthy, E. R., Scheiman, J., Kalhor, R., Yang, J. L., Ferrante, T. C., et al. (2014). Highly multiplexed subcellular RNA sequencing in situ. *Science* 343, 1360–1363. doi: 10.1126/science.1250212

Lehuede, C., Dupuy, F., Rabinovitch, R., Jones, R. G., and Siegel, P. M. (2016). Metabolic plasticity as a determinant of tumor growth and metastasis. *Cancer Res.* 76, 5201–5208. doi: 10.1158/0008-5472.can-16-0266

Lequeux, A., Noman, M. Z., Xiao, M., Sauvage, D., Van Moer, K., and Viry, E. (2019). Impact of hypoxic tumor microenvironment and tumor cell plasticity on the expression of immune checkpoints. *Cancer Lett.* 458, 13–20. doi: 10.1016/j.canlet.2019.05.021

Leung, E. L., Fiscus, R. R., Tung, J. W., Tin, V. P., Cheng, L. C., Sihoe, A. D., et al. (2010). Non-small cell lung cancer cells expressing CD44 are enriched for stem cell-like properties. *PLoS One* 5:e14062. doi: 10.1371/journal.pone.0014062

Lewis, P. W., Muller, M. M., Koletsky, M. S., Cordero, F., Lin, S., Banaszynski, L. A., et al. (2013). Inhibition of PRC2 activity by a gain-of-function H3 mutation found in pediatric glioblastoma. *Science* 340, 857–861. doi: 10.1126/science.1232245

Li, C., Heidt, D. G., Dalerba, P., Burant, C. F., Zhang, L., Adsay, V., et al. (2007). Identification of pancreatic cancer stem cells. *Cancer Res.* 67, 1030–1037.

Li, X., Jolly, M. K., George, J. T., Pienta, K. J., and Levine, H. (2019). Computational modeling of the crosstalk between macrophage polarization and tumor cell plasticity in the tumor microenvironment. *Front. Oncol.* 9:10. doi: 10.3389/fonc.2019.00010

Liberti, M. V., and Locasale, J. W. (2016). The warburg effect: how does it benefit cancer cells? *Trends Biochem. Sci.* 41, 211–218. doi: 10.1016/j.tibs.2015.12.001

Little, S. E., Popov, S., Jury, A., Bax, D. A., Doey, L., Al-Sarraj, S., et al. (2012). Receptor tyrosine kinase genes amplified in glioblastoma exhibit a mutual exclusivity in variable proportions reflective of individual tumor heterogeneity. *Cancer Res.* 72, 1614–1620. doi: 10.1158/0008-5472.can-11-4069

Liu, A., Yu, X., and Liu, S. (2013). Pluripotency transcription factors and cancer stem cells: small genes make a big difference. *Chin. J. Cancer* 32, 483–487.

Liu, L., Liu, C., Quintero, A., Wu, L., Yuan, Y., Wang, M., et al. (2019). Deconvolution of single-cell multi-omics layers reveals regulatory heterogeneity. *Nat. Commun.* 10:470.

Liu, P. P., Liao, J., Tang, Z. J., Wu, W. J., Yang, J., Zeng, Z. L., et al. (2014). Metabolic regulation of cancer cell side population by glucose through activation of the Akt pathway. *Cell Death Differ.* 21, 124–135. doi: 10.1038/cdd.2013.131

Liu, S., Cong, Y., Wang, D., Sun, Y., Deng, L., Liu, Y., et al. (2014). Breast cancer stem cells transition between epithelial and mesenchymal states reflective of their normal counterparts. *Stem Cell Rep.* 2, 78–91. doi: 10.1016/j.stemcr.2013.11.009

Liu, T. J., Sun, B. C., Zhao, X. L., Zhao, X. M., Sun, T., Gu, Q., et al. (2013). CD133+ cells with cancer stem cell characteristics associates with vasculogenic mimicry in triple-negative breast cancer. *Oncogene* 32, 544–553. doi: 10.1038/onc.2012.85

Liu, Z., Lee, Y., Jang, J., Li, Y., Han, X., Yokoi, K., et al. (2015). Microfluidic cytometric analysis of cancer cell transportability and invasiveness. *Sci. Rep.* 5:14272.

Lonardo, E., Cioffi, M., Sancho, P., Sanchez-Ripoll, Y., Trabulo, S. M., Dorado, J., et al. (2013). Metformin targets the metabolic achilles heel of human pancreatic cancer stem cells. *PLoS One* 8:e76518. doi: 10.1371/journal.pone.0076518

Luo, M., and Wicha, M. S. (2015). Metabolic plasticity of cancer stem cells. *Oncotarget* 6, 35141–35142.

Macaulay, I. C., Ponting, C. P., and Voet, T. (2017). Single-cell multiomics: multiple measurements from single cells. *Trends Genet* 33, 155–168. doi: 10.1016/j.tig.2016.12.003

Maiuthed, A., Chantarawong, W., and Chanvorachote, P. (2018). Lung cancer stem cells and cancer stem cell-targeting natural compounds. *Anticancer Res.* 38, 3797–3809. doi: 10.21873/anticanres.12663

Malta, T. M., Sokolov, A., Gentles, A. J., Burzykowski, T., Poisson, L., Weinstein, J. N., et al. (2018). Machine learning identifies stemness features associated with oncogenic dedifferentiation. *Cell* 173, 338–354.e5.

Mani, S. A., Guo, W., Liao, M. J., Eaton, E. N., Ayyanan, A., Zhou, A. Y., et al. (2008). The epithelial-mesenchymal transition generates cells with properties of stem cells. *Cell* 133, 704–715.

Marjanovic, N. D., Weinberg, R. A., and Chaffer, C. L. (2013). Cell plasticity and heterogeneity in cancer. *Clin. Chem.* 59, 168–179. doi: 10.1373/clinchem.2012.184655

Martano, G., Borroni, E. M., Lopci, E., Cattaneo, M. G., Mattioli, M., Bachi, A., et al. (2019). Metabolism of stem and progenitor cells: proper methods to answer specific questions. *Front. Mol. Neurosci.* 12:151. doi: 10.3389/fnmol.2019.00151

Martin, P., Liu, Y. N., Pierce, R., Abou-Kheir, W., Casey, O., Seng, V., et al. (2011). Prostate epithelial Pten/TP53 loss leads to transformation of multipotential progenitors and epithelial to mesenchymal transition. *Am. J. Pathol.* 179, 422–435. doi: 10.1016/j.ajpath.2011.03.035

McGranahan, N., and Swanton, C. (2017). Clonal heterogeneity and tumor evolution: past, present, and the future. *Cell* 168, 613–628. doi: 10.1016/j.cell.2017.01.018

McKenna, A., and Gagnon, J. A. (2019). Recording development with single cell dynamic lineage tracing. *Development* 146:dev169730. doi: 10.1242/dev.169730

Menendez, J. A., and Alarcon, T. (2014). Metabostemness: a new cancer hallmark. *Front. Oncol.* 4:262. doi: 10.3389/fonc.2014.00262

Mooney, S. M., Talebian, V., Jolly, M. K., Jia, D., Gromala, M., Levine, H., et al. (2017). The GRHL2/ZEB feedback loop-a key axis in the regulation of EMT in breast cancer. *J. Cell Biochem.* 118, 2559–2570. doi: 10.1002/jcb.25974

Moreira, M. P., Brayner, F. A., Alves, L. C., Cassali, G. D., and Silva, L. M. (2019). Phenotypic, structural, and ultrastructural analysis of triple-negative breast cancer cell lines and breast cancer stem cell subpopulation. *Eur. Biophys. J.* 48, 673–684. doi: 10.1007/s00249-019-01393-0

Morrison, S. J., and Spradling, A. C. (2008). Stem cells and niches: mechanisms that promote stem cell maintenance throughout life. *Cell* 132, 598–611. doi: 10.1016/j.cell.2008.01.038

Mourao, L., Jacquemin, G., Huyghe, M., Nawrocki, W. J., Menssouri, N., Servant, N., et al. (2019). Lineage tracing of Notch1-expressing cells in intestinal tumours reveals a distinct population of cancer stem cells. *Sci. Rep.* 9:888.

Nallanthighal, S., Heiserman, J. P., and Cheon, D. J. (2019). The role of the extracellular matrix in cancer stemness. *Front. Cell Dev. Biol.* 7:86. doi: 10.3389/fcell.2019.00086

Nath, B., Bidkar, A. P., Kumar, V., Dalal, A., Jolly, M. K., Ghosh, S. S., et al. (2019). Deciphering hydrodynamic and drug-resistant behaviors of metastatic EMT breast cancer cells moving in a constricted microcapillary. *J. Clin. Med.* 8:1194. doi: 10.3390/jcm8081194

Navin, N. E. (2015). The first five years of single-cell cancer genomics and beyond. *Genome Res.* 25, 1499–1507. doi: 10.1101/gr.191098.115

Ogden, A. T., Waziri, A. E., Lochhead, R. A., Fusco, D., Lopez, K., Ellis, J. A., et al. (2008). Identification of A2B5+CD133- tumor-initiating cells in adult human gliomas. *Neurosurgery* 62, 505–514.

Oshima, N., Yamada, Y., Nagayama, S., Kawada, K., Hasegawa, S., Okabe, H., et al. (2014). Induction of cancer stem cell properties in colon cancer cells by defined factors. *PLoS One* 9:e101735. doi: 10.1371/journal.pone.0101735

Papa, S., Choy, P. M., and Bubici, C. (2019). The ERK and JNK pathways in the regulation of metabolic reprogramming. *Oncogene* 38, 2223–2240. doi: 10.1038/s41388-018-0582-8

Pascual, G., Dominguez, D., and Benitah, S. A. (2018). The contributions of cancer cell metabolism to metastasis. *Dis. Model. Mech.* 11:dmm032920. doi: 10.1242/dmm.032920

Pastushenko, I., Brisebarre, A., Sifrim, A., Fioramonti, M., Revenco, T., Boumahdi, S., et al. (2018). Identification of the tumour transition states occurring during EMT. *Nature* 556, 463–468. doi: 10.1038/s41586-018-0040-3

Patel, A. P., Tirosh, I., Trombetta, J. J., Shalek, A. K., Gillespie, S. M., Wakimoto, H., et al. (2014). Single-cell RNA-seq highlights intratumoral heterogeneity in primary glioblastoma. *Science* 344, 1396–1401. doi: 10.1126/science.1254257

Pattabiraman, D. R., and Weinberg, R. A. (2014). Tackling the cancer stem cells – what challenges do they pose? *Nat. Rev. Drug Discov.* 13, 497–512. doi: 10.1038/nrd4253

Pavlides, S., Whitaker-Menezes, D., Castello-Cros, R., Flomenberg, N., Witkiewicz, A. K., Frank, P. G., et al. (2009). The reverse warburg effect: aerobic glycolysis in cancer associated fibroblasts and the tumor stroma. *Cell Cycle* 8, 3984–4001. doi: 10.4161/cc.8.23.10238

Peired, A. J., Sisti, A., and Romagnani, P. (2016). Renal cancer stem cells: characterization and targeted therapies. *Stem Cells Int.* 2016:8342625.

Peiris-Pages, M., Martinez-Outschoorn, U. E., Pestell, R. G., Sotgia, F., and Lisanti, M. P. (2016). Cancer stem cell metabolism. *Breast Cancer Res.* 18:55.

Peitzsch, C., Nathansen, J., Schniewind, S. I., Schwarz, F., and Dubrovska, A. (2019). Cancer stem cells in head and neck squamous cell carcinoma: identification, characterization and clinical implications. *Cancers (Basel)* 11:616. doi: 10.3390/cancers11050616

Peltanova, B., Raudenska, M., and Masarik, M. (2019). Effect of tumor microenvironment on pathogenesis of the head and neck squamous cell carcinoma: a systematic review. *Mol. Cancer* 18:63.

Poli, V., Fagnocchi, L., and Zippo, A. (2018). Tumorigenic cell reprogramming and cancer plasticity: interplay between signaling, microenvironment, and epigenetics. *Stem Cells Int.* 2018:4598195.

Prager, B. C., Xie, Q., Bao, S., and Rich, J. N. (2019). Cancer stem cells: the architects of the tumor ecosystem. *Cell Stem Cell* 24, 41–53. doi: 10.1016/j.stem.2018.12.009

Prasetyanti, P. R., and Medema, J. P. (2017). Intra-tumor heterogeneity from a cancer stem cell perspective. *Mol. Cancer* 16:41.

Prince, M. E., Sivanandan, R., Kaczorowski, A., Wolf, G. T., Kaplan, M. J., and Dalerba, P. (2007). Identification of a subpopulation of cells with cancer stem cell properties in head and neck squamous cell carcinoma. *Proc. Natl. Acad. Sci. U.S.A.* 104, 973–978. doi: 10.1073/pnas.0610117104

Puram, S. V., Parikh, A. S., and Tirosh, I. (2018). Single cell RNA-seq highlights a role for a partial EMT in head and neck cancer. *Mol. Cell Oncol.* 5:e1448244.

Puram, S. V., Tirosh, I., Parikh, A. S., Patel, A. P., Yizhak, K., Gillespie, S., et al. (2017). Single-cell transcriptomic analysis of primary and metastatic tumor ecosystems in head and neck cancer. *Cell* 171, 1611–1624.e24. doi: 10.1016/j.cell.2017.10.044

Qiu, Y., Wang, L., Zhong, X., Li, L., Chen, F., Xiao, L., et al. (2019). A multiple breast cancer stem cell model to predict recurrence of T1-3, N0 Breast Cancer. *BMC Cancer* 19:729. doi: 10.1186/s12885-019-5941-5

Quail, D. F., and Joyce, J. A. (2013). Microenvironmental regulation of tumor progression and metastasis. *Nat. Med.* 19, 1423–1437. doi: 10.1038/nm.3394

Quintana, E., Shackleton, M., Foster, H. R., Fullen, D. R., Sabel, M. S., Johnson, T. M., et al. (2010). Phenotypic heterogeneity among tumorigenic melanoma cells from patients that is reversible and not hierarchically organized. *Cancer Cell* 18, 510–523. doi: 10.1016/j.ccr.2010.10.012

Rheinbay, E., Suva, M. L., Gillespie, S. M., Wakimoto, H., Patel, A. P., Shahid, M., et al. (2013). An aberrant transcription factor network essential for Wnt signaling and stem cell maintenance in glioblastoma. *Cell Rep.* 3, 1567–1579. doi: 10.1016/j.celrep.2013.04.021

Ricci-Vitiani, L., Lombardi, D. G., Pilozzi, E., Biffoni, M., Todaro, M., Peschle, C., et al. (2007). Identification and expansion of human colon-cancer-initiating cells. *Nature* 445, 111–115. doi: 10.1038/nature05384

Rich, J. N. (2016). Cancer stem cells: understanding tumor hierarchy and heterogeneity. *Medicine (Baltimore)* 95(1 Suppl. 1), S2–S7.

Rios, A. C., Capaldo, B. D., Vaillant, F., Pal, B., van Ineveld, R., Dawson, C. A., et al. (2019). Intraclonal plasticity in mammary tumors revealed through large-scale single-cell resolution 3d imaging. *Cancer Cell* 35, 618–632.e6. doi: 10.1016/j.ccell.2019.02.010

Roesch, A., Fukunaga-Kalabis, M., Schmidt, E. C., Zabierowski, S. E., Brafford, P. A., Vultur, A., et al. (2010). A temporarily distinct subpopulation of slow-cycling melanoma cells is required for continuous tumor growth. *Cell* 141, 583–594. doi: 10.1016/j.cell.2010.04.020

Roy, L., and Cowden Dahl, K. D. (2018). Can stemness and chemoresistance be therapeutically targeted via signaling pathways in ovarian cancer? *Cancers (Basel)* 10:241. doi: 10.3390/cancers10080241

Roy Choudhury, A., Gupta, S., Chaturvedi, P. K., Kumar, N., and Pandey, D. (2019). Mechanobiology of cancer stem cells and their niche. *Cancer Microenviron.* 12, 17–27. doi: 10.1007/s12307-019-00222-4

Saliba, A. E., Saias, L., Psychari, E., Minc, N., Simon, D., Bidard, F. C., et al. (2010). Microfluidic sorting and multimodal typing of cancer cells in self-assembled magnetic arrays. *Proc. Natl. Acad. Sci. U.S.A.* 107, 14524–14529. doi: 10.1073/pnas.1001515107

Sancho, P., Barneda, D., and Heeschen, C. (2016). Hallmarks of cancer stem cell metabolism. *Br. J. Cancer* 114, 1305–1312. doi: 10.1038/bjc.2016.152

Sancho, P., Burgos-Ramos, E., Tavera, A., Bou Kheir, T., Jagust, P., Schoenhals, M., et al. (2015). MYC/PGC-1alpha balance determines the metabolic phenotype and plasticity of pancreatic cancer stem cells. *Cell Metab.* 22, 590–605. doi: 10.1016/j.cmet.2015.08.015

Santoro, A., Vlachou, T., Luzi, L., Melloni, G., Mazzarella, L., D'Elia, E., et al. (2019). p53 loss in breast cancer leads to Myc activation, increased cell plasticity, and expression of a mitotic signature with prognostic Value. *Cell Rep.* 26, 624–638.e8. doi: 10.1016/j.celrep.2018.12.071

Satija, R., Farrell, J. A., Gennert, D., Schier, A. F., and Regev, A. (2015). Spatial reconstruction of single-cell gene expression data. *Nat. Biotechnol.* 33, 495–502. doi: 10.1038/nbt.3192

Saxena, K., and Jolly, M. K. (2019). Acute vs. chronic vs. cyclic hypoxia: their differential dynamics, molecular mechanisms, and effects on tumor progression. *Biomolecules* 9:339. doi: 10.3390/biom9080339

Schmalhofer, O., Brabletz, S., and Brabletz, T. (2009). E-cadherin, beta-catenin, and ZEB1 in malignant progression of cancer. *Cancer Metastasis Rev.* 28, 151–166. doi: 10.1007/s10555-008-9179-y

Sehl, M. E., and Wicha, M. S. (2018). Modeling of interactions between cancer stem cells and their microenvironment: predicting clinical response. *Methods Mol. Biol.* 1711, 333–349. doi: 10.1007/978-1-4939-7493-1_16

Sellerio, A. L., Ciusani, E., Ben-Moshe, N. B., Coco, S., Piccinini, A., Myers, C. R., et al. (2015). Overshoot during phenotypic switching of cancer cell populations. *Sci. Rep.* 5:15464.

Shackleton, M., Quintana, E., Fearon, E. R., and Morrison, S. J. (2009). Heterogeneity in cancer: cancer stem cells versus clonal evolution. *Cell* 138, 822–829. doi: 10.1016/j.cell.2009.08.017

Shah, M., Cardenas, R., Wang, B., Persson, J., Mongan, N. P., Grabowska, A., et al. (2017). HOXC8 regulates self-renewal, differentiation and transformation of breast cancer stem cells. *Mol. Cancer* 16:38.

Sharma, A., Cao, E. Y., Kumar, V., Zhang, X., Leong, H. S., Wong, A. M. L., et al. (2018). Longitudinal single-cell RNA sequencing of patient-derived primary cells reveals drug-induced infidelity in stem cell hierarchy. *Nat. Commun.* 9:4931.

Shibue, T., and Weinberg, R. A. (2017). EMT, CSCs, and drug resistance: the mechanistic link and clinical implications. *Nat. Rev. Clin. Oncol.* 14, 611–629. doi: 10.1038/nrclinonc.2017.44

Singh, S. K., Hawkins, C., Clarke, D., Squire, J. A., Bayani, J., Hide, T., et al. (2004). Identification of human brain tumour initiating cells. *Nature* 432, 396–401.

Singla, M., Kumar, A., Bal, A., Sarkar, S., and Bhattacharyya, S. (2018). Epithelial to mesenchymal transition induces stem cell like phenotype in renal cell carcinoma cells. *Cancer Cell Int.* 18:57.

Skrtic, M., Sriskanthadevan, S., Jhas, B., Gebbia, M., Wang, X., Wang, Z., et al. (2011). Inhibition of mitochondrial translation as a therapeutic strategy for human acute myeloid leukemia. *Cancer Cell* 20, 674–688.

Skvortsov, S., Skvortsova, I. I., Tang, D. G., and Dubrovska, A. (2018). Concise review: prostate cancer stem cells: current understanding. *Stem Cells* 36, 1457–1474. doi: 10.1002/stem.2859

Skylaki, S., Hilsenbeck, O., and Schroeder, T. (2016). Challenges in long-term imaging and quantification of single-cell dynamics. *Nat. Biotechnol.* 34, 1137–1144. doi: 10.1038/nbt.3713

Snyder, V., Reed-Newman, T. C., Arnold, L., Thomas, S. M., and Anant, S. (2018). Cancer stem cell metabolism and potential therapeutic targets. *Front. Oncol.* 8:203. doi: 10.3389/fonc.2018.00203

Somasundaram, R., Villanueva, J., and Herlyn, M. (2012). Intratumoral heterogeneity as a therapy resistance mechanism: role of melanoma subpopulations. *Adv. Pharmacol.* 65, 335–359. doi: 10.1016/b978-0-12-397927-8.00011-7

Son, M. J., Woolard, K., Nam, D. H., Lee, J., and Fine, H. A. (2009). SSEA-1 is an enrichment marker for tumor-initiating cells in human glioblastoma. *Cell Stem Cell* 4, 440–452. doi: 10.1016/j.stem.2009.03.003

Srinivasan, S., Ashok, V., Mohanty, S., Das, A., Das, S., Kumar, S., et al. (2017). Blockade of Rho-associated protein kinase (ROCK) inhibits the contractility and invasion potential of cancer stem like cells. *Oncotarget* 8, 21418–21428.

Suhail, Y., Cain, M. P., Vanaja, K., Kurywchak, P. A., Levchenko, A., Kalluri, R., et al. (2019). Systems biology of cancer metastasis. *Cell Syst.* 9, 109–127.

Sun, J., Luo, Q., Liu, L., Zhang, B., Shi, Y., Ju, Y., et al. (2016). Biomechanical profile of cancer stem-like cells derived from MHCC97H cell lines. *J. Biomech.* 49, 45–52. doi: 10.1016/j.jbiomech.2015.11.007

Suva, M. L., Rheinbay, E., Gillespie, S. M., Patel, A. P., Wakimoto, H., Rabkin, S. D., et al. (2014). Reconstructing and reprogramming the tumor-propagating potential of glioblastoma stem-like cells. *Cell* 157, 580–594. doi: 10.1016/j.cell.2014.02.030

Suva, M. L., and Tirosh, I. (2019). Single-cell RNA sequencing in cancer: lessons learned and emerging challenges. *Mol. Cell* 75, 7–12. doi: 10.1016/j.molcel.2019.05.003

Swaminathan, V., Mythreye, K., O'Brien, E. T., Berchuck, A., Blobe, G. C., and Superfine, R. (2011). Mechanical stiffness grades metastatic potential in patient tumor cells and in cancer cell lines. *Cancer Res.* 71, 5075–5080. doi: 10.1158/0008-5472.can-11-0247

Swartz, M. A., Iida, N., Roberts, E. W., Sangaletti, S., Wong, M. H., Yull, F. E., et al. (2012). Tumor microenvironment complexity: emerging roles in cancer therapy. *Cancer Res.* 72, 2473–2480. doi: 10.1158/0008-5472.can-12-0122

Tang, D. G. (2012). Understanding cancer stem cell heterogeneity and plasticity. *Cell Res.* 22, 457–472. doi: 10.1038/cr.2012.13

Terris, B., Cavard, C., and Perret, C. (2010). EpCAM, a new marker for cancer stem cells in hepatocellular carcinoma. *J. Hepatol.* 52, 280–281. doi: 10.1016/j.jhep.2009.10.026

Tripathi, S. C., Fahrmann, J. F., Celiktas, M., Aguilar, M., Marini, K. D., Jolly, M. K., et al. (2017). MCAM mediates chemoresistance in small-cell lung cancer via the PI3K/AKT/SOX2 signaling pathway. *Cancer Res.* 77, 4414–4425. doi: 10.1158/0008-5472.can-16-2874

Tschaharganeh, D. F., Xue, W., Calvisi, D. F., Evert, M., Michurina, T. V., Dow, L. E., et al. (2014). p53-dependent Nestin regulation links tumor suppression to cellular plasticity in liver cancer. *Cell* 158, 579–592. doi: 10.1016/j.cell.2014.05.051

Turashvili, G., and Brogi, E. (2017). Tumor heterogeneity in breast cancer. *Front. Med. (Lausanne)* 4:227. doi: 10.3389/fmed.2017.00227

Vermeulen, L., de Sousa e Melo, F., Richel, D. J., and Medema, J. P. (2012). The developing cancer stem-cell model: clinical challenges and opportunities. *Lancet Oncol.* 13, e83–e89. doi: 10.1016/s1470-2045(11)70257-1

Wainwright, E. N., and Scaffidi, P. (2017). Epigenetics and cancer stem cells: unleashing, hijacking, and restricting cellular plasticity. *Trends Cancer* 3, 372–386. doi: 10.1016/j.trecan.2017.04.004

Wang, J., Sakariassen, P. O., Tsinkalovsky, O., Immervoll, H., Boe, S. O., Svendsen, A., et al. (2008). CD133 negative glioma cells form tumors in nude rats and give rise to CD133 positive cells. *Int. J. Cancer* 122, 761–768. doi: 10.1002/ijc.23130

Wang, K., and Sun, D. (2018). Cancer stem cells of hepatocellular carcinoma. *Oncotarget* 9, 23306–23314.

Wang, X., Huang, S., and Chen, J. L. (2017). Understanding of leukemic stem cells and their clinical implications. *Mol. Cancer* 16:2.

Warburg, O., Wind, F., and Negelein, E. (1927). The metabolism of tumors in the body. *J. Gen. Physiol.* 8, 519–530. doi: 10.1085/jgp.8.6.519

Wen, Y., Cai, J., Hou, Y., Huang, Z., and Wang, Z. (2017). Role of EZH2 in cancer stem cells: from biological insight to a therapeutic target. *Oncotarget* 8, 37974–37990.

Wolfson, B., Eades, G., and Zhou, Q. (2015). Adipocyte activation of cancer stem cell signaling in breast cancer. *World J. Biol. Chem.* 6, 39–47.

Yamaguchi, H., and Hung, M. C. (2014). Regulation and role of EZH2 in cancer. *Cancer Res. Treat.* 46, 209–222. doi: 10.4143/crt.2014.46.3.209

Yang, Y. C., Wang, S. W., Hung, H. Y., Chang, C. C., Wu, C., Huang, Y. L., et al. (2007). Isolation and characterization of human gastric cell lines with stem cell phenotypes. *J. Gastroenterol. Hepatol.* 22, 1460–1468.

Yu, L., Lu, M., Jia, D., Ma, J., Ben-Jacob, E., Levine, H., et al. (2017). Modeling the genetic regulation of cancer metabolism: interplay between glycolysis and oxidative phosphorylation. *Cancer Res.* 77, 1564–1574. doi: 10.1158/0008-5472.can-16-2074

Yuan, G. C., Cai, L., Elowitz, M., Enver, T., Fan, G., Guo, G., et al. (2017). Challenges and emerging directions in single-cell analysis. *Genome Biol.* 18:84.

Yuan, Y. (2016). Spatial heterogeneity in the tumor microenvironment. *Cold Spring Harb. Perspect. Med.* 6:a026583. doi: 10.1101/cshperspect.a026583

Zanotelli, M. R., Goldblatt, Z. E., Miller, J. P., Bordeleau, F., Li, J., VanderBurgh, J. A., et al. (2018). Regulation of ATP utilization during metastatic cell migration by collagen architecture. *Mol. Biol. Cell* 29, 1–9. doi: 10.1091/mbc.e17-01-0041

Zhang, S., Balch, C., Chan, M. W., Lai, H. C., Matei, D., Schilder, J. M., et al. (2008). Identification and characterization of ovarian cancer-initiating cells from primary human tumors. *Cancer Res.* 68, 4311–4320. doi: 10.1158/0008-5472.can-08-0364

Zhang, W., Kai, K., Choi, D. S., Iwamoto, T., Nguyen, Y. H., Wong, H., et al. (2012). Microfluidics separation reveals the stem-cell-like deformability of tumor-initiating cells. *Proc. Natl. Acad. Sci. U.S.A.* 109, 18707–18712. doi: 10.1073/pnas.1209893109

Zhang, Y., Sun, B., Zhao, X., Liu, Z., Wang, X., Yao, X., et al. (2013). Clinical significances and prognostic value of cancer stem-like cells markers and vasculogenic mimicry in renal cell carcinoma. *J. Surg. Oncol.* 108, 414–419. doi: 10.1002/jso.23402

Zhang, Y., Wu, M., Han, X., Wang, P., and Qin, L. (2015). High-throughput, label-free isolation of cancer stem cells on the basis of cell adhesion capacity. *Angew. Chem. Int. Ed. Engl.* 54, 10838–10842. doi: 10.1002/anie.201505294

Zheng, H., Pomyen, Y., Hernandez, M. O., Li, C., Livak, F., Tang, W., et al. (2018). Single-cell analysis reveals cancer stem cell heterogeneity in hepatocellular carcinoma. *Hepatology* 68, 127–140. doi: 10.1002/hep.29778

Zhou, Y., Xia, L., Wang, H., Oyang, L., Su, M., Liu, Q., et al. (2018). Cancer stem cells in progression of colorectal cancer. *Oncotarget* 9, 33403–33415.

Zomer, A., Ellenbroek, S. I., Ritsma, L., Beerling, E., Vrisekoop, N., and Van Rheenen, J. (2013). Intravital imaging of cancer stem cell plasticity in mammary tumors. *Stem Cells* 31, 602–606.

Conflict of Interest: The authors declare that the research was conducted in the absence of any commercial or financial relationships that could be construed as a potential conflict of interest.

Copyright © 2020 Thankamony, Saxena, Murali, Jolly and Nair. This is an open-access article distributed under the terms of the Creative Commons Attribution License (CC BY). The use, distribution or reproduction in other forums is permitted, provided the original author(s) and the copyright owner(s) are credited and that the original publication in this journal is cited, in accordance with accepted academic practice. No use, distribution or reproduction is permitted which does not comply with these terms.

frontiers in Cell and Developmental Biology

ORIGINAL RESEARCH
published: 08 May 2020
doi: 10.3389/fcell.2020.00288

Hybrid Stem Cell States: Insights Into the Relationship Between Mammary Development and Breast Cancer Using Single-Cell Transcriptomics

Tasha Thong[1†], Yutong Wang[2†], Michael D. Brooks[3], Christopher T. Lee[4], Clayton Scott[2,5], Laura Balzano[2], Max S. Wicha[3,5] and Justin A. Colacino[1,5,6]*

[1] Department of Environmental Health Sciences, School of Public Health, University of Michigan, Ann Arbor, MI, United States, [2] Department of Electrical Engineering and Computer Science, University of Michigan, Ann Arbor, MI, United States, [3] Department of Internal Medicine, Michigan Medicine, University of Michigan, Ann Arbor, MI, United States, [4] Department of Biostatistics, School of Public Health, University of Michigan, Ann Arbor, MI, United States, [5] Center for Computational Medicine and Bioinformatics, University of Michigan, Ann Arbor, MI, United States, [6] Department of Nutritional Sciences, School of Public Health, University of Michigan, Ann Arbor, MI, United States

OPEN ACCESS

Edited by:
Mohit Kumar Jolly,
Indian Institute of Science (IISc), India

Reviewed by:
Meisam Bagheri,
Dartmouth College, United States
Sagar S. Varankar,
National Centre for Cell Science, India
Sugandha Bhatia,
Queensland University of Technology, Australia

***Correspondence:**
Justin A. Colacino
colacino@umich.edu

[†] These authors have contributed equally to this work

Specialty section:
This article was submitted to Molecular and Cellular Oncology, a section of the journal Frontiers in Cell and Developmental Biology

Received: 13 December 2019
Accepted: 02 April 2020
Published: 08 May 2020

Citation:
Thong T, Wang Y, Brooks MD, Lee CT, Scott C, Balzano L, Wicha MS and Colacino JA (2020) Hybrid Stem Cell States: Insights Into the Relationship Between Mammary Development and Breast Cancer Using Single-Cell Transcriptomics. Front. Cell Dev. Biol. 8:288. doi: 10.3389/fcell.2020.00288

Similarities between stem cells and cancer cells have implicated mammary stem cells in breast carcinogenesis. Recent evidence suggests that normal breast stem cells exist in multiple phenotypic states: epithelial, mesenchymal, and hybrid epithelial/mesenchymal (E/M). Hybrid E/M cells in particular have been implicated in breast cancer metastasis and poor prognosis. Mounting evidence also suggests that stem cell phenotypes change throughout the life course, for example, through embryonic development and pregnancy. The goal of this study was to use single cell RNA-sequencing to quantify cell state distributions of the normal mammary (NM) gland throughout developmental stages and when perturbed into a stem-like state *in vitro* using conditional reprogramming (CR). Using machine learning based dataset alignment, we integrate multiple mammary gland single cell RNA-seq datasets from human and mouse, along with bulk RNA-seq data from breast tumors in the Cancer Genome Atlas (TCGA), to interrogate hybrid stem cell states in the normal mammary gland and cancer. CR of human mammary cells induces an expanded stem cell state, characterized by increased expression of embryonic stem cell associated genes. Alignment to a mouse single-cell transcriptome atlas spanning mammary gland development from *in utero* to adulthood revealed that NM cells align to adult mouse cells and CR cells align across the pseudotime trajectory with a stem-like population aligning to the embryonic mouse cells. Three hybrid populations emerge after CR that are rare in NM: *KRT18+/KRT14+* (hybrid luminal/basal), *EPCAM+/VIM+* (hybrid E/M), and a quadruple positive population, expressing all four markers. Pseudotime analysis and alignment to the mouse developmental trajectory revealed that E/M hybrids are the most developmentally immature. Analyses of single cell mouse mammary RNA-seq throughout pregnancy show that during gestation, there is an enrichment of hybrid E/M cells, suggesting that these cells play an important role in mammary morphogenesis during lactation. Finally, pseudotime analysis and alignment of TCGA breast cancer expression data revealed that breast cancer subtypes

express distinct developmental signatures, with basal tumors representing the most "developmentally immature" phenotype. These results highlight phenotypic plasticity of normal mammary stem cells and provide insight into the relationship between hybrid cell populations, stemness, and cancer.

Keywords: stem cells, breast cancer, single-cell RNA sequencing, hybrid, epithelial, mesenchymal, pregnancy

INTRODUCTION

As the field of cancer biology has evolved, a growing body of work has reinforced the critical role of stem-like cells in cancer. Due to long-observed similarities between embryonic development and oncogenesis, cancer is often considered a disease of "dysregulated development" (Ma et al., 2010; Reya et al., 2001). A characteristic shared by stem cells and cancer cells is cellular plasticity – the ability to transition and adopt alternative cell fates in response to environmental signals and stressors (Thong et al., 2019). Plasticity is crucial for stem cells during embryonic development, for example during gastrulation when epiblast cells undergo the epithelial to mesenchymal transition (EMT) to form mesoderm which gives rise to the mesenchyme (Kalluri and Weinberg, 2009). In adult stem cells, plasticity plays an important role in homeostasis and wound repair. This is demonstrated by adult tissue stem cells in the liver and intestinal epithelium which have been shown to de-differentiate or even *trans*-differentiate into cell types of a different lineage in order to replace damaged cells (Merrell and Stanger, 2016). For cancer cells in tumors of epithelial origin, EMT plasticity and its reverse MET, are crucial for primary tumors to be able to adopt mesenchymal characteristics in order to disseminate, metastasize, and re-epithelialize at the metastatic site (Tam and Weinberg, 2013).

Emerging evidence now suggests that these transitions occur along a continuum rather than as discrete switches in cell state. Transitioning hybrid cells exhibiting phenotypic markers of multiple cell states (epithelial/mesenchymal and luminal/basal) have been identified by us and others in both normal and carcinogenic breast tissue (Grosse-Wilde et al., 2015; Jolly et al., 2015; Colacino et al., 2018). These cellular states are defined by the co-expression of known marker genes, for example the epithelial marker *EPCAM* and the mesenchymal marker *VIM*, or the luminal marker *KRT18* and the basal/myoepithelial marker *KRT14*. Additionally, recent evidence shows that these hybrid cells exist in metastable states, not just as transient hybrids (Jolly et al., 2016). These hybrid populations are of particular interest due to their implicated role in promotion of tumorigenesis, metastasis, and aggressiveness of breast cancer (Jolly et al., 2015). There are a limited number of studies which have observed these hybrid populations in the normal breast, and of these, the low proportions of hybrid cells identified have made them challenging to characterize.

In this study, we integrate multiple single-cell RNA sequencing datasets from the human and mouse in order to characterize the cell state distributions of the normal mammary (NM) gland throughout the life course, as well as after being perturbed into an enriched stem cell state following *in vitro* culture using the conditional reprogramming (CR) method (Liu et al., 2017). Through a combined analysis of single cell RNA-seq data with bulk human breast cancer transcriptomics from the Cancer Genome Atlas (TCGA), we investigate mammary stem cell populations and hybrid cell states, elucidating roles for these cells in mammary gland development and cancer.

MATERIALS AND METHODS

Human Tissue Procurement

Tissue procurement was approved by the University of Michigan Institutional Review Board (HUM00042409). Normal mammary (NM) tissue was obtained from voluntary reduction mammoplasties performed at the University of Michigan hospital. Samples were processed following the protocol of Dontu et al. (2003) by enzymatic and mechanical digestion into single cell suspensions, as previously described (Colacino et al., 2016).

Conditional Reprogramming

NM cells isolated from mammoplasty dissociation were co-cultured with irradiated 3T3 J2 mouse fibroblasts (Kerafast) using F-media in adherent conditions according to the protocol of Liu et al. (2012, 2017). To establish an effective feeder layer, irradiated J2 fibroblasts were plated at a density of 12,000 cells per cm (Ma et al., 2010; Liu et al., 2017). Once plated, the co-cultured cells were incubated in a humidified incubator at 37°C/5% CO_2. Conditionally reprogrammed (CR) cells were allowed to grow up to 80% confluence and 0.05% trypsin/EDTA (Gibco, cat. no. 25300054) was used to differentially trypsinize cells from the adherent culture dishes. Differential trypsinization detaches irradiated J2s first, leaving behind an enriched population of CR mammary cells to be used for experimentation or cryopreservation.

To culture and irradiate J2 fibroblasts, cells were plated with J2 media in T-150 flasks (250,000–500,000 cells) and allowed to grow up to 80% confluence. J2s were carefully cultured to not exceed 90% confluence. Once confluent, J2s were trypsinized using 0.05% trypsin/EDTA, resuspended in J2 media, and placed on ice to be transported for irradiation. J2s were irradiated at 30 grays for 6 min, viability was assessed via acridine orange/propoidium iodide staining. Irradiated J2 cells were cryopreserved at 300,000–500,000 cells per vial in recovery cell culture freezing medium (Gibco, cat. no. 12648010). Following irradiation, 100,000 irradiated J2s and non-irradiated controls were plated for comparison in order to ensure success of irradiation in halting cell proliferation.

J2 media was prepared by combining 500 mL DMEM (Gibco, cat. no. 11965-092), 50 mL bovine calf serum (ATCC cat. no. 30-2030), 5.5 mL 200 mM L-glutamine (Gibco, cat. no. 25030081), and 5.5 mL 100X Pen-Strep (Gibco, cat. no. 15140122). F-media was made by combining 623.83 μL of 12 mM Rho-associated kinase (ROCK) inhibitor Y-27632 (Cayman Chemical, cat. no. 10005583), 194.48 μL of 96 μg/mL hydrocortisone (STEMCELL Technologies, cat. no. 07925), 8.98 μL of 10 μg/mL epidermal growth factor (STEMCELL Technologies, cat. no. 78006.1), 935 μL of 4 mg/mL insulin (Invitrogen-LifeTechnologies, cat. no. 12585014), and 62.83 μL of 1.2 μM cholera toxin (Sigma-Aldrich, cat. no. C8052) and 561 mL of complete DMEM (500 mL DMEM (Gibco, cat. no. 11965-092), 50 mL heat inactivated fetal bovine serum (Sigma-Aldrich cat. No F4135), 5.5 mL 200 mM L-glutamine (Gibco, cat. no. 25030081), and 5.5 mL 100X Pen-Strep (Gibco, cat. no. 15140122).

Single Cell RNA-Sequencing

NM cells and their CR counterparts (n = 3 pairs) were removed from liquid nitrogen storage and individually thawed, centrifuged, and counted. Cell mixtures were diluted with 0.01%FBS+PBS solution to achieve a final concentration of 100 cells/uL for each 5 mL sample (500,000 cells/sample). Samples were placed on ice and processed for drop-seq analysis according to the protocol of Macosko et al. (2015).

The drop-seq microfluidic device was assembled and calibrated to dispense oil droplets (Bio-Rad cat # 186-4006), cells, and Barcoded Bead SeqB (Chemgenes) beads at optimal velocity. Samples were loaded into the apparatus and the cell and microbead containing droplets were collected in 50 mL conical tubes (Falcon). Following droplet collection, a series of wash, transfer, and centrifuge steps were performed in order to prepare the microbeads for sequencing.

After bead purification the following workflow was performed in order to generate DNA for sequencing. To generate cDNA strands from RNA hybridized to bead primers, RT mix was added to the microbeads and incubated. Following incubation, microbeads were rinsed and resuspended in exonuclease mix to remove excess bead primers that did not capture any RNA, rinsed, and then prepped for PCR. A 13 cycle PCR program was run to amplify cDNA and the generated cDNA library was then purified and analyzed on a BioAnalyzer High Sensitivity Chip. The purified cDNA was then tagmented using Nextera XT, PCR amplified, analyzed again using the BioAnalyzer. Following these steps, the library was sequenced on a NextSeq 500 (Illumina) at the University of Michigan Advanced Genomics Core Facility.

Single-Cell Data Analyses

Raw Data Processing

The "Drop-seqAlignmentCookbookv1.2Jan2016" software was used to transform raw sequencing data into gene expression measurements for each individual cell. The paired end reads were aligned to a mixed human (hg19) and mouse (mm10) reference genome and then grouped by cell according to the cell bar code. Next, a digital expression matrix was generated from the unique molecular identifier (UMI) counts for each gene in each cell. We performed quality control (QC) filtering on the raw data, filtering out cells with greater than 5% of mitochondrial genes and fewer than 200 total genes. Following QC filtration, we performed global log-normalization, scaling by percent mitochondrial genes, detection of highly variable genes, and principal component analysis dimension reduction. QC and downstream data processing were performed using the Seurat R package v3 unless specified otherwise (Satija et al., 2015).

Unbiased Clustering and Cell Type Identification

Graph based unbiased clustering and PCA based tSNE dimension reduction were performed on NM, CR, and pooled NM and CR samples at a resolution of 0.5. Cell type identification was performed by identifying marker genes for individual clusters (**Supplementary Tables S1, S2**) as well as assessing expression of a pre-selected a panel of cell type marker genes. Cluster markers were identified using the FindMarkers function in Seurat and marker gene expression was assessed using the FeaturePlot and VlnPlot functions. Due to the differences in numbers of cells captured and analyzed between the NM and CR samples, we performed a normalized analysis by randomly down-sampling each individual sample to 200 cells and performing the same clustering and marker gene assessment as performed on the full dataset.

Differential Gene Expression Analysis

In order to isolate epithelial subsets of NM and CR cells for direct comparison, we filtered out stromal and immune cells from NM samples, and mouse cells were filtered out from CR samples. We performed differential expression analysis between pooled epithelial CR and NM samples with PQLseq, which uses a penalized quasilikelihood and a heredity correlation matrix (Sun et al., 2019). The hereditary matrix was designed with the hierarchical data structure in mind in order to account for random effects of individual samples. Doing so prevents any one individual with a large number of cells relative to any other to dominate the analysis, and provides a more powerful analysis compared to a naïve approach. Differential gene expression between the NM and CR cells within each individual was performed using the FindMarkers function in Seurat. DEGs between NM and CR for each individual were plotted by average log2FC and correlation coefficients were calculated for each comparison.

Embryonic Stem Cell Score

To estimate the similarities of the gene expression pattern of each cell to an embryonic stem cell, we calculated an "embryonic stem cell gene expression score." The proportion of total reads which belong to genes in the Embryonic Stem Cell Core set from the Gene Set Enrichment Analysis (GSEA) were calculated on a per cell basis (Wong et al., 2008). A higher stem cell score can be interpreted as a greater proportion of reads for a given cell being derived from embryonic stem cell-associated genes.

Transcription Factor and Enrichment Analyses

The top 1000 DEGs in CR compared to NM by log2FC were uploaded to the Enrichr web server to identify ENCODE

and ChEA transcription factors enrichment (Kuleshov et al., 2016). To characterize the enrichment of the mammary stem cell and luminal progenitor gene sets reported by Lim et al. (2009) and ROCK pathway gene signatures, each of these gene sets was overlapped with CR DEGs. The overlapped genes were then plotted by CR vs. NM log2FC to visualize gene signature enrichment.

Identification of Hybrid Populations

Hybrid populations were identified in using expression of *KRT14*, *KRT18*, *VIM*, and *EPCAM*. Cells expressing marker genes at the 50th percentile or greater were deemed "high expressors." High expressors for the *KRT14*/*KRT18* or *EPCAM*/*VIM* marker combinations were identified as "double positive" hybrids, and high expressors for all four marker genes were identified as "quadruple positive" hybrids. Differential gene expression analysis between quadruple hybrids and all other NM and CR epithelial cells was performed using FindMarkers in Seurat. Differentially expressed genes upregulated in quadruple hybrid cells were intersected with the MSigDB Hallmark Epithelial Mesenchymal Transition gene set ($n = 200$) in order identify EMT related genes expressed in quadruple hybrids.

Integration and Alignment of NM, CR, Bach, Nguyen, and the Cancer Genome Atlas (TCGA) Breast Cancer RNA-seq Samples to the Giraddi Mouse Mammary Transcriptome Atlas

Dataset Descriptions

To contextualize our findings in NM and CR cells, we also performed an integrated analysis with three other single cell RNA-seq mammary gland datasets generated from mice and humans, as well as a comparative analysis using bulk breast cancer RNA-seq data from TCGA. The "Bach" dataset contains single cell RNA-seq profiling of mouse mammary gland from four developmental stages: nulliparous, mid gestation, lactation, and post involution (Bach et al., 2017). The "Nguyen" dataset is comprising of single cell RNA-seq profiling of human mammary gland generated from adult voluntary reduction mammoplasty patients (Nguyen et al., 2018). The "Giraddi" dataset is comprized of single cell RNA-seq data from multiple timepoints during the lifecourse: embryonic day 16, embryonic day 18, postnatal day 0, postnatal day 4, and adult (Giraddi et al., 2018). Bulk RNA-seq counts of TCGA breast tumors were obtained from the National Cancer Institute's genomic data commons portal using the TCGAbiolinks R package (Colaprico et al., 2016).

Data Pre-processing

The raw counts data of NM, CR, Bach, and Nguyen cells were normalized using either the "multiBatchNorm" or the "normalize" function in the R package scran. For gene filtering, a modified version of the CORGI algorithm was used on the Nguyen and Giraddi datasets, hereinafter referred to as "CORGI genes" (Giraddi et al., 2018; Nguyen et al., 2018). The CORGI gene filtering algorithm works by randomly sampling subsets of genes and scoring the subsets based on the structuredness of the data (Wang et al., 2019a). Genes that lead to more structured data are encouraged and vice versa. The TCGA dataset was pre-processed in the same way as the single-cell samples.

Down-Sampling and Cell Selection

To generate the Giraddi reference dataset used for alignment, the full mouse mammary dataset was randomly down-sampled to 1000 cells spanning the four developmental stages (embryonic day 16, embryonic day 18, gestational day 4, and adult). Proportions of cells in the generated reference dataset reflect the proportions of cells from each developmental stage in the original dataset. The Bach mouse dataset was down-sampled by randomly selecting 250 cells from each of the four adult developmental stages (nulliparous, mid-gestation, lactation, and post-involution) for a total of 1000 cells. NM, CR, and Nguyen datasets were also randomly down-sampled to 1000 cells each.

Batch Correction

For batch correction, the "mnnCorrect" function in scran was used with default parameters on the logcounts on CORGI genes. The Giraddi dataset was input into the mnnCorrect as the first argument, i.e. as the reference atlas. Subsequently, the NM, CR, Bach, Nguyen, and TCGA samples were then projected onto the Giraddi developmental trajectory for comparative analysis.

Pseudotime Analysis

In order to place the various datasets onto a developmental timeline, we leveraged the Giraddi mouse atlas as a reference. Pseudotime is computed directly onto the two-dimensional PCA plots by taking the dot product with an "arrow-of-time" vector that differentiates between the adult and embryonic cell populations in the Giraddi dataset. The same arrow-of-time vector was then applied to the NM, CR, Bach, Nguyen, and TCGA samples. A generalized linear model was used to determine significantly different pseudotime means between TCGA subtypes.

Dataset Availability

The drop-seq data for the NM and CR samples are available on the Gene Expression Omnibus (GSE146792).

RESULTS

Normal Mammary Cells Contain a Mixture of Stromal and Epithelial Cells and Cluster by Subtype

As a first step toward characterizing the distribution of phenotypic states of epithelial cells in the human mammary gland, we performed unbiased clustering of NM scRNA-seq data to determine the cell types and proportions present in the samples. Samples were analyzed from three individuals, here termed "NM11", "NM15", and "NM23". tSNE visualization revealed that the majority of clusters contained cells from each individual (**Figure 1A**). To determine the identity of the six

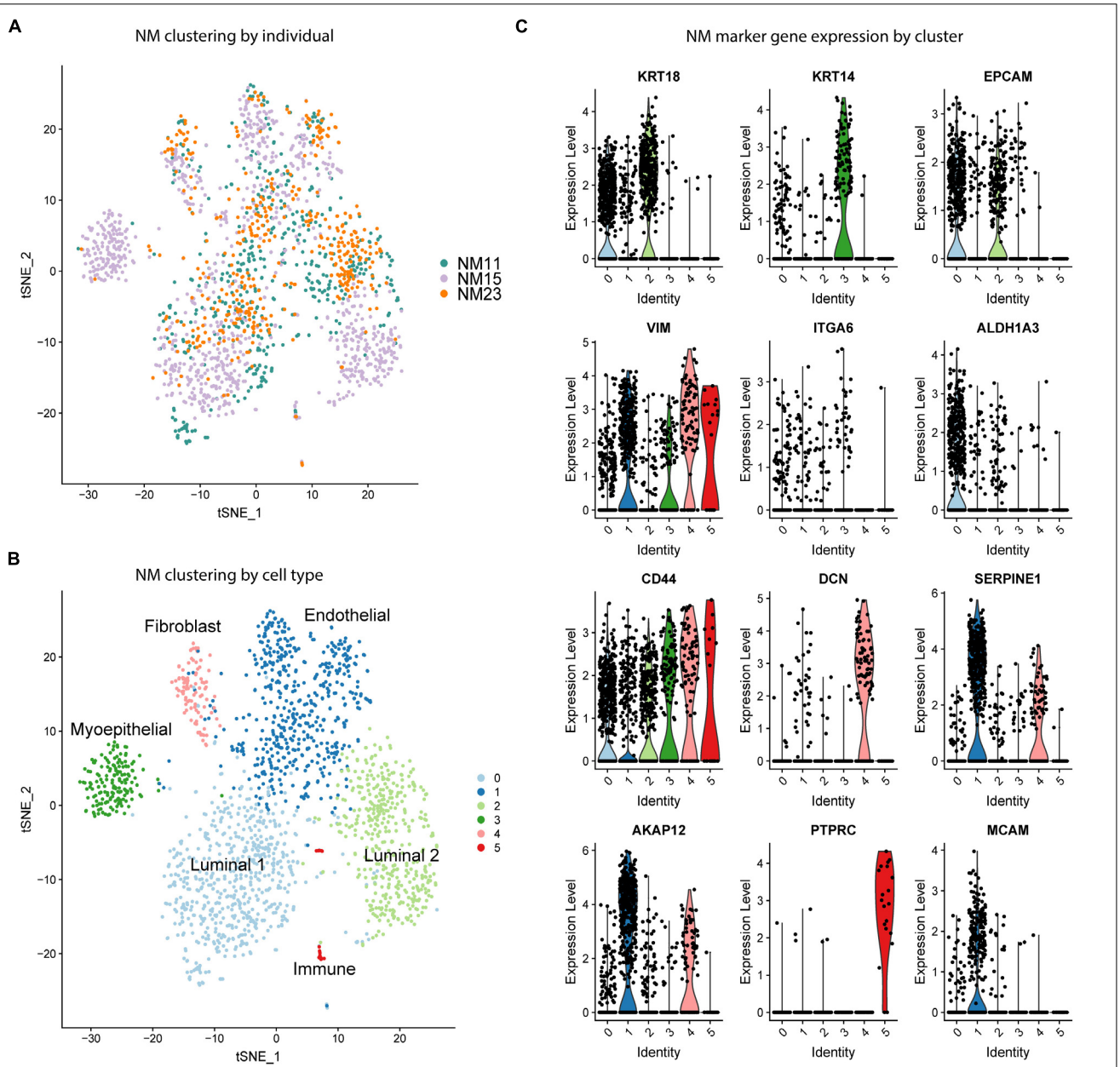

FIGURE 1 | Unbiased clustering and cell type identification of NM cells. **(A)** tSNE dimension reduction of NM samples colored by individual. **(B)** Unbiased clustering of NM samples colored by cell cluster. **(C)** Expression of known cell type marker genes by cluster across all NM samples.

clusters (**Figure 1B**), a panel of known breast cell type and stem cell marker genes (**Figure 1C**) along with the top marker genes for each cluster identified by Seurat (**Supplementary Table S1**), were used to characterize the clusters. The two major epithelial subtypes of the breast were identified by *KRT18* (luminal) and *KRT14* (myoepithelial) expression (**Figure 1C**; O'Hare et al., 1991; Abd El-Rehim et al., 2004). Clusters 0 and 2 (**Figure 1B**) represent two distinct luminal populations which both highly express epithelial marker *EPCAM* but differentially express stem cell marker *ALDH1A3*, which is preferentially expressed in cluster 0 (Trzpis et al., 2007; Marcato et al., 2011). Mammary stem cell markers *ITGA6* and *CD44* also exhibited varying expression by cluster, with *ITGA6* showing low expression in clusters 0-3 and *CD44* exhibiting moderate to high expression across all clusters (Al-Hajj et al., 2003). The myoepithelial Cluster 3 was almost entirely composed of cells from one individual (NM15), indicating variation in cell type proportions by individual. We identified cluster 4 identified as fibroblasts (*DCN*), cluster 1 as endothelial cells (*SERPINE1*, *AKAP12*), and cluster 5 as a small population of immune cells (*PTPRC*). Thus, prior to CR, normal mammary cells are composed of a mixture of stromal, immune, and epithelial cells and cluster primarily by cell type.

Conditionally Reprogrammed Mammary Cells Cluster by CR Status and by Individual

Marker analysis of the CR samples revealed that samples were depleted of fibroblasts, endothelial cells, and immune cells, but retained luminal and myoepithelial populations (**Supplementary Figures S1A,B**). We identified two clusters (7 and 8) of mouse fibroblasts, using the mouse gene *Gapdh* as a marker, which we excluded in downstream analyses (**Supplementary Figure S1B** and **Supplementary Table S2**). To characterize CR alterations specifically in epithelial cells, we grouped NM and CR epithelial cells together for analysis. Unbiased clustering of the NM and CR cells revealed that NM samples remained relatively well mixed amongst each other, whereas CR samples distinctly clustered by individual (**Figure 2A**). While CR11 and CR15 exhibited some overlap in clustering, CR23 remained distinct from the other samples. Samples clustered by CR status along tSNE_1 and both NM and CR samples clustered as myoepithelial and luminal cells (**Figures 2B,C**). *KRT14* was selectively expressed in NM and CR myoepithelial populations, however, *KRT18* expressing CR cells also co-expressed moderate levels of *KRT14*. To determine if this clustering behavior was representative of CR gene expression alterations or due to the greater proportion of CR to NM cells, the same clustering and marker gene identification was performed on a randomly down-sampled subset comprised of 200 cells from each NM and CR sample. This subset of cells displayed the same clustering patterns and marker gene expression as the full dataset (**Supplementary Figures S1C–F**). The co-expression (*KRT18*/*KRT14*) of luminal and myoepithelial markers was the first indication that the CR process could induce a hybrid state phenotype worthy of further investigation.

Conditionally Reprogrammed Mammary Cells Differentially Express Breast Cancer and Stem Cell Associated Genes

To gain mechanistic insight into the effects of the CR process, we compared gene expression patterns between NM and CR cells with differential gene expression (DGE) analysis. DGE between the NM and CR epithelial cells resulted in 3177 genes differentially expressed between the two cell populations (FDR < 0.05) (**Figure 2D**; **Supplementary Table S3**). DGE was also conducted between the NM and CR cells of each individual and the overlap of differentially expressed genes (DEGs) was compared between individuals (**Supplementary Figure S2A** and **Supplementary Table S4**). DEGs by individual were consistent with those found in combined NM and CR analysis, with both analyses identifying *LGALSI* as one of the most differentially upregulated genes in CR. Comparing DEGs between NM and

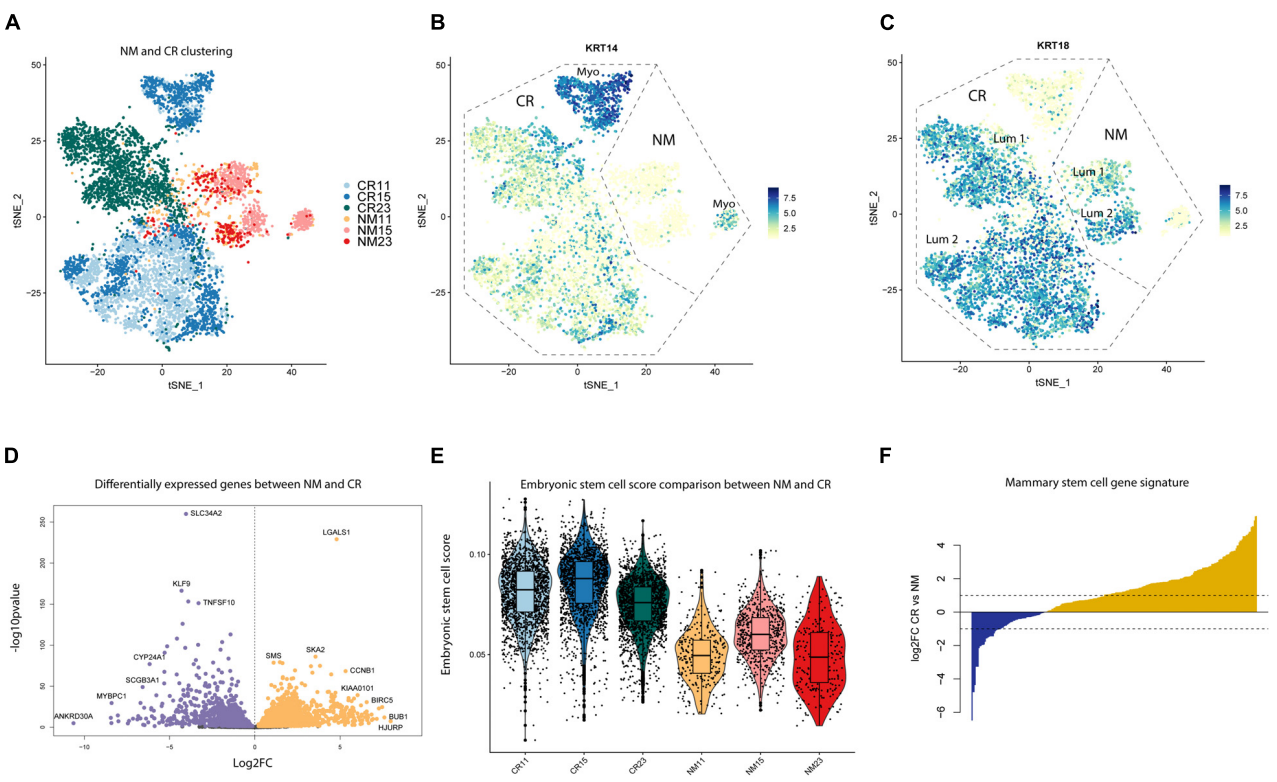

FIGURE 2 | Unbiased clustering and differential gene expression between NM and CR. **(A)** tSNE dimension reduction of NM and CR samples by individual. **(B)** FeaturePlots of myoepithelial marker gene (*KRT14*) and **(C)** luminal marker gene (*KRT18*) expression. **(D)** Differentially expressed genes between NM and CR epithelial cells. Significantly upregulated genes in CR (FDR < 0.05) are colored in orange. Significantly upregulated genes in NM are colored in purple. **(E)** Distribution of cells from NM and CR samples scored by embryonic stem cell gene expression. **(F)** Comparison of overlap between NM and CR differentially expressed genes and the mammary stem cell (MaSC) gene expression signature reported in Lim et al. (2009). Yellow genes indicate MaSC genes more highly expressed in CR vs. NM.

CR by individual also revealed that the DEGs between samples 11 and 15 are highly correlated with each other (r = 0.896) whereas DEGs between samples 11 and 23 (0.713) and between samples 15 and 23 (0.79) are less well correlated. Because the CR process requires the ROCK pathway small molecule inhibitor Y-27632, we assessed DEGs overlapping with ROCK associated pathway genes (**Supplementary Figure S2E** and **Supplementary Table S5**). Unsurprisingly, *ROCK2* was the most significantly downregulated gene in this pathway (log2FC = −1.25) in CR cells. We input the top 1000 upregulated DEGs in CR to the Enrichr web server to identify transcription factors likely driving this process. Gene targets of known stem cell associated transcription factors *E2F4, FOXM1, BRCA1, SOX2, KLF4,* and *MYC* were all identified as enriched in CR upregulated genes (**Supplementary Figure S2F** and **Supplementary Table S6**).

To further investigate whether NM and CR cells exhibit differences in expression of stem cell associated genes, we performed analyses using overall gene expression as well as NM and CR DEGs. We estimated how "embryonic stem cell-like" each cell was by calculating the proportion of total transcripts annotated to embryonic stem cell (ESC) associated genes (**Supplementary Table S7**) expressed in each NM and CR sample (Wong et al., 2008). CR samples had higher ESC scores than their NM counterparts (**Figure 2E**), providing further evidence that CR cells express a more developmentally immature phenotype. To further characterize this phenotype in comparison to stem and progenitor cells in the normal breast, we overlapped NM and CR DEGs with mammary stem cell (MaSC) and luminal progenitor gene expression signatures reported by Lim et al. (2009) (**Supplementary Tables S8, S9**) (Lim et al., 2009). Of the MaSC associated DEGs, 211/282 of the genes were upregulated in CR (**Figure 2F**), whereas only 68/144 luminal progenitor associated DEGs were upregulated in CR (**Supplementary Figure S2D**). Together, these analyses suggest that the CR process enriches for a stem cell-like state, and that the CR transcriptomic signature resembles ESCs and MaSCs.

Conditionally Reprogrammed Cells Reflect a More Developmentally Immature Phenotype

Due to the enrichment of stem cell associated genes in CR cells, we chose to further investigate this link in the context of mammary gland development. We integrated our data with the mouse mammary single-cell transcriptome atlas generated by Giraddi et al. (2018) which spans mouse mammary gland development from embryonic day 16 to adulthood (**Figure 3A**; Giraddi et al., 2018). We calculated pseudotime estimates for each cell across the mouse developmental trajectory. Pseudotime estimates correlate to the developmental timepoint during which each cell was isolated, the more negative the pseudotime estimate the more embryonic-like the cell (**Figure 3B**, **Supplementary Table S10**). Using the CORGI alignment algorithm, we used the Giraddi data as a reference to map our NM and CR samples onto the mammary gland developmental trajectory. The majority of NM cells aligned to the adult mouse cells, whereas CR cells spanned the trajectory with a distinct population aligning to the embryonic mouse cells (**Figure 3C**). When CR cells were labeled by individual, CR15 and CR23 had cells spanning the whole trajectory, whereas CR11 mapped mostly to mouse mammary gland at post-natal day 4 and adulthood (**Figure 3D**).

Hybrid Stem Cell Populations Emerge Following Conditional Reprogramming

A growing number of studies have characterized hybrid stem cell populations in the normal and cancerous breast and have linked these epithelial/mesenchymal (E/M) or luminal/basal (L/B) hybrid phenotypes to aggressiveness of cancer (Colacino et al., 2018; Gerdur Ísberg et al., 2019; Jolly et al., 2019). Additionally, emerging evidence shows that stem cells can stably exist in hybrid states and that these hybrid phenotypes may be metastable (Jolly et al., 2016). To investigate the presence of hybrid populations in normal mammary cells, we assessed the co-expression of the luminal and basal (here used interchangeably with myoepithelial) markers *KRT18*/*KRT14* (L/B) and the epithelial and mesenchymal markers *EPCAM*/*VIM* (E/M) to identify "double positive" hybrid cells. Overlap of *EPCAM*/*VIM* and *CDH1*/*VIM* double positive populations indicate that *EPCAM* and *CDH1* are both effective epithelial markers, however, *EPCAM* was ultimately chosen as the epithelial marker for hybrid identification due to its overall higher expression in NM and CR cells (**Supplementary Figures S1G,H**). Co-expression of all four markers *KRT18*/*KRT14*/*EPCAM*/*VIM* identified "quadruple positive" hybrid cells. "Triple positive" hybrid combinations were also assessed, however, we found these redundant and less informative than the double positive and quadruple positive marker combinations (**Supplementary Figure S4**). We identified L/B, E/M, and quadruple positive hybrid populations in the Giraddi dataset, NM, and CR cells, with CR cells expressing the highest proportions of both double positive hybrids and quadruple hybrids (**Supplementary Table S11**). CR15 expressed the highest proportion of hybrid cells among the individuals.

In the Giraddi dataset, E/M hybrids spanned both basal and luminal branches of the trajectory, L/B hybrids mostly mapped to adult luminal and post-natal day 4, and quadruple hybrids mapped along the luminal branch around embryonic day 18 and post-natal day 4 (**Figure 3E**). E/M hybrids were the only cells to map to the basal adult cells and the embryonic cells. To investigate the developmental maturity of hybrid CR cells, we mapped the E/M, L/B, and quadruple hybrids to the mouse developmental trajectory (**Figure 3F**). Almost all of the hybrid CR cells mapped to mouse cells spanning embryonic day 16 through post-natal day 4, with a few mapping to the adult populations. Interestingly, the hybrid E/M cells map along both the luminal and basal trajectories, however, the L/B hybrids almost exclusively map along the luminal trajectory. The majority of the quadruple hybrids also mapped along the luminal trajectory.

To further characterize the different cell types, pseudotime analysis was performed on the CR, NM, and hybrid populations. Pseudotime estimates for CR cells indicated a more developmentally immature phenotype relative to NM cells (**Figure 3G**). Pseudotime analysis of the Giraddi mouse hybrid populations revealed that hybrid E/M cells are the

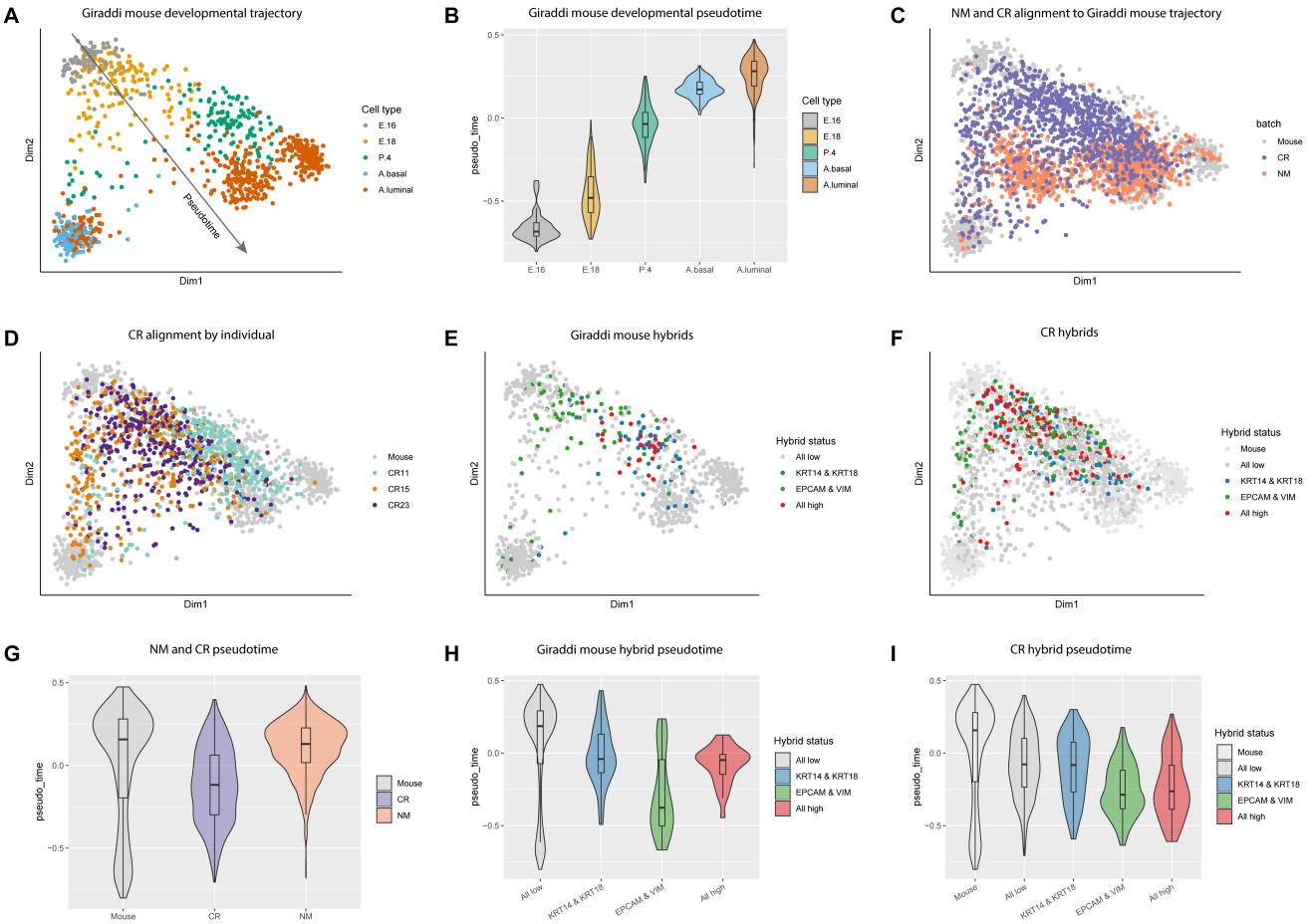

FIGURE 3 | Alignment of NM and CR cells to mouse mammary developmental trajectory and characterization of hybrid cells. **(A)** Principal component analysis plot of single cell RNA-seq data of mouse mammary gland at embryonic day 16 (E.16), embryonic day 18 (E. 18), post-natal day 4 (P.4), and adult basal (A. basal) and adult luminal (A.luminal) cells as reported in Giraddi et al. (2018). **(B)** Pseudotime estimates of mouse mammary developmental stages. **(C)** NM and CR cells mapped to the developmental trajectory with CoRGI. **(D)** CR samples mapped to the mouse mammary developmental trajectory labeled by individual. **(E)** Hybrid cell identification of mouse mammary cells along the developmental trajectory. Luminal/basal hybrids were identified by concurrent high *KRT14/KRT18* expression. Epithelial/mesenchymal hybrids were identified by concurrent high *EPCAM/VIM* expression. Quadruple positive hybrid cells were identified by high expression of all four marker genes *KRT14/KRT18,/EPCAM/VIM.* **(F)** CR cells mapped to mouse developmental trajectory and labeled by hybrid status. **(G)** Pseudotime estimates of NM and CR cells relative to the mouse mammary developmental trajectory cells. **(H)** Pseudotime estimates of mouse hybrid cells. **(I)** Pseudotime estimates of CR hybrid cells.

most developmentally immature, followed by the quadruple hybrids, and then hybrid L/B cells (**Figure 3H**). CR hybrids exhibited a similar pattern to the mouse hybrids, where hybrid E/M cells were the most developmentally immature, quadruple hybrids were intermediate, and L/B hybrids were the most mature (**Figure 3I**). Pseudotime differences between hybrid populations in the CR cells were less pronounced than in the mouse. We also calculated the embryonic stem cell score for the NM and CR hybrid cell populations and found that E/M and quadruple hybrids expressed a higher embryonic stem cell score, whereas L/B hybrids were less distinct (**Supplementary Figures S3A–C**). From this we concluded that the CR process causes an enrichment of hybrid cells and that these hybrid populations are transcriptionally similar to mammary cells in early development. Finally, E/M and L/B hybrids appear to represent distinct cellular populations with quadruple positive hybrid cells falling somewhere in between.

Differential gene expression analysis between quadruple positive hybrids and all other epithelial NM and CR cells identified 4052 genes upregulated and 2660 genes downregulated in quadruple hybrids (**Supplementary Figure S2B** and **Supplementary Table S12**). The most significant DEG upregulated in the quadruple positive hybrids was extracellular matrix gene *COL14A1* which has been found to be upregulated in cancerous breast stroma compared to normal breast stroma (Casey et al., 2009). We further investigated the DEGs from the quadruple hybrids by calculating the overlap of these genes with the MSIGDB EMT hallmark gene set (**Supplementary Table S13**). We found that 82 out of the 200 (41%) genes differentially expressed in the quadruple

hybrids were EMT related genes (**Supplementary Figure S2C**). Together, these data provide evidence for the presence of hybrid cells in the normal and developing breast, specifically early in development.

Hybrid Stem Cell Populations Are Enriched During Gestation and Lactation

The enrichment of these hybrid populations early in breast development aligns with the current understanding of the highly dynamic nature of mammary gland morphogenesis. This led us to investigate another highly dynamic and proliferative developmental stage of the breast: gestation and lactation. We incorporated the adult mouse mammary developmental dataset generated by Bach et al. (2017), which spans the nulliparous, mid-gestation, lactation, and post-involution time points (Bach et al., 2017). Alignment of the Bach dataset to the Giraddi developmental trajectory revealed a striking chronological pseudotime arc (**Figure 4A**). Beginning at the nulliparous stage, mammary cells exhibit a developmentally mature pseudotime, reflected by alignment to Giraddi mouse adult cells. Mammary cells during the gestation stage exhibit a more developmentally immature phenotype, indicated by a decrease in estimated pseudotime. Through the lactation and post-involution stages, pseudotime of mammary cells sequentially increases to stabilize at a pseudotime similar to the developmental maturity of the nulliparous stage. Mapping of these cells to the Giraddi trajectory demonstrated that the nulliparous and post-involution stages mapped most closely to the luminal and basal adult cells, the lactation stage mapped most closely to adult basal cells, and the gestation stage mapped most closely to the embryonic day 18 cells (**Figure 4B**). L/B, E/M, and quadruple hybrids were also identified in the Bach dataset and mapped to the Giraddi trajectory (**Figures 4C–E**). Proportions of hybrid cells were calculated for each stage (**Figure 4F**). The highest proportion of E/M hybrids were found in the gestation stage which also expressed the highest proportion of L/B hybrids, followed by the lactation stage. Interestingly, the lactation stage expressed the highest proportion of quadruple hybrids, followed by the gestation stage. Although the pseudotime estimates for the nulliparous and post-involution stages were similar, the post-involution stage had an approximately 5-fold lower proportion of hybrid cells. The enrichment of hybrid populations during the gestation and lactation stages suggests the importance of these cells during pregnancy-associated mammary gland morphogenesis.

To further extend and validate these findings in human patient samples, we also explored the distribution of hybrid cells in the Nguyen dataset, which is generated largely from nulliparous patients, and compared their alignment to the NM samples (**Supplementary Figure 5A**). We aligned the Nguyen data to the Giraddi developmental trajectory and found that cells largely clustered with the mouse adult luminal and basal cells (**Supplementary Figure S5B**). In the Nguyen dataset, there were approximately 11 and 12% of cells classified as E/M and L/B hybrids (**Supplementary Figures 5C–J**), respectively, which is comparable to the proportion of these hybrid cells in the nulliparous mice from the Bach dataset (10 and 16%). The proportion of these cells in the post-involution mouse cells from the Bach dataset were 3 and 2%, respectively.

Basal Breast Cancers Are the Most Transcriptionally Distinct and Developmentally Immature of Breast Cancer Subtypes

All our prior findings about hybrid cell states and developmental phenotypes were characterized in normal human and mouse mammary cells. Our next step was to leverage this data to inform our understanding of breast cancer subtype biology. To do this, we assessed gene expression of breast tumors from the Cancer Genome Atlas (TCGA). Principal component analysis of the TCGA tumors without any alignment showed that basal tumors clustered as the most distinct from the other subtypes, with luminal A and luminal B overlapping, and the other subtypes grouping between the luminal and basal subtypes (**Figure 5A**). We mapped the bulk TCGA tumor RNA expression data onto the Giraddi mouse developmental trajectory and found that normal, luminal A, and luminal B tumors mapped most closely to the adult cells, HER2 tumors mapped to slightly more immature cells, and basal tumors spanned pseudotime along the basal trajectory (**Figure 5B**). Pseudotime estimates by subtype revealed that the luminal A subtype exhibits a significantly more developmentally mature phenotype than the luminal B (p = 4.97E-07), Her2 (p = 0.0495), and basal (p < 2E-16) subtypes, with the basal subtype exhibiting the most immature pseudotime estimate (**Figure 5C**). As a next step, we assessed the link between the pseudotime estimates of gene expression and breast cancer outcomes. Of the top 10 annotated genes with the most negative pseudotime estimates, 5 were significantly associated with poor prognosis in breast cancer patients (**Figure 5D**). Our results suggest that "phenotypic developmental maturity" of cancer cells, particularly at timepoints strongly associated with the hybrid E/M state may be a distinguishing factor of the subtypes and that pseudotime-associated genes have prognostic implications for breast cancer patients.

DISCUSSION

Through our integrated analysis of normal human and mouse mammary data and TCGA tumor data, we witness an overarching theme – "developmentally immature" pseudotime is linked to the likelihood of hybrid cells which express a stem-like gene expression signature. We identify an increased proportion of hybrid cells at particular important timepoints during development: in particular the *in utero* period, gestation, and lactation. Others have found associations between an "embryonic stem-cell like" gene expression signature and aggressiveness of cancers (Malta et al., 2018). Hybrid E/M cells present a particularly interesting population to further explore in the context of aggressive cancers due to their low pseudotime estimates and their mapping along the basal mouse trajectory. Together, our results suggest that hybrid cells/states and their stem-like plasticity are important mediators in development

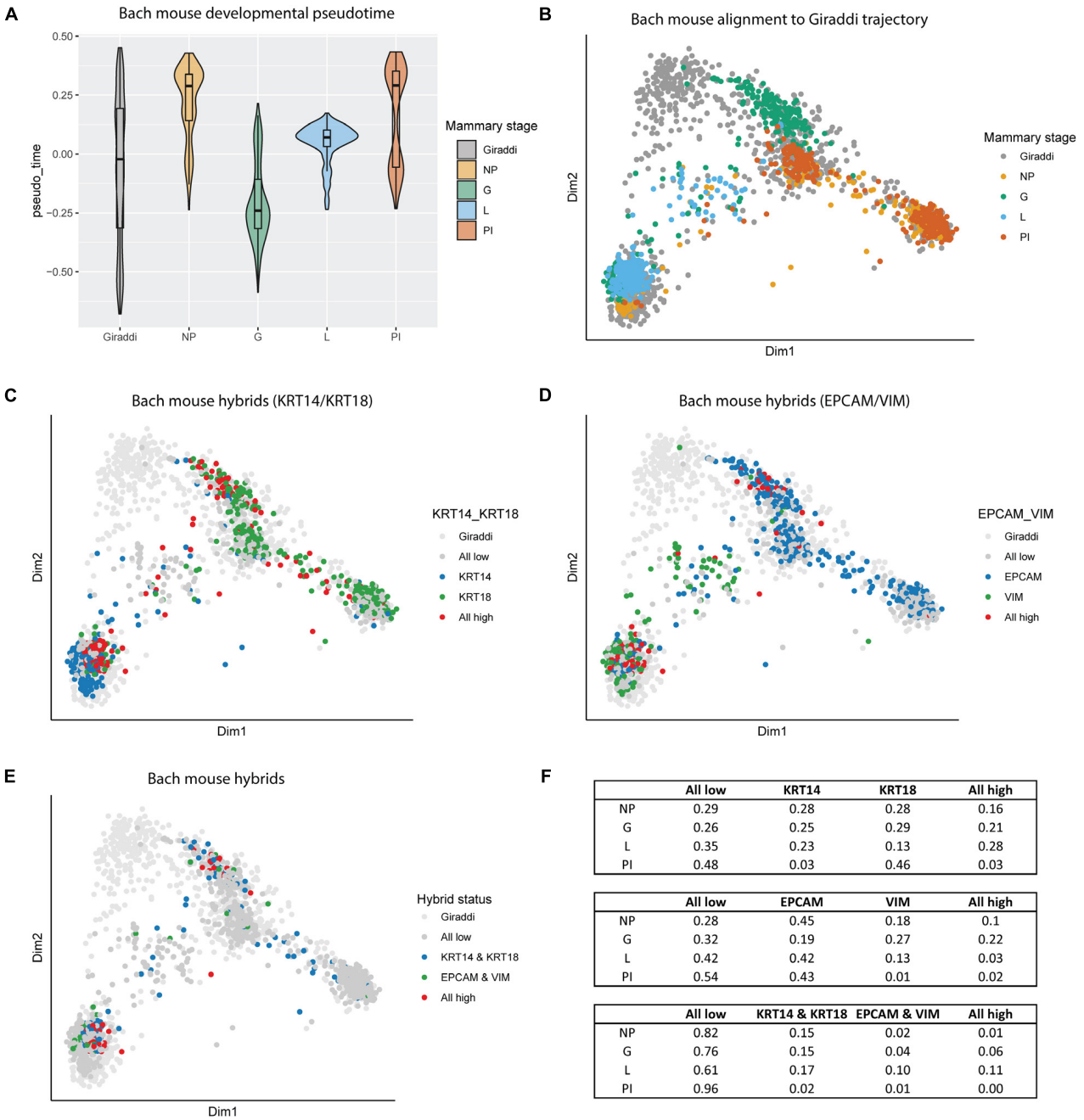

F

	All low	KRT14	KRT18	All high
NP	0.29	0.28	0.28	0.16
G	0.26	0.25	0.29	0.21
L	0.35	0.23	0.13	0.28
PI	0.48	0.03	0.46	0.03

	All low	EPCAM	VIM	All high
NP	0.28	0.45	0.18	0.1
G	0.32	0.19	0.27	0.22
L	0.42	0.42	0.13	0.03
PI	0.54	0.43	0.01	0.02

	All low	KRT14 & KRT18	EPCAM & VIM	All high
NP	0.82	0.15	0.02	0.01
G	0.76	0.15	0.04	0.06
L	0.61	0.17	0.10	0.11
PI	0.96	0.02	0.01	0.00

FIGURE 4 | Alignment of Bach mouse mammary developmental dataset to the Giraddi mammary trajectory. **(A)** Pseudotime estimates of Bach mammary developmental stages: nulliparous (NP), mid-gestation (G), lactation (L), and post-involution (PI). **(B)** Bach mammary cells mapped to the Giraddi trajectory with CoRGI. **(C)** Bach luminal/basal hybrid cells mapped to Giraddi trajectory. **(D)** Bach epithelial/mesenchymal hybrid cells mapped to Giraddi trajectory. **(E)** Bach quadruple positive hybrid cells mapped to Giraddi trajectory **(F)** Proportions of Bach hybrid cells by developmental stage.

and cancer and that this intersection is a promising future direction to explore.

The precision of single-cell RNA-seq allowed us to characterize NM tissue as comprized of stromal, immune, and epithelial cells. When we perturbed NM cells *in vitro* with the conditional reprogramming method, we identified that CR cells only contained luminal and myoepithelial populations, with a small subpopulation of mouse fibroblasts, which were used as a feeder layer to support the growth of the CR cells. The CR process appears to enhance inter-individual heterogeneity, where post-CR samples cluster much more distinctly by individual. Given that the CR samples and NM counterparts were derived from the same individual, the preferential clustering by CR status is indicative that the CR process likely induces major

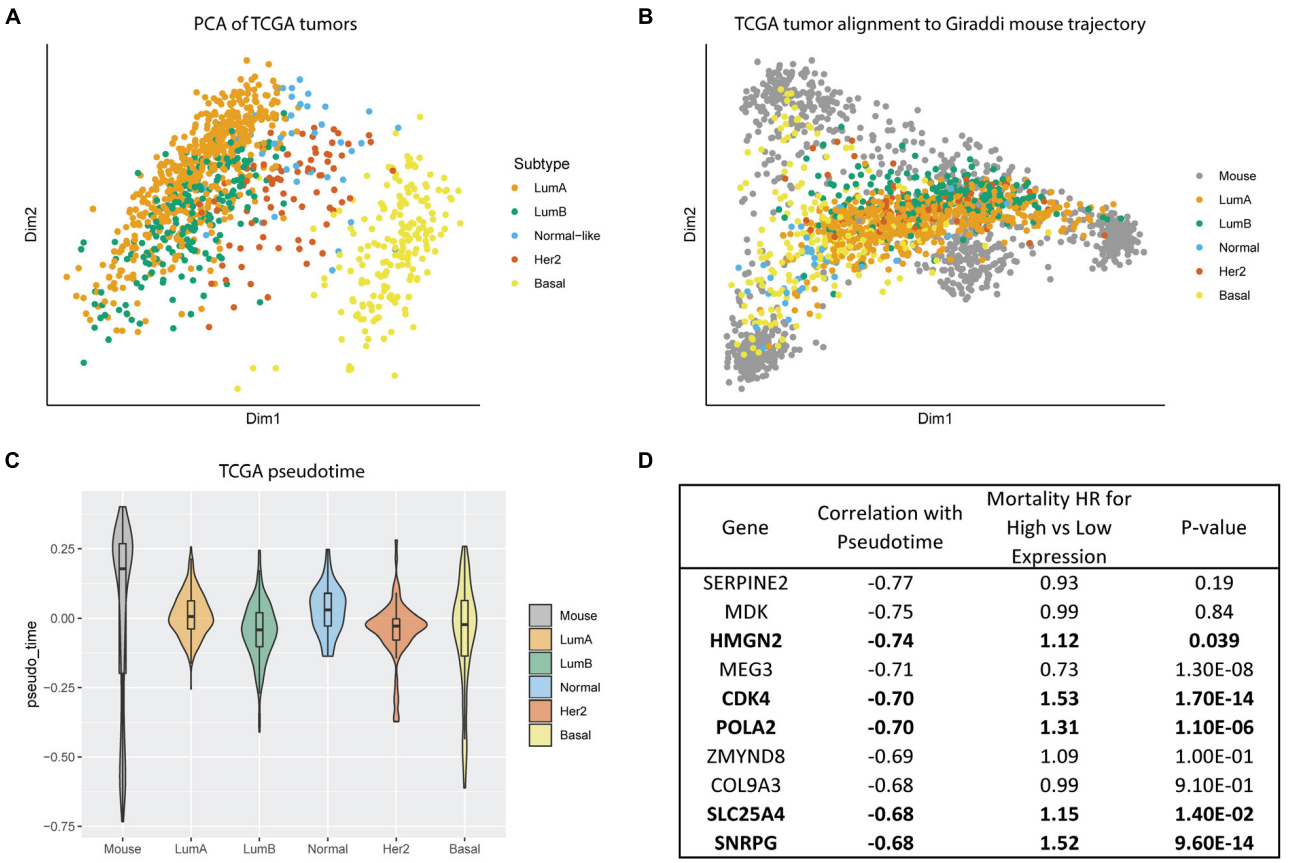

D

Gene	Correlation with Pseudotime	Mortality HR for High vs Low Expression	P-value
SERPINE2	-0.77	0.93	0.19
MDK	-0.75	0.99	0.84
HMGN2	**-0.74**	**1.12**	**0.039**
MEG3	-0.71	0.73	1.30E-08
CDK4	**-0.70**	**1.53**	**1.70E-14**
POLA2	**-0.70**	**1.31**	**1.10E-06**
ZMYND8	-0.69	1.09	1.00E-01
COL9A3	-0.68	0.99	9.10E-01
SLC25A4	**-0.68**	**1.15**	**1.40E-02**
SNRPG	**-0.68**	**1.52**	**9.60E-14**

FIGURE 5 | Alignment of TCGA tumors to Giraddi mammary trajectory. **(A)** Principal component analysis of TCGA bulk breast tumor RNA-seq labeled by subtype. **(B)** Alignment of TCGA tumors to Giraddi developmental trajectory. **(C)** Pseudotime estimates of TCGA tumor subtypes. **(D)** Mortality hazard ratio estimates relative to expression of the top 10 genes most negatively correlated with mouse pseudotime. The more negative the pseudotime estimate, the more highly expressed the gene is in the earliest timepoints during development.

transcriptomic alterations as well as depletion of immune and stromal cells.

DGE analysis between NM and CR samples allowed us to identify a number of significant genes. Understanding their molecular functions may provide crucial mechanistic insight into the CR process, the enrichment of the embryonic stem cell phenotype we observed, and the connection between stemness and cancer. Of these genes, *LGALS1* stands out due to its significant upregulation overall in CR cells as well as in comparisons of DEGs by sample. A member of the galectin family of proteins which modulate proliferation and cell-cell/cell-matrix interactions, upregulation of *LGALS1* expression in breast cancer adjacent fibroblasts has been linked to metastasis and is altered in lymph node metastases compared to primary breast tumors (Feng et al., 2007; Folgueira et al., 2013). Outside of the breast, *LGALS1* is linked to invasiveness and metastasis in oral cancer (Li et al., 2018). Amongst the other highly significant upregulated CR genes by *p*-value and log2FC, *SKA2*, *MKI67*, *HJURP*, *BIRC5*, and *CCNB1* are upregulated in breast cancer tissues and all five except for *SKA2* have been identified as prognostic markers for breast cancer (Li et al., 2013; Ding et al., 2014; Falato et al., 2014; Montes de Oca et al., 2015; Ren et al., 2019; Wang et al., 2019b). Additionally, *BUB1* and *BIRC5* have been linked to stemness, where depletion of *BUB1* reduced cancer stem cell potential in MDA-MB-231 and MCF-7 breast cancer cell lines and *BIRC5* is commonly expressed in embryonic tissues and cancer but not in adult tissues (Han et al., 2015; Ghaffari et al., 2016; Hamy et al., 2016). Experimental evidence continues to support the link between stemness and cancer, and our results showing enrichment of a stem-like phenotype and breast cancer related genes in CR cells adds to this body of work. It is striking that the induction of stem-like proliferation and de-differentiation of normal mammary adult cells by ROCK inhibitor Y-27632 upregulates numerous genes which overlap with breast cancer and metastasis, providing further experimental evidence that cancers are hijacking normal stem cell mechanisms.

Another key finding of our study was the emergence of hybrid cell populations post-CR. Our characterization of these populations is consistent previous reports and provides additional insight into the "developmental maturity" of these hybrid states. Hybrid E/M cells have been found in human primary tumors and lymph nodes where they exhibit enhanced tumor initiation and metastatic potential and are implicated in therapy resistance and poor survival (Yu et al., 2013;

Grosse-Wilde et al., 2015; Jolly et al., 2019). Similarly, L/B hybrids have been characterized in both normal and cancer tissue from humans and are believed to be derived from luminal progenitors (Abd El-Rehim et al., 2004; Gerdur Ísberg et al., 2019). This hypothesis of L/B hybrids being luminal in origin is consistent with our observations, where L/B hybrids in both human and mouse map only along the luminal trajectory of the mouse mammary gland developmental atlas, whereas E/M hybrids map to both luminal and basal trajectories. Sun et al. (2010) have shown that in the developing mouse mammary gland, *KRT5*/*KRT14* (L/B) hybrids are observed beginning from embryonic day 15.5 up until adulthood (8–12 weeks). While these populations decreased after 3 weeks, it is important to note that they were still present in the normal adult mouse mammary gland. Additionally, Sun et al. (2010) also identified a distinct population of cells expressing *KRT6*, a multipotent mammary epithelial progenitor marker, which emerged at embryonic day 16.5 and was localized to the nipple sheath. Expression of *KRT6* was also correlated to the boundary of the mammary mesenchyme, separate from luminal and basal localization. Considering the proximity to the mammary mesenchyme and its distinctness from luminal and basal progenitors, the *KRT6* population in the mouse mammary gland may be analogous to the E/M hybrids we identified in the CR population. The embryonic origin of hybrid populations in the developing mouse mammary gland and their persistence through adulthood suggests that hybrid populations in the human mammary gland also arise during embryogenesis and are maintained through adulthood.

Pseudotime analysis of mouse, NM, CR, and breast tumor samples suggest that the "developmental maturity" state of a cell or tumor plays a direct role in its biological behavior. Of the hybrid populations in both mouse and CR cells, the E/M hybrids exhibited the lowest estimated pseudotime. Based on prior knowledge implicating E/M hybrids in tumorigenesis and metastasis, this population may be of particular interest in the future to target for cancer prevention and therapy. To understand the impact of variation in pseudotime on our understanding of breast subtype biology, we calculated pseudotime estimates of bulk tumor RNA-seq data from TCGA samples. On average, none of the TCGA tumor subtypes exhibited pseudotime scores corresponding to adult mouse cells. Instead, average subtype scores corresponded to post-natal day 4 and earlier in development. While these are bulk samples being aligned to single-cell mouse samples, this suggests that regardless of cell type, a more developmentally immature phenotype is characteristic of cancers. Among the subtypes, basal cancers preferentially map to the most developmentally immature cells in the mammary gland and express the lowest pseudotime scores. This difference in "developmental maturity" may be a key distinction between basal cancers and other subtypes and may play a major role in the aggressiveness and low survival outcomes observed clinically and epidemiologically.

One of our most exciting findings was the characterization of hybrid cells in the adult mouse mammary gland during pregnancy. The enrichment of hybrid populations during gestation and lactation and their loss in the subsequent post-involution stage suggests that these hybrid states are inducible and transient. This transiency provides compelling evidence that these hybrid populations are instrumental to the dynamic modifications in breast morphogenesis which occur during pregnancy and lactation. This arc of mouse hybrid enrichment and stabilization parallels the transient increase in breast cancer risk during and immediately following pregnancy, which decreases over time. The time period during which hybrid populations are most prevalent in the mouse breast overlaps with pregnancy associated breast cancer (PABC) risk in humans, diagnosed between pregnancy and 1 year following birth (Ruiz et al., 2017). This overlap in time period, as well as the parallel transiency of mouse hybrid populations and PABC risk, supports the presence of these hybrid populations in the human breast during pregnancy and implicates their involvement in PABC. The pathophysiology of PABC is characterized by metastatic, high grade tumors, and survival is inversely correlated with time since birth (Ruiz et al., 2017). Consistent with this is the finding that ER-/PR-/HER2+, and triple-negative tumors are more common in women diagnosed with PABC compared to nulliparous women (Johansson et al., 2018). Based on our other findings that basal breast tumors exhibit the most "developmentally immature" pseudotime estimates and the link between hybrid cells and aggressive cancers, characterizing hybrid populations and "developmental maturity" of PABCs could inform prognostic and therapeutic treatment.

Our study had a number of limitations. One was the source and sample size of mammary tissue. Mammoplasty tissue has been critiqued as not being fully representative of the "normal" breast. Due to the de-identification of the samples we also lack demographic data on the women from whom they were obtained for our study, although we were able to supplement our findings with additional human data from the Nguyen study (Degnim et al., 2012). Moreover, the conditional reprogramming methodology only supports the outgrowth of epithelial cells from samples, a phenomenon which has been linked to the J2 fibroblast co-cultures since the 1970s (Rheinwatd and Green, 1975). A better understanding of stromal/epithelial interactions in regulating these hybrid stem cell states is an important future direction of research. These future experiments could, for example, assess the impact of adult fibroblasts or cancer associated fibroblasts on the reprogramming process. Future complementary analyses of conditional reprogramming using breast cancer samples could also provide important insights into the impacts of enhanced stemness and developmental immaturity on tumor characteristics. While single-cell technology is rapidly evolving and improving, we acknowledge that in this study we are only capturing expression of a subset of the genes expressed in each individual cell. Another limitation is the potential for unanticipated bias from using the subset of CORGI selected genes for alignment with the human mammary cells and TCGA tumor samples to the mouse developmental trajectory.

Overall, we showcase a computational analysis which leverages publicly available data to gain insight into the relationship between hybrid cell populations, stemness, and

cancer. We and others have identified significant inter-individual heterogeneity in proportions of stem cells in mammary tissue (Nakshatri et al., 2015; Colacino et al., 2018). Our ongoing work is utilizing single-cell RNA-seq of normal mammary tissue from epidemiologically well characterized women to understand how known epidemiological risk factors for cancer influence the "stemness" of breast epithelial cells. Quantification of reprogramming efficiency during conditional reprogramming across samples from diverse women could provide a functional readout of "stemness" or reprogramming capacity and their relations to known cancer risk factors, such as age, ethnicity, or genetic predisposition to cancer. Future work can focus on identifying the localization of these hybrid states in the adult mammary gland using advanced techniques, such as spatial transcriptomics. Overall, these results provide further evidence to support investigating the role of stem cells, and particularly hybrid E/M cells, in normal development and characterizing how this biology is hijacked during tumorigenesis. Understanding the biology of these cells will likely provide novel targets for the prevention and therapy of aggressive breast cancers.

DATA AVAILABILITY STATEMENT

The datasets generated for this study can be found in the Gene Expression Omnibus (GSE146792).

ETHICS STATEMENT

The studies involving human participants were reviewed and approved by the study protocol was reviewed and approved by the University of Michigan Institutional Review Board (HUM00042409). Written informed consent for participation was not required for this study in accordance with the national legislation and the institutional requirements.

AUTHOR CONTRIBUTIONS

TT conducted the experiments, analyzed the data, and wrote the manuscript. YW developed the analysis methods, analyzed the data, and wrote the manuscript. MB conducted the experiments, analyzed the data, and wrote the manuscript. CL analyzed the data. CS developed the analysis methods. LB developed the analysis methods. MW conceptualized the study and interpreted the data. JC conceptualized the study, analyzed the data, and wrote the manuscript. All authors reviewed and approved the final version of the manuscript.

FUNDING

This work was supported by grants from the National Institute of Environmental Health Sciences (R01ES028802, P30ES017885), the National Cancer Institute (P30CA046592, R35CA197585), the National Institutes of Health (UL1TR0022404), the University of Michigan Forbes Institute for Cancer Discovery, the University of Michigan Institute for Data Science, the National Science Foundation (CAREER CCF-1845076), and the Ravitz Family Foundation.

SUPPLEMENTARY MATERIAL

The Supplementary Material for this article can be found online at: https://www.frontiersin.org/articles/10.3389/fcell.2020.00288/full#supplementary-material

FIGURE S1 | Post-CR single cell unbiased clustering and gene expression. **(A)** tSNE dimension reduction of CR cells colored by cell cluster, identified by unbiased clustering **(B)** Expression of known cell type marker genes by cluster. Cluster 7 and 8 identified as mouse cells **(C)** tSNE dimension reduction of NM and CR samples by individual. Each individual sample was down-sampled to 200 cells. **(D)** NM and CR FeaturePlots of myoepithelial marker gene (*KRT14*) and **(E)** luminal marker gene (*KRT18*) expression **(F)** Expression of known cell type marker genes by down-sampled NM and CR individuals **(G)** Identification of NM and CR *CDH1/VIM* double positive cells and **(H)** *EPCAM/VIM* double positive cells. Table compares the overlap between the *CDH1/VIM* and *EPCAM/VIM* classifications.

FIGURE S2 | Post-CR differential gene expression and pathway analysis. **(A)** Comparison of differentially expressed genes between NM and CR cells of individual samples. DEGs are plotted by average log2FC. Positive values represent genes upregulated in CR and negative values represent genes downregulated in CR. **(B)** Differential gene expression of quadruple hybrids vs. all other NM and CR cells. Significantly upregulated genes in quadruple positive hybrids (FDR < 0.05) are colored in orange. Significantly downregulated genes in quadruple hybrids are colored in purple. **(C)** Overlap between quadruple hybrid upregulated genes and EMT related genes. Upregulated EMT genes in quadruple hybrids in orange, and downregulated EMT genes in purple. **(D)** Comparison of overlap between NM and CR differentially expressed genes and the luminal progenitor gene expression signature reported in Lim et al. (2009). Yellow genes indicate luminal progenitor genes more highly expressed in CR vs. NM. **(E)** Comparison of overlap between NM and CR differentially expressed genes and the ROCK pathway gene set. **(F)** Top 10 transcription factors associated with top 1000 genes overexpressed in CR cells.

FIGURE S3 | Embryonic stem cell gene signature of NM and CR hybrid cells. **(A)** ESC score of NM and CR cells labeled by *EPCAM/VIM* hybrids status, **(B)** *KRT14/KRT18* hybrid status, and **(C)** quadruple positive hybrid status.

FIGURE S4 | Comparison of triple positive Giraddi mammary cells and aligned CR cells. Localization of **(A)** mouse *KRT14/EPCAM/VIM* triple positive cells, **(B)** CR *KRT14/EPCAM/VIM* triple positive cells, **(C)** mouse *KRT14/KRT18/EPCAM* triple positive cells, **(D)** CR *KRT14/KRT18/EPCAM* triple positive cells, **(E)** mouse *KRT14/KRT18/VIM* triple positive cells, **(F)** CR *KRT14/KRT18/VIM* triple positive cells, **(G)** mouse *KRT14/EPCAM/VIM* triple positive cells, and **(H)** CR *KRT14/EPCAM/VIM* triple positive cells when aligned to the mouse mammary developmental trajectory with CoRGI.

FIGURE S5 | Comparison of hybrid NM cells and Nguyen human mammary cells. **(A)** Alignment of NM cells to Giraddi trajectory by individual. **(B)** Alignment of Nguyen mammary cells to Giraddi trajectory. **(C)** NM *EPCAM/VIM* hybrids. **(D)** Nguyen *EPCAM/VIM* hybrids. **(E)** NM KRT14/KRT18 hybrids **(F)** Nguyen KRT14/KRT18 hybrids. **(G)** NM quadruple positive hybrids. **(H)** Nguyen quadruple positive hybrids **(I)** Proportions of NM cells by hybrid status. **(J)** Proportions of Nguyen cells by hybrid status.

TABLE S1 | NM cluster markers. Most highly expressed genes for each individual NM cluster, orderd by log2FC.

TABLE S2 | CR cluster markers. Most highly expressed genes for each individual CR cluster, orderd by log2FC.

TABLE S3 | CR vs. NM differential gene expression. Differentially expressed genes between pooled epithelial NM and CR cells. Genes are ordered by log2FC, with higher numbers corresponding to genes up in CR and vice versa.

TABLE S4 | CR vs. NM differential gene expression by individual. Differentially expressed genes between the NM and CR cells of each individual ordered by log2FC.

TABLE S5 | ROCK gene set. Rho-associated kinase genes used to characterize ROCK enrichment between NM and CR.

TABLE S6 | CR transcription factors. ENCODE and CHEA transcription factors identified from the top 1000 differentially expressed genes in CR.

TABLE S7 | ESC gene set. List of genes from the Gene Set Enrichment Analysis used to calculated an embryonic stem cell gene expression score for NM and CR cells.

TABLE S8 | Mammary stem cell gene set. List of mammary stem cell genes used to characterize mammary stem cell enrichment between NM and CR.

TABLE S9 | Luminal progenitor gene set. List of luminal progenitor genes used to characterize luminal progenitor enrichment between NM and CR.

TABLE S10 | Mouse pseudotime genes. Arrow-of-time vector genes which most differentiate embryonic mouse mammary cells and adult cells from the Giraddi dataset. The lower the pseudotime score the more embryonically associated the gene and vice versa.

TABLE S11 | Hybrid proportions. Proportion of hybrid cells in Giraddi mouse dataset and NM and CR.

TABLE S12 | Quadruple hybrids vs. all other epithelial differential gene expression. Differentially expressed genes between quadruple hybrids and all other epithelial cells.

TABLE S13 | Overlap between differentially expressed genes in quadruple hybrids and EMT genes. A subset of differentially expressed genes between quadruple hybrids and all other epithelial cells which have been identified as EMT genes.

TABLE S14 | Mouse pseudotime vs. CR expression. Arrow-of-time mouse pseudotime genes applied to genes expressed in CR cells.

REFERENCES

Abd El-Rehim, D. M., Pinder, S. E., Paish, C. E., Bell, J., Blamey, R. W., Robertson, J. F., et al. (2004). Expression of luminal and basal cytokeratins in human breast carcinoma. *J. Pathol.* 203, 661–671. doi: 10.1002/path.1559

Al-Hajj, M., Wicha, M. S., Benito-Hernandez, A., Morrison, S. J., and Clarke, M. F. (2003). Prospective identification of tumorigenic breast cancer cells. *Proc. Natl. Acad. Sci. U.S.A.* 100, 3983–3988. doi: 10.1073/pnas.0530291100

Bach, K., Pensa, S., Grzelak, M., Hadfield, J., Adams, D. J., Marioni, J. C., et al. (2017). Differentiation dynamics of mammary epithelial cells revealed by single-cell RNA sequencing. *Nat Commun.* 8:2128. doi: 10.1038/s41467-017-02001-5

Casey, T., Bond, J., Tighe, S., Hunter, T., Lintault, L., Patel, O., et al. (2009). Molecular signatures suggest a major role for stromal cells in development of invasive breast cancer. *Breast Cancer Res. Treat.* 114, 47–62. doi: 10.1007/s10549-008-9982-8

Colacino, J. A., Azizi, E., Brooks, M. D., Harouaka, R., Fouladdel, S., McDermott, S. P., et al. (2018). Heterogeneity of human breast stem and progenitor cells as revealed by transcriptional profiling. *Stem Cell Rep.* 10, 1596–1609. doi: 10.1016/j.stemcr.2018.03.001

Colacino, J. A., McDermott, S. P., Sartor, M. A., Wicha, M. S., and Rozek, L. S. (2016). Transcriptomic profiling of curcumin-treated human breast stem cells identifies a role for stearoyl-coa desaturase in breast cancer prevention. *Breast Cancer Res. Treat.* 158, 29–41. doi: 10.1007/s10549-016-3854-4

Colaprico, A., Silva, T. C., Olsen, C., Garofano, L., Cava, C., Garolini, D., et al. (2016). TCGAbiolinks: an R/Bioconductor package for integrative analysis of TCGA data. *Nucleic Acids Res.* 44:e71. doi: 10.1093/nar/gkv1507

Degnim, A. C., Visscher, D. W., Hoskin, T. L., Frost, M. H., Vierkant, R. A., Vachon, C. M., et al. (2012). Histologic findings in normal breast tissues: comparison to reduction mammaplasty and benign breast disease tissues. *Breast Cancer Res. Treat.* 133, 169–177. doi: 10.1007/s10549-011-1746-1

Ding, K., Li, W., Zou, Z., Zou, X., and Wang, C. (2014). CCNB1 is a prognostic biomarker for ER+ breast cancer. *Med. Hypotheses* 83, 359–364. doi: 10.1016/j.mehy.2014.06.013

Dontu, G., Abdallah, W. M., Foley, J. M., Jackson, K. W., Clarke, M. F., Kawamura, M. J., et al. (2003). In vitro propagation and transcriptional profiling of human mammary stem/progenitor cells. *Genes Dev.* 17, 1253–1270. doi: 10.1101/gad.1061803

Falato, C., Lorent, J., Tani, E., Karlsson, E., Wright, P. K., Bergh, J., et al. (2014). Ki67 measured in metastatic tissue and prognosis in patients with advanced breast cancer. *Breast Cancer Res. Treat.* 147, 407–414. doi: 10.1007/s10549-014-3096-2

Feng, Y., Sun, B., Li, X., Zhang, L., Niu, Y., Xiao, C., et al. (2007). Differentially expressed genes between primary cancer and paired lymph node metastases predict clinical outcome of node-positive breast cancer patients. *Breast Cancer Res. Treat.* 103, 319–329. doi: 10.1007/s10549-006-9385-7

Folgueira, M. A. A. K., Maistro, S., Katayama, M. L. H., Roela, R. A., Mundim, F. G. L., Nanogaki, S., et al. (2013). Markers of breast cancer stromal fibroblasts in the primary tumour site associated with lymph node metastasis: a systematic review including our case series. *Biosci. Rep.* 33:e00085. doi: 10.1042/BSR20130060

Gerdur Ísberg, Ó, Kim, J., Fridriksdottir, A. J., Morsing, M., Timmermans-Wielenga, V., Rønnov-Jessen, L., et al. (2019). A CD146 FACS protocol enriches for luminal keratin 14/19 double positive human breast progenitors. *Sci. Rep.* 9:14843. doi: 10.1038/s41598-019-50903-9

Ghaffari, K., Hashemi, M., Ebrahimi, E., and Shirkoohi, R. (2016). BIRC5 genomic copy number variation in early-onset breast cancer. *Iran Biomed. J.* 20, 241–245. doi: 10.7508/ibj.2016.04.009

Giraddi, R. R., Chung, C.-Y., Heinz, R. E., Balcioglu, O., Novotny, M., Trejo, C. L., et al. (2018). Single-cell transcriptomes distinguish stem cell state changes and lineage specification programs in early mammary gland development. *Cell. Rep.* 24, 1653.e7–1666.e7. doi: 10.1016/j.celrep.2018.07.025

Grosse-Wilde, A., Fouquier d'Hérouël, A., McIntosh, E., Ertaylan, G., Skupin, A., Kuestner, R. E., et al. (2015). Stemness of the hybrid epithelial/mesenchymal state in breast cancer and its association with poor survival. *PLoS One* 10:e0126522. doi: 10.1371/journal.pone.0126522

Hamy, A. S., Bieche, I., Lehmann-Che, J., Scott, V., Bertheau, P., Guinebretière, J. M., et al. (2016). BIRC5 (survivin): a pejorative prognostic marker in stage II/III breast cancer with no response to neoadjuvant chemotherapy. *Breast Cancer Res. Treat.* 159, 499–511. doi: 10.1007/s10549-016-3961-2

Han, J. Y., Han, Y. K., Park, G. Y., Kim, S. D., and Lee, C. G. (2015). Bub1 is required for maintaining cancer stem cells in breast cancer cell lines. *Sci. Rep.* 5:15993. doi: 10.1038/srep15993

Johansson, A. L. V., Andersson, T. M. L., Hsieh, C. C., Jirström, K., Cnattingius, S., Fredriksson, I., et al. (2018). Tumor characteristics and prognosis in women with pregnancy-associated breast cancer. *Int. J. Cancer* 142, 1343–1354. doi: 10.1002/ijc.31174

Jolly, M. K., Boareto, M., Huang, B., Jia, D., Lu, M., Ben-Jacob, E., et al. (2015). Implications of the hybrid epithelial/mesenchymal phenotype in metastasis. *Front. Oncol.* 5:155. doi: 10.3389/fonc.2015.00155

Jolly, M. K., Somarelli, J. A., Sheth, M., Biddle, A., Tripathi, S. C., Armstrong, A. J., et al. (2019). Hybrid epithelial/mesenchymal phenotypes promote metastasis and therapy resistance across carcinomas. *Pharmacol. Ther.* 194, 161–184. doi: 10.1016/j.pharmthera.2018.09.007

Jolly, M. K., Tripathi, S. C., Jia, D., Mooney, S. M., Celiktas, M., Hanash, S. M., et al. (2016). Stability of the hybrid epithelial/mesenchymal phenotype. *Oncotarget* 7, 27067–27084. doi: 10.18632/oncotarget.8166

Kalluri, R., and Weinberg, R. A. (2009). The basics of epithelial-mesenchymal transition. *J. Clin. Invest.* 119, 1420–1428. doi: 10.1172/JCI39104

Kuleshov, M. V., Jones, M. R., Rouillard, A. D., Fernandez, N. F., Duan, Q., Wang, Z., et al. (2016). Enrichr: a comprehensive gene set enrichment analysis web server 2016 update. *Nucleic Acids Res.* 44, W90–W97. doi: 10.1093/nar/gkw377

Li, J.-M., Tseng, C.-W., Lin, C.-C., Law, C.-H., Chein, Y.-A., Kuo, W.-H., et al. (2018). Upregulation of LGALS1 is associated with oral cancer metastasis. *Ther. Adv. Med. Oncol.* 10:175883591879462. doi: 10.1177/1758835918794622

Li, Y., Chen, Y.-L., Xie, Y.-T., Zheng, L.-Y., Han, J.-Y., Wang, H., et al. (2013). Association study of germline variants in CCNB1 and CDK1 with breast cancer susceptibility, progression, and survival among chinese han women. *PLoS One* 8:e84489. doi: 10.1371/journal.pone.0084489

Lim, E., Vaillant, F., Wu, D., Forrest, N. C., Pal, B., Hart, A. H., et al. (2009). Aberrant luminal progenitors as the candidate target population for basal tumor development in BRCA1 mutation carriers. *Nat. Med.* 15, 907–913. doi: 10.1038/nm.2000

Liu, X., Krawczyk, E., Suprynowicz, F. A., Palechor-Ceron, N., Yuan, H., Dakic, A., et al. (2017). Conditional reprogramming and long-term expansion of normal and tumor cells from human biospecimens. *Nat. Protoc.* 12, 439–451. doi: 10.1038/nprot.2016.174

Liu, X., Ory, V., Chapman, S., Yuan, H., Albanese, C., Kallakury, B., et al. (2012). ROCK inhibitor and feeder cells induce the conditional reprogramming of epithelial cells. *Am. J. Pathol.* 180, 599–607. doi: 10.1016/j.ajpath.2011.10.036

Ma, Y., Zhang, P., Wang, F., Yang, J., Yang, Z., and Qin, H. (2010). The relationship between early embryo development and tumourigenesis. *J. Cell. Mol. Med.* 14, 2697–2701. doi: 10.1111/j.1582-4934.2010.01191.x

Macosko, E. Z., Basu, A., Satija, R., Nemesh, J., Shekhar, K., Goldman, M., et al. (2015). Highly parallel genome-wide expression profiling of individual cells using nanoliter droplets. *Cell* 161, 1202–1214. doi: 10.1016/J.CELL.2015.05.002

Malta, T. M., Sokolov, A., Gentles, A. J., Burzykowski, T., Poisson, L., Weinstein, J. N., et al. (2018). Machine learning identifies stemness features associated with oncogenic dedifferentiation. *Cell* 173, 338.e15–354.e15. doi: 10.1016/j.cell.2018.03.034

Marcato, P., Dean, C. A., Pan, D., Araslanova, R., Gillis, M., Joshi, M., et al. (2011). Aldehyde dehydrogenase activity of breast cancer stem cells is primarily due to isoform aldh1a3 and its expression is predictive of metastasis. *Stem Cells* 29, 32–45. doi: 10.1002/stem.563

Merrell, A. J., and Stanger, B. Z. (2016). Adult cell plasticity in vivo: de-differentiation and transdifferentiation are back in style. *Nat. Rev. Mol. Cell. Biol.* 17, 413–425. doi: 10.1038/nrm.2016.24

Montes de Oca, R., Gurard-Levin, Z. A., Berger, F., Rehman, H., Martel, E., Corpet, A., et al. (2015). The histone chaperone HJURP is a new independent prognostic marker for luminal A breast carcinoma. *Mol. Oncol.* 9, 657–674. doi: 10.1016/j.molonc.2014.11.002

Nakshatri, H., Anjanappa, M., and Bhat-Nakshatri, P. (2015). Ethnicity-dependent and -independent heterogeneity in healthy normal breast hierarchy impacts tumor characterization. *Sci. Rep.* 5:13526. doi: 10.1038/srep13526

Nguyen, Q. H., Pervolarakis, N., Blake, K., Ma, D., Davis, R. T., James, N., et al. (2018). Profiling human breast epithelial cells using single cell RNA sequencing identifies cell diversity. *Nat. Commun.* 9:2028. doi: 10.1038/s41467-018-04334-1

O'Hare, M. J., Ormerod, M. G., Monaghan, P., Lane, E. B., and Gusterson, B. A. (1991). Characterization in vitro of luminal and myoepithelial cells isolated from the human mammary gland by cell sorting. *Differentiation* 46, 209–221. doi: 10.1111/j.1432-0436.1991.tb00883.x

Ren, Z., Yang, T., Zhang, P., Liu, K., Liu, W., and Wang, P. (2019). SKA2 mediates invasion and metastasis in human breast cancer via EMT. *Mol. Med. Rep.* 19, 515–523. doi: 10.3892/mmr.2018.9623

Reya, T., Morrison, S. J., Clarke, M. F., and Weissman, I. L. (2001). Stem cells, cancer, and cancer stem cells. *Nature* 414, 105–111. doi: 10.1038/35102167

Rheinwatd, J. G., and Green, H. (1975). Seria cultivation of strains of human epidemal keratinocytes: the formation keratinizin colonies from single cell is. *Cell* 6, 331–343. doi: 10.1016/S0092-8674(75)80001-8

Ruiz, R., Herrero, C., Strasser-Weippl, K., Touya, D., St Louis, J., Bukowski, A., et al. (2017). Epidemiology and pathophysiology of pregnancy-associated breast cancer: a review. *Breast* 35, 136–141. doi: 10.1016/j.breast.2017.07.008

Satija, R., Farrell, J. A., Gennert, D., Schier, A. F., and Regev, A. (2015). Spatial reconstruction of single-cell gene expression data. *Nat. Biotechnol.* 33, 495–502. doi: 10.1038/nbt.3192

Sun, P., Yuan, Y., Li, A., Li, B., and Dai, X. (2010). Cytokeratin expression during mouse embryonic and early postnatal mammary gland development. *Histochem. Cell Biol.* 133, 213–221. doi: 10.1007/s00418-009-0662-5

Sun, S., Zhu, J., Mozaffari, S., Ober, C., Chen, M., and Zhou, X. (2019). Heritability estimation and differential analysis of count data with generalized linear mixed models in genomic sequencing studies. *Bioinformatics* 35, 487–496. doi: 10.1093/bioinformatics/bty644

Tam, W. L., and Weinberg, R. A. (2013). The epigenetics of epithelial-mesenchymal plasticity in cancer. *Nat. Med.* 19, 1438–1449. doi: 10.1038/nm.3336

Thong, T., Forté, C. A., Hill, E. M., and Colacino, J. A. (2019). Environmental exposures, stem cells, and cancer. *Pharmacol. Ther.* 204:107398. doi: 10.1016/j.pharmthera.2019.107398

Trzpis, M., McLaughlin, P. M. J., De Leij, L. M. F. H., and Harmsen, M. C. (2007). Epithelial cell adhesion molecule: more than a carcinoma marker and adhesion molecule. *Am. J. Pathol.* 171, 386–395. doi: 10.2353/ajpath.2007.070152

Wang, Y., Thong, T., Saligrama, V., Colacino, J., Balzano, L., and Scott, C. (2019a). A gene filter for comparative analysis of single-cell RNA-sequencing trajectory datasets. *bioRxiv* [Preprint]. doi: 10.1101/637488

Wang, Y., Zhang, C., Mai, L., Niu, Y., Wang, Y., and Bu, Y. (2019b). PRR11 and SKA2 gene pair is overexpressed and regulated by p53 in breast cancer. *BMB Rep.* 52, 157–162. doi: 10.5483/BMBRep.2019.52.2.207

Wong, D. J., Liu, H., Ridky, T. W., Cassarino, D., Segal, E., and Chang, H. Y. (2008). Module map of stem cell genes guides creation of epithelial cancer stem cells. *Cell Stem Cell* 2, 333–344. doi: 10.1016/j.stem.2008.02.009

Yu, M., Bardia, A., Wittner, B. S., Stott, S. L., Smas, M. E., Ting, D. T., et al. (2013). Circulating breast tumor cells exhibit dynamic changes in epithelial and mesenchymal composition. *Science* 339, 580–584. doi: 10.1126/science.1228522

Conflict of Interest: The authors declare that the research was conducted in the absence of any commercial or financial relationships that could be construed as a potential conflict of interest.

Copyright © 2020 Thong, Wang, Brooks, Lee, Scott, Balzano, Wicha and Colacino. This is an open-access article distributed under the terms of the Creative Commons Attribution License (CC BY). The use, distribution or reproduction in other forums is permitted, provided the original author(s) and the copyright owner(s) are credited and that the original publication in this journal is cited, in accordance with accepted academic practice. No use, distribution or reproduction is permitted which does not comply with these terms.

frontiers in Molecular Biosciences

REVIEW
published: 13 May 2020
doi: 10.3389/fmolb.2020.00063

Senescence-Associated Pro-inflammatory Cytokines and Tumor Cell Plasticity

*Jean Paul Vernot**

Facultad de Medicina, Universidad Nacional de Colombia, Bogotá, Colombia

The well-recognized cell phenotypic heterogeneity in tumors is a great challenge for cancer treatment. Dynamic interconversion and movement within a spectrum of different cell phenotypes (cellular plasticity) with the acquisition of specific cell functions is a fascinating biological puzzle, that represent an additional difficulty for cancer treatment and novel therapies development. The understanding of the molecular mechanisms responsible for moving or stabilizing tumor cells within this spectrum of variable states constitutes a valuable tool to overcome these challenges. In particular, cell transitions between epithelial and mesenchymal phenotypes (EMT-MET) and de-and *trans*-differentiation processes are relevant, since it has been shown that they confer invasiveness, drug resistance, and metastatic ability, due to the simultaneous acquisition of stem-like cell properties. Multiple drivers participate in these cell conversions events. In particular, cellular senescence and senescence-associated soluble factors have been shown to unveil stem-like cell properties and cell plasticity. By modulating gradually the composition of their secretome and the time of exposure, senescent cells may have differential effect not only on tumor cells but also on surrounding cells. Intriguingly, tumor cells that scape from senescence acquire stem-like cell properties and aggressiveness. The reinforcement of senescence and inflammation by soluble factors and the participation of immune cells may provide a dynamic milieu having varied effects on cell transitions, reprogramming, plasticity, stemness and therefore heterogeneity. This will confer different epithelial/mesenchymal traits (hybrid phenotype) and stem-like cell properties, combinations of which, in a particular cell context, could be responsible for different cellular functions during cancer progression (survival, migration, invasion, colonization or proliferation). Additionally, cooperative behavior between cell subpopulations with different phenotypes/stemness functions could also modulate their cellular plasticity. Here, we will discuss the role of senescence and senescence-associated pro-inflammatory cytokines on the induction of cellular plasticity, their effect role in establishing particular states within this spectrum of cell phenotypes and how this is accompanied by stem-like cell properties that, as the epithelial transitions, may also have a continuum of characteristics providing tumor cells with functional adaptability specifically useful in the different stages of carcinogenesis.

Keywords: Plasticity, senescence, proinflammatory cytokines, EMT, hybrid phenotypes, CSC

OPEN ACCESS

Edited by:
Mohit Kumar Jolly,
Indian Institute of Science, India

Reviewed by:
Joe Harvey Taube,
Baylor University, United States
Xuefei Li,
Shenzhen Institutes of Advanced Technology, China

***Correspondence:**
Jean Paul Vernot
jpvernoth@unal.edu.co

Specialty section:
This article was submitted to Molecular Diagnostics and Therapeutics, a section of the journal Frontiers in Molecular Biosciences

Received: *21 January 2020*
Accepted: *25 March 2020*
Published: *13 May 2020*

Citation:
Vernot JP (2020) Senescence-Associated Pro-inflammatory Cytokines and Tumor Cell Plasticity. Front. Mol. Biosci. 7:63. doi: 10.3389/fmolb.2020.00063

CELL HETEROGENEITY AND CANCER STEM CELL PLASTICITY

Phenotypic and functional intratumour heterogeneity occurs in cancer cells as a consequence of the clonal evolution and cancer stem cell models, genetic and epigenetic alterations, microenvironment cues, and importantly, reversible and dynamic modifications in cellular properties (Marjanovic et al., 2013; Meacham and Morrison, 2013; Mooney et al., 2016; Gupta et al., 2019). The high degree of genetic heterogeneity fuelled in part by genetic instability and clonal evolution is responsible for a good part of this phenotypic heterogeneity during tumor development (Loeb and Monnat, 2008; Mimori et al., 2018; Turajlic et al., 2019). Dynamic conversion between phenotypic states, bidirectional processes of differentiation and de-differentiation of cancer stem cells (CSC), contributes particularly to this heterogeneity and allows functional adaptation of cancer cells to the different hurdles imposed by the homeostatic and cell growth control processes (ElShamy and Duhé, 2013; Marjanovic et al., 2013; Nieto et al., 2016). An effective cancer treatment is enormously limited by this phenotypic heterogeneity and cellular plasticity, and particularly by the lack of understanding of the specific contribution of the different molecular and cellular mechanisms used for their establishment (Marusyk et al., 2012).

It is also recognized that cellular heterogeneity can also be found in other components of the tumor microenvironment (TME). Early studies have revealed distinct functional roles of the different stromal elements with the capacity to define a benign or transformed cell phenotype (Shekhar et al., 2001). Stroma-mediated epigenetic cues generate a permissive TME that may reverse breast cancer cell limitations and promote tumor cell plasticity and growth (Varga et al., 2014; Haynes et al., 2017).

On the other hand, it is now well recognized that cell identity is more ambiguous and cell fate less predictable as previously thought (Mills et al., 2019), and that in pathological conditions these features are much more complex. In fact, cell identity becomes more plastic and cell fate more uncertain when homeostasis of the microenvironment is perturbed, e.g., during injury, senescence, inflammation or cancer (Lamouille et al., 2014). Principally, two mechanisms responsible of tumor cell plasticity contributing not only to tumor initiation and progression (Varga et al., 2014) but also to chemoresistance and cancer relapse (Le Magnen et al., 2018) have been identified: the epithelial-mesenchymal transition (EMT) and de-differentiation or *trans*-differentiation processes. In this review, we discuss how senescence affect tumor cell plasticity through these mechanisms, generating tumor cells with particular stemness features that allow their functional adaptation during cancer progression. A particular emphasis is made on pro-inflammatory cytokines (IL-6 and IL-8) secreted by senescent/inflammatory cells, known to induce EMT, cell migration, and de-differentiation, and be responsible for propagating senescence and inflammation in the TME.

EMT/CSC AND TUMOR CELL PLASTICITY

One of the most well known examples of cellular plasticity is the epithelial-to-mesenchymal transition (EMT), which occurs in several contexts in normal development and disease, including cancer (Oft et al., 1996; Thiery, 2002; Kalluri and Weinberg, 2009; Thiery et al., 2009). The EMT has been associated with the appearance of cancer cells with stem-like cell properties or CSC (Mani et al., 2008; Morel et al., 2008) which are thought to be responsible for driving cancer growth, inducing radio- and chemotherapy resistance, causing metastasis and relapse (Clarke et al., 2006). The EMT can be induced by several of numerous pleiotropic growth factors or cytokines (EGF, HGF, FGF, TGF-β, NOTCH, IL-6, IL-8, among others) (Thiery et al., 2009; Kim et al., 2016) that can be produced by different cells present in the tumor. This leads to the redundant expression of the EMT-associated transcription factors (EMT-TF), including SNAIL1/2, TWIST1/2, ZEB1/2, and PRRX (Nieto et al., 2016; Yuan et al., 2019), and subsequent epithelial genes repression and mesenchymal genes induction (Lamouille et al., 2014; Dongre and Weinberg, 2019).

Intriguingly, a CSC signature could include epithelial gene expression within a mesenchymal cell context, or mesenchymal gene expression within a background of mostly epithelial tumor cells (Grosse-Wilde et al., 2015). In fact, CSC may exist in distinct mesenchymal- and epithelial-like states and possess a high degree of cellular plasticity enabling cells to dynamically transit between these two states based mainly on signals they receive from the TME (Liu et al., 2014). Cells displaying these dynamic changes have been called, plastic or metastable cells, cells in transition states, etc. (Mills et al., 2019). Therefore, cellular plasticity of tumor cells has been also associated with the reverse program MET (together with the EMT, better called epithelial-mesenchymal plasticity – EMP) (Guarino et al., 1999; Ford and Thompson, 2010; Lu et al., 2013; Nieto, 2013; Luo et al., 2015) and with the existence of the hybrid (E/M) phenotype (Christiansen and Rajasekaran, 2006; Grosse-Wilde et al., 2015; Jolly et al., 2015a). The E/M phenotype may appear in a fine-tuned manner allowing collective migration of cohesive epithelia (Revenu and Gilmour, 2009) and having multiple benefits that can be exploited by tumor cells during the different stages of cancer progression (Friedl et al., 2012; Jolly et al., 2015a). Since the hybrid phenotype may exist in different ranges between the pure E and M stages, it is particularly relevant that more cellular plasticity and tumorigenicity has been found in hybrid cells that tend to be more epithelial (Ocaña et al., 2012; Patsialou et al., 2012; Ombrato and Malanchi, 2014; Grosse-Wilde et al., 2015). A strong association between the expression of genes responsible for this hybrid E/M phenotype and breast cancer cell invasive behavior and aggressiveness has been found (Hendrix et al., 1997; Livasy

et al., 2006; Jolly et al., 2015a). In a TNBC model it was also found that CSC cells residing in an intermediate E/M phenotypic state had more stem-like cell properties, tumor-initiating capability and worse prognosis (Bierie et al., 2017). Although, the hybrid E/M phenotype has been considered metastable, stability factors of the hybrid E/M state have been described (Jia et al., 2015; Jolly et al., 2016). Intriguingly, stability was accompanied by a gain of stemness functions (Jolly et al., 2015b). Very recently, highly tumourigenic breast cancer cells in a stable intermediate E/M phenotype, driven by the mesenchymal SNAIL TF and the stemness-associated Wnt signaling pathway were more tumourigenic than a mixture of cells at the end of the spectrum of E or M phenotypes (Kröger et al., 2019). Nevertheless, the use of additional markers could eventually discern cell subpopulations of CSC within this E/M stable phenotype. Indeed, in another study using three different cell surface markers it was possible to distinguish different intermediate states, that were functionally distinct in invasion, clonogenicity, differentiation and importantly, plastic cell properties (Pastushenko et al., 2018).

Paradoxically, the EMT phenotype has also been shown to prevent the acquisition of stem-like cell properties (Korpal et al., 2011; Celià-Terrassa et al., 2012; Sarrio et al., 2012). Also, cooperation between EMT and non-EMT cells could favor lung metastasis by the non-EMT cells (Tsuji et al., 2008). More recently, in an *in vivo* breast cancer model it was shown that cells in a mesenchymal phenotype arriving at a secondary site adopt an epithelial state after very few cell divisions (Beerling et al., 2016), suggesting that differences in stemness between epithelial and mesenchymal states could be lost under certain circumstances and become irrelevant for metastatic outgrowth.

Thus the EMT and CSC programs that were originally described as coincident may appear separately, be regulated differentially and have gradual "intensities" (Beck et al., 2015; Schmidt et al., 2015; Batlle and Clevers, 2017). Stemness properties would be of different functional significance depending on the cell context and the cancer progression stage. In these scenarios, cellular plasticity allows tumor cells to adapt to the different circumstances of the tumor microenvironment, and to take advantage differentially of the functional properties conferred by the establishment of these programs (**Figure 1**).

Role of Senescence and Inflammation in EMP and CSC Properties Acquisition

The effect of senescent and inflammatory phenomena occurring in the TME on cellular plasticity and tumor progression is of great interest in cancer biology. Cellular senescence was recognized as a powerful anti-cancer mechanism (Campisi, 2005) since stressed or damaged cells are permanently withdrawn from the cell cycle. Nevertheless, early work has also shown that cancer cells can evade this tumor suppressive mechanism in different ways, for example, the p16 inactivation by CpG island methylation (Foster et al., 1998); this being just one of other evasion mechanisms that began to be revealed decades ago (Hollstein et al., 1991; Kim et al., 1994; Shay and Bacchetti, 1997; Jarrard et al., 1999). Currently, it is believed that cancer cell senescence override is necessary for full malignancy (Collado et al., 2005; Ohashi et al., 2010). Indeed, it was shown that human cancers express EMT-TF that are able to abrogate key regulators of senescence (for example, p53 and Rb) and cooperate with oncogenic signals allowing the complete induction of an EMT program and the acquisition of invasiveness properties (Ansieau et al., 2008; Tran et al., 2012). Some EMT-TF could also induce cellular plasticity and drug resistance through regulation of signaling pathways (NF-kB and MAPK) involved in stem cell maintenance (Lim et al., 2013; **Figure 2**). Also in an experimental model of TNBC, p53 deletion from the mammary epithelium inhibited the expression of differentiation markers, induced an early expansion of mammary stem/progenitor cells and accelerated the formation of TNBC tumors (Chiche et al., 2017).

Not only intrinsic senescence in the tumor cells and their scape from this condition is relevant for disease progression. Changes in the supportive stroma could also affect growth and homeostasis of tissues and be responsible for cancer progression and aggressiveness. Senescent cells induced by irradiation, drug treatment, oncogenic stimuli and other stressful insults can also exert detrimental effects on cancer cells and the surrounding tissues. The tumor stroma consists of non-malignant cells, including resident cells such as cancer-associate fibroblasts (CAF), endothelial cells and pericytes, immune cells, and mesenchymal stroma cells, among others (Eiro et al., 2019). All these cells can impact tumor growth in different modes. CAF, for example, can induce tumourigenesis of epithelial cells (Olumi et al., 1999; Shimoda et al., 2010). Additionally, because CSC can differentiate into supportive CAF-like cells they are able to induce and ensure, by this mean, survival of cancer cells in the TME (Nair et al., 2017). Tumour-associated macrophages (TAM) are the most abundant infiltrated leukocyte in the TME, in general they are polarized to the M2 phenotype and secrete IL-8, showing either anti- or pro-tumourigenic effects (Mantovani, 2004; Sica et al., 2006; Dominguez et al., 2017). TAM infiltration has a positive correlation with IL-8 expression and a negative correlation with patient survival (Chen et al., 2003). Although senescence-associated fibroblasts vary in different ways from CAF, they are also able to promote the proliferation and tumourigenesis of pre-neoplastic or neoplastic epithelial cells (Krtolica et al., 2001; Coppé et al., 2010).

Interestingly, these effects were independent of the senescence inducer and mainly due to factors secreted by senescent fibroblasts (cytokines, chemokines, growth factors and proteases) (Krtolica et al., 2001), collectively known as the senescence-associated secretory phenotype (SASP) (Coppé et al., 2008). The SASP was able to alter epithelial differentiation and to induce EMT (Parrinello et al., 2005; Bavik et al., 2006; Coppé et al., 2008). High levels of the pro-inflammatory cytokines IL-6 and IL-8, the main soluble factors present in the SASP, are responsible for augmenting the invasiveness of a panel of breast cancer cell lines (Coppé et al., 2008). Not surprisingly IL-6 and IL-8, having a central role in CSC formation (Korkaya et al., 2011) were highly upregulated in response to IL-1-beta (Lim et al., 2013) and responsible for SASP propagation in the TME (Coppé et al., 2010). The secretion of matrix metalloproteinases by senescent

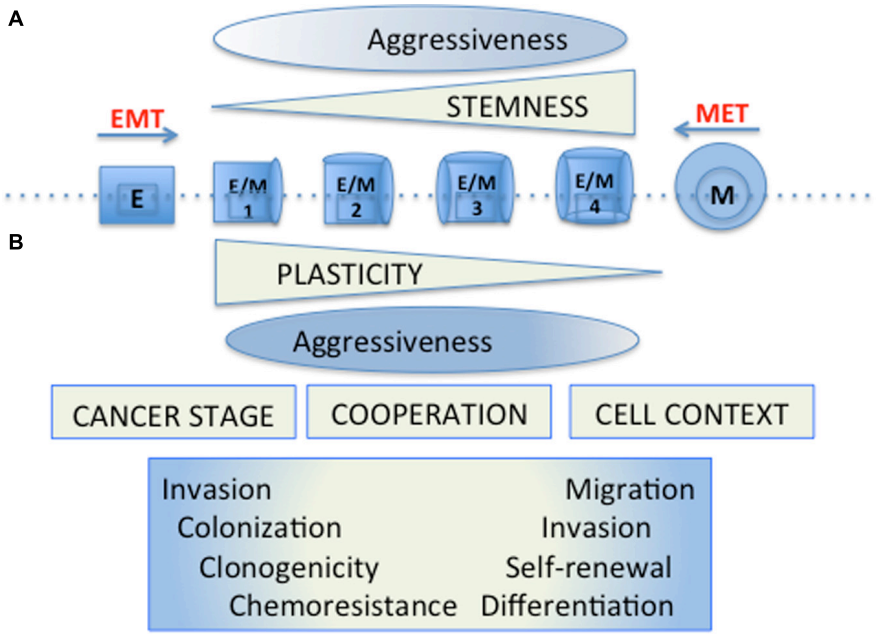

FIGURE 1 | Cellular plasticity and tumor cell aggressiveness. **(A)** The original model of cellular plasticity proposed that the EMT program was associated with the appearance of CSC properties and it was supposed that these mesenchymal-like cells were responsible for driving cancer cell growth, chemotherapy resistance, metastasis and relapse. **(B)** The new models of cellular plasticity propose that stemness properties would be of different functional significance depending on the cell context and the particular cancer progression stage. In these models, hybrid cells (E/M1-4) expressing both epithelial (E) and Mesenchymal (M) markers develop cellular plasticity with different stemness properties, allowing tumor cells to adapt to the diverse circumstances of the tumor microenvironment, and to take special advantages of the functional properties conferred by the establishment of these programs. The aggressiveness would be manifested by a wide spectrum of distinct hybrid cells, requiring particular properties according to the hurdles present during tumourigenesis.

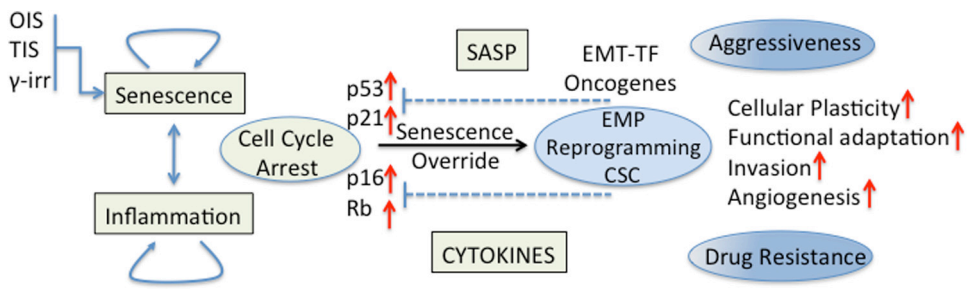

FIGURE 2 | Senescence/inflammation and cellular plasticity. Tumor cell senescence override is necessary for full malignancy. EMT-TF cooperate with oncogenic signals to abrogate key regulators of cell cycle for a complete induction of the EMT program and the acquisition of stemness properties. Some EMT-TF induce cellular plasticity and drug resistance through regulation of signaling pathways (NF-kB and MAPK) involved in stem cell maintenance. The final effect of senescence/inflammation in EMT/CSC plasticity depends on the contextual signals present in the TME, the stage of cancer progression and the functional heterogeneity reached.

cells also promotes the invasion of cancer cells (Parrinello et al., 2005; Liu and Hornsby, 2007).

Likewise, inflammation, an important physiological process in the TME can, on one hand, induce cell proliferation and survival of cancer cells, and promote angiogenesis (Mantovani et al., 2008) and on the other, attract immune cells, in particular TAM a key cell subset contributing to inflammation and resulting in anti-tumor activity (De Visser et al., 2006; Sica et al., 2006; Shigdar et al., 2014). These effects are also mediated by inflammatory cytokines (IL-1, IL-6, IL-8, TNF, TGF-ß, and others) and chemokines (CCL2 and CXCL8, for example) especially having an important effect during chronic inflammation (Tanno and Matsui, 2011). In particular, the EMT-inducing effect of TGF-ß has been well recognized (Hollier et al., 2009). IL-6 regulates the self-renewal of breast CSC through activation of STAT3 and NF-kB and further inducing an even greater secretion of IL-6 and IL-8 (Bromberg and Wang, 2009). IL-8 also increases breast CSC self-renewal by increasing the expression of the receptor CXCR1 (Ginestier et al., 2010). Elevated serum levels of both cytokines have been used independently as prognostic markers for breast

cancer (Bachelot et al., 2003; Benoy et al., 2004; Knüpfer and Preiß, 2007; Yao et al., 2007).

It is believed, that this senescent/inflammatory milieu contains the main contextual signals present in the TME, with the capability to affect pre- and malignant cells. In the post-crisis immortalized HEK cells model (Castro-Vega et al., 2013), cells with chromosomal instability, initially unable to induce tumors on their own in spite of displaying an EMT phenotype, become fully tumorigenic only in the presence of senescent fibroblasts (Castro-Vega et al., 2015). The acquisition of this tumor capacity was accompanied by the presence of enhanced stem-like cell properties. Interestingly, cells recovered from those tumors were now endowed with cell-autonomous tumorigenicity (in the absence of senescent cells), but they exhibited extensive heterogeneity in cell phenotype, differentiation status, gene expression profile and response to SASP (Castro-Vega et al., 2015). The capacity of SASP to modulate these phenotypes/functions (phenotypic interconversions, functional plasticity and adaptation) in pre- or fully malignant cells in the different stages of cancer progression must be very relevant *in vivo* (Chaffer and Weinberg, 2015).

From the known SASP composition and the inflammatory mediators it is clear that there is a close relationship between senescence and inflammation (Lasry and Ben-Neriah, 2015) and a strong effect of both processes in tumor progression. Prolonged exposure to inflammatory mediators can enhance tumor growth (Krtolica et al., 2001; Bavik et al., 2006). Also, chronic inflammation increased cancer risk by promoting tumourigenesis (Balkwill et al., 2005). The fact that the use of non-steroidal anti-inflammatory drugs after surgical removal of tumors decreases relapse and mortality in different types of cancer, suggests an important and broad role of inflammation in tumor progression (Fraser et al., 2014; Streicher et al., 2014). Due to their dual effect in cancer suppression and promotion, and their reciprocal influence, the final effect of senescence/inflammation in EMT/CSC plasticity would depend on the stage of cancer progression, the contextual signals present in the TME, the capacity of the tumor cells to escape senescence and the functional heterogeneity achieved (differentiation state, stemness attributes). Additionally, recent evidence supports the view that senescent and inflammatory mediators destabilize cancer cell genome, contributing to the accumulation of random genetic alterations and to the establishment of a genomically heterogeneous tumor cell population that can be further selected according to their new physiological properties and their relevance in the different stages of carcinogenesis (Colotta et al., 2009; Anuja et al., 2017).

DE- AND *TRANS*-DIFFERENTIATION PROCESSES AND CELLULAR PLASTICITY ACQUISITION

De- and *trans*-differentiation processes, by which cells adopt a different differentiation state from the original one or a more primitive state, influence cellular plasticity and cell fate options. Recent studies in breast cancer recognize a connection between genetics/epigenetics alterations (oncogenes, tumor suppressor genes or cell lineage specifiers) and the cell of origin, either luminal or basal subtypes (Chu et al., 2019). These alterations in a particular cell context can induce cell reprogramming in lineage-committed mammary epithelial cells. Based on this observation and the relationship between induced pluripotent stem cells and cancer cells, it was proposed that one or more reprogramming factors could be involved in the spontaneous de-differentiation and the acquisition of stemness function (Leis et al., 2012).

For example, over-expression of SOX2 increased both the amount of mammospheres in an *in vitro* culture model in low binding conditions and the formation of tumors in a xenograft model. It was argued that reactivation of SOX2 could explain tumor heterogeneity by placing the self-renewal ability and tumor-initiating capacity in any cell along the axis of mammary differentiation (Leis et al., 2012). Also, in the immortalized non-tumorigenic MCF10A mammary epithelial cell line, the introduction of reprogramming factors (SOX2, KLF4, OCT4, and c-Myc) endowed MCF10A cells with CSC properties and malignant traits both *in vitro* and *in vivo* (Nishi et al., 2014). Likewise, the expression of oncogenic PIK3CA in uni-potent basal cells gave rise to luminal-like cells, while its expression in uni-potent luminal cells produced basal-like cells, before progressing into invasive tumors with heterogeneous breast cancer cell types (Koren et al., 2015; Van Keymeulen et al., 2015). Additionally, c-Myc, part of the Yamanaka reprogramming factors (Takahashi et al., 2007) and a downstream effector of PIM1 and IL-6 stimulation (Gao et al., 2019) induced mammary tumourigenesis through cell reprogramming, which was attributed to MYC-mediated repression of luminal fate-specific enhancers (Poli et al., 2018a). On the other hand, MYC-driven de-differentiation induced a stem-like cell state with activation of *de novo* enhancers, driving the transcriptional activation of oncogenic pathways (Poli et al., 2018a). These studies and others (reviewed in Chu et al., 2019) have allowed unveiling the connections between the reprogramming of committed mammary epithelial cells and the tumorigenic capabilities of heterogeneous breast cancer cells (Dravis et al., 2018; Rodilla and Fre, 2018).

In breast cancer it is thought that cancer cells are derived from a common luminal progenitor cell type with stem-like properties that is able to develop into both luminal and basal tumors (Granit et al., 2014). The existence of unrestricted gene expression patterns in this bi-potential progenitor cells represents the developmental biology support for the occurrence of the hybrid phenotype (Fillmore and Kuperwasser, 2008). The hybrid signature was associated with stemness functions and with a poorest outcome in all breast cancer subtypes (luminal and basal breast cancer patients) (Grosse-Wilde et al., 2015). This strong relationship is based on the stemness appeal of the hybrid phenotype based on the cooperation between the E and M states complementing their functional attributes, cellular plasticity conveyed by the E state and self-renewal carried out by the M state (Grosse-Wilde et al., 2015). Also, in a transforming model of basal-like breast cancer it was shown that differentiated cells could give rise to CSC *in vitro* and *in vivo* (Chaffer and Weinberg, 2011). The authors argued that the plasticity of CSC

could be associated with the cell characteristics in their respective non-stem cell state and their capacity to produce new CSC.

Cellular Senescence and Cell Reprogramming

Recently, it was shown that senescent keratinocytes, in addition to the classical hallmark features of senescence (senescence-associated β-Galactosidase (SA-βGal) activity, cell cycle arrest, p53, p16, p21, and Rb expression, ROS production, H3K9me3 marks and others) also showed increased expression of genes usually associated with CSC (i.e., CD34, Prom1, CD44, and Nestin, among others) (Ritschka et al., 2017). This gene expression up-regulation was independent of the senescence inducer, and the transient exposure to SASP was found to be responsible for this stem-like cell markers. The authors propose that in these conditions, stem-like cells that reside in a more plastic dynamic state might be more prone to transformation (Ritschka et al., 2017). Cellular stemness functions obtained by reprogramming factors and/or EMT-TF must be able to cross-talk with the different controllers of the cell-cycle. In fact, cellular differentiation and senescence are regulated by the activity of major cell cycle repressors, such as p53, Rb, p16, Arf, and p21, the expression of which is targeted by the reprogramming factors and EMT-TF (Strauss et al., 2011). The stem-like cell transcriptional program is activated by alterations of the epigenetic machinery that favor self-renewal and pluripotency (Poli et al., 2018b). Among these, DNA methylation (by DNA methyltransferases, DNMT) and de-methylation (by Ten-eleven translocation proteins, TET) and histone modifiers define the cellular transcriptional program. For example, IL-6 increased the methylation of p53 and p21 in A549 cancer cells by expression of DNMT1 (Liu et al., 2015). Also, hypermethylation of a negative regulator of Wnt signaling is an early event during colorectal tumorigenesis (Zhang et al., 2008). In breast cancer it has been shown that EZH2 hyperactivation is sufficient for malignant transformation and aggressiveness, suggesting that H3K27me3 marks are necessary for the gaining of CSC properties (increased invasion) (Kleer et al., 2003). Recently, a complex role of these cell cycle regulators in senescence or reprogramming was established; while p16 and Arf were necessary for senescence induction, IL-6 secretion and reprogramming, p53 and p21, known to represent a barrier for cell reprogramming, were dispensable (Mosteiro et al., 2018). Since ROS is produced during senescence and is critical for cell reprogramming (Zhou et al., 2016) and activation of NF-kB (Escobar et al., 2012) a positive feedback loop may be induced by IL-6 stimulation (**Figure 3**).

Since cell reprogramming proceeds through sequential steps due to transcriptional regulation of reprogramming factors in a certain order and with a particular intensity, the effect of the TME (SASP, for instance) will depend on the spatial and temporal relationship between stimuli and functional targets. In this sense, their short- or long-term induction defines the outcome of cells toward cellular senescence or cell reprogramming (Mosteiro et al., 2016). The number of senescent cells and therefore the quantity and composition of SASP defines not only which cells are likely to be reprogrammed but also with which intensity. The specific microenvironments in which the tumor cells reside and the contextual signals produced are the most important determinants defining their reprogramming capabilities and stemness functions.

For example, in an *in vitro* model of breast cancer, the IL-6/Stat3 axis has been shown to be critical in the conversion of non-CSC into CSC (Kim et al., 2013). Also, in an *in vivo* mouse model a positive correlation between senescence and cell reprogramming was found and it was shown that this effect was mediated by soluble factors (Mosteiro et al., 2016). The authors found that Nanog+ cells generally appear in close proximity to clusters of senescent cells in similar reprogrammable mice. The communication between senescence and cell reprogramming was enabled by the cytokine-rich microenvironment associated with senescent cells, in which IL-6 was identified as the critical soluble factor responsible for promoting de-differentiation (Mosteiro et al., 2016). Pharmacological inhibition of NF-kB, a TF activated by inflammatory cytokines (including IL-6, the most prominent cytokine of the SASP) diminishes significantly cell reprogramming. Also inhibition of its downstream kinase effector PIM1 has the same effect (Mosteiro et al., 2016). In the breast cancer cell lines T47D and MCF-7, the stimulation with IL-6 induces the expression of PIM1 and the expression of EMT and stemness markers (Gao et al., 2019). Here again, knockdown of PIM1 or inhibition of the mediator STAT3 abrogates stemness markers and function, while overexpression of PIM1 increases invasion and EMT/CSC markers (Gao et al., 2019).

Also, in the immortalized HEK cells model (Castro-Vega et al., 2013), HEK cells stimulated with a senescent-conditioned media (SCM) upregulated the reprogramming factors KLF4, NANOG, and OCT4 and formed efficiently spheres in low-binding conditions (Castro-Vega et al., 2015). In the MCF-7 cell line, SCM stimulation not only induces the EMT-TF but also the reprogramming factors OCT4 and KLF4 (Ortiz-Montero et al., 2017). The SCM-abundant IL-8 and IL-6 cytokines on their own also induced the expression of NANOG, OCT4, and SOX2 or KLF4, respectively. Here again, immune neutralization of these cytokine in the SCM reduces the expression of EMT-TF and some of the reprogramming factors (Ortiz-Montero et al., 2017). In the study by Mosteiro et al. (2016) it was also shown *in vitro*, that cell reprogramming efficiency was strongly enhanced by the SCM obtained from damaged cells and that IL-6 immunodepletion from the SCM abolished cell reprogramming. Using a cellular model of immortalization and oncogenic transformation it was shown that the homeobox transcriptional regulator SIX1 has a pro-tumorigenic action induced by the repression of a senescence-related signature, including p16Ink4a (Oliveras-Ferraros et al., 2012; De Lope et al., 2019). SIX1 overexpression was accompanied by an increase in SOX2 levels and activity and the induction of a de-differentiated tumor phenotype.

These results show that senescence, and more exactly, specific soluble factors within SASP, can induce the reprogramming of cancer cells, and that this de-differentiation process is responsible in part for the cellular plasticity of cancer cells and undoubtedly for the several complications observed during cancer progression and treatment. In fact, prominent SASP expression and senescent cells accumulation have been shown to

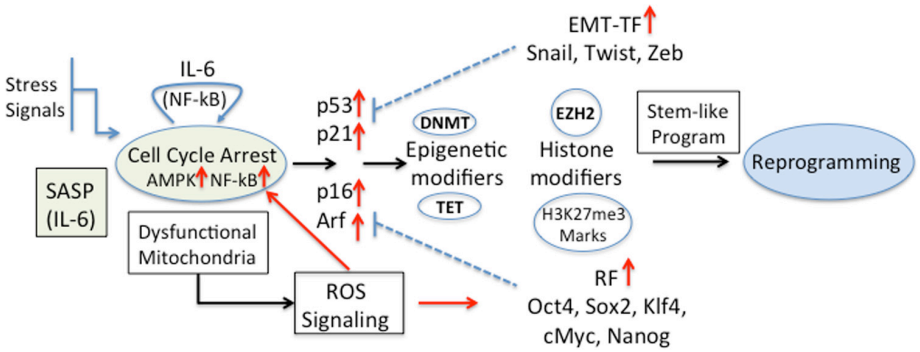

FIGURE 3 | Senescence and tumourigenic cell reprogramming. Different stress stimuli induce cellular senescence and cell cycle arrest with a concomitant expression of the regulators [p53, p21CIP1 (p21), p16INK4a (p16), p14Arf (p14)] and induction of SASP. In particular IL-6, being one of the main components within SASP, is a key player in cell reprogramming (Mosteiro et al., 2016). The higher expression of EMT-TF and reprogramming factors (RF) blocks some of the cell cycle regulators and modifies epigenetic marks and histones, and the appearance of stemness properties and the reprogramming of cells. The effect could be further reinforced by the fact that dysfunctional mitochondria induce the production of ROS, which are direct inducers of RF. Also, ROS-activated NF-kB contributes to the positive feedback loop originated by IL-6 stimulation.

be responsible for tumor progression and aggressiveness (Kang et al., 2011; Rodier and Campisi, 2011).

Chemotherapy-Induced Senescence and Cell Reprogramming

Cancer stem cells can survive and are able to proliferate after chemotherapy (Singh et al., 2004; Visvader and Lindeman, 2008; Alison et al., 2011; Kreso and Dick, 2014) and it is well established that the mechanisms of this resistance are multiple (Phi et al., 2018). Since senescent processes can be induced as a consequence of uncontrolled cell growth by oncogene stimulation or anti-cancer drug treatments, senescence occurring in the TME and intrinsically in the tumor cells can impact importantly cancer progression. In fact, in multiple myeloma it has been shown that SASP produced by senescent cells within the tumor induce the emergence, after therapy-induced genotoxic stress, of CSC with the characteristic self-renewal and differentiation capacities, and with the ability to migrate toward chemokines released by the senescent non-CSC (Cahu et al., 2012). Also, tumor cells with defective apoptosis respond to chemotherapy by entering to a premature senescent state and, contrary to the traditional perception of the irreversibility of this process, some of these cells spontaneously revert to a proliferating cell phenotype in culture (Beauséjour et al., 2003). These experiments, could explain in part early relapses after termination of drug treatment (Yang et al., 2015). Additionally, it has been shown that cancer cells emerging from senescence after drug therapy increased the expression of CSC markers, CD34 and CD117 in lung cancer cells (Sabisz and Skladanowski, 2009), and CD133 and the reprogramming factor OCT4 in breast cancer cells (Achuthan et al., 2011). Importantly, emergence, maintenance and migration of senescent cancer cells were likewise molded by SASP (Cahu et al., 2012).

Reactivation of antioxidant enzymes and the subsequent low reactive oxygen species (ROS) levels were also a principal characteristic of the cells that emerge from senescence (Achuthan et al., 2011). This is a meaningful finding, since it has been shown that low ROS levels allow stem cells to survive in adverse conditions (Chen et al., 2006). Importantly the senescence revertants displayed a gene expression profile different from the parental cells and had also increased migration and invasion capabilities (Yang et al., 2017). The results showed that in 80% of the tumors, the revertant cells outgrew the parental cells. Intriguingly, a subset of senescence-activated genes remains active in the revertants (although to a lesser extend) (Yang et al., 2017), suggesting that differential long lasting senescent imprinting could be responsible for a non-genetic heterogeneity. Also, in experimental models of acute leukemia, cells emerging from senescence showed enhanced expression of stem cells markers, clonogenic growth and tumor-initiation potential (Milanovic et al., 2018). In the same study it was shown that senescence provokes the cell-autonomous reprogramming of non-stem tumor cells into *de novo* CSC, not only in hematological malignancies but also in cancer tissues of different origins. Intriguingly, emerging clones with different combination of activated genes could also show dynamic cell conversion adding a new element to cell plasticity (Milanovic et al., 2018). Moreover, differential cellular reprogramming may also occur in tumor cells that have undergone senescence reversal, contributing to tumor heterogeneity and aggressiveness.

As indicated above, modifications of the host TME by the different drug treatments available for cancer play also an important role by providing survival and protective niches for tumor cells. Accumulation of senescent cells could induce a SASP-dependent survival niche that can favor senescence scape of premalignant cells or the survival of adjacent clones with lower fitness, eventually inducing disease relapse (Guillon et al., 2019). This is another important element related to EMP, stemness, cell reprogramming and the cell plasticity developed and its connection with the acquired drug resistance (Singh and Settleman, 2010; Holohan et al., 2013; Jolly et al., 2015a). Though it is difficult to prove that cellular plasticity is responsible for drug-resistance recent lineage tracing experiments, transplantation studies and functional analysis

have allowed finding indirect evidence of this (Le Magnen et al., 2018). For example, it was shown in advanced prostate cancer that drug resistance occurs by *trans*-differentiation of luminal adenocarcinoma into neuroendocrine-like cells (Zou et al., 2017). In non-small-cell lung tumors, resistant tumors with the original EGFR mutations show a phenotypic transition to small-cell neuroendocrine lung cancer suggesting a *trans*-differentiation process of the original adenocarcinoma (Oser et al., 2015). Also in other cancer models it has been shown that the plasticity of the hybrid E/M phenotypes not only favors collective migration, tumor initiation capabilities and metastatic potential, but also therapy resistance (Jolly et al., 2019). Cells that acquire a mesenchymal phenotype are in general resistant to drug treatment (Creighton et al., 2009; Oliveras-Ferraros et al., 2012; Shibue and Weinberg, 2017). The overexpression of EMT-TF in the luminal breast cancer cell line MCF-7 induced protection against the DNA-damaging agent doxorubicin (Kajita et al., 2004). In this work, the MCF-7 cells not only lost cell-cell contacts but also acquired invasive growth capabilities. A similar phenomenon was also reported for ovarian cancer (Haslehurst et al., 2012) and hepatocellular carcinoma (Dong et al., 2017). All these experiments demonstrate that cells that exhibit a high degree of cellular plasticity and stem-like cell functions are resistant to drug treatment.

In this sense, it has been suggested that blocking this cellular plasticity directly or by modulating the signals originated in the TME and responsible for this dynamic behavior could be important to increase susceptibility to therapy and control cancer progression (Yuan et al., 2019). Although the fundamental molecular mechanisms of drug resistance-induced cellular plasticity remain unsolved, it is believed that targeting the EMP pathways or the CSC maintenance programs, or particular E/M phenotypes with distinctive CSC attributes are thought to be valuable therapeutic strategies (Le Magnen et al., 2018). For example, the EMT phenotype can be manipulated by blocking the associated transcription factors (EMT-TF), inducing a reversal to an epithelial phenotype that in general is not linked to drug resistance in cancer cells (Li et al., 2009). Also relevant, prevention of CSC self-renewal function by inhibition of the PI3K/Akt/mTOR signaling axis may allow the evasion of chemotherapy resistance (Singh and Settleman, 2010).

Since cancer cell plasticity occurs by hijacking mechanisms present in the physiology of normal tissues, the pathways controlling it should be quite similar and susceptible to comparable blocking strategies. Cross-talk between CSC and the TME must be considered since during cancer progression they develop and share some characteristics that help functional adaptation of CSC, and therapeutic approaches must then target common cell plasticity properties of TME and CSC on one hand, but also some of the specificities found in the CSC.

CELLULAR SENESCENCE AND INFLAMMATION PROPAGATION

In general it is believed that senescent cells comprise a small fraction of tissues (Wiley et al., 2017). Nevertheless, the fact that senescence is a phenomenon that can be propagated in the TME by different stimuli suggests that its relevance in cancer progression could be more important than thought before. Also, there is a close relationship between senescence and inflammation and their role in tumor progression when the producing stimuli are long-lasting (Lasry and Ben-Neriah, 2015). The fact SCM can induce the secretion of pro-inflammatory cytokines and that this in turn induces senescence imply that a double reinforcing loops can be established (Acosta et al., 2008; Kojima et al., 2013; Ortiz-Montero et al., 2017). This type of senescence/inflammation dissemination involves not only tumor cells but also other cells within the TME (Acosta et al., 2013).

The relevance and consequences of the presence (or not) of senescent cells in breast cancer is clearly exemplified with the MCF-7 and MDA-MB-231 breast cancer cell lines. The MCF-7 luminal cancer cell line has been classified as a senescent-cell progenitor subtype showing lower expression of the SA-βGal (Mumcuoglu et al., 2010). This cell line can differentiate into luminal and myoepithelial cell types and do not secret the pro-inflammatory cytokines IL-6 or IL-8. This is opposed to the basal/mesenchymal cell line MDA-MB-231, a highly IL-6 and IL-8 secreting cell line, classified as an immortalized-cell progenitor cell line that do not express SA-βGal (Mumcuoglu et al., 2010). Breast cancer cells exposed to the pro-inflammatory IL-6 cytokine exhibited enhanced invasion capacity and increased drug resistance (Dethlefsen et al., 2013); also, inflammatory microenvironments are known to expand the CSC pool and increase tumor initiation (Shenoy et al., 2012). Exposure of the MCF-7 cell line to SCM or to the pro-inflammatory cytokines IL-6 and IL-8 induced stem-like cell properties and aggressiveness attributes of an otherwise low aggressive cell line (Ortiz-Montero et al., 2017). Moreover, exposure to the SCM induces senescence propagation in MCF-7 cell cultures and remarkably the secretion of the cytokines IL-6 and IL-8 by this supposedly non-secreting IL-6 and IL-8 breast cancer cell line, a phenomenon that allows reinforcement of senescence by inflammatory cytokines potentiating cellular plasticity (Ortiz-Montero et al., 2017).

On the other hand, addition of IL-6 and IL-8 had no effect on the MDA-MB-231 breast cancer line. But, neutralization of the IL-6 and IL-8 cytokines affected slightly cell morphology and cell migration capacity and induced the expression of epithelial cell markers, suggesting that in this "pre-set" mesenchymal subtype, neutralization of pro-inflammatory cytokines affected differentially cell functions. Nevertheless, this breast cancer cell line presented abnormal differentiation to the osteoblastic lineage and it was suggested that its aggressiveness was more related to its abnormal differentiation-induced cell heterogeneity (Ortiz-Montero et al., 2017). Also, IL-8 has been associated with CSC and enhanced migration, invasion and metastasis in breast cancer (Freund et al., 2003; Charafe-Jauffret et al., 2009). During persistent inflammation, senescent cells accumulated and spread, and abundant signal responsible for cell damage and cell reprogramming contribute importantly to CSC plasticity (Mosteiro et al., 2016; Ortiz-Montero et al., 2017). Recently, it was shown that senescent

cells are very heterogeneous in gene expression profiles (Wiley et al., 2017). One can imagine that surrounding cells will be affected in different ways depending on this cell heterogeneity.

In vivo, the situation should be more complicated and it would be very difficult to know how senescent cells evolve in TME with an immune system (IS) that could be partially effective in the beginning of the anti-tumoural immune response, but functionally impaired latter. Also, the appearance and maintenance of senescent cells would be influenced by the genetic instability induced by the continuous genotoxic stress, the rate at which senescence propagates in the TME and the persistence of inflammatory events. All these phenomena may also have important consequences on the robustness of the IS response, with serious consequences in the long-term. In this sense, the growth arrest observed by imagine techniques and interpreted as effective cytostatic responses will not always indicate a favorable response (Guillon et al., 2019), specially, if this guarantees the spread of senescence and the appearance of more aggressive CSC.

The IS also affect the TME in different ways; in particular it can contribute to an increased stress and to the accumulation of senescent cells. SASP of senescent cells facilitates leukocytes recruitment through various chemokines (Mantovani, 2004). Although in principle this would allow clearance of pre-malignant cells by the innate and/or adaptive IS, secretion of cytokines by immune cells (macrophages, neutrophils, myeloid-derived suppressors cells (MDSC), NK cells and lymphocytes) and their accumulation also affect significantly the TME. In particular, TGF-β secreted by TAM plays an important role. Although its effect has been shown to be highly context-dependent (Wahl, 2007), its secretion by macrophage or TAM induces senescence in primary and tumor cells (Katakura et al., 1999; Senturk et al., 2010). Also IL-6, secreted by tumor cells, infiltrating lymphocytes, TAM, MDSC and other myeloid cells, induces senescence and SASP dissemination in the TME (Coppé et al., 2010; Salminen et al., 2018). The immunosuppression induced by MDSC, through regulatory T-cells, impairs the clearance of senescent and cancer cells. IL-8, secreted by macrophages, epithelial cells, CAF and other infiltrating immune cells, induces senescence and promote recruitment of additional leucocytes, neutrophils and MDSC (Ginestier et al., 2010).

Additionally, SASP may also favor an immunosuppressive TME (Toso et al., 2014), resulting in an impaired immune surveillance, malfunctioning of immune cells and hence carcinoma progression (Kang et al., 2011). Since senescence may appear with different intensities (percentage of senescent cells or the presence of cells in different stages of senescence), and in different cell contexts (genetic or functional), its impact in the IS, via diverse SASP compositions, could change in the course of the disease. Of note, an impaired functionality of the IS with secretion of pro-inflammatory mediators (even in reduced amounts) in addition to SASP, contributes to the accumulation of senescent cells and the expansion of senescence due to a reduced cell clearance and the cytokine paracrine effect on the TME and also on immune cells (Prieto and Baker, 2019). In addition to causing the accumulation of senescent cells, SASP also allow the EMP, the cell reprogramming of tumor cells with the appearance of plastic CSC in a TME in which interactions between the different cells determine tumor growth and disease progression (Demaria et al., 2017; Milanovic et al., 2018).

Cooperation Between Different CSC Within a Senescent TME

As mentioned, SASP are responsible for spreading senescence in tumor cells and adjacent cells by a paracrine mechanism (Baker et al., 2011; Acosta et al., 2013; Campisi, 2013). In this manner, cells within the TME may display different levels of senescence and diverse stemness-associated features. Permanent fuelling with SASP would eventually allow cancer cells to acquire the ideal combination of stemness features with particular normal cell traits able to produce cells with special attributes responsible for increased aggressiveness. Gene expression signatures in senescent cells differ partially within the cell subpopulation present in TME (Wiley et al., 2017) and therefore one can imagine that their soluble secreted factors would have differential influence in the behavior of the tumor and surrounding cells. As already mentioned, CSC cultured in a conditioned medium obtained from senescent non-CSC remain in an undifferentiated state and develop enhanced migration capacity toward the same conditioned medium (Cahu et al., 2012), the latter event being a good example of cooperation between non-CSC and CSC. CSC with increased migration capacity would eventually migrate to new niche were SASP effect is reduced and could eventually differentiate into non-CSC rebuilding the bulk of tumor cells. The communication between the different cells present in the TME can be produced by protein matrix connections or soluble factors secretion from the different clones present and might produce benefit for all the participant cells, a sort of mutualism (Axelrod et al., 2006).

In a mouse model of breast cancer it was shown that interclonal cooperation is essential for the maintenance of tumors (Cleary et al., 2014). Abnormal secretion of signaling molecules generates tumors composed of basal and luminal cell subtypes. In conditions in which Wnt was withdrawn, basal subclones were able to recruit Wnt-secreting luminal subclones to restore tumor growth (Cleary et al., 2014). In a colorectal cancer model, it was shown that CSC-like cells and chemoresistant cells could confer chemoresistance on the surrounding naïve cancer cells (Bose et al., 2011). It was shown that this was mediated by soluble factors through the activation of growth and survival signaling pathways. In the immortalized HEK model, we have shown that explanted cells from tumors, that had acquired an autonomous tumorigenic capability (independent of the presence of senescent cells) expressed both epithelial and mesenchymal markers (hybrid E/M phenotype), but with variable expression of CD24. When these cells were tested for tumourigenicity, it was shown that those having increased stemness functions (CD24+) were not tumourigenic, while the CD24 negative cell population, having reduced stemness

functions, was as tumourigenic as the parental cell line (Ortiz-Montero et al., 2018) and presented homogeneous tumors with epithelioid morphology. Tumors formed by the simultaneous inoculation of a mixture of the non-tumourigenic CD24+ and the tumourigenic CD24 negative cell populations, were more heterogeneous with epithelioid and fibroblastoid cells and the presence of mesenchymal markers (alfa-SMA and vimentin). This suggests that non-tumourigenic cells may influence the differentiation of the tumors and contribute to cell heterogeneity. Although the mechanisms by which the presence of CD24+ cells contributes to cell heterogeneity within the tumor is unknown, it is interesting to appreciate that the CD24+ cell population has a more pro-inflammatory SASP. In fact both IL-6 and IL-8 were increased in a SCM obtained from CD24+ cells; this in turn could influence the CD24 negative population and clearly the TME (Ortiz-Montero et al., 2018).

These studies showed that phenotypically or genotypically distinct cell clones interact to the benefit of one or more clones within the tumor, contributing to heterogeneity and CSC plasticity (Neelakantan et al., 2015). All these cooperative processes should be very relevant also during the generation of metastatic clones or during the spread of the existing ones (Neelakantan et al., 2015). Intriguingly, tumor collapse can occur if the driver subclone gets outcompeted by the fast growing and less-fit dependent subclone (Marusyk et al., 2014). Mathematical modeling suggested that non-cell autonomous driving, together with clonal interference, stabilizes sub-clonal heterogeneity and enhancing inter-clonal interactions and the appearance of new phenotypic traits (Marusyk et al., 2014). This proposal is very relevant when its come to interpreting cancer genomic data. Some mutations detected at low allelic fractions and believed to represent late events in tumor progression may instead denote early events that allow interclonal cooperation and disease evolution (Cleary et al., 2014).

CONCLUSION

Phenotypic intratumour heterogeneity in cancer cells limits treatment against this disease. Cellular plasticity of cancer cells is a very complex process that can be induced by different mechanisms (EMP, de-and *trans*-differentiation processes, cell reprogramming, for example) and can be molded by the diverse stimuli present in the TME. In particular, the senescence and inflammation phenomena frequently occurring during cancer development and progression must have a very important role. Since this TME evolve permanently based on the incoming cells and the propagation of senescence and the composition of SASP, its effect is variable in the course of the disease. By this mean, cells are able to transit between different phenotypic states having different stemness properties and functions. Cancer cells with this dynamic behavior are more aggressive since they are more plastic and can respond/adapt more efficiently or faster to the diverse hurdles established during the different stages of carcinogenesis. These cells acquire/use particular functional properties, according to their needs, allowing them for example to proliferate, colonize a particular tissue and form a tumor; alternatively, these plastic cells may have other stem-associated features that allow them for example to migrate and invade new tissues; also they could be more prone to a cell cooperative behavior.

The acquisition of a specific set of stem cell features to overcome physical/physiological barriers may be sufficient or even more effective than to acquire a full-blown stemness program. Different stem-like cell properties would confer diverse cell advantages useful in the different stages of cancer progression. These features would be differentially influenced not only by the cell context (differentiation status, lineage background, etc.), the environmental cues (presence of inflammatory and senescent soluble factors) and immune status, but also, by radio- or chemotherapy. Intriguingly, they can be harbor by different subclones that cooperate to enhance they migration, colonization, growth, self-renewal and/or differentiation capabilities.

Stem cell functions (self-renewal, clonogenicity, multilineage differentiation capacity, migration, invasion, etc.) if adequately quantified and categorized according to the stage of cancer progression could give quantitative information about the adaptability of the tumor cell, and hence about CSC aggressiveness and tumor formation capacity. The phenomenon of cellular plasticity induced by a senescence-associated inflammatory milieu increases the difficulty of developing a suitable cancer therapy, and may explain the poor overall survival despite initial favorable responses to treatment. Blocking inflammation (Harrison et al., 2007; Loberg et al., 2007) and/or senescence (Myrianthopoulos et al., 2019; Zhang et al., 2019), or inhibiting the reversal of senescence in tumor cells (Yang et al., 2017), may reduce development, progression, and recurrence of cancer.

AUTHOR CONTRIBUTIONS

JV selected the topic, performed the revision and wrote the manuscript.

FUNDING

This work was supported by funds from the Departamento Administrativo de Ciencia, Tecnología e Innovación (Colciencias) – Contract 58257, and DIEB, Faculty of Medicine, Universidad Nacional de Colombia- Contract 38900.

ACKNOWLEDGMENTS

The author would like to thank Paola Fernanda Ruiz-Aparicio for her help in the preparation and revision of this manuscript.

REFERENCES

Achuthan, S., Santhoshkumar, T. R., Prabhakar, J., Nair, S. A., and Pillai, M. R. (2011). Drug-induced senescence generates chemoresistant stemlike cells with low reactive oxygen species. *J. Biol. Chem.* 286, 37813–37812. doi: 10.1074/jbc.M110.200675

Acosta, J. C., Banito, A., Wuestefeld, T., Georgilis, A., Janich, P., Morton, J. P., et al. (2013). A complex secretory program orchestrated by the inflammasome controls paracrine senescence. *Nat. Cell Biol.* 15, 978–990. doi: 10.1038/ncb2784

Acosta, J. C., O'Loghlen, A., Banito, A., Guijarro, M. V., Augert, A., Raguz, S., et al. (2008). Chemokine signaling via the CXCR2 receptor reinforces senescence. *Cell* 133, 1006–1018. doi: 10.1016/j.cell.2008.03.038

Alison, M. R., Lim, S. M. L., and Nicholson, L. J. (2011). Cancer stem cells: problems for therapy? *J. Pathol.* 223, 147–161. doi: 10.1002/path.2793

Ansieau, S., Bastid, J., Doreau, A., Morel, A. P., Bouchet, B. P., Thomas, C., et al. (2008). Induction of EMT by twist proteins as a collateral effect of tumor-promoting inactivation of premature senescence. *Cancer Cell* 14, 79–89. doi: 10.1016/j.ccr.2008.06.005

Anuja, K., Roy, S., Ghosh, C., Gupta, P., Bhattacharjee, S., and Banerjee, B. (2017). Prolonged inflammatory microenvironment is crucial for pro-neoplastic growth and genome instability: a detailed review. *Inflamm. Res.* 66, 119–128. doi: 10.1007/s00011-016-0985-3

Axelrod, R., Axelrod, D. E., and Pienta, K. J. (2006). Evolution of cooperation among tumor cells. *Proc. Natl. Acad. Sci. U.S.A.* 103, 13474–13479. doi: 10.1073/pnas.0606053103

Bachelot, T., Ray-Coquard, I., Menetrier-Caux, C., Rastkha, M., Duc, A., and Blay, J. Y. (2003). Prognostic value of serum levels of interleukin 6 and of serum and plasma levels of vascular endothelial growth factor in hormone-refractory metastatic breast cancer patients. *Br. J. Cancer* 88, 1721–1726. doi: 10.1038/sj.bjc.6600956

Baker, D. J., Wijshake, T., Tchkonia, T., Lebrasseur, N. K., Childs, B. G., Van De Sluis, B., et al. (2011). Clearance of p16 Ink4a-positive senescent cells delays ageing-associated disorders. *Nature* 479, ages232–ages236. doi: 10.1038/nature10600

Balkwill, F., Charles, K. A., and Mantovani, A. (2005). Smoldering and polarized inflammation in the initiation and promotion of malignant disease. *Cancer Cell* 7, 211–217. doi: 10.1016/j.ccr.2005.02.013

Batlle, E., and Clevers, H. (2017). Cancer stem cells revisited. *Nat. Med.* 23, 1124–1134. doi: 10.1038/nm.4409

Bavik, C., Coleman, I., Dean, J. P., Knudsen, B., Plymate, S., and Nelson, P. S. (2006). The gene expression program of prostate fibroblast senescence modulates neoplastic epithelial cell proliferation through paracrine mechanisms. *Cancer Res.* 66, 794–802. doi: 10.1158/0008-5472.CAN-05-1716

Beauséjour, C. M., Krtolica, A., Galimi, F., Narita, M., Lowe, S. W., Yaswen, P., et al. (2003). Reversal of human cellular senescence: roles of the p53 and p16 pathways. *EMBO J.* 2, 4212–4222. doi: 10.1093/emboj/cdg417

Beck, B., Lapouge, G., Rorive, S., Drogat, B., Desaedelaere, K., Delafaille, S., et al. (2015). Different levels of Twist1 regulate skin tumor initiation, stemness, and progression. *Cell Stem Cell* 16, 67–79. doi: 10.1016/j.stem.2014.12.002

Beerling, E., Seinstra, D., de Wit, E., Kester, L., van der Velden, D., Maynard, C., et al. (2016). Plasticity between epithelial and mesenchymal states unlinks EMT from metastasis-enhancing stem cell capacity. *Cell Rep.* 14, 2281–2288. doi: 10.1016/j.celrep.2016.02.034

Benoy, I. H., Salgado, R., Van Dam, P., Geboers, K., Van Marck, E., Scharpé, S., et al. (2004). Increased serum interleukin-8 in patients with early and metastatic breast cancer correlates with early dissemination and survival. *Clin. Cancer Res.* 10, 7157–7162. doi: 10.1158/1078-0432.CCR-04-0812

Bierie, B., Pierce, S. E., Kroeger, C., Stover, D. G., Pattabiraman, D. R., Thiru, P., et al. (2017). Integrin-β4 identifies cancer stem cell-enriched populations of partially mesenchymal carcinoma cells. *Proc. Natl. Acad. Sci. U.S.A.* 114, E2337–E2346. doi: 10.1073/pnas.1618298114

Bose, D., Zimmerman, L. J., Pierobon, M., Petricoin, E., Tozzi, F., Parikh, A., et al. (2011). Chemoresistant colorectal cancer cells and cancer stem cells mediate growth and survival of bystander cells. *Br. J. Cancer* 105, 1759–1767. doi: 10.1038/bjc.2011.449

Bromberg, J., and Wang, T. C. (2009). Inflammation and Cancer: IL-6 and STAT3 Complete the Link. *Cancer Cell* 15, 79–80. doi: 10.1016/j.ccr.2009.01.009

Cahu, J., Bustany, S., and Sola, B. (2012). Senescence-associated secretory phenotype favors the emergence of cancer stem-like cells. *Cell Death Dis.* 3:e446. doi: 10.1038/cddis.2012.183

Campisi, J. (2005). Suppressing cancer: the importance of being senescent. *Science (80-)* 309, 886–887. doi: 10.1126/science.1116801

Campisi, J. (2013). Aging, cellular senescence, and cancer. *Annu. Rev. Physiol.* 75, 685–705. doi: 10.1146/annurev-physiol-030212-183653

Castro-Vega, L. J., Jouravleva, K., Liu, W. Y., Martinez, C., Gestraud, P., Hupé, P., et al. (2013). Telomere crisis in kidney epithelial cells promotes the acquisition of a microRNA signature retrieved in aggressive renal cell carcinomas. *Carcinogenesis* 34, 1173–1180. doi: 10.1093/carcin/bgt029

Castro-Vega, L. J., Jouravleva, K., Ortiz-Montero, P., Liu, W. Y., Galeano, J. L., Romero, M., et al. (2015). The senescent microenvironment promotes the emergence of heterogeneous cancer stem-like cells. *Carcinogenesis* 34, 1173–1180. doi: 10.1093/carcin/bgv101

Celià-Terrassa, T., Meca-Cortés, Ó, Mateo, F., De Paz, A. M., Rubio, N., Arnal-Estapé, A., et al. (2012). Epithelial-mesenchymal transition can suppress major attributes of human epithelial tumor-initiating cells. *J. Clin. Invest.* 36, 1180–1192. doi: 10.1172/JCI59218

Chaffer, C. L., and Weinberg, R. A. (2011). A perspective on cancer cell metastasis. *Science (80-)* 122, 1849–1868. doi: 10.1126/science.1203543

Chaffer, C. L., and Weinberg, R. A. (2015). How does multistep tumorigenesis really proceed? *Cancer Discov.* 331, 1559–1564. doi: 10.1158/2159-8290.CD-14-0788

Charafe-Jauffret, E., Ginestier, C., Iovino, F., Wicinski, J., Cervera, N., Finetti, P., et al. (2009). Breast cancer cell lines contain functional cancer stem sells with metastatic capacity and a distinct molecular signature. *Cancer Res.* 69, 1302–1313. doi: 10.1158/0008-5472.CAN-08-2741

Chen, J. J. W., Yao, P. L., Yuan, A., Hong, T. M., Shun, C. T., Kuo, M. L., et al. (2003). Up-regulation of tumor interleukin-8 expression by infiltrating macrophages: its correlation with tumor angiogenesis and patient survival in non-small cell lung cancer. *Clin. Cancer Res.* 9, 729–737.

Chen, M. F., Lin, C. T., Chen, W. C., Yang, C. T., Chen, C. C., Liao, S. K., et al. (2006). The sensitivity of human mesenchymal stem cells to ionizing radiation. *Int. J. Radiat. Oncol. Biol. Phys.* 66, 244–253. doi: 10.1016/j.ijrobp.2006.03.062

Chiche, A., Moumen, M., Romagnoli, M., Petit, V., Lasla, H., Jézéquel, P., et al. (2017). P53 deficiency induces cancer stem cell pool expansion in a mouse model of triple-negative breast tumors. *Oncogene* 36, 2355–2365. doi: 10.1038/onc.2016.396

Christiansen, J. J., and Rajasekaran, A. K. (2006). Reassessing epithelial to mesenchymal transition as a prerequisite for carcinoma invasion and metastasis. *Cancer Res.* 66, 8319–8326. doi: 10.1158/0008-5472.CAN-06-0410

Chu, P. Y., Hou, M. F., Lai, J. C., Chen, L. F., and Lin, C. S. (2019). Cell reprogramming in tumorigenesis and its therapeutic implications for breast cancer. *Int. J. Mol. Sci.* 20:1827. doi: 10.3390/ijms20081827

Clarke, M. F., Dick, J. E., Dirks, P. B., Eaves, C. J., Jamieson, C. H. M., Jones, D. L., et al. (2006). Cancer stem cells – Perspectives on current status and future directions: AACR workshop on cancer stem cells. *Cancer Res.* 66, 9339–9344. doi: 10.1158/0008-5472.CAN-06-3126

Cleary, A. S., Leonard, T. L., Gestl, S. A., and Gunther, E. J. (2014). Tumour cell heterogeneity maintained by cooperating subclones in Wnt-driven mammary cancers. *Nature* 508, 113–117. doi: 10.1038/nature13187

Collado, M., Gil, J., Efeyan, A., Guerra, C., Schuhmacher, A. J., Barradas, M., et al. (2005). Tumour biology: senescence in premalignant tumours. *Nature* 436:642. doi: 10.1038/436642a

Colotta, F., Allavena, P., Sica, A., Garlanda, C., and Mantovani, A. (2009). Cancer-related inflammation, the seventh hallmark of cancer: links to genetic instability. *Carcinogenesis* 30, 1073–1081. doi: 10.1093/carcin/bgp127

Coppé, J.-P., Desprez, P.-Y., Krtolica, A., and Campisi, J. (2010). The senescence-associated secretory phenotype: the dark side of tumor suppression. *Annu. Rev. Pathol. Mech. Dis.* 5, 99–118. doi: 10.1146/annurev-pathol-121808-102144

Coppé, J. P., Patil, C. K., Rodier, F., Sun, Y., Muñoz, D. P., Goldstein, J., et al. (2008). Senescence-associated secretory phenotypes reveal cell-nonautonomous functions of oncogenic RAS and the p53 tumor suppressor. *PLoS Biol.* 6:2853–2868. doi: 10.1371/journal.pbio.0060301

Creighton, C. J., Li, X., Landis, M., Dixon, J. M., Neumeister, V. M., Sjolund, A., et al. (2009). Residual breast cancers after conventional therapy display

mesenchymal as well as tumor-initiating features. *Proc. Natl. Acad. Sci. U.S.A.* 106, 13820–13825. doi: 10.1073/pnas.0905718106

De Lope, C., Martín-Alonso, S., Auzmendi-Iriarte, J., Escudero, C., Mulet, I., Larrasa-Alonso, J., et al. (2019). SIX1 represses senescence and promotes SOX2-mediated cellular plasticity during tumorigenesis. *Sci. Rep.* 9:1412. doi: 10.1038/s41598-018-38176-0

De Visser, K. E., Eichten, A., and Coussens, L. M. (2006). Paradoxical roles of the immune system during cancer development. *Nat. Rev. Cancer* 6, 24–37. doi: 10.1038/nrc1782

Demaria, M., O'Leary, M. N., Chang, J., Shao, L., Liu, S., Alimirah, F., et al. (2017). Cellular senescence promotes adverse effects of chemotherapy and cancer relapse. *Cancer Discov.* 7, 165–176. doi: 10.1158/2159-8290.CD-16-0241

Dethlefsen, C., Højfeldt, G., and Hojman, P. (2013). The role of intratumoral and systemic IL-6 in breast cancer. *Breast Cancer Res. Treat.* 2:e94296. doi: 10.1007/s10549-013-2488-z

Dominguez, C., McCampbell, K. K., David, J. M., and Palena, C. (2017). Neutralization of IL-8 decreases tumor PMN-MDSCs and reduces mesenchymalization of claudin-low triple-negative breast cancer. *JCI Insight* 12:e0185088. doi: 10.1172/jci.insight.94296

Dong, J., Zhai, B., Sun, W., Hu, F., Cheng, H., and Xu, J. (2017). Activation of phosphatidylinositol 3-kinase/AKT/snail signaling pathway contributes to epithelial-mesenchymal transition-induced multi-drug resistance to sorafenib in hepatocellular carcinoma cells. *PLoS ONE* 20:e0185088. doi: 10.1371/journal.pone.0185088

Dongre, A., and Weinberg, R. A. (2019). New insights into the mechanisms of epithelial–mesenchymal transition and implications for cancer. *Nat. Rev. Mol. Cell Biol.* 34, 466–482.e6. doi: 10.1038/s41580-018-0080-4

Dravis, C., Chung, C. Y., Lytle, N. K., Herrera-Valdez, J., Luna, G., Trejo, C. L., et al. (2018). Epigenetic and transcriptomic profiling of mammary gland development and tumor models disclose regulators of cell state plasticity. *Cancer Cell* 11:664. doi: 10.1016/j.ccell.2018.08.001

Eiro, N., Gonzalez, L. O., Fraile, M., Cid, S., Schneider, J., and Vizoso, F. J. (2019). Breast cancer tumor stroma: cellular components, phenotypic heterogeneity, intercellular communication, prognostic implications and therapeutic opportunities. *Cancers (Basel)* 341, 2–8. doi: 10.3390/cancers11050664

ElShamy, W. M., and Duhé, R. J. (2013). Overview: cellular plasticity, cancer stem cells and metastasis. *Cancer Lett.* 341, 2–8. doi: 10.1016/j.canlet.2013.06.020

Escobar, J., Pereda, J., López-Rodas, G., and Sastre, J. (2012). Redox signaling and histone acetylation in acute pancreatitis. *Free Radic. Biol. Med.* 52, 819–837. doi: 10.1016/j.freeradbiomed.2011.11.009

Fillmore, C. M., and Kuperwasser, C. (2008). Human breast cancer cell lines contain stem-like cells that self-renew, give rise to phenotypically diverse progeny and survive chemotherapy. *Breast Cancer Res.* 10:R25. doi: 10.1186/bcr1982

Ford, H. L., and Thompson, E. W. (2010). Preface: mammary gland studies as important contributors to the cause of epithelial mesenchymal plasticity in malignancy. *J. Mammary Gland Biol. Neoplasia* 15, 113–115. doi: 10.1007/s10911-010-9182-0

Foster, S. A., Wong, D. J., Barrett, M. T., and Galloway, D. A. (1998). Inactivation of p16 in human mammary epithelial cells by CpG island methylation. *Mol. Cell. Biol.* 18, 1793–1801. doi: 10.1128/mcb.18.4.1793

Fraser, D. M., Sullivan, F. M., Thompson, A. M., and McCowan, C. (2014). Aspirin use and survival after the diagnosis of breast cancer: a population-based cohort study. *Br. J. Cancer* 111, 623–627. doi: 10.1038/bjc.2014.264

Freund, A., Chauveau, C., Brouillet, J. P., Lucas, A., Lacroix, M., Licznar, A., et al. (2003). IL-8 expression and its possible relationship with estrogen-receptor-negative status of breast cancer cells. *Oncogene* 22, 256–265. doi: 10.1038/sj.onc.1206113

Friedl, P., Locker, J., Sahai, E., and Segall, J. E. (2012). Classifying collective cancer cell invasion. *Nat. Cell Biol.* 14, 777–783. doi: 10.1038/ncb2548

Gao, X., Liu, X., Lu, Y., Wang, Y., Cao, W., Liu, X., et al. (2019). PIM1 is responsible for IL-6-induced breast cancer cell EMT and stemness via c-myc activation. *Breast Cancer* 26, 663–671. doi: 10.1007/s12282-019-00966-3

Ginestier, C., Liu, S., Diebel, M. E., Korkaya, H., Luo, M., Brown, M., et al. (2010). CXCR1 blockade selectively targets human breast cancer stem cells in vitro and in xenografts. *J. Clin. Invest.* 120, 485–497. doi: 10.1172/JCI39397

Granit, R. Z., Slyper, M., and Ben-Porath, I. (2014). Axes of differentiation in breast cancer: untangling stemness, lineage identity, and the epithelial to mesenchymal transition. *Wiley Interdiscip. Rev. Syst. Biol. Med.* 6, 93–106. doi: 10.1002/wsbm.1252

Grosse-Wilde, A., D'Hérouël, A. F., McIntosh, E., Ertaylan, G., Skupin, A., Kuestner, R. E., et al. (2015). Stemness of the hybrid epithelial/mesenchymal state in breast cancer and its association with poor survival. *PLoS ONE* 10:e0126522. doi: 10.1371/journal.pone.0126522

Guarino, M., Micheli, P., Pallotti, F., and Giordano, F. (1999). Pathological relevance of epithelial and mesenchymal phenotype plasticity. *Pathol. Res. Pract.* 195, 379–389. doi: 10.1016/S0344-0338(99)80011-9

Guillon, J., Petit, C., Toutain, B., Guette, C., Lelièvre, E., and Coqueret, O. (2019). Chemotherapy-induced senescence, an adaptive mechanism driving resistance and tumor heterogeneity. *Cell Cycle* 18, 2385–2397. doi: 10.1080/15384101.2019.1652047

Gupta, P. B., Pastushenko, I., Skibinski, A., Blanpain, C., and Kuperwasser, C. (2019). Phenotypic plasticity: driver of cancer initiation, progression, and therapy resistance. *Cell Stem Cell* 24, 65–78. doi: 10.1016/j.stem.2018.11.011

Harrison, M. L., Obermueller, E., Maisey, N. R., Hoare, S., Edmonds, K., Li, N. F., et al. (2007). Tumor necrosis factor α as a new target for renal cell carcinoma: two sequential phase II trials of infliximab at standard and high dose. *J. Clin. Oncol.* 25, 4542–4549. doi: 10.1200/JCO.2007.11.2136

Haslehurst, A. M., Koti, M., Dharsee, M., Nuin, P., Evans, K., Geraci, J., et al. (2012). EMT transcription factors snail and slug directly contribute to cisplatin resistance in ovarian cancer. *BMC Cancer* 12:91. doi: 10.1186/1471-2407-12-91

Haynes, B., Sarma, A., Nangia-Makker, P., and Shekhar, M. P. (2017). Breast cancer complexity: implications of intratumoral heterogeneity in clinical management. *Cancer Metastasis Rev.* 36, 547–555. doi: 10.1007/s10555-017-9684-y

Hendrix, M. J. C., Seftor, E. A., Seftor, R. E. B., and Trevor, K. T. (1997). Experimental co-expression of vimentin and keratin intermediate filaments in human breast cancer cells results in phenotypic interconversion and increased invasive behavior. *Am. J. Pathol.* 150, 483–495.

Hollier, B. G., Evans, K., and Mani, S. A. (2009). The epithelial-to-mesenchymal transition and cancer stem cells: a coalition against cancer therapies. *J. Mammary Gland Biol. Neoplasia* 14, 29–43. doi: 10.1007/s10911-009-9110-3

Hollstein, M., Sidransky, D., Vogelstein, B., and Harris, C. C. (1991). p53 mutations in human cancers. *Science (80-)* 253, 49–53. doi: 10.1126/science.1905840

Holohan, C., Van Schaeybroeck, S., Longley, D. B., and Johnston, P. G. (2013). Cancer drug resistance: an evolving paradigm. *Nat. Rev. Cancer* 13, 714–712. doi: 10.1038/nrc3599

Jarrard, D. F., Sarkar, S., Shi, Y., Yeager, T. R., Magrane, G., Kinoshita, H., et al. (1999). p16/pRb pathway alterations are required for bypassing senescence in human prostate epithelial cells. *Cancer Res.* 59, 2957–2956.

Jia, D., Jolly, M. K., Boareto, M., Parsana, P., Mooney, S. M., Pienta, K. J., et al. (2015). OVOL guides the epithelial-hybrid-mesenchymal transition. *Oncotarget* 6, 15436–15448. doi: 10.18632/oncotarget.3623

Jolly, M. K., Boareto, M., Huang, B., Jia, D., Lu, M., Onuchic, J. N., et al. (2015a). Implications of the hybrid epithelial/mesenchymal phenotype in metastasis. *Front. Oncol.* 5:155. doi: 10.3389/fonc.2015.00155

Jolly, M. K., Jia, D., Boareto, M., Mani, S. A., Pienta, K. J., Ben-Jacob, E., et al. (2015b). Coupling the modules of EMT and stemness: a tunable "stemness window" model. *Oncotarget* 194, 161–184. doi: 10.18632/oncotarget.4629

Jolly, M. K., Somarelli, J. A., Sheth, M., Biddle, A., Tripathi, S. C., Armstrong, A. J., et al. (2019). Hybrid epithelial/mesenchymal phenotypes promote metastasis and therapy resistance across carcinomas. *Pharmacol. Ther.* 194, 161–184. doi: 10.1016/j.pharmthera.2018.09.007

Jolly, M. K., Tripathi, S. C., Jia, D., Mooney, S. M., Celiktas, M., Hanash, S. M., et al. (2016). Stability of the hybrid epithelial/mesenchymal phenotype. *Oncotarget* 7, 27067–27084. doi: 10.18632/oncotarget.8166

Kajita, M., McClinic, K. N., and Wade, P. A. (2004). Aberrant expression of the transcription factors snail and slug alters the response to genotoxic stress. *Mol. Cell. Biol.* 24, 7559–7566. doi: 10.1128/mcb.24.17.7559-7566.2004

Kalluri, R., and Weinberg, R. A. (2009). The basics of epithelial-mesenchymal transition. *J. Clin. Invest.* 119, 1420–1428. doi: 10.1172/JCI39104

Kang, T. W., Yevsa, T., Woller, N., Hoenicke, L., Wuestefeld, T., Dauch, D., et al. (2011). Senescence surveillance of pre-malignant hepatocytes limits liver cancer development. *Nature* 479, 547–551. doi: 10.1038/nature10599

Katakura, Y., Nakata, E., Miura, T., and Shirahata, S. (1999). Transforming growth factor β triggers two independent-senescence programs in cancer cells. *Biochem. Biophys. Res. Commun.* 255, 110–115. doi: 10.1006/bbrc.1999.0129

Kim, J., Kong, J., Chang, H., Kim, H., and Kim, A. (2016). EGF induces epithelial-mesenchymal transition through phospho-Smad2/3-Snail signaling pathway in breast cancer cells. *Oncotarget* 7, 85021–85032. doi: 10.18632/oncotarget.13116

Kim, N. W., Piatyszek, M. A., Prowse, K. R., Harley, C. B., West, M. D., Ho, P. L. C., et al. (1994). Specific association of human telomerase activity with immortal cells and cancer. *Science (80-)* 266, 2011–2015. doi: 10.1126/science.7605428

Kim, S. Y., Kang, J. W., Song, X., Kim, B. K., Yoo, Y. D., Kwon, Y. T., et al. (2013). Role of the IL-6-JAK1-STAT3-Oct-4 pathway in the conversion of non-stem cancer cells into cancer stem-like cells. *Cell. Signal.* 25, 961–969. doi: 10.1016/j.cellsig.2013.01.007

Kleer, C. G., Cao, Q., Varambally, S., Shen, R., Ota, I., Tomlins, S. A., et al. (2003). EZH2 is a marker of aggressive breast cancer and promotes neoplastic transformation of breast epithelial cells. *Proc. Natl. Acad. Sci .U.S.A.* 100, 11606–11611. doi: 10.1073/pnas.1933744100

Knüpfer, H., and Preiß, R. (2007). Significance of interleukin-6 (IL-6) in breast cancer (review). *Breast Cancer Res. Treat.* 102, 129–135. doi: 10.1007/s10549-006-9328-3

Kojima, H., Inoue, T., Kunimoto, H., and Nakajima, K. (2013). IL-6-STAT3 signaling and premature senescence. *JAK-STAT* 2:e25763. doi: 10.4161/jkst.25763

Koren, S., Reavie, L., Couto, J. P., De Silva, D., Stadler, M. B., Roloff, T., et al. (2015). PIK3CAH1047R induces multipotency and multi-lineage mammary tumours. *Nature* 525, 114–118. doi: 10.1038/nature14669

Korkaya, H., Liu, S., and Wicha, M. S. (2011). Regulation of cancer stem cells by cytokine networks: attacking cancer's inflammatory roots. *Clin. Cancer Res.* 17, 6125–6129. doi: 10.1158/1078-0432.CCR-10-2743

Korpal, M., Ell, B. J., Buffa, F. M., Ibrahim, T., Blanco, M. A., Celià-Terrassa, T., et al. (2011). Direct targeting of Sec23a by miR-200s influences cancer cell secretome and promotes metastatic colonization. *Nat. Med.* 17, 1101–1108. doi: 10.1038/nm.2401

Kreso, A., and Dick, J. E. (2014). Evolution of the cancer stem cell model. *Cell Stem Cell* 14, 275–291. doi: 10.1016/j.stem.2014.02.006

Kröger, C., Afeyan, A., Mraz, J., Eaton, E. N., Reinhardt, F., Khodor, Y. L., et al. (2019). Acquisition of a hybrid E/M state is essential for tumorigenicity of basal breast cancer cells. *Proc. Natl. Acad. Sci. U.S.A.* 116, 7353–7362. doi: 10.1073/pnas.1812876116

Krtolica, A., Parrinello, S., Lockett, S., Desprez, P. Y., and Campisi, J. (2001). Senescent fibroblasts promote epithelial cell growth and tumorigenesis: a link between cancer and aging. *Proc. Natl. Acad. Sci. U.S.A.* 98, 12072–12077. doi: 10.1073/pnas.211053698

Lamouille, S., Xu, J., and Derynck, R. (2014). Molecular mechanisms of epithelial-mesenchymal transition. *Nat. Rev. Mol. Cell Biol.* 15, 178–179. doi: 10.1038/nrm3758

Lasry, A., and Ben-Neriah, Y. (2015). Senescence-associated inflammatory responses: aging and cancer perspectives. *Trends Immunol.* 36, 217–228. doi: 10.1016/j.it.2015.02.009

Le Magnen, C., Shen, M. M., and Abate-Shen, C. (2018). Lineage Plasticity in Cancer Progression and Treatment. *Annu. Rev. Cancer Biol.* 2, 271–289. doi: 10.1146/annurev-cancerbio-030617-050224

Leis, O., Eguiara, A., Lopez-Arribillaga, E., Alberdi, M. J., Hernandez-Garcia, S., Elorriaga, K., et al. (2012). Sox2 expression in breast tumours and activation in breast cancer stem cells. *Oncogene* 31, 1354–1365. doi: 10.1038/onc.2011.338

Li, Y., Vandenboom, T. G., Kong, D., Wang, Z., Ali, S., Philip, P. A., et al. (2009). Up-regulation of miR-200 and let-7 by natural agents leads to the reversal of epithelial-to-mesenchymal transition in gemcitabine-resistant pancreatic cancer cells. *Cancer Res.* 69, 6704–6712. doi: 10.1158/0008-5472.CAN-09-1298

Lim, S., Becker, A., Zimmer, A., Lu, J., Buettner, R., and Kirfel, J. (2013). SNAI1-mediated epithelial-mesenchymal transition confers chemoresistance and cellular plasticity by regulating genes involved in cell death and stem cell maintenance. *PLoS ONE* 8:e66558. doi: 10.1371/journal.pone.0066558

Liu, C. C., Lin, J. H., Hsu, T. W., Su, K., Li, A. F., Hsu, H. S., et al. (2015). IL-6 enriched lung cancer stem-like cell population by inhibition of cell cycle regulators via DNMT1 upregulation. *Int. J. Cancer* 136, 547–559. doi: 10.1002/ijc.29033

Liu, D., and Hornsby, P. J. (2007). Senescent human fibroblasts increase the early growth of xenograft tumors via matrix metalloproteinase secretion. *Cancer Res.* 67, 3117–3126. doi: 10.1158/0008-5472.CAN-06-3452

Liu, S., Cong, Y., Wang, D., Sun, Y., Deng, L., Liu, Y., et al. (2014). Breast cancer stem cells transition between epithelial and mesenchymal states reflective of their normal counterparts. *Stem Cell Rep.* 2, 78–91. doi: 10.1016/j.stemcr.2013.11.009

Livasy, C. A., Karaca, G., Nanda, R., Tretiakova, M. S., Olopade, O. I., Moore, D. T., et al. (2006). Phenotypic evaluation of the basal-like subtype of invasive breast carcinoma. *Mod. Pathol.* 19, 264–271. doi: 10.1038/modpathol.3800528

Loberg, R. D., Ying, C., Craig, M., Day, L. L., Sargent, E., Neeley, C., et al. (2007). Targeting CCL2 with systemic delivery of neutralizing antibodies induces prostate cancer tumor regression in vivo. *Cancer Res.* 67, 9417–9424. doi: 10.1158/0008-5472.CAN-07-1286

Loeb, L. A., and Monnat, R. J. (2008). DNA polymerases and human disease. *Nat. Rev. Genet.* 9, 594–604. doi: 10.1038/nrg2345

Lu, M., Jolly, M. K., Levine, H., Onuchic, J. N., and Ben-Jacob, E. (2013). MicroRNA-based regulation of epithelial-hybrid-mesenchymal fate determination. *Proc. Natl. Acad. Sci. U.S.A.* 110, 18144–18149. doi: 10.1073/pnas.1318192110

Luo, M., Brooks, M., and Wicha, M. (2015). Epithelial-mesenchymal plasticity of breast cancer stem cells: implications for metastasis and therapeutic resistance. *Curr. Pharm. Des.* 21, 1301–1310. doi: 10.2174/1381612826661412111 20604

Mani, S. A., Guo, W., Liao, M. J., Eaton, E. N., Ayyanan, A., Zhou, A. Y., et al. (2008). The epithelial-mesenchymal transition generates cells with properties of stem cells. *Cell* 133, 704–715. doi: 10.1016/j.cell.2008.03.027

Mantovani, A. (2004). Seminars in cancer biology: editorial. *Semin. Cancer Biol.* 14, 147–148. doi: 10.1016/j.semcancer.2003.10.010

Mantovani, A., Allavena, P., Sica, A., and Balkwill, F. (2008). Cancer-related inflammation. *Nature* 33(Suppl. 1), S79–S84. doi: 10.1038/nature07205

Marjanovic, N. D., Weinberg, R. A., and Chaffer, C. L. (2013). Cell plasticity and heterogeneity in cancer. *Clin. Chem.* 59, 168–179. doi: 10.1373/clinchem.2012.184655

Marusyk, A., Almendro, V., and Polyak, K. (2012). Intra-tumour heterogeneity: a looking glass for cancer? *Nat. Rev. Cancer* 12, 323–334. doi: 10.1038/nrc3261

Marusyk, A., Tabassum, D. P., Altrock, P. M., Almendro, V., Michor, F., and Polyak, K. (2014). Non-cell-autonomous driving of tumour growth supports sub-clonal heterogeneity. *Nature* 514, 54–58. doi: 10.1038/nature13556

Meacham, C. E., and Morrison, S. J. (2013). Tumour heterogeneity and cancer cell plasticity. *Nature* 553, 96–100. doi: 10.1038/nature12624

Milanovic, M., Fan, D. N. Y., Belenki, D., Däbritz, J. H. M., Zhao, Z., Yu, Y., et al. (2018). Senescence-associated reprogramming promotes cancer stemness. *Nature* 553, 96–100. doi: 10.1038/nature25167

Mills, J. C., Stanger, B. Z., and Sander, M. (2019). Nomenclature for cellular plasticity: are the terms as plastic as the cells themselves? *EMBO J.* 38:e103148. doi: 10.15252/embj.2019103148

Mimori, K., Saito, T., Niida, A., and Miyano, S. (2018). Cancer evolution and heterogeneity. *Ann. Gastroenterol. Surg.* 2, 332–338. doi: 10.1002/ags3.12182

Mooney, S., Jolly, M., Levine, H., and Kulkarni, P. (2016). Phenotypic plasticity in prostate cancer: role of intrinsically disordered proteins. *Asian J. Androl.* 18, 704–710. doi: 10.4103/1008-682X.183570

Morel, A. P., Lièvre, M., Thomas, C., Hinkal, G., Ansieau, S., and Puisieux, A. (2008). Generation of breast cancer stem cells through epithelial-mesenchymal transition. *PLoS ONE* 3:e2888. doi: 10.1371/journal.pone.0002888

Mosteiro, L., Pantoja, C., Alcazar, N., Marión, R. M., Chondronasiou, D., Rovira, M., et al. (2016). Tissue damage and senescence provide critical signals for cellular reprogramming in vivo. *Science (80-)* 354:aaf4445. doi: 10.1126/science.aaf4445

Mosteiro, L., Pantoja, C., de Martino, A., and Serrano, M. (2018). Senescence promotes in vivo reprogramming through p16INK4a and IL-6. *Aging Cell* 17:e12711. doi: 10.1111/acel.12711

Mumcuoglu, M., Bagislar, S., Yuzugullu, H., Alotaibi, H., Senturk, S., Telkoparan, P., et al. (2010). The ability to generate senescent progeny as a mechanism underlying breast cancer cell heterogeneity. *PLoS ONE* 5:e11288. doi: 10.1371/journal.pone.0011288

Myrianthopoulos, V., Evangelou, K., Vasileiou, P. V. S., Cooks, T., Vassilakopoulos, T. P., Pangalis, G. A., et al. (2019). Senescence and senotherapeutics: a new field in cancer therapy. *Pharmacol. Ther.* 193, 31–49. doi: 10.1016/j.pharmthera.2018.08.006

Nair, N., Calle, A. S., Zahra, M. H., Prieto-Vila, M., Oo, A. K. K., Hurley, L., et al. (2017). A cancer stem cell model as the point of origin of cancer-associated fibroblasts in tumor microenvironment. *Sci. Rep.* 7:6838. doi: 10.1038/s41598-017-07144-5

Neelakantan, D., Drasin, D. J., and Ford, H. L. (2015). Intratumoral heterogeneity: clonal cooperation in epithelial-to-mesenchymal transition and metastasis. *Cell Adhes. Migr.* 9, 265–276. doi: 10.4161/19336918.2014.972761

Nieto, M. A. (2013). Epithelial plasticity: a common theme in embryonic and cancer cells. *Science (80-)* 342:1234850. doi: 10.1126/science.1234850

Nieto, M. A., Huang, R. Y. Y. J., Jackson, R. A. A., and Thiery, J. P. P. (2016). EMT: 2016. *Cell* 166, 21–45. doi: 10.1016/j.cell.2016.06.028

Nishi, M., Sakai, Y., Akutsu, H., Nagashima, Y., Quinn, G., Masui, S., et al. (2014). Induction of cells with cancer stem cell properties from nontumorigenic human mammary epithelial cells by defined reprogramming factors. *Oncogene* 33, 643–652. doi: 10.1038/onc.2012.614

Ocaña, O. H., Córcoles, R., Fabra, Á, Moreno-Bueno, G., Acloque, H., Vega, S., et al. (2012). Metastatic colonization requires the repression of the epithelial-mesenchymal transition inducer Prrx1. *Cancer Cell* 22, 709–724. doi: 10.1016/j.ccr.2012.10.012

Oft, M., Peli, J., Rudaz, C., Schwarz, H., Beug, H., and Reichmann, E. (1996). TGF-β1 and Ha-Ras collaborate in modulating the phenotypic plasticity and invasiveness of epithelial tumor cells. *Genes Dev.* 10, 2462–2477. doi: 10.1101/gad.10.19.2462

Ohashi, S., Natsuizaka, M., Wong, G. S., Michaylira, C. Z., Grugan, K. D., Stairs, D. B., et al. (2010). Epidermal growth factor receptor and mutant p53 expand an esophageal cellular subpopulation capable of epithelial-to-mesenchymal transition through ZEB transcription factors. *Cancer Res.* 70, 4174–4184. doi: 10.1158/0008-5472.CAN-09-4614

Oliveras-Ferraros, C., Corominas-Faja, B., Vazquez-Martin, S. C. A., Martin-Castillo, B., Iglesias, J. M., López-Bonet, E., et al. (2012). Epithelial-to-mesenchymal transition (EMT) confers primary resistance to trastuzumab (Herceptin). *Cell Cycle* 11, 4020–4032. doi: 10.4161/cc.22225

Olumi, A. F., Grossfeld, G. D., Hayward, S. W., Carroll, P. R., Tlsty, T. D., and Cunha, G. R. (1999). Carcinoma-associated fibroblasts direct tumor progression of initiated human prostatic epithelium. *Cancer Res.* 59, 5002–5011.

Ombrato, L., and Malanchi, I. (2014). The EMT universe: space between cancer cell dissemination and metastasis initiation. *Crit. Rev. Oncog.* 19, 349–361. doi: 10.1615/CritRevOncog.2014011802

Ortiz-Montero, P., Liu-Bordes, W. Y., Londoño-Vallejo, A., and Vernot, J. P. (2018). CD24 expression and stem-associated features define tumor cell heterogeneity and tumorigenic capacities in a model of carcinogenesis. *Cancer Manage. Res.* 10, 5767–5784. doi: 10.2147/CMAR.S176654

Ortiz-Montero, P., Londoño-Vallejo, A., and Vernot, J. P. (2017). Senescence-associated IL-6 and IL-8 cytokines induce a self- and cross-reinforced senescence/inflammatory milieu strengthening tumorigenic capabilities in the MCF-7 breast cancer cell line. *Cell Commun. Signal.* 15:17. doi: 10.1186/s12964-017-0172-3

Oser, M. G., Niederst, M. J., Sequist, L. V., and Engelman, J. A. (2015). Transformation from non-small-cell lung cancer to small-cell lung cancer: molecular drivers and cells of origin. *Lancet Oncol.* 16, e165–e172. doi: 10.1016/S1470-2045(14)71180-5

Parrinello, S., Coppe, J. P., Krtolica, A., and Campisi, J. (2005). Stromal-epithelial interactions in aging and cancer: senescent fibroblasts alter epithelial cell differentiation. *J. Cell Sci.* 118(Pt 3), 485–496. doi: 10.1242/jcs.01635

Pastushenko, I., Brisebarre, A., Sifrim, A., Fioramonti, M., Revenco, T., Boumahdi, S., et al. (2018). Identification of the tumour transition states occurring during EMT. *Nature* 556, 463–468. doi: 10.1038/s41586-018-0040-3

Patsialou, A., Wang, Y., Lin, J., Whitney, K., Goswami, S., Kenny, P. A., et al. (2012). Selective gene-expression profiling of migratory tumor cells in vivo predicts clinical outcome in breast cancer patients. *Breast Cancer Res.* 14:R139. doi: 10.1186/bcr3344

Phi, L. T. H., Sari, I. N., Yang, Y. G., Lee, S. H., Jun, N., Kim, K. S., et al. (2018). Cancer stem cells (CSCs) in drug resistance and their therapeutic implications in cancer treatment. *Stem Cells Int.* 2018, 5416923. doi: 10.1155/2018/5416923

Poli, V., Fagnocchi, L., Fasciani, A., Cherubini, A., Mazzoleni, S., Ferrillo, S., et al. (2018a). MYC-driven epigenetic reprogramming favors the onset of tumorigenesis by inducing a stem cell-like state. *Nat. Commun.* 9:1024. doi: 10.1038/s41467-018-03264-2

Poli, V., Fagnocchi, L., and Zippo, A. (2018b). Tumorigenic cell reprogramming and cancer plasticity: interplay between signaling, microenvironment, and epigenetics. *Stem Cells Int.* 2018:4598195. doi: 10.1155/2018/4598195

Prieto, L. I., and Baker, D. J. (2019). Cellular senescence and the immune system in cancer. *Gerontology* 65, 505–512. doi: 10.1159/000500683

Revenu, C., and Gilmour, D. (2009). EMT 2.0: shaping epithelia through collective migration. *Curr. Opin. Genet. Dev.* 19, 338–342. doi: 10.1016/j.gde.2009.04.007

Ritschka, B., Storer, M., Mas, A., Heinzmann, F., Ortells, M. C., Morton, J. P., et al. (2017). The senescence-associated secretory phenotype induces cellular plasticity and tissue regeneration. *Genes Dev.* 31, 172–183. doi: 10.1101/gad.290635.116

Rodier, F., and Campisi, J. (2011). Four faces of cellular senescence. *J. Cell Biol.* 192, 547–556. doi: 10.1083/jcb.201009094

Rodilla, V., and Fre, S. (2018). Cellular plasticity of mammary epithelial cells underlies heterogeneity of breast cancer. *Biomedicines* 6:103. doi: 10.3390/biomedicines6040103

Sabisz, M., and Skladanowski, A. (2009). Cancer stem cells and escape from drug-induced premature senescence in human lung tumor cells: implications for drug resistance and in vitro drug screening models. *Cell Cycle* 8, 3208–3217. doi: 10.4161/cc.8.19.9758

Salminen, A., Kauppinen, A., and Kaarniranta, K. (2018). Myeloid-derived suppressor cells (MDSC): an important partner in cellular/tissue senescence. *Biogerontology* 19, 325–339. doi: 10.1007/s10522-018-9762-8

Sarrio, D., Franklin, C. K., Mackay, A., Reis-Filho, J. S., and Isacke, C. M. (2012). Epithelial and mesenchymal subpopulations within normal basal breast cell lines exhibit distinct stem cell/progenitor properties. *Stem Cells* 30, 292–303. doi: 10.1002/stem.791

Schmidt, J. M., Panzilius, E., Bartsch, H. S., Irmler, M., Beckers, J., Kari, V., et al. (2015). Stem-cell-like properties and epithelial plasticity arise as stable traits after transient twist1 activation. *Cell Rep.* 10, 131–139. doi: 10.1016/j.celrep.2014.12.032

Senturk, S., Mumcuoglu, M., Gursoy-Yuzugullu, O., Cingoz, B., Akcali, K. C., and Ozturk, M. (2010). Transforming growth factor-beta induces senescence in hepatocellular carcinoma cells and inhibits tumor growth. *Hepatology* 52, 966–974. doi: 10.1002/hep.23769

Shay, J. W., and Bacchetti, S. (1997). A survey of telomerase activity in human cancer. *Eur. J. Cancer Part A* 33, 787–791. doi: 10.1016/S0959-8049(97)00062-2

Shekhar, M. P. V., Werdell, J., Santner, S. J., Pauley, R. J., and Tait, L. (2001). Breast stroma plays a dominant regulatory role in breast epithelial growth and differentiation: implications for tumor development and progression. *Cancer Res.* 61, 1320–1326.

Shenoy, A. K., Fisher, R. C., Butterworth, E. A., Pi, L., Chang, L. J., Appelman, H. D., et al. (2012). Transition from colitis to cancer: high Wnt activity sustains the tumor-initiating potential of colon cancer stem cell precursors. *Cancer Res.* 72, 5091–5100. doi: 10.1158/0008-5472.CAN-12-1806

Shibue, T., and Weinberg, R. A. (2017). EMT, CSCs, and drug resistance: the mechanistic link and clinical implications. *Nat. Rev. Clin. Oncol.* 14, 611–629. doi: 10.1038/nrclinonc.2017.44

Shigdar, S., Li, Y., Bhattacharya, S., O'Connor, M., Pu, C., Lin, J., et al. (2014). Inflammation and cancer stem cells. *Cancer Lett.* 15, 2380–2386. doi: 10.1016/j.canlet.2013.07.031

Shimoda, M., Mellody, K. T., and Orimo, A. (2010). Carcinoma-associated fibroblasts are a rate-limiting determinant for tumour progression. *Semin. Cell Dev. Biol.* 21, 19–25. doi: 10.1016/j.semcdb.2009.10.002

Sica, A., Schioppa, T., Mantovani, A., and Allavena, P. (2006). Tumour-associated macrophages are a distinct M2 polarised population promoting tumour progression: potential targets of anti-cancer therapy. *Eur. J. Cancer* 42, 717–727. doi: 10.1016/j.ejca.2006.01.003

Singh, A., and Settleman, J. (2010). EMT, cancer stem cells and drug resistance: an emerging axis of evil in the war on cancer. *Oncogene* 29, 4741–4751. doi: 10.1038/onc.2010.215

Singh, S. K., Hawkins, C., Clarke, I. D., Squire, J. A., Bayani, J., Hide, T., et al. (2004). Identification of human brain tumour initiating cells. *Nature* 432, 396–401. doi: 10.1038/nature03128

Strauss, R., Li, Z. Y., Liu, Y., Beyer, I., Persson, J., Sova, P., et al. (2011). Analysis of epithelial and mesenchymal markers in ovarian cancer reveals phenotypic heterogeneity and plasticity. *PLoS ONE* 6:e16186. doi: 10.1371/journal.pone.0016186

Streicher, S. A., Yu, H., Lu, L., Kidd, M. S., and Risch, H. A. (2014). Case-control study of aspirin use and risk of pancreatic cancer. *Cancer Epidemiol. Biomarkers Prev.* 23, 1254–1263. doi: 10.1158/1055-9965.EPI-13-1284

Takahashi, K., Tanabe, K., Ohnuki, M., Narita, M., Ichisaka, T., Tomoda, K., et al. (2007). Induction of pluripotent stem cells from adult human fibroblasts by defined factors. *Cell* 131, 861–872. doi: 10.1016/j.cell.2007.11.019

Tanno, T., and Matsui, W. (2011). Development and maintenance of cancer stem cells under chronic inflammation. *J. Nippon Med. Sch.* 78, 138–145. doi: 10.1272/jnms.78.138

Thiery, J. P. (2002). Epithelial–mesenchymal transitions in tumour progression. *Nat. Rev. Cancer* 2, 442–454. doi: 10.1038/nrc822

Thiery, J. P., Acloque, H., Huang, R. Y. J., and Nieto, M. A. (2009). Epithelial-mesenchymal transitions in development and disease. *Cell* 139, 871–890. doi: 10.1016/j.cell.2009.11.007

Toso, A., Revandkar, A., DiMitri, D., Guccini, I., Proietti, M., Sarti, M., et al. (2014). Enhancing chemotherapy efficacy in pten-deficient prostate tumors by activating the senescence-associated antitumor immunity. *Cell Rep.* 9, 75–89. doi: 10.1016/j.celrep.2014.08.044

Tran, P. T., Shroff, E. H., Burns, T. F., Thiyagarajan, S., Das, S. T., Zabuawala, T., et al. (2012). Twist1 suppresses senescence programs and thereby accelerates and maintains mutant Kras-induced lung tumorigenesis. *PLoS Genet.* 8:e1002650. doi: 10.1371/journal.pgen.1002650

Tsuji, T., Ibaragi, S., Shima, K., Hu, M. G., Katsurano, M., Sasaki, A., et al. (2008). Epithelial-mesenchymal transition induced by growth suppressor p12 CDK2-AP1 promotes tumor cell local invasion but suppresses distant colony growth. *Cancer Res.* 68, 10377–10386. doi: 10.1158/0008-5472.CAN-08-1444

Turajlic, S., Sottoriva, A., Graham, T., and Swanton, C. (2019). Resolving genetic heterogeneity in cancer. *Nat. Rev. Genet.* 20, 404–416. doi: 10.1038/s41576-019-0114-6

Van Keymeulen, A., Lee, M. Y., Ousset, M., Brohée, S., Rorive, S., Giraddi, R. R., et al. (2015). Reactivation of multipotency by oncogenic PIK3CA induces breast tumour heterogeneity. *Nature* 525, 119–123. doi: 10.1038/nature14665

Varga, J., De Oliveira, T., and Greten, F. R. (2014). The architect who never sleeps: tumor-induced plasticity. *FEBS Lett.* 588, 2422–2427. doi: 10.1016/j.febslet.2014.06.019

Visvader, J. E., and Lindeman, G. J. (2008). Cancer stem cells in solid tumours: accumulating evidence and unresolved questions. *Nat. Rev. Cancer* 8, 755–768. doi: 10.1038/nrc2499

Wahl, S. M. (2007). Transforming growth factor-β: innately bipolar. *Curr. Opin. Immunol.* 19, 55–62. doi: 10.1016/j.coi.2006.11.008

Wiley, C. D., Flynn, J. M., Morrissey, C., Lebofsky, R., Shuga, J., Dong, X., et al. (2017). Analysis of individual cells identifies cell-to-cell variability following induction of cellular senescence. *Aging Cell.* 16, 1043–1050. doi: 10.1111/acel.12632

Yang, L., Fang, J., and Chen, J. (2017). Tumor cell senescence response produces aggressive variants. *Cell Death Discov.* 3:17049. doi: 10.1038/cddiscovery.2017.49

Yang, L., Song, T., Chen, L., Soliman, H., and Chen, J. (2015). Nucleolar repression facilitates initiation and maintenance of senescence. *Cell Cycle* 14, 3613–3623. doi: 10.1080/15384101.2015.1100777

Yao, C., Lin, Y., Ye, C. S., Bi, J., Zhu, Y. F., and Wang, S. M. (2007). Role of interleukin-8 in the progression of estrogen receptor-negative breast cancer. *Chin. Med. J. (Engl.)* 120, 1766–1772. doi: 10.1097/00029330-200710020-00007

Yuan, S., Norgard, R. J., and Stanger, B. Z. (2019). Cellular plasticity in cancer. *Cancer Discov.* 9, 837–851.

Zhang, B., Lam, E. W. F., and Sun, Y. (2019). Senescent cells: a new Achilles' heel to exploit for cancer medicine? *Aging Cell* 18:e12875. doi: 10.1111/acel.12875

Zhang, W., Glöckner, S. C., Guo, M., Machida, E. O., Wang, D. H., Easwaran, H., et al. (2008). Epigenetic inactivation of the canonical Wnt antagonist SRY-box containing gene 17in colorectal cancer. *Cancer Res.* 68, 2764–2772. doi: 10.1158/0008-5472.CAN-07-6349

Zhou, G., Meng, S., Li, Y., Ghebre, Y. T., and Cooke, J. P. (2016). Optimal ROS signaling is critical for nuclear reprogramming. *Cell Rep.* 15, 919–925. doi: 10.1016/j.celrep.2016.03.084

Zou, M., Toivanen, R., Mitrofanova, A., Floch, N., Hayati, S., Sun, Y., et al. (2017). Transdifferentiation as a mechanism of treatment resistance in a mouse model of castration-resistant prostate cancer. *Cancer Discov.* 7, 736–749. doi: 10.1158/2159-8290.CD-16-1174

Conflict of Interest: The author declares that the research was conducted in the absence of any commercial or financial relationships that could be construed as a potential conflict of interest.

Copyright © 2020 Vernot. This is an open-access article distributed under the terms of the Creative Commons Attribution License (CC BY). The use, distribution or reproduction in other forums is permitted, provided the original author(s) and the copyright owner(s) are credited and that the original publication in this journal is cited, in accordance with accepted academic practice. No use, distribution or reproduction is permitted which does not comply with these terms.

frontiers in Molecular Biosciences

REVIEW
published: 10 July 2020
doi: 10.3389/fmolb.2020.00130

Dynamics of Cellular Plasticity in Prostate Cancer Progression

*Ritika Tiwari, Nishat Manzar and Bushra Ateeq**

Molecular Oncology Laboratory, Department of Biological Sciences and Bioengineering, Indian Institute of Technology Kanpur, Kanpur, India

Despite the current advances in the treatment for prostate cancer, the patients often develop resistance to the conventional therapeutic interventions. Therapy-induced drug resistance and tumor progression have been associated with cellular plasticity acquired due to reprogramming at the molecular and phenotypic levels. The plasticity of the tumor cells is mainly governed by two factors: cell-intrinsic and cell-extrinsic. The cell-intrinsic factors involve alteration in the genetic or epigenetic regulators, while cell-extrinsic factors include microenvironmental cues and drug-induced selective pressure. Epithelial-mesenchymal transition (EMT) and stemness are two important hallmarks that dictate cellular plasticity in multiple cancer types including prostate. Emerging evidence has also pinpointed the role of tumor cell plasticity in driving anti-androgen induced neuroendocrine prostate cancer (NEPC), a lethal and therapy-resistant subtype. In this review, we discuss the role of cellular plasticity manifested due to genetic, epigenetic alterations and cues from the tumor microenvironment, and their role in driving therapy resistant prostate cancer.

Keywords: prostate cancer, ADT, cellular plasticity, EMT, stemness, drug resistance, NEPC

OPEN ACCESS

Edited by:
Satyendra Chandra Tripathi, All India Institute of Medical Sciences Nagpur, India

Reviewed by:
Letizia De Chiara, University of Florence, Italy
Saurav Kumar, Fred Hutchinson Cancer Research Center, United States

****Correspondence:***
Bushra Ateeq
bushra@iitk.ac.in

Specialty section:
This article was submitted to Molecular Diagnostics and Therapeutics, a section of the journal Frontiers in Molecular Biosciences

Received: *05 March 2020*
Accepted: *02 June 2020*
Published: *10 July 2020*

Citation:
Tiwari R, Manzar N and Ateeq B (2020) Dynamics of Cellular Plasticity in Prostate Cancer Progression. Front. Mol. Biosci. 7:130. doi: 10.3389/fmolb.2020.00130

INTRODUCTION

Prostate cancer (PCa) represents a highly heterogenous disease with diverse range of molecular alterations defining its subclasses. These molecular alterations include somatic or germline mutations, focal deletions, amplifications, and gene fusions that entail the intra- and inter-patient heterogeneity and confer variable clinical outcomes. The major molecular subclasses include a variety of gene fusions involving *ETS* family transcription factors, namely *ERG*, *ETV1/4*, *FLI1*, and *NDRG1*; or *RAF* kinase rearrangements, upregulation of secretory protein SPINK1 and somatic mutations in *SPOP*, *FOXA1,* and *IDH1* (Tomlins et al., 2005, 2008; Palanisamy et al., 2010; Cancer Genome Atlas Research, 2015; Bhatia and Ateeq, 2019). The androgen signaling plays a key role in development and maintenance of the prostate gland (Cunha et al., 1987; Cooke et al., 1991), while aberrant activation of this signaling has been linked to the initiation and metastatic progression of PCa (Gelmann, 2002; Culig and Santer, 2014; Tan et al., 2015). Thus, drugs that target biosynthesis of androgen or androgen receptor (AR) activity are often administered as the first line therapy also known as androgen deprivation therapy (ADT). However, the disease inadvertently progresses to an advanced stage, castrate-resistant prostate cancer (CRPC) (Cher et al., 1996; Gregory et al., 2001; Chen et al., 2004; Grasso et al., 2012; Robinson et al., 2015). At CRPC stage, the cancer cells bypass their dependency on the androgen signaling by various mechanisms such as somatic mutations or amplification of *AR* gene, constitutively active splice variants (AR-V7 and ARv567es), mutations in the ligand binding domain of AR (F877L and T878A), or activation

of androgen-regulated genes via glucocorticoid receptor (Taplin et al., 1995; Arora et al., 2013; Antonarakis et al., 2014). The androgen biosynthesis inhibitor, abiraterone and next-generation AR-antagonists, enzalutamide and apalutamide have been developed for the clinic management of CRPC patients (Scher et al., 2010; de Bono et al., 2011; Clegg et al., 2012). Although, AR-targeting therapies prolong the overall survival of the patients, nonetheless, resistance to these drugs often prevail leading to disease progression to an aggressive stage, also known as neuroendocrine prostate cancer (NEPC) (Aggarwal et al., 2018). The mechanism to overcome the acquired resistance toward anti-androgen therapy is frequently manifested by several molecular and phenotypic changes resulting in transition of androgen-independent CRPC to therapy-induced NEPC (Zou et al., 2017; Aggarwal et al., 2018; Soundararajan et al., 2018; Beltran et al., 2019). This dynamic transition provides multifaceted advantages to the cancer cells to overcome therapy-induced resistance and enable survival (Sun et al., 2012; Miao et al., 2017; Stylianou et al., 2019).

Cellular plasticity represents the dynamic transition of a cell between one state to another (Varga and Greten, 2017). The term "plasticity" was introduced to define the extensive reprogramming events happening in stem cells leading to cellular differentiation (Blau et al., 1985). This is a bidirectional process which involves changes both at the molecular and phenotypic levels of a cell. The cellular plasticity has been a key phenomenon that governs not only the developmental fate of the organism, but also serves as a driving force behind different malignancies, including PCa (Rothman and Jarriault, 2019; Yuan et al., 2019). During early embryonic development, the cellular plasticity helps the stem or progenitor cells to differentiate into different lineages while in the later stages of life, it maintains stem cell populations and regulates tissue repair (Wagers and Weissman, 2004). Several complex processes such as transcriptional regulation or epigenetic alterations are known to modulate the cellular identity and plasticity (Flavahan et al., 2017). Mounting evidence suggests that the genes involved in the embryonic development are frequently subverted or reactivated during malignant transformation of cells (Kalluri and Weinberg, 2009; Dempke et al., 2017). These acquired molecular attributes enable the tumor cells to elude the constraints of normal growth, thereby assisting them to thrive and sustain, escape therapeutic pressure and immune surveillance (Zou et al., 2017; Vitkin et al., 2019; Yuan et al., 2019). Likewise, in PCa, cellular plasticity aids the tumor cells to develop resistance against the targeted therapies in several different ways, for instance, by undergoing phenotypic conversions, cellular reprogramming and transition from one cell lineage to another (Beltran and Demichelis, 2015; Zou et al., 2017; Alumkal et al., 2020).

In this review, we discuss the importance of cellular plasticity in conferring intra-tumoral heterogeneity and its impact on disease progression and drug resistance. Further, we attempt to delineate the implications of cell-intrinsic and -extrinsic factors which govern the plasticity in tumor cells. Finally, we also summarize the novel therapeutic interventions used to target cellular plasticity in combating prostate cancer.

INTRA-TUMORAL HETEROGENEITY AND CELLULAR PLASTICITY

PCa exhibits high level of intra-tumor heterogeneity characterized by distinct sub-populations of the cancer cells, which is often a major confounding factor influencing disease progression (Boyd et al., 2012; Yadav et al., 2018). This intra-tumor heterogeneity offers a multifaceted advantage to the PCa cells such as disease progression, tumor dissemination, and driving resistance toward standard therapies such as chemotherapy, radiation or hormone therapy (Marjanovic et al., 2013). Two different models contributing to intra-tumoral heterogeneity in PCa have been generally accepted. In the clonal evolution model, tumors arise from a single cell of origin triggered in response to sequential oncogenic hits (Liu et al., 2009; Kreso and Dick, 2014). In cancer stem cell model, tumor cells originate from the differentiation of a small population of cancer stem cells (CSCs) or dedifferentiation of the existing cancer cells into CSCs to promote tumor growth and progression (Collins et al., 2005; Patrawala et al., 2006; Yadav et al., 2018). The neoplastic transformation via either of the proposed pathways give rise to genetically and phenotypically distinct cell types within same tumor (Poli et al., 2018). This morphological heterogeneity is responsible for the multifocality within the prostate tumor of the same patient. The multifocality has been reported in ∼50–90% of the PCa patients who underwent radical prostatectomy, and has been linked with higher grade, advanced stage and recurrence compared to unifocal prostate adenocarcinoma (Djavan et al., 1999). Multifocal tumors exhibit significant molecular heterogeneity in terms of copy number alterations (CNAs), single-nucleotide variants (SNVs), genomic rearrangements, and unique signatures of DNA damage and transcriptional dysregulation (Beltran and Demichelis, 2015; Boutros et al., 2015). Additionally, intra-tumoral variability involving distinct DNA methylation and histone modification patterns was found to be more pronounced in the advanced stage PCa, suggesting association of epigenetic heterogeneity with poor clinical outcome (Seligson et al., 2005; Bianco-Miotto et al., 2010; Brocks et al., 2014). Thus, deciphering the molecular basis of the intra-tumor heterogeneity may provide an insight for better prognosis and the clinical management of PCa patients.

EPITHELIAL-MESENCHYMAL TRANSITION MODULATES CELLULAR PLASTICITY IN PROSTATE CANCER

The epithelial-mesenchymal transition (EMT) is the key phenomenon in embryonic development, nonetheless, it plays a pivotal role in maintaining tissue homeostasis as well as cancer progression (Nauseef and Henry, 2011). This complex process involves transition of a epithelial cell into a mesenchymal phenotype, characterized by reduced cell-cell adhesion and increased migratory properties (Lu and Kang, 2019). Moreover, tumors often exhibit co-existence of a subpopulation of cells in hybrid state harboring both epithelial and mesenchymal phenotypes (hybrid E/M state), further aiding the cancer cells

to metastasize from primary to distant secondary sites (Tsai and Yang, 2013; Williams et al., 2019). During this reprogramming, the cancer cells secrete an array of enzymes which break down its attachment to the basement membrane followed by several phenotypic changes such as reorganization of actin cytoskeleton, leading to enhanced migratory and metastatic potential (Thiery et al., 2009). Multiple clinical evidence has associated enhanced mesenchymal features with high Gleason grade, shorter time to biochemical recurrence and increased metastasis in PCa (Cheng et al., 1996; Graham et al., 2008; Zhang et al., 2009; Figiel et al., 2017).

Several transcription factors (TFs) associated with EMT regulate cellular plasticity during embryonic development have been identified as the oncogenic determinants in the neoplastic transformation of prostate. For example, SRY-Box Transcription Factor 9 (SOX9) enables transition of fetal prostate epithelial cells into mesenchyme during embryogenesis and its high levels in advanced stage PCa has also been reported (Wang et al., 2008). Furthermore, Wnt/β-catenin signaling which is linked with the initiation and progression of multiple cancers is also known to regulate expression of Sox9 (Clevers, 2006). Another key feature of EMT is the loss of adherens junction protein, E-Cadherin (E-Cad), a tumor suppressor required for maintaining the epithelial phenotype (Loh et al., 2019). Moreover, downregulation of E-Cad via Notch signaling is also known to promote drug resistance in PCa cells (Wang et al., 2017). In addition, zinc finger proteins belonging to Snail family transcriptional repressors, SNAI1 (SNAIL) and SNAI2 (SLUG), and zinc finger E-box-binding homeobox 1 and 2 (ZEB1 and ZEB2) and Twist-related protein 1 (TWIST1) are the key TFs involved in EMT, which also downregulate E-Cad and upregulate various mesenchymal markers, namely N-Cadherin (N-Cad), Vimentin (VIM) and Fibronectin (Jennbacken et al., 2010; Zhu and Kyprianou, 2010; Sun et al., 2012; Shiota et al., 2014; Zhifang et al., 2015; Miao et al., 2017). In a recent study, a positive feedback loop has been demonstrated between SOX4 and a scaffold protein Cullin 4B (CUL4B), wherein CUL4B induces the SOX4 expression via PRC2-mediated silencing of miR-204 and in turn SOX4 positively regulates the transcription of CUL4B, leading to enhanced proliferation and invasion of PCa cells. In addition, the CUL4B+/SOX4+ subset of PCa patients show activation of Wnt/β-catenin signaling pathway and are associated with an aggressive disease and poor prognosis (Qi et al., 2019).

In PCa, the selection pressure imposed by ADT has been well-known to potentiate EMT and stemness (Sun et al., 2012; Tsai et al., 2018). Importantly, androgen deprivation in mice implanted with human LuCaP35 prostate tumor induces the increased expression of *N-Cadherin* (*CDH2*), *VIM*, *ZEB1*, *TWIST1*, and *SLUG*. Notably, a bidirectional negative feedback loop is generated between AR and Zeb1 which is involved in androgen deprivation induced EMT (Sun et al., 2012). Moreover, LNCaP cells treated with epigenetic drugs lead to upregulation of *ZEB1* and reduced AR levels, whereas siRNA mediated *ZEB1* silencing leads to increased expression of AR (Sun et al., 2012). Interestingly, enhanced expression of *ZEB1* due to copy number gain leads to direct transcriptional repression of miR-33a-5p in PCa cells, and contribute to an increase in EMT, invasion, migration and bone metastasis (Dai et al., 2019). Besides, miR-33a-5p indirectly inhibits ZEB1 expression via targeting TGFBR1 and suppressing TGF-β signaling, thus forming an indirect double-negative feedback loop. AR is also known to act as the direct transcriptional repressor of SNAIL, and its upregulation along with ZEB1/2, TWIST and Forkhead box protein C2 (FOXC2) has been reported as an adaptive response to androgen deprivation (Miao et al., 2017). Intriguingly, tumor grafts derived from PCa patients who underwent radical prostatectomy following neoadjuvant ADT (6–8 weeks of flutamide or lupron) exhibit mislocalization of E-Cad and elevated VIM expression (Zhao et al., 2013).

Conversely, ZEB2, another critical mediator of EMT shows AR mediated differential regulation in androgen dependent vs. independent manner. In androgen-dependent LNCaP cells, ZEB2 is positively regulated by AR and showed increased expression upon androgen stimulation while reduced expression in *AR*-silenced cells. In androgen-independent cell lines, such as PC3 and DU145, ectopic expression of AR leads to upregulation of miR-200a/miR-200b resulting in reduced expression of ZEB2 accompanied with diminished invasive potential (Jacob et al., 2014). This context-dependent AR mediated regulation of ZEB2 may be due to the differences in the levels and types of co-regulatory proteins which modulate AR activity as an activator or repressor (Van De Wijngaart et al., 2012). In another study, miR-145 has been shown to post-transcriptionally suppress the expression of ZEB2 resulting in decreased invasion, migration and stemness in PCa cells (Ren et al., 2014). Moreover, ZEB2 acts as a direct transcriptional repressor of miR-145 and its downregulation in PC3 cells results in reduced bone invasion in mouse models, suggesting a double-negative feedback loop between ZEB2 and miR-145. Unlike SNAIL, which is an AR repressed gene, the SLUG expression was found to be upregulated by constitutively active AR signaling in a ligand-independent manner. Additionally, SLUG also serves as a novel co-activator of AR and enhances its transcriptional activity even in the absence of androgens (Wu et al., 2012). Another study has shown that siRNA-mediated *AR* silencing in PCa cells promoted migration and invasion via C-C motif chemokine ligand 2 (CCL2)-dependent STAT3 activation and subsequent upregulation of EMT associated pathways (Izumi et al., 2013). In a follow-up study, targeting pSTAT3–CCL2 signaling with C-C chemokine receptor type 2 (CCR2) antagonists reversed the ADT induced cell invasion and macrophage infiltration in transgenic adenocarcinoma of the mouse prostate-C1 (TRAMP-C1) mouse tumors (Lin et al., 2013). One possible explanation could be that AR is known to directly regulate SPDEF (SAM pointed domain-containing ETS transcription factor), a transcriptional repressor of *CCL2*, and ADT leads to reduced SPDEF expression resulting in elevated CCL2 levels (Tsai et al., 2018). Thus, the importance of AR-signaling in EMT is context-dependent in PCa and needs to be further delineated in order to understand the pathobiology of this disease and develop effective therapeutic approaches.

While EMT helps with the initial dissemination of the tumor cells, clinical manifestation of the metastases depends upon mesenchymal-epithelial transition (MET), which is crucial for the effective seeding and colonization of the disseminated

tumor cells at the distant metastatic site (Nieto, 2013). For instance, the cross-talk between the metastasized PCa cells and stroma in liver show elevated expression of the E-Cad, possibly due to MET induced cellular plasticity (Yates et al., 2007). This dynamic transition through a spectrum of phenotypically different states could potentially regulate the initial dissemination of PCa cells followed by metastatic spread to the distant sites. However, more evidence is required to support the notion of EMT-MET axis in cellular reprogramming and may serve as a promising therapeutic strategy in targeting disease progression in prostate cancer.

STEMNESS IMPARTS CELLULAR PLASTICITY IN PROSTATE CANCER

The CSCs constitute a small population of tumor cells which has the potential to drive cancer progression, increased resistance to conventional therapies and ability to disseminate to distant organs (Soundararajan et al., 2018; Li and Shen, 2019). However, the theory about the exact origin of CSCs is still debatable. It has been suggested that CSCs are either derived directly from the normal stem cells or produced as a result of de-differentiation or trans-differentiation of the existing cancer cells (Friedmann-Morvinski and Verma, 2014; Plaks et al., 2015).

The role of EMT in imparting stemness is much in contrast to its significance in the normal embryonic development, wherein it primarily governs the differentiation of stem cells into multiple lineages (Wang and Unternaehrer, 2019). EMT promoting transcription factors, such as ZEB1 is known to promote stemness in PCa (Wellner et al., 2009; Orellana-Serradell et al., 2018). Moreover, ectopic expression of platelet-derived growth factor D (PDGF-D) in PC3 cells lead to morphological changes associated with acquisition of EMT and increased clonogenicity and sphere-forming abilities. These cells also show enhanced expression of TFs associated with stemness such as Nanog, Oct4 and Sox2, Lin28B and members of polycomb repressor complex 2 (PRC2) (Kong et al., 2010). Moreover, human PCa derived LuCaP35 xenografts when subjected to ADT show concomitant higher expression of EMT as well as stem cell markers, namely WNT5a and WNT5b (Sun et al., 2012). Although EMT is known to promote tumorigenesis, a subpopulation of tumor cells with epithelial phenotype are reported to have high metastatic potential (Celia-Terrassa et al., 2012). Also, cells undergoing EMT have increased invasive ability but diminished capacity of establishing distant metastasis (Tsuji et al., 2008; Floor et al., 2011). Furthermore, it has been demonstrated that a subpopulation of cells with epithelial phenotype and high E-Cad expression, also shows enhanced stemness and self-renewal ability (Celia-Terrassa et al., 2012). Intriguingly, a recent study has shown the tumor promoting role of E-Cad in invasive ductal carcinomas of breast, wherein it promotes tumor growth and metastases (Padmanaban et al., 2019). However, E-Cad has been implicated majorly as a tumor-suppressor across multiple cancer types, and its loss is directly involved in imparting various oncogenic traits especially stemness and metastases (Frixen et al., 1991; Berx et al., 1995; Guilford, 1999; Onder et al., 2008).

The CSCs express a broad range of cell surface markers which distinguish them from the cells of other origins. For instance, prostate CSCs (PCSCs) harbor expression of several cell surface markers such as $CD44^{+}\alpha2\beta1^{hi}CD133^{+}$ (Collins et al., 2005). The $CD44^{+}$ cell population derived from multiple PCa cell lines and xenograft tumors showed increased tumorigenic and metastatic potential along with enhanced expression of stemness promoting TFs factors namely, Oct-3/4, Bmi and β-catenin (Patrawala et al., 2006). The CD44 is considered as a putative marker for PCSCs and primarily expressed on the surface of basal and rare neuroendocrine cells, whereas the luminal cells lack its expression (Palapattu et al., 2009; Wang and Shen, 2011; Guo et al., 2012). The pluripotent basal cells differentiate to luminal and neuroendocrine cells, and hence been proposed to have high tumorigenic potential and could serve as cells of origin in prostate carcinogenesis (Goldstein et al., 2010; Taylor et al., 2012). It has also been reported that luminal multilineage progenitor cells are the cells of origin and basal cells transition to luminal cells in order to promote tumorigenesis (Karthaus et al., 2014; Wang et al., 2014). Further, ABCG2, a well-known ATP-binding cassette transporter (ABC transporter) associated with drug efflux is known to be highly expressed in PCSCs and drives resistance to therapeutic agents (Huss et al., 2005).

Similar to EMT, the dedifferentiated PCSCs show inverse correlation with AR signaling. For instance, $PSA^{-/lo}$ (PSA-negative or low) cell population exhibits gene expression profile similar to stem cells, harbors enhanced self-renewing potential and resistance to ADT and chemotherapeutic agents (Qin et al., 2012). The PCSCs isolated from AR-negative DU145 cells show higher expression of CD44, CD24, integrin α2β1, cellular reprogramming factor SOX2, and exhibit tumor-initiating potential and self-renewal ability (Rybak et al., 2011; Rybak and Tang, 2013). Similarly, a subpopulation of tumor cells isolated from prostatectomy specimens express higher levels of tumor-associated calcium signal transducer 2 (Trop2), CD44, and CD49f, and show increased sphere-forming ability and regeneration capability in mice (Garraway et al., 2010). Conclusively, a consensus regarding a specific set of markers to identify PCSCs is still lacking and in-depth study is warranted to identify the defined markers for multipotent tumor progenitor cells in order to develop better therapeutic strategies.

THERAPY-INDUCED CELLULAR PLASTICITY AND DISEASE PROGRESSION

The cancer cells evade the drug induced therapeutic pressure by modulating cellular plasticity which is one of the major mechanisms posing significant challenges for PCa treatment (Boumahdi and de Sauvage, 2019). The plasticity of the tumor cells provides a survival advantage by developing alternate adaptive pathways, independent of the targeted therapies. As mentioned previously, ADT is administered as the standard care for the treatment of men with prostate cancer. One of the main mechanisms of eluding AR-targeted therapy or ADT is the transdifferentiation of the AR-dependent PCa cells to AR-independent neuroendocrine (NE)-like phenotype (Lin et al.,

2014). Transdifferentiation is a process wherein a differentiated cell type transitions to another lineage to evade the therapy-associated drug pressure (Davies et al., 2018).

This transition process in response to therapy is often driven by a distinct transcriptional or epigenetic reprogramming of the tumor cells (Yuan et al., 2019). Recent evidence highlighted the role of EMT and stemness as important driving factors for the cellular plasticity during the neuroendocrine transdifferentiation (Soundararajan et al., 2018). Several transcription factors which are directly involved in regulating EMT are also key players involved in neuroendocrine transdifferentiation. For instance, overexpression of SNAIL imparts cellular plasticity by downregulating the E-Cad expression and enhancing the expression of neuroendocrine differentiation markers, namely, ENO2 and CHGA (McKeithen et al., 2010; Barnett et al., 2011). Similarly, neuroendocrine transdifferentiation of patient-derived LTL331 xenograft model also exhibits higher levels of SNAI1 and ZEB1 (Akamatsu et al., 2015).

The PCa cells have the ability to dedifferentiate into CSCs exhibiting tumor-initiating potential with an invasive phenotype and resistance to AR-antagonists. These reprogrammed cells when exposed to androgens in culture showed reactivation of the AR signaling, indicating the active dynamics of the cellular plasticity in response to the external cues (Nouri et al., 2017). The advanced neuroendocrine tumors such as small cell NE-like carcinomas are often characterized to have stem cell-like features (Ellis and Loda, 2015). Moreover, pluripotency factors, SOX2 and SOX11 have also been implicated in AR-independent NE-like tumors (Blee and Huang, 2019). Recent evidence suggested that BRN2 co-regulates the transcriptional landscape of the SOX2 and is essentially overexpressed in NEPC patients (Bishop et al., 2017). The elevated levels of EMT modulator ZEB1 also induces stem-cell like properties in PCa cells along with concomitant upregulation of SOX2 (Li et al., 2014). Apart from the critical role of EMT and CSCs in evading therapeutic pressure, several inherent factors also play an important role in imparting resistance to the therapy. For example, genetically engineered mouse (GEM) model with inactivation of Pten and Tp53 failed to show any response to abiraterone, and exhibited accelerated progression to treatment-induced neuroendocrine differentiation (Zou et al., 2017). A recent single-arm enzalutamide clinical trial revealed that non-responders to enzalutamide treatment exhibits a basal lineage, such as reduced AR transcriptional activity and a neurogenic/stemness program, while a luminal lineage program was activated in responders (Alumkal et al., 2020), indicating that there is need to explore the specific factors that regulate *de novo* enzalutamide resistance.

FACTORS GOVERNING CELLULAR PLASTICITY

Cell-Intrinsic Factors

In the past decade, multiple independent studies unraveled the diverse spectrum of molecular and other environmental factors governing the PCa lineage plasticity. Dramatic differences in the gene expression and copy number alterations has been reported to co-exist between the prostate adenocarcinoma and the NEPC, often within the same tumor foci (Beltran et al., 2011). Moreover, comprehensive molecular characterization of the NEPC tumors revealed the significance of divergent clonal evolution. Under the influence of therapy, CRPC cells give rise to new clones owing to epithelial plasticity, with distinct molecular profiles and genetic aberrations. Initially, few molecular alterations occur that drive and select clones for the cellular plasticity, followed by a series of passenger alterations which may result in the emergence of therapy-resistance NEPC (Beltran et al., 2016).

Most of the prostatic small cell carcinomas (SCC) harbor the *TMPRSS2-ERG* gene rearrangement confirming its involvement in the carcinogenesis. Although, *TMPRSS2-ERG* fusion is not reported in the SCC of non-prostatic origins, such as lung and urinary bladder, indicating that this genetic event can be used as a molecular marker to establish the prostatic origin of metastatic SCC (Guo et al., 2011). Of note, NEPC foci often lack the expression of ERG protein in the tumors harboring *TMPRSS2-ERG* fusion, which reaffirms the reduced or absent androgen signaling. A classic example of this ambiguity is the NEPC cell line model, NCI-H660 which harbors *TMPRSS2-ERG* fusion, but lacks expression of ERG protein (Beltran et al., 2011). Furthermore, ERG oncoprotein suppresses the expression of NEPC related genes in PCa which is relieved upon inhibition of AR signaling (Mounir et al., 2015).

The mutational landscape of NEPC patients has identified the role of *RB1* loss and mutated/deleted *TP53* in the SCC pathogenesis. In contrast to the CRPC-adenocarcinoma patients, CRPC-NE patients showed reduced frequency of genomic alterations associated with androgen receptor (AR), indicating the selection of AR-independent clonal subpopulation during NEPC progression (Beltran et al., 2016). Simultaneous aberration in various tumor suppressor genes (*RB1*, *TP53,* and/or *PTEN*) has been known to drive tumor plasticity in PCa (Aparicio et al., 2016). For instance, knockdown of *TP53* and *RB1* using short hairpin RNAs (shRNAs) in AR overexpressing LNCaP cells resulted in the enhanced expression of basal and neuroendocrine lineage markers thereby conferring resistance to anti-androgen therapy (Aparicio et al., 2016).

Overexpression of Aurora kinase A (AURKA) and oncogene N-Myc (MYCN) due to gene amplification was found in NEPC cases, where both proteins cooperate in driving the NE-transdifferentiation. Although, being located on different chromosomes, the mechanism involved in their co-amplification in NEPC remains unknown, but certainly hints toward their usefulness as diagnostic markers for early intervention in the high-risk population (Beltran et al., 2011). Interestingly, this discovery formed the basis to use Aurora kinase A inhibitors for the treatment of NEPC patients harboring AURKA amplification (Beltran et al., 2019). Moreover, activated AKT1 and MYCN are also known to drive the transformation of prostate epithelial cells to adenocarcinoma and differentiation to NE-like phenotype (Lee et al., 2016). MYCN in cooperation with PRC2 complex member, EZH2 and other cofactors suppress the AR signaling and PRC2 target genes (Beltran et al., 2011; Dardenne et al., 2016; Lee et al., 2016). Apart from EZH2, other PRC1 containing

proteins, such as members of CBX family have also been shown to be dysregulated in patient-tumor derived xenografts (PDX) and NEPC clinical samples, highlighting a role for dysregulated Polycomb Group (PcG)-mediated silencing during NE-transdifferentiation (Clermont et al., 2015).

Reduced expression of RE1 silencing transcription factor (REST), a master negative regulator of neuroendocrine differentiation accompanied with enrichment of the REST target NE-associated genes has been reported in the NEPC clinical samples (Lapuk et al., 2012). Interestingly, another member of REST transcriptional repressor complex, PHD finger protein 21A (PHF21A) is differentially spliced in NEPC cases compared to adenocarcinoma. PHDF21A loses the AT-hook domain which is involved in the DNA binding via alternative splicing (Lapuk et al., 2012). In LNCaP cells, androgen stimulation leads to co-occupancy of REST on the AR occupied chromatin regions and mediates transcriptional repression of a subset of genes. Further, siRNA mediated *REST* silencing leads to upregulation of genes associated with neuronal differentiation and maintenance of NE phenotype (Svensson et al., 2013). Moreover, activation of androgen signaling enhances REST protein levels by modulating the activity of β-TRCP ubiquitin ligase. Importantly, Casein kinase 1 (CK1) is known to phosphorylate REST and enhance the β-TRCP activity leading to ubiquitin-mediated proteasomal degradation of REST. Therefore, treatment of SPINK1-positive 22RV1 cells with CK1 inhibitor resulted in restoration of REST protein levels, accompanied with reduced SPINK1 levels and its oncogenic properties (Tiwari et al., 2020), thus emphasizing the repressive role of REST protein in the regulation of SPINK1 and disease progression toward NE-like phenotype.

Evaluation of the transcription factors involved in lineage plasticity in prostate tumors showed SRY-box transcription factor 2 (SOX2) to be highly upregulated in tumors with altered TP53 and RB1 ($TP53^{Alt}$, $RB1^{Alt}$) compared to wildtype TP53 and RB1 ($TP53^{WT}$, $RB1^{WT}$) tumors. Furthermore, *SOX2* silencing in the LNCaP cells overexpressing AR with inactivated RB1 and TP53 reversed the increased expression of basal (CK5, CK14, and TP63) and neuroendocrine (SYP, CHGA, and NSE) lineage markers induced due to *TP53* and *RB1* loss (Mu et al., 2017). Furthermore, the role of SOX2 has been reported in repressing adenocarcinoma specific genes by enhancing the expression and activity of lysine-specific demethylase 1A (LSD1/KDM1A) (Li et al., 2019), highlighting the potential of SOX2 as a lineage reprogramming factor in neuroendocrine prostate tumors. Moreover, a neural specific transcript variant of LSD1 also known as LSD1+8a, has been shown to be exclusively expressed in NEPC tissue samples and patient-derived xenograft samples, and LSD1+8a/SRRM4 co-upregulated gene signature was found to be exclusively activated in aggressive NEPC patient tumors, that are different from those regulated by the canonical LSD1 (Coleman et al., 2020). A recent study reported Serine Peptidase Inhibitor, Kazal type 1 (SPINK1) to be transcriptionally repressed by AR and its corepressor REST, and androgen deprivation resulted in its upregulation. Furthermore, SOX2 was shown to modulate the expression of SPINK1 during the NE-transdifferentiation of LNCaP cells (Tiwari et al., 2020). This study also confirmed the role of SPINK1 in EMT, stemness and NE-transdifferentiation. Additionally, a subset of NEPC patients exhibit elevated levels of SPINK1, suggesting its role in the maintenance of the NE-like phenotype (Tiwari et al., 2020).

Metabolic reprogramming plays a crucial role in cancer progression and therapy-resistance (Hanahan and Weinberg, 2011). The ground-breaking discovery by Warburg suggested the preference of aerobic glycolysis over oxidative phosphorylation in cancer cells which primarily rely on the mitochondrial oxidative phosphorylation for adenosine 5'-triphosphate (ATP) generation. This resulted in the higher rate of glucose uptake and lactate production in presence of oxygen (Vander Heiden et al., 2009). Early clinical studies have shown that fluorodeoxyglucose (FDG)-PET imaging which is based on increased glucose uptake by cancer cells failed to detect naïve localized PCa (Effert et al., 1996), but can detect the advanced stage small cell prostate cancer (SCPC) (de Carvalho Flamini et al., 2010), highlighting the metabolic differences underlying the adenocarcinoma and SCPC. Moreover, the higher uptake of glucose has been associated with the elevated expression of Glucose Transporter 1 (GLUT1) in poorly differentiated hormone-independent PCa (Effert et al., 2004). It has also been observed that PCa switch to aerobic glycolysis only at the advanced stages of the disease progression and correlates with poor clinical outcomes (Pertega-Gomes et al., 2015). Of interest, the gene expression profile of NEPC patients showed glycolysis and lactic acid production as the most significantly upregulated pathways in these tumors (Choi et al., 2018). It has been shown that higher expression of the plasma membrane transporter monocarboxylate transporter 4 (MCT4) facilitated the enhanced secretion of lactic acid, while antisense oligonucleotides mediated silencing of *MCT4* led to reduced lactic acid secretion, glucose metabolism and NEPC cell proliferation (Choi et al., 2018). Recently, reduced PKCλ/ι has been reported in *de novo* and treatment-related NEPC differentiation, which resulted in upregulated mTORC1/ATF4/PHGDH and promoted serine biosynthesis, leading to increased S-adenosyl methionine (SAM). Moreover, higher mTORC1 activity, stronger nuclear ATF4 staining and increased expression of PHGDH was also detected in NEPC tumors compared to adenocarcinoma, suggesting the critical role of mTORC1/ATF4/PHGDH metabolic axis in increased cell proliferation and epigenetic reprogramming during NEPC development (Reina-Campos et al., 2019).

Numerous factors have been shown to be involved in maintaining the tumor cell plasticity (**Table 1**), however, more comprehensive in-depth studies are required to dissect the specific drivers which can be targeted for therapeutic implications.

Cell-Extrinsic Factors

The external cues along with the cell intrinsic factors, such as transcriptional and epigenetics regulation, are the key determinants for the tumor heterogeneity in PCa patients (Davies et al., 2018). The cell extrinsic factors constitute the tumor microenvironment which dictates the process of cellular plasticity in most of the malignancies including prostate (Yates, 2011). The concept of influence of microenvironment on tumor cells was initially proposed by an English surgeon, Stephen Paget,

TABLE 1 | An overview of key molecular drivers involved in cell plasticity in the pathogenesis of prostate cancer.

Molecular drivers	Regulatory mechanism	Phenotypic features	References
EPITHELIAL-MESENCHYMAL TRANSITION (EMT)			
CDH1	Downregulated by Notch signaling	Silencing *CDH1* (E-Cad) promotes PCa cell migration, drug-resistance and metastasis	Wang et al., 2017; Loh et al., 2019
SOX9	Regulated by Wnt/β-catenin signaling	Enhances tumor cell proliferation and invasion	Wang et al., 2008
ZEB1	Shows bidirectional negative feedback loop with AR	Mediates androgen deprivation induced EMT	Sun et al., 2012
ZEB2	Differential regulation by AR	Potentiates cell invasion and migration	Jacob et al., 2014
SLUG	Androgen-responsive gene and AR coactivator	Facilitates PCa cell growth in androgen-deprived conditions	Wu et al., 2012
SNAIL	Transcriptionally repressed by AR	Plays a critical role in ADT induced epithelial-mesenchymal plasticity	Miao et al., 2017
CCL2	Silencing *AR* elevates CCL2 levels and STAT3 signaling	Promotes metastasis via macrophage recruitment	Izumi et al., 2013; Tsai et al., 2018
STEMNESS			
ABCG2	Membrane transporter found on prostate cancer stem cells	Maintain proliferative potential under hypoxic conditions, and efflux androgens	Huss et al., 2005
CD44	Cell-surface marker found on AR-independent basal prostate cells	CD44-positive PCa cells have high proliferative, clonogenic, tumorigenic, and metastatic potential	Liu et al., 1997; Patrawala et al., 2006
THERAPY-INDUCED CELLULAR PLASTICITY			
SNAIL	PEG10 regulates SNAIL expression via TGF-β signaling	Elevated levels found in tumor after castration in xenografts model and NEPC development	Akamatsu et al., 2015
ZEB1	Higher expression in castrated *PTEN* knockout mice and NEPC models	Induce stem cell-like properties and promotes androgen-independence in PCa	Li et al., 2014; Akamatsu et al., 2015
SOX11	Upregulated in *Pten* and *Trp53* inactivated mice model	Abiraterone treatment of *Pten/Trp53* inactivated mice lead to neuroendocrine differentiation	Zou et al., 2017
BRN2	AR repressed gene and regulates SOX2 expression	Key driver of aggressive tumor growth; higher levels found in NEPC compared to CRPC and adenocarcinomas	Bishop et al., 2017
CELL-INTRINSIC FACTORS			
AURKA	Amplified and overexpressed in NEPC	Functionally cooperate with N-MYC and drive neuroendocrine phenotype	Beltran et al., 2011; Lee et al., 2016
MYCN	Amplified and overexpressed in NEPC	Stabilizes AURKA, abrogates AR signaling, induces PRC2 silencing and serves as an oncogenic driver of NEPC	Beltran et al., 2011; Dardenne et al., 2016; Lee et al., 2016
EZH2	Highly expressed in advanced stage PCa and NEPC	Transforms the epigenetic landscape of PCa and NEPC	Varambally et al., 2008; Beltran et al., 2011; Clermont et al., 2015; Dardenne et al., 2016
REST	Downregulated in NEPC	Transcriptional corepressor of AR and implicated in NEPC development	Lapuk et al., 2012; Svensson et al., 2013; Tiwari et al., 2020
SOX2	Overexpressed in NEPC tumors consistent with RB1 and TP53 alterations	Required for lineage plasticity and antiandrogen resistance induced by inactivated RB1 and TP53	Bishop et al., 2017; Mu et al., 2017
SPINK1	Transcriptionally repressed by AR and REST and regulated by SOX2 in androgen deprived condition	Imparts cellular plasticity and maintenance of neuroendocrine phenotype	Tiwari et al., 2020
PKCλ/ι	Downregulated in NEPC	Its loss promotes serine biosynthesis, resulting in metabolic reprogramming to support cell proliferation and epigenetic changes	Reina-Campos et al., 2019
CELL-EXTRINSIC FACTORS			
TGF-β	Shows negative feedback loop with PMEPA1; cross talk with CXCR4; acts via both SMAD-dependent and independent pathways	Associated with PCa aggressiveness and bone metastasis	Derynck and Zhang, 2003; Bhowmick et al., 2004; Ao et al., 2007; Fournier et al., 2015
IL-6	Secreted by aggressive PCa cells	Elicits fibroblast activation and secrete MMPs	Giannoni et al., 2010
BMP6	Secreted by PCa cells and show feedback loop with IL-6	Upregulates IL-6 expression from macrophages, leading to neuroendocrine differentiation of PCa cells	Lee et al., 2011
IL-1 family genes	Secreted by prostate epithelial cells	Induce secretion of proinflammatory cytokines (CXCL-1,−2,−3 and IL-8) in stromal cells and facilitate cancer progression.	Kogan-Sakin et al., 2009
SPINK1	Regulated by NF-κB and C/EBP upon DNA damage in stromal cells	Serves as a senescence-associated secretory factor and a non-invasive biomarker of therapeutically damaged tumor microenvironment	Chen et al., 2018a

who laid the foundation that the conducive microenvironment is essential for the colonization of the disseminated tumor cells, also known as the seed and soil theory (Paget, 1889). The tumor microenvironment includes blood vessels, stromal cells namely, cancer-associated fibroblasts (CAFs), endothelial cells, neuroendocrine cells and infiltrating immune cells, growth factors and chemokines secreted by either tumor cells or stromal cells and many extracellular matrix proteins such as laminin, fibronectin, and collagen (Yates, 2011). Apart from the dynamic interaction between tumor and stromal cells, physical (elasticity and stiffness) and biochemical properties (protein composition) of the extracellular matrix (ECM), as well as access to nutrients and oxygen also governs the cellular plasticity of the tumor cells (Yates, 2011; Davies et al., 2018; Patel et al., 2019).

Among the different stromal cells, CAFs play a critical role in modulating the plasticity of the cancer cells. The CAFs are well-known to support tumor growth, resistance to therapy and metastasis by creating a tumor-promoting microenvironment for the cancer cells to proliferate, invade and evade the immune suppression (Cirri and Chiarugi, 2011). Moreover, CAFs mainly originate from the fibroblasts residing in tumor under the influence of the transforming growth factor (TGF-β) secreted by cancer cells (Massague, 2008; Bellomo et al., 2016). In addition, stromal cells such as pericytes or inflammatory cells may also transdifferentiate to CAFs via the process known as mesenchymal-to-mesenchymal transition (MMT) under the influence of TGF-β and other cytokines secreted in the tumor microenvironment (Bellomo et al., 2016). Similar to cancer cells, the CAFs also produce TGF-β which acts as an autocrine and paracrine factor and regulates the reorganization of the extracellular matrix and the interaction between tumor-stroma (Erdogan and Webb, 2017). Moreover, CAFs isolated from prostate carcinomas produce higher amounts of other cytokines namely, pro-inflammatory cytokines, interleukin-6 (IL6) and bone morphogenetic factor (BMP6), thereby promoting tumor progression (Doldi et al., 2015). There is a reciprocal interplay between CAFs and tumor cells, wherein tumor cells secrete IL6 and promotes CAFs to secrete matrix metalloproteases (MMPs) which in turn remodels the ECM, and further induces secretion of IL6 from tumor cells, thereby driving EMT. In addition, CAFs promote tumor forming ability and stemness when co-implanted with PCa cells in mice xenografts, and importantly, these tumor-repopulating cells were found to be CD44-positive and CD24-negative (Giannoni et al., 2010). The prostate stromal cells are also known to secrete proinflammatory and cancer-promoting chemokines such as CXCL-1, CXCL-2, CXCL-3, and interleukin (IL)-8, which are the key regulators of cellular plasticity, culminating in inflammation, and PCa progression

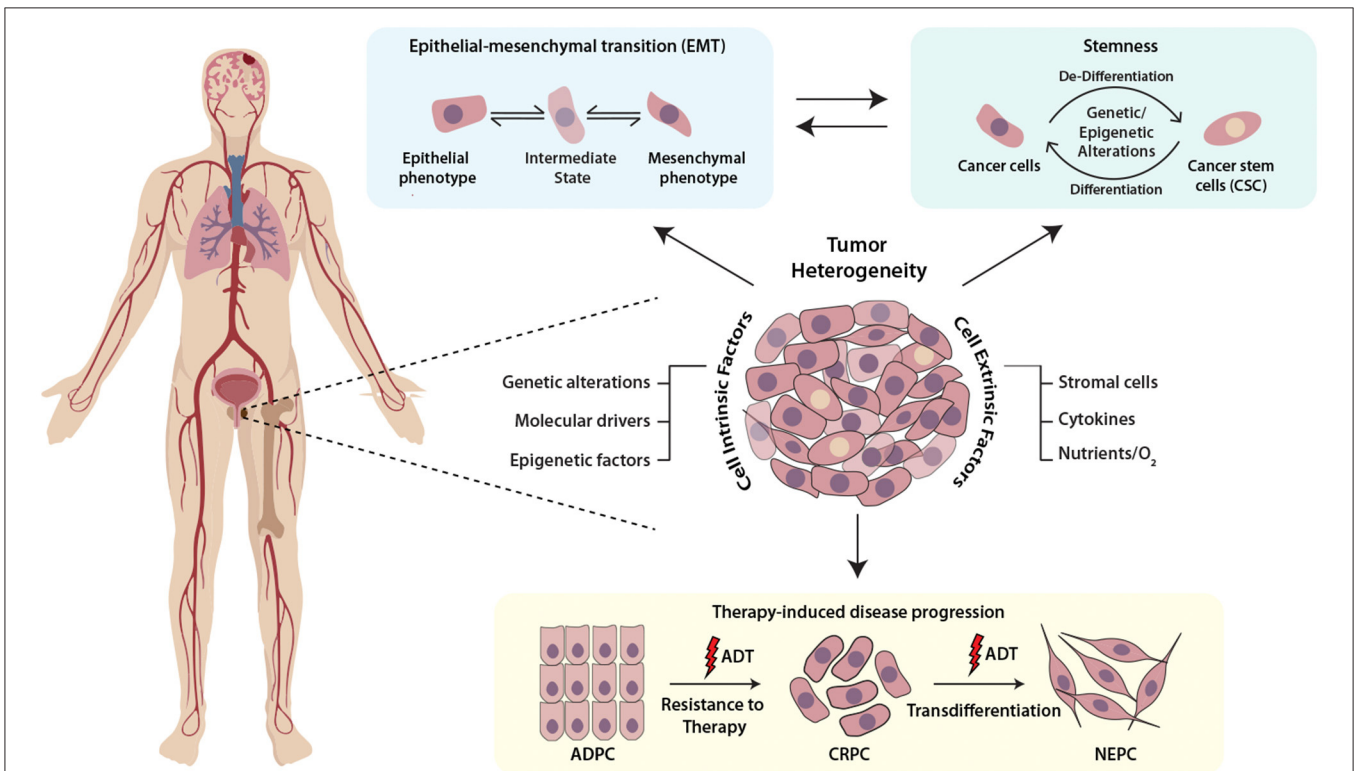

FIGURE 1 | Schematic representing the multifaceted role of cellular plasticity in progression of prostate cancer. Prostate tumor comprises of heterogenous cell populations where both cell-intrinsic and -extrinsic factors confer cellular plasticity to enable transition between different cell fates by facilitating different mechanisms like epithelial-mesenchymal transition (EMT), stemness and drug resistance. Prostate tumor cell plasticity imparts resistance toward androgen deprivation therapy (ADT) during the progression of prostate adenocarcinoma (ADPC) to castrate-resistant prostate cancer (CRPC) stage, which may also transdifferentiate to neuroendocrine prostate cancer (NEPC).

TABLE 2 | Therapeutic interventions targeting key molecular drivers involved in the cellular plasticity of prostate cancer.

Inhibitor	Target	Mechanism of action	Clinical trial and status	References
Siltuximab (CNTO 328)	IL6	Chimeric monoclonal antibody which neutralizes IL6 and prevents STAT3 activation	NCT00401765; Completed	Hudes et al., 2013
Lycopene	IL6	Attenuates IL6 activity and abrogates STAT3 phosphorylation	NCT01949519; Completed	Tang et al., 2011
Apitolisib (GDC-0980)	PI3K and mTOR kinase	Inhibits PI3K-AKT-mTOR signaling axis	NCT00854152; Completed	Dolly et al., 2016
CRLX101	HIF1α	Nanoparticle drug-conjugate with camptothecin, inhibits HIF1α and DNA Topoisomerase I activity	NCT03531827; Active	Tian et al., 2017; Chen et al., 2018b
CPI-1205	EZH2	Cofactor-competitive inhibitor of wild type and mutant EZH2 catalytic activity	NCT03480646; Active	Taplin et al., 2019
GSK2816126	EZH2	Inhibits EZH2 activity and reduces global methylation of H3K27me3 marks	NCT02082977; Terminated	Yap et al., 2016
PF-06821497	EZH2	Selective inhibitor of EZH2 activity	NCT03460977; Active	Kung et al., 2018
ZEN003694	N-MYC	Inhibits BET proteins and dysregulates N-MYC-mediated transcriptional programming	NCT02705469; Completed	Schafer et al., 2020
Alisertib (MLN8237)	AURKA	Inhibits interaction between AURKA and N-MYC, thereby disrupts N-MYC mediated signaling	NCT01799278; Completed	Beltran et al., 2019
Rovalpituzumab Tesirine (SC16LD6.5)	DLL3	Antibody–drug conjugate targeting DLL3 (a Notch ligand)	NCT02674568; Completed	Puca et al., 2019

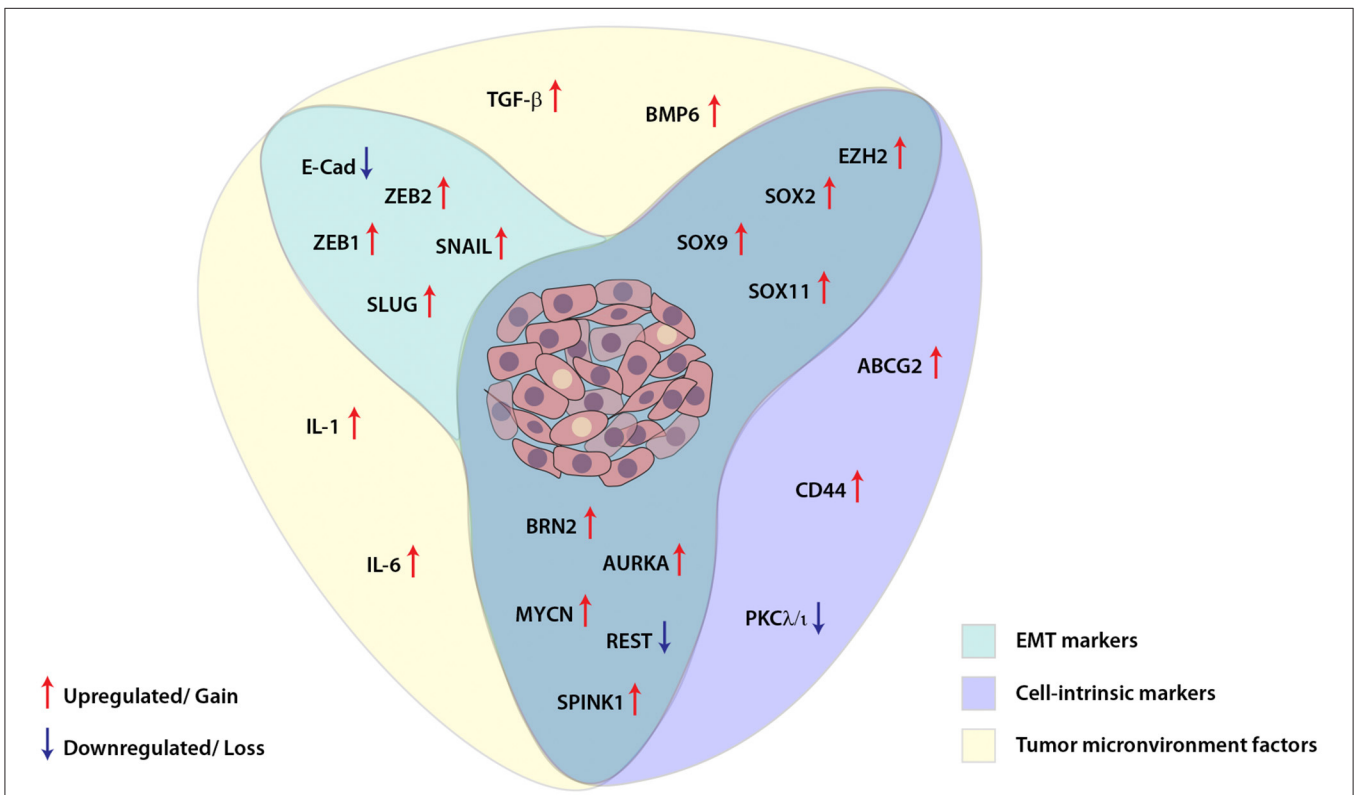

FIGURE 2 | Schematic showing interplay between key molecular players involved in cellular plasticity in prostate cancer. Molecular markers associated with epithelial-mesenchymal transition (EMT), cell-intrinsic factors and tumor microenvironment are deployed for imparting plasticity in prostate cancer cells. These EMT and cell-intrinsic factors are regulated by cytokines and other growth factors released in the tumor microenvironment, which in turn are modulated by different transcription factors, transcriptional/post-transcriptional events and dysregulated signaling pathways in the cancer cells.

(Kogan-Sakin et al., 2009). The prostatic CAFs also produce stromal glutamine as a result of epigenetic reprogramming and contribute to NE-transdifferentiation (Mishra et al., 2018). Interestingly, it has been known that genotoxic effect of chemo- and radiation therapies prompt stromal cells to produce SPINK1 as a secretory factor, which induces EGFR-mediated signaling and imparts chemoresistance in the adjacent prostate tumor cells (Chen et al., 2018a).

Tumor associated macrophages (TAMs) are also known to play important role in regulating cellular plasticity and NE-transdifferentiation. For instance, BPH-1 cells when co-cultured with THP-1 cells differentiated macrophages, led to increased expression of mesenchymal markers, such as N-Cad, Snail, and TGF-β2, and this phenotype was abrogated upon incubating with anti-TGF-β2 neutralizing antibody (Lu et al., 2012). Further, conditioned media collected from macrophages induce expression of NE-marker and parathyroid hormone-related peptide (PTHrP) in LNCaP and TRAMP-C2 cells. In this feedback loop, BMP6 secreted from the PCa cells induce production of IL6 from the macrophages, which in turn stimulates the NE-transdifferentiation of PCa cells (Lee et al., 2011).

Mounting evidence highlights the role of the physiochemical properties such as hypoxia or oxidative stress as key regulators of cellular plasticity in tumors. For instance, hypoxic stress leads to the upregulation of Hypoxia-inducible factor 1-α (HIF1α), which in cooperation with FOXA2, drives mesenchymal reprogramming and NE-transdifferentiation in PCa cells (Li et al., 2016). Another report indicates that hypoxia leads to reduced expression of transcriptional repressor REST, which in turn leads to hypoxia-induced neuroendocrine differentiation, followed by activation of associated AMPK pathway and autophagy (Lin et al., 2016). Multi-disciplinary approaches such as mathematical modeling and bioengineering tools, would allow fostering a hypoxic niche for exploring the events and mechanisms involved in adaptation of aggressive cancer behaviors, and would provide cues to disrupt the signaling pathways involved in crosstalk between cancer cells and tumor microenvironment (**Figure 1**).

TARGETING CELLULAR PLASTICITY AND ITS CLINICAL IMPLICATIONS

Current studies are focused on targeting the markers and pathways involved in upholding the cellular plasticity in prostate cancer. Previous investigations have recommended the use of aurora kinase inhibitors in NMYC overexpressing prostate cancer, wherein it disrupts the N-Myc-AURKA complex and results in reduced tumor burden (Beltran et al., 2011; Dardenne et al., 2016; Lee et al., 2016). However, recent phase II clinical trials of AURKA inhibitor (NCT01799278), alisertib used for the treatment of metastatic NEPC patients showed efficacy in select cases (Beltran et al., 2019). Furthermore, N-Myc has been shown to cooperate with EZH2 and play critical role in changing the epigenetic landscape of AR and N-Myc target genes during NEPC transition. Elevated levels of N-Myc showed enhanced sensitivity to EZH2 catalytic SET domain inhibitor GSK503 in mice harboring N-Myc overexpressing 22RV1 xenografts (Dardenne et al., 2016). The EZH2 inhibitor (CPI-1205) combined with enzalutamide or abiraterone/prednisone are currently under phase Ib/II clinical trials (NCT03480646) for the treatment of metastatic CRPC cases. Recently, one of the homeobox transcription factors, ONECUT2 has been shown to synergize with hypoxia signaling in promoting NEPC transition. Importantly, hypoxia-activated pro-drug TH-302 showed remarkable reduction of the tumor growth in PDX models with higher levels of ONECUT2, suggesting it as a promising treatment strategy for NEPC (Guo et al., 2019). A recent study showed the therapeutic potential of rovalpituzumab tesirine (SC16LD6.5) in NEPC cases with higher expression of Delta-like ligand 3 (DLL3) (Puca et al., 2019). There is no direct effective therapy for targeting cellular plasticity, however, therapeutic modalities targeting the known molecular drivers of NEPC using small molecule inhibitors in combination with immune checkpoint inhibitors are under development (**Table 2**).

CONCLUSION

Similar to other malignancies, in prostate cancer as well, cellular plasticity is induced as a result of different contributing factors and governs a diverse set of characteristics which are involved in facilitating tumor dissemination, metastatic spread to distant sites and conferring resistance toward therapy (**Figure 2**). Despite the clinical benefits of ADT for the treatment of PCa, emerging evidence has suggested that ADT propels the cancer cells toward therapy-induced resistance and emergence of aggressive AR-independent variants of prostate cancer. Therefore, understanding the dynamics of tumor cell plasticity during transition from androgen responsive to androgen non-responsive state holds a prime importance in targeting the PCa progression. Also, in order to discover new therapeutic avenues enormous efforts are required to explore the underlying mechanisms involved in ADT mediated resistance or chemotherapeutic drug resistance of cancer cells in the clinical spectrum of prostate cancer stages. In conclusion, therapies against the cell plasticity, alone or in combination with AR-antagonists might prove effective for the clinical management of advanced stage CRPC or NEPC patients.

AUTHOR CONTRIBUTIONS

RT, NM, and BA reviewed the literature and contributed to manuscript writing. All authors contributed to the article and approved the submitted version.

FUNDING

BA acknowledges the research funding from the Wellcome Trust/DBT India Alliance Fellowship (IA/I(S)/12/2/

500635 to BA), the Department of Biotechnology (BT/PR8675/GET/119/1/2015 to BA) and the Science and Engineering Research Board, Ministry of Science and Technology, Government of India (EMR/2016/005273 to BA). NM acknowledges fellowship support from the University Grants Commission (UGC), Government of India.

REFERENCES

Aggarwal, R., Huang, J., Alumkal, J. J., Zhang, L., Feng, F. Y., Thomas, G. V., et al. (2018). Clinical and genomic characterization of treatment-emergent small-cell neuroendocrine prostate cancer: a multi-institutional prospective study. *J. Clin. Oncol.* 36, 2492–2503. doi: 10.1200/JCO.2017.77.6880

Akamatsu, S., Wyatt, A. W., Lin, D., Lysakowski, S., Zhang, F., Kim, S., et al. (2015). The placental gene PEG10 promotes progression of neuroendocrine prostate cancer. *Cell Rep.* 12, 922–936. doi: 10.1016/j.celrep.2015.07.012

Alumkal, J. J., Sun, D., Lu, E., Beer, T. M., Thomas, G. V., Latour, E., et al. (2020). Transcriptional profiling identifies an androgen receptor activity-low, stemness program associated with enzalutamide resistance. *Proc. Natl. Acad. Sci. U.S.A.* 117, 12315–12323. doi: 10.1073/pnas.1922207117

Antonarakis, E. S., Lu, C., Wang, H., Luber, B., Nakazawa, M., Roeser, J. C., et al. (2014). AR-V7 and resistance to enzalutamide and abiraterone in prostate cancer. *N. Engl. J. Med.* 371, 1028–1038. doi: 10.1056/NEJMoa1315815

Ao, M., Franco, O. E., Park, D., Raman, D., Williams, K., and Hayward, S. W. J. C.R. (2007). Cross-talk between paracrine-acting cytokine and chemokine pathways promotes malignancy in benign human prostatic epithelium. *Cancer Res.* 67, 4244–4253. doi: 10.1158/0008-5472.CAN-06-3946

Aparicio, A. M., Shen, L., Tapia, E. L. N., Lu, J.-F., Chen, H.-C., Zhang, J., et al. (2016). Combined tumor suppressor defects characterize clinically defined aggressive variant prostate. *Cancers (Basel)*. 22, 1520–1530. doi: 10.1158/1078-0432.CCR-15-1259

Arora, V. K., Schenkein, E., Murali, R., Subudhi, S. K., Wongvipat, J., Balbas, M. D., et al. (2013). Glucocorticoid receptor confers resistance to antiandrogens by bypassing androgen receptor blockade. *Cell* 155, 1309–1322. doi: 10.1016/j.cell.2013.11.012

Barnett, P., Arnold, R. S., Mezencev, R., Chung, L. W., Zayzafoon, M., and Odero-Marah, V. (2011). Snail-mediated regulation of reactive oxygen species in ARCaP human prostate cancer cells. *Biochem. Biophys. Res. Commun.* 404, 34–39. doi: 10.1016/j.bbrc.2010.11.044

Bellomo, C., Caja, L., and Moustakas, A. J. B. J. O. C. (2016). Transforming growth factor β as regulator of cancer stemness and metastasis. *Br. J. Cancer* 115, 761–769. doi: 10.1038/bjc.2016.255

Beltran, H., and Demichelis, F. (2015). Intrapatient heterogeneity in prostate cancer. *Nat. Rev. Urol.* 12, 430–431. doi: 10.1038/nrurol.2015.182

Beltran, H., Oromendia, C., Danila, D. C., Montgomery, B., Hoimes, C., Szmulewitz, R. Z., et al. (2019). A phase II trial of the Aurora kinase A inhibitor alisertib for patients with castration-resistant and neuroendocrine prostate cancer: efficacy and biomarkers. *Clin. Cancer Res.* 25, 43–51. doi: 10.1158/1078-0432.CCR-18-1912

Beltran, H., Prandi, D., Mosquera, J. M., Benelli, M., Puca, L., Cyrta, J., et al. (2016). Divergent clonal evolution of castration-resistant neuroendocrine prostate cancer. *Nat. Med.* 22, 298–305. doi: 10.1038/nm.4045

Beltran, H., Rickman, D. S., Park, K., Chae, S. S., Sboner, A., Macdonald, T. Y., et al. (2011). Molecular characterization of neuroendocrine prostate cancer and identification of new drug targets. *Cancer Discov.* 1, 487–495. doi: 10.1158/2159-8290.CD-11-0130

Berx, G., Cleton-Jansen, A. M., Nollet, F., De Leeuw, W. J., Van De Vijver, M., Cornelisse, C., et al. (1995). E-cadherin is a tumour/invasion suppressor gene mutated in human lobular breast cancers. *EMBO J.* 14, 6107–6115. doi: 10.1002/j.1460-2075.1995.tb00301.x

Bhatia, V., and Ateeq, B. (2019). Molecular underpinnings governing genetic complexity of ETS-fusion-negative prostate cancer. *Trends Mol. Med.* 25, 1024–1038. doi: 10.1016/j.molmed.2019.07.001

Bhowmick, N. A., Chytil, A., Plieth, D., Gorska, A. E., Dumont, N., Shappell, S., et al. (2004). TGF-ß signaling in fibroblasts modulates the oncogenic potential of adjacent epithelia. *Science* 303, 848–851. doi: 10.1126/science.1090922

Bianco-Miotto, T., Chiam, K., Buchanan, G., Jindal, S., Day, T. K., Thomas, M., et al. (2010). Global levels of specific histone modifications and an epigenetic gene signature predict prostate cancer progression and development. *Cancer Epidemiol. Biomarkers Prev.* 19, 2611–2622. doi: 10.1158/1055-9965.EPI-10-0555

Bishop, J. L., Thaper, D., Vahid, S., Davies, A., Ketola, K., Kuruma, H., et al. (2017). The master neural transcription factor BRN2 is an androgen receptor–suppressed driver of neuroendocrine differentiation in prostate cancer. *Cancer Discov.* 7, 54–71. doi: 10.1158/2159-8290.CD-15-1263

Blau, H. M., Pavlath, G. K., Hardeman, E. C., Chiu, C. P., Silberstein, L., Webster, S. G., et al. (1985). Plasticity of the differentiated state. *Science* 230, 758–766. doi: 10.1126/science.2414846

Blee, A., and Huang, H. (2019). Lineage plasticity-mediated therapy resistance in prostate cancer. *Asian J. Androl.* 21, 241–248. doi: 10.4103/aja.aja_41_18

Boumahdi, S., and de Sauvage, F. J. (2019). The great escape: tumour cell plasticity in resistance to targeted therapy. *Nat Rev Drug Discov*. 19, 39–56. doi: 10.1038/s41573-019-0044-1

Boutros, P. C., Fraser, M., Harding, N. J., De Borja, R., Trudel, D., Lalonde, E., et al. (2015). Spatial genomic heterogeneity within localized, multifocal prostate cancer. *Nat. Genet.* 47, 736–745. doi: 10.1038/ng.3315

Boyd, L. K., Mao, X., and Lu, Y.-J. (2012). The complexity of prostate cancer: genomic alterations and heterogeneity. *Nat. Rev. Urol.* 9, 652–664. doi: 10.1038/nrurol.2012.185

Brocks, D., Assenov, Y., Minner, S., Bogatyrova, O., Simon, R., Koop, C., et al. (2014). Intratumor DNA methylation heterogeneity reflects clonal evolution in aggressive prostate cancer. *Cell Rep.* 8, 798–806. doi: 10.1016/j.celrep.2014.06.053

Cancer Genome Atlas Research, N. (2015). The molecular taxonomy of primary prostate cancer. *Cell* 163, 1011–1025. doi: 10.1016/j.cell.2015.10.025

Celia-Terrassa, T., Meca-Cortes, O., Mateo, F., Martinez De Paz, A., Rubio, N., Arnal-Estape, A., et al. (2012). Epithelial-mesenchymal transition can suppress major attributes of human epithelial tumor-initiating cells. *J. Clin. Invest.* 122, 1849–1868. doi: 10.1172/JCI59218

Chen, C. D., Welsbie, D. S., Tran, C., Baek, S. H., Chen, R., Vessella, R., et al. (2004). Molecular determinants of resistance to antiandrogen therapy. *Nat. Med.* 10, 33–39. doi: 10.1038/nm972

Chen, F., Long, Q., Fu, D., Zhu, D., Ji, Y., Han, L., et al. (2018a). Targeting SPINK1 in the damaged tumour microenvironment alleviates therapeutic resistance. *Nat. Commun.* 9, 1–19. doi: 10.1038/s41467-018-06860-4

Chen, G., Karzai, F., Madan, R. A., Cordes, L. M., Bilusic, M., Owens, H., et al. (2018b). CRLX101 plus olaparib in patients with metastatic castration-resistant prostate cancer. *J. Clin. Oncol.* 36 (Suppl. 15), TPS5096. doi: 10.1200/JCO.2018.36.15_suppl.TPS5096

Cheng, L., Nagabhushan, M., Pretlow, T. P., Amini, S. B., and Pretlow, T. G. (1996). Expression of E-cadherin in primary and metastatic prostate cancer. *Am. J. Pathol.* 148, 1375–1380.

Cher, M. L., Bova, G. S., Moore, D. H., Small, E. J., Carroll, P. R., Pin, S. S., et al. (1996). Genetic alterations in untreated metastases and androgen-independent prostate cancer detected by comparative genomic hybridization and allelotyping. *Cancer Res.* 56, 3091–3102.

Choi, S. Y. C., Ettinger, S. L., Lin, D., Xue, H., Ci, X., Nabavi, N., et al. (2018). Targeting MCT 4 to reduce lactic acid secretion and glycolysis for treatment of neuroendocrine prostate cancer. *Cancer Med.* 7, 3385–3392. doi: 10.1002/cam4.1587

Cirri, P., and Chiarugi, P. (2011). Cancer associated fibroblasts: the dark side of the coin. *Am. J. Cancer Res.* 1, 482–497.

Clegg, N. J., Wongvipat, J., Joseph, J. D., Tran, C., Ouk, S., Dilhas, A., et al. (2012). ARN-509: a novel antiandrogen for prostate cancer treatment. *Cancer Res.* 72, 1494–1503. doi: 10.1158/0008-5472.CAN-11-3948

Clermont, P.-L., Lin, D., Crea, F., Wu, R., Xue, H., Wang, Y., et al. (2015). Polycomb-mediated silencing in neuroendocrine prostate *cancer*. *Clin. Epigenetics* 7:40. doi: 10.1186/s13148-015-0074-4

Clevers, H. (2006). Wnt/beta-catenin signaling in development and disease. *Cell* 127, 469–480. doi: 10.1016/j.cell.2006.10.018

Coleman, D. J., Sampson, D. A., Sehrawat, A., Kumaraswamy, A., Sun, D., Wang, Y., et al. (2020). Alternative splicing of LSD1+8a in neuroendocrine prostate cancer is mediated by SRRM4. *Neoplasia* 22, 253–262. doi: 10.1016/j.neo.2020.04.002

Collins, A. T., Berry, P. A., Hyde, C., Stower, M. J., and Maitland, N. J. J. C.R. (2005). Prospective identification of tumorigenic prostate cancer stem cells. *Cancer Res,* 65, 10946–10951. doi: 10.1158/0008-5472.CAN-05-2018

Cooke, P. S., Young, P., and Cunha, G. R. (1991). Androgen receptor expression in developing male reproductive organs. *Endocrinology* 128, 2867–2873. doi: 10.1210/endo-128-6-2867

Culig, Z., and Santer, F. R. (2014). Androgen receptor signaling in prostate cancer. *Cancer Metastasis Rev.* 33, 413–427. doi: 10.1007/s10555-013-9474-0

Cunha, G. R., Donjacour, A. A., Cooke, P. S., Mee, S., Bigsby, R. M., Higgins, S. J., et al. (1987). The endocrinology and developmental biology of the prostate. *Endocr. Rev.* 8, 338–362. doi: 10.1210/edrv-8-3-338

Dai, Y., Wu, Z., Lang, C., Zhang, X., He, S., Yang, Q., et al. (2019). Copy number gain of ZEB1 mediates a double-negative feedback loop with miR-33a-5p that regulates EMT and bone metastasis of prostate cancer dependent on TGF-beta signaling. *Theranostics* 9, 6063–6079. doi: 10.7150/thno.36735

Dardenne, E., Beltran, H., Benelli, M., Gayvert, K., Berger, A., Puca, L., et al. (2016). N-Myc induces an EZH2-mediated transcriptional program driving neuroendocrine prostate cancer. *Cancer Cell* 30, 563–577. doi: 10.1016/j.ccell.2016.09.005

Davies, A. H., Beltran, H., and Zoubeidi, A. (2018). Cellular plasticity and the neuroendocrine phenotype in prostate cancer. *Nat. Rev. Urol.* 15, 271–286. doi: 10.1038/nrurol.2018.22

de Bono, J. S., Logothetis, C. J., Molina, A., Fizazi, K., North, S., Chu, L., et al. (2011). Abiraterone and increased survival in metastatic prostate cancer. *N. Engl. J. Med.* 364, 1995–2005. doi: 10.1056/NEJMoa1014618

de Carvalho Flamini, R., Yamaga, L., Mello, M. E., Wagner, J., Livorsi Da Cunha, M., Osawa, A., et al. (2010). F-18 FDG PET/CT imaging in small cell prostate cancer. *Clin. Nucl. Med.* 35, 452–453. doi: 10.1097/RLU.0b013e3181db4ce9

Dempke, W. C. M., Fenchel, K., Uciechowski, P., and Chevassut, T. (2017). Targeting developmental pathways: the achilles heel of cancer? *Oncology* 93, 213–223. doi: 10.1159/000478703

Derynck, R., and Zhang, Y. E. (2003). Smad-dependent and smad-independent pathways in TGF-beta family signalling. *Nature* 425, 577–584. doi: 10.1038/nature02006

Djavan, B., Susani, M., Bursa, B., Basharkhah, A., Simak, R., and Marberger, M. (1999). Predictability and significance of multifocal prostate cancer in the radical prostatectomy specimen. *Tech. Urol.* 5, 139–142. doi: 10.1016/S0022-5347(01)62084-6

Doldi, V., Callari, M., Giannoni, E., D'aiuto, F., Maffezzini, M., Valdagni, R., et al. (2015). Integrated gene and miRNA expression analysis of prostate cancer associated fibroblasts supports a prominent role for interleukin-6 in fibroblast activation. *Oncotarget* 6, 31441–31460. doi: 10.18632/oncotarget.5056

Dolly, S. O., Wagner, A. J., Bendell, J. C., Kindler, H. L., Krug, L. M., Seiwert, T. Y., et al. (2016). Phase I study of apitolisib (GDC-0980), dual phosphatidylinositol-3-kinase and mammalian target of rapamycin kinase inhibitor, in patients with advanced solid tumors. *Clin. Cancer Res.* 22, 2874–2884. doi: 10.1158/1078-0432.CCR-15-2225

Effert, P., Beniers, A. J., Tamimi, Y., Handt, S., and Jakse, G. (2004). Expression of glucose transporter 1 (Glut-1) in cell lines and clinical specimens from human prostate adenocarcinoma. *Anticancer Res.* 24, 3057–3063.

Effert, P. J., Bares, R., Handt, S., Wolff, J. M., Bull, U., and Jakse, G. J. T. J. O. U. (1996). Metabolic imaging of untreated prostate cancer by positron emission tomography with sup 18 fluorine-labeled deoxyglucose. *J. Urol.* 155, 994–998. doi: 10.1016/S0022-5347(01)66366-3

Ellis, L., and Loda, M. (2015). Advanced neuroendocrine prostate tumors regress to stemness. *Proc. Natl. Acad. Sci. U.S.A.* 112, 14406–14407. doi: 10.1073/pnas.1519151112

Erdogan, B., and Webb, D. J. (2017). Cancer-associated fibroblasts modulate growth factor signaling and extracellular matrix remodeling to regulate tumor metastasis. *Biochem. Soc. Trans.* 45, 229–236. doi: 10.1042/BST20160387

Figiel, S., Vasseur, C., Bruyere, F., Rozet, F., Maheo, K., and Fromont, G. (2017). Clinical significance of epithelial-mesenchymal transition markers in prostate cancer. *Hum. Pathol.* 61, 26–32. doi: 10.1016/j.humpath.2016.10.013

Flavahan, W. A., Gaskell, E., and Bernstein, B. E. (2017). Epigenetic plasticity and the hallmarks of cancer. *Science* 357:eaal2380. doi: 10.1126/science.aal2380

Floor, S., Van Staveren, W., Larsimont, D., Dumont, J. E., and Maenhaut, C. J. O. (2011). Cancer cells in epithelial-to-mesenchymal transition and tumor-propagating–cancer stem cells: distinct, overlapping or same populations. *Oncogene* 30, 4609–4621. doi: 10.1038/onc.2011.184

Fournier, P. G., Juárez, P., Jiang, G., Clines, G. A., Niewolna, M., Kim, H. S., et al. (2015). The TGF-β signaling regulator PMEPA1 suppresses prostate cancer metastases to *bone*. *Cancer Cell* 27, 809–821. doi: 10.1016/j.ccell.2015.04.009

Friedmann-Morvinski, D., and Verma, I. M. (2014). Dedifferentiation and reprogramming: origins of cancer stem cells. *EMBO Rep.* 15, 244–253. doi: 10.1002/embr.201338254

Frixen, U. H., Behrens, J., Sachs, M., Eberle, G., Voss, B., Warda, A., et al. (1991). E-cadherin-mediated cell-cell adhesion prevents invasiveness of human carcinoma cells. *J. Cell Biol.* 113, 173–185. doi: 10.1083/jcb.113.1.173

Garraway, I. P., Sun, W., Tran, C. P., Perner, S., Zhang, B., Goldstein, A. S., et al. (2010). Human prostate sphere-forming cells represent a subset of basal epithelial cells capable of glandular regeneration *in vivo*. *Prostate* 70, 491–501. doi: 10.1002/pros.21083

Gelmann, E. P. (2002). Molecular biology of the androgen receptor. *J. Clin. Oncol.* 20, 3001–3015. doi: 10.1200/JCO.2002.10.018

Giannoni, E., Bianchini, F., Masieri, L., Serni, S., Torre, E., Calorini, L., et al. (2010). Reciprocal activation of prostate cancer cells and cancer-associated fibroblasts stimulates epithelial-mesenchymal transition and cancer stemness. *Cancer Res.* 70, 6945–6956. doi: 10.1158/0008-5472.CAN-10-0785

Goldstein, A. S., Huang, J., Guo, C., Garraway, I. P., and Witte, O. N. (2010). Identification of a cell of origin for human prostate cancer. *Science* 329, 568–571. doi: 10.1126/science.1189992

Graham, T. R., Zhau, H. E., Odero-Marah, V. A., Osunkoya, A. O., Kimbro, K. S., Tighiouart, M., et al. (2008). Insulin-like growth factor-I-dependent up-regulation of ZEB1 drives epithelial-to-mesenchymal transition in human prostate cancer cells. *Cancer Res.* 68, 2479–2488. doi: 10.1158/0008-5472.CAN-07-2559

Grasso, C. S., Wu, Y. M., Robinson, D. R., Cao, X., Dhanasekaran, S. M., Khan, A. P., et al. (2012). The mutational landscape of lethal castration-resistant prostate cancer. *Nature* 487, 239–243. doi: 10.1038/nature11125

Gregory, C. W., He, B., Johnson, R. T., Ford, O. H., Mohler, J. L., French, F. S., et al. (2001). A mechanism for androgen receptor-mediated prostate cancer recurrence after androgen deprivation therapy. *Cancer Res.* 61, 4315–4319.

Guilford, P. (1999). E-cadherin downregulation in cancer: fuel on the fire? *Mol. Med. Today* 5, 172–177. doi: 10.1016/S1357-4310(99)01461-6

Guo, C., Liu, H., Zhang, B. H., Cadaneanu, R. M., Mayle, A. M., and Garraway, I. P. (2012). Epcam, CD44, and CD49f distinguish sphere-forming human prostate basal cells from a subpopulation with predominant tubule initiation capability. *PLoS ONE* 7:e34219. doi: 10.1371/journal.pone.0034219

Guo, C. C., Dancer, J. Y., Wang, Y., Aparicio, A., Navone, N. M., Troncoso, P., et al. (2011). TMPRSS2-ERG gene fusion in small cell carcinoma of the prostate. *Hum. Pathol.* 42, 11–17. doi: 10.1016/j.humpath.2010.05.026

Guo, H., Ci, X., Ahmed, M., Hua, J. T., Soares, F., Lin, D., et al. (2019). ONECUT2 is a driver of neuroendocrine prostate cancer. *Nat. Commun.* 10, 1–13. doi: 10.1038/s41467-018-08133-6

Hanahan, D., and Weinberg, R. A. (2011). Hallmarks of cancer: the next generation. *Cell* 144, 646–674. doi: 10.1016/j.cell.2011.02.013

Hudes, G., Tagawa, S. T., Whang, Y. E., Qi, M., Qin, X., Puchalski, T. A., et al. (2013). A phase 1 study of a chimeric monoclonal antibody against interleukin-6, siltuximab, combined with docetaxel in patients with metastatic castration-resistant prostate cancer. *Invest. New Drugs* 31, 669–676. doi: 10.1007/s10637-012-9857-z

Huss, W. J., Gray, D. R., Greenberg, N. M., Mohler, J. L., and Smith, G. J. J. C.R. (2005). Breast cancer resistance protein–mediated efflux of androgen in putative benign and malignant prostate stem cells. *Cancer Res.* 65, 6640–6650. doi: 10.1158/0008-5472.CAN-04-2548

Izumi, K., Fang, L. Y., Mizokami, A., Namiki, M., Li, L., Lin, W. J., et al. (2013). Targeting the androgen receptor with siRNA promotes prostate cancer metastasis through enhanced macrophage recruitment via

CCL2/CCR2-induced STAT3 activation. *EMBO Mol. Med.* 5, 1383–1401. doi: 10.1002/emmm.201202367

Jacob, S., Nayak, S., Fernandes, G., Barai, R., Menon, S., Chaudhari, U., et al. (2014). Androgen receptor as a regulator of ZEB2 expression and its implications in epithelial-to-mesenchymal transition in prostate cancer. *Endocr. Relat. Cancer* 21, 473–486. doi: 10.1530/ERC-13-0514

Jennbacken, K., Tešan, T., Wang, W., Gustavsson, H., Damber, J.-E., and Welen, K. (2010). N-cadherin increases after androgen deprivation and is associated with metastasis in prostate cancer. *Endocr. Relat. Cancer* 17, 469–479. doi: 10.1677/ERC-10-0015

Kalluri, R., and Weinberg, R. A. (2009). The basics of epithelial-mesenchymal transition. *J. Clin. Invest.* 119, 1420–1428. doi: 10.1172/JCI39104

Karthaus, W. R., Iaquinta, P. J., Drost, J., Gracanin, A., Van Boxtel, R., Wongvipat, J., et al. (2014). Identification of multipotent luminal progenitor cells in human prostate organoid cultures. *Cell* 159, 163–175. doi: 10.1016/j.cell.2014.08.017

Kogan-Sakin, I., Cohen, M., Paland, N., Madar, S., Solomon, H., Molchadsky, A., et al. (2009). Prostate stromal cells produce CXCL-1, CXCL-2, CXCL-3 and IL-8 in response to epithelia-secreted IL-1. *Carcinogenesis* 30, 698–705. doi: 10.1093/carcin/bgp043

Kong, D., Banerjee, S., Ahmad, A., Li, Y., Wang, Z., Sethi, S., et al. (2010). Epithelial to mesenchymal transition is mechanistically linked with stem cell signatures in prostate cancer cells. *PLoS ONE* 5:e12445. doi: 10.1371/journal.pone.0012445

Kreso, A., and Dick, J. E. J. C. S. C. (2014). Evolution of the cancer stem cell model. *Cell Stem Cell* 14, 275–291. doi: 10.1016/j.stem.2014.02.006

Kung, P. P., Bingham, P., Brooun, A., Collins, M., Deng, Y. L., Dinh, D., et al. (2018). Optimization of orally bioavailable enhancer of zeste homolog 2 (EZH2) inhibitors using ligand and property-based design strategies: identification of development candidate (R)-5,8-dichloro-7-(methoxy(oxetan-3-yl)methyl)-2-((4-methoxy-6-methyl-2-oxo-1,2-dihydropyridin-3-yl)methyl)-3,4-dihydroisoquinolin-1(2H)-one (PF-06821497). *J. Med. Chem.* 61, 650–665. doi: 10.1021/acs.jmedchem.7b01375

Lapuk, A. V., Wu, C., Wyatt, A. W., Mcpherson, A., Mcconeghy, B. J., Brahmbhatt, S., et al. (2012). From sequence to molecular pathology, and a mechanism driving the neuroendocrine phenotype in prostate cancer. *J. Pathol.* 227, 286–297. doi: 10.1002/path.4047

Lee, G. T., Kwon, S. J., Lee, J. H., Jeon, S. S., Jang, K. T., Choi, H. Y., et al. (2011). Macrophages induce neuroendocrine differentiation of prostate cancer cells via BMP6-IL6 loop. *Prostate* 71, 1525–1537. doi: 10.1002/pros.21369

Lee, J. K., Phillips, J. W., Smith, B. A., Park, J. W., Stoyanova, T., Mccaffrey, E. F., et al. (2016). N-Myc drives neuroendocrine prostate cancer initiated from human prostate epithelial cells. *Cancer Cell* 29, 536–547. doi: 10.1016/j.ccell.2016.03.001

Li, H., Wang, L., Li, Z., Geng, X., Li, M., Tang, Q., et al. (2019). SOX2 has dual functions as a regulator in the progression of neuroendocrine prostate cancer. *J. Tech. Methods Pathol.* 100, 570–582. doi: 10.1038/s41374-019-0343-5

Li, J. J., and Shen, M. M. (2019). Prostate stem cells and cancer stem cells. *Cold Spring Harb. Perspect. Med.* 9:ea030395. doi: 10.1101/cshperspect.a030395

Li, M., Wang, Y. X., Luo, Y., Zhao, J., Li, Q., Zhang, J., et al. (2016). Hypoxia inducible factor-1alpha-dependent epithelial to mesenchymal transition under hypoxic conditions in prostate cancer cells. *Oncol. Rep* 36, 521–527. doi: 10.3892/or.2016.4766

Li, P., Wang, J., Chu, M., Zhang, K., Yang, R., Gao, W.-Q. J. E. B., and Medicine (2014). Zeb1 promotes androgen independence of prostate cancer via induction of stem cell-like properties. 239, 813–822. doi: 10.1177/1535370214538727

Lin, D., Wyatt, A. W., Xue, H., Wang, Y., Dong, X., Haegert, A., et al. (2014). High fidelity patient-derived xenografts for accelerating prostate cancer discovery and drug development. *Cancer Res.* 74, 1272–1283. doi: 10.1158/0008-5472.CAN-13-2921-T

Lin, T. H., Izumi, K., Lee, S. O., Lin, W. J., Yeh, S., and Chang, C. (2013). Anti-androgen receptor ASC-J9 versus anti-androgens MDV3100 (Enzalutamide) or Casodex (Bicalutamide) leads to opposite effects on prostate cancer metastasis via differential modulation of macrophage infiltration and STAT3-CCL2 signaling. *Cell Death Dis.* 4:e764. doi: 10.1038/cddis.2013.270

Lin, T. P., Chang, Y. T., Lee, S. Y., Campbell, M., Wang, T. C., Shen, S. H., et al. (2016). REST reduction is essential for hypoxia-induced neuroendocrine differentiation of prostate cancer cells by activating autophagy signaling. *Oncotarget* 7, 26137–26151. doi: 10.18632/oncotarget.8433

Liu, A. Y., True, L. D., Latray, L., Nelson, P. S., Ellis, W. J., Vessella, R. L., et al. (1997). Cell–cell interaction in prostate gene regulation and cytodifferentiation. *Proc. Natl. Acad. Sci. U.S.A.* 94, 10705–10710. doi: 10.1073/pnas.94.20.10705

Liu, W., Laitinen, S., Khan, S., Vihinen, M., Kowalski, J., Yu, G., et al. (2009). Copy number analysis indicates monoclonal origin of lethal metastatic prostate cancer. *Nat. Med.* 15:559. doi: 10.1038/nm.1944

Loh, C.-Y., Chai, J. Y., Tang, T. F., Wong, W. F., Sethi, G., Shanmugam, M. K., et al. (2019). The E-cadherin and N-cadherin switch in epithelial-to-mesenchymal transition: Signaling, therapeutic implications, and challenges. *Cells* 8:1118. doi: 10.3390/cells8101118

Lu, T., Lin, W. J., Izumi, K., Wang, X., Xu, D., Fang, L. Y., et al. (2012). Targeting androgen receptor to suppress macrophage-induced EMT and benign prostatic hyperplasia (BPH) development. *Mol. Endocrinol.* 26, 1707–1715. doi: 10.1210/me.2012-1079

Lu, W., and Kang, Y. (2019). Epithelial-mesenchymal plasticity in cancer progression and metastasis. *Dev. Cell* 49, 361–374. doi: 10.1016/j.devcel.2019.04.010

Marjanovic, N. D., Weinberg, R. A., and Chaffer, C. L. (2013). Cell plasticity and heterogeneity in cancer. *Clin. Chem.* 59, 168–179. doi: 10.1373/clinchem.2012.184655

Massague, J. (2008). TGFbeta in Cancer. *Cell* 134, 215–230. doi: 10.1016/j.cell.2008.07.001

McKeithen, D., Graham, T., Chung, L. W., and Odero-Marah, V. (2010). Snail transcription factor regulates neuroendocrine differentiation in LNCaP prostate cancer cells. *Prostate* 70, 982–992. doi: 10.1002/pros.21132

Miao, L., Yang, L., Li, R., Rodrigues, D. N., Crespo, M., Hsieh, J.-T., et al. (2017). Disrupting androgen receptor signaling induces Snail-mediated epithelial–mesenchymal plasticity in prostate cancer. *Cancer Res.* 77, 3101–3112. doi: 10.1158/0008-5472.CAN-16-2169

Mishra, R., Haldar, S., Placencio, V., Madhav, A., Rohena-Rivera, K., Agarwal, P., et al. (2018). Stromal epigenetic alterations drive metabolic and neuroendocrine prostate cancer reprogramming. *J. Clin. Invest.* 128, 4472–4484. doi: 10.1172/JCI99397

Mounir, Z., Lin, F., Lin, V., Korn, J., Yu, Y., Valdez, R., et al. (2015). TMPRSS2: ERG blocks neuroendocrine and luminal cell differentiation to maintain prostate cancer proliferation. *Oncogene* 34:3815. doi: 10.1038/onc.2014.308

Mu, P., Zhang, Z., Benelli, M., Karthaus, W. R., Hoover, E., Chen, C.-C., et al. (2017). SOX2 promotes lineage plasticity and antiandrogen resistance in TP53-and RB1-deficient prostate cancer. *Science* 355, 84–88. doi: 10.1126/science.aah4307

Nauseef, J. T., and Henry, M. D. (2011). Epithelial-to-mesenchymal transition in prostate cancer: paradigm or puzzle? *Nat. Rev. Urol.* 8, 428–439. doi: 10.1038/nrurol.2011.85

Nieto, M. A. (2013). Epithelial plasticity: a common theme in embryonic and cancer cells. *Science* 342:1234850. doi: 10.1126/science.1234850

Nouri, M., Caradec, J., Lubik, A. A., Li, N., Hollier, B. G., Takhar, M., et al. (2017). Therapy-induced developmental reprogramming of prostate cancer cells and acquired therapy resistance. *Oncotarget* 8, 18949–18967. doi: 10.18632/oncotarget.14850

Onder, T. T., Gupta, P. B., Mani, S. A., Yang, J., Lander, E. S., and Weinberg, R. A. (2008). Loss of E-cadherin promotes metastasis via multiple downstream transcriptional pathways. *Cancer Res.* 68, 3645–3654. doi: 10.1158/0008-5472.CAN-07-2938

Orellana-Serradell, O., Herrera, D., Castellon, E. A., and Contreras, H. R. (2018). The transcription factor ZEB1 promotes an aggressive phenotype in prostate cancer cell lines. *Asian J. Androl.* 20, 294–299. doi: 10.4103/aja.aja_61_17

Padmanaban, V., Krol, I., Suhail, Y., Szczerba, B. M., Aceto, N., Bader, J. S., et al. (2019). E-cadherin is required for metastasis in multiple models of breast cancer. *Nature* 573, 439–444. doi: 10.1038/s41586-019-1526-3

Paget, S. (1889). The distribution of secondary growths in cancer of the breast. *Lancet* 133, 571–573. doi: 10.1016/S0140-6736(00)49915-0

Palanisamy, N., Ateeq, B., Kalyana-Sundaram, S., Pflueger, D., Ramnarayanan, K., Shankar, S., et al. (2010). Rearrangements of the RAF kinase pathway in prostate cancer, gastric cancer and melanoma. *Nat. Med* 16, 793–798. doi: 10.1038/nm.2166

Palapattu, G. S., Wu, C., Silvers, C. R., Martin, H. B., Williams, K., Salamone, L., et al. (2009). Selective expression of CD44, a putative prostate cancer stem cell

marker, in neuroendocrine tumor cells of human prostate cancer. *Prostate* 69, 787–798. doi: 10.1002/pros.20928

Patel, G. K., Chugh, N., and Tripathi, M. (2019). Neuroendocrine differentiation of prostate cancer-an intriguing example of tumor evolution at play. *Cancers (Basel)* 11:1405. doi: 10.3390/cancers11101405

Patrawala, L., Calhoun, T., Schneider-Broussard, R., Li, H., Bhatia, B., Tang, S., et al. (2006). Highly purified CD44+ prostate cancer cells from xenograft human tumors are enriched in tumorigenic and metastatic progenitor cells. *Oncogene* 25, 1696–1708. doi: 10.1038/sj.onc.1209327

Pertega-Gomes, N., Felisbino, S., Massie, C. E., Vizcaino, J. R., Coelho, R., Sandi, C., et al. (2015). A glycolytic phenotype is associated with prostate cancer progression and aggressiveness: a role for monocarboxylate transporters as metabolic targets for therapy. *J. Pathol.* 236, 517–530. doi: 10.1002/path.4547

Plaks, V., Kong, N., and Werb, Z. (2015). The cancer stem cell niche: how essential is the niche in regulating stemness of tumor cells? *Cell Stem Cell* 16, 225–238. doi: 10.1016/j.stem.2015.02.015

Poli, V., Fagnocchi, L., and Zippo, A. (2018). Tumorigenic cell reprogramming and cancer plasticity: interplay between signaling, microenvironment, and epigenetics. *Stem Cells Int.* 2018:4598195. doi: 10.1155/2018/4598195

Puca, L., Gavyert, K., Sailer, V., Conteduca, V., Dardenne, E., Sigouros, M., et al. (2019). Delta-like protein 3 expression and therapeutic targeting in neuroendocrine prostate cancer. *Sci. Transl. Med.* 11:eaav0891. doi: 10.1126/scitranslmed.aav0891

Qi, M., Hu, J., Cui, Y., Jiao, M., Feng, T., Li, X., et al. (2019). CUL4B promotes prostate cancer progression by forming positive feedback loop with SOX4. *Oncogenesis* 8:23. doi: 10.1038/s41389-019-0131-5

Qin, J., Liu, X., Laffin, B., Chen, X., Choy, G., Jeter, C. R., et al. (2012). The PSA(-/lo) prostate cancer cell population harbors self-renewing long-term tumor-propagating cells that resist castration. *Cell Stem Cell* 10, 556–569. doi: 10.1016/j.stem.2012.03.009

Reina-Campos, M., Linares, J. F., Duran, A., Cordes, T., L'hermitte, A., Badur, M. G., et al. (2019). Increased serine and one-carbon pathway metabolism by PKCλ/ι deficiency promotes neuroendocrine prostate cancer. *Cancer Cell* 35, 385–400.e389. doi: 10.1016/j.ccell.2019.01.018

Ren, D., Wang, M., Guo, W., Huang, S., Wang, Z., Zhao, X., et al. (2014). Double-negative feedback loop between ZEB2 and miR-145 regulates epithelial-mesenchymal transition and stem cell properties in prostate cancer cells. *Cell Tissue Res.* 358, 763–778. doi: 10.1007/s00441-014-2001-y

Robinson, D., Van Allen, E. M., Wu, Y.-M., Schultz, N., Lonigro, R. J., Mosquera, J.-M., et al. (2015). Integrative clinical genomics of advanced prostate cancer. *Cell* 161, 1215–1228. doi: 10.1016/j.cell.2015.05.001

Rothman, J., and Jarriault, S. (2019). Developmental Plasticity and Cellular Reprogramming in Caenorhabditis elegans. *Genetics* 213, 723–757. doi: 10.1534/genetics.119.302333

Rybak, A. P., He, L., Kapoor, A., Cutz, J. C., and Tang, D. (2011). Characterization of sphere-propagating cells with stem-like properties from DU145 prostate cancer cells. *Biochim. Biophys. Acta* 1813, 683–694. doi: 10.1016/j.bbamcr.2011.01.018

Rybak, A. P., and Tang, D. (2013). SOX2 plays a critical role in EGFR-mediated self-renewal of human prostate cancer stem-like cells. *Cell. Signal* 25, 2734–2742. doi: 10.1016/j.cellsig.2013.08.041

Schafer, J. M., Lehmann, B. D., Gonzalez-Ericsson, P. I., Marshall, C. B., Beeler, J. S., Redman, L. N., et al. (2020). Targeting MYCN-expressing triple-negative breast cancer with BET and MEK inhibitors. *Sci. Transl. Med.* 12:eaaw8275. doi: 10.1126/scitranslmed.aaw8275

Scher, H. I., Beer, T. M., Higano, C. S., Anand, A., Taplin, M. E., Efstathiou, E., et al. (2010). Antitumour activity of MDV3100 in castration-resistant prostate cancer: a phase 1-2 study. *Lancet* 375, 1437–1446. doi: 10.1016/S0140-6736(10)60172-9

Seligson, D. B., Horvath, S., Shi, T., Yu, H., Tze, S., Grunstein, M., et al. (2005). Global histone modification patterns predict risk of prostate cancer recurrence. *Nature* 435, 1262–1266. doi: 10.1038/nature03672

Shiota, M., Yokomizo, A., Takeuchi, A., Imada, K., Kashiwagi, E., Song, Y., et al. (2014). Inhibition of protein kinase C/Twist1 signaling augments anticancer effects of androgen deprivation and enzalutamide in prostate cancer. *Clin. Cancer Res.* 20, 951–961. doi: 10.1158/1078-0432.CCR-13-1809

Soundararajan, R., Paranjape, A. N., Maity, S., Aparicio, A., and Mani, S. A. (2018). EMT, stemness and tumor plasticity in aggressive variant neuroendocrine prostate cancers. *Biochim. Biophys. Acta Rev. Cancer* 1870, 229–238. doi: 10.1016/j.bbcan.2018.06.006

Stylianou, N., Lehman, M. L., Wang, C., Fard, A. T., Rockstroh, A., Fazli, L., et al. (2019). A molecular portrait of epithelial-mesenchymal plasticity in prostate cancer associated with clinical outcome. *Oncogene* 38, 913–934. doi: 10.1038/s41388-018-0488-5

Sun, Y., Wang, B.-E., Leong, K. G., Yue, P., Li, L., Jhunjhunwala, S., et al. (2012). Androgen deprivation causes epithelial–mesenchymal transition in the prostate: implications for androgen-deprivation therapy. *Cancer Res.* 72, 527–536. doi: 10.1158/0008-5472.CAN-11-3004

Svensson, C., Ceder, J., Iglesias-Gato, D., Chuan, Y.-C., Pang, S. T., Bjartell, A., et al. (2013). REST mediates androgen receptor actions on gene repression and predicts early recurrence of prostate *cancer*. *Nucleic Acids Res.* 42, 999–1015. doi: 10.1093/nar/gkt921

Tan, M. H., Li, J., Xu, H. E., Melcher, K., and Yong, E. L. (2015). Androgen receptor: structure, role in prostate cancer and drug discovery. *Acta Pharmacol. Sin.* 36, 3–23. doi: 10.1038/aps.2014.18

Tang, Y., Parmakhtiar, B., Simoneau, A. R., Xie, J., Fruehauf, J., Lilly, M., et al. (2011). Lycopene enhances docetaxel's effect in castration-resistant prostate cancer associated with insulin-like growth factor I receptor levels. *Neoplasia* 13, 108–119. doi: 10.1593/neo.101092

Taplin, M.-E., Hussain, A., Shah, S., Shore, N. D., Agrawal, M., Clark, W., et al. (2019). ProSTAR: a phase Ib/II study of CPI-1205, a small molecule inhibitor of EZH2, combined with enzalutamide (E) or abiraterone/prednisone (A/P) in patients with metastatic castration-resistant prostate cancer (mCRPC). *J. Clin. Oncol.* 37:TPS335. doi: 10.1200/JCO.2019.37.7_suppl.TPS335

Taplin, M. E., Bubley, G. J., Shuster, T. D., Frantz, M. E., Spooner, A. E., Ogata, G. K., et al. (1995). Mutation of the androgen-receptor gene in metastatic androgen-independent prostate cancer. *N. Engl. J. Med.* 332, 1393–1398. doi: 10.1056/NEJM199505253322101

Taylor, R. A., Toivanen, R., Frydenberg, M., Pedersen, J., Harewood, L., Australian Prostate Cancer, B., et al. (2012). Human epithelial basal cells are cells of origin of prostate cancer, independent of CD133 status. *Stem Cells* 30, 1087–1096. doi: 10.1002/stem.1094

Thiery, J. P., Acloque, H., Huang, R. Y., and Nieto, M. A. (2009). Epithelial-mesenchymal transitions in development and disease. *Cell* 139, 871–890. doi: 10.1016/j.cell.2009.11.007

Tian, X., Nguyen, M., Foote, H. P., Caster, J. M., Roche, K. C., Peters, C. G., et al. (2017). CRLX101, a nanoparticle-drug conjugate containing camptothecin, improves rectal cancer chemoradiotherapy by inhibiting DNA repair and HIF1alpha. *Cancer Res.* 77, 112–122. doi: 10.1158/0008-5472.CAN-15-2951

Tiwari, R., Manzar, N., Bhatia, V., Yadav, A., Nengroo, M. A., Datta, D., et al. (2020). Androgen deprivation upregulates SPINK1 expression and potentiates cellular plasticity in prostate cancer. *Nat. Commun.* 11:384. doi: 10.1038/s41467-019-14184-0

Tomlins, S. A., Rhodes, D. R., Perner, S., Dhanasekaran, S. M., Mehra, R., Sun, X. W., et al. (2005). Recurrent fusion of TMPRSS2 and ETS transcription factor genes in prostate cancer. *Science* 310, 644–648. doi: 10.1126/science.1117679

Tomlins, S. A., Rhodes, D. R., Yu, J., Varambally, S., Mehra, R., Perner, S., et al. (2008). The role of SPINK1 in ETS rearrangement-negative prostate cancers. *Cancer Cell* 13, 519–528. doi: 10.1016/j.ccr.2008.04.016

Tsai, J. H., and Yang, J. (2013). Epithelial-mesenchymal plasticity in carcinoma metastasis. *Genes Dev.* 27, 2192–2206. doi: 10.1101/gad.225334.113

Tsai, Y.-C., Chen, W.-Y., Abou-Kheir, W., Zeng, T., Yin, J. J., Bahmad, H., et al. (2018). Androgen deprivation therapy-induced epithelial-mesenchymal transition of prostate cancer through downregulating SPDEF and activating CCL2. *Biochim. Biophys. Acta Mol. Basis Dis.* 1864, 1717–1727. doi: 10.1016/j.bbadis.2018.02.016

Tsuji, T., Ibaragi, S., Shima, K., Hu, M. G., Katsurano, M., Sasaki, A., et al. (2008). Epithelial-mesenchymal transition induced by growth suppressor p12CDK2-AP1 promotes tumor cell local invasion but suppresses distant colony growth. *Cancer Res.* 68, 10377–10386. doi: 10.1158/0008-5472.CAN-08-1444

Van De Wijngaart, D. J., Dubbink, H. J., Van Royen, M. E., Trapman, J., and Jenster, G. (2012). Androgen receptor coregulators: recruitment via the coactivator binding groove. *Mol. Cell. Endocrinol.* 352, 57–69. doi: 10.1016/j.mce.2011.08.007

Vander Heiden, M. G., Cantley, L. C., and Thompson, C. B. (2009). Understanding the Warburg effect: the metabolic requirements of cell proliferation. *Science* 324, 1029–1033. doi: 10.1126/science.1160809

Varambally, S., Cao, Q., Mani, R. S., Shankar, S., Wang, X., Ateeq, B., et al. (2008). Genomic loss of microRNA-101 leads to overexpression of histone methyltransferase EZH2 in cancer. *Science* 322, 1695–1699. doi: 10.1126/science.1165395

Varga, J., and Greten, F. R. (2017). Cell plasticity in epithelial homeostasis and tumorigenesis. *Nat. Cell Biol.* 19, 1133–1141. doi: 10.1038/ncb3611

Vitkin, N., Nersesian, S., Siemens, D. R., and Koti, M. (2019). The tumor immune contexture of prostate cancer. *Front. Immunol.* 10:603. doi: 10.3389/fimmu.2019.00603

Wagers, A. J., and Weissman, I. L. (2004). Plasticity of adult stem cells. *Cell* 116, 639–648. doi: 10.1016/S0092-8674(04)00208-9

Wang, H., Leav, I., Ibaragi, S., Wegner, M., Hu, G.-F., Lu, M. L., et al. (2008). SOX9 is expressed in human fetal prostate epithelium and enhances prostate cancer invasion. *Cancer Res.* 68, 1625–1630. doi: 10.1158/0008-5472.CAN-07-5915

Wang, H., and Unternaehrer, J. J. (2019). Epithelial-mesenchymal transition and cancer stem cells: at the crossroads of differentiation and dedifferentiation. *Dev. Dyn.* 248, 10–20. doi: 10.1002/dvdy.24678

Wang, W., Wang, L., Mizokami, A., Shi, J., Zou, C., Dai, J., et al. (2017). Down-regulation of E-cadherin enhances prostate cancer chemoresistance via Notch signaling. *Chin J. Cancer* 36:35. doi: 10.1186/s40880-017-0203-x

Wang, Z. A., and Shen, M. M. (2011). Revisiting the concept of cancer stem cells in prostate cancer. *Oncogene* 30, 1261–1271. doi: 10.1038/onc.2010.530

Wang, Z. A., Toivanen, R., Bergren, S. K., Chambon, P., and Shen, M. M. (2014). Luminal cells are favored as the cell of origin for prostate cancer. *Cell Rep.* 8, 1339–1346. doi: 10.1016/j.celrep.2014.08.002

Wellner, U., Schubert, J., Burk, U. C., Schmalhofer, O., Zhu, F., Sonntag, A., et al. (2009). The EMT-activator ZEB1 promotes tumorigenicity by repressing stemness-inhibiting microRNAs. *Nat. Cell Biol.* 11, 1487–1495. doi: 10.1038/ncb1998

Williams, E. D., Gao, D., Redfern, A., and Thompson, E. W. (2019). Controversies around epithelial-mesenchymal plasticity in cancer metastasis. *Nat. Rev. Cancer* 19, 716–732. doi: 10.1038/s41568-019-0213-x

Wu, K., Gore, C., Yang, L., Fazli, L., Gleave, M., Pong, R.-C., et al. (2012). Slug, a unique androgen-regulated transcription factor, coordinates androgen receptor to facilitate castration resistance in prostate cancer. *Mol. Endocrinol.* 26, 1496–1507. doi: 10.1210/me.2011-1360

Yadav, S. S., Stockert, J. A., Hackert, V., Yadav, K. K., and Tewari, A. K. (2018). Intratumor heterogeneity in prostate cancer. *Urol. Oncol.* 36, 349–360. doi: 10.1016/j.urolonc.2018.05.008

Yap, T. A., Johnson, P. W. M., Winter, J., Leonard, J., Giulino-Roth, L., Horner, T., et al. (2016). A phase I, open-label study of GSK2816126, an enhancer of zeste homolog 2 (EZH2) inhibitor, in patients with relapsed/refractory diffuse large B-cell lymphoma (DLBCL), transformed follicular lymphoma (tFL), other non-Hodgkin's lymphomas (NHL), multiple myeloma (MM) and solid tumor. *J. Clin. Oncol.* 34(Suppl 15), TPS2595. doi: 10.1200/JCO.2016.34.15_suppl.TPS2595

Yates, C. (2011). "Prostate tumor cell plasticity: a consequence of the microenvironment," in *Human Cell Transformation* (New York, NY: Springer), 81–90.

Yates, C. C., Shepard, C. R., Stolz, D. B., and Wells, A. (2007). Co-culturing human prostate carcinoma cells with hepatocytes leads to increased expression of E-cadherin. *Br. J. Cancer* 96, 1246–1252. doi: 10.1038/sj.bjc.6603700

Yuan, S., Norgard, R. J., and Stanger, B. Z. (2019). Cellular plasticity in cancer. *Cancer Discov.* 9, 837–851. doi: 10.1158/2159-8290.CD-19-0015

Zhang, Q., Helfand, B. T., Jang, T. L., Zhu, L. J., Chen, L., Yang, X. J., et al. (2009). Nuclear factor-kappaB-mediated transforming growth factor-beta-induced expression of vimentin is an independent predictor of biochemical recurrence after radical prostatectomy. *Clin. Cancer Res.* 15, 3557–3567. doi: 10.1158/1078-0432.CCR-08-1656

Zhao, H., Thong, A., Nolley, R., Reese, S. W., Santos, J., Ingels, A., et al. (2013). Patient-derived tissue slice grafts accurately depict response of high-risk primary prostate cancer to androgen deprivation therapy. *J. Transl. Med.* 11:199. doi: 10.1186/1479-5876-11-199

Zhifang, M., Liang, W., Wei, Z., Bin, H., Rui, T., Nan, W., et al. (2015). The androgen receptor plays a suppressive role in epithelial-mesenchymal transition of human prostate cancer stem progenitor cells. *BMC Biochem.* 16:13. doi: 10.1186/s12858-015-0042-9

Zhu, M.-L., and Kyprianou, N. (2010). Role of androgens and the androgen receptor in epithelial-mesenchymal transition and invasion of prostate cancer cells. *FASEB J.* 24, 769–777. doi: 10.1096/fj.09-136994

Zou, M., Toivanen, R., Mitrofanova, A., Floch, N., Hayati, S., Sun, Y., et al. (2017). Transdifferentiation as a mechanism of treatment resistance in a mouse model of castration-resistant prostate cancer. *Cancer Discov.* 7, 736–749. doi: 10.1158/2159-8290.CD-16-1174

Conflict of Interest: The authors declare that the research was conducted in the absence of any commercial or financial relationships that could be construed as a potential conflict of interest.

Copyright © 2020 Tiwari, Manzar and Ateeq. This is an open-access article distributed under the terms of the Creative Commons Attribution License (CC BY). The use, distribution or reproduction in other forums is permitted, provided the original author(s) and the copyright owner(s) are credited and that the original publication in this journal is cited, in accordance with accepted academic practice. No use, distribution or reproduction is permitted which does not comply with these terms.

frontiers in Molecular Biosciences

PERSPECTIVE
published: 14 July 2020
doi: 10.3389/fmolb.2020.00138

Slug and E-Cadherin: Stealth Accomplices?

Esta Sterneck, Dipak K. Poria and Kuppusamy Balamurugan**

Laboratory of Cell and Developmental Signaling, Center for Cancer Research, National Cancer Institute, Frederick, MD, United States

During physiological epithelial-mesenchymal transition (EMT), which is important for embryogenesis and wound healing, epithelial cells activate a program to remodel their structure and achieve a mesenchymal fate. In cancer cells, EMT confers increased invasiveness and tumor-initiating capacity, which contribute to metastasis and resistance to therapeutics. However, cellular plasticity that navigates between epithelial and mesenchymal states and maintenance of a hybrid or partial E/M phenotype appears to be even more important for cancer progression. Besides other core EMT transcription factors, the well-characterized Snail-family proteins Snail (*SNAI1*) and Slug (*SNAI2*) play important roles in both physiological and pathological EMT. Often mentioned in unison, they do, however, differ in their functions in many scenarios. Indeed, Slug expression does not always correlate with complete EMT or loss of E-cadherin (*CDH1*). For example, Slug plays important roles in mammary epithelial cell progenitor cell lineage commitment and differentiation, DNA damage responses, hematopoietic stem cell self-renewal, and in pathologies such as pulmonary fibrosis and atherosclerosis. In this Perspective, we highlight Slug functions in mammary epithelial cells and breast cancer as a "non-EMT factor" in basal epithelial cells and stem cells with focus reports that demonstrate co-expression of Slug and E-cadherin. We speculate that Slug and E-cadherin may cooperate in normal mammary gland and breast cancer/stem cells and advocate for functional assessment of such Slug^{+}/E-cadherin$^{low/+}$ (SNAI2^{+}/CDH1$^{low/+}$) "basal-like epithelial" cells. Thus, Slug may be regarded as less of an EMT factor than driver of the basal epithelial cell phenotype.

Keywords: mammary gland, breast cancer, epithelial-mesenchymal transition (EMT), E-cadherin (CDH1), Slug (SNAI2), basal, luminal

OPEN ACCESS

Edited by:
Satyendra Chandra Tripathi, All India Institute of Medical Sciences Nagpur, India

Reviewed by:
Shivendra Vikram Singh, St. Jude Children's Research Hospital, United States
Wenjun Guo, Albert Einstein College of Medicine, United States
Saurav Kumar, Fred Hutchinson Cancer Research Center, United States

****Correspondence:***
Esta Sterneck
sternecg@nih.gov
Kuppusamy Balamurugan
k.kuppusamy@nih.gov

Specialty section:
This article was submitted to Molecular Diagnostics and Therapeutics, a section of the journal Frontiers in Molecular Biosciences

Received: *22 April 2020*
Accepted: *08 June 2020*
Published: *14 July 2020*

Citation:
Sterneck E, Poria DK and Balamurugan K (2020) Slug and E-Cadherin: Stealth Accomplices? Front. Mol. Biosci. 7:138. doi: 10.3389/fmolb.2020.00138

INTRODUCTION

Phenotypic plasticity refers to the ability of cells to change their phenotype such as transitioning from epithelial to mesenchymal characteristics or from stem cell to a differentiated state. This plasticity may be one-directional or reversible and transient or permanent. In addition, cells may inhabit any state between such defined phenotypes in a stable or metastable manner. The cellular plasticity of cancer cells relies on molecular mechanisms from the playbook of normal embryonic or postnatal development. The mammary gland is a particularly dynamic organ undergoing expansion and differentiation during pregnancy and early lactation, followed by cell death and remodeling during the course of weaning (Richert et al., 2000; Shamir and Ewald, 2015). One type of plasticity, the epithelial-mesenchymal transition (EMT) is an important process for normal development and tumor biology. During EMT cells lose their epithelial polarization and organization and E-cadherin

expression is drastically reduced through active inhibition of gene expression (Micalizzi et al., 2010). Thus, E-cadherin downregulation is often used as a (surrogate) marker for EMT. Snail and Slug are two transcription factors that can directly repress the E-cadherin gene (*CDH1*) promoter while activating the promoters of key mesenchymal genes such as ZEB1 and vimentin (Ye et al., 2015; Xu et al., 2019). For comprehensive background information, we refer the reader to a number of excellent recent reviews, which summarize Slug functions and regulation of expression (Zhou et al., 2019), regulation by posttranslational modifications (Xu et al., 2019), and the non-redundant functions of EMT factors (Stemmler et al., 2019).

Snail and Slug are often named in unison as if functionally synonymous, and expression of Slug alone suggested as indication of a mesenchymal gene program. However, the endogenous functions of Snail and Slug can vary significantly, in part due to differences in DNA-binding affinity and interaction partners. Thus, Slug and Snail have overlapping (e.g., *CDH1, VIM*) as well-distinct sets of target genes (e.g., *L1CAM, PTEN*) (Stemmler et al., 2019; Xu et al., 2019). Slug plays a role in maintaining the structure of the normal mammary gland and modulates the specific phenotypes of breast cancer subtypes (Phillips and Kuperwasser, 2014). Overexpression of ectopic Slug may lead to cellular responses that mimic Snail functions, such as inhibition of *CDH1* gene expression. However, at physiological levels, Slug and E-cadherin are often co-expressed. Thus, results from overexpression studies and cell culture paradigms, as has been noted before (Alves et al., 2009), have created the perception of Slug as an EMT transcription factor, when many times it is not. The above-mentioned reviews provide numerous examples for the role of Slug in EMT. Whether Slug can execute this role in the absence of its partner Snail, has perhaps not been addressed in detail. In experimental systems where Slug "inhibits expression of E-cadherin," it may be reduced but not abolished (e.g., Leong et al., 2007). The co-occurrence of Slug and E-cadherin may be particularly relevant for hybrid EMT and cellular plasticity, which are being recognized as important factors in cancer progression (Jolly et al., 2018; Aiello and Kang, 2019; Gupta et al., 2019), along with the role of E-cadherin in not only the establishment of metastases but also the process of dissemination (Rodriguez et al., 2012; Padmanaban et al., 2019; Voglstaetter et al., 2019). In this Perspective, we want to highlight examples of co-expression of Slug and E-cadherin and hypothesize on its relevance for tumor biology.

SLUG PROMOTES THE BASAL CELL PHENOTYPE AND STEMNESS IN THE MAMMARY EPITHELIUM: NOT WITHOUT E-CADHERIN?

The mammary gland epithelium is a bilayer of luminal epithelial cells and basal/myoepithelial cells that express unique sets of cytokeratins. Within each layer are subsets of cells with different characteristics based on e.g., expression of specific steroid hormone receptors and stem cell or lineage progenitors properties (Visvader and Stingl, 2014). To our knowledge, Slug protein expression has not been investigated in normal human mammary stem/progenitor cells. Mouse models have, however, provided significant insights about Slug's function in development. Slug is expressed in basal mammary epithelial cells (MECs) and is the only EMT factor that is enriched in both mouse and (by mRNA) human mammary stem cells (MaSC) that reside within this compartment (Lim et al., 2010; Guo et al., 2012; Nassour et al., 2012). Interestingly, *SNAI2*/Slug mRNA expression is detectable in human luminal progenitors (albeit at significantly lower levels compared to basal cells) but not in their mouse counterpart (Lim et al., 2010). Its functional significance has yet to be determined but may be relevant for the development of luminal breast cancer (see below). Slug plays an important role in maintaining stemness in cooperation with proteins such as Sox9 and the chromatin modifier LSD1 (Guo et al., 2012; Phillips et al., 2014; Bai et al., 2017). In addition, Slug determines progenitor cell lineage commitment and differentiation by actively repressing the luminal cell state (Phillips and Kuperwasser, 2014). Snail, on the other hand, is expressed in the mesenchymal stromal fibroblasts surrounding the mammary duct and not in normal mammary epithelial cells (Nassour et al., 2012; Ye et al., 2015). P-cadherin (*CDH3*), the classical myoepithelial cadherin (Shamir and Ewald, 2015), is a target gene of Slug and mediates many of its functions (Idoux-Gillet et al., 2018). E-cadherin is highly expressed in luminal cells, but Slug expressing basal cells also express E-cadherin (Ye et al., 2015). E-cadherin localizes to the lateral cell-junctions. Basal cells and luminal cells are very different in size and shape. Most likely, normal cells engage feedback mechanisms to regulate the levels of E-cadherin based on their cell-cell contacts. How should one compare the "functionally equivalent" amounts of E-cadherin cell-cell adhesions? For these reasons, here we use the term "E-cadherin+" to refer to cells that express any detectable amount of the protein.

Surprisingly, Slug-deficiency does not impair the regeneration capacity of transplanted mammary tissue fragments although lineage dynamics were compromised (Nassour et al., 2012). However, when the tissue was dissociated, the organoid-forming and gland-reconstituting activities of stem cells are dependent on Slug (Guo et al., 2012; Phillips et al., 2014). The apparent paradox might be explained by a pro-survival function of Slug in stem cells that becomes apparent in the dissociation paradigm and could also be relevant for cancer stem cell assays. Whether E-cadherin plays a role in MaSCs is not known (**Figure 1**). However, E-cadherin is important for pluripotency in embryonic stem cells through cooperation with the Wnt signaling pathway (Pieters and van Roy, 2014). Studies of the mechanisms leading to expansion of the mammary gland during pregnancy revealed that a TGFβ2/integrin-αvβ3 pathway induces Slug protein accumulation in MaSCs without affecting mRNA expression or overt EMT signatures. Knockdown of αvβ3 in MDA-MB-231 cells reduced Slug expression and compromised survival of tumor initiating cells (Desgrosellier et al., 2014). In addition, Slug has a role in genome maintenance. *Slug* knockout mice exhibited premature aging of mammary epithelium with loss of mammary stem cell activity, luminal differentiation of basal cells, and increased DNA damage due to replicative stress (Gross et al., 2019). Conceivably, this function could also contribute to cancer stem cell maintenance and resistance to chemotherapeutics.

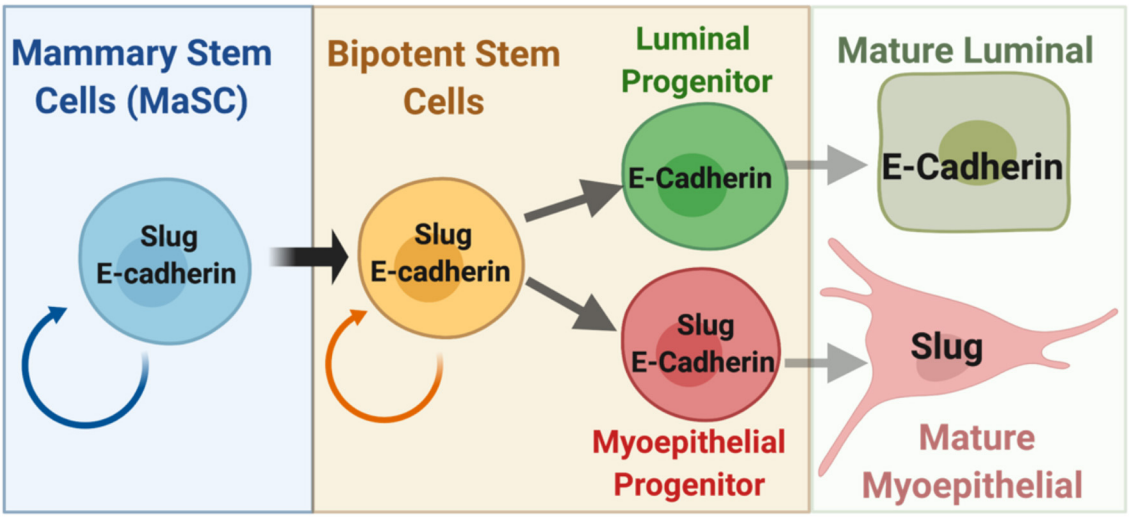

FIGURE 1 | Schematic of the mammary epithelial stem cell hierarchy depicting the known and proposed relationships of Slug and E-cadherin (see text for details). Relative differences in expression levels between cells can be assumed but are not depicted. Figure was created with BioRender.com.

Unexpectedly though, Slug knockout impairs MEC death during post-lactational mammary gland involution (Castillo-Lluva et al., 2015). The contrast of functions in developmental cell death vs. promoting cancer cell survival is not unique to Slug but also seen with STAT3 and C/EBPδ transcription factors (Balamurugan and Sterneck, 2013; Resemann et al., 2014). In summary, studies in mouse models demonstrate that Slug determines a basal MEC phenotype and promotes mammary stem cell self-renewal, genomic maintenance and cell survival, all of which is at least compatible with E-cadherin expression.

SLUG AND BREAST CANCER STEM CELLS: WHICH ONES, AND WHAT ABOUT E-CADHERIN?

Breast cancer (BC) is classified into subtypes based on expression of hormone receptors and HER2, which are usually associated with a luminal cell phenotype. Triple negative breast cancer (TNBC) lacking expression of these markers presents mostly with a basal or basal-like BC (BLBC) phenotype. Mesenchymal markers are enriched in a subset of TNBCs and are correlated with stemness properties (Dai et al., 2016). Despite controversies surrounding the cancer stem cell (CSC) theory, the concept has contributed to the identification of cancer cell plasticity and important mechanisms underlying tumor progression (Wang et al., 2015). Various cell surface molecules (e.g., CD44, CD24, CD133) and combinations thereof as well as ALDH activity have been used to enrich for cells with stemness properties and their frequency varies by BC subtype (Rodriguez et al., 2019). The $CD44^{+}/CD24^{-/low}$ CSCs are mesenchymal-like while $ALDH1^{+}$ and $CD44^{+}/CD24^{+}$ stem cells are epithelial-like. In node-positive BC, co-occurrence of ALDH1 and Slug in primary lesions was associated with shorter disease-free survival, though co-expression at the single cell level was not assessed (Ito et al., 2016). Transcriptomic analysis of patient-derived xenograft models showed that *SNAI2*/Slug mRNA was enriched in the mesenchymal CSCs "consistent" with its classification as an "EMT factor" (Liu et al., 2018). However, low levels of mRNA do not preclude Slug protein expression as shown for HMLER hybrid E/M cells (Kroger et al., 2019). Slug expression and its role in distinct types of tumor initiating cells with low proteasome activity, high STAT3, or SOX2/OCT4 activity has not been investigated (Vlashi et al., 2013; Wei et al., 2014; Tang et al., 2015). However, Slug was shown to be important for survival of integrin αvβ3/Src-induced CSCs that also express E-cadherin and exist across BC subtypes (Sun et al., 2018). Mesenchymal $CD44^{+}/CD24^{-/low}$ CSCs do not express E-cadherin but gain further tumor initiating capacity with the expression of the epithelial adhesion molecule EpCAM that marks "hybrid E/M" states (Dittmer, 2018). In BLBC cell lines, the p63 transcription factor, which is important for MaSCs (Memmi et al., 2015), promotes invasiveness through Slug without compromising E-cadherin expression (Dang et al., 2015). It is thus conceivable that E-cadherin may be important for a subset of breast CSCs. E-cadherin promotes BC cell mammosphere formation, a measure of stem cell self-renewal (Manuel Iglesias et al., 2013). E-cadherin can promote stemness in lung and gastric cancer cells (Tang et al., 2019; Ye et al., 2020) and signaling pathways that are known to support CSCs such as by EGFR (Rodriguez et al., 2012; Steelman et al., 2016), LIFR (del Valle et al., 2013), and Wnt (Pieters and van Roy, 2014). To our knowledge, the expression and potential function of E-cadherin in different types of BC stem cells has not been analyzed to date.

BRIEF UPDATE ON SLUG IN BREAST CANCER: QUITE BASAL AND TO THE BONE—ALONG WITH E-CADHERIN?

Not surprisingly, Slug expression is preferentially observed in basal/TNBC as are mesenchymal and stemness markers.

Compelling evidences for an important role of Slug in human breast cancer and mechanistic underpinnings have been reviewed (Phillips and Kuperwasser, 2014; Zhou et al., 2019). Here, we want to point out that the majority of basal/TNBC cancers do, however, not lose E-cadherin expression (Rodriguez et al., 2012; Horne et al., 2018). In support of the dissociation of Slug from the EMT processes, expression of Slug protein or E-cadherin (*CDH1*) mRNA were not correlated with the activation of a core EMT gene expression signature in breast cancer (Savci-Heijink et al., 2019). However, aberrant expression of Slug explains the emergence of basal tumor phenotypes from luminal progenitors (Phillips and Kuperwasser, 2014), or conversion of a luminal to basal phenotype through TGFβ (Sflomos et al., 2016). Furthermore, Slug contributes to treatment resistance of luminal cancers in part through promoting a phenotypic shift to a basal phenotype such as in HER2+ cells (Oliveras-Ferraros et al., 2012) and ER+ cells (Tsou et al., 2015; Geng et al., 2016; Alves et al., 2018). In addition, Slug expression in ER+ BC cell lines also promotes mammosphere formation, proliferation and invasive properties (Storci et al., 2010; Chimge et al., 2011; Mendoza-Villanueva et al., 2016; Manne et al., 2017). Interestingly, although *CDH1* mRNA levels increased with Slug knockdown in drug-resistant MCF-7 cells, total E-cadherin protein levels did not (Alves et al., 2018). A negative feedback loop between Slug and ER is seen in ER+ breast cancer cell lines, where estrogen inhibits TGFβ-induced EMT by suppressing Slug but not Snail expression (Liu et al., 2019). In the context of RUNX2/TGFβ/Wnt-signaling, a balanced expression of Slug and ERα is implicated in bone metastasis of ER+ BC cell lines (Chimge et al., 2011). Furthermore, in TNBC cell lines, Slug promotes bone metastasis but not lung infiltration (Ferrari-Amorotti et al., 2014). Given the implications of integrin αvβ3 in bone metastasis of various epithelial cancers (Kwakwa and Sterling, 2017), above-mentioned role of Slug in the integrin $\alpha v\beta 3^+$ breast CSCs that do express E-cadherin (Sun et al., 2018), and elevated E-cadherin expression in BC bone metastases (Saha et al., 2007; Matteucci et al., 2013), we hypothesize that E-cadherin expressing $\alpha v\beta 3^+/Slug^+$ stem-like cells could play a significant role in breast cancer bone metastasis.

SLUG AND EMT: GUILTY BY ASSOCIATION?

Without doubt, Slug's cousin Snail is a potent mediator of EMT. Slug and Snail are often coordinately expressed (Katoh, 2011), and Slug can thereby be implicated in EMT as "caught at the scene." For example, in breast cancers that show correlation of Slug and Snail with lymph node metastasis, only Slug expression was seen in more histologically semi-differentiated structures. The observation led the authors to the hypothesis (foresight?) that each drives distinct tumor invasion modes (Come et al., 2006). Investigations of the mouse MMTV-PyMT tumor model showed that Snail expressing cells are mesenchymal while Slug expressing cells exhibited an epithelial phenotype. Despite a large number of common target genes, only Snail occupied the promoters of key mesenchymal marker genes (Ye et al., 2015). In MDA-MB-231 cells, Snail was necessary for binding of Slug to the ZEB1 promoter and its activation indicating that Slug alone may not drive EMT in the absence of Snail (Ye et al., 2015). On the other hand, Slug can *attenuate* E-cadherin levels indirectly by post-transcriptional mechanisms through miR-221 and by promoting protein degradation (Pan et al., 2016; Anzai et al., 2017). Using oncogene-transformed human mammary epithelial cells (HMLER), Kroger et al. showed that Slug protein expression in such epithelial cells was similar to that in mesenchymal and hybrid E/M cells. Only epithelial cells expressed E-cadherin. Mesenchymal cells had the highest levels of ZEB1, while hybrid E/M cells exhibited the most Snail expression along with CSC activity. Interestingly, hybrid E/M cells showed significant downregulation of Slug mRNA but no change at the protein level, suggesting significant stabilization of Slug protein in these cells (Kroger et al., 2019). While the mRNA data are consistent with reports that Snail can repress Slug/*SNAI2* expression (Sundararajan et al., 2019), such results illustrate the importance of protein data even when mRNA expression is downregulated. Indeed, several mechanisms for stabilization of the Slug protein have been reported (Xu et al., 2019; Zhou et al., 2019). In the MMTV-PyMT mouse tumor model, $Slug^+$ populations also express E-cadherin and a subpopulation of $Slug^+$ cells also express EpCAM. Immunocytochemistry showed at the single cell level that among human basal breast cancer cell lines, there are various percentages of single and double positive cells for Slug and Snail protein (Ye et al., 2015). E-cadherin was not evaluated here, but these may be good models to mechanistically dissect the expression and function of E-cadherin in $Slug^+$ cells.

The specific position of a cell along the E-M continuum may depend in part on the expression levels of Snail vs. Slug and their fine-tuning of E-cadherin expression levels. Mutual regulation of Snail and Slug has also been described in other cell types. Snail inhibits Slug in ovarian cancer cell lines, i.e., Slug is downregulated during EMT (Sundararajan et al., 2019). Snail and Slug engage in mutual negative feedback of expression during bone development (Chen and Gridley, 2013). In oral squamous carcinoma cell lines, Snail and Slug can engage in mutual attenuation of expression although both are induced by TGFβ (Nakamura et al., 2018). Lastly, Slug can support its own gene transcription in cooperation with Sox9 during embryonic development, i.e., when SOX9 is induced by BMP and Wnt signaling, Slug expression self-amplifies (Sakai et al., 2006). These types of feedback regulation may not only balance their relative expression levels but play a role in generating a metastable cell phenotype with Slug/Snail ratios performing the function of an E/M rheostat and tuning the expression level of E-cadherin.

DISCUSSION: WHAT ARE THE FRONTIERS?

A comprehensive analysis of Slug's prognostic/predictive biomarker potential and correlation with E-cadherin expression at single cell resolution with well-validated antibodies is still outstanding. Stratification by subtype and additional clinical

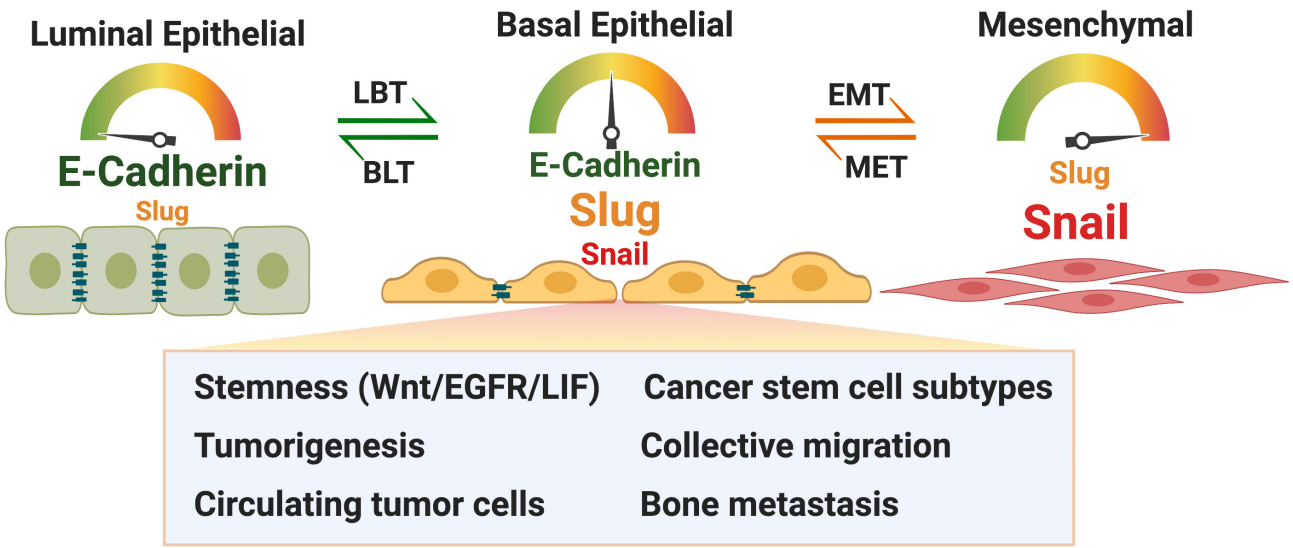

FIGURE 2 | Model describing expression of E-cadherin and Slug in luminal epithelial, basal epithelial and mesenchymal cancer cells and the proposed qualities of basal epithelial cancer cells due to co-expression of Slug and E-cadherin. Luminal basal transition (LBT) and basal luminal transition (BLT) are proposed terminologies in addition to EMT and MET. See text for details. Figure was created with BioRender.com.

criteria and biomarkers will be essential to gain significant insight. Because nuclear expression of Slug has also been correlated with cytoplasmic E-cadherin staining (Prasad et al., 2009), subcellular resolution may be important as well as consideration of E-cadherin isoforms (Ye et al., 2013; Konze et al., 2014; Wu et al., 2016). Similarly, sensitive single cell resolution analysis of Slug and E-cadherin *protein* expression among the diversity of cells in the mouse and human mammary epithelium and breast cancer may bring about new frontiers for functional studies.

Figure 2 summarizes cancer cell-related hypotheses on E-cadherin expression in relation to Slug and their potentially cooperative contribution to cancer progression. Due to the limited scope of this Perspective, the many other factors that are known to modulate these phenotypes were not included. A cell that expresses a moderate level of E-cadherin and Slug may be in a particular goldilocks state that facilitates these functions. Increasingly, a role for E-cadherin in cancer cell dissemination is being recognized (see Introduction). Collective migration/dissemination is one aspect in which Slug and E-cadherin may cooperate (Dang et al., 2015), and $Slug^{+}$/E-$cadherin^{+}$ cells may be particularly relevant in metastasis to the bone. In these contexts, the E-$cadherin^{+}$ cell may not be expressing high but still functionally relevant levels of E-cadherin. As hybrid E/M phenotypes in circulating tumor cells (CTCs) reveal strong association with tumor-initiation potential and metastasis (Fabisiewicz et al., 2020), $Slug^{+}$/E-$cadherin^{+}$ cells are likely contributors to disseminating CTCs as well, perhaps in part through inhibition of anoikis or E-cadherin's potential to support stemness promoting signaling pathways.

The epithelial cadherin EpCAM has received much attention for its expression and functions in tumor cells (Dittmer, 2018). It is time that E-cadherin emerges from its shadow and sheds the prevailing image of being (only) a tumor suppressor. Considering mesenchymal vs. epithelial state and luminal vs. basal state along with time of development (of the organ or tumor) and space (microenvironment), cells navigate at least these six dimensions to attain a particular phenotype, challenging our need for classification. Regard for $Slug^{+}$/E-$cadherin^{+/low}$ cells may in part address this challenge and contribute to better understanding of cancer biology.

AUTHOR CONTRIBUTIONS

ES and KB performed literature research and wrote the manuscript. DP reviewed literature, co-wrote the manuscript, and generated the figures. All authors contributed to the article and approved the submitted version.

FUNDING

The authors are supported by the Intramural Research Program of the NIH, National Cancer Institute.

ACKNOWLEDGMENTS

The authors apologize for not being able to discuss and cite a large body of relevant publications due to space limitations and the scope of the Perspective. Figures were created with BioRender.com.

REFERENCES

Aiello, N. M., and Kang, Y. (2019). Context-dependent EMT programs in cancer metastasis. *J. Exp. Med.* 216, 1016–1026. doi: 10.1084/jem.20181827

Alves, C. C., Carneiro, F., Hoefler, H., and Becker, K. F. (2009). Role of the epithelial-mesenchymal transition regulator Slug in primary human cancers. *Front. Biosci.* 14, 3035–3050. doi: 10.2741/3433

Alves, C. L., Elias, D., Lyng, M. B., Bak, M., and Ditzel, H. J. (2018). SNAI2 upregulation is associated with an aggressive phenotype in fulvestrant-resistant breast cancer cells and is an indicator of poor response to endocrine therapy in estrogen receptor-positive metastatic breast cancer. *Breast Cancer Res.* 20:60. doi: 10.1186/s13058-018-0988-9

Anzai, E., Hirata, K., Shibazaki, M., Yamada, C., Morii, M., Honda, T., et al. (2017). FOXA1 induces E-cadherin expression at the protein level via suppression of slug in epithelial breast cancer cells. *Biol. Pharm. Bull.* 40, 1483–1489. doi: 10.1248/bpb.b17-00307

Bai, J. W., Chen, M. N., Wei, X. L., Li, Y. C., Lin, H. Y., Chen, M., et al. (2017). The zinc-finger transcriptional factor Slug transcriptionally downregulates ERα by recruiting lysine-specific demethylase 1 in human breast cancer. *Oncogenesis* 6:e330. doi: 10.1038/oncsis.2017.38

Balamurugan, K., and Sterneck, E. (2013). The many faces of C/EBPδ and their relevance for inflammation and cancer. *Int. J. Biol. Sci.* 9, 917–933. doi: 10.7150/ijbs.7224

Castillo-Lluva, S., Hontecillas-Prieto, L., Blanco-Gomez, A., Del Mar Saez-Freire, M., Garcia-Cenador, B., Garcia-Criado, J., et al. (2015). A new role of SNAI2 in postlactational involution of the mammary gland links it to luminal breast cancer development. *Oncogene* 34, 4777–4790. doi: 10.1038/onc.2015.224

Chen, Y., and Gridley, T. (2013). Compensatory regulation of the Snai1 and Snai2 genes during chondrogenesis. *J. Bone Miner. Res.* 28, 1412–1421. doi: 10.1002/jbmr.1871

Chimge, N. O., Baniwal, S. K., Little, G. H., Chen, Y. B., Kahn, M., Tripathy, D., et al. (2011). Regulation of breast cancer metastasis by Runx2 and estrogen signaling: the role of SNAI2. *Breast Cancer Res.* 13:R127. doi: 10.1186/bcr3073

Come, C., Magnino, F., Bibeau, F., de Santa Barbara, P., Becker, K. F., Theillet, C., et al. (2006). Snail and slug play distinct roles during breast carcinoma progression. *Clin. Cancer Res.* 12, 5395–5402. doi: 10.1158/1078-0432.CCR-06-0478

Dai, X., Xiang, L., Li, T., and Bai, Z. (2016). Cancer hallmarks, biomarkers and breast cancer molecular subtypes. *J. Cancer* 7, 1281–1294. doi: 10.7150/jca.13141

Dang, T. T., Esparza, M. A., Maine, E. A., Westcott, J. M., and Pearson, G. W. (2015). ΔNp63α promotes breast cancer cell motility through the selective activation of components of the epithelial-to-mesenchymal transition program. *Cancer Res.* 75, 3925–3935. doi: 10.1158/0008-5472.CAN-14-3363

del Valle, I., Rudloff, S., Carles, A., Li, Y., Liszewska, E., Vogt, R., et al. (2013). E-cadherin is required for the proper activation of the Lifr/Gp130 signaling pathway in mouse embryonic stem cells. *Development* 140, 1684–1692. doi: 10.1242/dev.088690

Desgrosellier, J. S., Lesperance, J., Seguin, L., Gozo, M., Kato, S., Franovic, A., et al. (2014). Integrin alphavbeta3 drives slug activation and stemness in the pregnant and neoplastic mammary gland. *Dev. Cell* 30, 295–308. doi: 10.1016/j.devcel.2014.06.005

Dittmer, J. (2018). Breast cancer stem cells: features, key drivers and treatment options. *Semin. Cancer Biol.* 53, 59–74. doi: 10.1016/j.semcancer.2018.07.007

Fabisiewicz, A., Szostakowska-Rodzos, M., Zaczek, A. J., and Grzybowska, E. A. (2020). Circulating tumor cells in early and advanced breast cancer; biology and prognostic value. *Int. J. Mol. Sci.* 21:1671. doi: 10.3390/ijms21051671

Ferrari-Amorotti, G., Chiodoni, C., Shen, F., Cattelani, S., Soliera, A. R., Manzotti, G., et al. (2014). Suppression of invasion and metastasis of triple-negative breast cancer lines by pharmacological or genetic inhibition of slug activity. *Neoplasia* 16, 1047–1058. doi: 10.1016/j.neo.2014.10.006

Geng, C., Li, J., Ding, F., Wu, G., Yang, Q., Sun, Y., et al. (2016). Curcumin suppresses 4-hydroxytamoxifen resistance in breast cancer cells by targeting SLUG/Hexokinase 2 pathway. *Biochem. Biophys. Res. Commun.* 473, 147–153. doi: 10.1016/j.bbrc.2016.03.067

Gross, K. M., Zhou, W., Breindel, J. L., Ouyang, J., Jin, D. X., Sokol, E. S., et al. (2019). Loss of slug compromises DNA damage repair and accelerates stem cell aging in mammary epithelium. *Cell Rep. 28,* 394–407.e6. doi: 10.1016/j.celrep.2019.06.043

Guo, W., Keckesova, Z., Donaher, J. L., Shibue, T., Tischler, V., Reinhardt, F., et al. (2012). Slug and Sox9 cooperatively determine the mammary stem cell state. *Cell* 148, 1015–1028. doi: 10.1016/j.cell.2012.02.008

Gupta, P. B., Pastushenko, I., Skibinski, A., Blanpain, C., and Kuperwasser, C. (2019). Phenotypic plasticity: driver of cancer initiation, progression, and therapy resistance. *Cell Stem Cell* 24, 65–78. doi: 10.1016/j.stem.2018.11.011

Horne, H. N., Oh, H., Sherman, M. E., Palakal, M., Hewitt, S. M., Schmidt, M. K., et al. (2018). E-cadherin breast tumor expression, risk factors and survival: pooled analysis of 5,933 cases from 12 studies in the breast cancer association consortium. *Sci. Rep.* 8:6574. doi: 10.1038/s41598-018-23733-4

Idoux-Gillet, Y., Nassour, M., Lakis, E., Bonini, F., Theillet, C., Du Manoir, S., et al. (2018). Slug/Pcad pathway controls epithelial cell dynamics in mammary gland and breast carcinoma. *Oncogene* 37, 578–588. doi: 10.1038/onc.2017.355

Ito, M., Shien, T., Omori, M., Mizoo, T., Iwamoto, T., Nogami, T., et al. (2016). Evaluation of aldehyde dehydrogenase 1 and transcription factors in both primary breast cancer and axillary lymph node metastases as a prognostic factor. *Breast Cancer* 23, 437–444. doi: 10.1007/s12282-015-0583-1

Jolly, M. K., Mani, S. A., and Levine, H. (2018). Hybrid epithelial/mesenchymal phenotype(s): The 'fittest' for metastasis? *Biochim. Biophys. Acta Rev. Cancer* 1870, 151–157. doi: 10.1016/j.bbcan.2018.07.001

Katoh, M. (2011). Network of WNT and other regulatory signaling cascades in pluripotent stem cells and cancer stem cells. *Curr. Pharm. Biotechnol.* 12, 160–170. doi: 10.2174/138920111794295710

Konze, S. A., van Diepen, L., Schroder, A., Olmer, R., Moller, H., Pich, A., et al. (2014). Cleavage of E-cadherin and β-catenin by calpain affects Wnt signaling and spheroid formation in suspension cultures of human pluripotent stem cells. *Mol. Cell. Proteomics* 13, 990–1007. doi: 10.1074/mcp.M113.033423

Kroger, C., Afeyan, A., Mraz, J., Eaton, E. N., Reinhardt, F., Khodor, Y. L., et al. (2019). Acquisition of a hybrid E/M state is essential for tumorigenicity of basal breast cancer cells. *Proc. Natl. Acad. Sci. U.S.A.* 116, 7353–7362. doi: 10.1073/pnas.1812876116

Kwakwa, K. A., and Sterling, J. A. (2017). Integrin αvβ3 signaling in tumor-induced bone disease. *Cancers* 9:84. doi: 10.3390/cancers9070084

Leong, K. G., Niessen, K., Kulic, I., Raouf, A., Eaves, C., Pollet, I., et al. (2007). Jagged1-mediated Notch activation induces epithelial-to-mesenchymal transition through Slug-induced repression of E-cadherin. *J. Exp. Med.* 204, 2935–2948. doi: 10.1084/jem.20071082

Lim, E., Wu, D., Pal, B., Bouras, T., Asselin-Labat, M. L., Vaillant, F., et al. (2010). Transcriptome analyses of mouse and human mammary cell subpopulations reveal multiple conserved genes and pathways. *Breast Cancer Res.* 12:R21. doi: 10.1186/bcr2560

Liu, B. W., Yu, Z. H., Chen, A. X., Chi, J. R., Ge, J., Yu, Y., et al. (2019). Estrogen receptor- α-miR-1271-SNAI2 feedback loop regulates transforming growth factor-β-induced breast cancer progression. *J. Exp. Clin. Cancer Res.* 38:109. doi: 10.1186/s13046-019-1112-4

Liu, M., Liu, Y., Deng, L., Wang, D., He, X., Zhou, L., et al. (2018). Transcriptional profiles of different states of cancer stem cells in triple-negative breast cancer. *Mol. Cancer* 17:65. doi: 10.1186/s12943-018-0809-x

Manne, R. K., Agrawal, Y., Bargale, A., Patel, A., Paul, D., Gupta, N. A., et al. (2017). A MicroRNA/ubiquitin ligase feedback loop regulates slug-mediated invasion in breast cancer. *Neoplasia* 19, 483–495. doi: 10.1016/j.neo.2017.02.013

Manuel Iglesias, J., Beloqui, I., Garcia-Garcia, F., Leis, O., Vazquez-Martin, A., Eguiara, A., et al. (2013). Mammosphere formation in breast carcinoma cell lines depends upon expression of E-cadherin. *PLoS ONE* 8:e77281. doi: 10.1371/journal.pone.0077281

Matteucci, E., Maroni, P., Luzzati, A., Perrucchini, G., Bendinelli, P., and Desiderio, M. A. (2013). Bone metastatic process of breast cancer involves methylation state affecting E-cadherin expression through TAZ and WWOX nuclear effectors. *Eur. J. Cancer* 49, 231–244. doi: 10.1016/j.ejca.2012.05.006

Memmi, E. M., Sanarico, A. G., Giacobbe, A., Peschiaroli, A., Frezza, V., Cicalese, A., et al. (2015). p63 Sustains self-renewal of mammary cancer stem cells through regulation of Sonic Hedgehog signaling. *Proc. Natl. Acad. Sci. U.S.A.* 112, 3499–3504. doi: 10.1073/pnas.1500762112

Mendoza-Villanueva, D., Balamurugan, K., Ali, H. R., Kim, S. R., Sharan, S., Johnson, R. C., et al. (2016). The C/EBPδ protein is stabilized by estrogen receptor α activity, inhibits SNAI2 expression and associates with good prognosis in breast cancer. *Oncogene* 35, 6166–6176. doi: 10.1038/onc.2016.156

Micalizzi, D. S., Farabaugh, S. M., and Ford, H. L. (2010). Epithelial-mesenchymal transition in cancer: parallels between normal development and tumor progression. *J. Mammary Gland Biol. Neoplasia* 15, 117–134. doi: 10.1007/s10911-010-9178-9

Nakamura, R., Ishii, H., Endo, K., Hotta, A., Fujii, E., Miyazawa, K., et al. (2018). Reciprocal expression of slug and snail in human oral cancer cells. *PLoS ONE* 13:e0199442. doi: 10.1371/journal.pone.0199442

Nassour, M., Idoux-Gillet, Y., Selmi, A., Come, C., Faraldo, M. L., Deugnier, M. A., et al. (2012). Slug controls stem/progenitor cell growth dynamics during mammary gland morphogenesis. *PLoS ONE* 7:e53498. doi: 10.1371/journal.pone.0053498

Oliveras-Ferraros, C., Corominas-Faja, B., Cufi, S., Vazquez-Martin, A., Martin-Castillo, B., Iglesias, J. M., et al. (2012). Epithelial-to-mesenchymal transition (EMT) confers primary resistance to trastuzumab (herceptin). *Cell Cycle* 11, 4020–4032. doi: 10.4161/cc.22225

Padmanaban, V., Krol, I., Suhail, Y., Szczerba, B. M., Aceto, N., Bader, J. S., et al. (2019). E-cadherin is required for metastasis in multiple models of breast cancer. *Nature* 573, 439–444. doi: 10.1038/s41586-019-1526-3

Pan, Y., Li, J., Zhang, Y., Wang, N., Liang, H., Liu, Y., et al. (2016). Slug-upregulated miR-221 promotes breast cancer progression through suppressing E-cadherin expression. *Sci. Rep.* 6:25798. doi: 10.1038/srep25798

Phillips, S., and Kuperwasser, C. (2014). SLUG: Critical regulator of epithelial cell identity in breast development and cancer. *Cell Adh. Migr.* 8, 578–587. doi: 10.4161/19336918.2014.972740

Phillips, S., Prat, A., Sedic, M., Proia, T., Wronski, A., Mazumdar, S., et al. (2014). Cell-state transitions regulated by SLUG are critical for tissue regeneration and tumor initiation. *Stem Cell Rep.* 2, 633–647. doi: 10.1016/j.stemcr.2014.03.008

Pieters, T., and van Roy, F. (2014). Role of cell-cell adhesion complexes in embryonic stem cell biology. *J Cell Sci.* 127(Pt. 12), 2603–2613. doi: 10.1242/jcs.146720

Prasad, C. P., Rath, G., Mathur, S., Bhatnagar, D., Parshad, R., and Ralhan, R. (2009). Expression analysis of E-cadherin, Slug and GSK3β in invasive ductal carcinoma of breast. *BMC Cancer* 9:325. doi: 10.1186/1471-2407-9-325

Resemann, H. K., Watson, C. J., and Lloyd-Lewis, B. (2014). The Stat3 paradox: a killer and an oncogene. *Mol. Cell. Endocrinol.* 382, 603–611. doi: 10.1016/j.mce.2013.06.029

Richert, M. M., Schwertfeger, K. L., Ryder, J. W., and Anderson, S. M. (2000). An atlas of mouse mammary gland development. *J. Mammary Gland Biol. Neoplasia* 5, 227–241. doi: 10.1023/A:1026499523505

Rodriguez, D., Ramkairsingh, M., Lin, X., Kapoor, A., Major, P., and Tang, D. (2019). The Central contributions of breast cancer stem cells in developing resistance to endocrine therapy in estrogen receptor (ER)-positive breast cancer. *Cancers* 11:1028. doi: 10.3390/cancers11071028

Rodriguez, F. J., Lewis-Tuffin, L. J., and Anastasiadis, P. Z. (2012). E-cadherin's dark side: possible role in tumor progression. *Biochim. Biophys. Acta* 1826, 23–31. doi: 10.1016/j.bbcan.2012.03.002

Saha, B., Chaiwun, B., Imam, S. S., Tsao-Wei, D. D., Groshen, S., Naritoku, W. Y., et al. (2007). Overexpression of E-cadherin protein in metastatic breast cancer cells in bone. *Anticancer Res.* 27, 3903–3908.

Sakai, D., Suzuki, T., Osumi, N., and Wakamatsu, Y. (2006). Cooperative action of Sox9, Snail2 and PKA signaling in early neural crest development. *Development* 133, 1323–1333. doi: 10.1242/dev.02297

Savci-Heijink, C. D., Halfwerk, H., Hooijer, G. K. J., Koster, J., Horlings, H. M., Meijer, S. L., et al. (2019). Epithelial-to-mesenchymal transition status of primary breast carcinomas and its correlation with metastatic behavior. *Breast Cancer Res. Treat.* 174, 649–659. doi: 10.1007/s10549-018-05089-5

Sflomos, G., Dormoy, V., Metsalu, T., Jeitziner, R., Battista, L., Scabia, V., et al. (2016). A Preclinical model for ERα-positive breast cancer points to the epithelial microenvironment as determinant of luminal phenotype and hormone response. *Cancer Cell* 29, 407–422. doi: 10.1016/j.ccell.2016.02.002

Shamir, E. R., and Ewald, A. J. (2015). Adhesion in mammary development: novel roles for E-cadherin in individual and collective cell migration. *Curr. Top. Dev. Biol.* 112, 353–382. doi: 10.1016/bs.ctdb.2014.12.001

Steelman, L. S., Fitzgerald, T., Lertpiriyapong, K., Cocco, L., Follo, M. Y., Martelli, A. M., et al. (2016). Critical roles of EGFR family members in breast cancer and breast cancer stem cells: targets for therapy. *Curr. Pharm. Des.* 22, 2358–2388. doi: 10.2174/1381612822666160304151011

Stemmler, M. P., Eccles, R. L., Brabletz, S., and Brabletz, T. (2019). Non-redundant functions of EMT transcription factors. *Nat. Cell Biol.* 21, 102–112. doi: 10.1038/s41556-018-0196-y

Storci, G., Sansone, P., Mari, S., D'Uva, G., Tavolari, S., Guarnieri, T., et al. (2010). TNFalpha up-regulates SLUG via the NF-kappaB/HIF1α axis, which imparts breast cancer cells with a stem cell-like phenotype. *J. Cell. Physiol.* 225, 682–691. doi: 10.1002/jcp.22264

Sun, Q., Lesperance, J., Wettersten, H., Luterstein, E., deRose, Y. S., Welm, A., et al. (2018). Proapoptotic PUMA targets stem-like breast cancer cells to suppress metastasis. *J. Clin. Invest.* 128, 531–544. doi: 10.1172/JCI93707

Sundararajan, V., Tan, M., Tan, T. Z., Ye, J., Thiery, J. P., and Huang, R. Y. (2019). SNAI1 recruits HDAC1 to suppress SNAI2 transcription during epithelial to mesenchymal transition. *Sci. Rep.* 9:8295. doi: 10.1038/s41598-019-44826-8

Tang, B., Raviv, A., Esposito, D., Flanders, K. C., Daniel, C., Nghiem, B. T., et al. (2015). A flexible reporter system for direct observation and isolation of cancer stem cells. *Stem Cell Reports* 4, 155–169. doi: 10.1016/j.stemcr.2014.11.002

Tang, Y., Yang, G., Zhang, J., Li, X., Zhang, C., Wang, Y., et al. (2019). E-cadherin is required for the homeostasis of Lgr5(+) gastric antral stem cells. *Int. J. Biol. Sci.* 15, 34–43. doi: 10.7150/ijbs.28879

Tsou, S. H., Chen, T. M., Hsiao, H. T., and Chen, Y. H. (2015). A critical dose of doxorubicin is required to alter the gene expression profiles in MCF-7 cells acquiring multidrug resistance. *PLoS ONE* 10:e0116747. doi: 10.1371/journal.pone.0116747

Visvader, J. E., and Stingl, J. (2014). Mammary stem cells and the differentiation hierarchy: current status and perspectives. *Genes Dev.* 28, 1143–1158. doi: 10.1101/gad.242511.114

Vlashi, E., Lagadec, C., Chan, M., Frohnen, P., McDonald, A. J., and Pajonk, F. (2013). Targeted elimination of breast cancer cells with low proteasome activity is sufficient for tumor regression. *Breast Cancer Res. Treat.* 141, 197–203. doi: 10.1007/s10549-013-2688-6

Voglstaetter, M., Thomsen, A. R., Nouvel, J., Koch, A., Jank, P., Navarro, E. G., et al. (2019). Tspan8 is expressed in breast cancer and regulates E-cadherin/catenin signalling and metastasis accompanied by increased circulating extracellular vesicles. *J. Pathol.* 248, 421–437. doi: 10.1002/path.5281

Wang, T., Shigdar, S., Gantier, M. P., Hou, Y., Wang, L., Li, Y., et al. (2015). Cancer stem cell targeted therapy: progress amid controversies. *Oncotarget* 6, 44191–44206. doi: 10.18632/oncotarget.6176

Wei, W., Tweardy, D. J., Zhang, M., Zhang, X., Landua, J., Petrovic, I., et al. (2014). STAT3 signaling is activated preferentially in tumor-initiating cells in claudin-low models of human breast cancer. *Stem Cells* 32, 2571–2582. doi: 10.1002/stem.1752

Wu, S. M., Lin, W. Y., Shen, C. C., Pan, H. C., Keh-Bin, W., Chen, Y. C., et al. (2016). Melatonin set out to ER stress signaling thwarts epithelial mesenchymal transition and peritoneal dissemination via calpain-mediated C/EBPβ and NFκB cleavage. *J. Pineal Res.* 60, 142–154. doi: 10.1111/jpi.12295

Xu, R., Won, J. Y., Kim, C. H., Kim, D. E., and Yim, H. (2019). Roles of the phosphorylation of transcriptional factors in epithelial-mesenchymal transition. *J. Oncol.* 2019:5810465. doi: 10.1155/2019/5810465

Ye, T., Li, J., Sun, Z., Liu, D., Zeng, B., Zhao, Q., et al. (2020). Cdh1 functions as an oncogene by inducing self-renewal of lung cancer stem-like cells via oncogenic pathways. *Int. J. Biol. Sci.* 16, 447–459. doi: 10.7150/ijbs.38672

Ye, X., Tam, W. L., Shibue, T., Kaygusuz, Y., Reinhardt, F., Ng Eaton, E., et al. (2015). Distinct EMT programs control normal mammary stem cells and tumour-initiating cells. *Nature* 525, 256–260. doi: 10.1038/nature 14897

Ye, Y., Tian, H., Lange, A. R., Yearsley, K., Robertson, F. M., and Barsky, S. H. (2013). The genesis and unique properties of the lymphovascular tumor embolus are because of calpain-regulated proteolysis of E-cadherin. *Oncogene* 32, 1702–1713. doi: 10.1038/onc.2012.180

Zhou, W., Gross, K. M., and Kuperwasser, C. (2019). Molecular regulation of Snai2 in development and disease. *J. Cell Sci.* 132:jcs235127. doi: 10.1242/jcs. 235127

Conflict of Interest: The authors declare that the research was conducted in the absence of any commercial or financial relationships that could be construed as a potential conflict of interest.

Copyright © 2020 Sterneck, Poria and Balamurugan. This is an open-access article distributed under the terms of the Creative Commons Attribution License (CC BY). The use, distribution or reproduction in other forums is permitted, provided the original author(s) and the copyright owner(s) are credited and that the original publication in this journal is cited, in accordance with accepted academic practice. No use, distribution or reproduction is permitted which does not comply with these terms.

frontiers in Cell and Developmental Biology

ORIGINAL RESEARCH
published: 17 July 2020
doi: 10.3389/fcell.2020.00552

Id Proteins Promote a Cancer Stem Cell Phenotype in Mouse Models of Triple Negative Breast Cancer via Negative Regulation of Robo1

Wee S. Teo[1,2], Holly Holliday[1,2†], Nitheesh Karthikeyan[3†], Aurélie S. Cazet[1,2], Daniel L. Roden[1,2], Kate Harvey[1], Christina Valbirk Konrad[1], Reshma Murali[3], Binitha Anu Varghese[3], Archana P. Thankamony[3,4], Chia-Ling Chan[1,2], Andrea McFarland[1], Simon Junankar[1,2], Sunny Ye[1], Jessica Yang[1], Iva Nikolic[1,2], Jaynish S. Shah[5], Laura A. Baker[1,2], Ewan K. A. Millar[1,6,7,8], Matthew J. Naylor[1,2,9], Christopher J. Ormandy[1,2], Sunil R. Lakhani[10], Warren Kaplan[1,11], Albert S. Mellick[12,13], Sandra A. O'Toole[1,14], Alexander Swarbrick[1,2] and Radhika Nair[1,2,3]**

[1] Cancer Research Division, Garvan Institute of Medical Research, Darlinghurst, NSW, Australia, [2] Faculty of Medicine, St Vincent's Clinical School, UNSW Sydney, Sydney, NSW, Australia, [3] Cancer Research Program, Rajiv Gandhi Centre for Biotechnology, Thiruvananthapuram, India, [4] Manipal Academy of Higher Education, Manipal, India, [5] Gene & Stem Cell Therapy Program, Centenary Institute, The University of Sydney, Camperdown, NSW, Australia, [6] Department of Anatomical Pathology, NSW Health Pathology, St George Hospital, Kogarah, NSW, Australia, [7] School of Medical Sciences, UNSW Sydney, Kensington, NSW, Australia, [8] School of Medicine, Western Sydney University, Penrith, NSW, Australia, [9] School of Medical Sciences, Discipline of Physiology & Bosch Institute, University of Sydney, Sydney, NSW, Australia, [10] UQ Centre for Clinical Research, School of Medicine and Pathology Queensland, Royal Brisbane & Women's Hospital, The University of Queensland, Herston, QLD, Australia, [11] Peter Wills Bioinformatics Centre, Garvan Institute of Medical Research, Darlinghurst, NSW, Australia, [12] UNSW Medicine, University of NSW, Kensington, NSW, Australia, [13] Medical Oncology Group, Ingham Institute for Applied Medical Research, South Western Sydney Clinical School UNSW & CONCERT Translational Cancer Research Centre, Liverpool, NSW, Australia, [14] Department of Tissue Pathology and Diagnostic Oncology, Royal Prince Alfred Hospital, Camperdown, NSW, Australia

OPEN ACCESS

Edited by:
Herbert Levine,
Rice University, United States

Reviewed by:
Anantha Koteswararao Kanugula,
Northeast Ohio Medical University, United States
Erik Thompson,
Queensland University of Technology, Australia

***Correspondence:**
Alexander Swarbrick
a.swarbrick@garvan.org.au
Radhika Nair
radhikanair@rgcb.res.in

[†]These authors have contributed equally to this work

Specialty section:
This article was submitted to Molecular and Cellular Oncology, a section of the journal Frontiers in Cell and Developmental Biology

Received: 05 March 2020
Accepted: 10 June 2020
Published: 17 July 2020

Citation:
Teo WS, Holliday H, Karthikeyan N, Cazet AS, Roden DL, Harvey K, Konrad CV, Murali R, Varghese BA, Thankamony AP, Chan C-L, McFarland A, Junankar S, Ye S, Yang J, Nikolic I, Shah JS, Baker LA, Millar EKA, Naylor MJ, Ormandy CJ, Lakhani SR, Kaplan W, Mellick AS, O'Toole SA, Swarbrick A and Nair R (2020) Id Proteins Promote a Cancer Stem Cell Phenotype in Mouse Models of Triple Negative Breast Cancer via Negative Regulation of Robo1. Front. Cell Dev. Biol. 8:552. doi: 10.3389/fcell.2020.00552

Breast cancers display phenotypic and functional heterogeneity and several lines of evidence support the existence of cancer stem cells (CSCs) in certain breast cancers, a minor population of cells capable of tumor initiation and metastatic dissemination. Identifying factors that regulate the CSC phenotype is therefore important for developing strategies to treat metastatic disease. The Inhibitor of Differentiation Protein 1 (Id1) and its closely related family member Inhibitor of Differentiation 3 (Id3) (collectively termed Id) are expressed by a diversity of stem cells and are required for metastatic dissemination in experimental models of breast cancer. In this study, we show that ID1 is expressed in rare neoplastic cells within ER-negative breast cancers. To address the function of Id1 expressing cells within tumors, we developed independent murine models of Triple Negative Breast Cancer (TNBC) in which a genetic reporter permitted the prospective isolation of $Id1^+$ cells. $Id1^+$ cells are enriched for self-renewal in tumorsphere assays *in vitro* and for tumor initiation *in vivo*. Conversely, depletion of Id1 and Id3 in the 4T1 murine model of TNBC demonstrates that Id1/3 are required for cell proliferation and self-renewal *in vitro*, as well as primary tumor growth and metastatic colonization of the lung *in vivo*. Using combined bioinformatic analysis, we have defined a novel mechanism of Id protein function via negative regulation of the Roundabout Axon Guidance Receptor Homolog 1 (*Robo1*) leading to activation of a Myc transcriptional programme.

Keywords: Id proteins, Robo1, cancer stem cell, metastasis, Myc signature

INTRODUCTION

Several lines of evidence suggest that rare sub-populations of tumor cells, commonly termed cancer stem cells (CSCs), drive key tumor phenotypes such as self-renewal, drug resistance and metastasis and contribute to disease relapse and associated patient mortality (Li et al., 2008; Malanchi et al., 2011; Chen et al., 2012; Lawson et al., 2015; da Silva-Diz et al., 2018). Recent evidence points to the hypothesis that CSCs are not static, but they exist in dynamic states, driven by critical transcription factors and are highly dependent on the microenvironmental cues (Lee G. et al., 2016; Wahl and Spike, 2017; da Silva-Diz et al., 2018). Understanding the molecular networks that are critical to the survival and plasticity of CSCs is fundamental to resolving clinical problems associated with chemo-resistance and metastatic residual disease.

The Inhibitor of Differentiation (ID) proteins have previously been recognized as regulators of CSCs and tumor progression (Lasorella et al., 2014). These proteins constitute a family of four highly conserved transcriptional regulators (ID1-4) that act as dominant-negative inhibitors of basic helix–loop–helix (bHLH) transcription factors. ID proteins are expressed in a tissue-specific and stage-dependent manner and are required for the maintenance of self-renewal and multipotency of embryonic and many tissue stem cells (Liang et al., 2009; Hong et al., 2011; Stankic et al., 2013; Aloia et al., 2015). Previous studies have reported a functional redundancy among the four members of the mammalian Id family, in particular Id1 and Id3 (referred to collectively here as Id), and their overlapping expression patterns during normal development and cancer (Lyden et al., 1999; Gupta et al., 2007; Anido et al., 2010; O'Brien et al., 2012; Niola et al., 2013). Id2 and Id4 were not investigated in this work as they are found to have independent functions from Id1 and Id3.

A number of studies have implied a significant role for ID1 and ID3 in breast cancer progression and metastasis (Gupta et al., 2007). We have previously demonstrated that Id1 cooperates with activated Ras signaling and promotes mammary tumor initiation and metastasis *in vivo* by supporting long-term self-renewal and proliferative capacity (Swarbrick et al., 2008). Additional work has clearly implicated ID1 in regulating D- and E-type cyclins and their associated cyclin-dependant kinases, CDK4 and CDK2 in human breast epithelial cells, p21 (Swarbrick et al., 2005), the matrix metalloproteinase MT1-MMP (Fong et al., 2003), KLF17 (Gumireddy et al., 2009), Cyclin D1 (Tobin et al., 2011), Bcl-2 (Kim et al., 2008), and BMI1 (Qian et al., 2010) among others.

Even though several Id-dependent targets have been identified, we still lack a comprehensive picture of the downstream molecular mechanisms controlled by Id and their associated pathways mediating breast cancer progression and metastasis particularly in the poor prognostic TNBC subtype. In this study, we demonstrate using four independent mouse models of TNBC that Id is important for the maintenance of a CSC phenotype. We also describe a novel mechanism by which Id controls the CSC state by negatively regulating Robo1 to control proliferation and self-renewal via indirect activation of a Myc transcriptional programme.

Abbreviations: CSC, Cancer stem cell; TNBC, Triple Negative Breast Cancer; Id, Id1 and Id3.

MATERIALS AND METHODS

Plasmids

pEN_TmiRc3 parental entry plasmid, pSLIK-Venus and pSLIK-Neo destination vectors were obtained from the ATCC (Manassas, VA, USA).

Cell Culture

4T1 and HEK293T cells were obtained from the American Type Culture Collection (ATCC). 4T1 cells were maintained in RPMI 1640 (Gibco, Grand Island, NY, USA) supplemented with 10% (v/v) FBS (Thermo Fisher Scientific, Scoresby, Vic, Australia), 20 mM HEPES (Gibco, Grand Island, NY, USA), 1 mM sodium pyruvate (Gibco, Grand Island, NY, USA), and 0.25% (v/v) glucose. HEK293T cells were grown in DMEM (Gibco, Grand Island, NY, USA) supplemented with 10% (v/v) FBS (Thermo Fisher Scientific, Scoresby, Vic, Australia), 6 mM L-glutamine (Gibco, Grand Island, NY, USA), 1 mM sodium pyruvate (Gibco, Grand Island, NY, USA) and 1% (v/v) MEM Non-essential Amino Acids (Gibco, Grand Island, NY, USA). All cell lines were cultured at 37°C in a humidified incubator with 5% CO_2.

Animals

All experiments involving animal work were performed in accordance with the rules and regulations stated by the Garvan Institute Animal Ethics Committee. The BALB/c mice were sourced from the Australian BioResources Ltd. (Moss Vale, NSW, Australia). FVBN mice, p53 null mice, C3-Tag mice were a generous gift from Tyler Jacks, Cambridge, MA. Doxycycline (Dox) food, which contains 700 mg Dox/kg, was manufactured by Gordon's Specialty Stock Feed (Yanderra, NSW, Australia) and fed to the mice during studies involving Dox-induced knockdown of Id1/3.

mRNA and Protein Expression Analysis

Total RNA from the cells were isolated using Qiagen RNeasy minikit (Qiagen, Doncaster, VIC, Australia) and cDNA was generated from 500 ng of RNA using the Superscript III first strand synthesis system (Invitrogen, Mulgrave, VIC, Australia) according to the manufacturer's protocol. Quantitative real-time PCR was carried out using the TaqMan probe-based system (Applied Biosystems/Life Technologies, Scoresby, Vic, Australia) on the ABI Prism 7900HT Sequence Detection System (Biosystems/Life Technologies, Scoresby, Vic, Australia) according to manufacturer's instructions. The probes used for the gene expression analysis by TaqMan assay are; Mouse Id1- Mm00775963_g1, Mouse Id3- Mm01188138_g1, Mouse Robo1- Mm00803879_m1, Mouse Fermt1- Mm01270148_m1, mmu-mir-30a (TaqMan® Pri-miRNA Assays, Cat. #4427012), Mouse Gapdh- Mm99999915_g1 and Mouse β-Actin- Mm00607939_s1. For protein expression analysis, lysates were prepared in RIPA lysis buffer supplemented with complete ULTRA protease inhibitor cocktail tablets (Roche, Basel, Switzerland) and western

blotting was performed as demonstrated before (Nair et al., 2014a). The list of antibodies used for western blotting are given in **Supplementary Table 6**.

Immunohistochemistry

Immunohistochemistry analysis was performed as described earlier (Nair et al., 2014a). Briefly, 4 μm-thick sections of formalin-fixed, paraffin-embedded (FFPE) tissue blocks were antigen retrieved by heat-induced antigen retrieval and were incubated with respective primary and secondary antibodies (listed in **Supplementary Table 7**).

Id1GFP Reporter in the p53$^{-/-}$ and 4T1 Model

p53$^{-/-}$ tumors arise spontaneously following transplantation of Tp53-null mammary epithelium into the mammary fat pads of naïve FVB/n mice. The tumors were then transplanted into naïve recipients; this method has been previously used to study murine TNBC CSCs (Herschkowitz et al., 2007; Hochgrafe et al., 2010). We developed and validated an Id1/GFP molecular reporter construct in which 1.2 kb of the Id1 proximal promoter is placed upstream of the GFP cDNA. Cells with active Id1 promoter can be visualized and isolated based on GFP expression by FACS from primary mouse tumors and cell lines. A similar approach has been successfully used to isolate CSCs with active β-catenin signaling (Zhang et al., 2010). Using the reporter construct, we typically see between 2 and 15% of cancers cells are GFP^{+} by FACS, depending on the clone analyzed. We experimentally validated the Id1/GFP system to ensure that GFP expression accurately marks the Id1^{+} cells within the bulk tumor cell population. After transfection of the Id1/GFP reporter into cultured p53$^{-/-}$ tumor cells, both the sorted GFP^{+} and unsorted cells were able to generate new tumors when transplanted into wild-type recipient mice. Tumors were harvested, dissociated into single cells, expanded briefly *in vitro*, and then FACS sorted once more to collect GFP^{+} and GFP^{-} cell fractions. The 4T1 cells were transduced in a similar manner and characterized.

Generation of shRNA Lentiviral Vectors

Single stranded cDNA sequences of mouse Id1 and Id3 shRNAs were purchased from Sigma-Aldrich (Lismore, NSW, Australia). The Id1 shRNA sequence which targets 5′-GGGACCTGCAGCTGGAGCTGAA-3′ has been validated earlier (Gao et al., 2008). The Id3 sequence was adopted from Gupta et al. (2007) and targets the sequence 5′-ATGGATGAGCTTCGATCTTAA-3′. shRNA directed against EGFP was used as the control. The shRNA linkers were designed as described earlier (Shin et al., 2006). The sense and antisense oligonucleotides with BfuAI restriction overhangs were annealed and cloned into the BfuAI restriction siteofpEN_TmiRc3 entry plasmid. pSLIK lentiviral vectors expressing shRNA against Id1 and Id3 namely pSLIK-Venus-TmiR-shId1 and pSLIK-Neo-TmiR-shId3, were generated by Gateway recombination between the pEN_TmiR_Id1 or the pEN_TmiR_Id3 entry vector and the pSLIK-Venus or pSLIK-Neo destination vector, respectively. Control pSLIK vector expressing shRNA against EGFP (pSLIK-Neo-TmiR-shEGFP) was generated by recombination between the pEN_TmiR_EGFP vector and the pSLIK-Neo vector. The Gateway recombination was performed using the LR reaction according to the manufacturer's protocol (Invitrogen, Mulgrave, Vic, Australia).

Lentivirus Production

Lentiviral supernatant was produced by transfecting each lentiviral expression vector along with third-generation lentiviral packaging and pseudotyping plasmids (Dull et al., 1998) into the packaging cell line HEK293T. Briefly, 1.4×10^6 cells were seeded in a 60 mm tissue culture dish and grown to 80% confluence. Three microgram of expression plasmid was co-transfected with lentiviral packaging and pseudotyping plasmids (2.25 μg each of pMDLg/pRRE and pRSV-REV and 1.5 μg of pMD2.G), using Lipofectamine 2000 (Invitrogen, Mulgrave, Vic, Australia) according to the manufacturer's protocol. Cell culture medium was replaced after 24 h. The viral supernatant was collected 48 h post transfection and filtered using a 0.45 μm filter. The filtered lentiviral supernatant was concentrated 20-fold by using Amicon Ultra-4 filter units (100 kDa NMWL) (Millipore, North Ryde, NSW, Australia).

Lentiviral Infection

4T1 cells were plated at a density of 1.0×10^5 cells per well in 6-well tissue culture plates and culture medium was replaced after 24 h with medium containing 8 μg/mL of polybrene (Sigma-Aldrich, Lismore, NSW, Australia). The cells were infected overnight with the concentrated virus at 1:5 dilution. Culture medium was changed 24 h post infection and cells were grown until reaching confluence. Cells transduced with both pSLIK-Venus-TmiR-Id1 and pSLIK-Neo-TmiR-Id3 were sorted on FACS using Venus as a marker followed by selection with neomycin at 400 μg/mL for 5 days. Cells transduced with pSLIK-Neo-TmiR-EGFP were also selected with neomycin.

pSLIK Knock Down Conditions

For the Dox induction experiments, cells were treated with or without Dox for 5 days and the levels of Id1 and Id3 were checked on days 1, 3, and 5 (**Figure 2B**, **Supplementary Figure 3F**). For the Dox removal experiments, cells treated with or without Dox for days 1, 3, and 5 were cultured for another 2 days in the absence or presence of Dox and the levels of Id1 and Id3 were checked using western blotting (**Supplementary Figure 3G**). The Dox removal samples of cells treated with/without Dox for 1 day were collected on day 3, samples of 3 days treatment on day 5 and samples of 5 days treatment were collected on day 7.

Tumourigenesis and Metastasis Assays

For orthotopic transplantation, 4T1 cells were injected (7.0×10^3/10 μL/injection) into the fat pad of 4th mammary gland of 6-week old female BALB/c mice. Mice were weighed and imaged weekly. Palpable tumors were measured with Vernier calipers twice a week. Tumors were harvested at ethical end point which was determined by having a tumor which is >1 cm^3 in size or a deterioration of body condition score represented by the physical appearance of the mouse including having difficulty to breathe or a loss of body weight by >20% since last monitoring.

Primary tumor and organs including the lungs, liver, lymph node, spleen, pancreas, and brain were harvested and visually examined for metastatic lesions and foci. The lung and brain were also examined under the LEICA MZ16 FA fluorescence microscope (Leica Microsystems, Wetzlar, Germany) to detect and quantify the presence of any metastatic lesions.

For experimental metastasis, 5×10^5 4T1-GFP cells are injected via tail vein. Once the mice reach the ethical end point, mice were sacrificed. The primary tumor and metastases and normal breast tissue are harvested and processed for further experiments.

Tumorsphere Assay

Cells dissociated from modified 4T1 cells and $p53^{-/-}$ Id1/GFP, Id1C3-Tag tumors were put into tumorsphere assay as described previously (Nair et al., 2014a).

Limiting Dilution Assay

Single-cell suspensions of FACS sorted Id1/GFP^+ or unsorted viable tumor cells were prepared as described previously. Tumor cells were transplanted in appropriate numbers into the fourth mammary fat pad of 8- to 12-week-old FVB/N mice and aged till ethical end point. Extreme limiting dilution analysis software (Hu and Smyth, 2009) was used to calculate the TPF.

In vivo and *ex vivo* Imaging

The 4T1 cells were lentivirally modified with the pLV4311-IRES-Thy1.1 vector, a luciferase expressing vector (a kind gift from Dr. Brian Rabinovich, The University of Texas M.D. Anderson Cancer Center, Houston, TX, USA). Animals were imaged twice weekly. Briefly, mice were first injected intraperitoneally with 200 μL of 30% D-luciferin (Xenogen, Hopkinton, MA, USA) in PBS with calcium and magnesium (Life Technologies, Mulgrave, Vic, Australia) and imaged under anesthesia using the IVIS Imaging System 200 Biophotonic Imager (Xenogen, Alameda, CA, USA). Bioluminescent intensity was analyzed and quantified using the Image Math feature in Living Image 3.1 software (Xenogen, Alameda, CA, USA). For *ex vivo* imaging, 200 μL of 30% D-luciferin was injected into the mice just before autopsy. Tissues of interest were collected, placed into 6-well tissue culture plates in PBS, and imaged for 1–2 min. At ethical endpoint, lungs were harvested and visually examined to detect the presence of metastases and later quantified based on 4T1 GFP fluorescence under a dissecting microscope.

MTS Proliferation Assay

Cell viability assay (MTS assay) was carried out using the CellTiter 96 AQueous Cell Proliferation Assay (G5421; Promega, Alexandria, NSW, Australia) according to the manufacturer's recommendations.

Microarray and Bioinformatics Analysis

Total RNA from the samples were isolated using Qiagen RNeasy minikit (Qiagen, Doncaster, VIC, Australia. cDNA synthesis, probe labeling, hybridization, scanning, and data processing were all conducted by the Ramaciotti Center for Gene Function Analysis (The University of New South Wales). Gene expression profiling was performed using the Affymetrix GeneChip® Mouse Gene 2.0 ST Array. Normalization and probe-set summarization was performed using the robust multichip average method (Irizarry et al., 2003) implemented in the Affymetrix Power Tools apt-probeset-summarize software (version 1.15.0) (using the -a rma option). Differential expression between experimental groups was assessed using Limma (Smyth, 2004) via the limmaGP tool in GenePattern (Reich et al., 2006). Gene Set Enrichment Analysis (GSEA) (http://www.broadinstitute.org/gsea) (Subramanian et al., 2005) was performed using the GSEA Pre-ranked module on a ranked list of the limma moderated t-statistics, against gene-sets from v4.0 of the MSigDB (Subramanian et al., 2005) and custom gene-sets derived from the literature. Microarray data are freely available from GEO: GSE129790.

Next Generation Sequencing

3.5×10^4 4T1 K1 cells were seeded in 6-well plates in 4T1 media and treated with or without Doxorubicin (1 μg/mL) to induce Id1/3 knockdown. Cells were also transfected with non-targeting control siRNA (Dharmacon D-001810-10-05) or Robo1 siRNA (Dharmacon M-046944-01-0010). Cells were harvested after 48 h and total RNA was extracted using the automated QiaSymphony magnetic bead extraction system. The Illumina TruSeq Stranded mRNA Library Prep Kit was used to generate libraries with 1 μg of input RNA following the manufacturer's instructions. cDNA libraries were sequenced on the NextSeq system (Illumina), with 75 bp paired-end reads. Quality control was checked using FastQC (bioinformatics.babraham.ac.uk/projects/fastqc). Reads were then aligned to the mouse reference genome Mm10 using STAR ultrafast universal RNA-Seq aligner (Dobin et al., 2013). Gene feature counting was performed with RSEM (Li and Dewey, 2011). Replicate 3 from the Id1 KD group showed no KD of Id1 by qPCR and was therefore removed prior to down-stream differential expression analysis. Transcripts with expression counts of 0 across all samples were removed and then normalized using TMM (Robinson and Oshlack, 2010). The normalized counts were then log transformed using voom (Ritchie et al., 2015) and differential expression was performed with limma (Smyth, 2004). Differentially expressed genes were visualized and explored using Degust (http://degust.erc.monash.edu/). Genes with false discovery rate (FDR) <0.05 were considered significantly differentially expressed. For GSEA analysis, genes were ranked based on the limma moderated t-statistic and this was used as input for the GSEA desktop application (Subramanian et al., 2005). RNA sequencing data are freely available from GEO: GSE129858.

Microarray (GSE129790) and RNA-Seq (GSE129858) datasets are available in SuperSeries GSE129859.

Statistical Analysis

Statistical analyses were performed using GraphPad Prism 6. All *in vitro* experiments were done in 3 biological replicates each with 2 or more technical replicates. Five to ten mice were used per condition for the *in vivo* experiments. Data represented are means ± standard deviation. Statistical tests used are Unpaired student *t*-test and two-way-ANOVA. *p*-values < 0.05 were

considered statistically significant with $^{*}p < 0.05$, $^{**}p < 0.01$, $^{***}p < 0.001$, $^{****}p < 0.0001$.

RESULTS

Id Marks a Subset of Cells With Stem-Like Properties in TNBC Models

We investigated the role of Id in the context of CSC biology in the TNBC molecular subtype. Immunohistochemistry (IHC) analysis revealed that ID1 is expressed by a small minority of cells (range 0.5–6% of total cancer cells) in ∼50% of ER-negative disease, namely TNBC and Her2^{+} tumors (**Supplementary Figures 1A,B**). No significant difference in the distribution of ID3 expression was observed across different subtypes (data not shown).

To test the hypothesis that Id1^{+} cells have a unique malignant phenotype, we developed two murine models of TNBC that permit the prospective isolation of Id1^{+} cells for functional assays. In the first, we used the p53$^{-/-}$ TNBC tumor model where IHC analysis revealed that ∼ 5% of neoplastic cells expressed Id1, consistent with the observation in the clinical samples, while Id3 marked a majority of the tumor cells in this model (**Figure 1A**).

To create a genetic reporter cell line, p53$^{-/-}$ mammary tumor cells were transduced with a lentiviral GFP reporter construct under the control of the Id1 promoter (Id1/GFP), as described previously (Mellick et al., 2010) (**Supplementary Figure 1C**). FACS sorting for GFP expression followed by immunoblotting confirmed the ability of the Id1/GFP construct to prospectively enrich for Id1^{+} cells from this model (**Supplementary Figure 1D**). We next sought to understand if Id1 marked cells with high self-renewal capacity in this model using tumorsphere assays, a well-established surrogate for cells with high self-renewal capacity (Pastrana et al., 2011; Lee C. H. et al., 2016). We observed an increase in the self-renewal capacity of Id1/GFP^{+} cells when compared to the unsorted cell population in the p53$^{-/-}$ model (**Figure 1B**).

To establish the *in vivo* relevance of the increased self-renewal capacity of the Id1/GFP^{+} tumor cells observed *in vitro*, we determined the tumor initiating capacity (TIC) of the Id1/GFP^{+} cells using the limiting dilution assay (Nair et al., 2014a). Id1/GFP^{+} cells (1/68) showed more than a 4-fold significant increase (p-value 0.0221) in tumor initiating cell frequency over Id1/GFP^{-} cells (1/314) after serial passage (**Figure 1C**).

We used the Id1C3-Tag tumor model as a second murine model to assess the phenotype of Id1^{+} cells. In the C3-Tag tumor model, the expression of SV40-large T antigen in the mammary epithelium under the control of the C3 promoter leads to the development of TNBC in mice (Green et al., 2000; Pfefferle et al., 2013). These tumors (C3-Tag) closely model the TNBC subtype as assessed by gene expression profiling (Pfefferle et al., 2013). To generate a genetic reporter of Id1 promoter activity in TNBC, the C3-Tag model was crossed to a genetic reporter mouse model in which GFP is knocked into the intron 1 of the Id1 gene (Perry et al., 2007). The resulting Id1GFPC3-Tag mice (called Id1C3-Tag model) developed mammary tumors with similar kinetics as the parental C3-Tag mice and have a classical basal phenotype characterized by CK14^{+}/CK8^{-} phenotype (**Supplementary Figure 1E**). Five and sixty percentage of cells in the Id1C3-Tag tumor were stained positive for Id1 and Id3 expression, respectively, as observed by IHC (**Figure 1D**). We were able to isolate Id1^{+} tumor cells with a high degree of purity by FACS based on GFP expression followed by q-RT PCR (**Figure 1E**). The sorted cells were put into primary tumorsphere assay and the spheres were passaged to secondary spheres which robustly selects for self-renewing cell populations. Similar to the p53$^{-/-}$ Id1/GFP model, Id1^{+}/GFP^{+} cells from the Id1C3-Tag model were enriched for sphere-forming capacity (**Figure 1F**).

Using the Id1C3-Tag model, we also looked at the association of Id1/GFP expression with the expression of established CSC markers CD29, CD24, and CD61. CD29^{+}/CD24^{+} status was previously reported to mark the tumorigenic subpopulation of cells in murine mammary tumors (Zhang et al., 2008; Herschkowitz et al., 2012). The Id1^{+}/GFP^{+} cells in the Id1C3-Tag model are predominantly of the CD29^{+}/CD24^{+} phenotype (**Figure 1G**), with a 1.6-fold higher proportion of cells expressing both CD29 and CD24 compared to the Id1^{-}/GFP^{-} cells which comprise the bulk of the tumor. Interestingly, Id1^{+}/GFP^{+} cells are also highly enriched for CD24^{+}/CD61^{+} expression (more than 6-fold increase in Id1^{+}/GFP^{+} cells), which was also reported to mark a murine breast CSC population (Vaillant et al., 2008) (**Figure 1G**).

We found no correlation between Id1 expression (as indicated by GFP^{+}) and the CD29^{+}/CD24^{+} phenotype in the first transplantation round (T1) using the p53$^{-/-}$ model, as the percentage of CD29^{+}/CD24^{+} cells was similar across each gating group (**Supplementary Figure 1F**). Interestingly, the Id1^{+} cells, which are the putative cells that give rise to the increased TIC as shown in **Figure 1C**, showed 10 times less CD24^{+}/CD29^{+} cells in the second transplantation round (T2) (Vaillant et al., 2008). The ability of the markers like CD24, CD29, and CD61 to identify the CSC population is clearly model-dependent. In addition to CD29 and CD24, the percentage of GFP^{+} cells were also analyzed and a higher percentage of GFP^{+} cells was found in the second transplantation round of the p53$^{-/-}$ tumor compared to the first round tumor result (**Supplementary Figure 1G**), consistent with the increase in TICs reported in **Figure 1C**.

Id Requirement for Self-Renewal *in vitro* and Metastatic Competency *in vivo*

We next assessed the requirement for Id1 and Id3 in maintaining the CSC phenotypes. Numerous studies have shown that there exists a functional redundancy between Id1 and Id3, so studies typically require depletion of both the factors to reveal a phenotype (Konrad et al., 2017). Unfortunately we could not generate Id1 and Id3 double out knock mice for the C3-Tag and Id1/3 expressing reporter in the p53$^{-/-}$ tumor models due to technical reasons. Hence we decided to look at the role of both Id1 and Id3 in the context of a knock down model. We used the transplantable syngeneic 4T1 TNBC model, which has a high propensity to spontaneously metastasize to distant sites (including bone, lung, brain, and

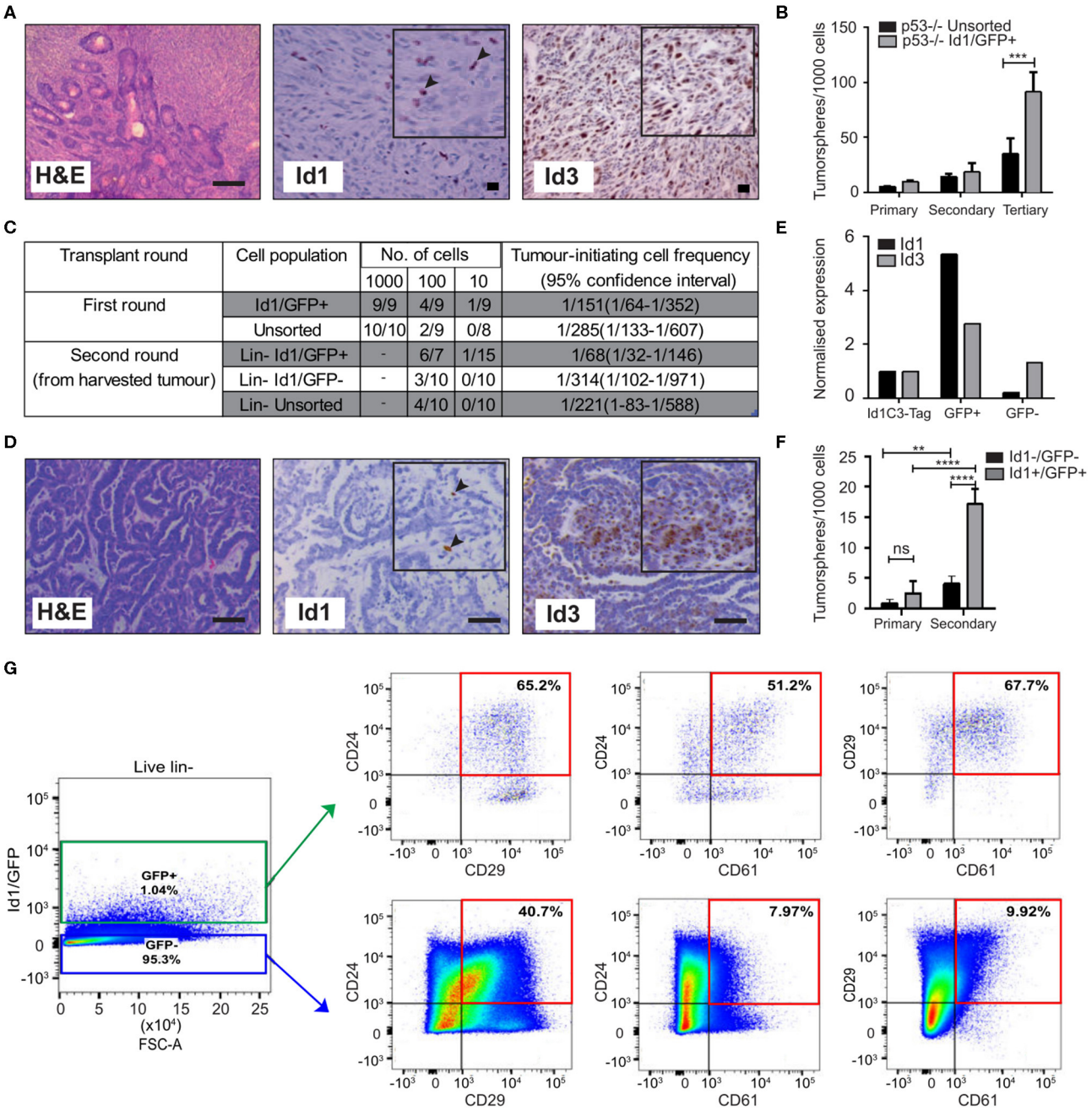

Transplant round	Cell population	No. of cells			Tumour-initiating cell frequency (95% confidence interval)
		1000	100	10	
First round	Id1/GFP+	9/9	4/9	1/9	1/151(1/64-1/352)
	Unsorted	10/10	2/9	0/8	1/285(1/133-1/607)
Second round (from harvested tumour)	Lin- Id1/GFP+	-	6/7	1/15	1/68(1/32-1/146)
	Lin- Id1/GFP-	-	3/10	0/10	1/314(1/102-1/971)
	Lin- Unsorted	-	4/10	0/10	1/221(1-83-1/588)

FIGURE 1 | Id1 marks tumor cells with high self-renewal in murine models of TNBC. **(A)** Representative IHC images of Id1 and Id3 expression in $p53^{-/-}$ tumor model. Black arrows in the inset indicate $Id1^{+}$ cells. Scale bars = 50 μm. **(B)** $p53^{-/-}$ tumor cells were transfected with the Id1/GFP reporter and subsequently sorted for GFP expression. The self-renewal capacity of Id1/GFP^{+} $p53^{-/-}$ cells was significantly higher than unsorted Id1/GFP $p53^{-/-}$ cells upon passage to tertiary tumorspheres. Data are means ± SD ($n = 3$) (***$p < 0.001$; Two-way ANOVA). **(C)** Id1 expressing cells were sorted from the $p53^{-/-}$ Id1/GFP tumor model and transplanted into recipient mice by limiting dilution assay. Based on limiting dilution calculations (ELDA), the $Id1^{+}$ cells demonstrated significant 4.6-fold enrichment in tumor initiating capacity (TIC) when compared to the $Id1^{-}$ cells in serial passage. *p*-values for $p53^{-/-}$ Id1GFP^{+} vs. Unsorted Round 1- 0.2920, $p53^{-/-}$ Id1GFP^{+} vs. Id1GFP- Round 2- 0.0221. **(D)** Representative IHC images of the Id1C3-Tag model, confirming its suitability as a model system. Black arrows in the inset indicate $Id1^{+}$ cells. Expression of Id1 was <5% as determined by IHC. Bars = 50 μm. **(E)** Tumor cells from the Id1C3-Tag tumor model were FACS sorted based on their GFP expression. qRT-PCR analyses on the sorted GFP^{+} and GFP^{-} cell populations showed a significant increase (more than 5-fold) for Id1 expression in the GFP^{+} cells compared to cells lacking GFP expression. **(F)** *In vitro* self-renewal capacity of GFP^{+} cells was measured using the tumorsphere assay. The secondary sphere forming capacity of $Id1^{+}$ tumor cells from the Id1C3-Tag model was significantly enriched in comparison to the $Id1^{-}$tumor cells. Data are means ± SD ($n = 3$) (**$p < 0.01$, ****$p < 0.0001$; Two-way ANOVA). **(G)** Representative FACS scatterplot and histograms from Id1C3-Tag tumors showing the expression of the CSC markers CD24, CD29, and CD61 in the $Id1^{-}$/GFP^{-} and $Id1^{+}$/GFP^{+} cancer cells. Putative CSC populations are highlighted within the red box.

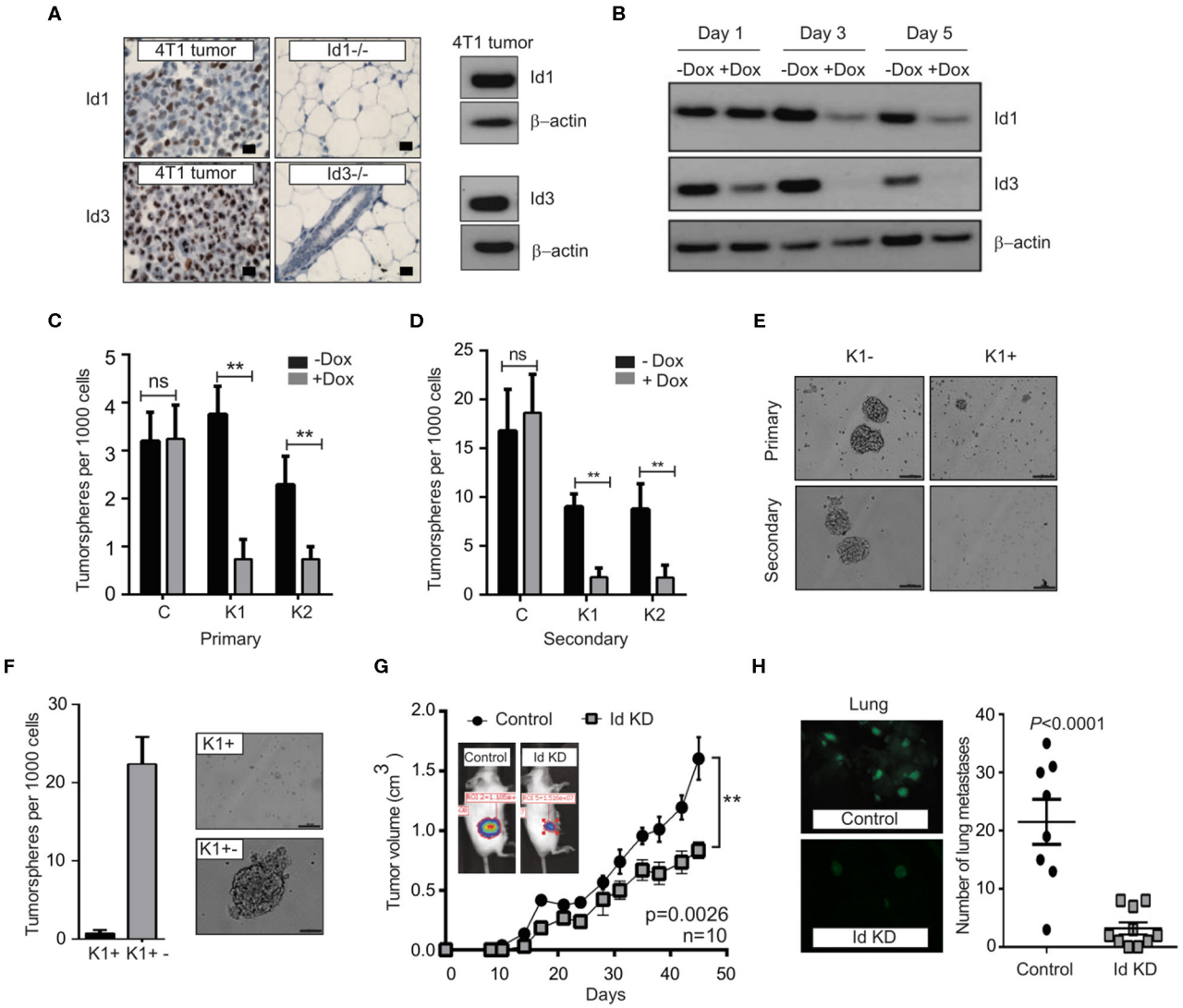

FIGURE 2 | Depletion of Id1 and Id3 leads to a reduced self-renewal capacity *in vitro* and metastatic potential *in vivo*. **(A)** Endogenous levels of Id1 and Id3 expression in 4T1 primary mammary tumors were determined. 4T1 were cells stained for Id1 and Id3 expression (brown) and counterstained with haematoxylin. Mammary gland tissue from Id1 and Id3 null ($Id1^{-/-}$ and $Id3^{-/-}$) mice served as negative controls. Scale bars = 50 μm. Western blot analysis of protein lysate from 4T1 tumor cells served as positive controls for Id1 and Id3 expression. **(B)** Kinetics of conditional Id knockdown in 4T1 cells. Representative Western blot analysis of Id protein levels in pSLIK K1 cells over time. Cells were cultured in the presence of 1 μg/ml of Doxycycline (Dox) for 1, 3, and 5 days. β-actin was used as loading control. **(C)** 4T1 Control, pSLIK K1 and K2 clones were assayed for their tumorsphere forming potential. Dox was added into the culture medium at day 0. Number of primary tumorspheres formed was quantified by visual examination on day 7. Id knockdown leads to a decrease in tumorsphere-forming ability of K1 and K2 cell lines. Data are means ± SD ($n = 3$) (**$p < 0.01$; Two-way ANOVA). **(D)** Primary tumorspheres were passaged and the number of secondary tumorspheres was quantified on day 14. Knockdown of Id significantly reduces the ability of the K1 and K2 cells to form secondary tumorspheres in the suspension culture. Data are means ± SD ($n = 3$) (**$p < 0.01$; Two-way ANOVA). **(E)** Representative images of primary and secondary tumorsphere formation for the clone K1 ± Dox. **(F)** Quantification and representative images of primary tumorsphere treated with Dox ($K1^{+}$) passaged to secondary spheres in Dox free conditions ($K1^{+-}$) allowing re expression of Id and restoration of self-renewal capacity. **(G)** Knockdown of Id significantly delays tumor growth in the 4T1 syngeneic model ($n = 10$ mice; **$p < 0.01$, Student's *t*-test). **(H)** Id knockdown suppresses spontaneous lung metastasis. Tumors depleted of Id expression generated fewer spontaneous lung macrometastatic lesions compared to the control despite growing in the host for a longer time. Inset shows representative images of lungs bearing the control (K1 - Dox) and Id KD (K1 + Dox) lung metastases at ethical end point. Control; $n = 8$ mice, Id KD; $n = 10$ mice. Scale bar = 50 μm.

liver), mimicking the aggressiveness of human breast cancers (Aslakson and Miller, 1992; Pulaski and Ostrand-Rosenberg, 1998; Lelekakis et al., 1999; Yoneda et al., 2000; Eckhardt et al., 2005; Tao et al., 2008). IHC analysis showed that 15% of 4T1 tumor cells express high levels of Id1, and 35% have intermediate levels of Id1 expression, whereas the expression of Id3 was found in most of the cells (**Figure 2A**).

In order to determine whether Id1 marks CSCs in the 4T1 TNBC model, 4T1 cells were transduced with a lentiviral GFP reporter construct under the control of the Id1 promoter (Id1/GFP) (**Supplementary Figure 2A**), as used in the $p53^{-/-}$ model and the cells were sorted based on GFP expression. Id1/GFP^{+} cells showed more than 2-fold increase in Id1 expression (**Supplementary Figure 2B**). Even though Id1/GFP^{+} and Id1/GFP- cells showed similar proliferation *in vitro* (**Supplementary Figure 2C**), a significant enrichment of *in vitro* self-renewal capacity was observed in Id1/GFP^{+} cells when compared to Id1/GFP- cells (**Supplementary Figures 2D,E**). Finally, we performed the LDT assay wherein we observed more than 40-fold increase in the metastatic propagating capacity of the Id1/GFP^{+} cells as compared to the control ($p = 0.000161$) (**Supplementary Figures 2F,G**).

We next used an inducible lentiviral shRNA system (Shin et al., 2006) that permits reversible knock down of Id1 and Id3 in response to doxycycline (Dox) treatment in 4T1 cells. Two clonal 4T1 cell lines, K1 and K2 were chosen along with a control line (C), based on the efficiency of Id knock down (**Figure 2B**, **Supplementary Figure 3A**). Id depletion resulted in a significant decrease in cell proliferation and migration *in vitro* when compared to the control (**Supplementary Figures 3B–D**).

We next interrogated the effect of Id depletion on the self-renewal capacity of the C, K1 and K2 cell lines. Dox-dependent shRNA induction significantly reduced the ability of the K1 and K2 cells to form primary tumorspheres in the suspension culture (**Figure 2C**). This effect was not observed in the control cell line (C; **Figure 2C**). A significant further decrease in self-renewal capacity of K1 and K2 lines was observed when primary tumorspheres were passaged to the secondary stage (**Figures 2D,E**). The Id depleted tumorspheres were also markedly smaller in size compared to controls (**Figure 2E**, **Supplementary Figure 3E**).

To assess if the self-renewal phenotype controlled by Id is reversible, we firstly passaged primary tumorspheres [previously treated with Dox (K^{+})] to secondary tumorspheres. The secondary tumorspheres were then cultured in the presence or absence of Dox, to maintain the Id knockdown status or to allow the re-expression of Id, respectively (**Supplementary Figures 3F,G**). The secondary tumorspheres cultured without Dox ($K1^{+-}$) re-established their self-renewal capacity as evidenced by the ability to form new tumorspheres (**Figure 2F**; **Supplementary Figures 3H,I**), suggesting that Id depletion does not lead to a permanent loss of self-renewal capacity.

To determine whether Id1 and Id3 are required for primary tumor and metastatic growth *in vivo*, K1 cells were orthotopically transplanted into the mammary fat pad of BALB/c mice. Dox-mediated knockdown of Id resulted in modest inhibition of primary tumor growth, with control tumors growing faster and reaching the ethical endpoint earlier than the Id knockdown group (**Figure 2G**). More significantly, mice transplanted with Id depleted K1 cells presented far fewer lung metastatic lesions compared to the control despite growing in the host for a longer time ($p < 0.0001$; **Figure 2H**).

To assess the role for Id in metastatic progression *in vivo*, we examined Id expression in lung metastasis compared to primary tumors in mice injected with K1 cells. An increase in the expression of Id1 was observed in the lung metastasis in all the samples, while no significant enrichment of Id3 expression was observed (**Supplementary Figure 4A**). This suggests that Id1 promotes lung metastatic dissemination in TNBC.

To determine whether altered expression patterns of ID1 are associated with metastasic progression in patients, ID1 IHC was performed on a cohort of 49 cases with matching primary tumor and brain metastatic lesions surgically removed from breast cancer patients. Amongst the 13 cases in which ID1 was detected by IHC in the primary tumor, an enrichment of ID1 expression was observed in brain metastases over the patient-matched primary tumor in 11 cases (**Supplementary Figure 4B**).

Identification of Genes and Pathways Regulated by Id

The canonical role for Id proteins is to regulate gene expression through association with transcription factors, yet a comprehensive analysis of Id transcriptional targets in cancer has not been reported. We performed gene expression profiling of Control (C) and Id depleted K1 cells. The gene expression profiles of four independent replicates (R1, R2, R3, and R4 ± doxycycline treatment) were compared by microarray analysis (**Supplementary Figure 5A**). 6081 differentially expressed genes were identified ($Q < 0.05$), with 3,310 up-regulated and 2,771 down-regulated genes in Id KD cells (**Supplementary Table 1**) shows the top 25 differentially regulated genes). Network and pathway enrichment analysis was conducted using the MetaCore™ software. Four thousand three hundred and one significant network objects were identified for the Id knockdown microarray data (adjusted p-value of ≤ 0.05). The top pathways affected by Id knockdown were mostly associated with the cell cycle (**Figures 3A,B**) consistent with the loss of proliferative phenotype described previously (**Supplementary Figures 3B,C**). Similar results were obtained using Gene Set Enrichment Analysis (GSEA) with significant down regulation of proliferative signatures (CELL_CYCLE_PROCESS) and mitosis (M_PHASE) (**Supplementary Table 2**). Genes such as CCNA2, CHEK1, and PLK1 in these gene sets are down-regulated by Id knockdown. This is consistent with our results (**Supplementary Figures 3B,C**) showing Id proteins are necessary for proliferation of 4T1 cells, as well as previous studies which reported a role of Id in controlling cell cycle progression and proliferation pathways (O'Brien et al., 2012; Nair et al., 2014b). Enrichment for genes involved in several oncogenic pathways such as Mek, Vegf, Myc, and Bmi1 signaling have also been highlighted (**Supplementary Table 3**). In order to identify whether Id specifically regulate genes controlling breast cancer metastasis, GSEA analysis was performed with a collection of custom "metastasis gene sets." This collection (**Table 1**) consists of several metastatic signatures from the C2 collection (MSigDB database; **Supplementary Table 4**), combined with a list of custom gene sets described in major studies (Dontu et al., 2003; Kang et al., 2003b; Minn et al., 2005a,b; Tang et al.,

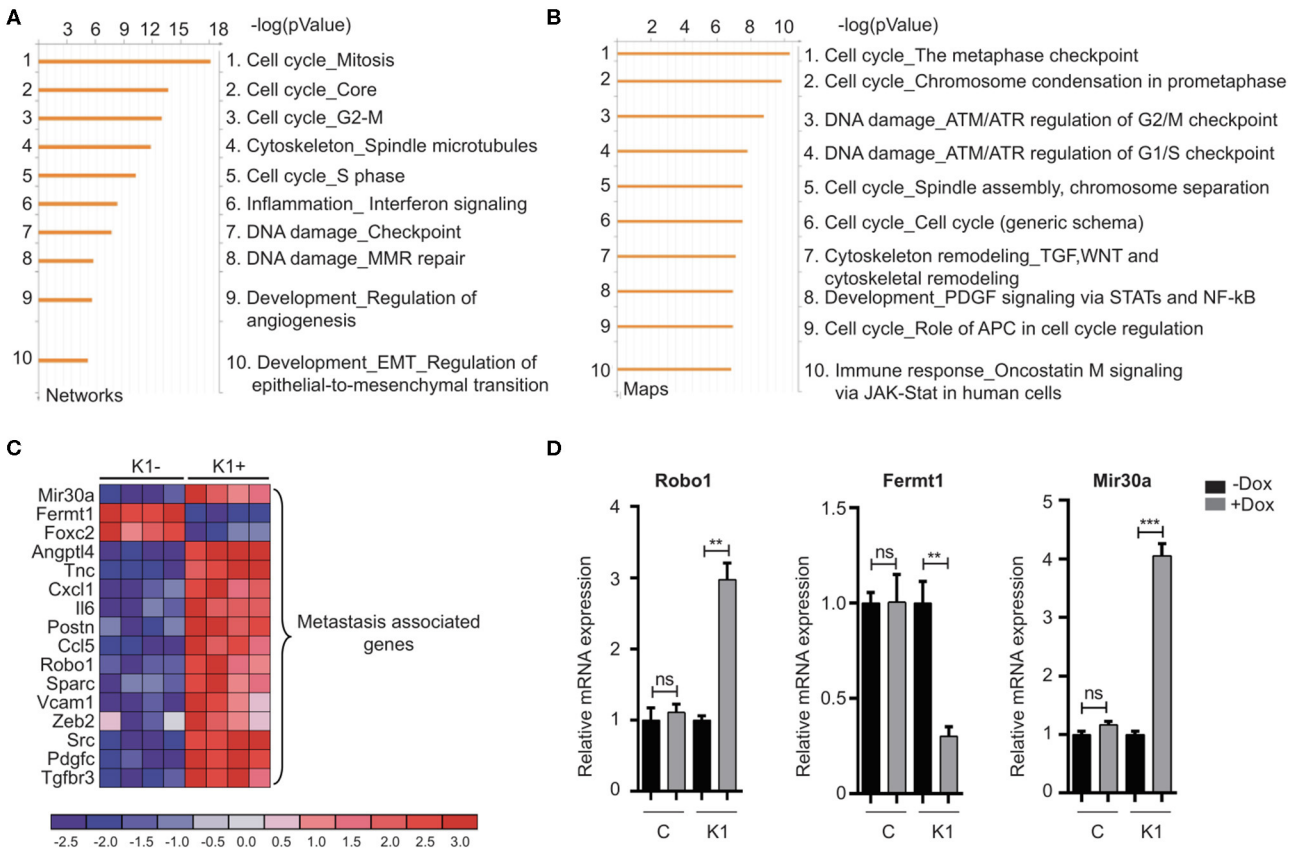

FIGURE 3 | Gene expression analysis reveals targets of Id in TNBC. **(A,B)** To characterize the network of genes regulated by Id, functional annotation analyses were performed on the gene array data from the 4T1 TNBC model. The Id depletion model attempted to identify downstream targets of Id through a loss of function approach. The gene expression profile of four independent replicates of the K1 shId clone, with and without doxycycline treatment, was compared by microarray analysis. This resulted in a list of differentially expressed genes between control and Id depleted cells, which by further network and map analysis using Metacore demonstrated was largely driven by genes controlling cell cycle pathways. **(C)** Gene expression analysis identified metastasis-related genes that were differentially expressed in response to Id knockdown. To determine if genes that mediate metastasis were enriched in the Id signature, gene expression analysis was performed using a manually curated set of metastasis gene sets. Genes differentially expressed in response to Id knockdown as well as associated with pathways regulating metastasis were identified based on reports from the literature which included Robo1. **(D)** Validation of expression profiling results by quantitative real-time-PCR using the Taqman® probe based system. Relative mRNA expression of Robo1, Fermt1, and Mir30a, in the 4T1 pSLIK shId Clonal cell line (K1) and pSLIK control (C), as indicated. Data are means ± SD ($n = 3$) (**$p < 0.01$, ***$p < 0.001$; unpaired t-test).

2007; Padua et al., 2008; Bos et al., 2009; Charafe-Jauffret et al., 2009; Liu et al., 2010; Aceto et al., 2014) as shown in **Figure 3C**. Genes differentially expressed in this set included *Robo1* (Chang et al., 2012; Qin et al., 2015), *Il6* (Chang et al., 2013), *Fermt1* (Landemaine et al., 2008), *Foxc2* (Mani et al., 2007), and Mir30a (Zhang et al., 2014). Three putative Id targets *Robo1, Fermt1*, and *Mir30a* were then validated using q-RT PCR (**Figure 3D**) and found to be differentially regulated in the K1 cell line upon Id KD.

Id Mediated Inhibition of Robo1 Controls the Proliferative Phenotype via Activation of Myc Transcription

Since Robo1 is known to have a tumor suppressor role in breast cancer biology (Chang et al., 2012; Shen et al., 2015), we next sought to determine if Robo1 has an epistatic interaction with Id loss of function using siRNA mediated knockdown of Robo1 followed by proliferation assays. Knockdown of *Robo1* ameliorated the requirement for Id and rescued ∼55% of the proliferative decrease induced by Id KD (**Figure 4A**).

To understand the mechanisms by which *Robo1* increases the proliferative potential of Id depleted cells *in vitro*, we performed RNA-Sequencing (RNA-Seq) experiments on K1 cells with dox-inducible Id KD and/or Robo1 depletion using siRNA. Four replicates per condition were generated and MDS plots presented in **Supplementary Figure 5B** showed that the replicates cluster together. Id KD alone in the K1 cells down regulated 4409 genes and up regulated 5236 genes (FDR <0.05), respectively. The majority of the differentially expressed genes determined by microarray were found by RNA-Seq analysis (**Supplementary Figure 5C**). Id depletion led to an increase in *Robo1* expression, as observed in the previous microarray experiment (**Figures 3C,D**, **4B**).

TABLE 1 | Gene expression signatures of breast cancer metastasis and breast cancer stem cells.

Study	Signature	Type	Available on GSEA MSigDB database?
Landemaine et al. A six-gene signature predicting breast cancer lung metastasis. Cancer Res. 2008 Aug 1;68(15):6092–9	Lung metastasis signature of breast cancer	Metastatic tissue tropism	Yes
Bild et al. Oncogenic pathway signatures in human cancers as a guide to targeted therapies. Nature 2006, 439:353–357.	Expression profile of 4 individual genes—Myc, E2F3, Ras, Src, β-catenin	Signaling pathway	Yes
van 't Veer et al. Gene expression profiling predicts clinical outcome of breast cancer. Nature 2002, 415:530–536.	Poor prognosis signature of breast cancer	Classifier that classifies patients as having good or poor prognosis	Yes
Wang et al. Gene-expression profiles to predict distant metastasis of lymph-node-negative primary breast cancer. Lancet 2005, 365:671–679.	Poor prognosis signature of breast cancer	Classifier	Yes
Ramaswamy et al. A molecular signature of metastasis in primary solid tumors. Nat Genet 2003, 33:49–54.	General metastasis	Classifier	Yes
Finak et al. Stromal gene expression predicts clinical outcome in breast cancer. Nat Med 2008, 14:518–527.	Breast tumor stromal gene expression signature	Classifier	Yes
Farmer et al. A stroma-related gene signature predicts resistance to neoadjuvant chemotherapy in breast cancer. Nat Med 2009, 15:68–74.	Stromal gene expression signature of breast tumor treated with chemotherapy	Classifier	Yes
Kang et al. A multigenic program mediating breast cancer metastasis to bone. Cancer Cell 2003, 3:537–549.	Bone metastasis signature of breast cancer	Metastatic tissue tropism	No
Minn et al. Genes that mediate breast cancer metastasis to lung. Nature 2005, 436:518–524	Lung metastasis signature of breast cancer	Metastatic tissue tropism	No
Bos et al. Genes that mediate breast cancer metastasis to the brain. Nature 2009, 459:1005–1009.	Bone metastasis signature of breast cancer	Metastatic tissue tropism	No
Padua et al. TGFbeta primes breast tumors for lung metastasis seeding through angiopoietin-like 4. Cell 2008, 133:66–77.	TGF-b signature in lung metastasis of breast cancer	Signaling pathway	No
Aceto et al. Tyrosine phosphatase SHP2 promotes breast cancer progression and maintains tumor-initiating cells via activation of key transcription factors and a positive feedback signaling loop. Nat Med. 2012 Mar 4;18(4):529–37.	Shp2 signature in breast cancer metastasis	Signaling pathway	No
Minn et al. Distinct organ-specific metastatic potential of individual breast cancer cells and primary tumors. J Clin Invest. 2005 Jan;115(1):44–55.	Poor prognosis signature of breast cancer; Breast cancer metastasis signature; Bone metastasis signature of breast cancer	Metastatic tissue tropism	No
Tang et al. Transforming growth factor-beta can suppress tumorigenesis through effects on the putative cancer stem or early progenitor cell and committed progeny in a breast cancer xenograft model. Cancer Res. 2007 Sep 15;67(18):8643–52.	TGF-b signature in lung metastasis of breast cancer	Signaling pathway	No
Liu et al. The prognostic role of a gene signature from tumorigenic breast-cancer cells. The New England journal of medicine. 2007. 356(3), 217–26.	Gene signatures of $CD44^{+}CD24^{-}$/low tumorigenic breast-cancer cell-lines and normal breast epithelium	Cancer stem cell	No
Charafe-Jauffret et al. Breast cancer cell lines contain functional cancer stem cells with metastatic capacity and a distinct molecular signature. 2009. Cancer research, 69(4), 1302–13.	Breast cancer stem cell signature	Cancer stem cell	No
Dontu, et al. *In vitro* propagation and transcriptional profiling of human mammary stem/progenitor cells. 2003. Genes & development, 17(10), 1253–70.	Gene signature of human mammary stem and progenitor cells	Cancer stem cell/differentiation	No

This table shows a collection of gene sets which comprised several metastatic signatures that were picked from the C2 collection on the MSigDB database and several other signatures that were manually curated. GSEA analysis was carried out to identify whether any of the Id1/3 targets from the profiling experiment are enriched in these signatures.

Given that Id repressed Robo1 expression, we sought to determine Robo1 target genes in the absence of Id. Remarkably, under Id depletion conditions, *Robo1* KD restored expression of a large subset (∼45%) of Id target genes to basal levels (**Figure 4C**). In comparison, knockdown of Id or Robo1 regulated few targets in the same direction (e.g., both up or both down). This implies that a large proportion of Id targets may be regulated via suppression of Robo1. Genes whose expression was repressed by Id KD and rescued by concomitant Robo1 KD were termed "Intersect 1" (**Figure 4C**, **Table 2**). Genes that were upregulated

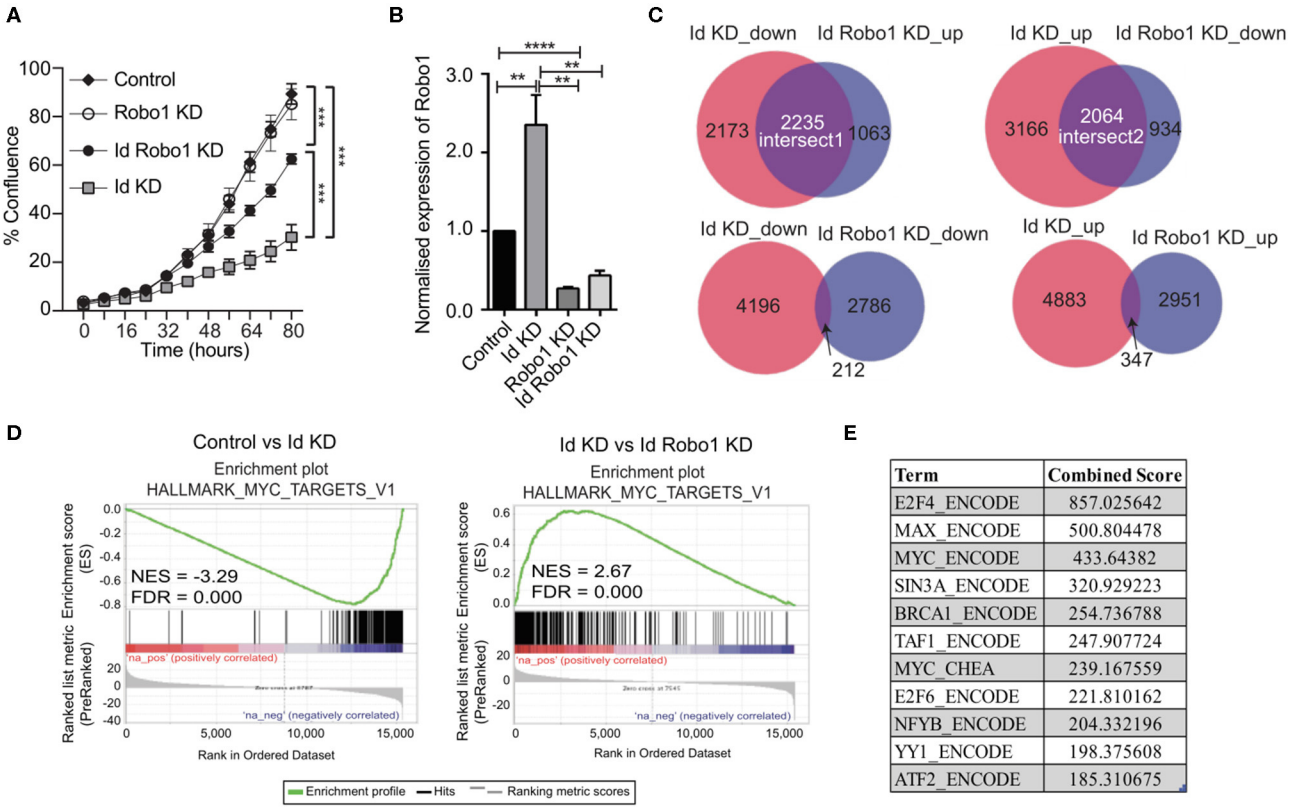

E

Term	Combined Score
E2F4_ENCODE	857.025642
MAX_ENCODE	500.804478
MYC_ENCODE	433.64382
SIN3A_ENCODE	320.929223
BRCA1_ENCODE	254.736788
TAF1_ENCODE	247.907724
MYC_CHEA	239.167559
E2F6_ENCODE	221.810162
NFYB_ENCODE	204.332196
YY1_ENCODE	198.375608
ATF2_ENCODE	185.310675

FIGURE 4 | Identification of Myc signature activation by Id via negative regulation of Robo1. **(A)** Proliferation of K1 cells treated with non-targeting (NT) control siRNA or Robo1 siRNA in the absence or presence of Doxycycline to induce Id knockdown was measured by the IncuCyte™ (Essen Instruments) live-cell imaging system. Data shown as mean ± SD ($n = 3$). (***$p < 0.001$; Unpaired two-tailed *t*-test). **(B)** Robo1 expression in Control, Id KD, Robo1 KD and Id Robo1 KD cells was measured by quantitative PCR. Ct values were normalized to β actin and GAPDH housekeeping genes. Data shown as mean ± SEM ($n = 4$) (**$p < 0.01$, ****$p <$ 0.0001; Unpaired two-tailed *t*-test). **(C)** Transcriptional profiling was performed on Control, Id KD, Robo1 KD, and Id Robo1 KD cells. Proportional Venn diagrams (BioVenn) were generated to visualize the overlapping genes between the different comparisons. **(D)** GSEA Enrichment plots of the hallmark Myc targets version 1 signature from MSigDB. NES, normalized enrichment score. **(E)** Consensus Transcription factor motif analysis using the Encyclopedia of DNA Elements (ENCODE) and ChIP enrichment analysis (ChEA) data sets determined using EnrichR. The combined score is a combination of the *p*-value and *z*-score.

by Id KD and downregulated by Robo1 KD (in the absence of Id) were annotated "intersect 2" (**Figure 4C**, **Table 3**). To investigate the function of these intersect group of genes, we performed GSEA analysis using the MSigDB hallmark gene set (Liberzon et al., 2015). The top signatures in Intersect 1 were involved in cell proliferation, with enrichment for G2M checkpoint, E2F and Myc targets as well as mTOR signaling (**Table 2**). Rank-based analysis revealed strong negative enrichment for the hallmark Myc targets signature upon Id knockdown alone, and strong positive enrichment upon Id and Robo1 knockdown (**Figure 4D**). This suggests that following Id KD, Robo1 is induced and exerts anti-proliferative effects via suppression of Myc and its target genes (**Supplementary Figures 5D,E**). Transcription factor motif analysis using EnrichR revealed that Myc and its binding partner Max, have a high combined score in the Intersect 1 gene list further implicating Myc as downstream effector of Robo1 and Id (**Figure 4E**).

We were interested in investigating the possibility that Robo1 may exert its negative effects on the Myc pathway via regulation of Myc co-factors, which can potently enhance or suppress Myc transcriptional activity (Gao et al., 2016). In order to test this hypothesis, we looked at known Myc co-factors from the literature in our RNA-Seq data to determine if they were differentially expressed in the Id1 and Robo1 KD conditions. As seen in **Supplementary Table 5**, we included negative (red) and positive (green) cofactors in the analysis. Scrutiny of this list suggests that there are numerous negative co-factors (7/10) being induced and activators being repressed (13/24) by Robo1. For example, putative activation of the gene Rlim which is an E3 ubiquitin ligase that suppresses the transcriptional activity of MYC (Gao et al., 2016).

In summary, we have demonstrated that Id depletion leads to a loss in the proliferative and self-renewal cancer stem cell phenotypes associated with TNBC. Id1 acts by negatively regulating Robo1 which in turn finally leads to the downstream activation of a Myc transcriptional program (**Figure 5**).

TABLE 2 | GSEA on the Intersect 1 genes from **Figure 4C** against the MSigDB hallmark gene sets.

INTERSECT 1 GSEA						
Gene set name	**# Genes in gene set (K)**	**Description**	**#Genes in overlap (k)**	**k/K**	***p*-value**	**FDR (*q*-value)**
HALLMARK_E2F_TARGETS	200	Genes encoding cell cycle related targets of E2F transcription factors.	158	0.79	5.02E-178	2.51E-176
HALLMARK_G2M_CHECKPOINT	200	Genes involved in the G2/M checkpoint, as in progression through the cell division cycle.	116	0.58	2.32E-105	5.80E-104
HALLMARK_MYC_TARGETS_V1	200	A subgroup of genes regulated by MYC—version 1 (v1).	113	0.565	7.79E-101	1.30E-99
HALLMARK_OXIDATIVE_ PHOSPHORYLATION	200	Genes encoding proteins involved in oxidative phosphorylation.	96	0.48	1.04E-76	1.30E-75
HALLMARK_MYC_TARGETS_V2	58	A subgroup of genes regulated by MYC—version 2 (v2).	42	0.7241	4.60E-45	4.60E-44
HALLMARK_MTORC1_SIGNALING	200	Genes up-regulated through activation of mTORC1 complex.	66	0.33	1.70E-40	1.42E-39
HALLMARK_MITOTIC_SPINDLE	200	Genes important for mitotic spindle assembly.	60	0.3	2.76E-34	1.97E-33
HALLMARK_DNA_REPAIR	150	Genes involved in DNA repair.	51	0.34	2.54E-32	1.59E-31
HALLMARK_UNFOLDED_ PROTEIN_RESPONSE	113	Genes up-regulated during unfolded protein response, a cellular stress response related to the endoplasmic reticulum.	31	0.2743	3.62E-17	2.01E-16
HALLMARK_FATTY_ ACID_METABOLISM	158	Genes encoding proteins involved in metabolism of fatty acids.	35	0.2215	5.10E-16	2.55E-15
HALLMARK_ADIPOGENESIS	200	Genes up-regulated during adipocyte differentiation (adipogenesis).	39	0.195	1.08E-15	4.89E-15
HALLMARK_CHOLESTEROL_ HOMEOSTASIS	74	Genes involved in cholesterol homeostasis.	24	0.3243	1.95E-15	8.11E-15
HALLMARK_ESTROGEN_RESPONSE_ LATE	200	Genes defining late response to estrogen.	35	0.175	8.70E-13	3.11E-12
HALLMARK_GLYCOLYSIS	200	Genes encoding proteins involved in glycolysis and gluconeogenesis.	35	0.175	8.70E-13	3.11E-12
HALLMARK_UV_RESPONSE_UP	158	Genes up-regulated in response to ultraviolet (UV) radiation.	28	0.1772	1.18E-10	3.95E-10
HALLMARK_SPERMATOGENESIS	135	Genes up-regulated during production of male gametes (sperm), as in spermatogenesis.	25	0.1852	4.39E-10	1.37E-09
HALLMARK_ANDROGEN_RESPONSE	101	Genes defining response to androgens.	20	0.198	7.15E-09	2.10E-08
HALLMARK_ESTROGEN_ RESPONSE_EARLY	200	Genes defining early response to estrogen.	28	0.14	2.76E-08	7.68E-08
HALLMARK_IL2_STAT5_SIGNALING	200	Genes up-regulated by STAT5 in response to IL2 stimulation.	25	0.125	1.31E-06	3.27E-06
HALLMARK_KRAS_ SIGNALING_UP	200	Genes up-regulated by KRAS activation.	25	0.125	1.31E-06	3.27E-06

DISCUSSION

There is increasing evidence that all cells within a tumor are not equal with some cells having the plasticity to adapt and subvert cellular and molecular mechanisms to be more tumorigenic than others. In this study, we demonstrate that Id1 and its closely related family member Id3 are important for the CSC phenotype in the TNBC subtype. Using four independent models of Id expression and depletion, we demonstrate that the properties of proliferation and self- renewal are regulated by Id proteins.

Transcription factors like the Id family of proteins can affect a number of key molecular pathways, allowing switching of phenotypes in response to local cues such as transforming growth factor-β (TGF-β) (Kang et al., 2003a; Stankic et al., 2013), receptor tyrosine kinase signaling (Tam et al., 2008), and steroid hormones (Lin et al., 2000) and therefore are able to transduce a multitude of cues into competency for proliferation and self-renewal. The CSC phenotype as marked by Id is plastic, fitting with the latest evidence that CSC are not necessarily hierarchically organized, but

TABLE 3 | GSEA on the Intersect 2 genes from **Figure 4C** against the MSigDB hallmark gene sets.

INTERSECT 2 GSEA						
Gene set name	**# Genes in gene set (K)**	**Description**	**# Genes in overlap (k)**	**k/K**	***p*-value**	**FDR (*q*-value)**
HALLMARK_INTERFERON_ GAMMA_RESPONSE	200	Genes up-regulated in response to IFNG [GeneID = 3458].	60	0.3	3.53E-38	1.76E-36
HALLMARK_INTERFERON_ ALPHA_RESPONSE	97	Genes up-regulated in response to alpha interferon proteins.	43	0.4433	4.26E-36	1.06E-34
HALLMARK_HYPOXIA	200	Genes up-regulated in response to low oxygen levels (hypoxia).	39	0.195	5.11E-18	8.51E-17
HALLMARK_P53_PATHWAY	200	Genes involved in p53 pathways and networks.	33	0.165	2.66E-13	3.33E-12
HALLMARK_APOPTOSIS	161	Genes mediating programmed cell death (apoptosis) by activation of caspases.	28	0.1739	4.49E-12	4.49E-11
HALLMARK_ESTROGEN_RESPONSE_ EARLY	200	Genes defining early response to estrogen.	31	0.155	7.51E-12	4.70E-11
HALLMARK_HEME_METABOLISM	200	Genes involved in metabolism of heme (a cofactor consisting of iron and porphyrin) and erythroblast differentiation.	31	0.155	7.51E-12	4.70E-11
HALLMARK_MYOGENESIS	200	Genes involved in development of skeletal muscle (myogenesis).	31	0.155	7.51E-12	4.70E-11
HALLMARK_PROTEIN_SECRETION	96	Genes involved in protein secretion pathway.	21	0.2188	2.31E-11	1.28E-10
HALLMARK_EPITHELIAL_ MESENCHYMAL_TRANSITION	200	Genes defining epithelial-mesenchymal transition, as in wound healing, fibrosis and metastasis.	30	0.15	3.77E-11	1.89E-10
HALLMARK_ESTROGEN_RESPONSE_ LATE	200	Genes defining late response to estrogen.	29	0.145	1.82E-10	8.29E-10
HALLMARK_APICAL_JUNCTION	200	Genes encoding components of apical junction complex.	28	0.14	8.47E-10	3.53E-09
HALLMARK_IL2_STAT5_ SIGNALING	200	Genes up-regulated by STAT5 in response to IL2 stimulation.	26	0.13	1.62E-08	5.77E-08
HALLMARK_KRAS_SIGNALING_DN	200	Genes down-regulated by KRAS activation.	26	0.13	1.62E-08	5.77E-08
HALLMARK_ALLOGRAFT_REJECTION	200	Genes up-regulated during transplant rejection.	25	0.125	6.63E-08	2.21E-07
HALLMARK_UNFOLDED_ PROTEIN_RESPONSE	113	Genes up-regulated during unfolded protein response, a cellular stress response related to the endoplasmic reticulum.	18	0.1593	1.16E-07	3.62E-07
HALLMARK_ADIPOGENESIS	200	Genes up-regulated during adipocyte differentiation (adipogenesis).	24	0.12	2.60E-07	6.83E-07
HALLMARK_TNFA_SIGNALING_ VIA_NFKB	200	Genes regulated by NF-kB in response to TNF [GeneID = 7124].	24	0.12	2.60E-07	6.83E-07
HALLMARK_XENOBIOTIC_ METABOLISM	200	Genes encoding proteins involved in processing of drugs and other xenobiotics.	24	0.12	2.60E-07	6.83E-07
HALLMARK_IL6_JAK_ STAT3_SIGNALING	87	Genes up-regulated by IL6 [GeneID = 3569] via STAT3 [GeneID = 6774], e.g., during acute phase response.	15	0.1724	4.51E-07	1.13E-06

rather represent a transient inducible state dependent on the local microenvironment.

We report the first comprehensive analysis of Id transcriptional targets. We go on to identify a novel epistatic relationship with Robo1, with Robo1 loss sufficient to remove the necessity for Id in proliferation, suggesting that suppression of Robo1 is an important function for Id in this setting. Robo1 is a receptor for SLIT1 and SLIT2 that mediates cellular responses to molecular guidance cues in cellular migration (Huang et al., 2015). Previous work with mammary stem cells showed that the

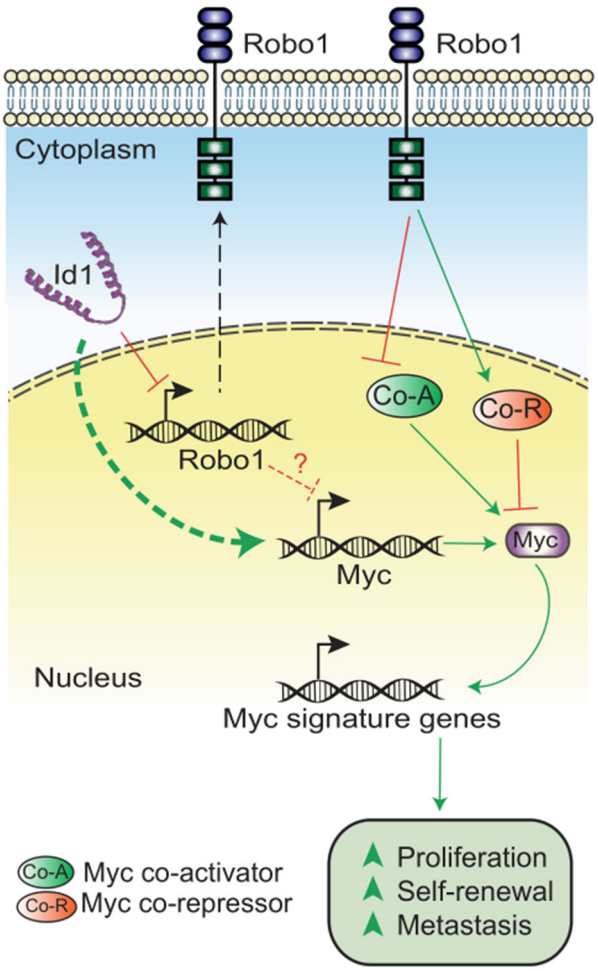

FIGURE 5 | Model showing the mechanism of Id-Robo1 action in cancer cells. The proposed model for the regulation of Myc by Id and Robo1. Co-A indicates representative Myc activator and Co-R indicates representative Myc repressor.

extracellular SLIT2 signals via ROBO1 to regulate the asymmetric self-renewal of basal stem cells through the transcription factor Snail during mammary gland development (Ballard et al., 2015). Our finding may have significant implications for tumor biology because SLIT/ROBO signaling is altered in about 40% of basal breast tumors (Ballard et al., 2015). Our work implicates a novel role for SLIT-ROBO signaling in CSC and shows a new mechanism by which Id proteins control the self-renewal phenotype by suppressing the Robo1 tumor suppressor role in TNBC.

The significant decrease in the Myc levels on Id knockdown suggest an Id/Robo1/Myc axis in TNBC (**Supplementary Figures 5D,E**). While the proposed model for regulation of Myc is not yet clear, we propose two possible modes of regulation of Myc: (1) Robo independent suppression of Myc expression and (2) Robo dependent regulation of Myc activity. Though the mechanism still needs to be elaborated, we hypothesize that in the absence of Id, Robo1 inhibits Myc activity via activation of Myc inhibitors (e.g., Rlim) and/or inhibition of Myc activators (e.g., Aurka). This is borne out by the analysis of Myc co-factors in the Id and Id Robo1 KD RNA Seq data (**Supplementary Table 5**). Further work is needed to determine whether, and which, Myc cofactors are epistatic to Id-Robo1 signaling. Our data provides further evidence that Robo1 is an important suppressor of proliferation and self-renewal in TNBC and future work includes extending this work to models of human TNBC. Prior work showing high Robo1 expression association with good outcome in breast cancer is consistent with our finding (Chang et al., 2012). There has been substantial interest in targeting Myc (Shen et al., 2015; Yang et al., 2017) and Id1, but until now has been very challenging (Fong et al., 2003; Dang et al., 2017). We show that Id1 is able to reprogram Myc activity possibly via Robo1 and may provide an alternative strategy to target Myc-dependent transcription.

CONCLUSION

We have demonstrated that breast cancer cells marked by Id expression have high propensity for key CSC phenotypes like proliferation and metastasis. We have uncovered a set of genes that are potential Id targets leading to identification of a mechanism which involves the negative transcriptional regulation of Robo1 by Id. This suggests an association between Id and Robo1 that correlates to the activation of a c-Myc driven proliferative and self-renewal program. Our observations suggest that we could exploit this pathway to target CSCs in the difficult to treat TNBC subtype.

DATA AVAILABILITY STATEMENT

The datasets generated for this study can be found in the GEO Database—GSE129790, GSE129858, and GSE129859.

ETHICS STATEMENT

The animal study was reviewed and approved by Animal Ethics Committee (AEC), Garvan Institute of Medical Research, Darlinghurst, New South Wales, Australia.

AUTHOR CONTRIBUTIONS

RN and AS contributed to the conceptualization and funding acquisition. WT, HH, AC, KH, and CK contributed to the methodology. DR and C-LC to the genomic analysis. RM, BV, AT, AM, SJ, JY, IN, JS, and LB contributed to the investigations. EM and SO'T carried out the analysis on patient samples. ASM contributed to the resources. RN and NK wrote the original draft of the manuscript. MN, CO, SL, and WK reviewed and edited the manuscript. NK contributed to the visualization. All authors read and approved the final manuscript.

FUNDING

This work was supported by funding from the National Health and Medical Research Council (NHMRC) of Australia, The National Breast Cancer Foundation and John and Deborah McMurtrie and in part by Early Career Research (ECR) Award from Science and Engineering Research Board (SERB), and Government of India (ECR/2015/000031). AS was the recipient of a Senior Research Fellowship from the NHMRC. SO'T was supported by NBCF Practitioner Fellowship and also acknowledges the Sydney Breast Cancer Foundation, the Tag family, Mr. David Paradice, ICAP and the O'Sullivan family and the estate of the late Kylie Sinclair. RN is the recipient of the Ramanujan Fellowship from the Government of India (SERB) (SB/S2/RJN/182/2014). WT was funded by International Postgraduate Research Scholarship and the Beth Yarrow Memorial Award in Medical Science. AT and BV were funded through CSIR-Junior Research Fellowship, and DST-INSPIRE Fellowship, respectively.

ACKNOWLEDGMENTS

We would like to thank the following people for their assistance with this manuscript: Ms. Nicola Foreman and Ms. Breanna Fitzpatrick for animal handling; Ms. Alice Boulghourjian and Ms. Anaiis Zaratzian for tissue processing and IHC staining; Mr. Rob Salomon and Mr. David Snowden for their help with flow sorting. This manuscript has been released as a pre-print at bioRxiv (Teo et al., 2018).

SUPPLEMENTARY MATERIAL

The Supplementary Material for this article can be found online at: https://www.frontiersin.org/articles/10.3389/fcell.2020.00552/full#supplementary-material

REFERENCES

Aceto, N., Bardia, A., Miyamoto, D. T., Donaldson, M. C., Wittner, B. S., Spencer, J. A., et al. (2014). Circulating tumor cell clusters are oligoclonal precursors of breast cancer metastasis. *Cell* 158, 1110–1122. doi: 10.1016/j.cell.2014.07.013

Aloia, L., Gutierrez, A., Caballero, J. M., and Di Croce, L. (2015). Direct interaction between Id1 and Zrf1 controls neural differentiation of embryonic stem cells. *EMBO Rep.* 16, 63–70. doi: 10.15252/embr.201439560

Anido, J., Saez-Borderias, A., Gonzalez-Junca, A., Rodon, L., Folch, G., Carmona, M. A., et al. (2010). TGF-beta receptor inhibitors target the CD44(high)/Id1(high) glioma-initiating cell population in human glioblastoma. *Cancer Cell* 18, 655–668. doi: 10.1016/j.ccr.2010.10.023

Aslakson, C. J., and Miller, F. R. (1992). Selective events in the metastatic process defined by analysis of the sequential dissemination of subpopulations of a mouse mammary tumor. *Cancer. Res.* 52, 1399–1405.

Ballard, M. S., Zhu, A., Iwai, N., Stensrud, M., Mapps, A., Postiglione, M. P., et al. (2015). Mammary stem cell self-renewal is regulated by Slit2/Robo1 signaling through SNAI1 and mINSC. *Cell. Rep.* 13, 290–301. doi: 10.1016/j.celrep.2015.09.006

Bos, P. D., Zhang, X. H., Nadal, C., Shu, W., Gomis, R. R., Nguyen, D. X., et al. (2009). Genes that mediate breast cancer metastasis to the brain. *Nature* 459, 1005–1009. doi: 10.1038/nature08021

Chang, P. H., Hwang-Verslues, W. W., Chang, Y. C., Chen, C. C., Hsiao, M., Jeng, Y. M., et al. (2012). Activation of Robo1 signaling of breast cancer cells by Slit2 from stromal fibroblast restrains tumorigenesis via blocking PI3K/Akt/beta-catenin pathway. *Cancer Res.* 72, 4652–4661. doi: 10.1158/0008-5472.CAN-12-0877

Chang, Q., Bournazou, E., Sansone, P., Berishaj, M., Gao, S. P., Daly, L., et al. (2013). The IL-6/JAK/Stat3 feed-forward loop drives tumorigenesis and metastasis. *Neoplasia* 15, 848–862. doi: 10.1593/neo.13706

Charafe-Jauffret, E., Ginestier, C., Iovino, F., Wicinski, J., Cervera, N., Finetti, P., et al. (2009). Breast cancer cell lines contain functional cancer stem cells with metastatic capacity and a distinct molecular signature. *Cancer Res.* 69, 1302–1313. doi: 10.1158/0008-5472.CAN-08-2741

Chen, J., Li, Y., Yu, T. S., McKay, R. M., Burns, D. K., Kernie, S. G., et al. (2012). A restricted cell population propagates glioblastoma growth after chemotherapy. *Nature* 488, 522–526. doi: 10.1038/nature11287

da Silva-Diz, V., Lorenzo-Sanz, L., Bernat-Peguera, A., Lopez-Cerda, M., and Munoz, P. (2018). Cancer cell plasticity: Impact on tumor progression and therapy response. *Semin.Cancer Biol.* 53, 48–58. doi: 10.1016/j.semcancer.2018.08.009

Dang, C. V., Reddy, E. P., Shokat, K. M., and Soucek, L. (2017). Drugging the 'undruggable' cancer targets. *Nat. Rev. Cancer* 17, 502–508. doi: 10.1038/nrc.2017.36

Dobin, A., Davis, C. A., Schlesinger, F., Drenkow, J., Zaleski, C., Jha, S., et al. (2013). STAR: ultrafast universal RNA-seq aligner. *Bioinformatics* 29, 15–21. doi: 10.1093/bioinformatics/bts635

Dontu, G., Al-Hajj, M., Abdallah, W. M., Clarke, M. F., and Wicha, M. S. (2003). Stem cells in normal breast development and breast cancer. *Cell Prolif.* 36(Suppl 1), 59–72. doi: 10.1046/j.1365-2184.36.s.1.6.x

Dull, T., Zufferey, R., Kelly, M., Mandel, R. J., Nguyen, M., Trono, D., et al. (1998). A third-generation lentivirus vector with a conditional packaging system. *J. Virol.* 72, 8463–8471. doi: 10.1128/JVI.72.11.8463-8471.1998

Eckhardt, B. L., Parker, B. S., van Laar, R. K., Restall, C. M., Natoli, A. L., Tavaria, M. D., et al. (2005). Genomic analysis of a spontaneous model of breast cancer metastasis to bone reveals a role for the extracellular matrix. *Mol. Cancer Res.* 3, 1–13.

Fong, S., Itahana, Y., Sumida, T., Singh, J., Coppe, J. P., Liu, Y., et al. (2003). Id-1 as a molecular target in therapy for breast cancer cell invasion and metastasis. *Proc. Natl. Acad. Sci. U.S.A.* 100, 13543–13548. doi: 10.1073/pnas.2230238100

Gao, D., Nolan, D. J., Mellick, A. S., Bambino, K., McDonnell, K., and Mittal, V. (2008). Endothelial progenitor cells control the angiogenic switch in mouse lung metastasis. *Science* 319, 195–198. doi: 10.1126/science.1150224

Gao, R., Wang, L., Cai, H., Zhu, J., and Yu, L. (2016). E3 ubiquitin ligase RLIM negatively regulates c-Myc transcriptional activity and restrains cell proliferation. *PLoS ONE* 11:e0164086. doi: 10.1371/journal.pone.0164086

Green, J. E., Shibata, M. A., Yoshidome, K., Liu, M. L., Jorcyk, C., Anver, M. R., et al. (2000). The C3(1)/SV40 T-antigen transgenic mouse model of mammary cancer: ductal epithelial cell targeting with multistage progression to carcinoma. *Oncogene* 19, 1020–1027. doi: 10.1038/sj.onc.1203280

Gumireddy, K., Li, A., Gimotty, P. A., Klein-Szanto, A. J., Showe, L. C., Katsaros, D., et al. (2009). KLF17 is a negative regulator of epithelial-mesenchymal transition and metastasis in breast cancer. *Nat. Cell. Biol.* 11, 1297–1304. doi: 10.1038/ncb1974

Gupta, G. P., Perk, J., Acharyya, S., de Candia, P., Mittal, V., Todorova-Manova, K., et al. (2007). ID genes mediate tumor reinitiation during breast cancer lung metastasis. *Proc. Natl. Acad. Sci. U.S.A.* 104, 19506–19511. doi: 10.1073/pnas.0709185104

Herschkowitz, J. I., Simin, K., Weigman, V. J., Mikaelian, I., Usary, J., Hu, Z., et al. (2007). Identification of conserved gene expression features between murine mammary carcinoma models and human breast tumors. *Genome Biol.* 8:R76. doi: 10.1186/gb-2007-8-5-r76

Herschkowitz, J. I., Zhao, W., Zhang, M., Usary, J., Murrow, G., Edwards, D., et al. (2012). Comparative oncogenomics identifies breast tumors enriched in functional tumor-initiating cells. *Proc. Natl. Acad. Sci. U.S.A.* 109, 2778–2783. doi: 10.1073/pnas.1018862108

Hochgrafe, F., Zhang, L., O'Toole, S. A., Browne, B. C., Pinese, M., Porta Cubas, A., et al. (2010). Tyrosine phosphorylation profiling reveals the signaling network characteristics of Basal breast cancer cells. *Cancer Res.* 70, 9391–9401. doi: 10.1158/0008-5472.CAN-10-0911

Hong, S. H., Lee, J. H., Lee, J. B., Ji, J., and Bhatia, M. (2011). ID1 and ID3 represent conserved negative regulators of human embryonic and induced pluripotent stem cell hematopoiesis. *J. Cell. Sci.* 124, 1445–1452. doi: 10.1242/jcs.077511

Hu, Y., and Smyth, G. K. (2009). ELDA: extreme limiting dilution analysis for comparing depleted and enriched populations in stem cell and other assays. *J. Immunol. Methods* 347, 70–78. doi: 10.1016/j.jim.2009.06.008

Huang, T., Kang, W., Cheng, A. S., Yu, J., and To, K. F. (2015). The emerging role of Slit-Robo pathway in gastric and other gastro intestinal cancers. *BMC Cancer* 15:950. doi: 10.1186/s12885-015-1984-4

Irizarry, R. A., Bolstad, B. M., Collin, F., Cope, L. M., Hobbs, B., and Speed, T. P. (2003). Summaries of Affymetrix GeneChip probe level data. *Nucl. Acids Res.* 31:e15. doi: 10.1093/nar/gng015

Kang, Y., Chen, C. R., and Massague, J. (2003a). A self-enabling TGFbeta response coupled to stress signaling: Smad engages stress response factor ATF3 for Id1 repression in epithelial cells. *Mol. Cell* 11, 915–926. doi: 10.1016/S1097-2765(03)00109-6

Kang, Y., Siegel, P. M., Shu, W., Drobnjak, M., Kakonen, S. M., Cordon-Cardo, C., et al. (2003b). A multigenic program mediating breast cancer metastasis to bone. *Cancer Cell* 3, 537–549. doi: 10.1016/S1535-6108(03)00132-6

Kim, H., Chung, H., Kim, H. J., Lee, J. Y., Oh, M. Y., Kim, Y., et al. (2008). Id-1 regulates Bcl-2 and Bax expression through p53 and NF-kappaB in MCF-7 breast cancer cells. *Breast Cancer Res. Treat.* 112, 287–296. doi: 10.1007/s10549-007-9871-6

Konrad, C. V., Murali, R., Varghese, B. A., and Nair, R. (2017). The role of cancer stem cells in tumor heterogeneity and resistance to therapy. *Can. J. Physiol. Pharmacol.* 95, 1–15. doi: 10.1139/cjpp-2016-0079

Landemaine, T., Jackson, A., Bellahcene, A., Rucci, N., Sin, S., Abad, B. M., et al. (2008). A six-gene signature predicting breast cancer lung metastasis. *Cancer Res.* 68, 6092–6099. doi: 10.1158/0008-5472.CAN-08-0436

Lasorella, A., Benezra, R., and Iavarone, A. (2014). The ID proteins: master regulators of cancer stem cells and tumour aggressiveness. *Nat. Rev. Cancer* 14, 77–91. doi: 10.1038/nrc3638

Lawson, D. A., Bhakta, N. R., Kessenbrock, K., Prummel, K. D., Yu, Y., Takai, K., et al. (2015). Single-cell analysis reveals a stem-cell program in human metastatic breast cancer cells. *Nature* 526, 131–135. doi: 10.1038/nature15260

Lee, C. H., Yu, C. C., Wang, B. Y., and Chang, W. W. (2016). Tumorsphere as an effective *in vitro* platform for screening anti-cancer stem cell drugs. *Oncotarget* 7, 1215–1226. doi: 10.18632/oncotarget.6261

Lee, G., Hall, R. R. 3rd, and Ahmed, A. U. (2016). Cancer stem cells: cellular plasticity, niche, and its clinical relevance. *J. Stem Cell Res. Ther.* 6:363. doi: 10.4172/2157-7633.1000363

Lelekakis, M., Moseley, J. M., Martin, T. J., Hards, D., Williams, E., Ho, P., et al. (1999). A novel orthotopic model of breast cancer metastasis to bone. *Clin. Exp. Metastasis* 17, 163–170. doi: 10.1023/A:1006689719505

Li, B., and Dewey, C. N. (2011). RSEM: accurate transcript quantification from RNA-Seq data with or without a reference genome. *BMC Bioinformatics* 12:323. doi: 10.1186/1471-2105-12-323

Li, X., Lewis, M. T., Huang, J., Gutierrez, C., Osborne, C. K., Wu, M. F., et al. (2008). Intrinsic resistance of tumorigenic breast cancer cells to chemotherapy. *J. Natl. Cancer Inst.* 100, 672–679. doi: 10.1093/jnci/djn123

Liang, Y. Y., Brunicardi, F. C., and Lin, X. (2009). Smad3 mediates immediate early induction of Id1 by TGF-beta. *Cell. Res.* 19, 140–148. doi: 10.1038/cr.2008.321

Liberzon, A., Birger, C., Thorvaldsdottir, H., Ghandi, M., Mesirov, J. P., and Tamayo, P. (2015). The molecular signatures database (MSigDB) hallmark gene set collection. *Cell Syst.* 1, 417–425. doi: 10.1016/j.cels.2015.12.004

Lin, C. Q., Singh, J., Murata, K., Itahana, Y., Parrinello, S., Liang, S. H., et al. (2000). A role for Id-1 in the aggressive phenotype and steroid hormone response of human breast cancer cells. *Cancer Res.* 60, 1332–1340.

Liu, H., Patel, M. R., Prescher, J. A., Patsialou, A., Qian, D., Lin, J., et al. (2010). Cancer stem cells from human breast tumors are involved in spontaneous metastases in orthotopic mouse models. *Proc. Natl. Acad. Sci. U.S.A.* 107, 18115–18120. doi: 10.1073/pnas.1006732107

Lyden, D., Young, A. Z., Zagzag, D., Yan, W., Gerald, W., O'Reilly, R., et al. (1999). Id1 and Id3 are required for neurogenesis, angiogenesis and vascularization of tumour xenografts. *Nature* 401, 670–677. doi: 10.1038/44334

Malanchi, I., Santamaria-Martinez, A., Susanto, E., Peng, H., Lehr, H. A., Delaloye, J. F., et al. (2011). Interactions between cancer stem cells and their niche govern metastatic colonization. *Nature* 481, 85–89. doi: 10.1038/nature10694

Mani, S. A., Yang, J., Brooks, M., Schwaninger, G., Zhou, A., Miura, N., et al. (2007). Mesenchyme Forkhead 1 (FOXC2) plays a key role in metastasis and is associated with aggressive basal-like breast cancers. *Proc. Natl. Acad. Sci. U.S.A.* 104, 10069–10074. doi: 10.1073/pnas.0703900104

Mellick, A. S., Plummer, P. N., Nolan, D. J., Gao, D., Bambino, K., Hahn, M., et al. (2010). Using the transcription factor inhibitor of DNA binding 1 to selectively target endothelial progenitor cells offers novel strategies to inhibit tumor angiogenesis and growth. *Cancer Res.* 70, 7273–7282. doi: 10.1158/0008-5472.CAN-10-1142

Minn, A. J., Gupta, G. P., Siegel, P. M., Bos, P. D., Shu, W., Giri, D. D., et al. (2005a). Genes that mediate breast cancer metastasis to lung. *Nature* 436, 518–524. doi: 10.1038/nature03799

Minn, A. J., Kang, Y., Serganova, I., Gupta, G. P., Giri, D. D., Doubrovin, M., et al. (2005b). Distinct organ-specific metastatic potential of individual breast cancer cells and primary tumors. *J. Clin. Invest.* 115, 44–55. doi: 10.1172/JCI22320

Nair, R., Roden, D. L., Teo, W. S., McFarland, A., Junankar, S., Ye, S., et al. (2014a). c-Myc and Her2 cooperate to drive a stem-like phenotype with poor prognosis in breast cancer. *Oncogene* 33, 3992–4002. doi: 10.1038/onc.2013.368

Nair, R., Teo, W. S., Mittal, V., and Swarbrick, A. (2014b). ID proteins regulate diverse aspects of cancer progression and provide novel therapeutic opportunities. *Mol. Ther.* 22, 1407–1415. doi: 10.1038/mt.2014.83

Niola, F., Zhao, X., Singh, D., Sullivan, R., Castano, A., Verrico, A., et al. (2013). Mesenchymal high-grade glioma is maintained by the ID-RAP1 axis. *J. Clin. Invest.* 123, 405–417. doi: 10.1172/JCI63811

O'Brien, C. A., Kreso, A., Ryan, P., Hermans, K. G., Gibson, L., Wang, Y., et al. (2012). ID1 and ID3 regulate the self-renewal capacity of human colon cancer-initiating cells through p21. *Cancer Cell* 21, 777–792. doi: 10.1016/j.ccr.2012.04.036

Padua, D., Zhang, X. H., Wang, Q., Nadal, C., Gerald, W. L., Gomis, R. R., et al. (2008). TGFbeta primes breast tumors for lung metastasis seeding through angiopoietin-like 4. *Cell* 133, 66–77. doi: 10.1016/j.cell.2008.01.046

Pastrana, E., Silva-Vargas, V., and Doetsch, F. (2011). Eyes wide open: a critical review of sphere-formation as an assay for stem cells. *Cell Stem Cell* 8, 486–498. doi: 10.1016/j.stem.2011.04.007

Perry, S. S., Zhao, Y., Nie, L., Cochrane, S. W., Huang, Z., and Sun, X. H. (2007). Id1, but not Id3, directs long-term repopulating hematopoietic stem-cell maintenance. *Blood* 110, 2351–2360. doi: 10.1182/blood-2007-01-069914

Pfefferle, A. D., Herschkowitz, J. I., Usary, J., Harrell, J. C., Spike, B. T., Adams, J. R., et al. (2013). Transcriptomic classification of genetically engineered mouse models of breast cancer identifies human subtype counterparts. *Genome Biol.* 14:R125. doi: 10.1186/gb-2013-14-11-r125

Pulaski, B. A., and Ostrand-Rosenberg, S. (1998). Reduction of established spontaneous mammary carcinoma metastases following immunotherapy with major histocompatibility complex class II and B7.1 cell-based tumor vaccines. *Cancer Res.* 58, 1486–1493.

Qian, T., Lee, J. Y., Park, J. H., Kim, H. J., and Kong, G. (2010). Id1 enhances RING1b E3 ubiquitin ligase activity through the Mel-18/Bmi-1 polycomb group complex. *Oncogene* 29, 5818–5827. doi: 10.1038/onc.2010.317

Qin, F., Zhang, H., Ma, L., Liu, X., Dai, K., Li, W., et al. (2015). Low expression of Slit2 and Robo1 is associated with poor prognosis and brain-specific metastasis of breast cancer patients. *Sci. Rep.* 5:14430. doi: 10.1038/srep14430

Reich, M., Liefeld, T., Gould, J., Lerner, J., Tamayo, P., and Mesirov, J. P. (2006). GenePattern 2.0. *Nat. Genet.* 38, 500–501. doi: 10.1038/ng0506-500

Ritchie, M. E., Phipson, B., Wu, D., Hu, Y., Law, C. W., Shi, W., et al. (2015). limma powers differential expression analyses for RNA-sequencing and microarray studies. *Nucl. Acids. Res.* 43:e47. doi: 10.1093/nar/gkv007

Robinson, M. D., and Oshlack, A. (2010). A scaling normalization method for differential expression analysis of RNA-seq data. *Genome Biol.* 11:R25. doi: 10.1186/gb-2010-11-3-r25

Shen, L., O'Shea, J. M., Kaadige, M. R., Cunha, S., Wilde, B. R., Cohen, A. L., et al. (2015). Metabolic reprogramming in triple-negative breast cancer through Myc suppression of TXNIP. *Proc. Natl. Acad. Sci. U.S.A.* 112, 5425–5430. doi: 10.1073/pnas.1501555112

Shin, K. J., Wall, E. A., Zavzavadjian, J. R., Santat, L. A., Liu, J., Hwang, J. I., et al. (2006). A single lentiviral vector platform for microRNA-based conditional RNA interference and coordinated transgene expression. *Proc. Natl. Acad. Sci. U.S.A.* 103, 13759–13764. doi: 10.1073/pnas.0606179103

Smyth, G. K. (2004). Linear models and empirical bayes methods for assessing differential expression in microarray experiments. *Stat. Appl. Genet. Mol. Biol.* 3:Article3. doi: 10.2202/1544-6115.1027

Stankic, M., Pavlovic, S., Chin, Y., Brogi, E., Padua, D., Norton, L., et al. (2013). TGF-beta-Id1 signaling opposes Twist1 and promotes metastatic colonization via a mesenchymal-to-epithelial transition. *Cell. Rep.* 5, 1228–1242. doi: 10.1016/j.celrep.2013.11.014

Subramanian, A., Tamayo, P., Mootha, V. K., Mukherjee, S., Ebert, B. L., Gillette, M. A., et al. (2005). Gene set enrichment analysis: a knowledge-based approach for interpreting genome-wide expression profiles. *Proc. Natl. Acad. Sci. U.S.A.* 102, 15545–15550. doi: 10.1073/pnas.0506580102

Swarbrick, A., Akerfeldt, M. C., Lee, C. S., Sergio, C. M., Caldon, C. E., Hunter, L. J., et al. (2005). Regulation of cyclin expression and cell cycle progression in breast epithelial cells by the helix-loop-helix protein Id1. *Oncogene* 24, 381–389. doi: 10.1038/sj.onc.1208188

Swarbrick, A., Roy, E., Allen, T., and Bishop, J. M. (2008). Id1 cooperates with oncogenic Ras to induce metastatic mammary carcinoma by subversion of the cellular senescence response. *Proc. Natl. Acad. Sci. U.S.A.* 105, 5402–5407. doi: 10.1073/pnas.0801505105

Tam, W. F., Gu, T. L., Chen, J., Lee, B. H., Bullinger, L., Frohling, S., et al. (2008). Id1 is a common downstream target of oncogenic tyrosine kinases in leukemic cells. *Blood* 112, 1981–1992. doi: 10.1182/blood-2007-07-103010

Tang, B., Yoo, N., Vu, M., Mamura, M., Nam, J. S., Ooshima, A., et al. (2007). Transforming growth factor-beta can suppress tumorigenesis through effects on the putative cancer stem or early progenitor cell and committed progeny in a breast cancer xenograft model. *Cancer Res.* 67, 8643–8652. doi: 10.1158/0008-5472.CAN-07-0982

Tao, K., Fang, M., Alroy, J., and Sahagian, G. G. (2008). Imagable 4T1 model for the study of late stage breast cancer. *BMC Cancer* 8:228. doi: 10.1186/1471-2407-8-228

Teo, W. S., Holliday, H., Karthikeyan, N., Cazet, A. S., Roden, D. L., Harvey, K., et al. (2018). Id proteins promote a cancer stem cell phenotype in triple negative breast cancer via negative regulation of Robo1. *bioRxiv. [preprint]*. 497313. doi: 10.1101/497313

Tobin, N. P., Sims, A. H., Lundgren, K. L., Lehn, S., and Landberg, G. (2011). Cyclin D1, Id1 and EMT in breast cancer. *BMC Cancer* 11:417. doi: 10.1186/1471-2407-11-417

Vaillant, F., Asselin-Labat, M. L., Shackleton, M., Forrest, N. C., Lindeman, G. J., and Visvader, J. E. (2008). The mammary progenitor marker CD61/beta3 integrin identifies cancer stem cells in mouse models of mammary tumorigenesis. *Cancer Res.* 68, 7711–7717. doi: 10.1158/0008-5472.CAN-08-1949

Wahl, G. M., and Spike, B. T. (2017). Cell state plasticity, stem cells, EMT, and the generation of intra-tumoral heterogeneity. *NPJ Breast Cancer* 3:14. doi: 10.1038/s41523-017-0012-z

Yang, A., Qin, S., Schulte, B. A., Ethier, S. P., Tew, K. D., and Wang, G. Y. (2017). MYC inhibition depletes cancer stem-like cells in triple-negative breast cancer. *Cancer Res* 77, 6641–6650. doi: 10.1158/0008-5472.CAN-16-3452

Yoneda, T., Michigami, T., Yi, B., Williams, P. J., Niewolna, M., and Hiraga, T. (2000). Actions of bisphosphonate on bone metastasis in animal models of breast carcinoma. *Cancer* 88, 2979–2988. doi: 10.1002/1097-0142(20000615)88:12+<2979::AID-CNCR13>3.0.CO;2-U

Zhang, M., Atkinson, R. L., and Rosen, J. M. (2010). Selective targeting of radiation-resistant tumor-initiating cells. *Proc. Natl. Acad. Sci. U.S.A.* 107, 3522–3527. doi: 10.1073/pnas.0910179107

Zhang, M., Behbod, F., Atkinson, R. L., Landis, M. D., Kittrell, F., Edwards, D., et al. (2008). Identification of tumor-initiating cells in a p53-null mouse model of breast cancer. *Cancer Res.* 68, 4674–4682. doi: 10.1158/0008-5472.CAN-07-6353

Zhang, N., Wang, X., Huo, Q., Sun, M., Cai, C., Liu, Z., et al. (2014). MicroRNA-30a suppresses breast tumor growth and metastasis by targeting metadherin. *Oncogene* 33, 3119–3128. doi: 10.1038/onc.2013.286

Conflict of Interest: The authors declare that the research was conducted in the absence of any commercial or financial relationships that could be construed as a potential conflict of interest.

Copyright © 2020 Teo, Holliday, Karthikeyan, Cazet, Roden, Harvey, Konrad, Murali, Varghese, Thankamony, Chan, McFarland, Junankar, Ye, Yang, Nikolic, Shah, Baker, Millar, Naylor, Ormandy, Lakhani, Kaplan, Mellick, O'Toole, Swarbrick and Nair. This is an open-access article distributed under the terms of the Creative Commons Attribution License (CC BY). The use, distribution or reproduction in other forums is permitted, provided the original author(s) and the copyright owner(s) are credited and that the original publication in this journal is cited, in accordance with accepted academic practice. No use, distribution or reproduction is permitted which does not comply with these terms.

frontiers in Molecular Biosciences

REVIEW
published: 21 August 2020
doi: 10.3389/fmolb.2020.00213

Spotlight on the Granules (Grainyhead-Like Proteins) – From an Evolutionary Conserved Controller of Epithelial Trait to Pioneering the Chromatin Landscape

*Vignesh Sundararajan[1], Qing You Pang[1,2], Mahesh Choolani[2] and Ruby Yun-Ju Huang[2,3,4]**

[1] Center for Translational Medicine, Cancer Science Institute of Singapore, National University of Singapore, Singapore, Singapore, [2] Department of Obstetrics and Gynaecology, National University of Singapore, Singapore, Singapore, [3] School of Medicine, College of Medicine, National Taiwan University, Taipei, Taiwan, [4] Graduate Institute of Oncology, College of Medicine, National Taiwan University, Taipei, Taiwan

OPEN ACCESS

Edited by:
Herbert Levine, Rice University, United States

Reviewed by:
Jason Somarelli, Duke University, United States
Geetha Durairaj, University of California, Irvine, United States

***Correspondence:**
Ruby Yun-Ju Huang
rubyhuang@ntu.edu.tw

Specialty section:
This article was submitted to Molecular Diagnostics and Therapeutics, a section of the journal Frontiers in Molecular Biosciences

Received: *07 June 2020*
Accepted: *03 August 2020*
Published: *21 August 2020*

Citation:
Sundararajan V, Pang QY, Choolani M and Huang RY-J (2020) Spotlight on the Granules (Grainyhead-Like Proteins) – From an Evolutionary Conserved Controller of Epithelial Trait to Pioneering the Chromatin Landscape. Front. Mol. Biosci. 7:213. doi: 10.3389/fmolb.2020.00213

Among the transcription factors that are conserved across phylogeny, the *grainyhead* family holds vital roles in driving the epithelial cell fate. In *Drosophila*, the function of *grainyhead* (*grh*) gene is essential during developmental processes such as epithelial differentiation, tracheal tube formation, maintenance of wing and hair polarity, and epidermal barrier wound repair. Three main mammalian orthologs of *grh*: Grainyhead-like 1-3 (GRHL1, GRHL2, and GRHL3) are highly conserved in terms of their gene structures and functions. GRHL proteins are essentially associated with the development and maintenance of the epithelial phenotype across diverse physiological conditions such as epidermal differentiation and craniofacial development as well as pathological functions including hearing impairment and neural tube defects. More importantly, through direct chromatin binding and induction of epigenetic alterations, GRHL factors function as potent suppressors of oncogenic cellular dedifferentiation program – epithelial-mesenchymal transition and its associated tumor-promoting phenotypes such as tumor cell migration and invasion. On the contrary, GRHL factors also induce pro-tumorigenic effects such as increased migration and anchorage-independent growth in certain tumor types. Furthermore, investigations focusing on the epithelial-specific activation of *grh* and GRHL factors have revealed that these factors potentially act as a pioneer factor in establishing a cell-type/cell-state specific accessible chromatin landscape that is exclusive for epithelial gene transcription. In this review, we highlight the essential roles of *grh* and GRHL factors during embryogenesis and pathogenesis, with a special focus on its emerging pioneering function.

Keywords: Grainyhead, Grh, Grainyhead-like 2, GRHL2, epithelial-to-mesenchymal transition, pioneer factor, epithelial differentiation, epigenetics

INTRODUCTION

The *grainyhead* (*grh*) transcription factor is a member of the ancestral LSF/Grainyhead gene family. Originally identified in *Drosophila* (previously known as Elf-1 or NTF-1) as an embryonic lethal locus, *grh* mutant *Drosophila* embryos show immature cuticle development, patchy tracheal network and the most notable 'granular' head skeleton aberration (Nüsslein-Volhard et al., 1984; Bray and Kafatos, 1991). The LSF/Grainyhead family of proteins are functionally distinctive by their nature of oligomerization and mechanism of DNA-binding module on cognate regulatory sites (Traylor-Knowles et al., 2010). Therefore, the gene family is subdivided into two branches: the LSF/CP2 subfamily and the Grainyhead subfamily, resulting from a major gene duplication event dated more than 700 million years ago (Wilanowski et al., 2002; Venkatesan et al., 2003). These transcription factors bind to *cis*-regulatory elements and control the expression of crucial genes during early embryonic development and tissue homeostasis. The LSF/CP2 subfamily has three mammalian orthologs and evolved from the ancestral gene *gemini* (*dCP2*) in *Drosophila*. Recent critical reviews have discussed the role of LSF/CP2 subfamily members (TFCP2, TFCP2L1, and UBP1) in various aspects of development and human diseases including cancer (Kotarba et al., 2018; Taracha et al., 2018). In this review, we elaborate on the essential functions of *grainyhead* in *Drosophila* and the three mammalian orthologs: Grainyhead-like proteins (GRHL1, GRHL2, and GRHL3). Additionally, we focus on human GRHL2 as an important determinant of the epithelial phenotype during development and as a gatekeeper of epithelial differentiation in several human cancers. Finally, we also discuss in detail the novel pioneering role of *grainyhead* and Grainyhead-like proteins in contouring the chromatin landscape during embryonic development and cancer progression.

The single *grh* gene in *Drosophila* and *Caenorhabditis elegans* exists as multiple orthologs in the vertebrates, which are denoted as *grainyhead-like* (*grhl*) genes. These genes remain evolutionarily conserved from insects to humans. In addition, a varying number of splice variants generated from alternative splicing events and alternative transcriptional initiation sites further highlight the underlying complexity and their gene regulatory networks operating during development and disease progression (Uv et al., 1997; Miles et al., 2017). Of note, three orthologs of *grainyhead* exist in humans: Grainyhead-like 1 (GRHL1), Grainyhead-like 2 (GRHL2) and Grainyhead-like 3 (GRHL3). Each protein contains three annotated functional domains: a transcriptional activation domain (TAD) at the N-terminus; a central DNA-binding domain (DBD) structurally similar to the equivalent of p53, and a dimerization domain (DD) at the C-terminus with unique ubiquitin-like folds. The TAD is the least conserved domain between *Drosophila* and mammalian orthologs, which could be partially due to the presence of an isoleucine-rich segment that has poor conservation across phylogeny (Attardi et al., 1993; Werth et al., 2010). With respect to the human GRHL2 amino acid sequence homology, the DBD holds higher level of sequence identity in all GRHL proteins, when compared to all other domains across the model organisms (**Table 1**).

Members of the grh/GRHL family share a similar palindromic DNA-binding motif (AACCGGTT), with different levels of variability for some target genes (**Table 2**). In *Drosophila*, Grh recognizes DNA regulatory sequences upstream of genes *Ddc* (TG**AACCGGTC**CTGCGG) and *en* (GTGAGCCGGCGA**AACCGGTT**), whereas the binding motif on *Ubx* and *ftz* promoters is (T/C)N**AAC(C/T)GGT(T/C)** (Bray et al., 1988; Soeller et al., 1988; Dynlacht et al., 1989; Wilanowski et al., 2002; Venkatesan et al., 2003). In mammals, GRHL binding motifs display as two adjacent repeats of Grainyhead consensus sequences, with two tandem core CNNG motifs set apart by five bases. For example, the mouse Grhl2 binding site in intron 2 of *Cdh1* (A**AA**C**CA**G**TC**A**AA**C**CA**G**TT**) and the promoter of *Cldn4* (A**AT**C**CA**G**AG**A**AA**C**TG**G**TC**) are strikingly similar to the human GRHL2 binding motif on the intron 2 of the *CDH1* (GCA**AA**C**CA**G**CC**A**AA**C**CA**G**TT**T) and the promoter of *CLDN4* (GGA**AT**C**CA**G**AG**AA**A**C**TG**G**TC**AG) (Werth et al., 2010; Chung et al., 2016). The invariant CNNG tandem motifs share similarity with the binding motif of Tfcp2l1 from the CP2 family suggesting a close phylogenetic relationship with members of the p53 family (two CNNG set apart by six bases) based on protein folding and the binding of DNA (Kokoszynska et al., 2008). A recent study on the crystal structure of Grhl1/2 DBDs shows that these domains share a common fold with p53, substantiating earlier computational predictions (Ming et al., 2018).

GRAINYHEAD AND GRHL FACTORS IN DEVELOPMENT

In metazoans, two major cell types form the basis of organ development: epithelium and mesenchyme. Epithelial cells are generated first during the embryonic development, while mesenchymal cells are derived from the pre-existing epithelial cells through a process called epithelial-to-mesenchymal transition (EMT) (Hay, 1995; Thiery and Sleeman, 2006; Kalluri and Weinberg, 2009). Epithelial cells usually maintain a strict, aligned cellular polarity (apical and basal surfaces) and remain closely connected to adjacent cells through specialized transmembrane structures, such as tight junctions, adherens junctions, and desmosomes. In contrast, due to their lack of stable cell-cell attachment and apical-basal polarity, mesenchymal cells possess higher migratory abilities and interact extensively with the surrounding extracellular matrix. The earliest developmental EMT occurs during gastrulation, where mesenchymal cells are generated from epithelial epiblast cells. The mesenchyme further condenses to form mesoderm (middle layer of the embryo) and endoderm (inner layer of the embryo), which eventually form the vertebral column, bony appendages and connective tissues (Hay, 2005). However, the epithelia is the stable state of cellular organization that forms the epidermis, the primary layer covering the external surface of the body that provides protection against external physical and mechanical stress. The following sections describe the vital roles of Grainyhead and Grainyhead-like proteins in the epidermis and epithelia.

TABLE 1 | Members of the grainyhead/Grainyhead-like transcription factor family and protein sequence homology in nematode, fruit fly, zebrafish, and mammals.

Species	Gene name (Official name)	Aliases	Gene location	Assembly	Splice variants	Amino acid sequence homology (% identity to human GRHL2)			
						Full length	TAD	DBD	DD
Round worm (*Caenorhabditis elegans*)	*CP2 domain-containing protein (grh1)*	–	Chr I: 1,259,374-1,268,155	WBcel235: BX284601.5	3	40.5	< 30	54.7	36.1
Fruit Fly (*Drosophila melanogaster*)	*grainy head (grh)*	Dmel\CG42311; DREB; EG:191D12.1; Elf-1; Grh; Ntf; Ntf1	Chr 2R: 17,801,132-17,842,820	BDGP6.28: AE013599.5	8	52.1	< 30	52.1	35.5
Zebrafish (*Danio rerio*)	*grainyhead-like 1 (grhl1)*	fc49a04; wu:fc49a04	Chr 17: 32,391,056-32,426,413	GRCz11: CM002901.2	7	56.9	63.3	73.4	68.2
	grainyhead-like 2a (grhl2a)	zgc:110324	Chr 16: 9,807,263-9,830,451	GRCz11: CM002900.2	1	61	63.7	78.9	59.8
	grainyhead-like 2b (grhl2b)	grhl2, si:dkey-21k18.2	Chr 19: 12,234,975-12,291,981	GRCz11: CM002903.2	2	70.5	59	86.1	70.7
	grainyhead-like 3 (grhl3)	cb467, sb:cb467, si:dkey-221l4.7, wu:fa01c12, wu:fb74c01	Chr 17: 26,965,351-26,977,183	GRCz11: CM002901.2	4	50.3	< 30	55.3	51.8
Mouse (*Mus musculus*)	*grainyhead-like 1 (Grhl1)*	LBP-32, Tcfcp2l2, p61 MGR, p70 MGR	Chr 12: 24,572,283-24,617,391	GRCm38:CM001005.2	4	56.7	59.1	73.4	59.2
	grainyhead-like 2 (Grhl2)	0610015A08Rik, BOM, Tcfcp2l3, clft3	Chr 15: 37,233,036-37,363,569	GRCm38:CM001008.2	6	94.7	96.2	98.7	93.2
	grainyhead-like 3 (Grhl3)	Get1, Som, ct	Chr 4: 135,541,888-135,573,630	GRCm38:CM000997.2	1	45.6	54.5	57.8	60
Human (*Homo sapiens*)	*grainyhead-like 1 (GRHL1)*	LBP-32, MGR, TFCP2L2	Chr 2: 9,951,693-10,002,277	GRCh38:CM000664.2	8	56.4	59.1	72.6	57.6
	grainyhead-like 2 (GRHL2)	BOM, DFNA28, FLJ13782, TFCP2L3	Chr 8: 101,492,439-101,669,726	GRCh38:CM000670.2	6	–	–	–	–
	grainyhead-like 3 (GRHL3)	SOM, TFCP2L4	Chr 1: 24,319,322-24,364,482	GRCh38:CM000663.2	9	45.7	50.5	57	64.1

TABLE 2 | A non-exhaustive list of transcriptional targets of Grh/GRHL factors in literature.

Target gene	Binding region	Species/ Model	Regulated by GRHL	Activation/ Repression	Function	References
Dopa decarboxylase *(Ddc)*	Promoter/ Enhancer	*Drosophila*	Grainyhead	Activation	Hardening of larval and adult cuticles	Bray and Kafatos, 1991; Venkatesan et al., 2003; Mace et al., 2005
Ultrabithorax (*Ubx*)	Promoter	*Drosophila*	Grainyhead	Activation	Differentiation of 'head skeleton'	Bray and Kafatos, 1991
Engrailed (*en*)	Promoter	*Drosophila*	Grainyhead	Activation	Posterior wing compartment identity	Soeller et al., 1988
Zerknüllt (*zen*), Tailless (*tll*), Scute (*sc*), Sex lethal (*Sxl*)	Promoter	*Drosophila*	Grainyhead	Repression	Developmental patterning, sex determination and cellularization	Harrison et al., 2010
Fasciclin 3 (*Fas3*), Coracle (*cora*), Sinuous (*Sinu*)	Intron 1	*Drosophila*	Grainyhead	Activation	Septate junction proteins that forms barrier epithelia	Narasimha et al., 2008
Stitcher (*stit*)	Intron 2	*Drosophila*	Grainyhead	Activation	Epidermal wound healing	Wang et al., 2009
Misshapen (*msn*), Krotzkopf verkehrt (*kkv*), Tyrosine hydroxylase (*ple*)	Enhancer	*Drosophila*	Grainyhead	Activation	Epidermal wound healing	Pearson et al., 2009
Claudin b (*cldnb*), Epithelial cell adhesion molecule (*epcam*)	Enhancer	Zebrafish	Grhl2b	Activation	Otic development and hearing ability	Han et al., 2011
Engrailed 2a (*eng2a*), CDC42 small effector 1 (*cdc42se1*)	Promoter	Zebrafish	Grhl2b	Activation	Midbrain-hindbrain morphogenesis	Dworkin et al., 2012
Engrailed-1 (*EN1*)	Promoter	Human	GRHL1	Activation	Morphogenesis	Wilanowski et al., 2002
Desmoglein 1 (*Dsg1/DSG1*)	Promoter	Human and Mouse	GRHL1	Activation	Desmosome organization	Wilanowski et al., 2008
Albumin (*Alb*), Carbamoylphosphate synthetase I (*1*), Hepatocyte nuclear factor 4α (*Hnf4α*), CCAAT/enhancer binding protein α (*Cebpa*)	Unknown	Mouse	Grhl2	Repression	Inhibition of hepatocytic differentiation	Tanimizu et al., 2013
Claudin 3 (*Cldn3*), Claudin 4 (*Cldn4*), E-cadherin (*Cdh1*)	Promoter – *Cldn4*, Intron 2 – *Cdh1*	Mouse	Grhl2	Activation	Maintenance of breast epithelial cell identity	Werth et al., 2010
miR-122	Promoter	Human	GRHL2	Repression	Ethanol induced liver injury and fibrosis	Satishchandran et al., 2018
miR-200b/-200a/429	Promoter	Human	GRHL2	Activation	Suppression of EMT	Cieply et al., 2012; Chung et al., 2016
Serine peptidase inhibitor, Kunitz type 1 (*SPINT1*)	Promoter	Human	GRHL2	Activation	Salivary gland development	Walentin et al., 2015; Matsushita et al., 2018
Matrix metalloproteinases (MMPs) - multiple	Unknown	Human	GRHL2	Repression	Suppression of invasion phenotype	Chung et al., 2016; Pifer et al., 2016; Xiang et al., 2017
Forkhead box M1B (*FOXM1B*)	Promoter	Human	GRHL2	Activation	Human papillomavirus associated oropharyngeal cancer development	Chen et al., 2018c, 2
Tumor protein p63 (*TP63/p63*)	Promoter	Human	GRHL2	Activation	Maintenance of epithelial phenotype in human keratinocytes	Mehrazarin et al., 2015
Ovo like zinc finger 2 (*Ovol2/OVOL2*)	Promoter	Human and Mouse	GRHL2	Activation	Epithelial barrier function and palatogenesis	Watanabe et al., 2014; Aue et al., 2015; Carpinelli et al., 2020
v-erb-b2 avian erythroblastic	Promoter	Human and Mouse	GRHL2	Activation	Suppression of EMT	Werner et al., 2013; Chung et al., 2016

(Continued)

TABLE 2 | Continued

Target gene	Binding region	Species/ Model	Regulated by GRHL	Activation/ Repression	Function	References
leukemia viral oncogene homolog 3 (*Erbb3/ERBB3*)						
member RAS oncogene family (*Rab25/RAB25*)	Promoter	Human and Mouse	GRHL2	Activation	Regulation of epithelial morphogenesis	Senga et al., 2012; Gao et al., 2013
Rho Guanine Nucleotide Exchange Factor 19 (*Arhgef19/ARHGEF19*)	Promoter	Human and Mouse	GRHL2 and GRHL3	Activation	Maintenance of epidermal differentiation	Caddy et al., 2010; Boglev et al., 2011; Gao et al., 2013
miR-21	Promoter	Human and Mouse	GRHL3	Repression	Maintenance of epidermal differentiation	Bhandari et al., 2013
Transglutaminase 1 (*Tgm1/TGM1*)	Promoter	Human and Mouse	GRHL3	Activation	Maintenance of epidermal differentiation	Ting et al., 2005; Boglev et al., 2011
Uroplakin 2 (*Upkll*)	Promoter	Mouse	GRHL3	Activation	Urothelial differentiation	Yu et al., 2009

The recurrence of EMT is also observed during the early development of the nervous system to generate neural crest cells. During the embryonic process termed neurulation, epithelial neural plate (neural ectoderm) bends, invaginates and fuses along the dorsal midline to form a cylindrical structure called the neural tube. Subsequent closure of the neural tube in anterior and posterior directions guides formation of the future brain and spinal cord (Wilde et al., 2014). Meanwhile, the dorsal neuroepithelial cells located close to the neural tube lose intercellular connections, undergo EMT, and migrate away to become neural crest cells (Acloque et al., 2009). Further delamination and migration of neural crest cells navigate to populate multiple niches throughout the embryo, ultimately progress toward terminal differentiation derivatives such as ganglia of the peripheral and enteric nervous system, cardiac valves, bone and cartilage of the facial skeleton (Simões-Costa and Bronner, 2013; Muñoz and Trainor, 2015). Members of the Grainyhead-like family provide distinct regional signals during neurulation, neural crest migration, and neural tube closure that are discussed in detail in an upcoming section.

Drosophila Grainyhead During Epidermal Morphogenesis

In *Drosophila*, the formation of protective exoskeleton called cuticle during the early stages of larval development serves many important functions during the adult life including the protection against water loss and the maintenance of structural framework for locomotion. *grh* remains to be essential for the development of the epidermal barrier and the repair of barriers after wounding. The embryonically lethal larval cuticles of *grh* mutants are multilayered and grossly inflated structures, generating the "blimp" phenotype that are functionally weaker when compared to wild-type cuticles (Uv et al., 1997; Ostrowski et al., 2002; Hemphälä et al., 2003). *grh* mutant embryos carrying induced aseptic epidermal wounds fail to restore the expression of Dopa decarboxylase *(Ddc* in the wound border*)*, one of the two key enzymes contributing for the formation and hardening of larval and adult cuticles. This results in the defective phosphorylation of *grh* by ERK which is required for wound-dependent regeneration of the epidermal barrier (Mace et al., 2005; Geiger et al., 2011; Kim and McGinnis, 2011). Other studies focusing on *Drosophila* epidermal wound healing and amnioserosa (defects in dorsal closure) have identified the direct regulation of Grh on major targets including *stit*, *msn*, *cora*, *sinu*, and *fas3* (Narasimha et al., 2008; Pearson et al., 2009; Wang and Samakovlis, 2012). In addition to controlling the epithelial and epidermal morphogenesis in *Drosophila*, Grh directly regulates the expression of key genes (**Table 2**) that are involved in the tracheal tube formation (Hemphälä et al., 2003), the maturation of central nervous system (Almeida and Bray, 2005; Khandelwal et al., 2017), and the maintenance of polarity in wing and hair (Lee and Adler, 2004).

GRHL Family in Epithelial Morphogenesis and Development

The GRHL family members play crucial roles during the development of several epithelial tissues (**Figure 1**). During the development of mouse circumvallate papilla (specialized dome shaped region located at the back of a tongue), knockdown of *Grhl3* significantly alters the epithelial structure and disrupts the epithelial integrity by having high proliferation, low apoptosis, and enhanced migration in epithelial tongues cells of embryonic mice (Adhikari et al., 2017). Several reports have claimed the prominent function of GRHL factors in epidermal integrity. Grhl1 directly controls the expression of the desmosomal cadherin, desmoglein 1 (*Dsg1*) and mice deficient of *Grhl1* show an abnormal desmosome phenotype in the interfollicular epidermis, ultimately delaying the initial skin coat growth and poor hair anchoring to the follicle (Wilanowski et al., 2008).

During early embryogenesis, Grhl2 expression is predominantly observed in several barrier-forming epithelial tissues, including the surface ectoderm, the otic ectoderm, and the gut tube (Auden et al., 2006; Werth et al., 2010). At the molecular level, Grhl2 binds to cis-regulatory elements and controls the timely expression of the apical junctional complex proteins such as the adherens junction component E-cadherin and the tight junction molecules claudin 3, claudin 4 (*Cldn3/4*), and an epithelial-specific member of small guanosine triphosphatase Rab25, which are crucial for epithelial differentiation (Werth et al., 2010; Senga et al., 2012;

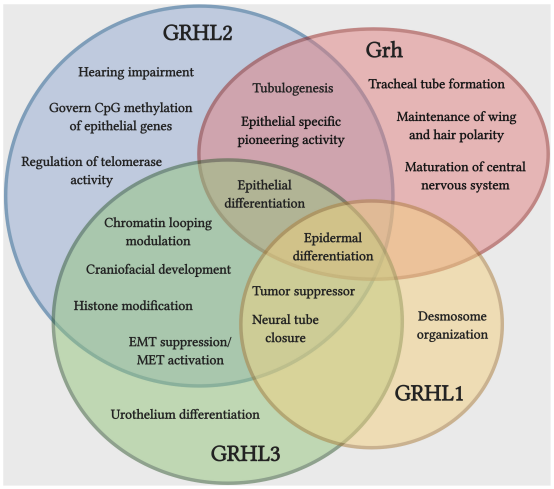

FIGURE 1 | Unique and cooperative functions of Grh and GRHL family during development and disease. Epidermal differentiation is the most common function shared by Grh and GRHL family, while a set of functions associated with epithelial differentiation is carried out by more than one member of the family. The overlapping function does not indicate that they are functionally redundant. Illustration created with Biorender.com.

Tanimizu and Mitaka, 2013). GRHL2 is involved in the epithelial morphogenesis of the lung epithelium and essential for the establishment and maintenance of the epithelial barrier of mucociliary airways. In primary human bronchial epithelial cells, GRHL2 directly or indirectly regulates the expression of proteins that form apical junction assembly and cell polarity (CDH1, TJP1, RAB25) as well as essential proteins that are required to establish barrier function (PVRL4, VAV1, and ESRP1/2). Mutant cells carrying dominant–negative GRHL2 protein consequently fail to form polarized epithelium with barrier function (Gao et al., 2013). Conditional deletion of *Grhl2* in mouse tracheal basal cells and *in vitro* CRISPR/Cas9 genome editing of *GRHL2* in human basal cells have been shown to disrupt the differentiation of ciliated cells via targeting multiple genes in the Notch signaling pathway and ciliogenesis such as *Mcidas*, *Rfx2*, and *Myb* (Gao et al., 2015). In cooperation with Nkx2-1, a homeobox transcription factor, Grhl2 regulates the expression of cell-cell interaction genes such as semaphorins and their receptors, which are crucial for maintaining the lung epithelial identity (Varma et al., 2012). Using mouse lung epithelial cells, the same study shows that Grhl2 binds to the *Nkx2-1* promoter regions and Nkx2-1 binds to the *Grhl2* intronic region and generates a positive feedback loop to reinforce lung epithelial phenotypes. Furthermore, a recent study reports that the loss of *Grhl2* in the developing mice lung epithelium reduces the expression of Elf5, an epithelial-specific transcription factor, and eventually leads to the impaired ciliated cell differentiation and the reduction of distal progenitor cells (Kersbergen et al., 2018).

Grhl3 controls epidermal differentiation and wound-repair by directly regulating the expression of two crucial genes: *Transglutaminase-1*, an enzyme that crosslinks structural components of the superficial epidermis (Ting et al., 2005), and *RhoGEF19*, a RhoA activator of the planar cell polarity (PCP) signaling pathway (Caddy et al., 2010). Grhl3 functionally interacts with the LIM-only protein LMO4 to regulate the differentiation of the epidermis, where mice lacking functional Grhl3 and LMO4 expression show severe defective skin barrier formation and failure of eyelid development affecting the expression of multiple genes linked to the epidermal terminal differentiation and F-actin cable formation (Yu et al., 2006, 2008; Hislop et al., 2008). Mice deleted for epidermal specific *Grhl3* have digit fusion (syndactyly) due to abnormal adhesion of the periderm covering the developing digits (Kashgari et al., 2020). In autosomal-recessive ectodermal dysplasia syndrome, whole exome-sequencing from affected individuals revealed the presence of homozygous mutations in the *GRHL2* locus. These mutant keratinocytes showed changes in the cellular phenotype and failure to form intact cell-cell junctions, partly due to the cytoplasmic translocation of GRHL2 (Petrof et al., 2014). Interestingly, cytoplasmic translocation of GRHL3 induces the activation of the non-canonical Wnt signaling pathway involving PCP genes, and eventually alters the mechanical properties essential for enduring tensile force during epithelial differentiation (Kimura-Yoshida et al., 2018). In additional to the pulmonary and epidermal epithelium, another major tissue that plays an important role in the barrier function is the urothelial membrane, which controls the selective movement of water and solutes between urine and tissues. Grhl3 is highly expressed in mature umbrella cells of the bladder epithelium. It directly targets the expression of *uroplakin II*, a major protein component of the asymmetric urothelial membrane plaques, thereby regulating the terminal differentiation and barrier function of the bladder epithelium (Yu et al., 2009).

GRHL Family in Neural Development

During neurulation, the single-layered neurepithelium distinguishes into two different cell fates: neural ectoderm and surface (non-neural) ectoderm prior to neural tube closure. The fate choice between neural and surface ectoderm is highly regulated through signaling interplay of Wnt, FGF and BMP activity (Murry and Keller, 2008). At the molecular level, canonical Wnt signaling mediated Grhl3 expression is essential for the specification of surface ectoderm cell fate, whereas, repression of Grhl3 by Dickkopf1 (Dkk1), a canonical Wnt signaling antagonist, leads to the specification of neural ectoderm cell fate (Ting et al., 2003; Kimura-Yoshida et al., 2015). Thus, the balance between Wnt controlled Grhl3 activation or repression regulates the binary cell fate choice of neural and surface ectoderm identity, which is essential for subsequent neural tube closure. The remodeling of five or more polarized epithelial cells converging radially around a central point of fusion to form transient "rosette" like structures are identified during the formation of multiple organ systems, including surface ectodermal lineage specification (Afonso and Henrique, 2006; Nishimura and Takeichi, 2008; Harding et al., 2014). Genetic fate mapping using $Grhl3^{Cre/+}$ mice have reported that the rosette forming cells of the surface ectoderm are Grhl3-expressing lineage cells, and Grhl3 mutants showed severe disruption of rosette formation, exhibiting fully penetrant spina

bifida (Molè et al., 2020; Zhou et al., 2020). Single-cell RNA sequencing of neural rosettes *in vitro*, generated from human induced pluripotent stem cells, showed GRHL2 and GRHL3 were highly expressed in early rosettes highlighting the role for GRHL TFs in neurulation in humans (Shang et al., 2018). Therefore, these findings denote an earlier role for GRHL factors in neurulation, such as lineage specification, prior to its contribution in neural tube closure.

Delamination and migration of neural crest cell from the border of the surface and neural ectoderm involves activation of EMT. Although GRHL factors are potent suppressors of EMT and associated phenotypes, depletion of *grhl3*/*Grhl3* in zebrafish and mouse embryos do not affect any stages of neural crest cell development and activity (Dworkin et al., 2014; Kimura-Yoshida et al., 2015). This might indicate that fate specification of surface ectoderm in the neural plate border is partly driven by GRHL factors. However, the involvement of other GRHL factors in neural crest cell migration remains to be explored.

Following the delineation of the neurepithelium, the developing neural tube converges and fuses along the midline to form complete the neural tube closure event. Among the GRHL family, disruption of GRHL2 and GRHL3 functions generated severe neural tube defects. Loss of Grhl2 expression in the surface ectoderm resulted in abnormal mesenchymal phenotypes, with increase in vimentin expression and downregulation of epithelial genes such as *Fermt1*, *Esrp1*, and *Tmprss2*, eventually resulting in neural tube closure defects (Pyrgaki et al., 2011; Ray and Niswander, 2016). In the Grhl2-null mutants, the expression levels of two Grhl2 direct targets, E-cadherin (*Cdh1*) and Claudin 4 (*Cldn4*), are significantly reduced in the surface ectoderm leading to neural tube defects (Werth et al., 2010). In contrast, overexpression of Grhl2 could also be the underlying cause of defective neural tube closure in Axial defects mutant mouse (Brouns et al., 2011). Similarly, Grhl3-null mutants exhibited fully penetrant spina bifida, and lack of Grhl3 expression in the hindgut caused curly tail phenotype, which occurs during the final stages of neural tube closure (Ting et al., 2003; Auden et al., 2006; Gustavsson et al., 2007). Moreover, Grhl2 and Grhl3 exhibit cooperative activity during neurulation closure at the forebrain/midbrain boundary and spinal closure from mid to lower thoracic region (Rifat et al., 2010). Taken together, members of the GRHL family play critical roles during several stages of neural development and dysregulation of these factors during neural development renders severe impact on neural tube closure.

GRHL IN PATHOPHYSIOLOGY

An array of studies has reported the implication of GRHL members in multiple human diseases including cancers. Essential functioning of GRHL factors are implicated during carcinogenesis as well as during tumor suppression indicating that these factors play complex and controversial roles in regulating different cancer entities. In the following section we highlight several prominent findings that describe the essential roles of GRHL factors in pathophysiology.

Tumor Promoting Roles of GRHL Members

Few recent studies have demonstrated the association of expression levels of GRHL members with patient outcomes during cancer progression. In colorectal cancer, higher expression levels of GRHL1 and GRHL3 are associated with worse disease-free survival, whereas low levels of all three members confer better overall survival of patients (Yuan et al., 2020). GRHL2 expression is enriched in human breast cancer stem cell-like subpopulation and is included in a 31-gene signature predictive of distant metastasis in estrogen receptor–negative breast cancer cohorts (Leth-Larsen et al., 2012). Gene correlation analysis of a breast cancer cohort showed that higher expression of GRHL2 is correlated with worse relapse-free survival in Luminal A, Luminal B, HER2$^+$, and Basal-like subtypes (Mooney et al., 2017). Furthermore, overexpression of GRHL2 in breast cancer cell lines showed significant increase in migration, invasion potential and also correlated with unfavorable breast cancer patient characteristics – grade III tumors and large tumor size at the time of diagnosis (Yang et al., 2013). High expression of GRHL2 is also observed in pancreatic cancer patients with worsened overall survival (Wang et al., 2019).

At the molecular level, GRHL2 directly regulates the expression of the EGFR family member *ERBB3* and the Wnt ligand *Wnt7A*, and overexpression of GRHL2 in metastatic breast cancer cells exhibit increased anchorage-independent growth, migratory and invasive potential (Xiang et al., 2012; Werner et al., 2013). Aberrant activation of ERBB3 potentially forms heterodimers with ERBB2 that directly contributes to decreased survival rate coupled with increased resistance to chemotherapy (Liu et al., 2007, 3; Sithanandam and Anderson, 2008; Garrett et al., 2011). Conditional deletion of *Grhl2* prevents oral cancer development in a chronic, chemically induced carcinogen model, when compared to the aggressive tumor formation in *Grhl2* wild-type mice (Chen et al., 2018b). In addition, the study also identifies that GRHL2 mediated activation of MAP kinase signaling and repression of TGF-β signaling in oral squamous cell carcinoma cell lines, dually render tumor promoting effects during the early stages of carcinogenesis. The role of GRHL2 in prostate cancer seems to be mainly oncogenic, as its expression is higher in prostate cancer tissue samples (Danila et al., 2014; Paltoglou et al., 2017). *Paltoglou et al.* showed that the loss of GRHL2 via silencing resulted in the loss of androgen receptor (AR) expression and demonstrated the presence of a positive feedback loop between GRHL2 and AR to promote prostate cancer growth (Paltoglou et al., 2017). In addition to driving AR expression, GRHL2 also acts as an AR transcriptional co-activator that enhances the oncogenic AR signaling pathway in prostate cancer progression. Furthermore, the oncogenic role of GRHL2 is observed in hepatocellular carcinoma (Tanaka et al., 2008), esophageal cancer (Shao et al., 2017), oral squamous cell carcinoma (Kang et al., 2009; Chen et al., 2016), and colorectal carcinoma (Quan et al., 2014, 2015).

GRHL Members as Tumor Suppressors

In squamous cell carcinoma, GRHL3 functions as a strong tumor suppressor, where the deletion of *Grhl3* in keratinocytes leads to hyper-proliferation epidermal keratinocytes that are more prone to chemical carcinogen induced spontaneous squamous cell carcinoma formation (Darido et al., 2011). Mechanistically, *Grhl3* depletion in keratinocytes leads to the loss of tumor suppressor *Pten* expression, which induces the activation of PI3K/AKT/mTOR signaling and the oncogenic miR-21 expression, culminating in the formation of aggressive and poorly differentiated squamous cell carcinoma. Oncogenic Ras-mediated *Grhl3*$^{-/-}$ mouse epidermal keratinocytes were more prone to tumorigenesis by upregulating the miR-21 levels (Bhandari et al., 2013). Similarly, in a two-stage chemical skin carcinogenesis model, over 40% of benign papilloma developed into squamous cell carcinoma in *Grhl1*$^{-/-}$ mice, when compared to one-fourth of such tumor formation in *Grhl1*$^{+/+}$ mice, due to the severe impairment of epidermal barrier and aberrant terminal differentiation of keratinocytes (Mlacki et al., 2014). In neuroblastoma, patients with high levels of GRHL1 expression show favorable prognosis, consistent with the suppressed tumor growth phenotype seen in the xenografts carrying forced GRHL1 expression in *MYCN*-amplified neuroblastoma cells (Fabian et al., 2014). At the molecular level, co-recruitment of MYCN and HDAC3 to the *GRHL1* promoter represses its transcription. Esophageal squamous cell carcinoma with low expression of GRHL1 levels show poor differentiation and the patients are associated with reduced overall survival rate (Li M. et al., 2019). The tumor suppressive role of GRHL2 is largely mediated though the suppression of EMT which is summarized in the following section.

GRHL Members as a Determinant for EMT and MET Execution During Cancer Progression

EMT and MET (mesenchymal to epithelial transition, the reversal of EMT) functionally dictate the cellular dedifferentiation and differentiation status respectively and determine the nature of cellular behavior. Although EMT/MET processes occur spontaneously during fundamental events such as gastrulation, neural crest dissemination and organogenesis, execution of EMT/MET is also observed during wound healing, fibrosis and cancer (Thiery and Sleeman, 2006). Overcoming years of speculations about the reactivation of reversible EMT and MET program during cancer progression, compelling evidences from *in vitro*, *in vivo* and clinical findings support the crucial roles of EMT and MET during cancer progression (McInnes et al., 2015; Santamaria et al., 2017; Francart et al., 2018; Rios et al., 2019; Williams et al., 2019). In brief, acquisition of mesenchymal trait through EMT is regarded as an essential feature for epithelial-derived cancer cells to successfully metastasize the surrounding tissues and distant organs. Being a pivotal gatekeeper of epithelial integrity, GRHL2 suppresses EMT in a multipronged manner across cancer entities. Firstly, multiple independent investigations have shown that GRHL2 controls the ZEB1/miR-200 regulatory axis. The EMT inducer ZEB1 and epithelial-phenotype reinforcing microRNA-200 (miR-200) family members reciprocally control the expression of each other generating a double-negative feedback loop (Brabletz and Brabletz, 2010). The expression of ZEB1 drives the cancer cells to undergo EMT, whereas restoration of miR-200 expression is vital for cells to undergo epithelial differentiation or MET. On one hand, GRHL2 directly suppresses the expression of the EMT inducer ZEB1 in breast (Cieply et al., 2012; Werner et al., 2013), ovarian (Chung et al., 2016), bladder cancers (Shen et al., 2020), and sarcoma (Somarelli et al., 2016). On the other hand, GRHL2 activates the expression of miR-200 family members through direct promoter binding in oral (Chen et al., 2016), ovarian (Chung et al., 2016) cancers and sarcoma (Somarelli et al., 2016).

Secondly, GRHL2 suppresses TGF-β mediated migratory and invasive capabilities of gastric (Xiang et al., 2017), breast (Cieply et al., 2012; Werner et al., 2013), and oral (Chen et al., 2018b) cancer cells, where the activation of TGF-β signaling cascade is a significant inducer of EMT in tumor progression (Heldin et al., 2012). Thirdly, re-expression of GRHL2 in mesenchymal-like cells induces MET effects by restoring the expression of epithelial components such as E-cadherin, ZO-1 and downregulating mesenchymal markers including Vimentin, Snail, Slug and ZEB1 (Chung et al., 2016; Yang et al., 2019; Shen et al., 2020). Fourthly, GRHL2 expression suppresses stemness properties in CD44^{high}/CD24^{low} mesenchymal subpopulation cells of breast cancer cells and restores the anoikis sensitivity by altering intracellular H_2O_2 ROS levels (Cieply et al., 2012; Farris et al., 2016).

EMT-TFs Snail and ZEB1 are known to recruit epigenetic remodelers such as the DNA methyltransferases (DNMTs) and/or polycomb repressive complex 2 (PRC2) to generate a repressive chromatin around epithelial genes (Dong et al., 2012; Fukagawa et al., 2015). GRHL2 also interacts with multiple epigenetic regulators to dually suppress EMT and to induce MET phenotypes. GRHL2 significantly inhibits the histone acetyltransferase coactivator p300 and its activity on mesenchymal genes, which interfered with the branching morphogenesis and EMT of Madin–Darby canine kidney (MDCK) cells (Pifer et al., 2016). In addition, GRHL2 interaction with the histone methyltransferases KMT2C and KMT2D induces MET and ICAM-1 expression in cancer cells, which sensitizes these cells for optimal natural killer (NK) cells mediated activation and target cell killing, suggesting a potential link between the epithelial phenotype and cellular susceptibility to NK killing (MacFawn et al., 2019). Furthermore, using a set of ovarian cancer cell lines, we have shown that during the reactivation of epithelial genes, the presence of GRHL2 is essential for the modification of the epigenetic landscape into a permissive chromatin to allow the transcription of key epithelial genes such as E-cadherin, ESRP1 and OVOL2 (Chung et al., 2019).

Evidences have shown that GRHL members are the gatekeepers of early phenotype transition. Our assessment on a heterogeneous ovarian cancer cell line panel revealed the presence of intermediate cellular phenotypes that dually expressed epithelial and mesenchymal markers (Huang et al., 2013). Consequently, the concept of an 'EMT spectrum' has emerged, whereby EMT is regarded as a continuum consisting of

multiple, transient intermediate phenotypes collectively referred as the EMT spectrum (Nieto et al., 2016; Yang et al., 2020). The prevalence of multiple intermediate EMT states is observed in breast (Grosse-Wilde et al., 2015; Yamashita et al., 2018), prostate (Ruscetti et al., 2015), and non-small lung cancer (Fustaino et al., 2017). GRHL2 knockdown in ovarian cancer cell lines harboring the epithelial phenotype results in a specific shift of subcellular E-cadherin localization with unaltered total E-cadherin protein abundance, generating a partial EMT phenotype (Chung et al., 2016). In lung cancer cells, GRHL2, OVOL2 and miR-145 play crucial roles in stabilizing the intermediate EMT phenotype (hybrid E/M), while transient knockdown of GRHL2 in cells with hybrid E/M phenotype switches to a complete EMT as evidenced by the disruption of partial EMT specific collective cell migration phenotype to a single cell migration phenotype (Jolly et al., 2016). Moreover, through computational modeling, the same study has predicted that GRHL2 promotes the association of hybrid E/M phenotype with high-tumor initiating stem-like traits, which might be helpful in stratifying patients with higher metastatic risk. Using a genetically engineered mouse model of squamous cell carcinoma, another recent study has identified spontaneous EMT and multiple intermediate EMT subpopulations with characteristic cell surface marker expressions (Pastushenko et al., 2018). Assay for transposase-accessible chromatin using sequencing (ATAC-seq) of these EMT subpopulations revealed the specific enrichment of a GRHL1 motif on the differentially expressed genes especially during the epithelial to early hybrid EMT state but not observed in the late hybrid EMT state or in mesenchymal subpopulations. Although tumor cells dynamically switch between epithelial, mesenchymal and intermediate E/M phenotypes through EMT and MET processes, mechanisms underlying the reversibility or irreversibility of such events are slowly emerging. In an inducible mammary EMT system (HMLE-Twist1-ER), epithelial clonal population (high GRHL2 expression) were susceptible to acquire a hybrid E/M phenotype and showed transient, reversible changes in chromatin accessibility when compared to the mesenchymal clonal population (low GRHL1/2 expression) (Eichelberger et al., 2020). In particular, ATAC-seq of the mesenchymal subpopulation revealed that the specific loss of chromatin accessibility along GRHL1/2 motifs governing loci of epithelial genes is crucial for these cells to enter an irreversible mesenchymal cell state or to resist trans-differentiation. Similarly, via mathematical modeling, another independent study has proposed two mechanisms that drive epithelial cells to resist undergoing EMT or enabling irreversible MET: (i) GRHL2 mediated epigenetic feedback on inhibition of ZEB1 and (ii) stochastic partitioning of biomolecules during cell division to generate different phenotypic subpopulations in regards to EMT (Jia et al., 2020). Altogether, these studies have unraveled that GRHL factors play crucial roles in establishing the EMT spectrum and moderating the EMT/MET dynamics during cancer progression. Importantly, comprehending the biology of such intermediate or hybrid trans-differentiation states is essential to combat clinically challenging issues such as metastatic aggressiveness and therapeutic resistance (Santamaria et al., 2017; Jolly et al., 2018, 2019; Williams et al., 2019).

GRHL Family in Other Human Diseases

Craniofacial development encompasses the patterning of bones, muscles and vasculatures of face, skull and jaws, governed by highly coordinated migration signals and spatiotemporal regulation of genetic and molecular factors. Owing to the gene nomenclature, *Drosophila* larvae carrying *grh* mutations have pronounced deformation in the chitinous head-skeleton morphology generating a granular head appearance (Bray and Kafatos, 1991). Similarly, deregulation of Grhl/GRHL factors are also heavily associated in the etiology of craniofacial malformations in mammals (Carpinelli et al., 2017). The failure of cranial neural tube closure in these mutants resulted in anterior spina bifida, prematurely apposed skull bones, split-face, defective neural fold elevation, cranioschisis and exencephaly, lumbosacral spina bifida (open neuropore) and a curled tail phenotype. Accordingly, multiple independent reports have observed that patients with craniofacial malformations are associated with microdeletions of a gene cluster at the chromosomal region 8q22.2-q22.3, comprising clinically relevant genes including *GRHL2* (Kuechler et al., 2011; Kuroda et al., 2014; Sinajon et al., 2015; Chen et al., 2017; Hoebel et al., 2017; de Vries et al., 2020). Dominant-negative mutations in *GRHL3* have been reported in the congenital disorder Van Der Woude syndrome, which is characterized by cleft lip and/or cleft palate (Peyrard-Janvid et al., 2014; Wang et al., 2016; Eshete et al., 2018).

Defects in neural tube closure generate severe congenital morbidity and mortality in human, which occurs at a high rate of 1 in every 1000 human pregnancies (Bhandari and Thada, 2020). Murine models carrying *Grhl2* and *Grhl3* conditional deletions are embryonically lethal with severe defects in organogenesis, dorso-lateral hinge point formation during neurulation and neural tube closure (Ting et al., 2003; Rifat et al., 2010; Werth et al., 2010; Pyrgaki et al., 2011; Menke et al., 2015; Goldie et al., 2016). Gene targeting in mice have demonstrated that the lack or surplus of Grhl2/Grhl3 expression could interfere with spinal neural tube closure (Gustavsson et al., 2007; Brouns et al., 2011; Nikolopoulou et al., 2017; De Castro et al., 2018). In particular, Grhl2 mediates the upregulation of cell-cell junction proteins via modulating the local actomyosin-dependent mechanical stress, which is essential for spinal neural tube closure (Nikolopoulou et al., 2019). The regulation of GRHL2 in the transactivation of OVOL1/2, ESRP1/2, miR-200 family and the suppression of ZEB1 expression during MET is also recapitulated during palate closure (Carpinelli et al., 2020). Furthermore, mouse models carrying *Grhl3* dependent gene manipulation in the surface ectoderm showed severe defects in neural tube closure and open spina bifida (Camerer et al., 2010; Kimura-Yoshida et al., 2015; Molè et al., 2020).

Hearing impairment is another pathologic condition linked to *GRHL2* mutation, where sequencing of the gene loci DFNA28 on chromosome 8q22 in a large American family is associated with progressive autosomal dominant hearing loss (Peters et al., 2002). The study initially identified a frameshift mutation 1609-1610insC generating the *GRHL2* transcript with a premature stop codon in exon 14. A decade later, a second novel splice site mutation in *GRHL2* – c.1258-1G > A resulting in p. Gly420Glufs0111 frameshift mutation in exon 10 was

associated with age-related, post-lingual hearing loss (Vona et al., 2013). Subsequent studies have reported that mutations and/or gene polymorphisms in *GRHL2* are implicated in hereditary and acquired hearing loss such as age-related hearing impairment, non-syndromic hearing loss, sudden sensorineural hearing loss and noise-induced hearing loss in Chinese, Korean, Roma and Hungarian populations (Kim et al., 2015; Zhang et al., 2015; Lin et al., 2016; Xu et al., 2016; Li X. et al., 2019; Matyas et al., 2019; Wu et al., 2020). Although mutations and gene polymorphisms of *GRHL2* are associated with multiple hearing abnormalities, substantial association of *GRHL2* in the development of the inner ear is not yet demonstrated. However, a recent examination of deafness genes in the non-human primate model marmoset (*Callithrix jacchus*) has revealed that GRHL2 expression is prevalent in cochlear duct lining cells, hair cells, and supporting cells of the inner ear (Hosoya et al., 2016), denoting that the definitive role of GRHL2 in the inner ear development needs further investigations.

EPIGENETIC CONTROL OF GRAINYHEAD AND GRHL MEMBERS

On top of gene expression regulations through *cis*- and *trans*-regulatory elements, epigenetic modifications such as methylation of DNA cytosine and extensive post-translational modifications occur on the core octamer histone proteins collectively modulate chromatin landscape of underlying genes, and thereby regulate gene expression. Although methylation of DNA is a global phenomenon, concentrated methylation on short patches of CpG dinucleotide repeats (CpG islands) are often observed in genes that are suppressed at a particular cell state/type (Suzuki and Bird, 2008). A staggering number of histone modifications occur on the flexible N- and C-terminal 'tail' domains. These include prominent alterations such as lysine acetylation, lysine/arginine methylation, serine/threonine/tyrosine phosphorylation as well as many under-examined, minor changes such as lysine ubiquitination/sumoylation, citrullination, ADP-ribosylation, and proline isomerization (Bannister and Kouzarides, 2011). Alterations of CpG methylation patterns and histone modifications are observed in a variety of important cellular processes such as during cellular growth, differentiation, and cancer progression (Rothbart and Strahl, 2014; Audia and Campbell, 2016). GRHL factors have been shown to induce changes in CpG methylation levels and histone modifications during development.

In mouse kidney cells, depletion of active histone marks H3K4me3 and H3K9/14ac are observed at the E-cadherin promoter region exclusively in Grhl2-knockdown cells, denoting that Grhl2 expression is essential to sustain activating histone marks at the promoter (Werth et al., 2010). Selective expression of uroplakin II (*UpkII*) in mouse bladder epithelial cells is also regulated through Grhl3-mediated active H3K9ac mark enrichment on the *UpkII* promoter (Yu et al., 2009). During the development of kidney ureteric buds and collecting ductal epithelia, GRHL2 strongly associates with the active H3K4me3 mark of target genes (*Cdh1*, *Rab25*, *Ovol2*, and *Cldn4*) that are essential for lumen expansion and barrier formation (Aue et al., 2015). Besides direct transcription controls, GRHL2 imposes several epigenetic modifications on selected epidermal differentiation genes. GRHL2 overexpression in normal human epidermal keratinocytes leads to the inhibition of methylation at the CpG island of the *hTERT* promoter and restores hTERT expression, potentially by hindering the activity of DNA methyltransferase DNMT1 (Chen et al., 2010). In addition, GRHL2 overexpression in normal human epidermal keratinocytes also leads to the enrichment of H3K27me3 repressive mark, while simultaneously inhibiting the recruitment of histone demethylase Jmjd3 to the cognate promoters of epidermal differentiation genes such as involucrin (*IVL*), keratin 1 (*KRT1*), filaggrin (*FLG*) and cyclin dependent kinase inhibitor 2A (*INK4A*) (Chen et al., 2012). During epidermal differentiation, GRHL3 binds directly to the *TGM1* promoter to control the expression of transglutaminase (*TGM1*) (Hopkin et al., 2012), a Ca^{2+}-dependent enzyme is essential for the formation of cornified cell envelope (Eckert et al., 2005). GRHL3 further recruits the Trithorax complex components MLL2 and WDR5 to the target promoter and increases the active H3K4 methylation mark and drives *TGM1* expression during epidermal differentiation (Hopkin et al., 2012). These studies substantiate the notion that GRHL factors have the potential to epigenetically modify chromatin states during cellular differentiation.

PIONEER ACTIVITY OF GRAINYHEAD AND GRHL FAMILY

About two meters long, the double stranded DNA is condensed and packed into a typical eukaryotic interphase nucleus that only measures about six micrometers in diameter. This composite level of condensation starts primarily by wrapping the DNA around an octameric protein complex made of four core histones into a structure called nucleosome. Arrays of nucleosomes undergo further condensation into higher-order chromatin structures that functionally demarcate the chromatin boundaries into densely condensed heterochromatin and relatively less compressed euchromatin units. Although the high level of DNA packaging significantly deals with containing the genetic material in a miniscule space, DNA access to gene regulatory proteins during key cellular process such as transcription is greatly restricted. In this context, one crucial question is "How do TFs find their way to gene regulatory elements that are repressed or latent amidst these convoluted nucleosomal barriers in order to initiate transcription for diverse cellular processes?" A new set of regulatory proteins called 'pioneer factors' have been identified to accomplish this phenomenal task (Zaret and Carroll, 2011).

Pioneer factors belong to a unique class of TFs that can recognize and bind specific *cis*-regulatory units within permissive heterochromatin, and subsequently prime the chromatin for additional factors to bind, prior to transcription initiation (Zaret and Mango, 2016; Mayran and Drouin, 2018). The pioneer factors display few salient characteristics that are usually lacking in general TFs: (i) the ability to destabilize chromatin

compaction (nucleosomes) and to bind to otherwise inaccessible heterochromatin regions, in a cell type/state-specific manner; (ii) the potential to alter pre-existing epigenetics modifications (such as DNA methylation and histone modification) to enhance DNA accessibility; and (iii) the remodeling of adjacent chromatin landscape to facilitate the binding of non-pioneer TFs prior to transcription initiation. In mammals, pioneer factors such as FOXA1, FOXD3, GATA-3, and PU.1 have crucial roles in development, cell fate conversions and deregulation of such factors in also implicated in cancer (Magnani et al., 2011; Iwafuchi-Doi and Zaret, 2016). Compelling evidences have accumulated to illustrate the novel role of Grainyhead and GRHL family proteins as pioneer factors in multiple cellular contexts.

Pioneering Role of Grainyhead and GRHL in Remodeling Target Enhancers

Pioneer factors can remodel the chromatin landscape to expose functional *cis*-regulatory elements (such as enhancers) that recruit the binding of transcription factors, cofactors and collectively form a stable regulatory complex. Promoters are usually a minimal stretch of DNA sequences, located in proximity to the transcription start sites within a nucleosome-free chromatin landscape to enable easy access to the transcription machinery. In contrast, enhancers tend to be located far (either upstream or downstream) from the cognate promoters and enhance transcriptional outputs in a cell-type/state specific and spatiotemporal manner (Wittkopp and Kalay, 2012; Long et al., 2016). As a pioneer factor, Grainyhead and GRHL proteins bind to enhancers and regulate chromatin accessibility at the target genes during several developmental processes. During *Drosophila* eye development, the unbiased genome-wide characterization of direct TF interactions with enhancer regions of target genes have revealed a significant enrichment of Grainyhead in large fraction of active enhancer regions, which further elucidates the abundant Grh expression in the eye disc (Potier et al., 2014). The utilization of high-throughput genome-wide association methods such as the single-cell assay for transposable-accessible chromatin using sequencing (scATAC-seq) and quantitative trait loci for chromatin accessibility (caQTL) across a panel of *Drosophila* strains have revealed that the pioneer binding of Grh is essential for the opening and accessibility of epithelial cell enhancers (Jacobs et al., 2018). In these Grh binding sites, about 75% of Grh target sites are inaccessible due to the lack of *Grh* expression in the non-epithelial larval brain, whereas the ectopic overexpression of *grh* in the larval brain tissue profoundly increases the chromatin accessibility of these regions (Jacobs et al., 2018). These findings reiterate that, in *Drosophila*, Grh is the chief pioneer factor of the epithelial chromatin landscape. It potentially binds to the recognition sites and alters the closed chromatin landscape of non-epithelial tissues. In addition, the pioneering activity of Grh is also subjected to spatio-temporal and tissue specific regulation. Its pioneering activity has been reported to become essential during and after gastrulation but not during early embryogenesis (Nevil et al., 2020).

Investigations in mammalian GRHL factors also showed such pioneering roles in modulating the chromatin landscape of enhancers. During the early transition from the mouse naive embryonic stem cells (ESCs) to the primed pluripotent epiblast-like cells (EpiLCs), GRHL2 binds to latent enhancers (regions with low or no histone marks) and restores the epigenetic landscape toward an activation state (high levels of H3K4me1, H3K27ac histone marks and depletion of nucleosomes) of key genes that control the epithelial state and cell adhesion (Chen et al., 2018a; **Figure 2**). Importantly, in the ESC state, a different set of enhancers and TFs (such as KLF4, KLF5, and EKLF) controls the expression of the above mentioned genes, whereas in the EpiLCs, the control of gene expression switches toward the GRHL2-bound enhancers. Assaying across 47 human cell types, the positional distribution of TF binding motifs within the nucleosome-depleted enhancer sites have shown that GRHL1 is one of the six transcription factors that modulate DNA accessibility (Grossman et al., 2018). This study further elucidates that GRHL1 stably binds to the DNA with prolonged occupancy denoting that it may act in generating central anchor regions for potential transcription initiation. These results posit that in addition to pioneering the chromatin architecture, GRHL factors potentially mediate a major enhancer-switching phenomenon during cellular differentiation.

GRHL proteins also exhibit the role of pioneering the enhancer landscape in human cancers. Chromatin states that denote the accessibility of the genomic region (such as active, repressed, heterochromatin, bivalent and poised) could be annotated using an automated ChromHMM algorithm (Ernst and Kellis, 2012). In ovarian cancer, using experimental ChIP-seq data derived from five major histone marks (H3K4me3, H3K4me1, H3K9me3, H3K27me3, and H3K27ac), our group has utilized this pipeline to show that upon the loss of GRHL2, a radical shift from an active chromatin state toward a latent, poised/bivalent, or repressed chromatin state occur across intronic and intergenic regions at the GRHL2 binding sites of epithelial genes such as *MARVELD3*, *ESRP1, GRHL1, RAB25, OVOL2* and *MUC20* (Chung et al., 2019). Upon re-expressing GRHL2 by using the inducible system, the chromatin changes of these GRHL2 binding sites located at the promoter and enhancer regions further shine the light on the pioneering function of GRHL2. GRHL2 is highly effective to induce MET in ovarian cancer cells with the intermediate phenotype. This is achieved via the suppression of PRC2 activity and to remove the repressive histone mark (H3K27me3) at the promoters with the corresponding suppression of HDAC activity at the enhancers to restore the H3K27ac mark (Chung et al., 2019). However, the pioneering capacity of GRHL2 might differ depending on cellular states along the EMT spectrum. The MET reversibility of GRHL2 in the highly mesenchymal cells has been quite limited suggesting that there would be state-specific pioneering reprogramming mechanisms. In human breast cancer cells, transient siRNA-mediated knockdown of all three GRHL orthologs show a reduced chromatin accessibility on GRHL-regulated enhancer elements that encode proteins required for cell-cell adhesion such as protocadherin-1 (*PCDH1*) and serine peptidase inhibitor 1 (*SPINT1*) (Jacobs et al., 2018). After priming the chromatin into an accessible regulatory landscape mediated by pioneer factors, tissue specific transcription factors

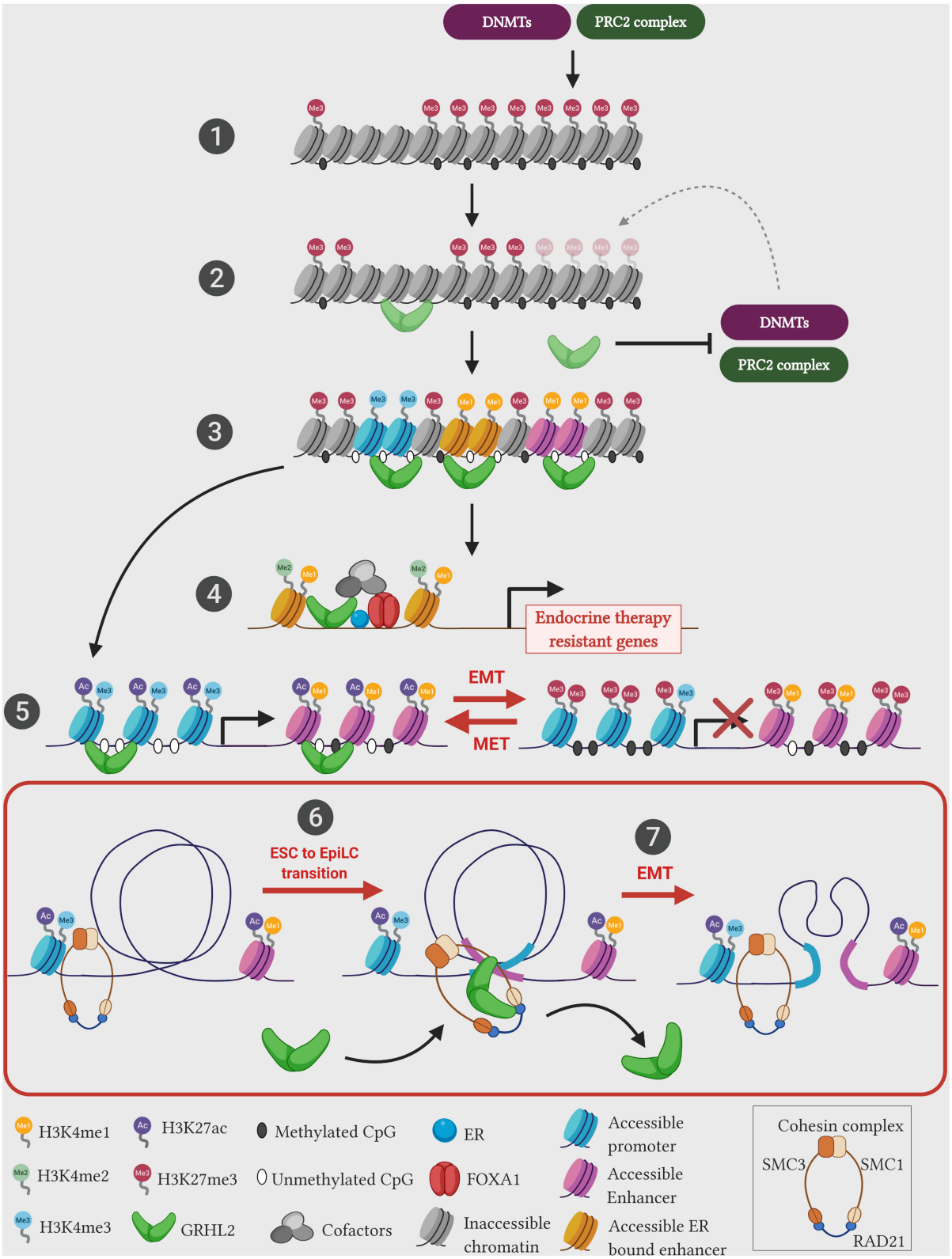

FIGURE 2 | Continued

FIGURE 2 | Emerging pioneering functions of GRHL2 during pathophysiology. Recent studies unearth the novel function of GRHL2 as a leading pioneer factor. (1) Typical chromatin landscape comprises cellular DNA wrapped around the core histone complex to form a nucleosome. Over half of the genome remains either in a latent/poised state with no histone marks/methylation status or in a repressed state studded with repressive chromatin marks (H3K27me3)/methylated CpG sites. These epigenetic marks are mediated through epigenetic repressors such as polycomb repressive complex 2 (PRC2) complex, and DNA methyltransferases (DNMTs). (2) Pioneer factors such as GRHL2 can potentially bind and activate latent chromatin in the context of ESC to EpiLC transition (6), or inhibit the activities of epigenetic repressors in the context of EMT (5). (3) GRHL2 primed regions generate accessible chromatin with unmethylated CpG islands and permissive histone marks (H3K4me3 – promoter; H3K4me1 – enhancer). (4) GRHL2 cooperates with pioneer factor FOXA1 at ER bound-active enhancer regions (studded with active histone H3K4me1/me2 marks) to drive transcription of endocrine therapy resistant genes. (5) In the presence of GRHL2, epigenetic landscape of epithelial genes are modified into a permissive chromatin (studded with H3K27ac and H3K4me3) at promoter and enhancer regions, whereas during cellular differentiation such as EMT, lack of GRHL2 expression results in change of chromatin setting of epithelial genes to a repressed state (hypermethylated promoters and enrichment of repressive H3K27me3 mark). (6) During ESC to EpiLC transition, GRHL2 associates with the cohesin component SMC1 on EpiLC-specific enhancer sites to facilitate transition. (7) In epithelial ovarian cancer cells, GRHL2 associates with the cohesin component RAD21 and brings distantly located gene regulatory elements in close proximity, to drive the expression of early epithelial genes such as *ERBB3* and *PERP*. However, SNAI1-mediated EMT induction in these cells downregulates GRHL2 expression potentially disassembles cohesin structure, leading to reduced epithelial gene expression. Illustration created with Biorender.com.

and additional cofactors assemble to carryout gene expression. Such regulation is observed in the specific recruitment of GRHL factors to control steroid hormone-mediated gene expression in hormone-dependent cancers. Estrogen receptor α (ER) is a nuclear hormone receptor that drives over 70% of aggressive breast cancers. GRHL2 expression significantly correlates with ER-positive breast cancer tumors (Carroll et al., 2005; Xiang et al., 2012; Werner et al., 2013). ChIP-seq profiling of ER and phosphorylated ER at S118 (pS118-ER) occupancy sites shows a significant overlap with GRHL2 binding motifs (Helzer et al., 2018; Holding et al., 2019). This indicates that GRHL2 occupancy in the ER binding sites potentially drives ER transcription complex. The ER chromatin interaction and the subsequent gene expression changes are mediated through the pioneering activity of FOXA1 on cognate regulatory sites, independent of estrogen hormone signaling (Hurtado et al., 2011; Glont et al., 2019). Indeed, GRHL2 has been identified as the FOXA1 interaction partner at the ER bound-active enhancer regions demarcated with H3K4me1/me2 marks to promote tumor progression (Jozwik et al., 2016). This cooperation between FOXA1 and GRHL2 in ER driven breast cancer cells also contributes toward the resistance to endocrine therapy via the upregulation of LYPD/AGR2 (a receptor/ligand complex) making it a promising targetable frontier in endocrine therapy-resistant tumors (Cocce et al., 2019; **Figure 2**). These data clearly indicate the inevitable role of Grainyhead and GRHL proteins in the remodeling of gene regulatory units at the targeted sites.

Pioneering Role of GRHL Proteins in Altering Chromatin Conformation

As mentioned earlier, folding of the chromatin into three-dimensional structures are not only crucial for packaging DNA but also contribute toward fine-tuning of spatiotemporal gene regulation. For instance, in regulation of gene activity by cell-specific enhancers, distal enhancers are brought into close contact with its cognate promoters via DNA looping. Typically, DNA loops can occur between genomic loci which are tens to hundreds of kilobase pairs apart and are referred to as topological associated domains (TADs). The presence of TADs is evident across many species, ranging from *Drosophila* to mammals, and is a conserved feature of the three-dimensional chromatin architecture (Dixon et al., 2012; Hou et al., 2012; Nora et al., 2012; Sexton et al., 2012). These domains are demarcated by boundaries and often enriched in binding of architectural proteins: (i) sequence-specific CCTC-binding factor (CTCF) and (ii) cohesin protein complex, that serves to constrain the DNA loops within the TADs (Parelho et al., 2008; Stedman et al., 2008; Dixon et al., 2012; Rao et al., 2014). Therefore, TADs provide a structural and functional architecture across the genome, which permit short- and long-range chromatin interactions between regulatory elements within the same TADs (intradomain), while limiting interactions that span across the TAD boundaries (interdomain) to ensure proper gene regulation (Lupiáñez et al., 2015, 2016; Flavahan et al., 2016; Hnisz et al., 2016; Weischenfeldt et al., 2017; Beagan and Phillips-Cremins, 2020). The functional consequence of DNA loops in engaging promoters with its distal enhancers to drive transcriptional output of genes have been studied and reviewed (Sanyal et al., 2012; Long et al., 2016). In the context of the Grh family, a handful of studies indicate that GRHL factors have the potential to modulate chromatin looping structures and eventually affect gene expression. During mouse early embryonic development, intron 2 of the *Cdh1* locus potentially functions as an enhancer element that control epithelium-specific E-cadherin expression (Stemmler et al., 2005). Using chromatin conformation capture-based techniques, it was revealed that the recruitment of Grhl2, Grhl3 and Hnf4α to multiple enhancers within intron 2 of *Cdh1* resulted in functional DNA-loops to the Cdh1 promoter, thereby increasing the expression of the epithelial gene (Werth et al., 2010; Alotaibi et al., 2015). Formation of such DNA loops are essential for activating E-cadherin expression in mouse inner medullary collecting duct cells and thereby to induce epithelial differentiation in non-tumorigenic mouse mammary gland cells.

The formation of DNA loops is mainly mediated by the ring-shaped cohesin complex, which consists of four subunits – SMC1, SMC3, SCC1/RAD21, and SCC3/SA1/SA2 that topologically clasps chromatin into looping structures. As revealed by single-molecule imaging studies, the cohesin complex binds to DNA in a ring-shaped conformation and translocate along the chromatin in an ATPase-dependent fashion until it is impeded by CTCF (Davidson et al., 2016; Kanke et al., 2016; Stigler et al., 2016). It has been shown the transient degradation of cohesin resulted in the loss of DNA loops or loop domains, while CTCF degradation lead to the loss of DNA loops at the TAD boundaries, leading to subsequent loss of TAD insulation (Nora et al., 2017; Rao et al.,

2017). Therefore, this highlights the role of cohesin complex lies heavily in the formation of loops linking two genomic loci and modulation of cohesin binding affects gene regulation during development and disease (Remeseiro et al., 2013). Recent studies have shown the direct interaction between GRHL factors and members of the cohesin complex. During the transition process of mouse ESCs to EpiLCs, Grhl2 predominantly associates with the cohesin subunit SMC1 to perform its pioneering function at enhancer regions of key epithelial genes to drive the transition process (Chen et al., 2018a). In the investigation on ovarian cancer cell lines, we also show that the co-occupancy of cohesin subunit RAD21 and GRHL2 on the promoter and enhancer elements of early epithelial genes (*ERBB3* and *PERP*) is crucial for their expressions (Sundararajan et al., 2020; **Figure 2**). Moreover, we show that the recruitment of RAD21 on such enhancer regions are dependent on endogenous GRHL2 expression and the gradual loss of GRHL2 expression along the EMT spectrum of ovarian cancer cell lines might loosen up or alter the chromatin loop structures, which eventually lead to epithelial dedifferentiation. These observations highlight the identification of novel crosstalk between GRHL factors and the chromatin architectural complexes, where the pioneering activity of GRHL factors along the regulatory regions of epithelial genes potentially serve as loop anchors to mediate long-range functional chromatin interactions. Therefore, this mechanism appears to be an essential phenomenon in establishing the epithelial identity in development, while such interactions could be altered during cancer progression under conditions such as EMT. For example, in human sarcoma cells, ZEB1-associated chromatin remodeling factor BRG1 suppresses E-cadherin expression by blocking its promoter region (Somarelli et al., 2016). Depletion of BRG1 in the context of GRHL2 expression further upregulates E-cadherin expression, indicating that ZEB1-mediated chromatin remodeling interferes with GRHL factors associated pioneering function.

CONCLUSION AND FUTURE PERSPECTIVES

Almost three decades ago, foundation studies using *Drosophila* as a model organism have shown that the transcription factor *Grainyhead* is a crucial determinant of the epithelial phenotype and is involved in the development of vital fly organs such as epidermis, trachea, wings, and exoskeleton. Subsequent studies have identified that Grh potentially acts as a transcriptional activator and a repressor to regulate target gene expression, depending on the signaling events and its association with other transcription factors or co-factors. Interestingly, a recent study in the German cockroach (*Blattella germanica*) model has showed that Grh functions as a transcriptional repressor to regulate genes essential for the development of epithelium and molting of old integument (ecdysis) (Zhao et al., 2020). This indicates that the role of Grh in epithelial and epidermal differentiation is fundamental and evolutionarily conserved. Future Grh functional studies on other insect model systems might generate the possibility of Grh-mediated pest control management.

The three mammalian descendants of Grh – Grainyhead like 1-3 are also heavily implicated in the development of vital organs such as the neural tube, epidermis, and craniofacial skeleton. Although mutations and gene polymorphisms in *Grhl* genes were implicated in multiple human abnormalities such as hearing impairment, ectodermal dysplasia syndrome, and cleft palate formation, somatic mutations in *GRHL* genes in human cancer samples occur at a very low frequency (Kotarba et al., 2020). Moreover, the dual functioning of GRHL factors in carcinogenesis and tumor suppression indicate that GRHL factors impose a greater level of control over their target genes and miRNAs. In addition to directly controlling the target gene expression through promoter/enhancer binding, recent studies have shown that GRHL factors are potent modulators of the epigenetic landscape of target genes, which facilitate their spatiotemporal and cell type specific control. Such regulation is prevalent in the maintenance of epithelial barrier functions and the restoration of epithelial phenotypes during EMT/MET fluidity.

Recent studies underline how Grhl factors are essential during surface ectodermal neural lineage specification. Also, members of the GRHL family are potent repressors of the EMT program during development and cancer. These indicate that GRHL factors are at the crossroads of controlling epithelial, mesenchymal and neural-like phenotypes that determine cell lineage and transdifferentiation programs. It is therefore fair to hypothesize that tipping this balance during pathogenesis such as cancer might derail lineage specification, resulting in adverse phenotypes. Therefore, future studies on delineating GRHL factors-mediated of cellular and lineage plasticity through lineage tracing is worth exploring. Such investigations would shed light on the contribution of GRHL factors to the generation of neuroendocrine-like phenotypes, neuroendocrine differentiation observed in several cancers.

Genome-wide research progress in the last decade has brought a novel role of Grh/GRHL members as pioneer factors in limelight. Being pioneer factors, Grh/GRHL2 potentially gain access to the latent and repressed chromatin landscape of epithelial genes and prime such chromatin elements toward transcription initiation. Furthermore, GRHL2/3 associate with protein complexes that control chromatin 3D conformation structures (e.g., cohesins) and potentially regulate their access along the epithelial gene loci during cellular differentiation/dedifferentiation. Of note, chromatin conformational changes during EMT/MET programs during development and cancer progression are starting to emerge recently (Essafi et al., 2011; Yun et al., 2016; Sundararajan et al., 2020). Since GRHL2/3 are recently implicated in modulating the 3D chromatin architecture, future studies employing advanced sequencing techniques like ATAC-seq, FAIRE-seq, and Hi-C or Hi-ChIP would help us comprehend the interplay between GRHL factors and the chromatin accessibility during EMT/MET programs. Such investigations would also clarify our understanding on the dynamic changes of chromatin architecture along the EMT spectrum and eventually pave way toward improved cancer diagnostics and therapeutics.

AUTHOR CONTRIBUTIONS

VS and RH conceptualized and wrote the complete first version of the manuscript. All authors contributed to the manuscript revision, read, and approved the final version.

FUNDING

This work was supported by the National University Cancer Centre of Singapore (NCIS) Research Grant, Theme: EMT in Cancer and the Yushan Scholar Program by the Ministry of Education, Taiwan (NTU-109V0402) to RH.

REFERENCES

Acloque, H., Adams, M. S., Fishwick, K., Bronner-Fraser, M., and Nieto, M. A. (2009). Epithelial-mesenchymal transitions: the importance of changing cell state in development and disease. *J. Clin. Invest.* 119, 1438–1449. doi: 10.1172/JCI38019

Adhikari, N., Neupane, S., Gwon, G.-J., Kim, J.-Y., An, C.-H., Lee, S., et al. (2017). Grhl3 modulates epithelial structure formation of the circumvallate papilla during mouse development. *Histochem. Cell Biol.* 147, 5–16. doi: 10.1007/s00418-016-1487-7

Afonso, C., and Henrique, D. (2006). PAR3 acts as a molecular organizer to define the apical domain of chick neuroepithelial cells. *J. Cell Sci.* 119, 4293–4304. doi: 10.1242/jcs.03170

Almeida, M. S., and Bray, S. J. (2005). Regulation of post-embryonic neuroblasts by *Drosophila* grainyhead. *Mech. Dev.* 122, 1282–1293. doi: 10.1016/j.mod.2005.08.004

Alotaibi, H., Basilicata, M. F., Shehwana, H., Kosowan, T., Schreck, I., Braeutigam, C., et al. (2015). Enhancer cooperativity as a novel mechanism underlying the transcriptional regulation of E-cadherin during mesenchymal to epithelial transition. *Biochim. Biophys. Acta* 1849, 731–742. doi: 10.1016/j.bbagrm.2015.01.005

Attardi, L. D., Seggern, D. V., and Tjian, R. (1993). Ectopic expression of wild-type or a dominant-negative mutant of transcription factor NTF-1 disrupts normal *Drosophila* development. *PNAS* 90, 10563–10567. doi: 10.1073/pnas.90.22.10563

Auden, A., Caddy, J., Wilanowski, T., Ting, S. B., Cunningham, J. M., and Jane, S. M. (2006). Spatial and temporal expression of the Grainyhead-like transcription factor family during murine development. *Gene Express. Patterns* 6, 964–970. doi: 10.1016/j.modgep.2006.03.011

Audia, J. E., and Campbell, R. M. (2016). Histone modifications and Cancer. *Cold Spring Harb. Perspect. Biol.* 8:a019521. doi: 10.1101/cshperspect.a019521

Aue, A., Hinze, C., Walentin, K., Ruffert, J., Yurtdas, Y., Werth, M., et al. (2015). A grainyhead-like 2/Ovo-Like 2 pathway regulates renal epithelial barrier function and lumen expansion. *JASN* 26, 2704–2715. doi: 10.1681/ASN.2014080759

Bannister, A. J., and Kouzarides, T. (2011). Regulation of chromatin by histone modifications. *Cell Res.* 21, 381–395. doi: 10.1038/cr.2011.22

Beagan, J. A., and Phillips-Cremins, J. E. (2020). On the existence and functionality of topologically associating domains. *Nat. Genet.* 52, 8–16. doi: 10.1038/s41588-019-0561-1

Bhandari, A., Gordon, W., Dizon, D., Hopkin, A. S., Gordon, E., Yu, Z., et al. (2013). The Grainyhead transcription factor Grhl3/Get1 suppresses miR-21 expression and tumorigenesis in skin: modulation of the miR-21 target MSH2 by RNA-binding protein DND1. *Oncogene* 32, 1497–1507. doi: 10.1038/onc.2012.168

Bhandari, J., and Thada, P. K. (2020). *Neural Tube Disorders*. Treasure Island, FL: StatPearls Publishing.

Boglev, Y., Wilanowski, T., Caddy, J., Parekh, V., Auden, A., Darido, C., et al. (2011). The unique and cooperative roles of the Grainy head-like transcription factors in epidermal development reflect unexpected target gene specificity. *Dev. Biol.* 349, 512–522. doi: 10.1016/j.ydbio.2010.11.011

Brabletz, S., and Brabletz, T. (2010). The ZEB/miR-200 feedback loop—a motor of cellular plasticity in development and cancer? *EMBO Rep.* 11, 670–677. doi: 10.1038/embor.2010.117

Bray, S. J., Johnson, W. A., Hirsh, J., Heberlein, U., and Tjian, R. (1988). A cis-acting element and associated binding factor required for CNS expression of the *Drosophila melanogaster* dopa decarboxylase gene. *Embo J.* 7, 177–188. doi: 10.1002/j.1460-2075.1988.tb02798.x

Bray, S. J., and Kafatos, F. C. (1991). Developmental function of Elf-1: an essential transcription factor during embryogenesis in *Drosophila*. *Genes Dev.* 5, 1672–1683. doi: 10.1101/gad.5.9.1672

Brouns, M. R., De Castro, S. C. P., Terwindt-Rouwenhorst, E. A., Massa, V., Hekking, J. W., Hirst, C. S., et al. (2011). Over-expression of Grhl2 causes spina bifida in the Axial defects mutant mouse. *Hum. Mol. Genet.* 20, 1536–1546. doi: 10.1093/hmg/ddr031

Caddy, J., Wilanowski, T., Darido, C., Dworkin, S., Ting, S. B., Zhao, Q., et al. (2010). Epidermal wound repair is regulated by the planar cell polarity signaling pathway. *Dev. Cell* 19, 138–147. doi: 10.1016/j.devcel.2010.06.008

Camerer, E., Barker, A., Duong, D. N., Ganesan, R., Kataoka, H., Cornelissen, I., et al. (2010). Local protease signaling contributes to neural tube closure in the mouse embryo. *Dev. Cell* 18, 25–38. doi: 10.1016/j.devcel.2009.11.014

Carpinelli, M. R., de Vries, M. E., Jane, S. M., and Dworkin, S. (2017). Grainyhead-like transcription factors in craniofacial development. *J. Dent. Res.* 96, 1200–1209. doi: 10.1177/0022034517719264

Carpinelli, M. R., Vries, M. E., de, Auden, A., Butt, T., Deng, Z., et al. (2020). Inactivation of Zeb1 in GRHL2-deficient mouse embryos rescues mid-gestation viability and secondary palate closure. *Dis. Models Mech.* 13:dmm042218. doi: 10.1242/dmm.042218

Carroll, J. S., Liu, X. S., Brodsky, A. S., Li, W., Meyer, C. A., Szary, A. J., et al. (2005). Chromosome-wide mapping of estrogen receptor binding reveals long-range regulation requiring the forkhead protein FoxA1. *Cell* 122, 33–43. doi: 10.1016/j.cell.2005.05.008

Chen, A. F., Liu, A. J., Krishnakumar, R., Freimer, J. W., DeVeale, B., and Blelloch, R. (2018a). GRHL2-Dependent enhancer switching maintains a pluripotent stem cell transcriptional subnetwork after exit from naive pluripotency. *Cell Stem Cell* 23, 226.e4–238.e4. doi: 10.1016/j.stem.2018.06.005

Chen, W., Kang, K. L., Alshaikh, A., Varma, S., Lin, Y.-L., Shin, K.-H., et al. (2018b). Grainyhead-like 2 (GRHL2) knockout abolishes oral cancer development through reciprocal regulation of the MAP kinase and TGF-β signaling pathways. *Oncogenesis* 7:38. doi: 10.1038/s41389-018-0047-5

Chen, W., Shimane, T., Kawano, S., Alshaikh, A., Kim, S. Y., Chung, S. H., et al. (2018c). Human papillomavirus 16 E6 induces FoxM1B in oral keratinocytes through GRHL2. *J. Dent. Res.* 97, 795–802. doi: 10.1177/0022034518756071

Chen, C.-P., Chang, T.-Y., Hung, F.-Y., Chern, S.-R., Wu, P.-S., Chen, S.-W., et al. (2017). Prenatal diagnosis of an 8q22.2-*q*23.3 deletion associated with bilateral cleft lip and palate and intrauterine growth restriction on fetal ultrasound. *Taiwanese J. Obstetr. Gynecol.* 56, 843–846. doi: 10.1016/j.tjog.2017.10.026

Chen, W., Dong, Q., Shin, K.-H., Kim, R. H., Oh, J.-E., Park, N.-H., et al. (2010). Grainyhead-like 2 enhances the human telomerase reverse transcriptase gene expression by inhibiting DNA methylation at the 5'-CpG Island in normal human keratinocytes. *J. Biol. Chem.* 285, 40852–40863. doi: 10.1074/jbc.M110.103812

Chen, W., Xiao Liu, Z., Oh, J.-E., Shin, K.-H., Kim, R. H., Jiang, M., et al. (2012). Grainyhead-like 2 (GRHL2) inhibits keratinocyte differentiation through epigenetic mechanism. *Cell Death Dis.* 3:e450. doi: 10.1038/cddis.2012.190

Chen, W., Yi, J. K., Shimane, T., Mehrazarin, S., Lin, Y.-L., Shin, K.-H., et al. (2016). Grainyhead-like 2 regulates epithelial plasticity and stemness in oral cancer cells. *Carcinogenesis* 37, 500–510. doi: 10.1093/carcin/bgw027

Chung, V. Y., Tan, T. Z., Tan, M., Wong, M. K., Kuay, K. T., Yang, Z., et al. (2016). GRHL2-miR-200-ZEB1 maintains the epithelial status of ovarian cancer through transcriptional regulation and histone modification. *Sci. Rep.* 6:19943. doi: 10.1038/srep19943

Chung, V. Y., Tan, T. Z., Ye, J., Huang, R.-L., Lai, H.-C., Kappei, D., et al. (2019). The role of GRHL2 and epigenetic remodeling in epithelial–mesenchymal plasticity in ovarian cancer cells. *Commun. Biol.* 2:272. doi: 10.1038/s42003-019-0506-3

Cieply, B., Riley, P., Pifer, P. M., Widmeyer, J., Addison, J. B., Ivanov, A. V., et al. (2012). Suppression of the epithelial–mesenchymal transition by grainyhead-like-2. *Cancer Res.* 72, 2440–2453. doi: 10.1158/0008-5472.CAN-11-4038

Cocce, K. J., Jasper, J. S., Desautels, T. K., Everett, L., Wardell, S., Westerling, T., et al. (2019). The lineage determining factor GRHL2 collaborates with FOXA1 to establish a targetable pathway in endocrine therapy-resistant breast cancer. *Cell Rep.* 29, 889.e10–903.e10. doi: 10.1016/j.celrep.2019.09.032

Danila, D. C., Anand, A., Schultz, N., Heller, G., Wan, M., Sung, C. C., et al. (2014). Analytic and clinical validation of a prostate cancer–enhanced messenger RNA detection assay in whole blood as a prognostic biomarker for survival. *Eur. Urol.* 65, 1191–1197. doi: 10.1016/j.eururo.2013.07.006

Darido, C., Georgy, S. R., Wilanowski, T., Dworkin, S., Auden, A., Zhao, Q., et al. (2011). Targeting of the tumor suppressor GRHL3 by a miR-21-dependent proto-oncogenic network results in PTEN loss and tumorigenesis. *Cancer Cell* 20, 635–648. doi: 10.1016/j.ccr.2011.10.014

Davidson, I. F., Goetz, D., Zaczek, M. P., Molodtsov, M. I., Huis In 't Veld, P. J., Weissmann, F., et al. (2016). Rapid movement and transcriptional re-localization of human cohesin on DNA. *Embo J.* 35, 2671–2685. doi: 10.15252/embj.201695402

De Castro, S. C. P., Hirst, C. S., Savery, D., Rolo, A., Lickert, H., Andersen, B., et al. (2018). Neural tube closure depends on expression of Grainyhead-like 3 in multiple tissues. *Dev. Biol.* 435, 130–137. doi: 10.1016/j.ydbio.2018.01.016

de Vries, M., Carpinelli, M., Rutland, E., Hatzipantelis, A., Partridge, D., Auden, A., et al. (2020). Interrogating the Grainyhead-like 2 (Grhl2) genomic locus identifies an enhancer element that regulates palatogenesis in mouse. *Dev. Biol.* 459, 194–203. doi: 10.1016/j.ydbio.2019.11.015

Dixon, J. R., Selvaraj, S., Yue, F., Kim, A., Li, Y., Shen, Y., et al. (2012). Topological domains in mammalian genomes identified by analysis of chromatin interactions. *Nature* 485, 376–380. doi: 10.1038/nature11082

Dong, C., Wu, Y., Yao, J., Wang, Y., Yu, Y., Rychahou, P. G., et al. (2012). G9a interacts with Snail and is critical for Snail-mediated E-cadherin repression in human breast cancer. *J. Clin. Invest.* 122, 1469–1486. doi: 10.1172/JCI57349

Dworkin, S., Darido, C., Georgy, S. R., Wilanowski, T., Srivastava, S., Ellett, F., et al. (2012). Midbrain-hindbrain boundary patterning and morphogenesis are regulated by diverse grainy head-like 2-dependent pathways. *Development* 139, 525–536. doi: 10.1242/dev.066522

Dworkin, S., Simkin, J., Darido, C., Partridge, D. D., Georgy, S. R., Caddy, J., et al. (2014). Grainyhead-like 3 regulation of endothelin-1 in the pharyngeal endoderm is critical for growth and development of the craniofacial skeleton. *Mech. Dev.* 133, 77–90. doi: 10.1016/j.mod.2014.05.005

Dynlacht, B. D., Attardi, L. D., Admon, A., Freeman, M., and Tjian, R. (1989). Functional analysis of NTF-1, a developmentally regulated *Drosophila* transcription factor that binds neuronal cis elements. *Genes Dev.* 3, 1677–1688. doi: 10.1101/gad.3.11.1677

Eckert, R. L., Sturniolo, M. T., Broome, A.-M., Ruse, M., and Rorke, E. A. (2005). Transglutaminase function in epidermis. *J. Invest. Dermatol.* 124, 481–492. doi: 10.1111/j.0022-202X.2005.23627.x

Eichelberger, L., Saini, M., Moreno, H. D., Klein, C., Bartsch, J. M., Falcone, M., et al. (2020). Maintenance of epithelial traits and resistance to mesenchymal reprogramming promote proliferation in metastatic breast cancer. *bioRxiv* doi: 10.1101/2020.03.19.998823

Ernst, J., and Kellis, M. (2012). ChromHMM: automating chromatin-state discovery and characterization. *Nat. Methods* 9, 215–216. doi: 10.1038/nmeth.1906

Eshete, M. A., Liu, H., Li, M., Adeyemo, W. L., Gowans, L. J. J., Mossey, P. A., et al. (2018). Loss-of-function GRHL3 variants detected in african patients with isolated cleft palate. *J. Dent. Res.* 97, 41–48. doi: 10.1177/0022034517729819

Essafi, A., Webb, A., Berry, R. L., Slight, J., Burn, S. F., Spraggon, L., et al. (2011). A wt1-controlled chromatin switching mechanism underpins tissue-specific wnt4 activation and repression. *Dev. Cell* 21, 559–574. doi: 10.1016/j.devcel.2011.07.014

Fabian, J., Lodrini, M., Oehme, I., Schier, M. C., Thole, T. M., Hielscher, T., et al. (2014). GRHL1 acts as tumor suppressor in neuroblastoma and is negatively regulated by MYCN and HDAC3. *Cancer Res.* 74, 2604–2616. doi: 10.1158/0008-5472.CAN-13-1904

Farris, J. C., Pifer, P. M., Zheng, L., Gottlieb, E., Denvir, J., and Frisch, S. M. (2016). Grainyhead-like 2 reverses the metabolic changes induced by the oncogenic epithelial–mesenchymal transition: effects on anoikis. *Mol. Cancer Res.* 14, 528–538. doi: 10.1158/1541-7786.MCR-16-0050

Flavahan, W. A., Drier, Y., Liau, B. B., Gillespie, S. M., Venteicher, A. S., Stemmer-Rachamimov, A. O., et al. (2016). Insulator dysfunction and oncogene activation in IDH mutant gliomas. *Nature* 529, 110–114. doi: 10.1038/nature16490

Francart, M.-E., Lambert, J., Vanwynsberghe, A. M., Thompson, E. W., Bourcy, M., Polette, M., et al. (2018). Epithelial-mesenchymal plasticity and circulating tumor cells: travel companions to metastases. *Dev. Dyn.* 247, 432–450. doi: 10.1002/dvdy.24506

Fukagawa, A., Ishii, H., Miyazawa, K., and Saitoh, M. (2015). δEF1 associates with DNMT1 and maintains DNA methylation of the E-cadherin promoter in breast cancer cells. *Cancer Med.* 4, 125–135. doi: 10.1002/cam4.347

Fustaino, V., Presutti, D., Colombo, T., Cardinali, B., Papoff, G., Brandi, R., et al. (2017). Characterization of epithelial-mesenchymal transition intermediate/hybrid phenotypes associated to resistance to EGFR inhibitors in non-small cell lung cancer cell lines. *Oncotarget* 8, 103340–103363. doi: 10.18632/oncotarget.21132

Gao, X., Bali, A. S., Randell, S. H., and Hogan, B. L. M. (2015). GRHL2 coordinates regeneration of a polarized mucociliary epithelium from basal stem cells. *J. Cell Biol.* 211, 669–682. doi: 10.1083/jcb.201506014

Gao, X., Vockley, C. M., Pauli, F., Newberry, K. M., Xue, Y., Randell, S. H., et al. (2013). Evidence for multiple roles for grainyhead-like 2 in the establishment and maintenance of human mucociliary airway epithelium. *PNAS* 110, 9356–9361. doi: 10.1073/pnas.1307589110

Garrett, J. T., Olivares, M. G., Rinehart, C., Granja-Ingram, N. D., Sánchez, V., Chakrabarty, A., et al. (2011). Transcriptional and posttranslational up-regulation of HER3 (ErbB3) compensates for inhibition of the HER2 tyrosine kinase. *Proc. Natl. Acad. Sci. U.S.A.* 108, 5021–5026. doi: 10.1073/pnas.1016140108

Geiger, J. A., Carvalho, L., Campos, I., Santos, A. C., and Jacinto, A. (2011). Hole-in-one mutant phenotypes link EGFR/ERK signaling to epithelial tissue repair in *Drosophila*. *PLoS One* 6:e28349. doi: 10.1371/journal.pone.0028349

Glont, S.-E., Chernukhin, I., and Carroll, J. S. (2019). Comprehensive genomic analysis reveals that the pioneering function of FOXA1 is independent of hormonal signaling. *Cell Reports* 26, 2558.e3–2565.e3. doi: 10.1016/j.celrep.2019.02.036

Goldie, S. J., Arhatari, B. D., Anderson, P., Auden, A., Partridge, D. D., Jane, S. M., et al. (2016). Mice lacking the conserved transcription factor Grainyhead-like 3 (Grhl3) display increased apposition of the frontal and parietal bones during embryonic development. *BMC Dev. Biol.* 16:37. doi: 10.1186/s12861-016-0136-7

Grosse-Wilde, A., Fouquier, d'Hérouël, A., McIntosh, E., Ertaylan, G., Skupin, A., et al. (2015). Stemness of the hybrid epithelial/mesenchymal state in breast cancer and its association with poor survival. *PLoS One* 10:e0126522. doi: 10.1371/journal.pone.0126522

Grossman, S. R., Engreitz, J., Ray, J. P., Nguyen, T. H., Hacohen, N., and Lander, E. S. (2018). Positional specificity of different transcription factor classes within enhancers. *PNAS* 115, E7222–E7230. doi: 10.1073/pnas.1804663115

Gustavsson, P., Greene, N. D. E., Lad, D., Pauws, E., de Castro, S. C. P., Stanier, P., et al. (2007). Increased expression of Grainyhead-like-3 rescues spina bifida in a folate-resistant mouse model. *Hum. Mol. Genet.* 16, 2640–2646. doi: 10.1093/hmg/ddm221

Han, Y., Mu, Y., Li, X., Xu, P., Tong, J., Liu, Z., et al. (2011). Grhl2 deficiency impairs otic development and hearing ability in a zebrafish model of the progressive dominant hearing loss DFNA28. *Hum. Mol. Genet.* 20, 3213–3226. doi: 10.1093/hmg/ddr234

Harding, M. J., McGraw, H. F., and Nechiporuk, A. (2014). The roles and regulation of multicellular rosette structures during morphogenesis. *Development* 141, 2549–2558. doi: 10.1242/dev.101444

Harrison, M. M., Botchan, M. R., and Cline, T. W. (2010). Grainyhead and Zelda compete for binding to the promoters of the earliest-expressed Drosophila genes. *Dev. Biol.* 345, 248–255. doi: 10.1016/j.ydbio.2010.06.026

Hay, E. D. (1995). An overview of epithelio-mesenchymal transformation. *Acta Anat.* 154, 8–20. doi: 10.1159/000147748

Hay, E. D. (2005). The mesenchymal cell, its role in the embryo, and the remarkable signaling mechanisms that create it. *Dev. Dyn.* 233, 706–720. doi: 10.1002/dvdy.20345

Heldin, C.-H., Vanlandewijck, M., and Moustakas, A. (2012). Regulation of EMT by TGFβ in cancer. *FEBS Lett.* 586, 1959–1970. doi: 10.1016/j.febslet.2012.02.037

Helzer, K. T., Szatkowski Ozers, M., Meyer, M. B., Benkusky, N. A., Solodin, N., Reese, R. M., et al. (2018). The phosphorylated estrogen receptor α (ER) cistrome identifies a subset of active enhancers enriched for direct ER-DNA binding and the transcription factor GRHL2. *Mol. Cell Biol.* 39, e417–e418. doi: 10.1128/MCB.00417-18

Hemphälä, J., Uv, A., Cantera, R., Bray, S., and Samakovlis, C. (2003). Grainy head controls apical membrane growth and tube elongation in response to Branchless/FGF signalling. *Development* 130, 249–258. doi: 10.1242/dev.00218

Hislop, N. R., Caddy, J., Ting, S. B., Auden, A., Vasudevan, S., King, S. L., et al. (2008). Grhl3 and Lmo4 play coordinate roles in epidermal migration. *Dev. Biol.* 321, 263–272. doi: 10.1016/j.ydbio.2008.06.026

Hnisz, D., Weintraub, A. S., Day, D. S., Valton, A.-L., Bak, R. O., Li, C. H., et al. (2016). Activation of proto-oncogenes by disruption of chromosome neighborhoods. *Science* 351, 1454–1458. doi: 10.1126/science.aad9024

Hoebel, A. K., Drichel, D., van de Vorst, M., Böhmer, A. C., Sivalingam, S., Ishorst, N., et al. (2017). Candidate genes for nonsyndromic cleft palate detected by exome sequencing. *J. Dent. Res.* 96, 1314–1321. doi: 10.1177/0022034517722761

Holding, A. N., Giorgi, F. M., Donnelly, A., Cullen, A. E., Nagarajan, S., Selth, L. A., et al. (2019). VULCAN integrates ChIP-seq with patient-derived co-expression networks to identify GRHL2 as a key co-regulator of ERa at enhancers in breast cancer. *Genome Biol.* 20:91. doi: 10.1186/s13059-019-1698-z

Hopkin, A. S., Gordon, W., Klein, R. H., Espitia, F., Daily, K., Zeller, M., et al. (2012). GRHL3/GET1 and trithorax group members collaborate to activate the epidermal progenitor differentiation program. *PLoS Genet.* 8:e1002829. doi: 10.1371/journal.pgen.1002829

Hosoya, M., Fujioka, M., Ogawa, K., and Okano, H. (2016). Distinct expression patterns of causative genes responsible for hereditary progressive hearing loss in non-human primate cochlea. *Sci. Rep.* 6:22250. doi: 10.1038/srep22250

Hou, C., Li, L., Qin, Z. S., and Corces, V. G. (2012). Gene density, transcription, and insulators contribute to the partition of the *Drosophila* genome into physical domains. *Mol. Cell* 48, 471–484. doi: 10.1016/j.molcel.2012.08.031

Huang, R. Y.-J., Wong, M. K., Tan, T. Z., Kuay, K. T., Ng, A. H. C., Chung, V. Y., et al. (2013). An EMT spectrum defines an anoikis-resistant and spheroidogenic intermediate mesenchymal state that is sensitive to e-cadherin restoration by a src-kinase inhibitor, saracatinib (AZD0530). *Cell Death Dis.* 4:e915. doi: 10.1038/cddis.2013.442

Hurtado, A., Holmes, K. A., Ross-Innes, C. S., Schmidt, D., and Carroll, J. S. (2011). FOXA1 is a key determinant of estrogen receptor function and endocrine response. *Nat. Genet.* 43, 27–33. doi: 10.1038/ng.730

Iwafuchi-Doi, M., and Zaret, K. S. (2016). Cell fate control by pioneer transcription factors. *Development* 143, 1833–1837. doi: 10.1242/dev.133900

Jacobs, J., Atkins, M., Davie, K., Imrichova, H., Romanelli, L., Christiaens, V., et al. (2018). The transcription factor Grainy head primes epithelial enhancers for spatiotemporal activation by displacing nucleosomes. *Nat. Genet.* 50, 1011–1020. doi: 10.1038/s41588-018-0140-x

Jia, W., Tripathi, S., Chakraborty, P., Chedere, A., Rangarajan, A., Levine, H., et al. (2020). Epigenetic feedback and stochastic partitioning during cell division can drive resistance to EMT. *Oncotarget* 11, 2611–2624. doi: 10.18632/oncotarget.27651

Jolly, M. K., Mani, S. A., and Levine, H. (2018). Hybrid epithelial/mesenchymal phenotype(s): the 'fittest' for metastasis? *Biochim. Biophys. Acta* 1870, 151–157. doi: 10.1016/j.bbcan.2018.07.001

Jolly, M. K., Somarelli, J. A., Sheth, M., Biddle, A., Tripathi, S. C., Armstrong, A. J., et al. (2019). Hybrid epithelial/mesenchymal phenotypes promote metastasis and therapy resistance across carcinomas. *Pharmacol. Therap.* 194, 161–184. doi: 10.1016/j.pharmthera.2018.09.007

Jolly, M. K., Tripathi, S. C., Jia, D., Mooney, S. M., Celiktas, M., Hanash, S. M., et al. (2016). Stability of the hybrid epithelial/mesenchymal phenotype. *Oncotarget* 7, 27067–27084. doi: 10.18632/oncotarget.8166

Jozwik, K. M., Chernukhin, I., Serandour, A. A., Nagarajan, S., and Carroll, J. S. (2016). FOXA1 directs H3K4 monomethylation at enhancers via recruitment of the methyltransferase MLL3. *Cell Rep.* 17, 2715–2723. doi: 10.1016/j.celrep.2016.11.028

Kalluri, R., and Weinberg, R. A. (2009). The basics of epithelial-mesenchymal transition. *J. Clin. Invest.* 119, 1420–1428. doi: 10.1172/JCI39104

Kang, X., Chen, W., Kim, R. H., Kang, M. K., and Park, N.-H. (2009). Regulation of the hTERT promoter activity by MSH2, the hnRNPs K and D, and GRHL2 in human oral squamous cell carcinoma cells. *Oncogene* 28, 565–574. doi: 10.1038/onc.2008.404

Kanke, M., Tahara, E., Huis In't, Veld, P. J., and Nishiyama, T. (2016). Cohesin acetylation and Wapl-Pds5 oppositely regulate translocation of cohesin along DNA. *Embo J.* 35, 2686–2698. doi: 10.15252/embj.201695756

Kashgari, G., Meinecke, L., Gordon, W., Ruiz, B., Yang, J., Ma, A. L., et al. (2020). Epithelial migration and non-adhesive periderm are required for digit separation during mammalian development. *Dev. Cell* 52, 764.e–778.e. doi: 10.1016/j.devcel.2020.01.032

Kersbergen, A., Best, S. A., Dworkin, S., Ah-Cann, C., de Vries, M. E., Asselin-Labat, M.-L., et al. (2018). Lung morphogenesis is orchestrated through Grainyhead-like 2 (Grhl2) transcriptional programs. *Dev. Biol.* 443, 1–9. doi: 10.1016/j.ydbio.2018.09.002

Khandelwal, R., Sipani, R., Govinda Rajan, S., Kumar, R., and Joshi, R. (2017). Combinatorial action of grainyhead, extradenticle and notch in regulating Hox mediated apoptosis in *Drosophila larval* CNS. *PLoS Genet.* 13:e1007043. doi: 10.1371/journal.pgen.1007043

Kim, M., and McGinnis, W. (2011). Phosphorylation of grainy head by ERK is essential for wound-dependent regeneration but not for development of an epidermal barrier. *Proc. Natl. Acad. Sci. U.S.A.* 108, 650–655. doi: 10.1073/pnas.1016386108

Kim, Y.-R., Kim, M.-A., Sagong, B., Bae, S.-H., Lee, H.-J., Kim, H.-J., et al. (2015). Evaluation of the contribution of the EYA4 and GRHL2 genes in korean patients with autosomal dominant non-syndromic hearing loss. *PLoS One* 10:e0119443. doi: 10.1371/journal.pone.0119443

Kimura-Yoshida, C., Mochida, K., Ellwanger, K., Niehrs, C., and Matsuo, I. (2015). Fate specification of neural plate border by canonical Wnt signaling and Grhl3 is crucial for neural tube closure. *Ebio Med.* 2, 513–527. doi: 10.1016/j.ebiom.2015.04.012

Kimura-Yoshida, C., Mochida, K., Nakaya, M.-A., Mizutani, T., and Matsuo, I. (2018). Cytoplasmic localization of GRHL3 upon epidermal differentiation triggers cell shape change for epithelial morphogenesis. *Nat. Commun.* 9:4059. doi: 10.1038/s41467-018-06171-8

Kokoszynska, K., Ostrowski, J., Rychlewski, L., and Wyrwicz, L. S. (2008). The fold recognition of CP2 transcription factors gives new insights into the function and evolution of tumor suppressor protein p53. *Cell Cycle* 7, 2907–2915. doi: 10.4161/cc.7.18.6680

Kotarba, G., Krzywinska, E., Grabowska, A. I., Taracha, A., and Wilanowski, T. (2018). TFCP2/TFCP2L1/UBP1 transcription factors in cancer. *Cancer Lett.* 420, 72–79. doi: 10.1016/j.canlet.2018.01.078

Kotarba, G., Taracha-Wisniewska, A., and Wilanowski, T. (2020). Grainyhead-like transcription factors in cancer – Focus on recent developments. *Exp. Biol. Med.* 245, 402–410. doi: 10.1177/1535370220903009

Kuechler, A., Buysse, K., Clayton-Smith, J., Caignec, C. L., David, A., Engels, H., et al. (2011). Five patients with novel overlapping interstitial deletions in 8q22.2*q*22.3. *Am. J. Med. Genet. Part A* 155, 1857–1864. doi: 10.1002/ajmg.a.34072

Kuroda, Y., Ohashi, I., Saito, T., Nagai, J., Ida, K., Naruto, T., et al. (2014). Refinement of the deletion in 8q22.2–*q*22.3: the minimum deletion size at 8q22.3 related to intellectual disability and epilepsy. *Am. J. Med. Genet. Part A* 164, 2104–2108. doi: 10.1002/ajmg.a.36604

Lee, H., and Adler, P. N. (2004). The grainy head transcription factor is essential for the function of the frizzled pathway in the *Drosophila* wing. *Mech. Dev.* 121, 37–49. doi: 10.1016/j.mod.2003.11.002

Leth-Larsen, R., Terp, M. G., Christensen, A. G., Elias, D., Kühlwein, T., Jensen, O. N., et al. (2012). Functional heterogeneity within the CD44 high human breast cancer stem cell-like compartment reveals a gene signature predictive of distant metastasis. *Mol. Med.* 18, 1109–1121. doi: 10.2119/molmed.2012.00091

Li, M., Li, Z., Guan, X., and Qin, Y. (2019). Suppressor gene GRHL1 is associated with prognosis in patients with oesophageal squamous cell carcinoma. *Oncol. Lett.* 17, 4313–4320. doi: 10.3892/ol.2019.10072

Li, X., Zhu, Z., Li, W., Wei, L., Zhao, B., and Hao, Z. (2019). Polymorphism in GRHL2 gene may contribute to noise-induced hearing loss susceptibility: a

meta-analysis. *Braz. J. Otorhinolaryngol.* 86, 370–375. doi: 10.1016/j.bjorl.2019.01.003

Lin, X., Teng, Y., Lan, J., He, B., Sun, H., and Xu, F. (2016). GRHL2 genetic polymorphisms may confer a protective effect against sudden sensorineural hearing loss. *Mol. Med. Rep.* 13, 2857–2863. doi: 10.3892/mmr.2016.4871

Liu, B., Ordonez-Ercan, D., Fan, Z., Edgerton, S. M., Yang, X., and Thor, A. D. (2007). Downregulation of erbB3 abrogates erbB2-mediated tamoxifen resistance in breast cancer cells. *Int. J. Cancer* 120, 1874–1882. doi: 10.1002/ijc.22423

Long, H. K., Prescott, S. L., and Wysocka, J. (2016). Ever-changing landscapes: transcriptional enhancers in development and evolution. *Cell* 167, 1170–1187. doi: 10.1016/j.cell.2016.09.018

Lupiáñez, D. G., Kraft, K., Heinrich, V., Krawitz, P., Brancati, F., Klopocki, E., et al. (2015). Disruptions of topological chromatin domains cause pathogenic rewiring of gene-enhancer interactions. *Cell* 161, 1012–1025. doi: 10.1016/j.cell.2015.04.004

Lupiáñez, D. G., Spielmann, M., and Mundlos, S. (2016). Breaking TADs: how alterations of chromatin domains result in disease. *Trends Genet.* 32, 225–237. doi: 10.1016/j.tig.2016.01.003

Mace, K. A., Pearson, J. C., and McGinnis, W. (2005). An epidermal barrier wound repair pathway in *Drosophila* is mediated by grainy head. *Science* 308, 381–385. doi: 10.1126/science.1107573

MacFawn, I., Wilson, H., Selth, L. A., Leighton, I., Serebriiskii, I., Bleackley, R. C., et al. (2019). Grainyhead-like-2 confers NK-sensitivity through interactions with epigenetic modifiers. *Mol. Immunol.* 105, 137–149. doi: 10.1016/j.molimm.2018.11.006

Magnani, L., Eeckhoute, J., and Lupien, M. (2011). Pioneer factors: directing transcriptional regulators within the chromatin environment. *Trends Genet.* 27, 465–474. doi: 10.1016/j.tig.2011.07.002

Matsushita, T., Sakai, M., Yoshida, H., Morita, S., Hieda, Y., and Sakai, T. (2018). Grhl2 regulation of SPINT1 expression controls salivary gland development. *Biochem. Biophys. Res. Commun.* 504, 263–269. doi: 10.1016/j.bbrc.2018.08.166

Matyas, P., Postyeni, E., Komlosi, K., Szalai, R., Bene, J., Magyari, L., et al. (2019). Age-related hearing impairment associated NAT2, GRM7, GRHL2 susceptibility gene polymorphisms and haplotypes in roma and hungarian populations. *Pathol. Oncol. Res.* 25, 1349–1355. doi: 10.1007/s12253-018-0388-6

Mayran, A., and Drouin, J. (2018). Pioneer transcription factors shape the epigenetic landscape. *J. Biol. Chem.* 293, 13795–13804. doi: 10.1074/jbc.R117.001232

McInnes, L. M., Jacobson, N., Redfern, A., Dowling, A., Thompson, E. W., and Saunders, C. M. (2015). Clinical implications of circulating tumor cells of breast cancer patients: role of epithelial-mesenchymal plasticity. *Front. Oncol.* 5:42. doi: 10.3389/fonc.2015.00042

Mehrazarin, S., Chen, W., Oh, J.-E., Liu, Z. X., Kang, K. L., Yi, J. K., et al. (2015). The p63 gene is regulated by Grainyhead-like 2 (GRHL2) through reciprocal feedback and determines the epithelial phenotype in human keratinocytes. *J. Biol. Chem.* 290, 19999–20008. doi: 10.1074/jbc.M115.659144

Menke, C., Cionni, M., Siggers, T., Bulyk, M. L., Beier, D. R., and Stottmann, R. W. (2015). Grhl2 is required in nonneural tissues for neural progenitor survival and forebrain development. *Genesis* 53, 573–582. doi: 10.1002/dvg.22875

Miles, L. B., Dworkin, S., and Darido, C. (2017). Alternative splicing and start sites: lessons from the Grainyhead-like family. *Dev. Biol.* 429, 12–19. doi: 10.1016/j.ydbio.2017.06.018

Ming, Q., Roske, Y., Schuetz, A., Walentin, K., Ibraimi, I., Schmidt-Ott, K. M., et al. (2018). Structural basis of gene regulation by the Grainyhead/CP2 transcription factor family. *Nucl. Acids Res.* 46, 2082–2095. doi: 10.1093/nar/gkx1299

Mlacki, M., Darido, C., Jane, S. M., and Wilanowski, T. (2014). Loss of Grainy head-like 1 is associated with disruption of the epidermal barrier and squamous cell carcinoma of the skin. *PLoS One* 9:e89247. doi: 10.1371/journal.pone.0089247

Molè, M. A., Galea, G. L., Rolo, A., Weberling, A., Nychyk, O., De Castro, S. C., et al. (2020). Integrin-mediated focal anchorage drives epithelial zippering during mouse neural tube closure. *Dev. Cell* 52, 321.e6–334.e6. doi: 10.1016/j.devcel.2020.01.012

Mooney, S. M., Talebian, V., Jolly, M. K., Jia, D., Gromala, M., Levine, H., et al. (2017). The GRHL2/zeb feedback loop—a key axis in the regulation of EMT in breast cancer. *J. Cell. Biochem.* 118, 2559–2570. doi: 10.1002/jcb.25974

Muñoz, W. A., and Trainor, P. A. (2015). "Chapter One - Neural crest cell evolution: how and when did a neural crest cell become a neural crest cell," in *Current Topics in Developmental Biology Neural Crest and Placodes*, ed. P. A. Trainor (London: Academic Press), 3–26. doi: 10.1016/bs.ctdb.2014.11.001

Murry, C. E., and Keller, G. (2008). Differentiation of embryonic stem cells to clinically relevant populations: lessons from embryonic development. *Cell* 132, 661–680. doi: 10.1016/j.cell.2008.02.008

Narasimha, M., Uv, A., Krejci, A., Brown, N. H., and Bray, S. J. (2008). Grainy head promotes expression of septate junction proteins and influences epithelial morphogenesis. *J. Cell. Sci.* 121, 747–752. doi: 10.1242/jcs.019422

Nevil, M., Gibson, T. J., Bartolutti, C., Iyengar, A., and Harrison, M. M. (2020). Establishment of chromatin accessibility by the conserved transcription factor Grainy head is developmentally regulated. *Development* 147:dev185009. doi: 10.1242/dev.185009

Nieto, M. A., Huang, R. Y.-J., Jackson, R. A., and Thiery, J. P. (2016). EMT: 2016. *Cell* 166, 21–45. doi: 10.1016/j.cell.2016.06.028

Nikolopoulou, E., Galea, G. L., Rolo, A., Greene, N. D. E., and Copp, A. J. (2017). Neural tube closure: cellular, molecular and biomechanical mechanisms. *Development* 144, 552–566. doi: 10.1242/dev.145904

Nikolopoulou, E., Hirst, C. S., Galea, G., Venturini, C., Moulding, D., Marshall, A. R., et al. (2019). Spinal neural tube closure depends on regulation of surface ectoderm identity and biomechanics by Grhl2. *Nat. Commun.* 10, 1–17. doi: 10.1038/s41467-019-10164-6

Nishimura, T., and Takeichi, M. (2008). Shroom3-mediated recruitment of Rho kinases to the apical cell junctions regulates epithelial and neuroepithelial planar remodeling. *Development* 135, 1493–1502. doi: 10.1242/dev.019646

Nora, E. P., Goloborodko, A., Valton, A.-L., Gibcus, J. H., Uebersohn, A., Abdennur, N., et al. (2017). Targeted degradation of CTCF decouples local insulation of chromosome domains from genomic compartmentalization. *Cell* 169, 930.e22–944.e22. doi: 10.1016/j.cell.2017.05.004

Nora, E. P., Lajoie, B. R., Schulz, E. G., Giorgetti, L., Okamoto, I., Servant, N., et al. (2012). Spatial partitioning of the regulatory landscape of the X-inactivation centre. *Nature* 485, 381–385. doi: 10.1038/nature11049

Nüsslein-Volhard, C., Wieschaus, E., and Kluding, H. (1984). Mutations affecting the pattern of the larval cuticle in *Drosophila melanogaster*. *Wilhelm. Roux'. Archiv.* 193, 267–282. doi: 10.1007/BF00848156

Ostrowski, S., Dierick, H. A., and Bejsovec, A. (2002). Genetic control of cuticle formation during embryonic development of *Drosophila melanogaster*. *Genetics* 161, 171–182.

Paltoglou, S., Das, R., Townley, S. L., Hickey, T. E., Tarulli, G. A., Coutinho, I., et al. (2017). Novel androgen receptor coregulator GRHL2 exerts both oncogenic and antimetastatic functions in prostate cancer. *Cancer Res.* 77, 3417–3430. doi: 10.1158/0008-5472.CAN-16-1616

Parelho, V., Hadjur, S., Spivakov, M., Leleu, M., Sauer, S., Gregson, H. C., et al. (2008). Cohesins functionally associate with CTCF on mammalian chromosome arms. *Cell* 132, 422–433. doi: 10.1016/j.cell.2008.01.011

Pastushenko, I., Brisebarre, A., Sifrim, A., Fioramonti, M., Revenco, T., Boumahdi, S., et al. (2018). Identification of the tumour transition states occurring during EMT. *Nature* 556, 463–468. doi: 10.1038/s41586-018-0040-3

Pearson, J. C., Juarez, M. T., Kim, M., Drivenes, Ø, and McGinnis, W. (2009). Multiple transcription factor codes activate epidermal wound-response genes in *Drosophila*. *Proc. Natl. Acad. Sci. U.S.A.* 106, 2224–2229. doi: 10.1073/pnas.0810219106

Peters, L. M., Anderson, D. W., Griffith, A. J., Grundfast, K. M., San Agustin, T. B., Madeo, A. C., et al. (2002). Mutation of a transcription factor, TFCP2L3, causes progressive autosomal dominant hearing loss, DFNA28. *Hum. Mol. Genet.* 11, 2877–2885. doi: 10.1093/hmg/11.23.2877

Petrof, G., Nanda, A., Howden, J., Takeichi, T., McMillan, J. R., Aristodemou, S., et al. (2014). Mutations in GRHL2 result in an autosomal-recessive ectodermal dysplasia syndrome. *Am. J. Hum. Genet.* 95, 308–314. doi: 10.1016/j.ajhg.2014.08.001

Peyrard-Janvid, M., Leslie, E. J., Kousa, Y. A., Smith, T. L., Dunnwald, M., Magnusson, M., et al. (2014). Dominant mutations in GRHL3 cause Van der Woude Syndrome and disrupt oral periderm development. *Am. J. Hum. Genet.* 94, 23–32. doi: 10.1016/j.ajhg.2013.11.009

Pifer, P. M., Farris, J. C., Thomas, A. L., Stoilov, P., Denvir, J., Smith, D. M., et al. (2016). Grainyhead-like 2 inhibits the coactivator p300, suppressing

tubulogenesis and the epithelial–mesenchymal transition. *MBoC* 27, 2479–2492. doi: 10.1091/mbc.E16-04-0249

Potier, D., Davie, K., Hulselmans, G., Naval Sanchez, M., Haagen, L., Huynh-Thu, V. A., et al. (2014). Mapping gene regulatory networks in *Drosophila* eye development by large-scale transcriptome perturbations and motif inference. *Cell Rep.* 9, 2290–2303. doi: 10.1016/j.celrep.2014.11.038

Pyrgaki, C., Liu, A., and Niswander, L. (2011). Grainyhead-like 2 regulates neural tube closure and adhesion molecule expression during neural fold fusion. *Dev. Biol.* 353, 38–49. doi: 10.1016/j.ydbio.2011.02.027

Quan, Y., Jin, R., Huang, A., Zhao, H., Feng, B., Zang, L., et al. (2014). Downregulation of GRHL2 inhibits the proliferation of colorectal cancer cells by targeting ZEB1. *Cancer Biol. Ther.* 15, 878–887. doi: 10.4161/cbt.28877

Quan, Y., Xu, M., Cui, P., Ye, M., Zhuang, B., and Min, Z. (2015). Grainyhead-like 2 promotes tumor growth and is associated with poor prognosis in colorectal cancer. *J. Cancer* 6, 342–350. doi: 10.7150/jca.10969

Rao, S. S. P., Huang, S.-C., Glenn, St Hilaire, B., Engreitz, J. M., Perez, E. M., et al. (2017). Cohesin loss eliminates all loop domains. *Cell* 171, 305.e24–320.e24. doi: 10.1016/j.cell.2017.09.026

Rao, S. S. P., Huntley, M. H., Durand, N. C., Stamenova, E. K., Bochkov, I. D., Robinson, J. T., et al. (2014). A 3D map of the human genome at kilobase resolution reveals principles of chromatin looping. *Cell* 159, 1665–1680. doi: 10.1016/j.cell.2014.11.021

Ray, H. J., and Niswander, L. A. (2016). Grainyhead-like 2 downstream targets act to suppress epithelial-to-mesenchymal transition during neural tube closure. *Development* 143, 1192–1204. doi: 10.1242/dev.129825

Remeseiro, S., Cuadrado, A., and Losada, A. (2013). Cohesin in development and disease. *Development* 140, 3715–3718. doi: 10.1242/dev.090605

Rifat, Y., Parekh, V., Wilanowski, T., Hislop, N. R., Auden, A., Ting, S. B., et al. (2010). Regional neural tube closure defined by the Grainy head-like transcription factors. *Dev. Biol.* 345, 237–245. doi: 10.1016/j.ydbio.2010.07.017

Rios, A. C., Capaldo, B. D., Vaillant, F., Pal, B., van Ineveld, R., Dawson, C. A., et al. (2019). Intraclonal plasticity in mammary tumors revealed through large-scale single-cell resolution 3D imaging. *Cancer Cell* 35:953. doi: 10.1016/j.ccell.2019.02.010

Rothbart, S. B., and Strahl, B. D. (2014). Interpreting the language of histone and DNA modifications. *Biochim. Biophys. Acta* 1839, 627–643. doi: 10.1016/j.bbagrm.2014.03.001

Ruscetti, M., Quach, B., Dadashian, E. L., Mulholland, D. J., and Wu, H. (2015). Tracking and functional characterization of epithelial-mesenchymal transition and mesenchymal tumor cells during prostate cancer metastasis. *Cancer Res.* 75, 2749–2759. doi: 10.1158/0008-5472.CAN-14-3476

Santamaria, P. G., Moreno-Bueno, G., Portillo, F., and Cano, A. (2017). EMT: present and future in clinical oncology. *Mol. Oncol.* 11, 718–738. doi: 10.1002/1878-0261.12091

Sanyal, A., Lajoie, B. R., Jain, G., and Dekker, J. (2012). The long-range interaction landscape of gene promoters. *Nature* 489, 109–113. doi: 10.1038/nature11279

Satishchandran, A., Ambade, A., Rao, S., Hsueh, Y.-C., Iracheta-Vellve, A., Tornai, D., et al. (2018). MicroRNA 122, regulated by GRLH2, protects livers of mice and patients from ethanol-induced liver disease. *Gastroenterology* 154, 238.e–252.e. doi: 10.1053/j.gastro.2017.09.022

Senga, K., Mostov, K. E., Mitaka, T., Miyajima, A., and Tanimizu, N. (2012). Grainyhead-like 2 regulates epithelial morphogenesis by establishing functional tight junctions through the organization of a molecular network among claudin3, claudin4, and Rab25. *Mol. Biol. Cell* 23, 2845–2855. doi: 10.1091/mbc.E12-02-0097

Sexton, T., Yaffe, E., Kenigsberg, E., Bantignies, F., Leblanc, B., Hoichman, M., et al. (2012). Three-dimensional folding and functional organization principles of the *Drosophila* genome. *Cell* 148, 458–472. doi: 10.1016/j.cell.2012.01.010

Shang, Z., Chen, D., Wang, Q., Wang, S., Deng, Q., Wu, L., et al. (2018). Single-cell RNA-seq reveals dynamic transcriptome profiling in human early neural differentiation. *Gigascience* 7:giy117. doi: 10.1093/gigascience/giy117

Shao, C., Ji, C., Wang, X., and Hu, B. (2017). Expression and significance of GRHL2 in esophageal cancer. *Onco Targets Ther.* 10, 2025–2031. doi: 10.2147/OTT.S128294

Shen, J., Lv, X., and Zhang, L. (2020). GRHL2 acts as an anti-oncogene in bladder cancer by regulating ZEB1 in Epithelial-Mesenchymal Transition (EMT) process. *Onco Targets Ther.* 13, 2511–2522. doi: 10.2147/OTT.S239120

Simões-Costa, M., and Bronner, M. E. (2013). Insights into neural crest development and evolution from genomic analysis. *Genome Res.* 23, 1069–1080. doi: 10.1101/gr.157586.113

Sinajon, P., Gofine, T., Ingram, J., and So, J. (2015). Microdeletion 8q22.2-q22.3 in a 40-year-old male. *Eur. J. Med. Genet.* 58, 569–572. doi: 10.1016/j.ejmg.2015.10.004

Sithanandam, G., and Anderson, L. M. (2008). The ERBB3 receptor in cancer and cancer gene therapy. *Cancer Gene Ther.* 15, 413–448. doi: 10.1038/cgt.2008.15

Soeller, W. C., Poole, S. J., and Kornberg, T. (1988). In vitro transcription of the *Drosophila* engrailed gene. *Genes Dev.* 2, 68–81. doi: 10.1101/gad.2.1.68

Somarelli, J. A., Shetler, S., Jolly, M. K., Wang, X., Dewitt, S. B., Hish, A. J., et al. (2016). Mesenchymal-epithelial transition in sarcomas is controlled by the combinatorial expression of MicroRNA 200s and GRHL2. *Mol. Cell. Biol.* 36, 2503–2513. doi: 10.1128/MCB.00373-16

Stedman, W., Kang, H., Lin, S., Kissil, J. L., Bartolomei, M. S., and Lieberman, P. M. (2008). Cohesins localize with CTCF at the KSHV latency control region and at cellular c-myc and H19/Igf2 insulators. *Embo J.* 27, 654–666. doi: 10.1038/emboj.2008.1

Stemmler, M. P., Hecht, A., and Kemler, R. (2005). E-cadherin intron 2 contains cis-regulatory elements essential for gene expression. *Development* 132, 965–976. doi: 10.1242/dev.01662

Stigler, J., Çamdere, G. Ö, Koshland, D. E., and Greene, E. C. (2016). Single-molecule imaging reveals a collapsed conformational state for DNA-bound cohesin. *Cell Rep.* 15, 988–998. doi: 10.1016/j.celrep.2016.04.003

Sundararajan, V., Tan, M., Zea Tan, T., Pang, Q. Y., Ye, J., Chung, V. Y., et al. (2020). SNAI1-driven sequential EMT changes attributed by selective chromatin enrichment of RAD21 and GRHL2. *Cancers* 12:1140. doi: 10.3390/cancers12051140

Suzuki, M. M., and Bird, A. (2008). DNA methylation landscapes: provocative insights from epigenomics. *Nat. Rev. Genet.* 9, 465–476. doi: 10.1038/nrg2341

Tanaka, Y., Kanai, F., Tada, M., Tateishi, R., Sanada, M., Nannya, Y., et al. (2008). Gain of GRHL2 is associated with early recurrence of hepatocellular carcinoma. *J. Hepatol.* 49, 746–757. doi: 10.1016/j.jhep.2008.06.019

Tanimizu, N., and Mitaka, T. (2013). Role of grainyhead-like 2 in the formation of functional tight junctions. *Tissue Barr.* 1:e23495. doi: 10.4161/tisb.23495

Tanimizu, N., Nakamura, Y., Ichinohe, N., Mizuguchi, T., Hirata, K., and Mitaka, T. (2013). Hepatic biliary epithelial cells acquire epithelial integrity but lose plasticity to differentiate into hepatocytes in vitro during development. *J. Cell Sci.* 126, 5239–5246. doi: 10.1242/jcs.133082

Taracha, A., Kotarba, G., and Wilanowski, T. (2018). Neglected functions of TFCP2/TFCP2L1/UBP1 transcription factors may offer valuable insights into their mechanisms of action. *Int. J. Mol. Sci.* 19:2852. doi: 10.3390/ijms19102852

Thiery, J. P., and Sleeman, J. P. (2006). Complex networks orchestrate epithelial–mesenchymal transitions. *Nat. Rev. Mol. Cell Biol.* 7, 131–142. doi: 10.1038/nrm1835

Ting, S. B., Caddy, J., Hislop, N., Wilanowski, T., Auden, A., Zhao, L., et al. (2005). A homolog of drosophila grainy head is essential for epidermal integrity in mice. *Science* 308, 411–413. doi: 10.1126/science.1107511

Ting, S. B., Wilanowski, T., Auden, A., Hall, M., Voss, A. K., Thomas, T., et al. (2003). Inositol- and folate-resistant neural tube defects in mice lacking the epithelial-specific factor Grhl-3. *Nat. Med.* 9, 1513–1519. doi: 10.1038/nm961

Traylor-Knowles, N., Hansen, U., Dubuc, T. Q., Martindale, M. Q., Kaufman, L., and Finnerty, J. R. (2010). The evolutionary diversification of LSF and Grainyhead transcription factors preceded the radiation of basal animal lineages. *BMC Evol. Biol.* 10:101. doi: 10.1186/1471-2148-10-101

Uv, A. E., Harrison, E. J., and Bray, S. J. (1997). Tissue-specific splicing and functions of the *Drosophila* transcription factor Grainyhead. *Mol. Cell. Biol.* 17, 6727–6735. doi: 10.1128/MCB.17.11.6727

Varma, S., Cao, Y., Tagne, J.-B., Lakshminarayanan, M., Li, J., Friedman, T. B., et al. (2012). The transcription factors Grainyhead-like 2 and NK2-Homeobox 1 form a regulatory loop that coordinates lung epithelial cell morphogenesis and differentiation. *J. Biol. Chem.* 287, 37282–37295. doi: 10.1074/jbc.M112.408401

Venkatesan, K., McManus, H., and Mello, C. (2003). Functional conservation between members of an ancient duplicated transcription factor family, LSF/Grainyhead. *Nucl. Acids Res.* 31, 4304–4316. doi: 10.1093/nar/gkg644

Vona, B., Nanda, I., Neuner, C., Müller, T., and Haaf, T. (2013). Confirmation of GRHL2 as the gene for the DFNA28 locus. *Am. J. Med. Genet. A* 161A, 2060–2065. doi: 10.1002/ajmg.a.36017

Walentin, K., Hinze, C., Werth, M., Haase, N., Varma, S., Morell, R., et al. (2015). A Grhl2-dependent gene network controls trophoblast branching morphogenesis. *Development* 142, 1125–1136. doi: 10.1242/dev.113829

Wang, G., Pan, J., Zhang, L., and Wang, C. (2019). Overexpression of grainyhead-like transcription factor 2 is associated with poor prognosis in human pancreatic carcinoma. *Oncol. Lett.* 17, 1491–1496. doi: 10.3892/ol.2018.9741

Wang, S., and Samakovlis, C. (2012). Grainy head and its target genes in epithelial morphogenesis and wound healing. *Curr. Top. Dev. Biol.* 98, 35–63. doi: 10.1016/B978-0-12-386499-4.00002-1

Wang, S., Tsarouhas, V., Xylourgidis, N., Sabri, N., Tiklová, K., Nautiyal, N., et al. (2009). The tyrosine kinase stitcher activates grainy head and epidermal wound healing in *Drosophila*. *Nat. Cell Biol.* 11, 890–895. doi: 10.1038/ncb1898

Wang, Y., Sun, Y., Huang, Y., Pan, Y., Jia, Z., Ma, L., et al. (2016). Association study between Van der Woude Syndrome causative gene GRHL3 and nonsyndromic cleft lip with or without cleft palate in a Chinese cohort. *Gene* 588, 69–73. doi: 10.1016/j.gene.2016.04.045

Watanabe, K., Villarreal-Ponce, A., Sun, P., Salmans, M. L., Fallahi, M., Andersen, B., et al. (2014). Mammary morphogenesis and regeneration require the inhibition of EMT at terminal end buds by Ovol2 transcriptional repressor. *Dev. Cell* 29, 59–74. doi: 10.1016/j.devcel.2014.03.006

Weischenfeldt, J., Dubash, T., Drainas, A. P., Mardin, B. R., Chen, Y., Stütz, A. M., et al. (2017). Pan-cancer analysis of somatic copy-number alterations implicates IRS4 and IGF2 in enhancer hijacking. *Nat. Genet.* 49, 65–74. doi: 10.1038/ng.3722

Werner, S., Frey, S., Riethdorf, S., Schulze, C., Alawi, M., Kling, L., et al. (2013). Dual roles of the transcription factor Grainyhead-like 2 (GRHL2) in breast cancer. *J. Biol. Chem.* 288, 22993–23008. doi: 10.1074/jbc.M113.456293

Werth, M., Walentin, K., Aue, A., Schönheit, J., Wuebken, A., Pode-Shakked, N., et al. (2010). The transcription factor grainyhead-like 2 regulates the molecular composition of the epithelial apical junctional complex. *Development* 137, 3835–3845. doi: 10.1242/dev.055483

Wilanowski, T., Caddy, J., Ting, S. B., Hislop, N. R., Cerruti, L., Auden, A., et al. (2008). Perturbed desmosomal cadherin expression in grainy head-like 1-null mice. *Embo J.* 27, 886–897. doi: 10.1038/emboj.2008.24

Wilanowski, T., Tuckfield, A., Cerruti, L., O'Connell, S., Saint, R., Parekh, V., et al. (2002). A highly conserved novel family of mammalian developmental transcription factors related to *Drosophila* grainyhead. *Mech. Dev.* 114, 37–50. doi: 10.1016/S0925-4773(02)00046-1

Wilde, J. J., Petersen, J. R., and Niswander, L. (2014). Genetic, epigenetic, and environmental contributions to neural tube closure. *Annu. Rev. Genet.* 48, 583–611. doi: 10.1146/annurev-genet-120213-092208

Williams, E. D., Gao, D., Redfern, A., and Thompson, E. W. (2019). Controversies around epithelial–mesenchymal plasticity in cancer metastasis. *Nat. Rev. Cancer* 19, 716–732. doi: 10.1038/s41568-019-0213-x

Wittkopp, P. J., and Kalay, G. (2012). Cis -regulatory elements: molecular mechanisms and evolutionary processes underlying divergence. *Nat. Rev. Genet.* 13, 59–69. doi: 10.1038/nrg3095

Wu, D., Huang, W., Xu, Z., Li, S., Zhang, J., Chen, X., et al. (2020). Clinical and genetic study of 12 Chinese Han families with nonsyndromic deafness. *Mol. Genet. Genomic Med.* 8:e1177. doi: 10.1002/mgg3.1177

Xiang, J., Fu, X., Ran, W., and Wang, Z. (2017). Grhl2 reduces invasion and migration through inhibition of TGFβ-induced EMT in gastric cancer. *Oncogenesis* 6:e284. doi: 10.1038/oncsis.2016.83

Xiang, X., Deng, Z., Zhuang, X., Ju, S., Mu, J., Jiang, H., et al. (2012). Grhl2 determines the epithelial phenotype of breast cancers and promotes tumor progression. *PLoS One* 7:e50781. doi: 10.1371/journal.pone.0050781

Xu, X., Yang, Q., Jiao, J., He, L., Yu, S., Wang, J., et al. (2016). Genetic variation in POU4F3 and GRHL2 associated with noise-induced hearing loss in Chinese population: a case-control study. *Int. J. Environ. Res. Public Health* 13:561. doi: 10.3390/ijerph13060561

Yamashita, N., Tokunaga, E., Iimori, M., Inoue, Y., Tanaka, K., Kitao, H., et al. (2018). Epithelial paradox: clinical significance of coexpression of E-cadherin and vimentin with regard to invasion and metastasis of breast cancer. *Clin. Breast Cancer* 18, e1003–e1009. doi: 10.1016/j.clbc.2018.02.002

Yang, J., Antin, P., Berx, G., Blanpain, C., Brabletz, T., Bronner, M., et al. (2020). Guidelines and definitions for research on epithelial–mesenchymal transition. *Nat. Rev. Mol. Cell Biol.* 21, 341–352. doi: 10.1038/s41580-020-0237-9

Yang, X., Vasudevan, P., Parekh, V., Penev, A., and Cunningham, J. M. (2013). Bridging cancer biology with the clinic: relative expression of a GRHL2-mediated gene-set pair predicts breast cancer metastasis. *PLoS One* 8:e56195. doi: 10.1371/journal.pone.0056195

Yang, Z., Wu, D., Chen, Y., Min, Z., and Quan, Y. (2019). GRHL2 inhibits colorectal cancer progression and metastasis via oppressing epithelial-mesenchymal transition. *Cancer Biol. Ther.* 20, 1195–1205. doi: 10.1080/15384047.2019.1599664

Yu, Z., Bhandari, A., Mannik, J., Pham, T., Xu, X., and Andersen, B. (2008). Grainyhead-like factor Get1/Grhl3 regulates formation of the epidermal leading edge during eyelid closure. *Dev. Biol.* 319, 56–67. doi: 10.1016/j.ydbio.2008.04.001

Yu, Z., Lin, K. K., Bhandari, A., Spencer, J. A., Xu, X., Wang, N., et al. (2006). The Grainyhead-like epithelial transactivator Get-1/Grhl3 regulates epidermal terminal differentiation and interacts functionally with LMO4. *Dev. Biol.* 299, 122–136. doi: 10.1016/j.ydbio.2006.07.015

Yu, Z., Mannik, J., Soto, A., Lin, K. K., and Andersen, B. (2009). The epidermal differentiation-associated Grainyhead gene Get1/Grhl3 also regulates urothelial differentiation. *Embo J.* 28, 1890–1903. doi: 10.1038/emboj.2009.142

Yuan, M., Wang, J., and Fang, F. (2020). Grainyhead-like genes family may act as novel biomarkers in colon cancer. *Onco Targets Ther.* 13, 3237–3245. doi: 10.2147/OTT.S242763

Yun, J., Song, S.-H., Kim, H.-P., Han, S.-W., Yi, E. C., and Kim, T.-Y. (2016). Dynamic cohesin-mediated chromatin architecture controls epithelial–mesenchymal plasticity in cancer. *Embo Rep.* 17, 1343–1359. doi: 10.15252/embr.201541852

Zaret, K. S., and Carroll, J. S. (2011). Pioneer transcription factors: establishing competence for gene expression. *Genes Dev.* 25, 2227–2241. doi: 10.1101/gad.176826.111

Zaret, K. S., and Mango, S. (2016). Pioneer transcription factors, chromatin dynamics, and cell fate control. *Curr. Opin. Genet. Dev.* 37, 76–81. doi: 10.1016/j.gde.2015.12.003

Zhang, X., Liu, Y., Zhang, L., Yang, Z., Yang, L., Wang, X., et al. (2015). Associations of genetic variations in EYA4, GRHL2 and DFNA5 with noise-induced hearing loss in Chinese population: a case- control study. *Environ. Health* 14:77. doi: 10.1186/s12940-015-0063-2

Zhao, Z., Li, L., Cheng, M., Jing, A.-D., Liu, S.-N., Zhu, S.-M., et al. (2020). Grh signaling regulates epithelium development and ecdysis in Blattella germanica. *Insect Sci.* doi: 10.1111/1744-7917.12780

Zhou, C. J., Ji, Y., Reynolds, K., McMahon, M., Garland, M. A., Zhang, S., et al. (2020). Non-neural surface ectodermal rosette formation and F-actin dynamics drive mammalian neural tube closure. *Biochem. Biophys. Res. Commun.* 526, 647–653. doi: 10.1016/j.bbrc.2020.03.138

Conflict of Interest: The authors declare that the research was conducted in the absence of any commercial or financial relationships that could be construed as a potential conflict of interest.

Copyright © 2020 Sundararajan, Pang, Choolani and Huang. This is an open-access article distributed under the terms of the Creative Commons Attribution License (CC BY). The use, distribution or reproduction in other forums is permitted, provided the original author(s) and the copyright owner(s) are credited and that the original publication in this journal is cited, in accordance with accepted academic practice. No use, distribution or reproduction is permitted which does not comply with these terms.

Advantages of publishing in Frontiers

OPEN ACCESS
Articles are free to read for greatest visibility and readership

FAST PUBLICATION
Around 90 days from submission to decision

HIGH QUALITY PEER-REVIEW
Rigorous, collaborative, and constructive peer-review

TRANSPARENT PEER-REVIEW
Editors and reviewers acknowledged by name on published articles

Frontiers
Avenue du Tribunal-Fédéral 34
1005 Lausanne | Switzerland

Visit us: www.frontiersin.org
Contact us: frontiersin.org/about/contact

REPRODUCIBILITY OF RESEARCH
Support open data and methods to enhance research reproducibility

DIGITAL PUBLISHING
Articles designed for optimal readership across devices

FOLLOW US
@frontiersin

IMPACT METRICS
Advanced article metrics track visibility across digital media

EXTENSIVE PROMOTION
Marketing and promotion of impactful research

LOOP RESEARCH NETWORK
Our network increases your article's readership